



## **27<sup>th</sup> International QUENCH Workshop**

27-29 September 2022  
Karlsruhe Institute of Technology  
Karlsruhe, Germany

**Editor: Martin Steinbrück**

DOI: [10.5445/IR/1000152245](https://doi.org/10.5445/IR/1000152245)



## AGENDA

### 27<sup>th</sup> International QUENCH Workshop\*

Karlsruhe Institute of Technology, Campus North, H.-von-Helmholtz-Platz 1, 76344 Egg.-Leopoldshafen, Germany  
27-29 September 2022

**Meeting Location:** Fortbildungszentrum für Technik und Umwelt (FTU), Auditorium (Aula)

**Tuesday, 27 Sep 2022**

8:10	<b>Pick-up at the hotel Kübler</b>	
8:30	<b>Registration</b>	
9:00	Welcome	W. Tromm/M. Steinbrück, KIT
	<b><u>QUENCH PROGRAM: RECENT RESULTS</u></b> (Chair: M. Steinbrück, KIT)	
9:20	Update of the QUENCH Program	M. Steinbrück, KIT
9:40	Preparation of the QUENCH ATF1 bundle test with Cr coated optimized ZIRLO claddings and results of the reference test QUENCH LOCA 3HT	J. Stuckert, KIT
10:10	Post-test examinations of the QUENCH tests simulating LOCA by means of neutron imaging	M. Grosse, KIT
10:30	<b>Coffee break (Group Photo)</b>	
	<b><u>ATF CLADDING I</u></b> (Chair: M. Grosse, KIT)	
11:00	ATF related activities at OECD/NEA	J.-F. Martin, OECD-NEA
11:20	Accident Tolerant Fuel: Cr Coated Cladding Development at Westinghouse	L. Czerniak, WEC
11:40	Degradation mechanisms of the most promising ATF cladding concepts	M. Steinbrück, KIT
12:10	High-temperature behavior of accident-tolerant control rods clad with Zr alloy during BDBA and SA leading to reaction with molten fuel	K. Nakamura, CRIEPI
12:30	<b>Lunch</b>	
	<b><u>ATF CLADDING II</u></b> (Chair: J.-F. Martin, OECD-NEA)	
13:30	Safety envelop study of Cr-coated Zircaloy ATF via SNU's integral LOCA experiment	Y. Lee, SNU
14:00	Effect of Cr content on the on-cooling phase transformations and induced prior- $\beta$ Zr mechanical hardening and failure mode (in relation with E-ATF Cr Coated Zr-based claddings behavior upon and after high temperature transients)	J.-C. Brachet, CEA

\* In Cooperation with the International Atomic Energy Agency (IAEA)



14:30	UHT Test Facility Updates and Oxidation Tests for Accident Tolerant Fuel Developments	G. Wang, WEC
15:00	<b>Coffee break</b>	
	<b>EXPERIMENTS</b> (Chair: J. Stuckert, KIT)	
15:30	Burst and oxidation tests on bare and pre-oxidized claddings	C. Duriez, IRSN
16:00	Ballooning and Burst Measurement of Nuclear Fuel Claddings	R. Nagy, CER-EK
16:30	Overview on COSMOS Facility on thermal-hydraulic phenomena in nuclear reactors	S. Gabriel, KIT
17:00	<b>Bus transfer to the hotel</b>	

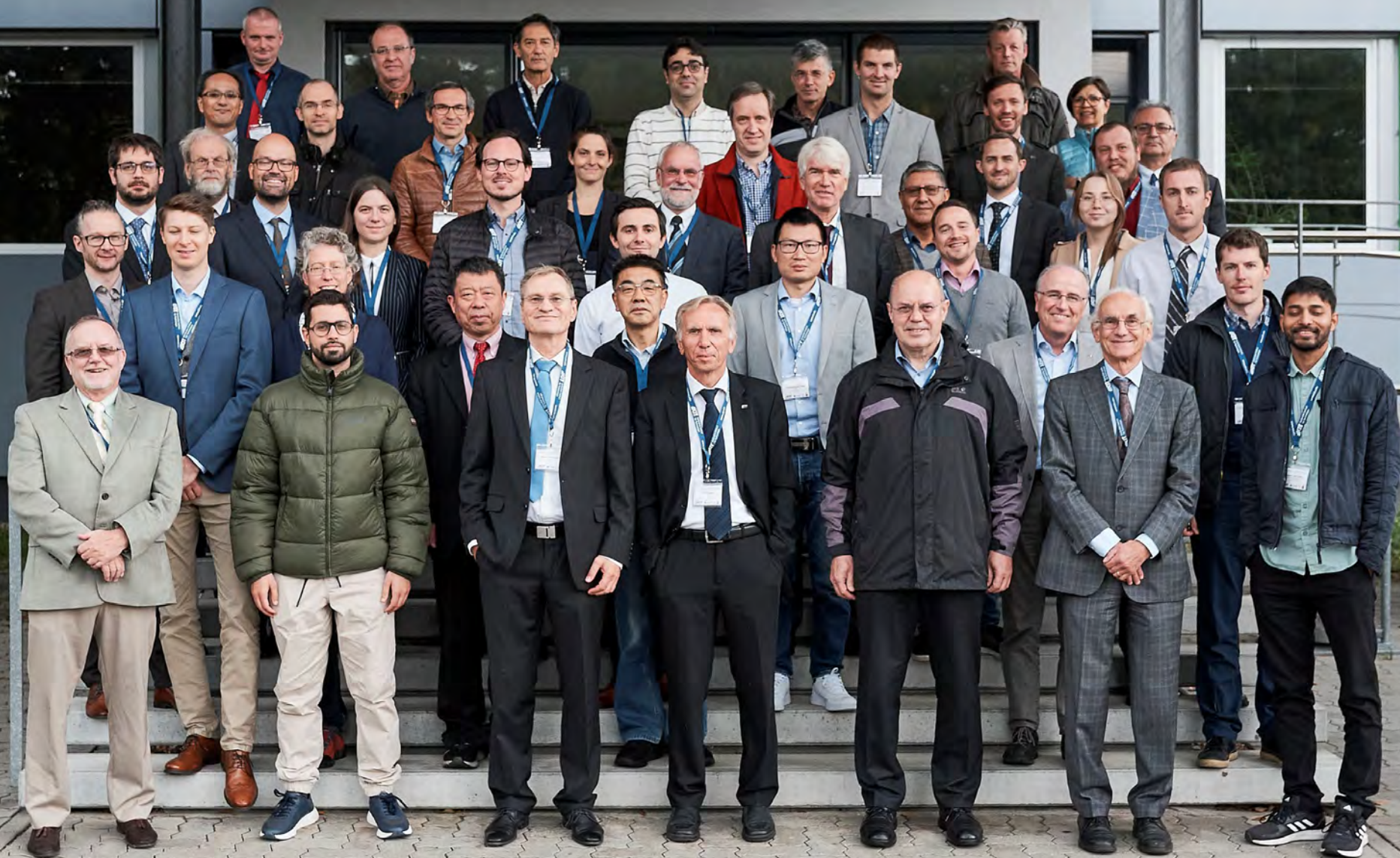
**Wednesday, 28 Sep 2022**

8:30	<b>Pick-up at the hotel Kübler</b>	
	<b>MODELLING AND CODE APPLICATION I</b> (Chair: C. Allison, ISS)	
9:00	Preliminary simulation results of the experiments QUENCH-L3HT and QUENCH-ATF-1 regarding high-temperature oxidation mechanisms using the system code AC <sup>2</sup>	G.T. Stahlberg, RUB
9:20	Preliminary Analysis of the QUENCH-19 Test by means of the ASTEC Code	F. Gabrielli, KIT
9:40	Simulation of QUENCH-19 and QUENCH-20 with AC <sup>2</sup> /ATHLET-CD	T. Hollands, GRS (L. Tiborcz)
10:10	Preliminary Modelling Results Of QUENCH-20 Test Using RELAP/SCDAPSIM code	T. Kaliatka, LEI
10:30	<b>Coffee break</b>	
	<b>MODELLING AND CODE APPLICATION II</b> (Chair: L. Tiborcz, GRS)	
11:00	First assessment of PSI nitriding model against QUENCH-air experiments	B. Jäckel, PSI
11:30	Evolution of Pressure-assisted Mis-fit Stress During the Clad Corrosion: The Materials Selection	A. Aryanfar, AUB
12:00	Estimates of the VVER-1000 Fuel Assembly Behavior and Possible In-Vessel Instrument Responses during SBO-like Conditions	C. Allison, ISS
12:30	<b>Lunch</b>	
13:30	Overview on LWR nuclear safety research at KIT	W. Tromm, KIT
14:00-17:00	Technical visit of QUENCH, COSMOS and SET labs	KIT
17:30	<b>Bus to Höpfner Brewery</b>	
ca. 21:30	<b>Arrival at KIT and in hotel</b>	

**Thursday, 29 Sep 2022**

8:30	<b>Pick-up at the hotel Kübler</b>	
	<b>LONG-TERM DRY STORAGE</b> (Chairs: M. Grosse, KIT/F. Boldt, GRS)	
9:00	Overview of spent fuel ageing studies and testing at JRC Karlsruhe	T. Wiss, JRC KA
9:30	SPIZWURZ project: Benchmark Update and Progress	F. Boldt, GRS
10:00	Update of the investigations on the hydrogen solubility and diffusivity in cladding tube materials in the framework of the SPIZWURZ project	S. Weick, KIT
10:25	<b>Coffee break</b>	
10:55	Understanding mechanical integrity of hydrided Zircaloy cladding for extended spent fuel management	Y. Lee, SNU
11:25	Use of advanced imaging methods for characterizing hydrogen related cladding degradation	A. Colldeweih, PSI
11:55	New test facilities at KIT for investigation of hydrogen/hydride behavior in Zr alloys	M. Grosse, KIT
12:20	<b>Closure of the Workshop</b>	M. Steinbrück, KIT
12:30	<b>Lunch</b>	
13:30	<b>Bus for train station and hotel</b>	
14:00	<b>QUENCH ATF Program Review Group Meeting</b> Building 681, Room 214 <i>Only for QUENCH-ATF PRG Members</i>	
Friday	<b>QUENCH ATF Management Board Meeting</b> Building 681, Room 214 <i>Only for QUENCH-ATF MB Members</i>	
9:00		

# 27th International QUENCH Workshop





**W. Tromm**  
**KIT**

### **Welcome address**

The head of the nuclear safety program at KIT (NUSAFE) gave an overview on the program status and perspectives.



# Welcome Address: 27th QUENCH workshop at KIT

## Outlook Programme NUSAFE at KIT and Helmholtz Association

Th. Walter Tromm, Programme Nuclear Waste Management, Safety and Radiation Research



## NUSAFE Topic 2, EU-projects

- In the Euratom Call NFRP-2021-2022 in October 2021, a total of 10 proposals with KIT participation were submitted, 1 of which was coordinated by KIT
- Evaluation results in February 2022: 9 of the 10 submitted proposals were approved, including the one coordinated by KIT - success rate: 90%
- Approved funding amount for KIT: about 2.9 million euros over 4 years

Acronym	EC funding for KIT	Full title
<i>bewilligt:</i>		
ANSELMUS	68.719,00	Advanced Nuclear Safety Evaluation of Liquid Metal Using Systems
ASSAS	358.313,00	Artificial intelligence for the Simulation of Severe AccidentS
ENEN2plus	105.000,00	Building European Nuclear Competence through continuous Advanced and Structured Education and Training Actions
ESFR-SIMPLE	578.774,00	European Sodium Fast Reactor - Safety by Innovative Monitoring, Power Level flexibility and Experimental research
INNUMAT (Koord.: KIT)	1.021.986,00	Innovative Structural Materials for Fission and Fusion
OFFERR	42.500,00	eurOpean platForm For accEssing nucleaR R&d facilities
SASPAM-SA	247.032,00	Safety Analysis of SMR with PASSive Mitigation strategies - Severe Accident
SCORPION	249.930,00	SiC composite claddings: LWR performance optimization for nominal and accident conditions
SEAKNOT	192.047,00	SEvere Accident research and KNOWledge management for LWRs
<i>bewilligte Summe</i>	<b>2.864.301,00</b>	
<i>nicht bewilligt:</i>		
ARMSTRONG		Advanced Robust Multiphysics Simulation Tools for Reactors Of New Generation

# Program NUSAFE/Topic 2: Excerpt of the recommendations

- The NUSAFE program of KIT provides an enormously important contribution to the urgently needed maintenance of nuclear competences in Germany, regardless of the nuclear phase-out.
- The COSMOS, KALLA, and QUENCH facilities represent major investments, and belong to the leading facilities of their kind worldwide.
- QUENCH specifically delivers important inputs for ATF and to the issues of long-term dry storage, which is particularly imminent in Germany. This is why the SAB supports the continuation of the facility.
- The JRODOS code is a flagship development of KIT.
- International interest in advanced small reactors growing, even with closed fuel cycle.
- International cooperation with many countries is well developed by KIT. This also will help to keep competence in the relevant research fields and to contribute to specific questions pertaining to international nuclear safety.

## NUSAFE Topic 2: Highlights

- Development of advanced safety analysis tools for Small Modular reactors (SMR)
- ASTEC and JRODOS: Assessment of the radiological consequences of severe accidents in nuclear power plants
- Helmholtz QUENCH Test Facility: Conduction of experiments on accident tolerant fuels (ATF) cladding materials as OECD/NEA Joint Undertaking, see lab visit

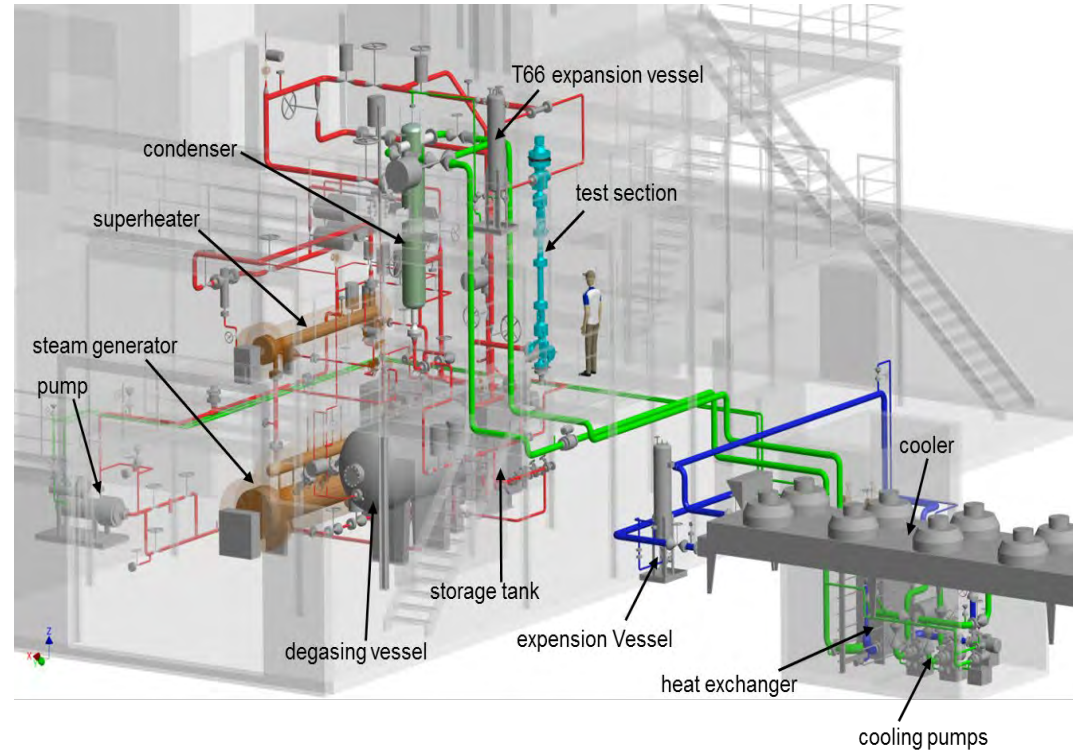


# Development of advanced safety analysis tools for Small Modular reactors (SMR)



- **EU-project McSAFER:**  
Improving safety analysis methodologies
- Increased deployment of different SMR-design in EU and worldwide
- BMBF-initiative „Innovationspool-Projekts „**Sicherheitsbewertung generischer kleiner modularer Reaktoren (SMR)**“ to support:
  - Develop advanced simulation tools for safety analysis of SMR to be build in Europe
  - Contribute to the validation of numerical simulation tools using experimental data relevant for SMR e.g. data generated at KIT COSMOS-H facility
  - KIT Focus:
    - advanced neutronic (MC and transport) and thermal hydraulics (two-phase, porous-media) for the core and plant behavior of SMR
    - Experimental investigations at COMSOS-H facility (safety-relevant TH phenomena e.g. boiling, CHF)

- Experiments in McSAFER (High-Performance Advanced Methods and Experimental Investigations for the Safety Evaluation of Generic Small Modular Reactors)
- Two series of experiments are planned to investigate the thermal hydraulics in different SMR concepts
  - Investigation of flow boiling up to the critical heat flux under reactor typical conditions

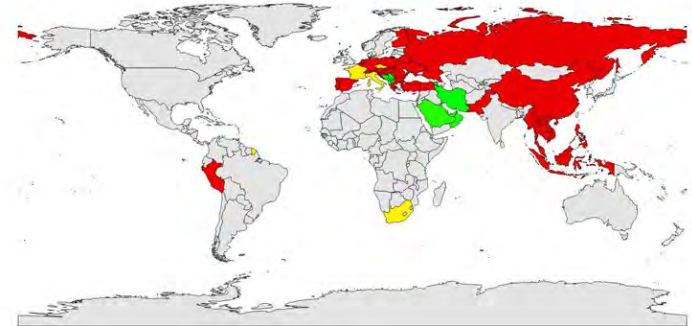




# JRODOS

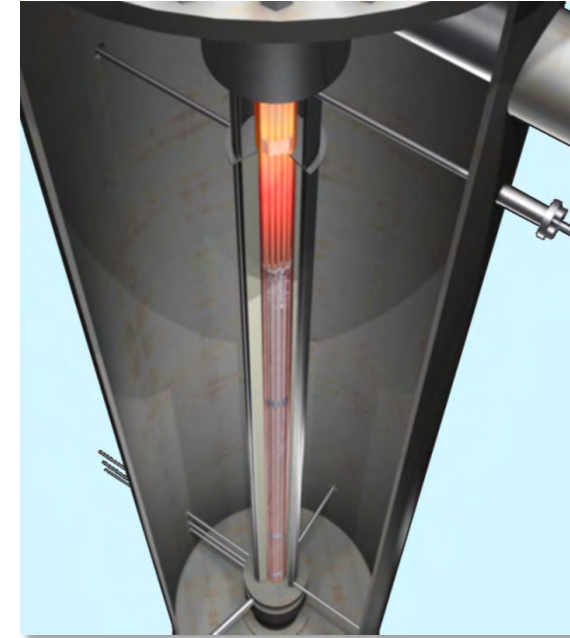
- JRODOS is used operational in many European countries and since more than 15 years in Germany
- It is installed – partly with the support the European Commission – in about 40 countries worldwide
- Ongoing installations are in the ASEAN countries, six Gulf states, six West-Balkan states, Armenia and Iran

- RODOS installation
  - RODOS installation – started
  - RODOS local users
- 2020 Installation in West Balkan countries, GCC countries, Armenia and Iran





- Three bundle experiments with ATF cladding in the QUENCH facility
- Time frame: 2021-2024
- Costs: 1.5 M€ (approx. 500 000 €/test) + NEA fee
  - 50% covered by KIT/Germany, 50% covered by collaborators



# Many thanks for your attention

**Th. Walter Tromm**  
**Karlsruhe Institute of Technology**  
**Programme Nuclear Waste Management,**  
**Safety and Radiation Research**

**walter.tromm@kit.edu**



**M. Steinbrück**

**KIT**

## **Update of the QUENCH Program**

The main objective of the QUENCH program at KIT is the investigation of the hydrogen source term and materials interactions during LOCA and the early phase of severe accidents including reflood. Bundle experiments as well as separate-effects tests are conducted to provide data for the development of models and the validation of severe fuel damage code systems.

The QUENCH bundle facility is a unique out-of-pile bundle facility with electrically heated fuel rod simulators and extensive instrumentation. So far, 20 experiments with various severe accident (SA) scenarios as well as a series of eight DBA LOCA experiments were conducted. The QUENCH-LOCA series was completed in 2016. One of the main results is the definition of the conditions for secondary hydriding around the burst position and its influence on the mechanical properties of the cladding rods.

The most recent QUENCH bundle tests was conducted in July 2022 with ATF cladding tubes in the framework of the OECD-NEA Joint Undertaking QUENCH-ATF.

Separate-effects tests during 2020/21 were focused on the high-temperature behavior of various ATF cladding candidates as well as on the behavior of hydrogen in Zr alloys under long-term dry storage conditions.

QUENCH bundle tests are part of the validation matrices of most SFD code systems, which was also reflected during the session “Modelling and code validation”.

A long-duration test (8 month) is planned in the framework of the German SPIZWURZ project on long-term dry intermediate storage of used fuel elements, after which the two remaining bundle experiments with ATF cladding in the framework of the NEA project are foreseen.

Most activities of the QUENCH group are embedded in international cooperation in the framework of the EC, OECD-NEA and IAEA.

Finally, the status of reporting and publishing as well as the numerous national and international cooperations were briefly described and acknowledged.



# Update of the QUENCH Program

**M. Steinbrück, J. Stuckert, M. Große et al.**

*27th International QUENCH Workshop, Karlsruhe Institute of Technology, 27-29 Sept 2022*

Institute for Applied Materials, Programme NUSAFE





## Outlook

- Motivation
- Experimental facilities
- ATF activities
- Long-term dry intermediate storage activities
- Modelling / Code validation
- Reporting
- Cooperation
- Future planning

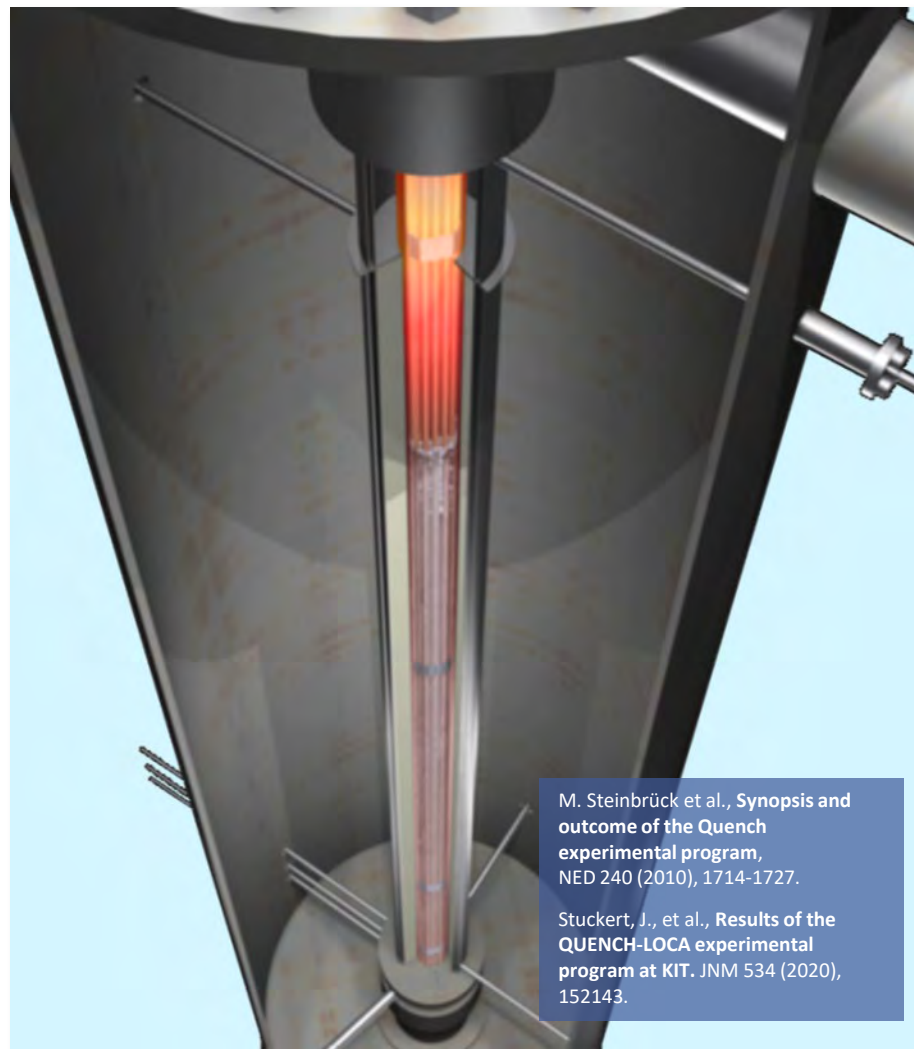


- Reflood is a prime accident management measure to terminate a nuclear accident
- Reflood may cause temperature excursion connected with increased hydrogen and FP release (severe accidents) and embrittlement of cladding and secondary hydriding (LOCA)
- Coolability of a degraded core is a matter of high priority (Fukushima)
- ➡ QUENCH experiments (bundle+SET) provide data for development of models and validation of SFD code systems

- Accident tolerant fuel (ATF) cladding
  - Characterization of promising ATF cladding concepts at (very) high temperatures
  - Degradation mechanisms and kinetic data
  - Max. temperature and coping time for AMMs
- Long-term dry intermediate storage
  - Hydrogen/hydride behavior in Zr cladding during 50-100 years storage e.g. in CASTOR casks
  - Hydride reorientation and its effect on mechanical properties

# QUENCH/LICAS facility

- Unique out-of-pile bundle facility to investigate reflood of an overheated reactor core
- 21-31 electrically heated fuel rod simulators; T up to >2000°C
- Extensive instrumentation for T, p, flow rates, level, etc. + MS
- So far, 20 experiments on SA performed (1996-today)
  - Influence of pre-oxidation, initial temperature, flooding rate
  - B<sub>4</sub>C, Ag-In-Cd control rods
  - Air ingress; debris formation
  - Advanced cladding alloys
- 7+1 DBA LOCA experiments with separately pressurized fuel rods



# Upgrade of the QUENCH facility

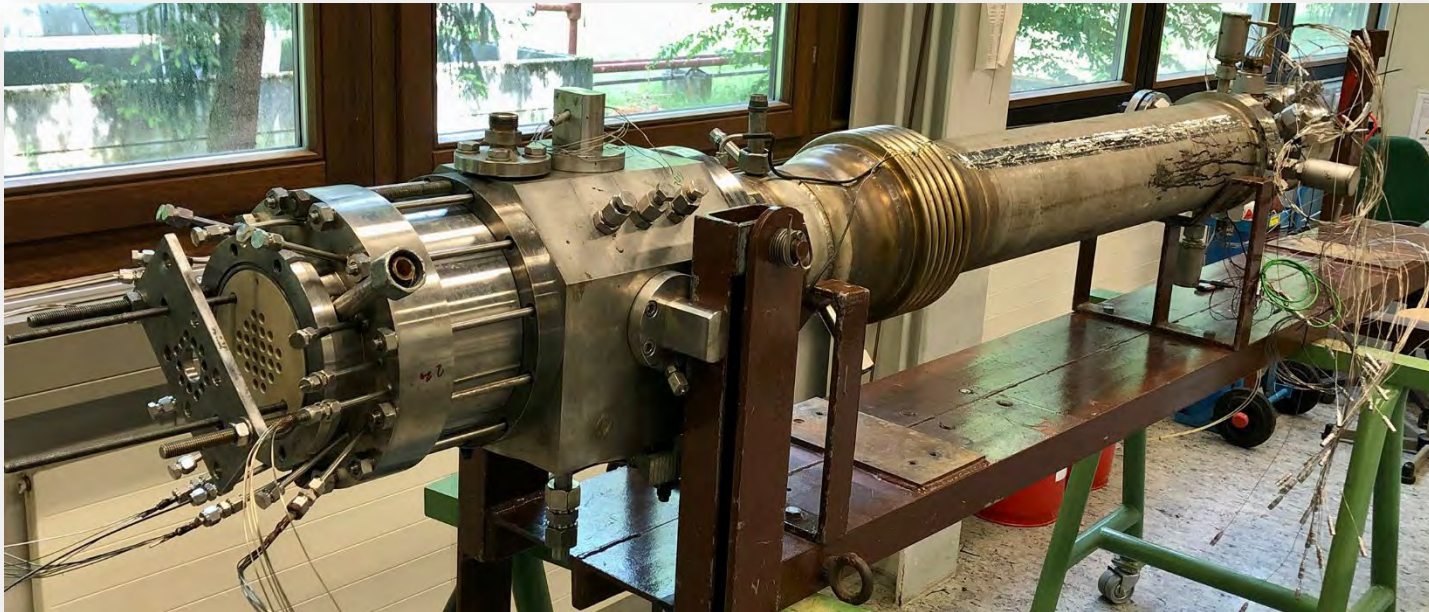
- New power supply system
  - Two DC generators with a maximum power of 80 kW each (4000 A, 20 V)
  - Improved precision of power adjustment
- New design of electric connections to fuel rod simulators
  - Allowing measurement of resistance and power of every single rod
- Improved and simplified design of fuel rod simulators
  - Easier assembly and disassembly of fuel rod simulators
- Thermostatic control of the cooling jacket temperature
  - Especially for long-term SPIZWURZ test





## QUENCH-ATF1 bundle test

- Conducted in July 2022 in the framework of the OECD-NEA Joint Undertaking QUENCH-ATF
- Scenario: Slightly beyond DBA-LOCA with QUENCH-LOCA3HT as reference test
- PTE and blind benchmark exercise ongoing





- Three bundle experiments with ATF cladding in the QUENCH facility
  - Focus on Cr-coated Zr alloys
  - Option for SiC cladding in second phase of project
  - Tubes provided by Westinghouse (US) (and others?)
  - Design basis and beyond design basis accident conditions
  
- Supporting separate-effects tests
  - at KIT
  - Complementary tests at IRSN (France)
  
- Code support for test preparation and code benchmark exercises, coordinated by GRS

## QUENCH-ATF #1 (July 2022)

- **Cr coated Zr** (provided by Westinghouse)
- Bundle with 24 heated rods, 12.6mm pitch
- **Extended LOCA** conditions: similar conditions as QUENCH-L3HT (LOCA 3 High Temperature) with optimized ZIRLO™, which will allow for comparison

## QUENCH-ATF #2 (2023)

- **Cr coated Zr**
- **Severe accident conditions**  
(above Zr-Cr eutectic)
- ATCR under discussion

## QUENCH-ATF #3 (~S1 2024)

- Cr coated Zr or SiC
- GO/NOGO on SiC in 2023
- Scenario depending on material and results of previous tests

# QUENCH-ATF Objectives

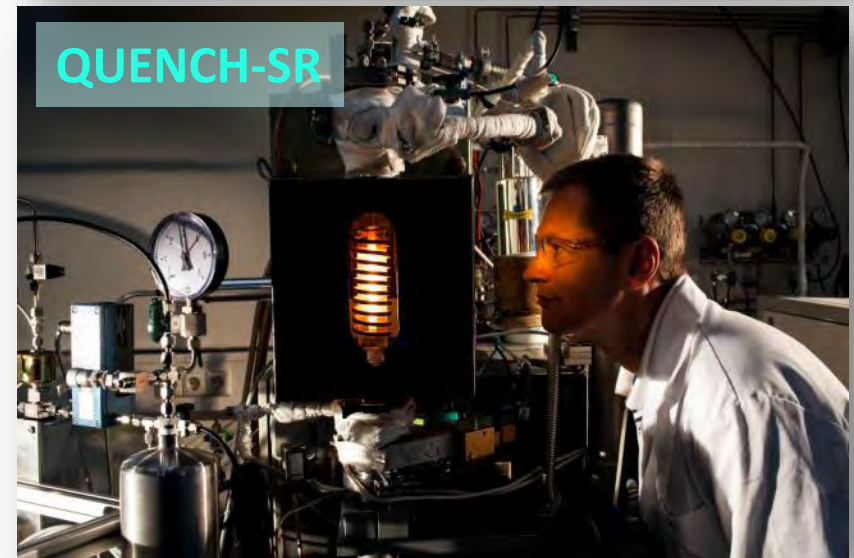
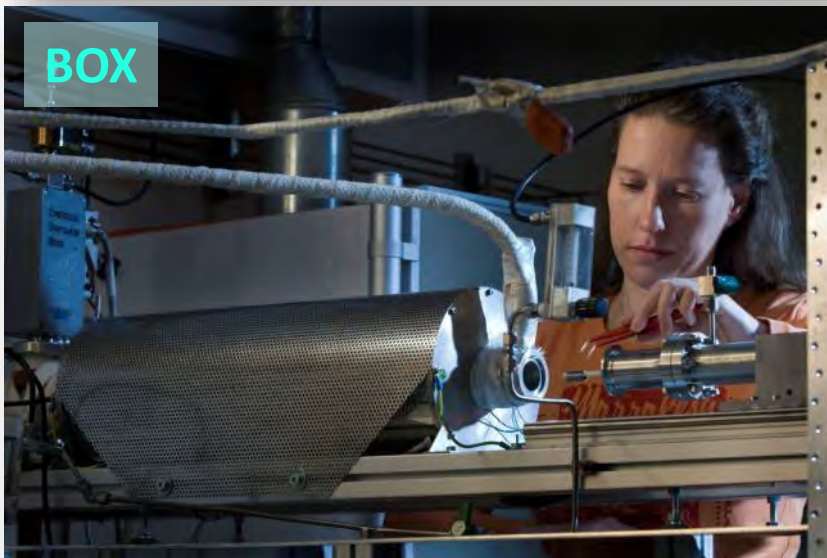
## DBA LOCA tests

- Claddings ballooning and burst, and bundle blockage by ballooned claddings
- Secondary hydrogenation via the uncoated inner Zry surface of the claddings through the burst opening
- Influence of the quenching on the rods integrity and residual ductility of the claddings after the reflood
- Comparison e.g. with the QUENCH-L3HT bundle test with uncoated ZIRLO™ cladding

## BDBA severe accident (SA, DEC) tests

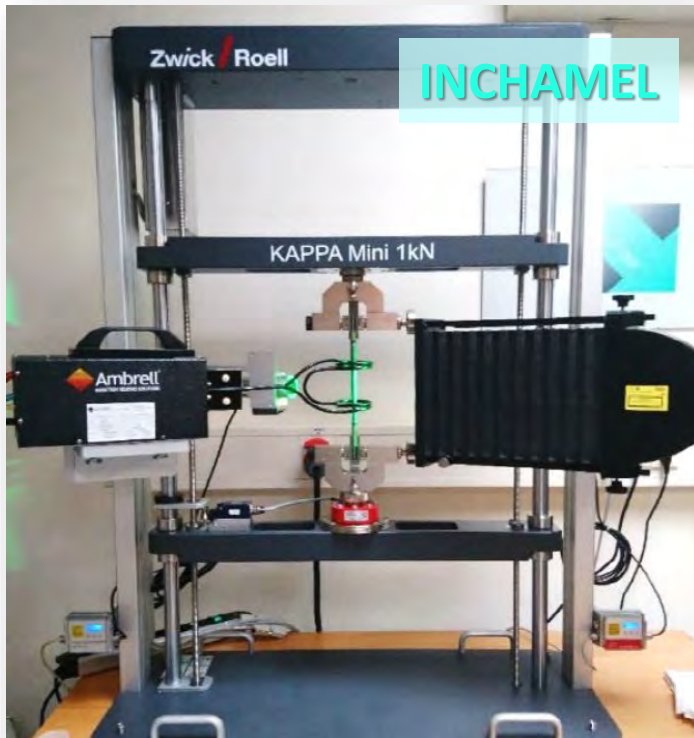
- Oxidation and hydrogen source term
- High-temperature materials interactions between Zry and Cr coating as well as between cladding and other FE structures (e.g. absorber rods)
- Potential increase of coping time
- Comparison e.g. with the QUENCH-15 experiment with uncoated ZIRLO cladding

# QUENCH Separate-effects tests: Main setups





# New test facilities



Apparatus for in-situ neutron radiography experiments under defined mechanical load and temperature



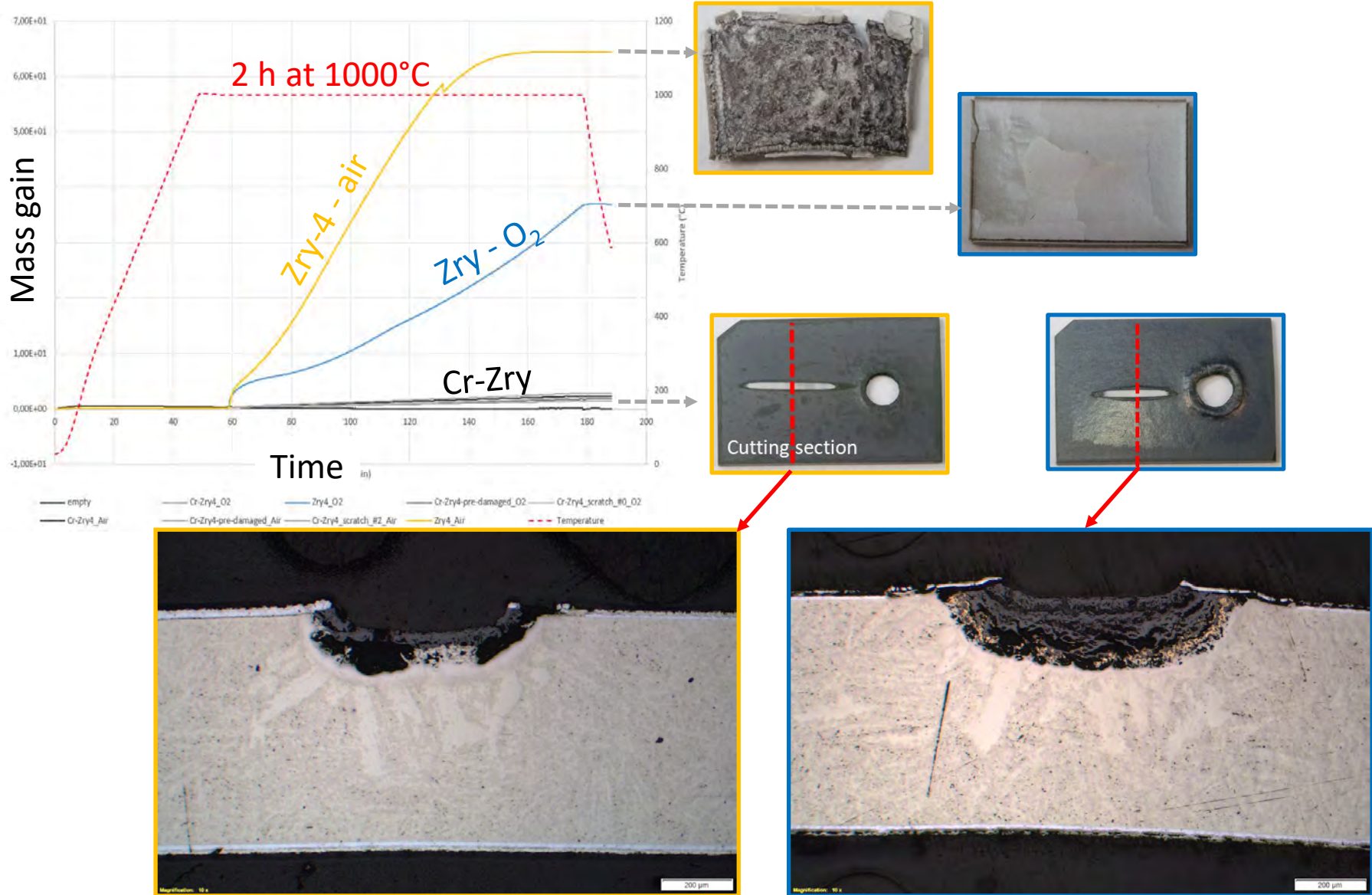
2.5 m long furnace for hydrogen pre-loading of cladding tubes for bundle tests

## QUENCH SET activities on ATF cladding materials

- Single-rod oxidation and quench tests various ATF cladding segment samples
- High-temperature furnace tests in various atmospheres for analysis of degradation mechanisms
- Development of MAX phase coatings
  
- Participation in various international collaborations on ATF
  - EC IL TROVATORE (Coordinator of WP “Coolant-cladding-fuel interaction”)
  - EC SCORPION (Coord. of WP “Coolant/cladding/fuel interaction tests”)
  - IAEA ATF-TS (Coordinator of Benchmark QU-19 and exp. program)
  - OECD NEA QUENCH-ATF (KIT is Operating Agent)
  - OECD NEA TCOFF-2
  - Various bilateral collaborations with CNL, CEA, CTU Prague, KONICOF, ...



# Oxidation of pre-damaged Cr-Zry in O<sub>2</sub> and air



## Long-term intermediate storage activities

- Work embedded in the German project SPIZWURZ (GRS, KIT) and the HGF HOVER infrastructure program
  - 8 month lasting bundle test in preparation
  - Various SETs on the system Zr-H
- Operation of a Sieverts type chamber for hydrogen loading of small samples (SICHA)
  - Investigation of the hydrogen uptake at temperatures relevant for dry storage of spent fuel
- Commissioning of the INCHAMEL test facility
  - Apparatus for in-situ neutron radiography experiments under defined mechanical load and temperature
- Commissioning of the HOKI test facility
  - 2.5 m long furnace for hydrogen pre-loading of cladding tubes for bundle tests

## Modelling and code validation

- QUENCH bundle tests are part of validation matrices of most SFD code systems
- Post-test calculations of QUENCH-19 (FeCrAl) in the framework of the IAEA ATF-TS project
- Post-test calculations for QUENCH-20 (BWR) by various partners
- Pre-test calculation of QUENCH-ATF-1 and LICAS-01 by GRS
- Benchmark exercise (blind & open phase) on QUENCH-ATF1 test coordinated by GRS
- Separate-effects test data are used by various institutions for model development



# Reporting

■ Papers and conference contributions (18 Scopus references in 2021/22)

■ QUENCH-19 (FeCrAl) report published

■ QUENCH-20 (BWR) report published

Nuclear Engineering and Design  
Contents lists available at ScienceDirect  
ELSEVIER  
journal homepage: [www.elsevier.com/locate/nuengdes](http://www.elsevier.com/locate/nuengdes)

Effect of steam and oxygen starvation on severe accident progression with air ingress  
Róbert Farkas<sup>a,\*</sup>, Zoltán Hózer<sup>a</sup>, Inre Nagy<sup>a</sup>, Nóra Vér<sup>a</sup>, Márta Horváth<sup>a</sup>, Martin Steinbrück<sup>b</sup>, Juri Stuckert<sup>c</sup>, Mirco Grosse<sup>b</sup>

<sup>a</sup> Center for Energy Research (ER), Budapest, Hungary  
<sup>b</sup> Karlsruhe Institute of Technology (KIT), Karlsruhe, Germany

ARTICLE INFO  
ABSTRACT

Keywords: Severe accident test; Core degradation; VVER reactor

The CODEX-ATF experiment simulated an air vessel air ingress scenario after failure of bottom head of a nuclear reactor. 1400 °C maximum temperature was reached with the electrical heated bundle and after steel-clad down sea

Journal of Nuclear Materials 564 (2022) 119319

Journal of Nuclear Materials  
Contents lists available at ScienceDirect  
ELSEVIER  
journal homepage: [www.elsevier.com/locate/jnucmat](http://www.elsevier.com/locate/jnucmat)

## 1. Introduction

Severe reactor accidents during heat and low heat integration and rod cladding between core degradation and degradation progress in the core still maintain rod TM-2 accident (1). The failure of the access to heat fuel

## Oxidation mechanism and kinetics of nuclear-grade FeCrAl alloys in the temperature range of 500–1500 °C in steam

Chaewon Kim<sup>a,b</sup>, Chongchong Tang<sup>a</sup>, Mirco Grosse<sup>a</sup>, Yunhwan Maeng<sup>c</sup>, Changheui Jang<sup>b,d</sup>, Martin Steinbrück<sup>b,e</sup>

<sup>a</sup> Institute for Applied Materials (IAM), Karlsruhe Institute of Technology (KIT), Karlsruhe D-76021, Germany  
<sup>b</sup> Department of Nuclear and Quantum Engineering, Korea Advanced Institute of Science and Technology (KAIST), Daejeon 34141, Republic of Korea  
<sup>c</sup> Korea Electric Power Corporation-Engineering & Construction Company (KEPCO-E&C), Gyeongju 39664, Republic of Korea

## ARTICLE INFO

Article history:  
Received 5 December 2021  
Received in revised form 24 February 2022  
Accepted 29 March 2022  
Available online 7 April 2022

Keywords:  
ATF claddings  
Nuclear-grade FeCrAl  
High-temperature steam oxidation  
Oxidation kinetics

\* Corresponding author.  
E-mail address: [chaewon.kim@kaist.ac.kr](mailto:chaewon.kim@kaist.ac.kr) (C. Kim).

## 1. Introduction

Since the Fukushima nuclear accident, worldwide efforts have been made for the development of accident tolerant fuel (ATF) cladding materials to mitigate the excessive hydrogen production from the oxidation of current Zr-alloy claddings [1–5]. Among ATF cladding candidates, Fe-based alloys such as FeCrAl exhibited superior oxidation resistance and good mechanical properties [1]. However, Fe-based cladding materials should have a thinner thickness due to the higher neutron absorption cross-section of Fe and Cr compared to Zr. High Cr and Al contents have benefit for the corrosion and oxidation resistance. However, high Al content makes steels brittle, which makes it difficult to produce thin cladding tubes. High Cr content also makes alloys susceptible to thermal and irradiation embrittlement owing to the accelerated phase decomposition. Thus, Oak Ridge National Laboratory (ORNL) developed nuclear-grade FeCrAl alloys containing lower Cr content compared to commercial Kanthal alloys to mitigate the embrittlement issue [6].

While commercial FeCrAl alloys show slow oxidation kinetics by forming a protective alumina layer in high-temperature steam environments [7,8], nuclear-grade FeCrAl alloys also have superior oxidation resistance in spite of their lower Cr content [6,8]. As

\* Corresponding authors.  
E-mail addresses: [chang@kate.ac.kr](mailto:chang@kate.ac.kr) (C. Jang), [martin.steinbrueck@kit.edu](mailto:martin.steinbrueck@kit.edu) (M. Steinbrück).

<https://doi.org/10.1016/j.jnucmat.2022.119319>  
0022-3113/© 2022 Elsevier B.V. All rights reserved.

Journal of Nuclear Materials 559 (2022) 119470  
Contents lists available at ScienceDirect  
ELSEVIER  
journal homepage: [www.elsevier.com/locate/jnucmat](http://www.elsevier.com/locate/jnucmat)

High-temperature oxidation and quenching of chromium-coated zirconium alloy ATF cladding tubes with and w/o pre-damage  
M. Steinbrück<sup>a,\*</sup>, U. Stegmaier<sup>a</sup>, M. Große<sup>a</sup>, L. Czerniak<sup>a</sup>, E. Lahoda<sup>a</sup>, R. Daum<sup>a</sup>, K. Yueh<sup>b</sup>

<sup>a</sup> Karlsruhe Institute of Technology, Germany  
<sup>b</sup> Westinghouse Electric Company, USA  
<sup>c</sup> Electric Power Research Institute, USA

ARTICLE INFO  
ABSTRACT

Article history:  
Received 7 October 2021  
Received in revised form 20 November 2021  
Accepted 12 December 2021  
Available online 13 April 2022

Chromium-coated zirconium alloys are one of the promising candidates for accident-tolerant fuel cladding (ATF) tubes for light water reactors (LWRs). In this study, the high temperature oxidation and degradation

Journal of Nuclear Materials 563 (2022) 119318

Corrosion Science  
Contents lists available at ScienceDirect  
ELSEVIER  
journal homepage: [www.elsevier.com/locate/corsci](http://www.elsevier.com/locate/corsci)

## 1. Introduction

Systematic investigations on the coating degradation mechanism during the steam oxidation of Cr-coated Zry-4 at 1200 °C  
Junkai Liu<sup>a,b,c</sup>, Martin Steinbrück<sup>a</sup>, Mirco Große<sup>a</sup>, Ulrike Stegmaier<sup>a</sup>, Chongchong Tang<sup>a</sup>, Di Yu<sup>b,c,d</sup>, Jianqiao Yang<sup>e</sup>, Yanguang Cui<sup>d</sup>, Hans Jürgen Seifert<sup>a</sup>

<sup>a</sup> Institute for Applied Materials (IAM), Karlsruhe Institute of Technology (KIT), D-76021 Karlsruhe, Germany  
<sup>b</sup> School of Nuclear Science and Technology, Xi'an Jiaotong University, Xi'an 710049, China  
<sup>c</sup> Key Laboratory of Thermal-Radiation Science and Engineering of MOE, School of Energy and Power Engineering, Xi'an Jiaotong University, Xi'an 710049, China  
<sup>d</sup> Shanghai Nuclear Engineering Research & Design Institute, Shanghai 200333, China

## ARTICLE INFO

Keywords:  
Accident-tolerant fuel (ATF) cladding  
High-temperature steam oxidation  
Diffusion  
Oxidation kinetics transition  
Coating degradation

## 1. Introduction

After the Fukushima nuclear power plant accidents in 2011, the concept of Accident-tolerant fuels (ATFs) was proposed to improve the safety of nuclear reactors under design basic accident (DBA) and beyond design basic accident (BDBA) conditions by improving or replacing the current Zircaloy cladding–UO<sub>2</sub> fuel system [1–4]. Among different ATF concepts, Zircaloy substrates with surface protective coatings have attracted much attention owing to their low R&D costs and short R&D time [5–13]. Among the numerous candidate materials for surface coatings on Zircaloy, pure Cr is considered as the most promising coating material due to its excellent oxidation resistance [14] and adhesion property with Zircaloy substrate [15], relative low thermal neutron absorption cross-section [6], favorable thermo-mechanical properties [15–17], and irradiation resistance [18,19]. Up to date, the oxidation behavior and oxidation mechanism of the Cr-coated Zircaloy under high-temperature steam atmospheres have been extensively investigated by different research groups, and almost all the results show that the Cr coating can effectively protect the Zircaloy substrate from oxidation during the steam exposure up to 1200–1300 °C for a certain time [15,20–25].

However, although a large number of oxidation experiments with Cr-coated Zircaloy were conducted under steam atmosphere at different

temperatures, the coating degradation mechanism of the Cr-coated Zircaloy and the oxidation kinetics transition mechanism during the high-temperature steam oxidation are still ambiguous. Up to present, there are mainly two widely accepted mechanisms related to coating failure and degradation. One is proposed by Brachet et al. [26], the mechanism focuses on the failure of the unoxidized Cr coating beneath the outer Cr<sub>2</sub>O<sub>3</sub> scale. During steam oxidation, Zr diffuses from the Zircaloy substrate towards the outer Cr coating and is further oxidized into ZrO<sub>2</sub> on the Cr grain boundaries. The ZrO<sub>2</sub> grain inside the Cr coating connect with each other and finally form networks, which can act as paths for the inward diffusion of oxygen. Then the coating failure occurs and a large amount of oxygen reaches the Zircaloy substrate. Another mechanism is proposed by Han et al. [26,27] concentrating on the failure of the outer dense Cr<sub>2</sub>O<sub>3</sub> scale of the Cr coating during oxidation. The thickness of the Cr<sub>2</sub>O<sub>3</sub> scale first increases by the oxidation of Cr coating. When the Cr coating is completely oxidized and the thickness of the Cr<sub>2</sub>O<sub>3</sub> scale reaches its maximum value, the Cr<sub>2</sub>O<sub>3</sub> scale will be reduced by the redox reaction between Cr<sub>2</sub>O<sub>3</sub> and the Zircaloy substrate. The thickness decrease of the Cr<sub>2</sub>O<sub>3</sub> scale results in the fast inward diffusion of oxygen into the inner coating and the substrate through the outer Cr<sub>2</sub>O<sub>3</sub> scale. In our previous work on the transient oxidation behavior of the Cr-coated Zircaloy under steam atmosphere up to 1600 °C [23] and in later studies of Han et al. [20] and

\* Corresponding authors at: School of Nuclear Science and Technology, Xi'an Jiaotong University, Xi'an 710049, China.  
E-mail addresses: [liu1478@xjtu.edu.cn](mailto:liu1478@xjtu.edu.cn) (J. Liu), [dyun1979@xjtu.edu.cn](mailto:dyun1979@xjtu.edu.cn) (D. Yu).

<https://doi.org/10.1016/j.corsci.2022.119318>  
Received 25 January 2022; Received in revised form 28 March 2022; Accepted 9 April 2022  
Available online 13 April 2022  
0010-938X/© 2022 Elsevier Ltd. All rights reserved.

# Co-operations

## Programs

- NUGENIA
- HORIZON 2020
- IAEA
- OECD-NEA



## Bilateral

- PSI
- MTA EK
- IRSN, CEA, EdF
- RUB-LEE
- GRS
- Westinghouse
- USNRC
- KONICOF
- NECSA, BAM, HMI
- NRA, JAEA
- ISS
- ORNL
- CNL
- Various Chinese Organizations





- SPIZWURZ bundle experiment
  - Long-term intermediate storage test
  - 250 days, starting from 400°C with 1 K/d cooling rate
  - Three cladding types, two hydrogen concentrations, two pressures
  - Hydrogen pre-loading is ongoing
- QUENCH-ATF2 experiment
  - Severe accident test with Cr-coated Optimized ZIRLO cladding
- Post-test examinations of QUENCH-ATF1
- SETs on various topics, mainly on ATF cladding and Zry/H

## Acknowledgement

- Helmholtz Association for funding program NUSAFE at KIT
- Program NUSAFE and IAM institute's management for broad support of our activities
- BMWK for funding of the SPIZWURZ project
- EC for funding the projects IL TROVATORE and SCORPION
- OECD-NEA and partners for support of QUENCH-ATF
  
- And last but not least the QUENCH team:  
J. Laier, J. Moch, H. Muscher, U. Peters, **C. Roessger**,  
U. Stegmaier, C. Tang, S. Weick



**J. Stuckert**  
**KIT**

## **Preparation of the QUENCH-ATF1 bundle test with Cr coated optimized ZIRLO claddings and results of the reference test QUENCH-LOCA-3HT**

The first bundle test *QUENCH-ATF1* with Cr coated cladding tubes was prepared and successfully carried out on July 18, 2022. The test scenario was comparable to the earlier reference test *QUENCH-LOCA-3HT* with uncoated opt. ZIRLO cladding tubes with maximum temperatures of 1300 °C and thus slightly above design basis accident conditions. The post-test investigations will be performed similar to *QUENCH-LOCA-3HT*: profilometry with laser scanner, endoscope observations, ultrasound measurements of wall thickness, measurement of burst opening sizes by optical methods, metallography, neutron radio- and tomography, measurement of hydrogen concentration by hot extraction, tensile tests.

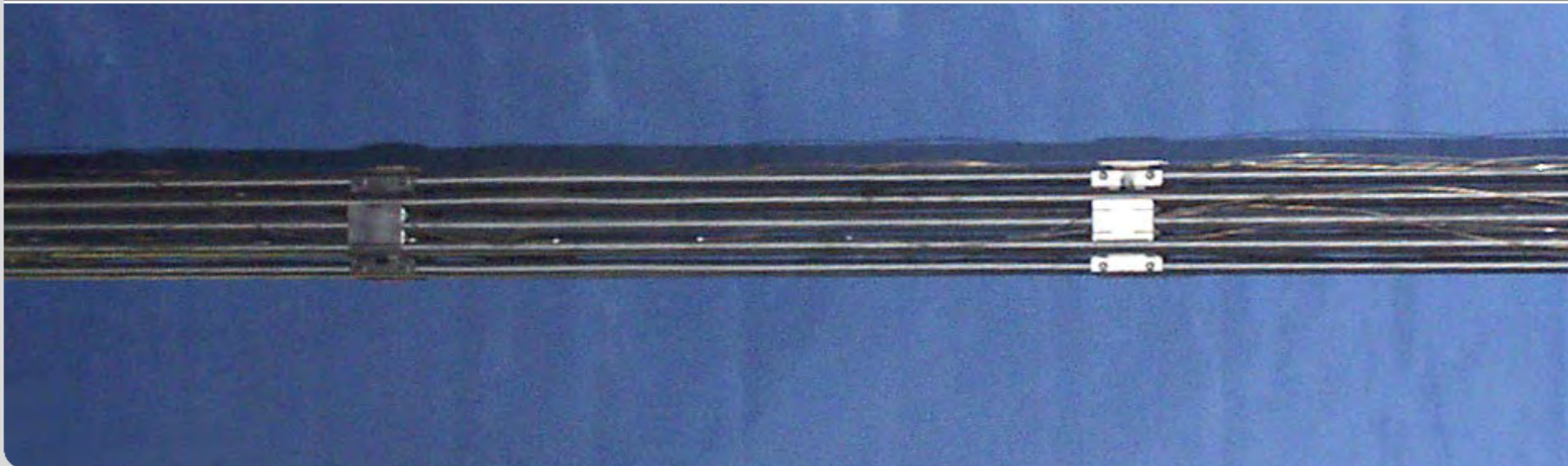
The evaluation of the *QUENCH-LOCA-3HT* results showed that the maximum of virtual coplanar blockage ratio of cooling channel was 35%. Due to moderate blockage a good bundle coolability was kept for both bundles. The cladding burst occurred at temperatures between 1030 and 1200 K; the average burst temperature was  $1127 \pm 48$  K. The inner rod pressures relief to the system pressure during about 30 s. During quenching, following the high-temperature phase, no fragmentation of claddings was observed (residual ductility is sufficient).

# Preparation of the QUENCH-ATF1 bundle test with Cr coated optimized ZIRLO claddings and results of the reference test QUENCH-LOCA-3HT

J. Stuckert, M. Große, J. Laier, J. Moch, U. Peters, C. Rössger, U. Stegmaier, M. Steinbrück

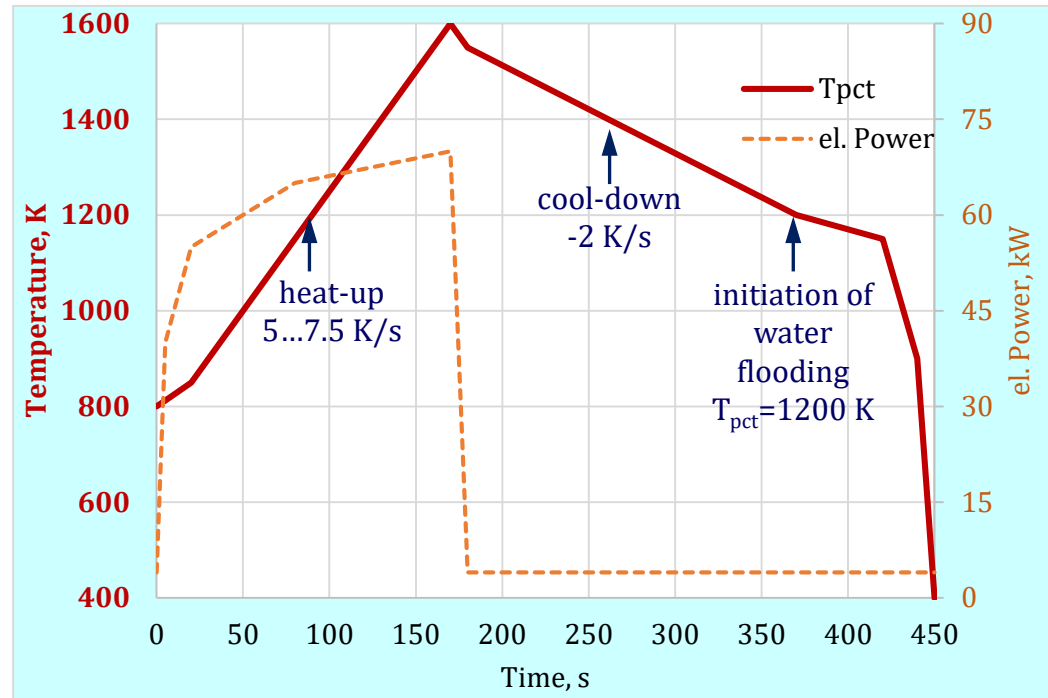
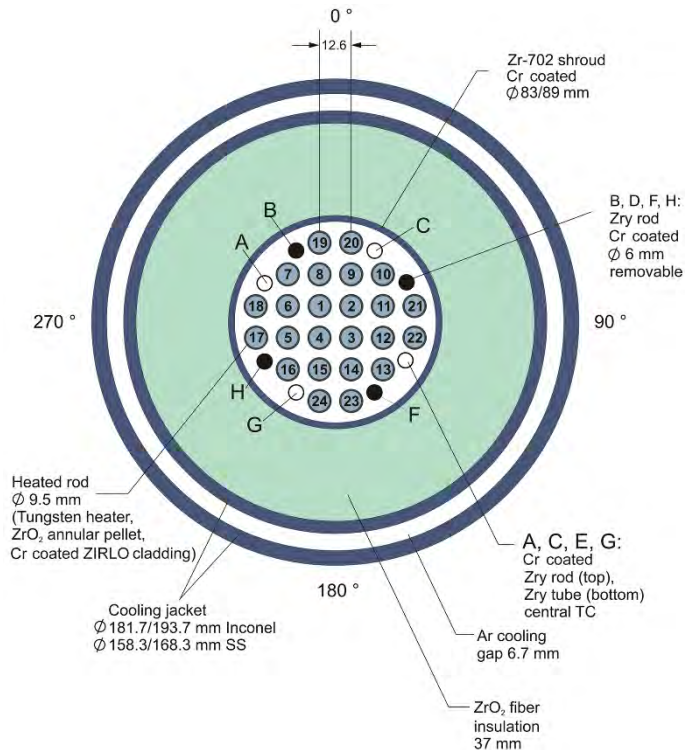
*QWS-27, Karlsruhe*

Institute for Applied Materials; Program NUSAFE



# QUENCH-ATF-1 bundle and proposed test scenario

- Test bundle with 24 heated rods, pitch 12.6 mm
- Heating-up rate during heating in superheated steam: 5 K/s
- Peak cladding temperature at the end of the heat-up stage:  $T_{pct}^{max} = 1600$  K (extended DBA conditions)
- Duration of cool-down stage during cooling from 1600 K to 1200 K in saturated steam:  $\approx 200$  s
- Rate of water flooding after cool-down stage:  $\approx 4$  g/s/rod



Test scenario according to the reference test QUENCH-LOCA-3HT



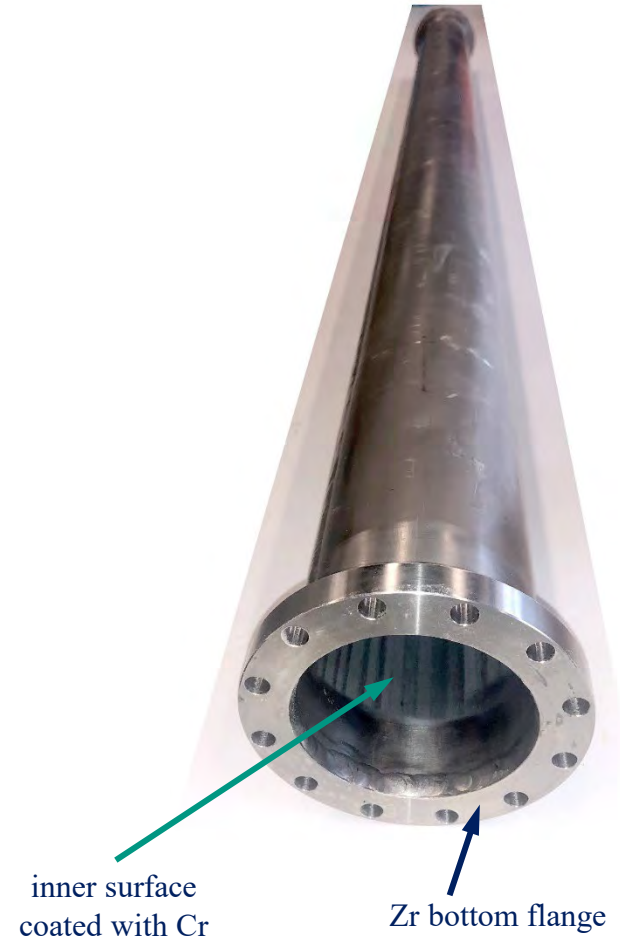
# Zr shroud coated internally with Cr



Zr sheet (thickness 3 mm)  
PVD coated at OERLIKON BALZERS GmbH  
with Cr (10  $\mu\text{m}$ , X-ray measured) at one side



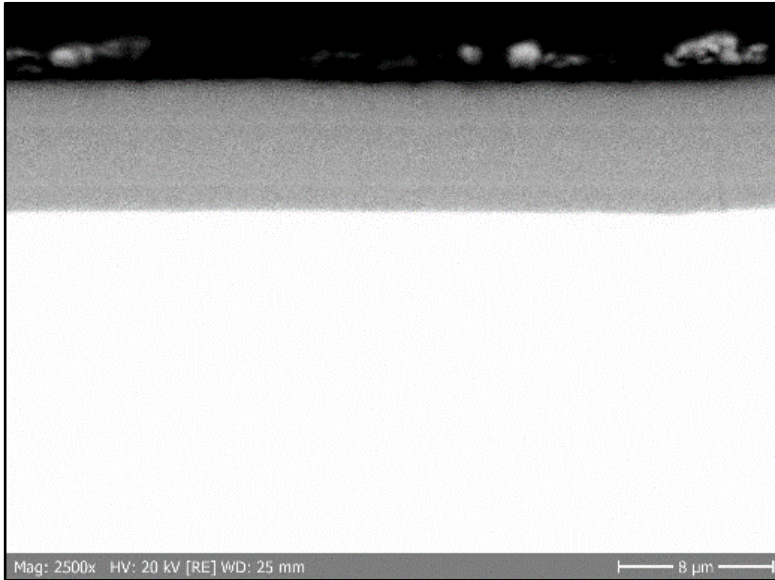
weld seam



inner surface  
coated with Cr

Zr bottom flange

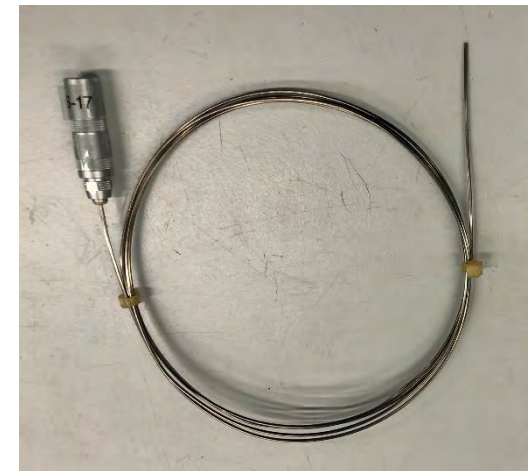
# Corner rods and instrumentation



PVD coating at OERLIKON BALZERS GmbH:  
homogeneous Cr layer before test (Cr layer 10 μm)



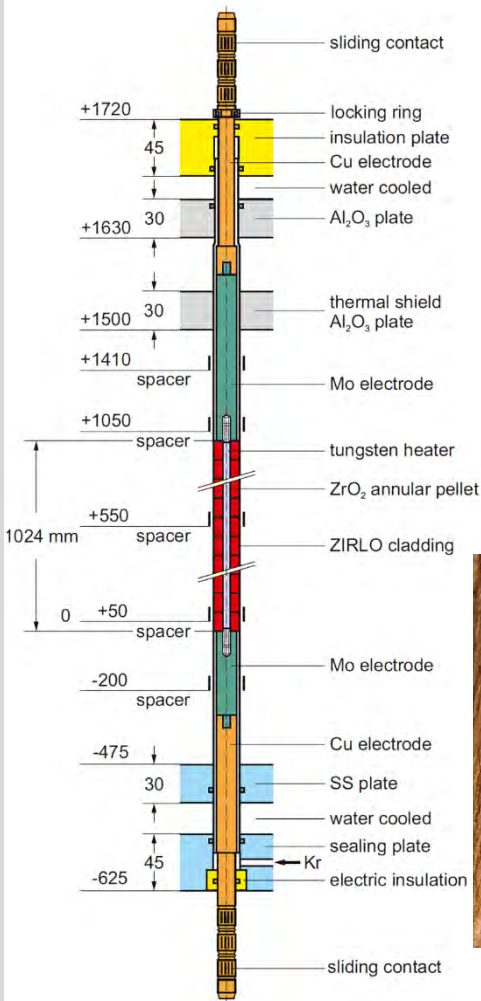
corner rods and tubes (OD 6 mm)  
PVD coated with Cr (10 μm)



75 NiCr/Ni thermocouples  
sheathed with stainless steel



# Heated rod parts: heaters, electrodes, pellets



24 heated rods



24 W heaters, OD 4.6 mm



2234 ZrO<sub>2</sub> pellets  
OD=7.93 mm,  
ID=4.75 mm



24 Mo/Cu upper electrodes  
partially coated by ZrO<sub>2</sub> (200 μm)  
OD 7.75 mm in coated region



24 Mo/Cu lower electrodes  
partially coated by ZrO<sub>2</sub> (200 μm)  
OD 7.75 mm in coated region



opt. ZIRLO claddings coated with Cr layer

*cladding tube parameters:*

OD without coating  $9.144 \pm 0.038$  mm;

ID 8.092 mm;

wall thickness 526  $\mu\text{m}$ ;

length in test bundle 2300 mm;

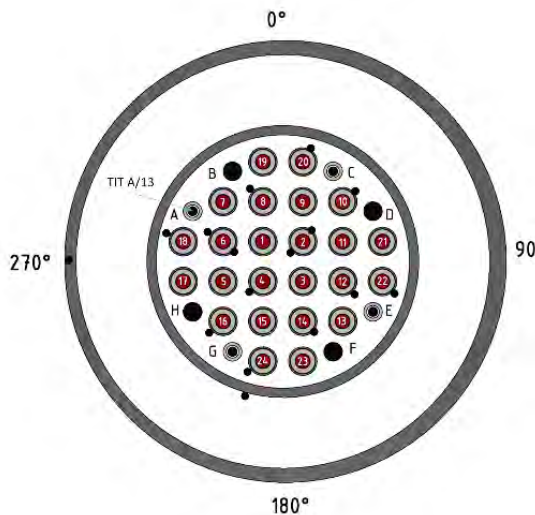
Cr layer thickness about 25  $\mu\text{m}$ .



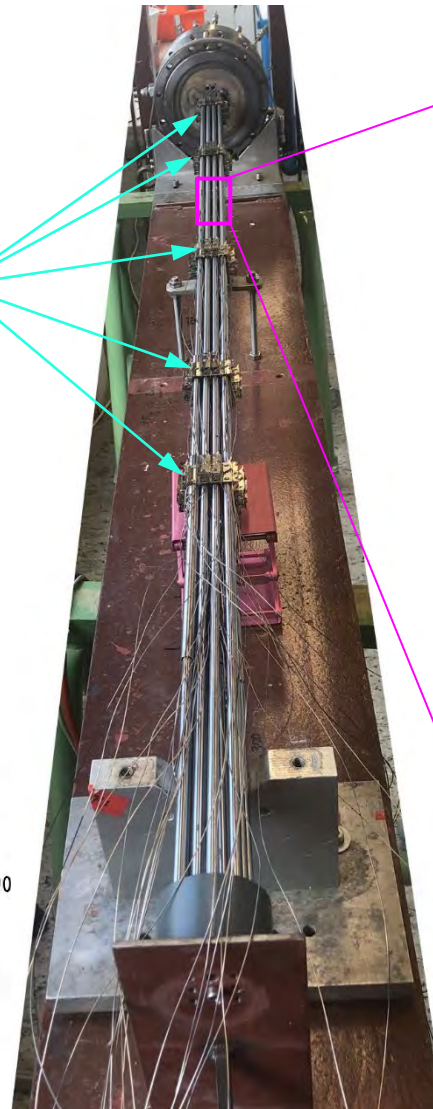
# Bundle assembly and instrumentation



eroded grid spacer  
pitch 12.6 mm



thermocouples at 950 mm



bottom view  
of bundle part with 16 rods



TCs at  
rod #10

850 mm

TC at rod #8

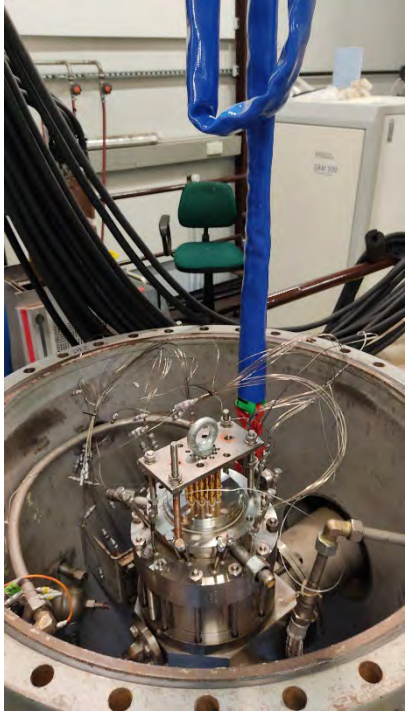
no scratches  
while dragging  
of tubes through  
the spacers

750 mm

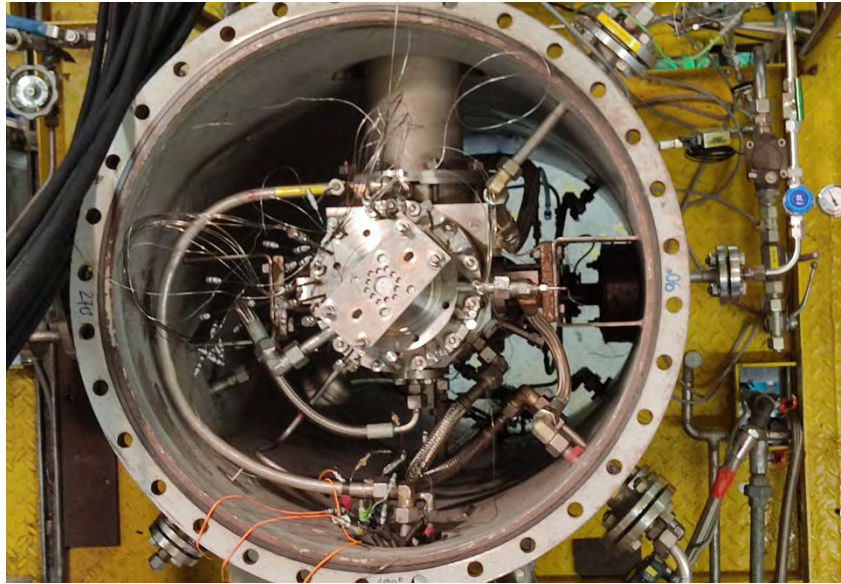
sheathed Ni/CrNi thermocouples attached  
to cladding surface with Pt/Rh wire wrapped around the rod



# QUENCH-ATF1 bundle in the test section



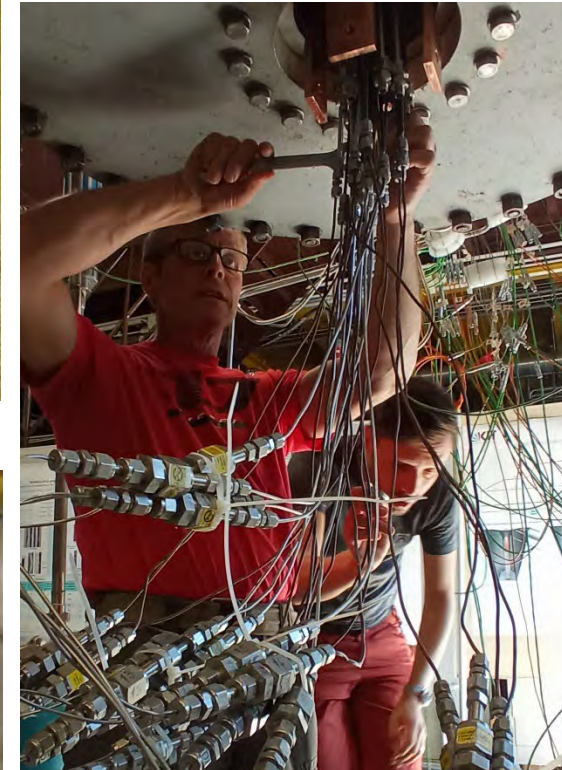
Inserting the bundle into the test section



Test section top



Electrical connections for current measurements at each rod



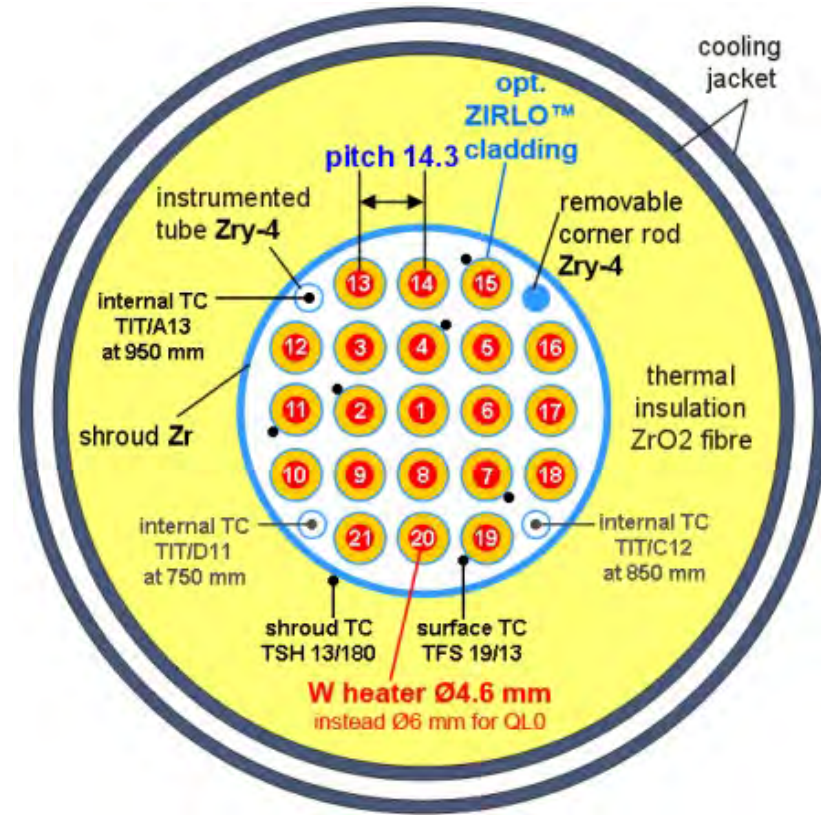
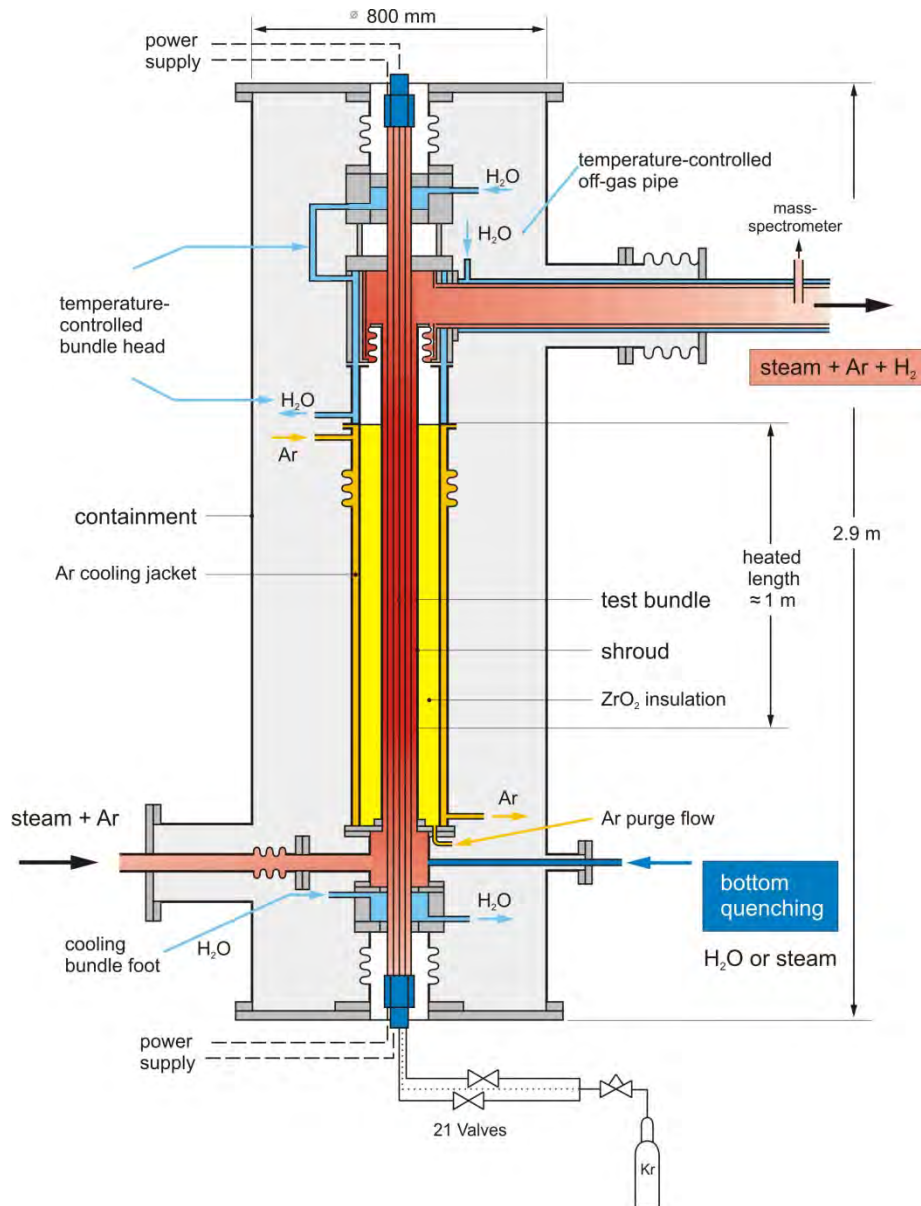
Test section bottom with individual gas connections to each rod

# QUENCH-LOCA bundle tests: boundary conditions and results

Test	Type of cladding tubes	Max heat-up rate, K/s	Max T on the end of heat-up, K	Duration of inner clad. oxidation at T > 1123 K, s	Secondary cladding hydrogenation	Post-test fracture due to second. hydrogenation
<b>Commissioning QUENCH-L0</b> July 22, 2010	Zry-4	2.5	1350	110	yes	yes
<b>Reference QUENCH-L1</b> Feb. 02, 2012	Zry-4	7	1373	105	yes	no
<b>QUENCH-L2</b> July 30, 2013	M5 <sup>®</sup>	8	1373	88	yes	no
<b>QUENCH-L3HT</b> March 21, 2014	Opt. ZIRLO <sup>™</sup>	8	<u>1623</u>	252	yes	yes
<b>QUENCH-L4</b> July 30, 2014	Pre-hydr. M5 <sup>®</sup> (100 wppm H)	8	1385	100	yes	yes
<b>QUENCH-L3</b> March 17, 2015	Opt. ZIRLO <sup>™</sup>	8	1346	84	yes	no
<b>QUENCH-L5</b> Feb. 17, 2016	Pre-hydr. opt. ZIRLO <sup>™</sup> (300 wppm H)	8	1257	45	no	-

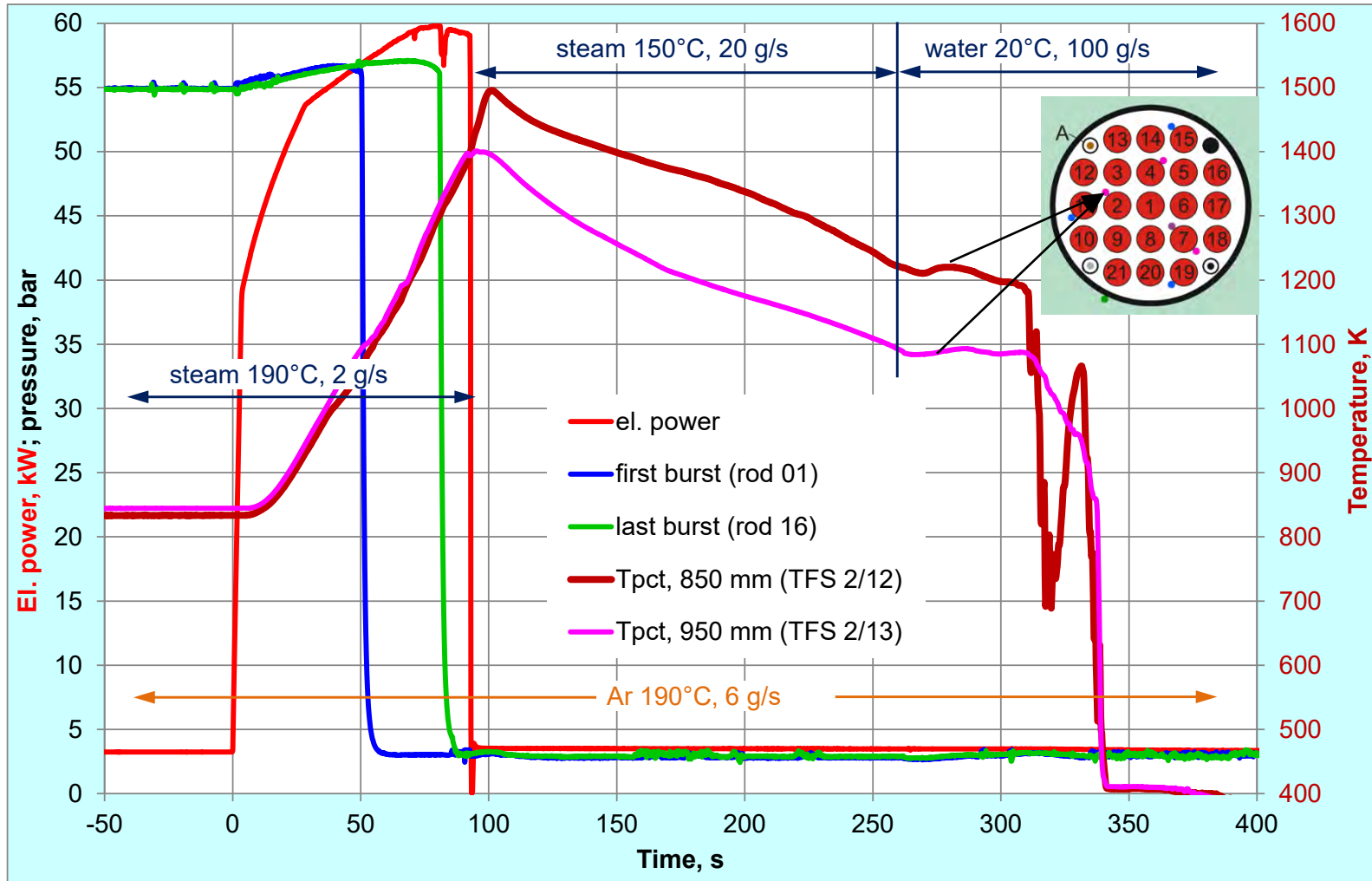


# QUENCH-LOCA test section



cross section of QUENCH-LOCA bundles with 21 heated rods

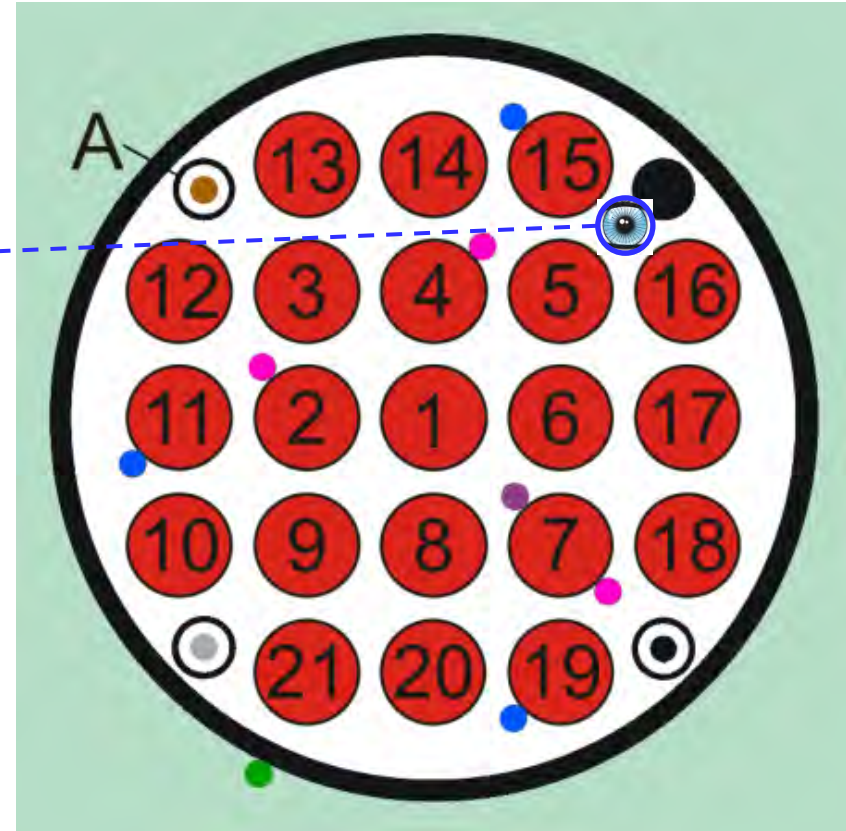
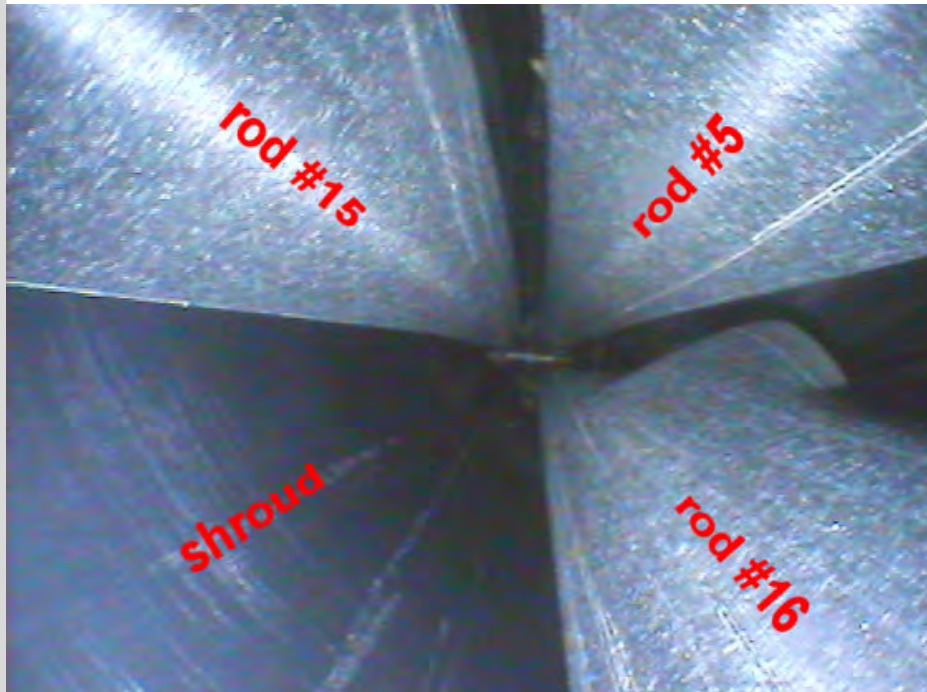
# Progress of the high temperature QUENCH-L3HT test



1) Temperature escalation at 850 mm on 91.4 s

2) Max temperature measured with TFS 7/12i (readings not shown): 1623 K

# QL3HT: videoscope observations of the bundle at the position of withdrawn corner rod

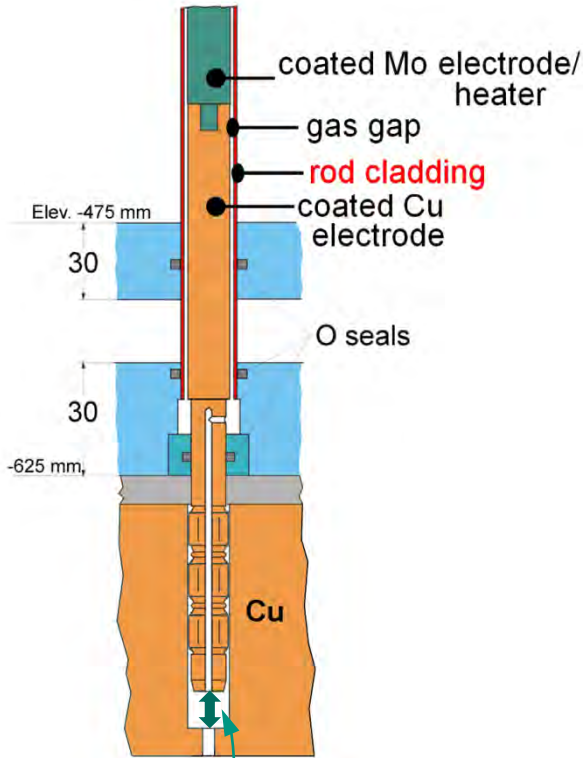


ballooning and burst of cladding tubes at elevation 950 mm



# QUENCH-L3HT: bundle between spacers GS3 (550 mm) and GS4 (1050 mm).

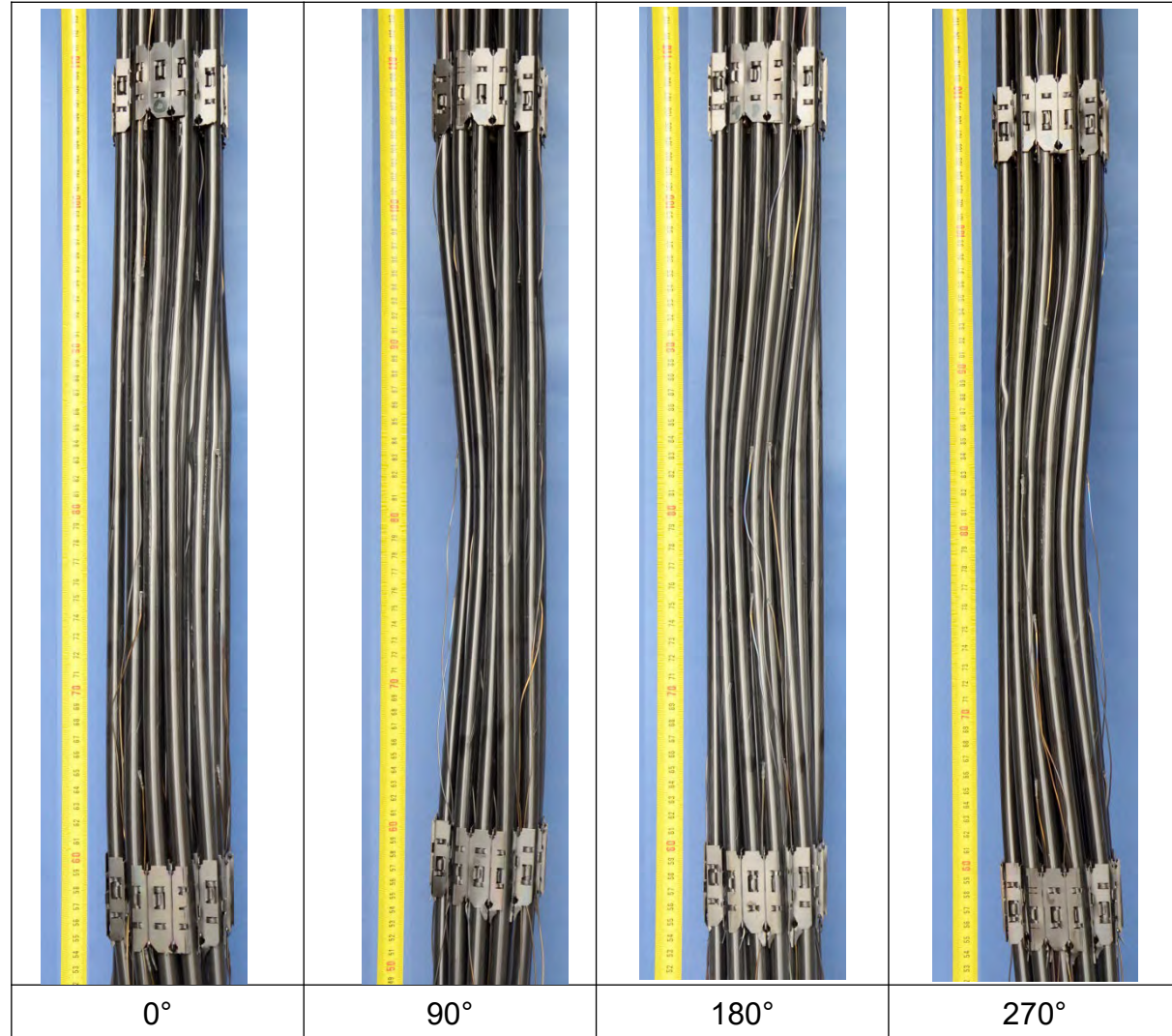
*Rod bending due to 1) limitation of axial thermal expansion of W-Mo heater ( $T_{pct} > 1250^{\circ}\text{C}$ ); 2) non-uniform cladding axial expansion.*



gap must be:

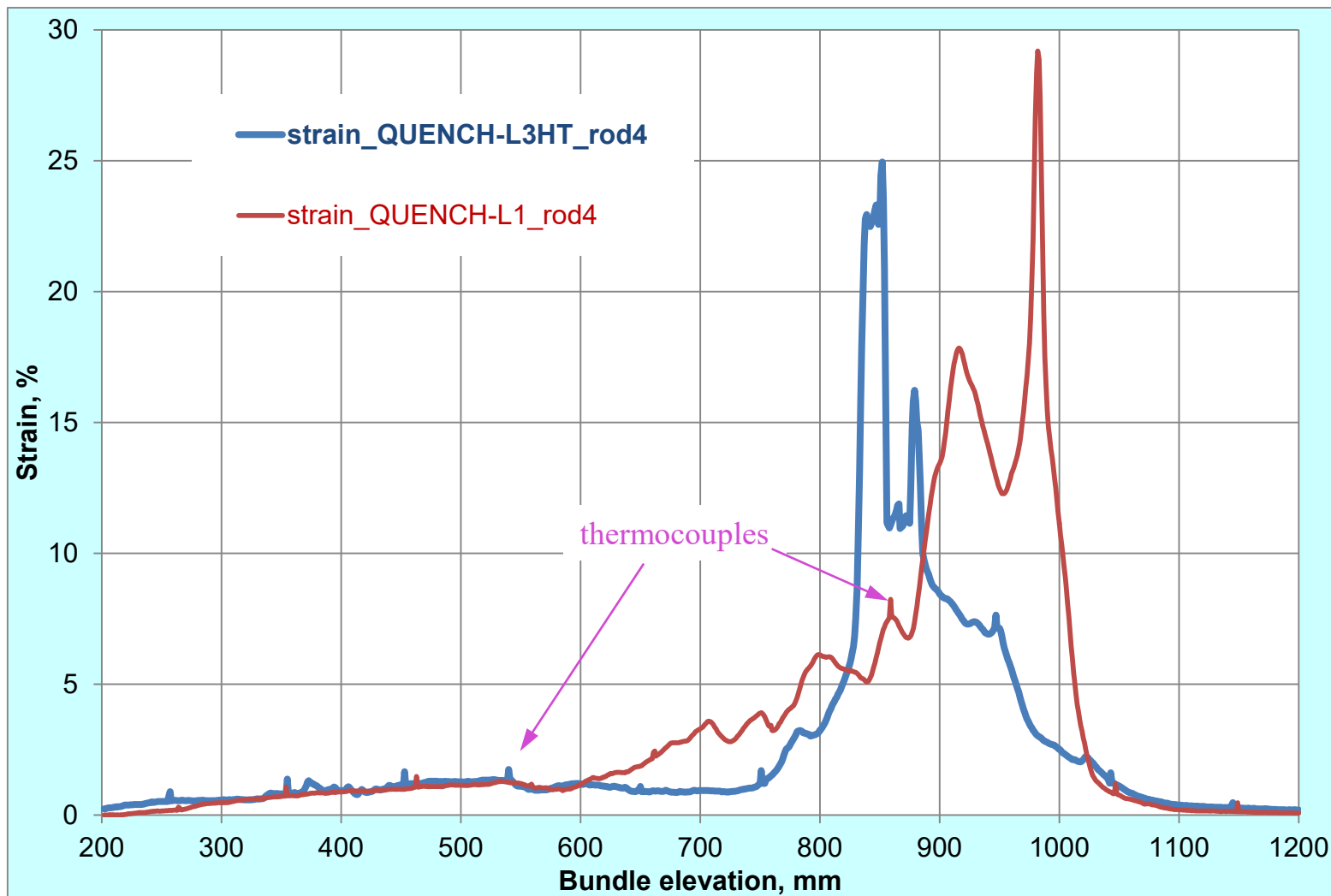
>6.5 mm for QL3HT.

real gap was 5 mm




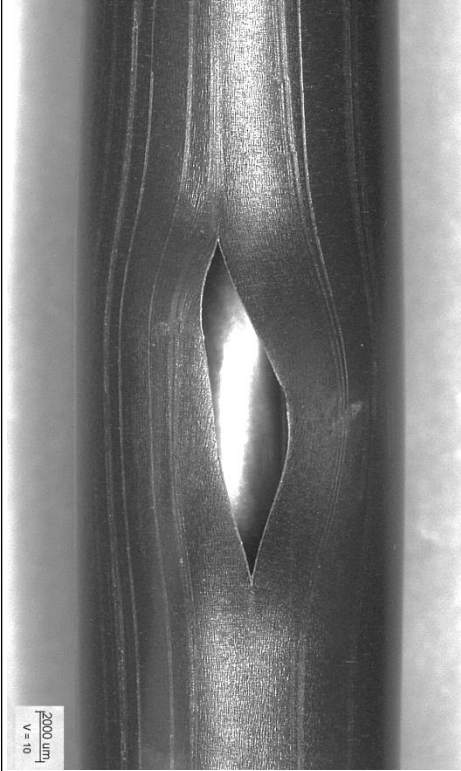
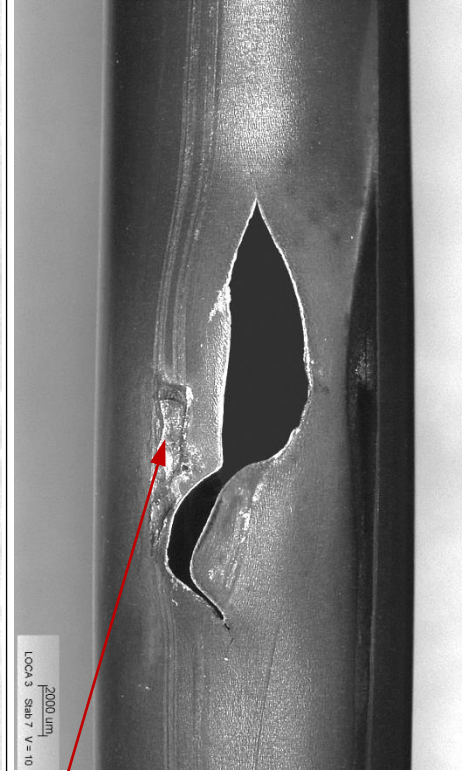
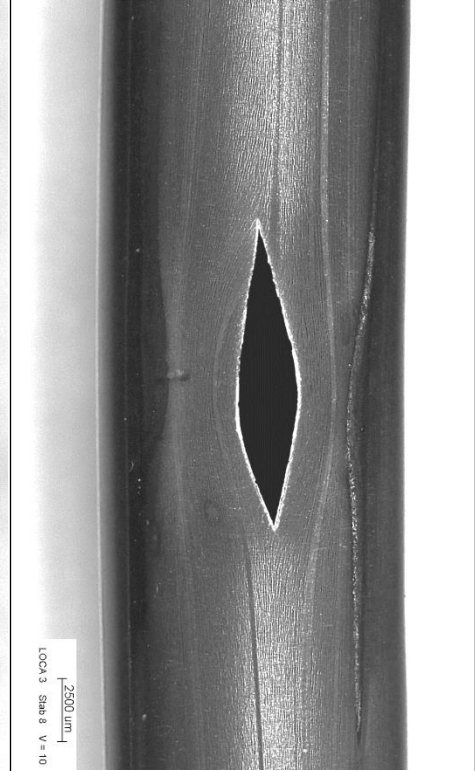
# Laser profilometer: axial strain distribution for rod #4.

## Comparison between QUENCH-L3HT (opt. ZIRLO) and QUENCH-L1 (Zry-4)



**For coplanar positions of all 21 burst openings:  $B_{QL1} = 46\%$ ;  $B_{QL3HT} = 35\%$  (B - max blockage)**

# QUENCH-L3HT: burst openings of several claddings

			
<p>rod #2: elevation 900 mm  <math>H_{op} = 17.2</math> mm  <math>\max W_{op} = 4.7</math> mm  <math>A_{op} = 50.7</math> mm<sup>2</sup></p>	<p>rod #5: elevation 908 mm  <math>H_{op} = 13.5</math> mm  <math>\max W_{op} = 3.0</math> mm  <math>A_{op} = 24.0</math> mm<sup>2</sup></p>	<p>rod #7: elevation 850 mm  <math>H_{op} = 16.6</math> (10.6) mm  <math>\max W_{op} = 3.4</math> mm  <math>A_{op} = 29.7</math> (25.2) mm<sup>2</sup></p>	<p>rod #8: elevation 837 mm  <math>H_{op} = 11.6</math> mm  <math>\max W_{op} = 2.3</math> mm  <math>A_{op} = 15.9</math> mm<sup>2</sup></p>

welding traces of  
TC TFS 7/12 i

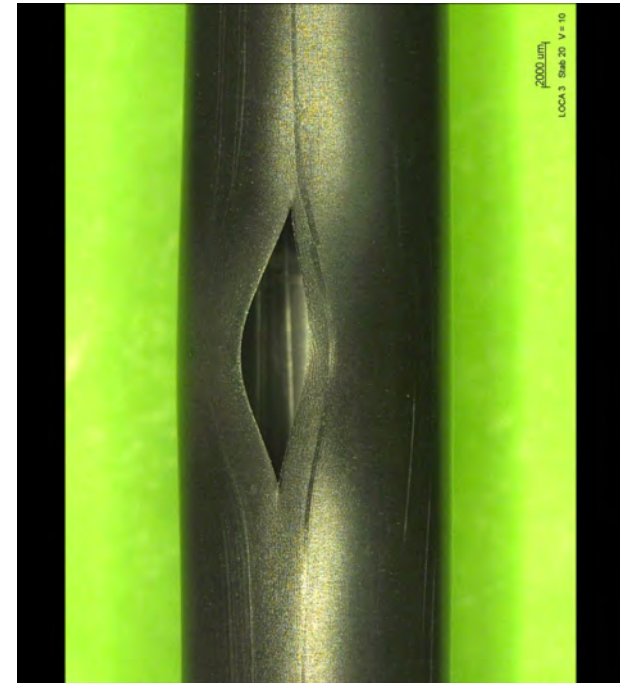


# QUENCH-L3HT videos of ballooning regions: balloonings are not symmetrical due to circumferential temperature gradient



**rod 5**

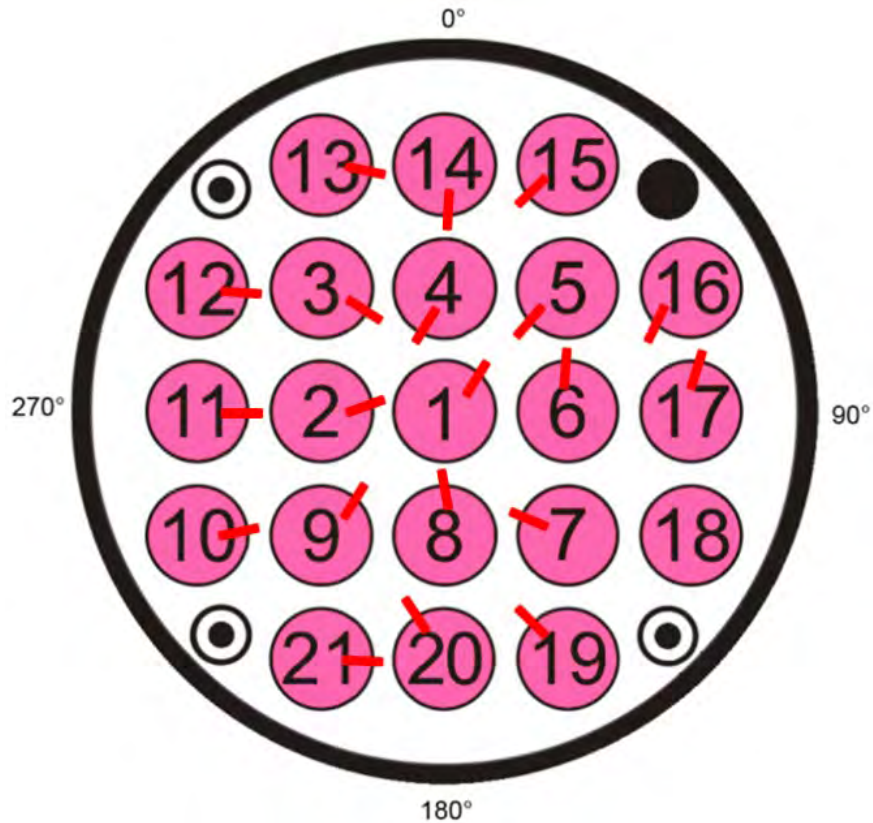
[https://www.iam.kit.edu/awp/downloads/QL3\\_rod5.wmv](https://www.iam.kit.edu/awp/downloads/QL3_rod5.wmv)



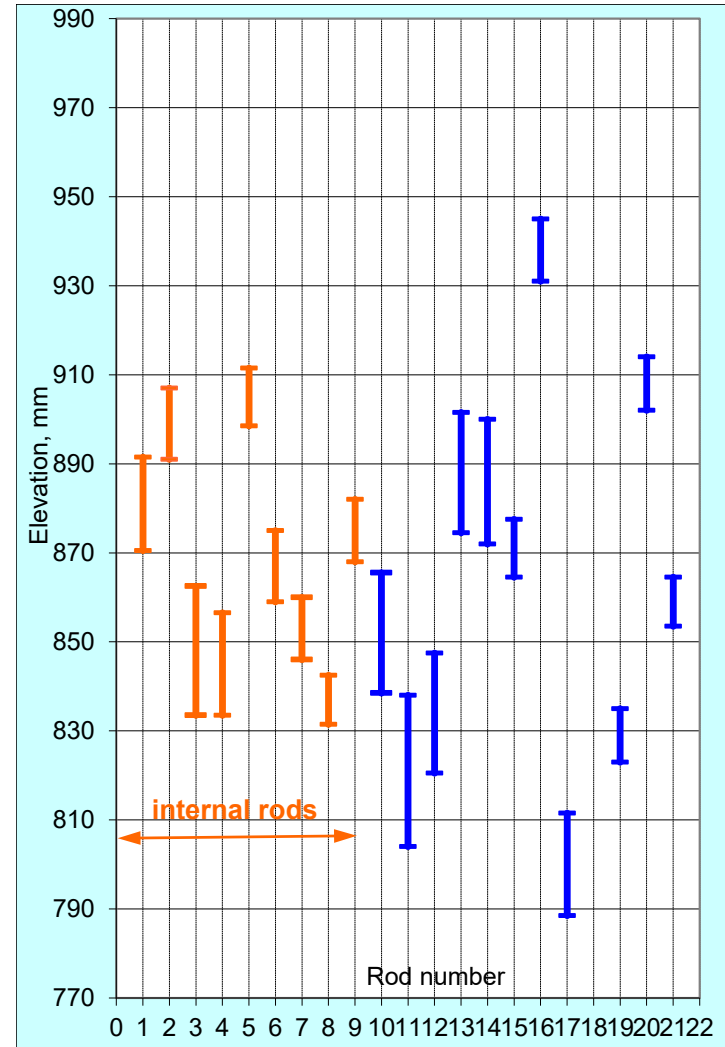
**rod 20**

[https://www.iam.kit.edu/awp/downloads/QL3\\_rod20.wmv](https://www.iam.kit.edu/awp/downloads/QL3_rod20.wmv)

# QUENCH-L3HT: circumferential and axial positions of burst openings



mostly orientation  
to bundle center



burst openings located between 790 and 950 mm



# Burst parameters of different claddings

## LOCA-1 (Zry-4)

Rod group	Rod #	Burst time, s	Burst temperature, interpolated, K
Inner rods	4	55.2	1154
	6	55.2	1110
	1	55.6	1169 (Max)
	5	57.2	1104
	2	57.2	1132
	8	58.6	1132
	3	59.0	1118
	7	59.8	1074 (Min)
	9	62.6	1162
Outer rods	15	64.4	1159
	17	67.6	1104
	11	67.6	1056
	14	68.6	1154
	16	68.8	1156
	18	72.6	1081
	13	73.6	1147
	20	76.0	1105
	12	76.8	1092
	21	80.6	1140
	19	83.6	1163
	10	87.6	1143

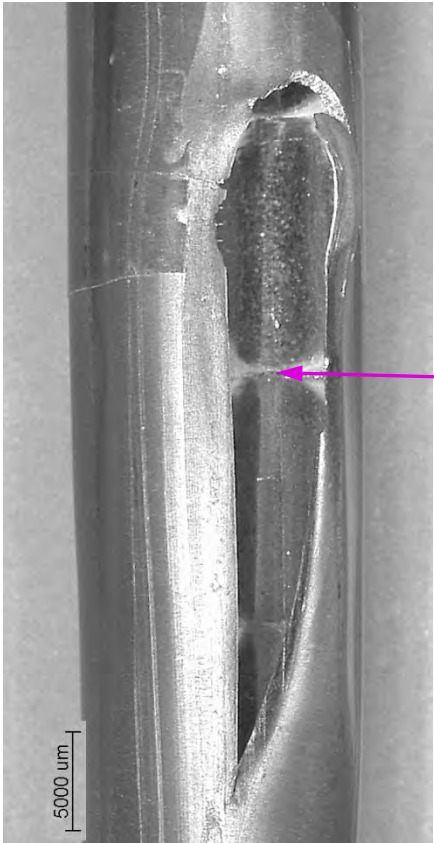
average burst T:  $1126 \pm 33 \text{ K} = 853 \pm 33 \text{ }^\circ\text{C}$

## LOCA-3HT (opt. ZIRLO)

Rod group	Rod #	Burst time, s	Burst temperature, interpolated, K
Inner rods	1	50.2	1112
	4	51.4	1123
	6	51.6	1030
	5	54.4	1121
	2	54.6	1122
	3	55.6	1153
	8	56.2	1167
	7	57	1169
	9	58.2	1147
Outer rods	15	56.4	1114
	14	63	1155
	13	65.8	1143
	11	68.2	1176
	12	68.6	1187
	17	69	1090
	18	71 (short circuit)	-
	21	73.6	1039
	10	75.2	1161
	20	75.2	1066
	19	77	1073
	16	81	1198

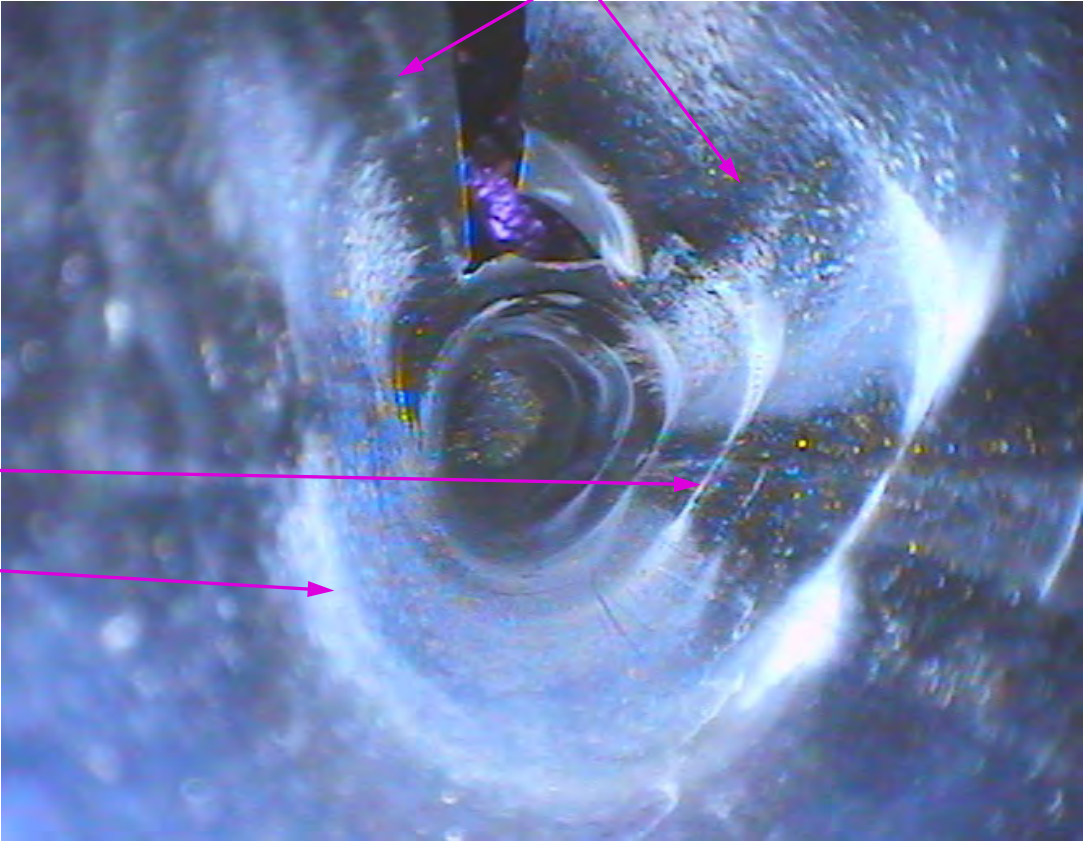
average burst T:  $1127 \pm 48 \text{ K} = 854 \pm 48 \text{ }^\circ\text{C}$

# QUENCH-L3HT: endoscope observation of the inner surface of cladding #3



outer view of burst

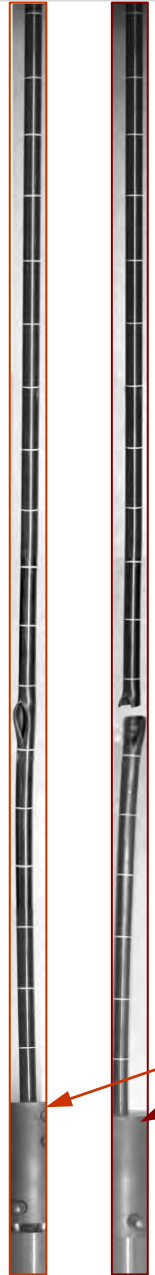
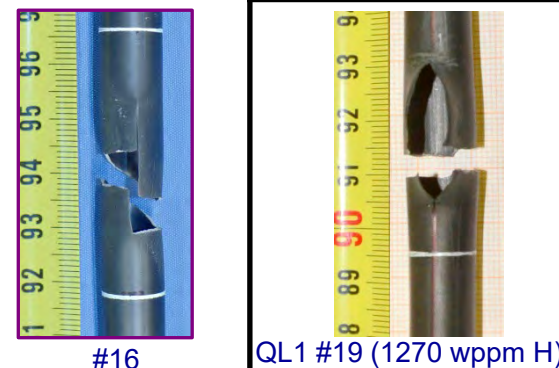
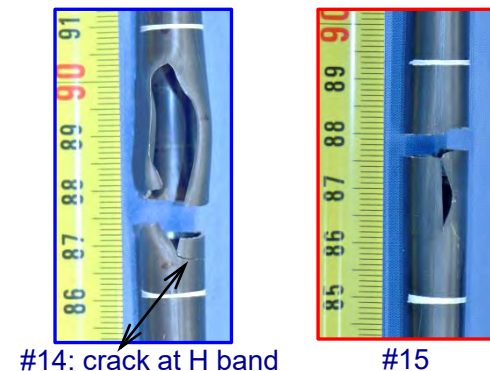
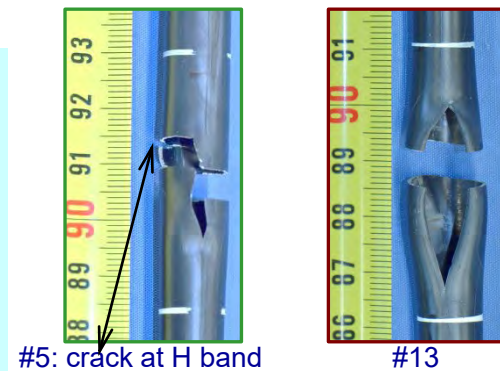
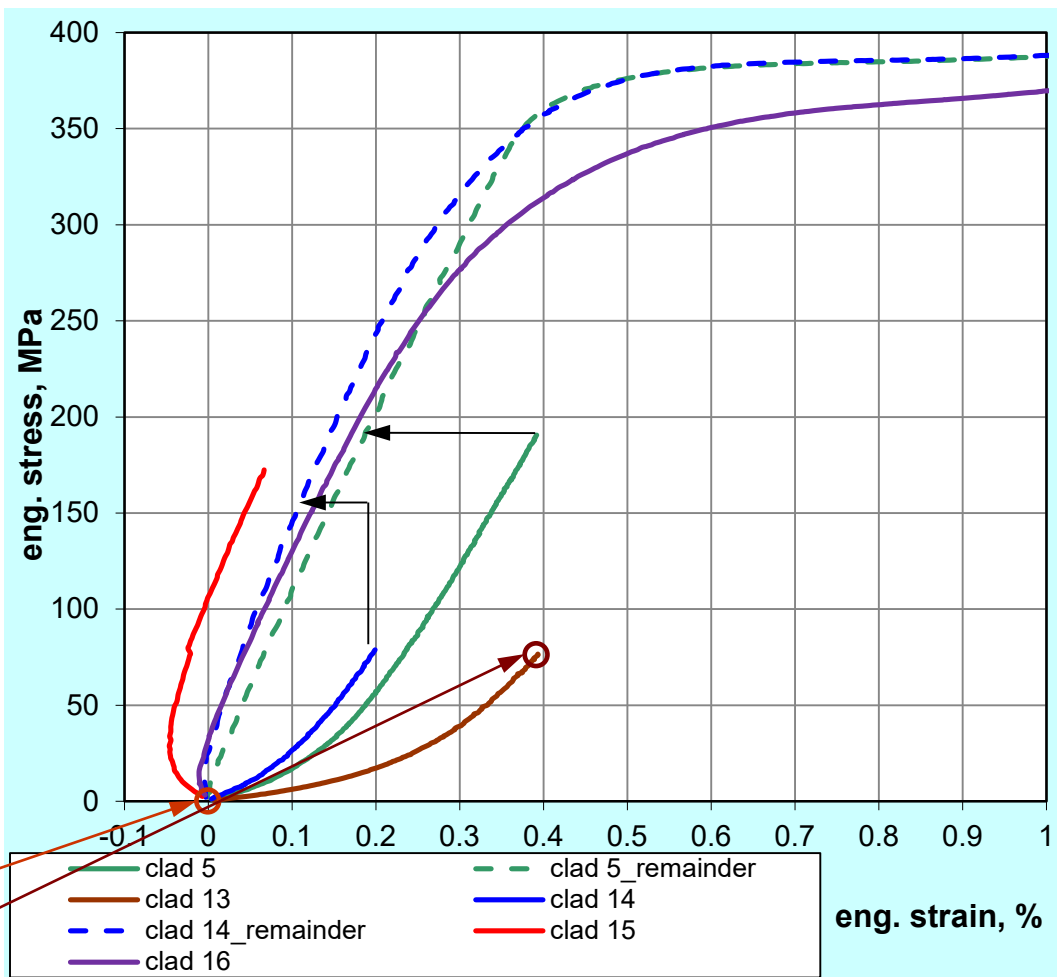
oxidation rings  
at the positions  
of contacts  
between pellets



less oxidized area  
near to the burst opening

inner cladding surface in the vicinity of burst opening

# QL3HT tensile tests: ruptures due to stress concentration, cracks at hydrogen bands



# Summary and conclusions

- The first bundle test QUENCH-ATF1 with Cr coated cladding tubes was prepared and successfully carried out on July 18, 2022. The test scenario was comparable to the earlier *reference test QUENCH-LOCA-3HT* with uncoated opt. ZIRLO cladding tubes with maximum temperatures of approx. 1300 °C and thus slightly above design basis accident conditions. The post-test investigations will be performed similar to *QUENCH-LOCA-3HT*: profilometry with laser scanner, endoscope observations, ultrasound measurement of wall thickness, measurement of burst opening sizes by optical methods, metallography, neutron radio- and tomography, measurement of hydrogen concentration by hot extraction, tensile tests.
- *QUENCH-LOCA-3HT: the maximum of virtual coplanar blockage ratio of cooling channel was 35%. Due to moderate blockage a good bundle coolability was kept for both bundles.*
- *The cladding burst occurred at temperatures between 1030 and 1200 K; the average burst temperature was  $1127 \pm 48$  K. The inner rod pressure relief to the system pressure during about 30 s.*
- *During quenching, following the high-temperature phase, no fragmentation of claddings was observed (residual ductility is sufficient).*



# Acknowledgment

The QUENCH-ATF1 experiment was performed in the framework of the OECD QUENCH-ATF program and supported by the KIT program NUSAFE. Personal thanks to Ms. Fiona-Martin (NEA), Mr. Lahoda and Mr. Chernyak (Westinghouse), Mr. Esmaili (NRC) for their help and fruitful cooperation. The coated cladding tubes and prototypical grid spacers were provided by Westinghouse. The coating of Zr shroud and Zry corner rods was performed by Oerlikon Balzers GmbH.

The authors would like to thank all colleagues involved in the pre-test calculations.

*Thank you for your attention*

<http://www.iam.kit.edu/awp/666.php>  
<http://quench.forschung.kit.edu/>



**M. Große**  
**KIT**

## **Post-Test Examinations of the QUENCH tests simulating LOCA by means of neutron imaging**

The paper gives an introduction into the investigation of hydrogen in zirconium alloys by means of neutron imaging methods. Due to the strong differences between the total neutron cross sections of hydrogen (very high) and zirconium (very low), even small hydrogen concentrations can be measured quantitatively.

On the examples of the results of neutron tomography measurements at cladding tubes of the QUENCH-L3 and QUENCH-L3HT tests, two typical types of hydrogen enrichments in the claddings were described:

- Bended bands with high hydrogen concentrations (>1500 ppm) oriented non-perpendicular to the tube axis
- Axial oriented hydrogen enriched strips where the pellets touch the cladding

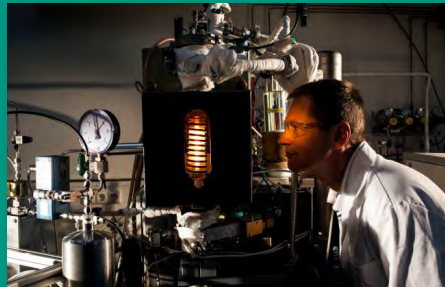
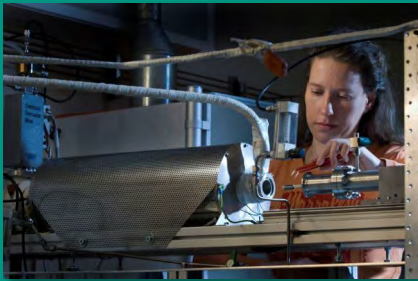
Hydrogen enrichments were only found in rods exceeding temperatures of about 1000°C during the LOCA simulation tests. This threshold temperature corresponds with the monoclinic – tetragonal phase transformation in zirconia. Obviously, the oxide layer with tetragonal structure is much more transparent for hydrogen than the monoclinic one.

The paper ends with an outlook to the investigations at chromium coated cladding tubes tested in the QUENCH-ATF-1 test with similar temperature protocol than the QUENCH-L3HT test. First neutron radiography measurements of these cladding tubes were already performed. Results of these investigations are still restricted to the members of the QUENCH-ATF consortia.

# Post-Test Examinations of the QUENCH tests simulating LOCA by means of neutron imaging

**M. Grosse, S. Weick, C. Roessger**

KIT / Institute for Applied Materials – Applied Material Physics / Program NUSAFE



# Introduction

- 7 QUENCH-LOCA tests were performed applying uncoated claddings made of Zry-4, M5™, as well as ZIRLO®
- Development of ATF claddings. Cr coated zirconium alloys is a very promising near term solution.
- Testing the behaviour of Cr coated ZIRLO is the aim of the first test of the QUENCH-ATF program of the consortia coordinated by the OECD-NEA. Repeating the QUENCH-ATF-03HT test (optm. ZIRLO) with Cr coated ZIRLO.
- Post test examinations of the secondary hydriding by means of neutron imaging



# Determination of hydrogen concentrations by means of neutron imaging

X-ray radiography



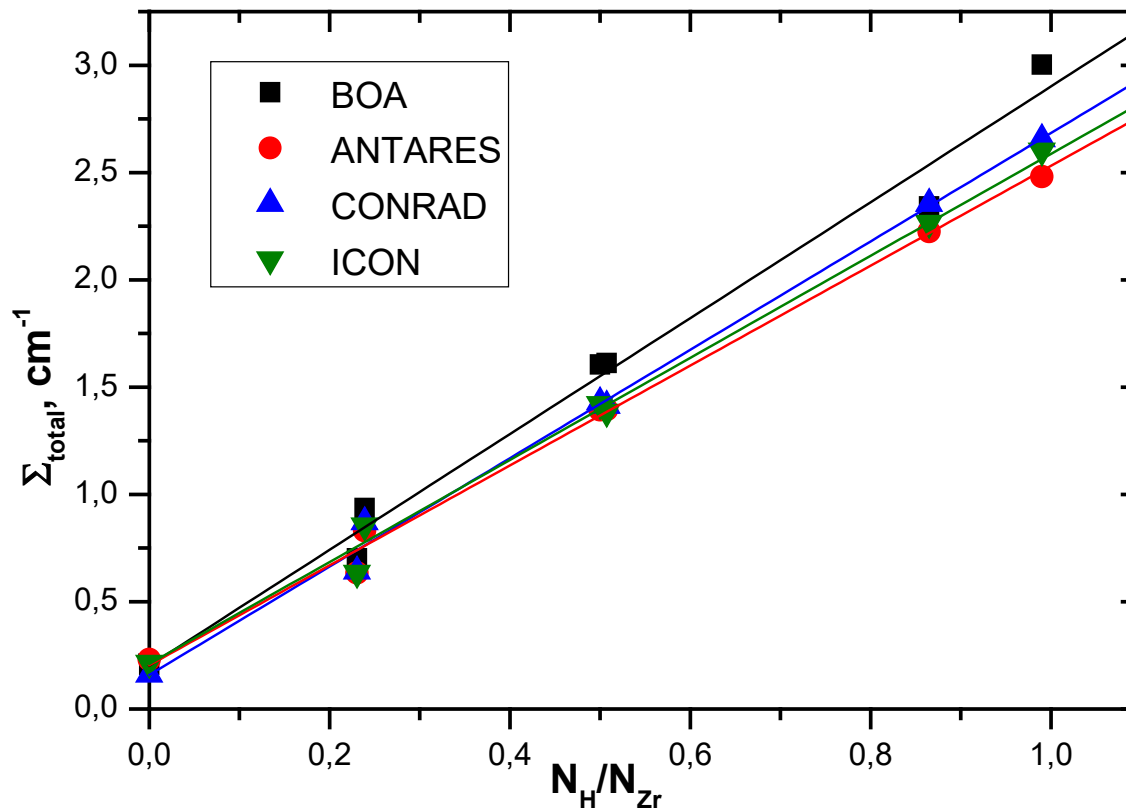
neutron radiography



GKSS Geesthacht 1991

# Calibration of the measurements

$$\Sigma_{total} = \frac{-\ln\left(\frac{I - I_B}{I_0 - I_B}\right)}{s} = \sum_i N_i \sigma_i = \underbrace{N_{Zr} \sigma_{Zr} + \dots + N_H \sigma_H}_{\Sigma_{Zry}} + N_O \sigma_O$$

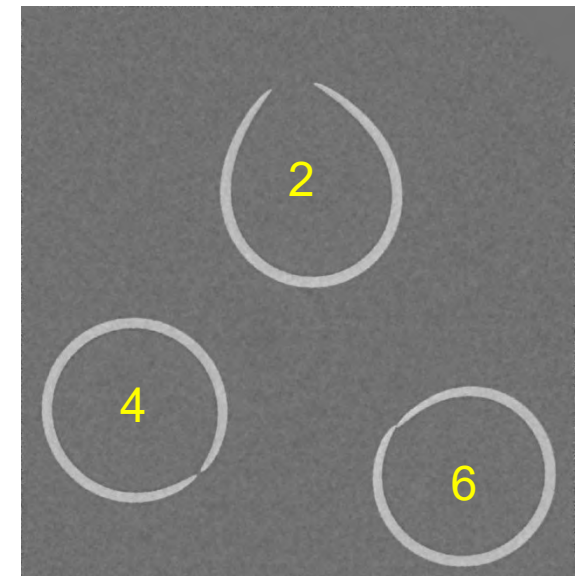
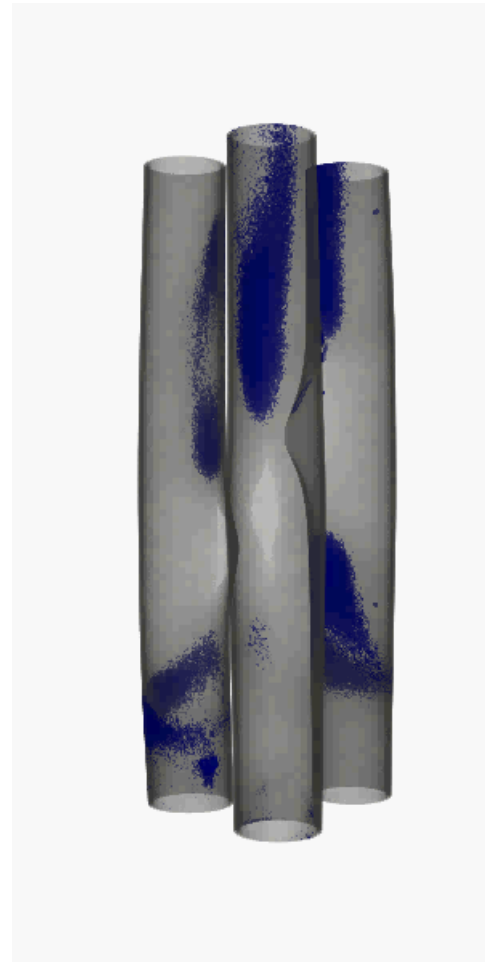


# Neutron Imaging Experiments at Q-LOCA claddings

Date	Facility	Source	Method	Spatial Resolution	Time/Sample
March 19 - 23 2015	ANTARES	FRM 2 Garching Germany	Tomography QL4	~ 50 $\mu\text{m}$	4 h / Tomography
May 26 2015	BOA	SINQ PSI Villigen Switzerland	Radiography QL3	~ 80 $\mu\text{m}$	5 min / image 25 min / rod
July 8 - 13 2015	CONRAD	BER Berlin Germany	Radiography Tomography QL3	~ 80 $\mu\text{m}$	5 min /image 17 min / rod 14 h / Tomo.
July 30 - Aug. 02 2015	ICON	SINQ PSI Villigen Switzerland	Tomography QL3HT	~ 60 $\mu\text{m}$	15 h / Tomography
Sept. 10 - 14 2015	BOA	SINQ PSI Villigen Switzerland	Tomography QL4	~80 $\mu\text{m}$	30 h / Tomography

# Simultaneous tomography of 3 claddings

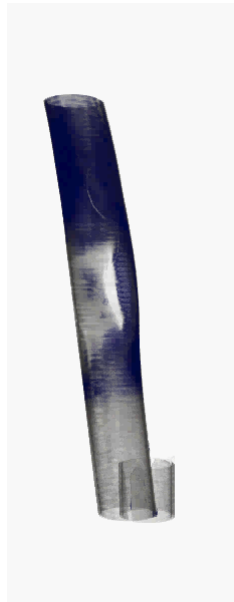
Investigating of three  
times more rods



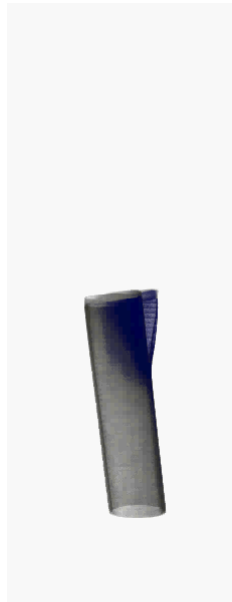


# Results QUENCH-L3HT rods

inner rods



02



03



04



05



07



08

The data obtained for the QUENCH-3HT claddings are not yet quantitatively analyzed.

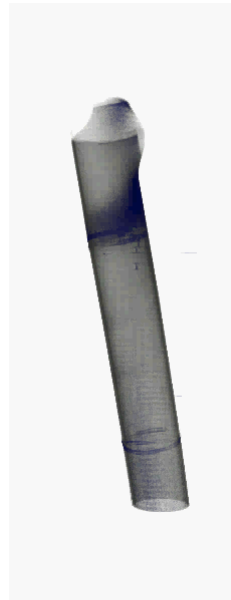
Fracture during dismounting of the sample at hydrogen enrichments of the rods 03, 04 and 05.

# Results QUENCH-L3HT rods

peripheral rods



13



16



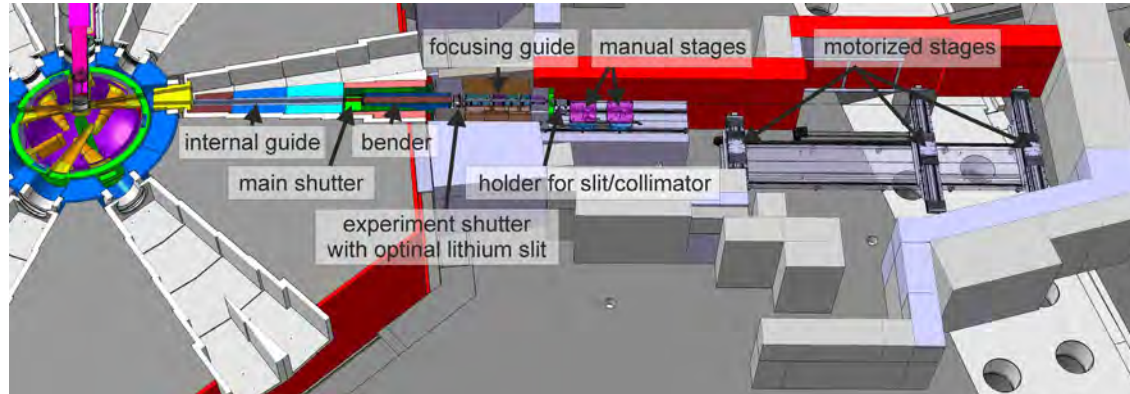
21

# Conclusions

- Post test examinations by means of neutron imaging provides very valuable information about the hydrogen distribution and with it about the secondary hydriding during the QUENCH LOCA simulation tests.
- Main results concerning the secondary hydriding are:
  - Bended bands with high hydrogen concentrations (>1500 ppm) non-perpendicular to the tube axis
  - Axial oriented hydrogen enriched strips where the pellets touch the cladding
  - Formation of hydrogen enrichments only beyond a threshold temperature (~1000°C, corresponds with the monoclinic to tetragonal phase transition)
- How is the secondary hydrogenation of Cr coated cladding tubes?

# Neutron Radiography Measurements

- 24 h beamtime at the BOA facility at the Swiss Neutron Source (SINQ – PSI Villigen, Switzerland) at September 9 – 10 2022

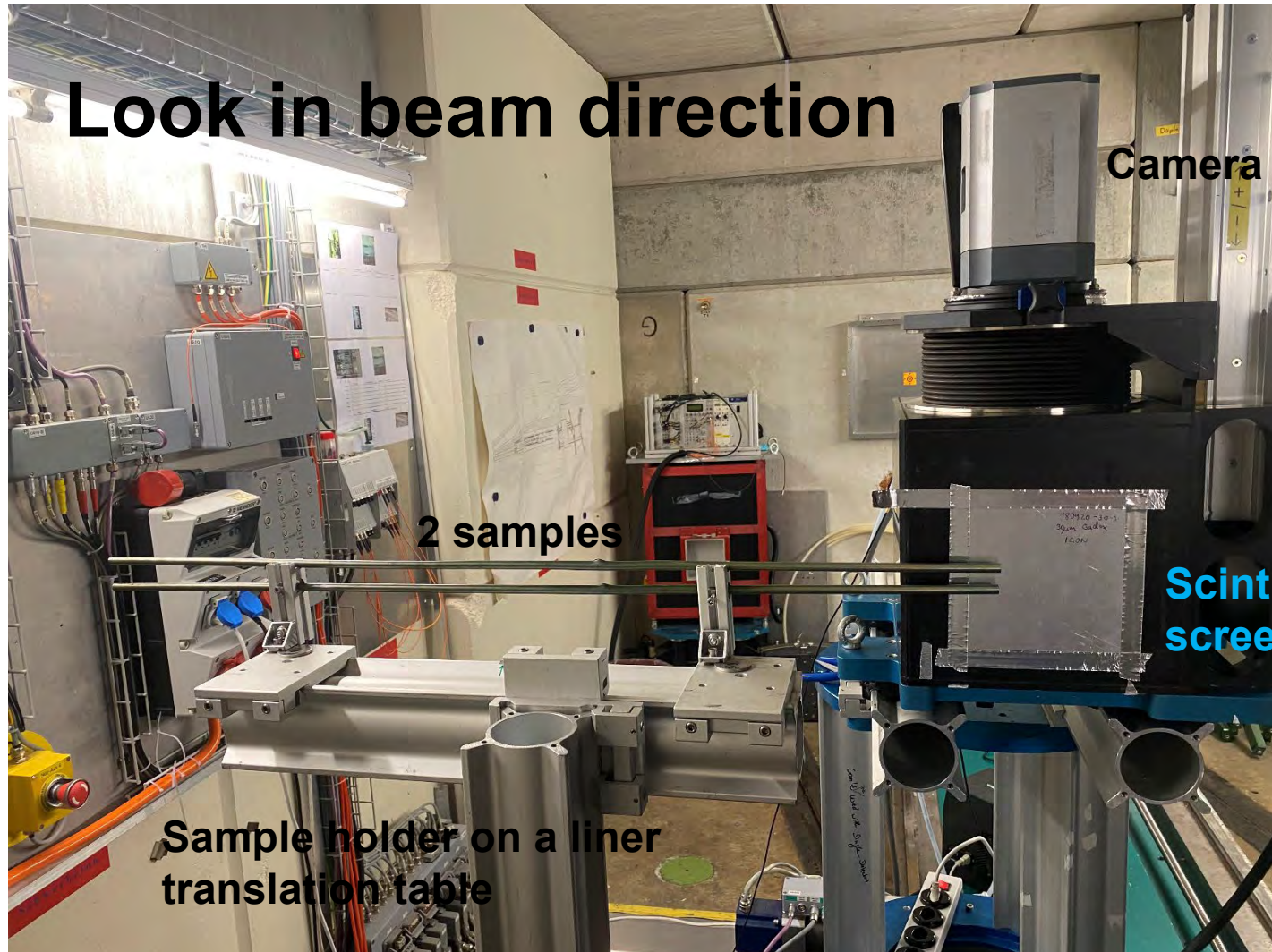


## ■ Experimental Setup:

- FoV: 65 mm x 65 mm
- Pixel size: 32  $\mu\text{m}$
- Spatial resolution:  $\sim 50 \mu\text{m}$
- L/d: 290
- Illumination time: 9 x 30 s = 4.5 min per position
- Step with scan: 55 mm  $\rightarrow$  19 positions per scan



# Neutron Radiography Measurements



## Neutron Radiography Measurements

- Neutron radiography measurements at cladding tubes used in the QUENCH-ATF-1 test were successfully.
- Similarities as well differences to the results of the QUENCH-LOCA-3HT using uncoated claddings were found. Further PTE are needed to confirm that the features detected are hydrogen enrichments.
- Results are restricted yet to the consortia members.
- Do you want becoming a member? – Ask Julie Martin

## Next steps

- Neutron tomography investigations at chosen tubes (on proposal basis at PSI Villigen or together with CEA at ILL Grenoble?)
- Verifying the hydrogen enrichments by means of hot extraction measurements at KIT
- Metallographic analysis KIT
- Applying other methods?

# Acknowledgement

OECD-NEA for coordinating the project and all members of the consortia for their support.

PSI for providing beamtime and particularly David Mannes and Matteo Busi support during the measurements and data transfer.

# Thank you for your attention





**J.-F. Martin**  
**OECD-NEA**

## **OECD Nuclear Energy Agency's Activities related to Accident Tolerant Fuels**

The OECD Nuclear Energy Agency (NEA) is an intergovernmental agency set up in February 1958 which aim is to support its member countries through international cooperation in the scientific, technological and legal aspects of nuclear energy to support a safe, environmentally sound and economical use for peaceful applications.

The efforts towards the development of accident tolerant fuel for enhanced safety and resilience to off-normal conditions have been supported by the NEA since their early developments, in the aftermath of the Fukushima event in March 2011. This presentation reviews recent outcome and on-going efforts dedicated to ATF developments.

Notably, a State-of-the-Art Report on Light Water Reactor Accident Tolerant Fuels was published in 2018 [NEA (2018), OECD Publishing, Paris], providing a complete review of the most promising ATF designs including an assessment of their respective technology readiness levels. Further to this report, a Technical Opinion Paper on the Applicability of Nuclear Fuel Safety Criteria to Accident Tolerant Fuel Designs was released in 2022 [NEA (2022), OECD Publishing, Paris] focusing on existing fuel design and performance requirements with a view to their applicability to such new designs; and identifies needs for new or different performance metrics and design requirements. Both reports are freely available on the NEA's website ([www.oecd-nea.org](http://www.oecd-nea.org)).

Complementary to the work of the NEA's standing technical committees and the reports that are thereby produced, the NEA supports dedicated programs involving interested participants through the mechanism of "Joint Undertakings", which are cost-sharing endeavours and allow notably to undertake experimental studies. A review of half a dozen joint undertakings of relevance to the development of ATF designs, currently supported by the NEA, is provided. These projects enable the acquisition of new experimental data, such as with the QUENCH-ATF project (see resp. contributions by M. Steinbrück, J. Stuckert, M. Grosse); as well as the development of databases such as the TAF-ID project, which results in a comprehensive thermodynamic database for advanced fuel materials; and finally the development and improvement of modelling and simulation tools through accompanying analytical exercises.

The NEA continues to fulfil its mission of supporting its member countries through the establishment and sharing of best practices and state of the art methods and approaches, as well as the support of experimental facilities for the shared benefit of its membership.

*The author acknowledges contributions from fellow NEA colleagues Michelle Bales, Markus Beilmann, Alice Dufresne, Didier Jacquemain.*

# OECD/NEA Activities related to Accident Tolerant Fuels

**Julie-Fiona Martin**

with input from M. Bales, M. Beilmann,  
A. Dufresne, D. Jacquemain





# The NEA mission

To assist its member countries in maintaining and further developing, through **international co-operation**, the **scientific, technological and legal bases** required for a safe, environmentally sound and economical use of nuclear energy for peaceful purposes.

To provide authoritative assessments and to forge **common understandings** on key issues as **input to government decisions on nuclear energy policy** and to broader OECD policy analyses in areas such as energy and the sustainable development of low-carbon economies.

# Seeking excellence in nuclear safety, technology and policy

**34** member countries + partners  
(e.g. China, India, Brazil, etc.)

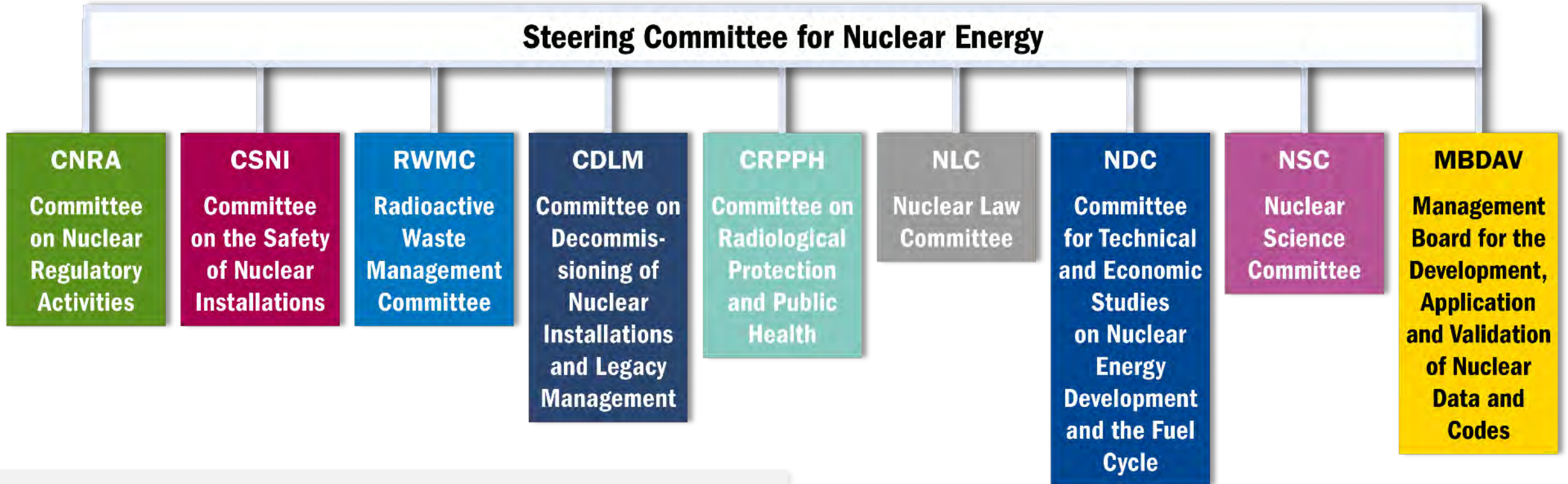
**8** standing technical committees  
**1** management board  
**74** working parties and expert groups

**26** international joint projects

**The NEA Data Bank** – a major international resource

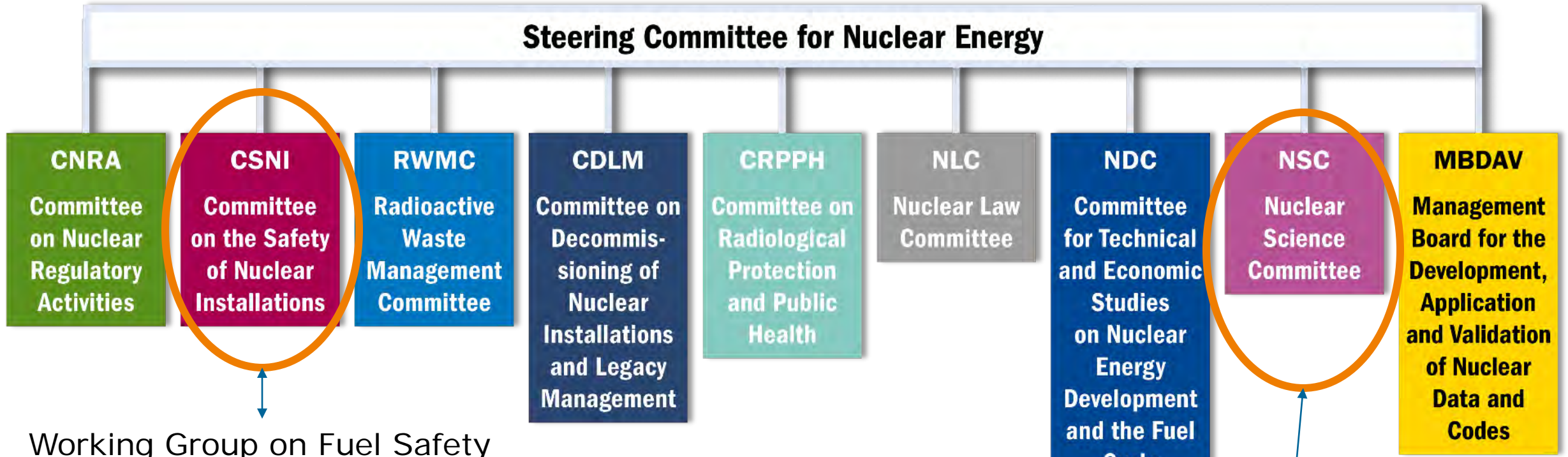


# NEA committees (as of 1 January 2022)



**8** standing technical committees  
**1** management board  
**74** working parties and expert groups

# NEA committees (as of 1 January 2022)

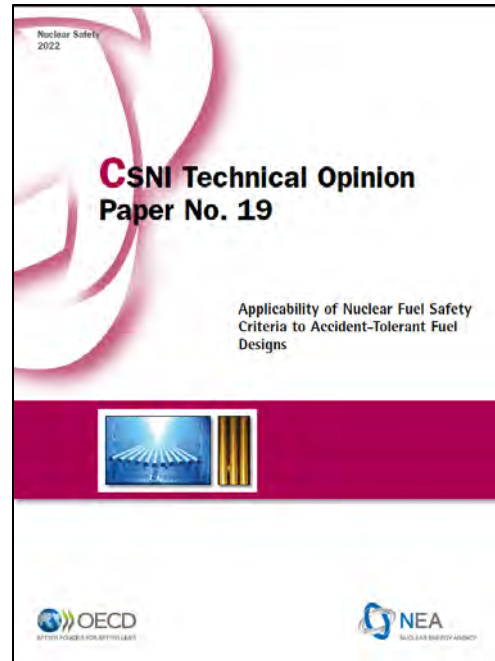
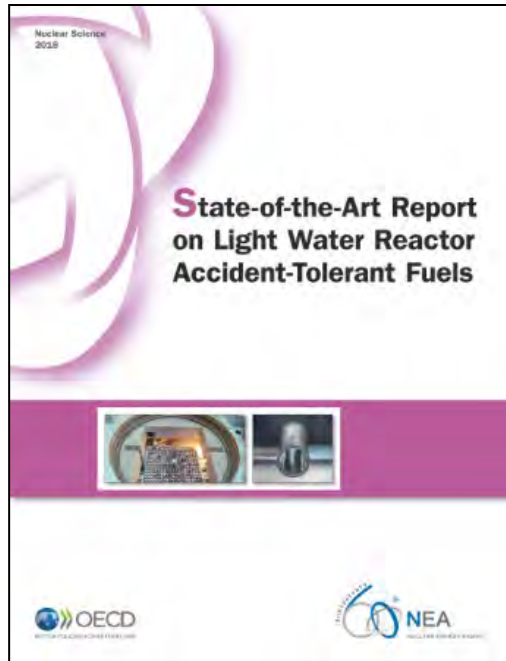


Working Group on Fuel Safety

- 8** standing technical committees
- 1** management board
- 74** working parties and expert groups

Expert group on Reactor Fuel Performance

# Recently or soon-to-be published NEA reports on ATF



- CSNI and NSC both main contributors to ATF related studies with complementary approaches
- State-of-the-Art Report on Light Water Reactor Accident-Tolerant Fuels, 2018
- **!NEW!** Technical Opinion Paper No 19 on Applicability of Nuclear Fuel Safety Criteria to ATFs, 2022

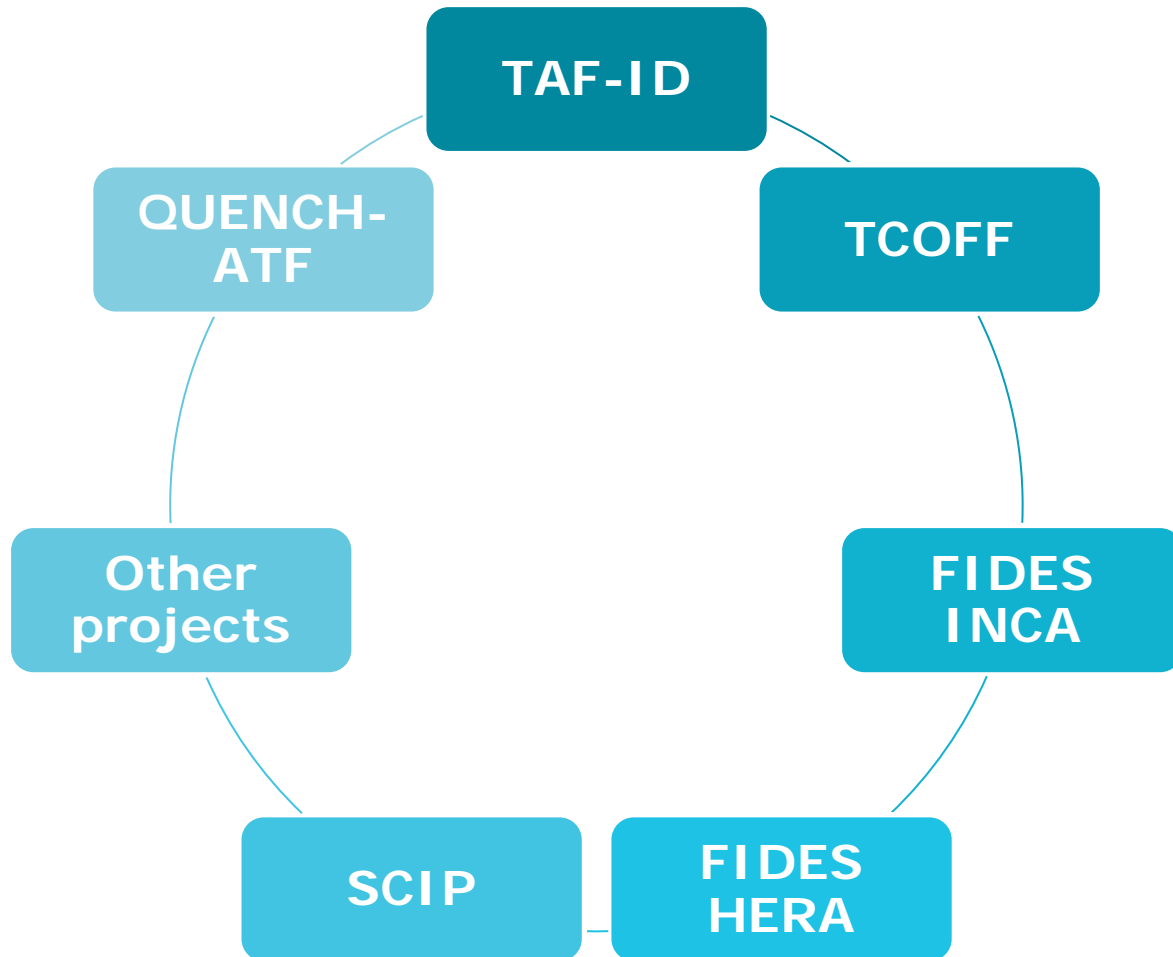
**!NEW!** Status report on fuel safety implication of extended enrichment, in press

ATF design concept	EGATFL technology readiness level*	Relative impact on existing fuel safety criteria	Number of new phenomena	Relative magnitude of data gaps
Coated zirconium alloy cladding	4	Low	3	Low
FeCrAl cladding	3-4	Medium	2	Medium
Silicon carbide cladding	< 3	High	3	High
Doped UO <sub>2</sub> ceramic pellets	8	Low	0	Low
Uranium silicide ceramic pellets	< 3	High	1	High

\* In 2018, the EGATFL report defined a TRL for each ATF design concept from 1 to 9, with 9 defined as *routine commercial-scale operation. Multiple reactors operating.*

From CSNI TOP#19, NEA(2022)

# NEA Joint Projects addressing ATF



On-going OECD/NEA joint undertakings tackling ATF

- FIDES/HERA (2021-24)
- FIDES/INCA (2021-24)
- QUENCH-ATF (2021-24)
- Halden Fuel & Materials (2021-23)
- SCIP-IV (2019-24)
- CIP (2011-25)
- TCOFF (2017-20, 2022-...)
- TAF-ID (2013-2017, 2018-2021, 2022-...)



# TAF ID –Thermodynamic of Advanced Fuel International Database

## Objectives

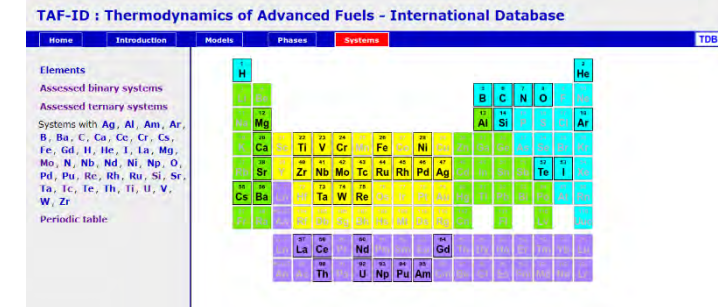
- Develop a thermodynamic database (phase diagrams + thermodynamic properties of the phases) for advanced fuel materials using the Calphad method

## Systems of interest: materials for Generation II, III, IV

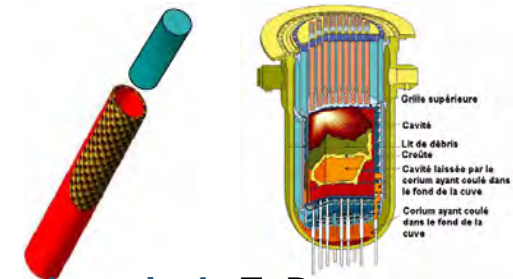
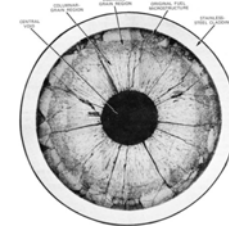
- Fuels:  $UO_2$ ,  $(U,Pu,Am,Np)O_2$ ,  $(U,Th)O_2$ ,  $(U,Pu,Zr,Am,Np)$ , **UN**, **(U,Pu)C**
- Fission products: Ba, Sr, Mo, Zr, Lanthanides (Ce, La, Nd, Gd), metallic FPs (Pd, Ru, Rh, Te, Tc), Volatile (Ag, Cs, I, Te)
- Structural materials: Fe-Cr-Ni, Zr alloys, Fe-Cr-Al-Y, Concrete ( $SiO_2$ -CaO- $FexOy$ - $Al_2O_3$ -MgO), SiC, B<sub>4</sub>C

## Status of the project

- Phase 2 focusing on SA and irradiated fuels is approaching completion (Nov. 2022)
- Phase 3 under preparation: **increased focus on ATF materials** (UN,  $U_3Si_2$ , encapsulated fuels) and ATF cladding materials (Cr-coated Zry, FeCrAl, SiC) and their interactions with fission products, coolants, and structural materials



<https://www.oecd-nea.org/science/taf-id/>



**Chair** C. Gueneau (FR), **vice-chair** T. Besmann (US), **secretariat** A. Dufresne

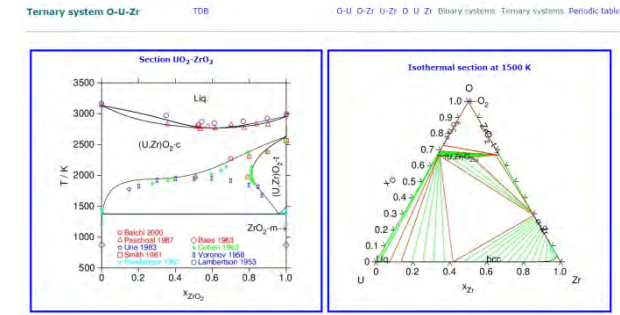
# TCOFF – Thermodynamic Characterization Of Fuel Debris and Fission Products based on Scenario Analysis of Severe Accident Progression at Fukushima-Daiichi NPS

## Objectives

- Improve the quality/expand existing thermodynamic databases & degradation models used for severe accident analyses
- Joint thermodynamic evaluation of the FDNPS severe accident progression
- Development of fuel/core degradation models and FP-behaviour models for SA analysis codes
- Fuel debris characterization for FDNPS

## Status of the project

- Phase 1 completed (July 2020)
- Phase 2 launched Sept. 2022: broadened scope in terms of reactor design (not limited to BWR) and materials (the effect **of potential deployment of ATF materials** will be evaluated): U<sub>3</sub>Si<sub>2</sub>, UN, Cr<sub>2</sub>O<sub>3</sub> doped UO<sub>2</sub>, Cr-coated Zry, FeCrAl, SiC/SiC
  - Task-1: Prioritisation of the material science issues related to the severe accidents study
  - Task-2: Improvement of the materials science knowledge on fuel core degradation and FP release (UO<sub>2</sub>-Zry and ATFs)
  - Task-3: Implementation of improved knowledge for the simulation of the accident behavior (UO<sub>2</sub>-Zry and ATFs)
  - Task-4: Leaching
  - Task-5: Training and Education



Phase relations in U-Zr-Fe-O system (metallic/oxidic melts in corium)



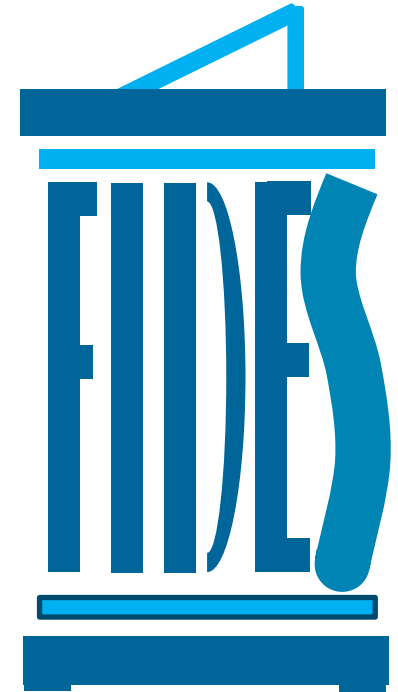
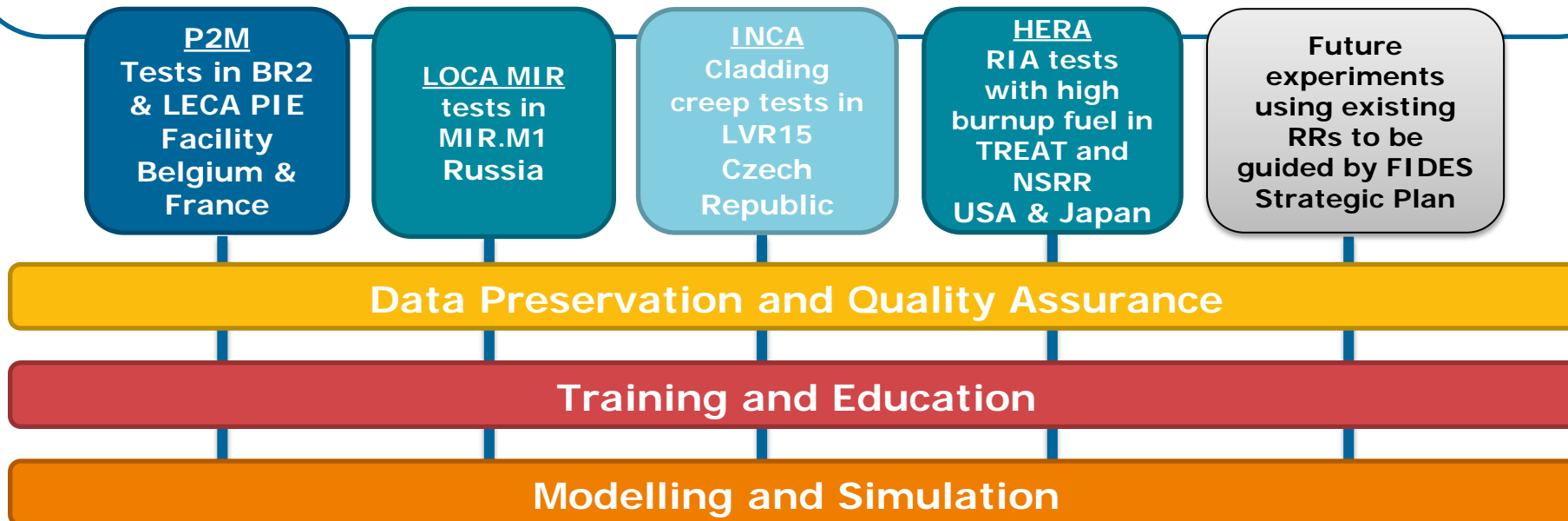
Phase relations in U-Zr-Fe-O system (oxidic/metallic melts in corium)

**MB Chair** H. Esmaili (US), C. Journeau (FR), **PRG Chair** M. Kurata (JPN), L. Lovasz (GER) **Secretariat** M. Bales

# Enhancing Testing Capabilities: NEA Framework for Irradiation Experiments (FIDES)

## Framework for Irradiation Experiments – FIDES

- NEA joint undertaking, established pursuant to Article 5 of the NEA Statue in co-ordination with the NSC and the CSNI
- A stable, sustainable, reliable platform for fuel and material testing using nuclear research reactors (RRs) in NEA member countries
- Generates experimental results and expertise for shared costs
- **PoW 2021-2024 includes 4 Joint Experimental Programmes (JEEPs) and 3 cross cutting pillars**



**Chair** R. Furstenau (US), G. Bignan (FR)  
**Secretariat** M. Beilmann, M. Bales

# JEEP INCA

## In-pile Creep Studies of ATF Claddings



Facility: LVR-15 reactor and hot cells, ÚJV Řež, Czech Republic

Scenario: Steady state conditions

Materials: Coated ATF claddings

Objective: Provide comparative data on the irradiation induced creep of current Zr alloys and Cr coated samples; and between RR and NPP irradiation

Experiment Status: Irradiation began May 2022

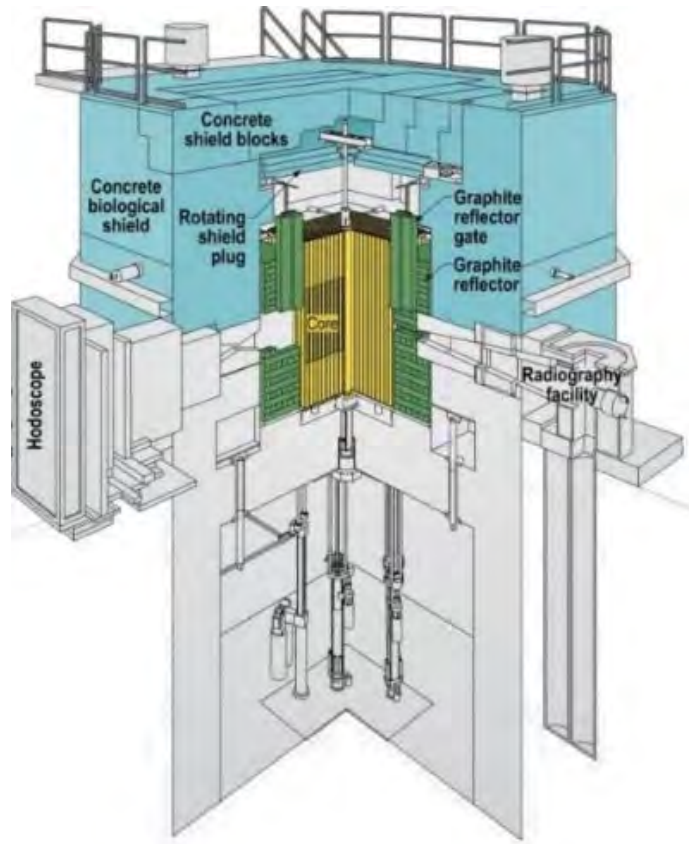
LVR-15 reactor. Court. ÚJV Řež

**Programme Manager** M. Miklos (CZ) **Secretariat** M. Bales & M. Beilmann



# JEEP HERA

## High Burnup Experiments in Reactivity Initiated Accidents



TREAT reactor. Court. INL

Facility: TREAT reactor and hot cells, INL USA and NSRR Japan

Scenario: 6 RIA tests with pre-hydride cladding and oversized UO<sub>2</sub> pellets + 4 RIA test with actual HBU fuels

Materials: High burnup fuels (& ATF in later phase)

Objective: Investigate performance of modern high burnup fuel (lower corrosion / hydrogen pickup than some previous RIA tests) at representative pulse widths

Experiment Status: Pre-hydride and pre-irradiated tests planned for 2022/23

**Programme Manager D. Kamerman (US)**  
**Secretariat M. Bales & M. Beilmann**

# SCIP - Studsvik Cladding Integrity Project

## Objectives:

- Understanding the fuel and cladding performance in interim storage conditions
- Investigate the fuel behavior during LOCA
- Analysis of the influence of the microstructure on PCI
- Support the experimental investigations with pre- and post-test modeling

## Status of the project:

- Phases 1-3 completed (start in 2004)
- Phase 4 ongoing (2019-2024), Back-end topics were included for the first time
- Participants: 38 Organisations from 15 Countries
- Broad range of materials are used for the investigations (PWR, BWR, VVER, non-standard) including doped fuel (ADOPT, ALSi, GD, IFBA)

**Programme Manager** Per Magnusson (SWE)  
**MB Chair** Davis Shrire (SWE) **PRG Chair** Kurt Atkinson (UK) **Secretariat** M. Beilmann

## Other projects investigating ATF materials

### Halden Fuels & Materials (2021-2023)

- ATF investigation have been performed and were planned
  - Cr, CrAl and FeCrAl coated claddings
  - UN, U<sub>3</sub>Si<sub>2</sub>, doped UO<sub>2</sub>
- LOCA testing to be done via Studsvik's SPARE project
- Programme manager: Jon Kvaalem (NOR), Secretariat: D. Jacquemain

### CIP Cabri International Programme

- 12 tests in CABRI reactor (IRSN, France)
- 4 tests dedicated to advanced fuels (Cr doped UO<sub>2</sub>) a/o advanced cladding (liners)
- 2011-2025
- Operating agent contact: F. Barré (FR), Secretariat: D. Jacquemain

# QUENCH-ATF (See presentations by M. Steinbrück, J. Stuckert, M. Grosse)

A joint project to investigate **ATF claddings** for enhanced performance and safety:

- Three large-scale bundle tests performed at the QUENCH facility (KIT, Germany)
- with ATF cladding materials:
- Simulating design-basis and severe accident scenarios
- Supporting separate-effects tests
- Complementary tests performed by IRSN
- Numerical simulation exercise: blind post-test benchmark coordinated by GRS

Participants: 19 organisations from 9 NEA countries

Project started in Autumn 2021, for 4 years

**Programme Manager** M. Steinbrück (GER),  
**MB Chair** H. Esmaili (US), **PRG Chair** Y. Nemoto (JPN), **Secretariat** J.-F. Martin



## QUENCH-ATF #1 (Jul. 2022)

- Cr coated Zr (Westinghouse US)
- Bundle with 24 heated rods
- Extended LOCA conditions
- Peak local temperature 1600 K
- Compares with QUENCH-L3HT

## QUENCH-ATF #2 (S1 2023)

- Cr coated Zr
- Severe accident conditions
- Above Zr-Cr eutectic

## QUENCH-ATF #3 (2024)

- Cr coated Zr, or SiC
- Scenario depending on material and results of previous tests



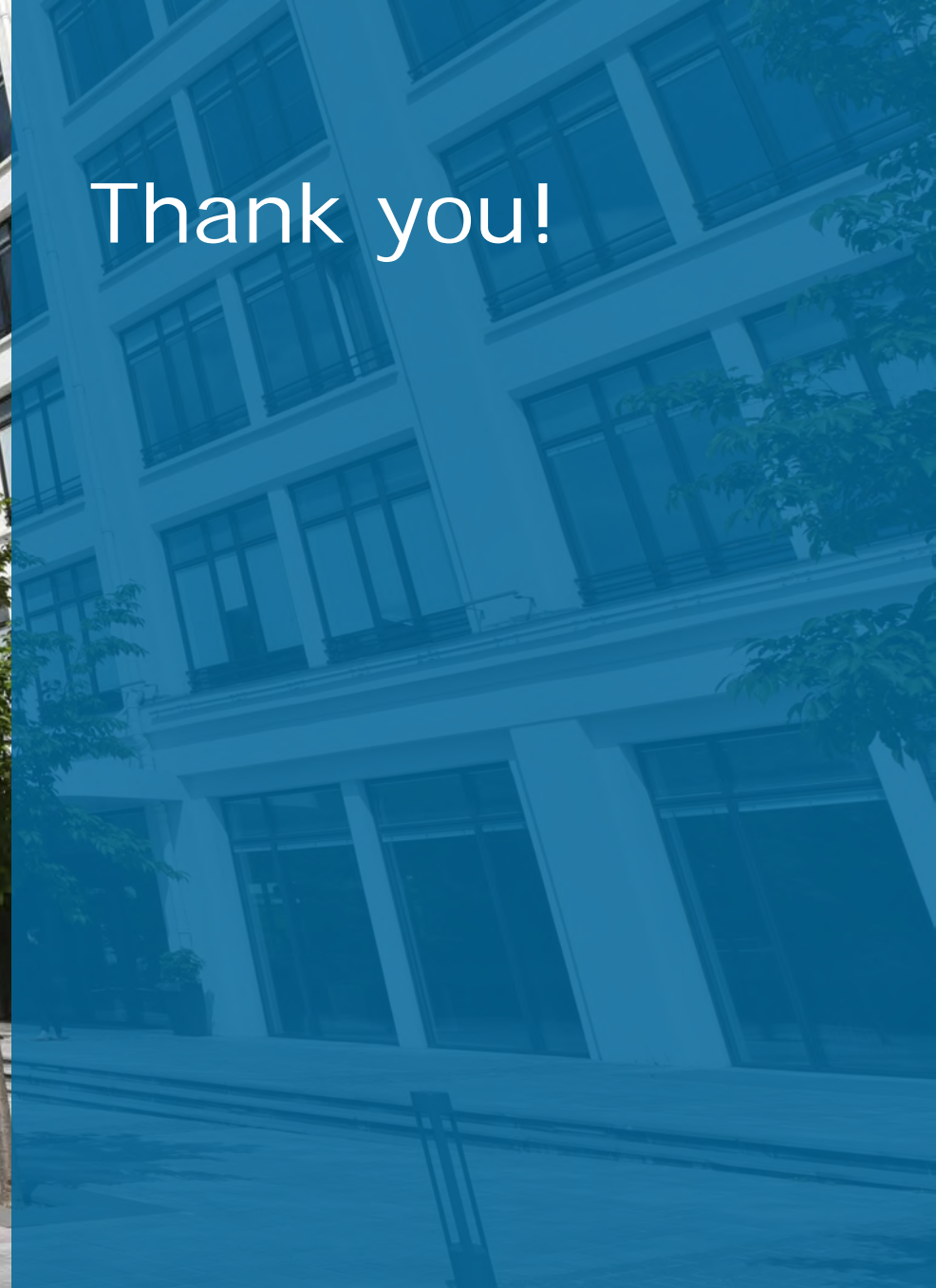
# Looking ahead

NEA assists its members with promoting international collaboration to support advanced fuel technologies by:

- Ensuring information exchanges between relevant international initiatives in the field
- Updating research priorities for ATF development, integrating, as far as feasible, state-of-the-art knowledge from R&D and implementation plans in NEA member countries
- Enhancing testing capabilities and developing FIDES as a framework for fuel testing in key research reactors
- Coupling experimentation with advanced modeling and simulation
- Preserving key experimental data and competencies



Thank you!







**L. Czerniak**

**Westinghouse Electric Company LLC**

## **Accident Tolerant Fuel: Cr Coated Cladding Development at Westinghouse**

In response to the nuclear industry's desire for longer coping times following the Fukushima accident in Japan in 2011, Westinghouse's **EnCore**<sup>®</sup>\* accident tolerant fuel (ATF) program, is developing and commercializing an advanced fuel cladding and fuel pellet with the main goals of improving safety and economic performance. The program is a two-pathway approach, cladding and fuel, with each pathway having an intermediate product and long-term product; both of which are in testing and development phases. The cladding pathway will be the emphasis of this presentation as it is directly tied to the Quench testing being performed by KIT. The chrome coated cladding is undergoing testing in various settings and at various facilities. LTR and LTAs campaigns are currently underway with utility partners and future LTR and LTAs are planned for the upcoming year. These campaigns provide real-world data on the performance of the coating. Supporting testing at both the Westinghouse Churchill and Columbia facilities are occurring in parallel to provide valuable results in the development of the design and specification of the chrome coating.

This material is based upon work supported by the Department of Energy under Award Number DE-NE0009033.

This report was prepared as an account of work sponsored by an agency of the United States Government. Neither the United States Government nor any agency thereof, nor any of their employees, makes any warranty, express or implied, or assumes any legal liability or responsibility for the accuracy, completeness, or usefulness of any information, apparatus, product, or process disclosed, or represents that its use would not infringe privately owned rights. Reference herein to any specific commercial product, process, or service by trade name, trademark, manufacturer, or otherwise does not necessarily constitute or imply its endorsement, recommendation, or favoring by the United States Government or any agency thereof. The views and opinions of authors expressed herein do not necessarily state or reflect those of the United States Government or any agency thereof.

© 2022 Westinghouse Electric Company LLC. All rights reserved

\*EnCore is a registered trademark of Westinghouse Electric Company LLC, its affiliates and/or its subsidiaries in the United States of America and may be registered in other countries throughout the world. All rights reserved. Unauthorized use is strictly prohibited. Other names may be trademarks of their respective owners.

# Accident Tolerant Fuel: Cr Coated Cladding Development at Westinghouse

Luke Czerniak

September 27, 2022

27<sup>th</sup> International Quench Workshop





Westinghouse **VISION & VALUES**

**together**

we advance technology  
& services to power a  
clean, carbon-free future.

• Customer Focus & Innovation

• Speed & Passion to Win

• Teamwork & Accountability

Safety • Quality • Integrity • Trust



# Outline

- Westinghouse **EnCore**<sup>®</sup> Fuel Program
- Coated Cladding Updates
- Coated Cladding Testing
- 2<sup>nd</sup> Test ATF-Quench

ADOPT, EnCore, AXIOM, ZIRLO, Optimized Zirlo are trademarks or registered trademarks of Westinghouse Electric Company LLC, its affiliates and/or its subsidiaries in the United States of America and may be registered in other countries throughout the world. SiGA is a registered trademark of General Atomics, its affiliates and/or its subsidiaries in the United States of America and may be registered in other countries throughout the world. All rights reserved. Unauthorized use is strictly prohibited. Other names may be trademarks of their respective owners.

# Westinghouse's EnCore<sup>®</sup> Fuel Program

*The EnCore<sup>®</sup> Fuel program is developing and commercializing advanced fuel products to improve safety and economic performance*

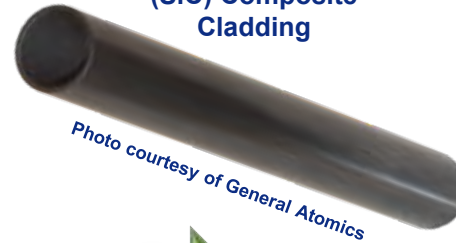
## Advanced Cladding

- Cr-Coated Zirconium – increases safety and operational margin, and may enable high burnup
- Silicon Carbide Cladding – safety and operational benefits

Chromium-Coated Zr Cladding



SiGA<sup>®</sup> Silicon Carbide (SiC) Composite Cladding



*Photo courtesy of General Atomics*

ATF Product Evolution

Enables HEF

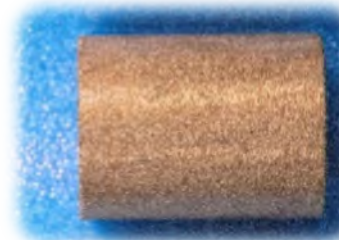
## Advanced Fuel

- ADOPT fuel pellets – higher density,
- Advanced Pellet (UN) - benefits to fuel cycle costs, and may support high burnup improved fuel cycle economics, thermal properties, and lower operating temperatures

ADOPT Pellets



Uranium Nitride (UN) Pellets



U<sup>15</sup>N Fuel

*Photo courtesy of Los Alamos National Lab*

Step 1: ~68 GWd/MTU for rods that do not rupture in a LOCA or experience DNB beyond 62 GWd/MTU

Step 2: Entire core to ~75 GWd/MTU with enrichment increase



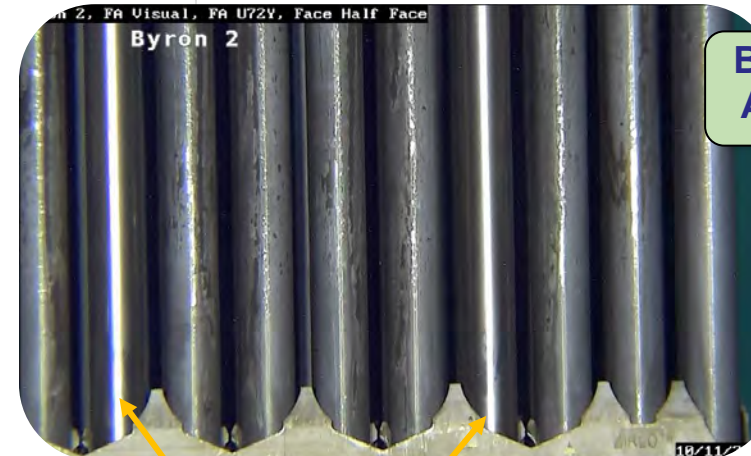
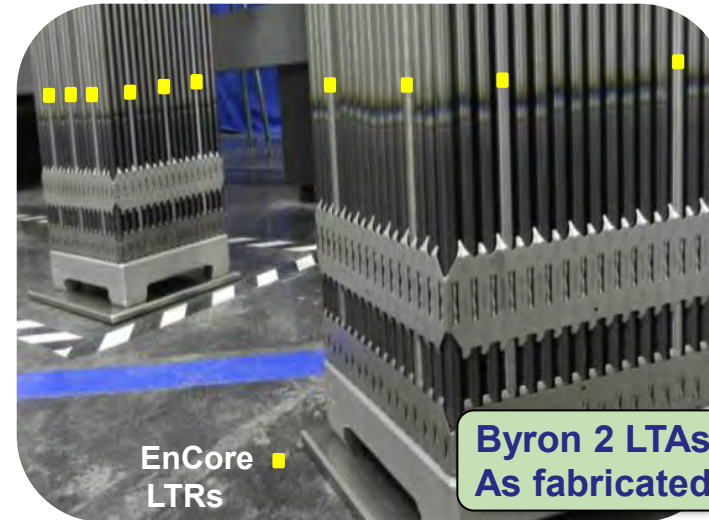
# LTA and LTR Status



# Lead Test Rod & Lead Test Assembly Programs

LTA Campaigns with Utility Partners provide data to support fuel qualification

- Byron 2: inserted Spring 2019
  - Two 17x17 assemblies
  - 16 rods with Cold Spray Cr Coated Cladding
    - 4 rods with **ADOPT** pellets
  - 4 rods with 12" segments of high-density pellets
  - 1st & 2nd cycle Poolside exam show excellent adherence
  - 1st cycle hot cell examination underway at ORNL
- Doel Unit 4: inserted Spring 2020
  - Four 17x17 RFA XL assemblies
  - 32 rods with Cold Spray Cr Coated Cladding with  $UO_2$
- Vogtle Unit 2: Insertion planned for 2023
  - Full assemblies of ATF product (**ADOPT** pellets and coated cladding)
  - 6%  $^{235}U$  rods lead industry in higher enrichment
- EDF: Insertion planned for 2023
  - Lead Test Rods of Cr Coated Cladding
  - This marks the largest R&D program on enhanced fuel that Westinghouse has conducted in Europe
- 3rd cycle Reinsertion in Byron Unit 2:
  - Fuel Assembly, U72Y (**ADOPT** pellets, Pure Cr Coating), Cycle 25
  - Supplies essential high-burnup data for coated cladding, **ADOPT**, and standard fuel licensing



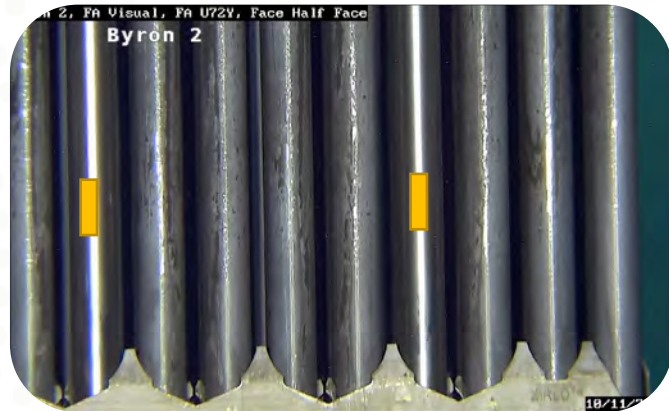
Byron 2 LTAs After 1 cycle

- Limited apparent crud accumulation (easily brushed off)
- No significant oxidation
- No deformation
- No apparent wear

# Visual Inspections from LTR Programs Complete

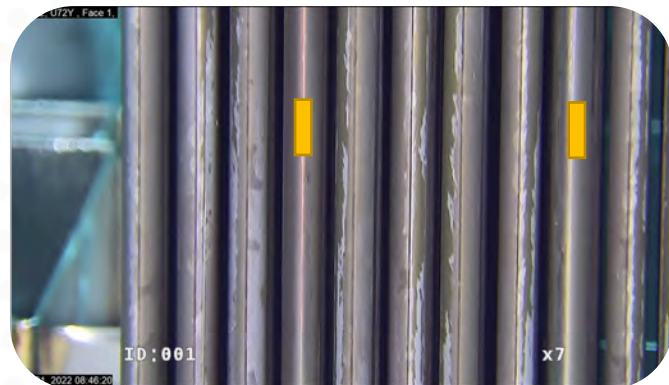
## Byron Unit 2 LTRs

EOC 1



Cr Coated Cladding

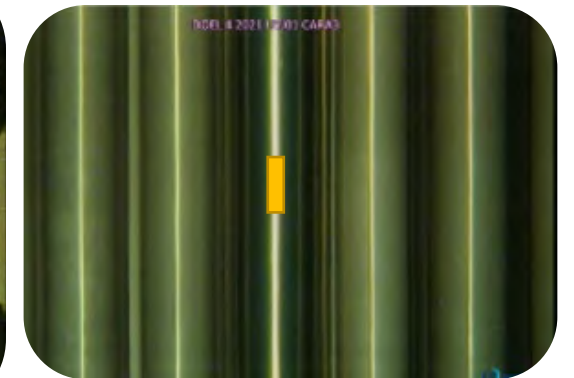
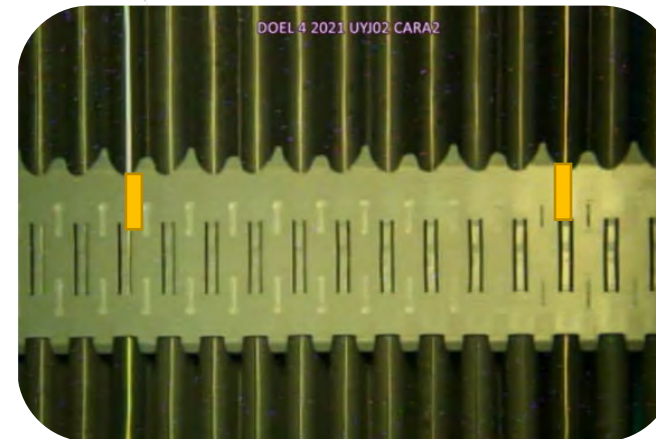
EOC 2



Photos courtesy of Constellation

## Doel Unit 4 LTRs

EOC 1



Photos courtesy of Electrabel

- 1<sup>st</sup> and 2<sup>nd</sup> cycle visuals: Excellent adherence, rods remain shiny with little indication of crud
- Byron 1<sup>st</sup> cycle visuals, fiberscope, rod length, profilometry, eddy current complete
- Byron 2<sup>nd</sup> cycle pool side rod extraction with rod length, fiberscope profilometry, and eddy current scheduled for November. Doel 2<sup>nd</sup> Cycle poolside exam scheduled Spring 23

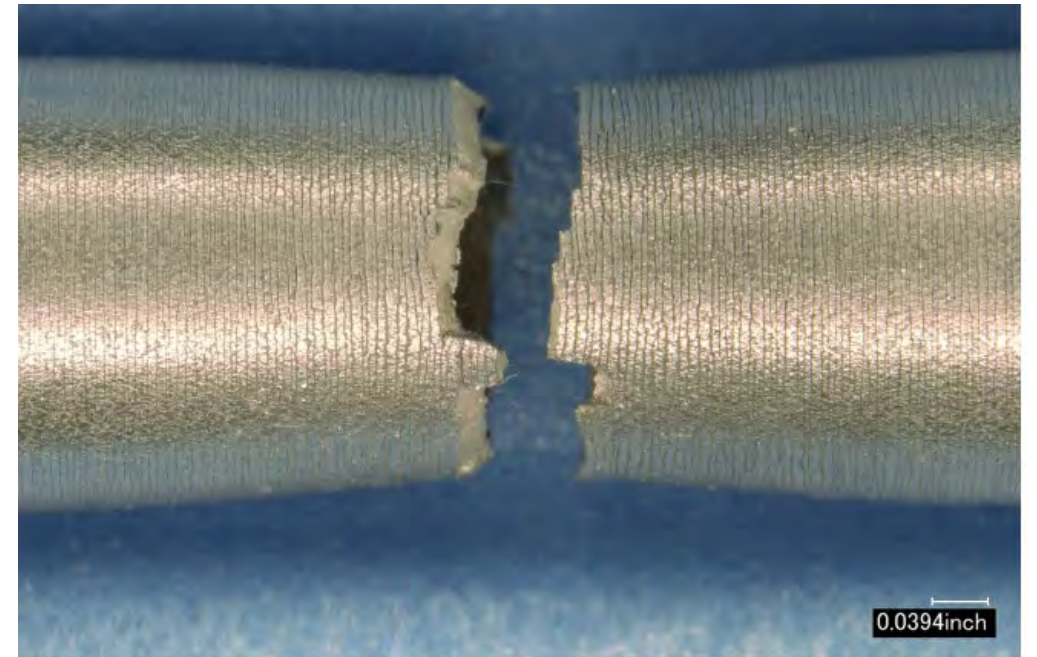
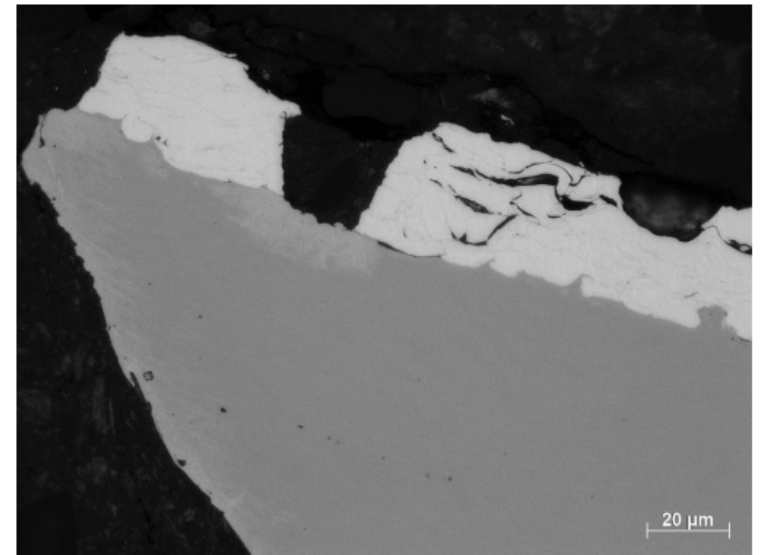


# Coated Cladding Testing



# Tensile Testing

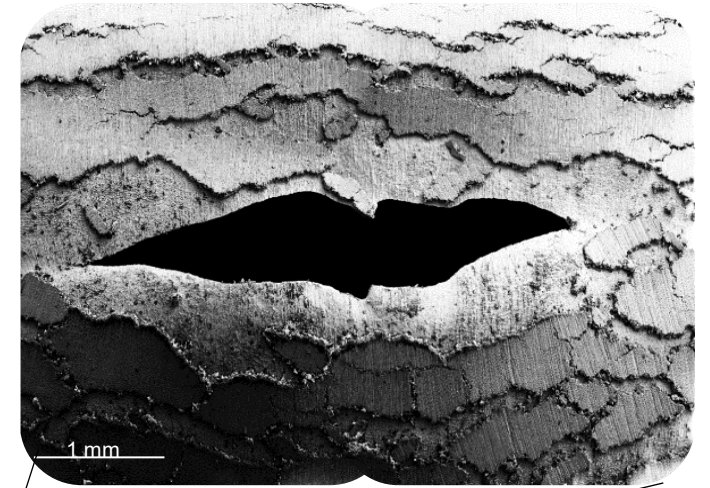
- NCS demonstrated similar adhesion with no delamination in comparison to HCS
- Cracking of the coating begins to occur around ~3% strain
- Increase in elastic modulus and tensile strength
  - ~25% and ~12% respectively





# Burst Testing

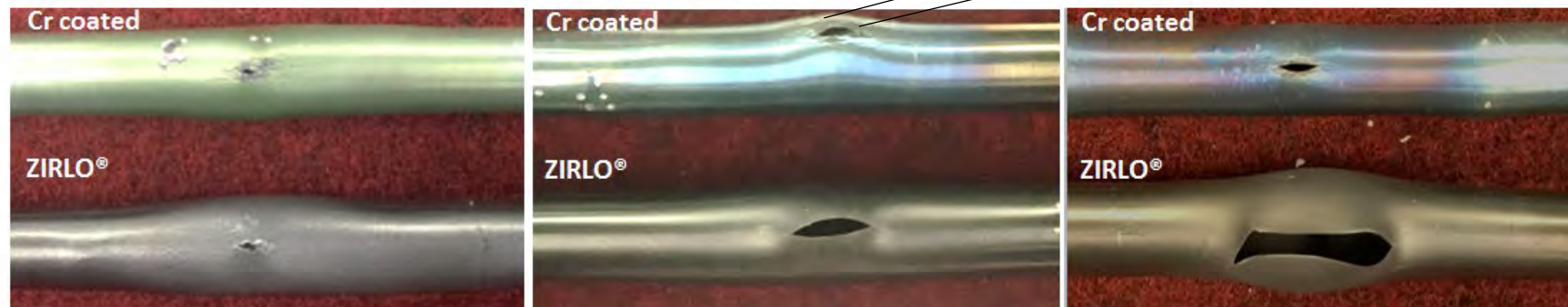
- Chromium coating increases burst temperature and reduces ballooning and burst opening
  - No coating spallation observed
  - Minor cracking and crack opening in burst region
- Increases safety and operational margin and enables high burnup



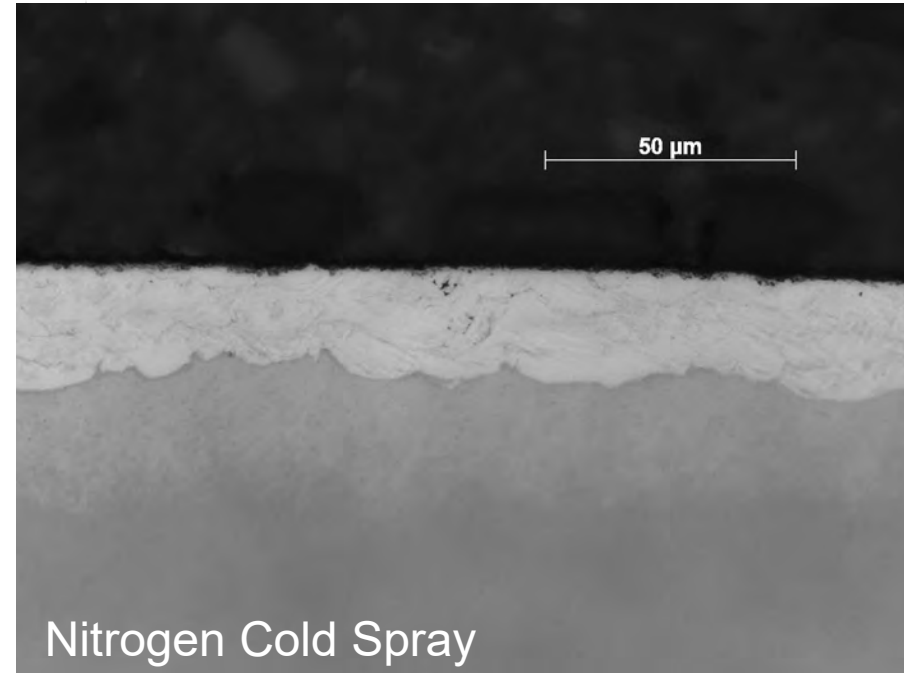
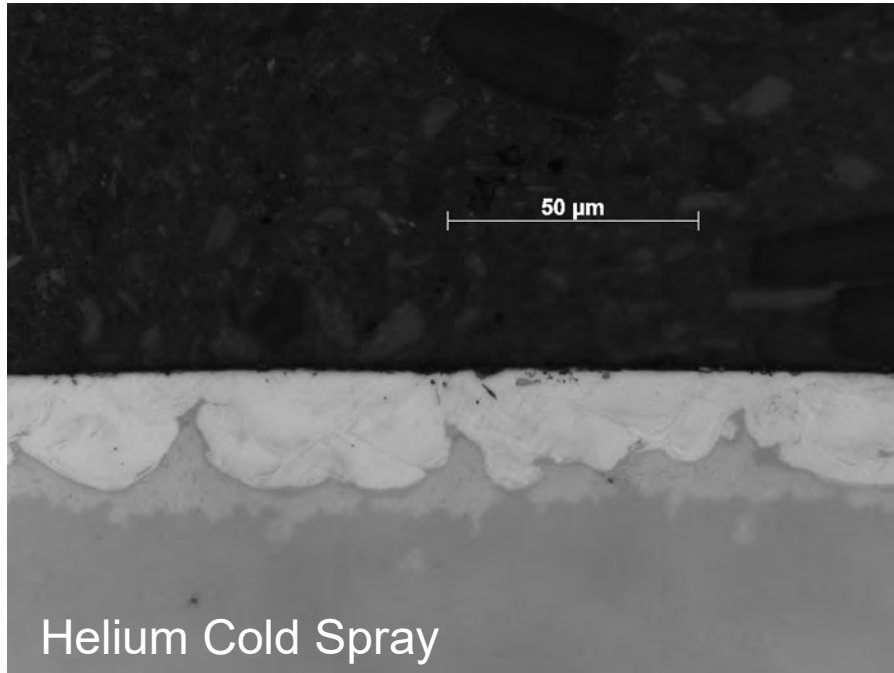
200 psi (1.4 Mpa)

800 psi (5.5 Mpa)

1800 psi (12.4 Mpa)



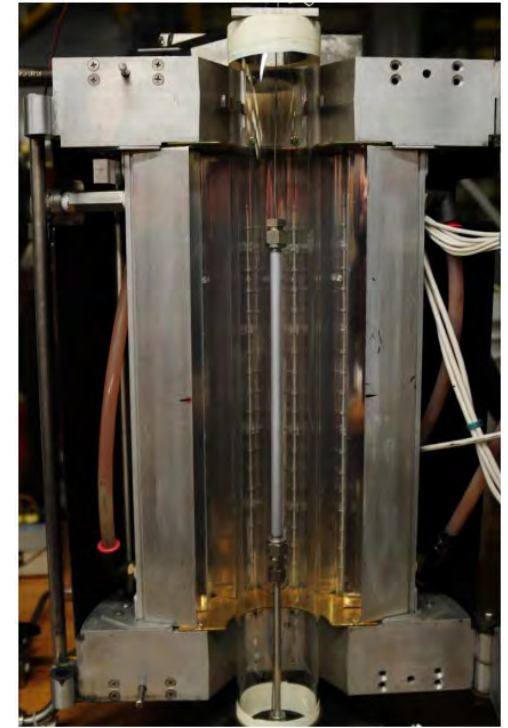
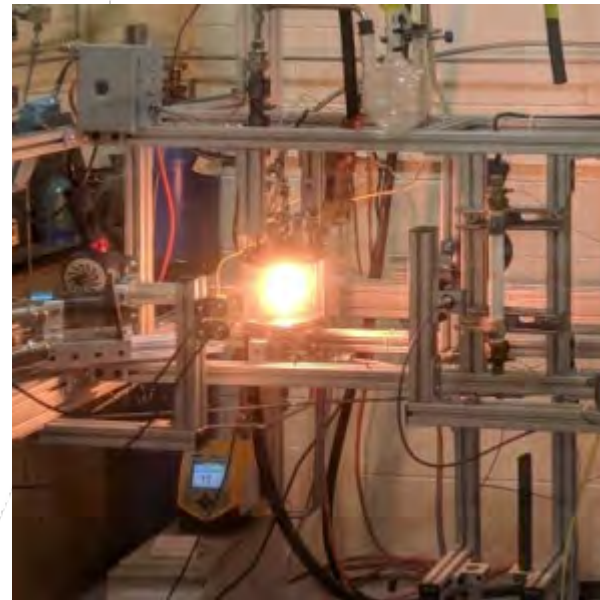
# Helium vs. Nitrogen Cold Spray



- Both gases result in deposits that are highly dense with low porosity
- HeCS yields a rougher interface compared to N2CS because of higher particle velocity
- Greater interfacial roughness is a disadvantage because it requires a thicker coating to meet minimum thickness requirements

# Ongoing/Future Testing

- Fatigue Testing
- Corrosion Studies
- High Temperature Oxidation
- Ring Compression Testing
- Ultra-High Temperature Testing
- DNB Testing
- Burst Testing
- PIE Analysis



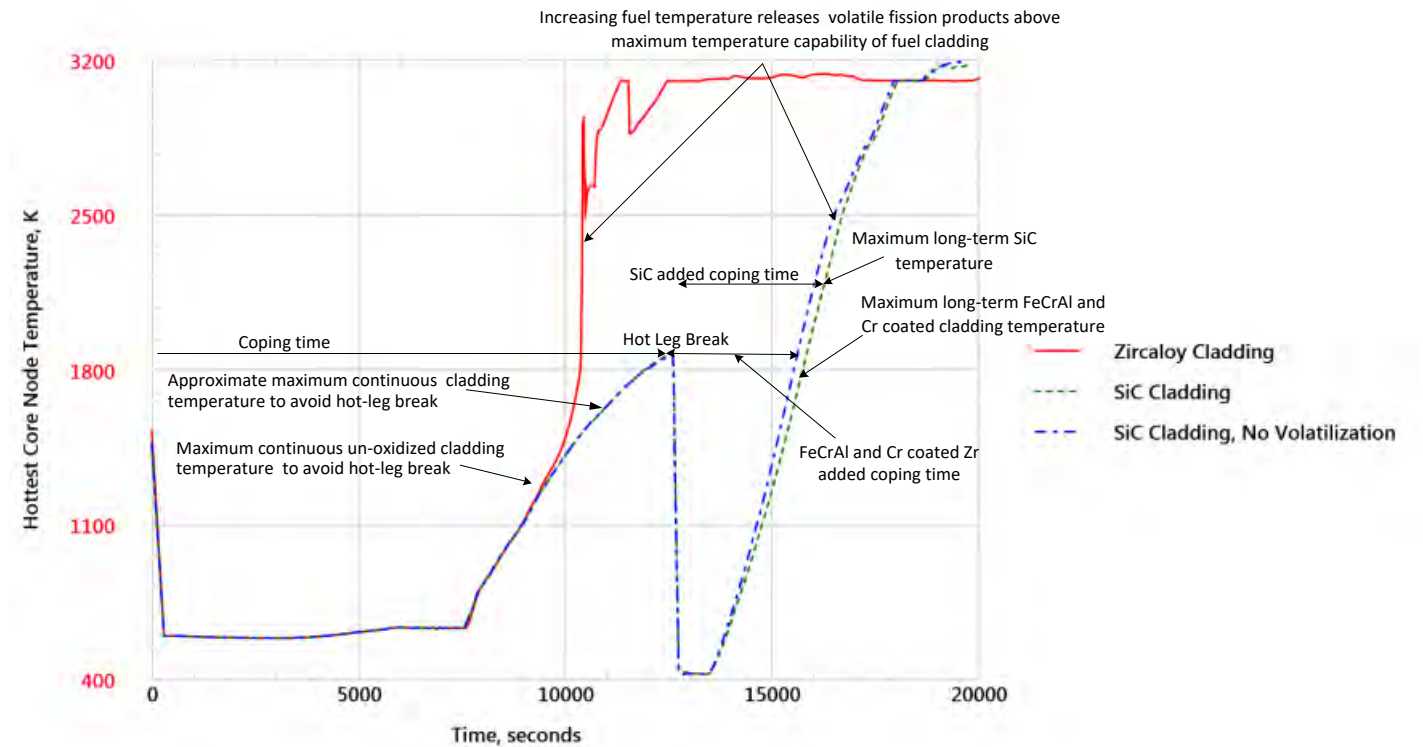


# 2<sup>nd</sup> Test ATF-Quench Program



# Projected Test Parameters

- Beyond Design Basis Accident
  - Max Temperature
    - 1600°C
  - Heat Rate
    - 10°C/min
  - Quench at 1600°C



# Sample Delivery and Planning

- Tubes
  - 30 full length tubes (~2.5m in length)
  - Chromium cold spray coating
    - NCS and HCS tubes
- Grids
  - 17x17 grind construction
  - Standard plant mid-grid
- Projected shipment to KIT is October 2022

# Thank You



Westinghouse  
Electric Company



@WECNuclear



Westinghouse  
Electric Company



wecchinanuclear

[westinghousenuclear.com](http://westinghousenuclear.com)



Westinghouse



**M. Steinbrück**

**KIT**

## **Limiting degradation mechanisms for high-temperature oxidation resistance of promising ATF cladding solutions**

Eleven years after the Fukushima Daiichi accidents, three material systems are considered the most promising solutions for accident-tolerant fuel cladding (ATF). These are (1) chromium-coated zirconium alloys as an evolutionary short-term solution as well as (2) FeCrAl alloys and (3) SiC-based ceramic matrix composites (CMC) as revolutionary long-term alternatives to classical Zr alloys.

The new cladding materials should exhibit at least the same excellent properties as Zr alloys during operation and design-basis accidents, but ATF materials should also show improved behavior in terms of high-temperature oxidation resistance during severe accidents, resulting in reduced hydrogen and chemical heat release and extended coping time.

The presentation briefly discusses the high-temperature degradation mechanisms for the three ATF cladding materials mentioned above, which result in different maximum "survival" temperatures. Illustrative examples from recent experimental work at the Karlsruhe Institute of Technology are given for all systems.

In conclusion from international and KIT's research on ATF cladding, the maximum survival temperatures for the ATF cladding materials are:

- 1200-1300°C for Cr-coated Zr-based cladding
- 1300-1400°C for FeCrAl alloys, and
- >1700°C for SiC<sub>f</sub>-SiC composites.



# Degradation mechanisms of the most promising ATF cladding concepts

M. Steinbrück, M. Große, C. Tang, J. Stuckert

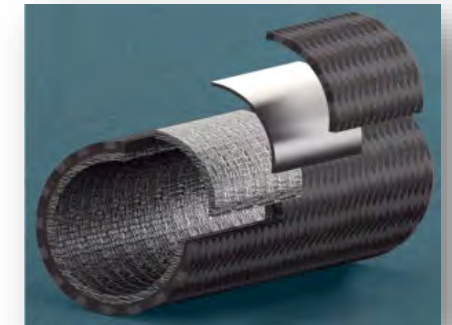
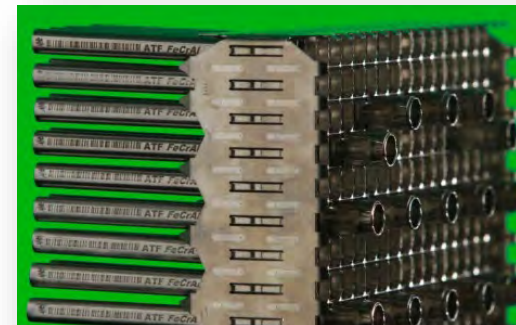
*27th International QUENCH Workshop, Karlsruhe Institute of Technology, 27-29 Sept 2022*

Institute for Materials Research IAM-AWP / Program Nuclear Safety



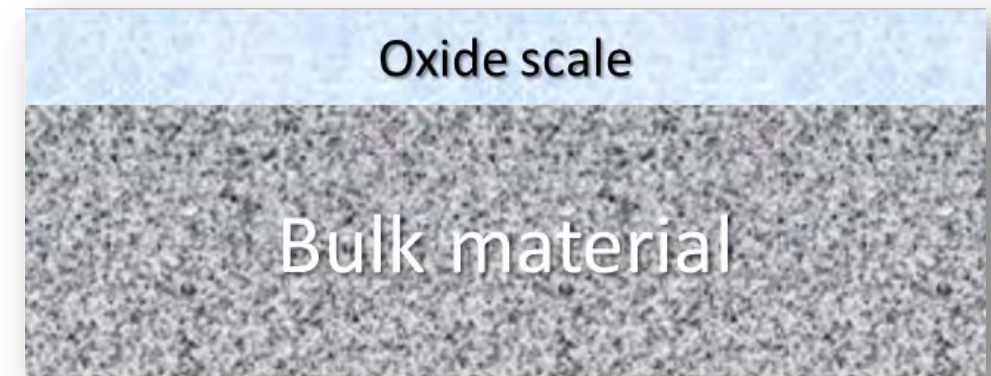
# ATF cladding research

- Worldwide research on accident tolerant fuel (ATF) materials after Fukushima accidents
- ATF materials should reduce release of hydrogen and heat (oxidation kinetics) and increase coping time for accident management measures
- After ten years of international research, the most promising ATF cladding concepts are:
  - Cr-coated Zr alloys
  - FeCrAl alloys
  - SiC<sub>f</sub>-SiC ceramic matrix composites

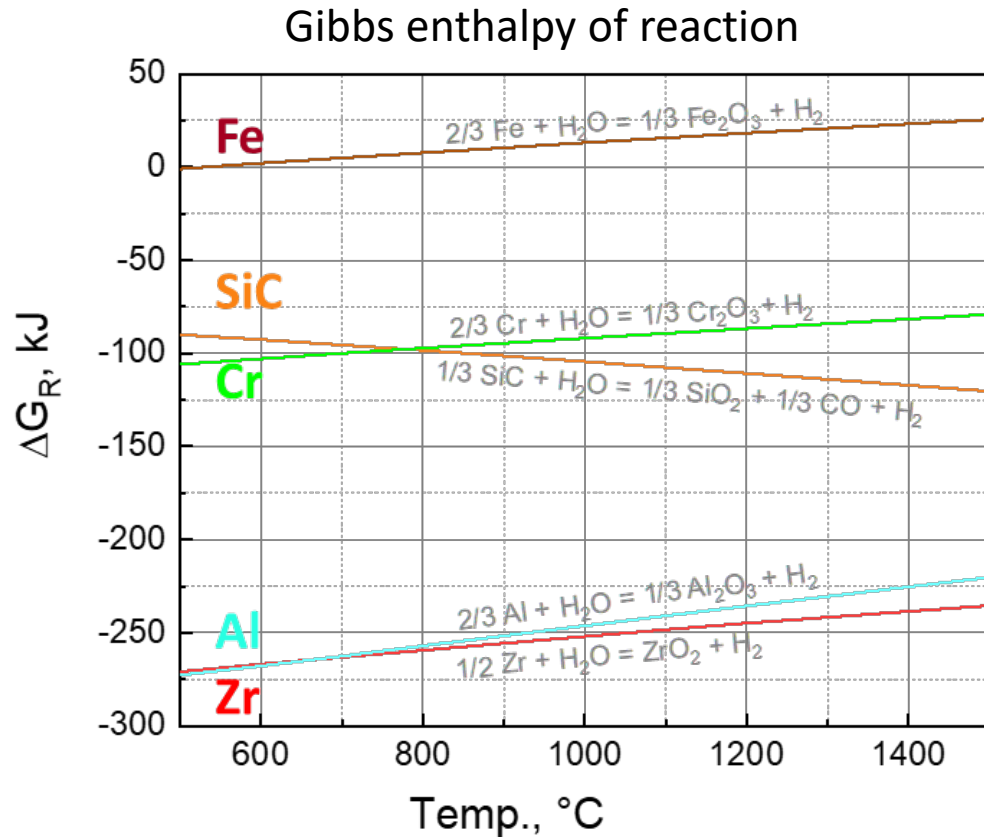


# Oxidation and degradation mechanisms

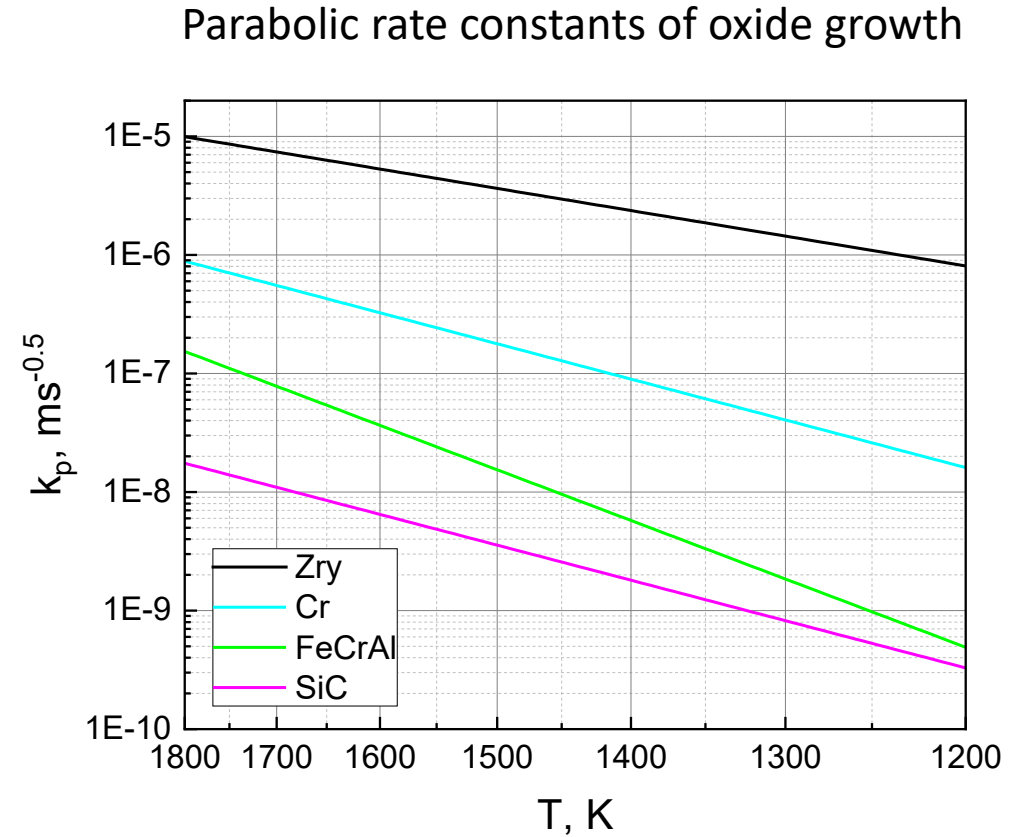
- HT oxidation resistance relies on the formation of thermodynamically stable oxides with low diffusion constants of oxygen and/or metal ions
  - $\text{Al}_2\text{O}_3$ ,  $\text{Cr}_2\text{O}_3$ ,  $\text{SiO}_2$
- Degradation of these protective oxides may be caused by consumption of the oxidizing species due to:
  - Volatilization of the oxide in steam atmosphere
  - Diffusion
    - Depletion of oxidizing species in the bulk material (alloy)
    - of coating into bulk
- Melting of bulk material or oxide scale, eutectic interactions



# Comparison of oxidation data



➔  $\text{Al}_2\text{O}_3$  and  $\text{ZrO}_2$  are thermo-dynamically most stable



➔  $\text{Al}_2\text{O}_3$  and  $\text{SiO}_2$  have the slowest growth kinetics



# Melting temperatures

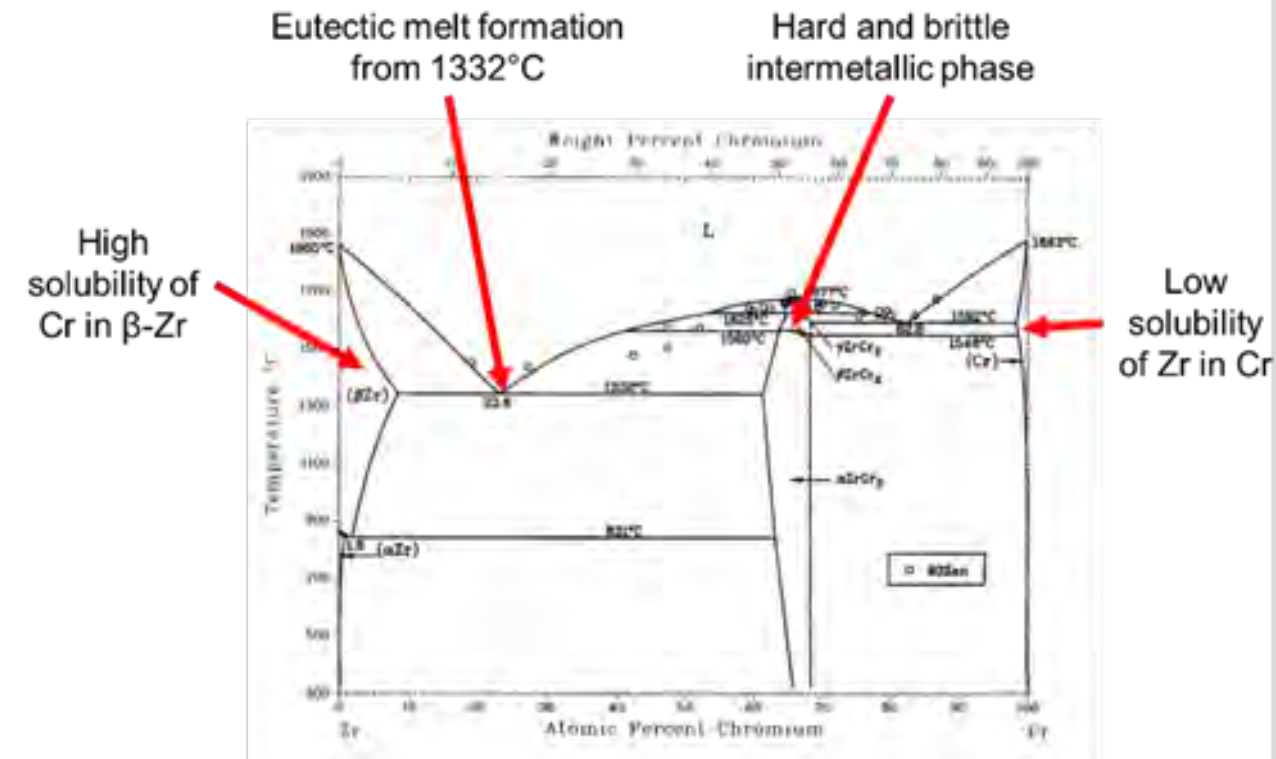
- Determining the ultimate application/survival temperatures of the materials

Zry	1850°C	ZrO <sub>2</sub>	2715°C
Cr	1907°C	Cr <sub>2</sub> O <sub>3</sub>	2435°C
FeCrAl	1425-1500°C	Al <sub>2</sub> O <sub>3</sub>	2072°C
		FeO	1377°C*
SiC	2700°C (subl.)	SiO <sub>2</sub>	1710°C

\* Potential interaction with UO<sub>2</sub>

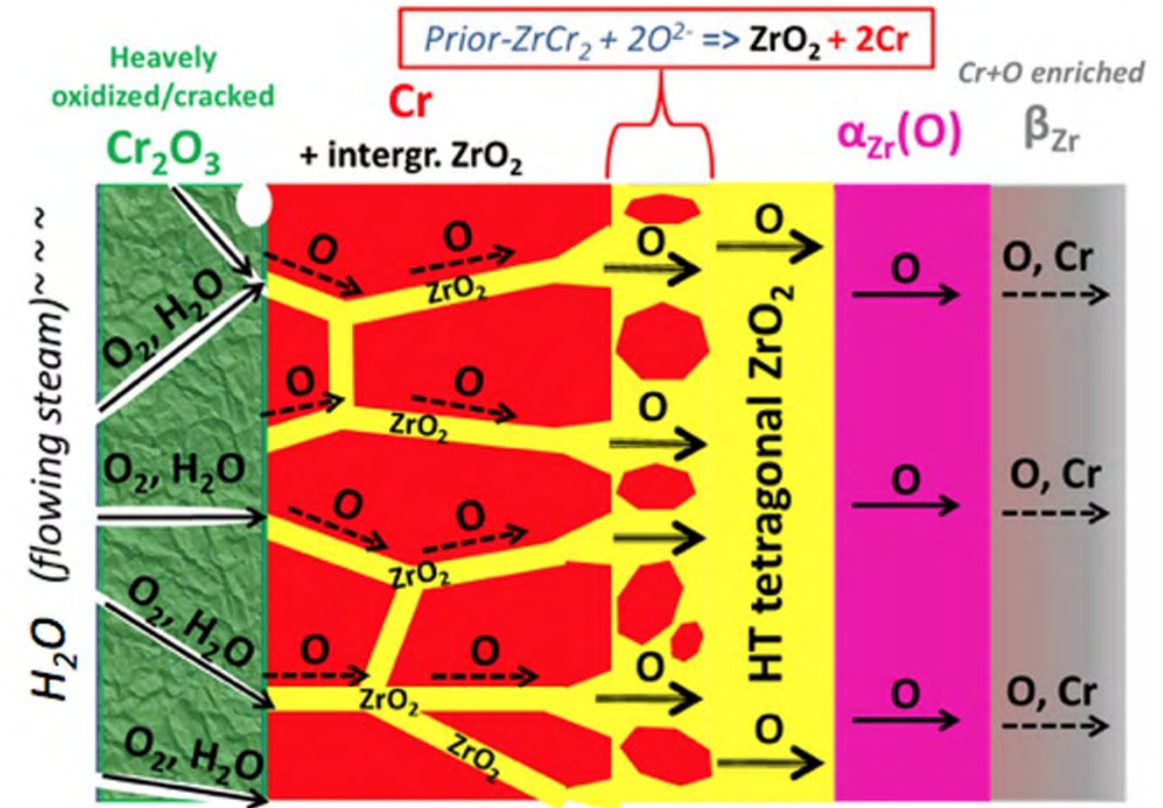
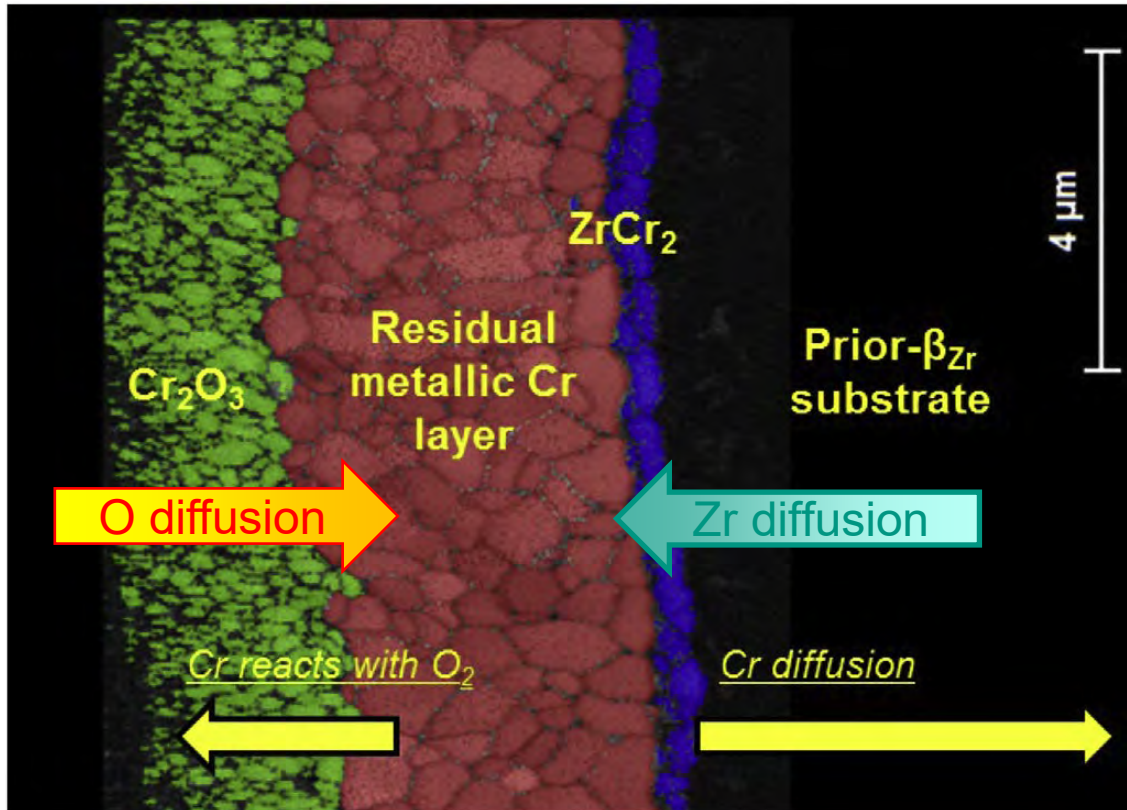
# Cr-coated Zr alloys

- $2 \text{Cr} + 3 \text{H}_2\text{O} \rightarrow \text{Cr}_2\text{O}_3 + 3 \text{H}_2$ 
  - ➔ Adherent and well protective oxide scale
  - ➔ Consumption of Cr layer
- Zr-Cr eutectic melt formation at 1332°C
  - ➔ Ultimate upper limit of application
- $\text{Zr} + 2 \text{Cr} \rightarrow \text{ZrCr}_2$ 
  - ➔ Consumption of Cr coating by diffusion into Zr bulk and formation of a brittle intermetallic layer
- $\text{Cr}_2\text{O}_3 + 1.5 \text{O}_2 \rightarrow 2 \text{CrO}_3(\text{g}) \uparrow$   
 $\text{Cr}_2\text{O}_3 + 2 \text{H}_2\text{O} + 1.5 \text{O}_2 \rightarrow 2 \text{CrO}_2(\text{OH})_2(\text{g}) \uparrow$ 
  - ➔ Potential consumption of Cr layer at HT by formation of volatile species

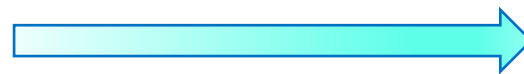


Zr-Cr phase diagram

# Interaction Cr-coating with Zry bulk



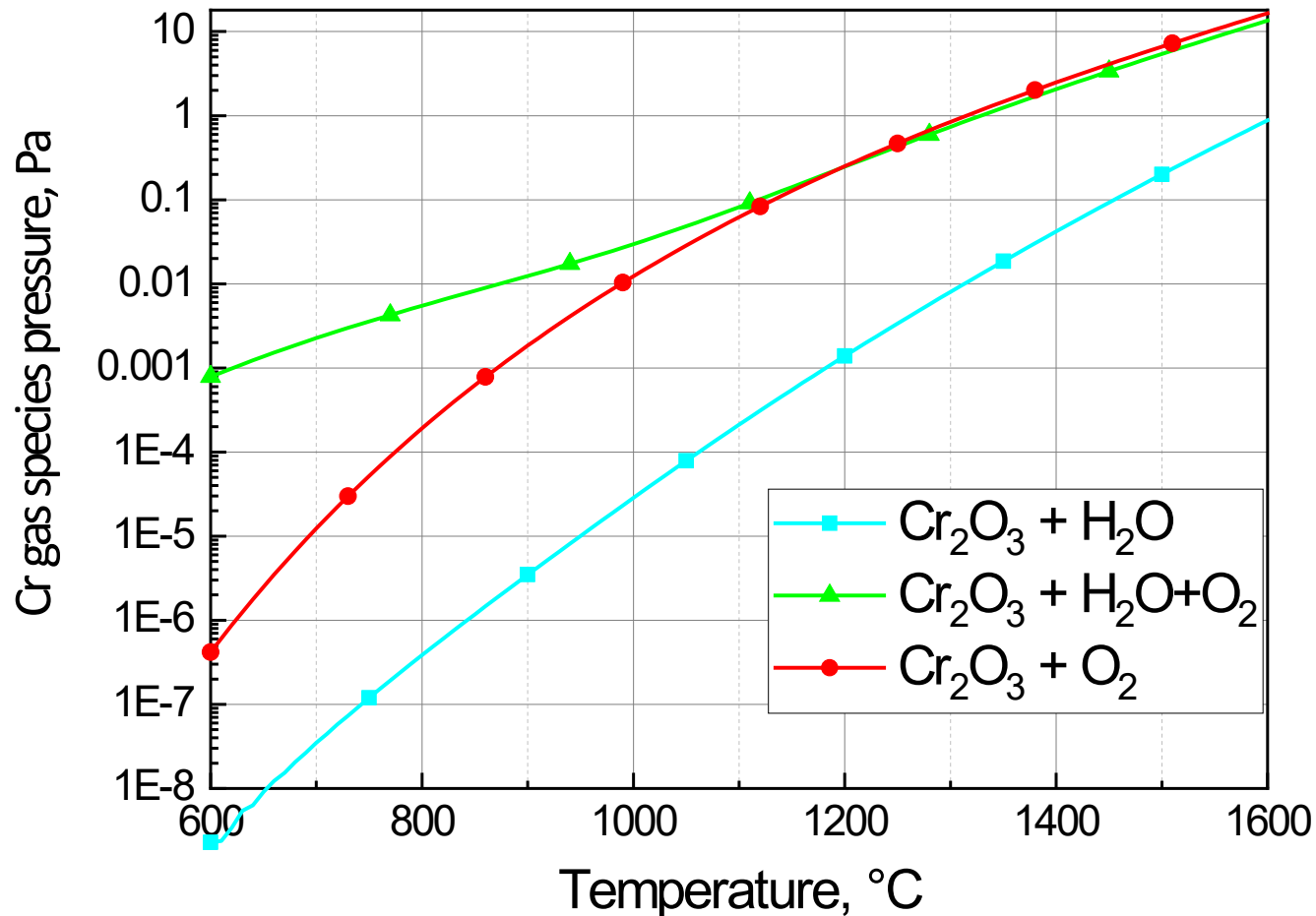
Protective coating



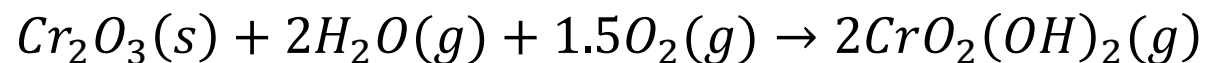
Non-protective coating

Due to the formation of O conducting ZrO<sub>2-x</sub> channels along Cr grain boundaries

# Volatility of chromia

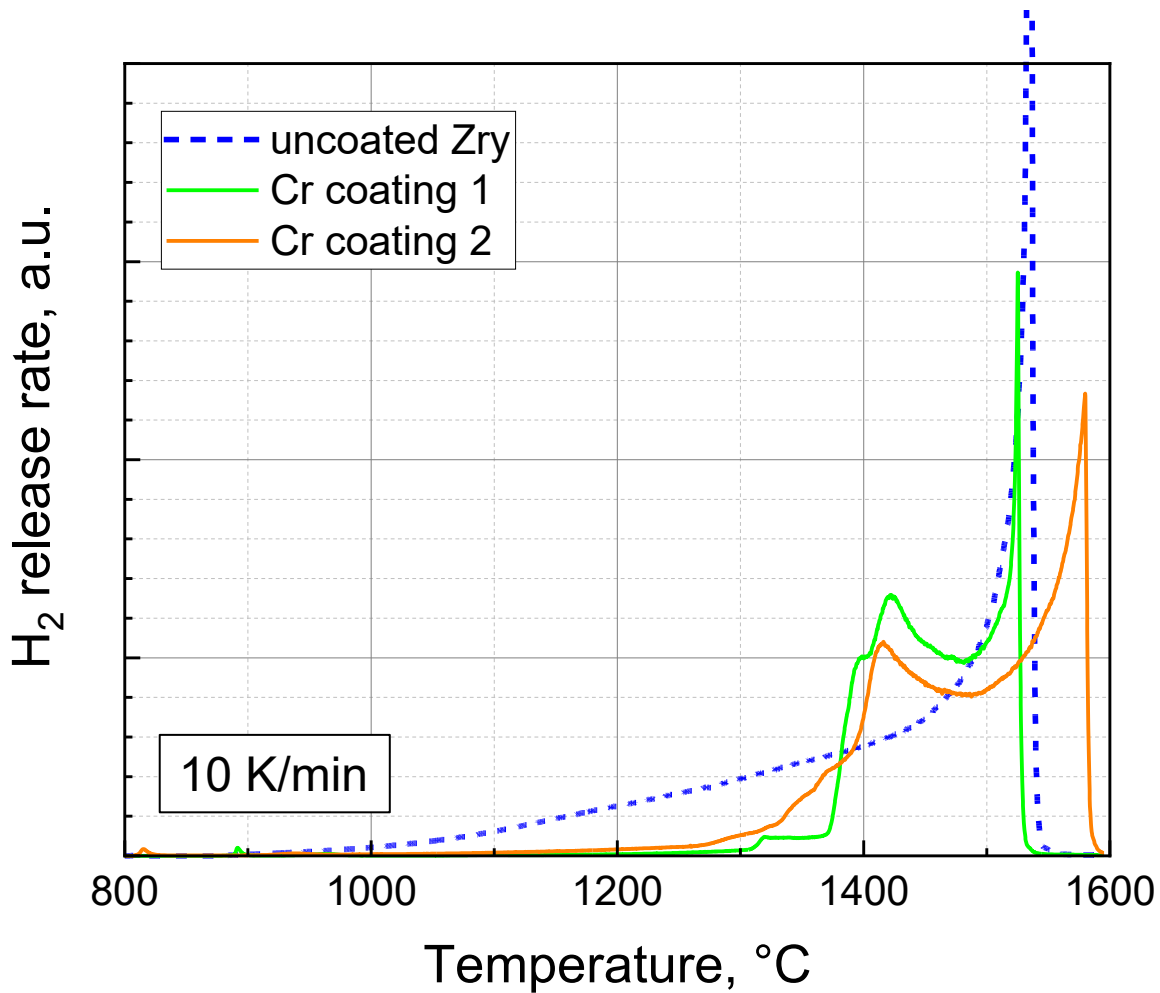


- ➔ Low volatility in pure water vapor
- ➔ Significant volatility only at temperatures >1300°C, i.e., after failure of Cr coating due to other reasons





# Transient tests from 800°C until failure



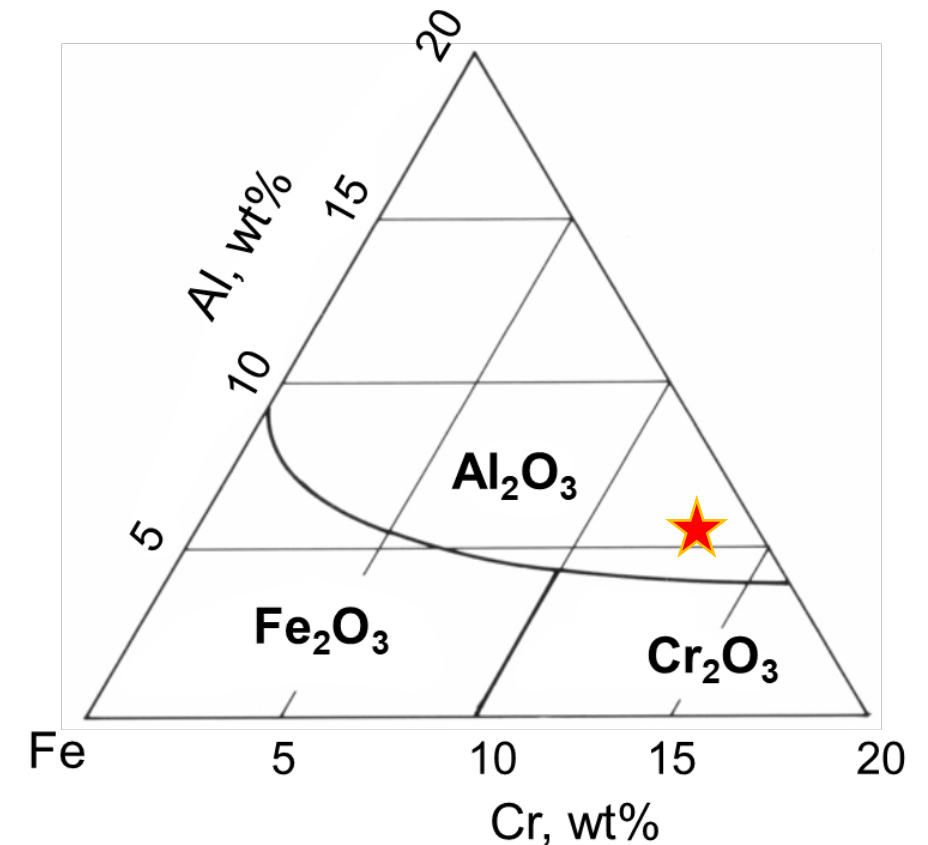
Oxidation kinetics of Cr coated and non-coated Zr alloy

- ➔ Protective behavior of Cr coating up to ~1300°C
- ➔ Serious failure at ~1350°C
- ➔ **Faster oxidation of coated samples after coating failure compared to Zry!**



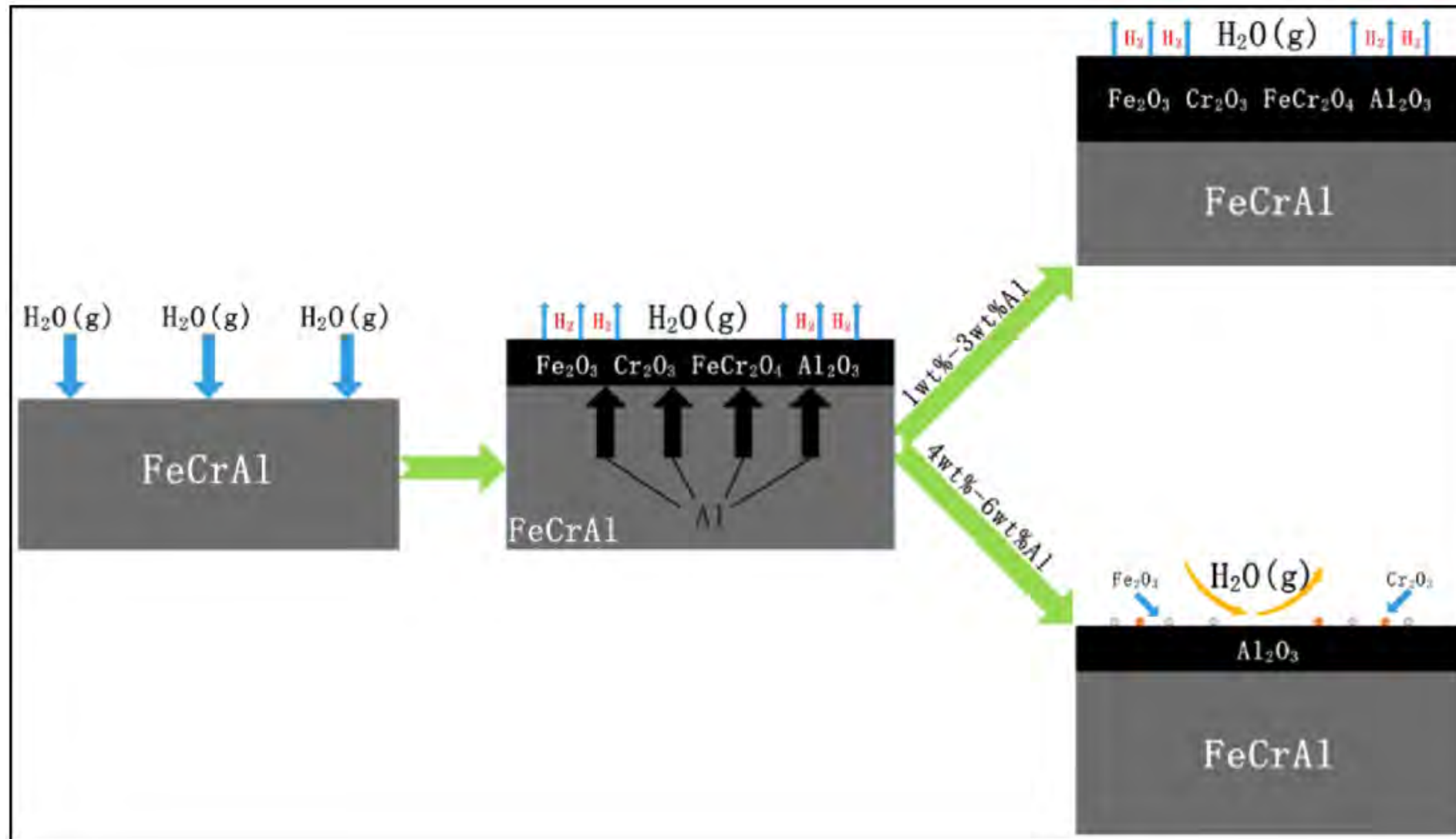
# FeCrAl alloys

- $2 M + 3 H_2O \rightarrow M_2O_3 + 3 H_2$
- Thermodynamic stability:  
 $Al_2O_3 > Cr_2O_3 > FeO_x$
- Diffusion in metal:  $Al > Fe \approx Cr$   
 Diffusion in oxide:  $Fe^{3+} > Cr^{3+} > Al^{3+}$
- Volatility:  
 $Cr_2O_3 \gg Al_2O_3 \approx FeO_x$
- Formation of stable and very protective  $\alpha-Al_2O_3$  scale
  - At  $T > 800-1000^\circ C$
  - Depending on composition
  - “Third element effect” of Cr
- Nuclear grade FeCrAl with low Cr content (Fe13Cr6Al)

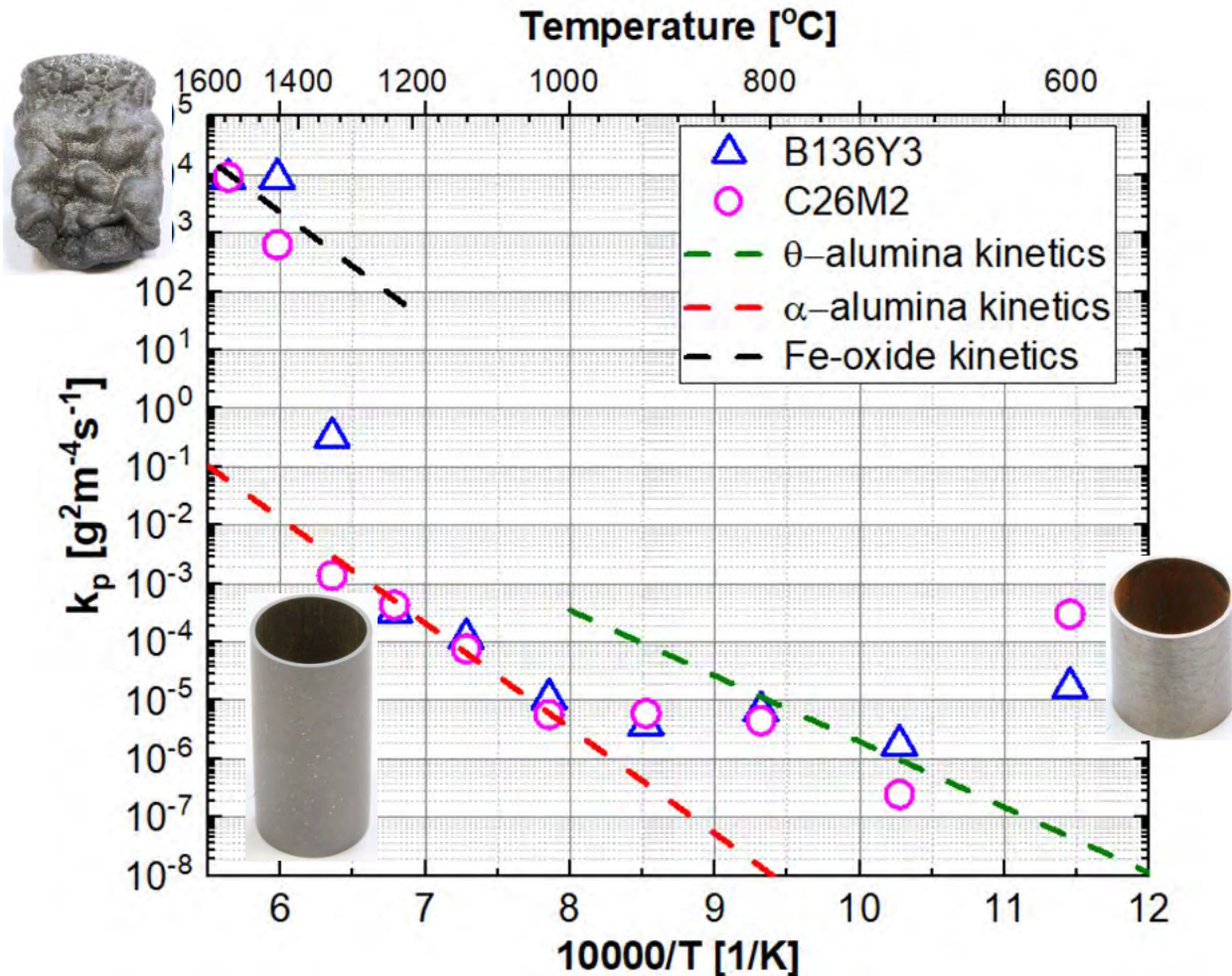


Oxide map at 1000°C

# HT oxidation mechanism of FeCrAl alloys



# Oxidation kinetics of nuclear grade FeCrAl alloys

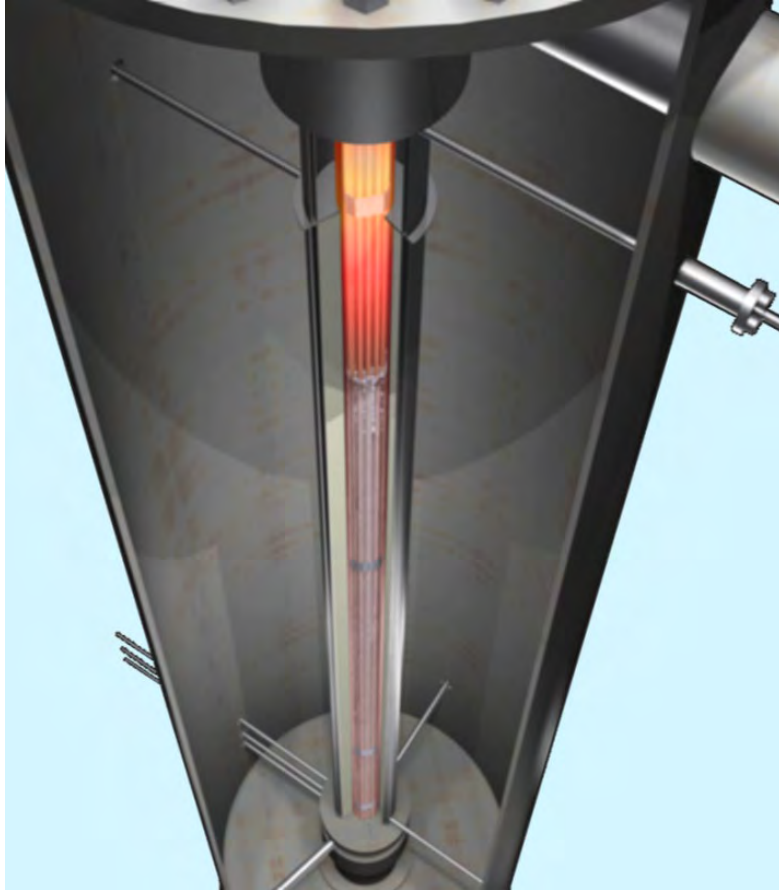


Steam oxidation kinetics of nuclear-grade FeCrAl alloys with kinetics of  $\theta$ - and  $\alpha$ -alumina and Fe-oxide

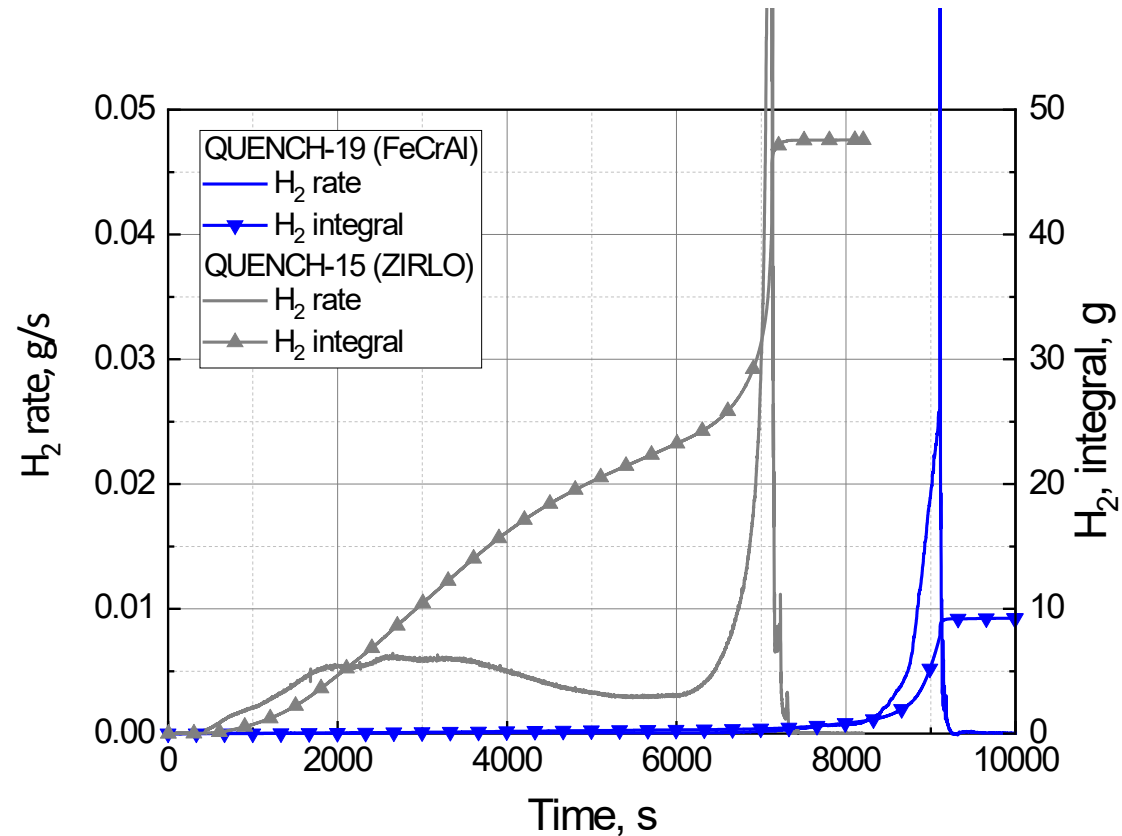
- ➔  $600^\circ\text{C}$ :  
Fast oxidation of inner tube surface (Fe-rich)
- ➔  $700^\circ\text{C} < T < 900^\circ\text{C}$ :  
 $\theta$ -alumina kinetics
- ➔  $1000^\circ\text{C} < T < 1350^\circ\text{C}$ :  
 **$\alpha$ -alumina kinetics**
- ➔  $T \geq 1400^\circ\text{C}$ :  
Fe-oxide kinetics resulting in catastrophic oxidation
- ➔ Transition temperature from protective  $\alpha$ -alumina kinetics to catastrophic oxidation is dependent on composition, surface finish and heating rate, etc.



# QUENCH-19 bundle test with FeCrAl cladding



QUENCH Facility



Hydrogen release during QU-19 test compared with reference test QU-15 with ZIRLO

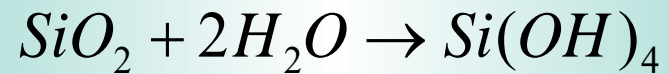


QUENCH-19 bundle post-test

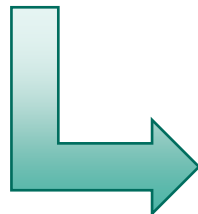
# SiC reaction with steam at very high temperatures



Parabolic oxidation  $\rightarrow$  scale growth



Linear volatilization  $\rightarrow$  material loss



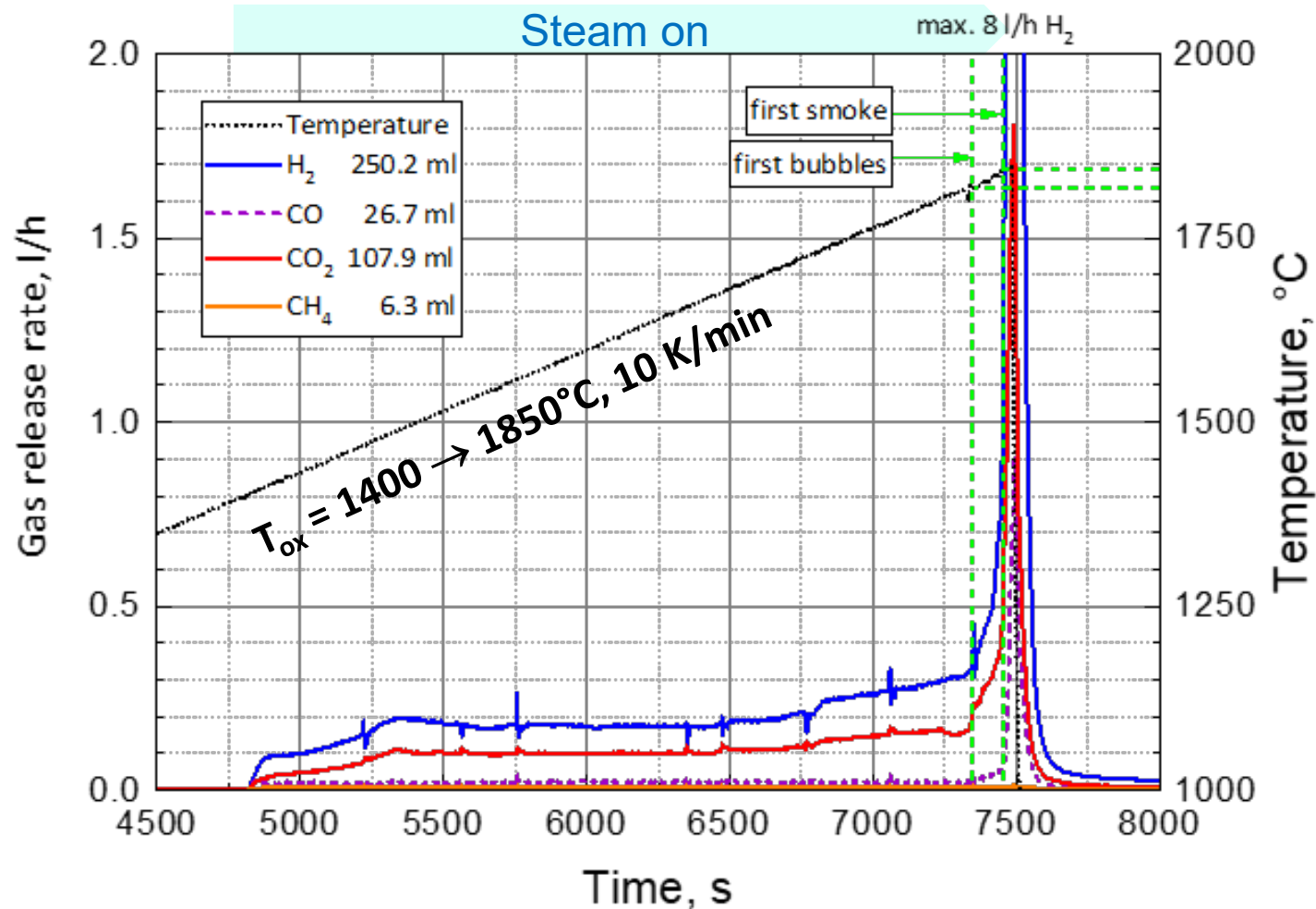
$$\frac{dx}{dt} = \frac{k_p}{2x} - k_l$$

Paralinear kinetics

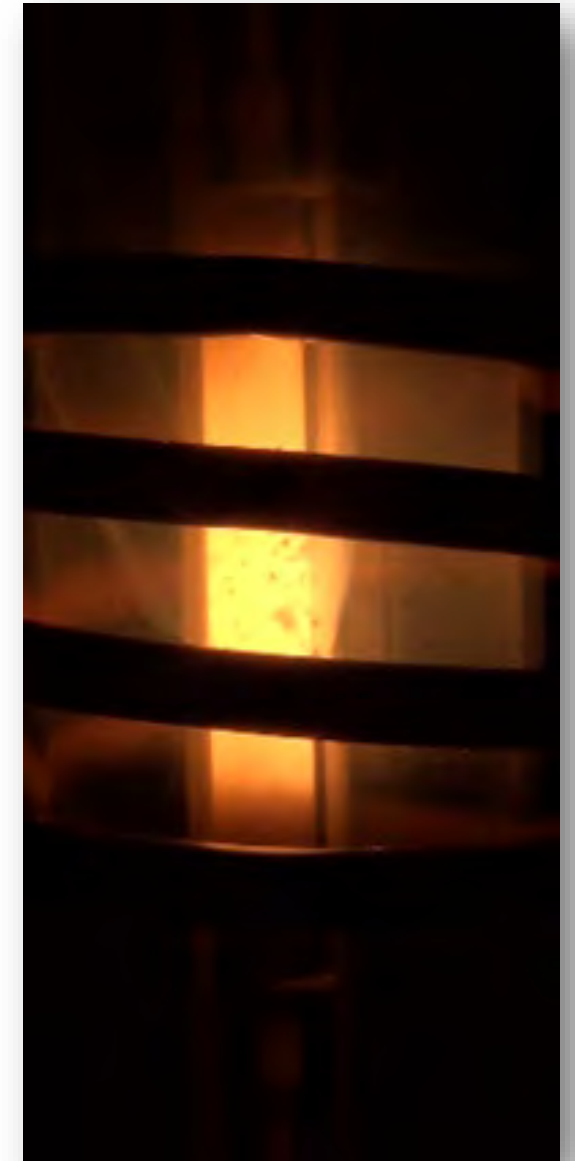
$$T_{\text{melt}}(\text{SiO}_2) \approx 1710^\circ\text{C}$$



# Transient test with SiC: Conduct and MS results

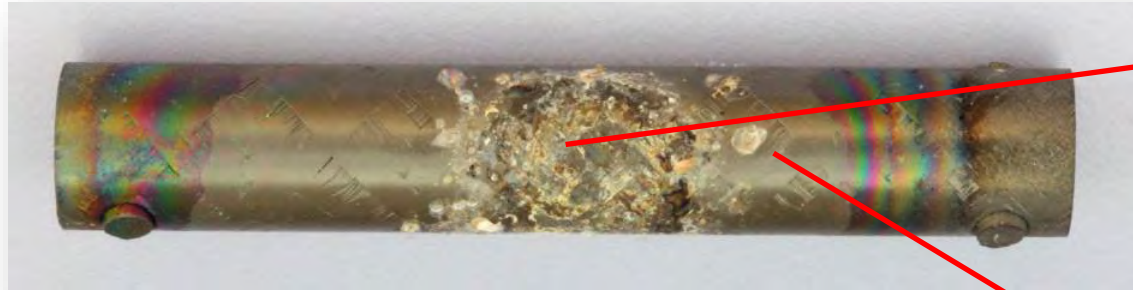


- ➔ Low oxidation kinetics up to ca. 1750°C
- ➔ Bubble formation, strong gas release, SiO<sub>x</sub> volatilization above ~1750°C

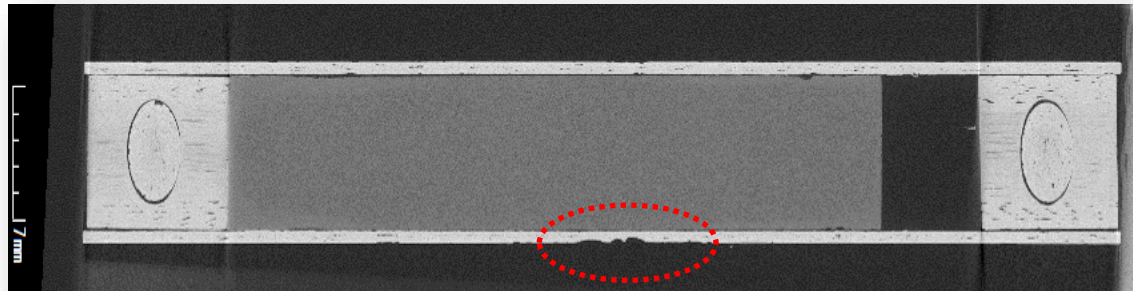


Video snapshot at 1845°C

# Transient tests: Post-test appearance

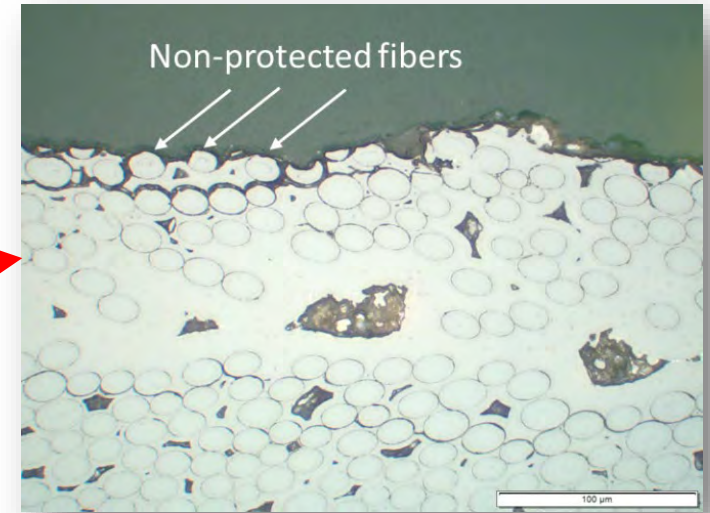


Sample after the transient test up to 1845°C

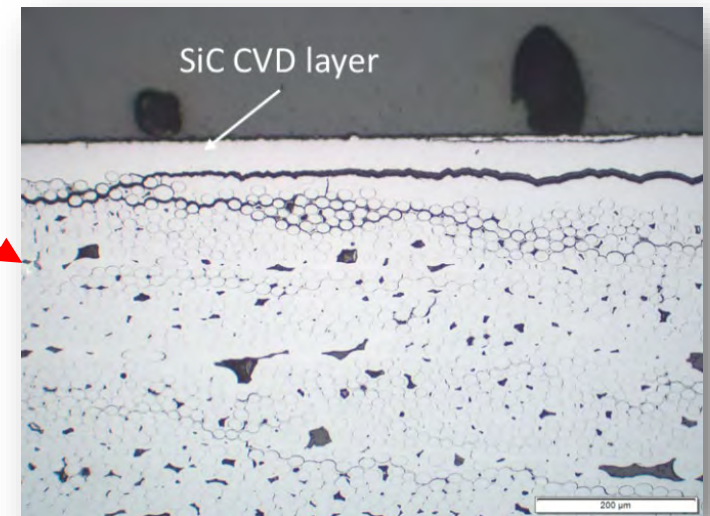


X-ray tomography, longitudinal cut

➔ Local failure of the CVI seal-coat above 1750°C and attack of SiC fibers



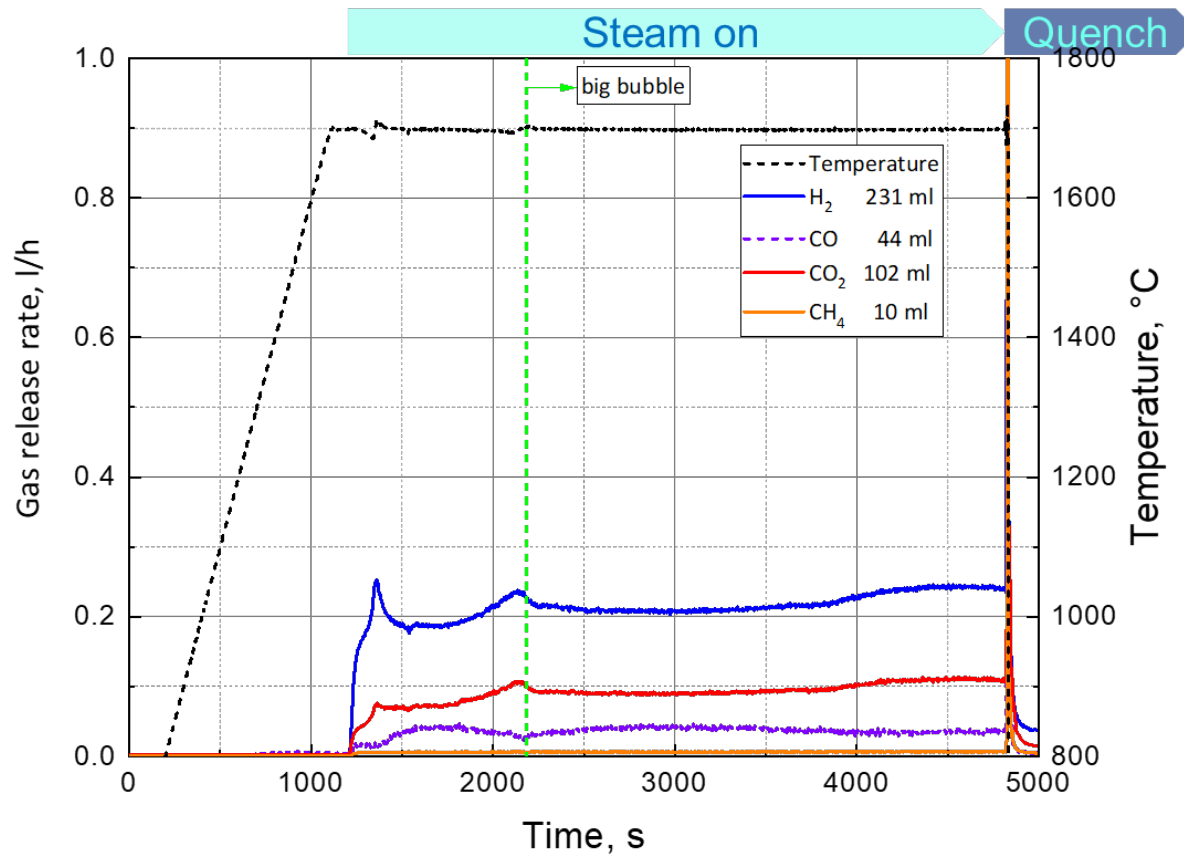
OM from the failure region



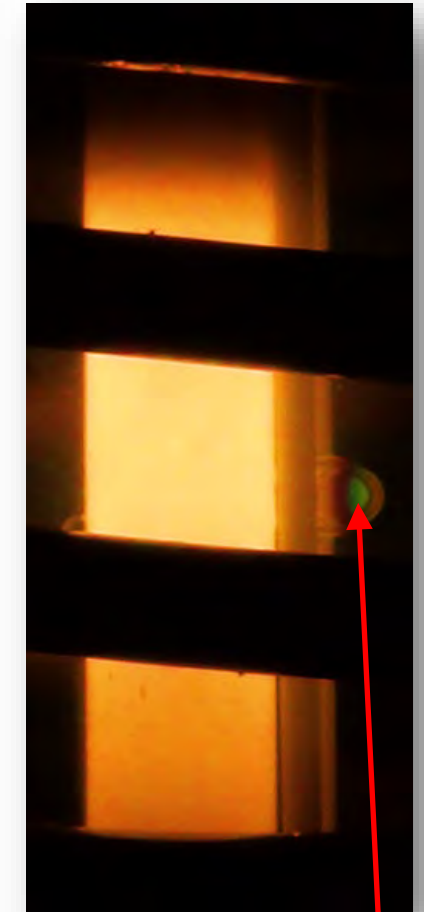
OM from the non-failure region



# Isothermal test 1 hour at 1700°C: Gas release and post-test appearance



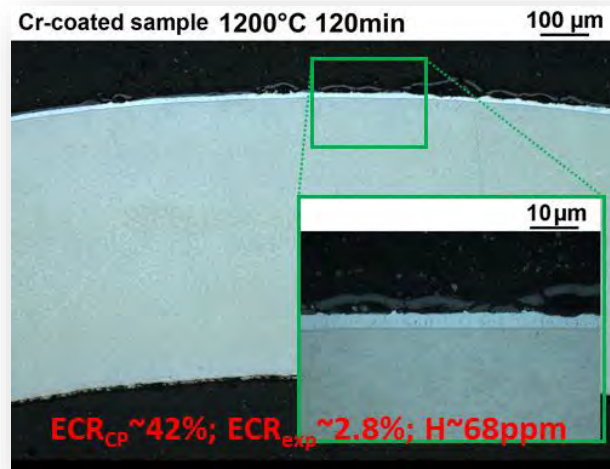
- ➔ Very limited oxidation of the SiC<sub>f</sub>/SiC cladding at 1700°C
- ➔ Recession rate 15-25 μm/h
- ➔ Generally strongly dependent on boundary conditions and impurities



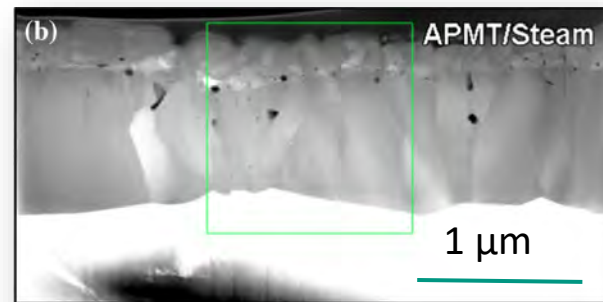
Bubble

# Conclusion I

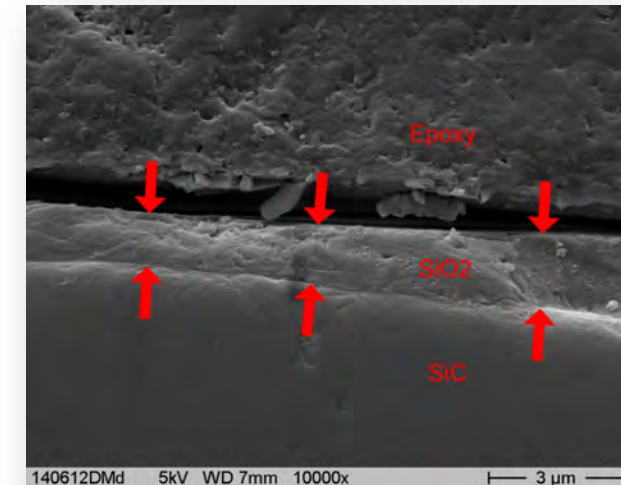
- ATF claddings provide much lower HT oxidation rates compared to Zr alloys and therefore decrease the risk of temperature escalation and hydrogen detonation during severe accidents as well as significantly increase the coping time for AMMs



**Cr-Zry**  
 2 h 1200°C  
 steam  
 4 µm Cr<sub>2</sub>O<sub>3</sub>  
 ZrO<sub>2</sub>: 250 µm



**FeCrAl**  
 4 h 1200°C  
 steam  
 1 µm Al<sub>2</sub>O<sub>3</sub>  
 ZrO<sub>2</sub>: 350 µm



**SiC**  
 1 h 1700°C  
 steam  
 1 µm SiO<sub>2</sub>  
 ZrO<sub>2</sub>: 2400 µm

# Conclusion II

- Degradation mechanisms of the three most promising ATF cladding concepts are different and result in the following max. survival temperatures:
  - **Cr-coated Zr-based cladding: 1200-1300°C**
    - Determined mainly by Cr-Zr eutectic and diffusion processes leading to the loss of protective effect of coating
    - Depending on thickness (and quality) of Cr coating
  - **FeCrAl alloys: 1300-1400°C**
    - Determined mainly by the competition between bulk Al diffusion and the kinetics of  $\alpha$ -alumina formation
    - Depending on composition and heating rate
  - **SiC<sub>f</sub>-SiC composites: >1700°C (with monolithic external layer)**
    - Determined mainly by the volatilization kinetics of silica at HT in steam atmosphere
    - Depending on the thickness of the external monolithic SiC layer and thermo-hydraulic boundary conditions
- However, this presentation provided a simplified view on the complex oxidation and degradation processes at high temperatures



**K. Nakamura**  
**CRIEPI**

## **High-temperature behavior of accident-tolerant control rods clad with Zr alloy during BDBA and SA leading to reaction with molten fuel**

ATF deployment is one of the integrated and innovative solutions to improve the safety, economy, and flexibility of current light water reactors leading to continue nuclear power generation toward the realization of a carbon-neutral society. In the practical use of ATF with extended accident coping times, there is a concern about a potential increase in falling into uncontrollable recriticality conditions where conventional control rods (CRs) such as Ag-In-Cd alloy or B<sub>4</sub>C clad with stainless steel tubes are discharged from the core while the fuel rods still maintain a coolable geometry in the temperature range of 1200 to 1400°C. If non-borated water is injected into the core without CRs, the risk of uncontrollable recriticality will be further increased by introduction of the ATF technology. Thus, CRIEPI has pointed out since 2013 that both CRs and fuel rods should be developed in parallel with each other to enhance accident tolerance. CRIEPI has been contributing to the development of accident-tolerant control rod (ATCR) that can be also expected to improve economic efficiency and reduce the number of spent CRs, considering neutronic and irradiation properties, physico-chemical characteristic, and manufacturability & applicability.

Assuming the application of coated Zr alloy to both fuel and CR cladding tube, high temperature integrity test of a novel neutron absorber Eu<sub>2</sub>O<sub>3</sub>-50mol% HfO<sub>2</sub> clad with uncoated Zr alloy was carried out under the beyond DBA condition in this study. An unpressurized ATCR rod assembled with eight Zr alloy fuel rods was inductively heated to 1700°C at a heating rate of 2-3 K/s in a steam environment and cooled down in Ar gas flow without water quenching. Embrittlement was observed in all Zr alloy cladding tubes, but no reaction layer was formed at the interface between the inner surface of the Zr alloy and the outer surface of the absorber pellet. Almost no dimensional change was also observed in the absorber pellets. The results showed that the ATCR concept clad with Zr alloy cladding tube had good integrity without deformation to at least 1700°C compared with the conventional CRs.

To confirm the miscibility of the novel neutron absorber and the molten fuel under severe accident (SA) conditions, the reaction test between Eu<sub>2</sub>O<sub>3</sub>-50mol% HfO<sub>2</sub> pellet as absorber candidate and UO<sub>2</sub>-50mol% ZrO<sub>2</sub> pellet as molten fuel simulant was carried out in Ar atmosphere in the temperature range of 2200°C to 2600°C. After holding for 60 minutes at 2200°C, where solid-solid interdiffusion is expected, fcc-(Eu,Hf,U,Zr)O<sub>2</sub> solid solution was formed at the interface with a thickness of approximately 30µm. When held at about 2600°C for 3 min, the Eu<sub>2</sub>O<sub>3</sub>-50mol%HfO<sub>2</sub> melt enveloped the entire UO<sub>2</sub>-50mol% ZrO<sub>2</sub> pellet and partially dissolved it to form a homogeneous fcc-(Eu,Hf,U,Zr)O<sub>2</sub> solid solution. Increasing the holding time to 10 min resulted in complete melting of both pellets to form a homogeneous liquid phase. From the above, it was clarified that the Zr-based alloy-clad ATCR concept such as rare earth (RE)-Zr mixed oxide or RE-Hf mixed oxide is highly compatible with oxidic melt containing U and is likely to significantly reduce the risk of recriticality during and after SA.



# High-temperature behavior of **A**ccident-**T**olerant **C**ontrol **R**ods clad with Zr alloy during BDBA and SA leading to reaction with molten fuel

Kinya Nakamura<sup>1</sup>, Hirokazu Ohta<sup>1</sup>, and Masahide Takano<sup>2</sup>

<sup>1</sup> Central Research Institute of Electric Power Industry (CRIEPI)

<sup>2</sup> Japan Atomic Energy Agency (JAEA)

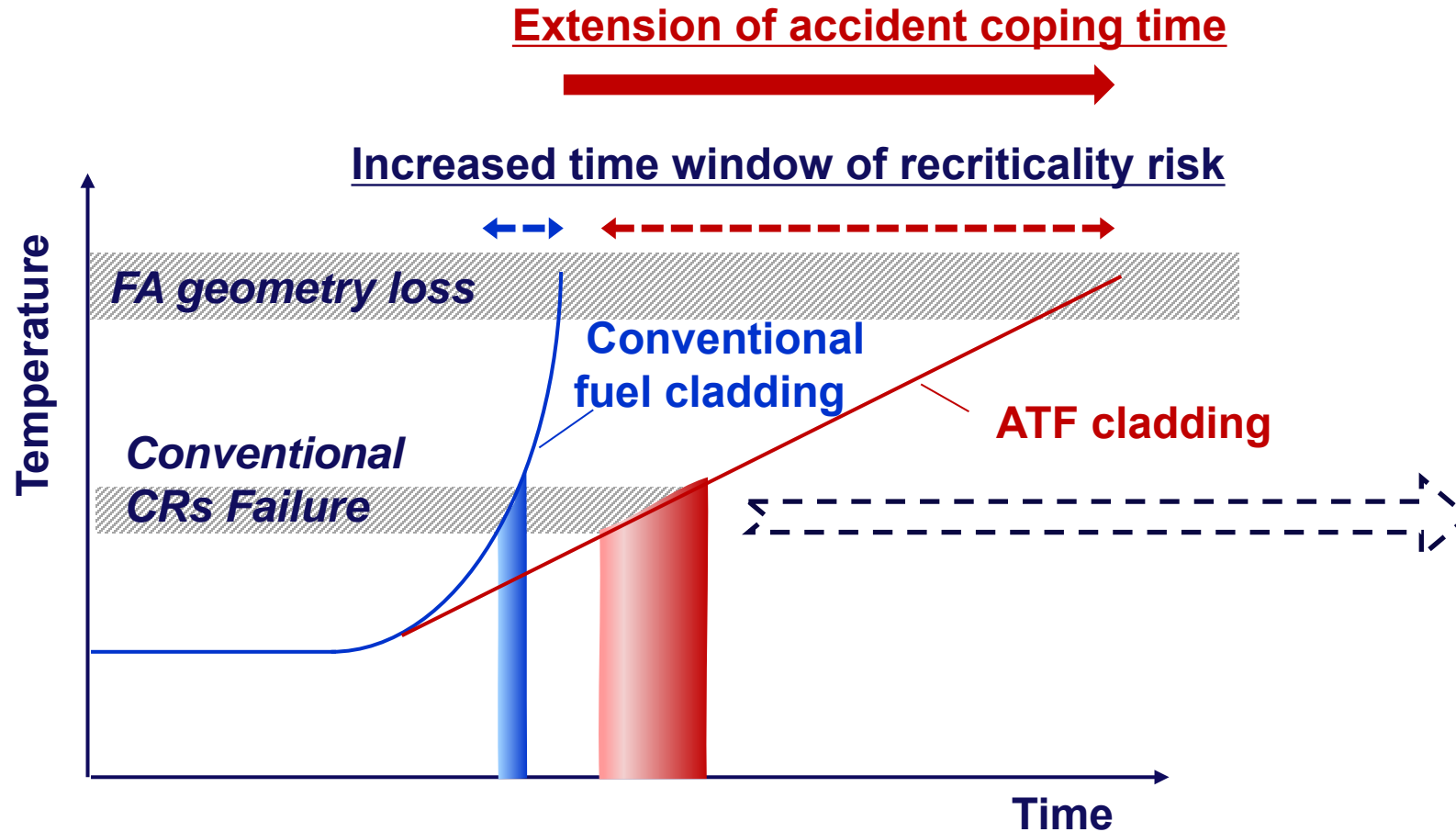
*27th International QUENCH Workshop*

Karlsruhe Institute of Technology, Germany

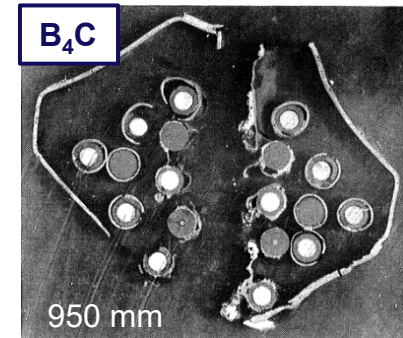
27 - 29 September 2022

# Motivation for ATCR Development

Image of temperature history in case of deployment of ATF with conventional CRs in a hypothetical accident scenario

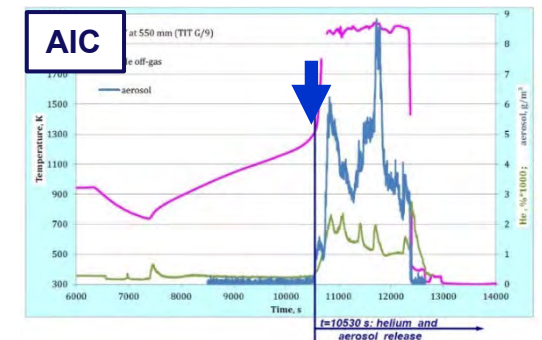


## Failure of conventional CRs



CORA-16

L. Sepold, FZKA 7447.



QUENCH-18

J. Stuckert, et al., QWS-23, Karlsruhe 2017.

# Basic Concept of ATCR

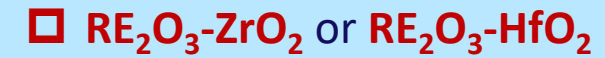
➤ The ATCR concept designed by CRIEPI has the potential to bring a lot of benefits to the safety, economy, and flexibility of the LWR core during NO, AOO, DB, and beyond DB accidents.

## REQUIREMENT

- ❑ Sufficient neutron absorption effect equivalent to or higher than conventional CRs,
- ❑ **Higher failure temperature than conventional CRs,**
- ❑ High melting points comparable to fuel failure temperatures, and
- ❑ **Favorable miscibility with molten and resolidified fuel materials**

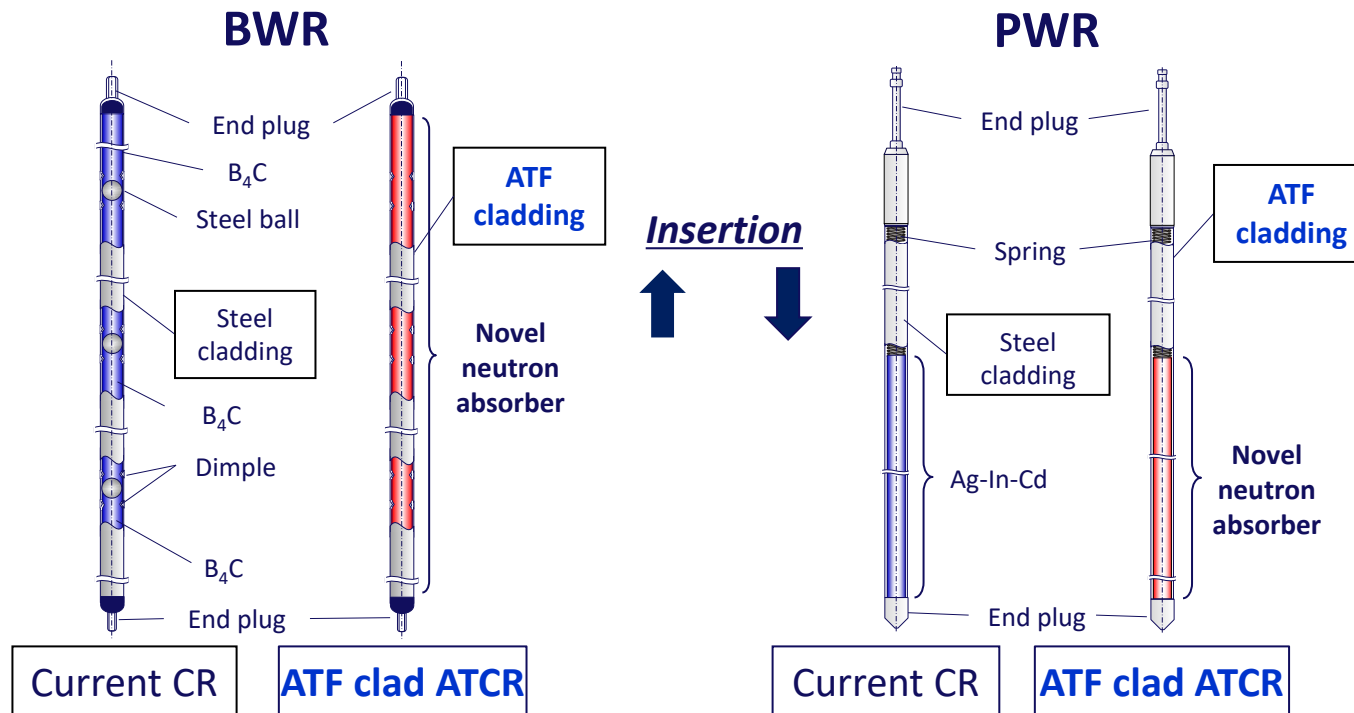
## NOVEL NEUTRON ABSORBERS

Both for BWR & PWR

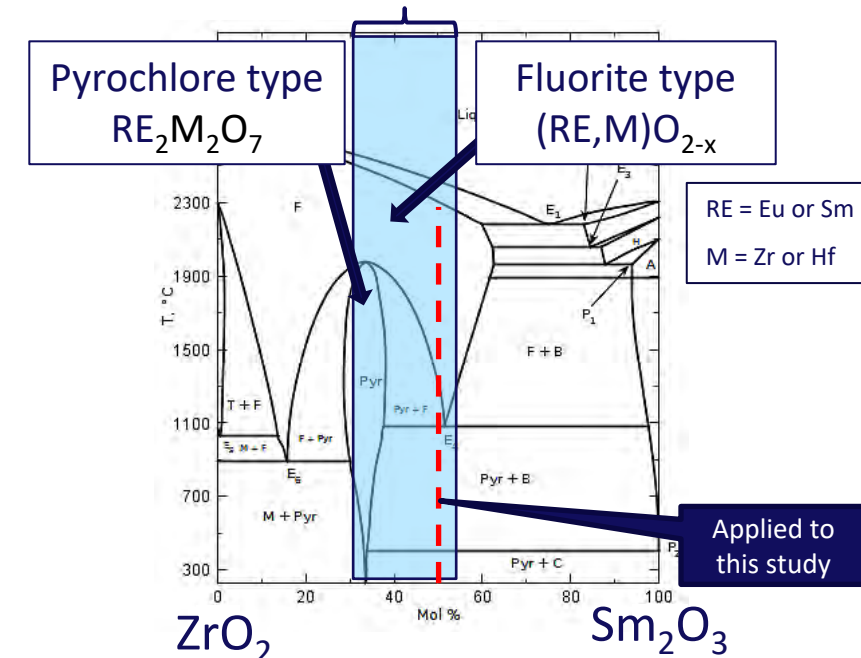


RE = Sm or Eu

- ❑ Composition range 30-50 mol%  $RE_2O_3$



## Composition range



K. Nakamura, H. Ohta, 11th Annual EPRI/DOE/INL Joint Workshop on ATF, EPRI & WebEx, March 28–29, 2022.

O. B. Fabrichnaya and H. J. Seifert, *J. Alloys Compd.*, **475** [1-2] 86-95 (2009).

# Benefits & Issues of ATCR

**Bold : Confirmed**

*Italic : Not confirmed*

## Benefits

### Neutronic & Irradiation Properties

- ❑ **Higher CR worth (higher thermal neutron capture cross section) than conventional CRs**
- ❑ **Extended lifetime as the neutron capture products are also neutron absorbers** (*Reduction of number and storage space of used CRs*)
- ❑ *Improvement of robustness of CRs during NO & AOO due to no additional production of non-condensable gases from neutron absorption*

### Physico-chemical characteristic

- ❑ **Favorable compatibility with primary coolant** (*Potential continuous use even for a leak CR*)
- ❑ **Favorable compatibility with core structural materials such as SS & Zry and ATF candidate cladding such as coated Zry, FeCrAl(-ODS) and SiC/SiC composite up to 2000°C with limited corrosion**
- ❑ *Potential favorable coexistence with fuel & corium (reduction of re-criticality risk during SA)*

### Manufacturability & Applicability

- ❑ **Utilization of conventional production technique such as high density neutron absorber pellets**
- ❑ *Utilization of conventional CR assembly design without significant impact on the reactor design and operation*

### Practical utilization

- ❑ *Improvement of core safety from NO to accident conditions by simultaneous deployment of ATF & ATCR*

## Issues to be developed

- ❑ Confirmation of period availability for the absorbers under practical neutron irradiation condition
- ❑ Reactivity worth analysis at normal & SA conditions
- ❑ Shape stability under neutron irradiation

- ❑ Accumulation of physical, chemical and mechanical property dataset
- ❑ **Performance improvement during BDBA**
- ❑ **Coexistence with molten and resolidified fuel materials even after core damage**

- ❑ Quality-controlled manufacturing processes
- ❑ Increased radioactivity of used CRs
- ❑ Insertability of CRs and flow vibration characteristics due to coolant flow
- ❑ Resource risk of rare earth raw materials

- ❑ Reactivity measurement under NO conditions
- ❑ Domestic standards and criteria of LUA for irradiation tests
- ❑ Demonstration by LUA





## Updates on ATCR development

- 1. HT compatibility of the upright ATCR geometry**
2. HT coexistence of novel neutron absorber with molten fuel

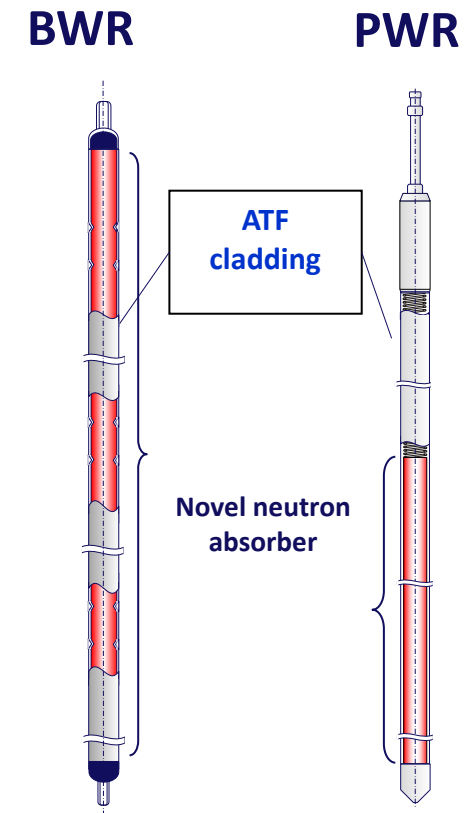
# Background

- Under hypothetical BDBA conditions at 2000°C or less, the novel neutron absorber has been confirmed to have good compatibility with the candidate ATF cladding materials such as coated Zr alloy, FeCrAl alloy, and SiC without significant damage.

*K. Nakamura, AESJ annual meeting, Mar. 17-19, 2021.  
K. Nakamura, AESJ annual meeting, Mar. 16-18, 2022.*

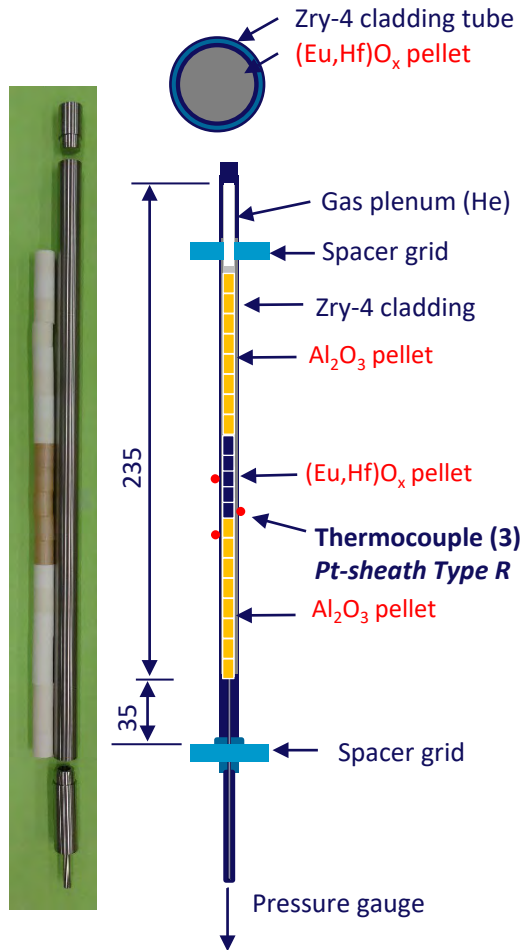
# Purpose

- To confirm HT compatibility of the upright ATCR geometry under BDBA conditions, *assuming that coated Zr alloy cladding tube is applied to both the fuel and control rods.*

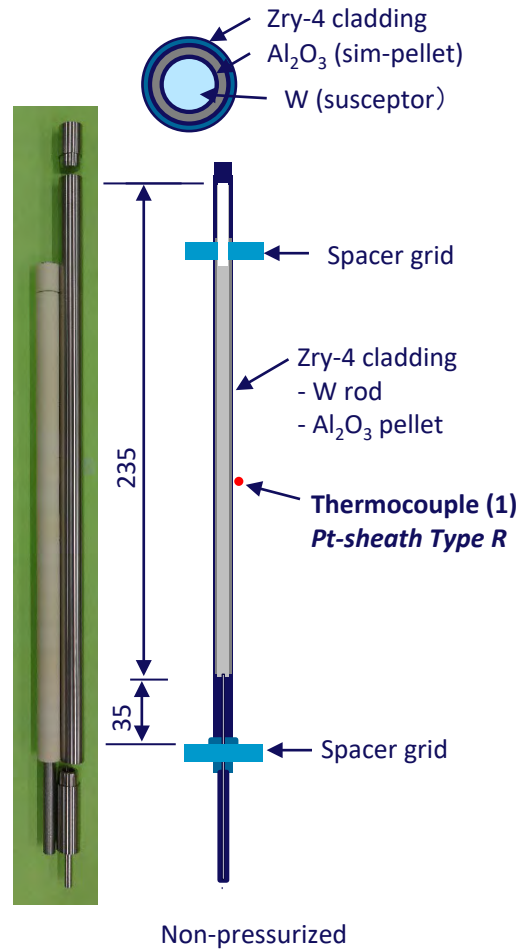


# Test Rod

## ATCR (Center rod)

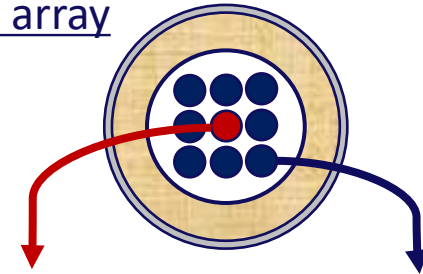


## Fuel rod (Outer heater rod)



## Specification of test rod components

Bundle array

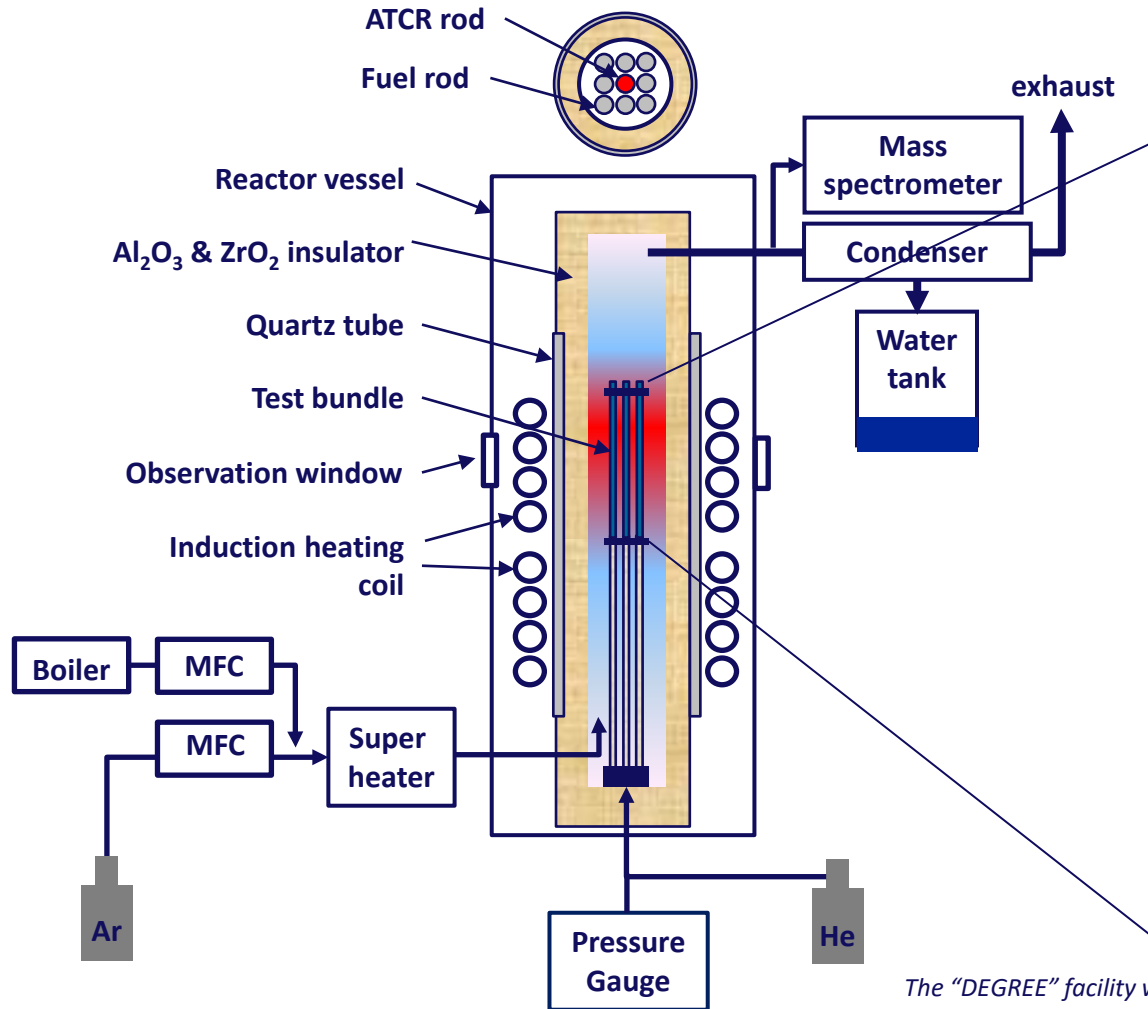


Item		ATCR	Fuel rod
Cladding tube	Material	Uncoated Zircaloy-4	Uncoated Zircaloy-4
	Dimension	OD9.5 × 0.57t × L235 mm	OD9.5 × 0.57t × L235 mm
Pellet	Material	(1) $Eu_2O_3$ -50mol%HfO <sub>2</sub> (2) $Al_2O_3$	$Al_2O_3$
	Dimension	(1)(2) $\Phi 8.2 \times h9.5mm$	$\Phi 8.2 \times \Phi 5.7 \times h50mm$
Rod	Pellet stack	(1) 47.5mm, (2)152mm	200mm
	Plenum volume	9 cm <sup>3</sup>	10 cm <sup>3</sup>
	Rod internal pressure	<b>0.003 MPa (He) at RT</b>	<b>0.003 MPa (He)</b>
	Number of rods	1	8
Heater	Materials	-	Tungsten
	Dimension	-	$\Phi 5.5 \times 200mm$



# Set-up of the HT compatibility test

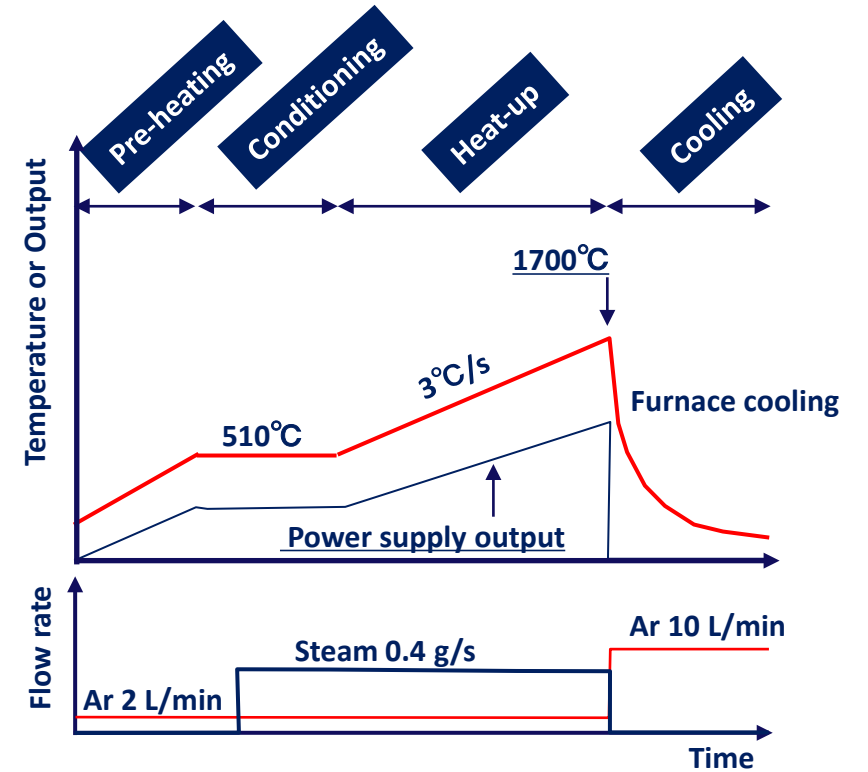
## Test set-up



## Bundle

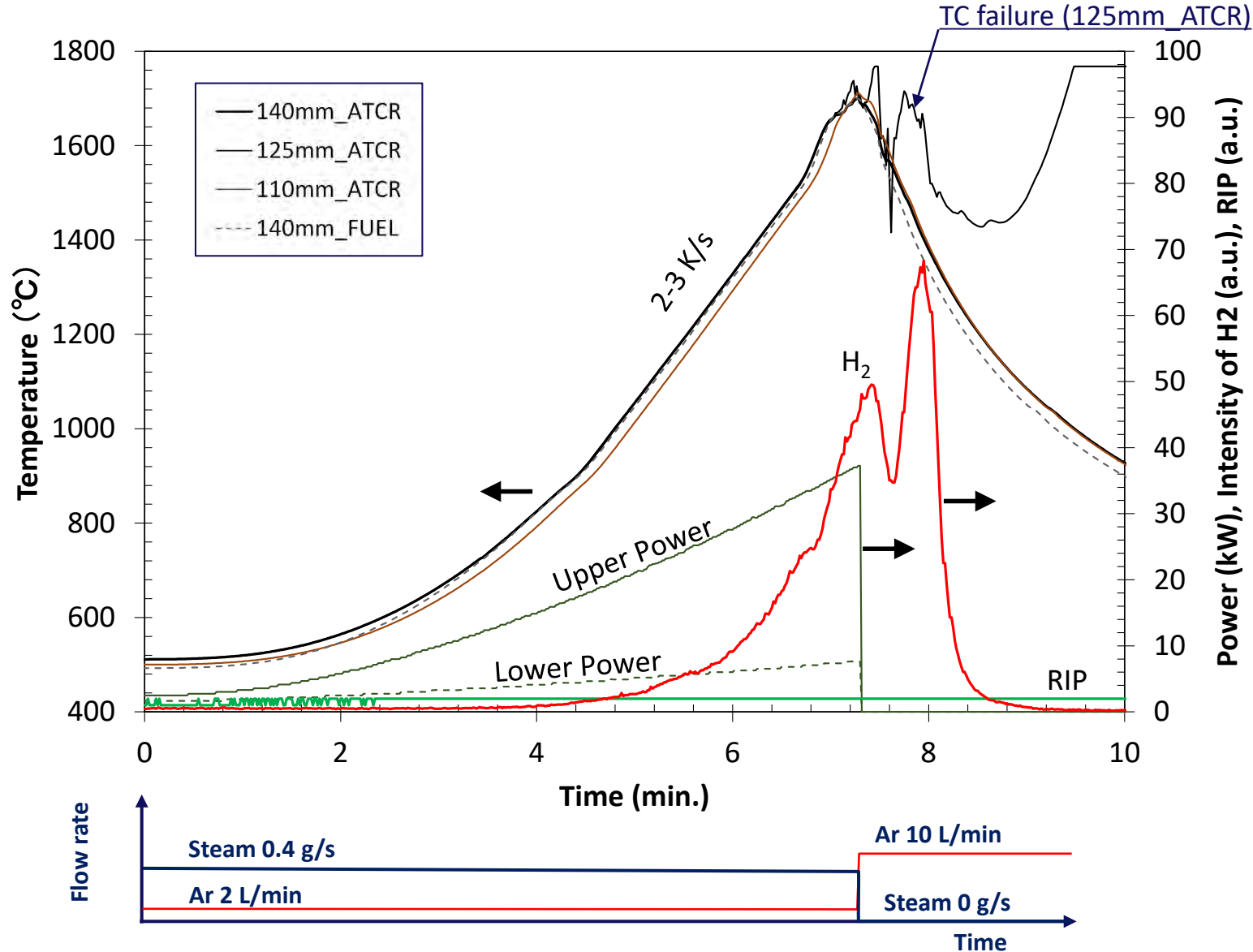


## Time History



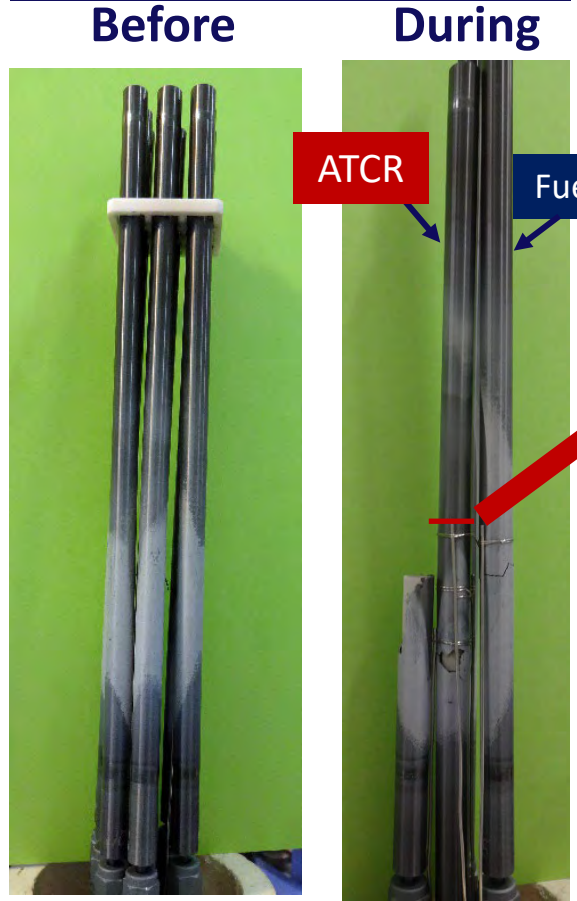
The "DEGREE" facility was built in 2015 within the framework of "Advanced Multi-scale Modeling and Experimental Test of Fuel Degradation in Severe Accident Conditions" supported by Ministry of Economy, Trade and Industry, Japan.

# Temperature Profile

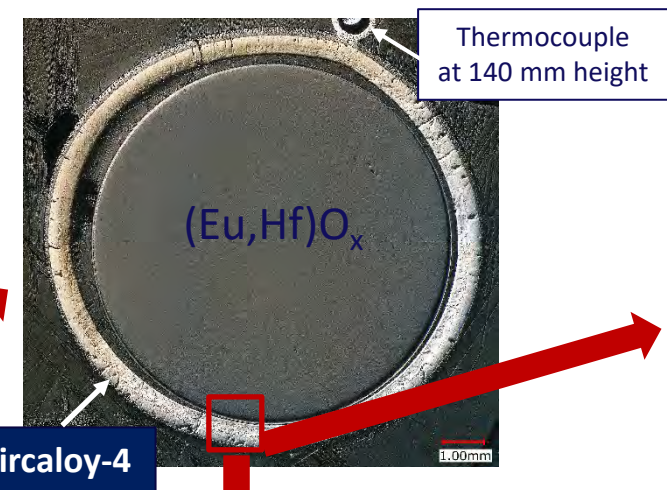


# Cross-section of boundary between Zr alloy and absorber

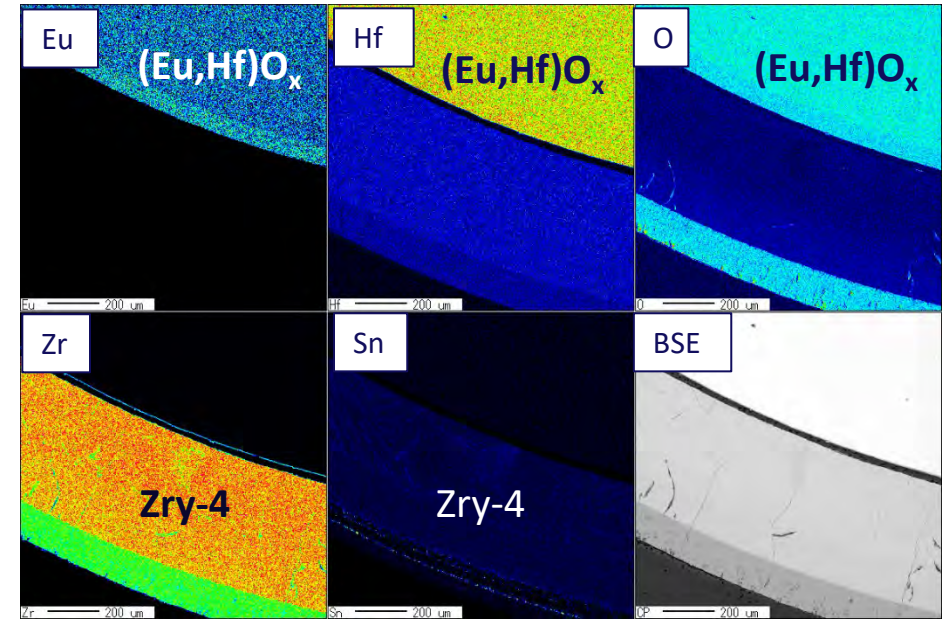
## Dismantling



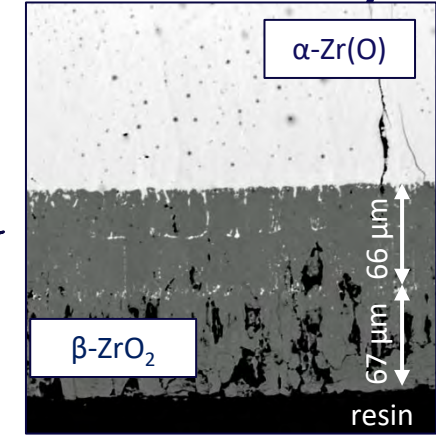
## Optical microscope image at the hottest region



## At the Zry-4 - absorber interface



## Outside Zircaloy-4



$\beta\text{-ZrO}_2 + \alpha\text{-Zr(O)}$  eutectoid structure transformed from  $\gamma\text{-ZrO}_{2-x}$  indicating  $T > 1520^\circ\text{C}$

- Embrittlement in all Zry-4 cladding tubes
- No solid-solid interdiffusion layer formation at the Zry-4 - absorber interface
- Almost no dimensional change in the absorber pellets

The concept of ATCR clad with Zr alloy had good geometry integrity with negligible deformation to at least  $1700^\circ\text{C}$ .

## Updates on ATCR development

1. HT compatibility of the upright ATCR geometry
- 2. HT coexistence of novel neutron absorber with molten fuel**

*This research was conducted at the Nuclear Science Research Institute of JAEA Tokai as a joint research between the CRIEPI and the JAEA.*



# Purpose

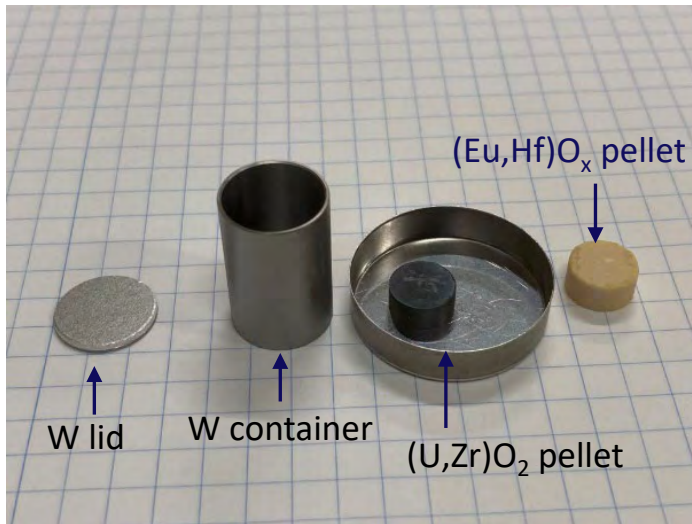
---

To confirm coexistence of novel neutron absorbers and molten/resolidified fuel materials even after core damage

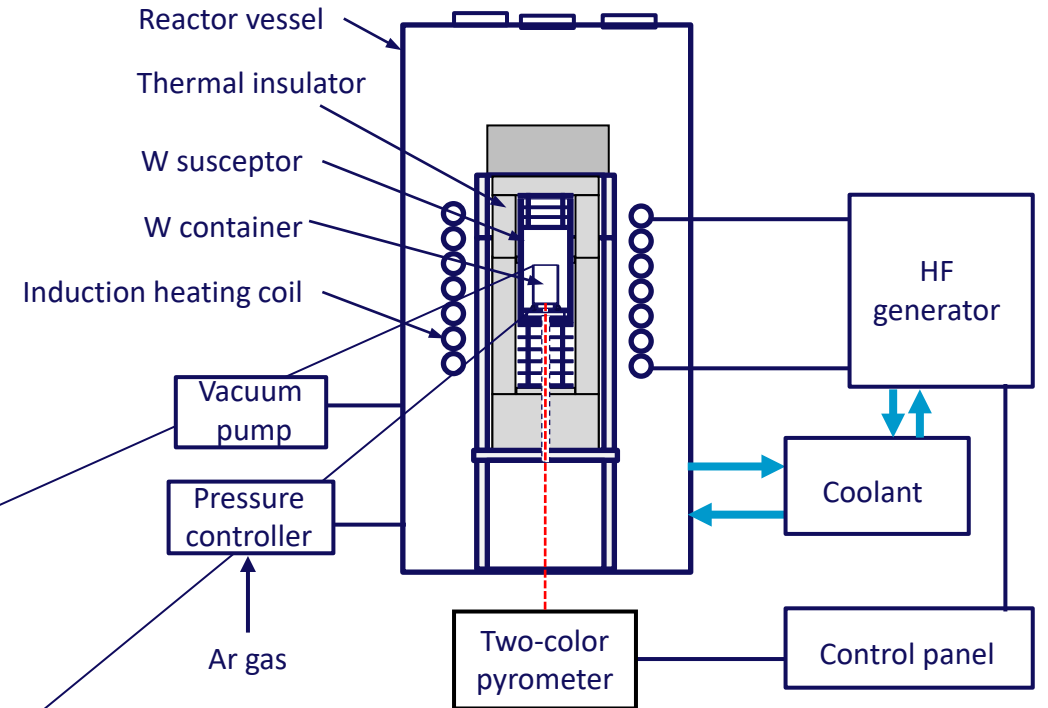
# Experimental

## Sample

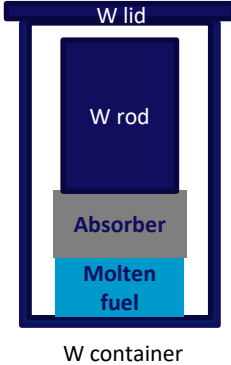
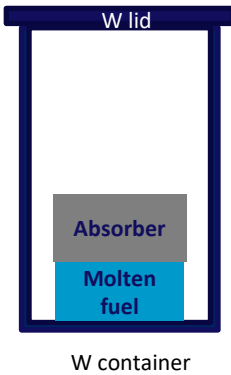



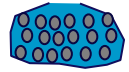
Item	Molten fuel simulant	Absorber candidate
Composition	$\text{UO}_2\text{-50mol\%ZrO}_2$ hereinafter $(\text{U,Zr})\text{O}_2$	$\text{Eu}_2\text{O}_3\text{-50mol\%HfO}_2$ hereinafter $(\text{Eu,Hf})\text{O}_x$
Crystal structure	fcc $(\text{U}_{0.70}\text{Zr}_{0.30})\text{O}_2$ + tetragonal $(\text{U}_{0.23}\text{Zr}_{0.77})\text{O}_2$	fcc
Pellet	Diameter	8.54 mm
	Height	3.82 mm
	Density	8.49 g/cm <sup>3</sup>
Liquidus temp	~ 2500°C	~ 2300°C



## Experimental set-up



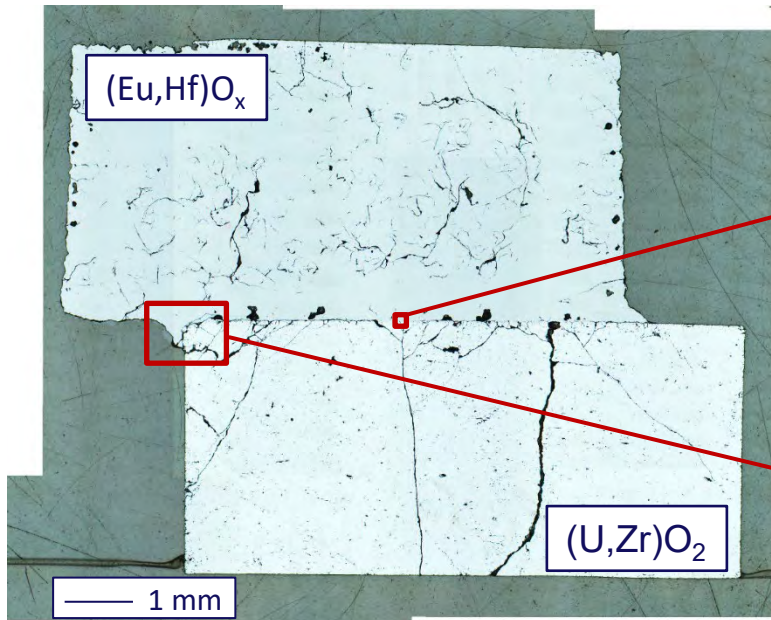
# HT compatibility test condition

Item	Test #1	Test #2	Test #3
Holding temperature (°C)	<b>2200</b>	<b>2400</b>	<b>2600</b>
Holding time (min.)	<b>60</b>	<b>10</b>	<b>3</b>
Atmosphere	Argon	Argon	Argon
Layout			
Expected reaction type	Solid-Solid interdiffusion 	Solid-Liquid reaction 	Liquid-Liquid reaction 

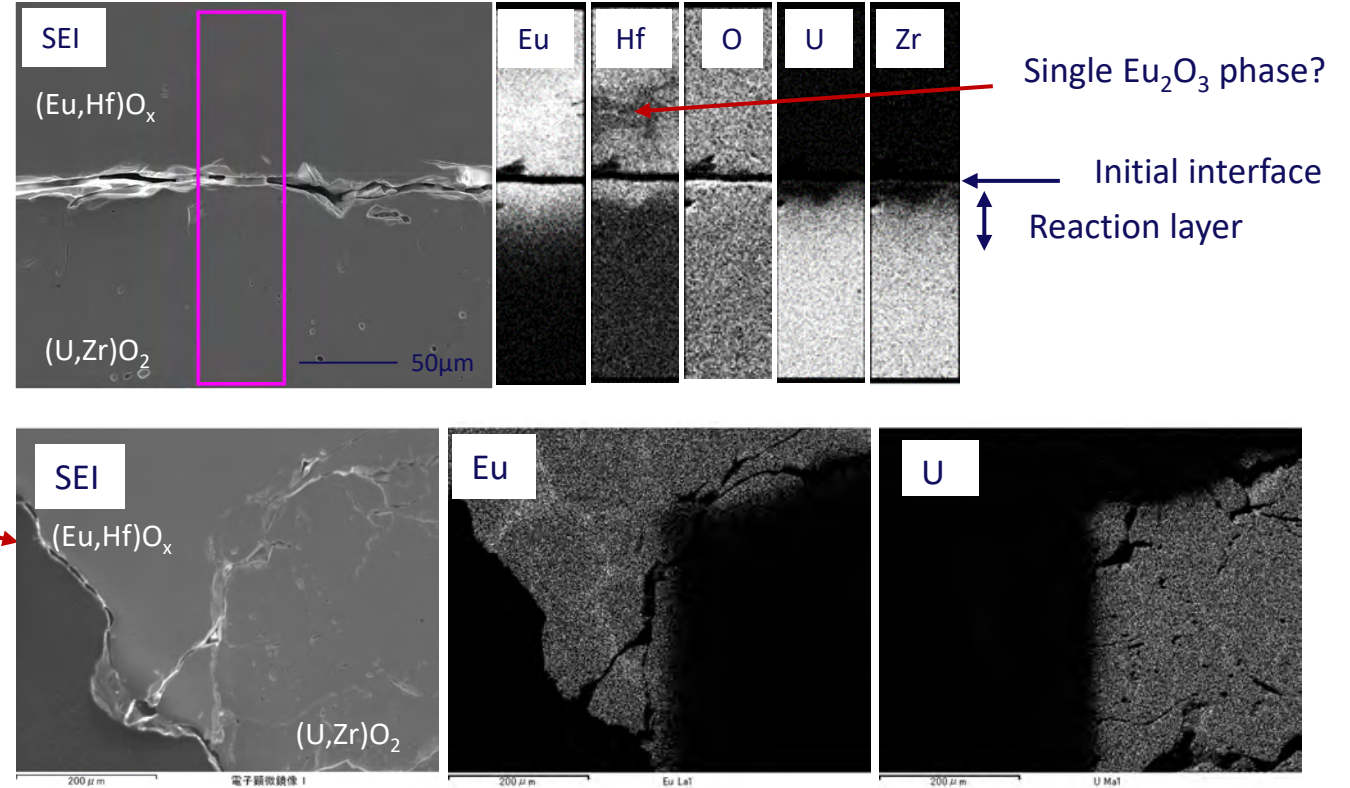
- A very low weight loss of less than 0.04 wt% was observed through the tests.
- The results suggest that evaporation losses below 2600°C are negligible for this oxide system.

# Cross section **Test #1** at 2200°C for 60 min

## Whole sample region (OM)



## Reaction layer at the interface

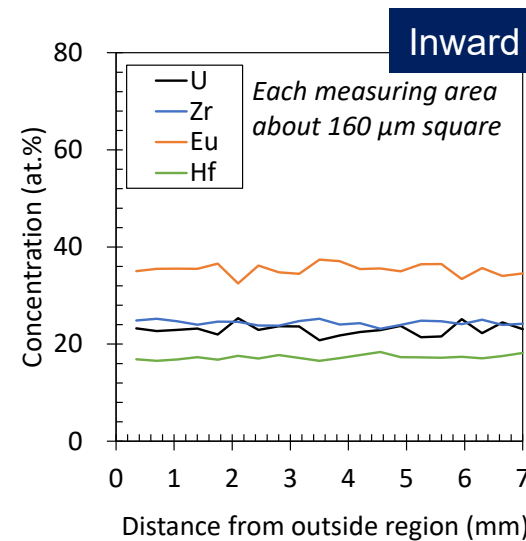
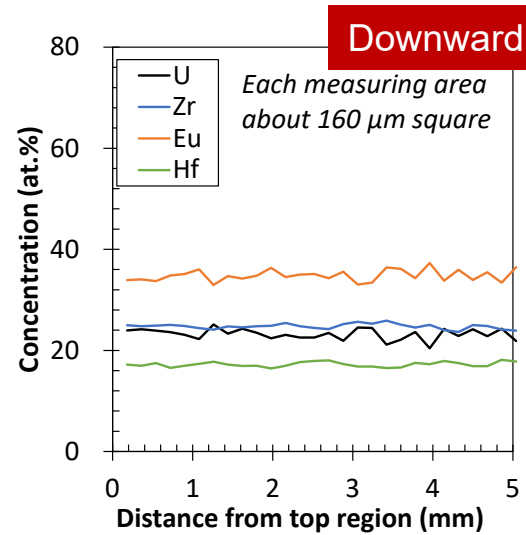


- **Limited reaction layer formation at the interface** (about 30μm thickness)
- Preferential diffusion of Eu and Hf to the (U,Zr)O<sub>2</sub> side to form a reaction layer, not vice versa  
(Composition : U/Zr/Eu/Hf = 21-31/25-37/30-44/3-10 at.%)
- Cracking throughout the pellet due to rapid cooling
- Formation of Eu-rich region on the absorber side of the initial interface, suggesting the formation of a single Eu<sub>2</sub>O<sub>3</sub>

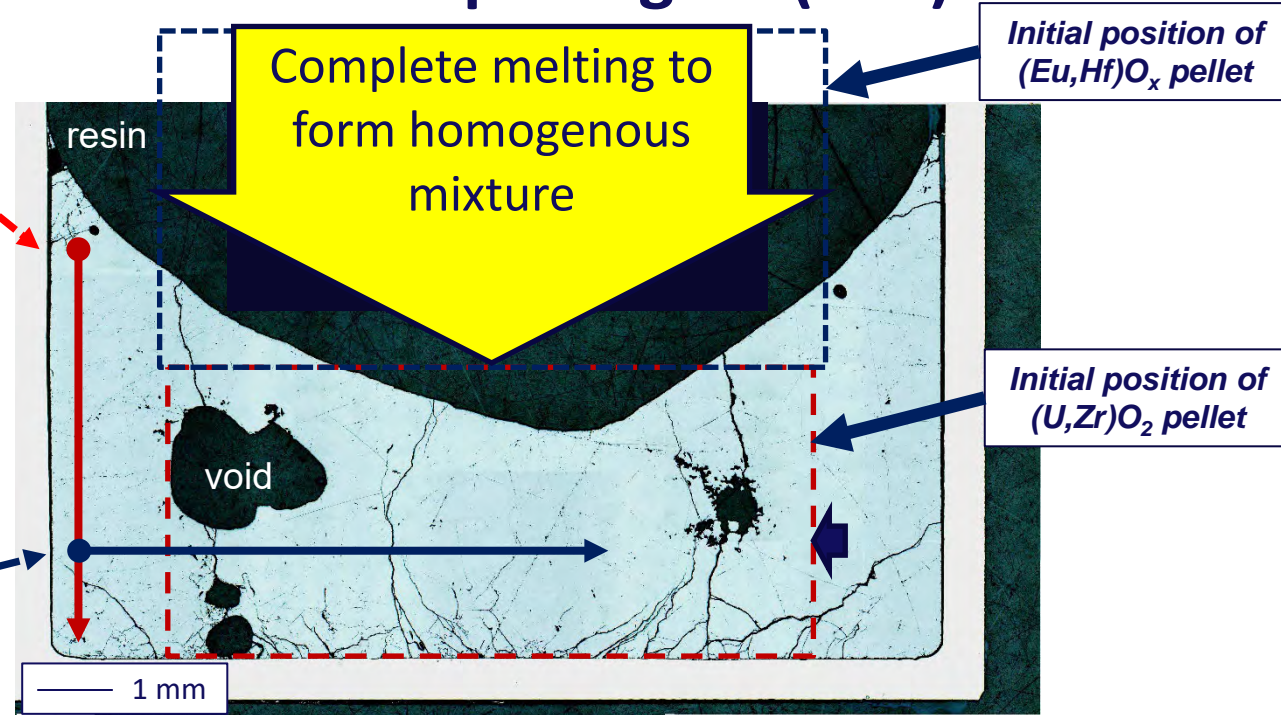


# Cross section Test #2 at 2400°C for 10 min

## Concentration profile



## Whole sample region (OM)

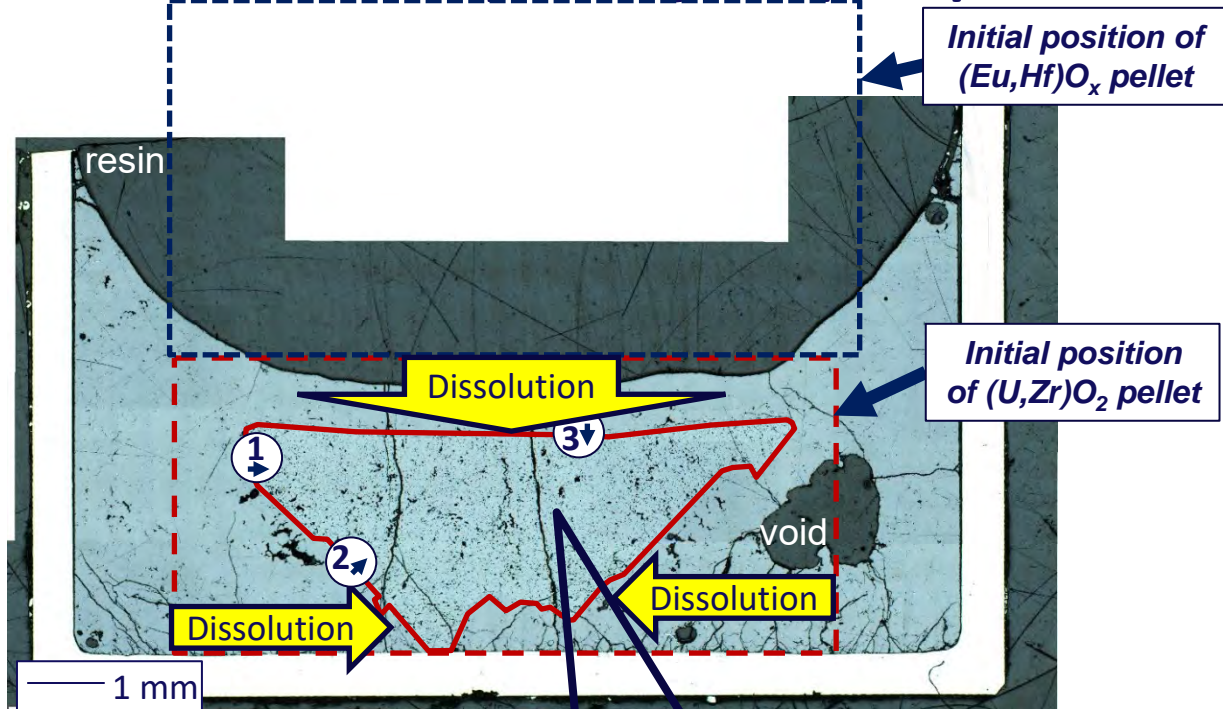


- Formation of uniform oxidic melt and solidified  $\text{fcc-}(\text{Eu,Hf,U,Zr})\text{O}_2$  single phase in whole region
- Suggesting that **the concept of ATCR clad with Zr-based alloy** is
  - **Good miscibility with molten and resolidified fuel materials** and
  - Likely to significantly reduce the risk of recriticality during and after core damage.

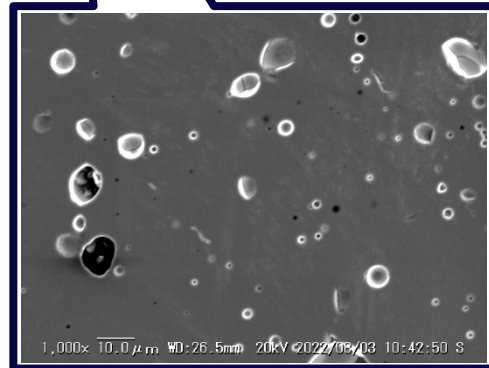
*Based on the high-frequency power output history, there is a possibility that it was heated to about 2600 ° C.*

# Cross section Test #3 at 2600°C for 3 min

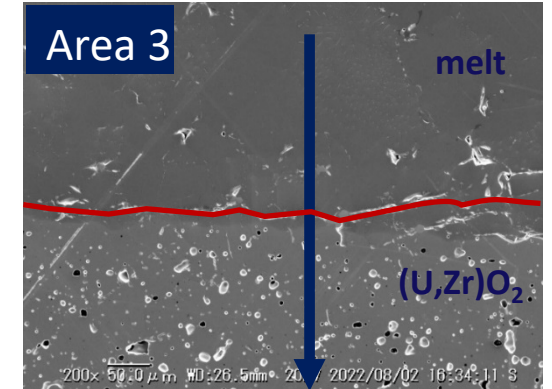
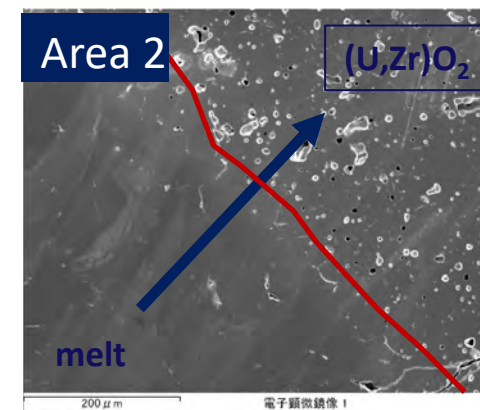
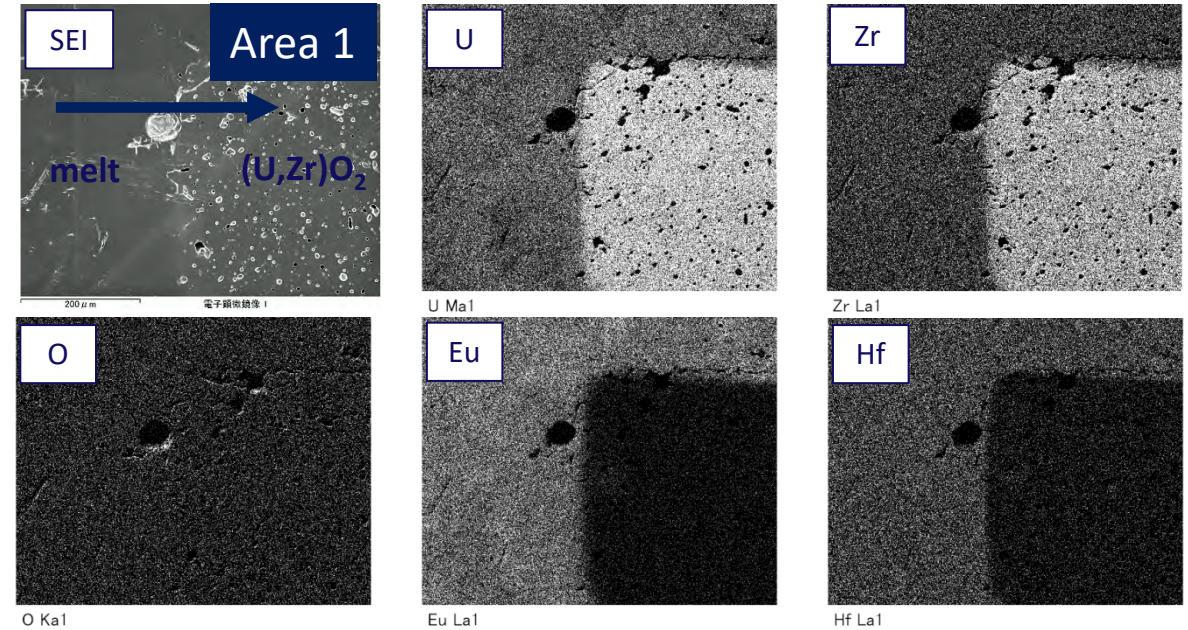
## Whole sample region (OM)



Unreacted solid  $(U,Zr)O_2$



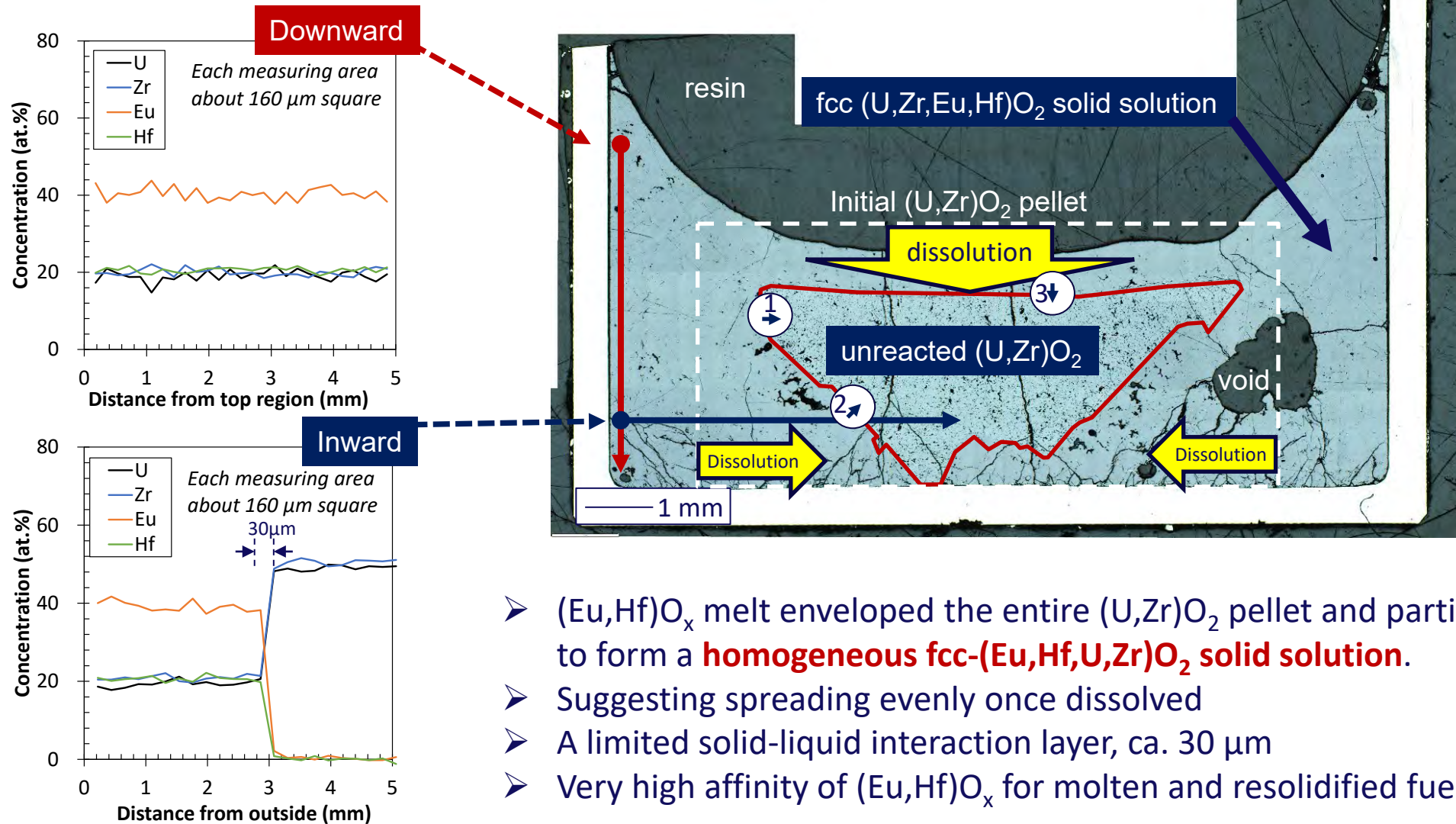
## Reaction layer at the interface





# Cross section Test #3 at 2600°C for 3 min

## Concentration profile



- (Eu,Hf) $\text{O}_x$  melt enveloped the entire (U,Zr) $\text{O}_2$  pellet and partially dissolved it to form a **homogeneous fcc-(Eu,Hf,U,Zr) $\text{O}_2$  solid solution**.
- Suggesting spreading evenly once dissolved
- A limited solid-liquid interaction layer, ca. 30  $\mu\text{m}$
- Very high affinity of (Eu,Hf) $\text{O}_x$  for molten and resolidified fuel materials

# Conclusion

The following tests were performed:

- (1) HT compatibility test of the upright ATCR geometry
- (2) HT coexistence test of neutron absorber with molten fuel

As a result, it was clarified that the concept of ATCR clad with Zr-based alloy

- had good geometry integrity with negligible deformation to at least 1700°C,
- is favorable miscibility with molten and resolidified fuel materials;
- is likely to significantly reduce the risk of recriticality during and after core damage;
- is assumed to bring the same performance to candidate combination of  $\text{Eu}_2\text{O}_3\text{-ZrO}_2$ ,  $\text{Sm}_2\text{O}_3\text{-ZrO}_2$ , and  $\text{Sm}_2\text{O}_3\text{-HfO}_2$  systems with similar chemical properties.





**Y. Lee**

**Seoul National University**

## **Safety envelop study of Cr-coated Zircaloy ATF via SNU's integral LOCA experiment**

In the first part of the presentation, an integral LOCA facility that allows to test fuel dispersal phenomena is discussed with preliminary results. Loaded with fragmented surrogate pellets with various sizes (i.e., 0.5mm in diameter, and mixed particles), the cladding material, heated by inductive heating method, undergoes ballooning, burst, and pellet dispersal. These moments were recorded using a high speed video camera. The result demonstrates that a significant fraction of fragmented surrogate pellets were dispersed, indicating the need for further analyses with caution that fuel fragmentation, relocation, dispersal (FFRD) may pose a serious problem for discharge burnup increase.

The second part of the presentation addresses key embrittlement mechanisms of Cr-coated Zircaloy. Inner side oxidation caused by steam ingress through the burst hole embrittles the coated cladding, and its embrittlement limit was found to 14% Equivalent Cladding Reacted (ECR). The lower ECR limit for Cr-coated cladding versus the conventional uncoated cladding (18%) is due to the nature of Ring Compression Test (RCT) that induces peak tensile stress at the inner surface at which the crack starts to propagate from brittle phase ( $ZrO_2$  and  $\alpha(O)$ -Zr). For the same level of ECR, the Cr-coated cladding has a thicker brittle phase at the inner surface, thereby becoming more prone to failure under RCT. This result illuminates that the nature of RCT biasedly lowers the ECR limit for Cr-coated cladding. Results of published journal by the presenter are used (Journal of Nuclear Materials 558 (2022) 153354). The matrix hardening with presence of  $ZrCr_2$  phase resulted by Cr diffusion into Zr matrix was observed, and is another embrittlement mechanism. Eutectic reaction was shown to occur at  $\sim 1310^\circ\text{C}$  regardless of the coating thickness. It was found significantly deteriorate structural integrity of the cladding, indicating that it may serve as the ultimate peak cladding temperature limit.

# **Safety envelope study of Cr-coated Zircaloy ATF via SNU's integral LOCA experiment**

**Department of Nuclear Engineering  
Seoul National University, Korea**

27<sup>th</sup> International QUENCH Workshop  
Karlsruhe Institute of Technology, Germany

**Youho Lee, Hyunwoo Yook, Dongju Kim, Sunghoon Jeong**

[leeyouho@snu.ac.kr](mailto:leeyouho@snu.ac.kr)



# Contents

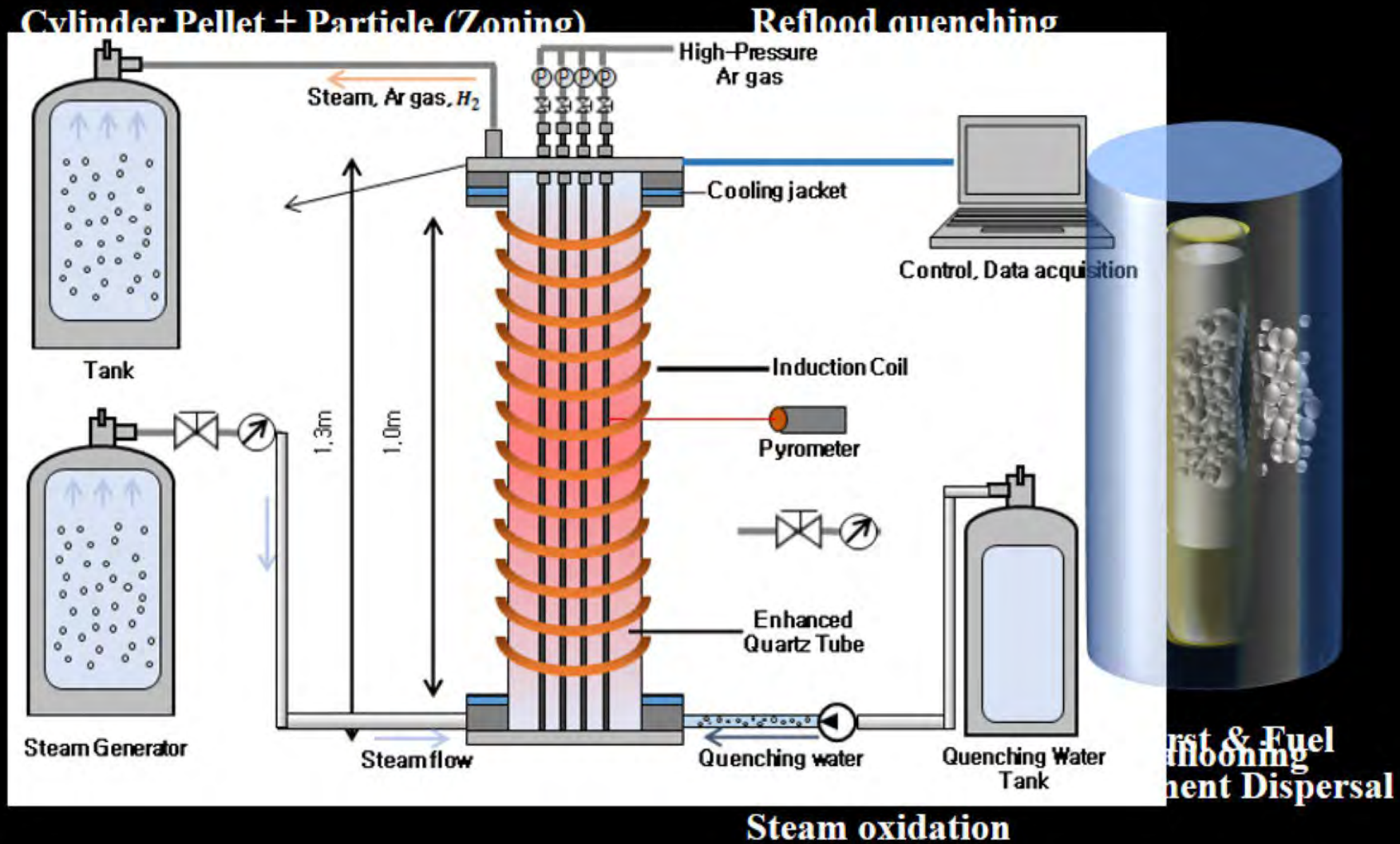
- 1. Integral LOCA experiments**
- 2. Cr-coated cladding embrittlement study**
- 3. Conclusions**



# 1. Integral LOCA experiment



# Schematic of SNU's integral LOCA experiment

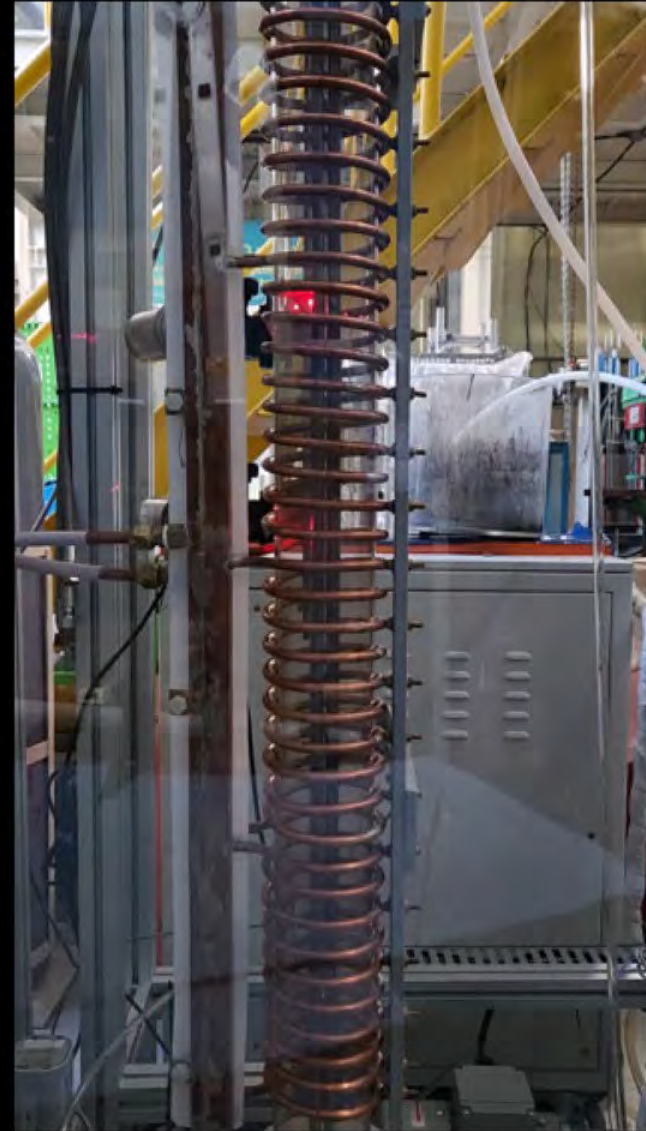


# Integral experiment

---



<Single Rod LOCA experiment>

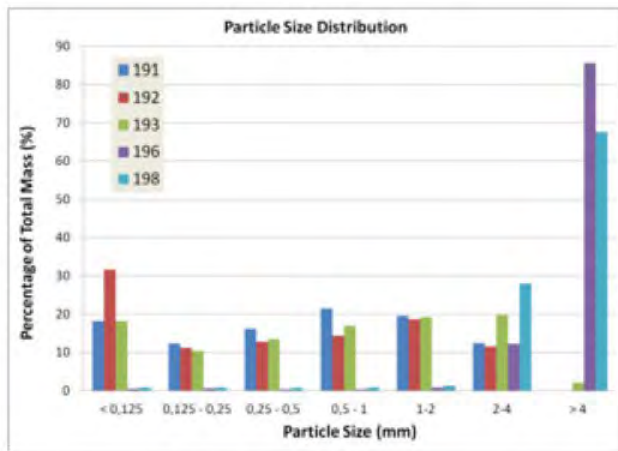


<Multiple Rods (4 rods) LOCA experiment>



# Fuel Dispersal Experiment

- **Surrogate  $ZrO_2$  particle/particle mixture for fragmented pellets**



<Studsvik LOCA Program  
(Burnup ~72 GWd/MTU)>

- **Surrogate  $ZrO_2$  powder type pellet were used to simulate disposal of high burnup fuel (~72 GWd/MTU)**

①



<Single  $ZrO_2$  particle (d=0.5mm)>

②



<Mixed  $ZrO_2$  powder

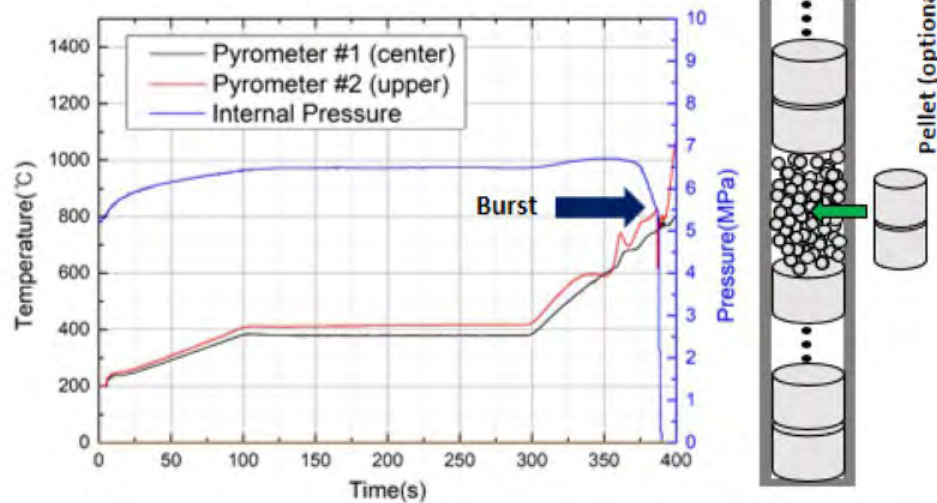
(d=0.3,1,2,3,5 mm, with the same mass fraction)>



<Particle loaded into cladding>

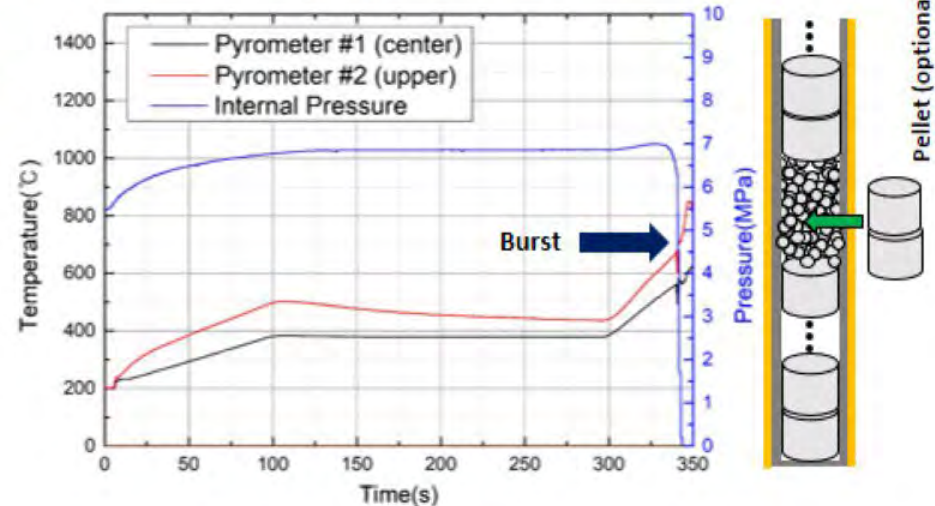
# Fuel dispersal experiment

## ① Zr-Nb-Sn cladding



<ZIRLO with powder pellet burst test>

## ② Cr-coated (18 $\mu$ m) Zr-Nb cladding



<Cr coated cladding (Zr-Cr-1.1Nb) with powder pellet burst test>

- **Surrogate pellet:** 0.5mm  $ZrO_2$  particles loaded in the burst region / Pellet
- **Initial Pressure at room T:** 50 bar
- **Cold void volume:**  $\sim 30\text{cm}^3$  (in consistent with typical PWR fuel)
- **Steam oxidation**
- **Burst occurrence temperature:** 700~800°C



# Fuel dispersal recorded

---

110087+: +0.000 ms



<Zr-Nb-Sn cladding with 0.5mm diameter

ZrO<sub>2</sub> particles>

18691+: +0.000 ms



<Cr-coated Zr-Nb cladding with 0.5mm diameter

ZrO<sub>2</sub> particles>

# Burst hole sizes

## “Pellet inserted in the burst region”



< Zr-Nb-Sn cladding with  
cylinder pellet in  
burst region >

Width: 2 [mm]  
Length: 11 [mm]  
Elevation: 103 [cm]

<Cr coated cladding (Zr-Nb)  
with cylinder pellet in burst  
region >

Width: 3 [mm]  
Length: 10 [mm]  
Elevation : 98 [cm]

## “0.5mm particle inserted in the burst region”



< Zr-Nb-Sn cladding with  
0.5mm particles  
in burst region >

Width: 10 [mm]  
Length: 26 [mm]  
Elevation : 104 [cm]

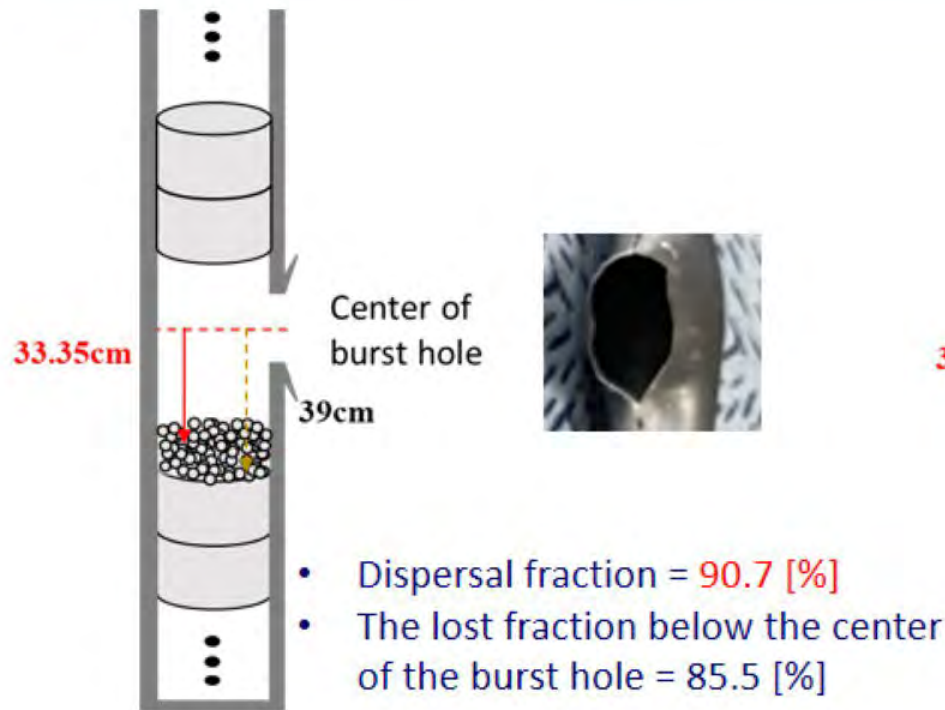
<Cr coated cladding (Zr-Nb)  
0.5mm particles in  
burst region >

Width: 11 [mm]  
Length: 25 [mm]  
Elevation : 99 [cm]

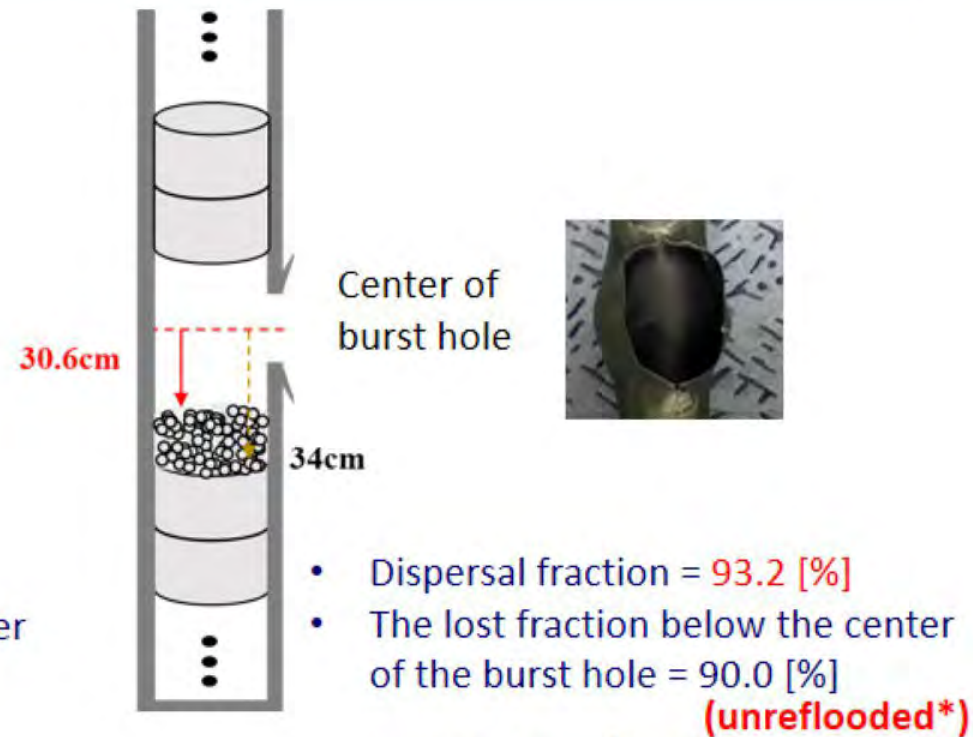
- No appreciable difference in burst hole size and location between uncoated and Cr-coated cladding
- The larger burst hole with the 0.5mm particle case may be due to potentially the larger initial void volume. Despite the attempt to maintain the same void volume for all test cases, the statistical nature of packing fraction of randomly distributed particles and resulting uncertainties may have led the tests with greater initial void volume. We plan to check it.



# Dispersal fraction analysis



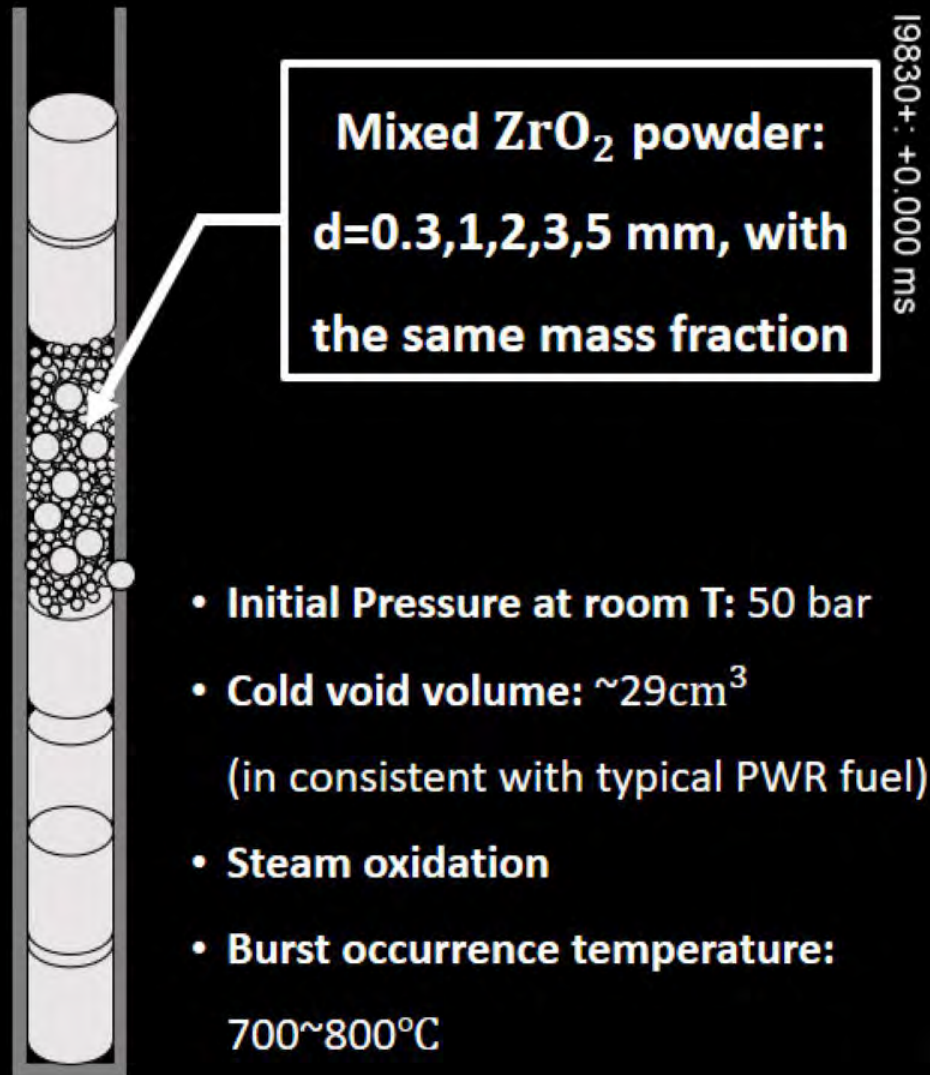
< Zr-Nb-Sn cladding with 0.5mm particles in burst region >



< Cr coated cladding (Zr-Nb) 0.5mm particles in burst region >

- >90% of loaded  $ZrO_2$  particles (0.5mm) are lost for both cases.
- All particles above the burst holes are lost. Particles below ~30cm of the center of burst hole are lost.
- Most particles are lost upon burst. Such that reflood has limited influence on test result.

# Mixed particle dispersal experiment



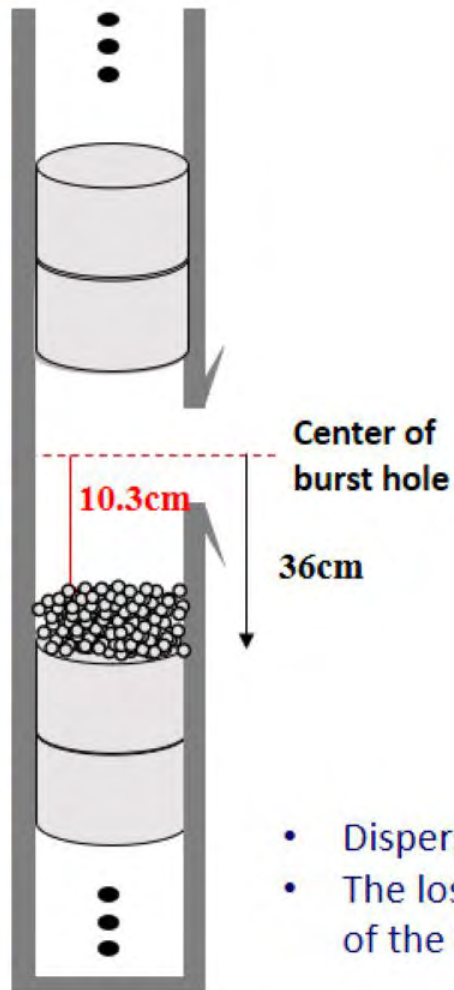
<Schematic of mixed powder  
pellet loading condition>



<Zr-Nb-Sn cladding with mixed  
 $ZrO_2$  particles>



# Dispersal fraction analysis – Mixed particle



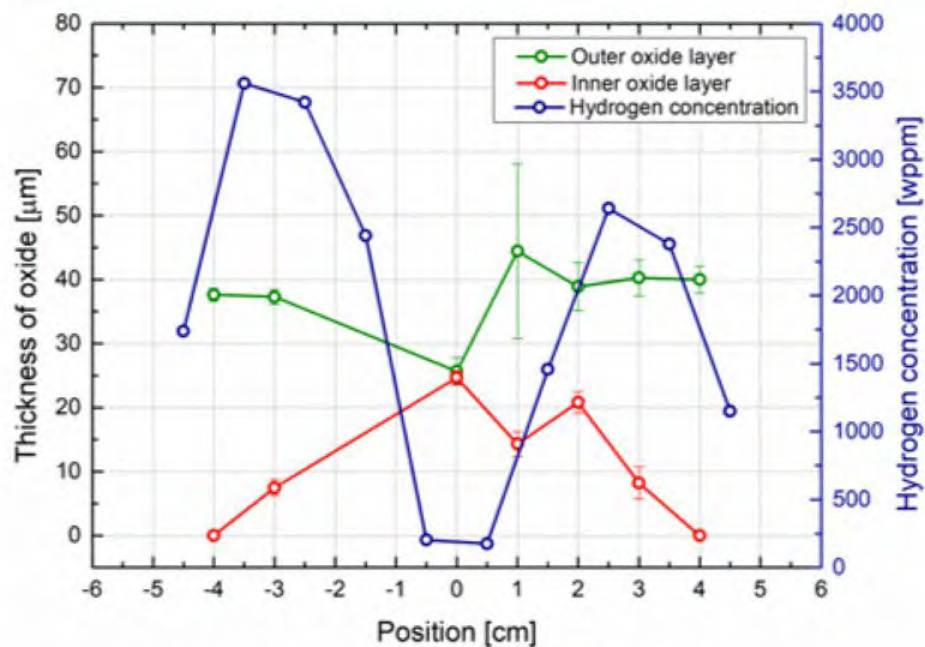
- Compared to the sole 0.5mm particle case, a significantly increased fraction of particles is retained in the fuel rod.
- Particles smaller than size of the burst holes can be retained in the rod.
- Yet, the effect of reflood remains to be seen in this case.

- Dispersal fraction = 42.8 [%]
- The lost fraction below the center of the burst hole = 28.6 [%]

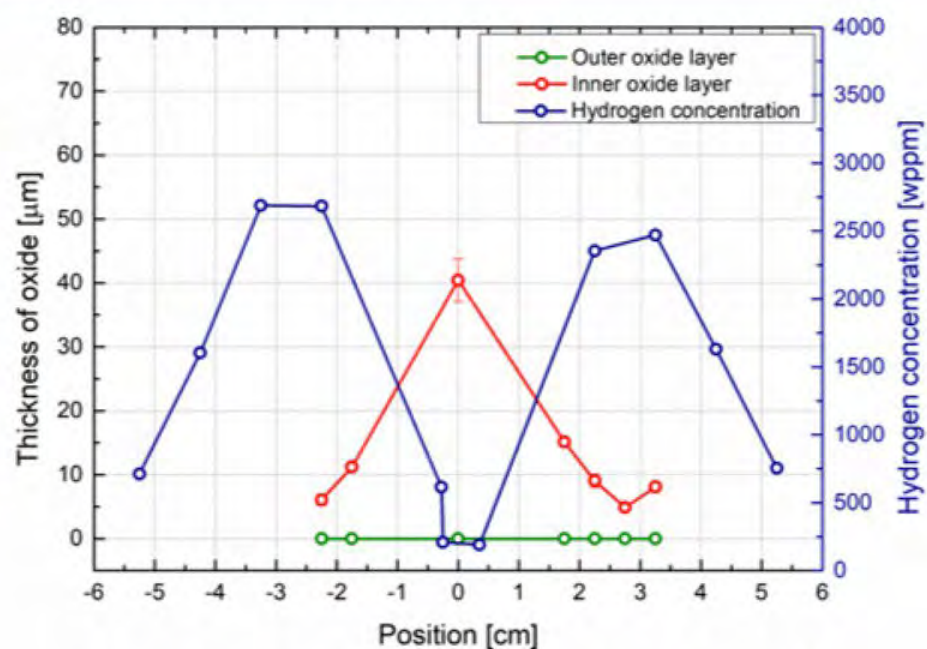
(unreflooded\*)

<Zr-Nb-Sn cladding with mixed  
ZrO<sub>2</sub> particles>

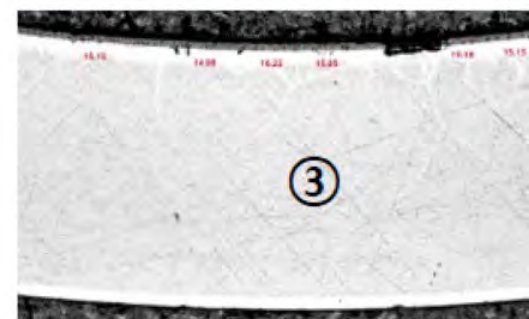
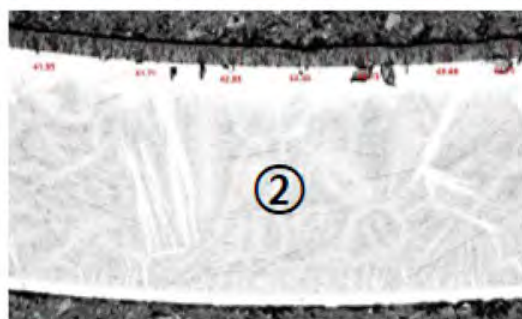
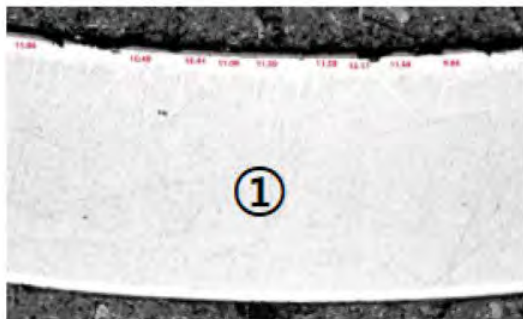
# Post-LOCA characterization



<Uncoated Zircaloy, pellet inserts>

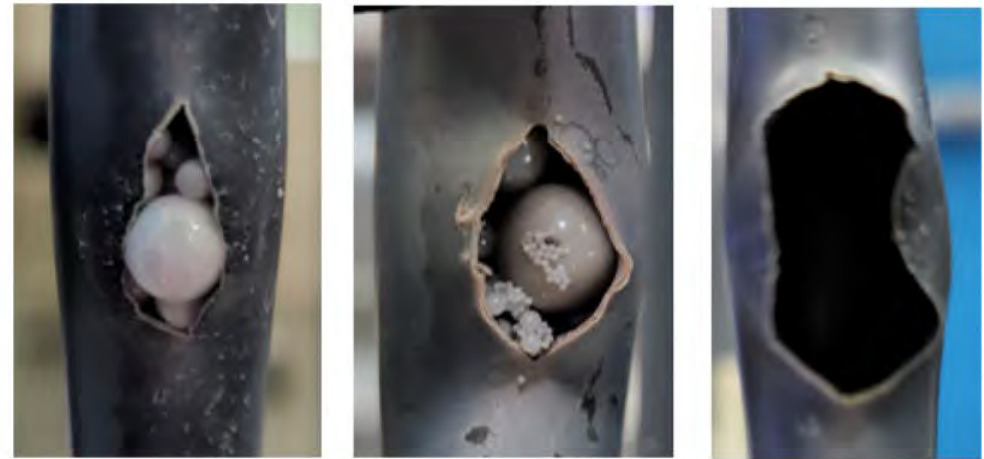


<Cr(18μm) coated Zircaloy, pellet inserts>

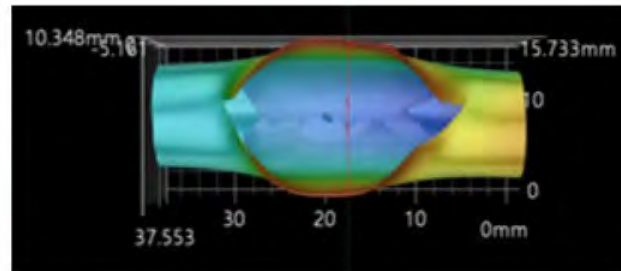




## Multi-rod (4 rod) tests are underway



<Burst hole and post-LOCA mixed particles >



<Left: Strain fields measurements in 3D scanner, Right: bursted fuel rods held by a ceramic spacer grid>

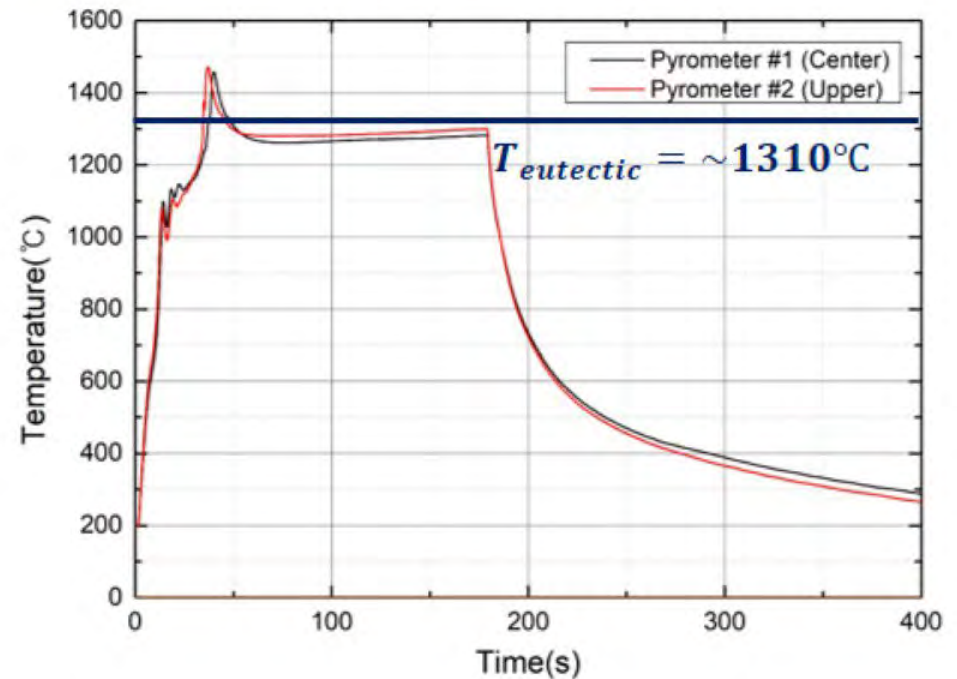
- Multi-rod tests are underway.
- It allows to investigate potential cascade of fuel burst and damage resulted by ejected fuel particles.

<Zr-Nb-Sn fuel rods (four) with mixed  $ZrO_2$  particles>

# Zr-Cr eutectic ( $>1320^{\circ}\text{C}$ ) experiments: Will fuel rods melt down via eutectic melting?



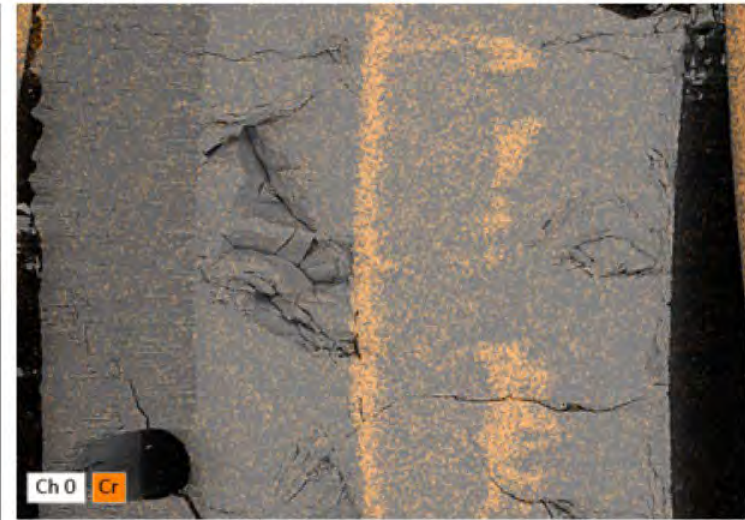
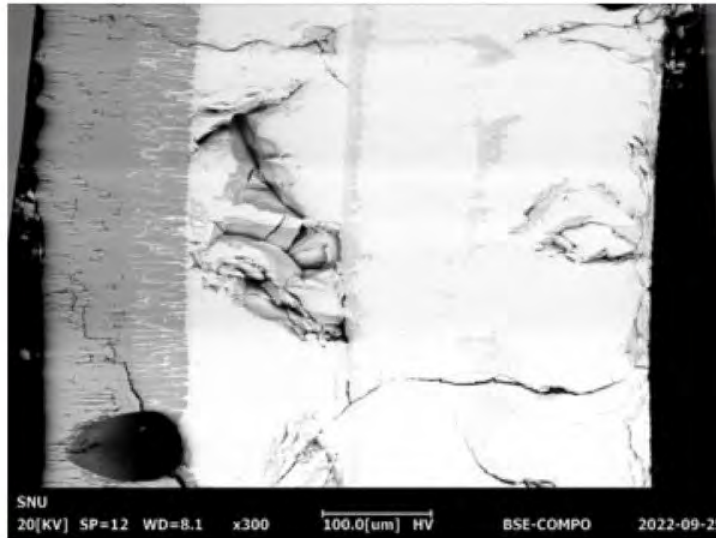
<Cr coated cladding (Zr-Cr-1.1Nb )  
high temperature exposure test>



- To simulate eutectic of Cr-coated cladding in BDBA, high temperature steam exposure experiment was conducted
- Peak temperature was 1458 $^{\circ}\text{C}$ .
- Tubes were not pressurized.



# Zr-Cr eutectic (>1320°C) experiments: Results



<SEM-EDS image of Cr-coated cladding showing Cr-Zr eutectic occurrence>



<Surface morphology of Cr-coated cladding after high temperature steam exposure>

- Fuel rods did not collapse with melting even well above the eutectic temperature.
- Significant embrittlement resulted in as a consequence of eutectic reaction. Practically no structural integrity should be expected above eutectic melting point.

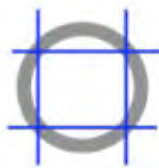
# Characterization of eutectic reaction

## ① DSC equipment



- NETZSCH DSC 404-F3
  - Environment: 99.9999% Ar gas with an Oxygen Trap System.
  - Temperature range: 25-1500 °C
  - Maximum heating rate: 0.001K/min to 50 K/min

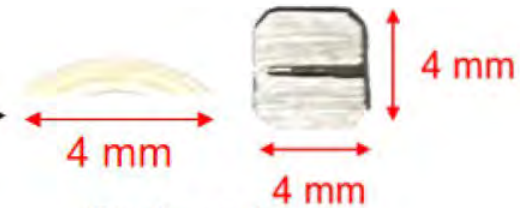
## ② Specimen preparation



Cutting into 4 segments



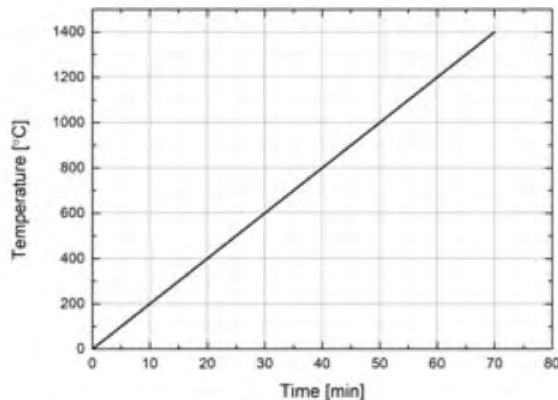
Mechanical polishing



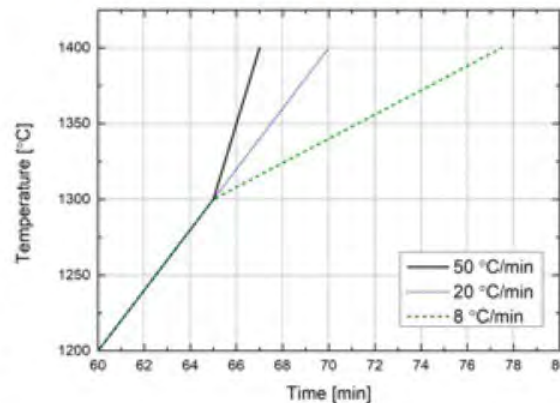
Final specimen

## ③ Temperature program

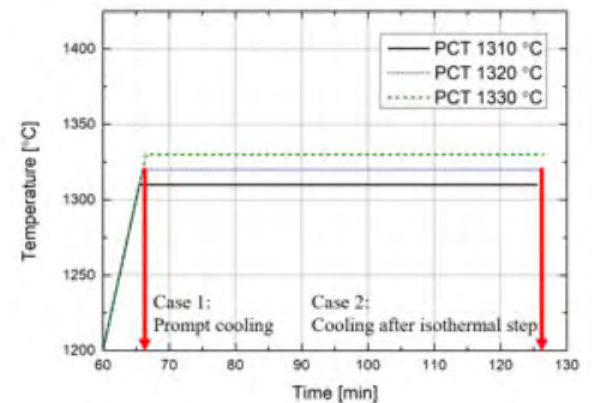
1. Reference case (1400°C, 20°C/min)



2. Various heating rate(8-50°C/min)



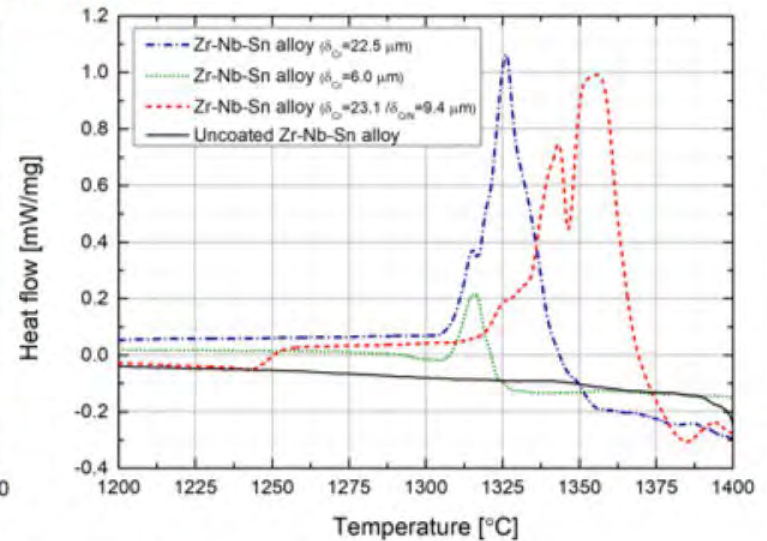
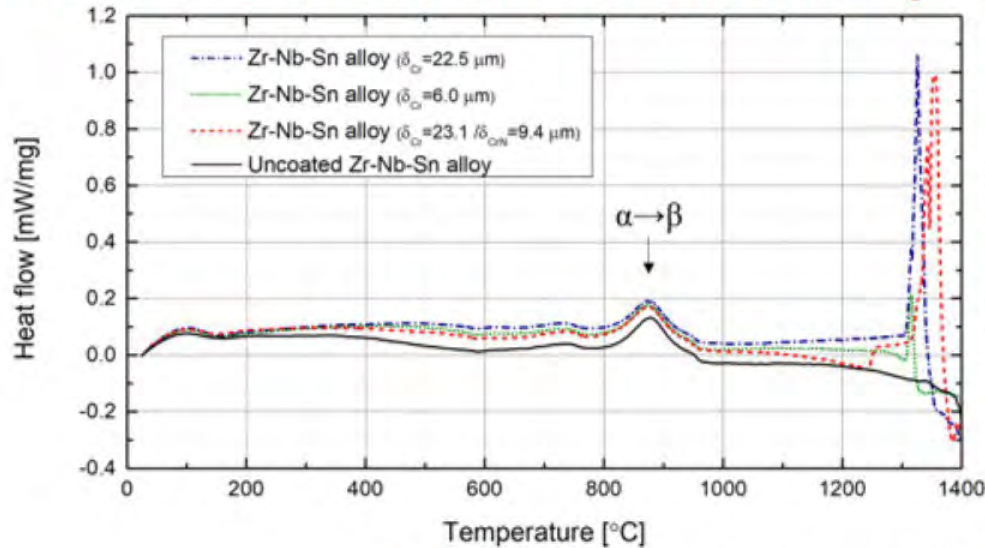
3. Various PCT (1310-1330°C) and time



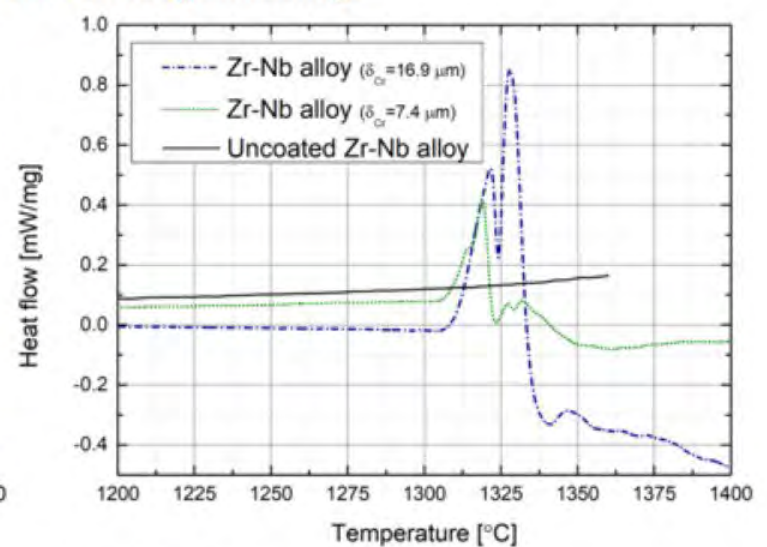
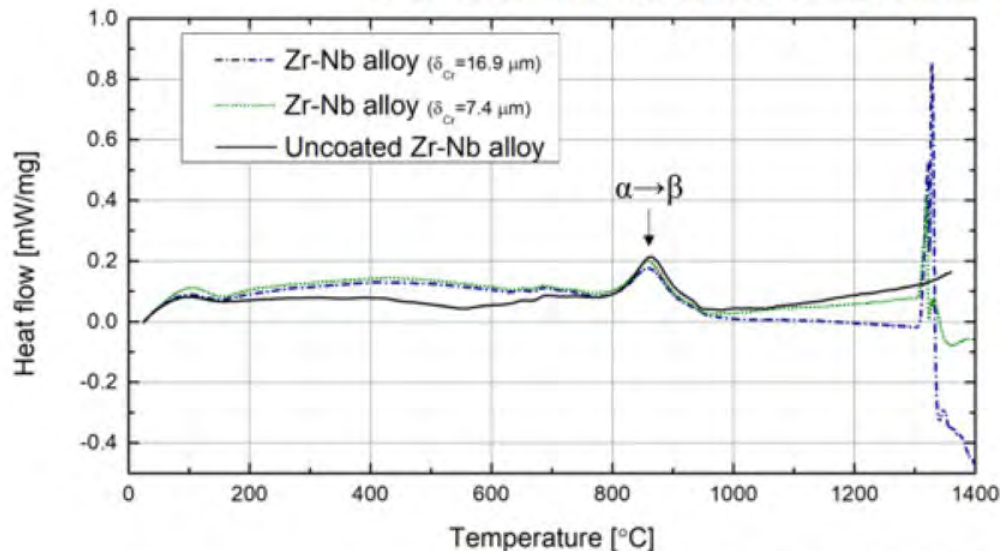


# Characterization of eutectic reaction

## Result 1: Eutectic reaction of each specimen



<DSC heat flow curve for Cr-coated Zr-Nb-Sn alloy cladding>



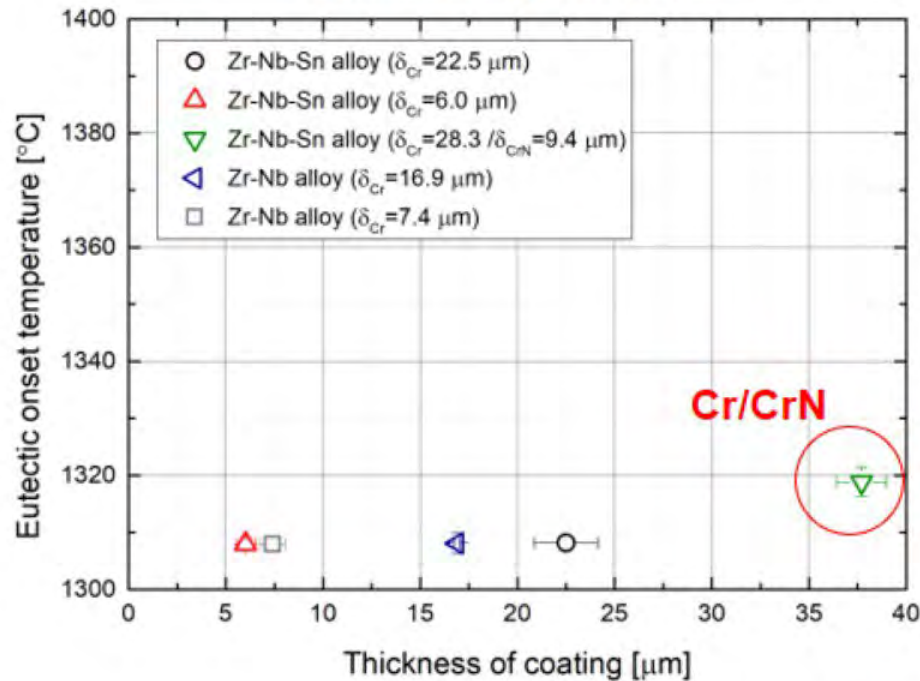
<DSC heat flow curve for Cr-coated Zr-Nb alloy cladding>

# Characterization of eutectic reaction

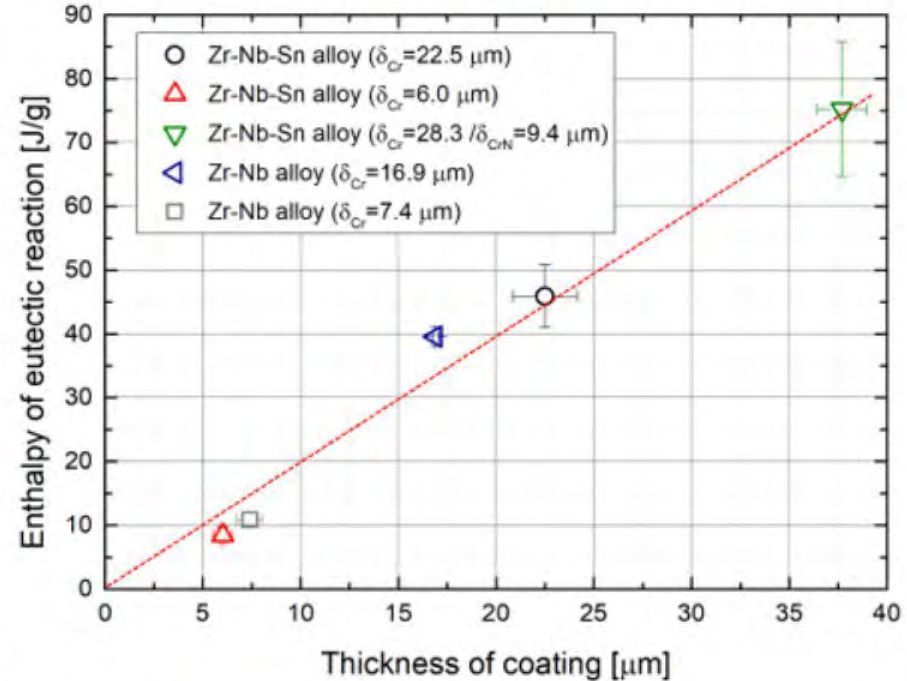
## Result 2: Coating sensitivity on eutectic reaction

- In the case of Cr single-layer coating, the eutectic temperature was almost identical at about 1308 °C, regardless of the coating thickness (6~22.5 μm) or the base material
- Cr/CrN bilayer coated specimen has a slightly (~ 10 °C) higher eutectic temperature compared to the Cr single layer coated specimen
- Enthalpy of the eutectic reaction increases linearly with the coating thickness

<Onset temperature>



<Enthalpy>



<Eutectic onset temperature and enthalpy of eutectic reaction>

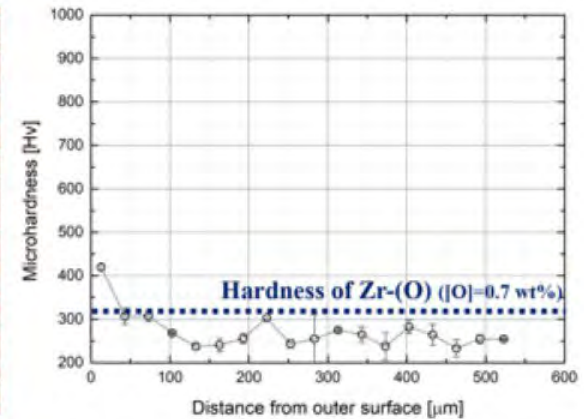
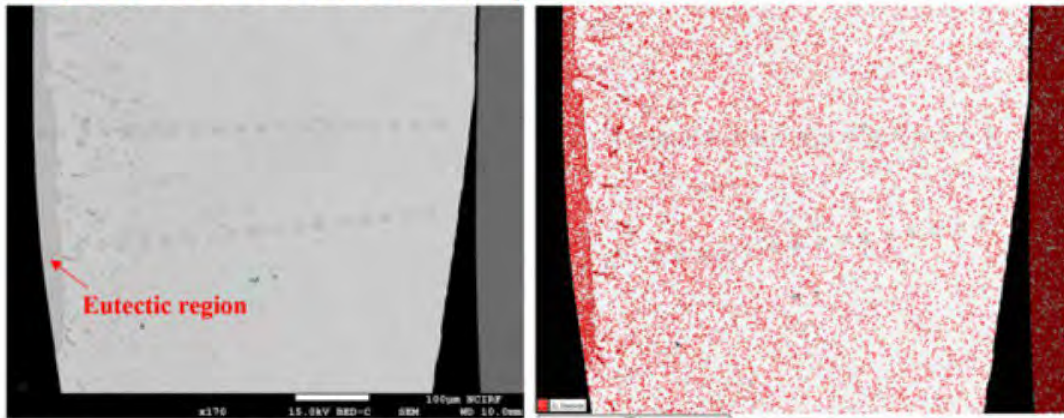


# Characterization of eutectic reaction

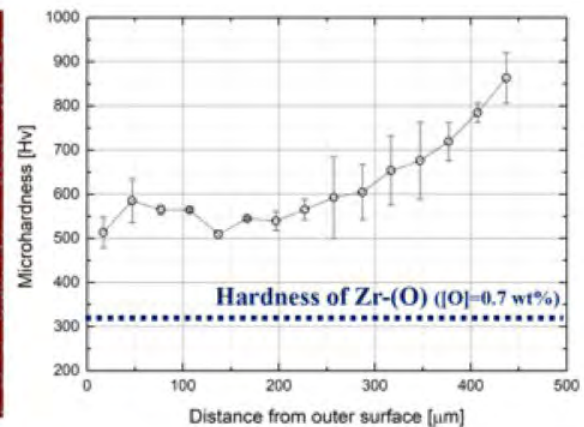
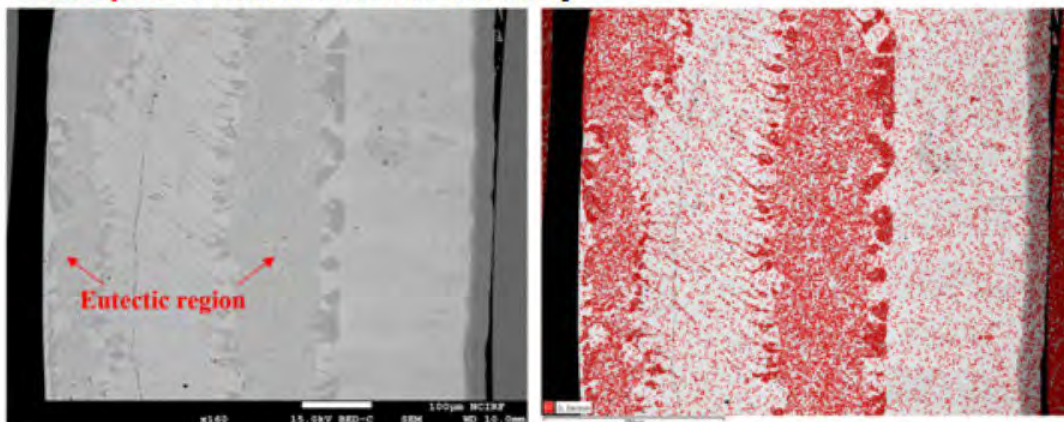
## • Result 3: Embrittlement of the cladding

- Eutectic region with  $ZrCr_2$  precipitation is formed.
- For thicker coating, the area of eutectic region and microhardness are greater.

<6  $\mu\text{m}$  Cr coated Zr-Nb-Sn alloy>



<22.5  $\mu\text{m}$  Cr coated Zr-Nb-Sn alloy >



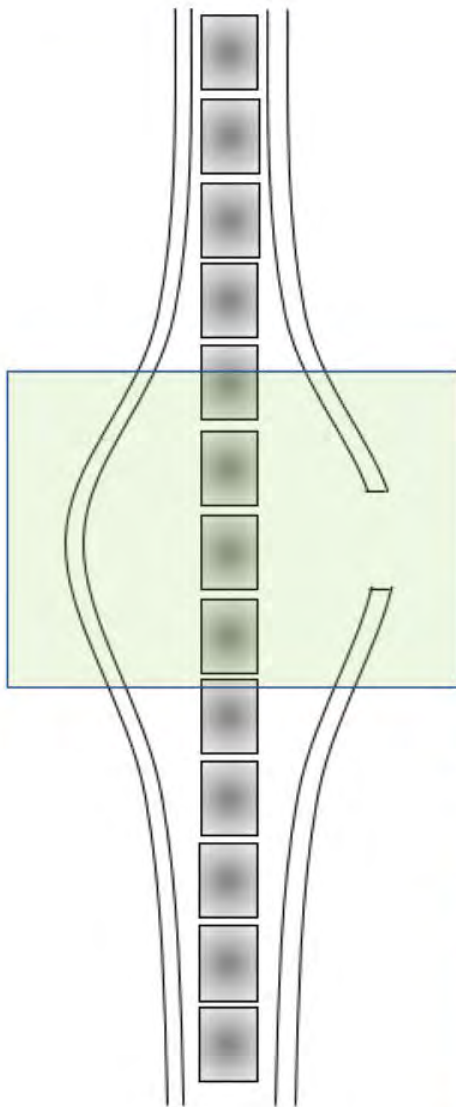
<BE-SEM and EDS image with hardness measurements>



## **2. Cr-coated cladding embrittlement study**



# Post-Quench ductility near the burst hole: a key DBA limit



Exacerbated embrittlement near the burst region

① Double side oxidation

② Thinning of the wall



$$ECR_{double-sided} = 87.8 * \frac{\Delta W_{CP}}{\delta_{avg,deformed}}$$

**NUREG 2119, U.S NRC**

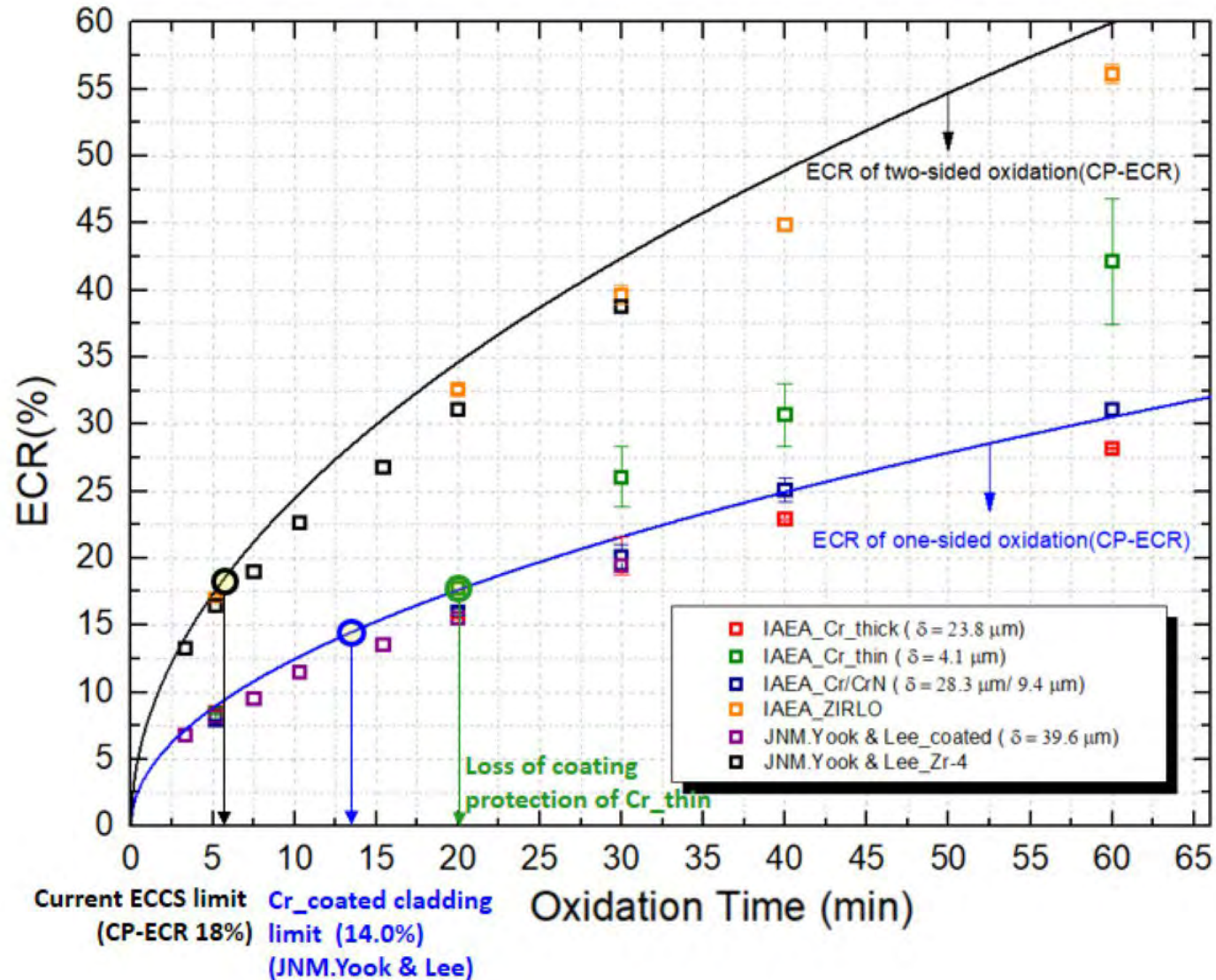
Therefore, the Office of Nuclear Regulatory Research recommendation for how to treat the ballooned region is that the time-at-temperature limit developed based on ring-compression data to limit oxidation is applied uniformly to the entire rod, with the provisions for the balloon outlined in the existing rule to use the average wall thickness in the rupture region to calculate the CP-ECR.

**ATF-ISG-2020-01, U.S NRC**

Differences in oxidation kinetics between zirconium-based cladding and chromium-coated cladding change the relationship between oxygen diffusion and oxide growth. This issue is further complicated within the burst region where cladding inner diameter oxidation is based on zirconium alloy kinetics and cladding outer diameter oxidation would be based on chromium coating kinetics. Hence, the applicability of the 17-percent equivalent cladding reacted analytical limit and, more generally, the use of maximum local oxidation as a surrogate SAFDL for cladding embrittlement is questionable.

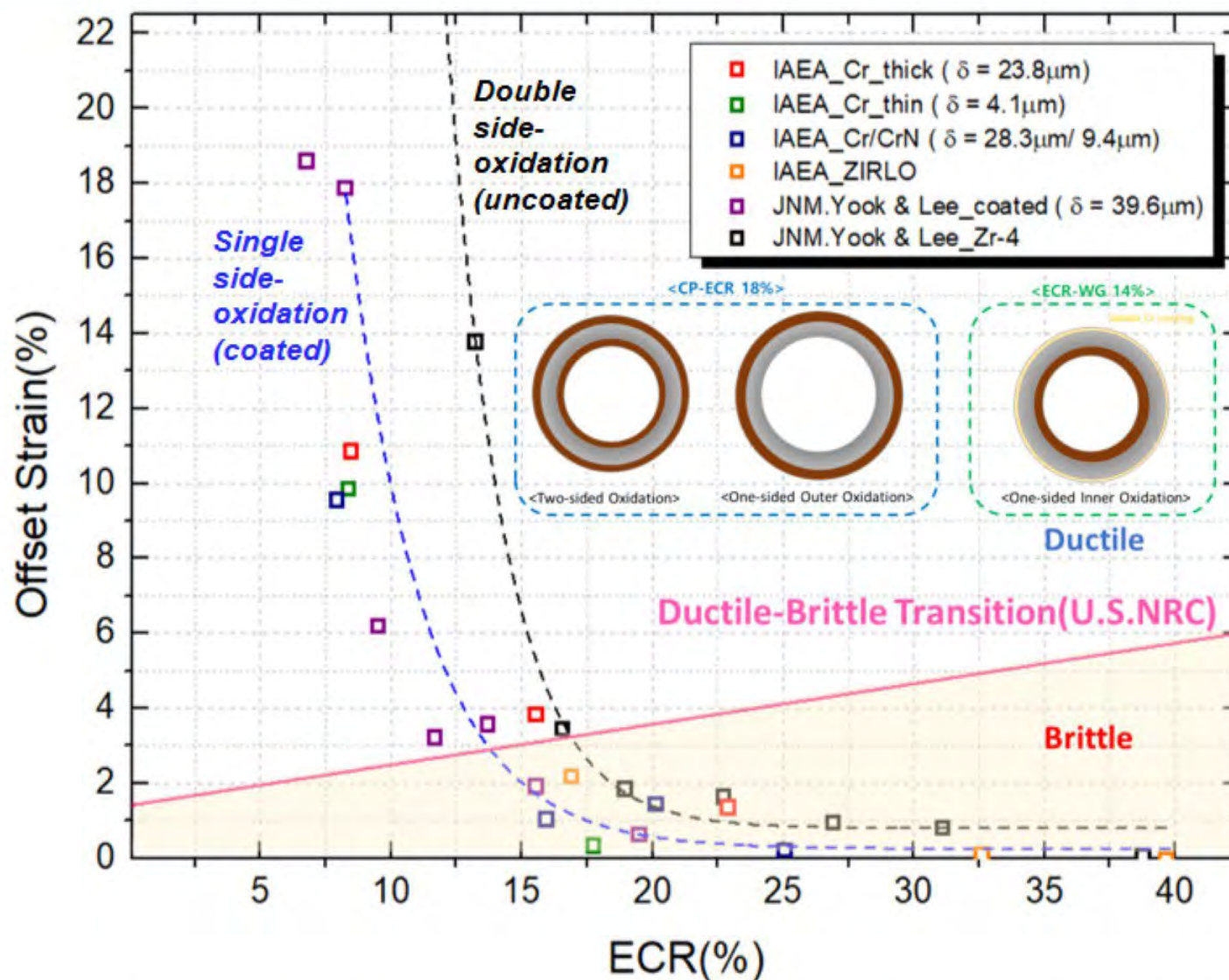
The NRC staff should ensure that, if the applicant elects to ignore the potential benefits expected with chromium coatings and continues to use the existing 10 CFR 50.46 analytical limits, then supporting evidence has been provided to demonstrate residual ductility of the coated cladding up to these analytical limits.

# Coated cladding: effectively single side oxidation for DBA consideration



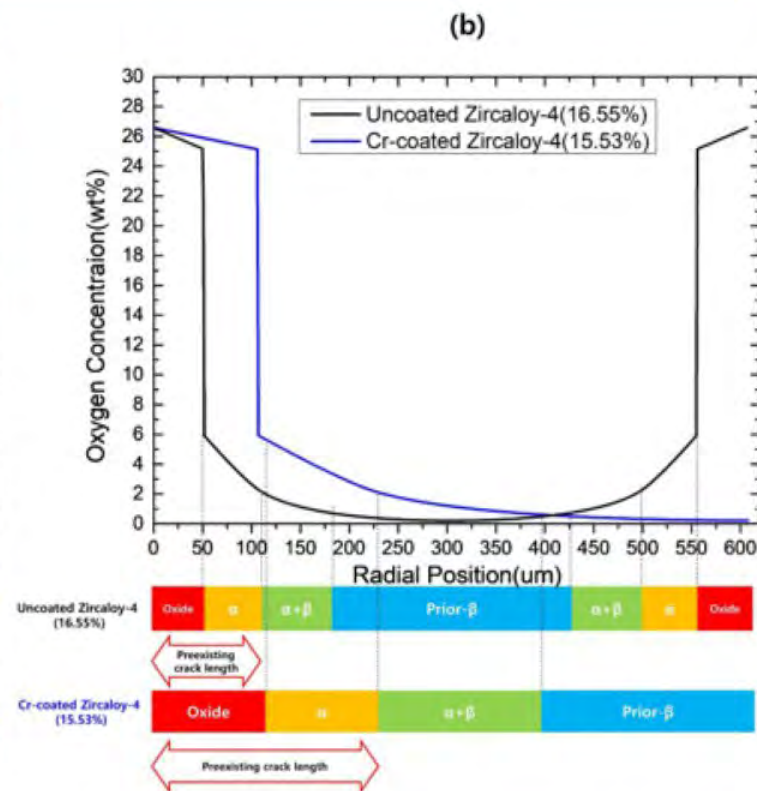
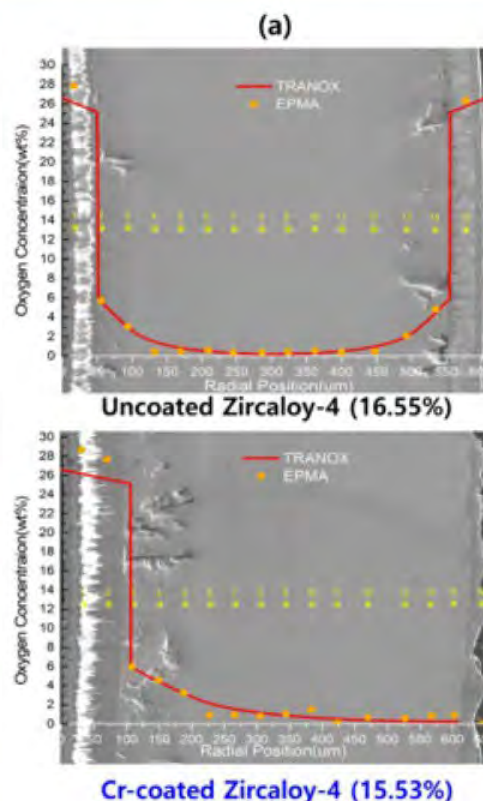
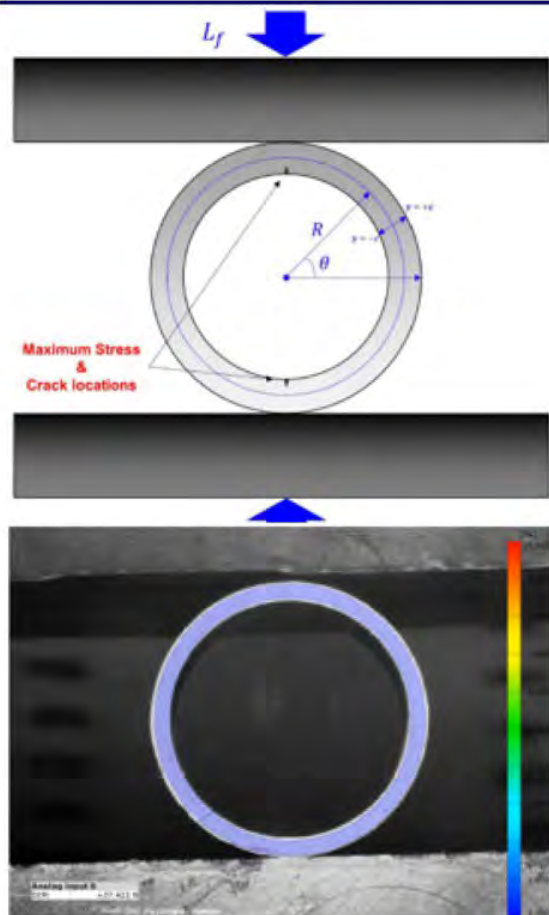


# ECCS Criteria (DBA limit) study: Embrittlement limit



Premature ductile-to-brittle transition of Cr-coated cladding

# ECCS Criteria (DBA limit) study



<Difference in inner side the brittle phase thickness for the similar level of ECR  
 (a) Comparison of oxygen distributions in coated and uncoated specimens. (b)  
 Pre-existing crack lengths (oxide + alpha layer) of specimens for RCT.>

## Key deliverables:

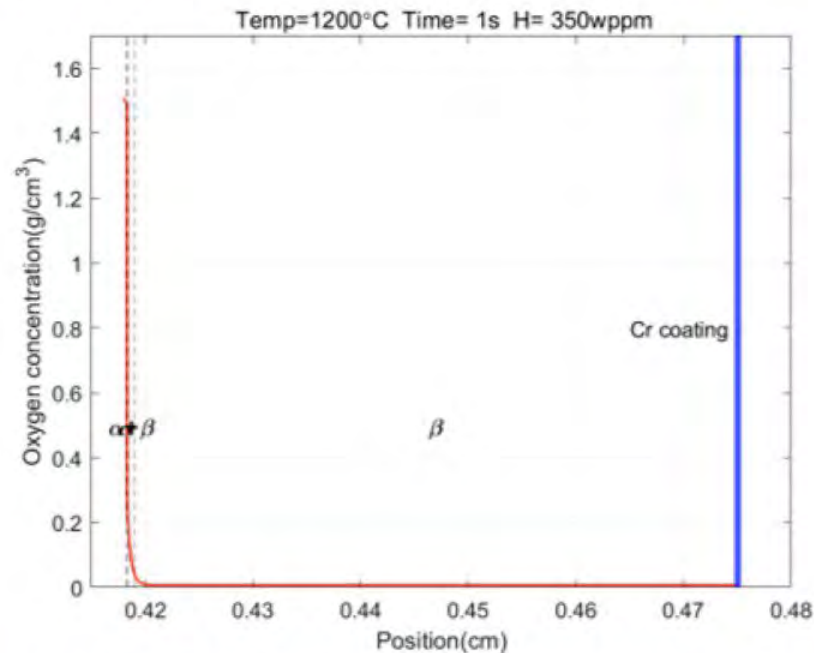
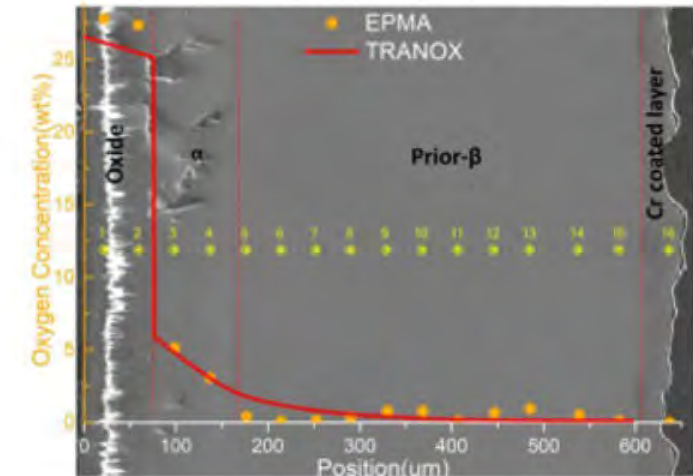
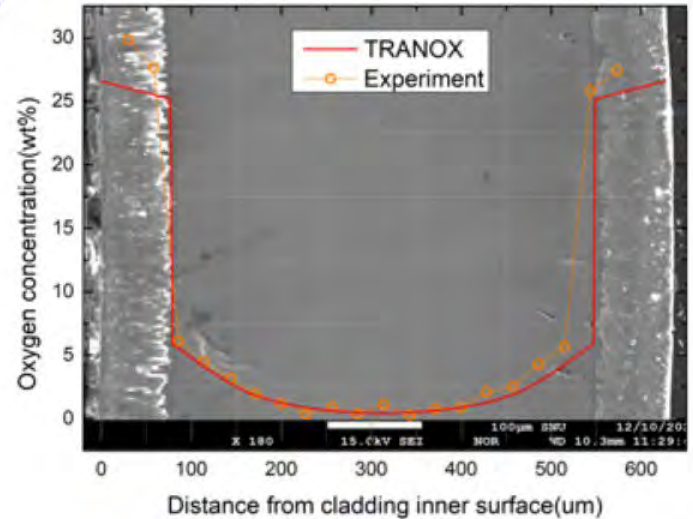
- Nature of RCT biasedly lowers the ECR limit for coated cladding: the lower ECR limit for coated cladding is not due to the ductility carrying phase (prior-  $\beta$ ). Even with thicker prior-  $\beta$  phase, coated cladding undergoes premature ductile to brittle transition under RCT. This is primarily because it has thicker brittle phases ( $ZrO_2 + \alpha-Zr(O)$ ) at the inner surface compared to uncoated cladding for the same ECR



# TRANOX : Mechanistic model of Zircaloy oxidation

## Current TRANOX 2.0 Capability

- Oxygen distribution, ECR,  $\alpha$  and  $\beta$ -phase thickness
- Transient temperature
- Presence of hydrogen (high burnup)
- Pre-transient oxide layer (high burnup)
- Coated cladding



[1] 2021. D. Kim et al., TRANOX: Model for Non-Isothermal Steam Oxidation of Zircaloy Cladding. *Journal of Nuclear Materials*, 556, 153153.

[2] 2022. H. Yook, et al., Post-LOCA Ductility of Cr-coated cladding and its embrittlement limit. *Journal of Nuclear Materials*, 558, 153354.

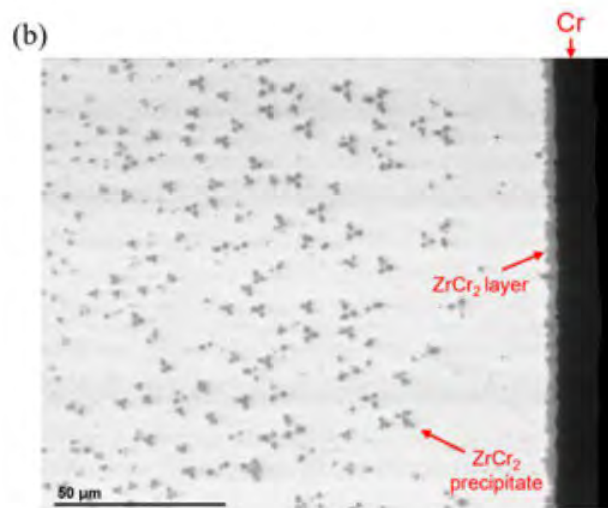
[3] 2022. D. Kim et al., Study of high burnup effect on steam oxidation of Zircaloy and its regulatory implications via the development of pre-transient oxide model of TRANOX. *Journal of Nuclear Materials*, 567, 15 153801

# Chromium diffusion and model development

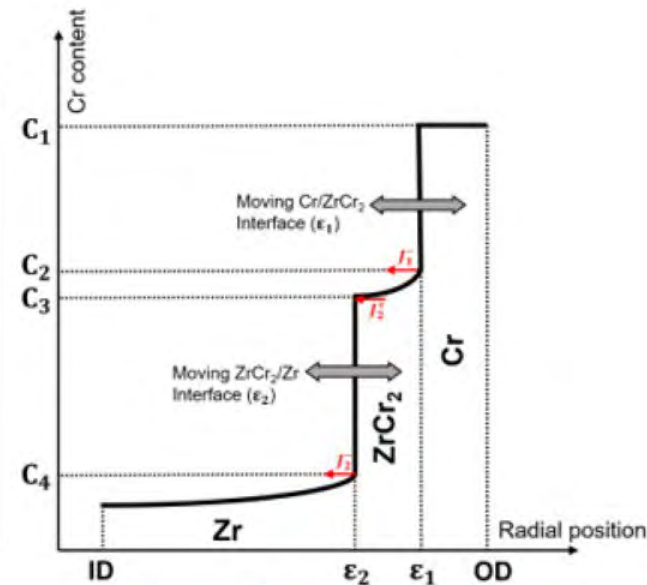
- Upgrading TRANOX to handle Zr-Cr system
  - Modeling distribution of  $ZrCr_2$  phase



<As-received Cr-coated specimen>



<Cr-diffused after high T annealing >

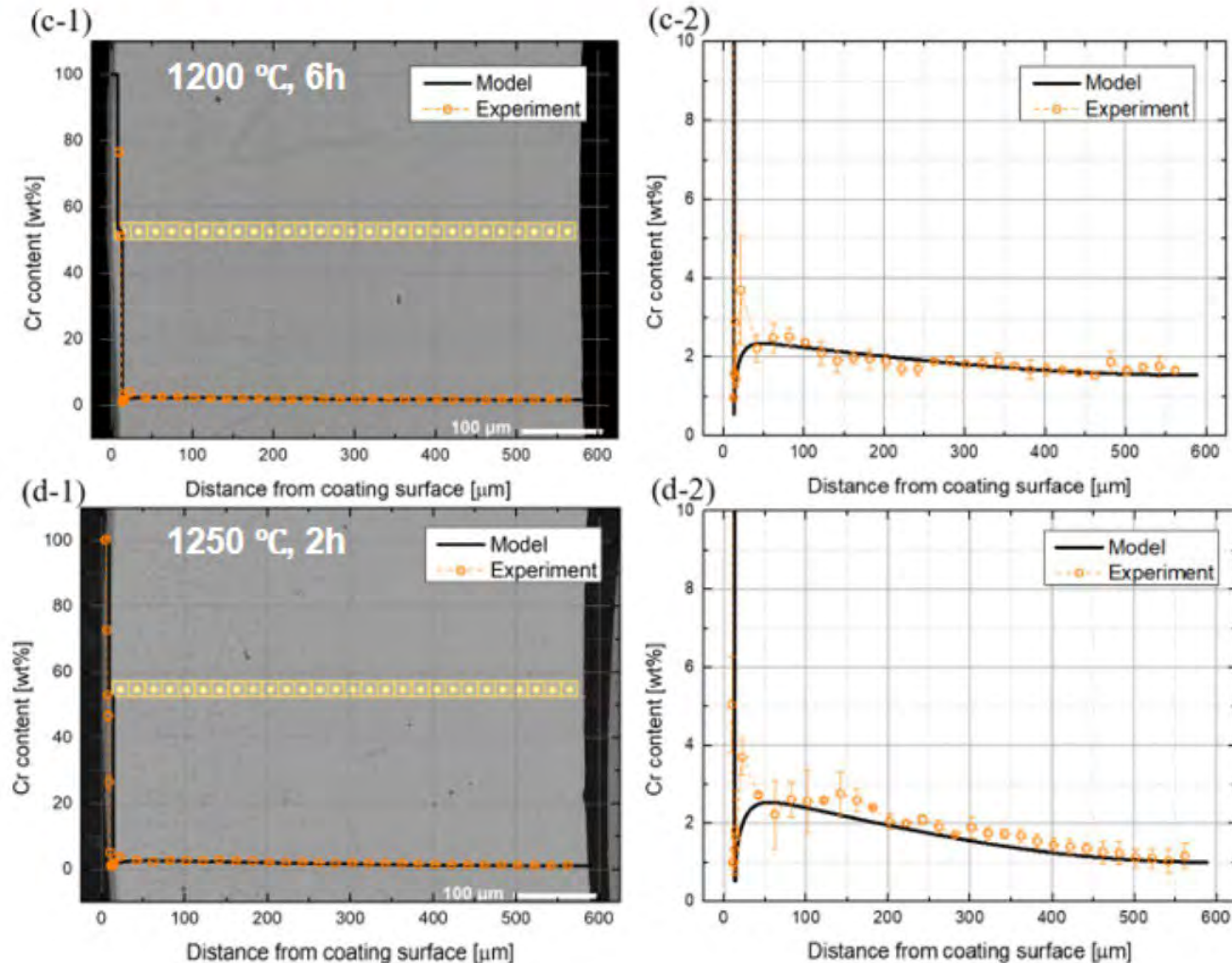


<Schematic of Cr diffusion and resulting phases due to high T annealing>



# Experimental validation of the Cr diffusion model 1

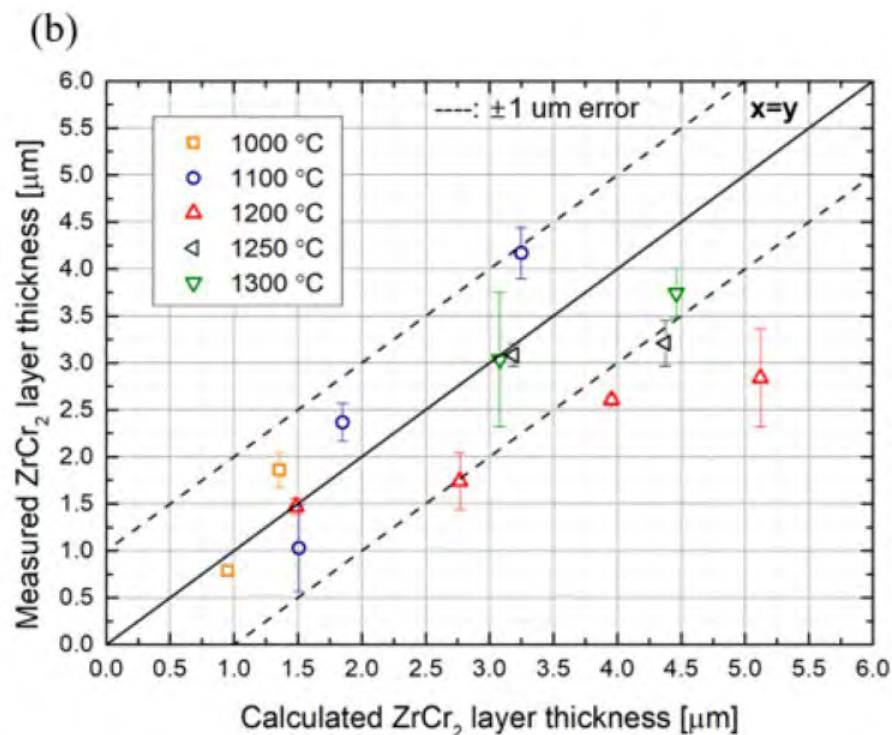
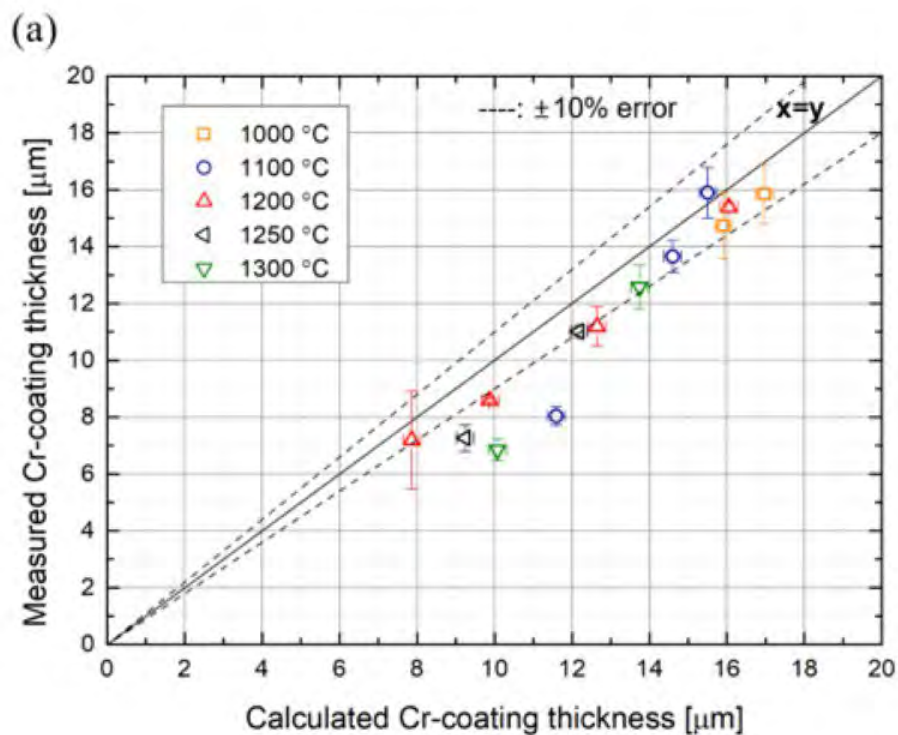
- **EPMA measurement of Cr distribution**
  - In-house experimental validation



<Cr distribution after high T annealing>

# Experimental validation of the Cr diffusion model 2

- Thickness of Cr and  $ZrCr_2$  phase
  - In-house experimental validation

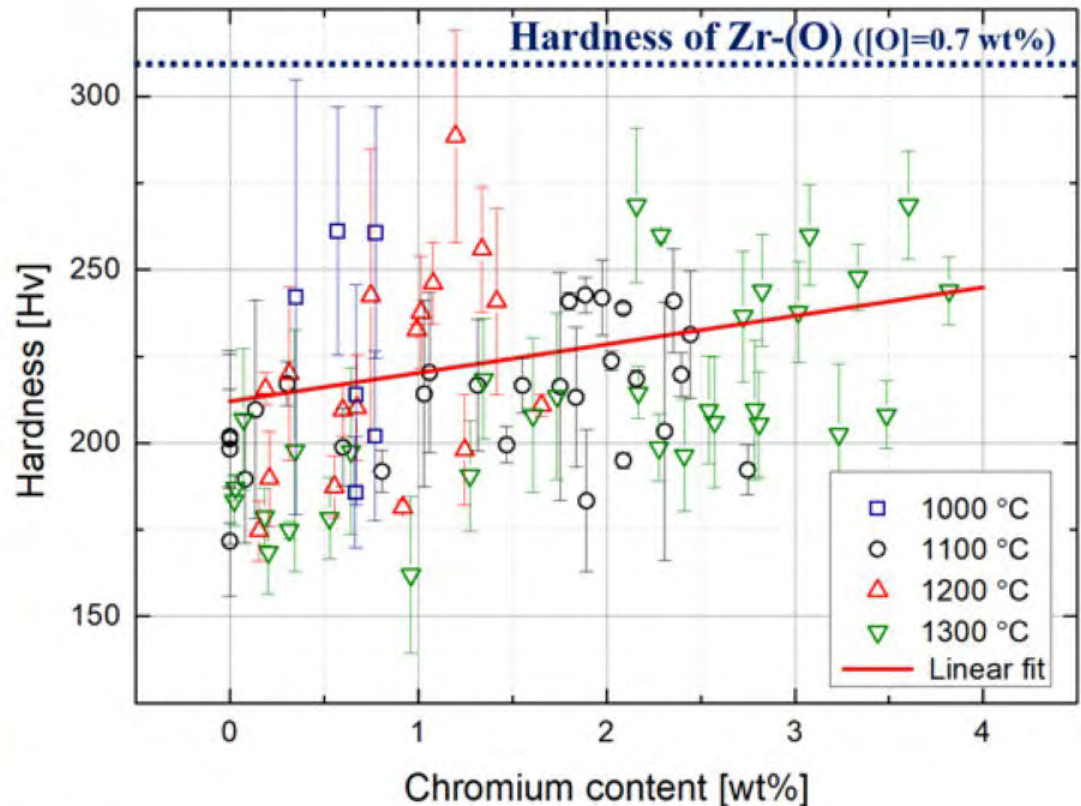
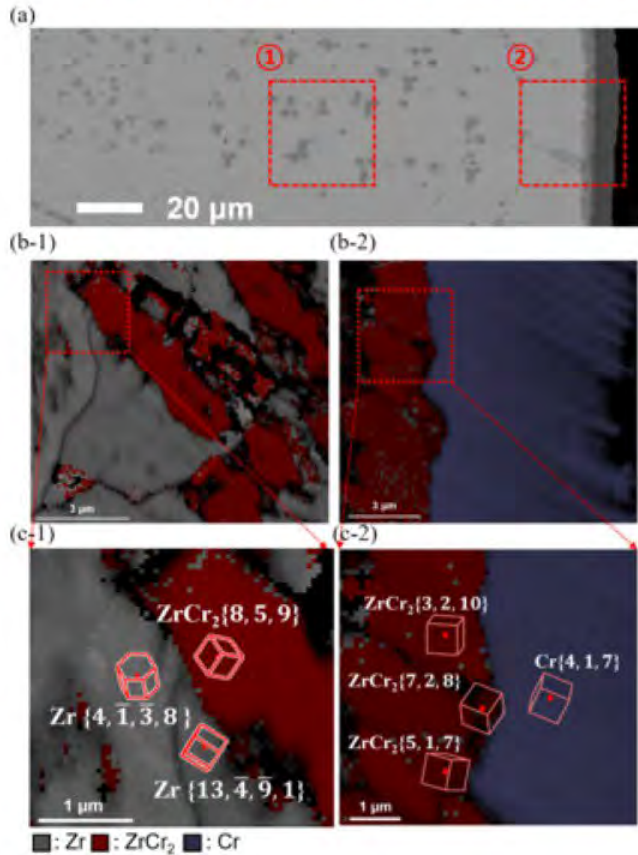


<Cr coating thickness validation after high T annealing>



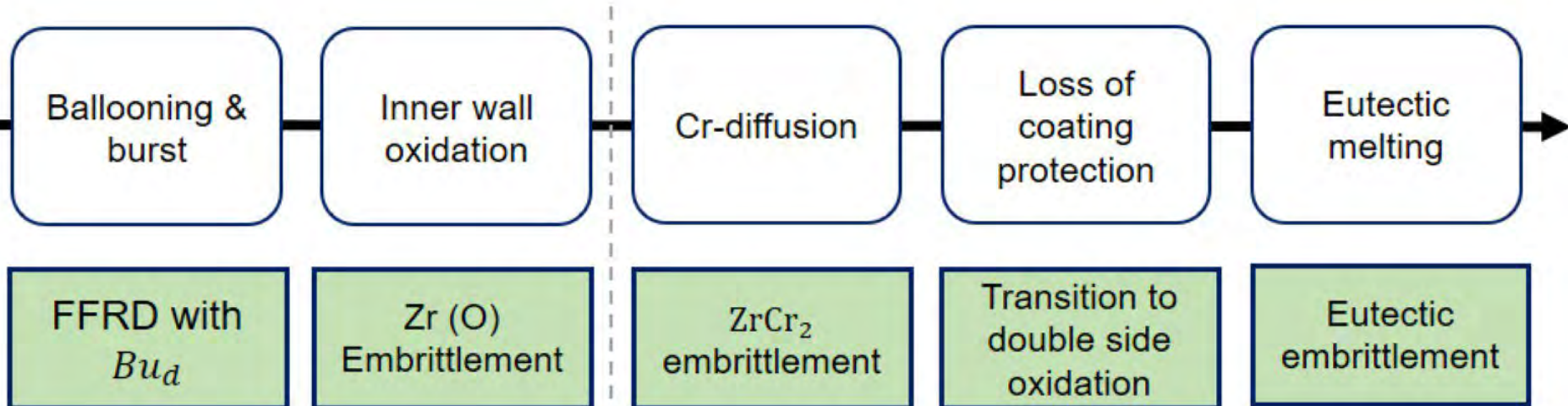
# Hardness change with Chromium precipitation

- Cr precipitation-induced embrittlement



- Increasing embrittlement via formation of two-phase aggregate with incoherent interface.
- Its quantitative effect on cladding embrittlement in macroscopic behavior in comparison with oxygen solid solution hardening remains to be investigated.

# Conclusions: tentative findings and understanding



## Tentative understanding:

Confirmed serious fuel dispersal... (further investigation needed!)

ECR=14% (single side oxidation)  
PCT = 1204°C (2200F)

Needs minimum tens of mins to be appreciable. Modeling capability ready.

If coating is >20μm, it is hard to occur. It is likely to be resulted by eutectic melting.

Once it happens at >1310°C, no structural integrity should be expected. The ceiling of possible PCT limits. Coating-design insensitive.

DBA-relevant (i.e., ECCS Criteria 10 CFR 50.46)

**+10 min accident coping time at 1204°C (2200F)**  
*[It may be critical for discharge burnup increase beyond 60MWd/kgU]*

BDBA progression-relevant





**Thank you**

Discharge burnup

Core Damage Frequency (CDF)

Severe Accident Progression

“Integral LOCA experiment”

Steady-state strain limit (Allowable coating failure)

Cr-Coated DBA limit (PCT, ECR (oxidation))

High burnup FFRD criteria

SNU-developed Fuel code 'GIFT'

Steady-state corrosion

Steady-state creep deformation

Steady-state T & P

Irradiation axial growth

Burnup-initialized conditions

Uncovered area

Strain

Strain

Burnup-initialized conditions

Coating failure / effective uncovered area

Uncovered area

Double side oxidation, Clad thickness

Strain

High T oxidation and Cr diffusion

Ballooning & Burst

Cr-Zr Eutectic reaction

Oxidation rate

Burst hole size

FFRD

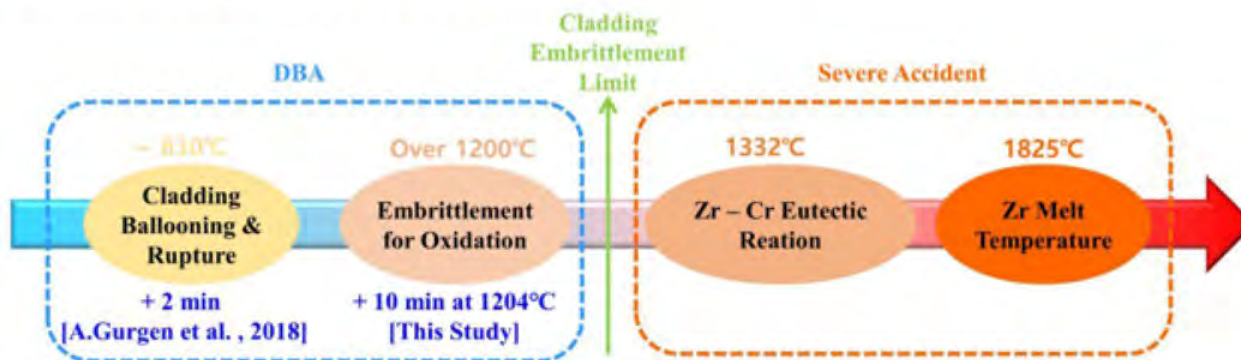
Hydrogen generation



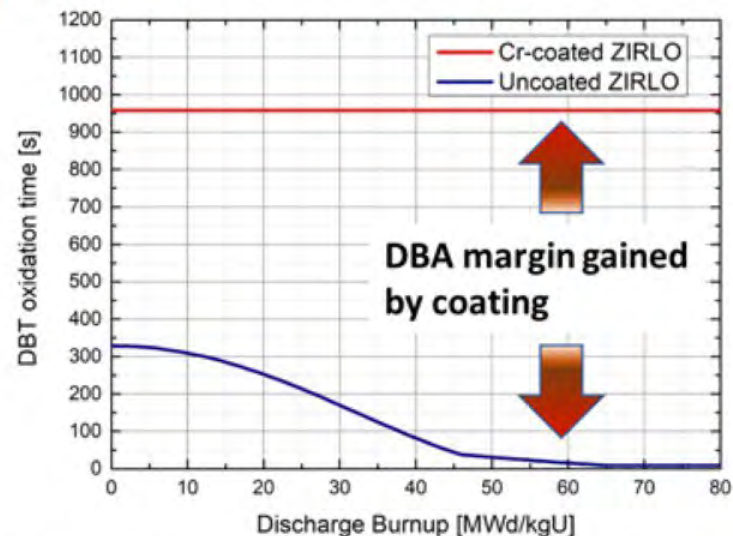
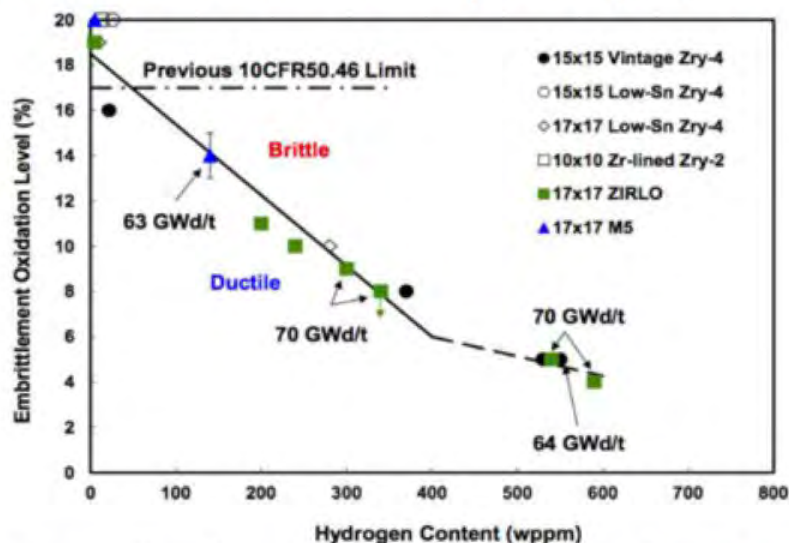
# Implications on accident coping time

## Preliminary ramifications:

- ~ 10 minutes of extra accident coping time (at 1204°C)



- It means a lot from the viewpoint of potential burnup extension



<Decreasing allowable ECR limit with  $Bu_d(H)$ , U.S. NRC>

<Time required to reach ductile to brittle transition (DBT) by exposure to 1200 °C steam, Cr-coated ECR Limit: 14% Uncoated ECR Limit: decreasing with  $Bu_d$ >

# Characterization of eutectic reaction

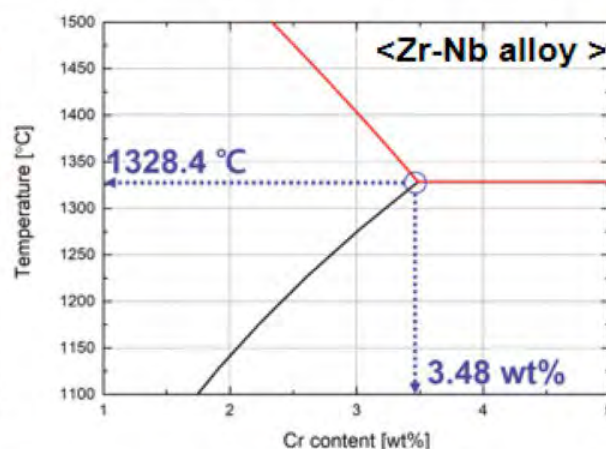
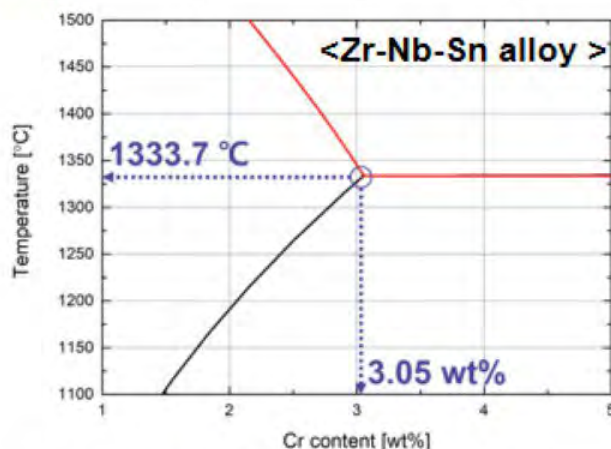
## Cr-coated ATF specimen

<Specimen used to eutectic reaction experiment>

Specimen	Base material	Coating material	Coating thickness [ $\mu\text{m}$ ]
Zr-Nb-Sn alloy ( $\delta_{Cr} = 6\mu\text{m}$ )	Zr-Nb-Sn alloy	Cr	$6.0 \pm 0.47$
Zr-Nb-Sn alloy ( $\delta_{Cr} = 22.5\mu\text{m}$ )			$22.5 \pm 1.65$
Zr-Nb-Sn alloy ( $\delta_{Cr} = 28.3/\delta_{CrN} = 9.4\mu\text{m}$ )		Cr/CrN	$23.1 \pm 0.64/9.4 \pm 0.63$
Zr-Nb alloy ( $\delta_{Cr} = 7.4\mu\text{m}$ )	Zr-Nb alloy	Cr	$7.4 \pm 0.65$
Zr-Nb alloy ( $\delta_{Cr} = 16.9\mu\text{m}$ )			$16.9 \pm 0.13$

<Chemical composition of each Zr alloy>

Element [wt%]	Sn	Fe	O	Nb	Cu	Hf	Zr
Zr-Nb-Sn alloy	0-0.99	0.11	0.11	0.98	-	0.004	98.3 (bal.)
Zr-Nb alloy	-	-	-	1.1	0.05	-	98.85 (bal.)



<Predicted eutectic temperature and composition using ThermoCalc and TCZR1 database >

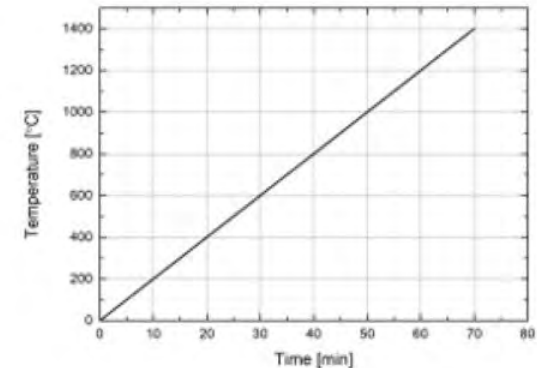


# Characterization of eutectic reaction

## Testing scope

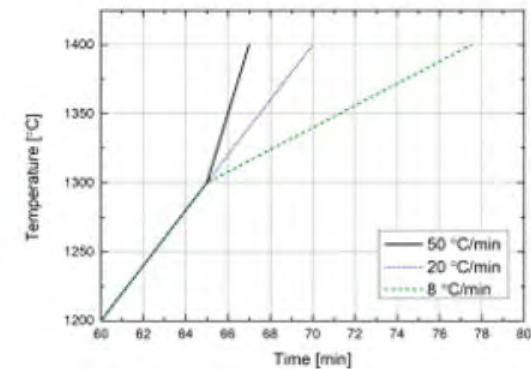
### ① Reference case

- Analyze **differences in eutectic reaction** between specimens
- Heating up to **1400 °C** with heating rate of **20 °C/min**



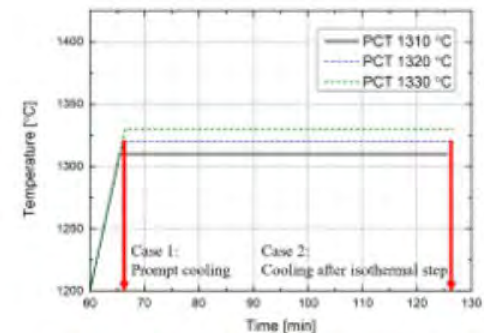
### ② Variable heating rate for kinetics of eutectic reaction

- Analyze the **kinetics of the eutectic reaction**
- Heating up to 1300 °C with heating rate of 20 °C/min (same as ①), heating up to 1400 °C with heating rate or **8, 20, 50 °C/min**



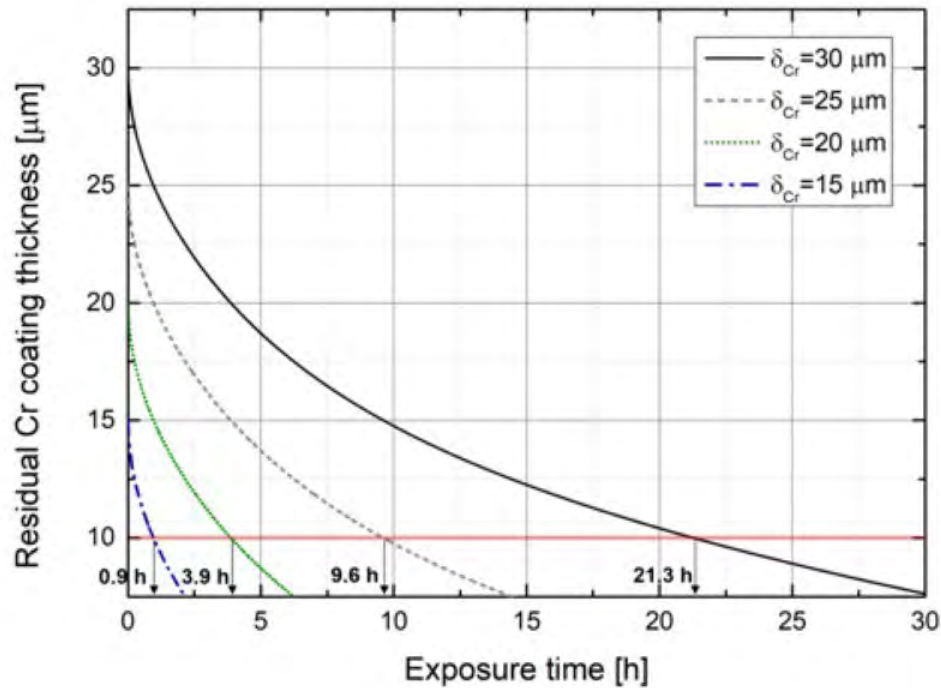
### ③ Variable PCT and holding time

- Analyze the response to **holding time and peak temperature**
- Heating up to **various PCT (1310, 1320, 1330 °C)** with heating rate of 20 °C/min, and controlling the holding time (**0h or 1h**)

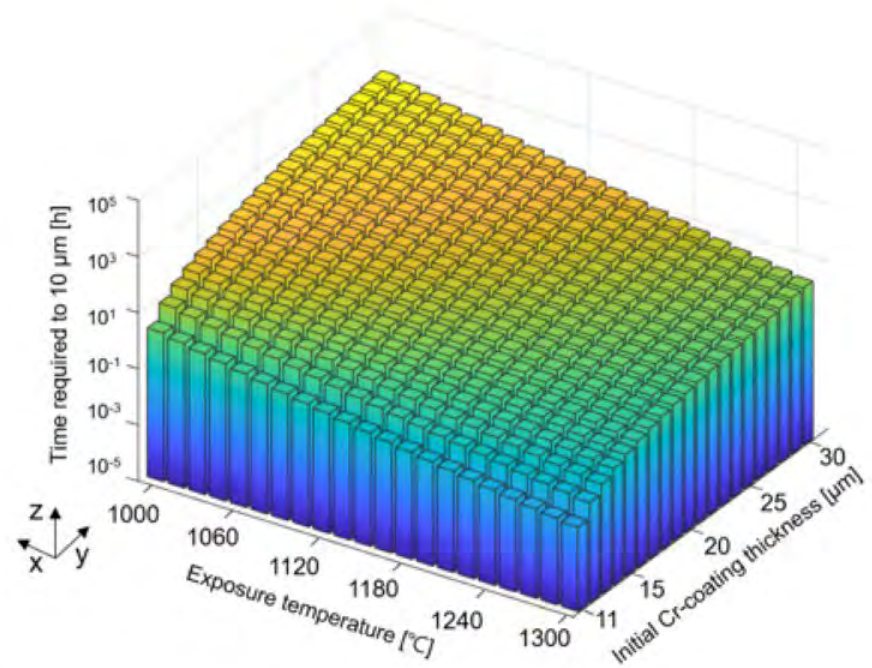


# Required coating thickness against diffusional loss

## Application of the developed model



<Model prediction of Cr coating reduction due to diffusion>

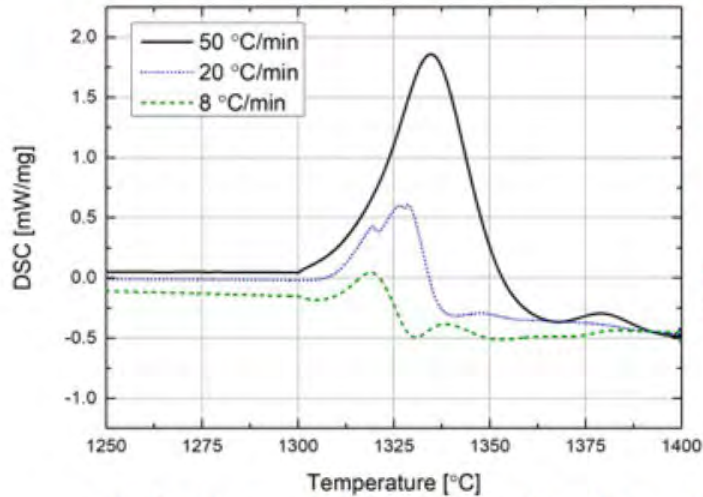


<Time to reduce initial Cr thickness ( $>10 \mu\text{m}$ ) to  $10 \mu\text{m}$ >



# Characterization of eutectic reaction

## Result 2: Variable heating rate for kinetics of eutectic reaction

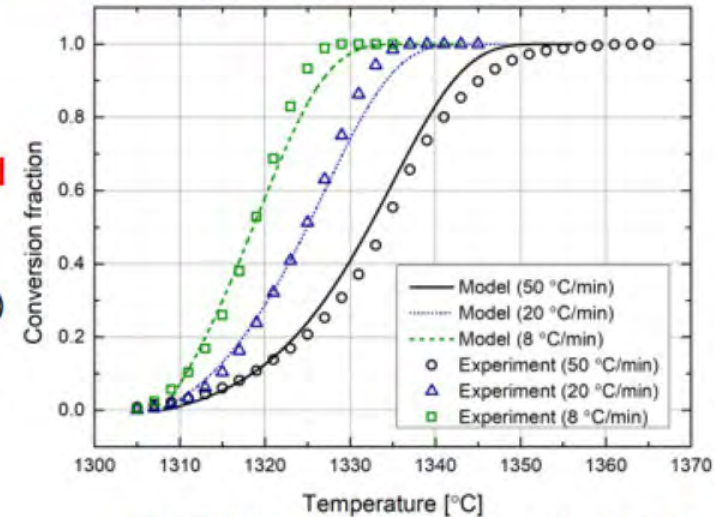


<Eutectic peak for various heating rate>

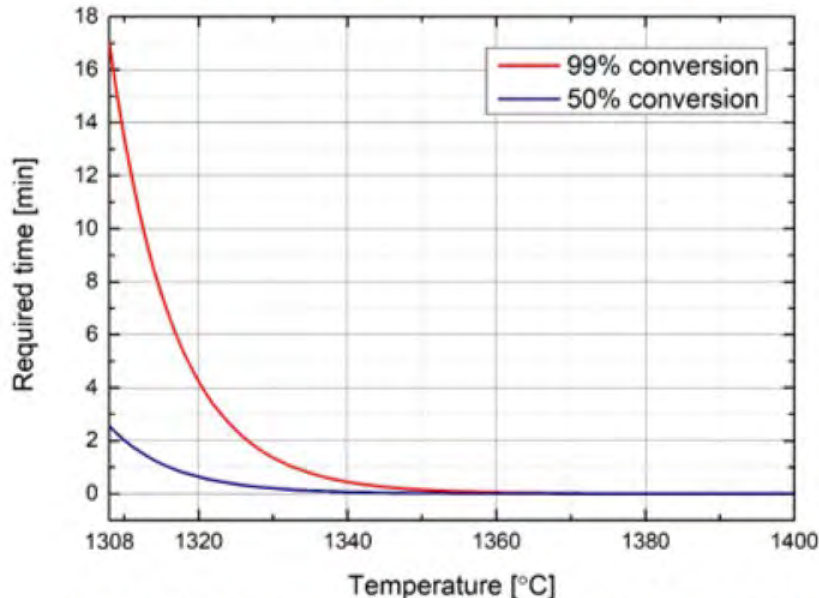
Fitting to kinetics model

$$\frac{d\alpha}{dt} = K_0 \exp\left(-\frac{E_a}{kT}\right) \cdot (1 - \alpha)$$

$$K_0 = e^{115.85}, E_a = -1043365J$$



<Model-to-experiment comparison for conversion curve>



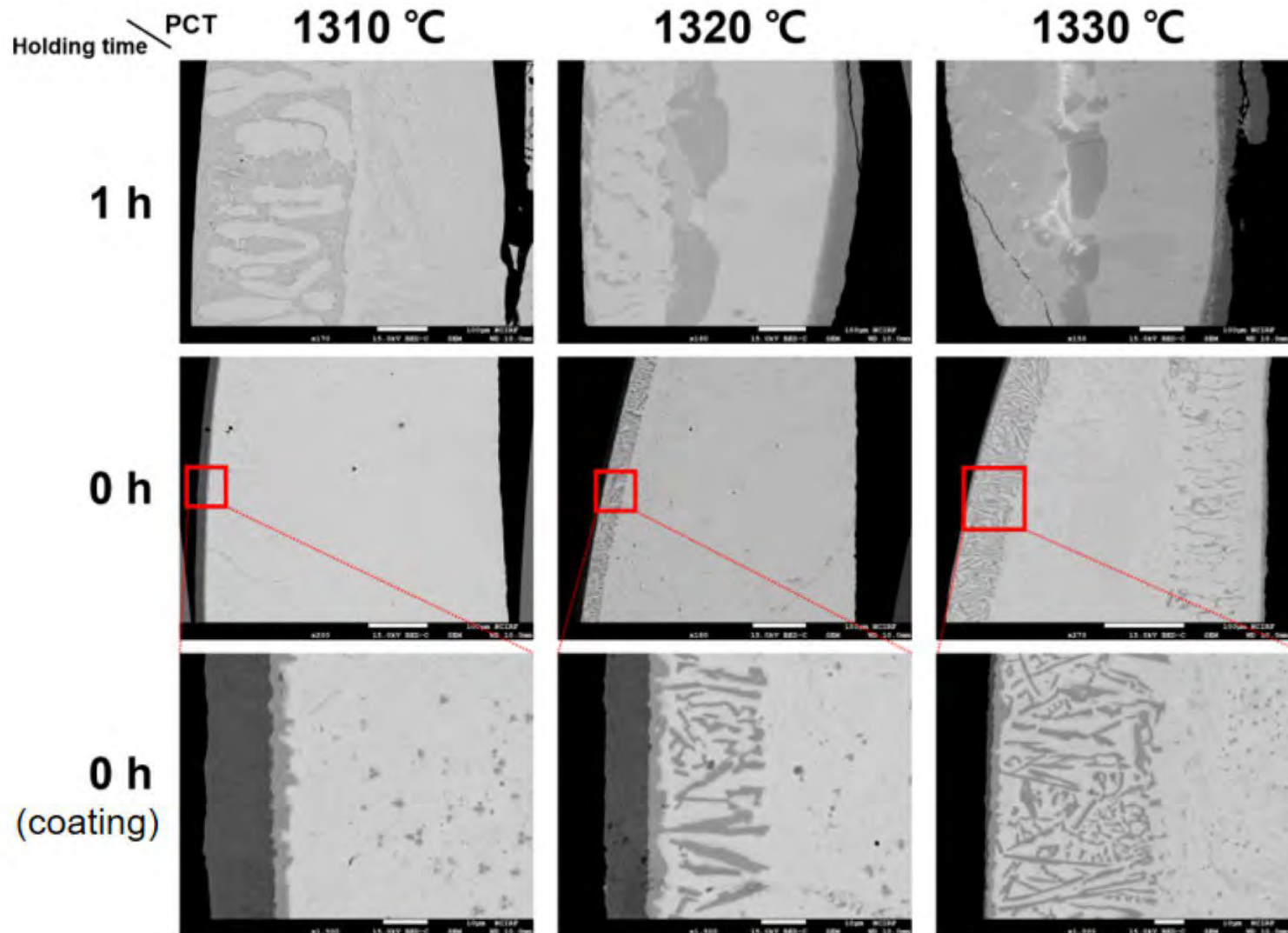
<Calculated time to reach 99% and 50% conversion>

- There could be a several minutes of coping time for PCT about 10 °C higher than onset temperature
- Above PCT of 1350 °C, the eutectic reaction will be completed in a few seconds.

# Characterization of eutectic reaction

## Result 3: Variable PCT and holding time

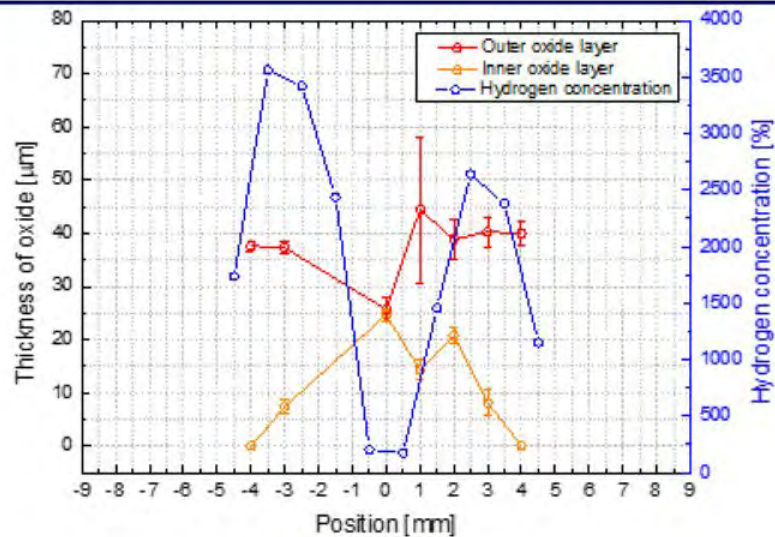
- Until PCT of 1320 °C , immediate cooling can maintain coating with heating rate of 20 °C/min



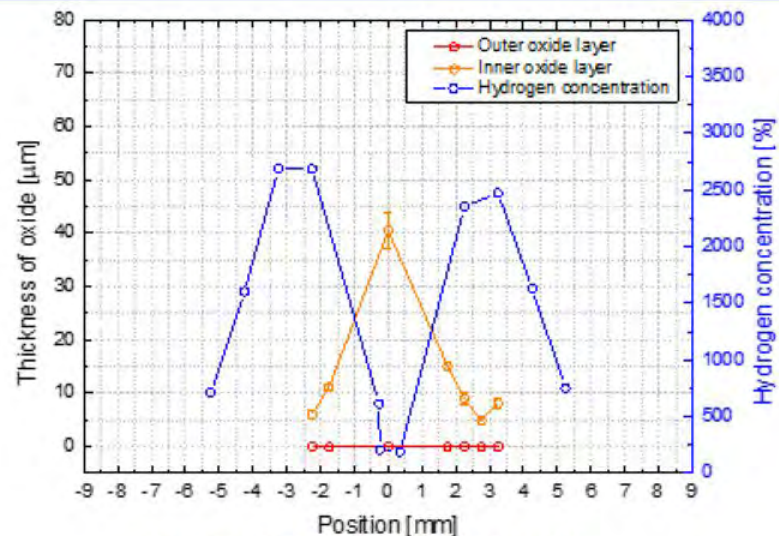
<BE-SEM image of specimen with various PCT and holding time>



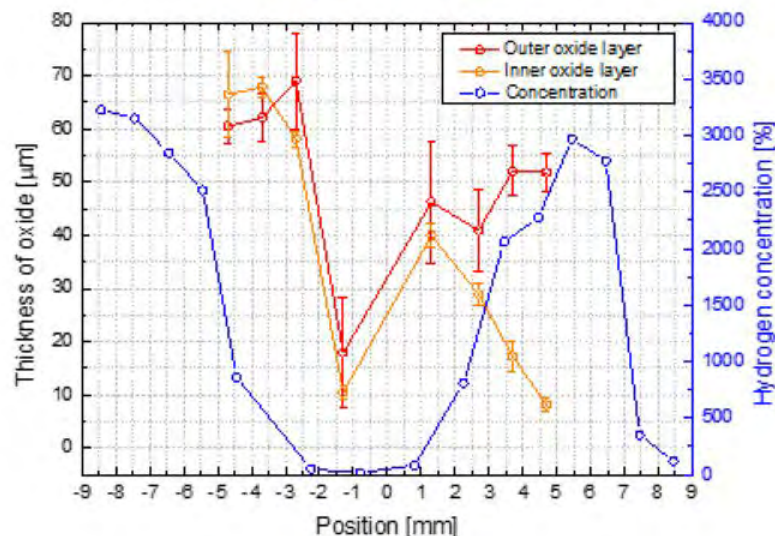
# 11.



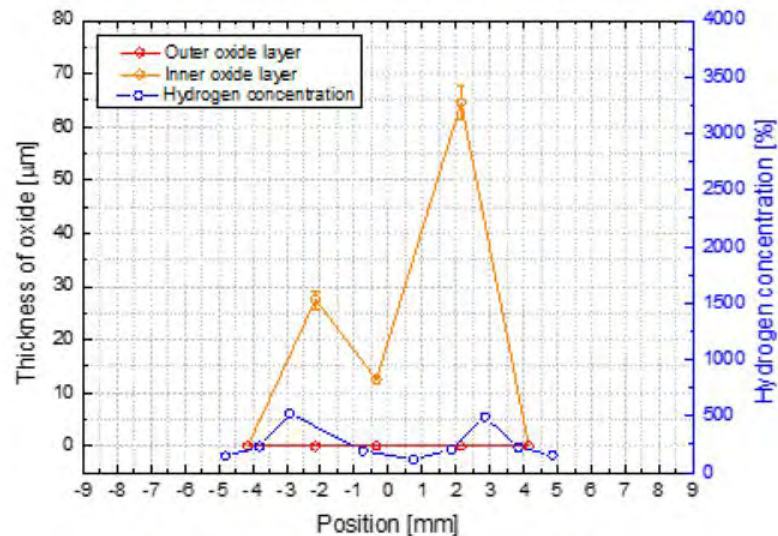
**< ZIRLO with  
cylinder pellet burst test >**



**<Cr coated cladding (Zr-Cr-1.1Nb)  
with cylinder pellet burst test>**



**< ZIRLO with  
powder pellet burst test >**



**<Cr coated cladding (Zr-Cr-1.1Nb)  
with powder pellet burst test>**



**J.-C. Brachet**

**Univ. Paris-Saclay, CEA**

**Effect of Cr content on the on-cooling phase transformations and induced prior- $\beta_{Zr}$  mechanical hardening and failure mode (*in relation with E-ATF Cr Coated Zr-based claddings behavior upon and after high temperature (LOCA) transients*)**

Chromium coated zirconium based nuclear fuel claddings are studied within the CEA-Framatome-EDF French nuclear fuel joint program as a short-term “Enhanced Accident Tolerant Fuel” (EATF) concept. It has already been demonstrated that, in hypothetical accident conditions such as Loss-of-Coolant-Accident (LOCA), 10-20  $\mu\text{m}$  thick Cr coating slows down the High Temperature (HT) steam oxidation overall kinetics and improves induced Post-Quenching (PQ) cladding strength and ductility. However, upon HT steam oxidation of Cr-coated Zr based nuclear fuel claddings, chromium diffusion occurs within the  $\beta_{Zr}$  metallic substrate, thus contributing to the overall Cr-coating consumption kinetics.

In the present study, it is shown that, depending of the cooling scenario from the high oxidation temperature applied, the mechanical response of the Cr-enriched prior- $\beta_{Zr}$  layer of Cr-coated Zr based alloy is quite different. Among the different results obtained and thanks to preliminary thermodynamic calculations and study of Cr-doped Zr1Nb(O) model alloys, it is shown that:

- after direct water quenching from high oxidation temperature (*i.e.*,  $\beta_{Zr}$  temperature range), the observed hardening and potential embrittlement at RT of the chromium enriched prior- $\beta_{Zr}$  metallic substrate should be related to martensitic Cr-supersaturated prior- $\beta_{Zr}$  structure formation, with a linear chromium solid-solution strengthening effect up to 1.5 wt.% Cr. Beyond 2.5 wt.% Cr, a smooth decrease of prior- $\beta_{Zr}$  hardness is observed.
- improved Cr-enriched prior- $\beta_{Zr}$  layer ductility has been observed following more LOCA-prototypical “two-steps” cooling scenario (*with a final water quenching from 700°C*), and has been related to the early precipitation of most of the available chromium as coarse ZrCr<sub>2</sub> Second Precipitated Phases (SPPs), upon cooling from the prior- $\beta_{Zr}$  temperature range.

*Communication based on a presentation done at the 20<sup>th</sup>. Int. ASTM Symposium on Zr in the Nuclear Industry, Ottawa, Canada, June 2022. Associated paper to be published in ASTM STP*



27th. Int. QUENCH Workshop, KIT,  
Karlsruhe, Germany, Sept. 27-29, 2022



**Effect of Cr content on the on-cooling  
phase transformations and induced  
prior- $\beta_{Zr}$  mechanical hardening and  
failure mode (*in relation with LOCA  
behavior of Cr coated  
(E-ATF) Zr based claddings*)**

DE LA RECHERCHE À L'INDUSTRIE

- ⇒ *Presentation already done at the 20TH INTERNATIONAL SYMPOSIUM ON ZIRCONIUM IN THE NUCLEAR INDUSTRY, June 20-23, 2022, Ottawa, Ontario, Canada*
- ⇒ *Associated full-length paper to be published in next-coming ASTM-STP*

*J.-C. Brachet, P. Gokelaere, T. Guilbert, C. Toffolon-Masclat, S. Urvoy, M. Dumerval, G. Nony, J. Braun, H. Palancher, K. Buchanan, E. Pouillier, T.M. Vu, J.-M. Joubert*



*Cr coated M5<sub>Framatome</sub> upon LOCA*

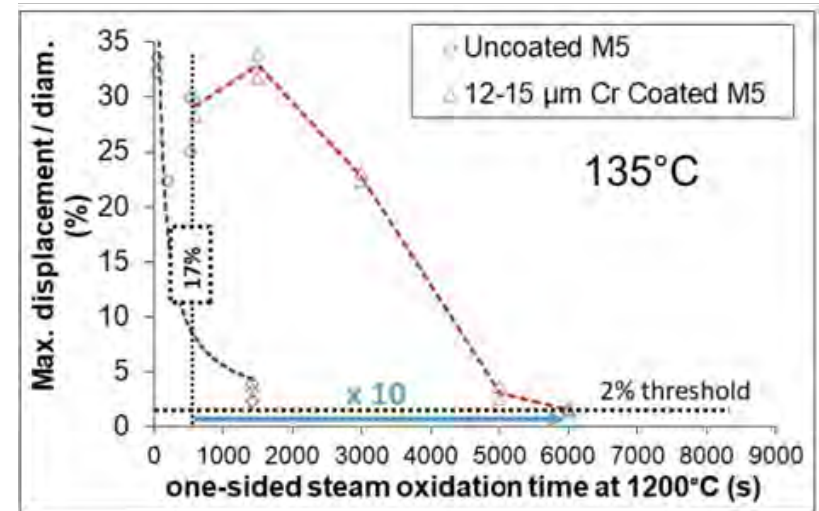
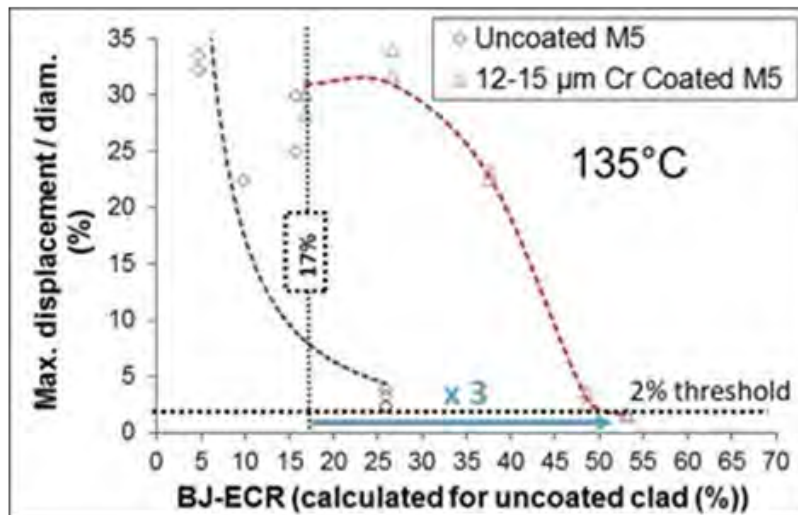
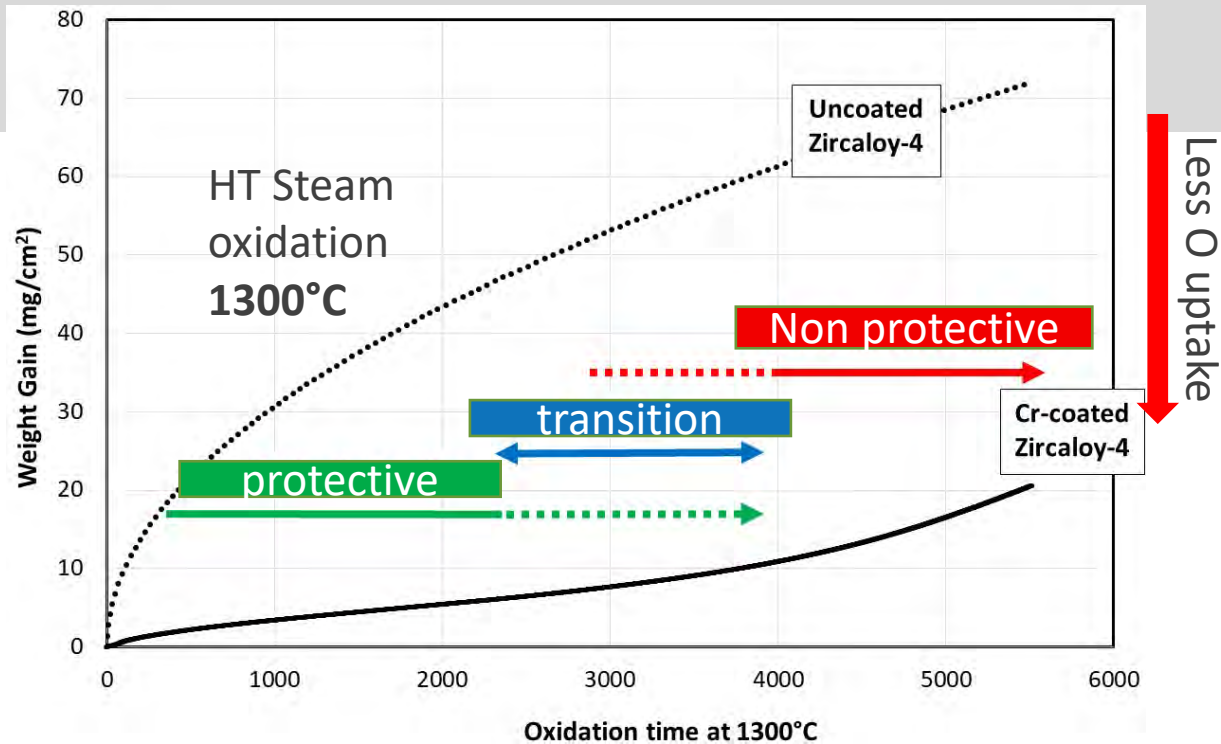
*Study of “model” materials : Zr1Nb(O)+Cr*

*Conclusions and on-going/further work*

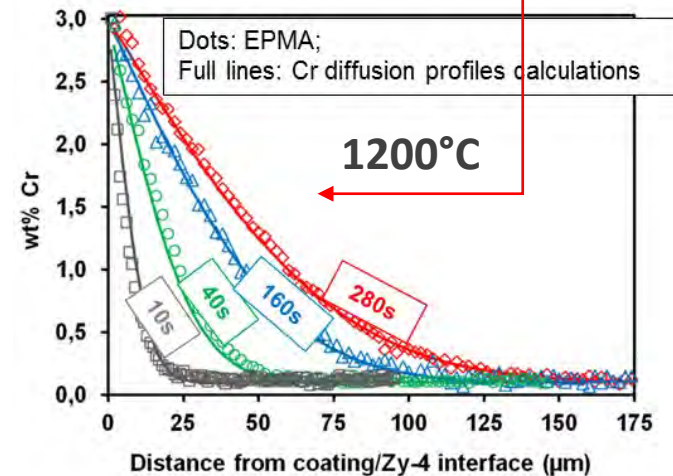
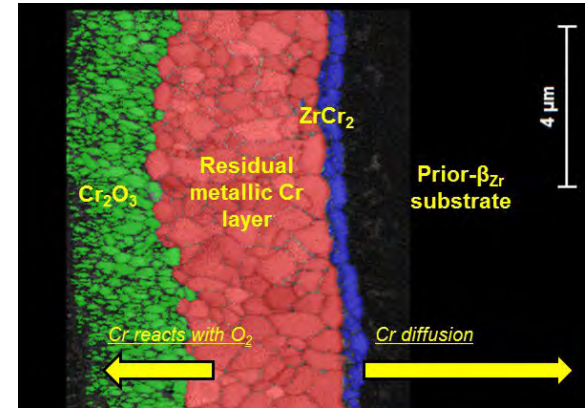
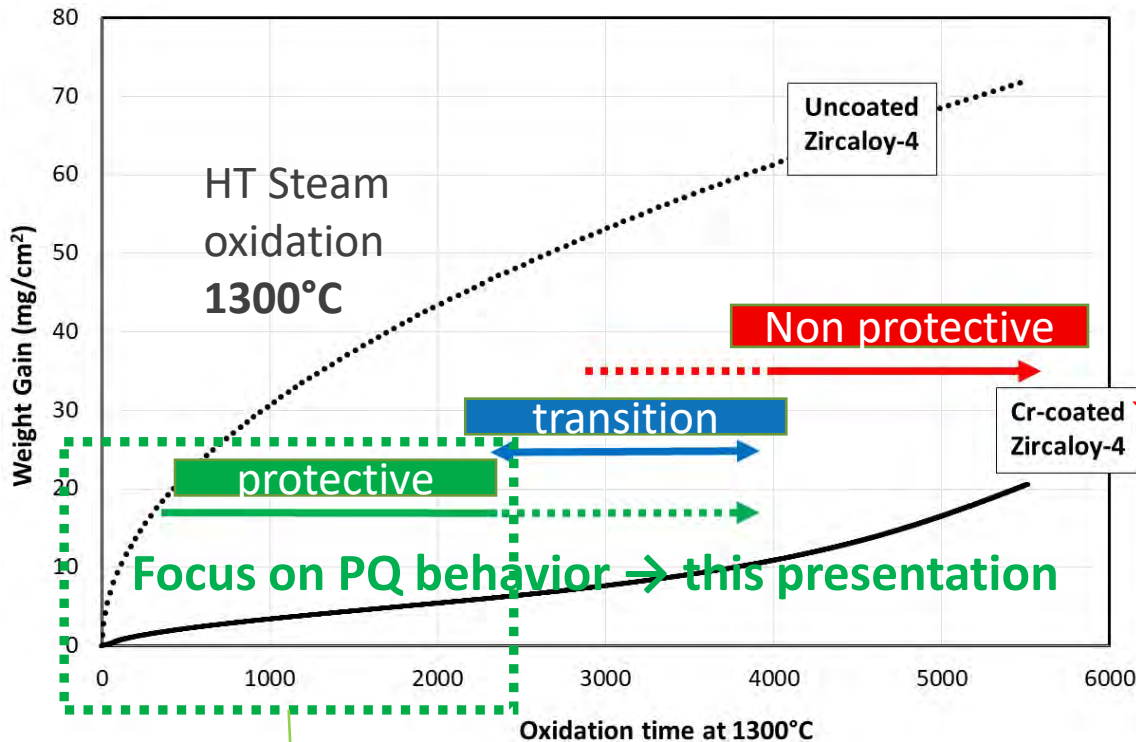


Coated zirconium claddings were developed to specifically slow down HT oxidation in steam and thus to delay the PQ clad hardening & embrittlement

Steam oxidation at 1200°C + direct water quenching down to RT, PQ RCT:

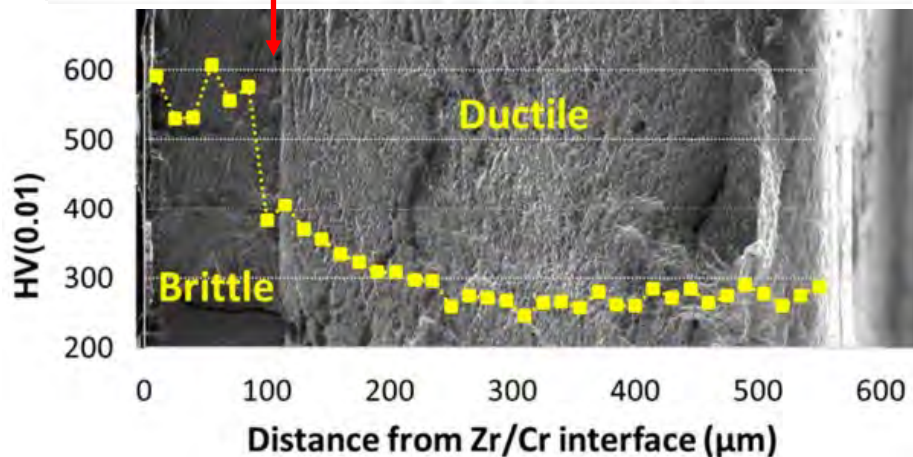
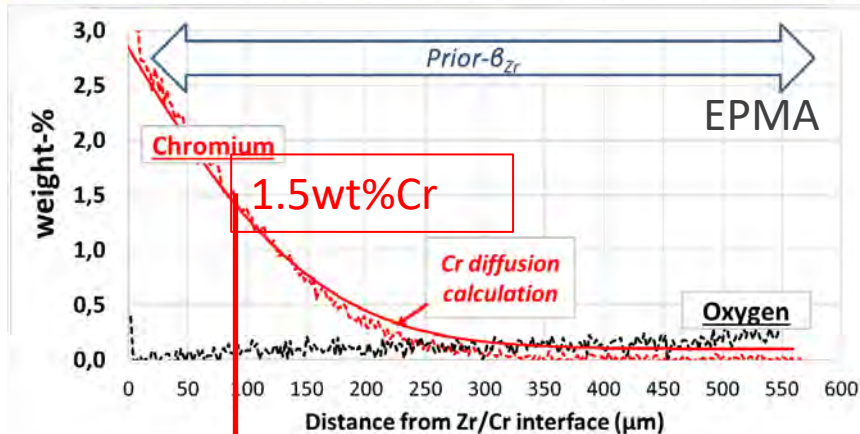
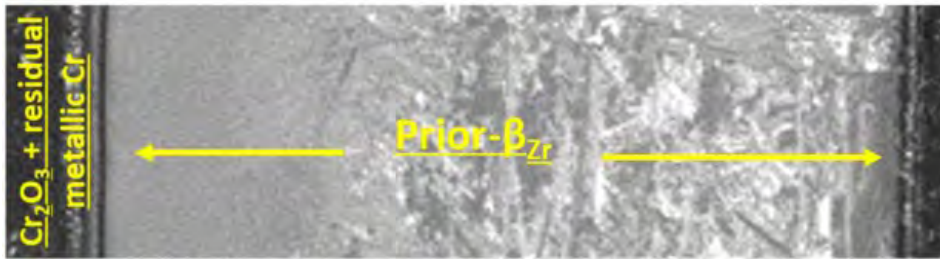


Coated zirconium claddings were developed to specifically slow down HT oxidation in steam and thus to delay the PQ clad hardening & embrittlement



As long as the Cr coating is protective, Oxidation kinetics, overall parabolic, almost 10 times slower than uncoated Zr ;

1. outer Cr<sub>2</sub>O<sub>3</sub> scale formation,
2. Inward Cr diffusion into the β<sub>Zr</sub> substrate.

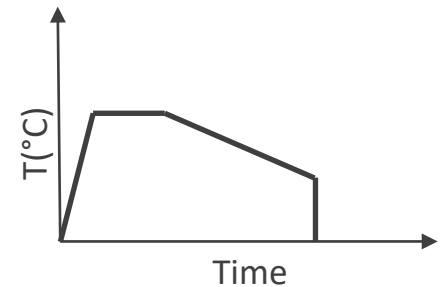
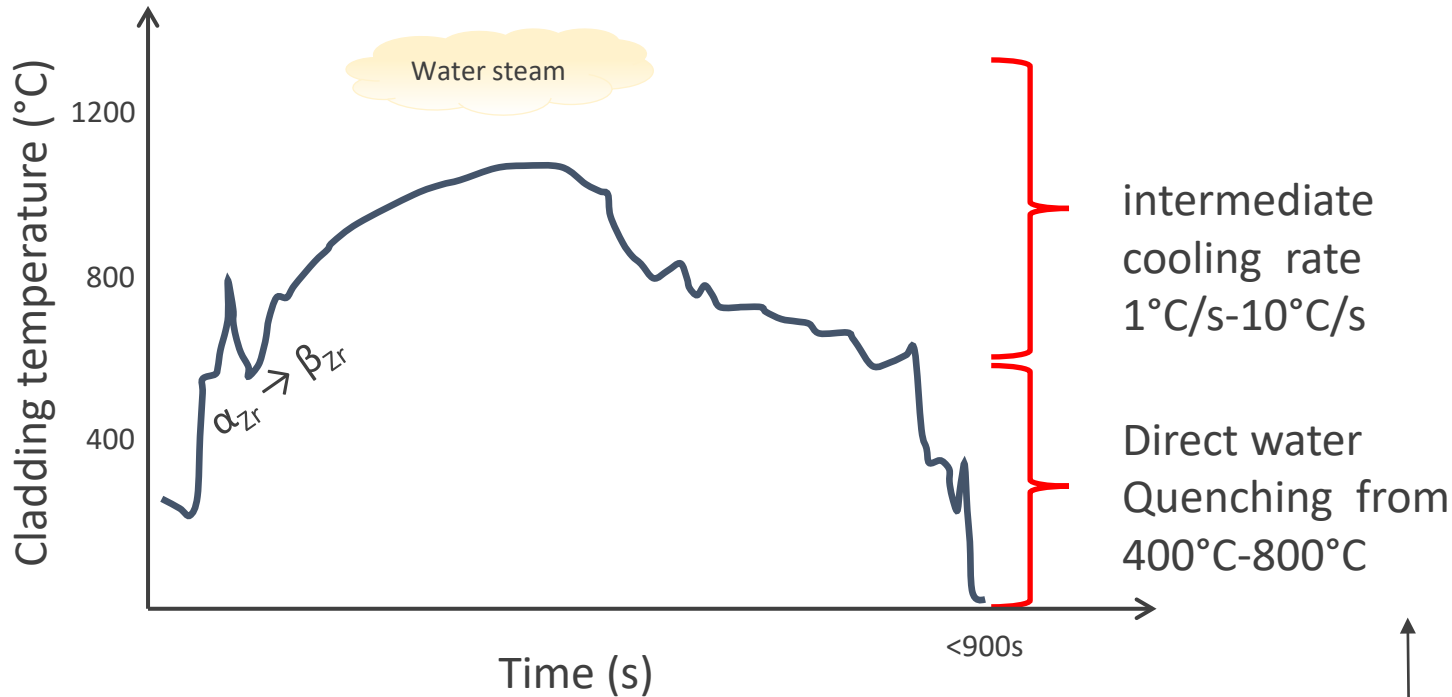


- After oxidation at 1200°C for 1500s (ECR<sub>Bj</sub> 27%): ~15μm thick Cr coating is fully protective
  - No formation of ZrO<sub>2</sub> and α(O) brittle layers,
  - No O ingress/diffusion in β<sub>Zr</sub>
- Chromium has diffused throughout the cladding inducing a diffusion profile,
- Fractographic analysis shows a **brittle behavior at RT** in the region where the Cr content is **beyond 1,5wt%Cr** and ductile elsewhere,
- Sharp DBT with HV transition

- After direct water quenching following HT oxidation, Cr enrichment in prior-β<sub>Zr</sub> induces PQ clad hardening, and embrittlement beyond 1,5wt%

M5<sub>Framatome</sub> is a trademark or registered trademark of Framatome or its affiliates, in the USA or other countries.

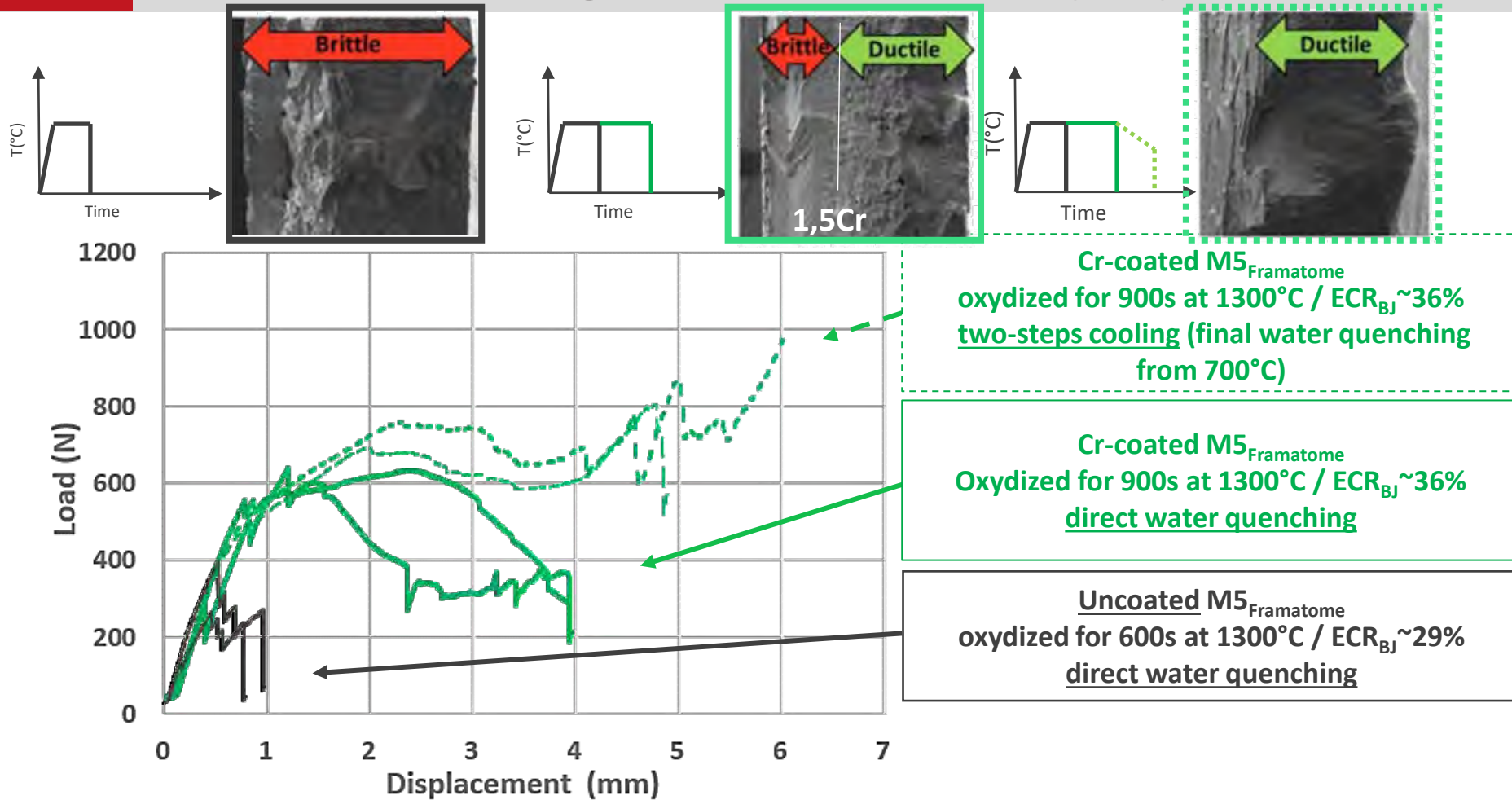
Schematic typical LOCA transient



What would be the effect of a “two steps cooling” (\*) scenario on PQ mechanical properties of Cr-coated Zr based claddings ((\*) *more prototypical of LOCA transient*) ?



# PQ Ring Compression Testing (RCT) after steam oxidation at 1300°C “Design Extension Conditions (DEC)”



- Enhanced residual ductility of Cr coated vs uncoated M5<sub>Framatome</sub>
- Significant effect of the cooling scenario on residual Cr-coated clad ductility

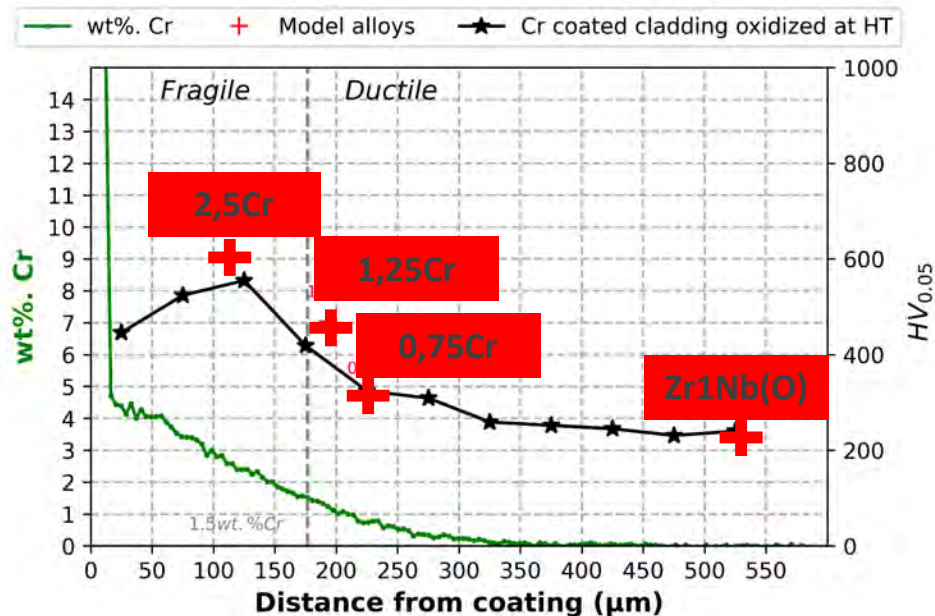
*Cr coated M5<sub>Framatome</sub> upon LOCA*

*Study of “model” materials : Zr1Nb(O)+Cr*

*Conclusions and on-going/further work*

## Dynamic conditions

- Study of Cr enriched Zr1Nb(O) alloys, in dynamic conditions more prototypical of LOCA transient (CCT...).



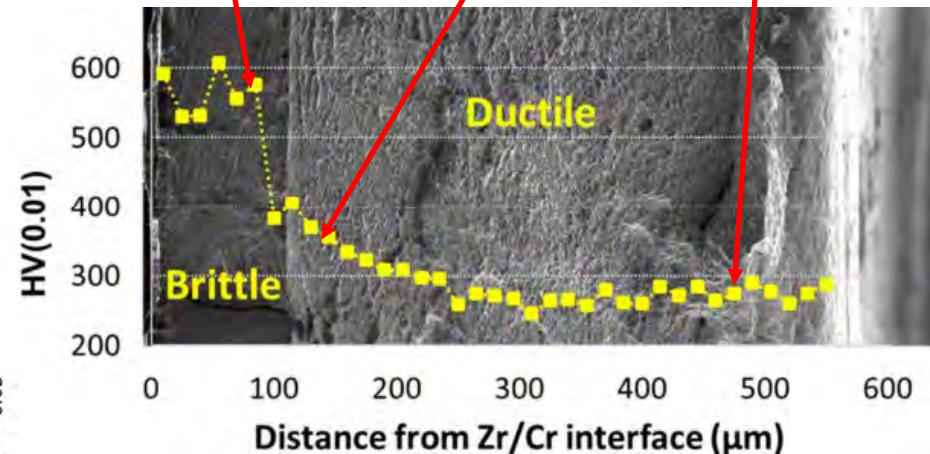
PQ hardness of model alloys being consistent with the local hardening of “real” Cr-coated claddings following HT oxidation and direct water quenching

## Model alloys (as cast):

Zr1Nb(O)  
+2,5wt%Cr

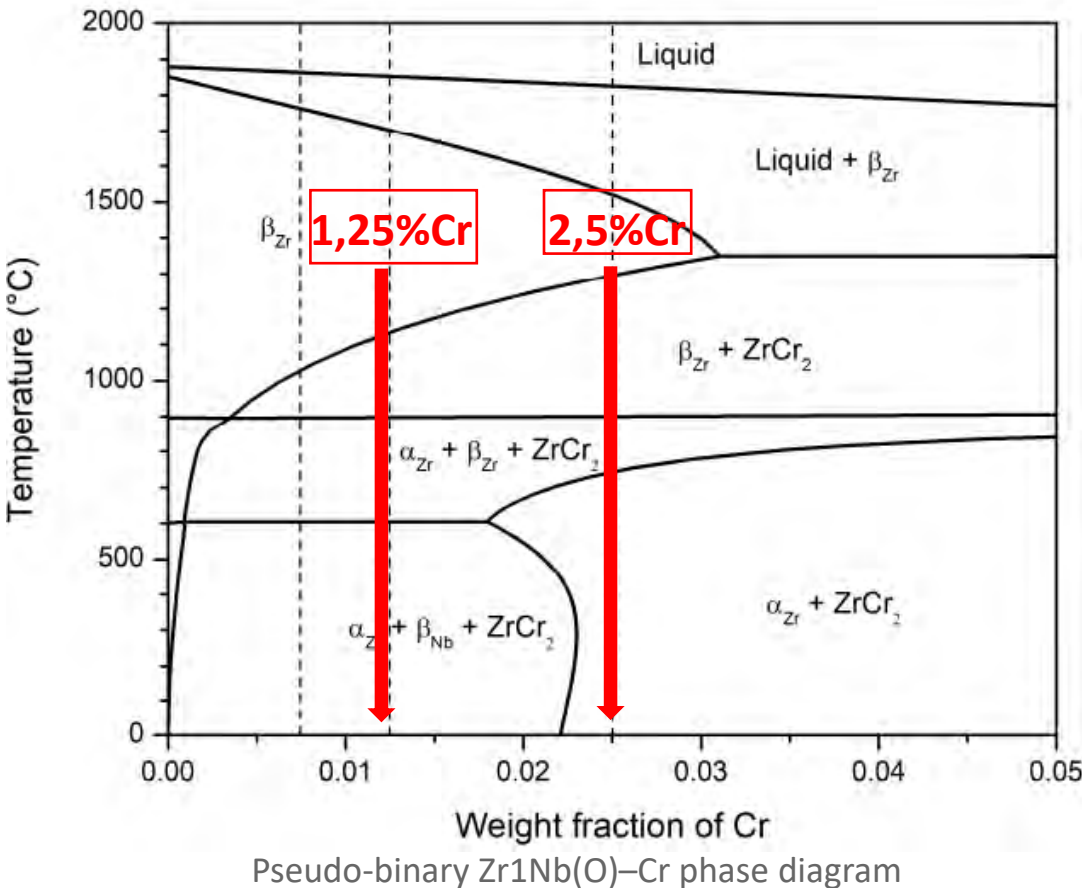
Zr1Nb(O)  
+1,25wt%Cr

Zr1Nb(O)  
M5<sub>Framatome</sub>

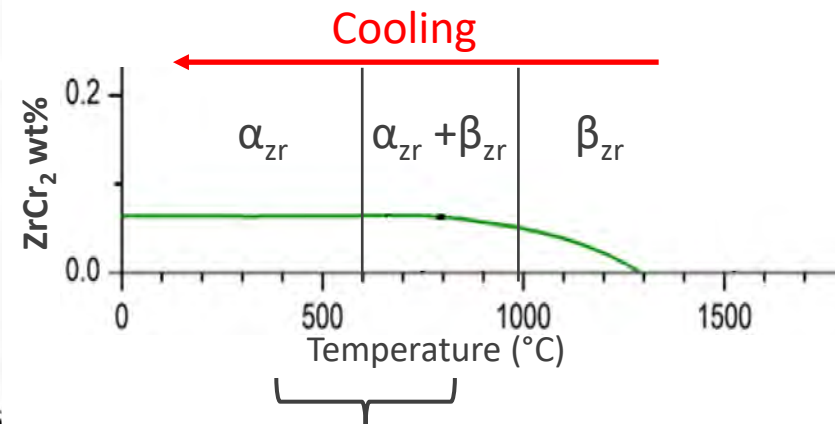


### Thermodynamics at equilibrium

- Zr-Cr-O-(Nb) equilibrium phase diagram: Experimental study and Calphad modelling (*on going PhD work, not developed here... further work by T-M. VU and P. GOKELAERE*)



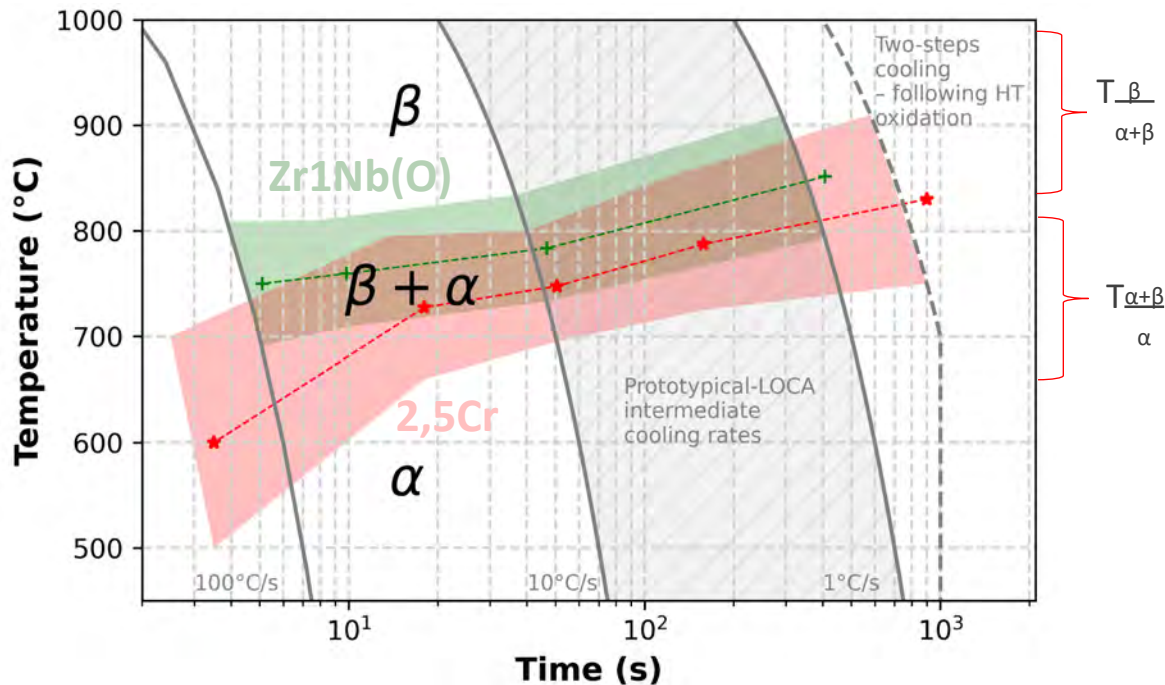
- Full Cr precipitation as LAVES-C15  $ZrCr_2$  at RT,
- Precipitation starts in the  $\beta_{Zr}$  temperature range,
- Upon cooling from  $\beta_{Zr}$  when reaching intermediate temperatures [800°C;400°C] most of the Cr has precipitated.



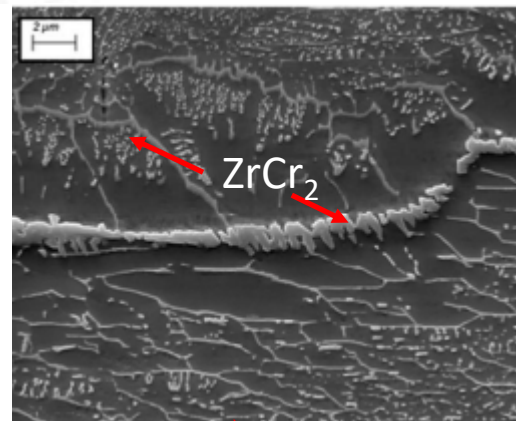
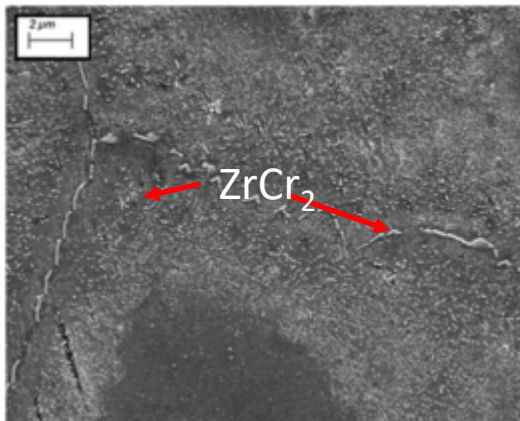
Intermediate LOCA Temperatures



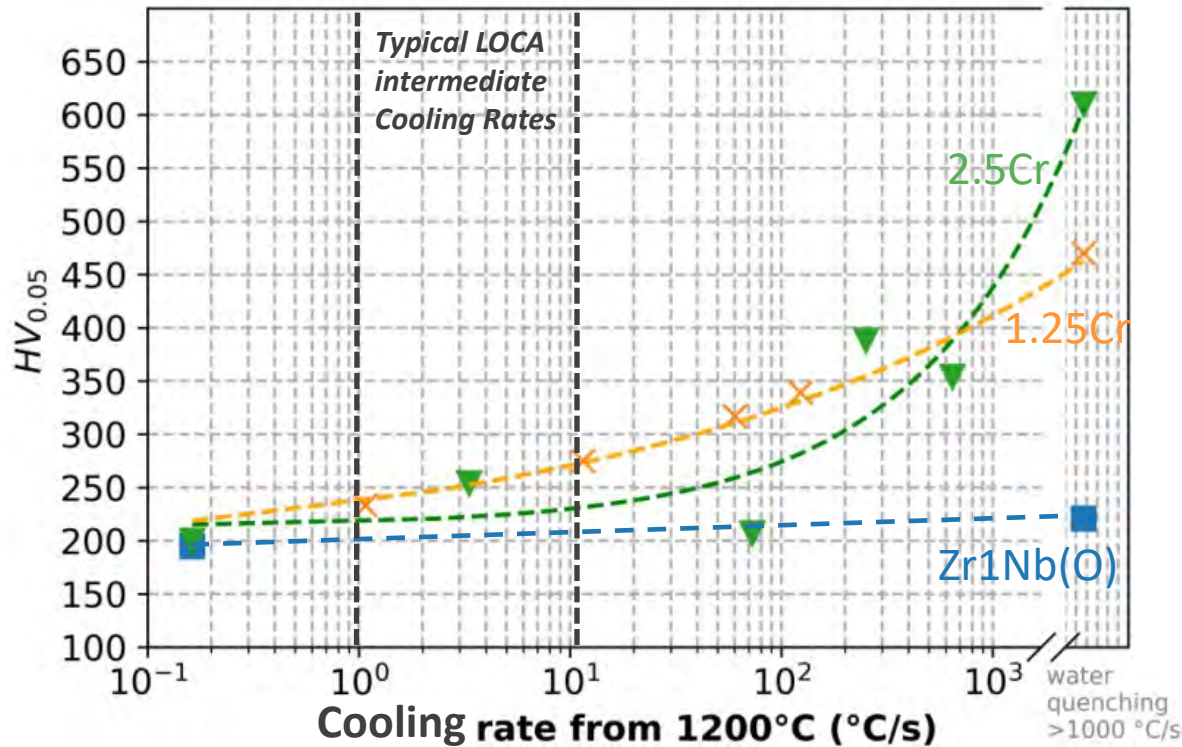
# Evolution of transformations temperatures from prior- $\beta_{Zr}$ in dynamic conditions: CCT diagram (dilatometry)



- Transformation temperatures decrease when cooling rates increase,
- Addition of Cr decreases  $\beta_{Zr} \rightarrow \alpha_{Zr}$  temperatures,
- Coarser  $ZrCr_2$  SPPs for lower cooling rates,
- Preferential and coarser precipitation at prior- $\beta$  grain boundaries, *consistent with thermodynamics calculations predicting early  $ZrCr_2$  precipitation in the  $\beta_{Zr}$  temperature range.*



Decreasing cooling rates



Evolution of Hv with respect to quenching rates from 1200°C

How to explain the hardening ?

- Solid solution strengthening ?
- SPPs strengthening ?
- Displacive martensitic-like  $\alpha'$  transformation ?
- Metastable  $\Omega$  phase formation ?
- ...

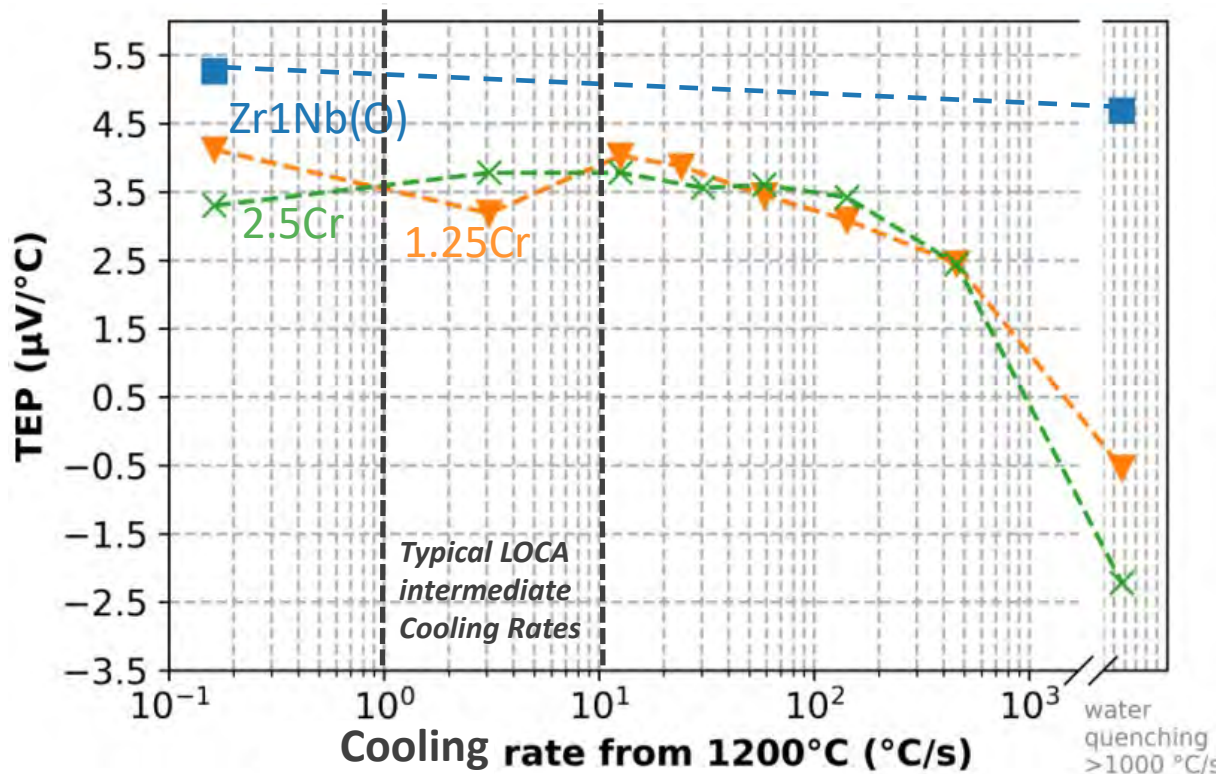
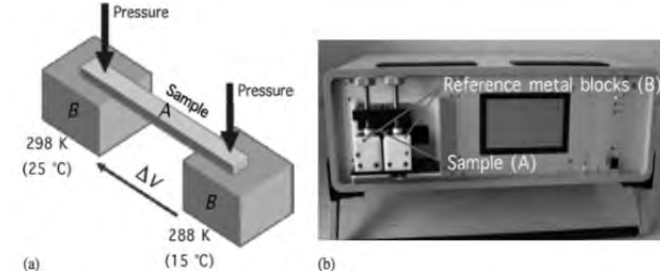
### Zr1NbO

- Limited hardness evolution with respect to the quenching rates

### Zr1NbO+Cr

- The higher quenching rate, the higher  $Hv_{0,05}$
- Limited evolution for a rate  $\in ]0; 100]^{\circ}\text{C/s}$
- Drastic increase for water quenching

- TEP measurements known to be sensitive to chemical composition of metallic solid solution,
- Already use to quantify iron, tin and oxygen in solid solution of Zr based alloys.



Evolution of TEP with respect to quenching rates from 1200°C

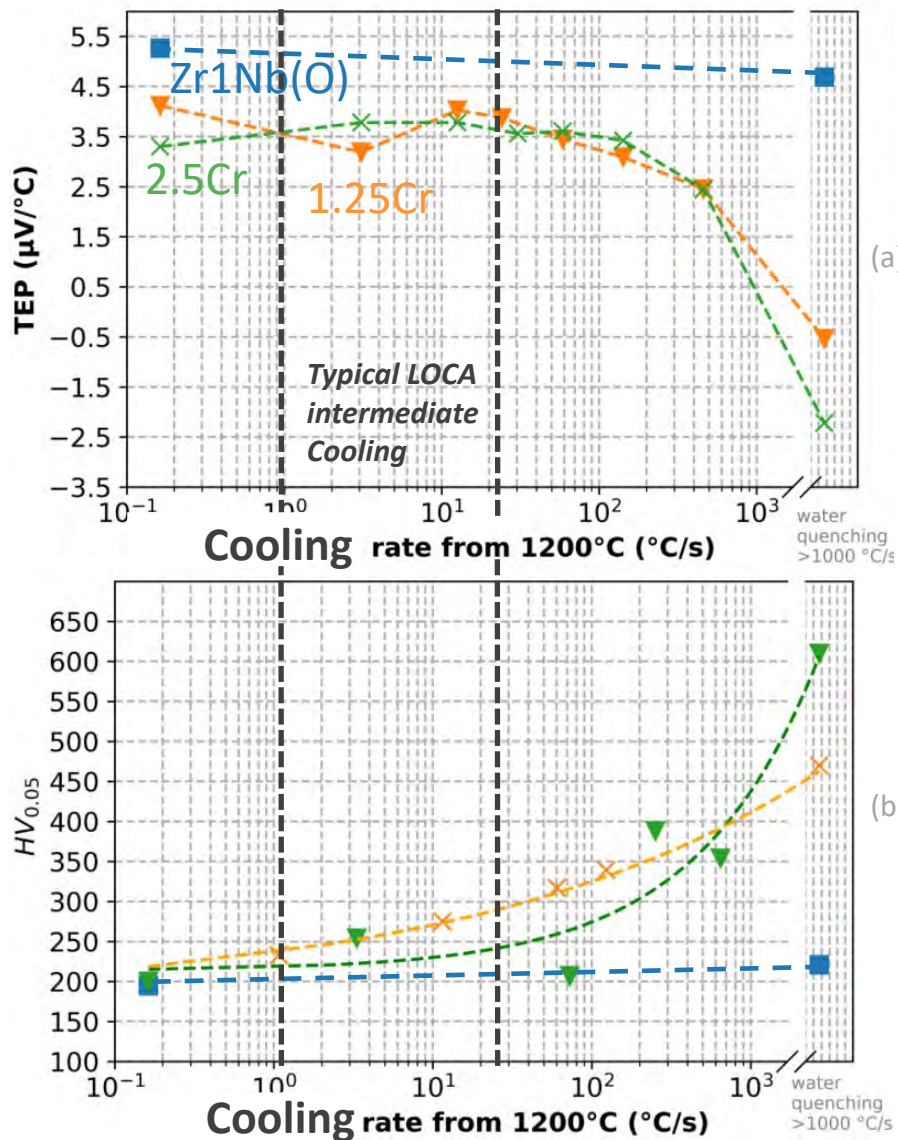
## Zr1NbO

- Doesn't seem to change much with the quenching rates

## Zr1NbO+Cr

- The higher quenching rate, the lower TEP
- Limited evolution for a rate  $< \sim 100^\circ\text{C/s}$
- Drastic decrease for water quenching



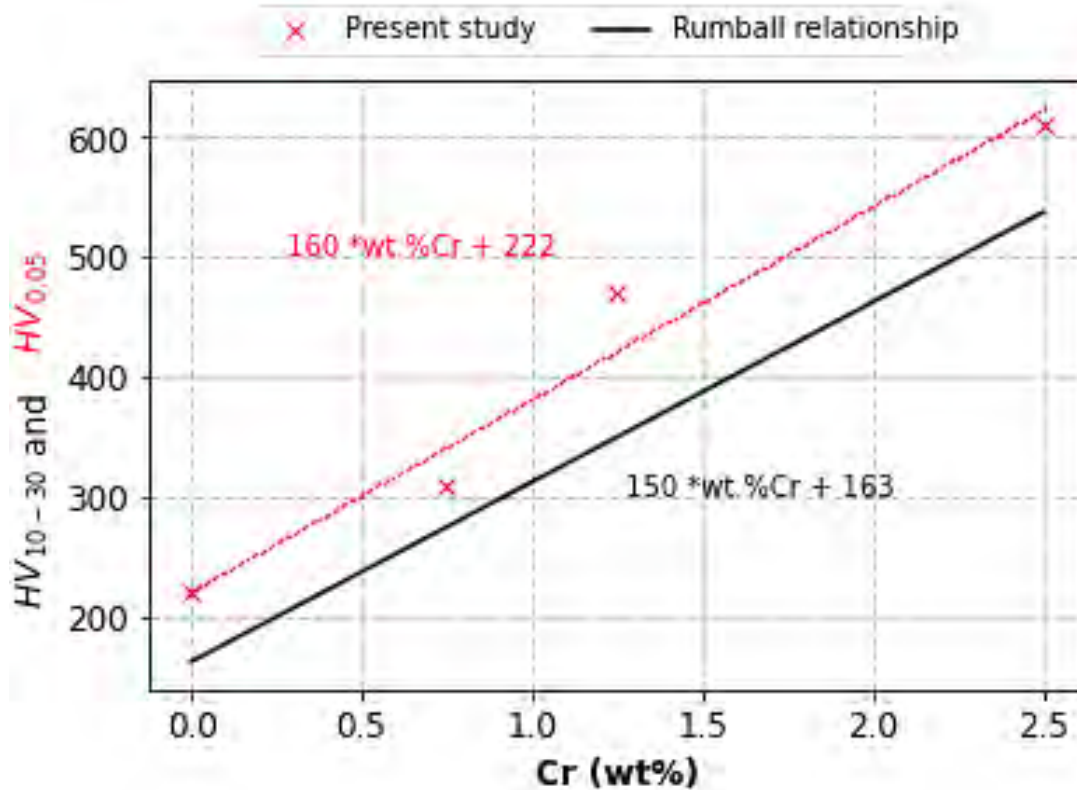


- Zr1Nb(O) shows limited evolution
- Both experiments show Limited evolution until a few hundreds of  $^\circ\text{C}/\text{s}$ ,
- Abrupt increase/decrease is observed when reaching water quench cooling rates,
- Since TEP is sensitive to solid solution, at first it is assumed that prior- $\beta$  strengthening hardness is mainly due to solid solution strengthening effect of Cr (PQ supersaturated prior- $\beta_{\text{Zr}}$ ).
- Upon prototypical LOCA “two-steps” cooling scenario, less Cr in PQ prior- $\beta_{\text{Zr}}$  supersaturated solid-solution

➔ ductile behavior

Evolution of Vickers hardness (a) and TEP (b) with respect to quenching rates from 1200°C





## Rumball study

Empirical relationship for  $\beta$ - quenched ZrCrO alloys

## Present study:

Hardness of **water quenched** model alloys Zr1Nb(O) + Cr assuming that all the available Cr in solid solution, consistent with Rumball prediction

However: the existence of other potential  $\mu$ structural hardening mechanisms (thinner grain sizes,  $\mu$ twinning, Omega phase precipitation... will need further investigations...

$$VPN = (0,05 \times ppm O) + (150 \times wt\% Cr) + \Delta h_i + \Delta h_s + 65$$

**Solid solution**

**Structure ( $\alpha^*$ ,  $\alpha'$ ,  $\Omega$ )**

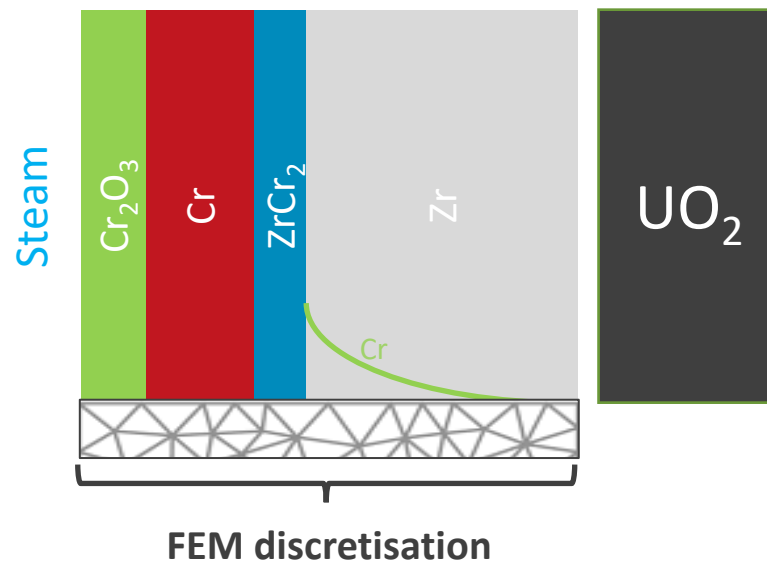
*Cr coated M5<sub>Framatome</sub> upon LOCA*

*Study of “model” materials : Zr1Nb(O)+Cr*

**Conclusions and on-going/further work**

- Upon HT steam oxidation (LOCA) of Cr-coated Zr based nuclear fuel claddings, Cr diffusion in  $\beta_{Zr}$  metallic substrate → significant PQ hardening and DBT of water quenched prior- $\beta_{Zr}$  failure mode at RT beyond 1.5 wt.% Cr;
- Applying a more LOCA-prototypical “two-steps” cooling scenario → significant ductility restoration;
- Both thermodynamic predictions and experimental study of Cr enriched Zr1Nb(O) alloys showed that it may rely mostly on the residual prior  $\beta_{Zr}$  Cr content in supersaturated solid solution (*need however further investigations...*)
- After HT oxidation, even while considering the most penalizing cooling scenario (*direct water quenching from  $\beta_{Zr}$* ), PQ Cr-coated materials behave significantly better than the uncoated ones;
- Under the same critical conditions, the thickness affected by Cr diffusion is much lower than the one affected by O diffusion in uncoated reference cladding.

- Better thermodynamic assessment of Zr-Cr-O-(Nb) phase diagram,
- Further characterizations of quenched Cr enriched prior  $\beta_{Zr}$  microstructures (XRD, TEM, APT ...)
- Further mechanical characterization on model alloys for different cooling scenario in order to derive constitutive mechanical laws vs. prior- $\beta_{Zr}$  Cr content...
- Final objective : link microstructural features to mechanical behavior (FE calculations ...)






# Thank you for your attention

## Some CEA references:

Journal of Nuclear Materials 517 (2019) 268–285

Contents lists available at ScienceDirect




**Journal of Nuclear Materials**

journal homepage: [www.elsevier.com/locate/jnucmat](http://www.elsevier.com/locate/jnucmat)

Early studies on Cr-Coated Zircaloy-4 as enhanced accident tolerant nuclear fuel claddings for light water reactors

Corrosion Science 167 (2020) 108537

Contents lists available at ScienceDirect




**Corrosion Science**

journal homepage: [www.elsevier.com/locate/corsci](http://www.elsevier.com/locate/corsci)

High temperature steam oxidation of chromium-coated zirconium-based alloys: Kinetics and process

Journal of Nuclear Materials 533 (2020) 152106

Contents lists available at ScienceDirect




**Journal of Nuclear Materials**

journal homepage: [www.elsevier.com/locate/jnucmat](http://www.elsevier.com/locate/jnucmat)

Evaluation of Equivalent Cladding Reacted parameters of Cr-coated claddings oxidized in steam at 1200 °C in relation with oxygen diffusion/partitioning and post-quench ductility

Journal of Nuclear Materials 550 (2021) 152953

Contents lists available at ScienceDirect



**Journal of Nuclear Materials**

journal homepage: [www.elsevier.com/locate/jnucmat](http://www.elsevier.com/locate/jnucmat)

DLI-MOCVD Cr<sub>x</sub>C<sub>y</sub> coating to prevent Zr-based cladding from inner oxidation and secondary hydriding upon LOCA conditions

Journal of Nuclear Materials 504 (2018) 289–299

Contents lists available at ScienceDirect



**Journal of Nuclear Materials**

journal homepage: [www.elsevier.com/locate/jnucmat](http://www.elsevier.com/locate/jnucmat)

HRTEM and chemical study of an ion-irradiated chromium/zircaloy-4 interface

*J Mater Sci* (2018) 53:9879–9895

**Review**

**Atomic-scale interface structure of a Cr-coated Zircaloy-4 material**



Article

**Radiation-Induced Sharpening in Cr-Coated Zirconium Alloy**

Journal of Nuclear Materials 558 (2022) 153332

Contents lists available at ScienceDirect



**Journal of Nuclear Materials**

journal homepage: [www.elsevier.com/locate/jnucmat](http://www.elsevier.com/locate/jnucmat)

Mechanical behavior of a chromium coating on a zirconium alloy substrate at room temperature

Acta Materialia 200 (2020) 570–580

Contents lists available at ScienceDirect



**Acta Materialia**

journal homepage: [www.elsevier.com/locate/actamat](http://www.elsevier.com/locate/actamat)

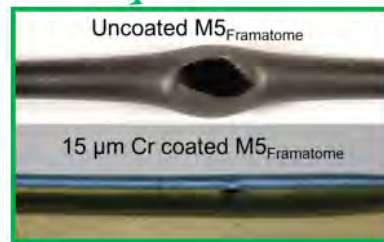
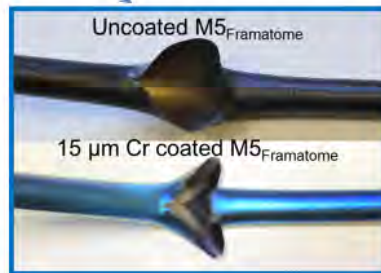
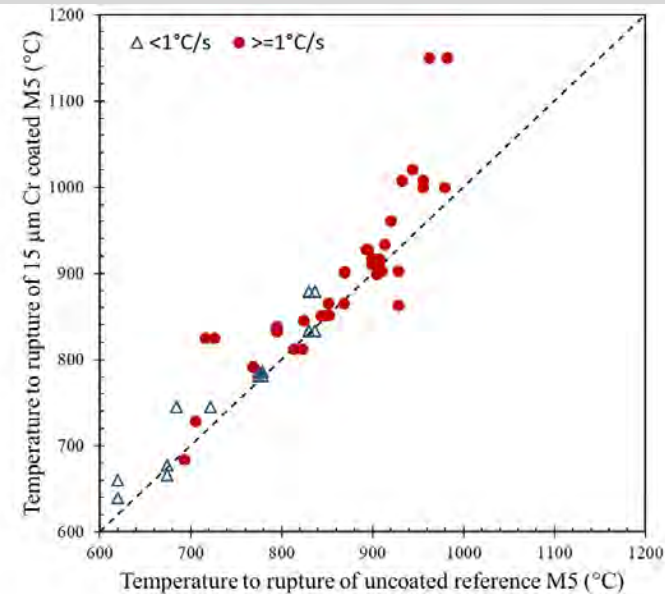
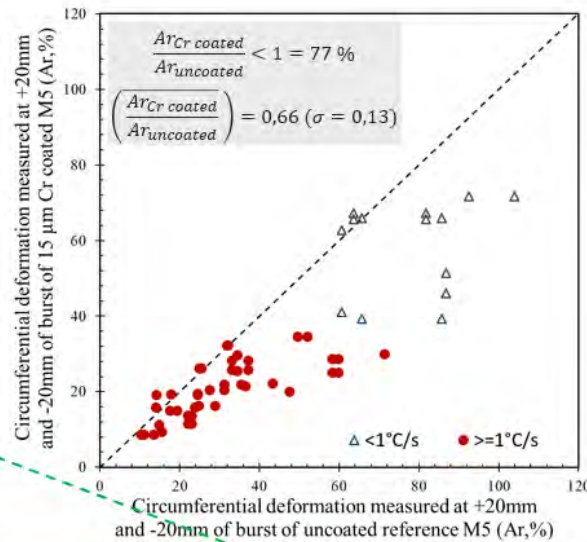
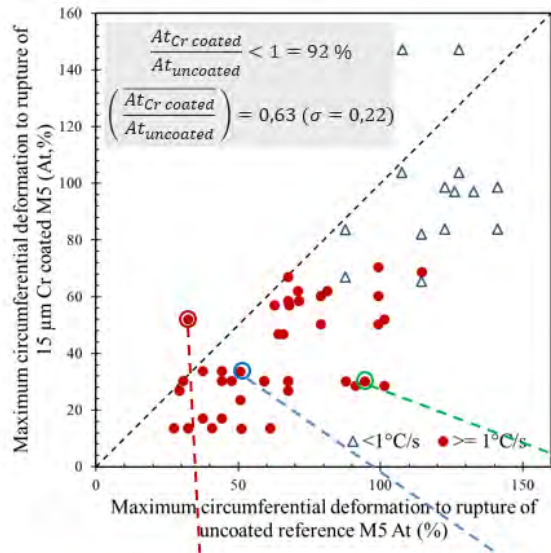
Full length article

Impact of magnetism on screw dislocations in body-centered cubic chromium

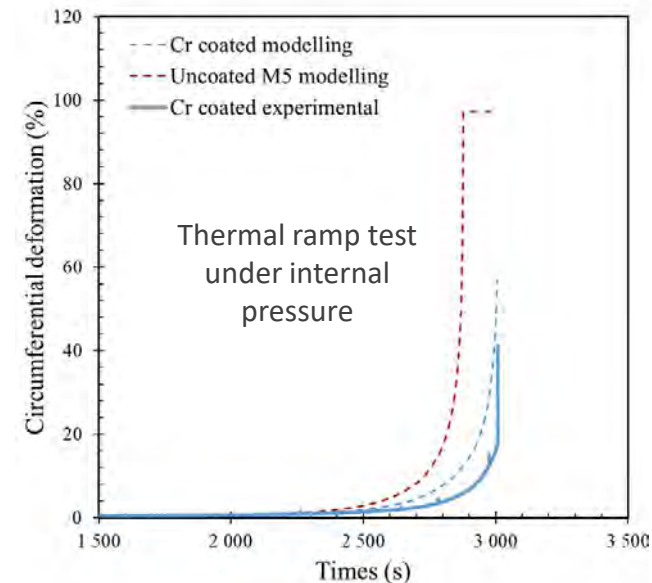
énergies

***Back slides...***

---



- **Lower ballooning and strengthening effect** are confirmed upon internal pressure (“EDGAR”) LOCA ramp tests
- Significant amount of experimental data
- **Modelling** efforts are on-going

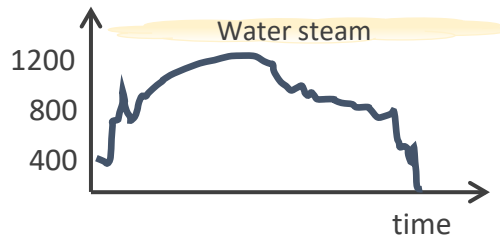


M5<sub>Framatome</sub> is a trademark or registered trademark of Framatome or its affiliates, in the USA or other countries.



# Uncoated Zr based cladding behavior upon LOCA: post HT oxidation residual strength and ductility

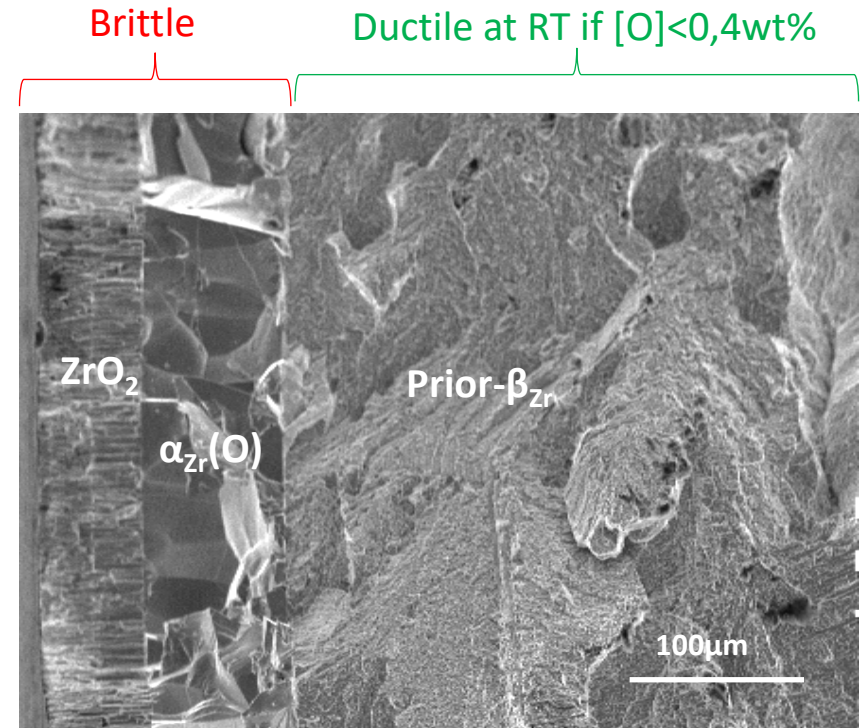
- Upon LOCA conditions, nuclear fuel assembly needs to maintain their integrity ( $ECR_{BJ} < 17\%$ ),



- Once the amount of oxygen is significant, the  $\alpha_{Zr}(O)$  is stabilized at high temperature,

Aim of E-ATF Cr-coated claddings:

- delay brittle  $ZrO_2$  and  $\alpha_{Zr}(O)$  layers formation and the O diffusion in  $\beta_{Zr}$



Fractography of Zy-4 oxidized for  $\sim 3$  min at  $1200^\circ\text{C}$  and quenched, mechanically tested at  $20^\circ\text{C}$

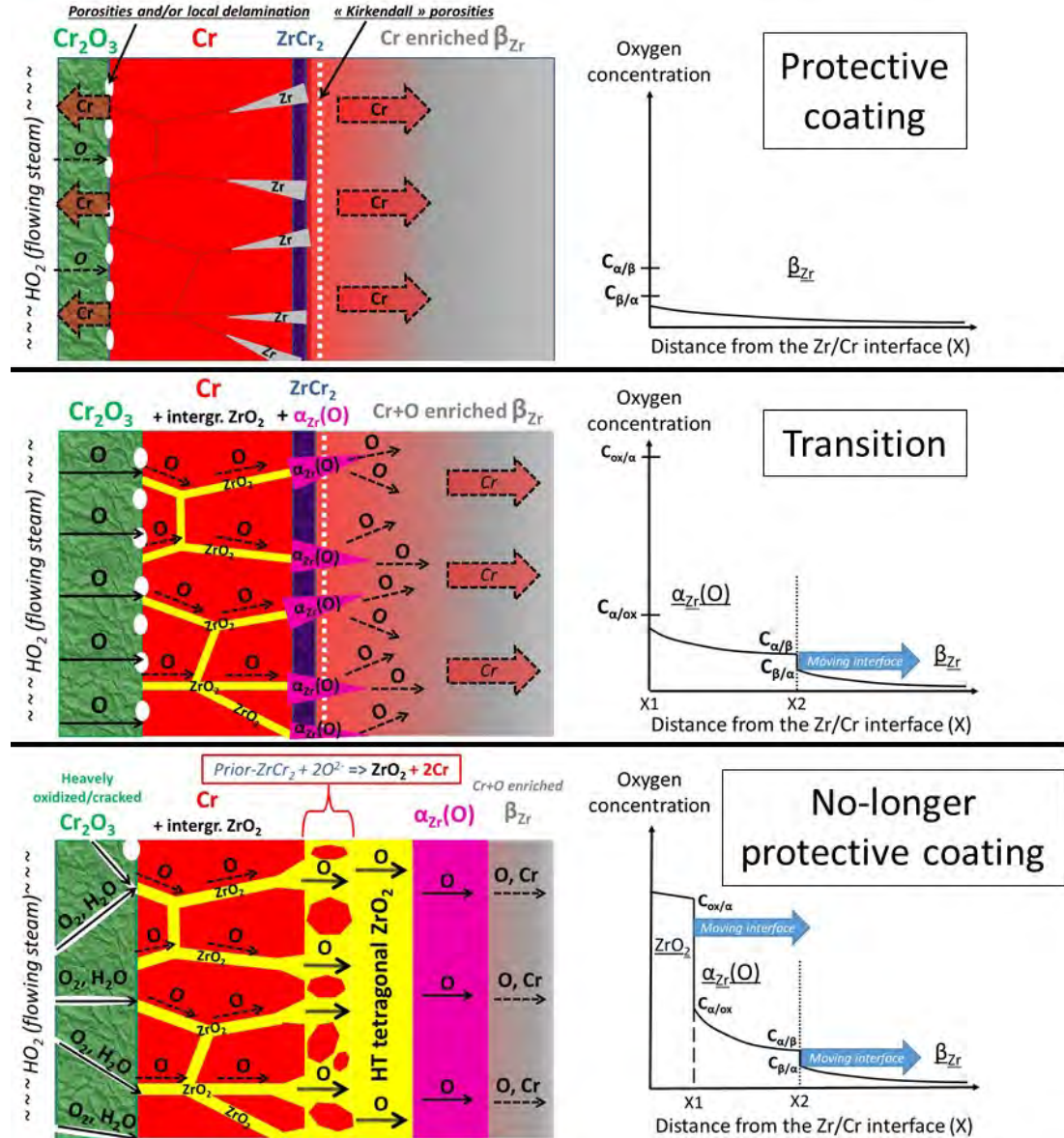
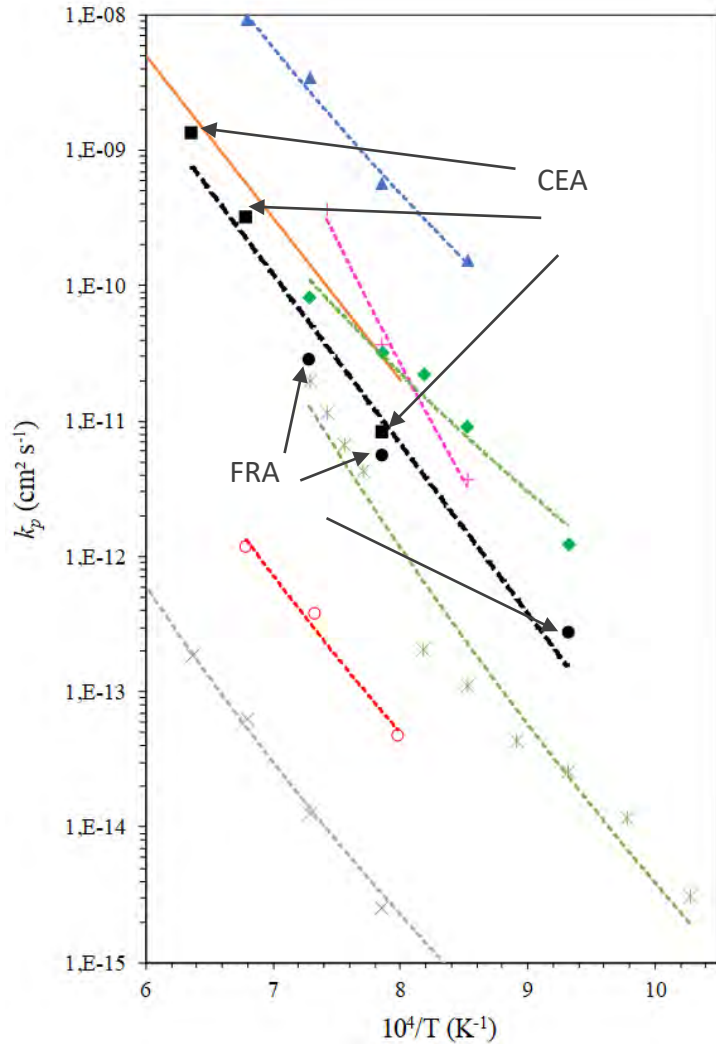
Réf. : Cabrera (2012)

## EATF evolutive solution: metallic Cr coating

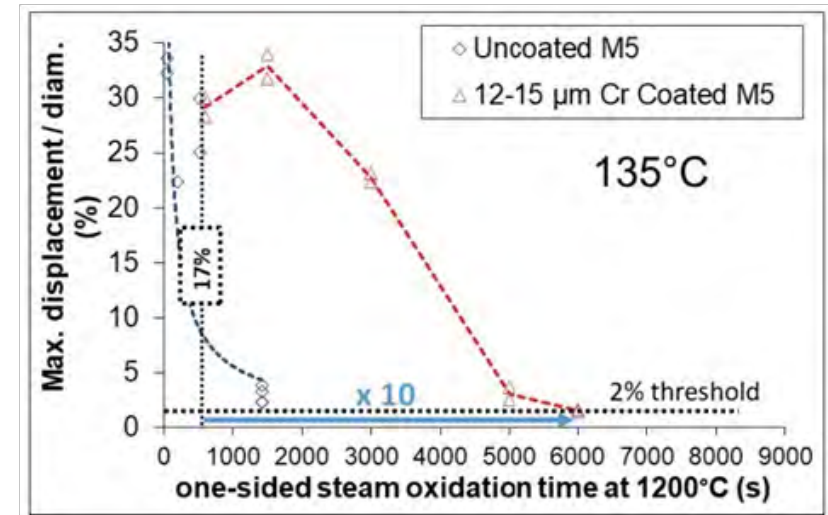
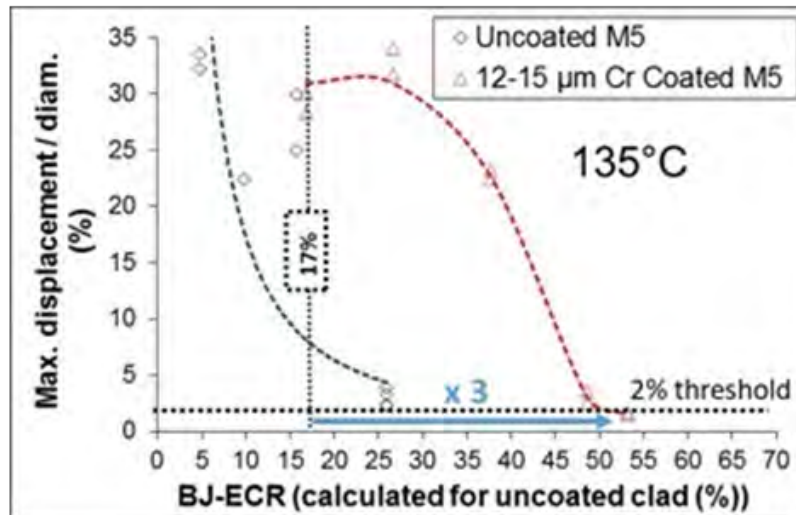
- In service condition : very limited corrosion, higher wear resistance ...
- In LOCA condition : At HT strengthening & lower balloon and burst openings sizes + significant additional copying time before loss of clad integrity upon HT steam oxidation and final quenching.



## Chromia scale ( $Cr_2O_3$ ) thickening kinetics upon steam oxidation at HT:

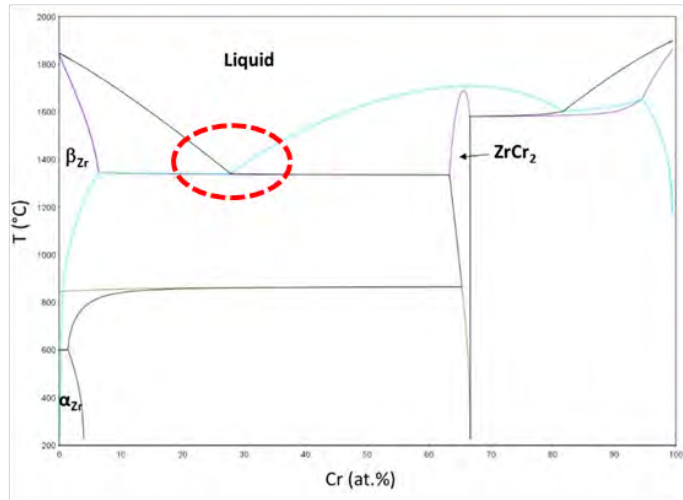


One-sided steam oxidation at **1200°C** + direct water quenching down to RT => PQ mechanical properties improvement



For one-sided oxidation, **current LOCA regulatory “clad embrittlement” criteria**, based on calculated BJ-ECR(uncoated clad)=17%, **seems highly conservative** regarding the resistance to quenching and the PQ behavior of Cr-coated M5<sub>Framatome</sub> oxidized at HT (up to 1300°C).

HT oxidation + quenching tests performed up to 1500 ° C to evaluate the consequences of the potential Zr/Cr eutectic reaction occurrence



Calculated pseudo-binary M5-Cr phase diagram

Cr-coated or not?	T(°C) of steam introduction upon heating at 1°C/s	Temperature range achieved (°C)	Oxidation time (s)	Measured Weight Gain (mg/cm <sup>2</sup> )	Failed or not upon quenching?
No	600°C	1310 ± 10	600	24.8	No
Yes		1310 ± 10	600	2.8-2.9	No
No		1410 ± 10	100	20	No
Yes		1425 ± 25	100	19.0	No
No		1515 ± 15	50	28.7	Yes or No
Yes		1525 ± 25	50	Not measured	No
No	1300°C	1325 ± 25	600	31.1	Yes
Yes		1305 ± 5	600	2.4	No
No		1425 ± 25	100	25.8	Yes
Yes		1425 ± 25	100	19.6	No

Steam oxidation at T > 1300 ° C (above Zr/Cr eutectic temp.)



### Encouraging/reassuring results:

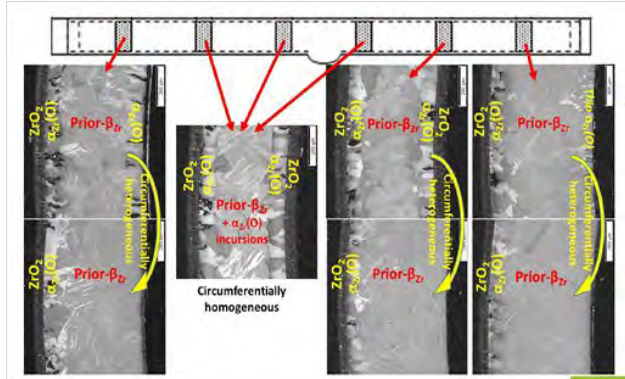
- **No temperature escalation / limited temperature overshoot**
- **Cr-coated M5<sub>Framatome</sub> clad segments tested kept their integrity upon the final water quenching (even if eutectic reaction had occurred), while some uncoated reference claddings did not**



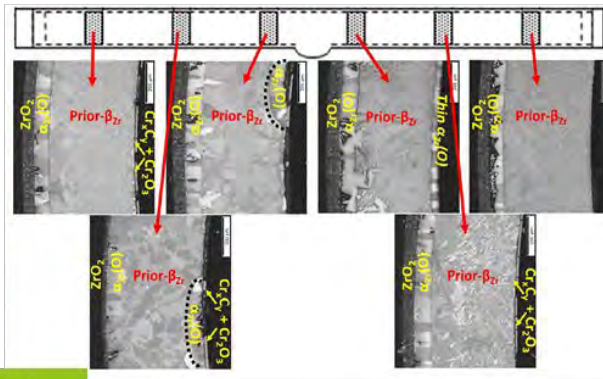
# CEA prospective studies on inner coated Zr-based claddings: => Encouraging results obtained after HT oxidation up to $ECR_{BJ} \sim 35\%$

HT oxidation: @  
1200° C for 600s

## Uncoated



## INNER Coated

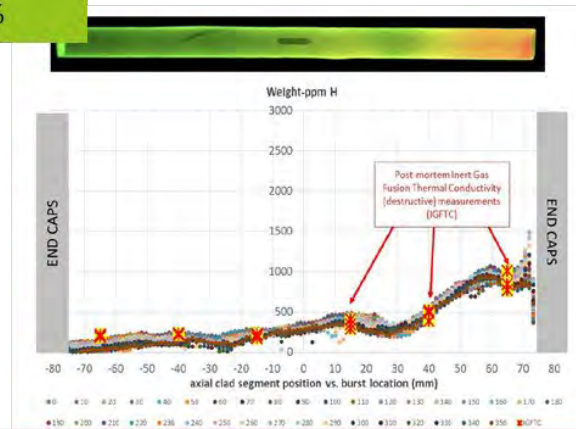
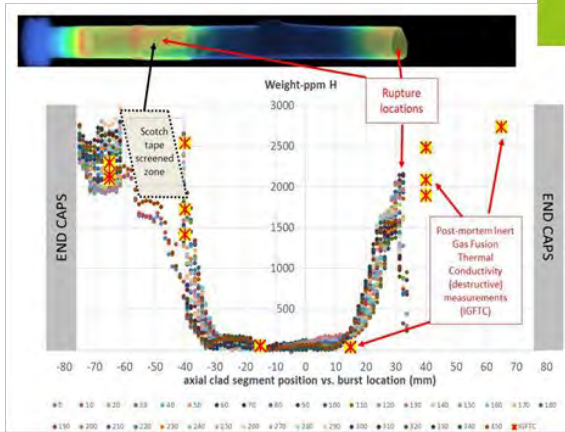


J-C. Brachet,  
J. Nucl. Mater. (2021)

⇒ Inner coated Zy4 clad kept its integrity

⇒ Much thinner inner oxidation scale with inner coating

$ECR_{BJ} = 30-35\%$



⇒ Much lower H concentration in inner coated Zy4 clad (neutron tomography and IGFTC)

Un-irradiated CVD-DLIMO inner clad coatings:  
some mitigation capacity vs. 2<sup>nd</sup>ary hydriding at HT





**G. Wang**

**Westinghouse Electric Company LLC**

## **UHT Test Facility Updates and Oxidation Tests for Accident Tolerant Fuel Developments**

Research and development on accident tolerant fuel (ATF) have been widely pursued by the nuclear industry around the world. Westinghouse is changing nuclear energy again with its revolutionary new accident tolerant fuel design, EnCore<sup>®1</sup> Fuel. Chromium (Cr) coated zirconium alloy and silicon-carbide (SiC) fuel cladding are the excellent candidates for application in fuel cladding of light water reactors (LWRs). Nuclear energy technology is being improved with this revolutionary new accident tolerant fuel design. The ATF fuel is being developed to deliver beyond-design-basis (BDB) and design-basis-altering (DB) safety margins, withstanding far more severe conditions than the current fuel. The products in this portfolio have enhanced temperature performance enabling survival during BDB and DB accidents. The products also minimize interactions of fuel and fuel rod materials with water. The Cr-coated zirconium alloy cladding exhibits sustained high temperature performance and inhibits the detrimental effects of the zirconium-steam reaction. Westinghouse's silicon-carbide (SiC) fuel cladding offers game-changing safety benefits in severe accident conditions, particularly compared to the significant hydrogen- and-heat producing reactions that occur above 1200° C for zirconium fuel cladding. These advancements will increase safety margins and enable the transition to high burnup facilities as well.

To support the accident tolerant fuel (ATF) development, the Westinghouse Ultra High Temperature (UHT) test facility was built at the Westinghouse Churchill site in early 2016. The UHT test facility has been upgraded recently. The current UHT reactor was designed to promote better sealing of the reaction chamber and a smaller uncertainty on cladding temperature measurement. Simulating large break LOCA steam conditions, the UHT oxidation tests have been performed with SiC, Optimized ZIRLO<sup>®1</sup> and Cr-coated zirconium alloy cladding. In the EnCore Fuel program, one of the key tasks is to test the safety features and margin gain of the EnCore Fuel. This presentation describes the designs, safety features and baseline commissioning tests for the upgraded Ultra High Temperature (UHT) test facility.

---

<sup>1</sup>Optimized ZIRLO<sup>™</sup> or EnCore<sup>®</sup> is a trademark or registered trademark of Westinghouse Electric Company LLC, its Affiliates and/or its Subsidiaries in the United States of America and may be registered in other countries

# Acknowledgement

This material is based upon work supported by the Department of Energy under Award Number DE-NE0008222, DE-NE0008824, and DE-NE0009033.

Disclaimer: This slide package was prepared as an account of work sponsored by an agency of the United States Government. Neither the United States Government nor any agency thereof, nor any of their employees, makes any warranty, express or implied, or assumes any legal liability or responsibility for the accuracy, completeness, or usefulness of any information, apparatus, product, or process disclosed, or represents that its use would not infringe privately owned rights. Reference herein to any specific commercial product, process, or service by trade name, trademark, manufacturer, or otherwise does not necessarily constitute or imply its endorsement, recommendation, or favoring by the United States Government or any agency thereof. The views and opinions of authors expressed herein do not necessarily state or reflect those of the United States Government or any agency thereof.



# UHT Test Facility Updates and Oxidation Tests for Accident Tolerant Fuel Developments

(27<sup>th</sup> International QUENCH Workshop at KIT)

Guoqiang Wang, and Art Byers

(Reviewed by Ed Lahoda)

Westinghouse Electric Company LLC

September 27-29, 2022

# Overview of UHT Test Facility Development



# UHT Testing for EnCore<sup>®</sup> Fuel

- Westinghouse Ultra-High Temperature (UHT) Test Facility developed for ATF cladding testing since October 2016
- Completed or Future UHT Projects
  - EPRI ATF Licensing Gap
  - UHT Tests for **AXIOM**<sup>™</sup>
  - UHT Tests for ATF Projects
    - ❑ Cr-coated Cladding, and
    - ❑ SiC Cladding
  - Project for the Canadian Nuclear Safety Commission (CNSC)



ADOPT, EnCore, ZIRLO, AXIOM are trademarks or registered trademarks of Westinghouse Electric Company LLC, its affiliates and/or its subsidiaries in the United States of America and may be registered in other countries throughout the world. All rights reserved. Unauthorized use is strictly prohibited. Other names may be trademarks of their respective owners.

**EnCore<sup>®</sup>**  
**Fuel**

*We're changing nuclear  
energy ... again*



UHT Test Facility

# UHT-ATF Test Facility Buildup

- Single heater rod or tube in a ceramic tube
- Noncontact Infrared Temperature Measurement
- Heater Rod Length of 29.7cm (11.7")
- Heater Rod OD of 0.95cm (0.374")
- Decay power still ~7% of the original power at reactor shutdown
- System Pressure 0.0 psig
- Steam with Water Drop Entrainment
- Simulate Large Break LOCA conditions



High Temperature  
Sensor Head and Box



High Temperature  
Sensor Head with  
Laser

# Key Parameters of the UHT-ATF Test Section

Parameters	Values
System pressure, psig	0.0 psig
Heater Rod Power, W/cm <sup>2</sup>	12 W/cm <sup>2</sup>
Heat Removal, kW	1.1 kW
Steam Flow, mg/s-cm <sup>2</sup>	0.5 to 30 mg/s-cm <sup>2</sup>
Cladding temperature, °C	1200 ~ 1600 °C



# WATCH Facility (in 301)

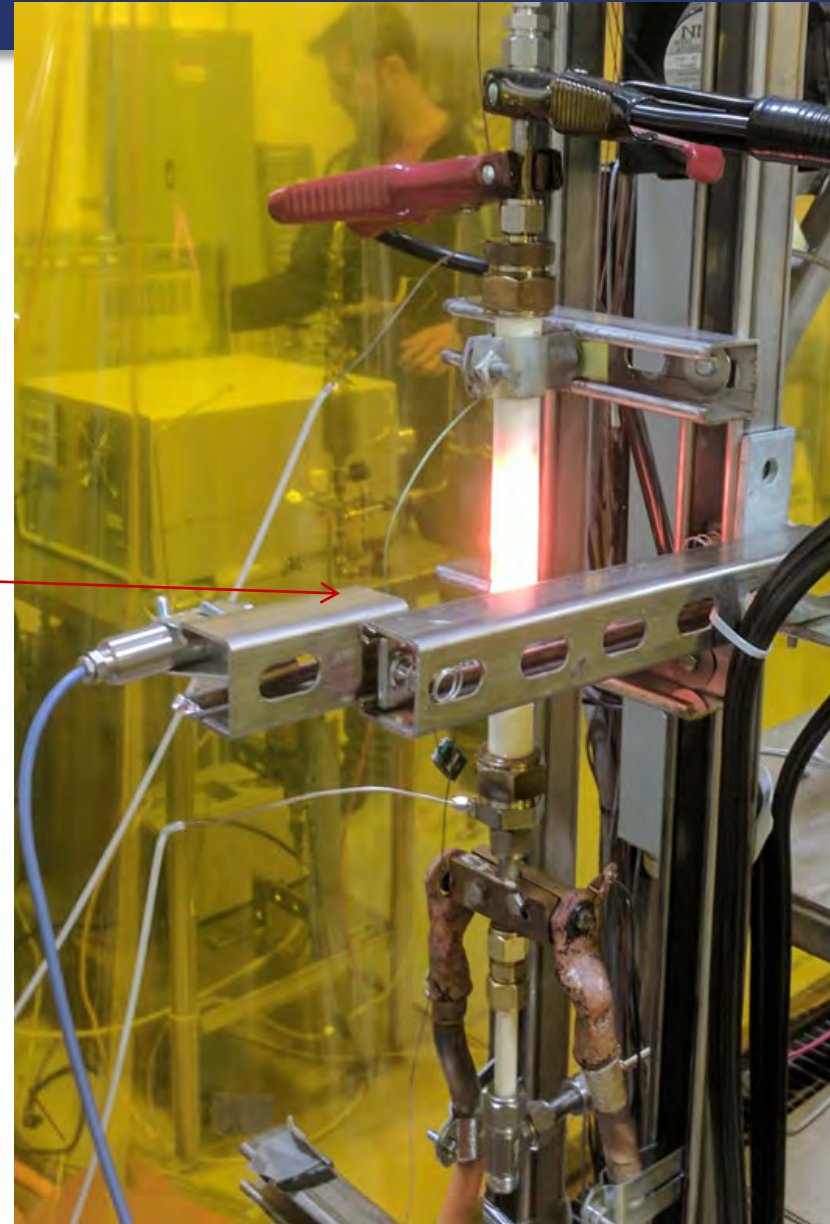
- WATCH Loop
- New HT-ATF Test Facility Location (to be placed)



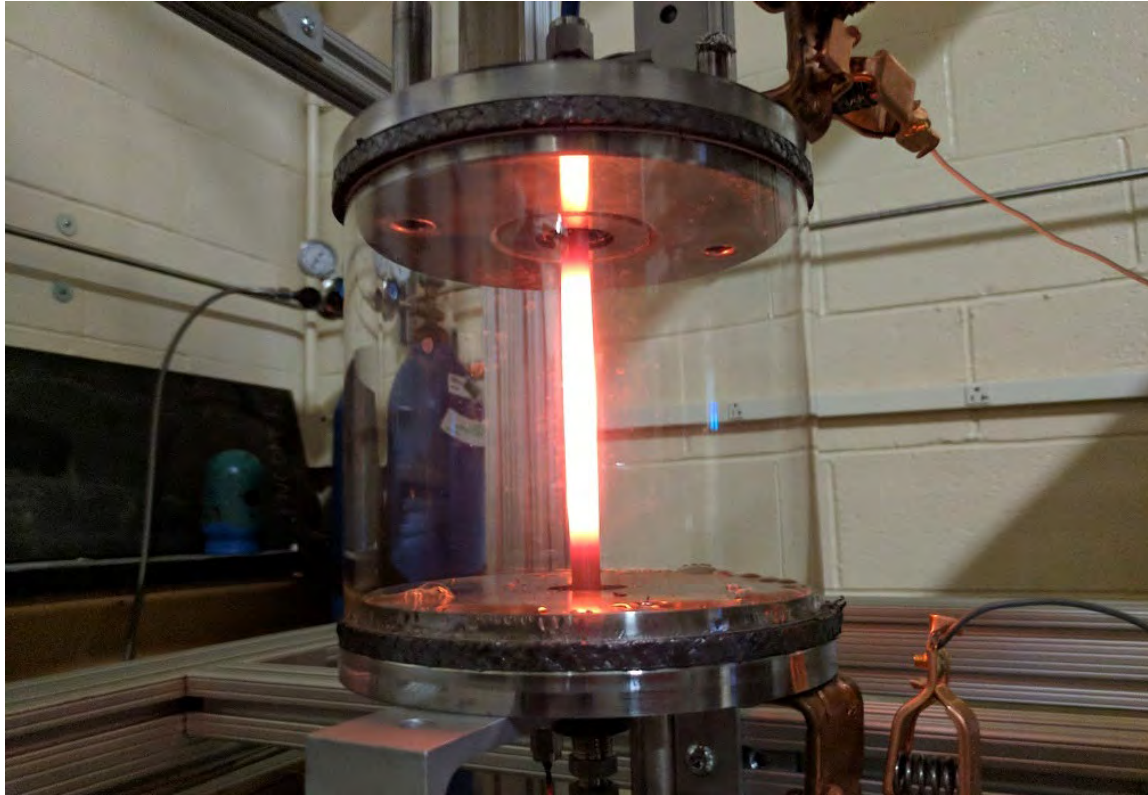


# UHT-1 Test Facility

- UHT-ATF Test Facility Located near the WATCH Loop



# UHT-2 and UHT-3 Test Facility



**UHT-2 Reaction Chamber testing Coated or SiC cladding using indirect heating from the rod ID**



***UHT-3 Reaction Chamber Photo***



# New UHT Test Facility

- The New UHT Test Facility Located in a standalone frame
- Infrared Sensor





# Westinghouse Zirconium Oxidation Experiment (ZOE) Test Facility



# Zirconium Oxidation Experiment (ZOE)

- The ZOE test unit provides high temperature steam exposures of numerous specimens simultaneously
- Multiple specimens are exposed to flowing steam for predetermined times at temperatures up to 1200°C (2192°F)
- A water quench of the specimens is typically performed immediately after steam exposure.
- To evaluate the behavior of new fuel cladding alloys under development by

Westinghouse and to support new regulator



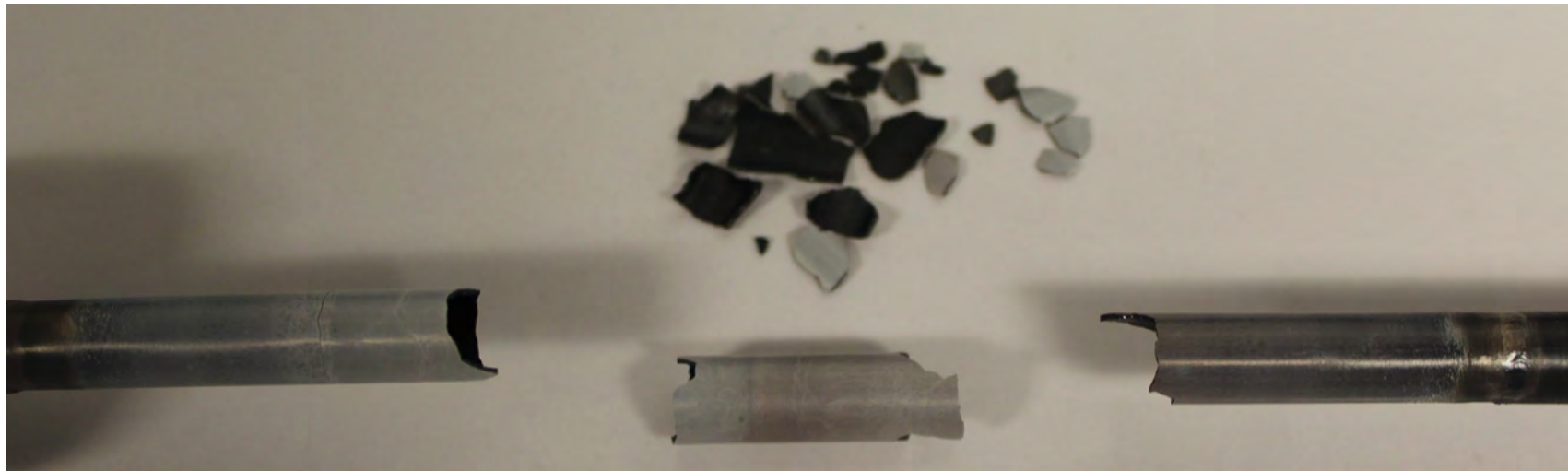


# Early UHT-ATF Test Results

# UHT-ATF Test Results



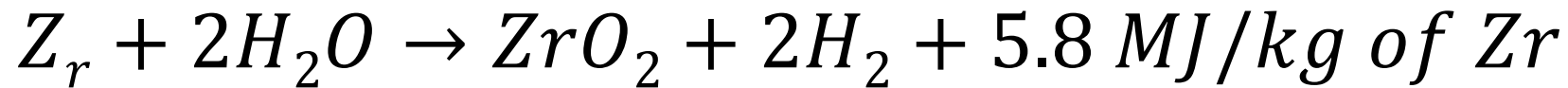
UHT-1 Test Section (During a Post-LOCA Test)



UHT-1 Test Result (Temp > 1400 °C, After a Post-LOCA Test)

# UHT-1 Test Results (cont.)

- Zr oxidation begins at about 1000°C – releasing heat and hydrogen from Zr-steam reaction

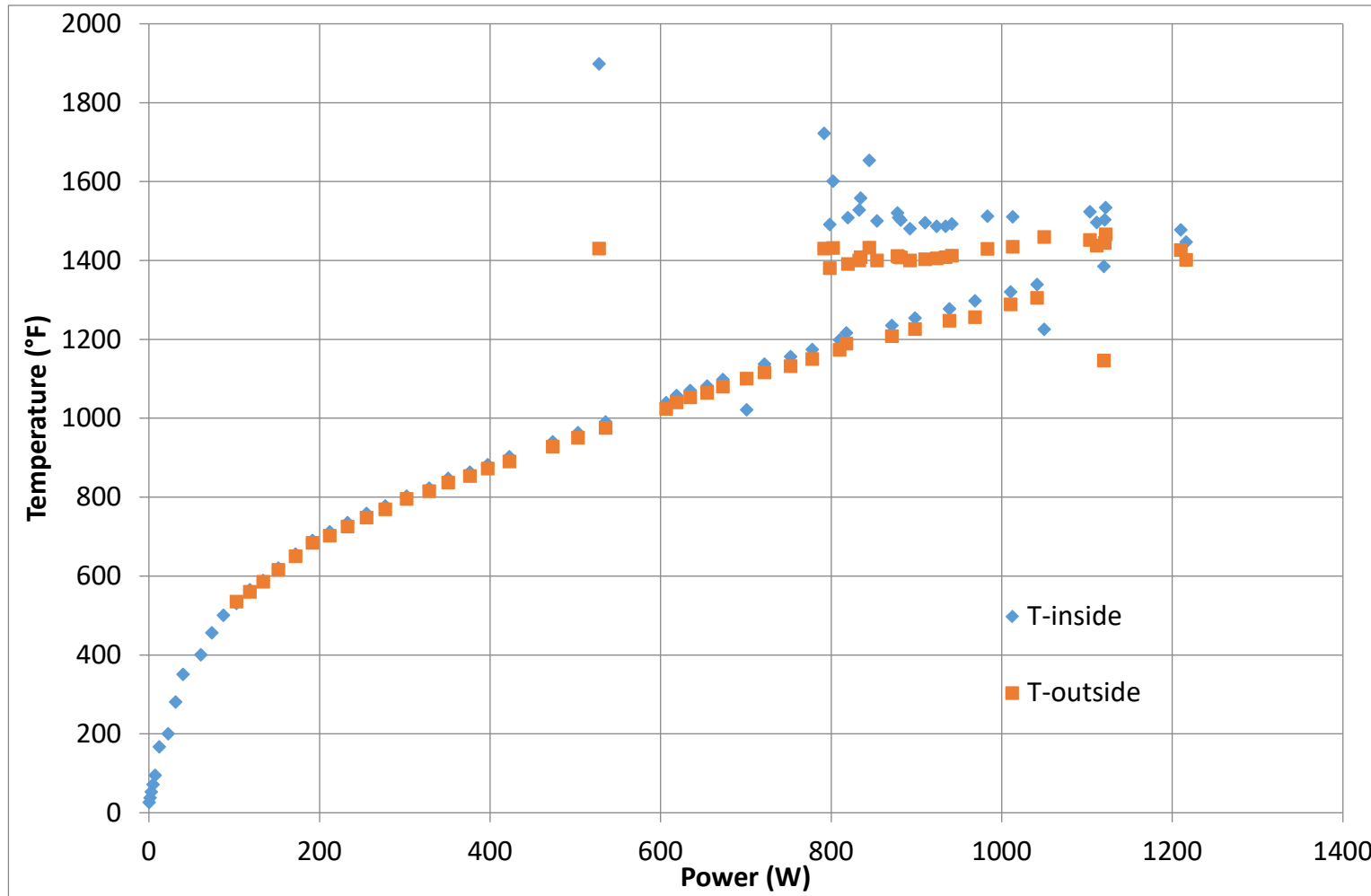


- The Zr cladding melts at about 1850°C
- The cladding becomes very brittle
  - ❑ Black color inside (with helium in the tube)
  - ❑ Grey color outside (reacted with steam)



# UHT-1 Test Results (cont.)

- Cladding Inside and Outside Temperatures vs Power

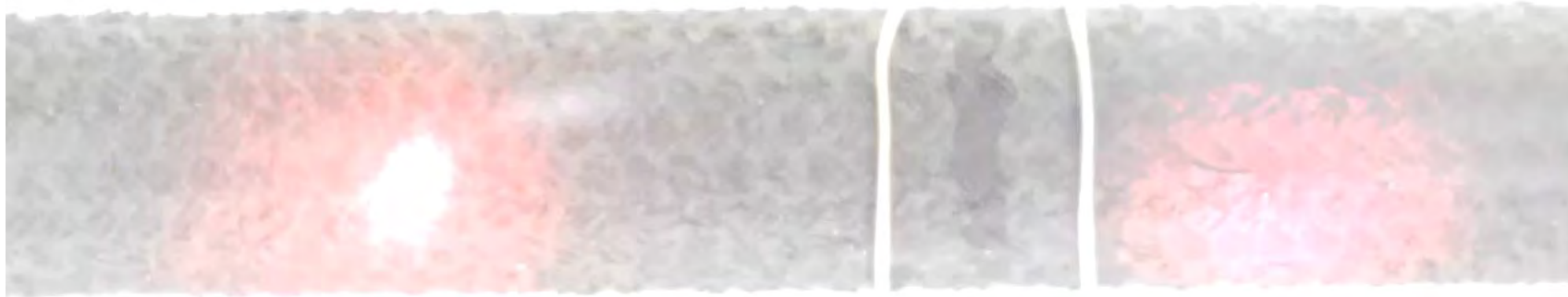


# UHT-1 Test Results and Discussions

- Oxidation of the Zr cladding in the presence of steam produces hydrogen exothermically
  - Energy release 5.8 MJ/kg of Zr
  - Exacerbates the fuel decay power dissipation problem
- Need to avoid accelerating temperature rise rate due to added energy release from oxidation of Zr

# UHT Updates, Calibrations and More Results

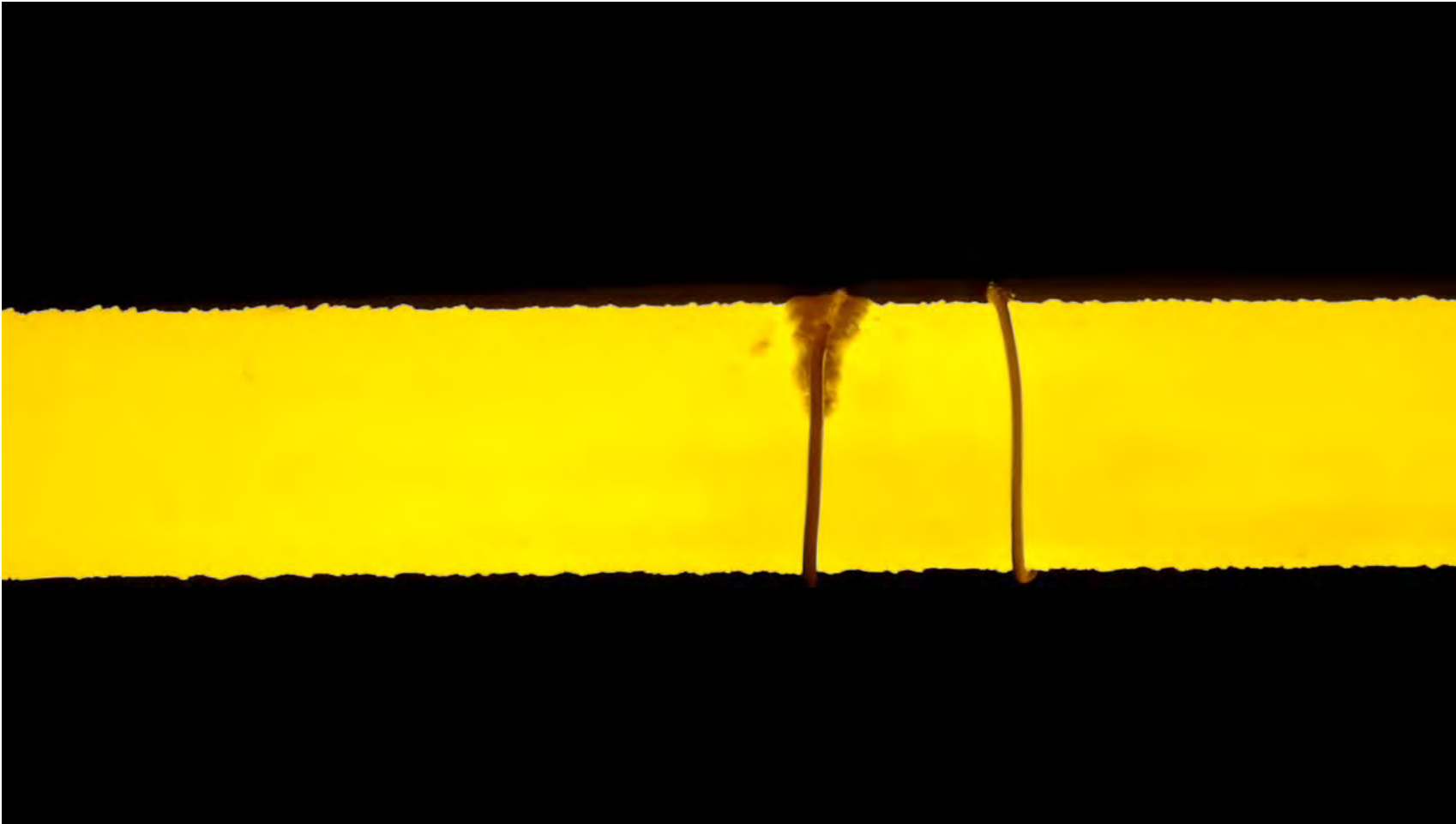
# Pyrometer Calibration Check During a SiC Run



- This video shows the setting of the pyrometer measurement location.
- The size of the laser spot shows the size of the sampled surface temperature
- The copper and platinum wire are used to check the pyrometer calibration. High purity materials are used to get a sharp melting point



# Pyrometer Calibration Check During a SiC Run



- This video shows the copper calibration wire as it melts.
- The bubbling is from carbon monoxide escaping from the silicon carbide under the liquid copper

# Pyrometer Calibration Check During a SiC Run



- This video shows final stage of the experiment after the platinum wire has melted
- The video goes dark and the exposure is readjusted showing the chamber has filled with smoke.
- Later analysis showed the smoke was composed of silicon oxide.

# Pyrometer Calibration Check During a SiC Run

Sensor	Uncalibrated Temperature (°C)	Calibrated Temperature (°C)	Error (°C)
Omega 1	1771.2	1788.1	15.1
Omega 2	1747.7	1771.1	-1.9
Micro Epsilon 3	1731.5	1756.7	-16.3
Micro Epsilon 4	1736.1	1763.9	-9.1

Note- The true melting point of platinum is 1773°C.

# Results at 1200°C in ZOE Tests Show Effectiveness of Coatings in Reducing Oxidation

After ZOE\* LOCA1062



## Weight Gain

LOCA#	Sample	Description	Weight Gain (mg/dm <sup>2</sup> )		Deviation (%)
			C-P Predicted For Zr Tube	Measured	
1060	CCR1	Reference bare Zr tube	1143	1096	-4.2
	FM2C	FeCrAl on Mo tube	1143	530	-53.6
1061	FM9C	FeCrAl on Mo tube	1188	549	-53.8
1062	C1C	Cr coated Zr tube	1179	508	-56.9
1063	C8C	Cr coated Zr tube	1172	554	-52.7

\*Zirconium Oxidation Experiment (ZOE) is a standard NRC 1200 °C LOCA test rig

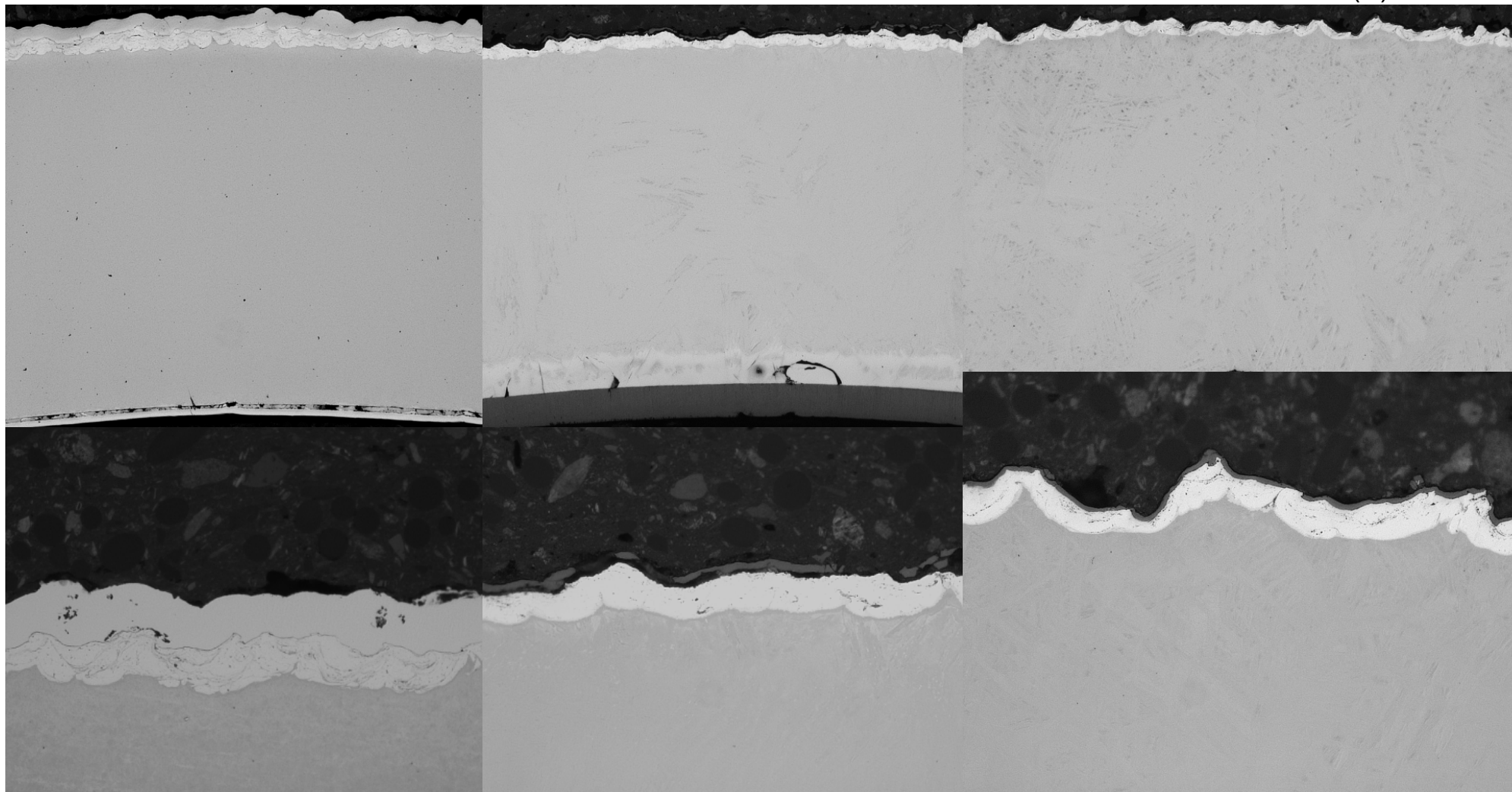


# Comparable Results at 1200°C for Cr Coated Zr Tube

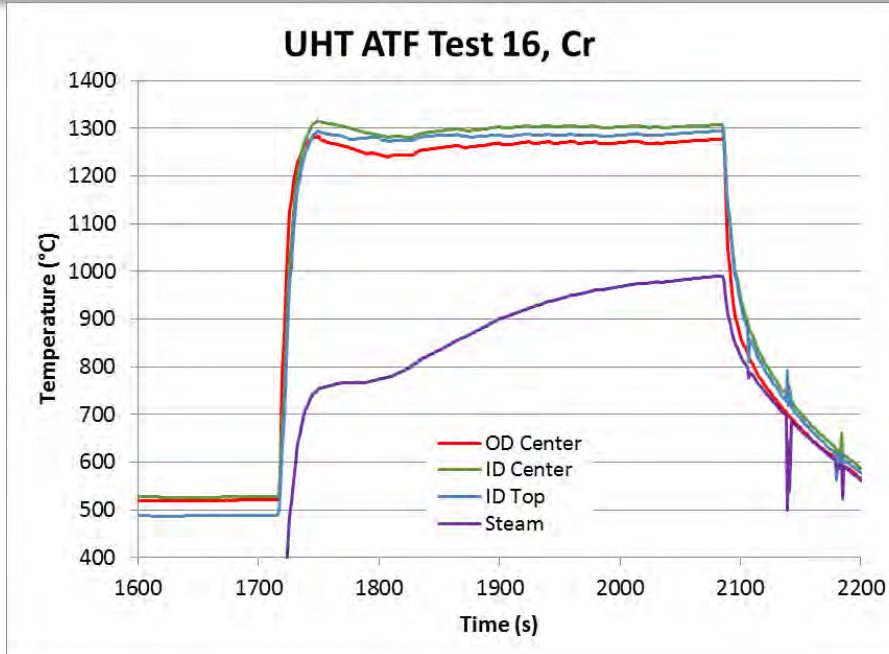
As-Received

After ZOE LOCA1062

After UHT Test 14 (B)



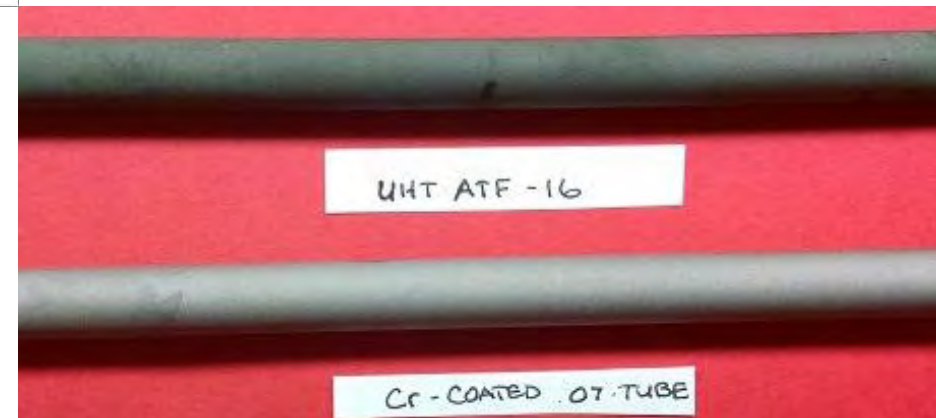
# UHT Test Results at 1300°C for Cr Coated Zr Tube



- Ultra High Temperature (UHT) Test to simulate large break LOCA conditions
- Sample surface temperature 1300°C
- Test duration ~350 s

Sample after UHT Test →

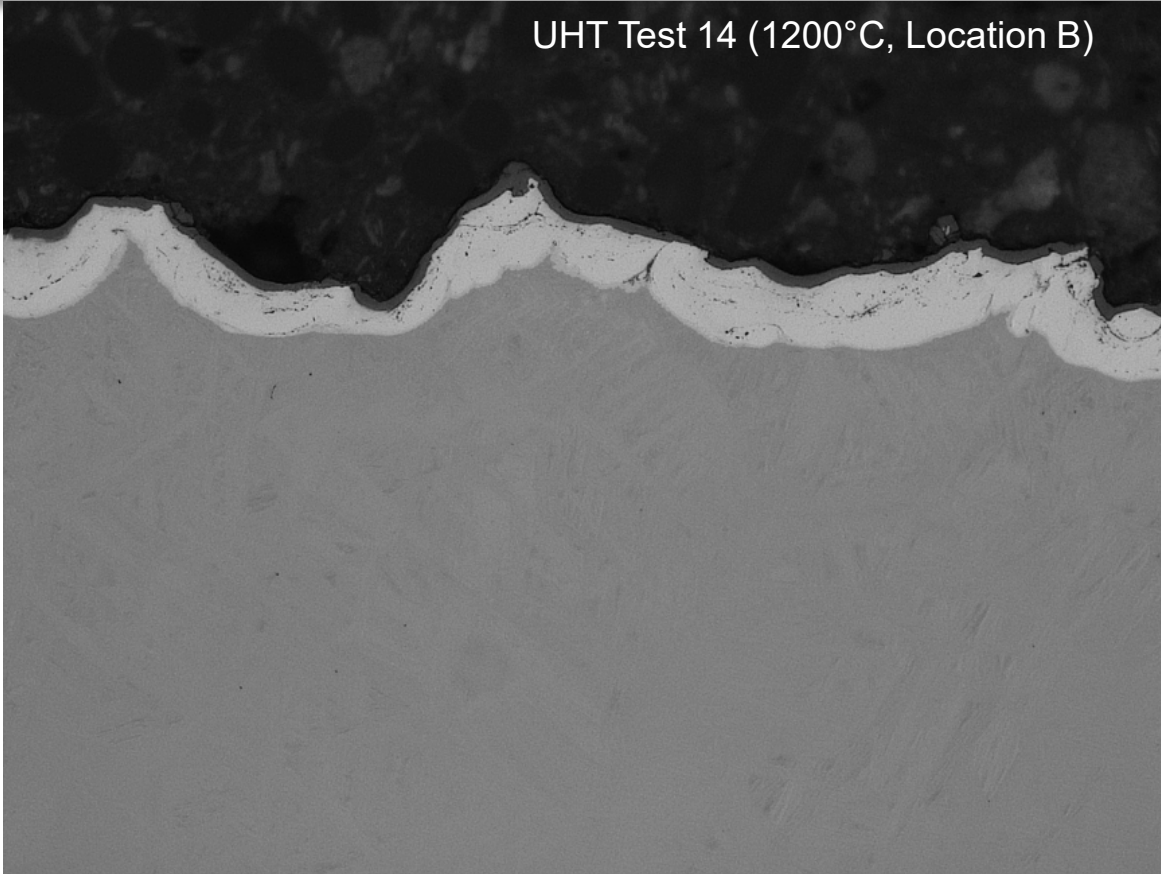
Sample before UHT Test →



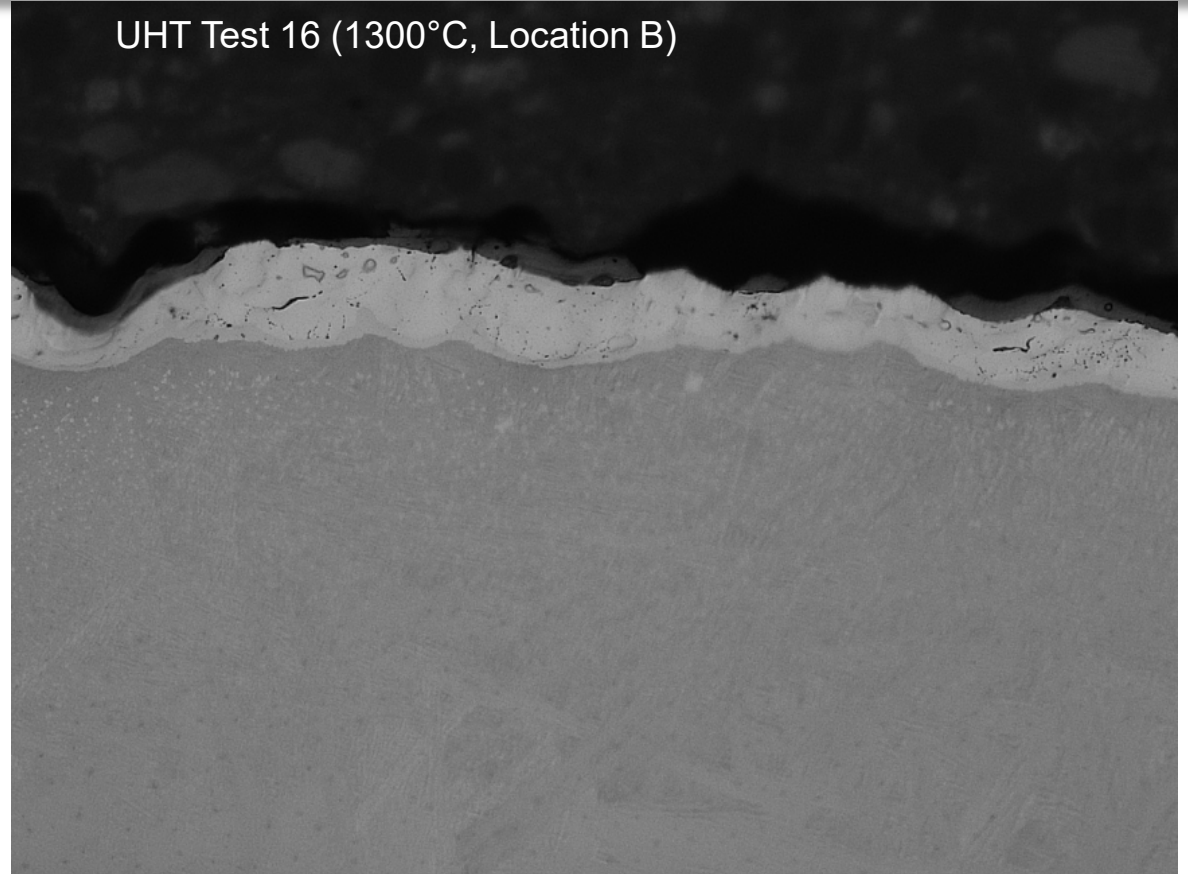


# Cr Coated Zr Tube UHT Results at 1200°C and 1300°C

UHT Test 14 (1200°C, Location B)



UHT Test 16 (1300°C, Location B)



- With a Cr-coating layer, the substrate claddings were protected at 1200 °C and 1300 °C

# Summary

- FeCrAl on Mo Tube appears acceptable up to 1200°C
  - With local spots with loss of Mo and interdiffusion
- Cr appears acceptable up to 1300°C
  - Slight interdiffusion observed
  - Peeling of chromia needs evaluation
- More tests are planned at higher temperatures
- Comparison of tests with ZOE test results suggests no issues with UHT



# UHT Test Plans in Next Phase

## UHT Tests and Evaluations:

- Optimize measurement of the PCT and duration time
- Perform evaluation of cladding degradation vs. time and temperature
- Evaluate eutectic formation and effect on oxidation rate
- Compare high temperature performance of cladding types, **ZIRLO™/AXIOM/Cr-Coated Zr**
- Develop Corrosion/Eutectic Oxidation Model

## Exploration of Other Measurements:

- Measure cladding physical properties, e.g., thermal conductivity
- Repeat runs to seek and prove PCT margin by simulating best estimated LOCA transient conditions
- Determine oxidation rates for coated Zr vs **AXIOM** cladding
- Perform post-quench ductility (PQD) tests



**C. Duriez**

**IRSN**

### **Burst and oxidation tests on bare and pre-oxidized claddings**

A device to test cladding ballooning/burst under steam environment, based on induction heating of 250 mm long rods filled with alumina pellets, has been developed at IRSN. Strain and temperature in the balloon region are measured online by stereo Digital Image Correlation (3D-DIC) and an Infrared camera respectively. The hoop creep rate versus cladding temperature can therefore be determined. Illustrative results obtained on thermal ramp tested M5 rods showed limited influence of the pre-transient oxidation on the creep rate.

Ballooned specimens are fast-cooled, dismantled and afterwards high temperature steam oxidized in a separate resistive furnace, the samples being finally water quenched by dropping them in a water bath. After very long steam exposure times, spontaneous ruptures without applied load in the secondary hydriding region have sometimes been observed during quenching. For non-ruptured rods, four point bending tests are performed usually resulting in rupture in the ballooned region.

Post-test metallographic examinations and hydrogen measurement by hot vacuum extraction have led to some highlights on the secondary hydriding process. Among others, a thin inner pre-transient zirconia layer, aiming to simulate the layer formed at high burn-up by pellet-clad interaction, can be dissolved during the high temperature oxidation phase and therefore doesn't prevent secondary hydriding.

# Burst and oxidation tests on bare and pre-oxidized claddings

C. Duriez, Q. Ferrand, J. Desquines, M. Kpemou, T. Taurines

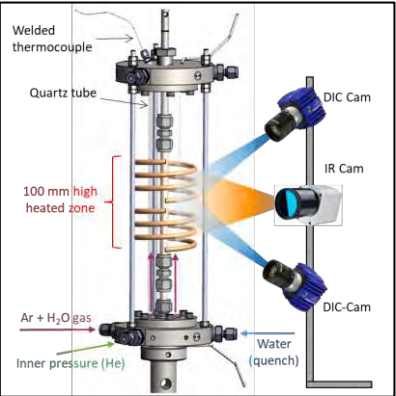
**IRSN**

PSN-RES/SEREX  
Centre de Cadarache, 13115 St Paul-Lez-Durance  
France

*27th International QUENCH Workshop, Karlsruhe, September 27-29, 2022.*



## STEP 1 Ballooning/burst tests in steam



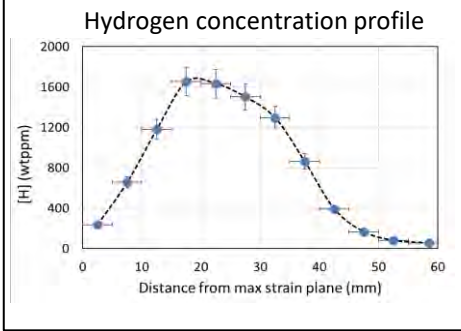
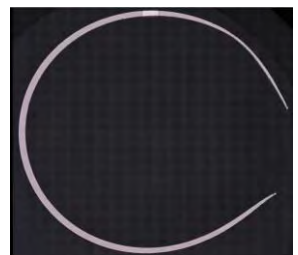
## STEP 2 High temperature steam oxidation



## STEP 3 4 points bending tests



## STEP 4 Post-test examinations

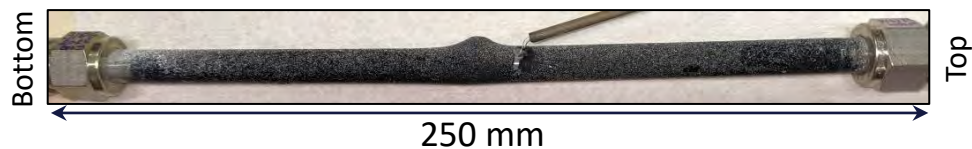
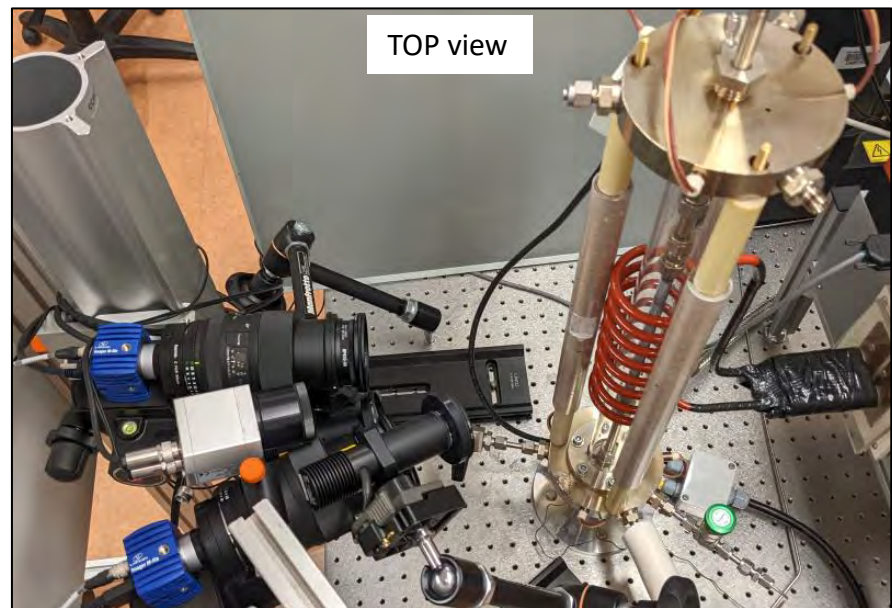
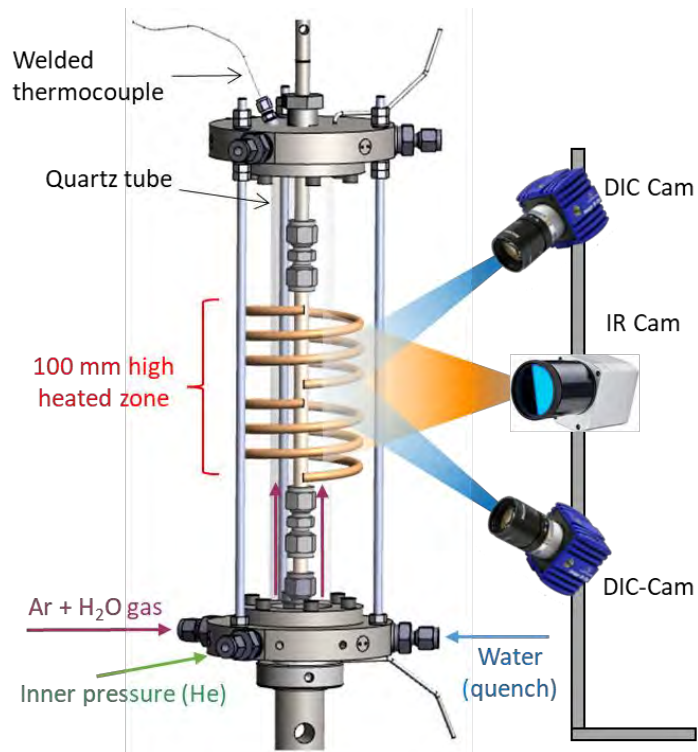




# Step 1

## ballooning/burst tests in steam

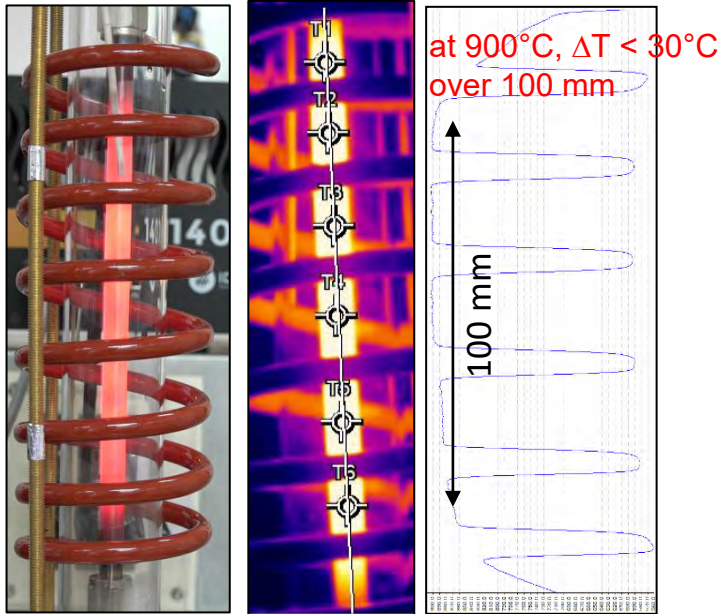
# Device for ballooning/burst tests in steam



# Induction heating

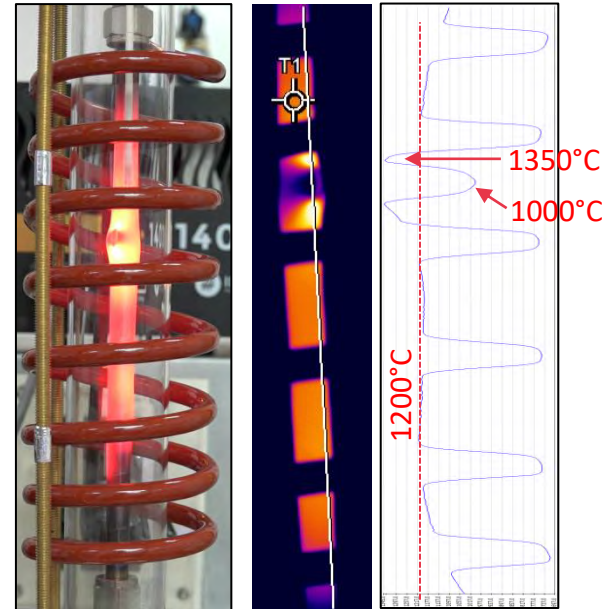


- Fast heating, high T
- Good control of the temperature axial profile
- The specimen is viewable → T from IR cam

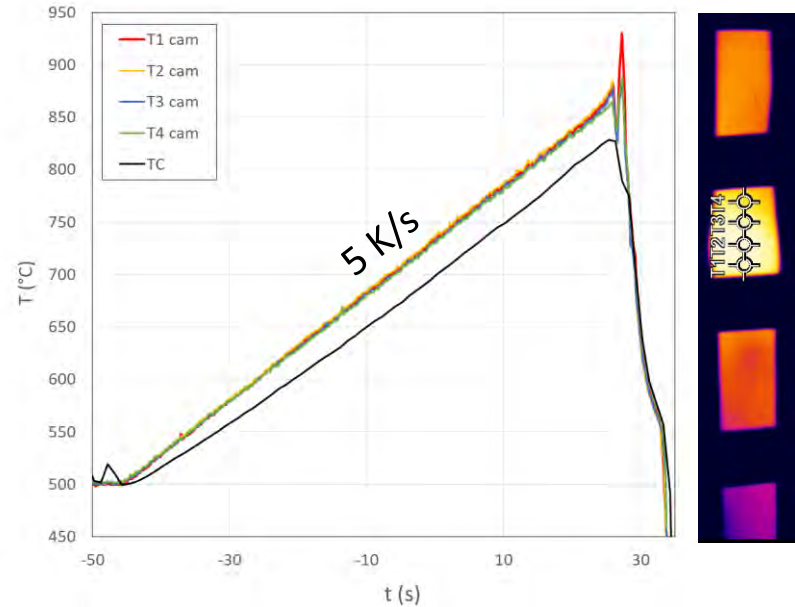
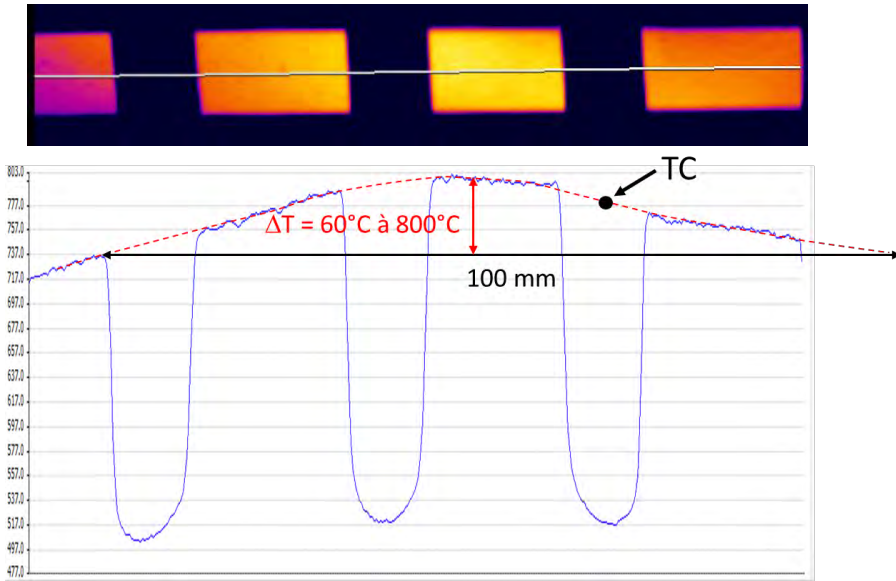


After burst, heating is not anymore homogeneous !

- Cold zone in the burst opening region
- Hot spots on both sides of the opening



# Temperature profile for burst tests



- $\Delta T = 60^\circ\text{C}$  over 100 mm (for non ballooned tubes).
- T ramp regulated from IR cam measurement in the balloon.
- Thermocouple welded close to the balloon to calibrate the IR cam.



# Burst test matrix

Alloy	Initial state	Inner pressure	Ramp rate
Zy4	As-received	20, 30, 50 bar	1 K/s 5 K/s
	Pre-ox 40/30 $\mu$ m, [H] $\sim$ 250 wtppm	10, 20, 30, 50 bar	5 K/s
M5 FRAMATOME	As-received	20, 50 bar	5 K/s 10 K/s
	Pre-ox 10/0 $\mu$ m, [H] = $19 \pm 5$ wtppm Pre-ox 10/10 $\mu$ m, [H] = $40 \pm 5$ wtppm	20, 50 bar	5 K/s

Pre-oxidation was performed at 425°C in O<sub>2</sub> + H<sub>2</sub>O

→ 25 burst tests  
20 tests at 5 K/s

M5 and M5<sub>Framatome</sub> are trademarks or registered trademarks of Framatome or its affiliates, in the USA or other countries.



As-received M5, 20 bar, 5 K/s

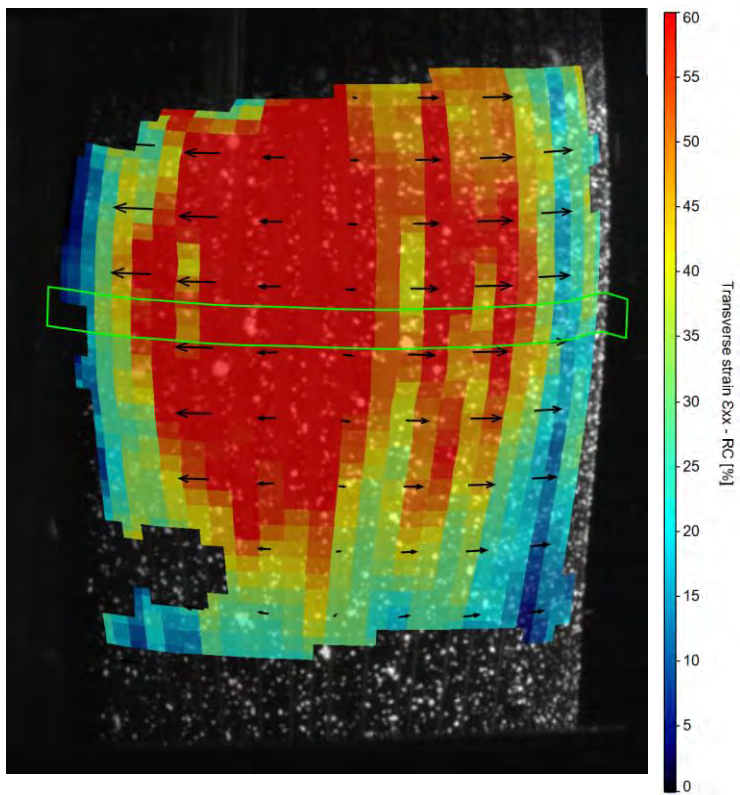


Pre-ox 10/0 $\mu$ m M5 , 50 bar, 5 K/s

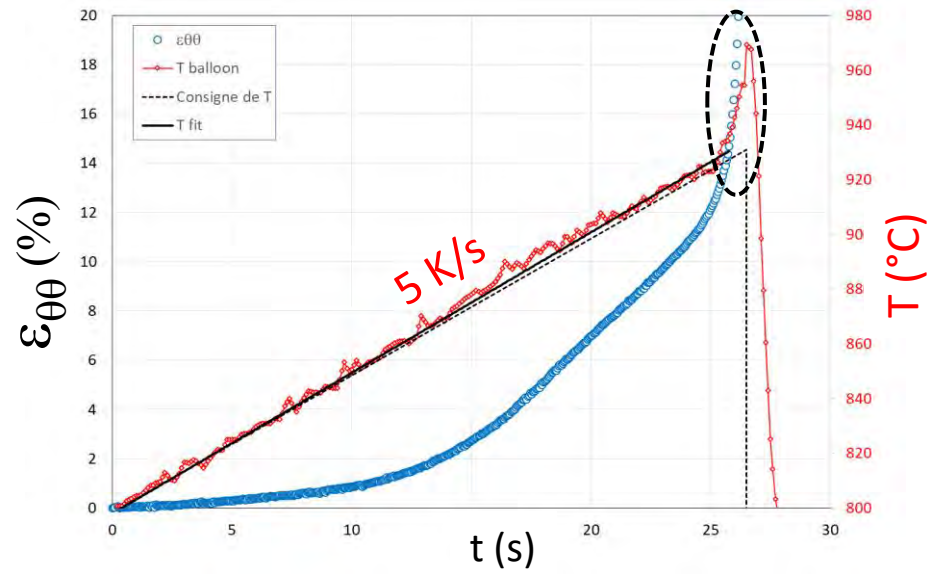


At 50 bar, slight bending likely due to gas ejection at burst

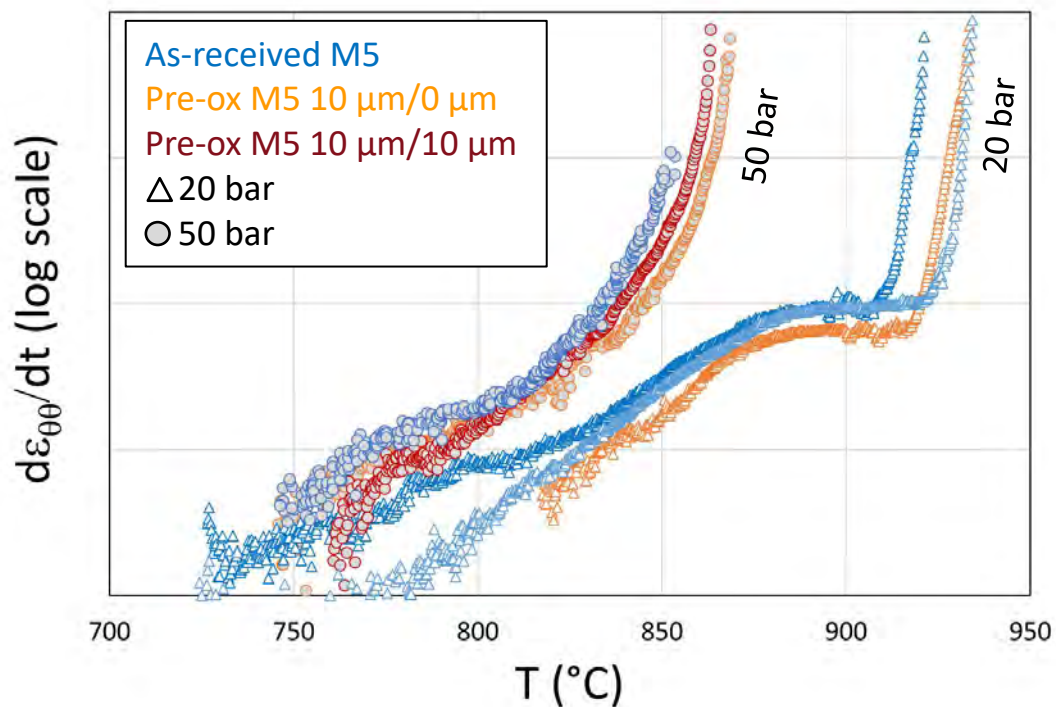
# The use of 3D-DIC for ballooning/burst tests



Burst test at 20 bar, 5 K/s

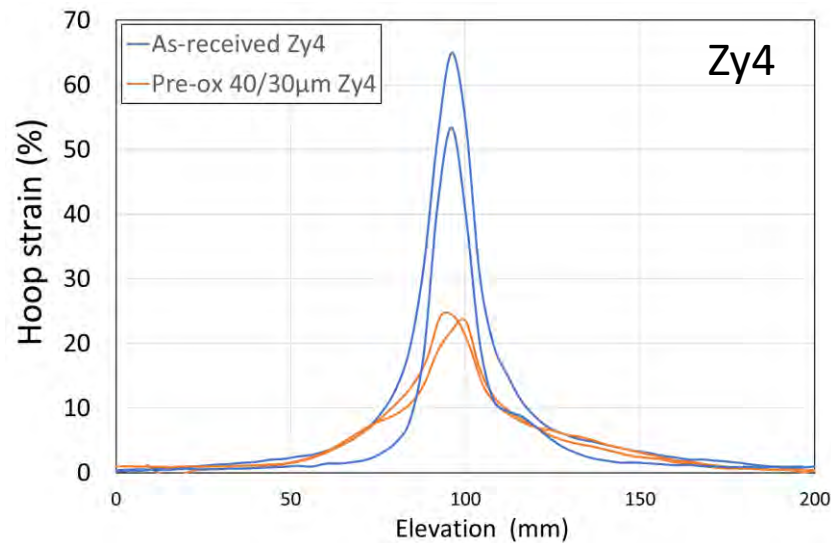
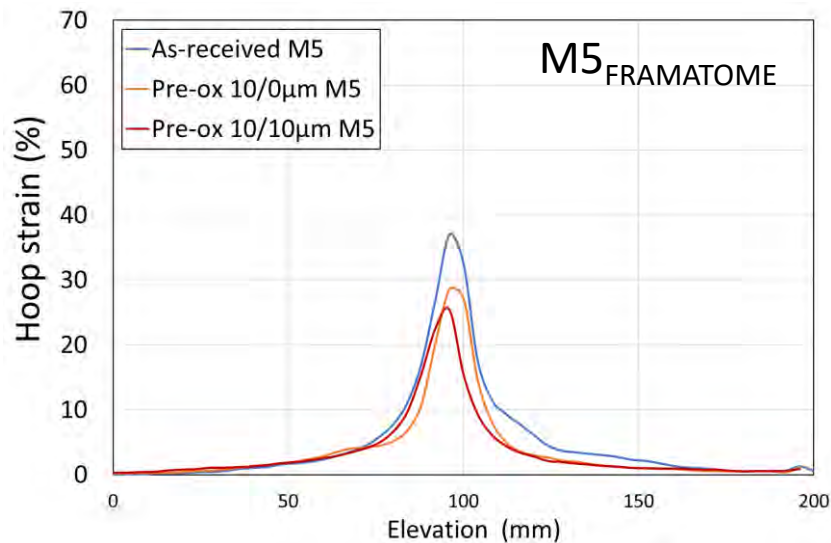


- From DIC  $\rightarrow \epsilon_{\theta\theta} = f(T)$
  - From IR cam  $\rightarrow T = f(T)$
- $\} \rightarrow \dot{\epsilon}_{\theta\theta} = f(T)$
- T follows the setup ramp, except for the last two seconds.



- The creep rate slows down as the  $\beta$ -Zr fraction increases.
- Limited influence of pre-oxidation.

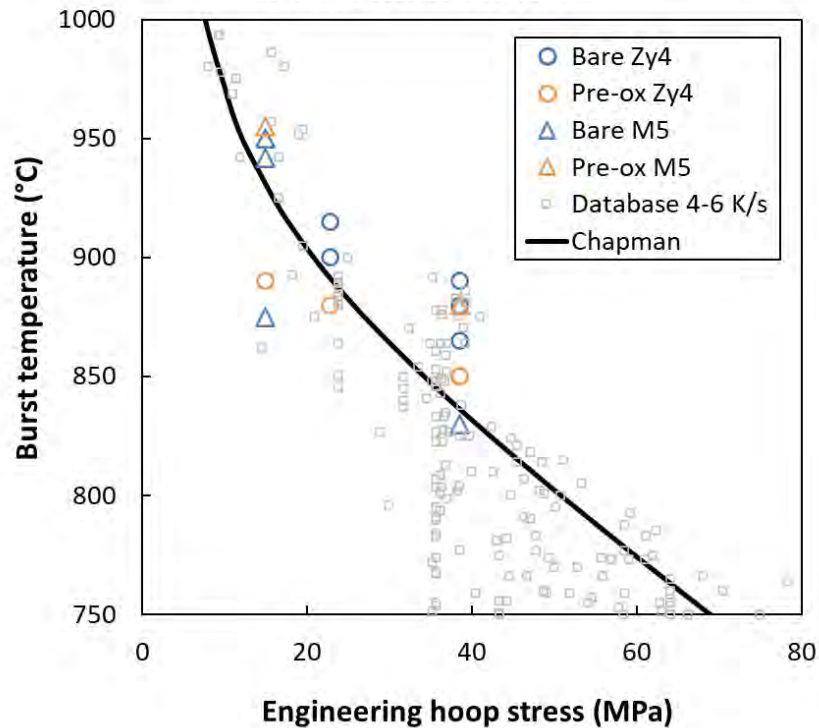
## Results at 50 bar and 5 K/s



- Lower strain for M5<sub>FRAMATOME</sub> than for Zy4
- Limited effect of a thin pre-oxidation scale (M5)
- Significant influence of thick pre-oxidation scales (Zy4)



# Burst temperature at 5 K/s



For Zy-4, burst temperatures are lower for pre-oxidised rods  
→ probable effect of hydrogen (~250 wtppm)

*R.H. Chapman et al., from US-NRC NUREG-0630, 1980.*

## Step 2

# High temperature steam oxidation

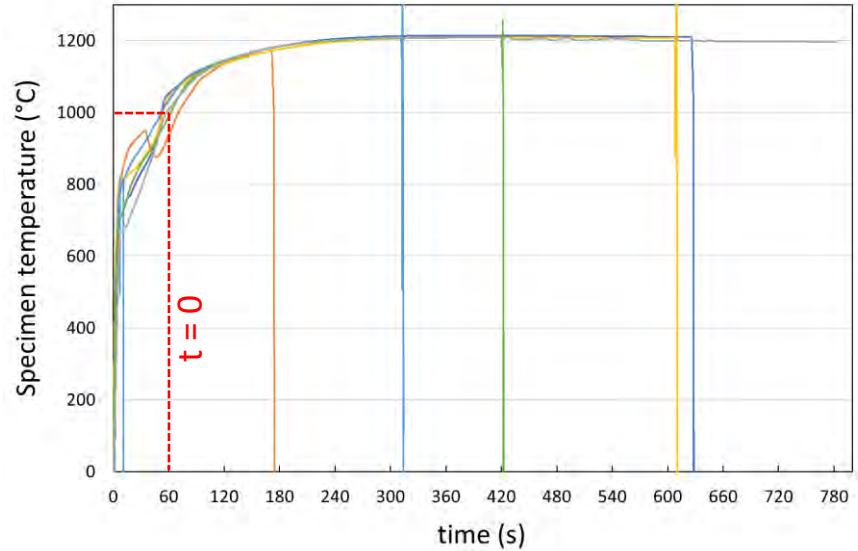
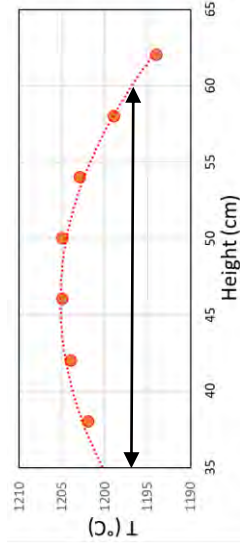
# HT steam oxidation in a resistive, open furnace



10% Ar  
90% Steam (500 g/h)



1200 ± 5°C  
over 25 cm



- Heat-up rate is rather slow, due to thermal inertia of  $\text{Al}_2\text{O}_3$  pellets → no overshoot !
- $\text{ECR}_{\text{BJ}}$  in the balloon is calculated considering double side oxidation, and taking into account the thermal history, the strain and the pre-oxidation

$\Delta t = 90 \text{ s to } 12 \text{ min} \rightarrow \text{ECR}_{\text{BJ}}$  in the range 10-40%

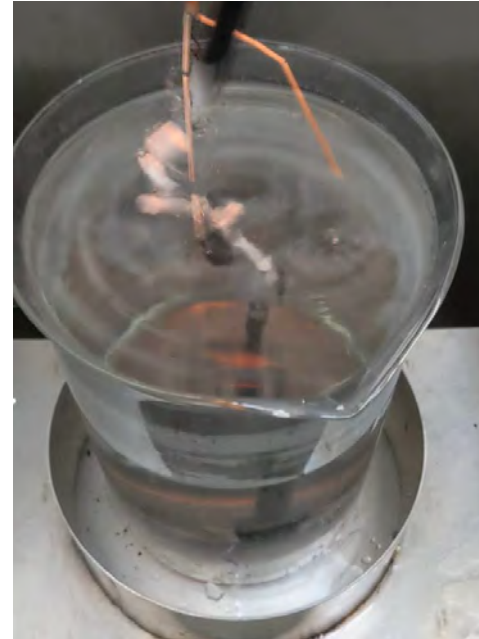
# Spontaneous rupture during quench

At very high ECR (ECR-BJ  $\approx$  40%, i.e. ECR-CP  $\approx$  30%), rupture without applied load occurs in the secondary hydriding region during quench. This was observed both for M5 and Zy4 rods

Quench @ t = 0



Rupture @ t = 23s

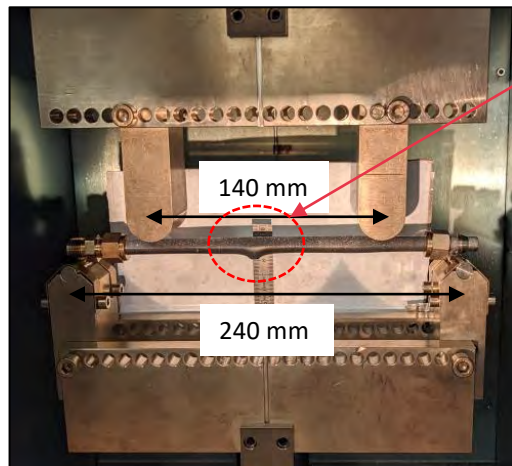




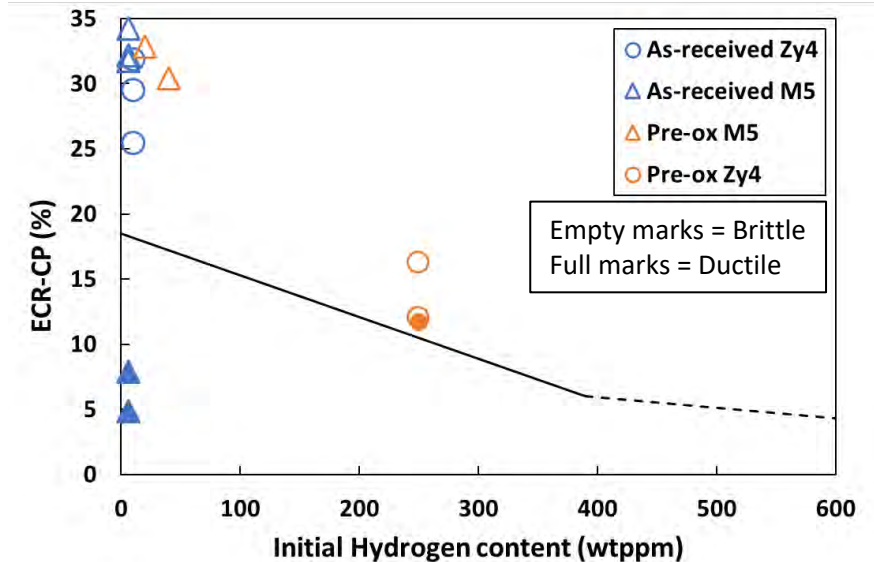
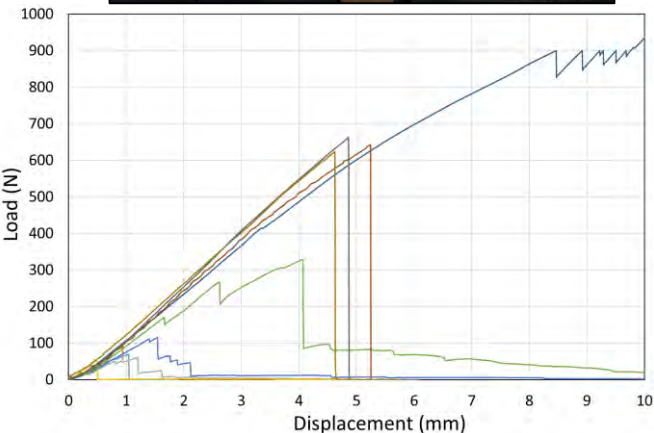
## **Step 3**

### **4 points bending tests**

# Four-points bending tests (4PBT) at 135°C



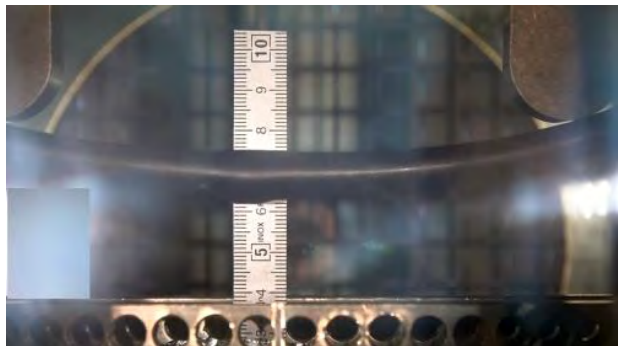
The opening points downward



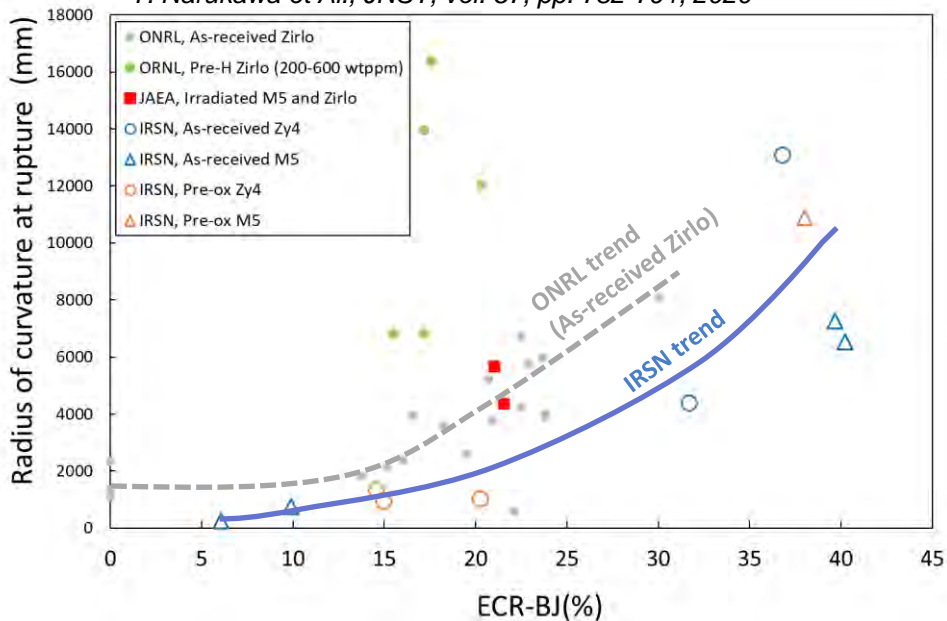
- ⇒
- Most of the rods were brittle, results are consistent with the ductile/brittle limit derived from Argonne RCTs.
  - All rupture during 4PBT occurred in the balloon, even for rods having high H content.

# Four point bending tests at 135°C

Radius of curvature at rupture is calculated from the rod deflexion at rupture



M. C. Billone et Al. NUREG-7219, 2016.  
T. Narukawa et Al., JNST, vol. 57, pp. 782-791, 2020



Better behaviour than for as-received Zirlo ?

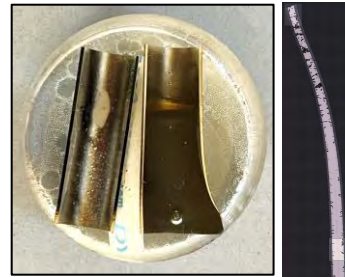
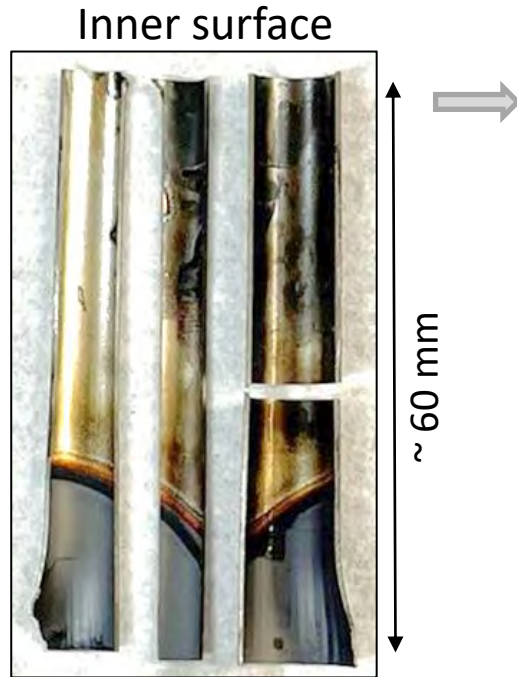
## **Step 4**

### **Post-test examinations**

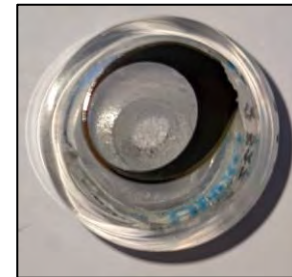
**Thanks to Alice Viretto and Gaëlle Villevieille for the post-test exams**



# Post-test destructive examinations



Axial cross-section



Radial cross-section(s)

- At balloon center
- At failure location



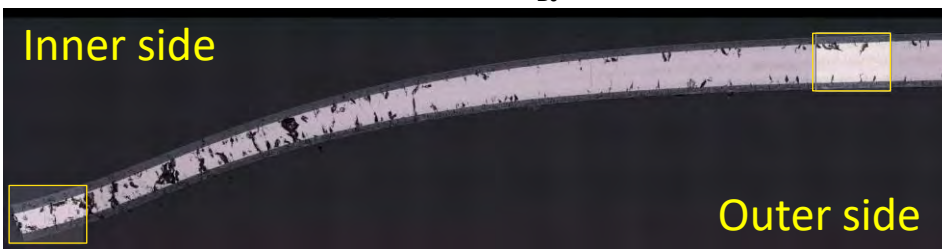
Band cut at the opposite side of the opening for [H] measurements by hot vacuum extraction (LECO)



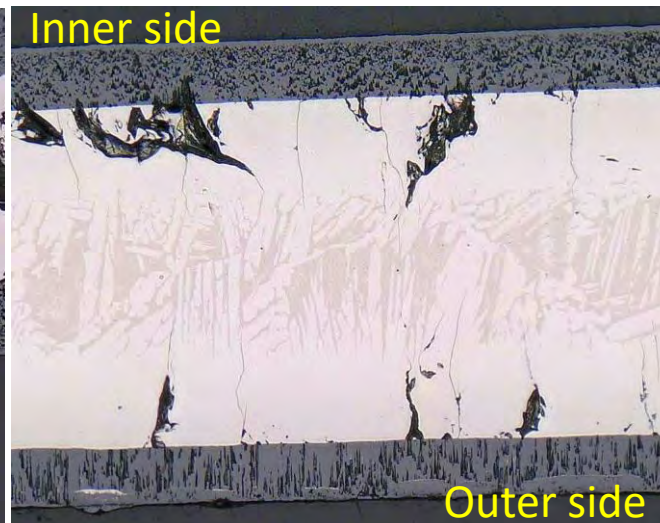
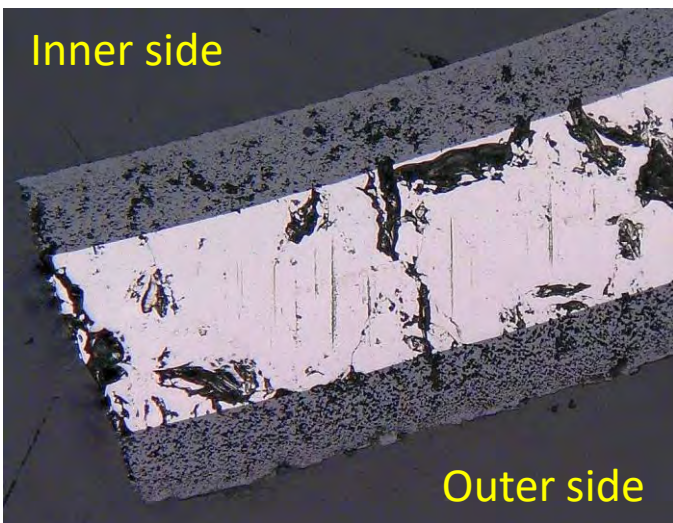
→ Axial Hydrogen distribution

# Impact of the painting on the HT oxidation ?

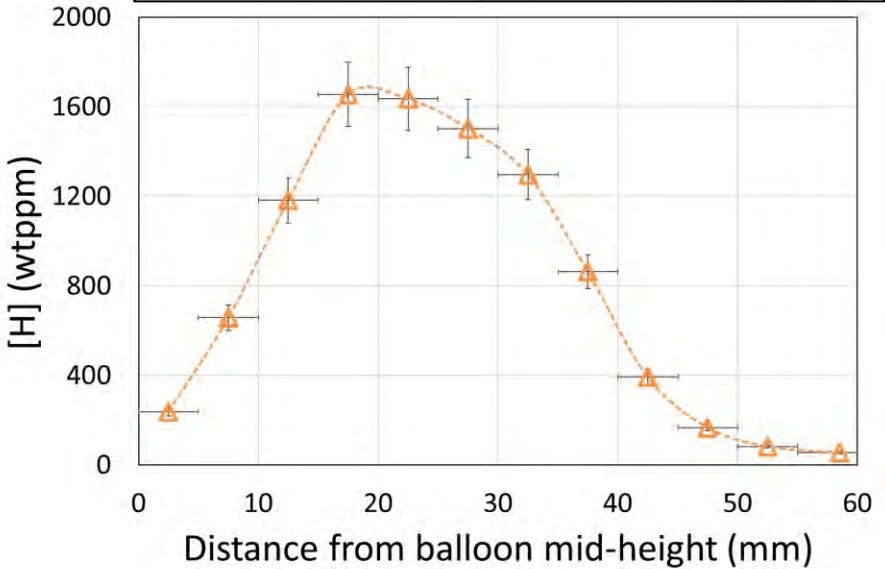
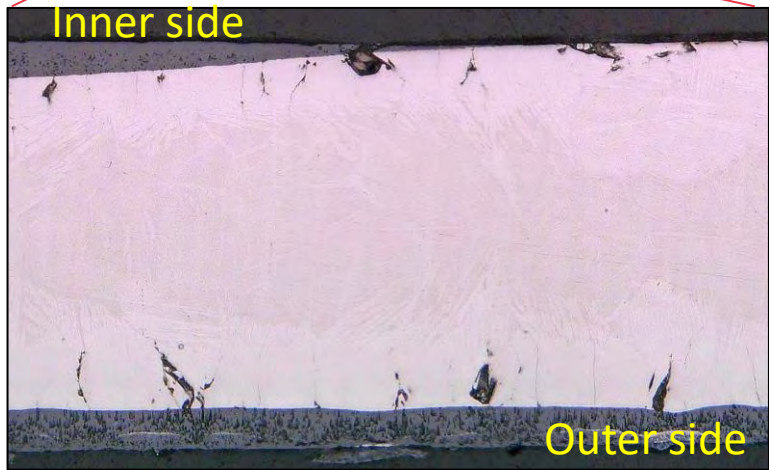
As-received M5,  $ECR_{BJ} = 40.2\%$



Close to the opening, same oxide thickness outside and inside → no or limited influence of the painting.

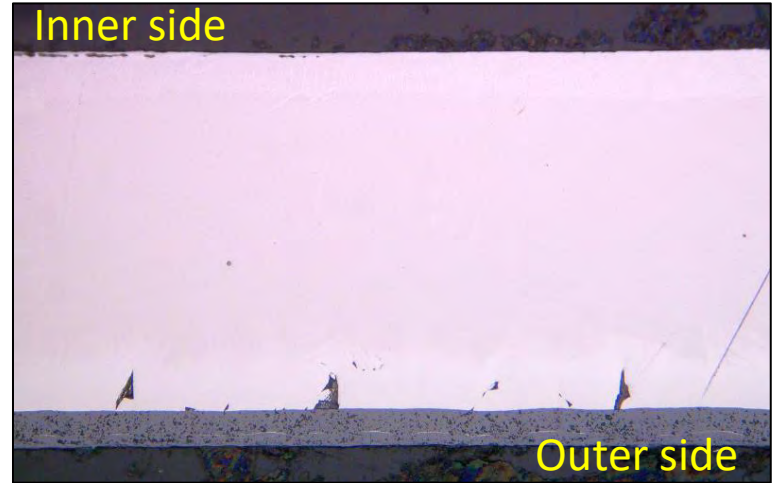
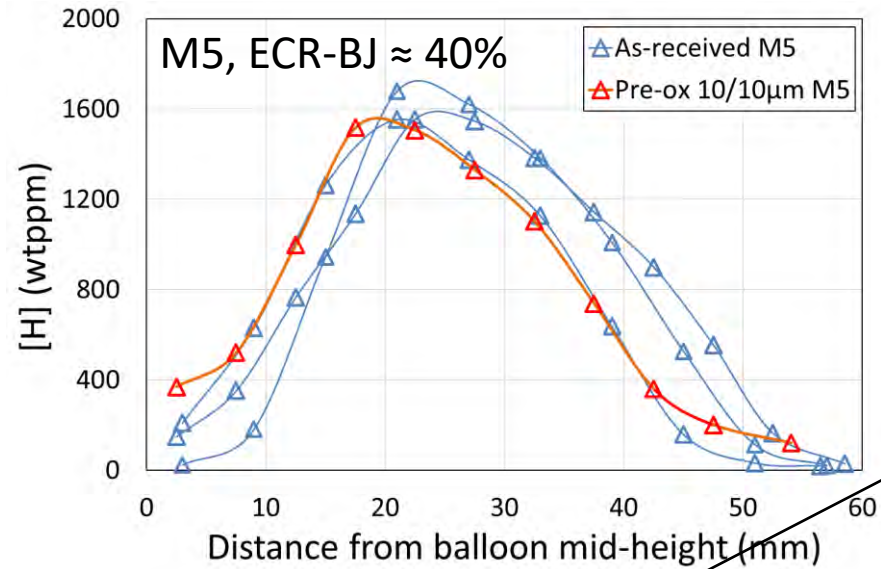


# Hydrogen axial distribution



- The colour change corresponds to the end of the inner oxide layer.
- Clear link between the colour change and the hydrogen axial distribution.
- H peak maximum is located few mm from the end of the inner oxide layer.

# Effect of the inner pre-oxidation on H pick-up

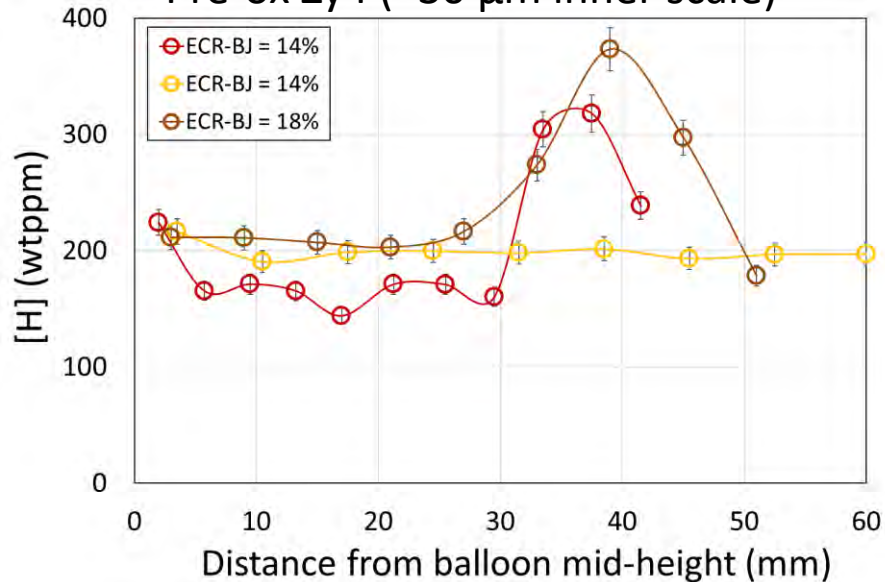


- For high ECR, a thin (10 µm) inner pre-oxide scale dissolves and doesn't prevent secondary hydriding.



# Effect of the inner pre-oxidation on H pick-up

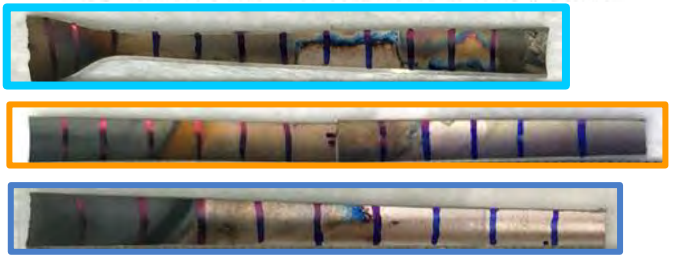
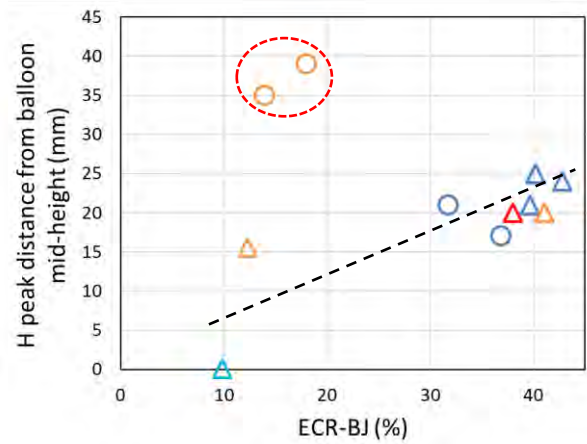
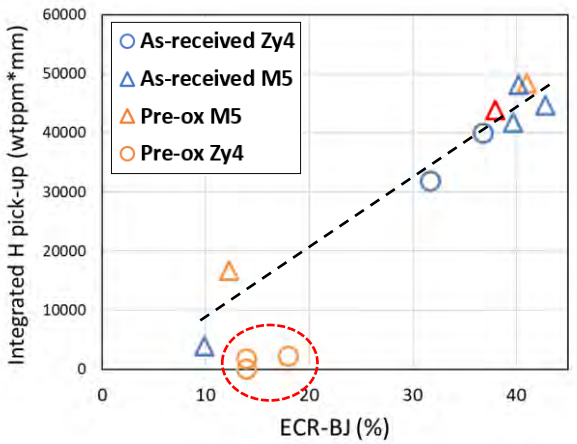
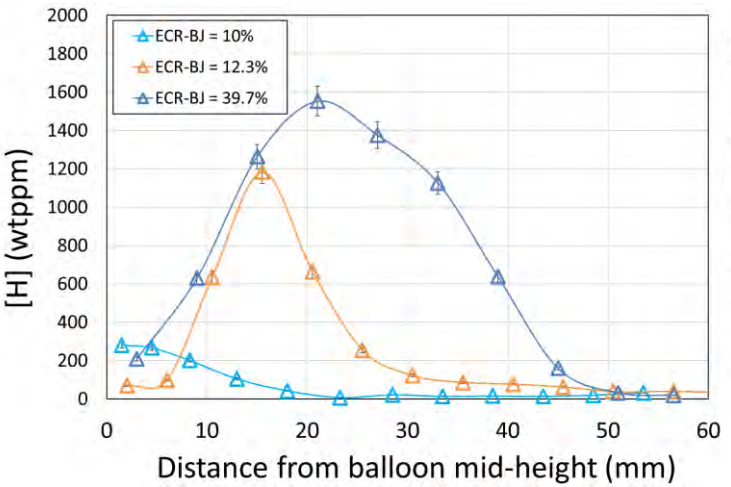
Pre-ox Zy4 (~30  $\mu\text{m}$  inner scale)




For Pre-ox Zy4 (30  $\mu\text{m}$  inner scale):

- Moderate (but non zero) H-pick-up.
- Pick-up occurred away from the opening.
- Inner zirconia scale is darker (but not fully dissolved) where H pick-up occurred.

# Amount of H picked-up and H-peak/balloon distance



 = thick inner pre-oxide scale

- The amount of incorporated hydrogen increases with ECR.
- The H-peak maximum may shift away from the balloon mid-height as ECR increases.

# Conclusions (preliminary)

## Regarding the strain in the ballooned region

- Lower strain for M5<sub>Framatome</sub> than for Zy4,
- Thick pre-oxide layers (40/30 $\mu\text{m}$ ) significantly decreases the strain (Zy4),
- Thin pre-oxidation layers (10/0 or 10/10 $\mu\text{m}$ ) have much lower influence (M5<sub>Framatome</sub>).

## Regarding rupture after HT oxidation

- At very high ECRs, rupture without applied load sometimes occurred in the secondary hydriding region during quench.

## Regarding secondary hydriding

- A thin inner pre-oxide scale can be dissolved and doesn't prevent secondary hydriding.
- The amount of H incorporated increases with ECR (i.e. with exposure time),
- The H-peak maximum shifts away from the opening as exposure time increases.

More data needed, specifically at intermediate ECRs.

**We are ready to test Cr-coated ATF claddings !**

Thank you for your attention





**R. Nagy**

**Centre for Energy Research, Budapest**

## **Ballooning and burst measurement of nuclear fuel cladding**

A new experimental series was launched at MTA EK to investigate the dynamics of cladding ballooning of VVER fuel claddings. Our goal was to reproduce the previously measured VVER data regarding burst pressure at different pressurization rates using the isothermal method, and to observe the ballooning and burst phenomena in detail using regular and high-speed, and also infrared video recording in the high temperature furnace.

The experimental setup consisted of four parts: a modified tube furnace, an optical system, the pressure system and the control and data acquisition unit. The inside of the electrically heated furnace was 520 mm long and 104 mm in diameter. The high pressure argon gas was fed into the cladding samples by a needle valve, in order to maintain a certain rate of internal pressure increment. It was tested between 1 kPa/s and 0.5 MPa/s and the accuracy and linearity was over 99%. For data acquisition and control, we used a Measurement Computing USB-2408 multifunction measurement device. Two identical optical telescopes have been constructed to observe and record the behavior of the cladding samples during the tests, which were operable at 1000 °C. The telescopes consisted of a flat-corrected condenser objective lens group (3 lenses, 27 mm in diameter) and an ocular or eyepiece lens (40 mm in diameter) made of high purity quartz. A regular camera was used to record the kinetics of the ballooning and a high-speed camera to record the crack opening and propagation during the burst. A near-infrared camera (2-5  $\mu\text{m}$ ) was used to proof a hot spot appearance on the sample during ballooning phase. We used different shareware programs and codes to process the recorded videos and to measure the diameter increase of samples without human interventions. A self-developed code determined the contours of the cladding tube samples in the video frames.

The burst pressure was found to highly depend on the temperature and the internal pressure increment rate. The diameter of the cladding samples increased in two phases. A global increase in diameter at the beginning, then a local bulge formation was observed prior to the burst. Every burst was preceded by a local heat-up and an axial bend simultaneously. The hot spot appeared not earlier than 1–1.5 s, bend was observable 2-3 s prior to the crack opening and burst [2].

We observed by a high speed camera that the time scale of the crack propagation lasts about 0,16 ms. A crack edge become slightly hotter. High speed camera recording also revealed that small debris fly within the furnace after burst.

Infrared camera observation showed that oxide and pure metal has slight difference emission coefficient and the hot spot is about 20 degrees warm. The hottest point of the sample seems always to be located at the tip of the propagating crack.

New Zr plug geometry was proposed and new frequency converter was used to slow down the welding, more time for the tube and the plug to melt, stronger bonding.

Coated samples (E110, E110opt (G), Iranian E110, Zirlo, Zry-4, and those Cr-coated and CrN coated versions, optimal Zirlo) were tested in the facility. Generally can be told that the coating does not effect significantly on burst pressure. Cracks forming in the coating layer, parallel to the opening. Cr-CrN coating prevents the most coat layer-crackings.



Centre for Energy Research

# Ballooning and burst measurement of nuclear fuel cladding

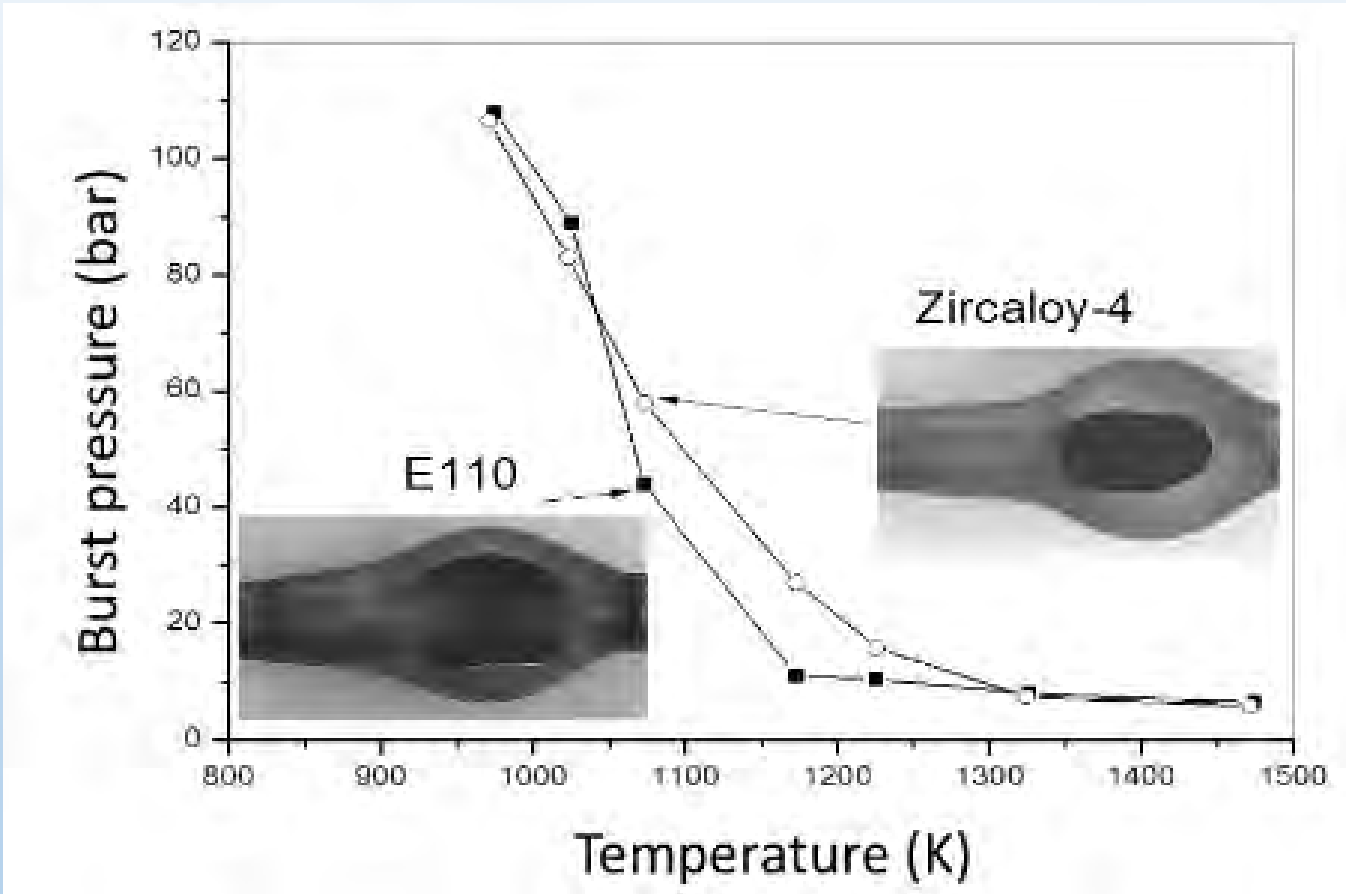
Richárd Nagy, Márton Király, Tamás Szepesi  
Zoltán Hózer, Péter Petrik

Karlsruhe, 27-29 September 2022.



# Loss of Coolant Accidents (LOCA)

when pressure of coolant drops, temperature increases, and internal pressure pushes the wall of the tube, plastic deformation occurs, finally a crack opens up





Retort: heat resistant steel

Length: 520 mm / Diameter: 104 mm

Kaolin insulating wall: 80 mm

Accuracy: 800 °C within 300 mm  $\pm 1$  °C

Three zones electric wire

PID controller (LTP-F 3X16A)

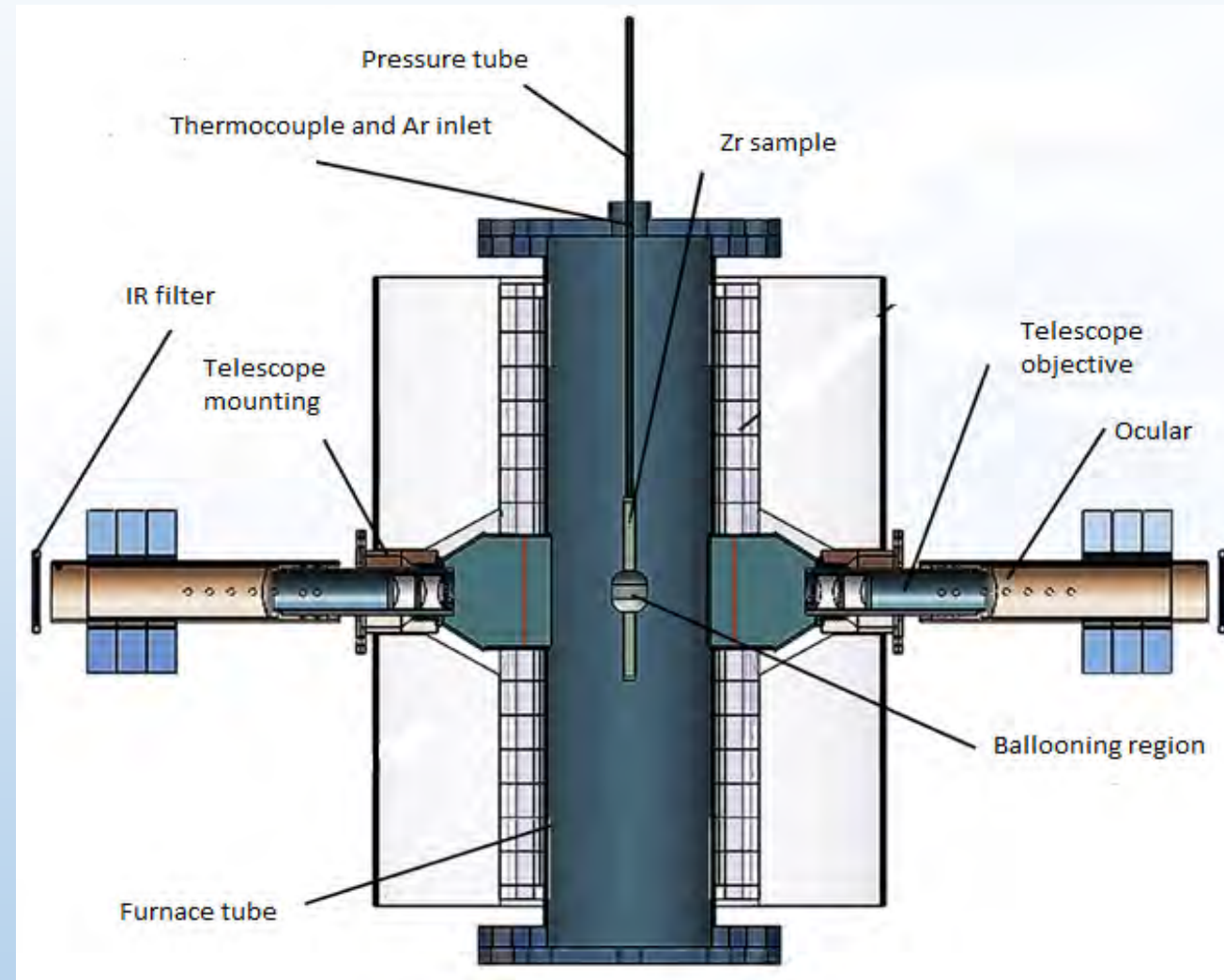
K type thermocouple

Argon atmosphere

Camera mount: 30 mm

Length of samples: 85 mm

Diameter: 9,1 – 30 mm

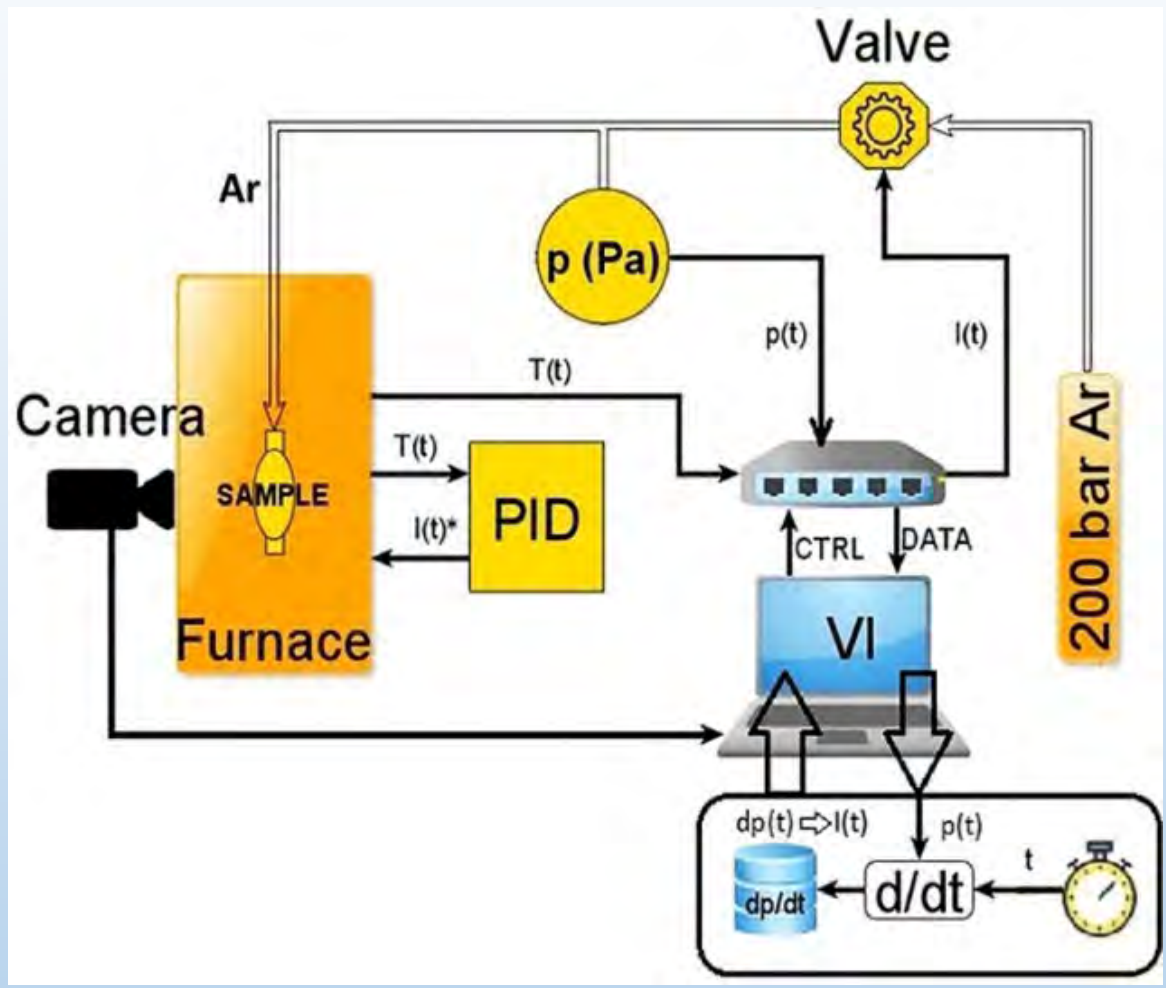
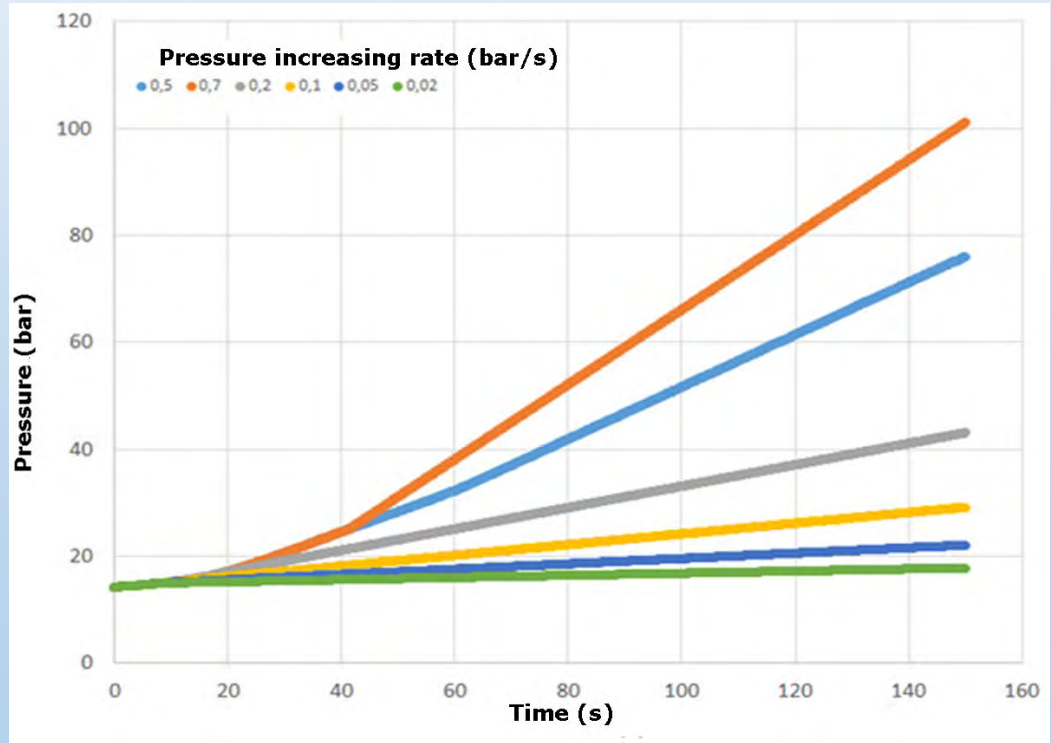


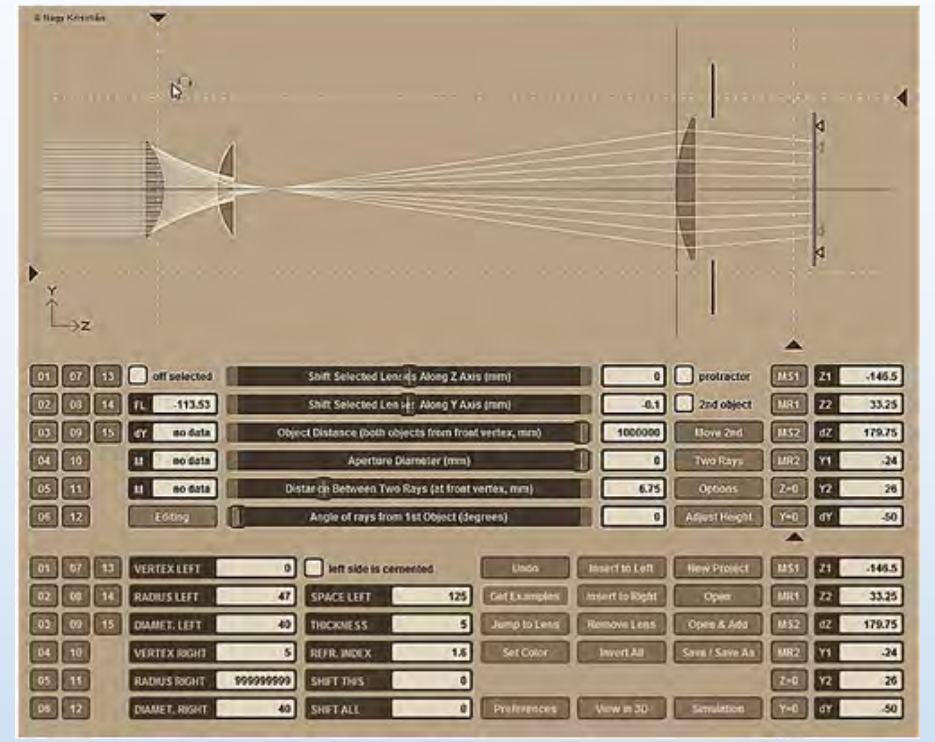
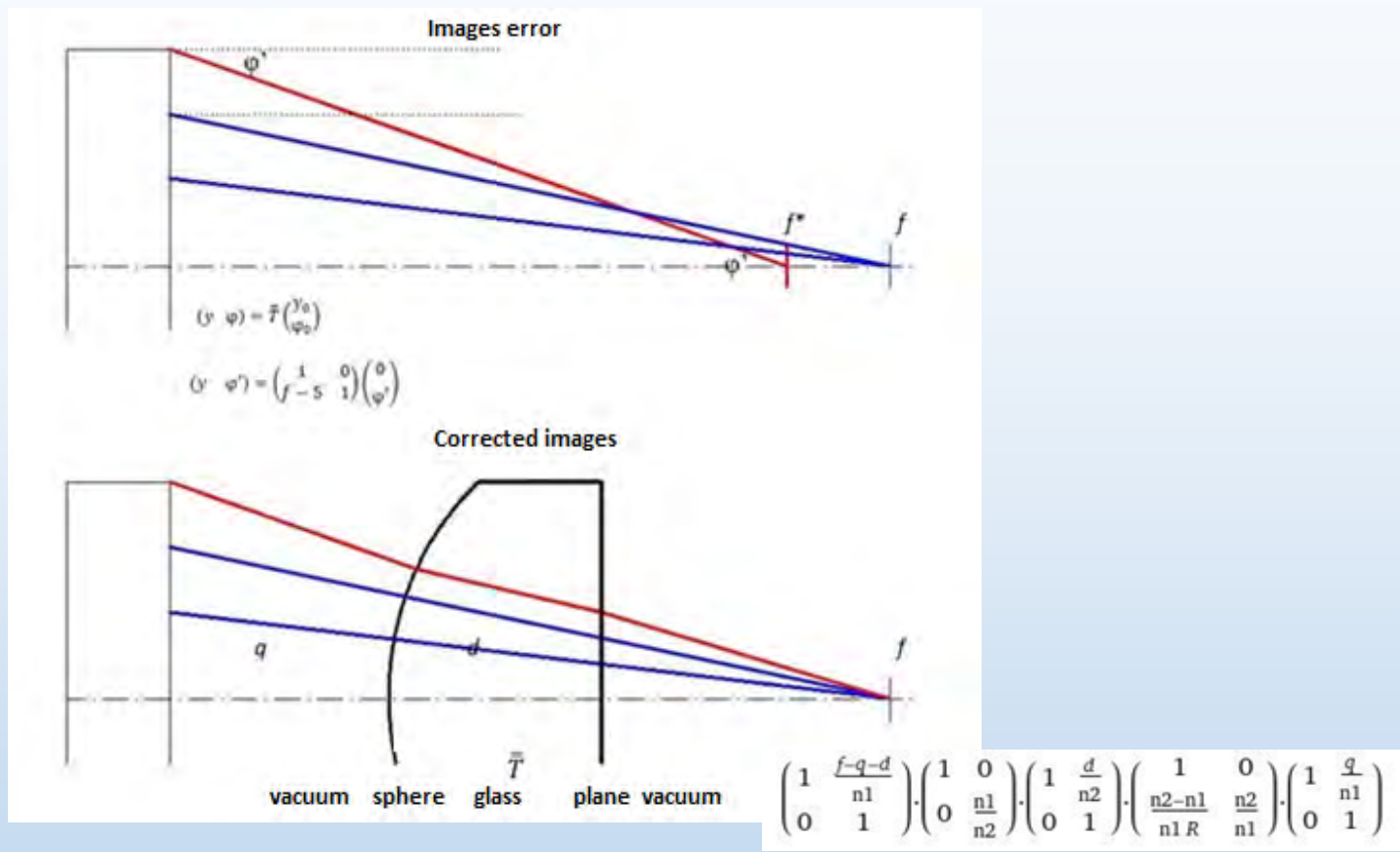


LabView VI + own designed electronics

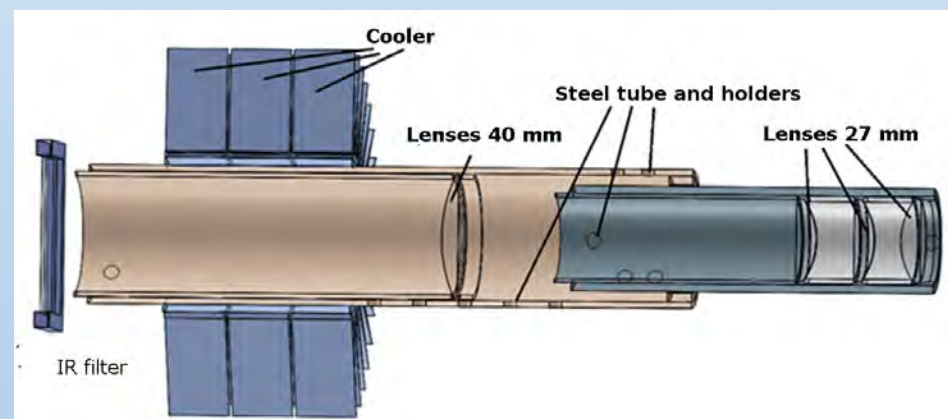
Needle valve operated by stepper motor (0,02 bar/s – 6 bar/s pressure increment)

Eliminating sealing problems





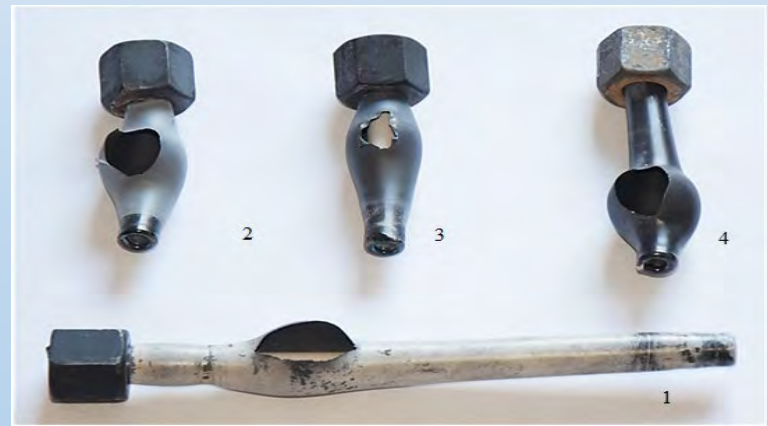
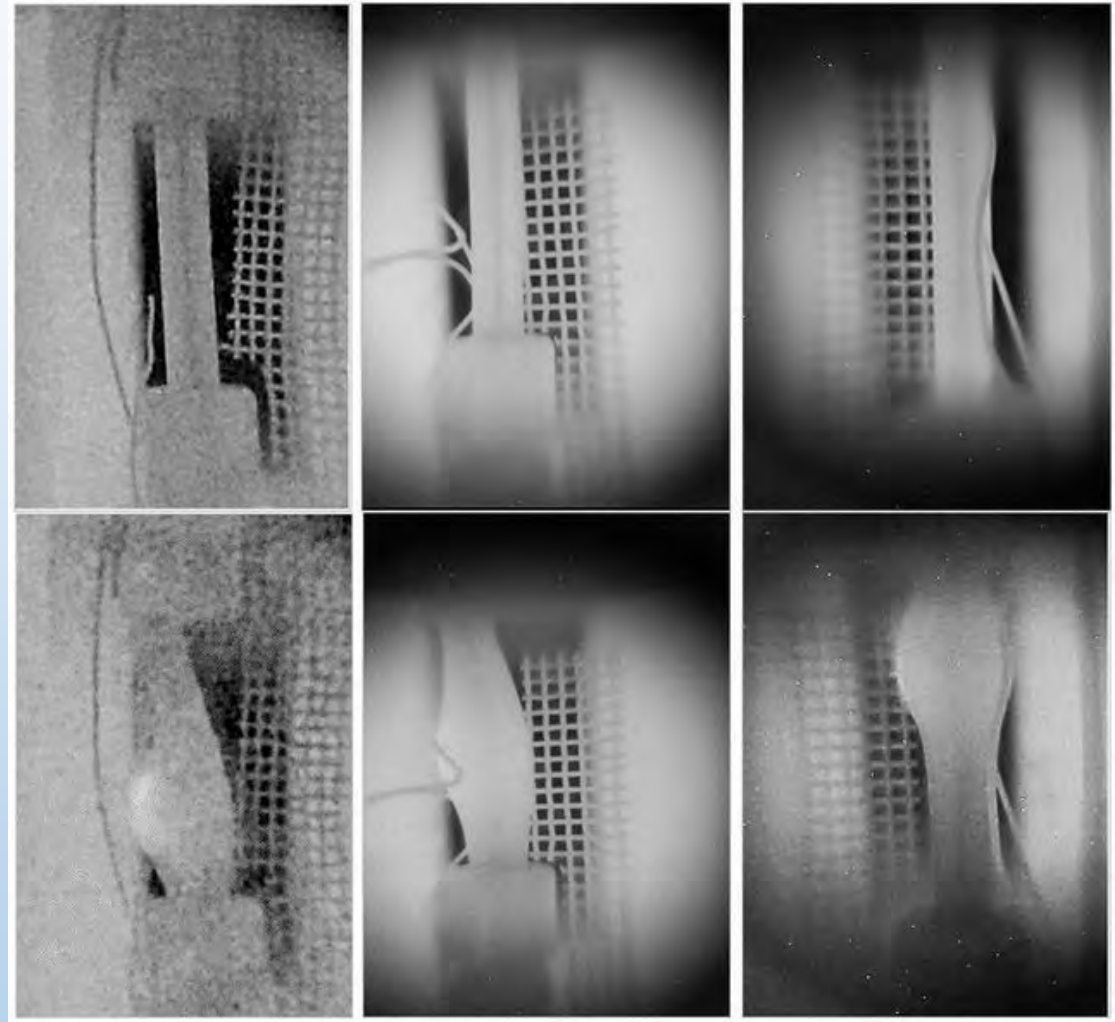
Heraeus Suprasil-1 quartz  $v = 1,467$   
 Objective lens  $f = 42 \text{ mm} / d = 27 \text{ mm}$   
 ( $R = 22 \text{ mm}, 6,6 \text{ mm}$ )  
 Distance of corrector lens  $21,596 \text{ mm}$   
 (measured actual:  $20 \text{ mm}$ )





# HD camera measurements hot spot and axial bending were observed

Data No.	Length (mm)	PIR (bar/s)	Temperature (°C)	Burst (bar)	Alloy
1.	150	0,48	795	76,9	E110G
2.	65	0,43	755	91,1	E110G
3.	70	0,69	805	94,1	E110G
4.	85	0,39	820	89,9	E110G





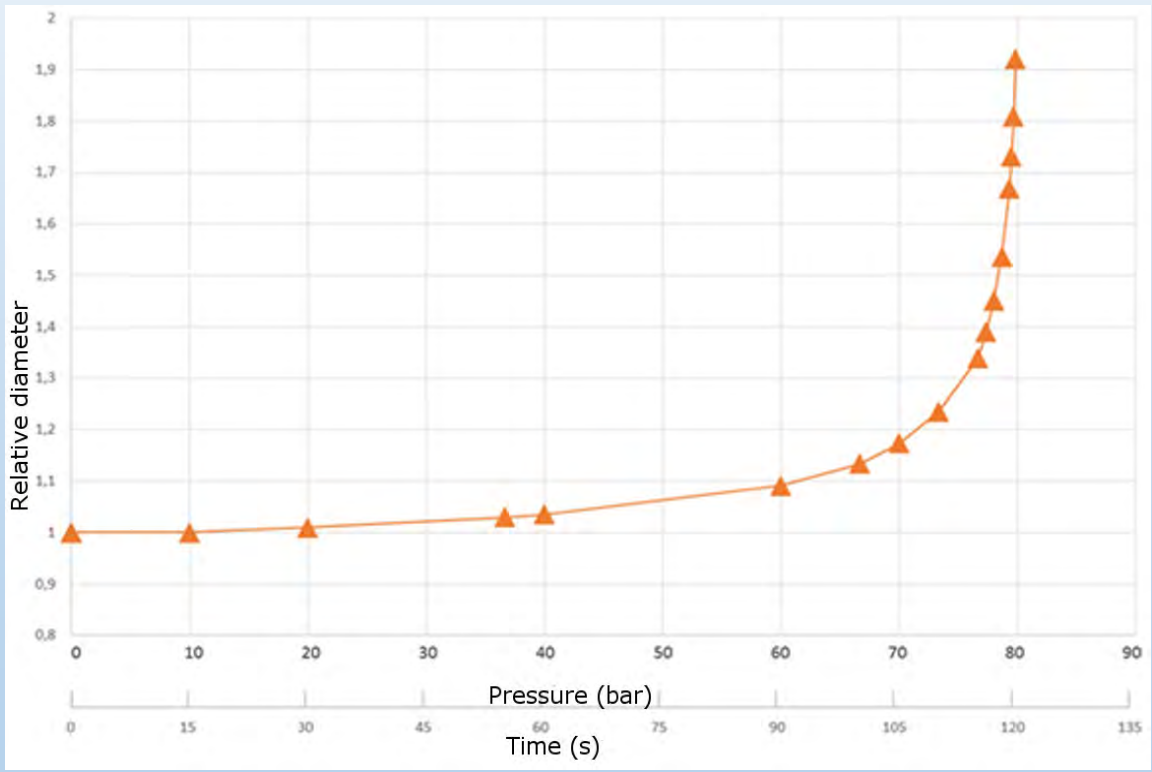




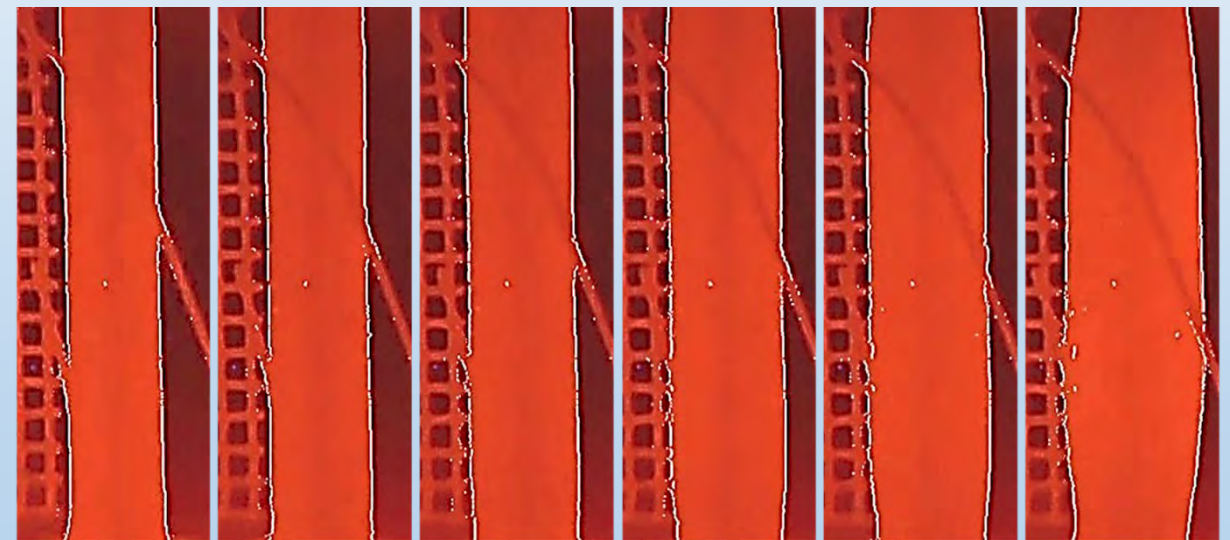
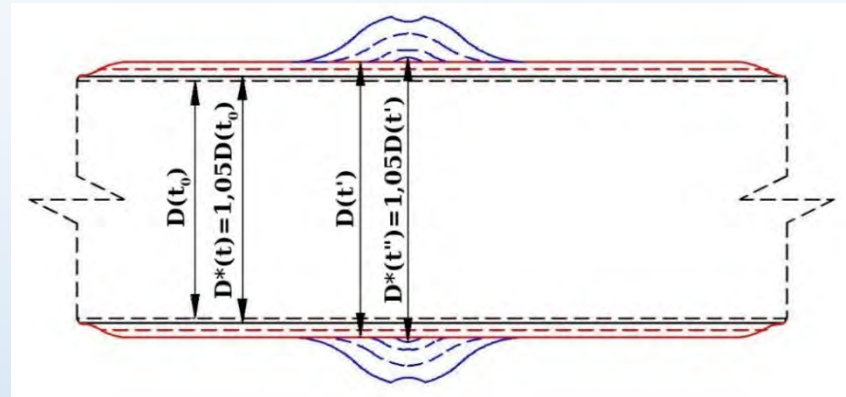


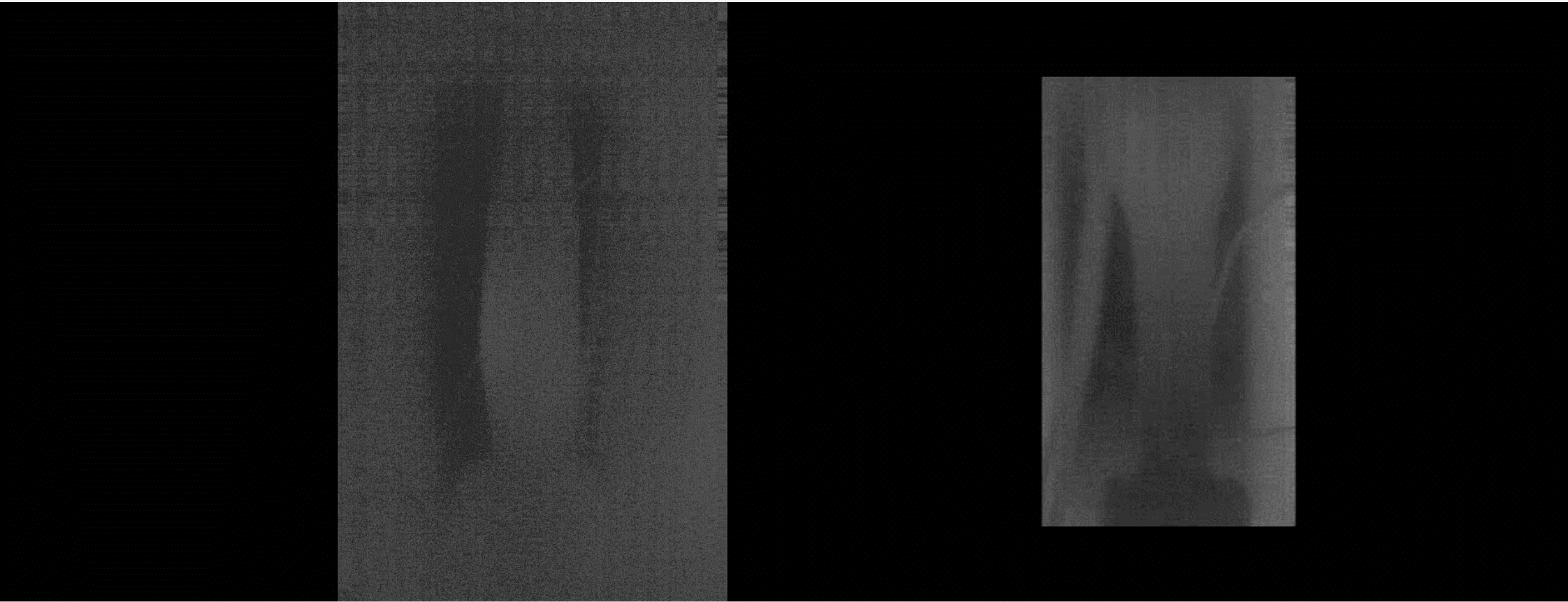
# HD camera measurements

## Developing contour seeker algorithm Based on comparing pixel RGB values



### Definition of different diameter growing (unique and bulge)

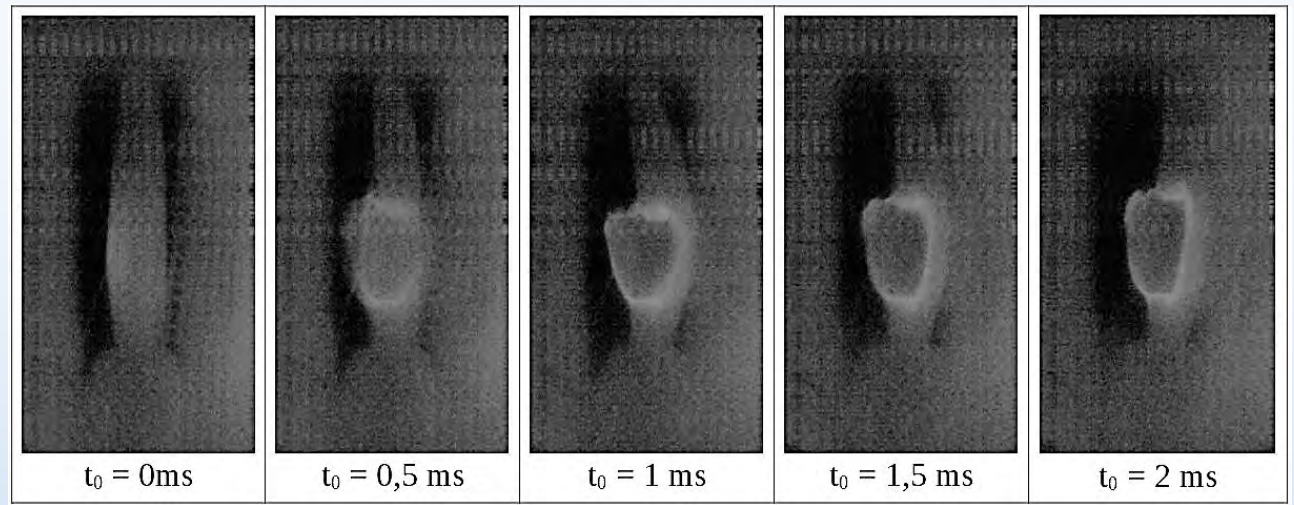




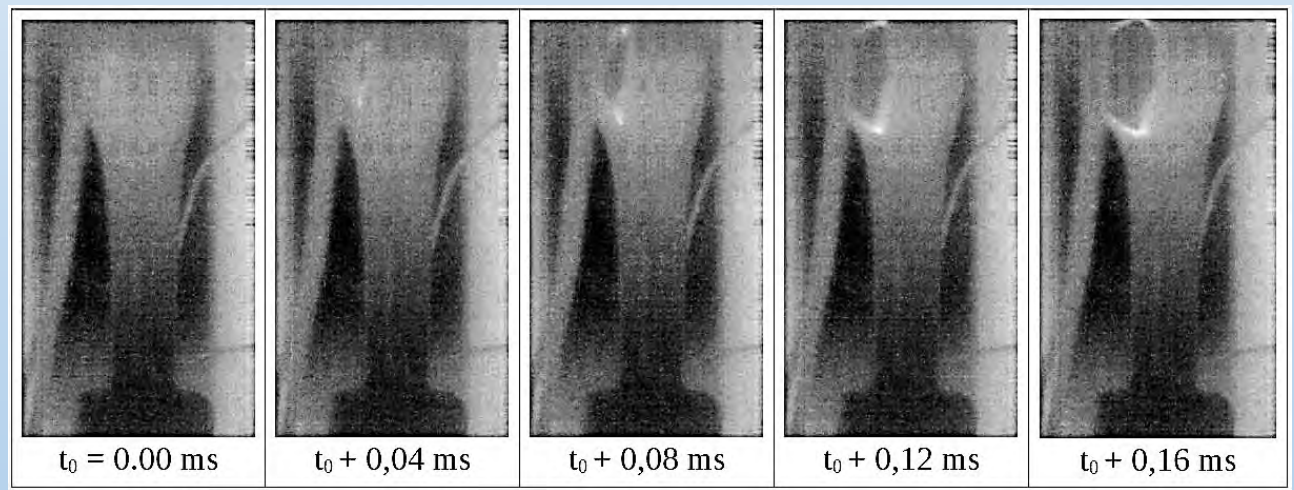




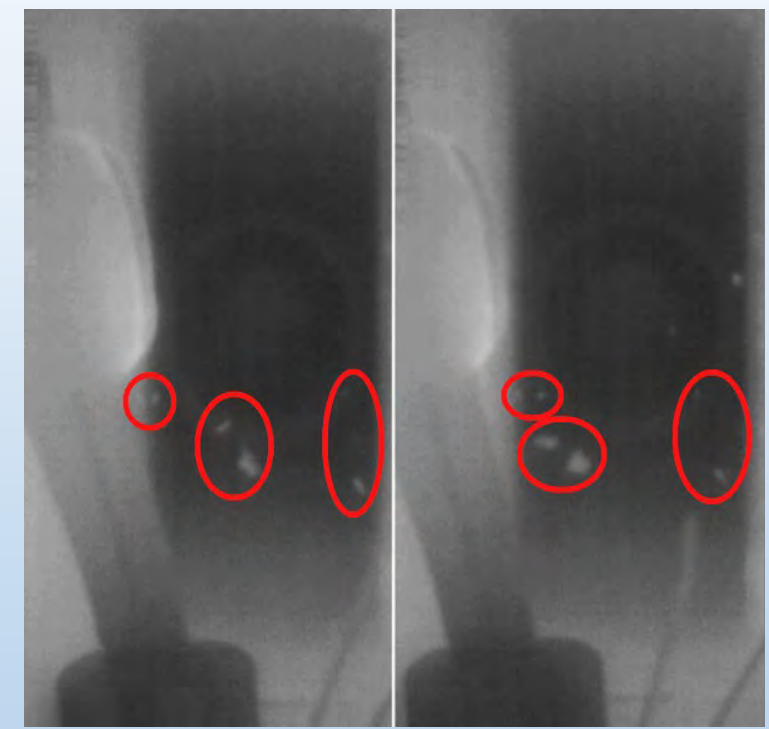
## 2000 FPS

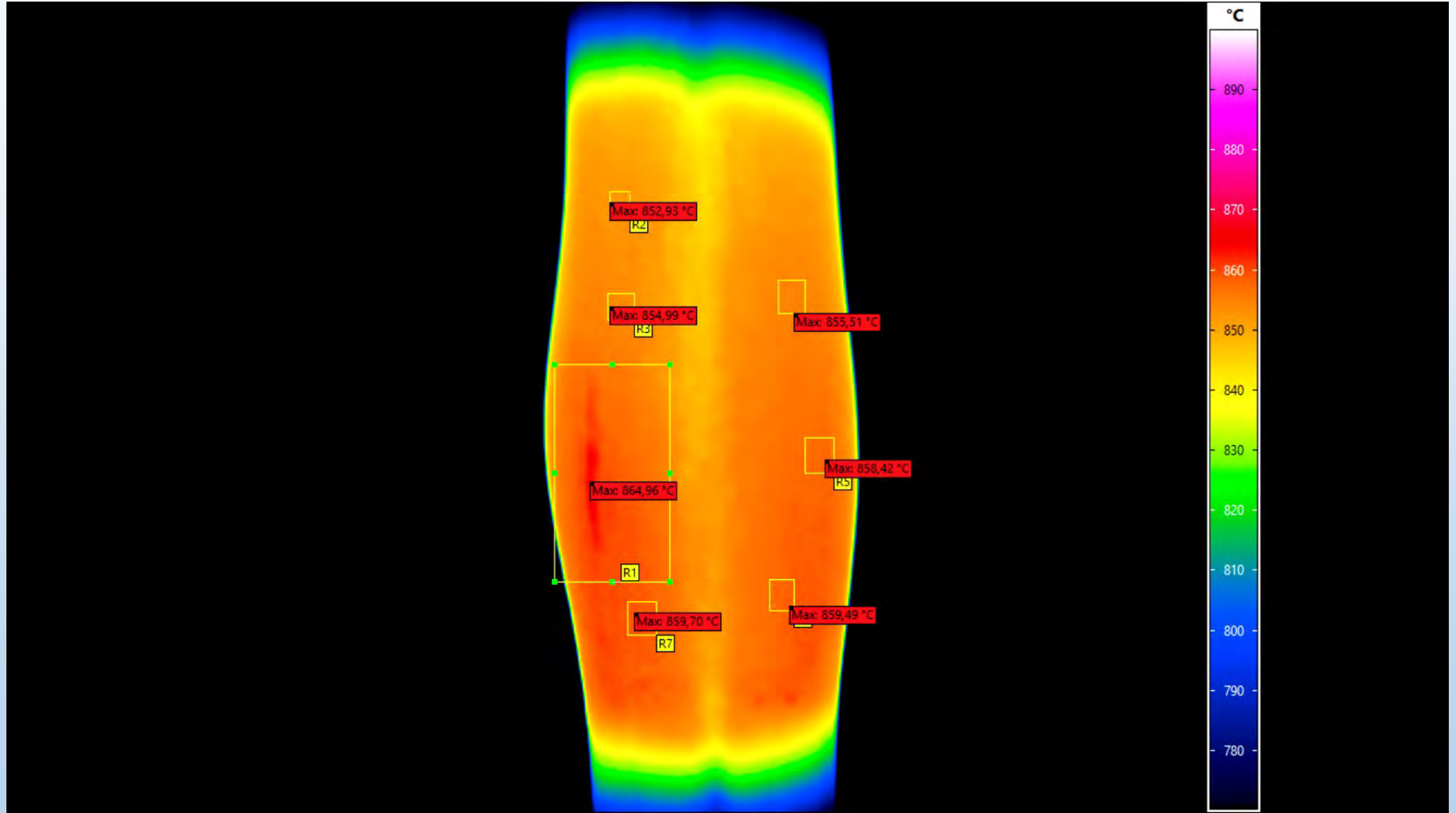


## 25000 FPS



## 100000 FPs

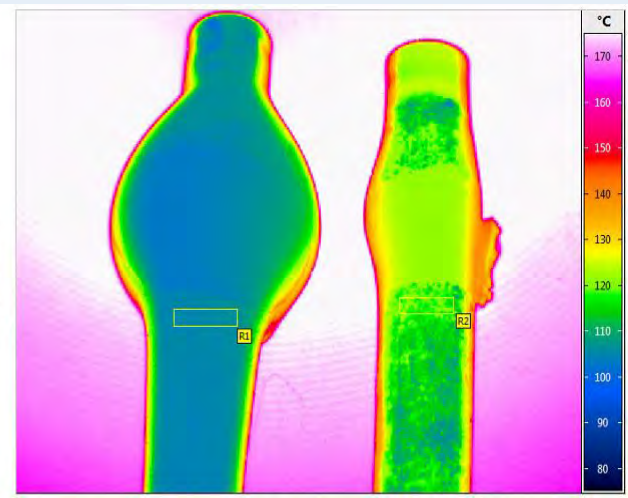
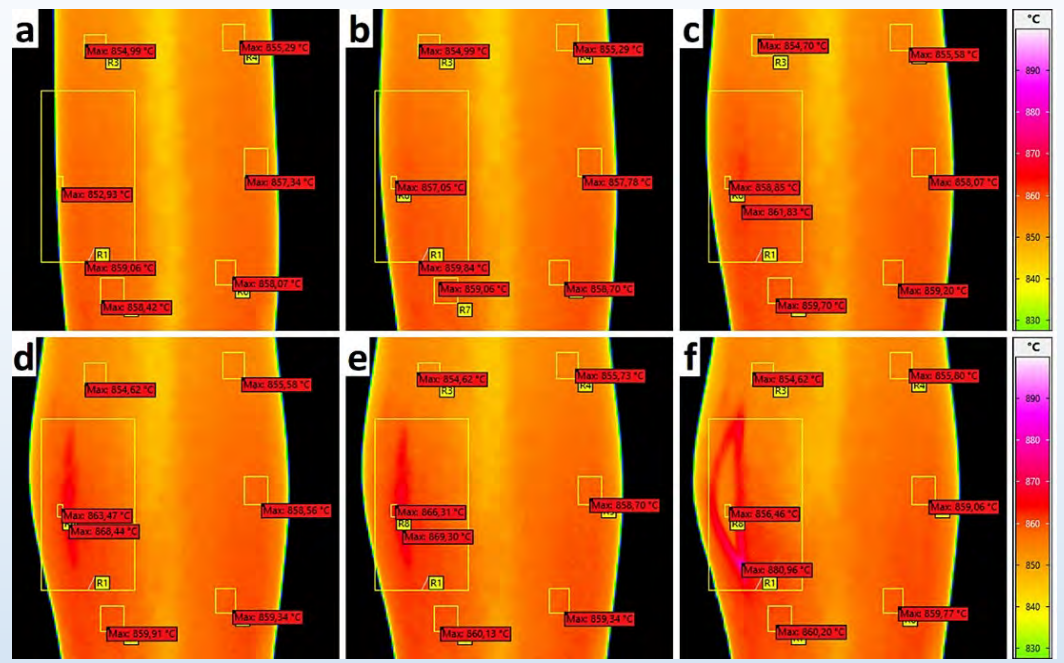




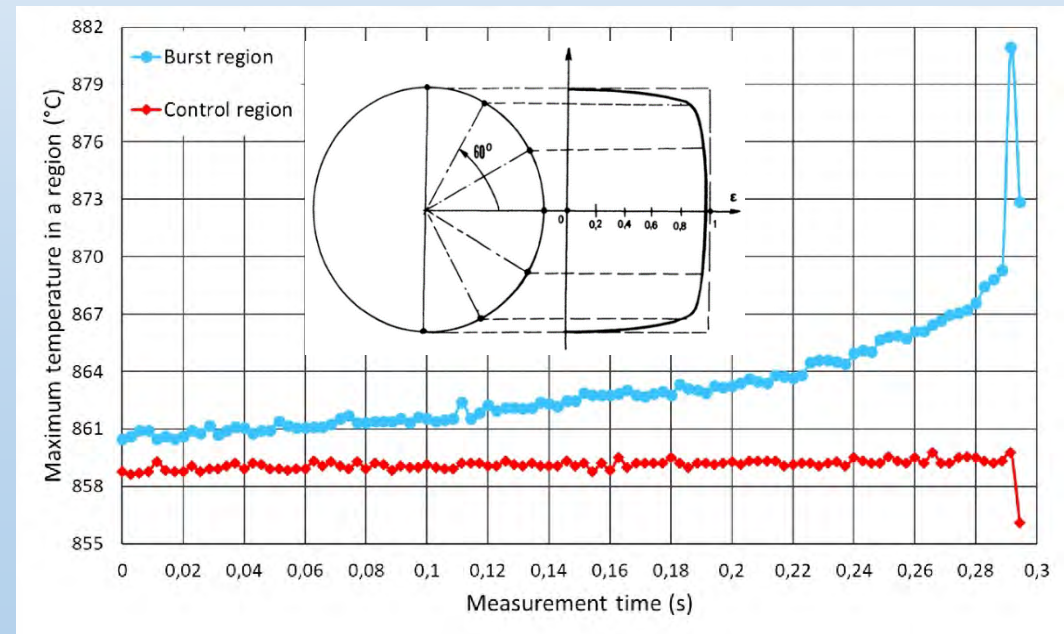




350 FPS infra-camera (2-5  $\mu\text{m}$  QWIP detector)  
 Sample at 800 °C  
 Calibration of emission coefficient by the factory  
 Hot spot is real with 20 °C temperature increment

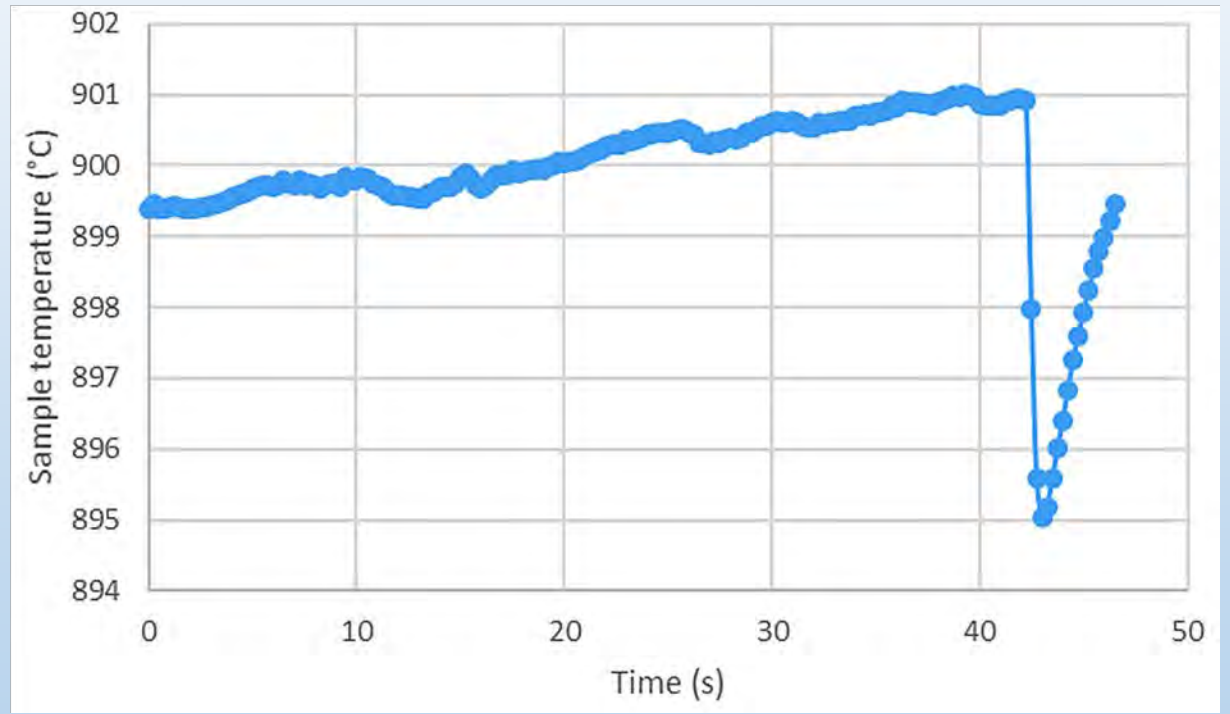
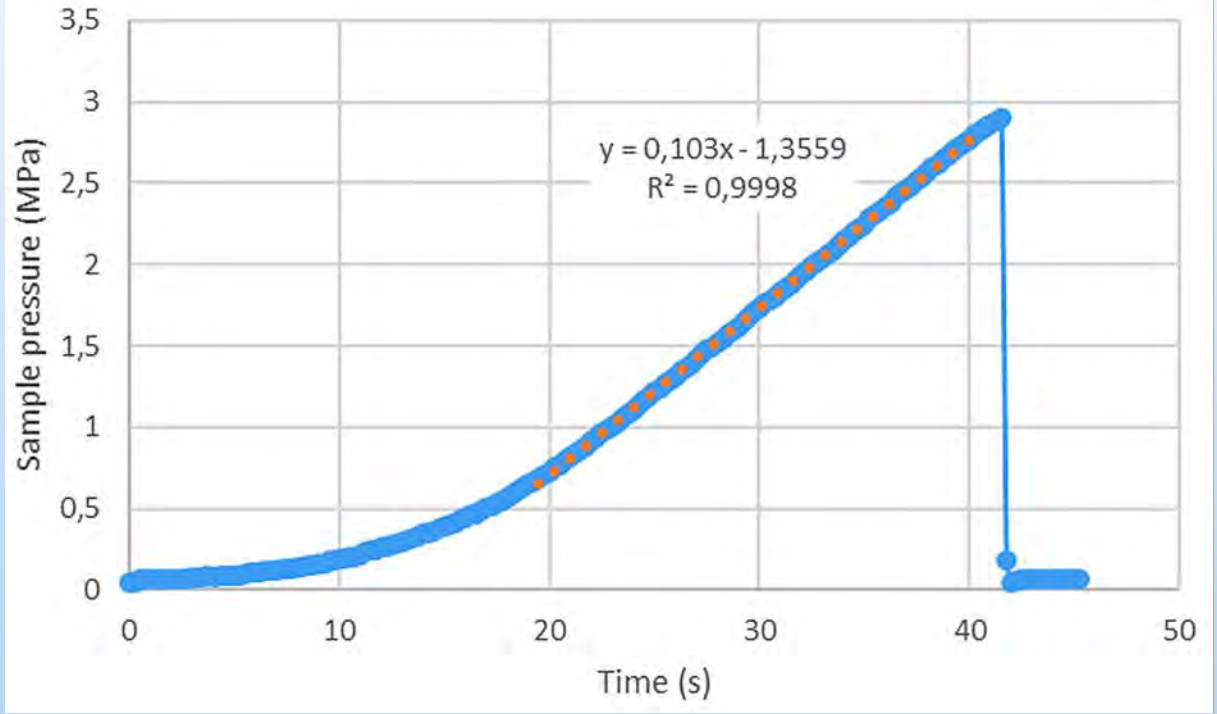


Sample	Pure metallic area		Oxidized area	
	measured $\epsilon$ (direct)	measured $\epsilon$ (indirect)	measured $\epsilon$ (direct)	measured $\epsilon$ (indirect)
Emission	0,91-0,98	0,89-0,94	0,74-0,93	0,8-0,93





Burst conditions: pressure increment (0.1 Mpa/s) and temperature ( $\approx 900$  °C)



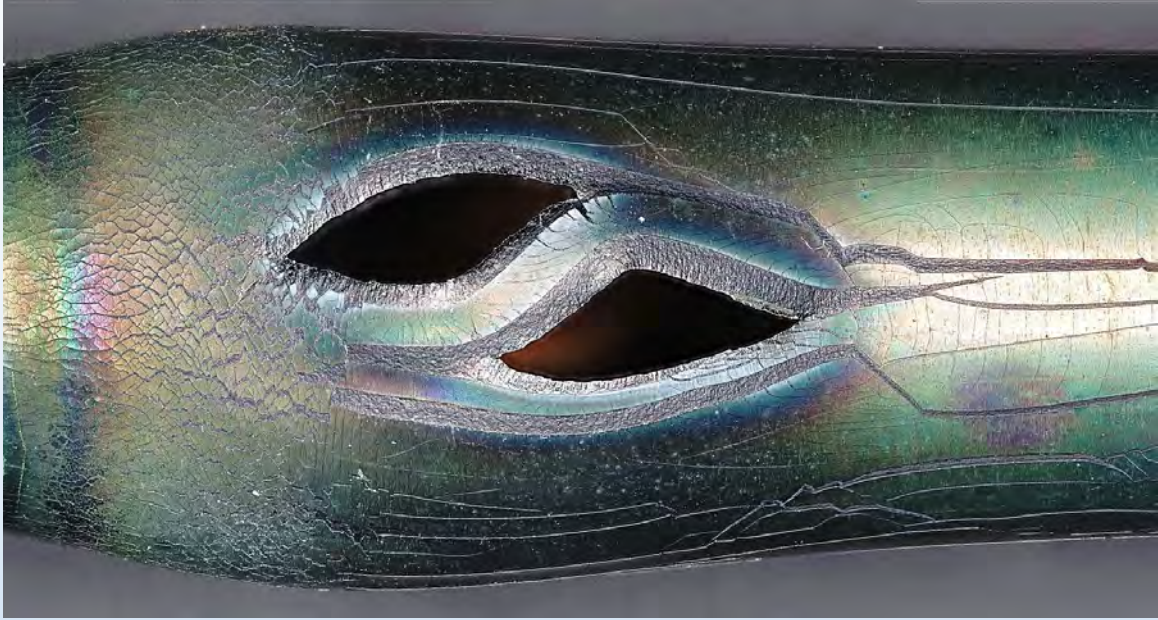


Results, 2022, 900 °C and 100 kPa/s

Sample No.	Institute	Cladding material (coating)	Temperature (°C)	Pressure increase rate (kPa/s)	Burst pressure (MPa)
ATFTS-28	AEOI	E110 (as-received)	892	65	2,89
ATFTS-29	AEOI	E110 (as-received)	899	64	2,69
ATFTS-30	AEOI	E110 (Cr)	898	80	2,76
ATFTS-31	AEOI	E110 (Cr)	892	104	2,80
ATFTS-32	AEOI	E110 (CrN)	895	103	3,13
ATFTS-33	AEOI	E110 (CrN)	900	101	2,92
ATFTS-34	AEOI	E110 (Cr-CrN)	899	103	2,75
ATFTS-35	AEOI	E110 (Cr-CrN)	890	103	2,90

No significant effect of the coating on the burst pressure.





The CrN-coated AEOL E110 cracked moderately, no spalling.

The Cr-coated AEOL E110, with smaller cracks by the burst location and no cracks along the rest of the sample







Centre for Energy Research

Thank you for your  
attention!



**S. Gabriel**  
**KIT**

## **Overview on COSMOS Facility on thermal-hydraulic phenomena in nuclear reactors**

The presentation gives an overview on the research activities at the experimental facilities COSMOS-L and COSMOS-H. For the low-pressure water loop COSMOS-L, selected results on the boiling experiments performed so far up to critical heat (critical heat flux/departure from nucleate boiling) were shown. Different test sections were used with heaters in the form of a single tube in an annular gap, rod bundles and flat heaters. The predominant heater materials used include Zircalloy-4 and stainless steel. The facility has a rapid shutoff system to protect the heater and allows repetition of experiments with identical heater. It shows that the critical heat in the up to 54 times per measurement point occurs as a frequency distribution comparable to a Gaussian distribution. The series of experiments on heat transfer of boiling flows up to CHF on a flat heater (In Vessel Retention by Ex-Vessel Cooling) show a significant dependence of the critical power on the orientation of the heater with respect to the vertical.

In the second part of the presentation, COSMOS-H was presented, a water circuit with about 2 MW thermal power that can reach power plant conditions. The performance data include max. 170 bar, 360°C and a mass flow of 1.4 kg/s water/steam. The facility is currently in the process of completion or commissioning. The test section for the first series of tests within the framework of the McSAFER project contains a single heated tube in the annular gap and later also a bundle of five tubes was equipped with a high degree of instrumentation. The modular design of the test section allows flexible adaptation of the test arrangement and instrumentation. Furthermore, a high-pressure sight glass for use in the experiments on SMR reactor concepts was presented.

## **27th International QUENCH Workshop**

### Overview on COSMOS Facility on thermal-hydraulic phenomena in nuclear reactors

**Stephan Gabriel, Giancarlo Albrecht, Wilson Heiler, Felix Heineken, Nicolas Wefers**  
**27.09.2022**

Institute for Thermal Energy Technology and Safety (ITES)

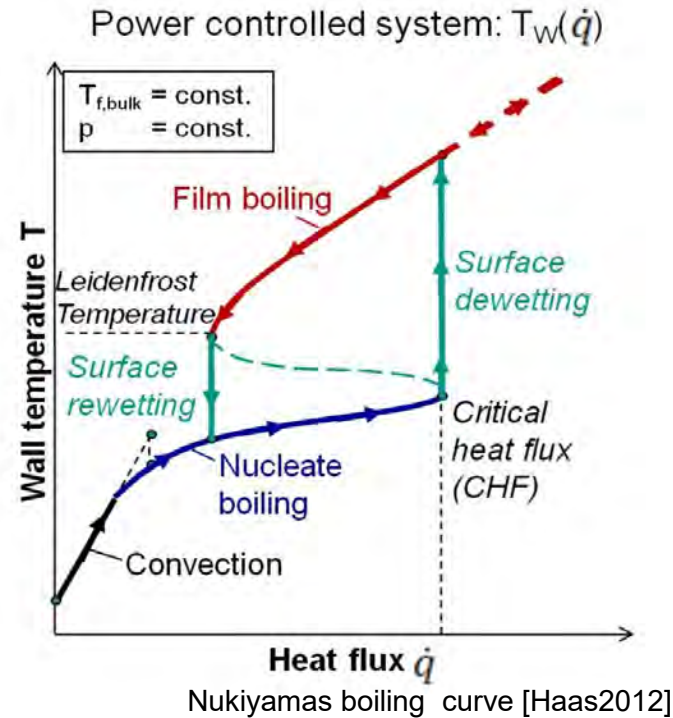
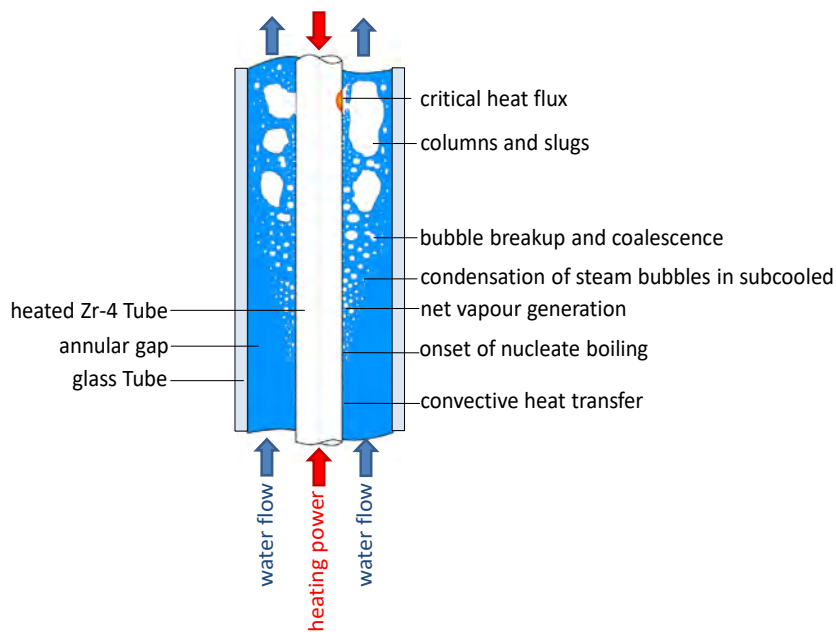


# Outline

- Motivation
  - Flow boiling under forced convection and boiling crisis
  - Single tube and bundle tests
  - IVR / ERVC
- COSMOS-L
  - Facility
  - Single tube in annular gap / rod bundle
  - Flat heater
- COSMOS-H
  - Facility
  - McSafer testsection
- Conclusions / Outlook

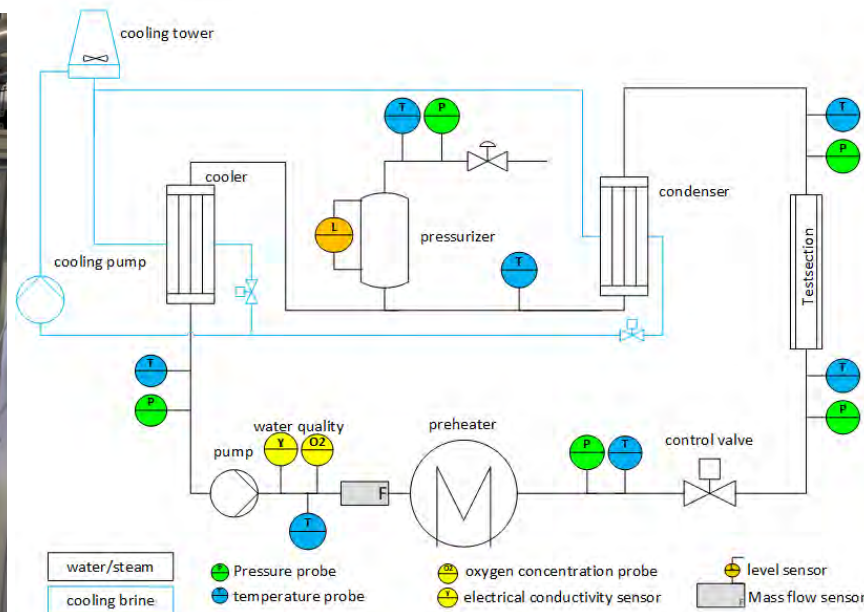


# Motivation



- Boiling under forced convection is a very powerful heat transfer mechanism
- It is relevant for many different operating conditions and reactor concepts
- The heat transfer by flow boiling is limited by the boiling crisis or critical heat flux (CHF). This can occur either as dryout or as departure from nucleate boiling (DNB)
- The main influencing variables are pressure, temperature, mass flow, heater geometry and cooling medium

# COSMOS-L

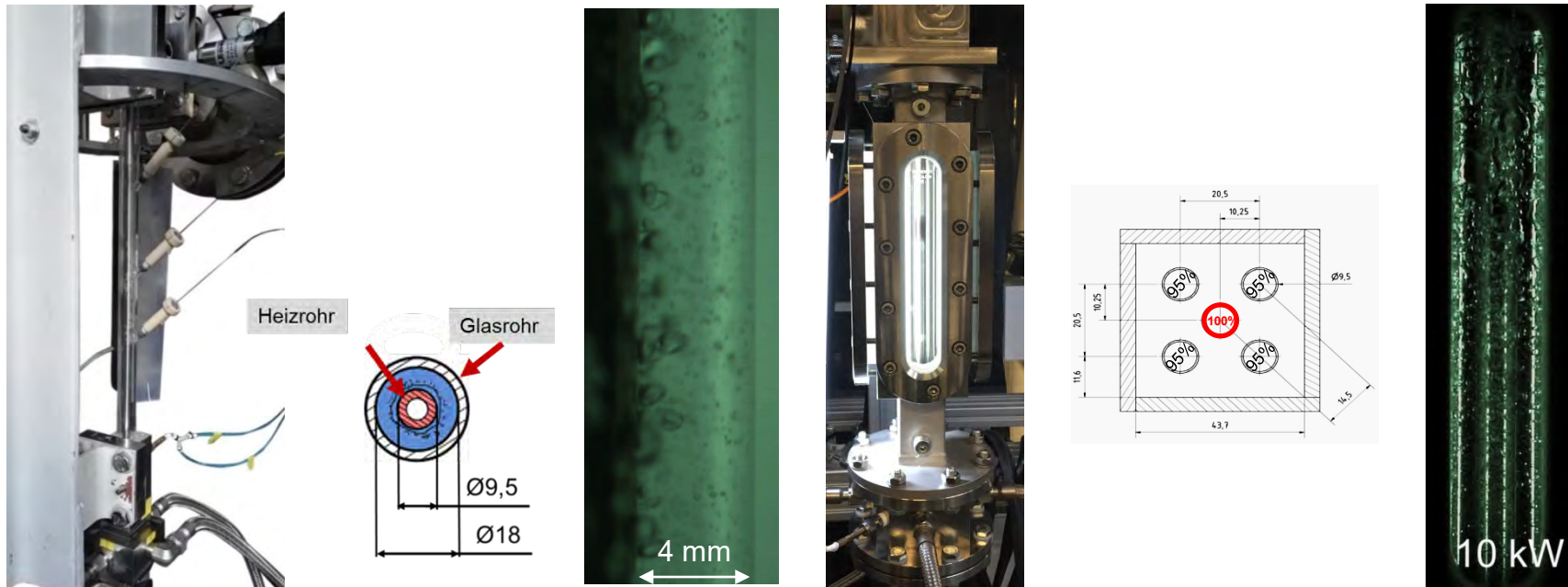


simplified flow chart

Variable	Value
test medium	water
mass flow	0,01 – 0,8 kg/s
inlet subcooling	5 – 100 K
pressure	1 - 6 bar
thermal power	ca. 180 kW
thermal power test section	3-75 kW, 50-300 kW

- In COSMOS-L we try to observe flow boiling and CHF under conditions as close as possible to the application
- The low pressure system offers a good measurement access to the flow and the possibility to use optical methods
- Due to its fast data acquisition, we are able to detect CHF and suspend the heating power in a short time

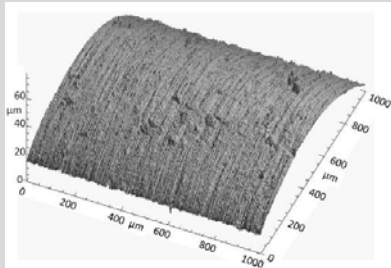
# COSMOS-L – NUBEKS test sections



- Two test sections are currently in use for the experiments:
  - a single heated tube in an annular gap
  - a rod bundle test section of 5 tubes (independently heated)
- The modular pressure housing allows flexible adaption of new measurement technologies like optical fibre probes (void) or optical measurement methods like PIV or LDA
- Thus COSMOS-L is very well suited for measurement technology development, preliminary studies for the high-pressure tests and highly detailed studies on boiling flows up to CHF

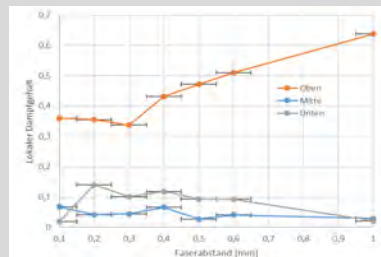
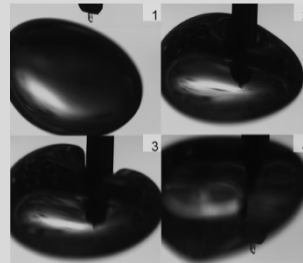
# COSMOS-L NUBEKS results

## Heater characterisation



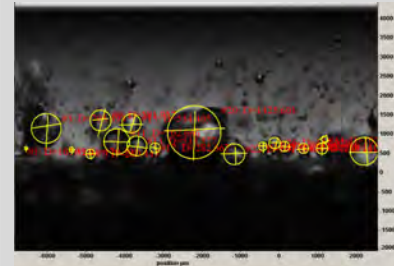
- detailed investigation of the used heater tubes:
  - surface structure and porosity,
  - rewetting and contact angle,
  - thermal conductivity and oxidation
- The Zr-4 tubes have been studied and their boiling behaviour was characterised

## the fibre optic void sensor



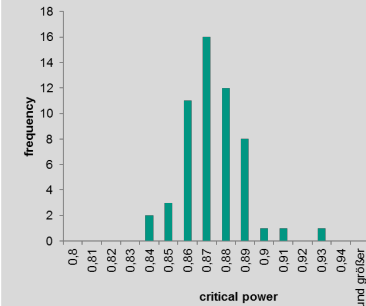
- a fiber optic void sensor was developed and validated, it is now ready to use to measure local void profiles

## Flow characterisation



- flow boiling was studied with a particle characterisation method results are:
  - local bubble velocity profiles
  - bubble size distributions
  - characteristic bubble trajectories/condensation data

## CHF statistics

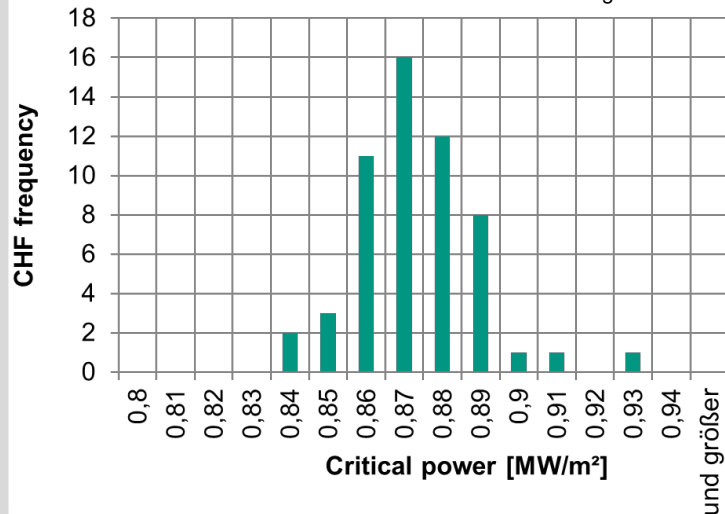


- Extensive statistical studies of the critical CHF power were completed
- The result is a significant dataset for CHF critical power in dependence of the major boundary conditions like system pressure, temperature/ subcooling and mass flow

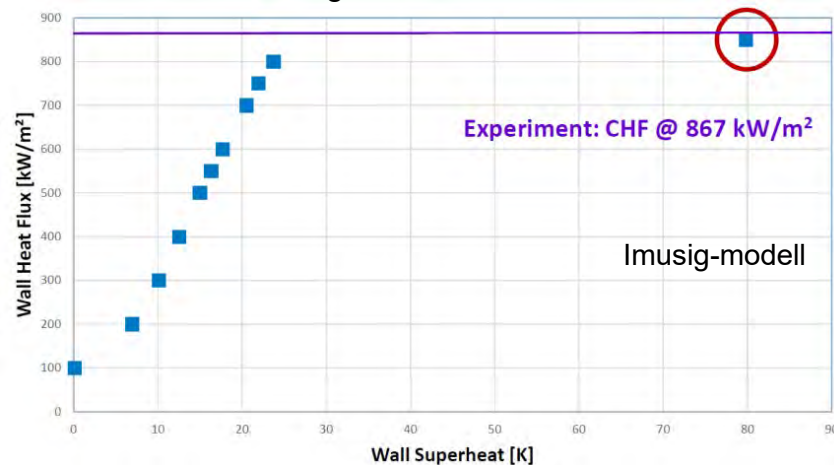


# Validation results in NUBEKS

Test conditions: T = 80°C P = 1200 mbar M = 400 kg/m<sup>2</sup>s



Simulation using CFX 18.1 + Customized Solver

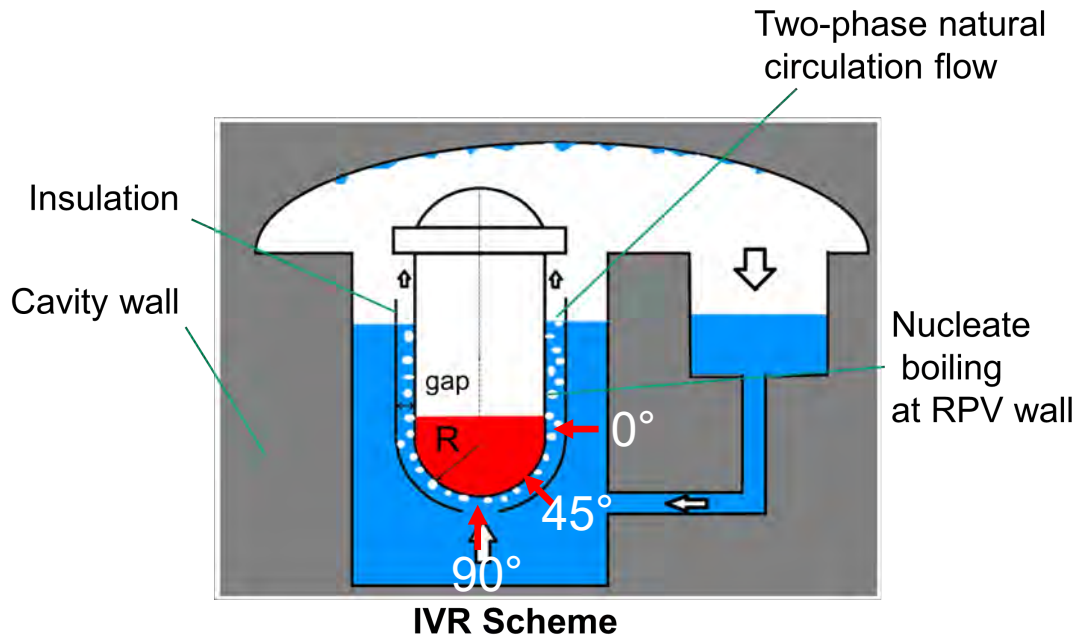


From: Thomas Frank(1), Amine Ben Hadj Ali(1), Conxita Lifante(1), Florian Kaiser(2), Stephan Gabriel(2), Henning Eickenbusch(1) (1) ANSYS Germany GmbH/ (2)KIT\_IKET, Erkoftag 2018, Stuttgart

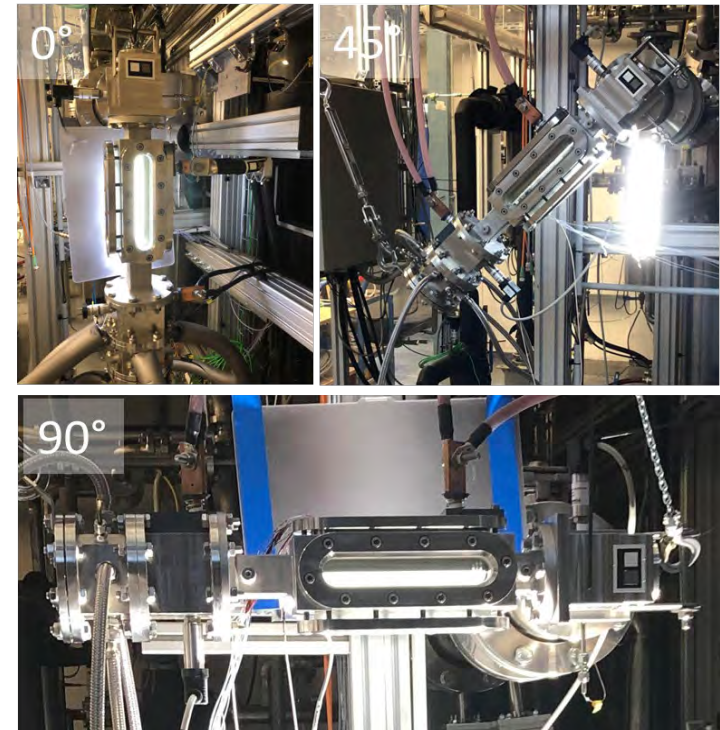


- The experimentally measured heat flux at which CHF occurs is about 867 kW/m<sup>2</sup> with a standard deviation equal to 16 kW/m<sup>2</sup>
- This is in good agreement with the ANSYS CFX results – Temperature excursion in the heater rod obtained at 850 kW/m<sup>2</sup> in the simulations – Liquid cooling of Zircaloy cladding breaks down at the very end of the heater rod

# Project KEK -SIMA



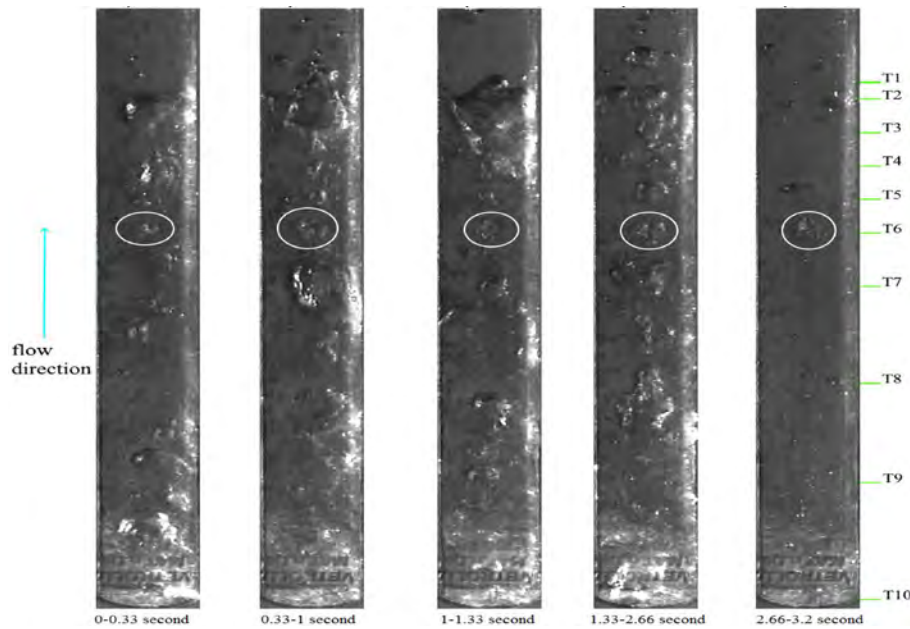
Stelios Michaelides



Stelios Michaelides

- In the KEK-SIMA project, the heat transfer up to the boiling crisis is investigated together with KIT/IATF under the aspect of in-vessel retention by external cooling (IVR/ERV)C
- In addition, more test parameters such as periodically fluctuating mass flows (period duration and amplitude are variable) as well as the test section inclination were investigated

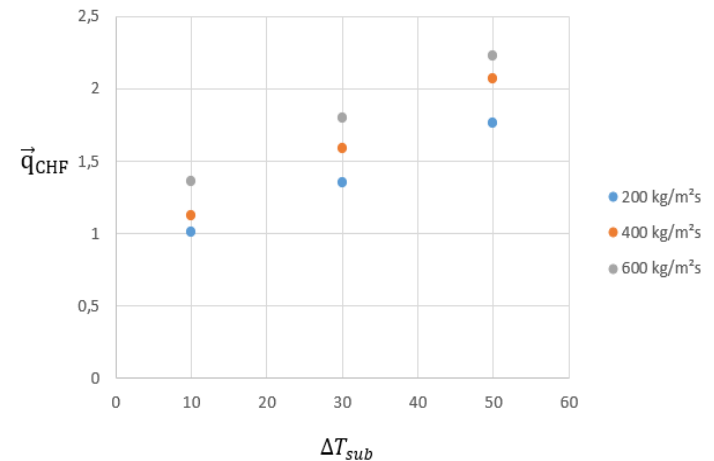
# Project KEK-SIMA



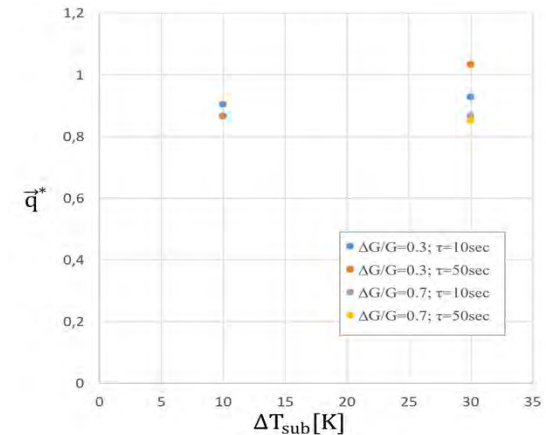
Stelios Michaelides

- It can be seen that the boundary conditions have a strong effect on the critical heat
- The CHF increases with subcooling, but pressure fluctuations also increase
- Mass flow oscillations do not necessarily lead to a decrease of the CHF. The thermal inertia of the heater must also be considered here

Test conditions:  $T = 80^{\circ}\text{C}$   $P = 1200$  mbar  
 steady mass flow

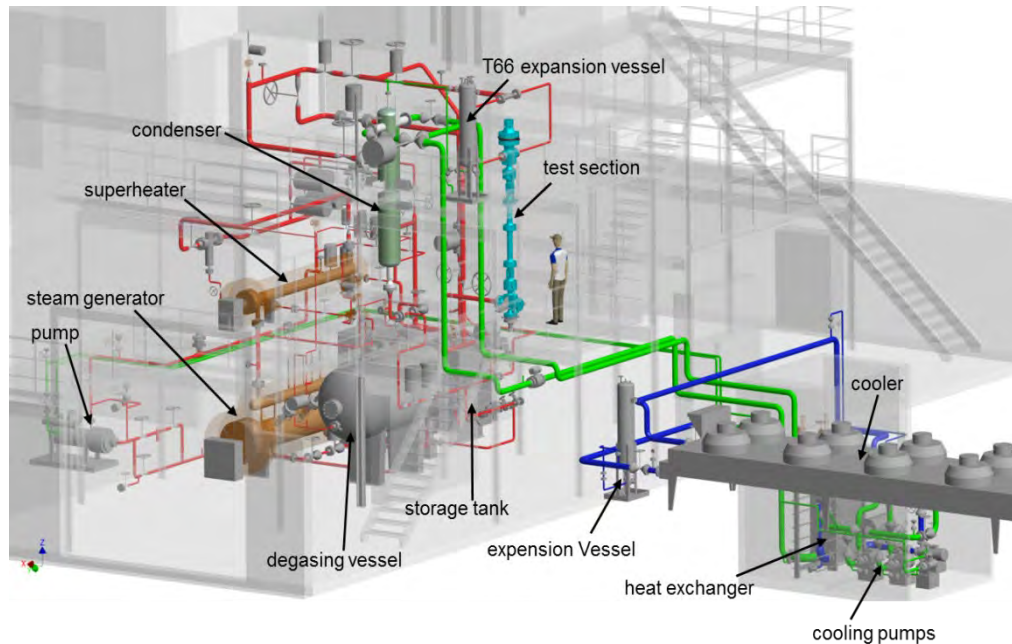


oscillating mass flow  $G = 400$  kg/m<sup>2</sup>s



Stelios Michaelides

# COSMOS-H thermohydraulic facility

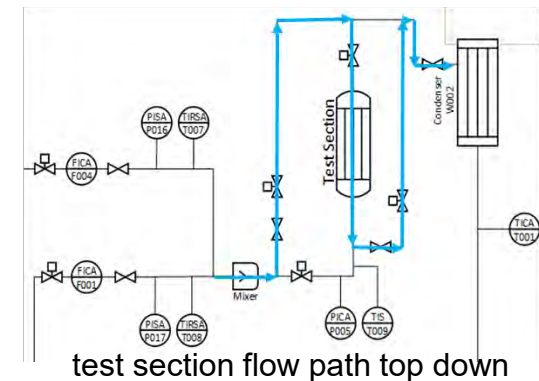
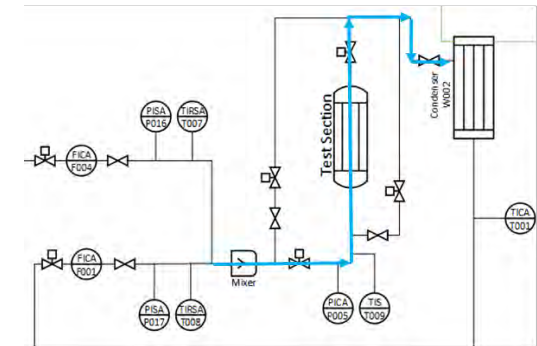
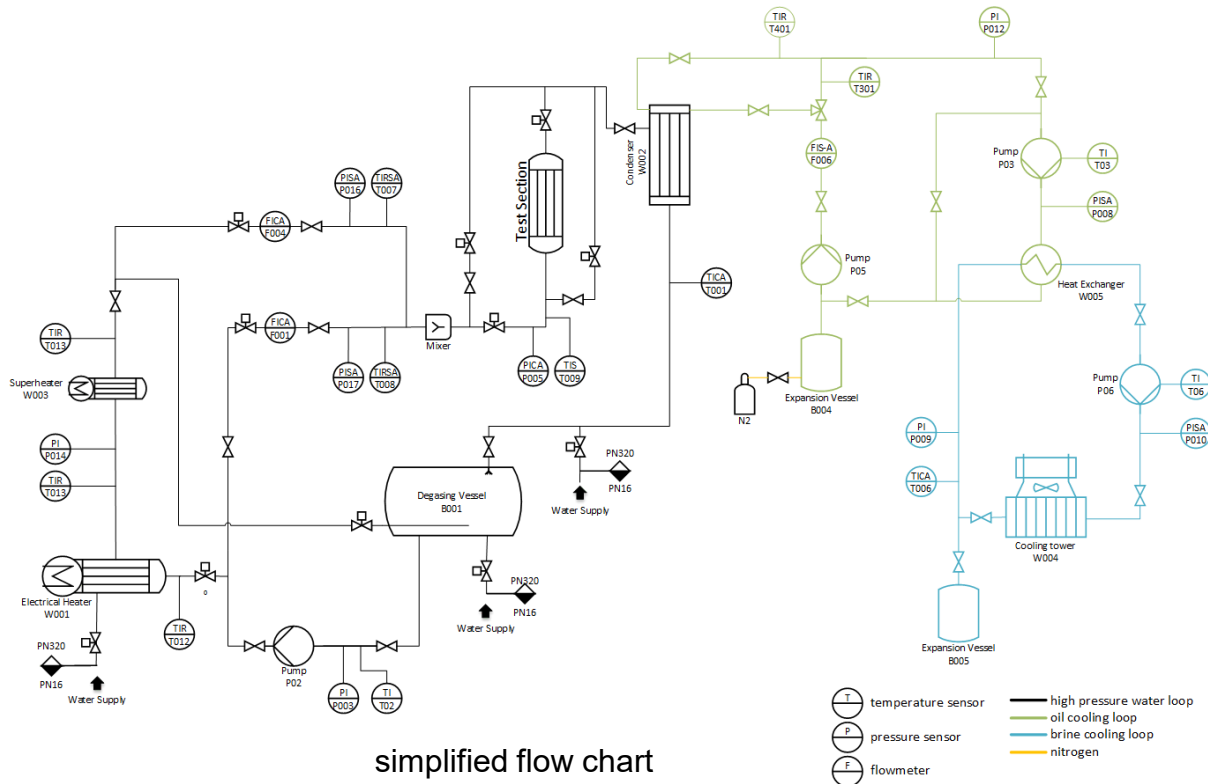


Parameter	Value	Unit
System pressure	70-170	bar
Max. pressure difference (pump)	10	bar
Steam mass fraction (test section inlet)	0-30%	-
Mass flow test section (steam + liquid water)	~1,4	kg/s
Mass flow density	4.000	kg/m <sup>2</sup> s
Max. test section inlet temperature	360	°C
Max. heating power	1,8	MW

- The aim of the facility is to be able to perform precise measurements on thermohydraulic issues under power plant conditions (e.g. boiling water reactor or pressurized water reactor)
- The test facility consists of a test loop (water + steam) and two cooling loops (thermal oil and cooling brine)
- Approx. 600 kW are available for heating the test section, which can be disconnected within 0.15 s when the boiling crisis is detected

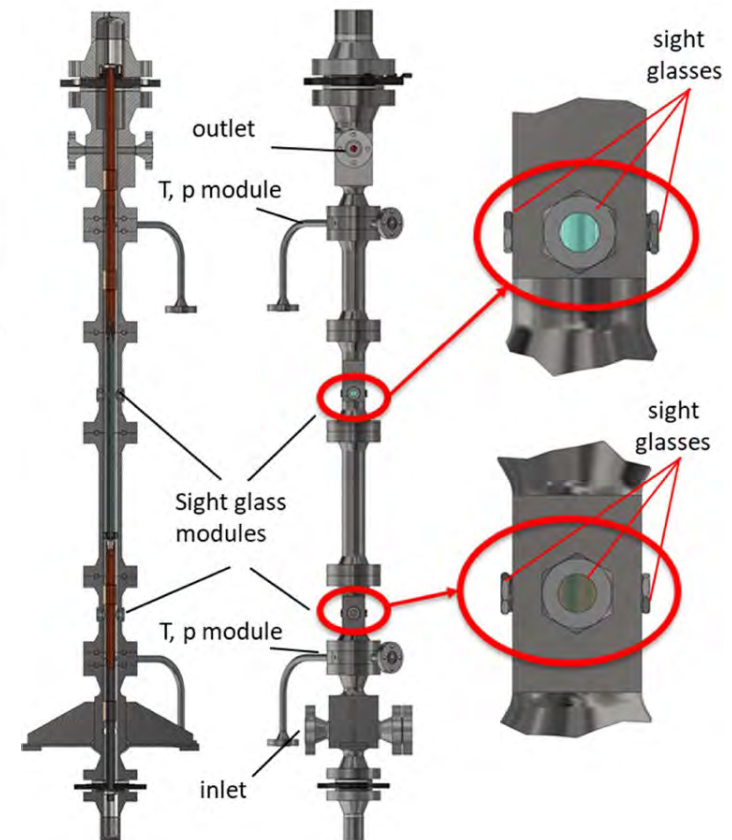
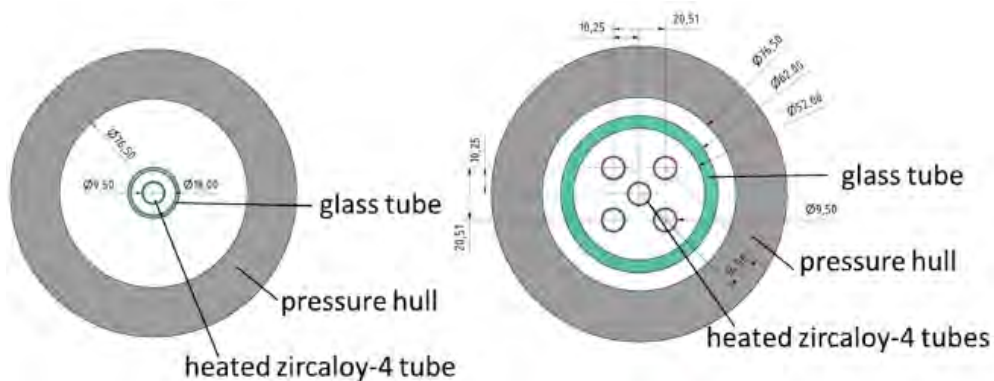


# COSMOS-H Thermohydraulic Facility



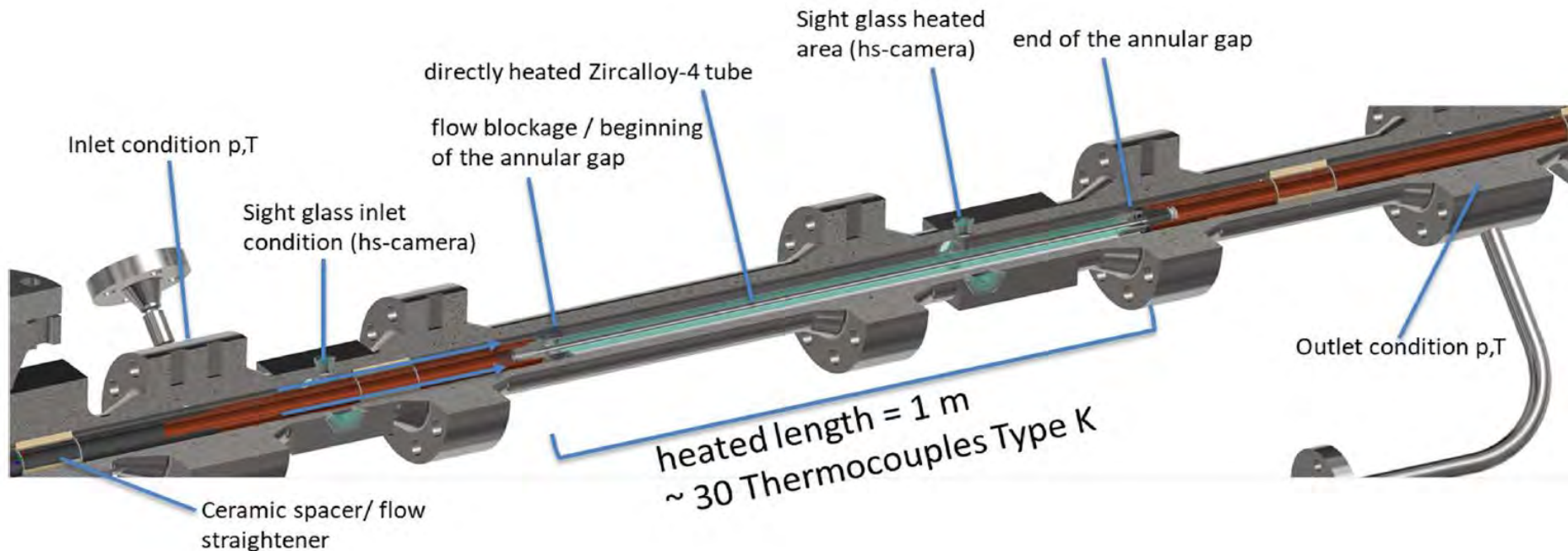
- The system can be operated with pure steam, pure water or mixtures
- A temperature- or power-controlled trace heating system enables operation with very low heat losses
- The flow path through the test section can be from top to down or from bottom to top

# COSMOS-H – McSAFER test section



- The objective of McSAFER is to measure CHF values under SMR typical conditions
- In order to be flexible regarding different measuring tasks, a modular measuring section was developed in which various test setups can be integrated
- In addition to various measuring modules, sight glass modules are also available

# COSMOS-H – McSAFER test section



- For the first series of experiments, a simple experimental setup with a heated tube in an annular gap is designed
- The instrumentation with numerous thermocouples in the heated tube allows temperature distributions to be measured and the CHF to be detected before it damages the heater as in the low-pressure system

# High pressure sight glass



- The sight glasses in the test track are a major safety hazard during the trials. That is why we have set up a small test rig to investigate the operating behavior in advance
- It consists of a short pipe of pressure class 32 MPa with an inner diameter of approx. 65 mm and a volume of 2.7 litres. A trace heating with thermal insulation was added. The instrumentation consists of a few p,T-sensors
- First results show that the glasses work in principle up to 10 MPa and approx. 310°C. However, the operation of the system is important, cause rapid temperature changes can lead to glass breakage



# Conclusion

- We use the low pressure loop COSMOS-L as a flexible system to observe flow boiling and boiling crisis in different scenarios
- The past experiments showed the numerous influencing variables of pressure, temperature, mass flow, material and geometry
- Outlook: Next, we will investigate the boiling and CHF behavior of different ATF-materials
- COSMOS-H is currently in commissioning and will be able to perform investigations under non-scaled conditions up to 17 MPa and 360°C
- Despite high safety requirements, we are striving to build an equally flexible system that can be used for different applications
- In the first project McSafer, boiling tests up to CHF will be performed on the single rod and also on a small bundle

■ Thank for your interest!

# CFD Setup Characteristics – iMUSIG

Extended RPI wall boiling model ↔ Inhomogeneous MUSIG ↔ CHT

<b>Version</b>	18.1 + Customized Solver	
<b>Analysis Type</b>	Steady runs with fluid time scale $\Delta t = 0.005$ [s]	
<b>Material Properties</b>	IAPWS IF-97 Library	
<b>Interfacial forces</b>	Lift	Tomiyama
	Drag	Grace
	Turbulent Dispersion	FAD turbulent dispersion model
<b>Boiling Model</b>	Equilibrium RPI model	Maximum Area Fraction of Bubble Influence = 10
	Bubble Departure Diameter	Tolubinski et al. (default)
	Nucleation Site Density	Lemmert et al. (default) / Modified Reference Site Density
<b>Vapor heat transfer</b>	Thermal Energy	
<b>Turbulence model</b>	SST	Homogeneous Turbulence
<b>iMUSIG</b>	Breakup Coeff. = 1.0 ; Turb. Coalescence Coefficient = 10.0	
	Boundary Conditions: Size Fraction of the smallest group = 1 @ Domain Openings and Domain Initialization	



**G. Stahlberg**

**Ruhr-Universität Bochum**

## **Preliminary simulation results of the experiments QUENCH-L3HT and QUENCH-ATF-1 regarding high-temperature oxidation mechanisms using the system code AC<sup>2</sup>**

Within the framework of a national research project, PSS aims at a more in-depth analysis of the behaviour of accident tolerant cladding materials as well as further development of the model basis of the severe accident analysis code AC<sup>2</sup> – ATLET-CD, developed by GRS gGmbH. As an essential part of these analyses, PSS performs calculations of the large-scale bundle test QUENCH-L3HT as well as first simulations of QUENCH-ATF-1 using a preliminary oxidation model currently being under development.

The investigated experiments were conducted at the QUENCH test facility of KIT under a loss of coolant accident scenario in light water reactors with subsequent re-flooding. The main focus of the test QUENCH-L3HT is the examination of e.g. strain, bursting, oxidation and secondary hydrogenation. In the OECD NEA research project “QUENCH-ATF”, experiments with accident tolerant materials like QUENCH-ATF-1 are conducted and accompanied by benchmark simulations. The experiments include chromium(Cr)-coated Zircaloy (Zry) rods and the investigation of the influence on a postulated accident progression. In the bundle tests QUENCH-L3HT and -ATF-1 peak temperatures of 1,500 K and 1,600 K respectively are reached. In consequence of several technical defects the high temperatures in L3HT create comparability and thus suitability as a reference for ATF-1. Distinguishing characteristics between the experiments are found in the design of the bundle and in the experimental procedure. In contrast to QUENCH-L3HT, a thin Cr-layer is applied to the QUENCH-ATF-1 rods and shroud by using the cold spray deposition technique. In a steam atmosphere the Cr-coating inhibits the inward oxygen diffusion and forms a protective chrome(III)-oxide layer (Cr<sub>2</sub>O<sub>3</sub>) which is intended to reduce hydrogen release and oxidation heat compared to uncoated Zry. Furthermore, the Cr-coating can possibly increase the coping time for accident management measures, which is essential for reactor safety. Regarding the protective effectiveness of the coating, several influencing factors like the coating thickness, degradation mechanisms or heating rate amongst others can be identified.

The analyses of the simulation results focus primarily on the code’s capability to represent the thermal behaviour of the rods as well as the oxidation behaviour under the given experimental conditions. The simulation of QUENCH-L3HT shows a good accordance to the experimental data considering the technical particularities. The reproduction of the hydrogen release matches the experimental data quantitatively and qualitatively. However, the delayed temperature decrease in saturated steam cannot be represented. The tentative simulation using the Cr-oxidation test-model for QUENCH-ATF-1 shows overall higher temperatures than the reference scenario L3HT. The hydrogen release rate is lower compared to the experimental data.





RUB

RUHR-UNIVERSITÄT BOCHUM


CONFIDENTIAL

## Preliminary simulation results of the experiments QUENCH-L3HT and QUENCH-ATF-1 regarding high-temperature oxidation mechanisms using the system code AC<sup>2</sup>

Gregor T. Stahlberg, Christoph Brattfisch, Marco K. Koch

27<sup>th</sup> QUENCH Workshop | Karlsruhe Institute of Technology

September 27 – 29, 2022

 Plant Simulation and Safety  
Prof. Dr.-Ing. Marco K. Koch

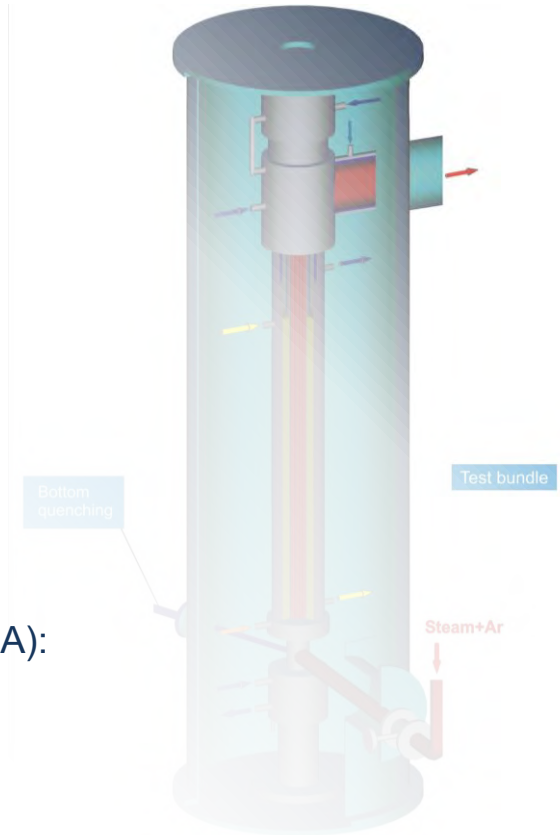
# **Introduction**

Motivation and objective

# Motivation and objective

## Overview

- National funded project (BMUV)
    - Analysis and validation of the AC<sup>2</sup> model approaches currently under development regarding **Accident Tolerant Fuel (ATF)**
    - *Available option so far: FeCrAl oxidation based on QUENCH-19 as well as an oxidation model with user input*
  - OECD-NEA „QUENCH-ATF“ Joint Project
    - Experiments with ATF under postulated accident conditions: **QUENCH-ATF-1, -2 with Cr-Coating and -3 with SiC** (tbd)
    - Reference experiments with similar boundary conditions (LOCA, BDBA): **QUENCH-L3HT/Q-L3 and QUENCH-15**
- A model for Cr-Oxidation is under development

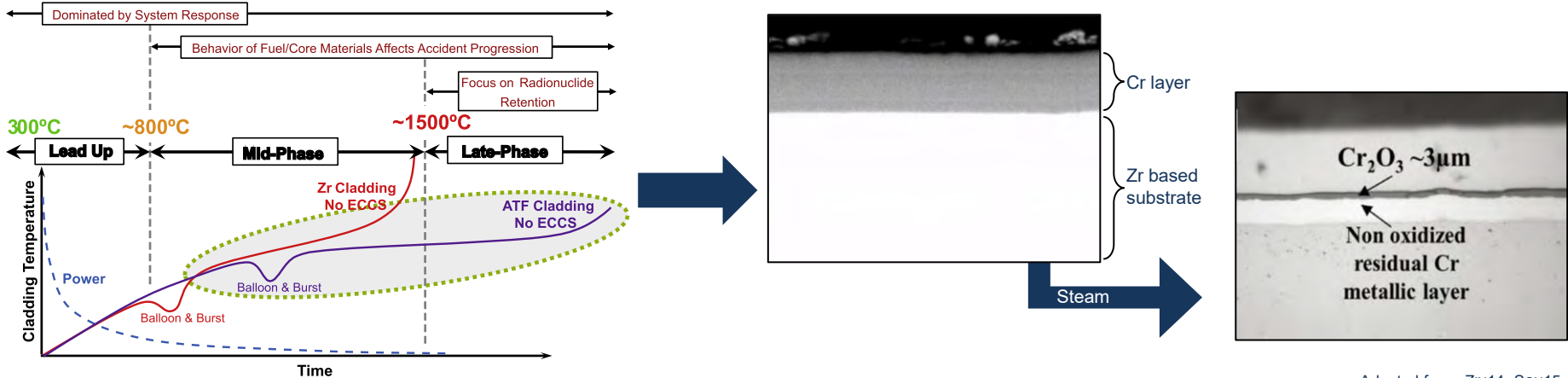
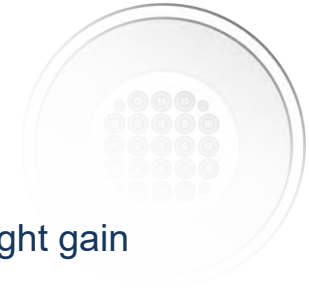


Adapted from: STU18

# Motivation and objective

## Importance of Cr-coating

- Excellent corrosion resistance due to Chromium(III)oxide layer ( $\text{Cr}_2\text{O}_3$ ) with overall low weight gain
  - Oxygen diffusion barrier protects underlying metal
  - Similar CTE to Zr-based alloys, high melting point as well as low embrittlement
- (Limited) Increase of coping time and reduced load on ECCS (generated heat ↓)



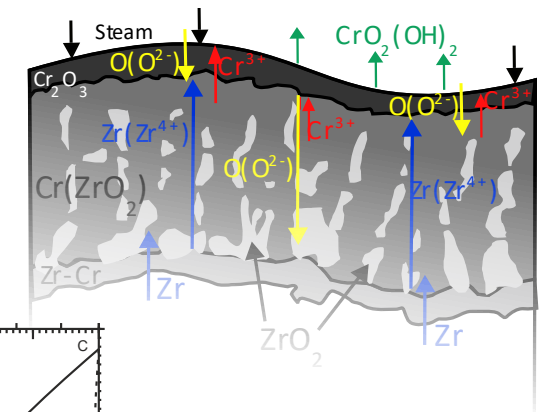
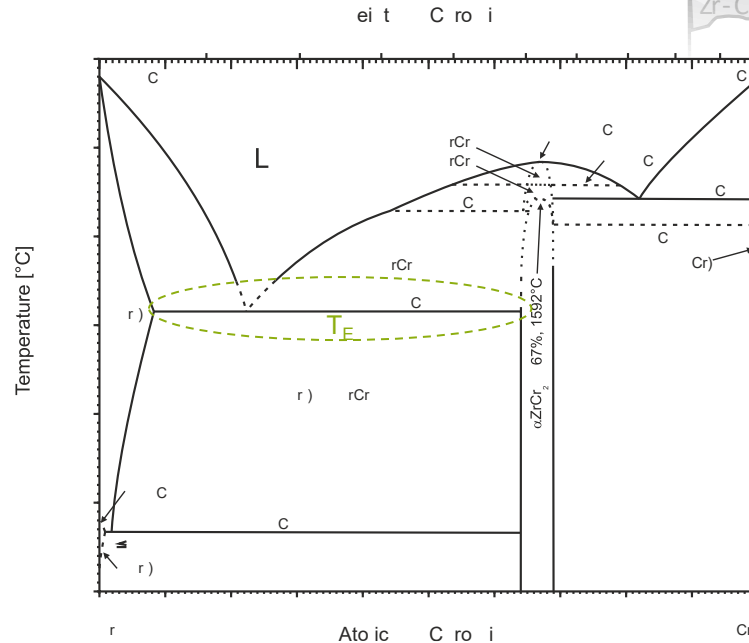
Adapted from: ZIN14, SCH15, Viz21



# Motivation and objective

## Coating degradation

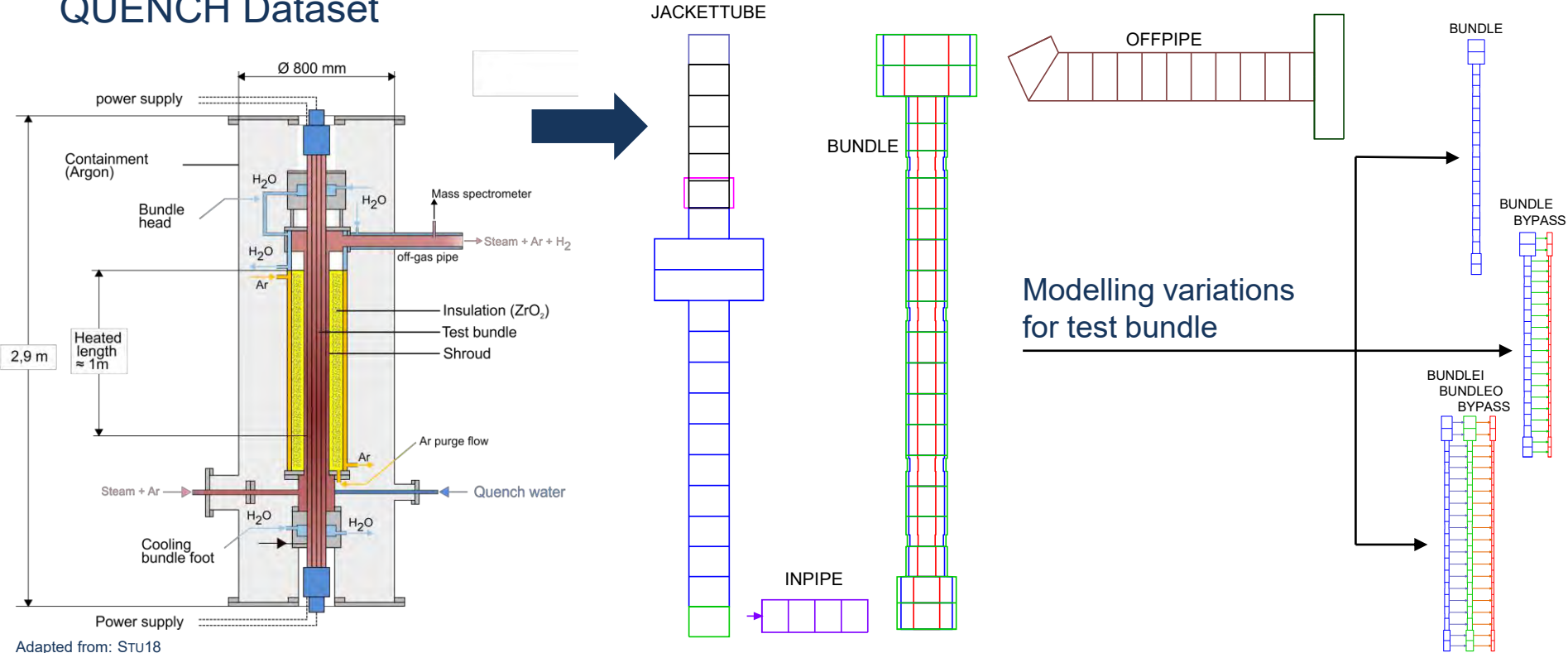
- Protective effect and coating failure mainly depends on:
  - Microstructure (Deposition)
  - Applied layer thickness
  - Duration of oxidation
  - Heating rate
  - Temperature (PCT)
    - eutectic Temperature  $T_E$
  - Degradation mechanisms



Adapted from: LIU21, ARI86

# Modelling Dataset and BC

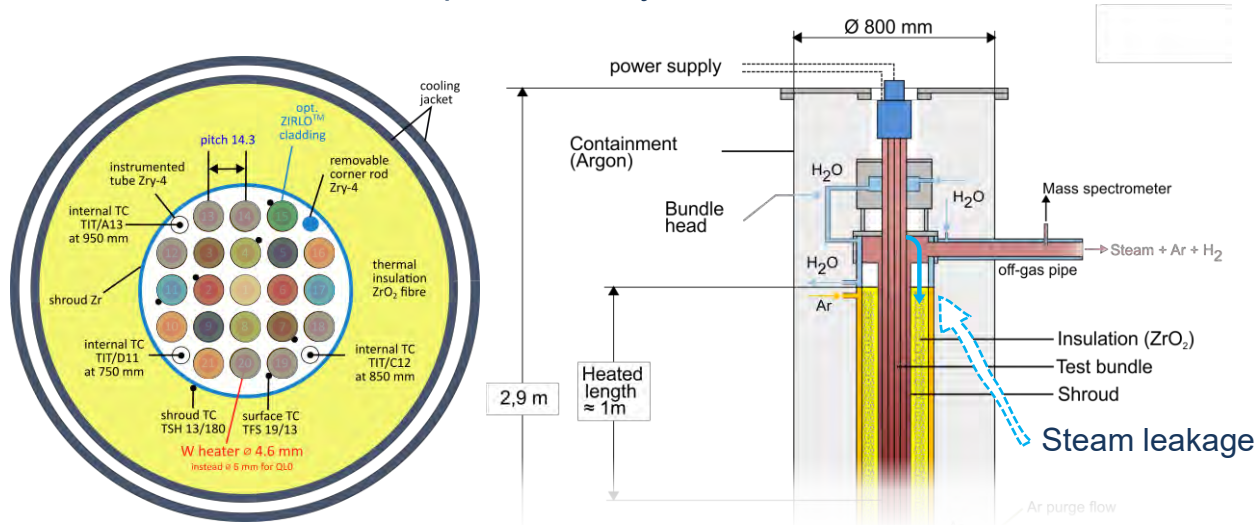
# Modelling QUENCH Dataset



# Modelling

## QUENCH-L3HT

- Simulation of QUENCH-L3HT under DBA conditions (LOCA), PCT ~1500 K (~1600 K TFS i at 850 mm)
  - **Q-L3HT** → Reference for QUENCH-ATF-1, PWR, 21 rods, ZIRLO
  - **ECORE Module** → Bundle is represented by 9 RODs to address characteristics



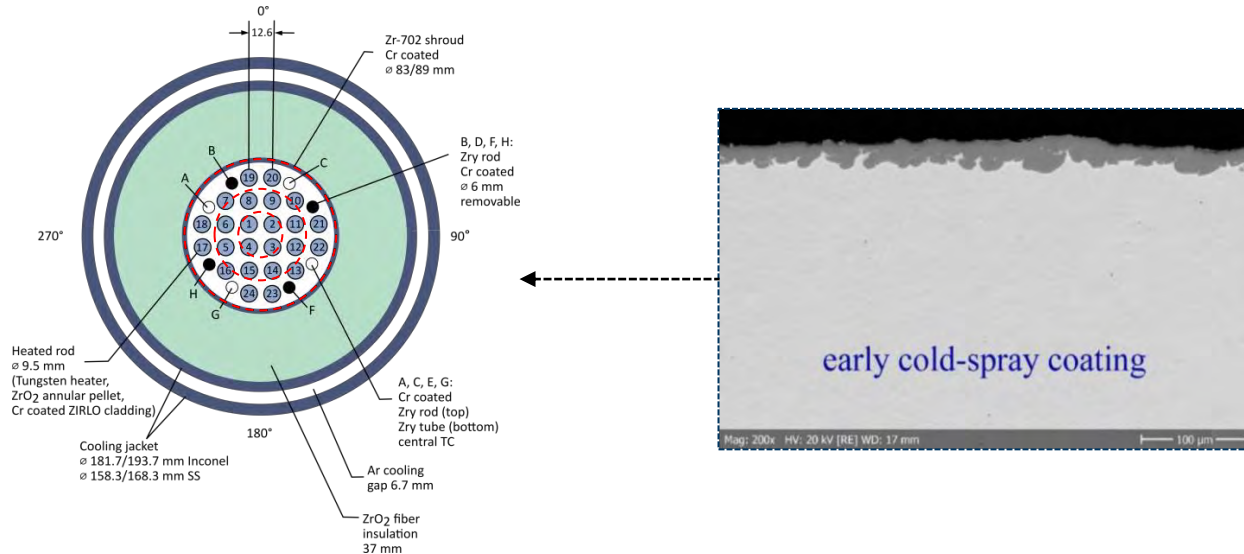
Adapted from: STU14 & STU18



# Modelling

## QUENCH-ATF-1

- Preliminary simulation of the ATF-1 experiment with extended DBA conditions (LOCA)
  - **Q-ATF-1** → P R rods, Cr-coated ZIRLO (Cold Spray, Westinghouse)
  - **ECORE Module** → B ndle is represented by 3 RODs (concentric rings) in current dataset

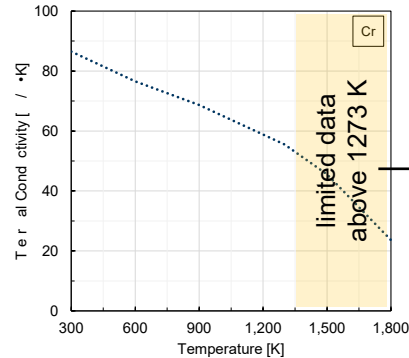
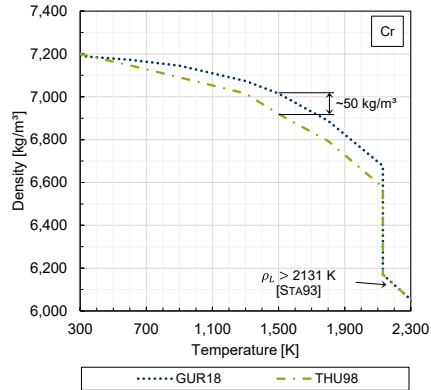


STU22

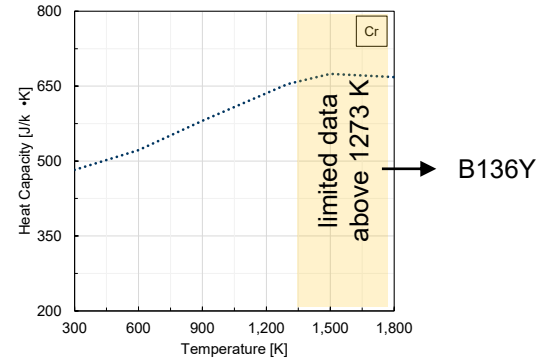
# Modelling

## Material properties

- Molar masses:  $M_{Cr} = 51.996 \text{ g/mole}$  and  $M_{Cr_2O_3} = 151.990 \text{ g/mole}$ , for oxide layer calculation
- Density, thermal conductivity and heat capacity of Cr\*
  - Material properties ( $c_p$  and  $\lambda$ ) above 1273 K comparable to other metals (e.g., B136Y)



\* $c_p$  and  $\lambda$  for Cr valid for 300-1273 K



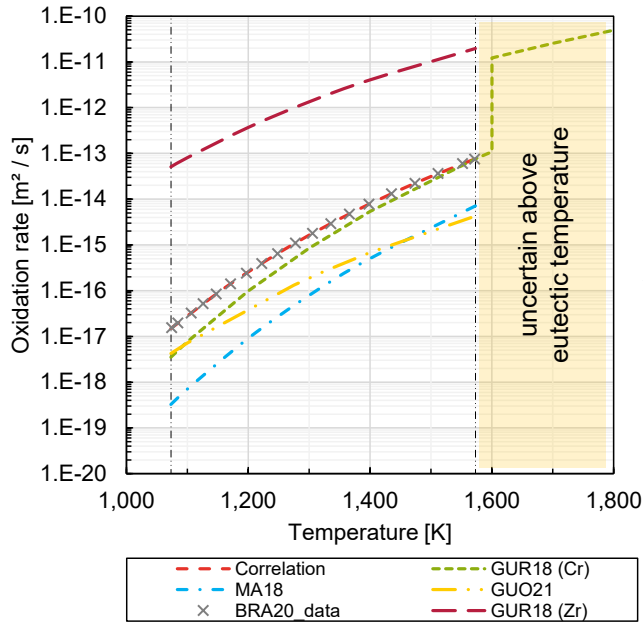
- Density, thermal conductivity and heat capacity of  $Cr_2O_3$ 
  - $\rho_{RT} \approx 5,220 \text{ [kg/m}^3\text{]}; \lambda_{RT} \approx 10 - 32.9 \text{ [W/m}\cdot\text{K]}; c_{p,1073-1373K} \approx 0.773 - 0.785 \text{ [kJ/kg}\cdot\text{K]}$

CONFIDENTIAL

# Modelling

## Oxidation-specific quantities

### ■ Oxidation (Arrhenius)



Brachet et al. [BRA20]  
800-1300 C

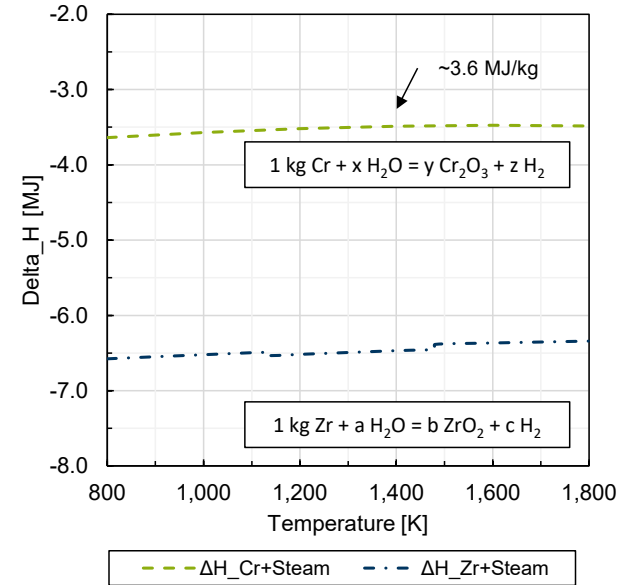
$$X_{Cr_2O_3} = (K(T) * t)^{1/2} \text{ [cm]}$$

With  $K(T) = A * \exp(-B/RT)$

$$K(T) \begin{cases} A \approx 7,085 * 10^{-06} \text{ [m}^2\text{/s]} \\ B \approx 28,85 * 10^3 \text{ (240 [kJ/mol])} \end{cases}$$

[<sup>2</sup>/s] → [k<sup>2</sup> / <sup>4</sup>s] calculated via molar masses of Cr, O<sub>2</sub> and density

### ■ Oxidation Heat



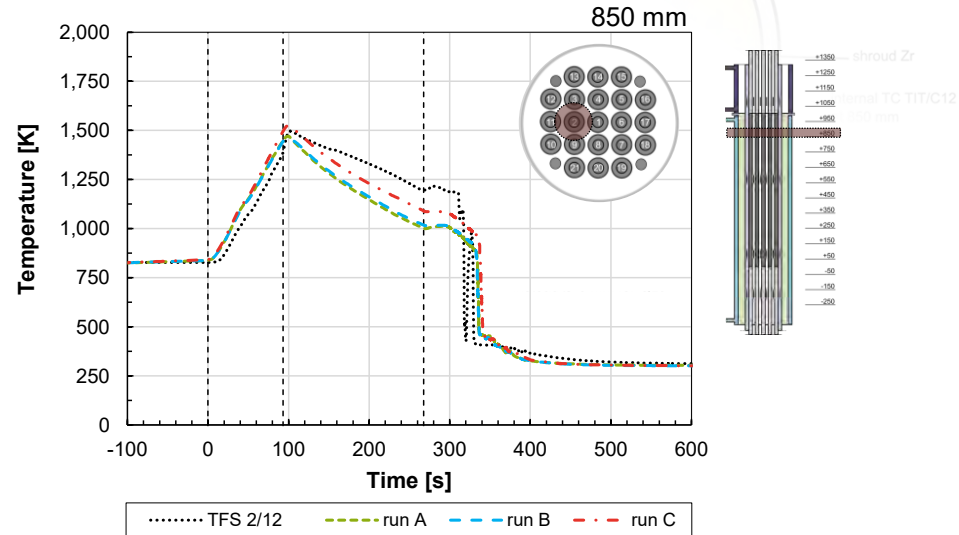
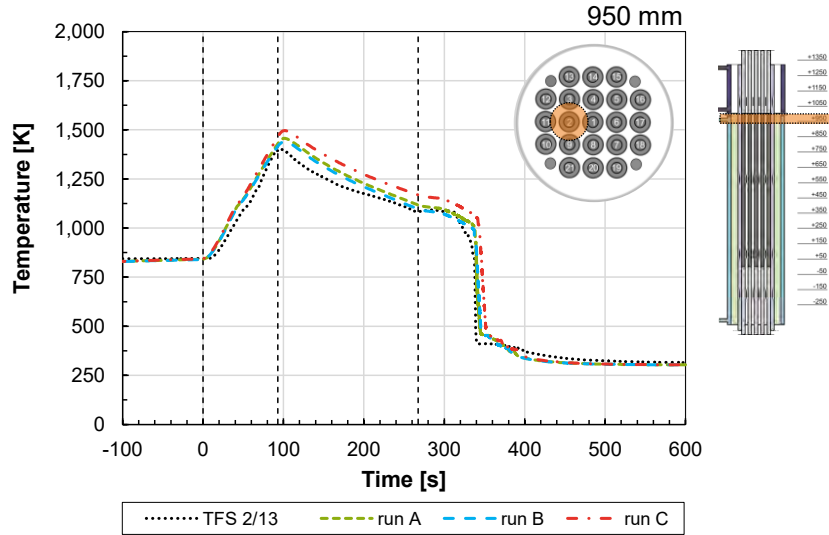
Reaction calculated by Software / Steinbrück, M. (HSC Chemistry)

# Preliminary simulation results with AC<sup>2</sup>



# Reference Experiment

## QUENCH-L3HT

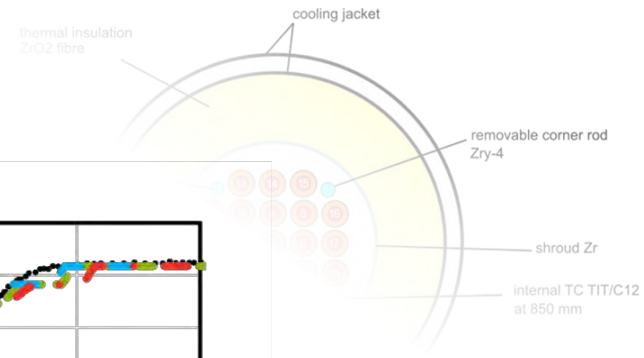
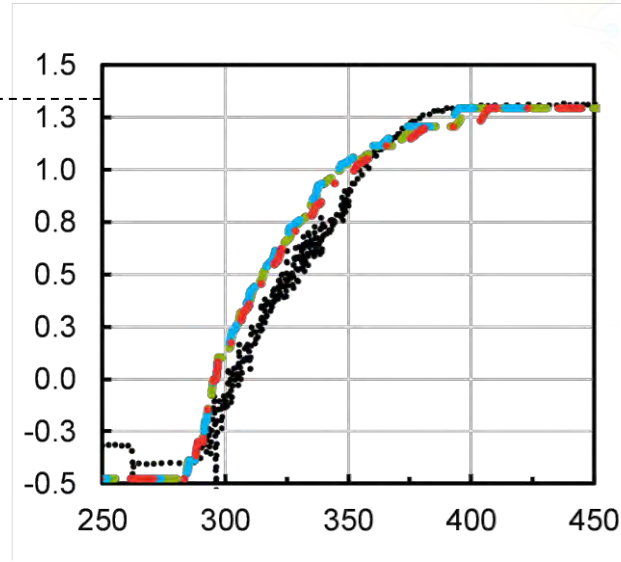
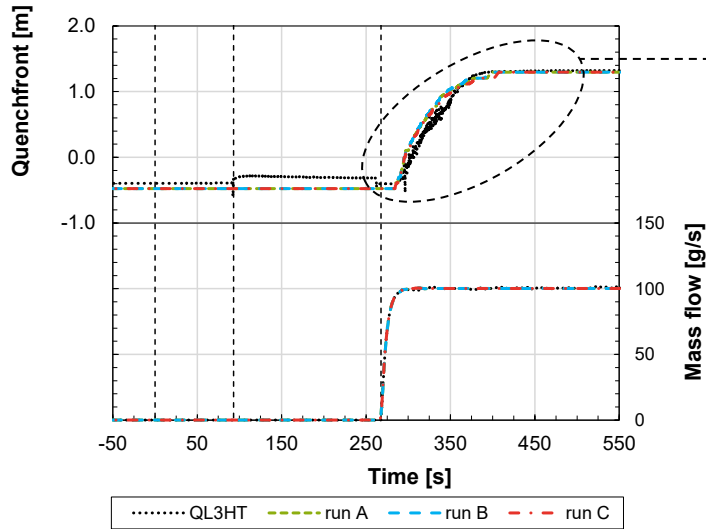


- B: Additional heat losses, C: Steam leakage and condensate injection, A: combines B and C
- Thermocouples of #ROD2 at 850 and 950 mm, no representation of slower cooling (850 mm)
- Minor temperature deviations in stabilization phase for modeled RODs / TFOs, respectively

Adapted from: STU18

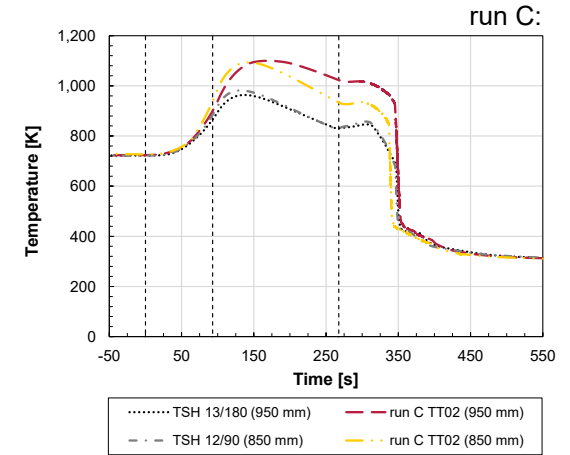
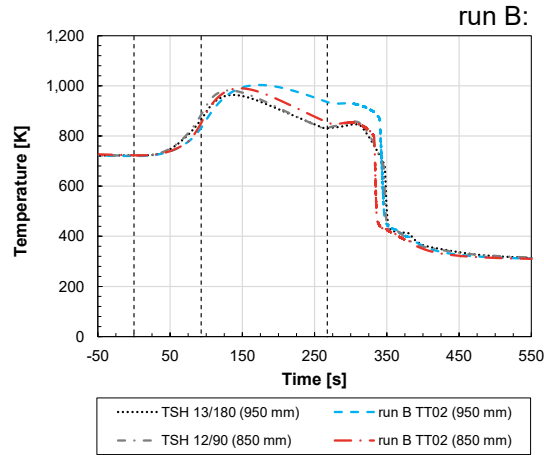
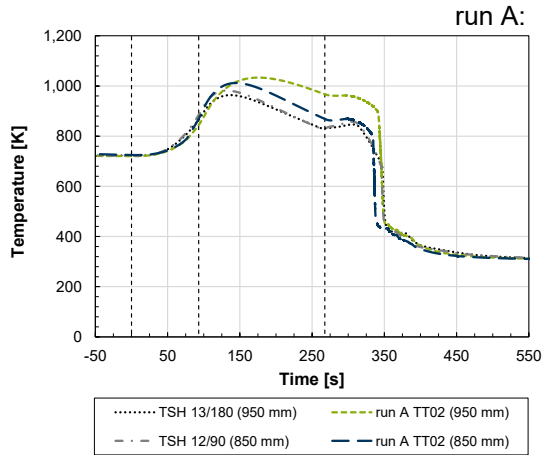
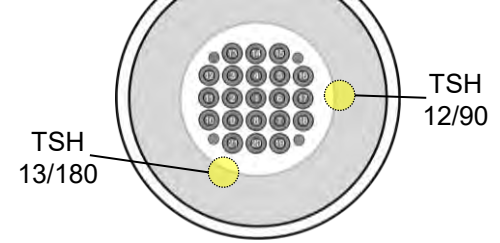
# Reference Experiment

## QUENCH-L3HT



- Quenchfront as well as the modeled quench water input (table) simulated in good agreement
- Increase in water level from 250 s is not calculated possibly model related “C QUENCHCORE”)
- Neglectable differences concerning calculation of the quench water level

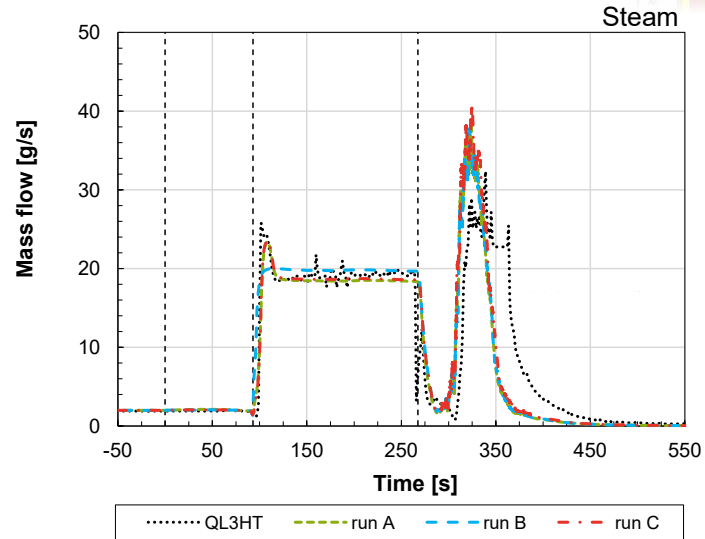
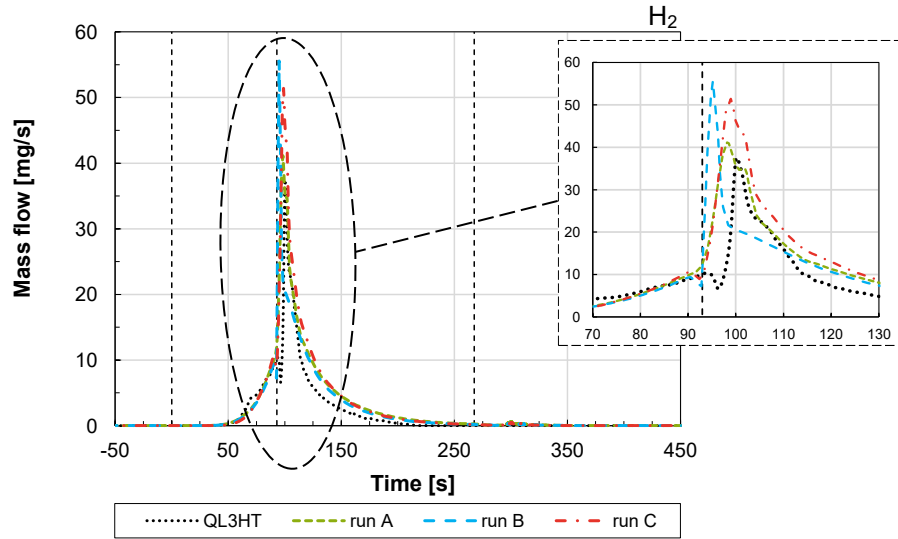
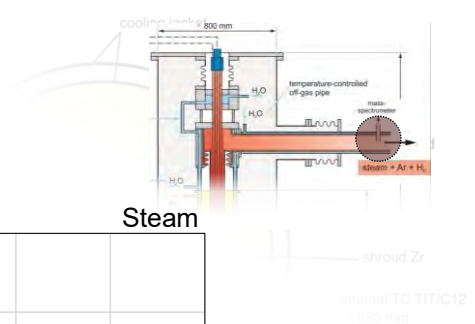
# Reference Experiment QUENCH-L3HT



- Thermocouples TSH 13/180 and TSH 12/90 are best represented by run B with consideration of reduced heating power in the outer fuel rod simulators
- In contrast, significantly higher temperatures are calculated in run C

# Reference Experiment

## QUENCH-L3HT



- Hydrogen release overestimated, improved representation in run A and C
- Injected condensate has a small influence on the time of maximum H<sub>2</sub> release (run A, C)
- Overall qualitative representation of experimental data with deviations regarding steam/H<sub>2</sub>



# First results of QUENCH-ATF

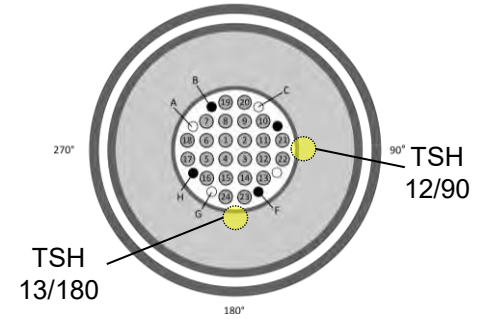
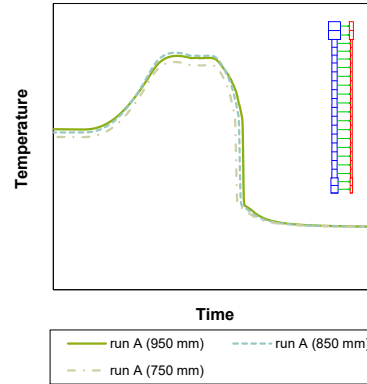
## QUENCH-ATF-1\*

- Temperature profiles HECU Object “S rod” as presented in L3HT

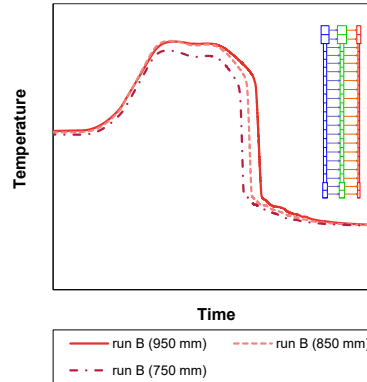
→ Deviating tables for water/steam and power as well as oxidation specific input

- Variations for bundle are tested, different onset of quenching between runs (run B like QL3HT dataset)
  - Temperature decrease is calculated later in run B with a more detailed bundle modelling

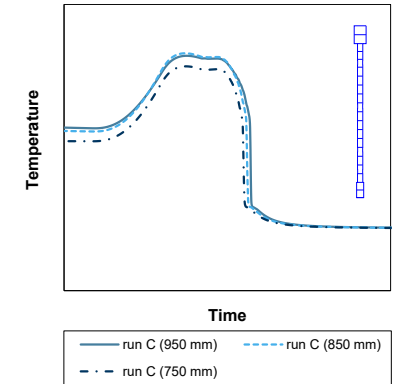
run A:



run B:



run C:

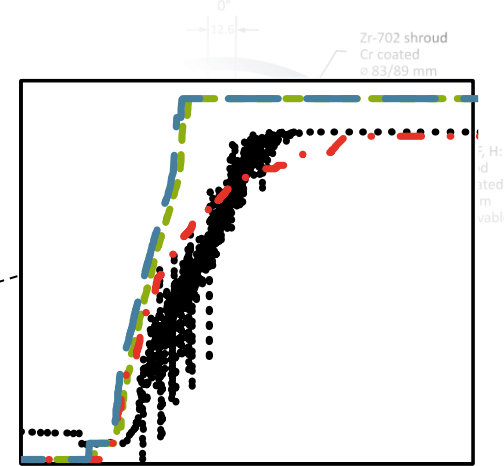
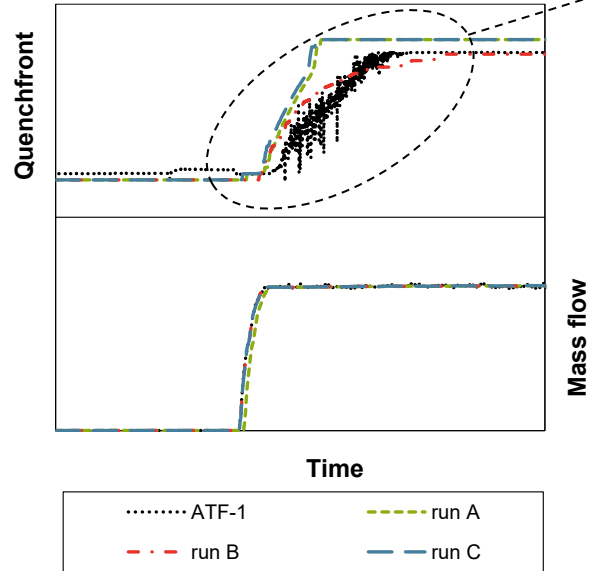


\*No quantitative results are shown due to QUENCH-ATF Agreement

# First results of QUENCH-ATF

## QUENCH-ATF-1\*

- Significant differences in water level calculation → investigation of bundle power and quenching modelling
- In addition to the deviating quenchfront calculation, the steam mass flow rate is lower with run B (offpipe/mass spectrometry)
- Quenchfront as well as the modelled quench water injection calculated sufficiently with run B

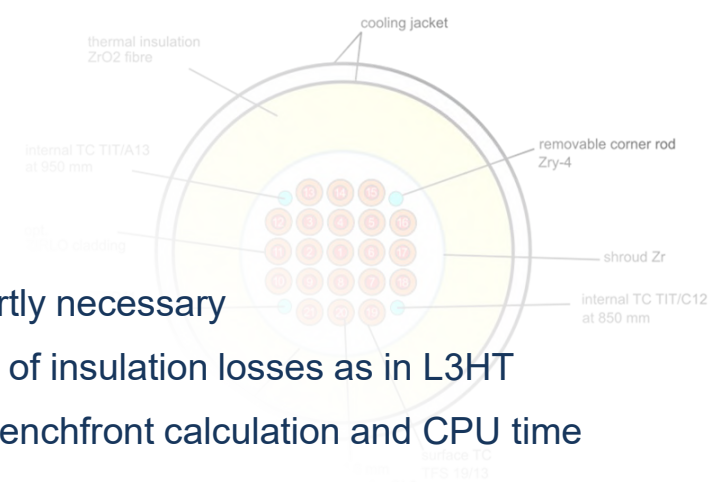


\*No quantitative results are shown due to QUENCH-ATF Agreement

# Conclusion and Outlook

# Conclusion

- Simulation of reference test Q-L3HT shows good agreement, but
  - Further improvements regarding local technical defects are partly necessary
  - Delayed steam cooling is not calculated (850 mm), due to lack of insulation losses as in L3HT
  - Detailed test bundle with two channels + bypass influences quenchfront calculation and CPU time

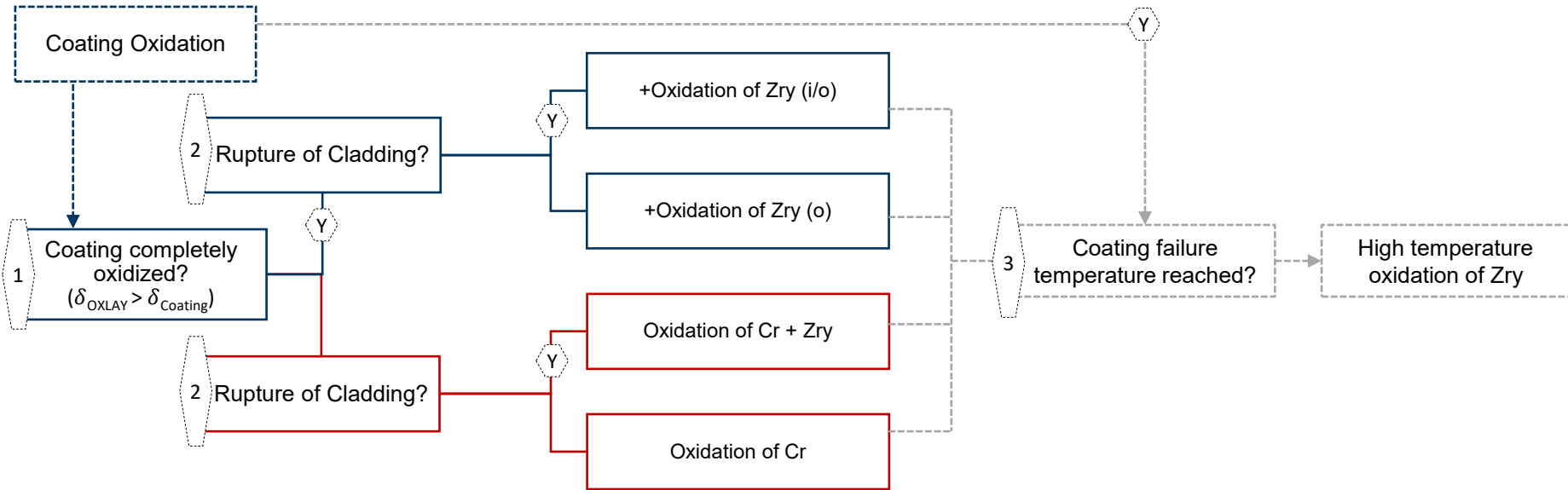


- First insights into the ATF bundle test Q-ATF-1
  - Modelling approach for the representation of the oxidation kinetics of chromium implemented
  - Bundle modelling based on L3HT influences quenchfront as well as temperature progression (decrease)
- Source code modifications were required for correct calculation of the oxide layer (own test version)
  - Molar Masses and new option for Cr-oxidation
  - Further development underway regarding coating degradation / oxidation model above eutectic



# Outlook

## Coating oxidation approach



- Analyzing influences on coating failure in depth → Identifying relevance to performance in
- Additional material properties and oxidation of Cr besides Zry for fuel rods as well as HECU structures

# Acknowledgement

This work is funded by the German Federal Ministry for the Environment, Nature Conservation, Nuclear Safety and Consumer Protection (BMUV) under grant number 1501629 based on a decision by the German Bundestag. Responsibility for the content lies with the authors.

The authors are grateful for the support of the participating countries to the joint project QUENCH-ATF\* run under the auspices of the Nuclear Energy Agency (NEA) within the Organization for Economic Cooperation and Development (OECD).

The results were obtained using the GRS software package AC<sup>2</sup> 2021.0.

Supported by:



Federal Ministry  
for the Environment, Nature Conservation,  
Nuclear Safety and Consumer Protection

based on a decision of  
the German Bundestag

\*No quantitative results are shown due to non-disclosure policy set on project results as per the QUENCH-ATF Agreement



**RUB**

**Thank you for your attention!**

**Gregor T. Stahlberg**

Gregor.Stahlberg@pss.rub.de



**Christoph Bratfisch**

Christoph.Bratfisch@pss.rub.de



**Marco K. Koch**

Marco.Koch@pss.rub.de



**RUHR-UNIVERSITÄT BOCHUM**

**PSS** Plant Simulation and Safety  
Prof. Dr.-Ing. Marco K. Koch

Building: Wasserstr. 223 | Floor 1  
Universitätsstr. 150 | D-44801 Bochum

**[pss.rub.de](https://pss.rub.de)**

# References

- [ARI86] Arias, D.; Abriata J P : Te Cr-r C ro i -Zirconium) system. Bulletin of Alloy Phase Diagrams 7, S. 237–244, 1986. DOI: 10.1007/BF02868997.
- [BRA20A] Brachet, J.-C.; Rouesne, E.; Ribis, J.; Guilbert, T.; Urvoy, Stéphane; N., Guillaume; Toffolon-Masclet, C.; Le Saux, M.; Chaabane, N.; Palancher, H.; David, A.; Bischoff, J.; Augereau, J.; Pouillier, E.: High temperature steam oxidation of chromium-coated zirconium-based alloys: Kinetics and process. Corrosion Science 167, 2020. DOI: 10.1016/j.corsci.2020.108537.
- [GUO21] Guo, Z.; Dailey, R.; Feng, T.; Zhou, Y.; Sun, Z.; Corradini, M. L.; Wang, J.: Uncertainty analysis of ATF Cr-coated-Zircaloy on BWR in-vessel accident progression during a station blackout. Reliability Engineering & System Safety 213, 2021. DOI: 10.1016/j.ress.2021.107770.
- [GUR18] Gurgen, A.; Shirvan, K.: Estimation of coping time in pressurized water reactors for near term accident tolerant fuel claddings. Nuclear engineering and design, 337, S. 38–50, 2018. DOI: 10.1016/j.nucengdes.2018.06.020.
- [LIU21] Liu, J.; Tang, C.; Steinbrück, M.; Yang, J.; Stegmaier, U.; Große, M.; Di Yun; Seifert, H. J.: Transient experiments on oxidation and degradation of Cr-coated Zircaloy in steam up to 1600 °C. Corrosion Science 192, 2021. DOI: 10.1016/j.corsci.2021.109805.
- [MA18] Ma, Z.; Parisi, C.; Zhang, H.; Mandelli, D.; Blakely, C.; Yu, J.; Youngblood, R.; Anderson, N.: Plant-Level Scenario-Based Risk Analysis for Enhanced Resilient PWR – SBO and LBLOCA. U.S. Department Of Energy, INL/EXT-18-51436, Idaho Falls, USA, 2018. DOI: 10.2172/1495192.
- [SCH15] Schuster, F.; Lomello, F.; Billard, Alain; et al.: On-going studies at CEA on chromium coated zirconium based nuclear fuel claddings for enhanced accident tolerant LWRS fuel, Top Fuel 2015 - Reactor Fuel Performance Meeting, Zurich, Switzerland, 2015.
- [STA93] Stankus, S. V.: The density of vanadium and chromium at high temperatures. Teplofizika Vysokikh Temperatur (TVT), S. 565–568, 1993.
- [STU14] Stuckert, J.; Große, M.; Moch, J.; Rössger, C.; Steinbrück, M.; Walter, M.: First results of the high temperature bundle test QUENCH-L3HT with optimized ZIRLO™ claddings, 2014.
- [STU18] Stuckert, J.; Große, M.; Rössger, C.; Steinbrück, M.; Walter, M.: Results of the LOCA bundle test QUENCH-L3 with optimised ZIRLO™ claddings (SR-7737), 2018. DOI: 10.5445/IR/1000083087.
- [STU22] Stuckert, J.; Grosse, M.; Steinbrück, M.: Report on the preparation and execution of the QUENCH-ATF-1 test, 3<sup>rd</sup> Management Board Meeting OECD NEA “QUENCH-ATF” Joint Undertaking, 20.07.2022.
- [THU98] Thurnay, K.: Thermal properties of transition metals, FZKA 6095, Forschungszentrum Karlsruhe, Karlsruhe, Germany, 1998. DOI: 10.5445/IR/270043419.
- [VIZ21] Vizelkova, K.; Stuckert, J.; Stegmaier, U.: The results of high temperature single rod tests with chromium coated cladding. 26th. International QUENCH Workshop. Karlsruher Institut für Technologie (KIT), Karlsruhe, Germany, 2021.
- [ZIN14] Zinkle, S. J.; Terrani, K. A.; Gehin, J. C.; Ott, L. J.; Snead, L. L.: Accident tolerant fuels for LWRs: A perspective. Journal of Nuclear Materials, 448, S. 374–379, 2014. DOI: 10.1016/j.jnucmat.2013.12.005.

CONFIDENTIAL

**Preliminary simulation results of the experiments QUENCH-L3HT and -ATF-1 regarding high-temperature oxidation mechanisms using AC<sup>2</sup> | 27<sup>th</sup> QWS 2022**





**F. Gabrielli (pres. by V. Sanchez)**

**KIT**

## **Preliminary Analysis of the QUENCH-19 Test by means of the ASTEC Code**

The Accident Tolerant Fuel (ATF) and Cladding (ATC) materials are under development worldwide because of their potential for improving the safety performance of large and integral Light Water Reactors during normal/transient operations and severe accident scenarios. Compared with the Zirconium based claddings used for decades in typical light water reactors, such new ATC materials show significantly slower oxidation kinetics at high temperatures in steam or air environments. It results in a strong reduction of the hydrogen generation rate due to the oxidation of the in-vessel components after the core uncovering, leading to an increase of time available for the activation of the accident mitigation measures. Having this in mind, efforts are going on at the Karlsruhe Institute of Technology to extend the capabilities of the Accident Source Term Evaluation Code, developed by IRSN and co-developed by KIT to model the ATC materials in order to employ the code for performing analyses of severe accident scenarios in innovative reactor concepts employing such materials.

The paper describes the results of the most recent research activities performed at KIT related to the implementation of the steam/FeCrAl oxidation behavior in the ASTEC code. In order to validate such new implementations, the QUENCH-19 experiment performed at KIT in 2018 is considered. In the paper, the ASTEC model of the QUENCH-19 test is described and the simulation results of the main figure of merits of the test, i.e. component temperatures and hydrogen production, are compared with the experimental data. The results show that ASTEC is able to qualitatively reproduce the QUENCH-19 experimental data with respect to the time- and space-dependent behavior of the cladding temperature, while an overestimation of ~100 degree is observed. On the contrary, a quite acceptable agreement is observed concerning the temperature of the shroud. The total amount of hydrogen produced during the QUENCH-19 test is rather well reproduced by the ASTEC code. Additional efforts are necessary in the ASTEC modeling to properly reproduce the kinetics of the hydrogen mass produced during the power escalation.

# Preliminary Analysis of the QUENCH-19 Test by means of the ASTEC Code

F. Gabrielli, V.H. Sanchez-Espinoza

Institute for Neutron Physics and Reactor Technology



# Motivation

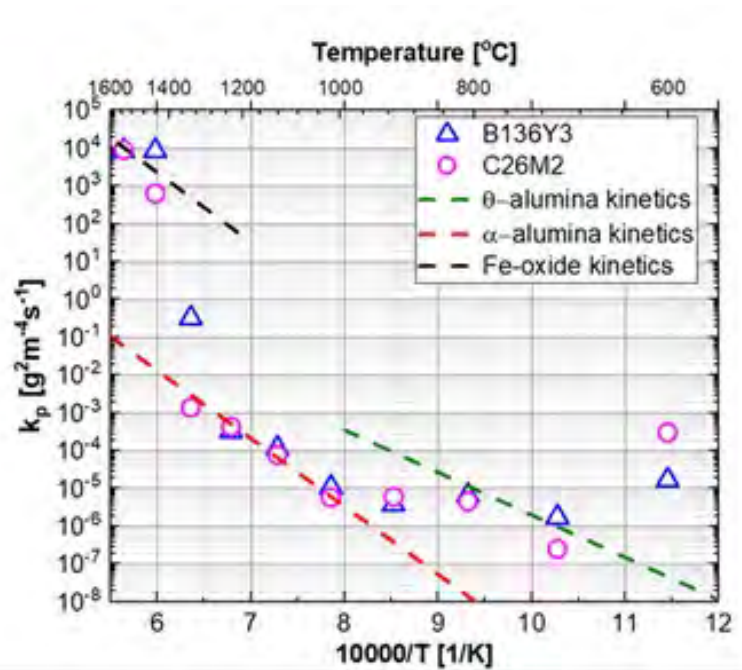
- KIT strategy for severe accident (SA) analyses → continuous improvement of the codes to evaluate the radiological consequences of SAs in current and innovative NPPs.
- ATFs have the potential for improving the safety performance of large and integral LWRs during normal/transient operations and SA scenarios.
- **Efforts going on at KIT/INR to extend the ATF-related modelling capabilities (cladding) of the ASTEC code** to enable the safety assessment of the innovative reactor concepts employing such materials.
- Activities triggered by the KIT participation to the OECD/NEA QUENCH-ATF project and the IAEA CRP ATF-TS.
- **Focus on the implementation of the Steam/FeCrAl oxidation laws in ASTEC and analysis of the QUENCH-19 test.**

# Modeling New Materials in the ASTEC Code

- User usually employs the data stored in the available material database, i.e. for Zry/ZrO<sub>2</sub>
  - Thermo-physical properties.
  - Oxidation models, i.e. Cathcart, Prater-Courtright, Urbanic, Best-fit,...
- ASTEC is flexible enough to introduce new materials either by adjusting the properties of a default material or to fully define behavior and properties by scratch.
- **Approach:**
  - Implementation of the Steam/FeCrAl oxidation laws provided by the Quench experimental team in the ASTEC database (v2.2\_b employed)
  - Same approach for KANTHAL APM



# ASTEC: FeCrAl Oxidation Model



➤ Fitting functions for weight gain provided by J. Stuckert (IAEA CRP ATF-TS)

$$K = \begin{cases} 9.62 \times 10^{-12} [\text{g}^2/\text{cm}^4\text{s}], & T \leq 1473 \text{ K} \\ A_B \exp\left(\frac{-E_B}{RT}\right), & 1473 < T < 1648 \text{ K} \\ A_{Fe} \exp\left(\frac{-E_{Fe}}{RT}\right), & T \geq 1648 \text{ K (melting point of FeO)} \end{cases}$$

$$A_B = 3 \cdot 10^9 \text{ g}^2/\text{cm}^4 \text{ s}$$

$$E_B = 594354 \text{ J/mol}$$

$$A_{Fe} = 2.4 \cdot 10^6 \text{ g}^2/\text{cm}^4 \text{ s}$$

$$E_{Fe} = 352513 \text{ J/mol}$$

# ASTEC: FeCrAl Oxidation Model

- Modifying the laws for oxygen mass gain in the database.
- **Assumptions:**
  - **No information on the oxide thickness growth (similar law as mass gain used)**
  - **$\Delta h$  of Zr employed**

$$m_o(t + dt) = S \cdot \left( \left( \frac{m_o(t)}{S} \right)^{\frac{1}{model}} + AGAIN \cdot e^{-\frac{BGAIN}{R \cdot T}} dt \right)^{model}$$

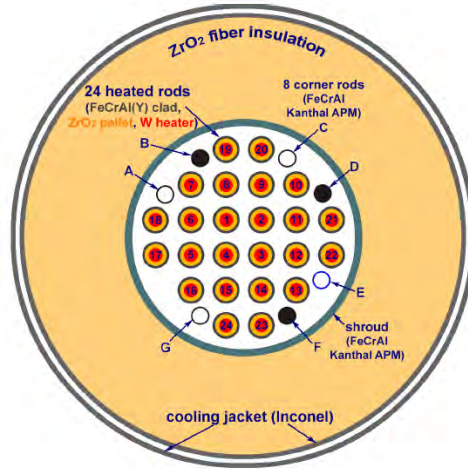
$$e_{ZrO_2}(t + dt) = \left( \left( e_{ZrO_2}(t) \right)^{\frac{1}{model}} + ATHIC \cdot e^{-\frac{BTHIC}{R \cdot T}} dt \right)^{model}$$

... .

```

STRUCTURE MODEL NAME 'BEST-FIT' LAW 'COEFF' VARIABLE 'T' VUNIT 'K' RUNLOW 0. RUNUPP 5000.
  SRG VALUE AGAIN 9.62D-10 BGAIN 0.0 ATHIC 2.252D-13 BTHIC 0.0 MODEL 0.5 TERM
  X 1473.K
  SRG VALUE AGAIN 3.0D+11 BGAIN 5.94354D5 ATHIC 3.371D3 BTHIC 5.94354D5 MODEL 0.5 TERM
  X 1648.K
  SRG VALUE AGAIN 2.4D+08 BGAIN 3.52513D5 ATHIC 0.008682D0 BTHIC 3.52513D5 MODEL 0.5 TERM
END
  
```

# QUENCH-19 Test Conduct



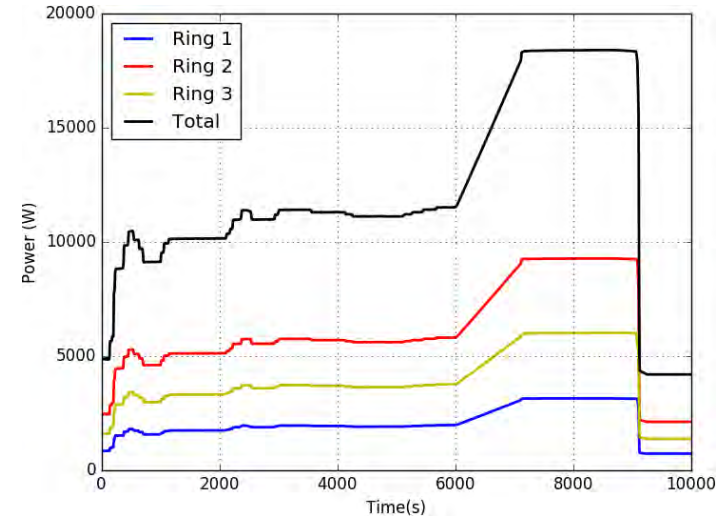
Phase 1: heating up to  $\sim 600$  °C (4 kW).

Phase 2: power increase up to 11.5 kW (pre-oxidation).

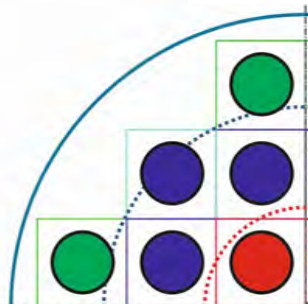
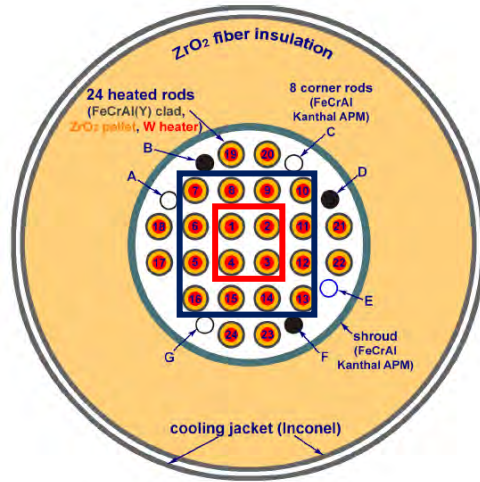
Phase 3: power increased up to 18.12 kW (5 W/s) ( $T_{pct} \sim 1500$  °C).

Phase 4: power reduced to 4.1 kW.

- Atmosphere of Ar (3.45 g/s) and superheated steam (3.6 g/s).
- Reflooding at  $\sim 9100$  s
  - Fast initial injection of 4 kg of water
  - Slow injection 48 ~ g/s of water



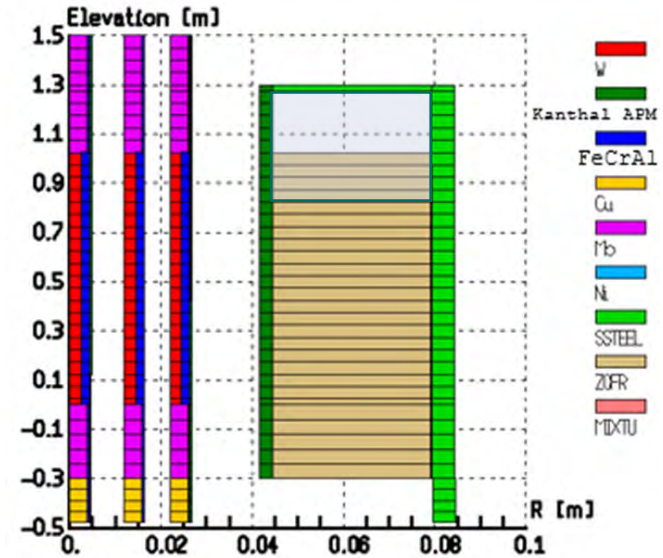
# ASTEC Model of the QUENCH-19 Test



Ch. 3, 8 rods,  $r_{\text{ext}} = 41.5$  cm

Ch. 2, 12 rods,  $r_{\text{ext}} = 28.4$  cm

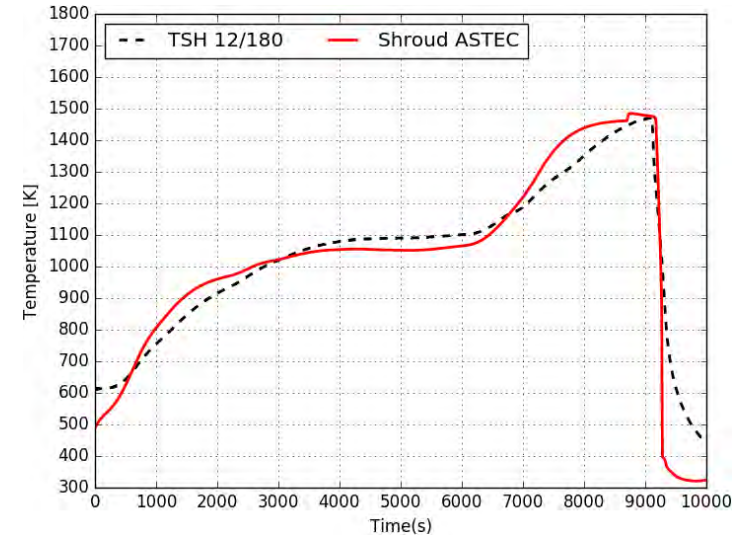
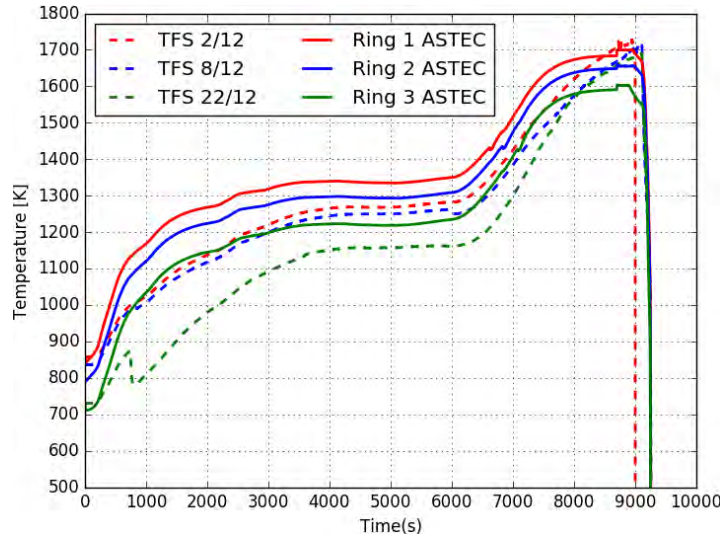
Ch. 1, 4 rods,  $r_{\text{ext}} = 14.2$  cm



- Accidental presence of 4 l water the gap between the shroud and the cooling jacket modelled (J. Stuckert).



# Results: Clad and Shroud Temp. @850 mm Height



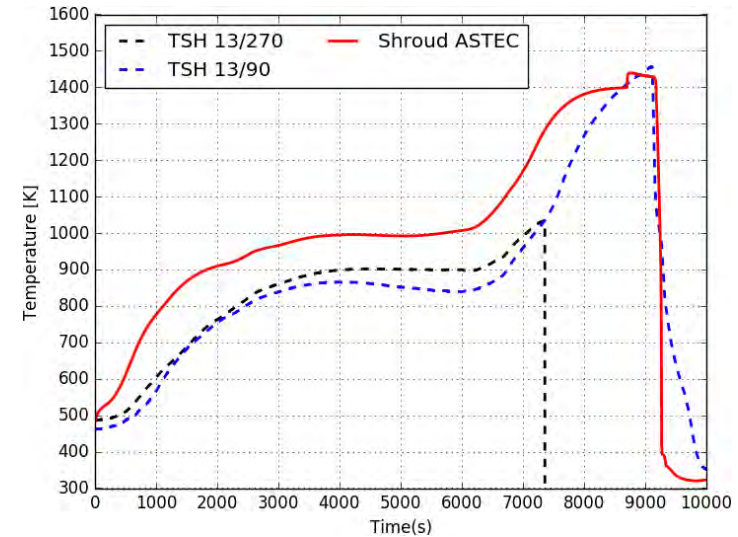
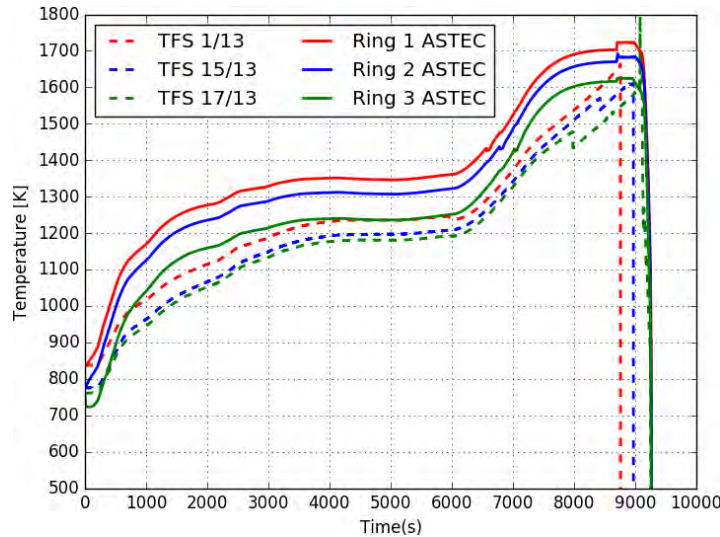
## ➤ Clad

- Results exceed the exp. of about 100 degree in the pre-oxidation phase in Ring 1.
- Better agreement in Ring 2 and 3.
- Max. temperatures reasonably well reproduced in Ring 1 and 2 (deviation of ~ 100 degree in Ring 3).

## ➤ Shroud

- Experimental results reasonably well reproduced.

# Results: Clad and Shroud Temp. @950 mm Height



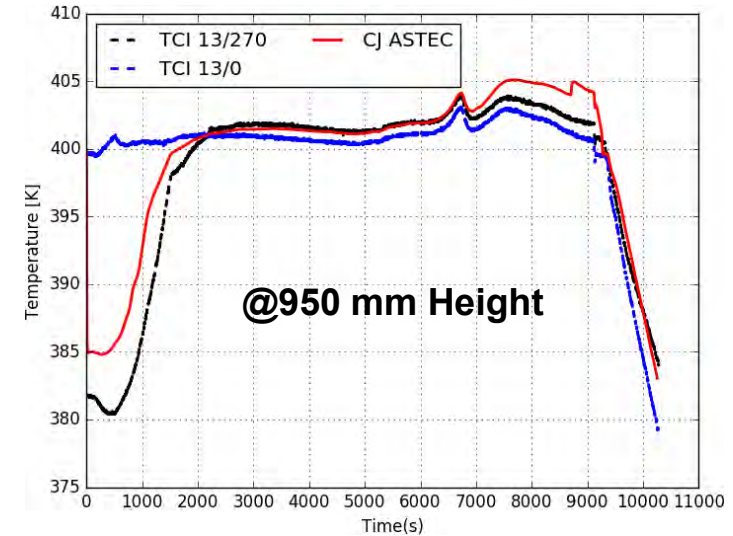
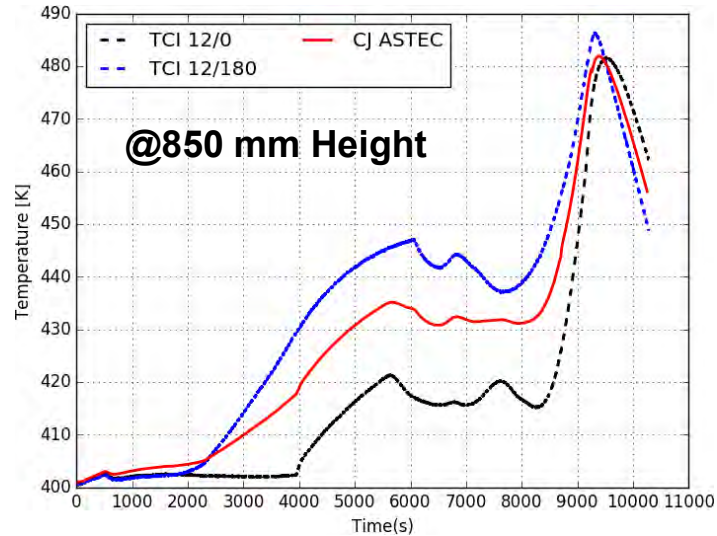
## ➤ Clad

- Results exceed the exp. of about 100 degree in the pre-oxidation phase in Ring 1 and 2.
- Better agreement in Ring 3.
- Max. temperature reasonably well reproduced in Ring 1 and 3 (deviation of ~ 100 degree in Ring 2).

## ➤ Shroud

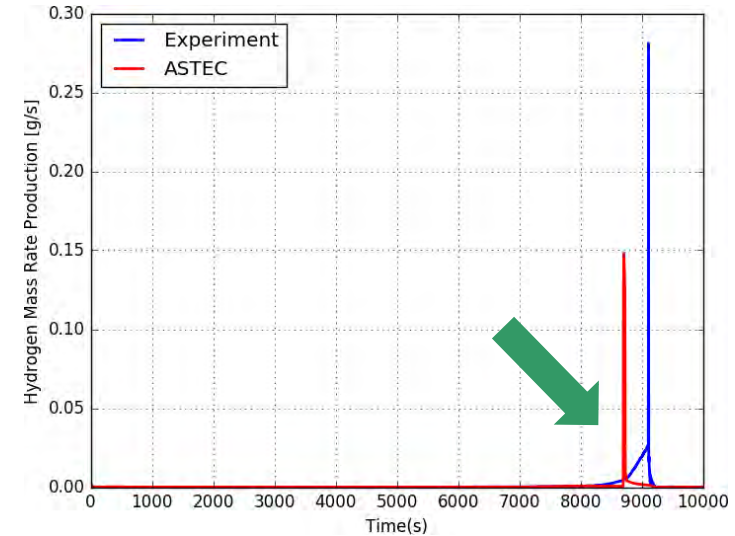
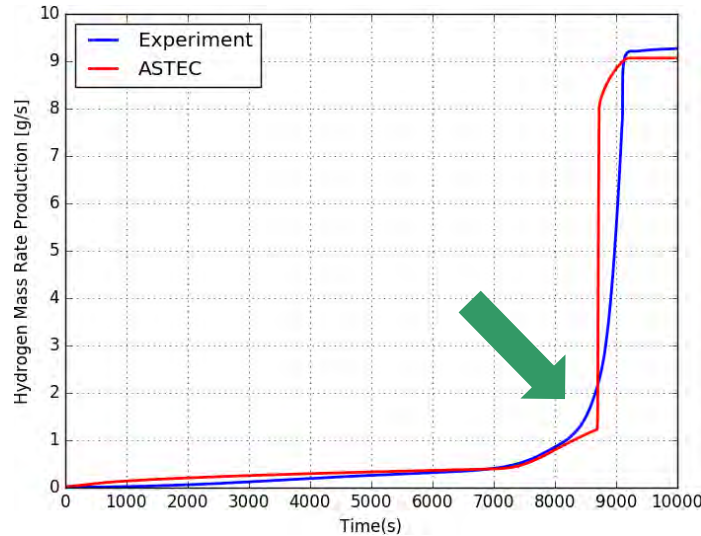
- Results exceed the exp. of about 100 degree in the pre-oxidation phase.
- Max. temperature reasonably well reproduced.

# Results: Cooling Jacket Temperature



➤ **Experimental results reasonably well reproduced.**

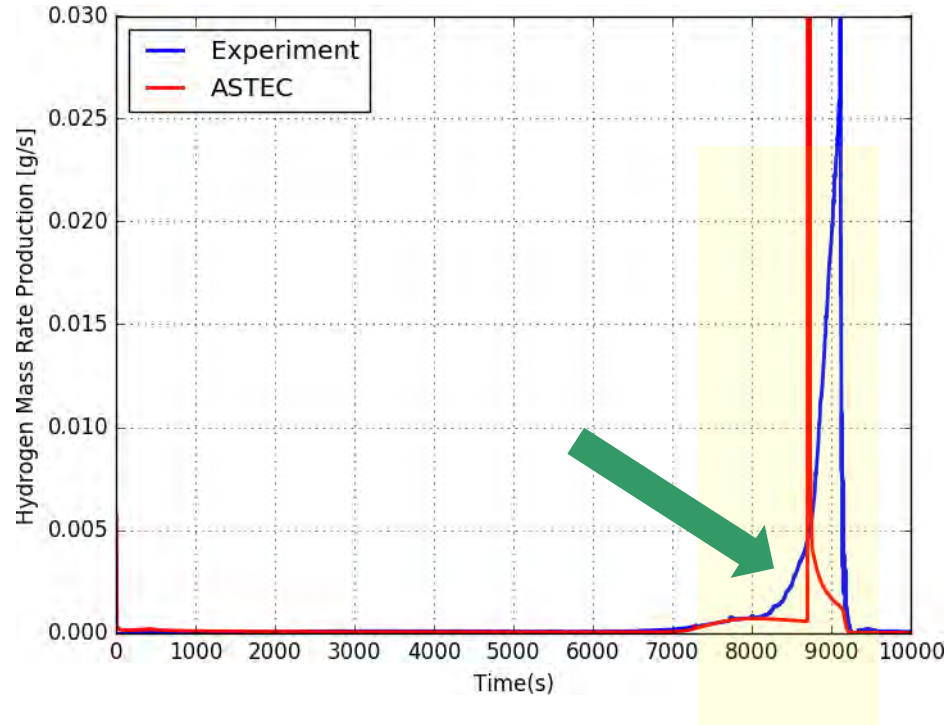
# Results: Hydrogen Production



- **The final amount of H<sub>2</sub> is reasonably well reproduced.**
- ASTEC results show a good agreement with exp. up about 8000 s.
- Escalation is anticipated in time with about 50% of the mass rate compared with the exp.
- **Transition to the escalation is not well reproduced.**



# Results: Hydrogen Production



- **‘Smooth’ kinetics behavior is not reproduced.**
- **Updating of the model related to the oxide thickness gain may improve the ASTEC vs. exp. agreement.**

# Conclusion

- Efforts are going on to extend the capabilities of the ASTEC to model the ATFs.
- The Steam/FeCrAl oxidation laws implemented in the material database of the code (v2.2\_b).
- The QUENCH-19 test has been analyzed
- **Overestimation of the clad temperatures (~100 degree) and acceptable agreement on the radial profile**
- **Acceptable ASTEC/Exp. agreement concerning the shroud temperatures**
- **H<sub>2</sub> generation** – ASTEC vs. Exp.
  - **Total amount reasonable well reproduced**
  - **The kinetics of the escalation is not well predicted**
- **Outlook**
  - **Refinement of the oxide thickness law necessary.**
  - **Participation to the OECD/NEA benchmark (blind phase) on ATF-1 experiment.**



**T. Hollands (pres. by L. Tiborcz)**

**GRS**

## **Simulation of QUENCH-19 and QUENCH-20 with AC<sup>2</sup>/ATHLET-CD**

In contrast to the experiments QUENCH-00 to QUENCH-18 which dealt with PWR configurations and Zr-based claddings, in QUENCH-19 the Accident Tolerant Fuel (ATF) FeCrAl in a PWR configuration and in QUENCH-20 a BWR like configuration were investigated. For both tests pre- and post-test were performed with AC<sup>2</sup>/ATHLET-CD in the respective current version because QUENCH-19 was performed in 2018 and QUENCH-20 in 2019. The latest post-test simulations were performed with AC<sup>2</sup> 2021, which includes ATHLET-CD 3.3.0.

The model base of ATHLET-CD was improved to consider also FeCrAl components and their oxidation. There are two correlations for the FeCrAl oxidation hard-coded based on KANTHAL APM, which was used for all components in the pre- and former post-tests analyses. Currently, there is an option available to implement own correlations via the input deck to consider the characteristics of the oxidation of dedicated material compositions. For QUENCH-19 an oxidation correlation for B136Y3 claddings was used, while for corner rods, grid spacers and shroud the standard correlation was applied like in the test. With respect to the temperatures the results of the simulations show that the qualitative evolution is generally captured well for all elevations, but the observed radial gradient due to the wetted insulation is not captured. By application of the dedicated correlations the measured integral hydrogen mass is predicted in very good agreement with a slightly different qualitative evolution over time. Some parameter studies show that hydrogen generation strongly depends on the chosen correlation, which differ significantly depending on FeCrAl composition. ATF will play a major role for future developments and safety assessments, and the models need to be further improved for ATF concepts to allow robust predictions. This requires also an expanded experimental database.

For the BWR configuration of QUENCH-20, the reactor-like option was used in ATHLET-CD including the oxidation of the absorber material B<sub>4</sub>C, which could have a significant impact on accident progression. The results of the post-test simulations show a good agreement with the experimental observations. The thermal behaviour is generally well captured for the cladding, while the BWR components are underestimated particularly in the middle and lower bundle heights. This could be caused by the underestimation of B<sub>4</sub>C oxidation, which has also an exothermal character with an additional heat impact. Furthermore, melting and relocation of BWR components is not calculated, which could also have an impact on the temperatures in the lower bundle region. Based on post-test examinations the analyses will be continued and a detailed investigation and review of the BWR model including B<sub>4</sub>C oxidation is foreseen.

# **Simulation of QUENCH-19 and QUENCH-20 with AC<sup>2</sup>/ATHLET-CD**

**Thorsten Hollands, Livia Tiborcz**

GRS gGmbH, Boltzmannstr. 14, 85748 Garching, Germany

**27th International QUENCH Workshop**

**Karlsruhe Institute of Technology, Campus North, H.-von-Helmholtz-Platz 1, 76344 Egg-  
Leopoldshafen, Germany 27-29 September 2022**



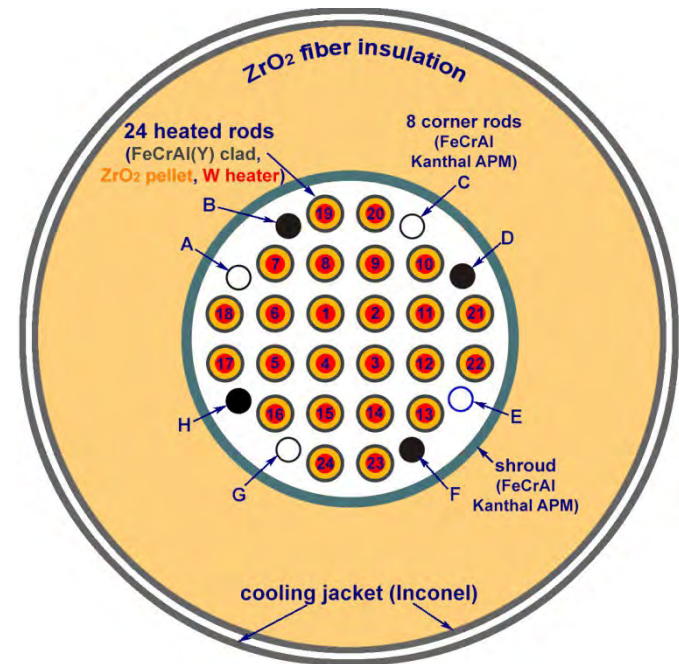
# Content

- QUENCH-19
  - Bundle Configuration and Test Conduct
  - ATF Modelling in AC<sup>2</sup>
  - Simulation Results
  - Main Findings
- QUENCH-20
  - Bundle Configuration and Test Conduct
  - Modelling in AC<sup>2</sup>
    - Simulation Results
    - Main Findings
- Conclusions and Outlook

# QUENCH-19

# QUENCH-19 – Bundle Configuration –

- Performed at KIT 2018
- FeCrAl claddings to investigate the cladding material behaviour under SA conditions
- Scenario: similar to QUENCH-15 with Zirlo cladding
  - same bundle geometry
  - same electrical power input
- Bundle configuration made of different FeCrAl compositions:
  - 24 heated rods with tungsten heater and  $ZrO_2$  pellet
  - 8 corner rods
  - 5 spacer grid
  - Shroud

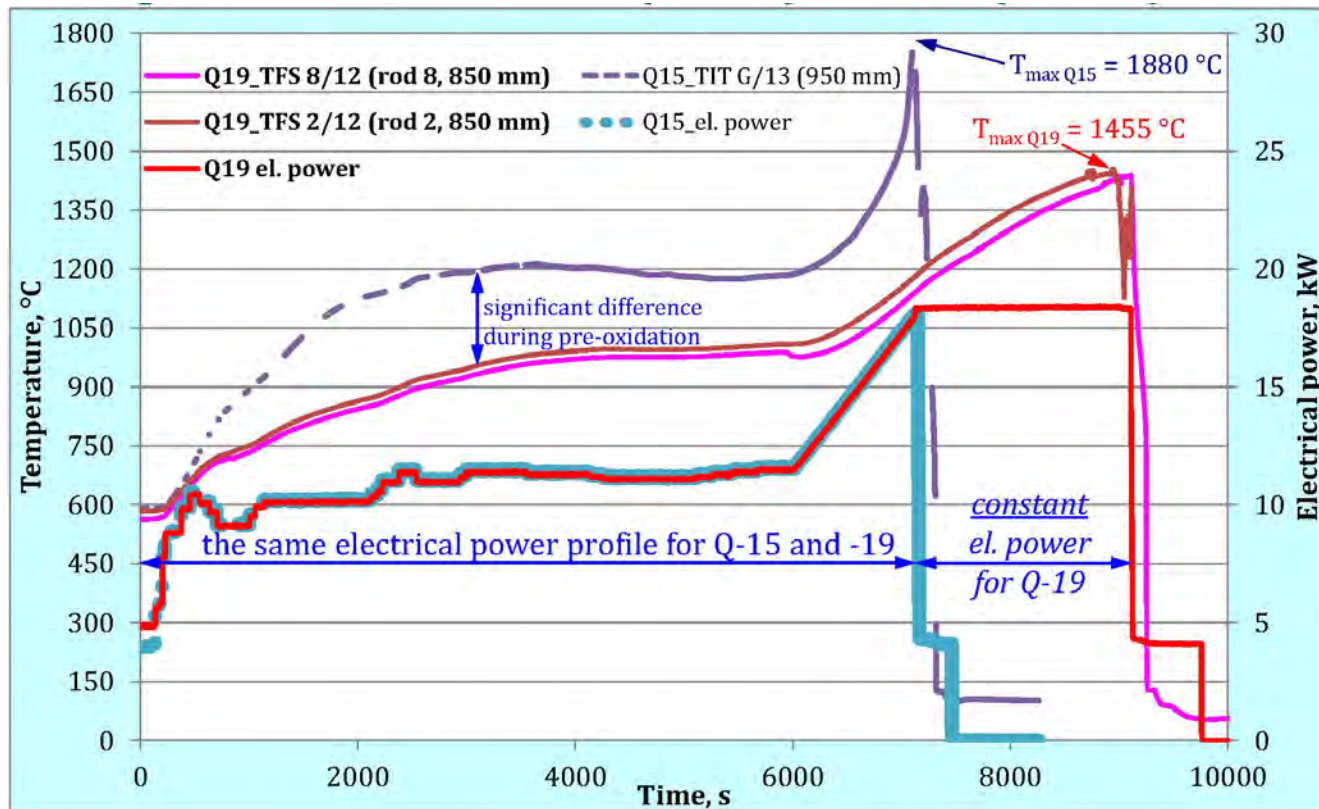


Source: KIT

# QUENCH-19

## – Test Conduct –

- Pre-Oxidation Phase      0 – 6020 s
- Transient Phase          6020 – 9106 s
- Quench Phase              9106 – 10000 s

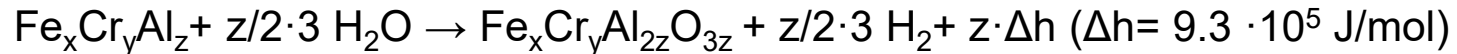


Source: KIT



# ATF Modelling in AC<sup>2</sup> (I)

- Assumption: Al oxidized only



- Oxidation Rate  $\rightarrow$  Parabolic law derived from the analytical solution of the diffusion equation (as for Zr):

$$dW^2 = K(T) \cdot dt$$

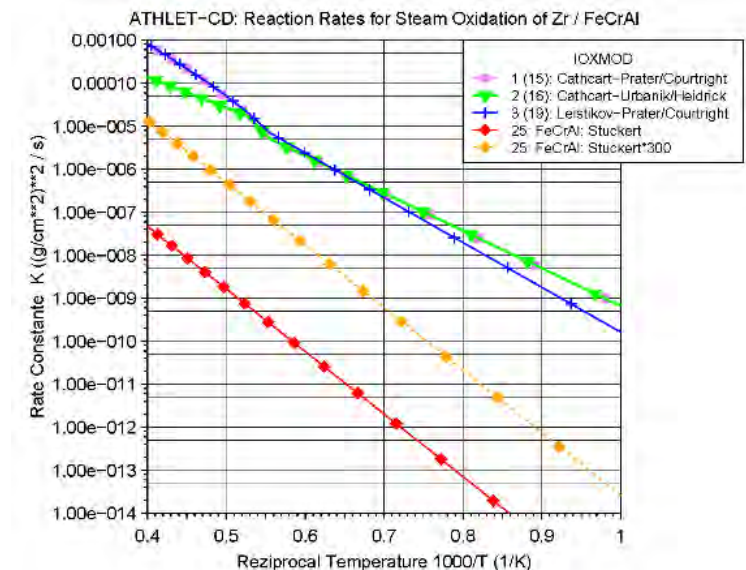
W:  $m_{\text{Ox}}/A$  [kg/m<sup>2</sup>], K: reaction rate [kg<sup>2</sup>/m<sup>4</sup> s], t: time [s]

- Reaction rate from the Arrhenius formulation:

$$K = A \cdot e^{-B/(RT)}$$

R = 8.134 J/mol K, T: cladding Temperature [K],

A, B: rate constants

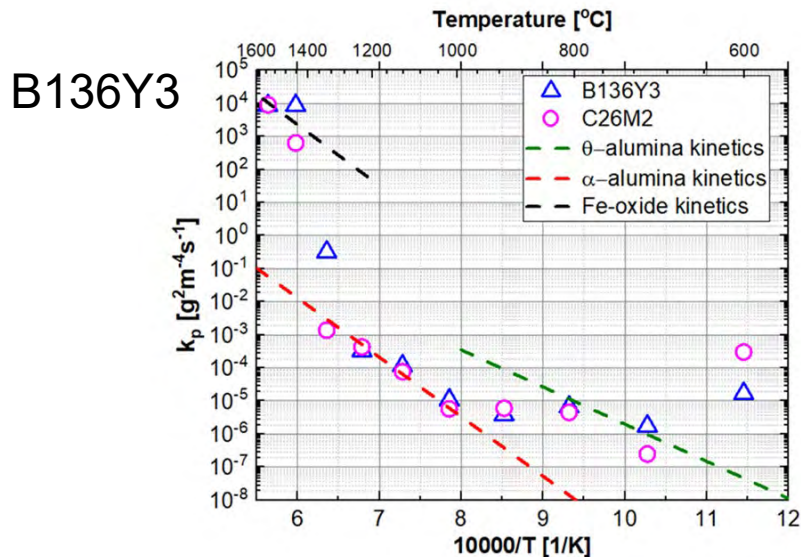


# ATF Modelling in AC<sup>2</sup> (II)

- For the current investigations the following correlation is used in AC<sup>2</sup>/ATHLET-CD:

$$K = \begin{cases} 9.62 \times 10^{-12} [\text{g}^2 / \text{cm}^4 \text{ s}], & T \leq 1473 \text{ K} \\ A_B \exp\left(\frac{-E_B}{RT}\right), & 1473 < T < 1648 \text{ K} \\ A_{Fe} \exp\left(\frac{-E_{Fe}}{RT}\right), & T \geq 1648 \text{ K (melting point of FeO)} \end{cases}$$

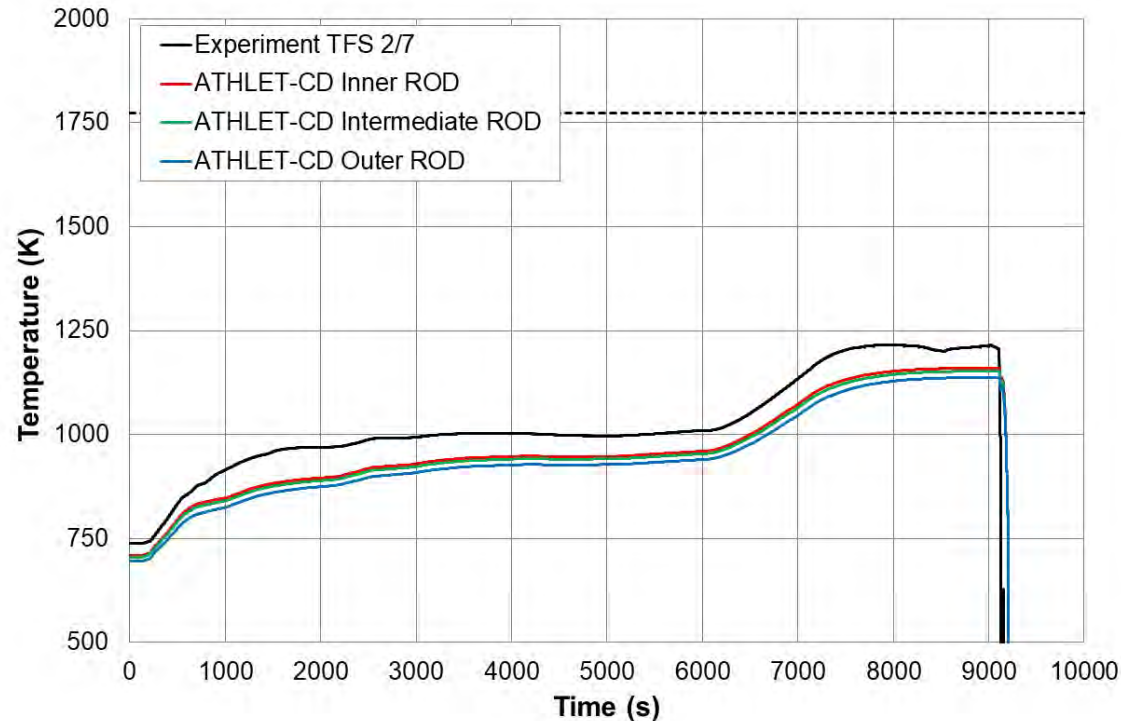
*J. Stuckert. Suggestion for IAEA  
CRP ATF-TS*



*C. KIM et al.: OXIDATION KINETICS OF NUCLEAR  
GRADE FeCrAl ALLOYS IN STEAM IN THE  
TEMPERATURE RANGE 600-1500°C, TopFuel 2021*

# Simulation Results

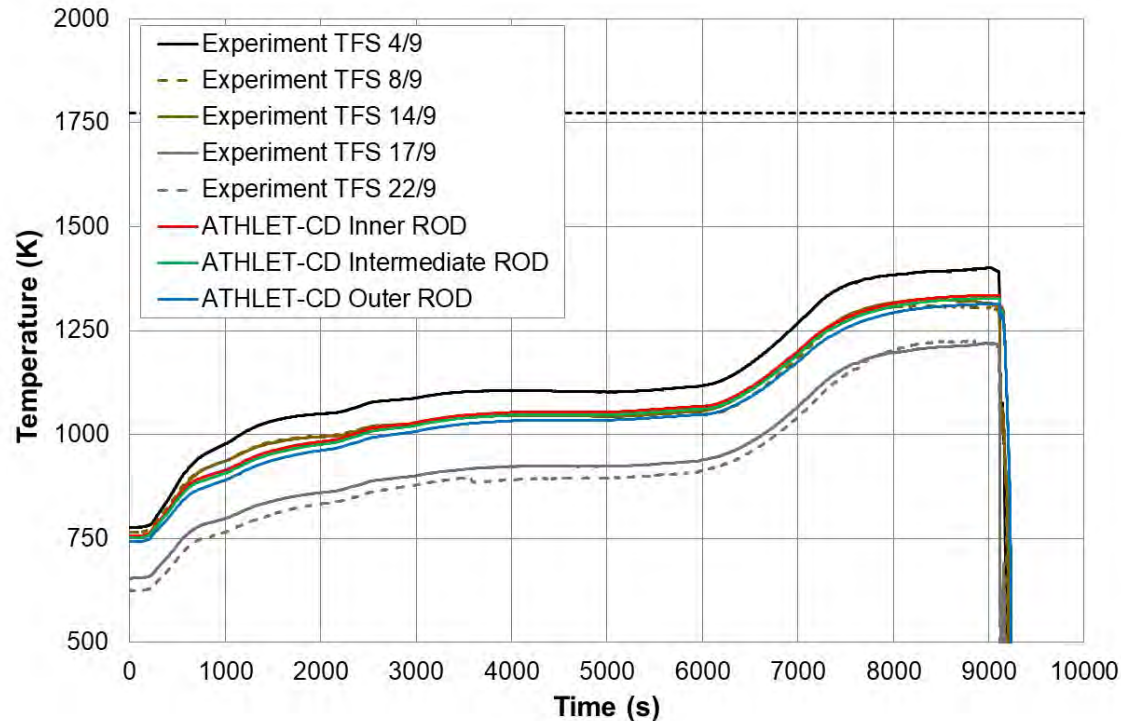
## – Cladding Temperatures at 350 mm –



- The simulations predict the measured temperatures in the lower bundle elevation qualitatively well, without temperature escalation as in the test, but
  - underestimate the experimental values

# Simulation Results

## – Cladding Temperatures at 550 mm –

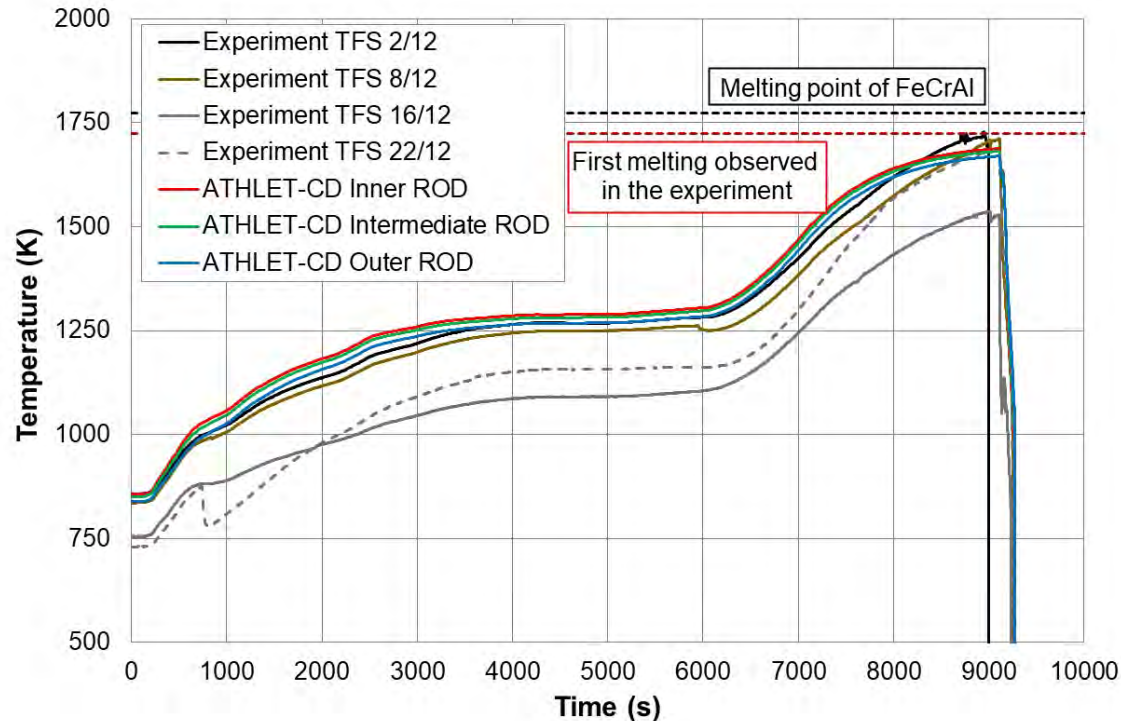


- The simulation predicts the measured temperature in the middle bundle elevation qualitatively well without temperature escalation as in the test
- The simulated cladding temperatures capture the temperatures of the inner rods
- The strong radial profile in the experiment is not captured



# Simulation Results

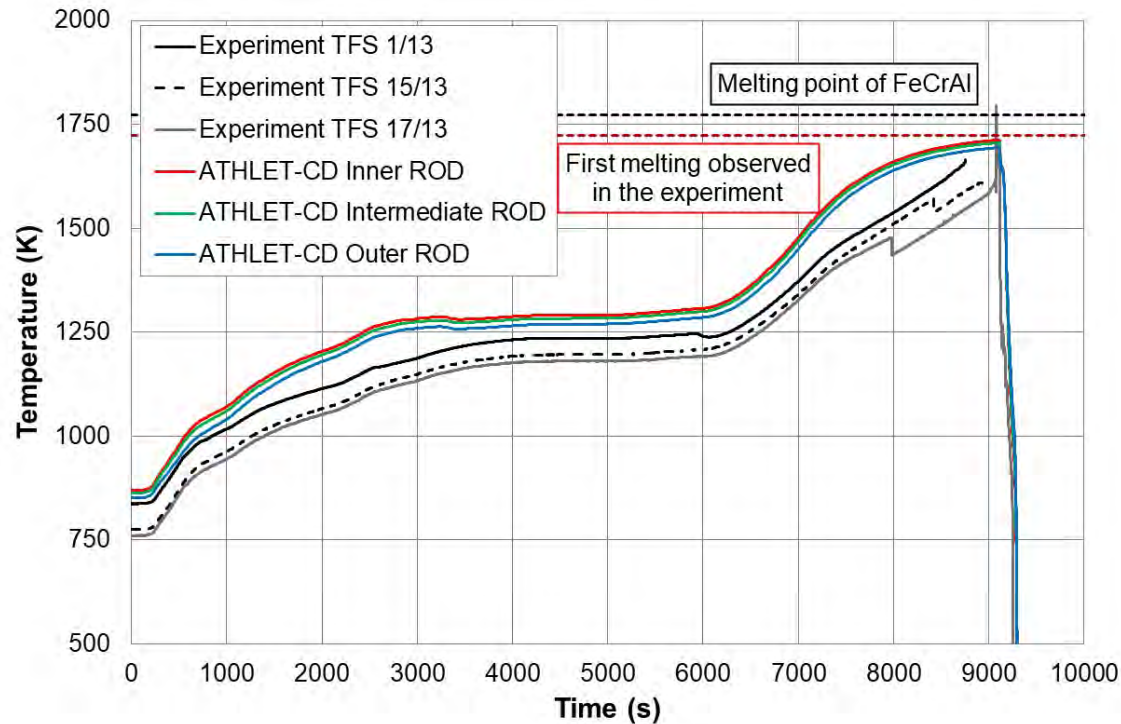
## – Cladding Temperatures at 850 mm –



- The qualitative evolution of the measured temperatures is predicted well by the code without temperature escalation at the end of the transient and quenching phase
- The strong radial profile in the experiment is not captured

# Simulation Results

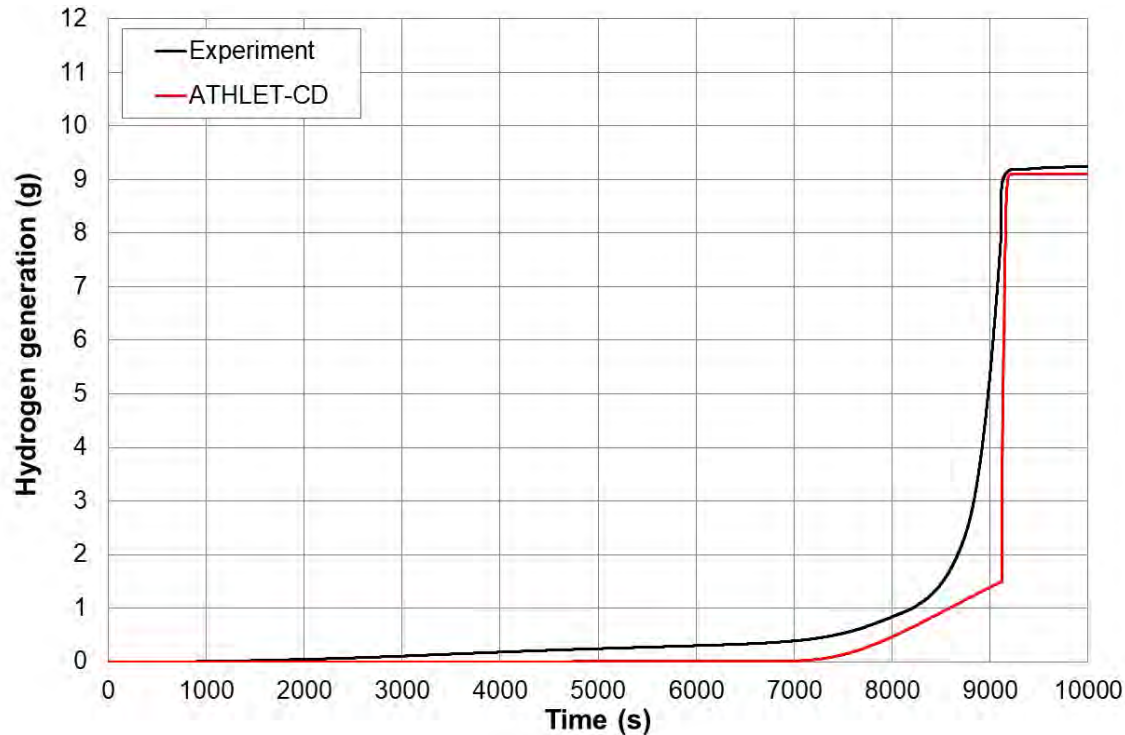
## – Cladding Temperatures at 950 mm –



- Simulation overestimates the measured temperatures
- No escalation is predicted
- The strong radial profile in the experiment is not captured

# Simulation Results

## – Hydrogen Generation –



- The measured integrated hydrogen mass is well predicted by ATHLET-CD
- The quantitative evolution is underestimated until the final reflooding phase

# Main Findings

## QUENCH-19

- The capabilities of the AC<sup>2</sup>/ATHLET-CD were extended to simulate ATFs
- Dedicated models to calculate FeCrAl material and its oxidation has been implemented
- The experiment QUENCH-19 performed at KIT was considered to validate the recently implemented models
- With respect to the temperatures the results of the simulations show that
  - The qualitative evolution is generally captured well for all elevations
  - The observed radial gradient due to the wetted insulation is not captured
- The results show that the hydrogen generation strongly depends on the chosen correlation, which differ significantly depending on the FeCrAl composition
- ATF will play a major role for future developments and safety assessments
- Models need to be further improved for ATF concepts to allow robust predictions
- Therefore, also the experimental basis needs to be expanded

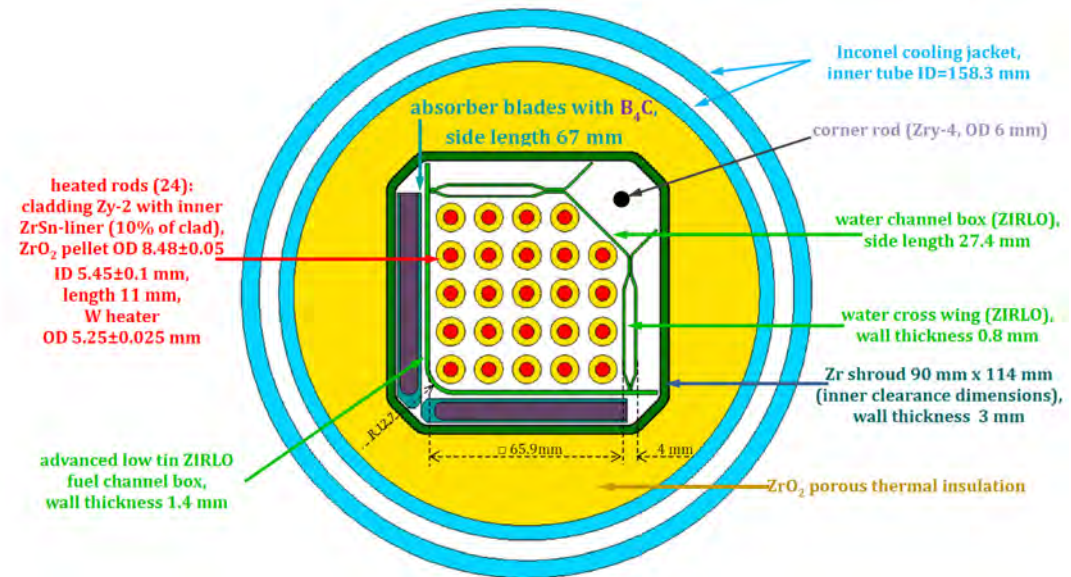


# QUENCH-20

# QUENCH-20

## – Bundle Configuration –

- Performed at KIT 9<sup>th</sup> October 2019
- BWR configuration
- Westinghouse bundle parts (clad, channel box, spacer grids, absorber blades, B<sub>4</sub>C pins)
- Quadratic Zr shroud
- Bundle configuration:
  - 24 heated rods with tungsten heater
  - ZrO<sub>2</sub> pellets
  - Zy-2 clad with ZrSn inner liner
  - 1 corner rod (withdrawn after pre-oxidation)
  - 5 spacer grids

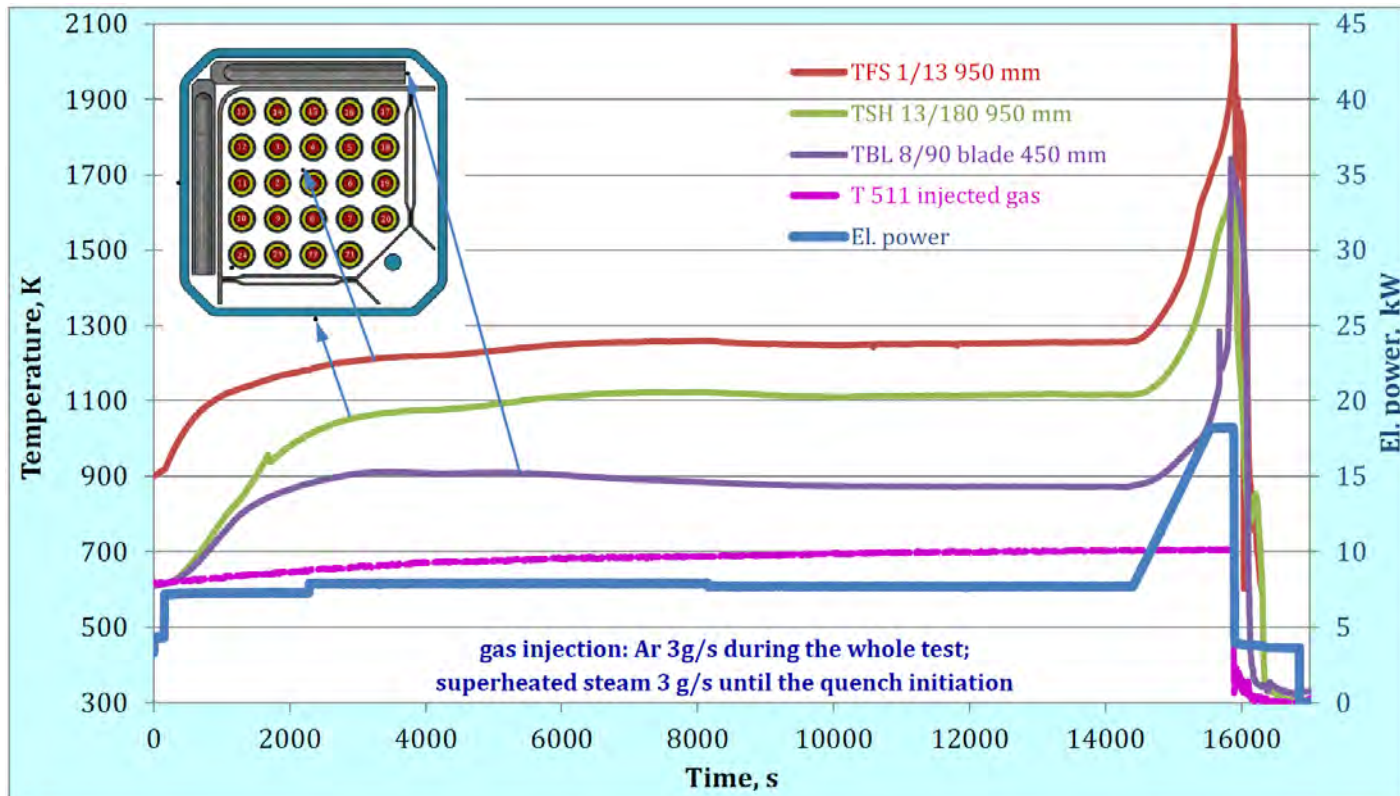


Source: KIT

# QUENCH-20

## – Test Conduct –

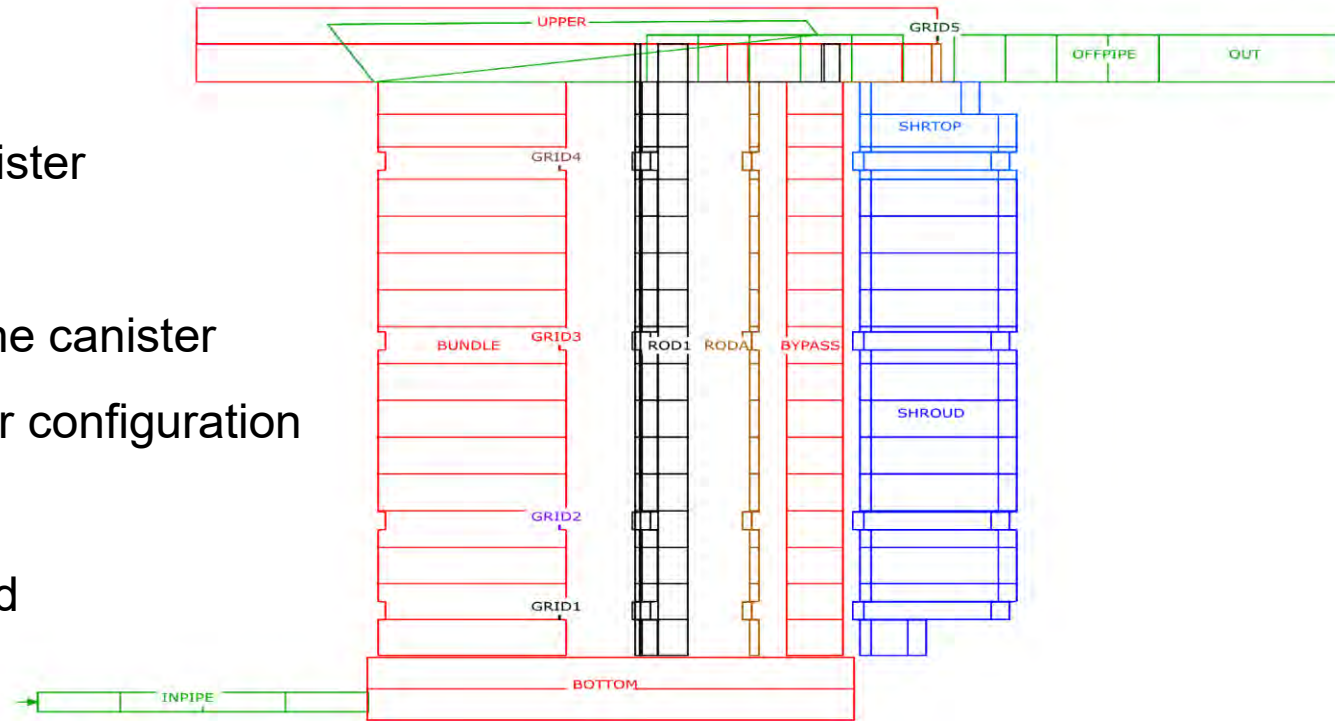
- Pre-Oxidation Phase      0 – 14416 s
- Transient Phase          14416 – 15882 s
- Quench Phase              15882 – 16 375 s



Source: KIT

# Nodalisation and Model Options

- Standard QUENCH input deck adopted for QUENCH-20 BWR configuration
- Bundle configuration implemented as given by KIT
- Two fluid channels
  - BUNDLE
    - 53 % within the canister
  - BYPASS
    - 47 % surrounding the canister
- BWR model for reactor configuration is applied
  - All rods are summed up to ROD1
- Corner rod RODA

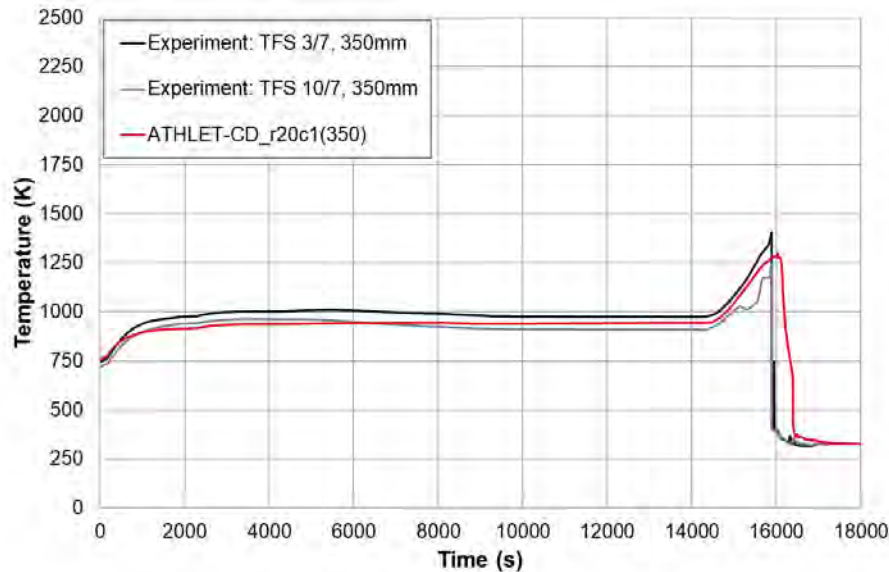




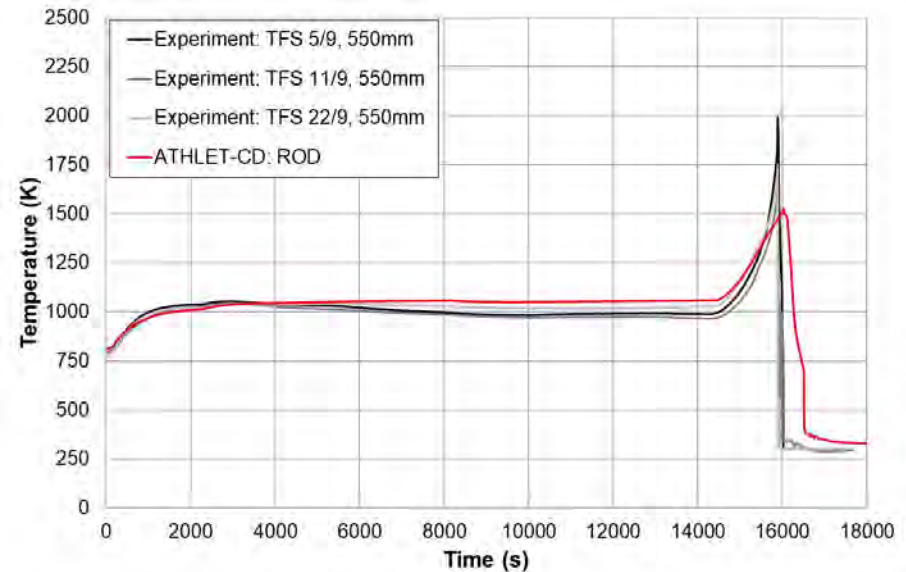
# Simulation Results

## – Cladding Temperatures at Lower Elevations –

350 mm



550 mm

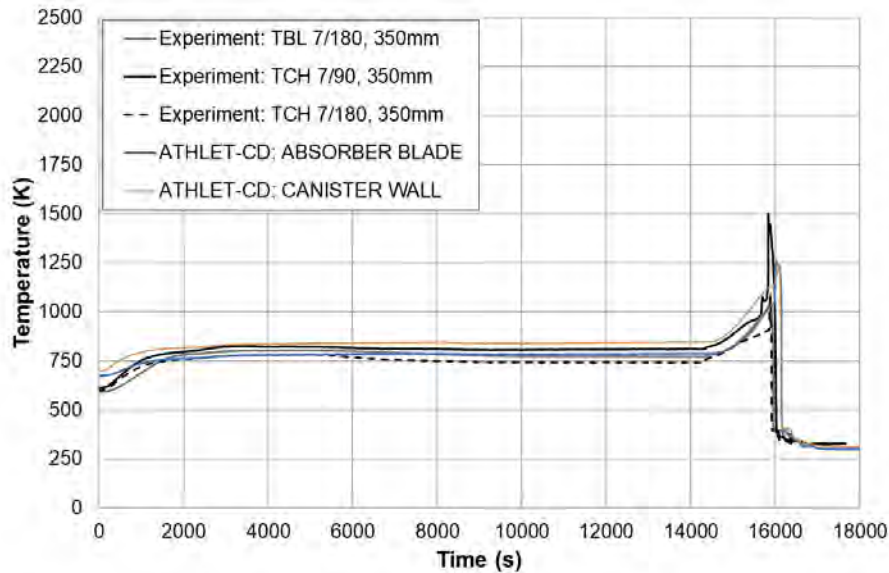


- Good agreement during pre-oxidation
- Underestimation in the middle bundle elevation during transient and quench phases due to underestimation of  $B_4C$  oxidation, which triggers the temperature escalation of the cladding in the experiment

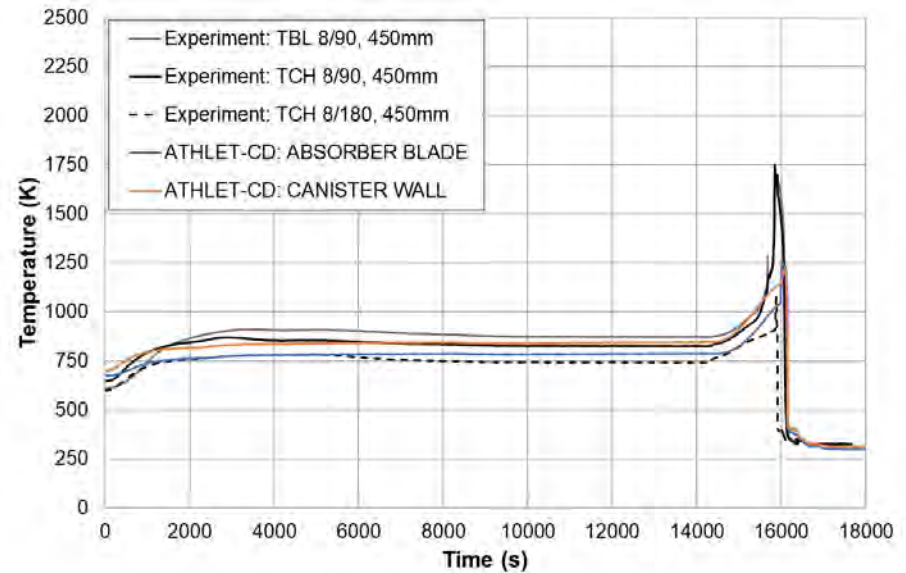
# Simulation Results

## – Absorber/Canister Temperatures at Lower Elevations –

350 mm



450 mm

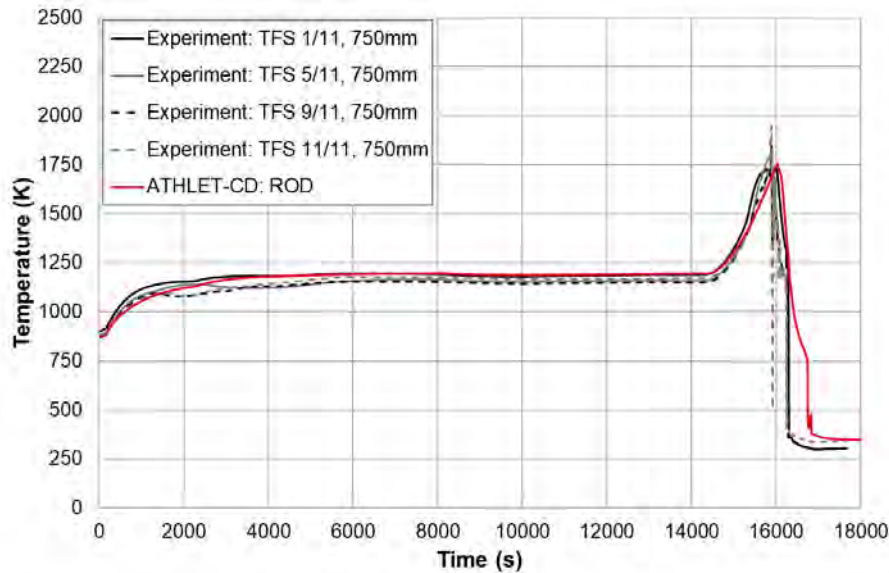


- During the pre-oxidation the numerical results are within the experimental range
- The relocation of absorber material is not calculated which leads – besides the underestimated  $B_4C$  oxidation of intact structures – to an underestimation of the oxidation and the corresponding heat impact

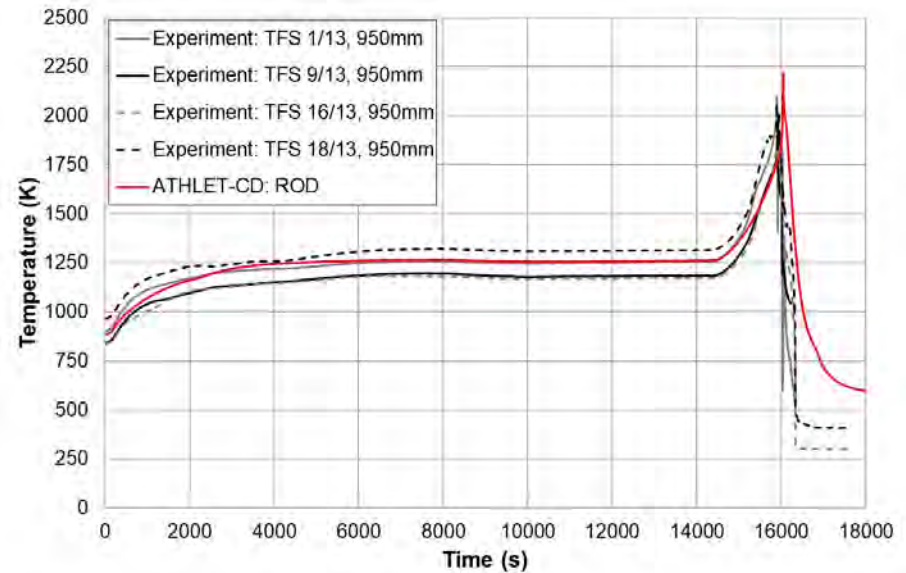
# Simulation Results

## – Cladding Temperatures at Higher Elevations –

750 mm



950 mm

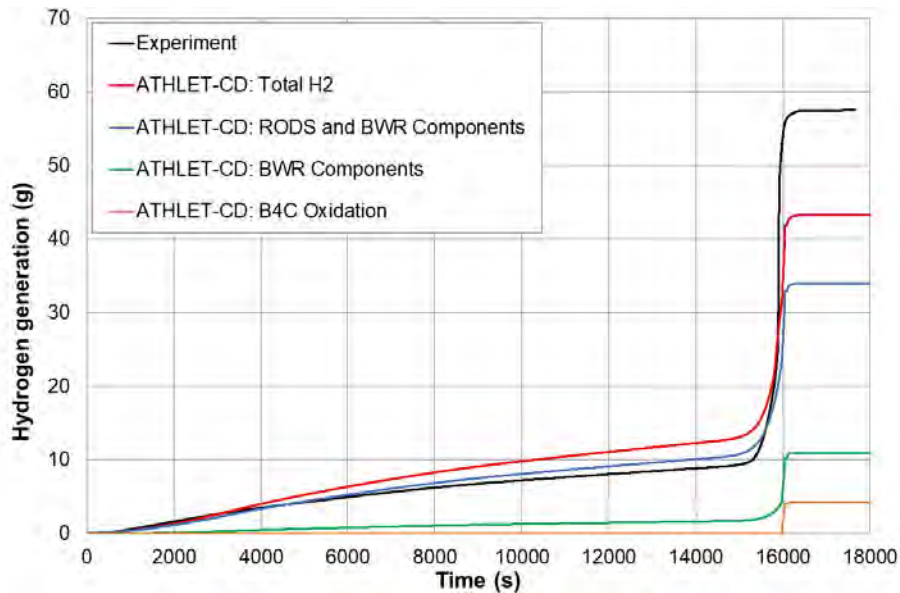


- Simulation results are within the band of measured temperatures
- The observed azimuthal spreading can not be captured by the code due to the assumption that each rod has the same behavior

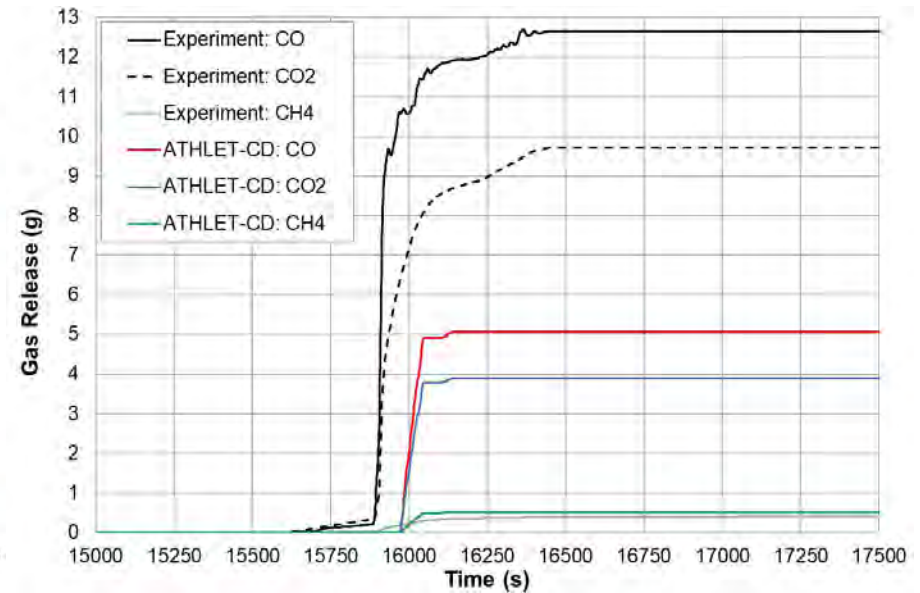
# Simulation Results

## – Gas Analysis –

### Hydrogen



### CO, CO<sub>2</sub> and CH<sub>4</sub>



- Total H<sub>2</sub> generation is underpredicted
- B<sub>4</sub>C oxidation is underestimated in the simulation by 50 % (10 g H<sub>2</sub> in the experiment), which leads to a comparable underestimation of CO, CO<sub>2</sub> and CH<sub>4</sub>
  - Improvement of B<sub>4</sub>C oxidation necessary



# Main Findings

## QUENCH-20

- The experiment QUENCH-20 was performed at KIT in 2019
- The results of the experiment show that the cladding reaches the melting point only for a short time at a very high elevation while the absorber blade temperatures in the lower elevations are above the melting temperature
- The thermal behavior is generally well captured for the cladding, while the BWR components are underestimated especially in the middle and lower bundle heights
- $B_4C$  oxidation which has also an exothermal character with an additional heat impact is underestimated by the code
- Furthermore, melting and relocation of BWR components is not calculated by ATHLET-CD for QUENCH-20, which could also have an impact on the temperatures in the lower bundle region
- Based on post-test examinations the analyses will be continued and a detailed investigation and review of the BWR model including  $B_4C$  oxidation is necessary

# Conclusions and Outlook

- AC<sup>2</sup>/ATHLET-CD was successfully applied on new QUENCH topics ATF (FeCrAl) and BWR (reactor configuration, not like CORA)
- The FeCrAl simulation show, that the results are very sensitive to the chosen oxidation correlation, which belongs to the cladding composition
- For BWR core degradation processes the impact of absorber melting and relocation is significant
  
- Further ATF concepts needs to be considered
  - oxidation needs to be analyzed in detail and general as well as dedicated models have to be developed
- The BWR model in AC<sup>2</sup>/ATHLET-CD needs to be improved for absorber behaviour and B<sub>4</sub>C oxidation

# Acknowledgements

- The work of GRS is sponsored by the German Federal Ministry for the Environment, Nature Conservation, Nuclear Safety and Consumer Protection (BMUV).

Supported by:



Federal Ministry  
for the Environment, Nature Conservation,  
Nuclear Safety and Consumer Protection

based on a decision of  
the German Bundestag

# Thank you for your Attention!



**T. Kaliatka**

**Lithuanian Energy Institute**

## **Preliminary Modelling Results of QUENCH-20 Test Using RELAP/SCDAPSIM code**

Lithuanian Energy Institute (LEI) used severe accident analysis computer codes ASTEC and RELAP/SCDAPSIM to simulate several QUENCH tests (QUENCH-03, 06, 10, 18) to analyze the main phenomena in these tests. Applying this extensive experience, several different approaches, numerical models of QUENCH-20 were developed to evaluate the main processes occurring in this test.

From QUENCH matrix was found that the boundary conditions of QUENCH-6 and QUENCH-20 tests are similar. The main difference is in the test bundle structure. Thus, the first modeling approach was - to use similar modelling scheme as QUENCH-6 test with modifying the test bundle according to QUECH-20 bundle geometry. Using this simple approach different RELAP/SCDAPSIM versions were also tested. However, absorber blades were not considered in this modeling approach. In the second modelling approach, absorber blades were modeled using SCDAP components: "bladebox" or "shroud". Different nodalization schemes were applied as well. Parametric analysis of QUENCH-20 test were provided to investigate the influence of absorber blades on the calculation results.

This presentation observes the main challenges of modeling the QUENCH-20 test. Comparison of the RELAP/SCDAPSIM code modeling results with experimental data is discussed. Part of the presented work was done in the framework of the International Atomic Energy Agency Coordinated Research Project titled "Advancing the State-of-Practice in Uncertainty and Sensitivity Methodologies for Severe Accident Analysis in Water Cooled Reactors" where LEI is participating in the QUENCH working group of this project.



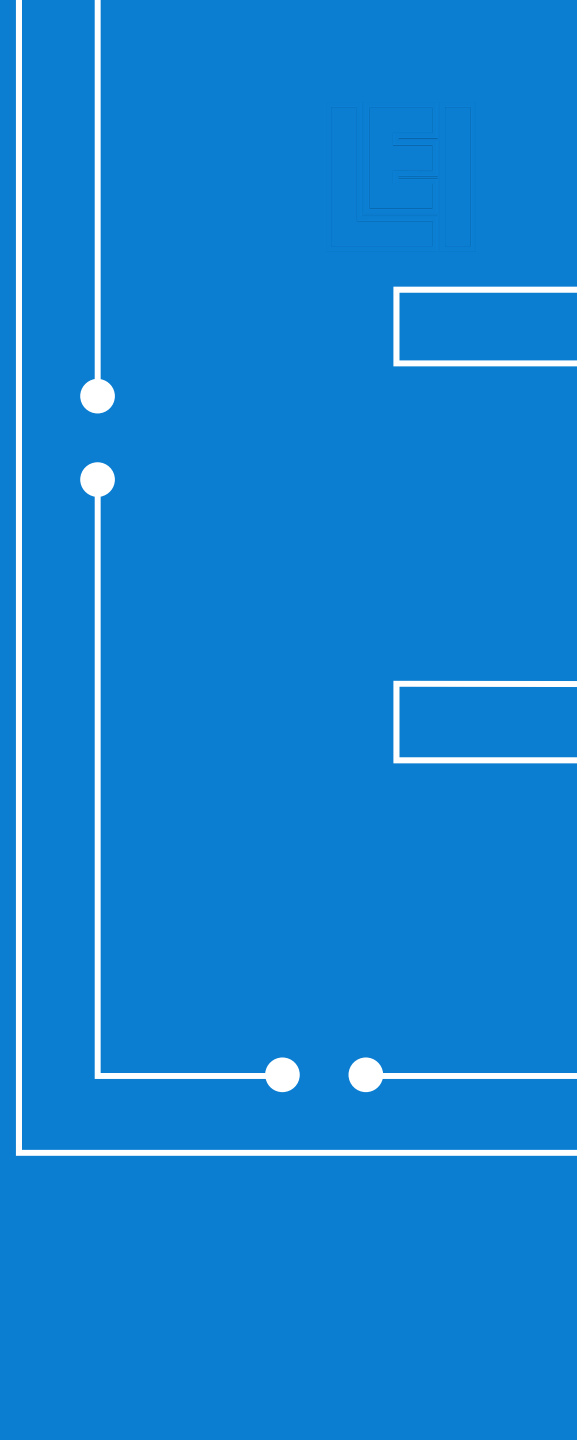


LITHUANIAN  
ENERGY  
INSTITUTE

# Preliminary Modelling Results Of QUENCH-20 Test Using RELAP/SCDAPSIM code

T. Kaliatka, N. Elsalamouny . Lithuanian Energy Institute

2022-09-27, 27th International QUENCH Workshop

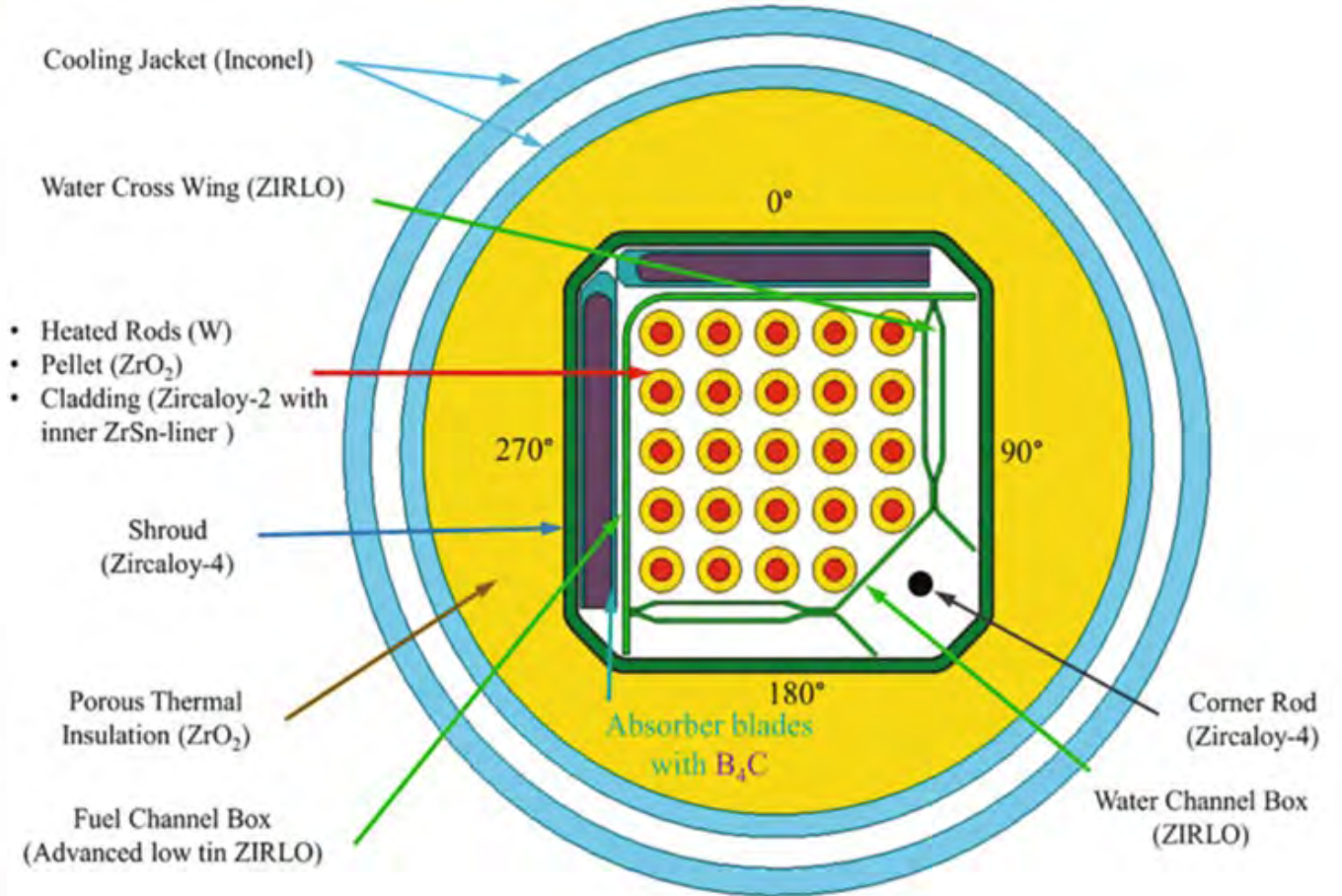
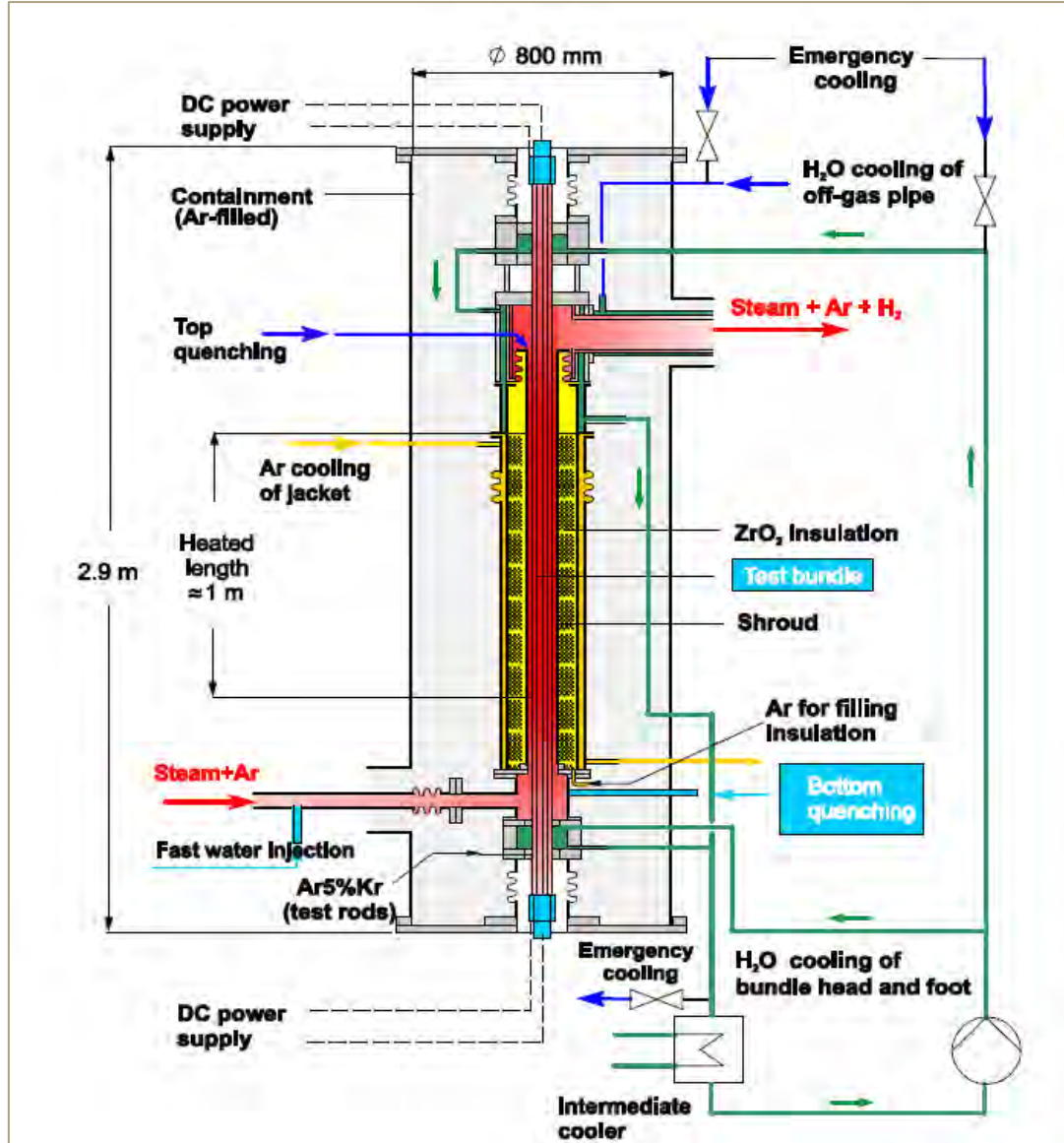


# Content



- Introduction, QUENCH-20 test
- Model development for RELAP/SCDAPSIM
  - Different modelling approaches
  - Calculation results
  - Parametric analysis
- Conclusion

# QUENCH-20 test facility

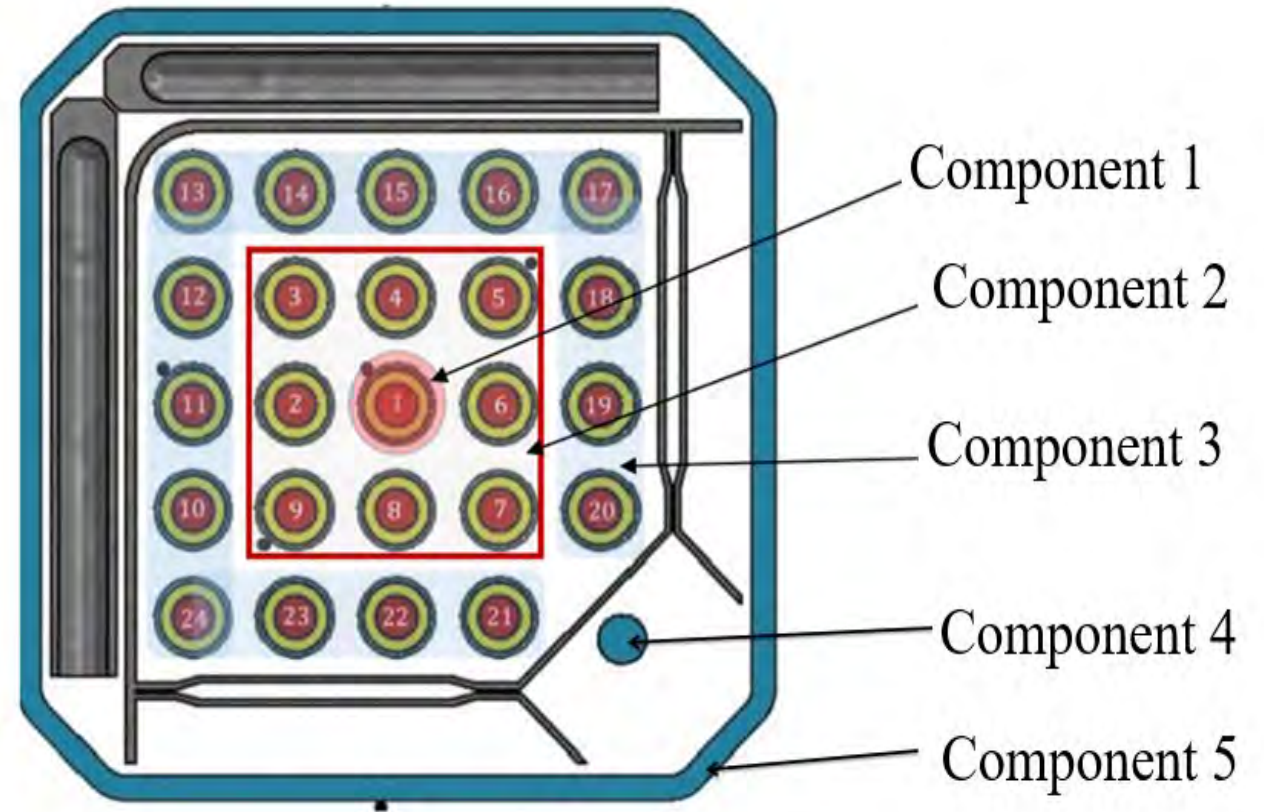
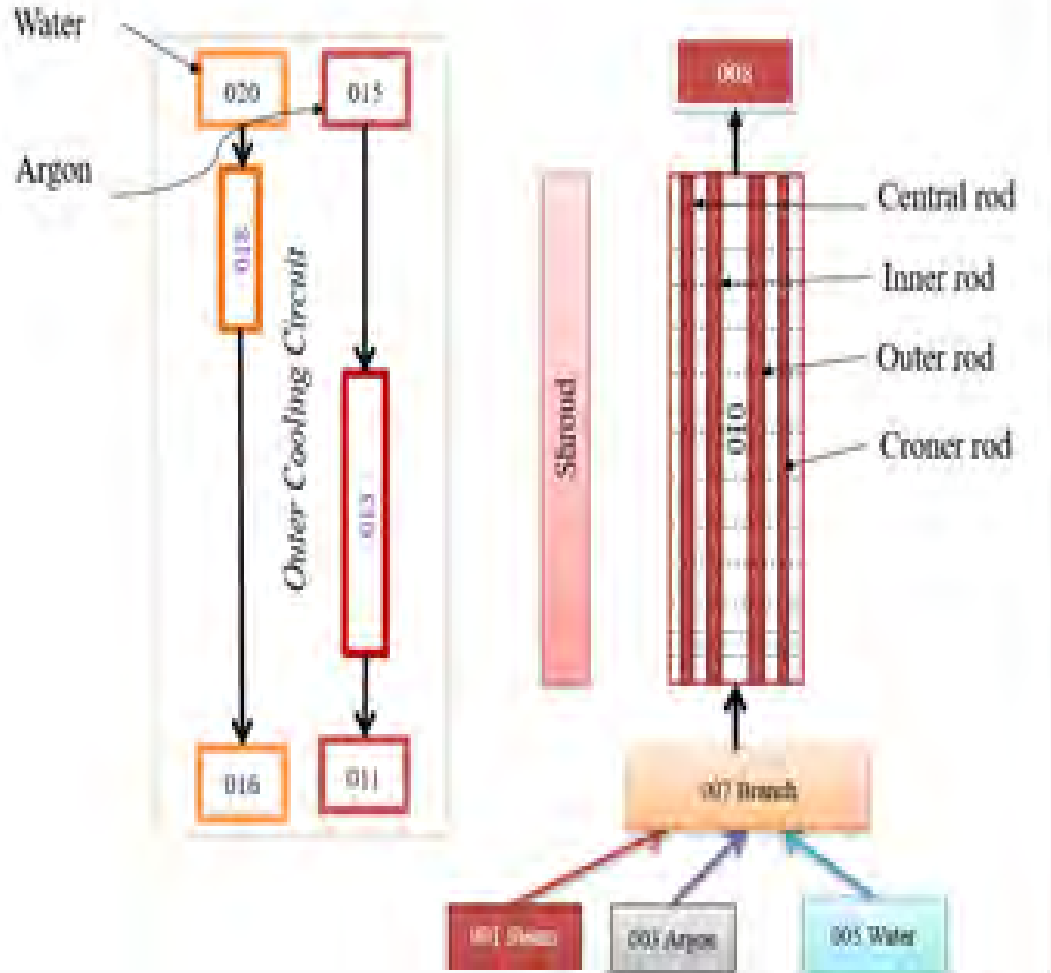


QUENCH-20 test bundle

# Development of QUENCH-20 Model for RELAP/SCDAPSIM



Based on QUENCH-06 model



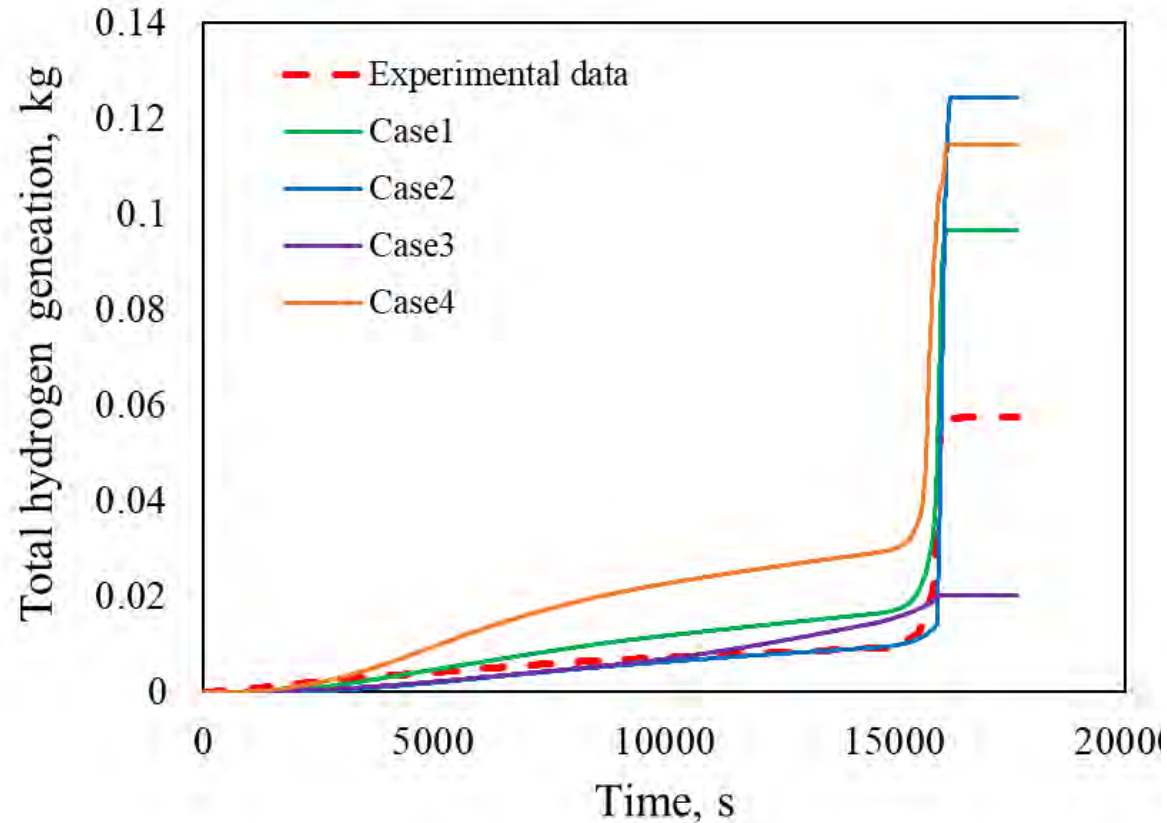


# Preliminary Results of Modelling QUENCH-20 Test

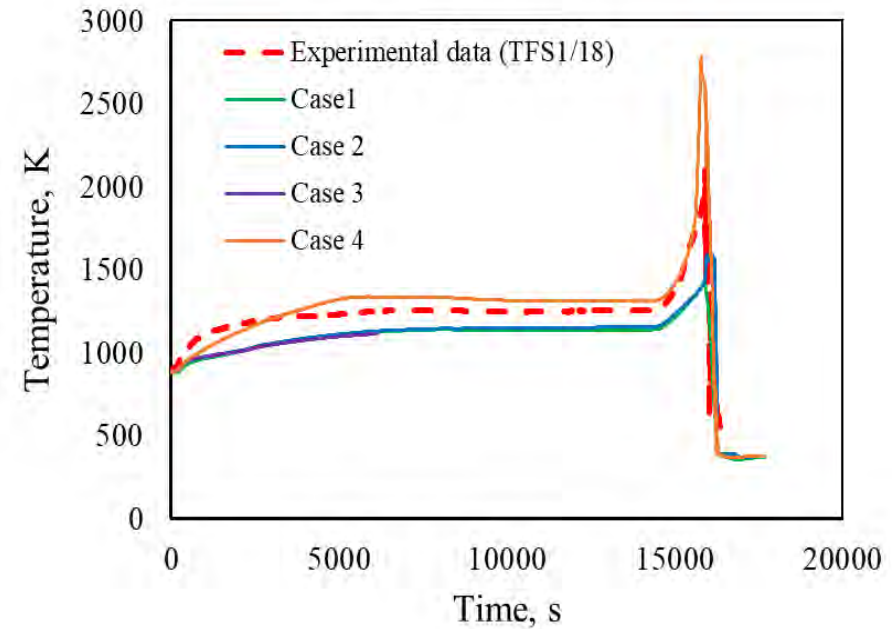


- Two different versions (mod 3.4 & 3.6) of RELAP/SCDAPSIM code were used.
- The RELAP/SCDAPSIM mod 3.6 version has many improvements and modeling options for the SCDAP part:
  - improvements of fuel gap conductance model;
  - improvements in the model of the electrically heated rod simulator;
  - shroud model improvements.
  - models to treat the influence of air ingress.
- **Case1:** calculations performed using RELAP/SCDAPSIM mod 3.4.
- **Case2:** calculations performed using RELAP/SCDAPSIM mod 3.6.
- **Case3:** calculations performed using RELAP/SCDAPSIM mod 3.6. PSI developed model for oxidation was activated.
- **Case4:** calculations performed using RELAP/SCDAPSIM mod 3.6, with activated improvements of fuel gap conductance model.

# Preliminary Results of Modelling Quench-20 Test



Cladding temperature at 950mm elevation



16th INTERNATIONAL CONFERENCE ON HEAT TRANSFER, FLUID MECHANICS AND THERMODYNAMICS

**LEI QUENCH TESTS MODELLING EXPERIENCE AND THE PRELIMINARY  
MODELLING RESULTS OF QUENCH-20 TEST USING RELAP/SCDAPSIM**

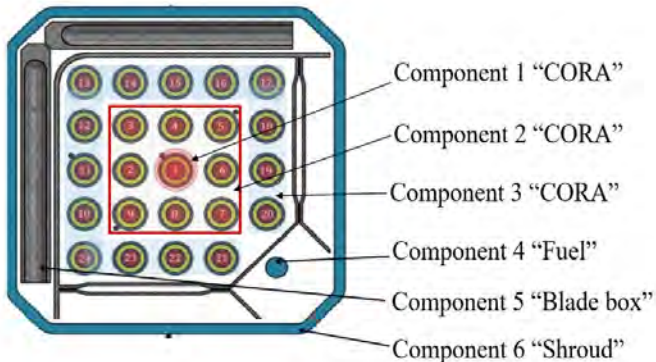
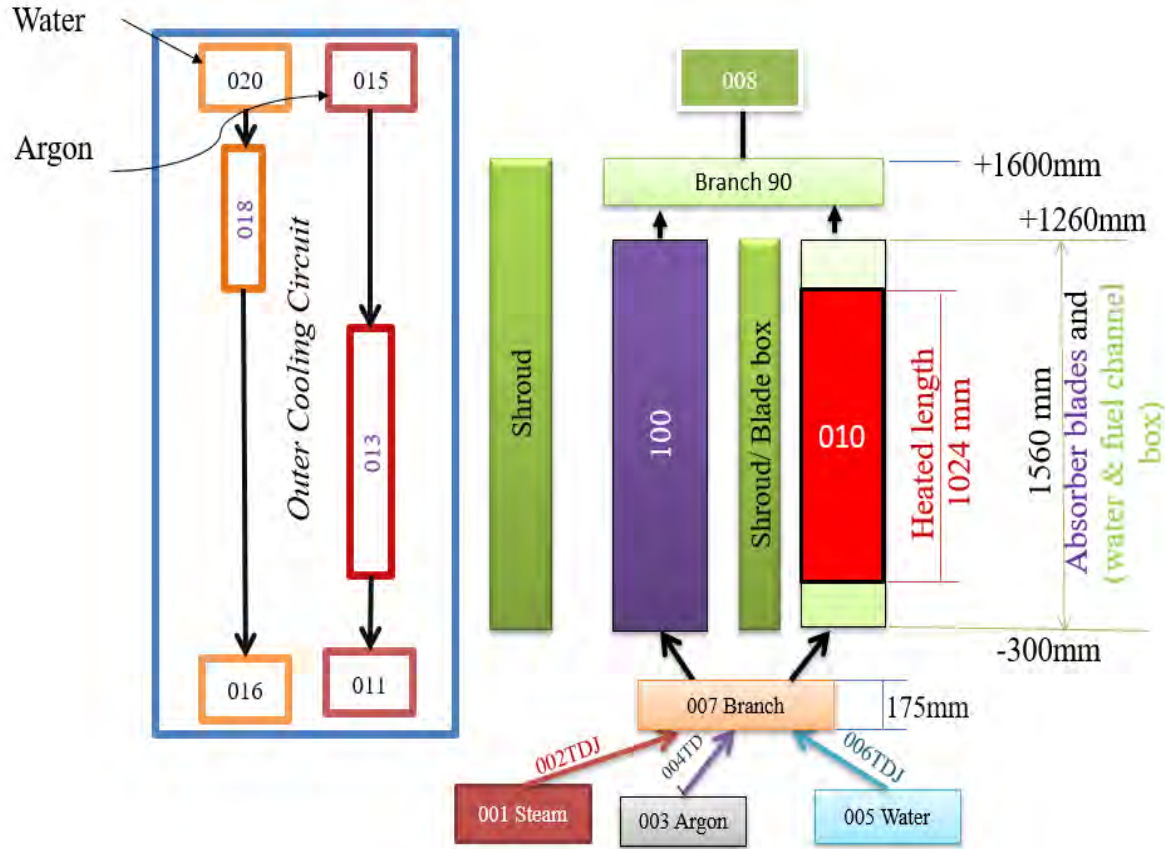
Elsalamouny N.\*, Kaliatka T., Kaliatka A.

\*Author for correspondence

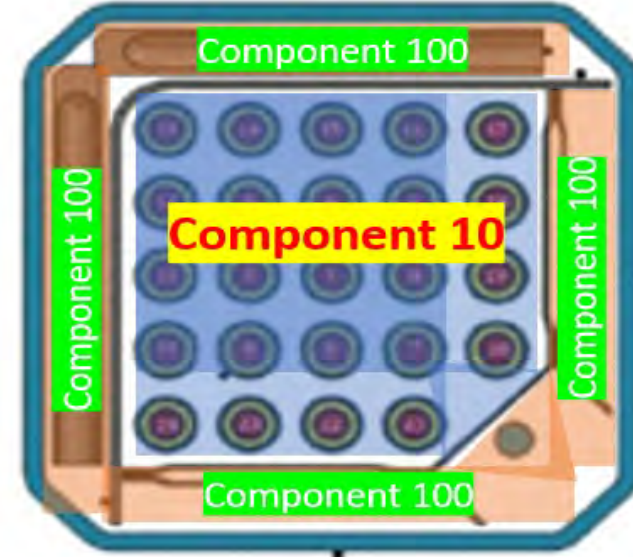
Laboratory of Nuclear Installation Safety,  
Lithuanian Energy Institute,  
Kaunas,  
Lithuania,

E-mail: [noura.elsalamouny@lei.lt](mailto:noura.elsalamouny@lei.lt)

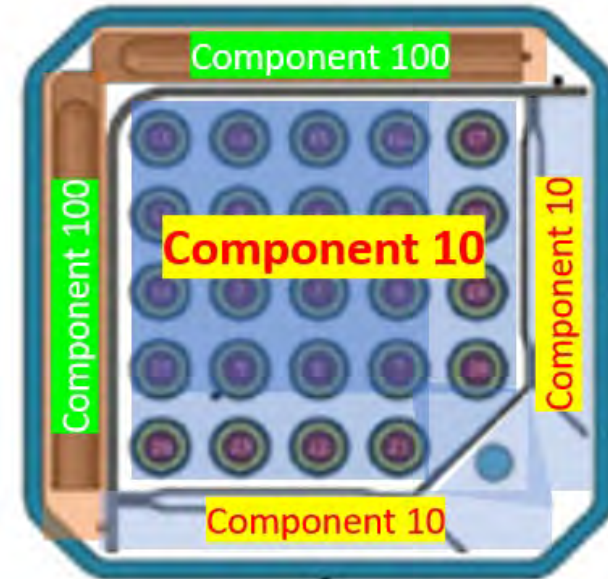
# Updated model



## Approach 1



## Approach 2



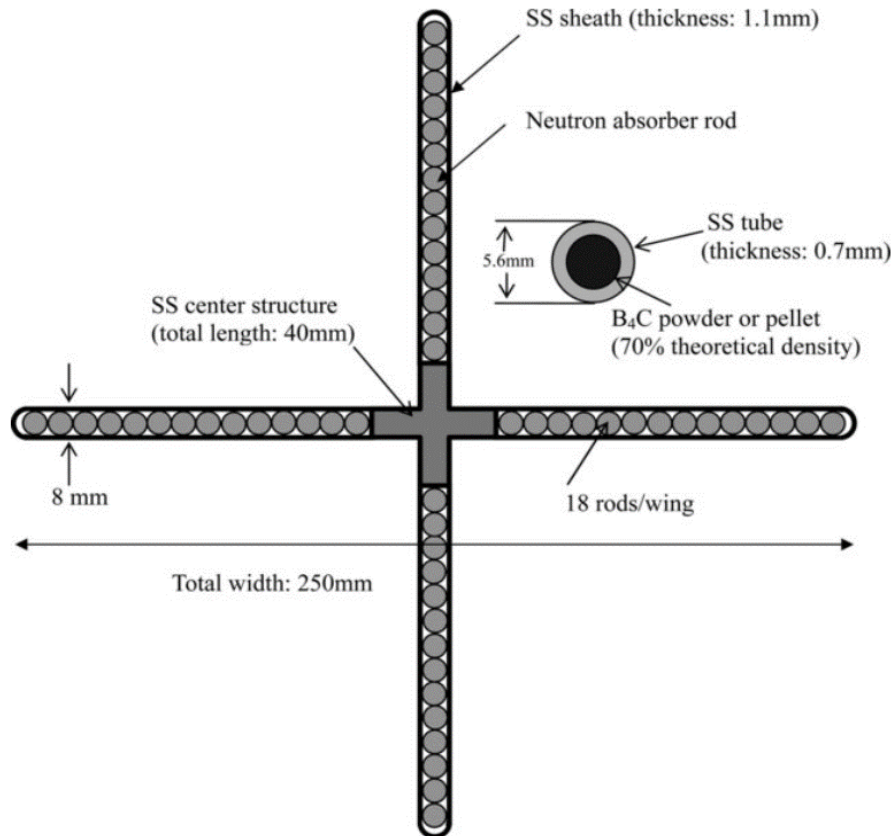
# Component 5 “bladebox”



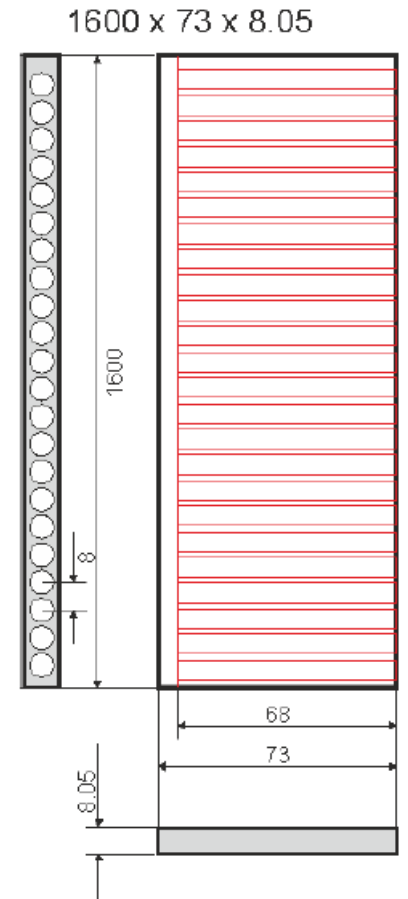
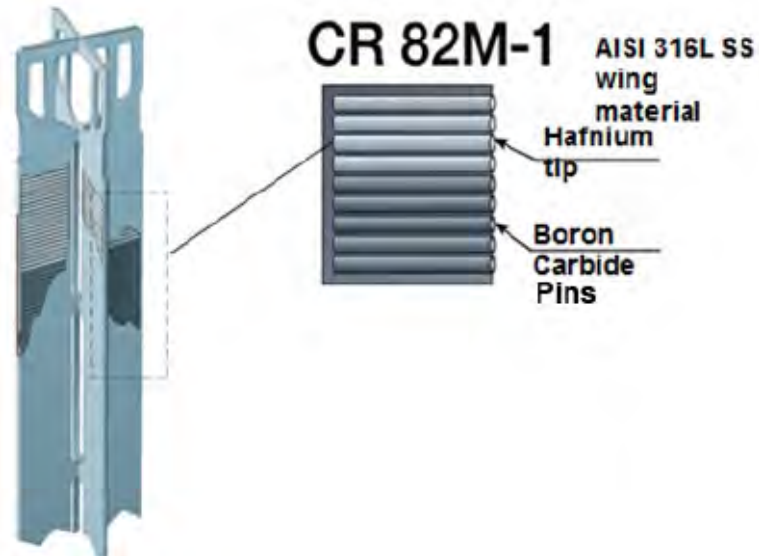
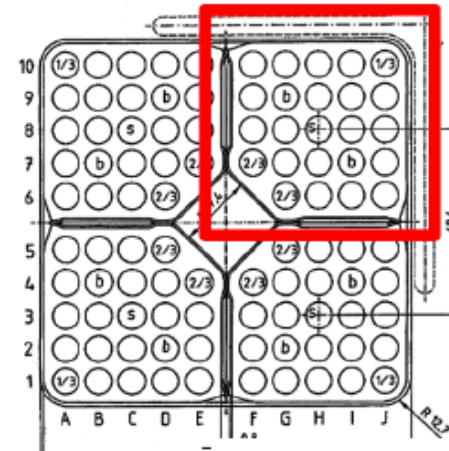
LITHUANIAN  
ENERGY  
INSTITUTE

In SCDAP coded principal geometry

SEVA-96 Optima 2 (QUENCH-20)



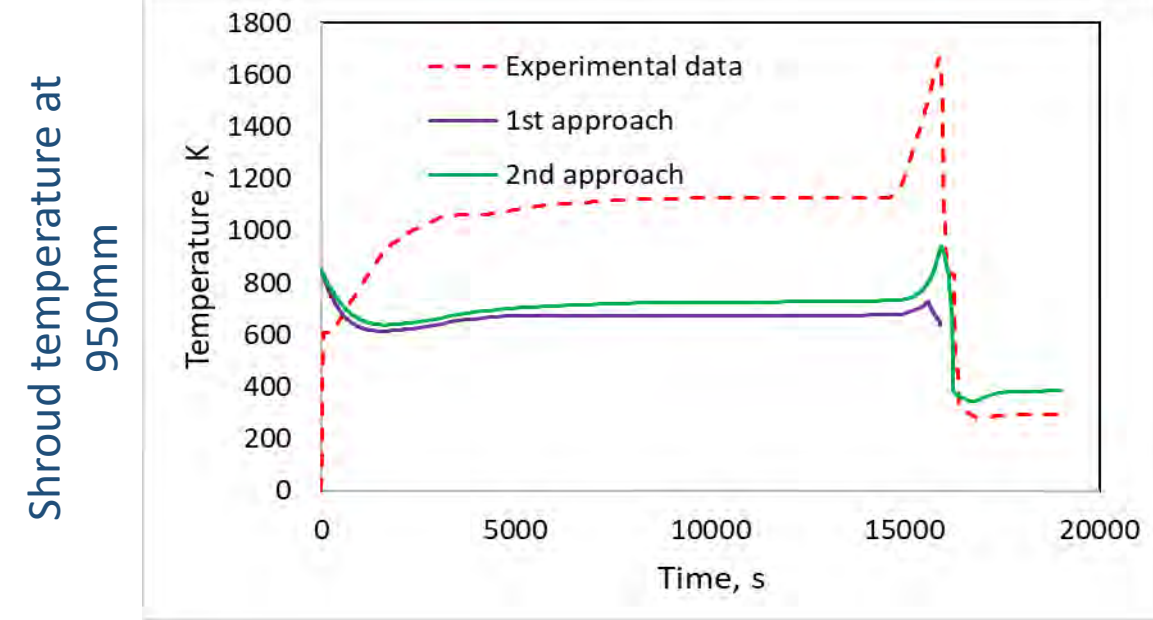
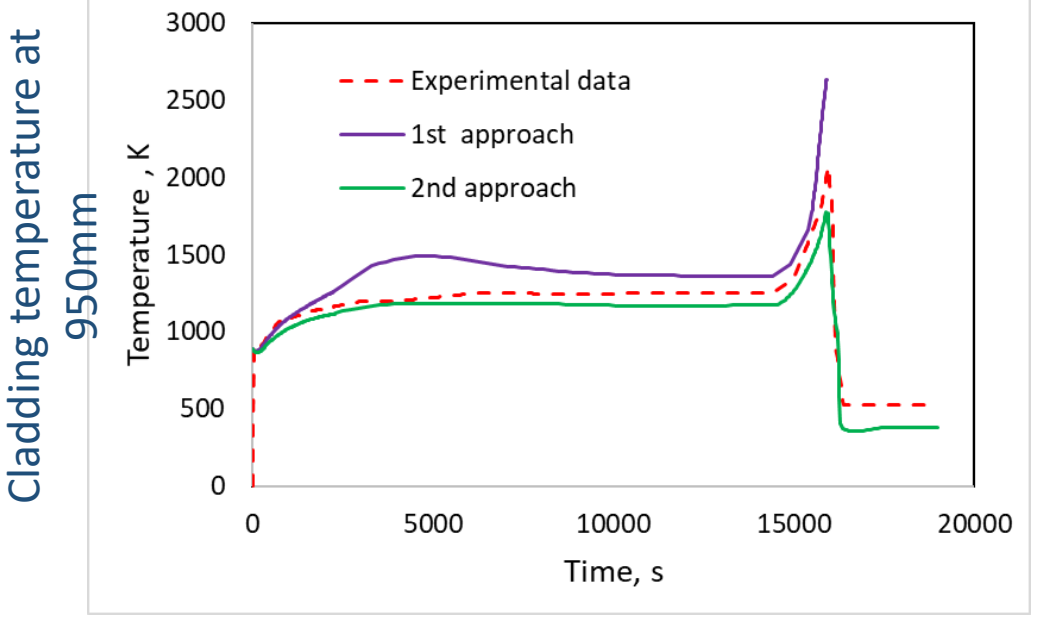
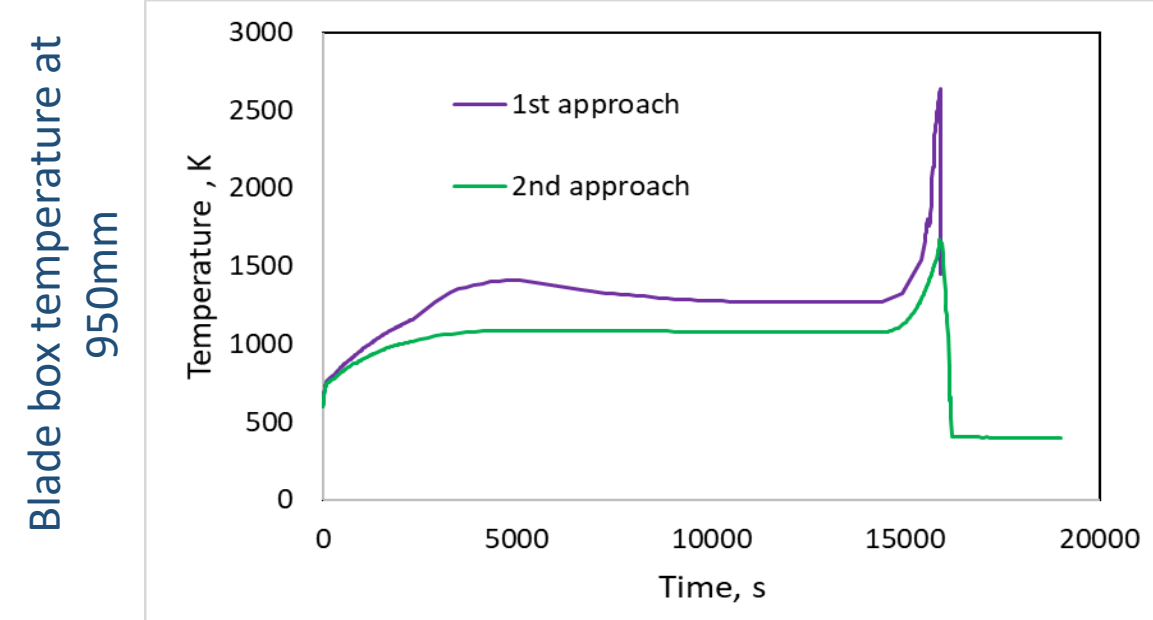
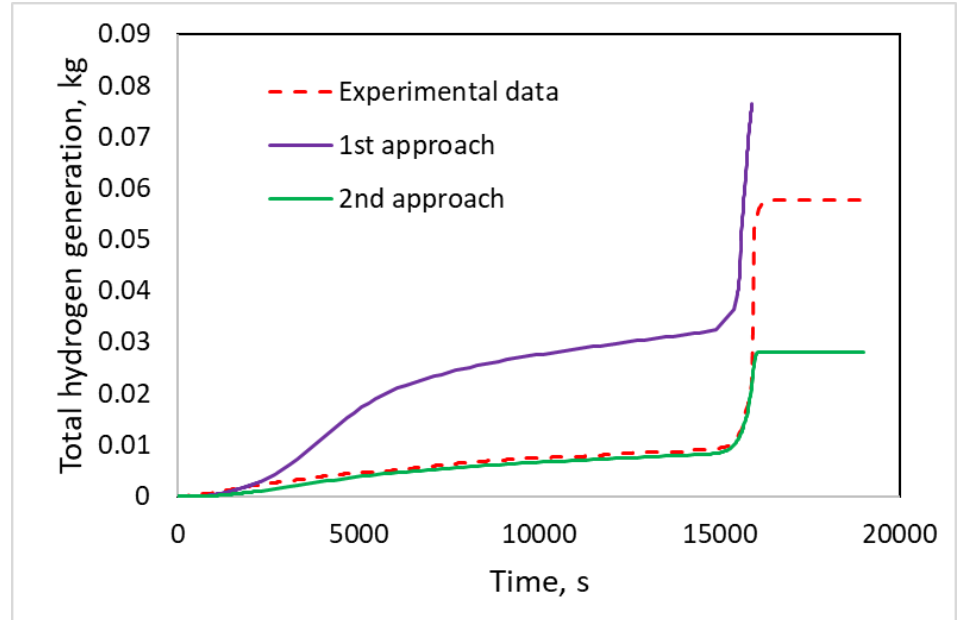
Recalculated values





# Comparison of Results

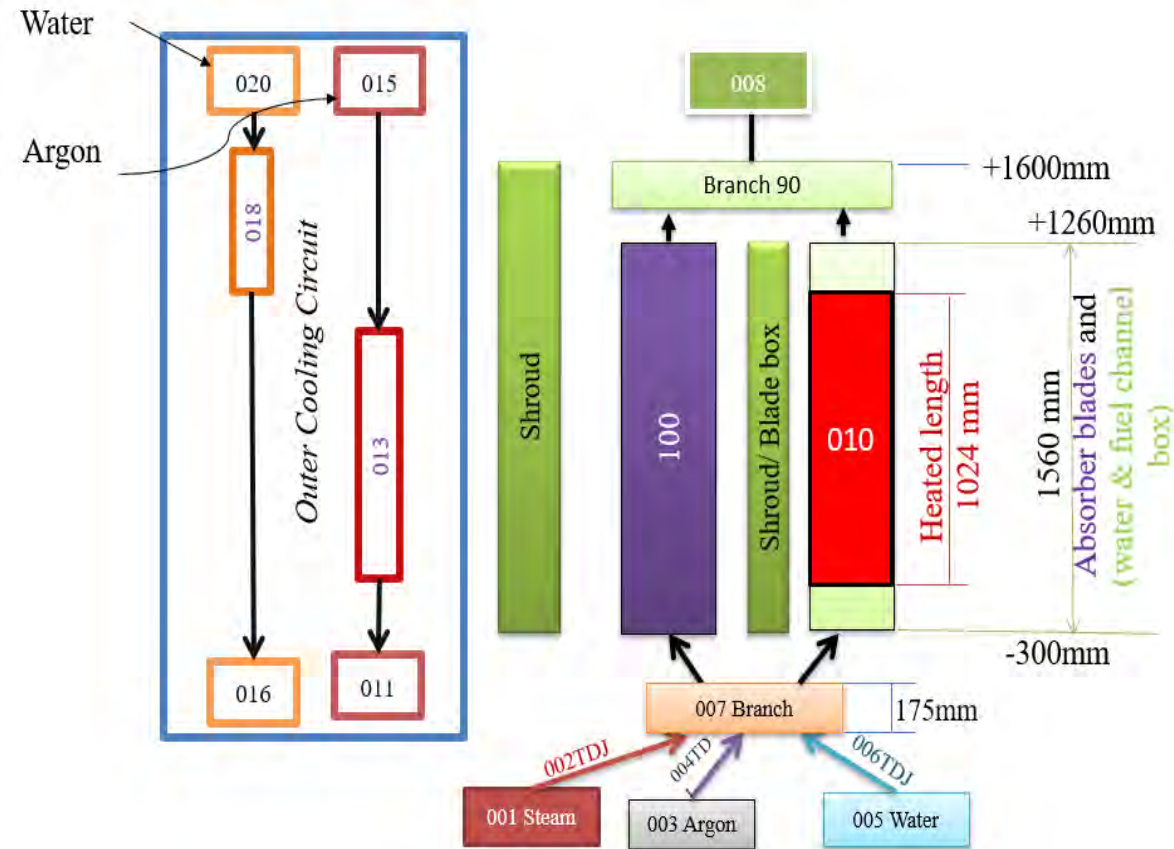
# Component 5 - "Bladebox"



View factors according to Q-6 with small modifications was assumed in the model



# Component 5 - “shroud”



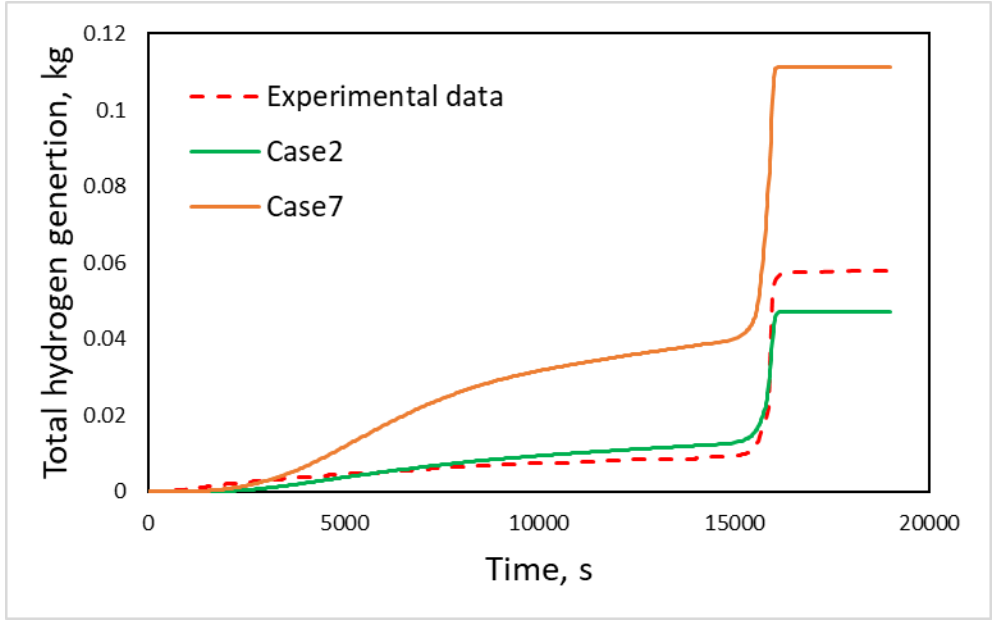
# Comparison of Results

## Component 5 - "shroud"

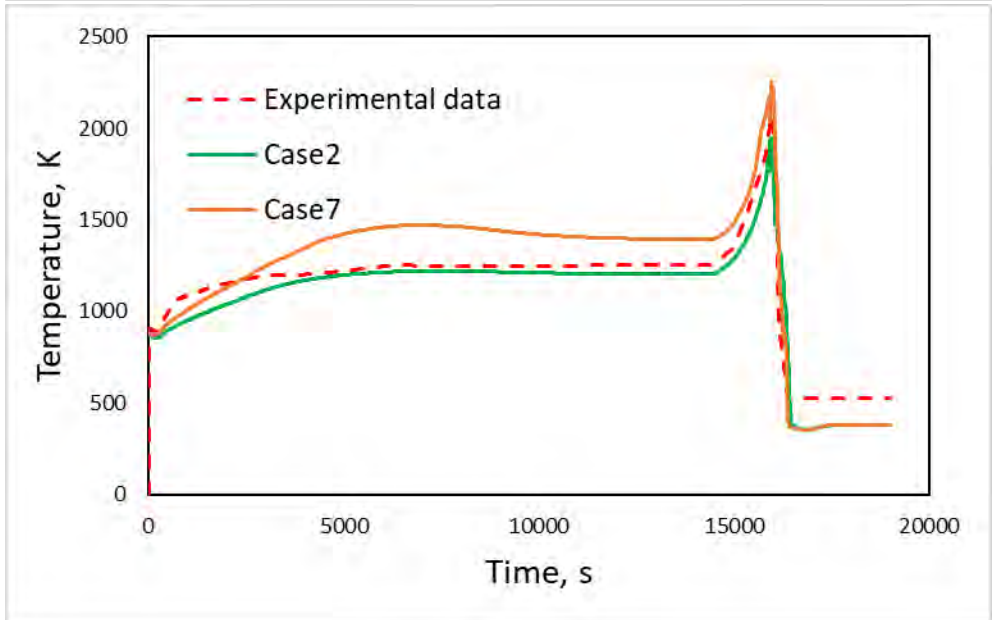
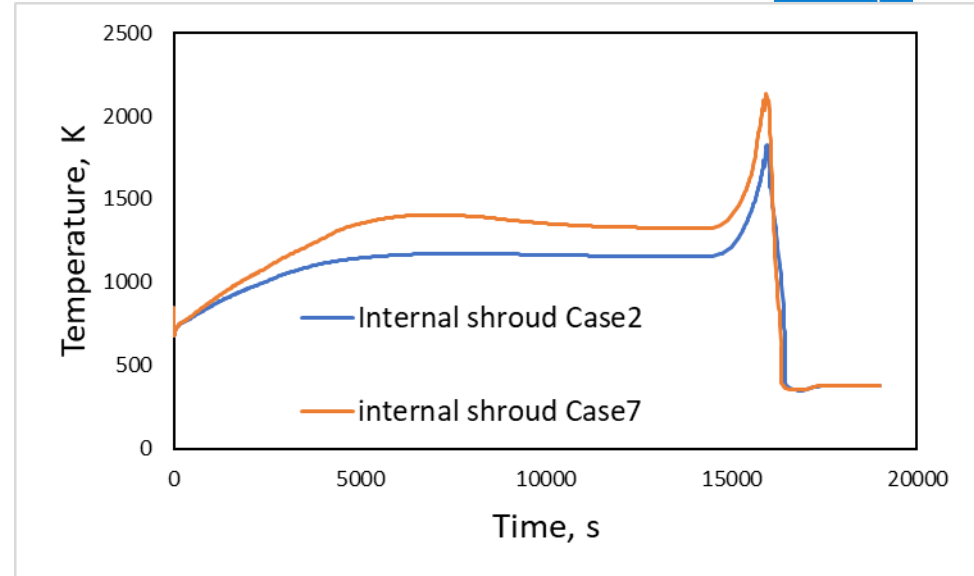


- **Case2:** Based on 2<sup>nd</sup> approach
- **Case7:** Based on 1<sup>st</sup> approach

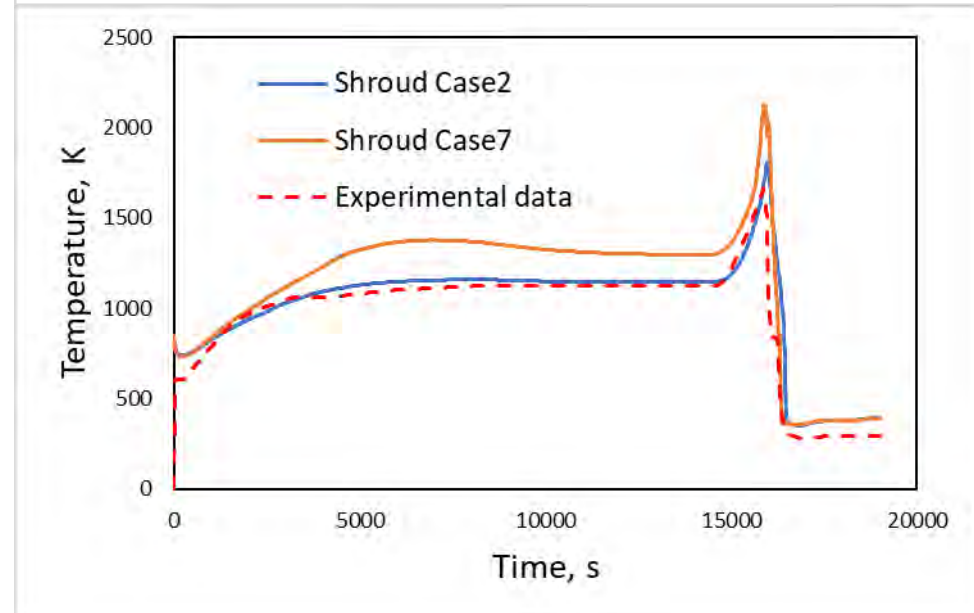
Cladding temperature at 950mm



Internal shroud temperature at 950mm



Shroud temperature at 950mm



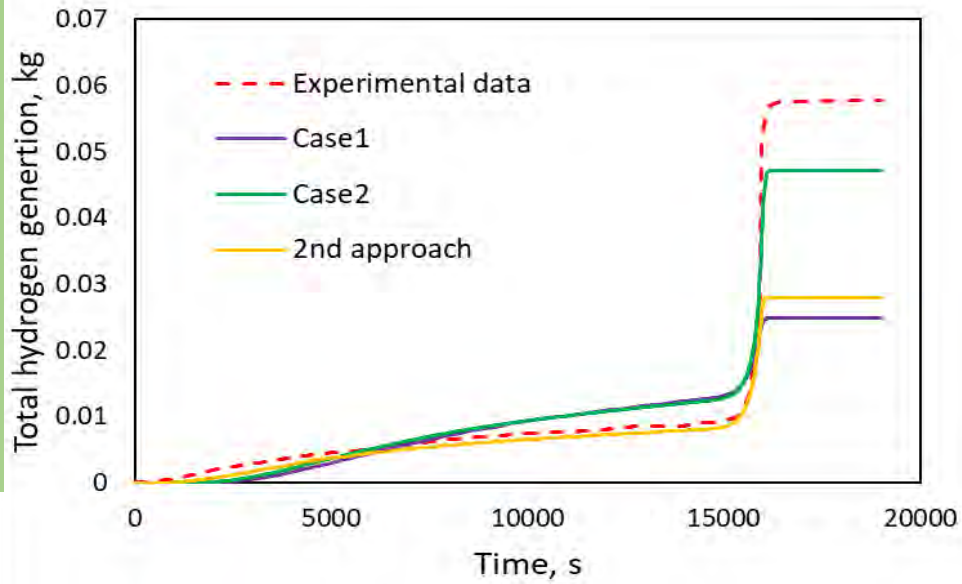
# Parametric analysis

- *Thermal material properties of internal shroud*
- *Contact resistance*
- *Thickness of internal shroud*
- *Form losses of bypass channel (component 100)*
- *Radiation properties: path length and view factors*

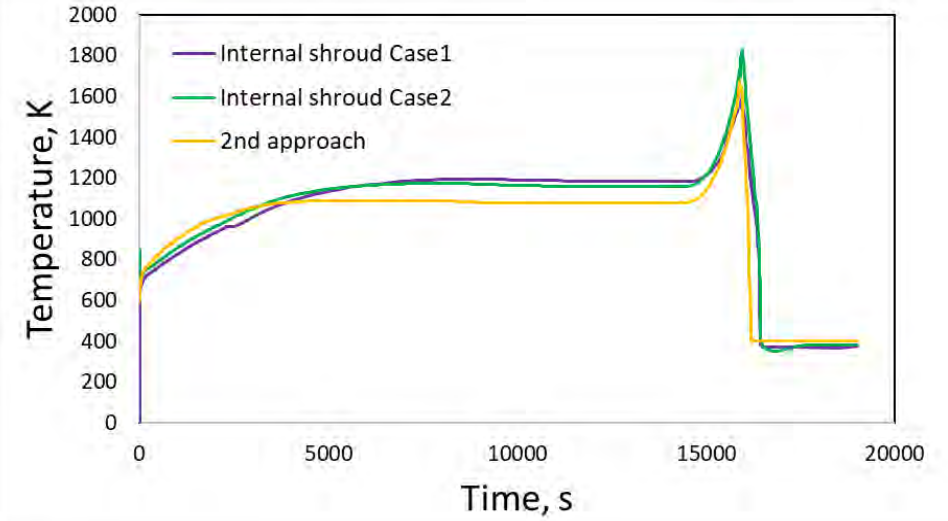


# Internal shroud *material properties*

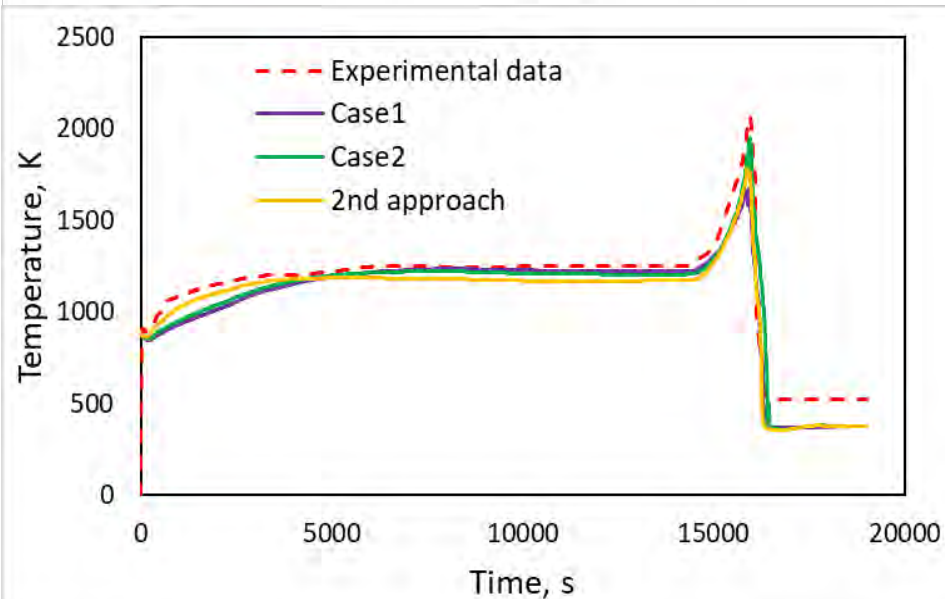
- **Case1:**  
Based on 2<sup>nd</sup> approach and internal shroud material (SS+Zr)
- **Case2:**  
Based on 2<sup>nd</sup> approach and internal shroud material (SS+B4C+Zr)



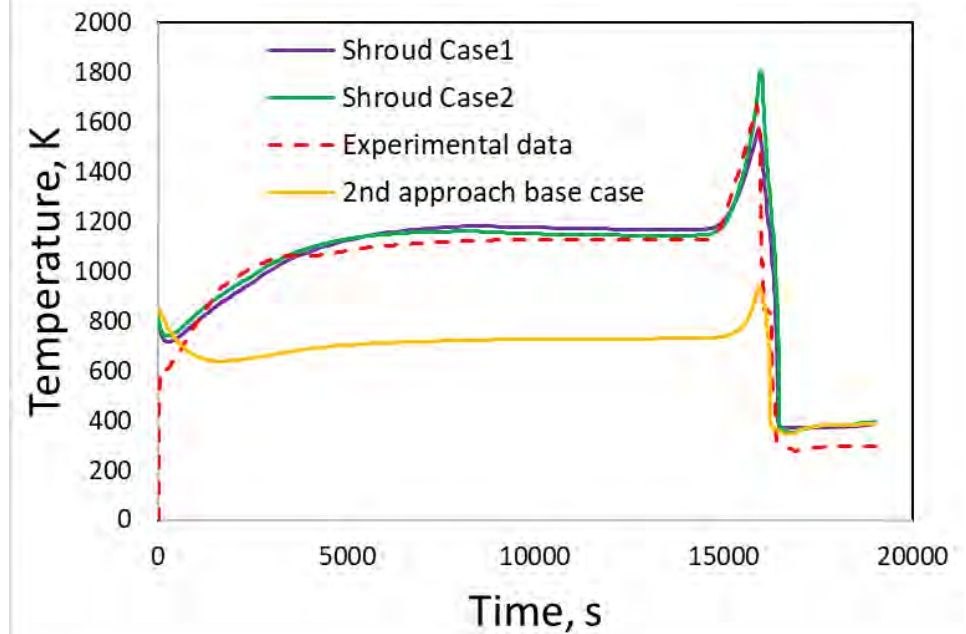
Internal shroud  
temperature at 950mm



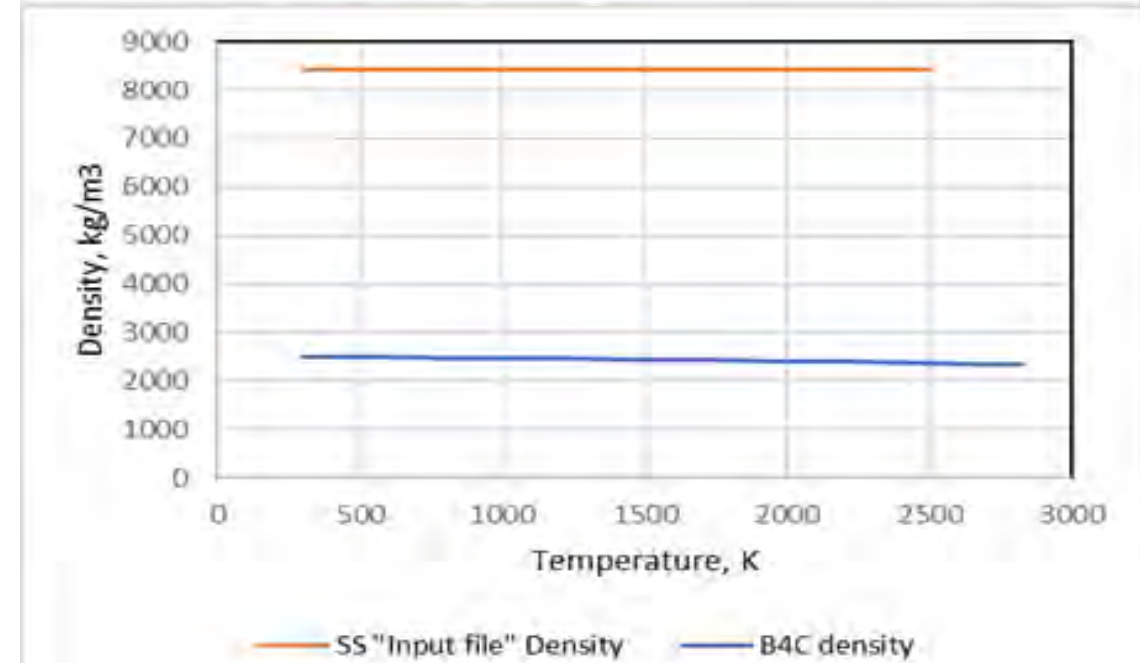
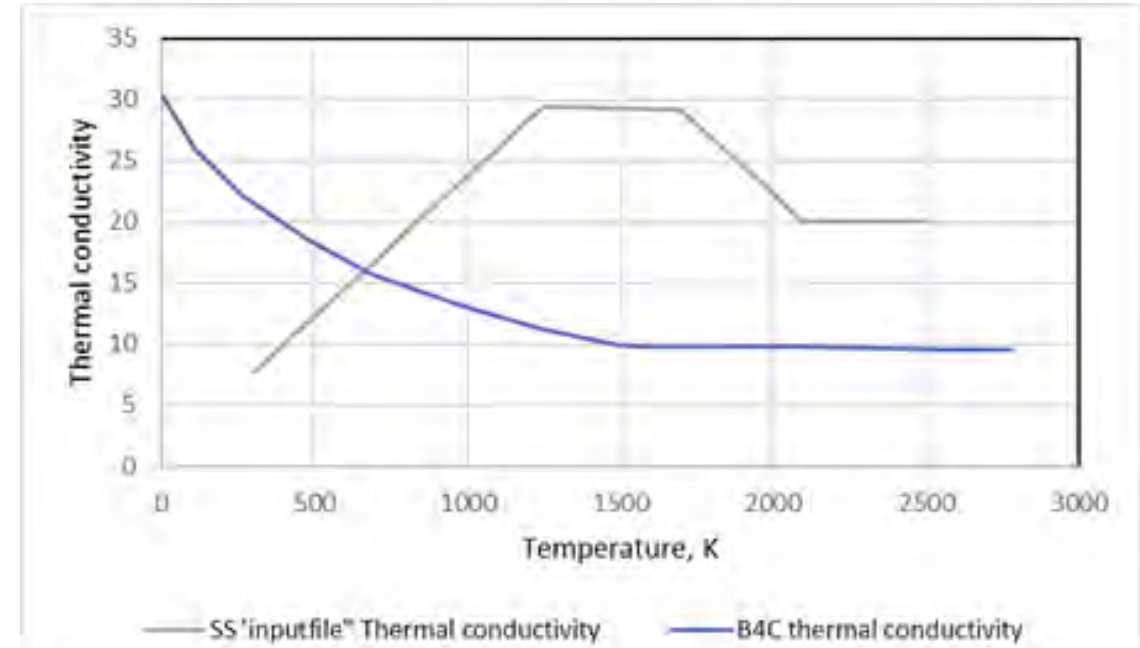
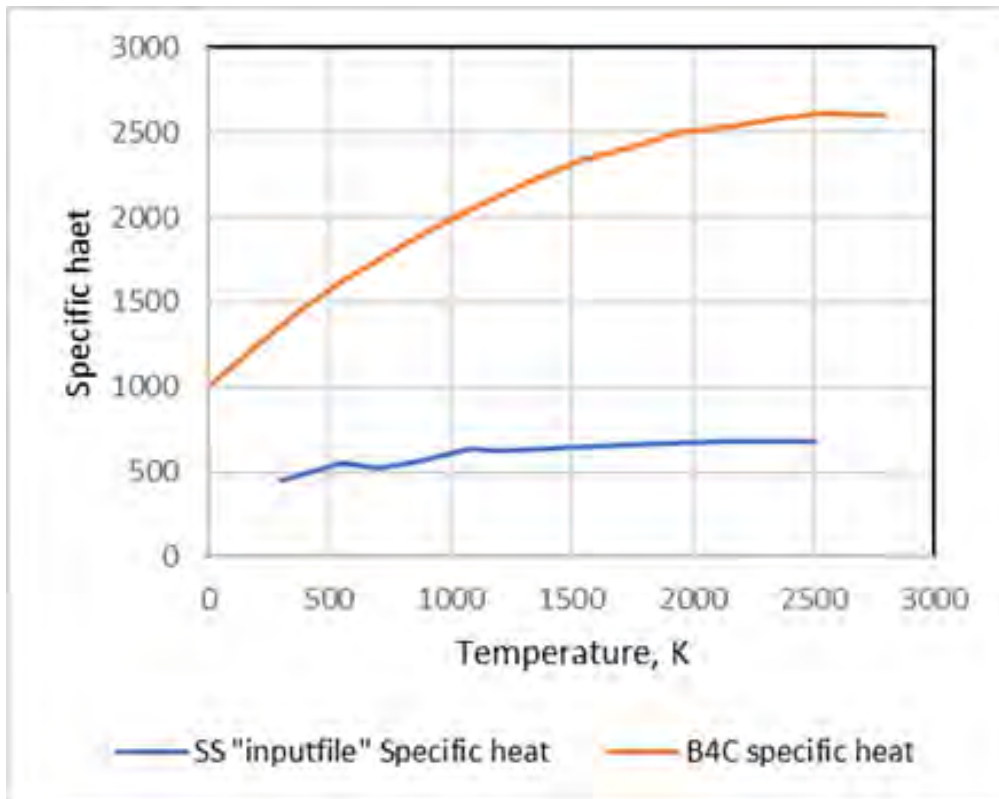
Cladding  
temperature at  
950mm



Shroud temperature at  
950mm



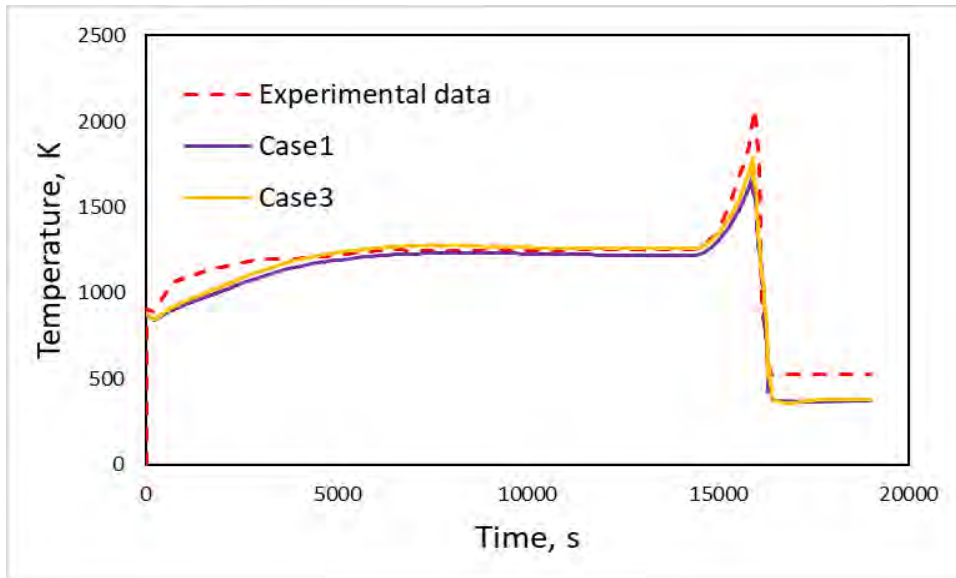
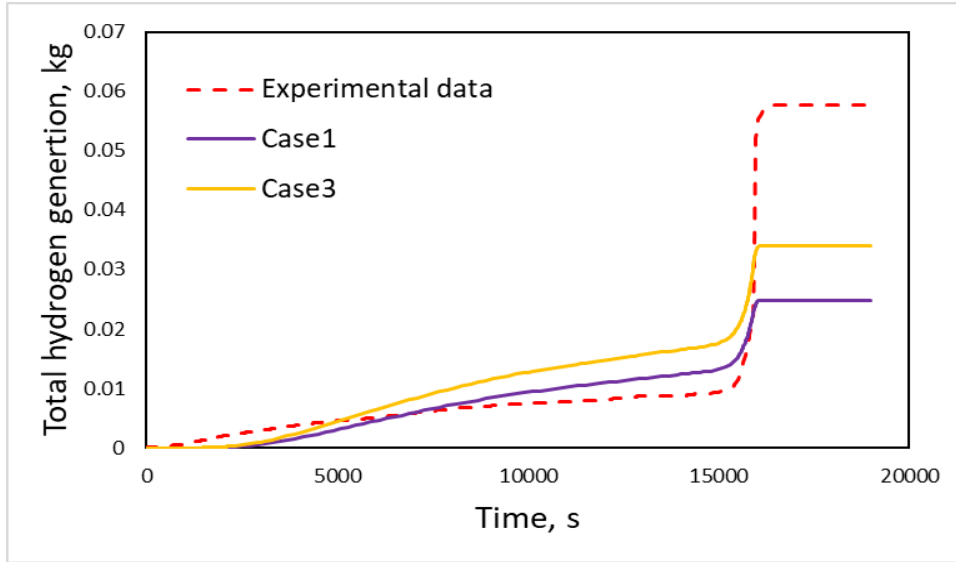
# Thermal material properties From SCDAP material library (MATPRO)



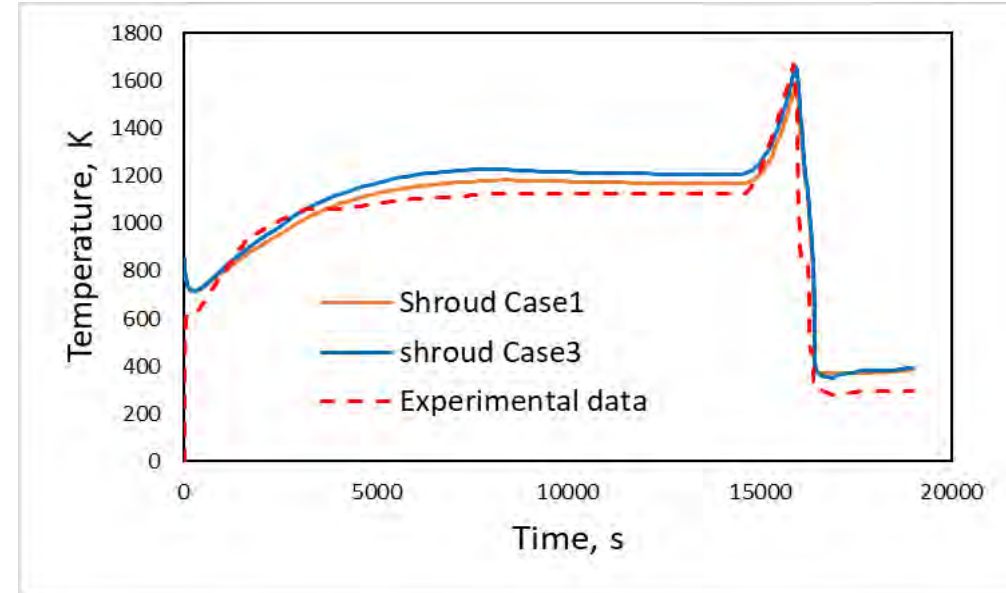
# Comparison based on *contact resistance*

- **Case1:** Based on 2<sup>nd</sup> approach and contact resistance = 0.0048
- **Case3:** Based on 2<sup>nd</sup> approach and contact resistance = 0.0036

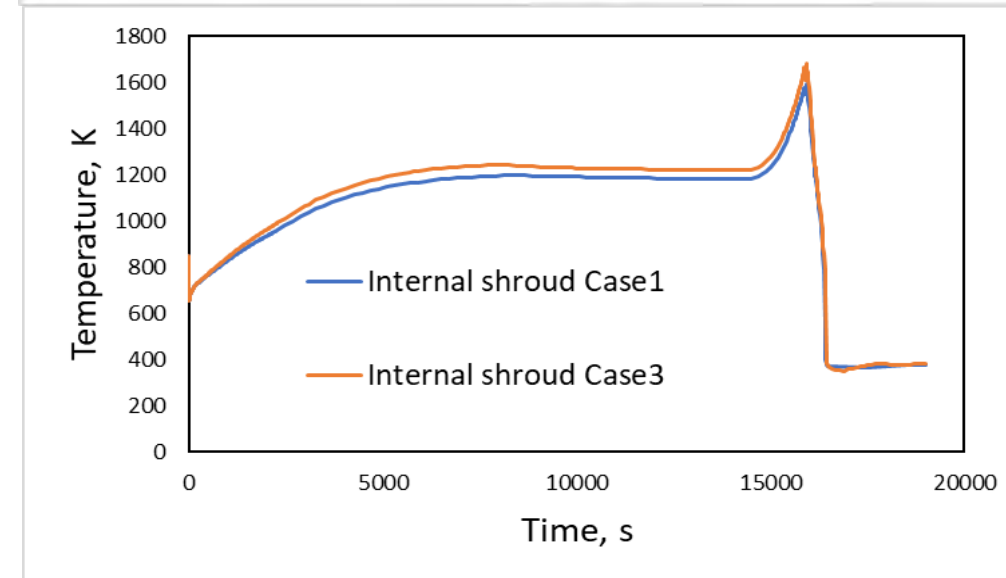
Cladding temperature at 950mm



Shroud temperature at 950mm

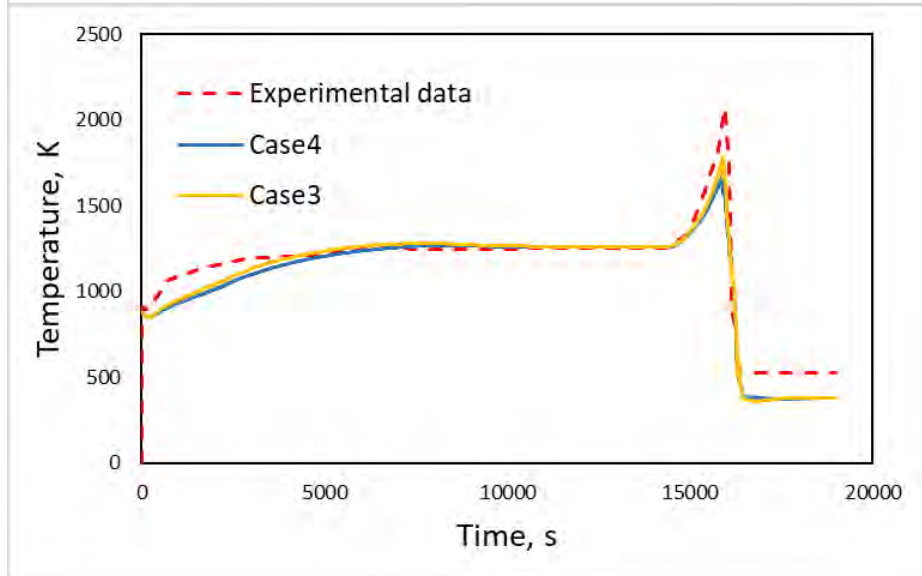
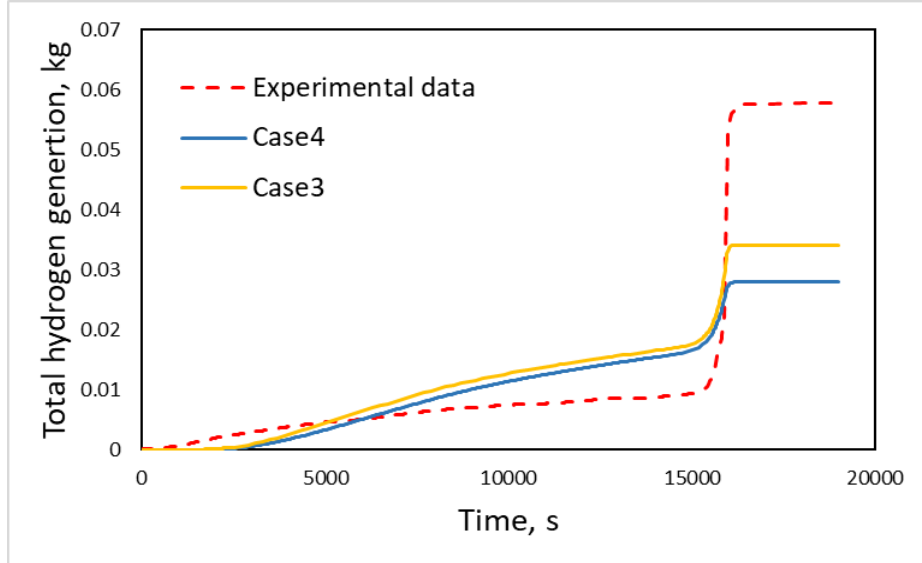


Internal shroud temperature at 950mm

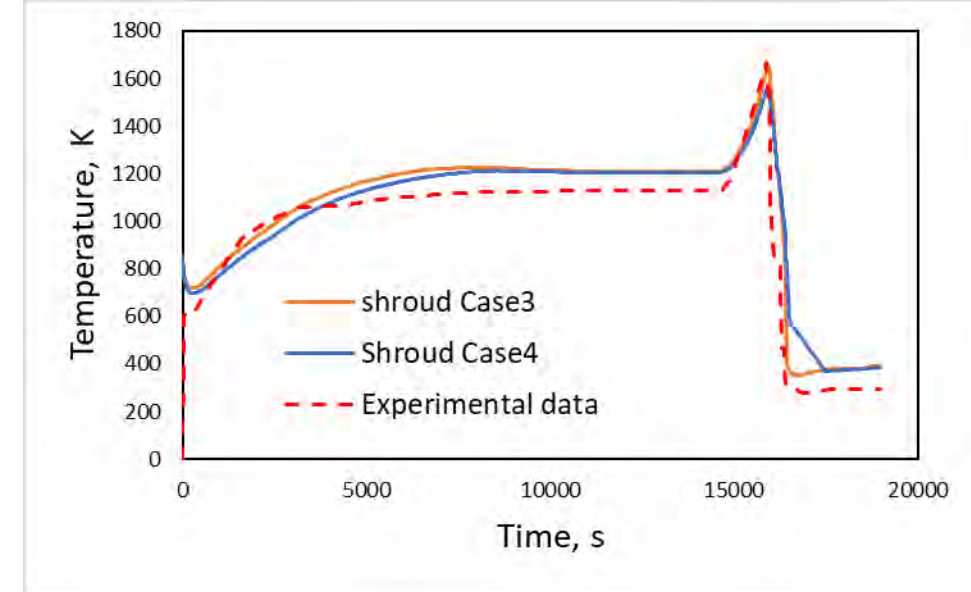


# Comparison based on *the thickness of internal shroud*

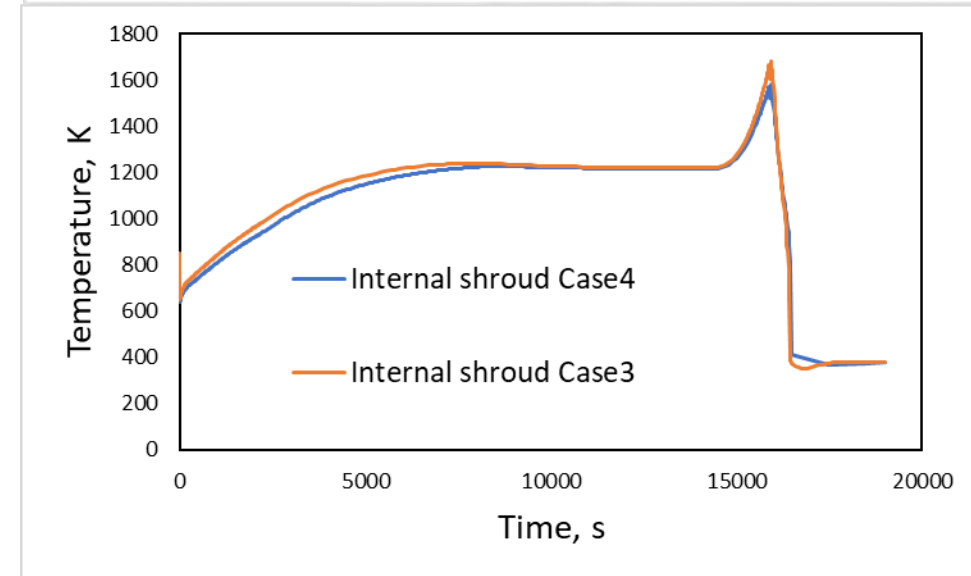
Cladding temperature at 950mm



Internal shroud temperature at 950mm



Shroud temperature at 950mm

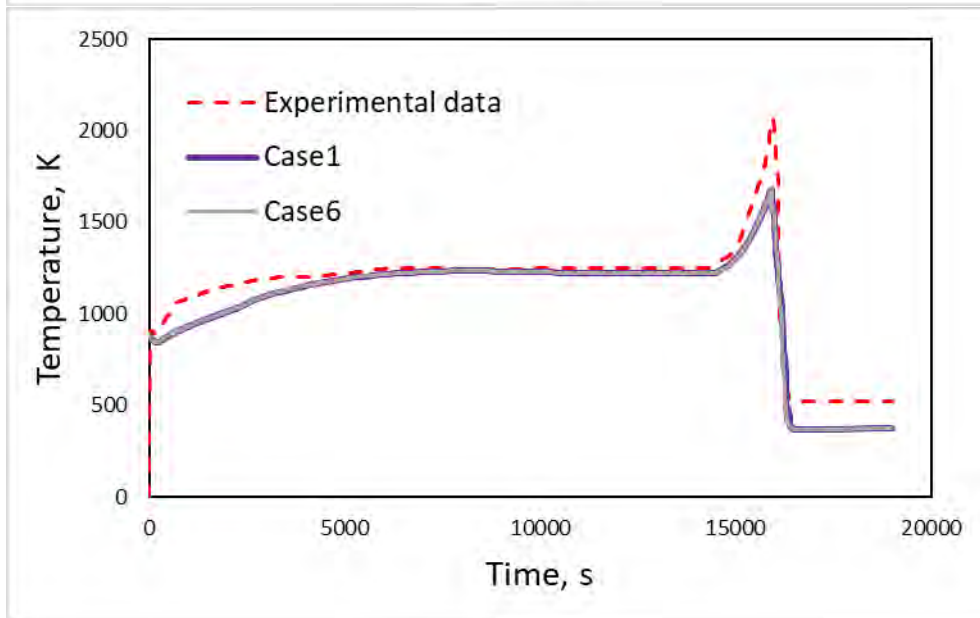
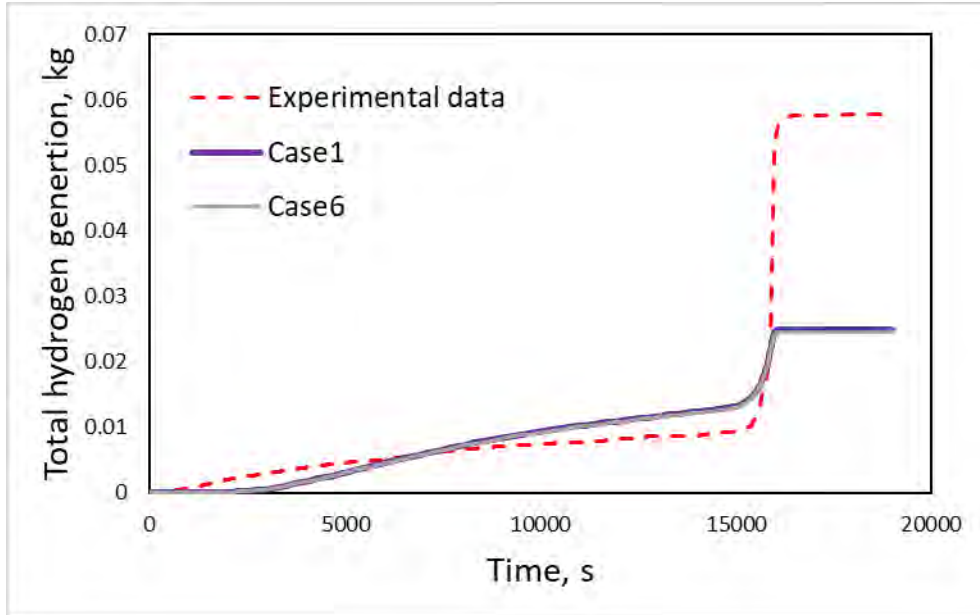




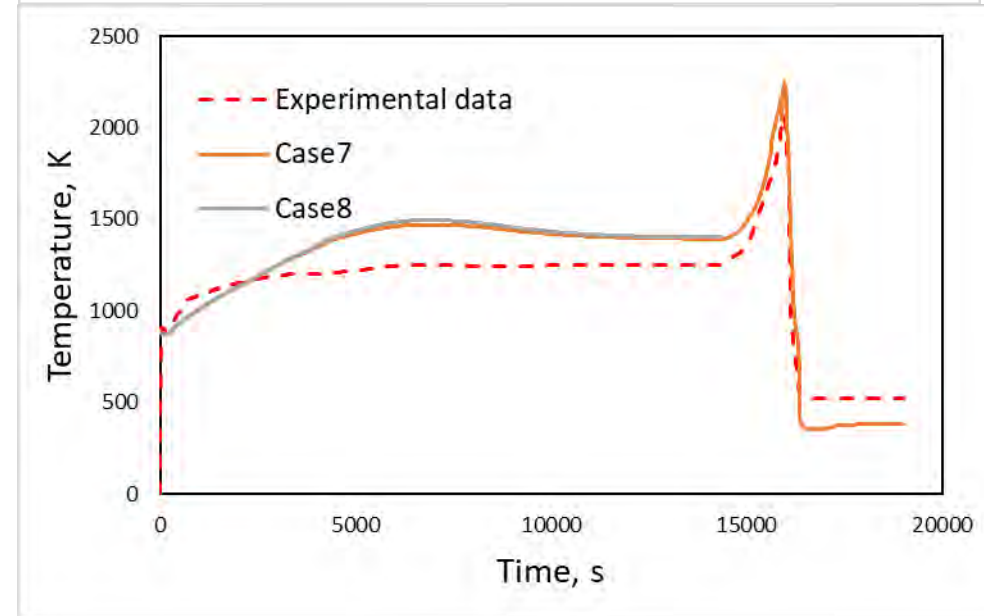
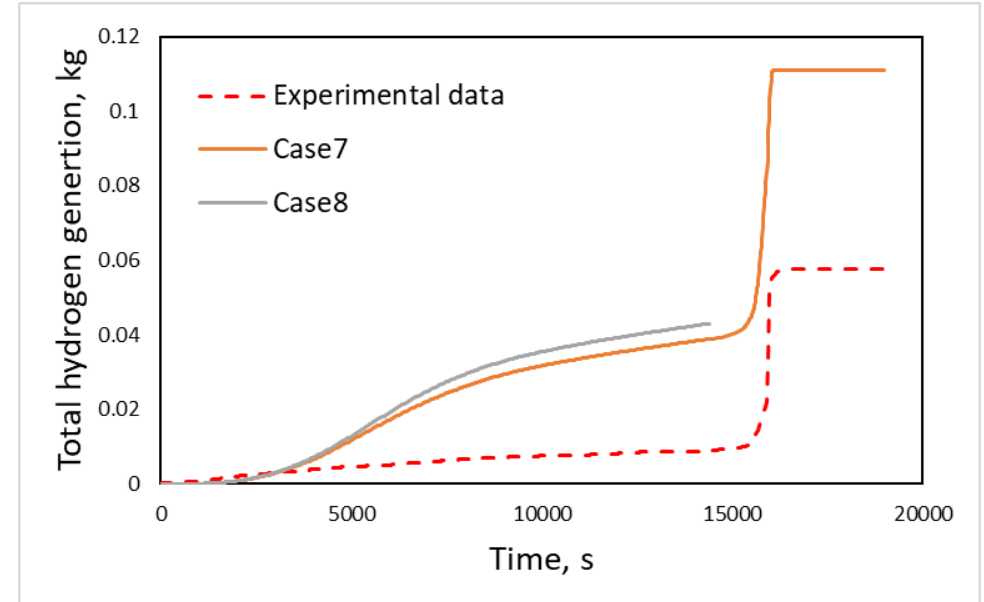
# Comparison of *Form losses*



- Approach 2 Foam losses increased by 10 at the component 10



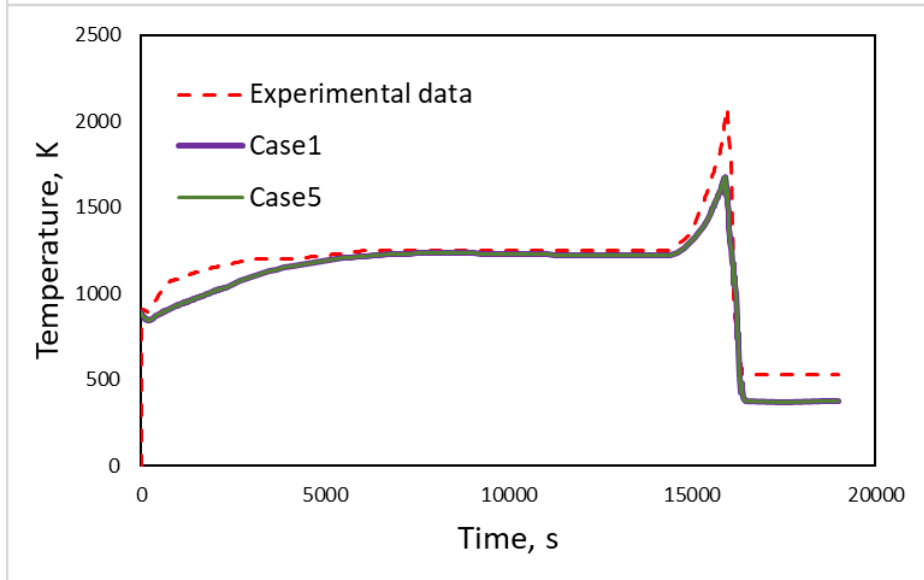
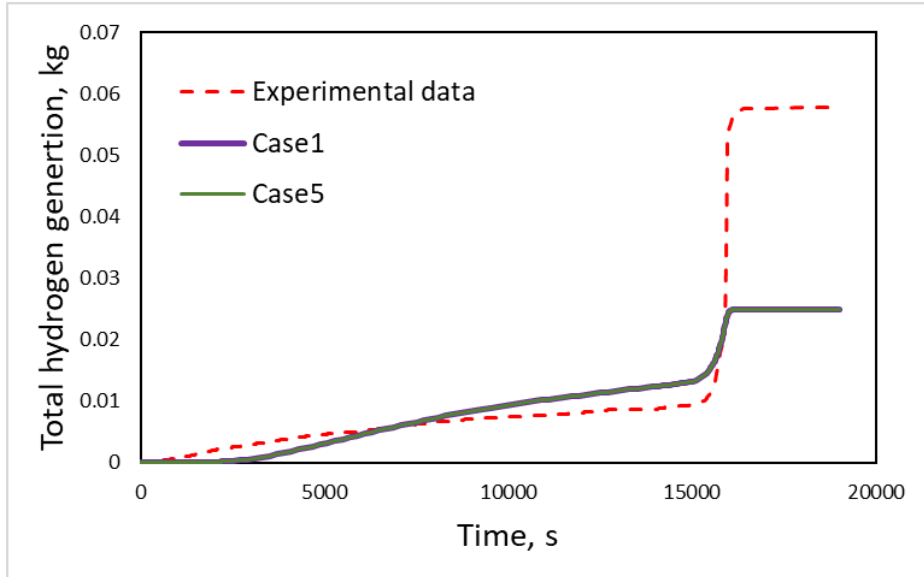
- Approach 1 Foam losses increased by 10 at the component 10



# Comparison for *path length*

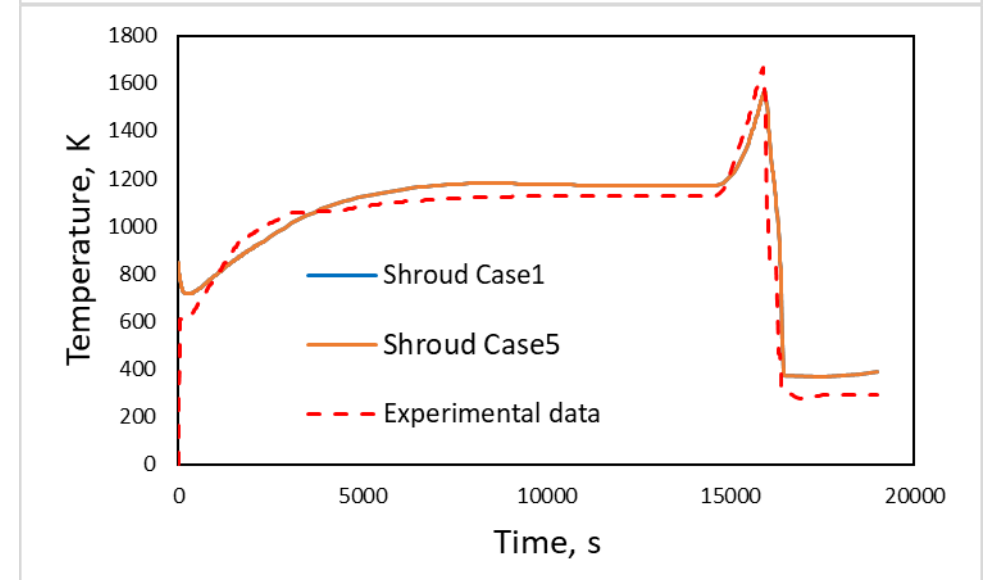
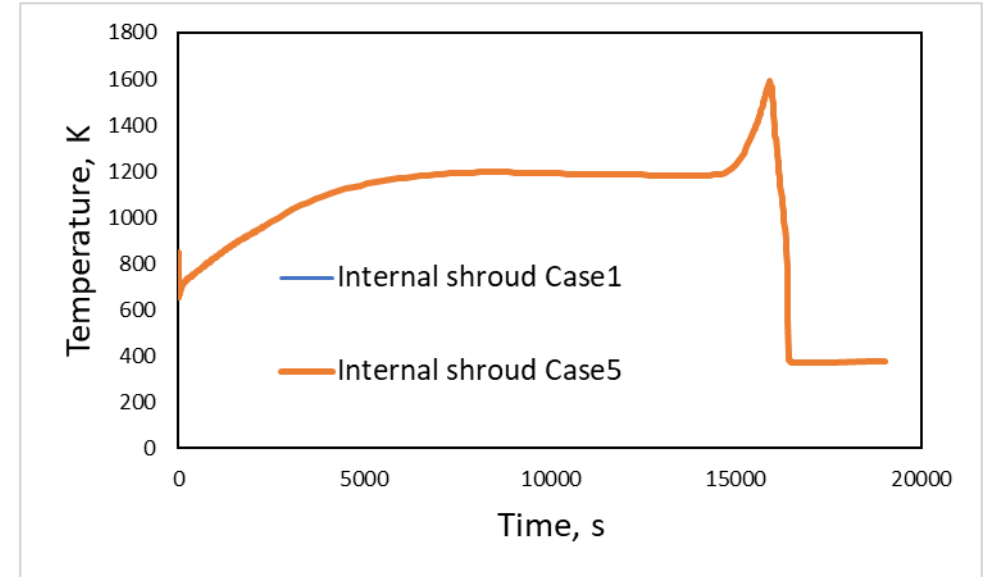


Cladding temperature at 950mm

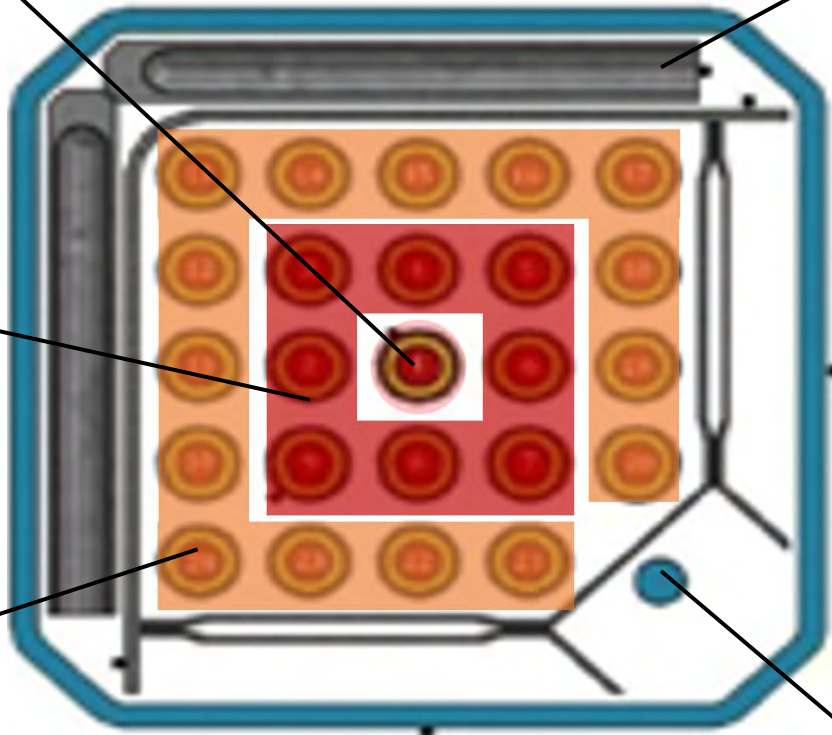
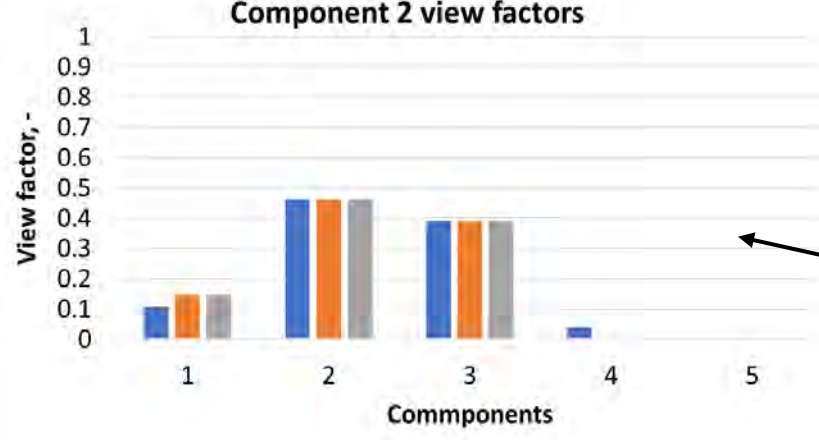
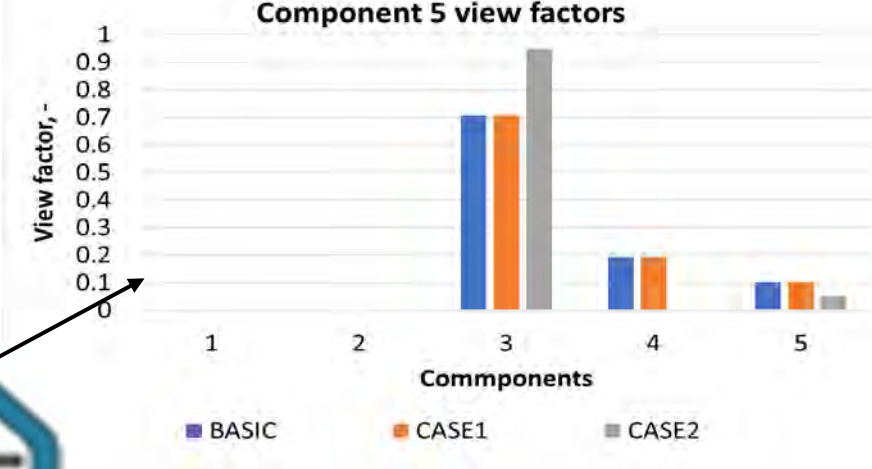
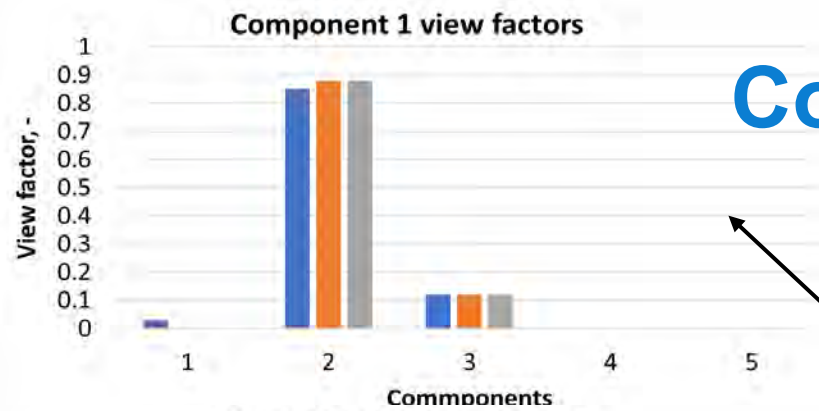


Internal shroud temperature at 950mm

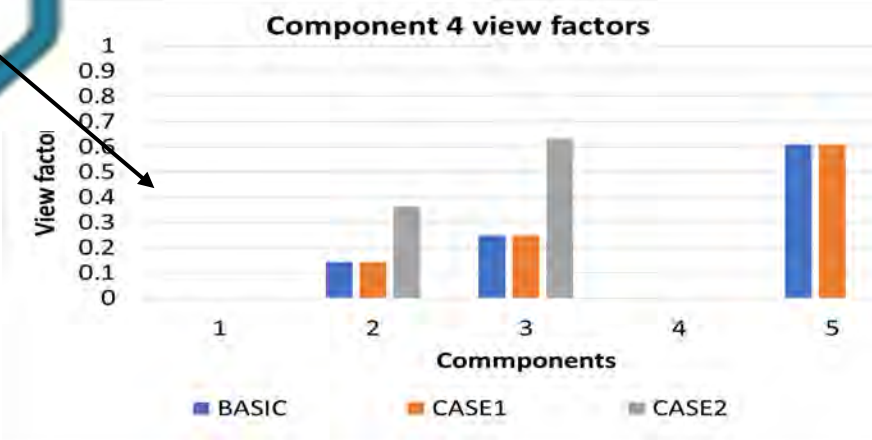
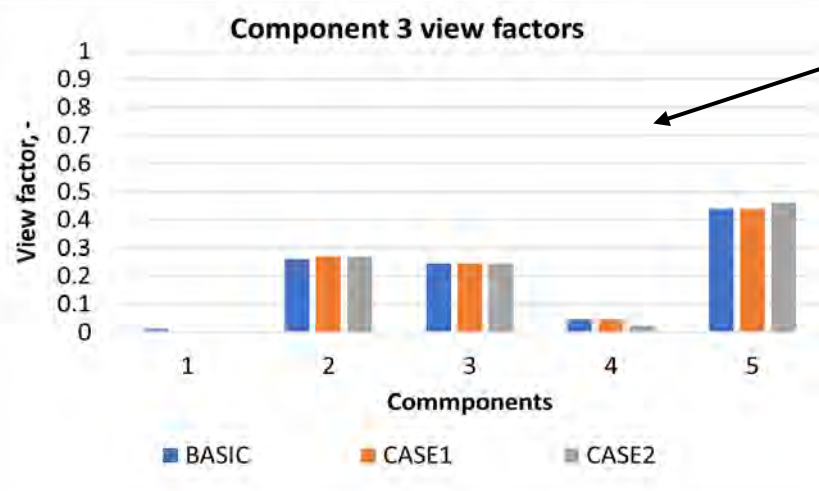
Shroud temperature at 950mm



# Comparison of *view factors*



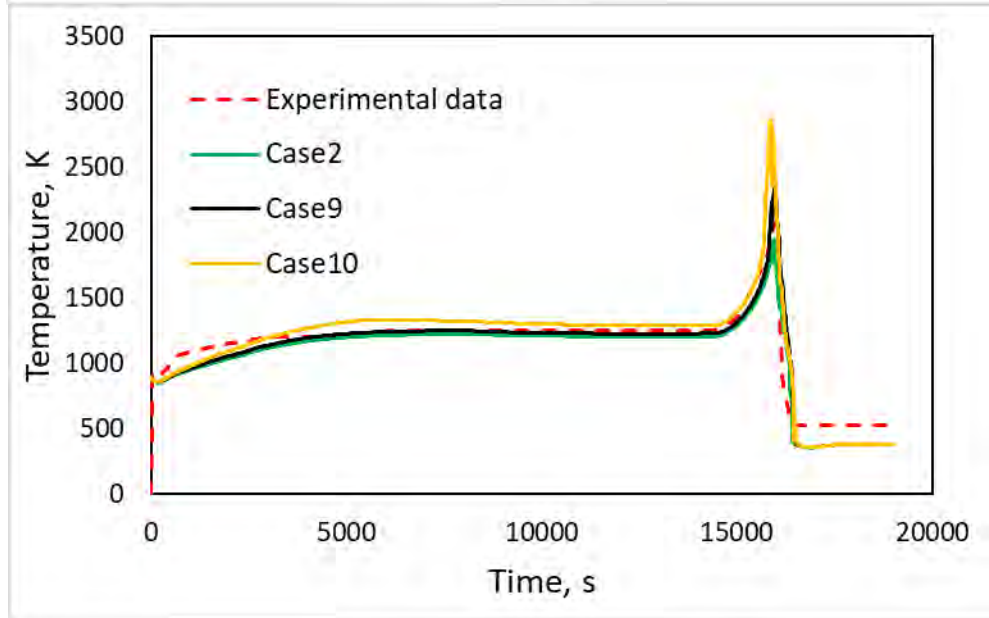
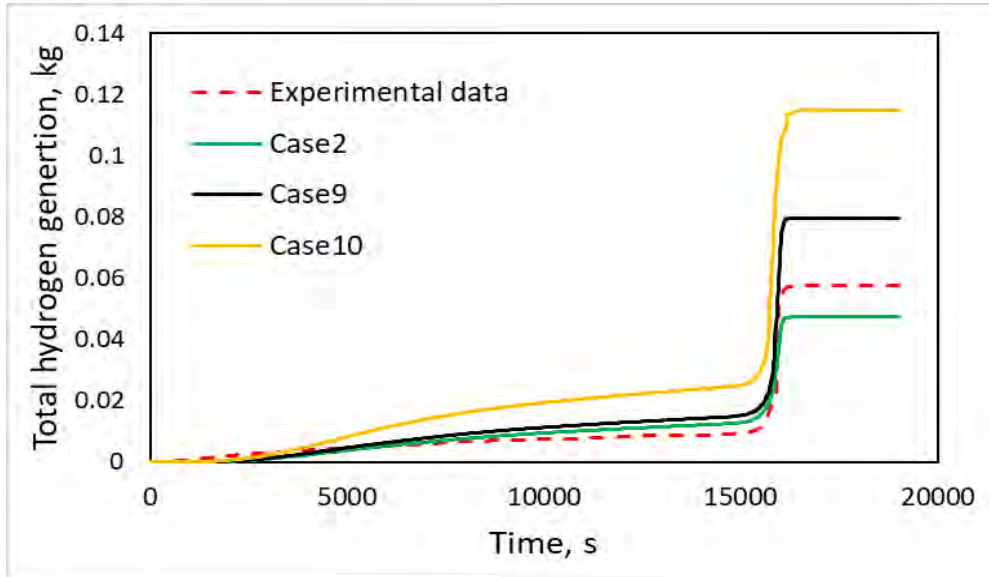
CASE1 – considered component 5 around heated rods, small difference from BASIC case  
 CASE2 - considered component 5 as in experiment



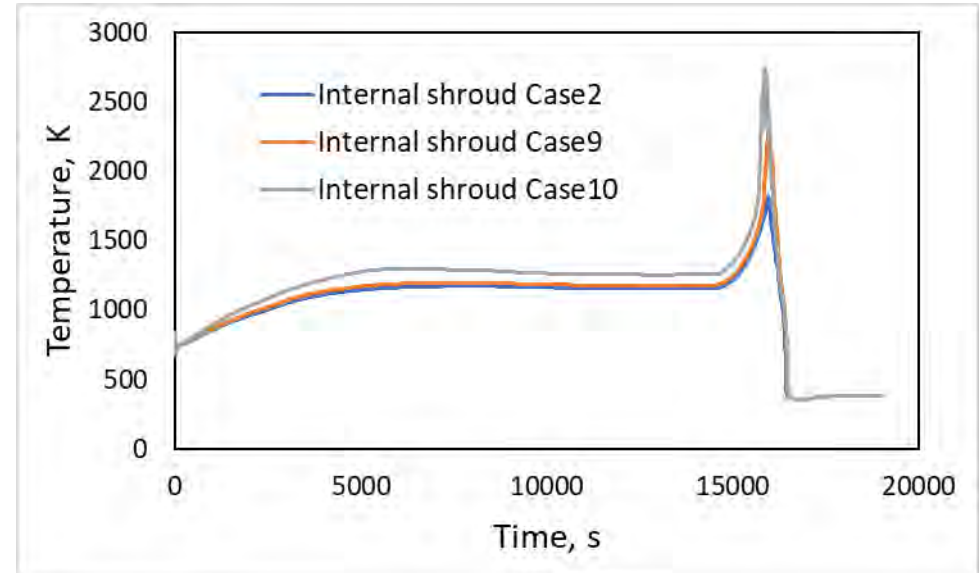
# Comparison of *view factors*



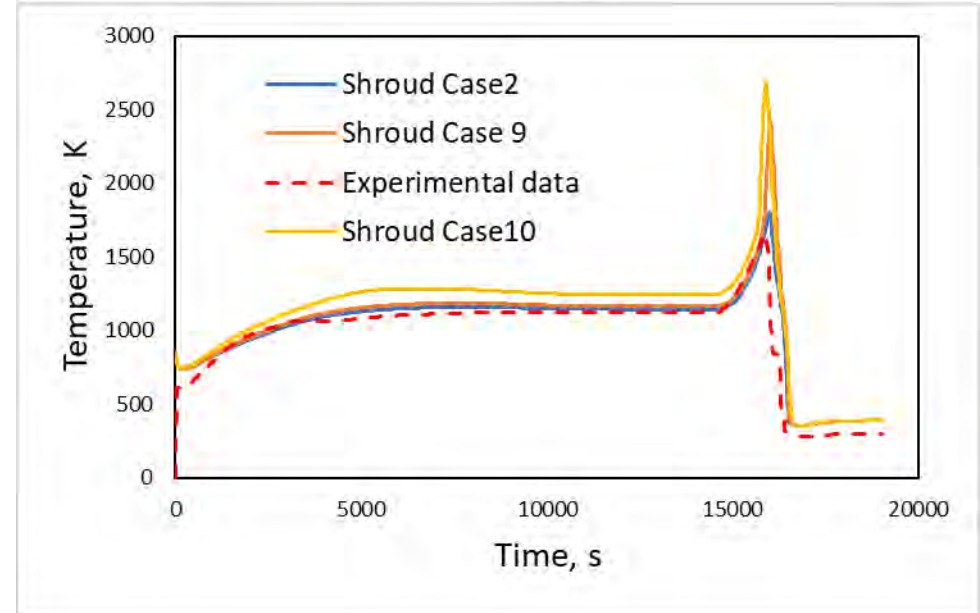
Cladding temperature at 950mm



Internal shroud temperature at 950mm



Shroud temperature at 950mm

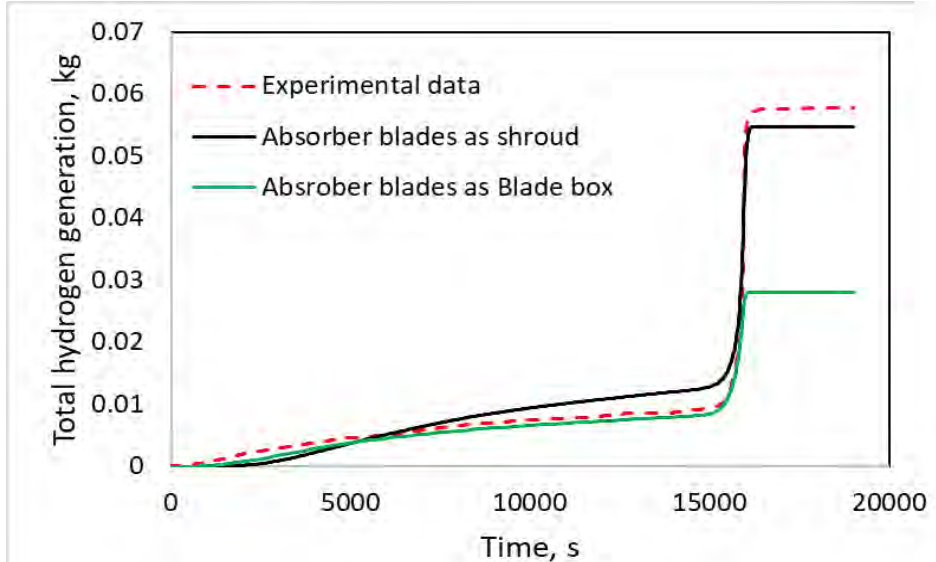
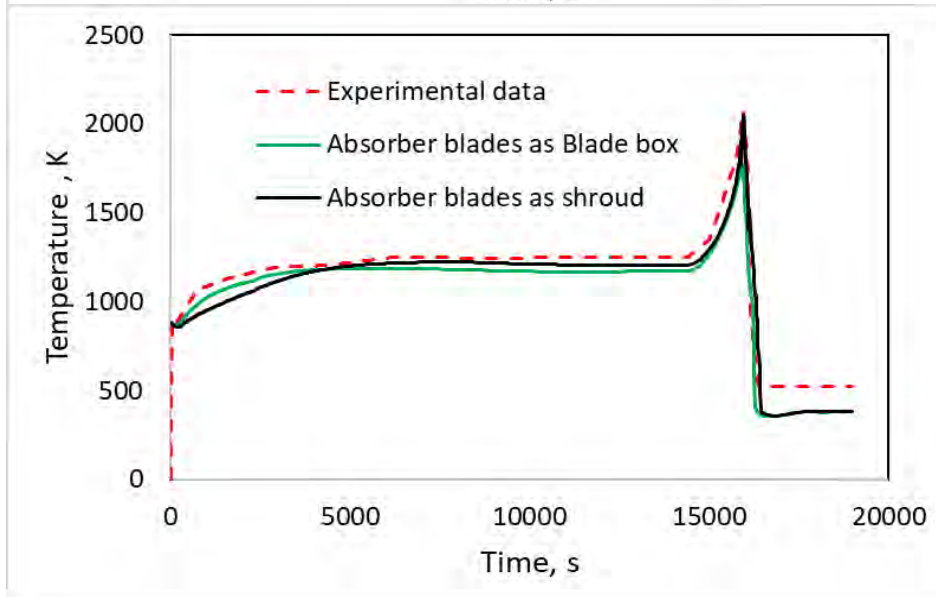




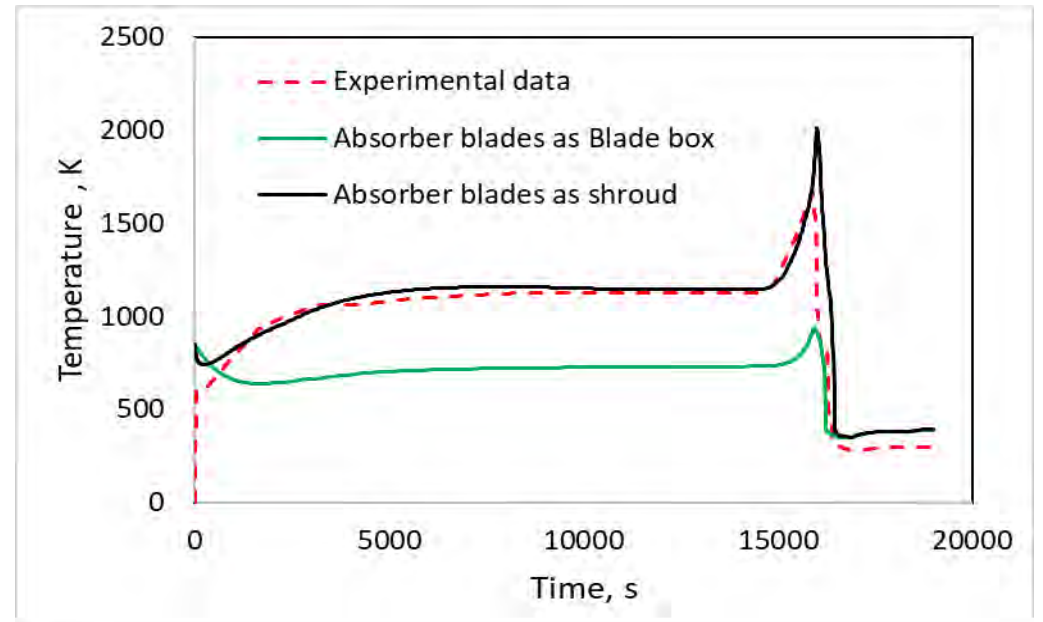
# Best calculations results



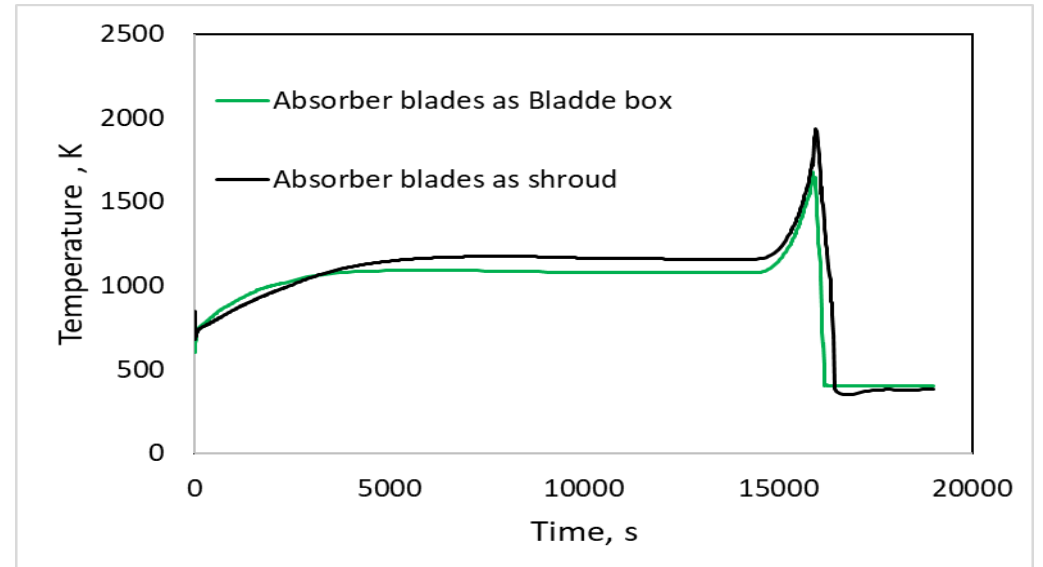
Cladding temperature at 950mm



Shroud temperature at 950mm



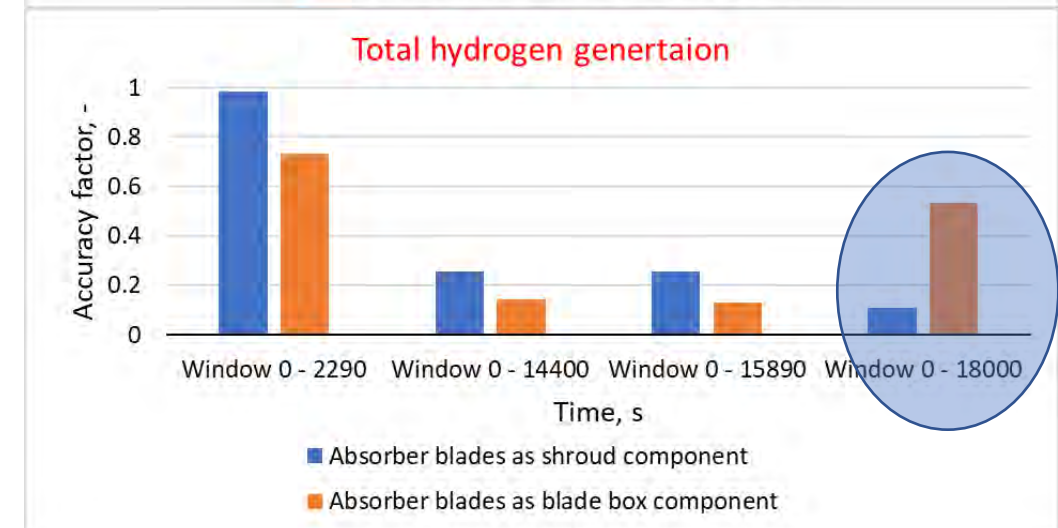
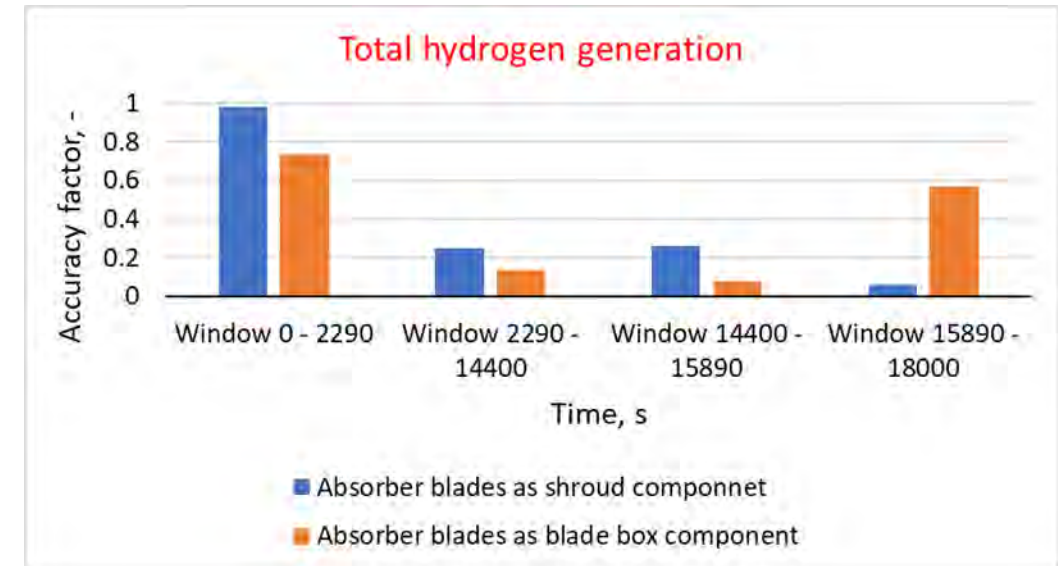
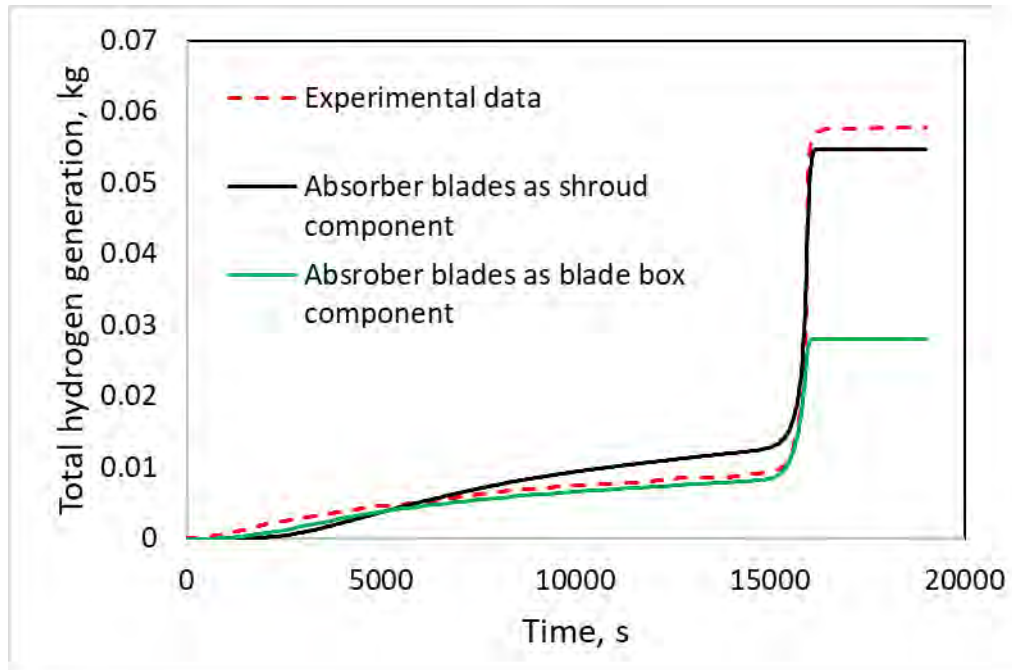
Component 5 temperature at 950mm





# FFTBM method for evaluating the accuracy of calculation results

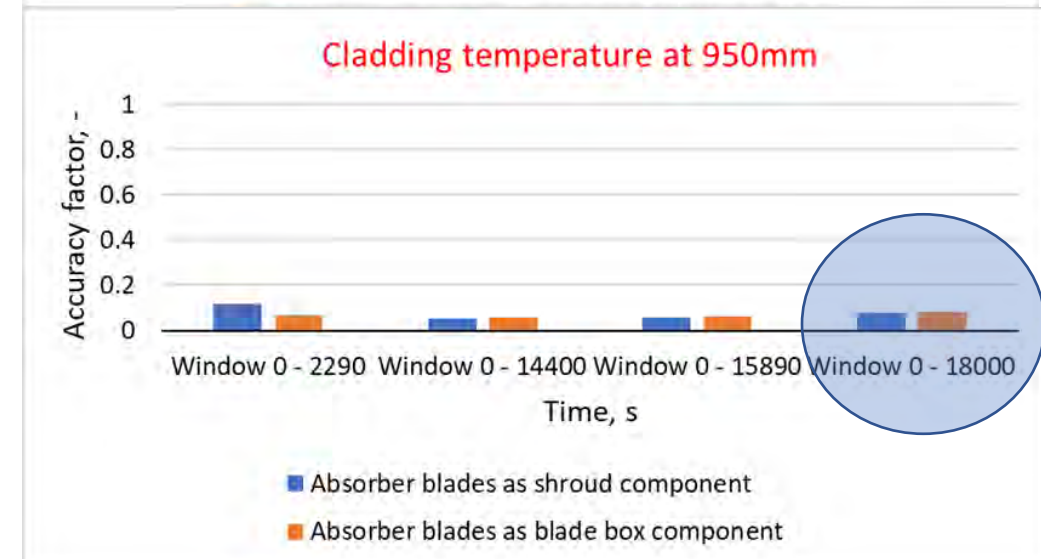
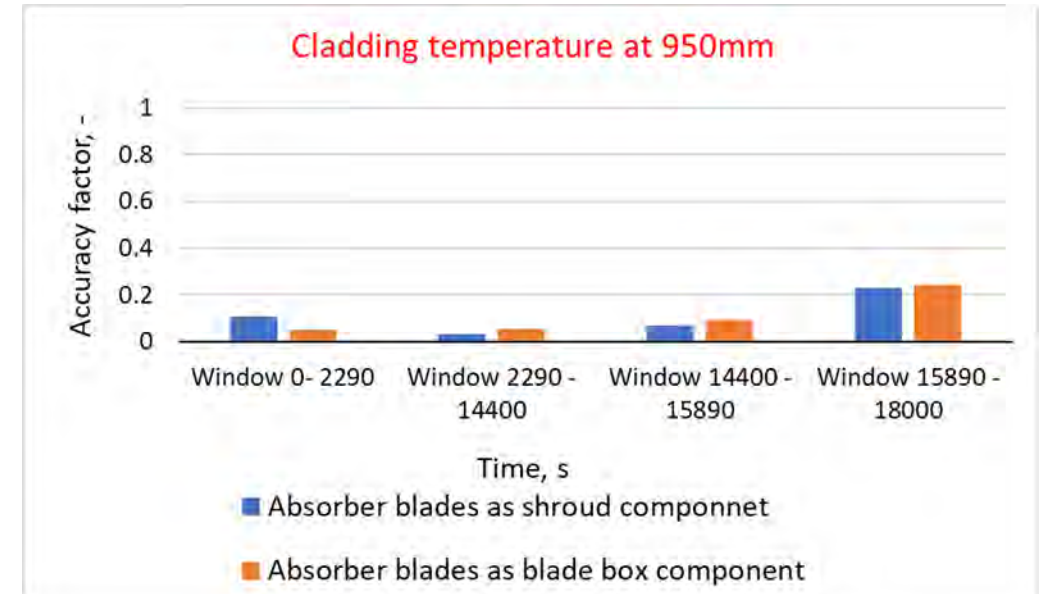
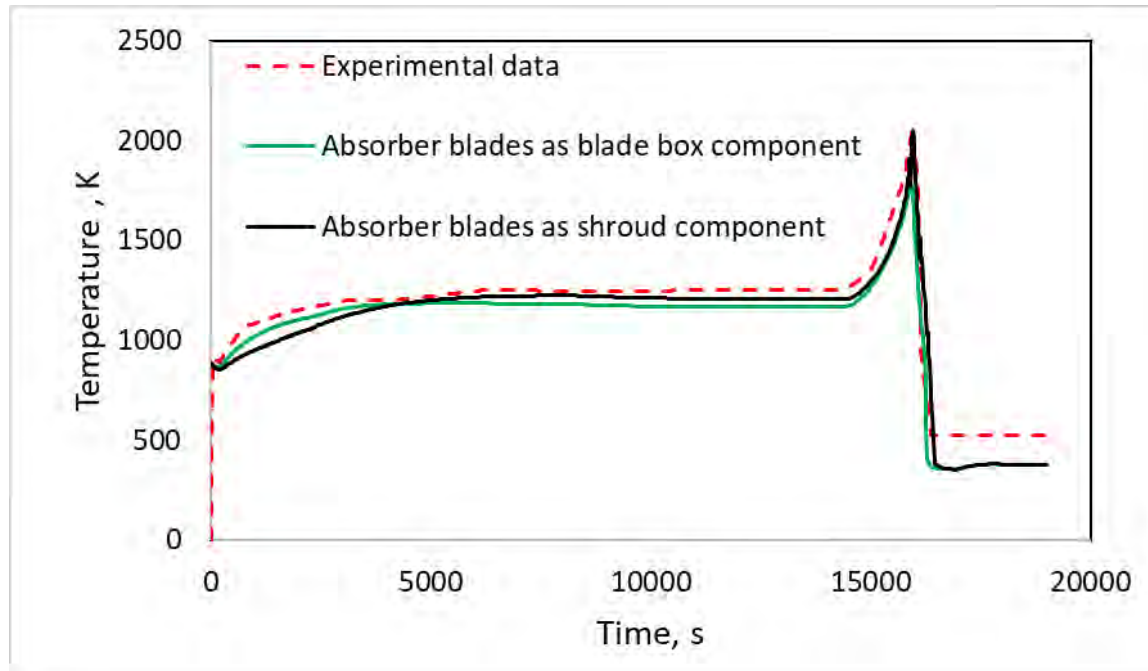
## Hydrogen generation





# FFTBM method for evaluating the accuracy of calculation results

## Inner rod cladding temperature



# Conclusions



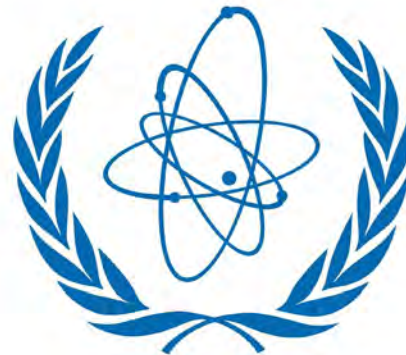
- The modelling process passed through different stages:
  - First: using the similar nodalization scheme as QUENCH-06 test, in this case the calculation were performed using different versions of RELAP/SCDAPSIM (mod3.4 & 3.6). RELAP/SCDAPSIM Mod 3.6 showed better results. In this modeling stage absorber blades was not considered.
  - Second: new nodalization scheme was prepared for two different structure in the SCDAP part.
    - The first - the absorber blades is modelled as blade box component.
    - The second - the absorber blades is modelled as shroud component.
- Calculation results for both calculation schemes showed quantitatively good agreement with experimental data. However, calculation results using blade box component showed not adequate heat transfer from blade box component to the shroud. Modelling schematics in the RELAP/SCDAPSIM code should be improved.
- Parametric analysis were performed.
  - Different calculations were performed for different cases to investigate the influence of material properties, thickness of the internal shroud, contact resistance, form losses, path length and view factors.
  - The parameters that have higher influence on calculation results are view factors, contact resistance, material properties (thermal conductivity).
- Best calculation results agreement with experimental data was achieved. FFTBM method for evaluating the accuracy of calculation results was used.





# Acknowledgement

- This work is done as a part of the International Atomic Energy Agency (IAEA) Coordinated Research Project (CRP), titled “Advancing the State-of-Practice in Uncertainty and Sensitivity Methodologies for Severe Accident Analysis in Water Cooled Reactors”, launched in 2019.



**IAEA**

International Atomic Energy Agency

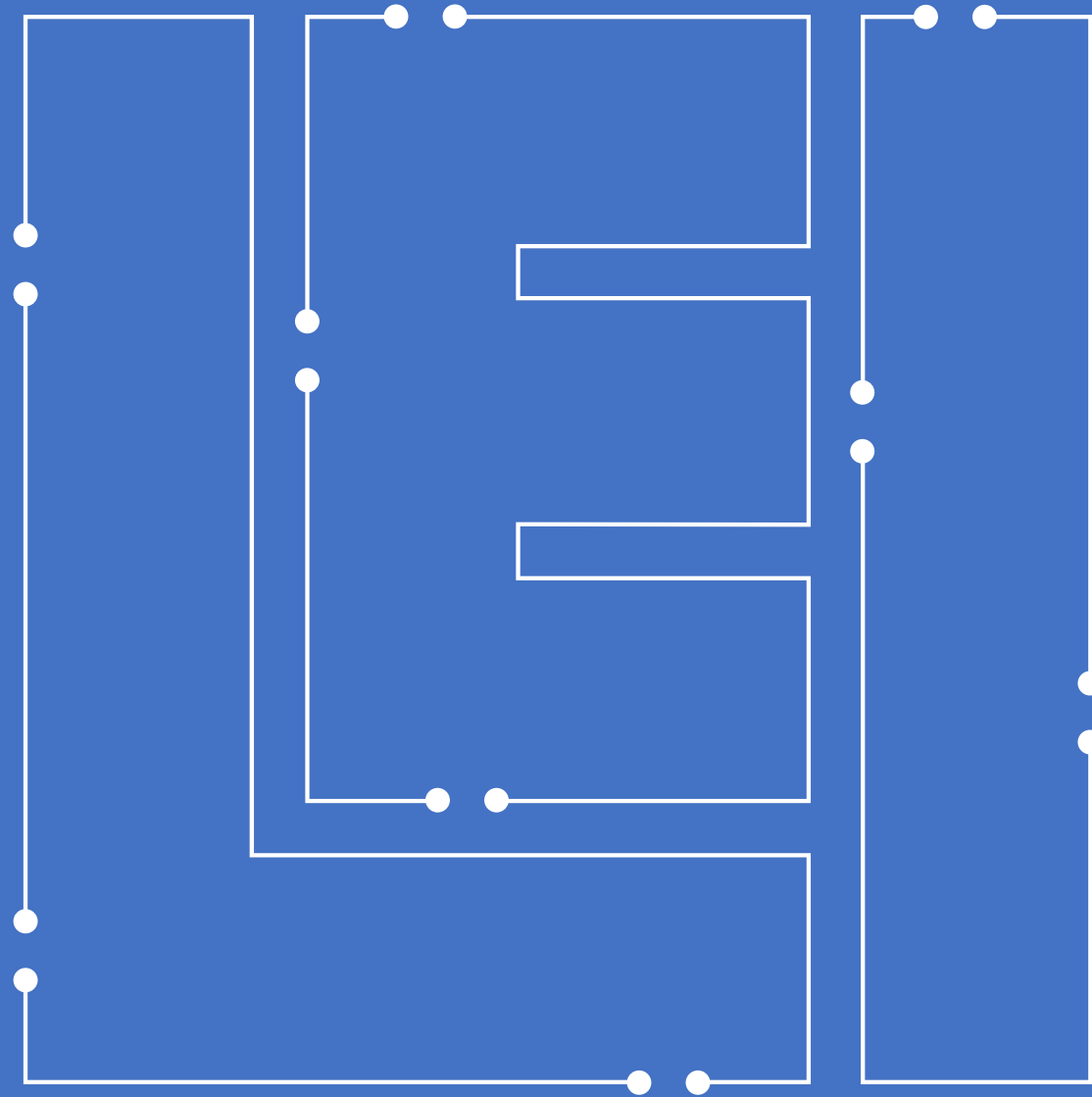


LITHUANIAN  
ENERGY  
INSTITUTE

Thank you for your attention !

[Tadas.Kaliatka@lei.lt](mailto:Tadas.Kaliatka@lei.lt)

2022-09-28, LEI, Kaunas, Lithuania





**J. Birchley (pres. by B. Jäckel)**  
**PSI (retired)**

## **First assessment of PSI nitriding model against air ingress experiments QUENCH-16 and “-18”**

A first assessment of the PSI nitriding model has been performed against the air ingress experiments QUENCH -16 and -18. The study continues the experimental investigation on nitriding/reoxidation performed by Park in the frame of a joint PSI/KIT PhD study, followed by the development of a model based on the experimental results and its implementation into a PSI version of MELCOR/1.8.6. The work was motivated by the extensive nitriding observed in previous integral experiments that were originally performed to address oxidation in air.

QUENCH-16 was performed to address the impact of an air environment on cladding oxidation and fuel damage, and on the subsequent escalation during oxidant starvation when all the oxygen has been consumed. QUENCH-18 was an approximate counterpart experiment in which the environment was a mixture of steam and air.

Comparison between the QUENCH-16 data and MELCOR simulations with and without the nitriding model show how the model captures the additional reaction and heat generation after all the oxygen is consumed, resulting in the uptake of nitrogen and formation of zirconium nitride (ZrN). No significant uptake of nitrogen was observed before oxygen starvation, in either the experiment or simulation.

The effect of a mixture of steam and air, addressed in QUENCH-18, is investigated qualitatively by repeating the QUENCH-16 simulation with the additional of steam flow corresponding to the QUENCH-18 conditions. It is noted that a direct quantitative comparison between the -16 and -18 results is not possible because of numerous differences in bundle configuration. Both the experiment and simulation demonstrate no noticeable consumption of steam before oxygen starvation. The continuing presence of steam therefore results in a slightly reduced thermal escalation prior to oxygen starvation, and a sharp increase afterwards as the steam is consumed, also captured by the model. Also, as observed in the experiment, no significant nitrogen uptake occurs until both the oxygen and steam are fully consumed.

Some calculational difficulties emerged with the model, apparently numerical, during the late stages of the simulations, including reflood. There is also a difference in the calculated oxidation kinetics during pre-oxidation because the nitriding model results in a lower oxide thickness as some of the uptaken oxygen produces alpha-Zr(O).

# First assessment of PSI nitrating model against QUENCH-air experiments



Gustave Courbet  
"The Stone Breakers" (1849)

27th International QUENCH Workshop  
Karlsruhe Institute of Technology  
September, 2022

Jonathan Birchley, Bernd Jaeckel



# Outline

- Background PSI nitriding model implemented in MELCOR and presented at QWS 2021
  - Integral experiments (QUENCH-air, etc) reveal need for nitriding model
- Introduction to study
- Simulations of QUENCH-16
  - MELCOR-186/PSI calculation from SARNET benchmark on QUENCH-air
  - Calculations with MELCOR-186/PSI/pre-NT and /NT
  - Option for nitrogen-promoted accelerated oxidation, on/off
- Simulations of “QUENCH-18”
  - QUENCH-16 with similar boundary conditions to -18 to examine effect of air+steam compared with air
- Summary of results
- Conclusions and outlook

# Background and aim

- Air oxidation model implemented in MELCOR-186 and SCDAPSim-3.5
  - Successfully reproduced the air oxidation in QUENCH-16/-18
  - Simulations of revealed need for nitriding model
- Nitriding model in MELCOR presented at QWS 2021
- Present study aims:
  - First assessment of model for integral transient analysis
  - Assessment of ability to capture trends and phenomena
  - Comparison with simulations with previous PSI version and cases with air oxidation and nitriding models not activated
  - Verification that model works as intended
  - Check of model robustness under transient conditions
  - Not primarily assessment against the experimental data

# Introduction to study

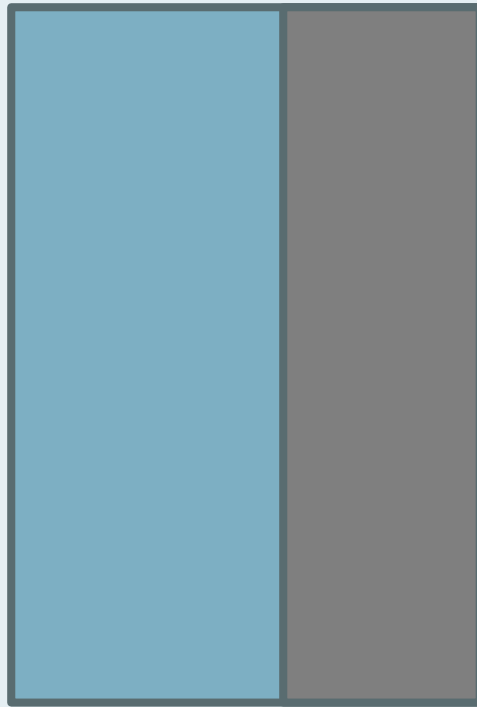
- Summary of nitriding model
- QUENCH-16/-18 used as reference cases
  - Investigating the model rather than analysing the experiments themselves
  - Starting point was ERMSAR benchmark simulation, an idealised description of QUENCH-16
  - Likewise, an idealised variant of using same QUENCH-16 input deck plus QUENCH-18 steam flow during air flow
- Code/model versions (all based on MELCOR/1.8.6/PSI)
  - Pre-nitriding version (pre-NT)
  - Nitriding version (NT) with model activated/not activated
  - Cases with and without nitrogen promoted oxidation kinetics
  - Main focus on pre-oxidation and air ingress phases

# Summary of nitriding model: Oxidation

- $\text{Zr} + \text{oxidant} = x\text{ZrO}_2 + (1-x)\text{Zr(O)}$ 
  - Oxidant may be steam and/or oxygen, with nitrogen present
  - Model assumes  $\text{Zr(O)}$  is  $\text{ZrO}_{0.4}$  which corresponds to oxygen-stabilised alpha-Zr at near-saturation dissolved oxygen
    - In reality, the alpha-Zr is not necessarily at saturation, except at the interface with the oxide
  - Oxide production rate determined by standard parabolic correlations, possibly modified by breakaway or presence of nitrogen
  - Oxide thickness, not mass gain, used as controlling quantity for kinetics
  - Production of alpha-Zr is by diffusion from oxide to metal, at a rate that would correspond to standard correlation during “normal” oxidation
  - However, alpha-Zr(O) production continues during oxidant starvation, reducing the oxide thickness (potentially homogenising the Zr/ZrO<sub>2</sub> layers)

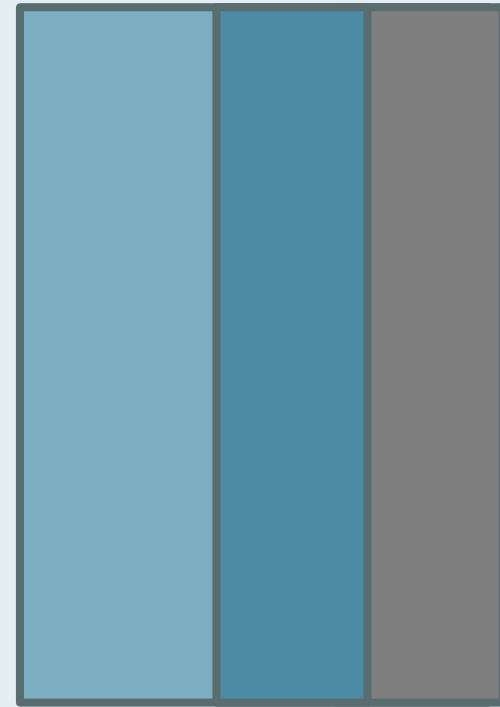


# Schematic of oxidation in nitriding model



Zr

ZrO<sub>2</sub>



Zr

Zr(O)

ZrO<sub>2</sub>

- Classical and double layer representation of oxidation with same mass gain
- Reduced thickness ( $\delta$ ) in double layer representation causes faster oxidation kinetics when used with parabolic correlation:  $d/dt (\delta^* \delta) = F(T)$

# Summary of nitriding model: Nitriding

- In presence of nitrogen but not oxidant
- If  $Zr_{0.4}$  remains
  - $2ZrO_{0.4} + N_2 = 2ZrN + 0.8[O]$
  - The oxygen released is taken up half-half by remaining  $ZrO_{0.4}$  to produce  $ZrO_2$ , and by Zr to partially replenish the  $ZrO_{0.4}$  consumed in the nitriding
  - Kinetics are comparatively rapid
- If Zr remains but no  $Zr_{0.4}$ 
  - $2Zr + N_2 = 2ZrN$
  - Kinetics are slow
- Otherwise no reaction and nitrogen not uptaken
- Oxygen is not displaced from the cladding during nitriding

# Summary of nitrating model: Reoxidation

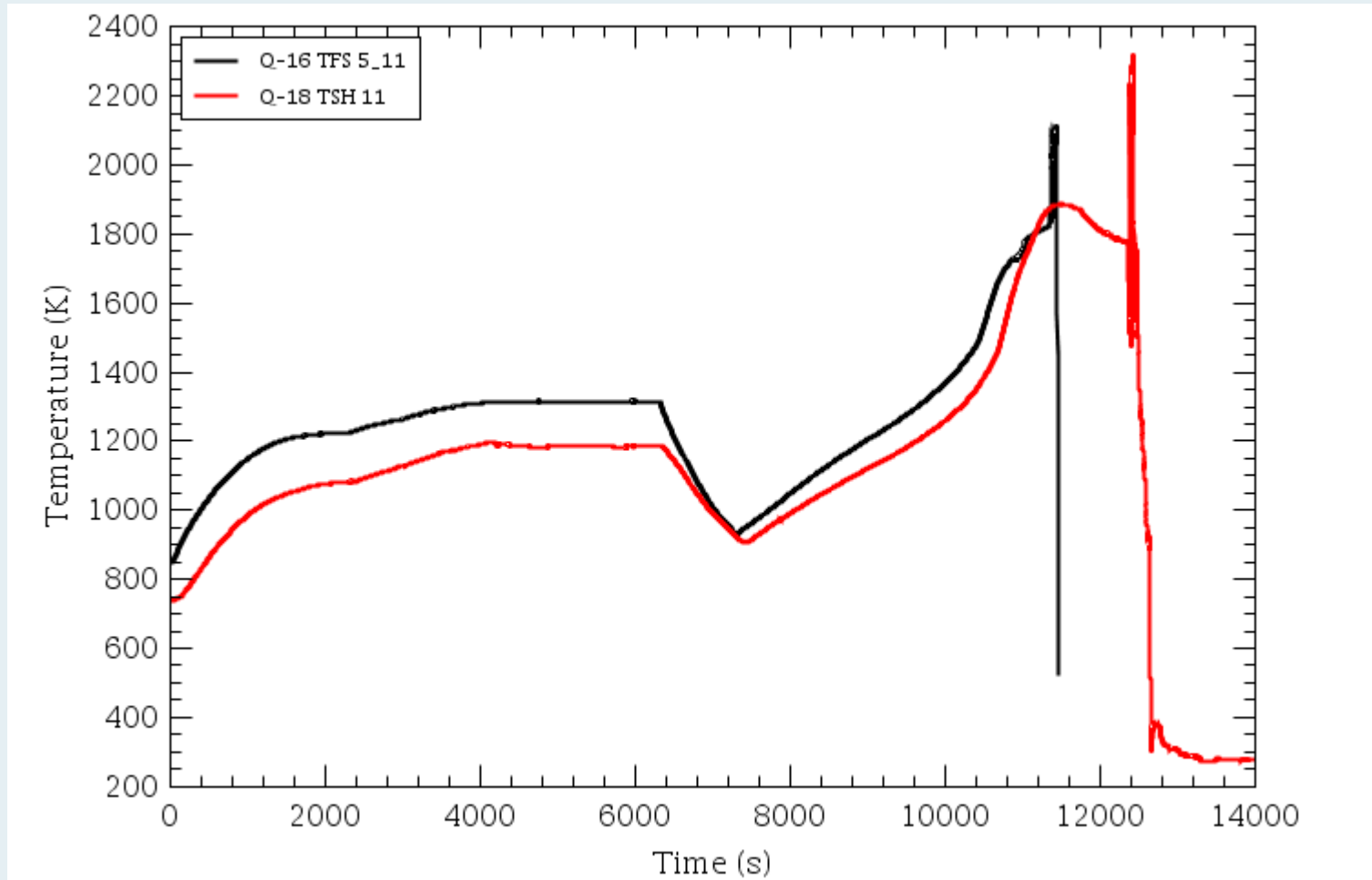
- In presence of oxygen or steam, ZrN is oxidised to ZrO<sub>2</sub>
  - $2\text{ZrN} + 2\text{O}_2 = 2\text{ZrO}_2 + \text{N}_2$
  - $2\text{ZrN} + 4\text{H}_2\text{O} = 2\text{ZrO}_2 + 4\text{H}_2 + \text{N}_2$
- Reaction with oxygen takes precedence over steam
  - Assumption: in reality there is gas-phase reaction  $2\text{H}_2 + \text{O}_2 = 2\text{H}_2\text{O}$
- Nitrogen is displaced from the cladding
  - Potential conflict when nitrogen and oxidant are both present
  - If oxidant supply is limited, the nitrogen released can react with Zr(O) or Zr in oxidant-starved region
  - Programming logic needs to be handled very carefully

# Recap of experiment results

- Approximate counterpart air ingress experiments in 3 phases
  - 1) Oxidation in steam 2) air flow 3) reflood
  - QUENCH-16 phase 2 was air alone
  - QUENCH-18 phase 2 was air+steam
- In both experiments
  - Extended period of oxidant starvation
  - Significant nitriding in both
  - Nitrogen release and significant oxidation reflood excursion
  - Shroud breached
- Differences in bundle configuration hinders direct assessment of effect of air+steam compared with air

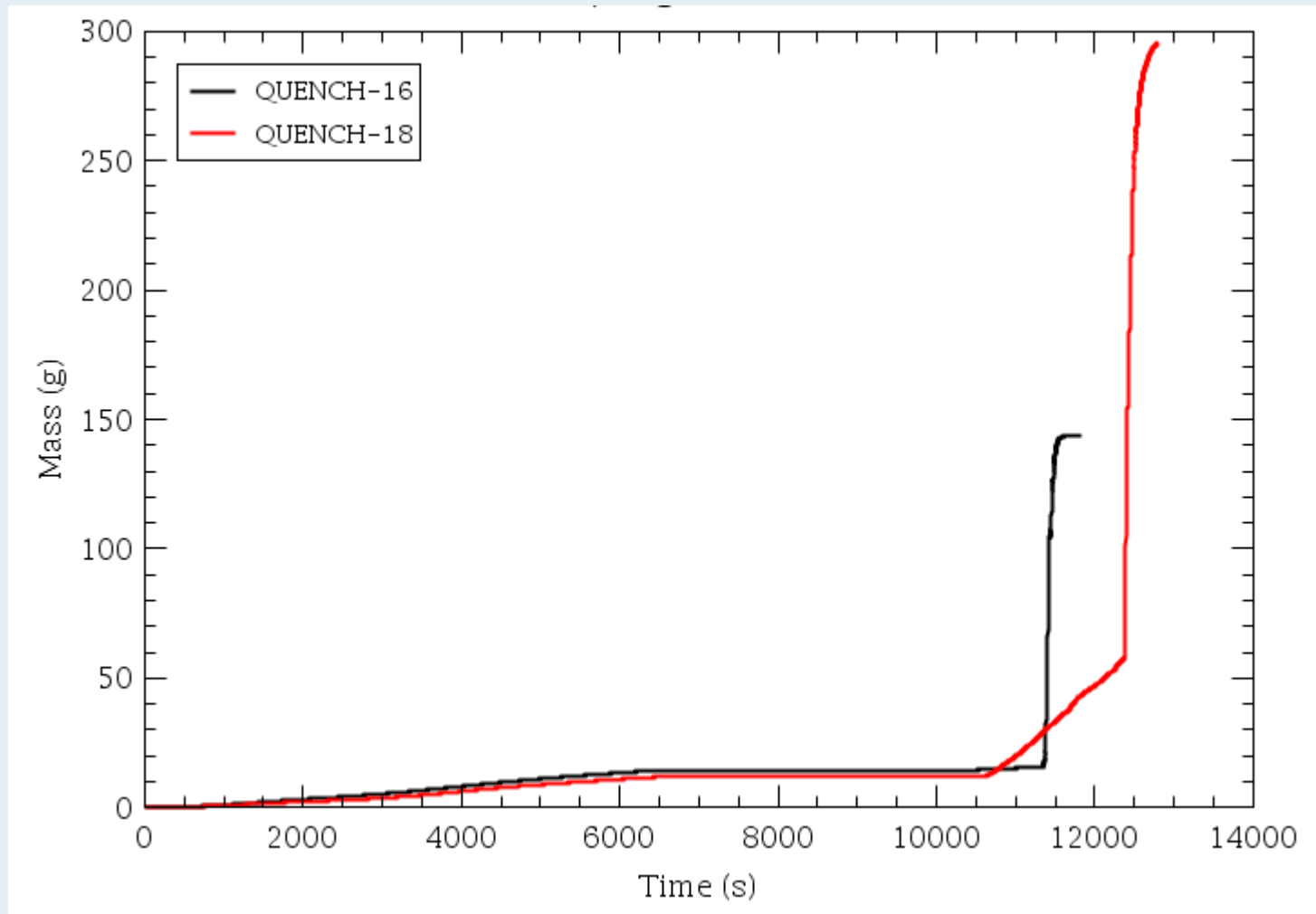


# Comparison of thermal response (750 mm)



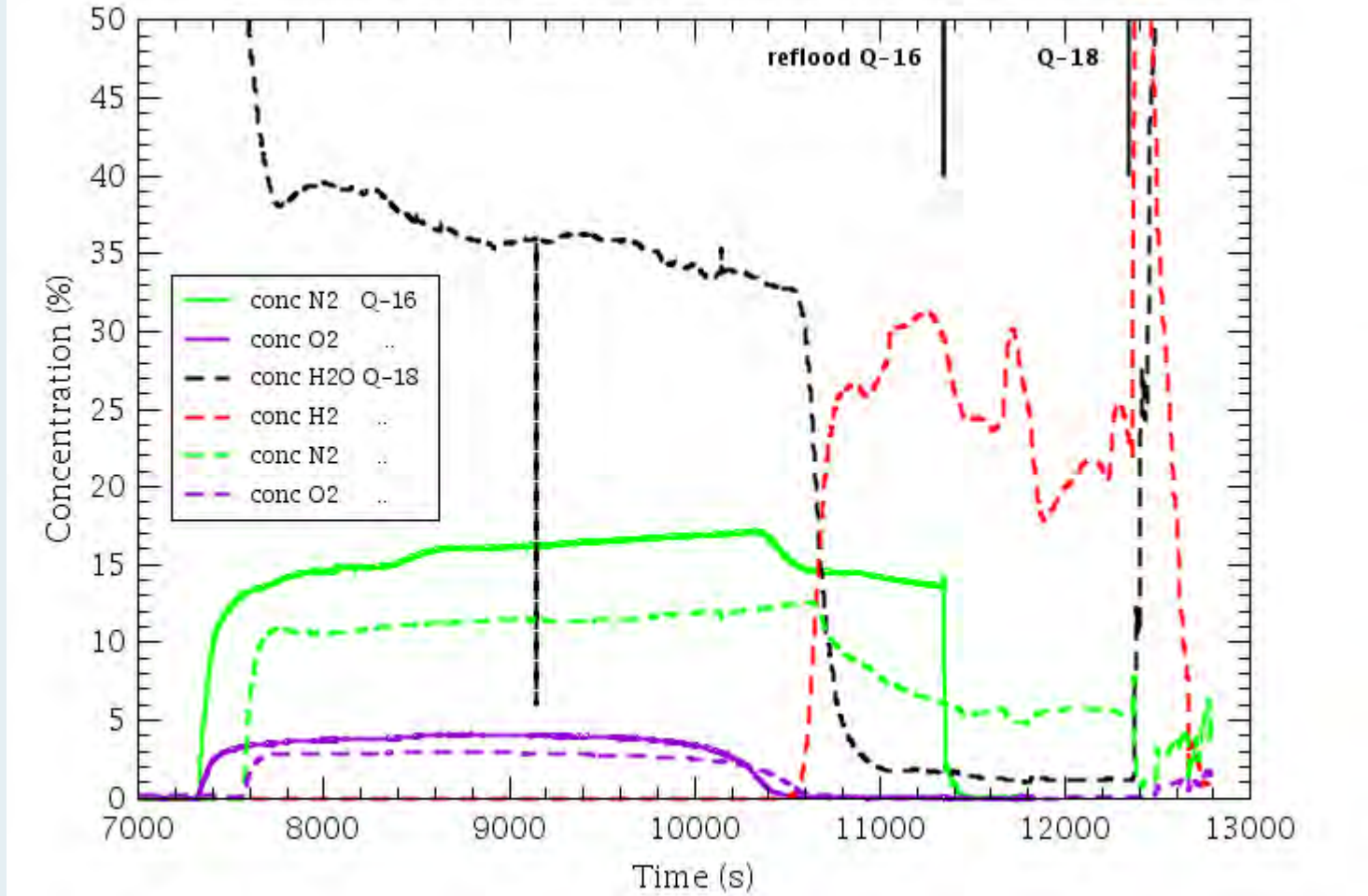
- Lower QUENCH-18 temperature may be due to bundle difference and shroud location
- Indication of additional heating from nitriding after ca. 10500 s

# Comparison of hydrogen generation



- Hydrogen release does not fully represent the oxidation
- Hydrogen production in QUENCH-18 during period of oxygen starvation

# Steam, H<sub>2</sub>, N<sub>2</sub>, O<sub>2</sub> offgas concentrations



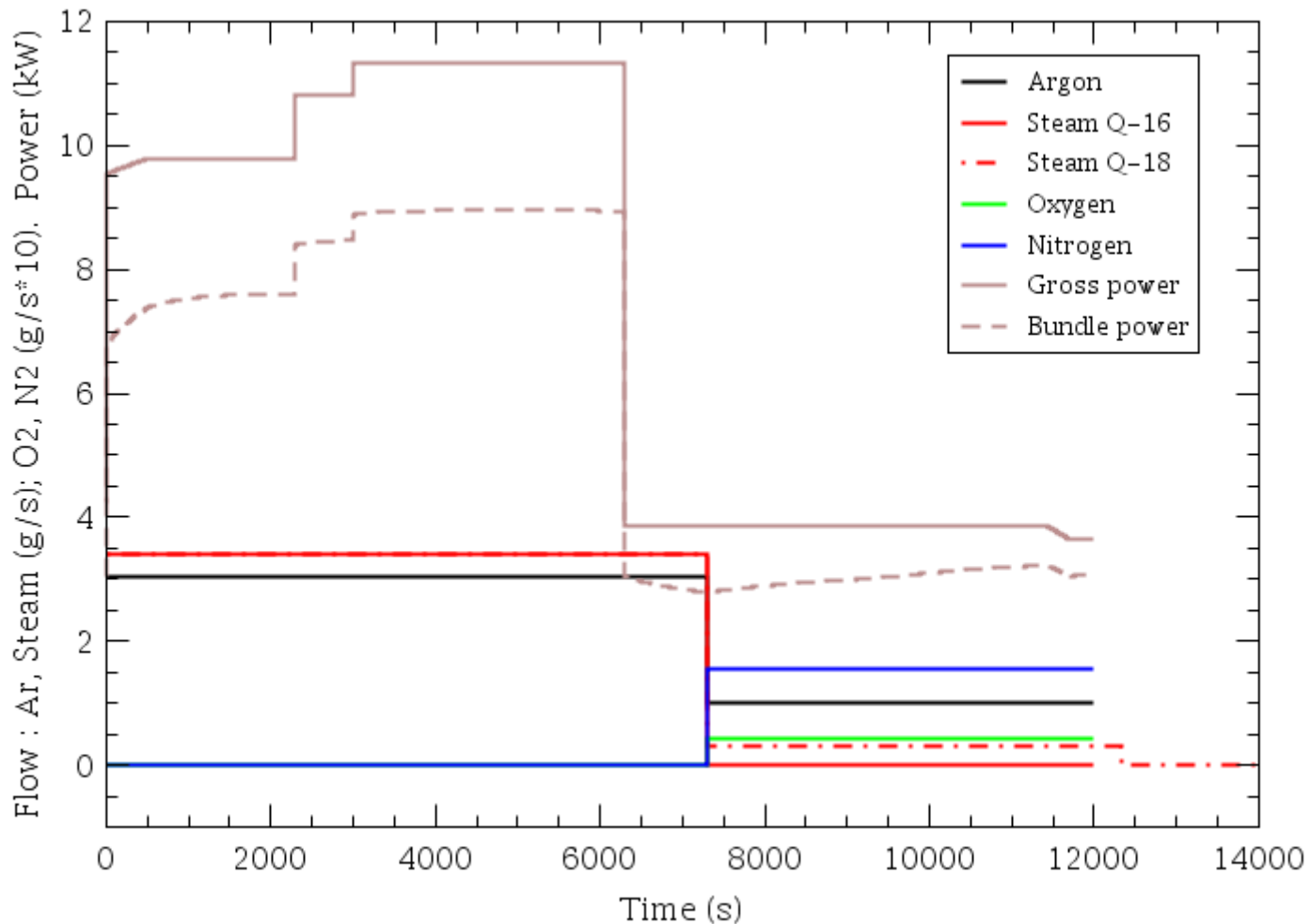
- Nitrogen consumption starts only after oxygen almost fully consumed
- Nitrogen consumption starts before steam fully consumed in QUENCH-18

# Simulations of QUENCH-16, -18

- Boundary conditions
- Code versions
  - MELCOR 1.8.6/PSI/pre-NT
  - MELCOR 1.8.6/PSI/NT
- Model choices
  - PSI model on or off (PSI=1 or 0)
  - Nitrogen-promoted oxidation kinetics on or off (nb =1 or 2)
  - Exit mole fractions: oxygen, nitrogen
  - Cathcart-Pawel/Urbanic-Heidrick and Uetsuga-Hoffman correlations used for oxidation in steam and oxygen, respectively, with PSI modification in presence of nitrogen
- Comparisons with data and between models
  - Thermal response
  - H<sub>2</sub> generation
  - Exit composition
  - Cladding composition



# Idealised boundary conditions used

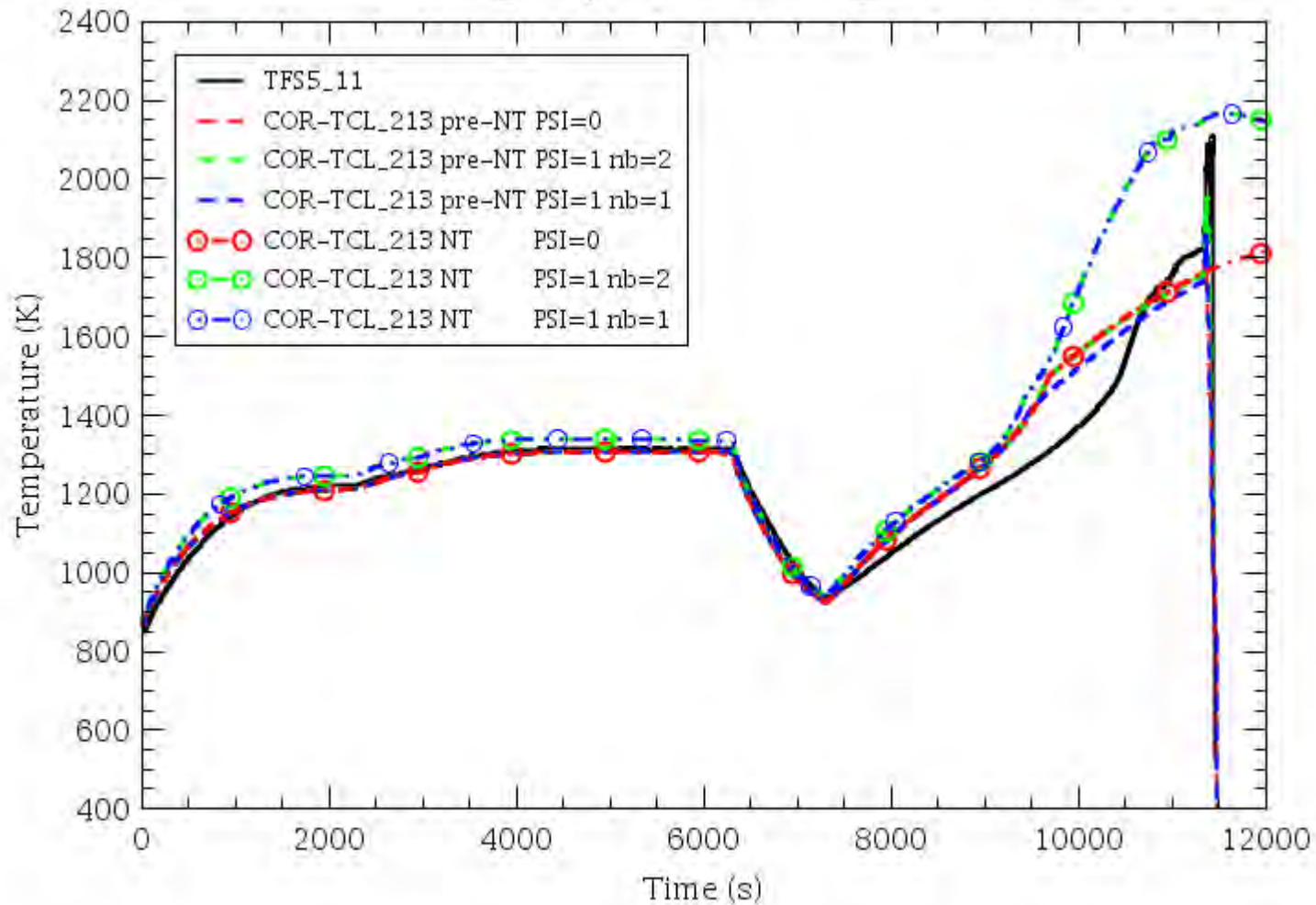


- Nominal QUENCH-16 conditions correspond to PSI benchmark simulation
- Replicated for "QUENCH-18" with inclusion of 0.3 g/s steam during air phase

# Simulations of QUENCH-16

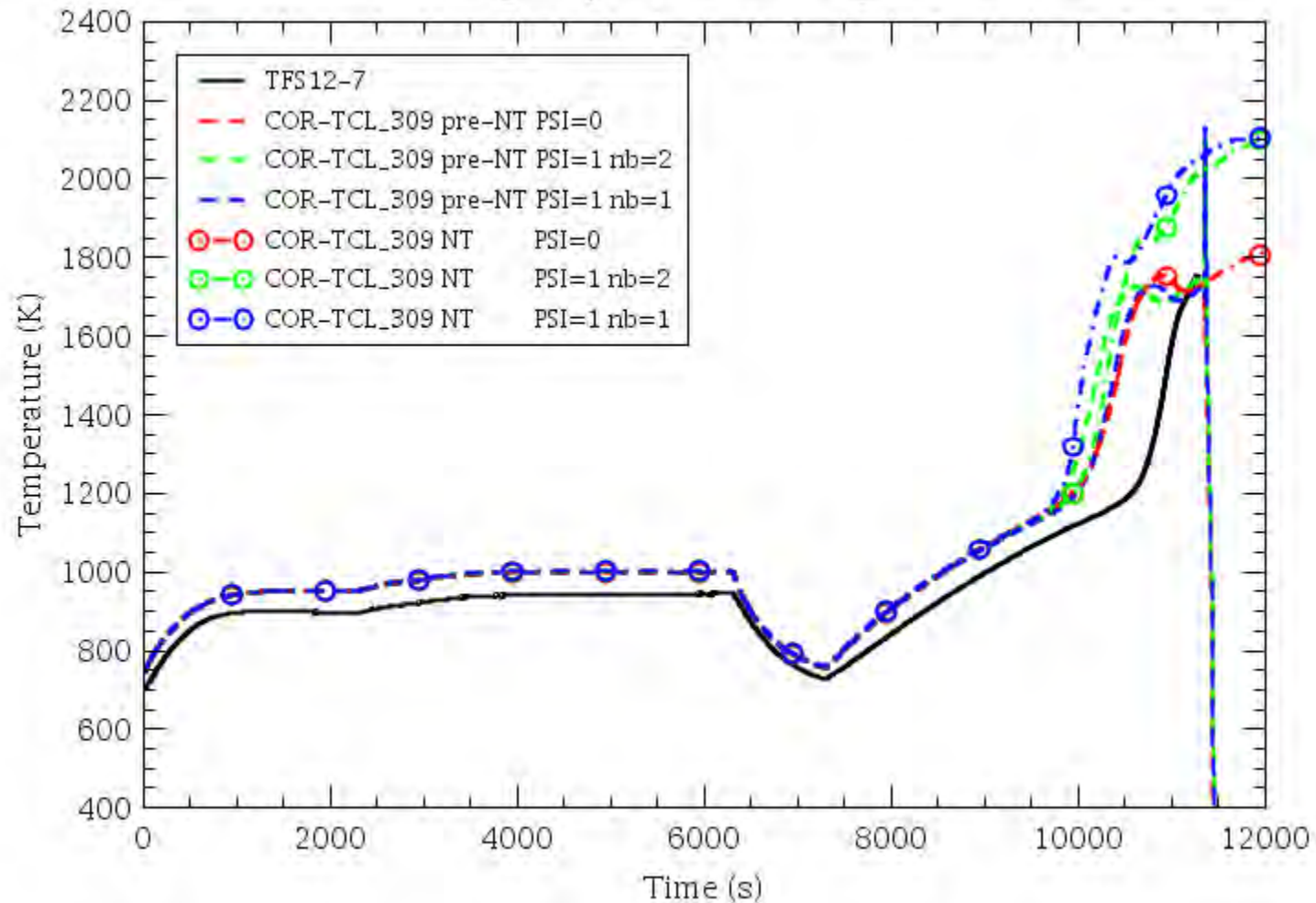
- Concentrate on comparison with experiment and effect of NT model
- Verify consistency between code versions when NT model not used
- Assess robustness and ability of code to calculate nitriding as intended

# QUENCH-16 temperature at 750 mm inner rod (5)



- No significant difference between cases without nitriding
- Clear effect of nitriding on cladding temperature
- Slightly higher pre-oxidation temperature with nitriding model

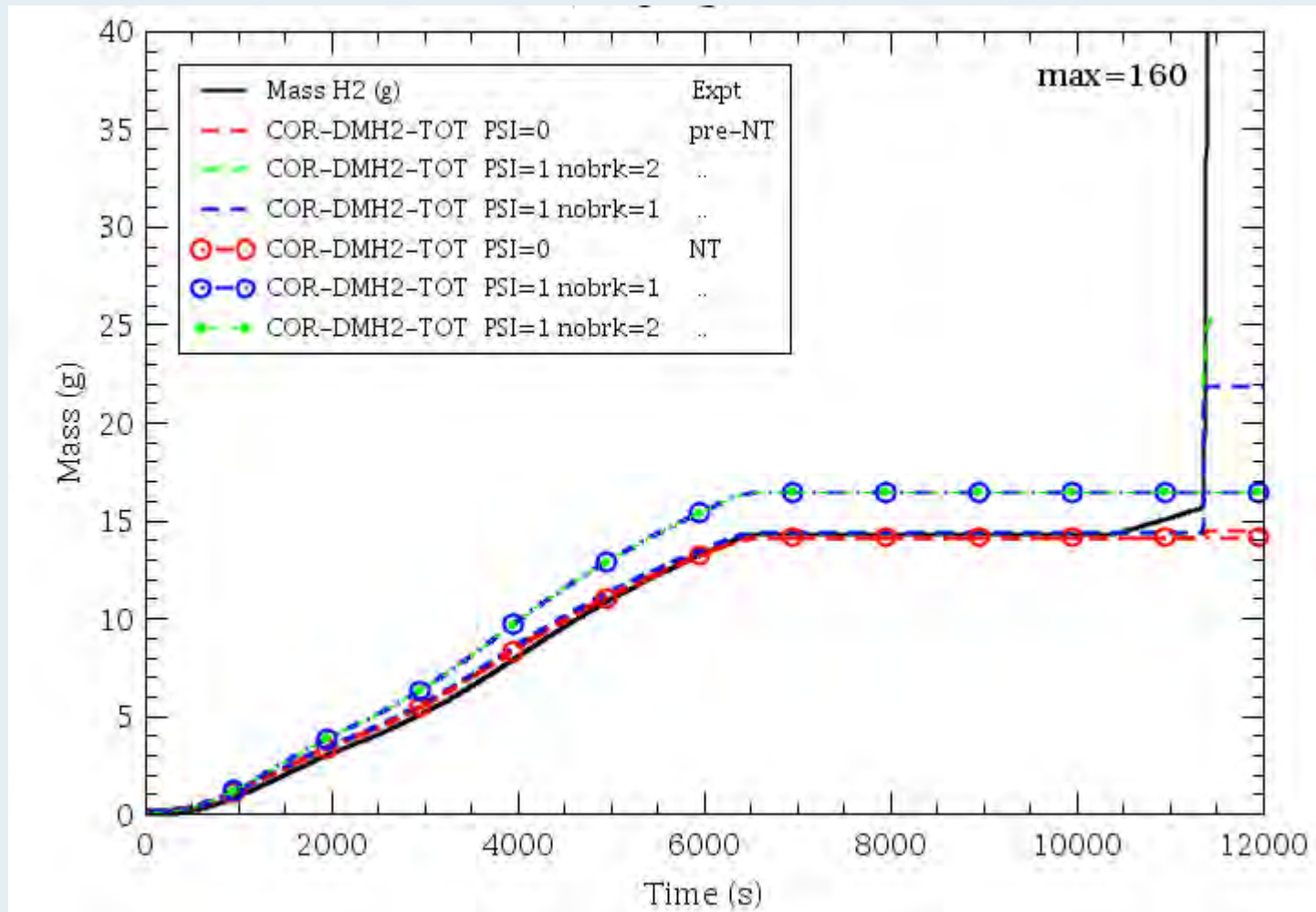
# QUENCH-16 temperature at 350 mm outer rod (12)



- Temperatures slightly overestimated; earlier escalation
- Reduced effect nitriding at 350 mm due to later calculated oxygen starvation
- Oxygen starvation might not have occurred at this location in experiment

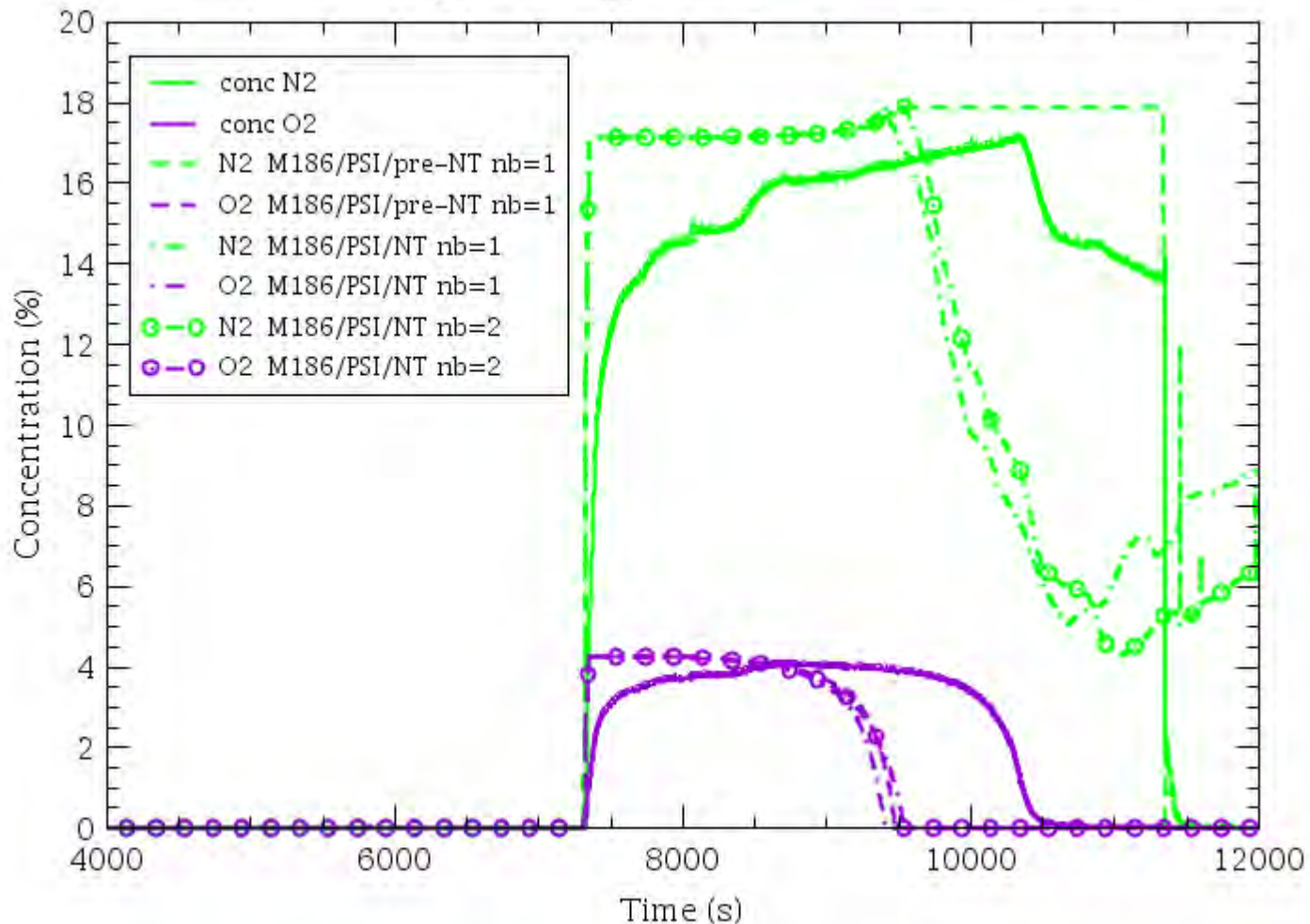


# QUENCH-16 hydrogen generation



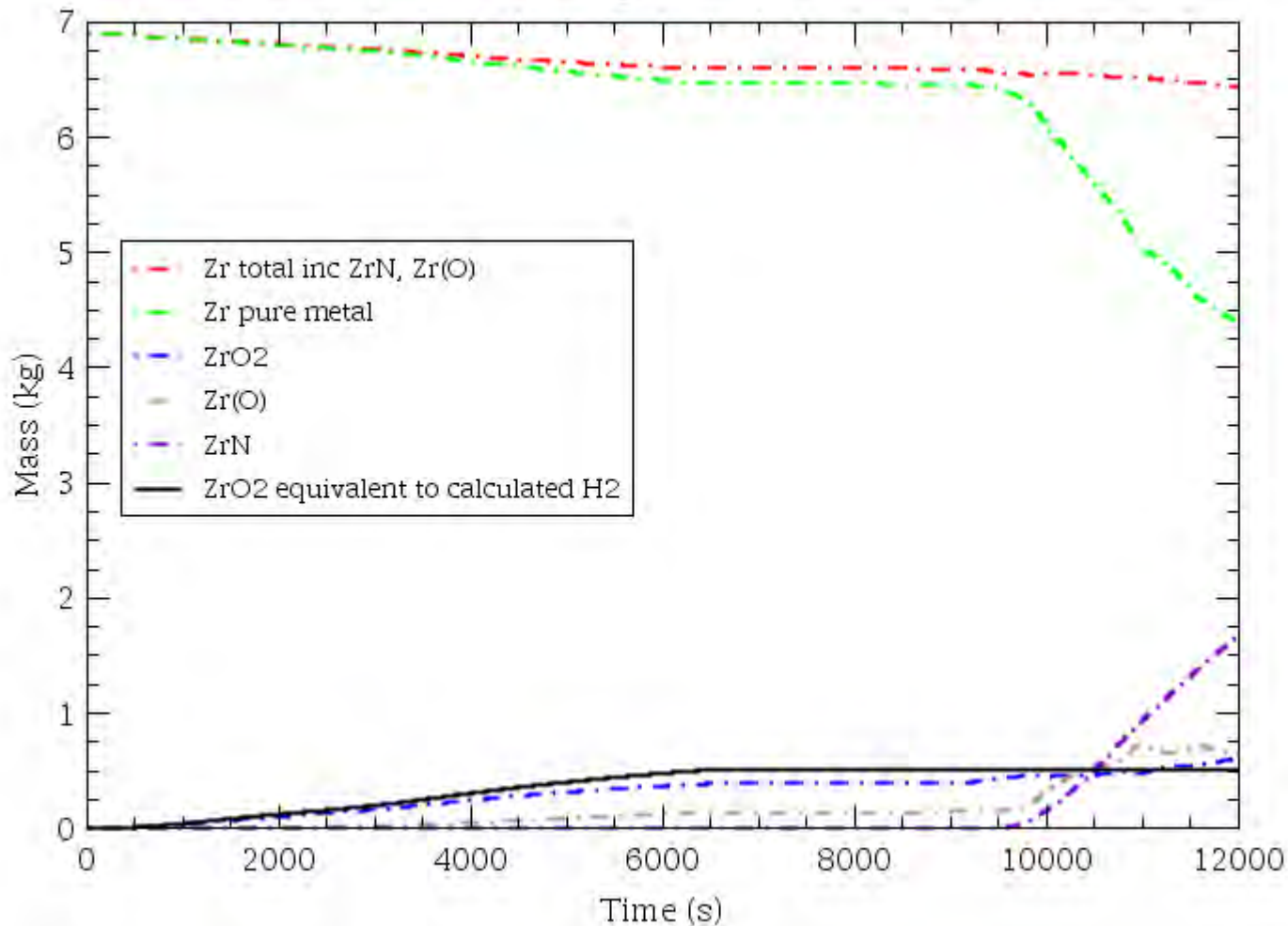
- Excellent agreement pre-reflood without NT model, but overestimated by NT
- No effect of nitrogen-promoted oxidation
- Hydrogen in experiment after oxygen starvation (steam flow in bundle not included)
- Reflood excursion greatly underestimated or not calculated at all

# QUENCH-16 exit oxygen and nitrogen concentration



- Considers only cases with nitriding
- Oxygen and nitrogen consumption trends captured consumption rates overestimated
- Likely effect of oxygen dilution (observed in KIT SETs) not modelled

# QUENCH-16 NT cladding composition



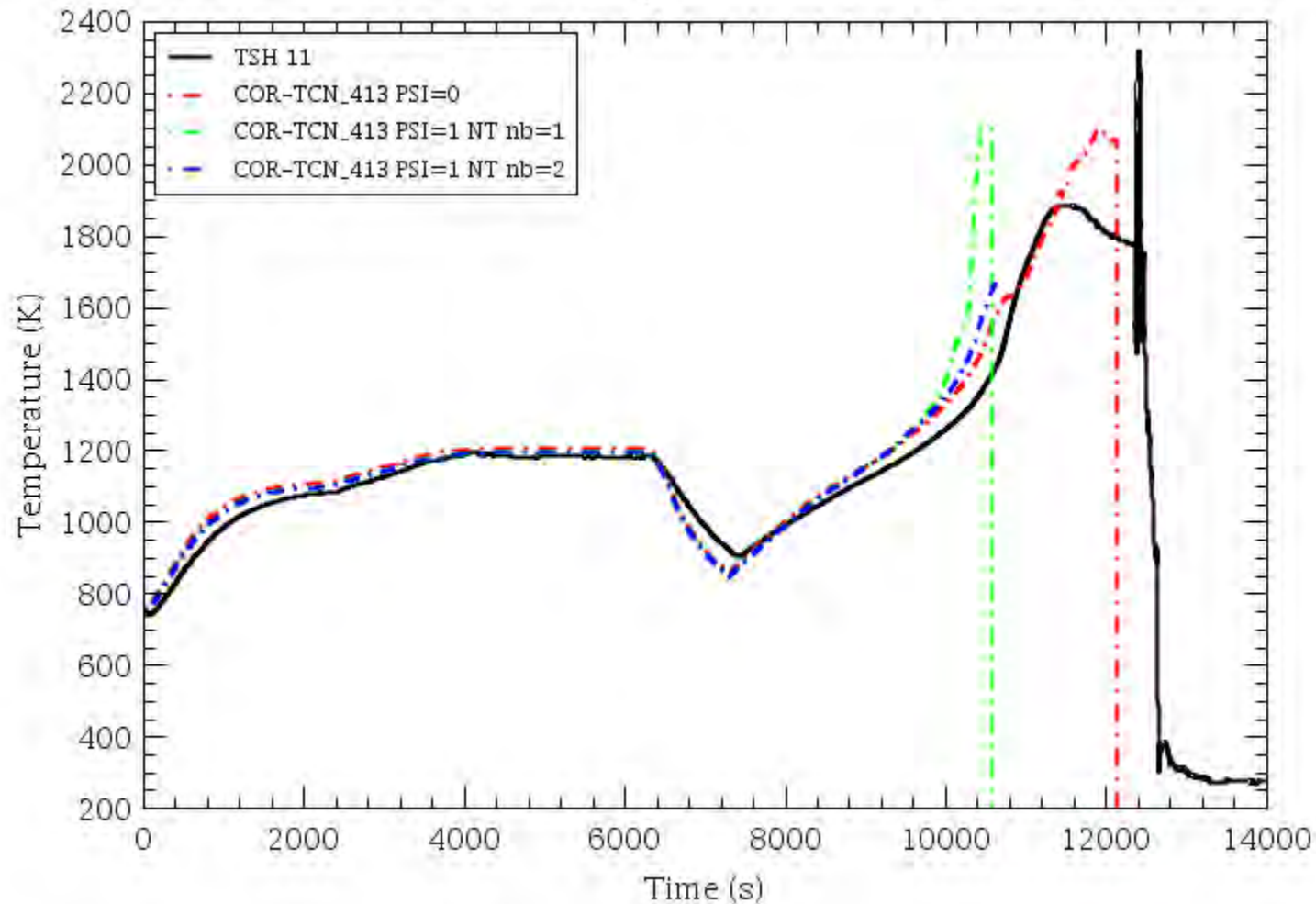
- One case: NT/q16\_11
- Zr(O) formation alongside ZrO<sub>2</sub> and from oxidation of ZrN
- As expected, difference between NT calculated ZrO<sub>2</sub> mass and H<sub>2</sub> equivalent mass
- Strong nitride formation after oxygen starvation; exceeds oxide mass

# Simulations of "QUENCH-18"

- Essentially as QUENCH-16
- Focus on effect of model and differences between QUENCH-16 and -18 flow conditions
- Assess robustness and ability of code to calculate nitriding as intended
- Direct comparison with experiment of peripheral importance

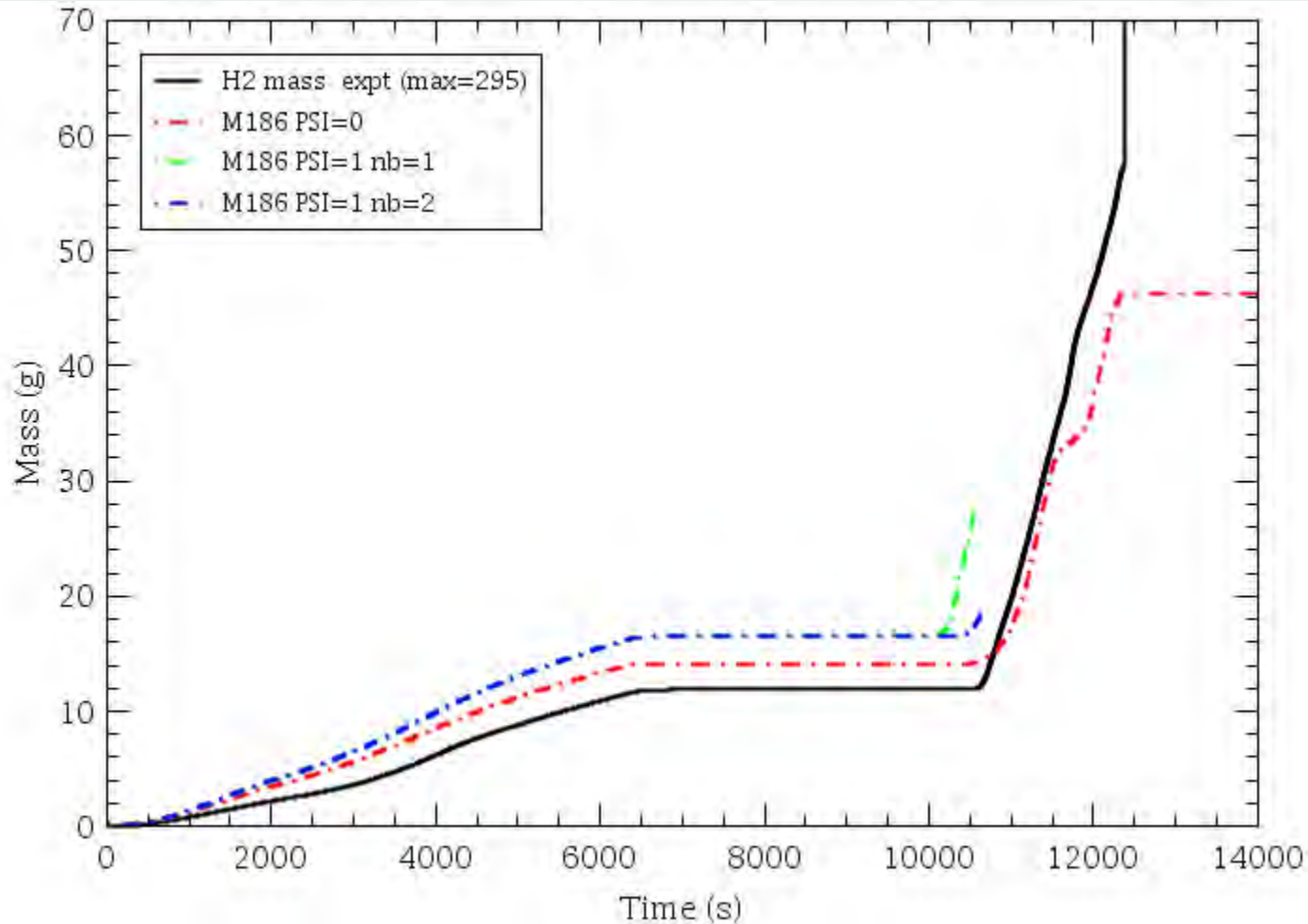


# "QUENCH-18" temperature at 750 mm shroud



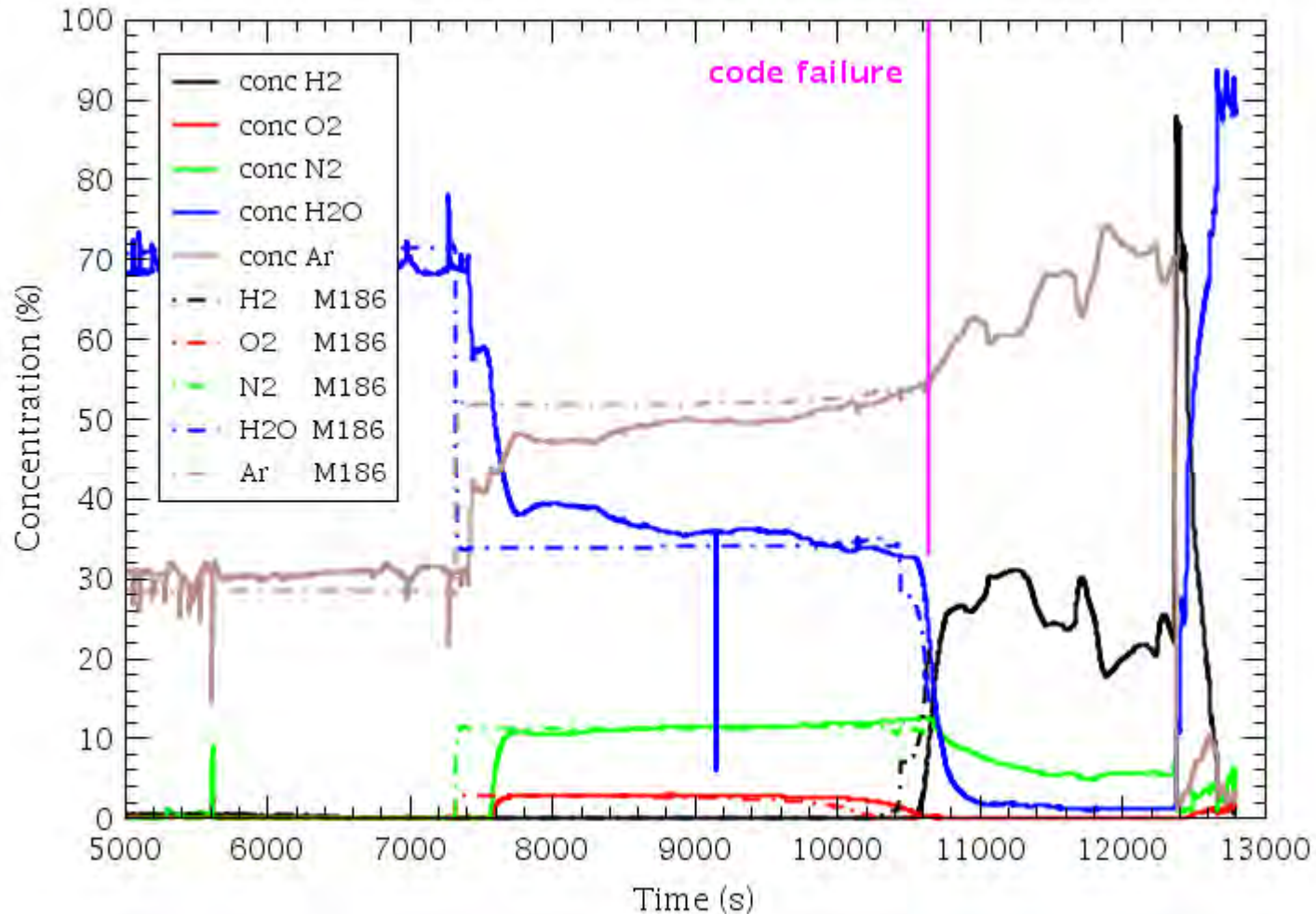
- Agreement during pre-oxidation may be due to cancelling effects
- Faster temperature rise due to nitriding and to nitrogen-promoted oxidation
- Some overprediction during air phase
- Code fails soon after start of nitriding, due to numerical issues

# "QUENCH-18" hydrogen generation



- Comparison affected by input model so focus on trends rather than quantitative values
- Pre-oxidation hydrogen generation increased with NT model.
- Effect of nitrogen-promoted oxidation

# QUENCH-18 exit composition



- Correctly reproduces trends and phenomena until code failure
- Unable to assess nitrogen consumption during steam+air phase
- Oxygen and nitrogen consumption rates overestimated as before with QUENCH-16
- Possible effect of oxygen dilution (observed in KIT SETs) not modelled

# Summary

- Model works well in air environment with PSI oxidation model
  - Production of alpha-Zr(O), ZrN
  - Consistency between all pre-NT cases or when NT model not activated
- NT model calculates faster (ca. 15%) oxidation during pre-oxidation compared with pre-NT code versions or with NT not activated
  - Reason is the reduced oxide thickness (the controlling factor with parabolic kinetics) compared with standard correlation, due to some of the oxygen taken up in alpha-Zr(O)
- Oxygen and nitrogen consumption rates overestimated
  - May be an effect of low reactant concentration
- Code failed early during nitriding in air+steam environment (Q-18)
  - Minor amount of ZrN formed and no significant oxidation of ZrN
- Code failed at start of reflood in all cases with nitriding model



# Conclusions and outlook

- The newly developed and implemented model successfully captures the main trends and phenomena for nitriding under transient conditions
  - The formation of alpha-Zr(O) is a key precursor to nitride formation
  - The consequently diminished oxide thickness during and after pre-oxidation should also make it possible to reproduce the observed reflood excursion following prolonged steam starvation
  - The “alpha-modified” thickness is the correct quantity for the oxidation kinetics
  - However, the model needs reworking to recover consistency with chosen oxidation correlation in a “normal” steam environment
- For both NT and air oxidation models, there is a case for modifying the kinetics to take account of low oxygen/nitrogen concentrations
- The numerical solution algorithm should be examined and modified to avoid code failures during reflood and in steam+air environments
- Despite these limitations, the demonstrated success implies significant progress towards an effective model for reactor and spent fuel air ingress sequences

# Acknowledgments

The authors are pleased to acknowledge the financial support from the Swiss Nuclear Safety Organisation (ENSI) to facilitate the model development, and technical support and provision of experimental data from Karlsruhe Institute of Technology

The first author wishes to acknowledge Hythe Computers, without whose IT help this work would not have been possible

**Thank you for your attention**



**A. Aryanfar**

**American University of Beirut**

## **Evolution of Compressive Stress During the Corrosion of Metals. The Materials Selection**

The formation of an oxide layer on the surface of metals leads to mechanical failure, cracks, and spalling. We develop a real-time framework for computing the evolution of interfacial misfit stress within both oxide and metal throughout the corrosion of thin films. Subsequently, we anticipate the onset of mechanical failure due to accumulation of compressive stress in both media. These results are useful for anticipating the failure mode and state in various metals based on their physical and mechanical properties.

# Evolution of Compressive Stress During the Corrosion of Metals

## The Materials Selection

**Asghar Aryanfar**

Assistant Professor  
Mechanical Engineering  
American University of Beirut  
Visiting Associate, Caltech

Jaime Marian (UCLA)

**QUENCH Workshop**

September 28, 2022

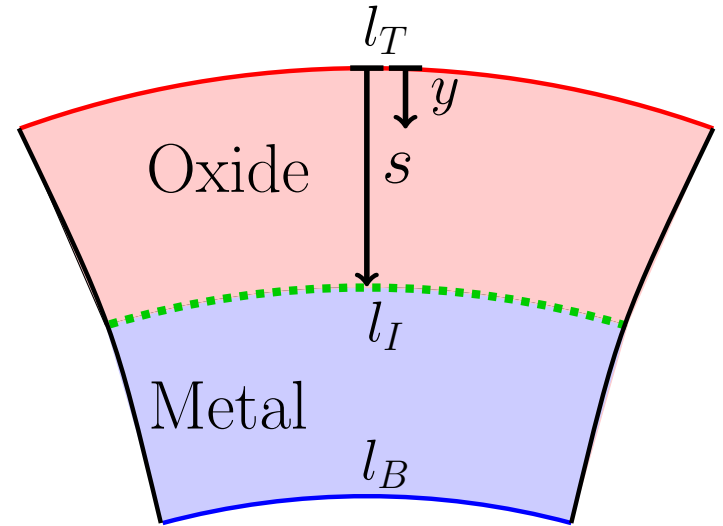




# Volume Relationships

- Parameters:  $M + \frac{n}{2}O_2 \rightarrow MO_n$  ( $V \uparrow$ )

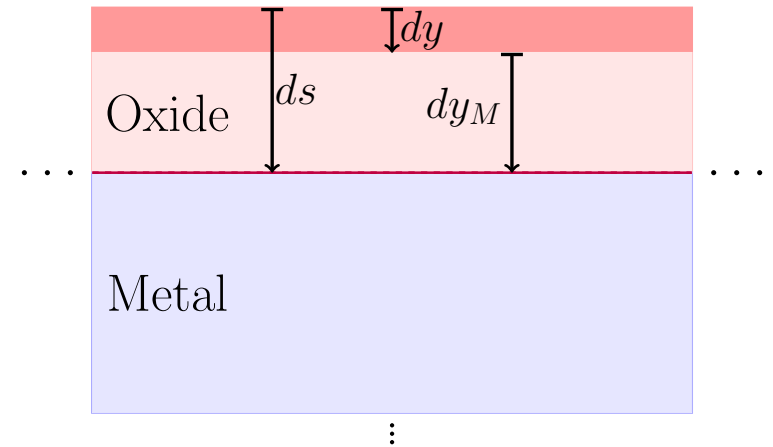
$$\begin{cases} R_{PB} = \frac{V_O}{V_M} \\ \nu = -\frac{\epsilon_\theta}{\epsilon_r} \end{cases} \rightarrow \begin{cases} \sigma_\theta < 0 & \text{Oxide} \\ \sigma_\theta > 0 & \text{Metal} \end{cases}$$



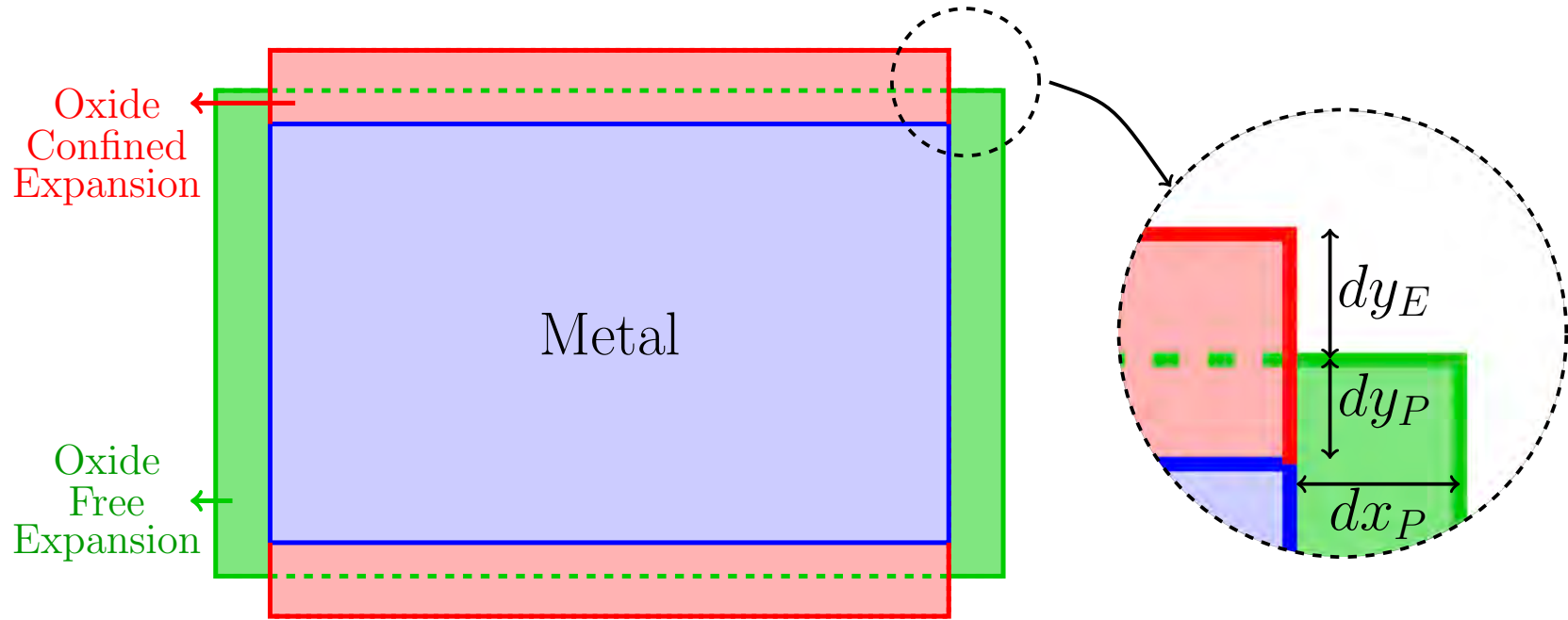
- Infinitesimal Swelling:

$$\delta s = R_{PB} \delta y_M \quad , \quad \delta y = \delta s - \delta y_M$$

$$\delta y = \frac{R_{PB} - 1}{R_{PB}} \delta s \rightarrow y = l + \frac{R_{PB} - 1}{R_{PB}} s$$



## Poisson Effect (thin films)



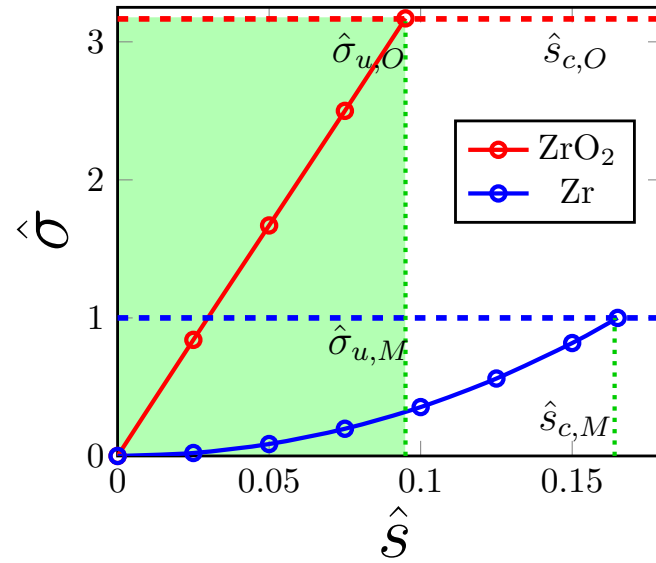
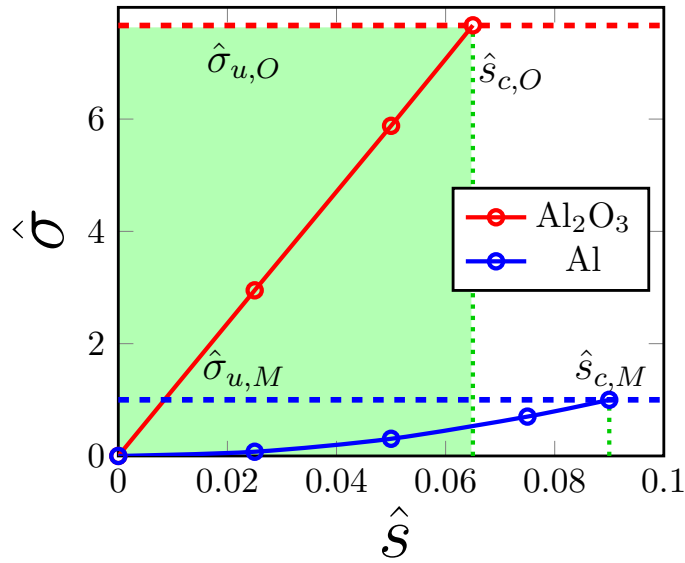
$$\frac{dy}{y} = \frac{dy_P}{y} + \frac{\delta y_E}{y}, \quad \frac{\delta y_E}{y} = \nu \frac{\delta x_P}{x}, \quad \epsilon = \frac{\delta y_P}{y} = \frac{\delta x_P}{x} \rightarrow \frac{\delta y_E}{y} = \frac{\nu}{1+\nu} \frac{\delta y}{y}$$

$$\int_0^\sigma \delta \sigma_O \approx \int_0^s K_O \frac{\delta y_E}{y} \rightarrow \sigma_O = K_O \frac{\nu}{1+\nu} \ln \left( 1 + \frac{R_{PB} - 1s}{R_{PB} l} \right)$$

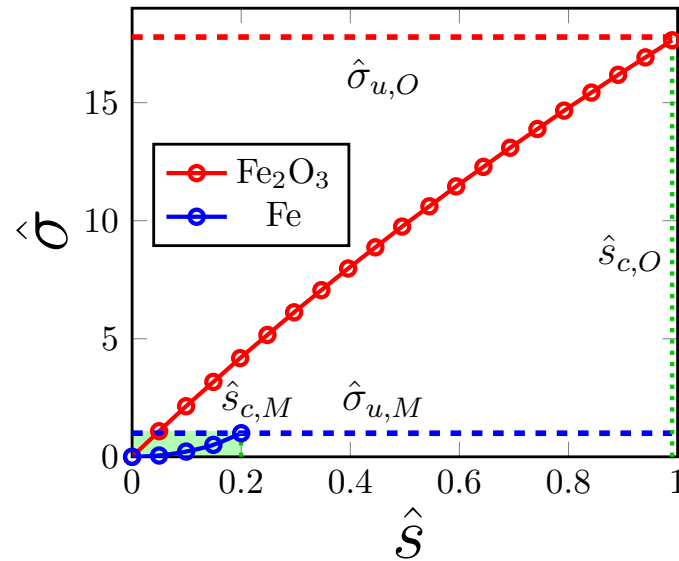
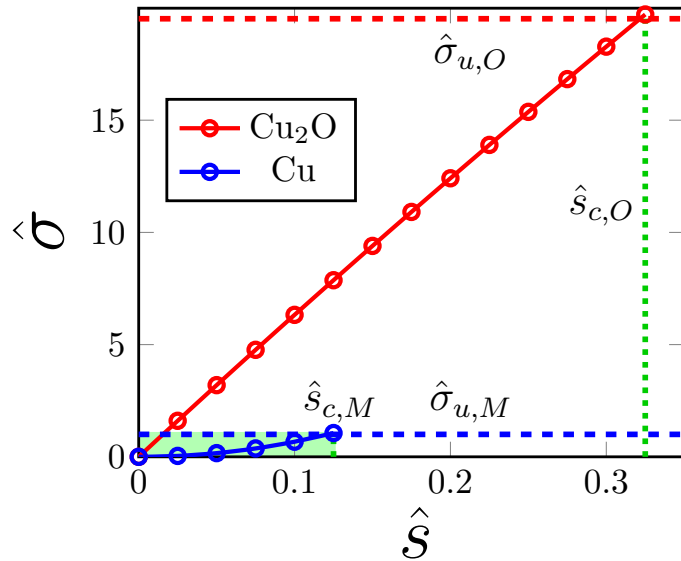
$$\int \sigma_O dy = \int \sigma_M dy \rightarrow \sigma_M = K_O \frac{\nu}{1+\nu} \frac{R_{PB} s}{R_{PB} l - s} \ln \left( 1 + \frac{R_{PB} - 1s}{R_{PB} l} \right)$$

# Stress Evolution

Oxide Earlier Yielding:  $\hat{\sigma} = \frac{\sigma}{\sigma_{ut,M}}$ ,  $\hat{s} = \frac{s}{l}$



Metal Earlier Yielding:



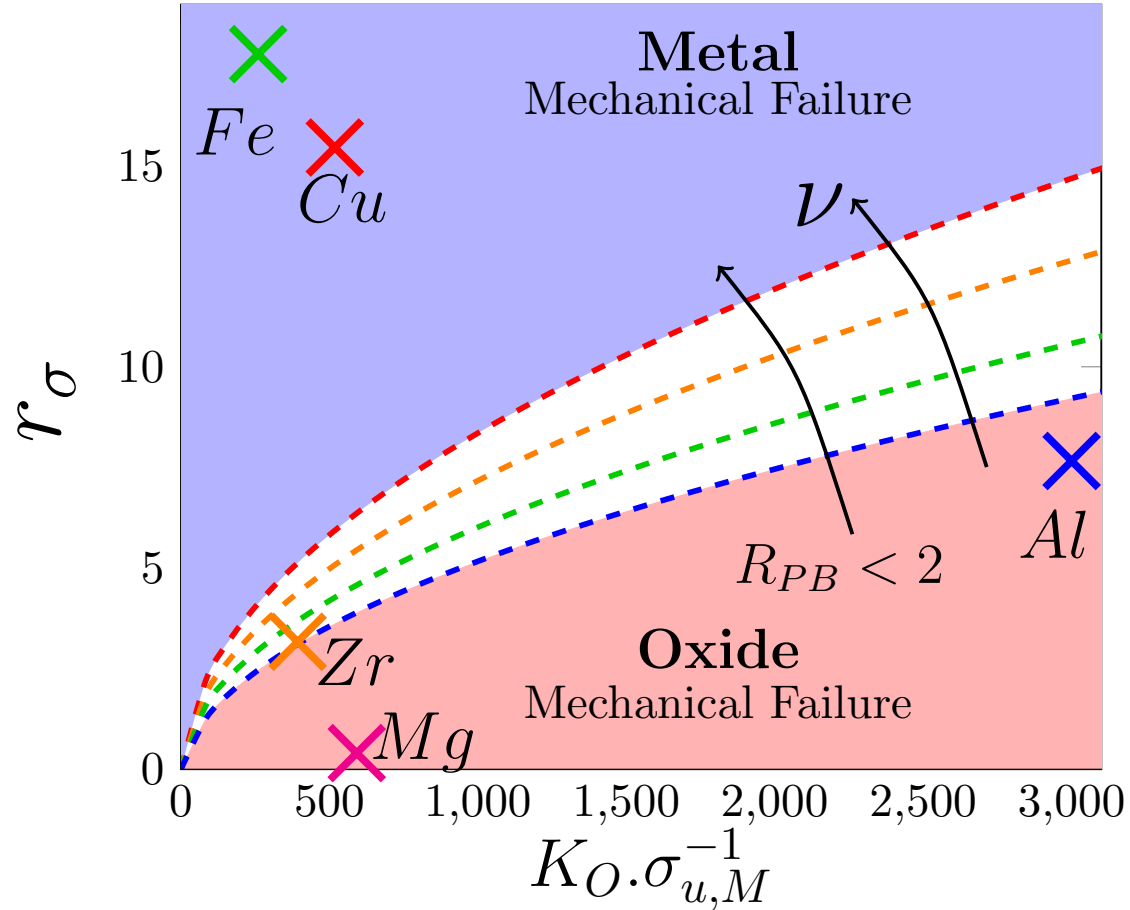
# Characterization

$$r_\sigma := \frac{\sigma_O}{\sigma_M}$$

$$\hat{s}_{c,O} \approx \frac{\sigma_{uc,O} 1 + \nu}{K_O \nu} \frac{R_{PB}}{R_{PB} - 1}$$

$$\hat{s}_{c,M} = \frac{\sqrt{1+2\alpha}-1}{\alpha}$$

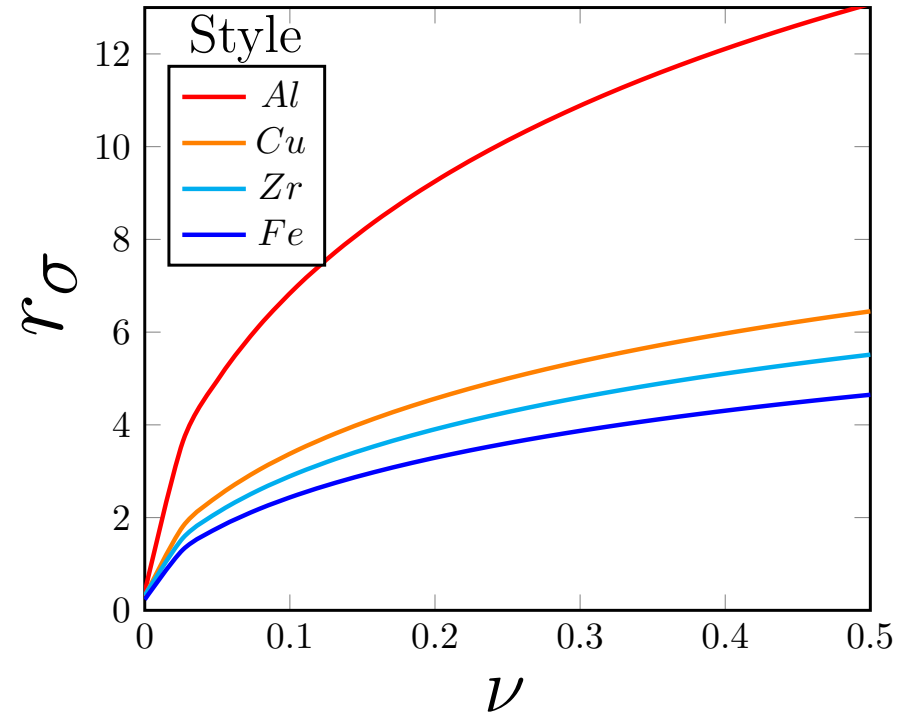
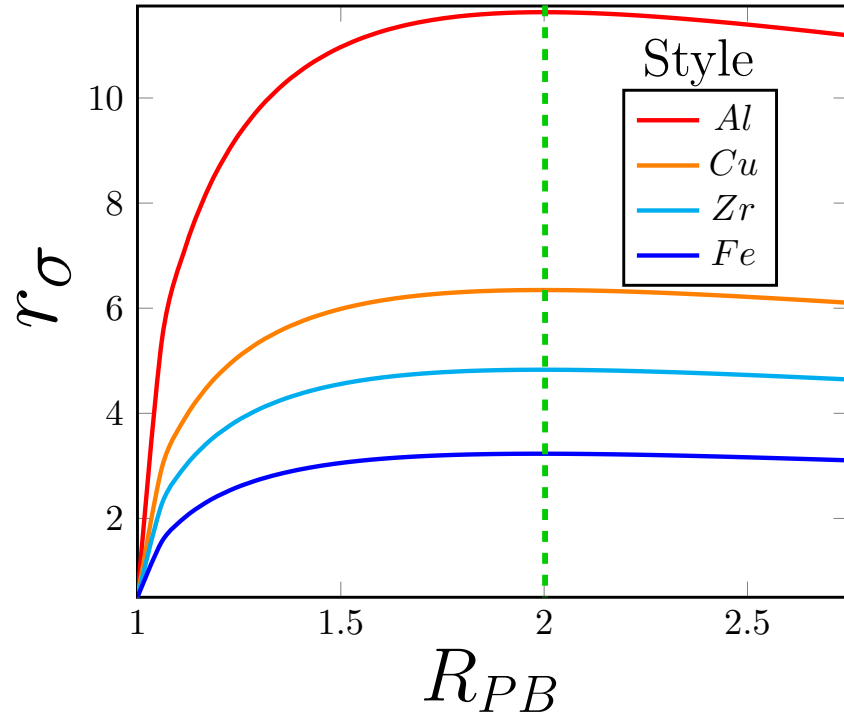
$$\alpha = 2 \frac{K_O \nu}{\sigma_{ut,M} (1 + \nu)} (R_{PB} - 1)$$



$$\hat{s}_{c,M} := \hat{s}_{c,O} \rightarrow r_{\sigma,c} \approx \frac{1}{2R_{PB}} \left( \sqrt{1 + 4 \frac{K_O \nu}{\sigma_{ut,M} (1 + \nu)} (R_{PB} - 1)} - 1 \right)$$



# $R_{PB}$ vs. $\nu$



$$r_{\sigma,c} \sim \frac{1}{R_{PB}} \sqrt{R_{PB} - 1} \quad , \quad \frac{\partial r_{\sigma,c}}{\partial R_{PB}} = 0 \quad \rightarrow \quad R_{PB} \approx 2$$

$$r_{\sigma,c} \sim \sqrt{\frac{\nu}{1+\nu}} \quad \rightarrow \quad \frac{\partial r_{\sigma,c}}{\partial \nu} \sim \frac{1}{2\sqrt{\nu(1+\nu)^3}} > 0$$

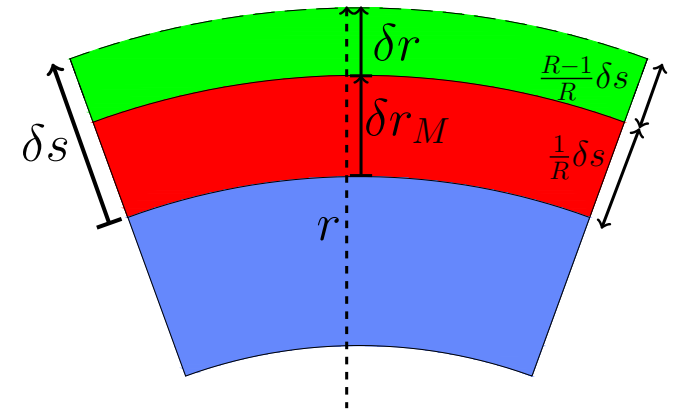
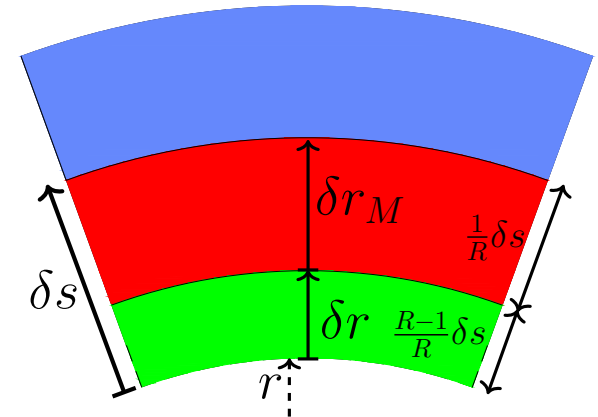
# Curved Boundary (Pipes)

## • Inner / Outer Corrosion

$$\begin{cases} r = R_I - \frac{R_{PB}-1}{R_{PB}}s \\ r = R_O + \frac{R_{PB}-1}{R_{PB}}s \end{cases} \rightarrow \sigma_{EL} = \int_0^s K \frac{dA}{A}$$

$$\begin{cases} dA = 2\pi \left( R_I - \frac{R_{PB}-1}{R_{PB}}s \right) \frac{R_{PB}-1}{R_{PB}} ds & \text{Inner} \\ dA = 2\pi \left( R_O + \frac{R_{PB}-1}{R_{PB}}s \right) \frac{R_{PB}-1}{R_{PB}} ds & \text{Outer} \\ A = \pi \left( R_O^2 - \left( R_I - \frac{R_{PB}-1}{R_{PB}}s \right)^2 \right) & \text{Inner} \\ A = \pi \left( \left( R_O + \frac{R_{PB}-1}{R_{PB}}s \right)^2 - R_I^2 \right) & \text{Outer} \end{cases}$$

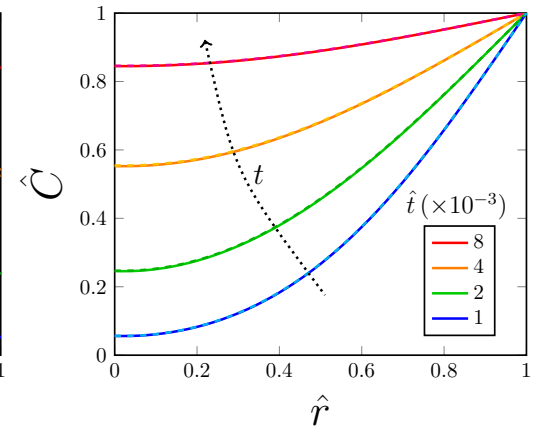
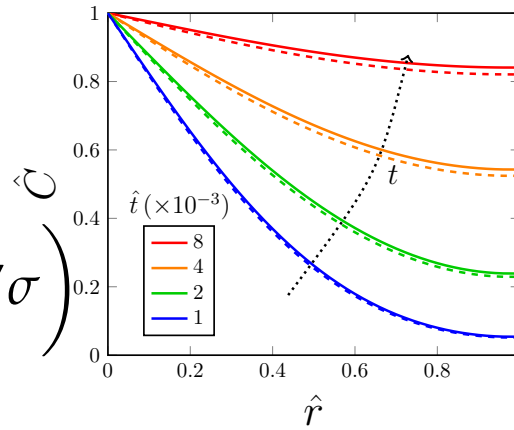
$$\begin{cases} \sigma_{EL} = K \frac{\nu}{1+\nu} \ln \left( 1 + \frac{R_{PB}-1}{R_{PB}} \left( \frac{2R_I}{R_O^2 - R_I^2} \right) s + \left( \frac{R_{PB}-1}{R_{PB}} \right)^2 \frac{s^2}{R_O^2 - R_I^2} \right) & \text{Inner} \\ \sigma_{EL} = K \frac{\nu}{1+\nu} \ln \left( 1 + \frac{R_{PB}-1}{R_{PB}} \left( \frac{2R_O}{R_O^2 - R_I^2} \right) s + \left( \frac{R_{PB}-1}{R_{PB}} \right)^2 \frac{s^2}{R_O^2 - R_I^2} \right) & \text{Outer} \end{cases}$$



# Diffusion - Reaction Framework

$$\hat{C} = \frac{C}{C_0}, \hat{r} = \frac{r}{R_O - R_I}, \hat{s} = \frac{s}{l}, \hat{t} = \frac{D}{R_O^2} s$$

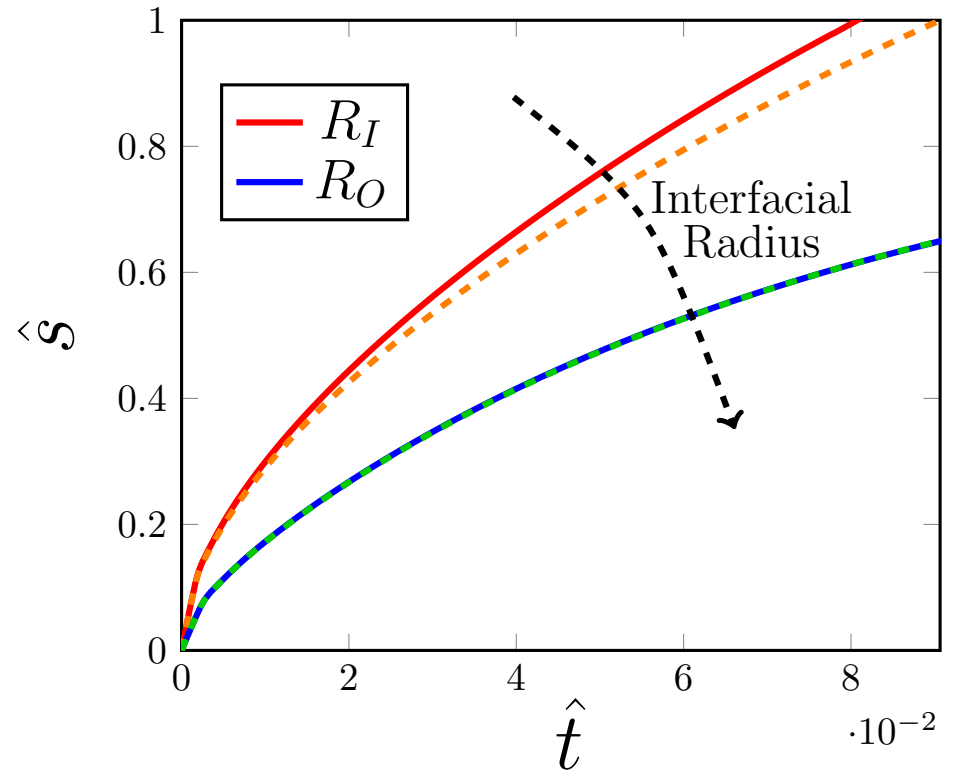
$$\begin{cases} \left( \frac{dC}{dt} \right)_{\text{Diff}} = -D \nabla \cdot \left( \nabla C + \frac{f\Omega}{R_u T} C \nabla \sigma \right) \\ \left( \frac{dC}{dt} \right)_{\text{Rxn}} = -kC \end{cases}$$



$$\begin{cases} \left( \frac{dC}{dt} \right)_{\text{Diff}} \sim D \frac{C_0}{R_O} \sim 10^{-15} \text{ mol.s}^{-1} \\ \left( \frac{dC}{dt} \right)_{\text{Rxn}} \sim kC_0 \sim 10^{-1} \text{ mol.s}^{-1} \end{cases}$$

→ All the oxygen consumed upon arrival.

$$\rightarrow s = \frac{\Omega}{2\pi r} \int_{R_I}^{R_O} C dA$$



# Thick Medium

$$\sum F_x = 0 \quad \tau = G\gamma \quad \int \sigma dy = \int \tau dx$$

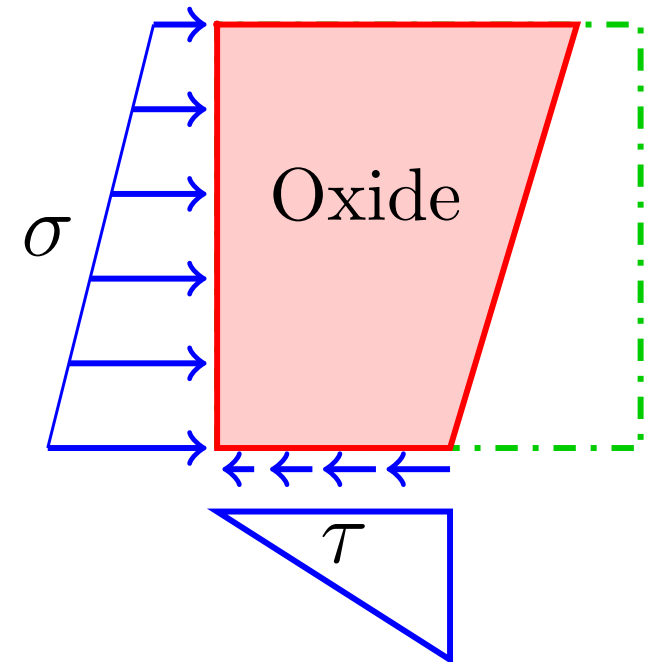
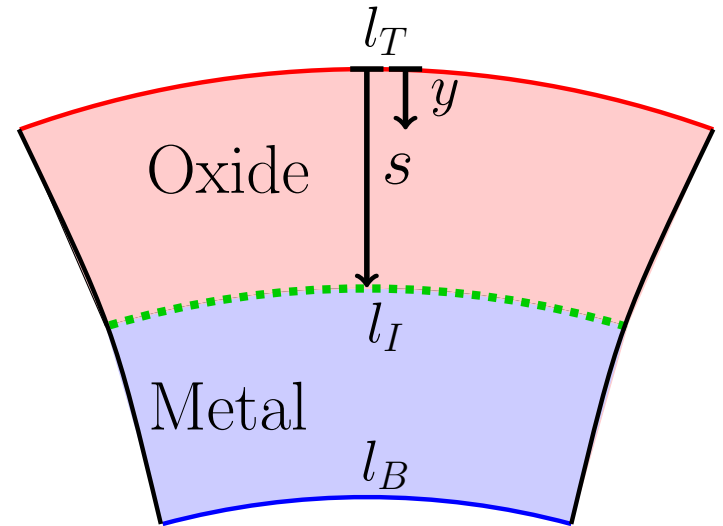
$$\begin{cases} el_T + (e + ra)l_I + ral_B = 2l_M a (e + r) \\ grl_T - (1 + gr)l_I + l_B = 0 \\ \left(\frac{G_O}{4s}\right)l_I^2 - \left(\frac{G_O l_T}{4s} + \frac{E_O s}{al_M}\right)l_I + \frac{E_O s}{al_M}(2al_M - l_T) = 0 \end{cases}$$

where:

$$e = \frac{E_O}{E_M}, g = \frac{G_O}{G_M}, r = \frac{l}{s} - \frac{1}{R_{PB}}, a = \sqrt[3]{R_{PB}}$$

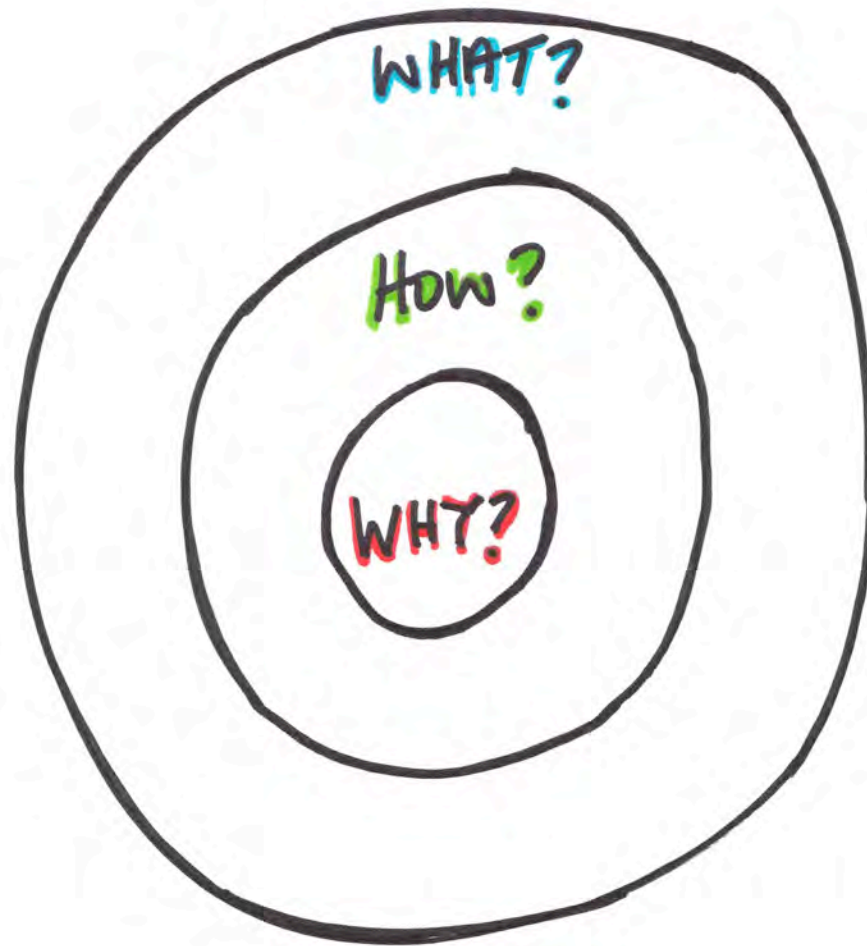
$$\rightarrow Al_I^2 + Bl_I + C = 0$$

$$\begin{cases} A = \frac{G_O}{2s}(e + ra) \\ B = \frac{2E_O s}{al_M}(r^2 ga + ra) - \frac{G_O al_M}{2s}(r + e) \\ C = -2E_O s(r^2 ga + r) \end{cases}$$





THANK YOU!



Email: [aryanfar@caltech.edu](mailto:aryanfar@caltech.edu)



**C. Allison**  
**ISS**

## **Estimates of the VVER-1000 Fuel Assembly Behavior and Possible In-Vessel Instrument Responses during SBO-like Conditions**

After the Russian invasion of Ukraine in February 2022 and attack on their nuclear power plants (NPPs), Innovative Systems Software LLC (ISS), contacted the Energy Safety Group LLC (ESG) in Ukraine, and offered their support in the event that any accident management strategies might need to be updated in light of the increased risk of station blackout (SBO) conditions. ESG had recently published the results of their "Post-Fukushima" safety analysis of the Zaporizhzhya NPP Unit 1 using a combination of RELAP5 and MELCOR. ISS, and other collaborators had provided similar support for the emergency assessment of the Fukushima Daiichi accident using RELAP/SCDAPSIM.

In preparation for any analysis that might have been required on an accelerated time frame, it was decided to perform a series of baseline calculations that could then be used to provide preliminary assessments of the reactor and containment behavior in the event of an SBO with the added possibility of externally caused damage to the containment, reactor coolant system (RCS), or associated safety systems. This approach is similar to that used in support of the IAEA emergency response team as the Fukushima Daiichi accident was in progress. It was also decided that a combination of RELAP/SCDAPSIM and ASYST would be used. RELAP/SCDAPSIM/MOD3.4 would be used for the initial baseline studies since it is the widely used version of RELAP/SCDAPSIM and has been used in the analysis in the widest range of historical and ongoing experiments as well as our initial Fukushima Daiichi calculations. However, it is limited in its ability to consider response of the containment under severe accident conditions. ASYST VER 3.5, which has containment modelling options being developed in conjunction with our Japanese collaborators, will be able to provide direct comparisons with the original ESG calculations using RELAP5 and MELCOR. This paper describes the basic features of RELAP/SCDAPSIM/MOD3.4 and ASYST VER 3.5, the VVER-1000 input models that are being used, and a brief presentation and discussion of some of the key results from these baseline calculations.



# Baseline Calculations - Estimates of the VVER-1000 Fuel Assembly Behavior and Possible In-Vessel Instrument Responses during SBO-like Conditions

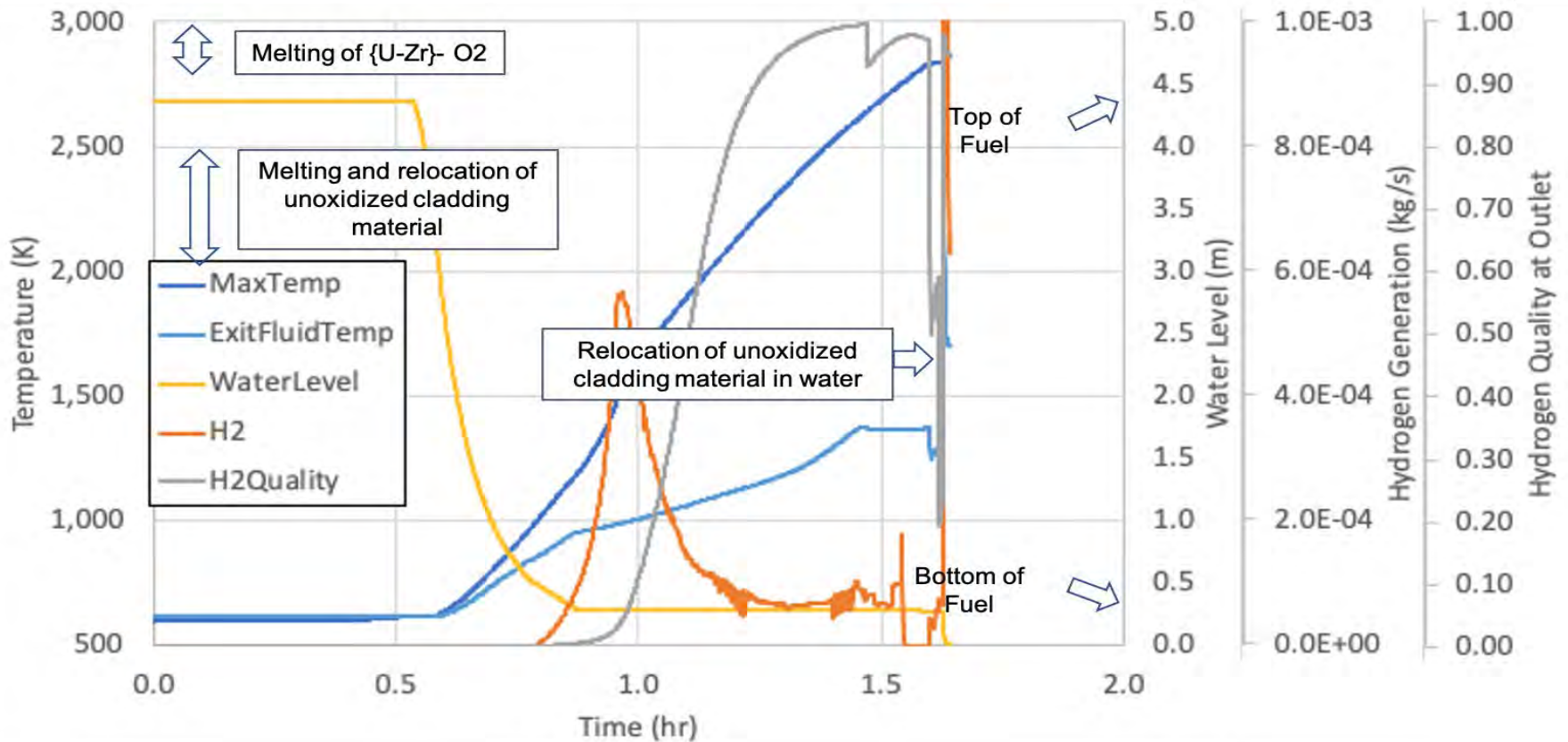
Dr. Chris Allison  
Innovative Systems Software (ISS)  
with support from  
INRNE and Worley Parsons (Bulgaria)  
University of Alexandria (Egypt)  
Energy Safety Group LLC (Ukraine)  
ENSO (Spain)

# Presentation will focus on assessment of VVER fuel assembly behavior during initial heating and fuel melting under Fukushima-Daichi-like SBO

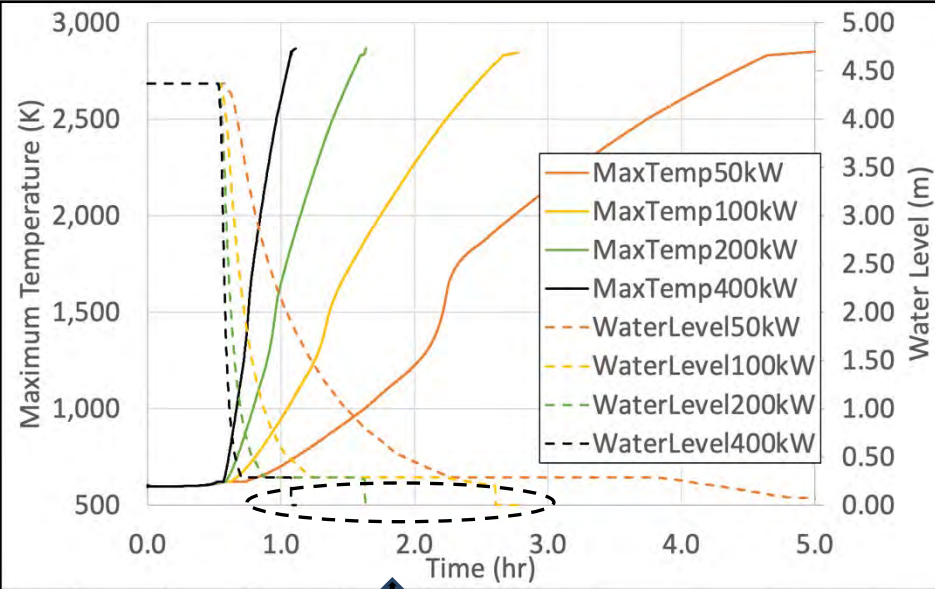
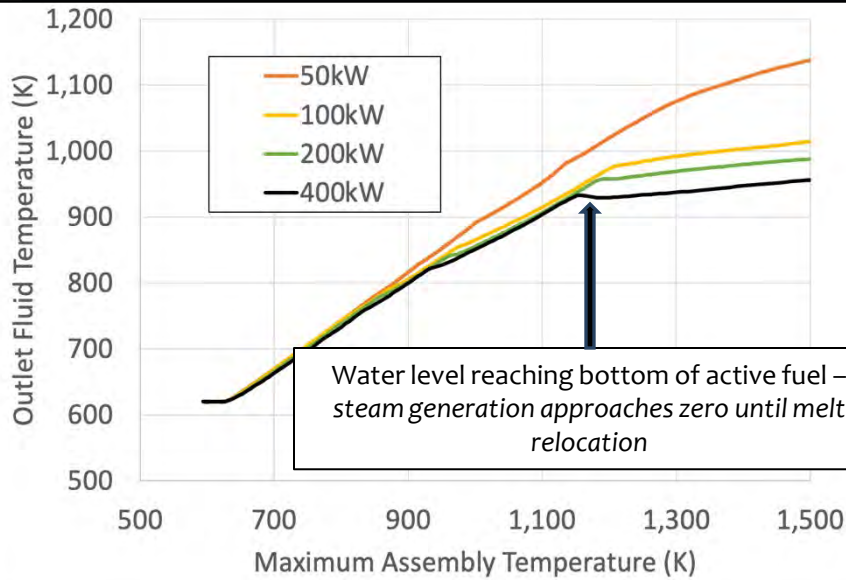
- \* **Background** (Presented at HND-2022 meeting – June 2022)
  - \* Input models include representative fuel assembly, full core, and plant models developed for and by VVER user community over past several years
  - \* Sensitivity studies looking at influence of wide variation in possible TH conditions and **possible indicators observable by operators (water level, exit fluid temperatures, instrumentation failures)**
- \* **Impact on behavior and indicators** from intentional and unintentional depressurization with accumulator water injection
  - \* *Uncertainties in depressurization and misleading water level indicators major factors in FD-SBO*



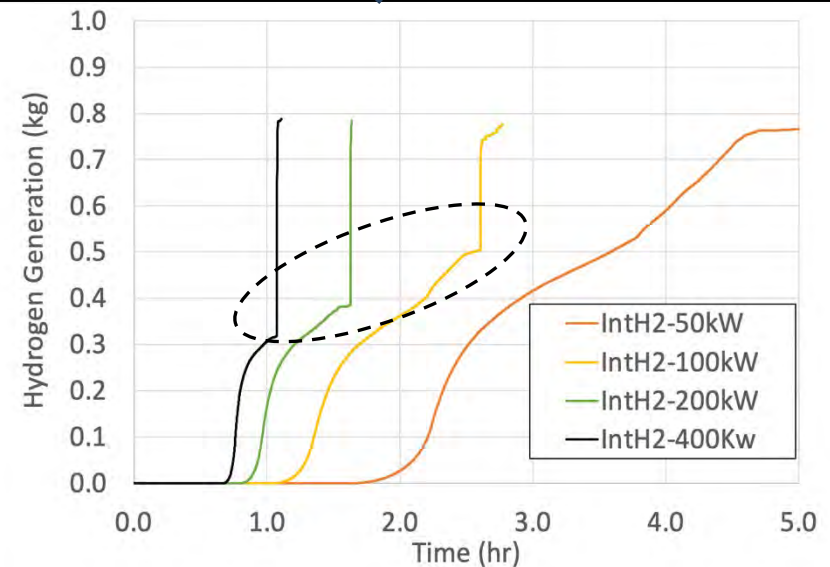
# Expected behavior of a representative VVER fuel assembly at constant pressure (TMI-2 like conditions - No accumulator water injection)



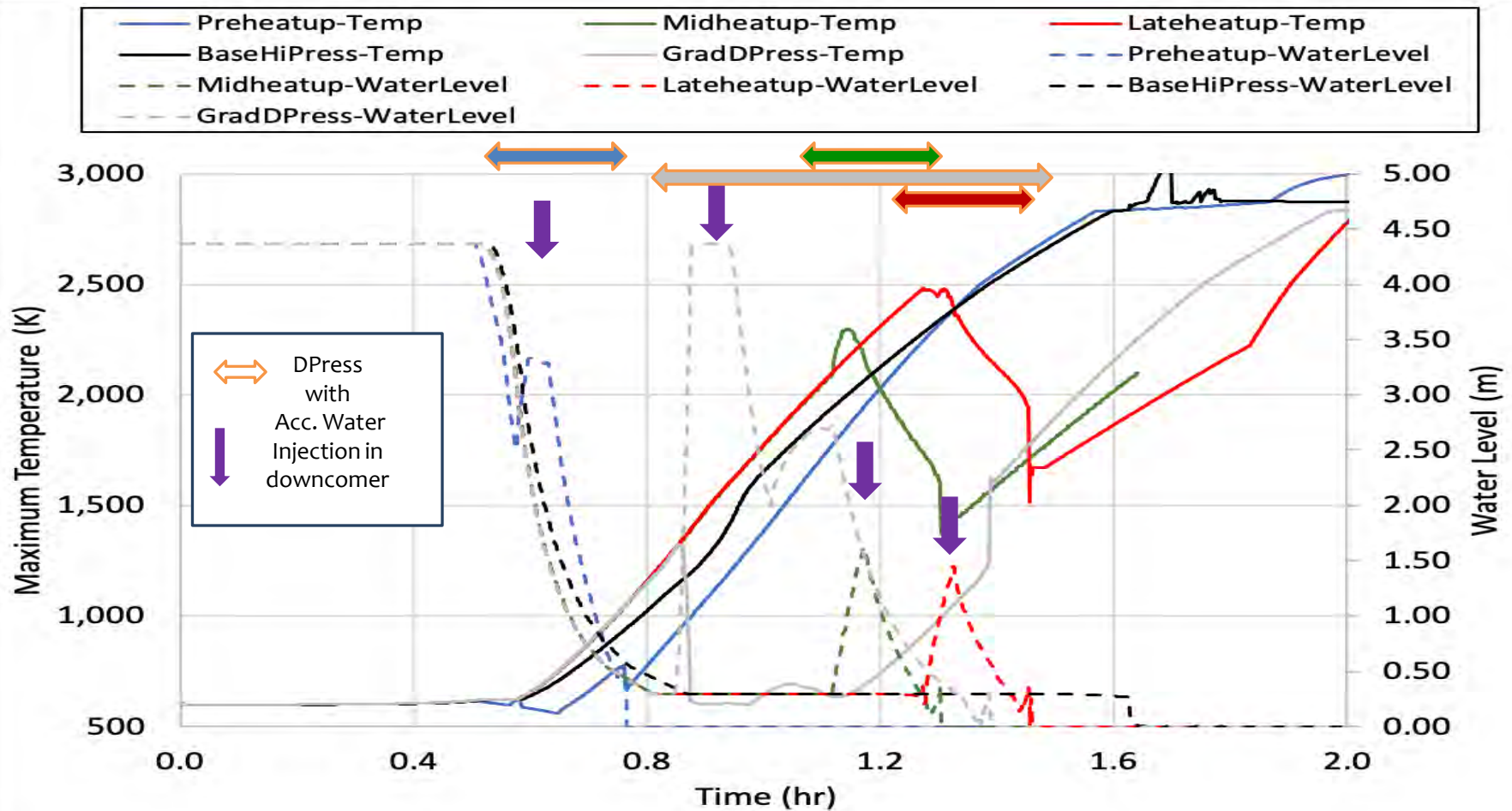
Good correlation between key parameters and indicators for variation in peak assembly power – Hi-Pressure



Relocation of material into water at bottom of assembly



# Behavior more complex with variation in depressurization conditions with associated accumulator injection

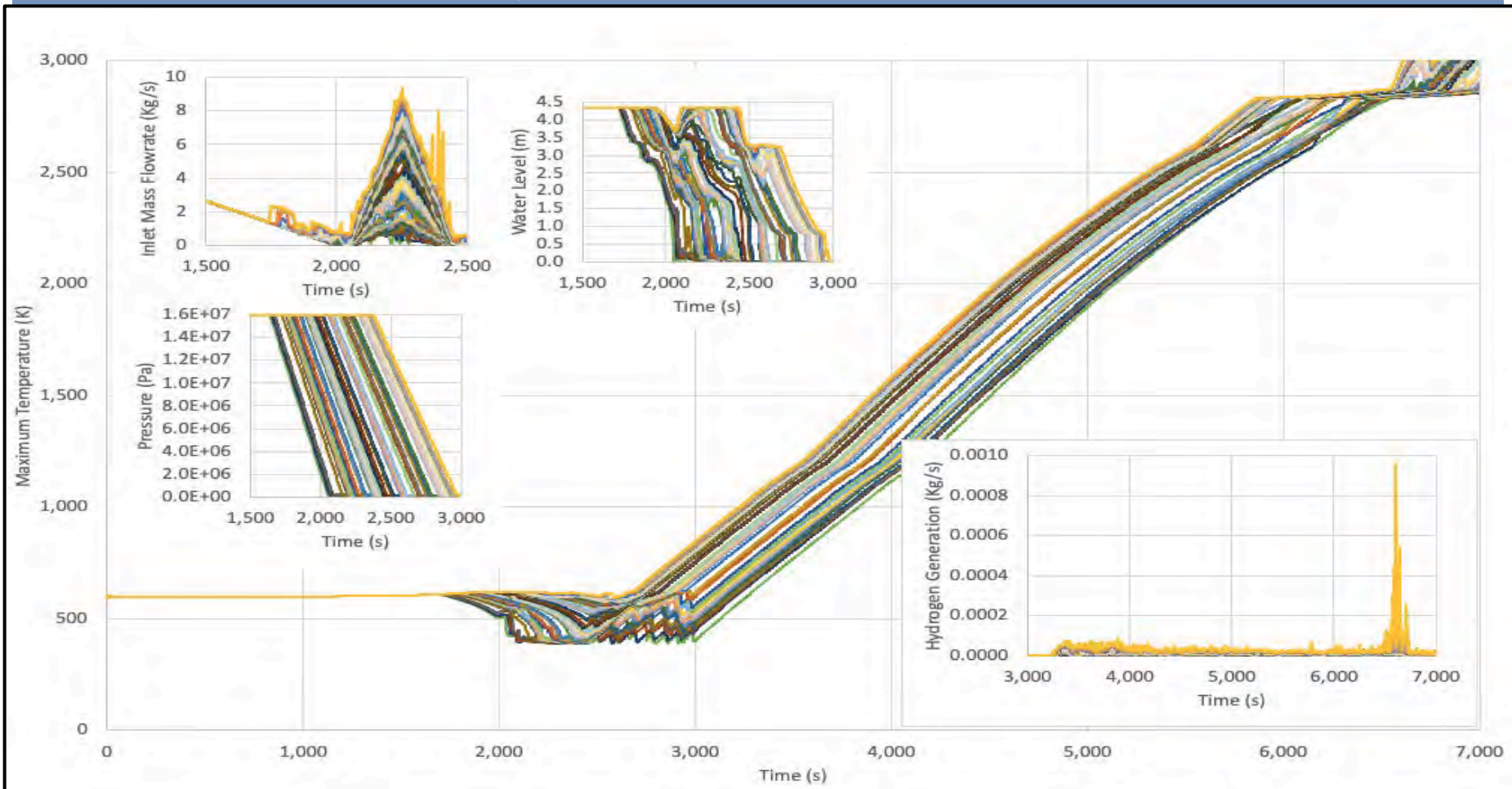


Results are relatively insensitive to local variations in timing of start of depression and magnitude at water injection in early stages of core uncovering ( $T < \text{DBA limits}$ ) – see examples in next slides



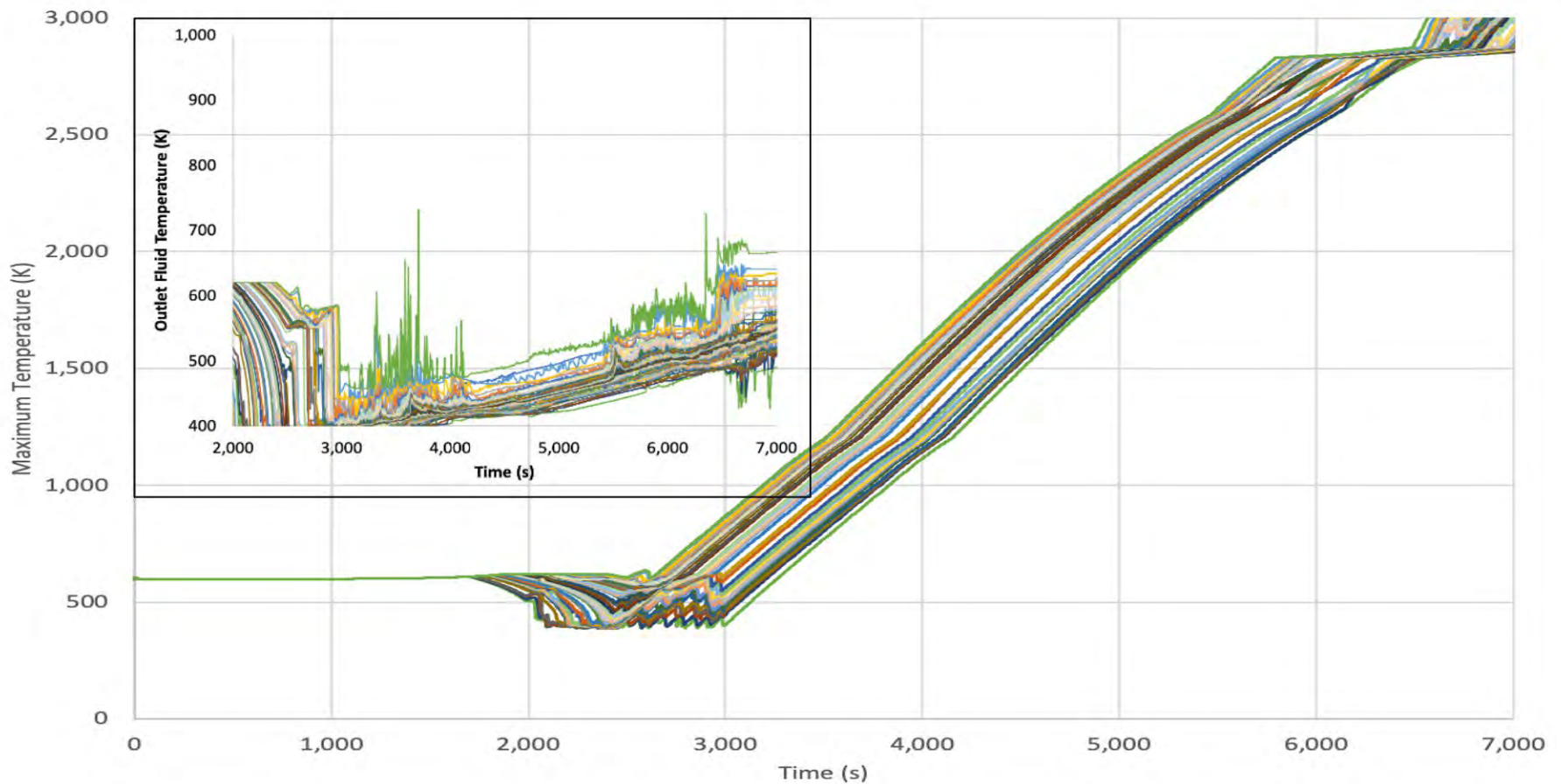
# Sensitivity to variation in depressurization times and magnitude of water injection - at beginning of core uncover

(Automated Sensitivity Analysis results)

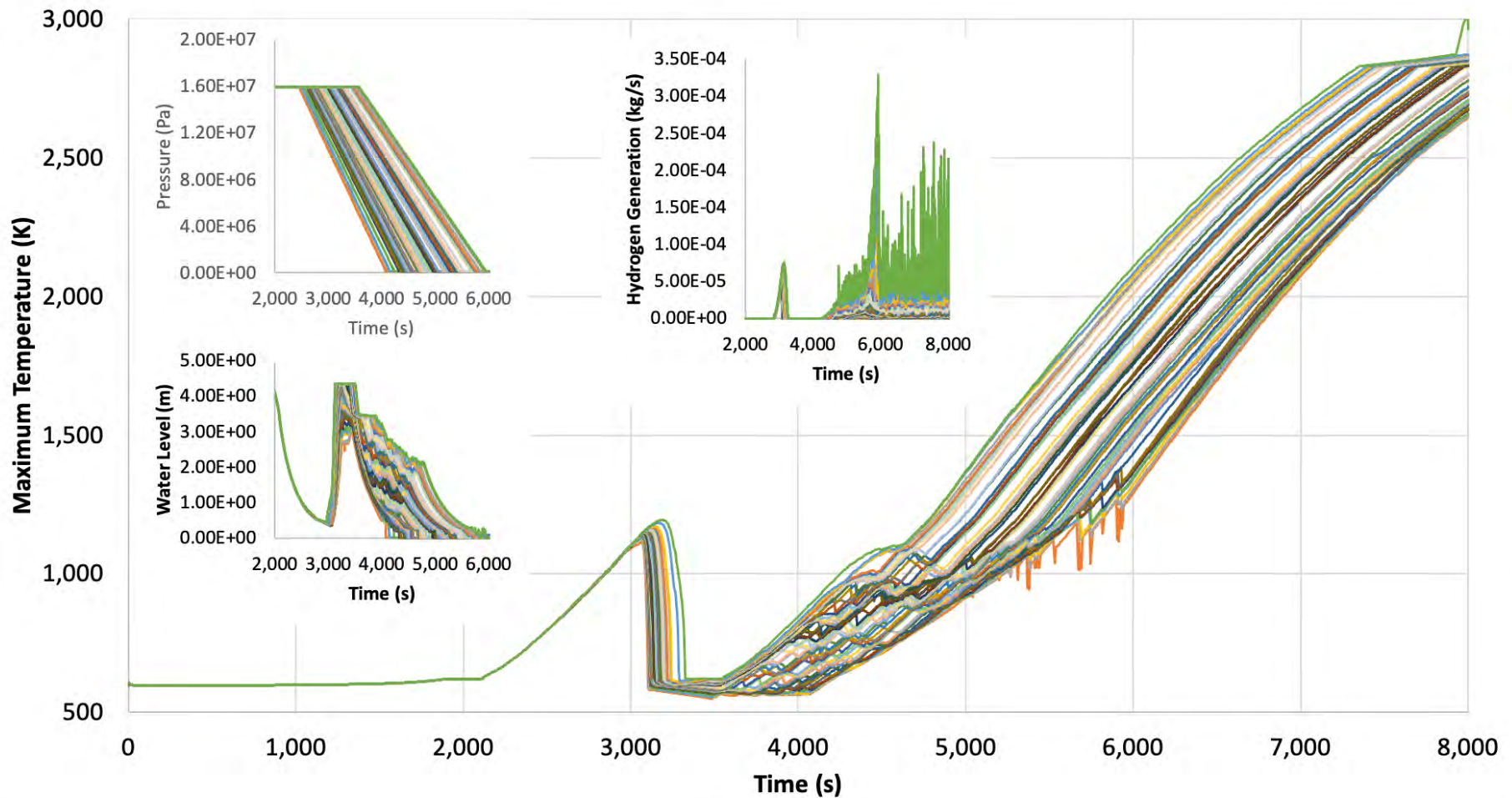


# Variation in relationship between outlet fluid and peak assembly temperatures - at beginning of core uncover

(Automated Sensitivity Analysis results)

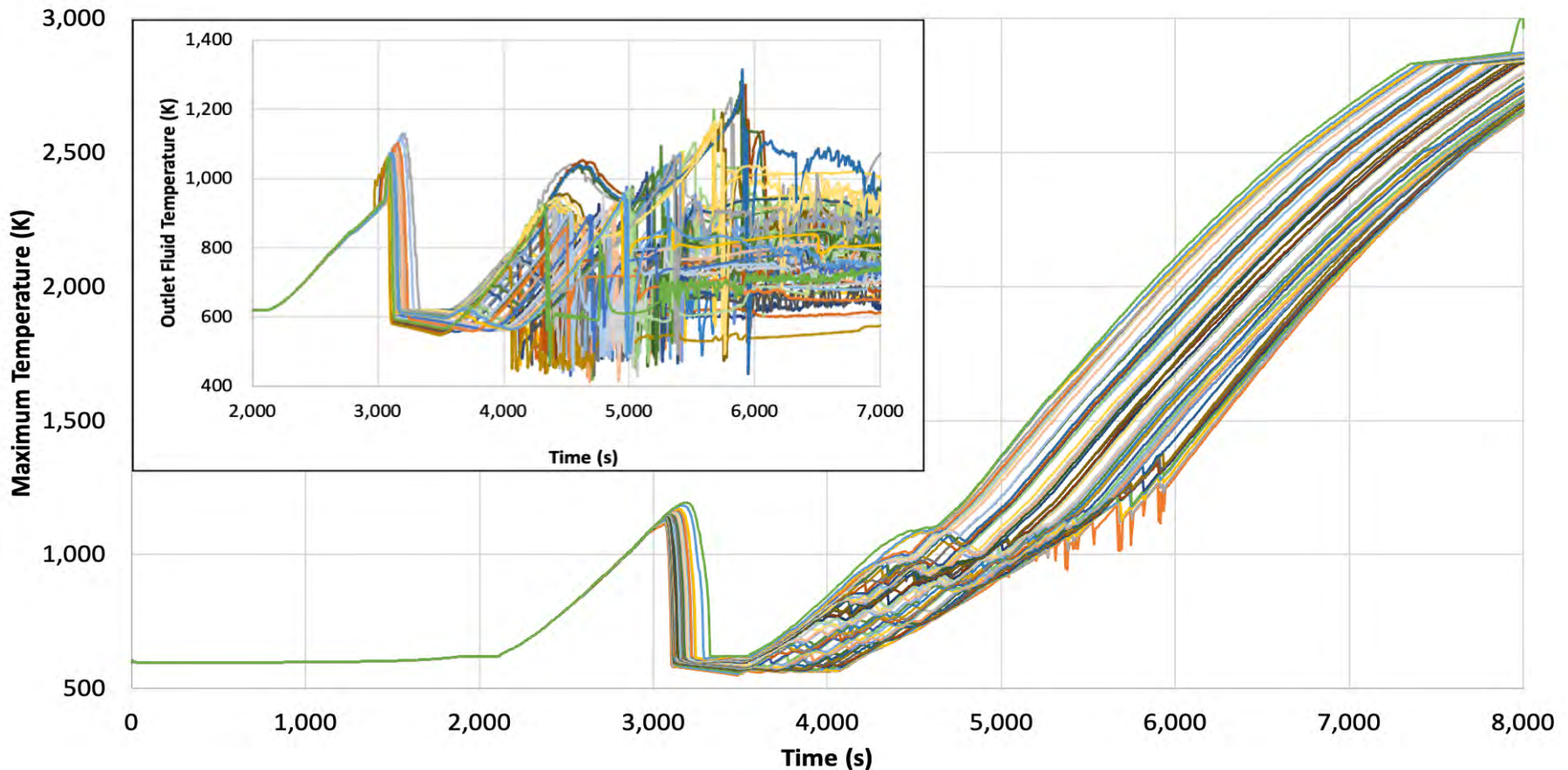


# Sensitivity to variation in depressurization times and magnitude of water injection – gradual depressurization starting within DBA limits





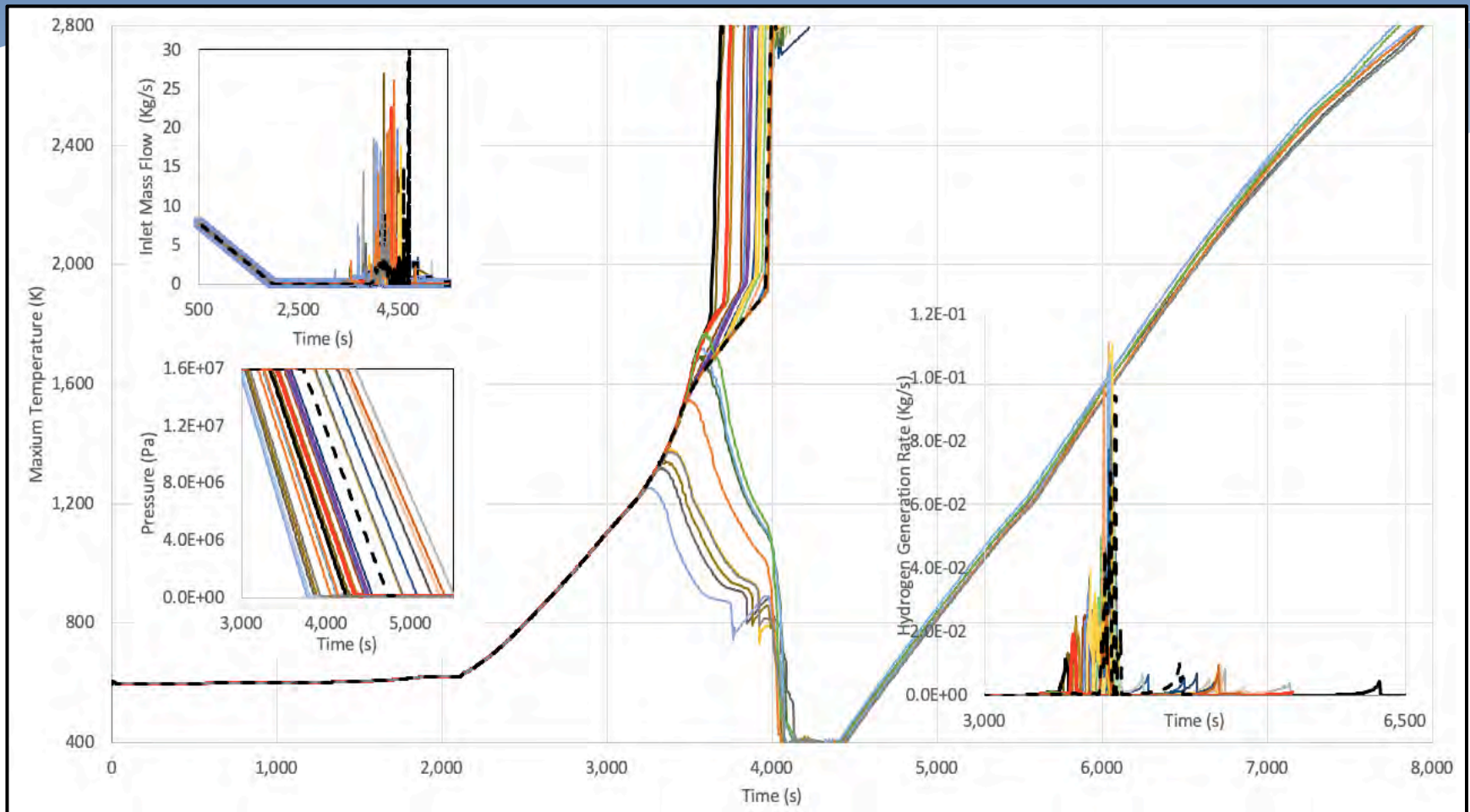
# Variation in relationship between outlet fluid and peak assembly temperatures – gradual depressurization starting within DBA





# Sensitivity to variation in depressurization times and magnitude of water injection - at transition from DBA limits

(Automated Sensitivity Analysis results)



# General conclusions and closing remarks

- \* **Our detailed analysis using generic VVER-1000 models can provide some guidance** on how the system will respond during an SBO with uncertainties in TH conditions similar to those of Fukushima Daiichi
- \* However **plant specific design features and conditions – radial/axial power peaking, system set points, and general SAM strategy, needs to be used in final analysis** to
  - \* Best optimize the strategies
  - \* Develop specific correlations/relationships between key parameters (heating rates, time to reach fuel melting... and observable indicators
- \* The various observable indicators, **exit fluid temperatures, water levels, instrumentation failures (melting) can be significant factors in helping reduce uncertainties associated TH boundary conditions**
  - \* Cross-correlation of relationships between the observable indicators, ie fluid temperatures vs water level, can minimize the impact of misleading indicators such as those observed in FD
  - \* ***Transition to instrumentation qualified for BDBA conditions, ie similar to those used in SA experiments like KIT QUENCH could reduce uncertainties in current SAM strategies***

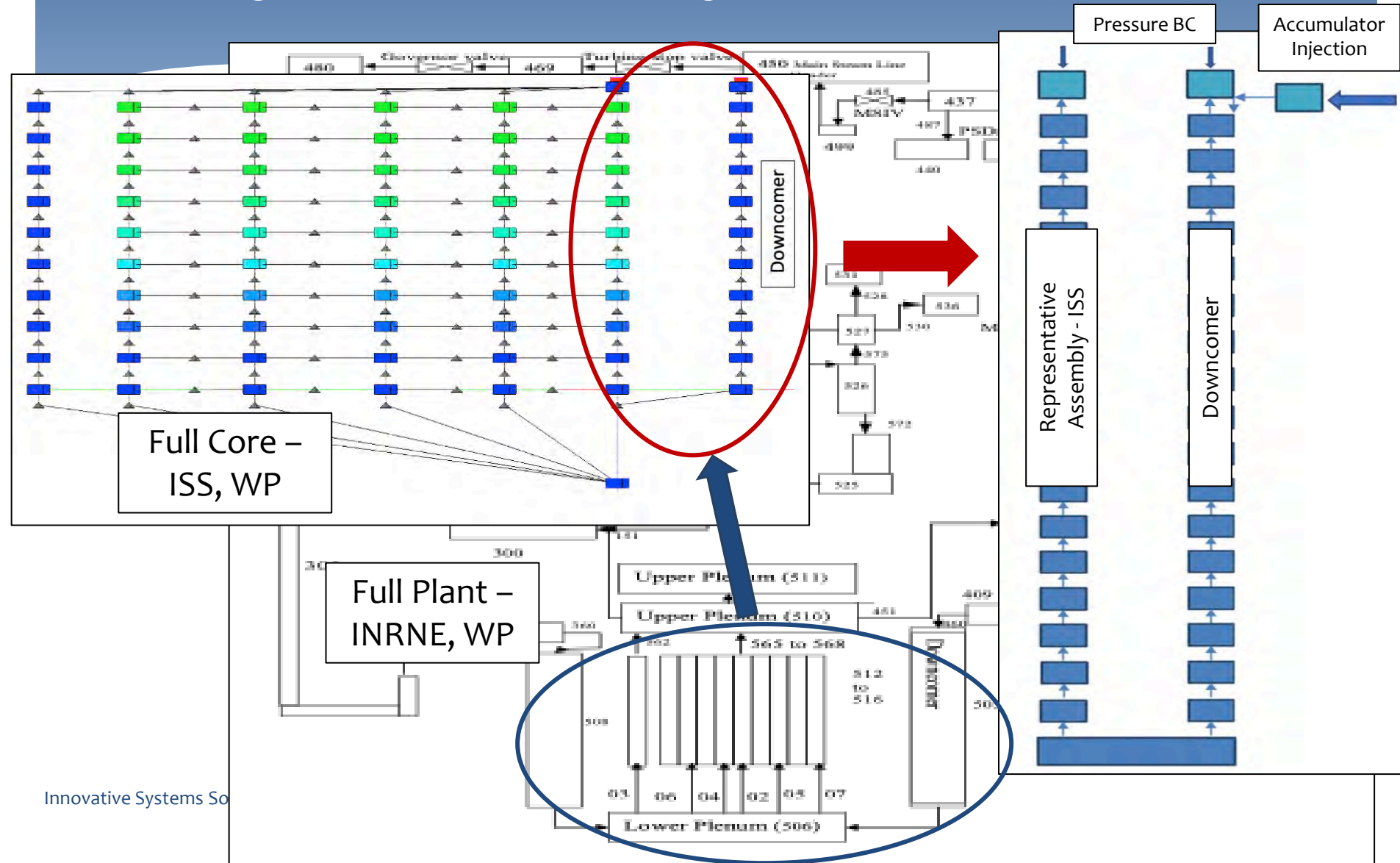
# Extra Slides

## Analysis and sensitivity studies are consistent with results of experiments and DBA/BDBA conditions including Zr melting and relocation and [U-Zr]-O<sub>2</sub> liquefaction ( $\geq 2900$ K)

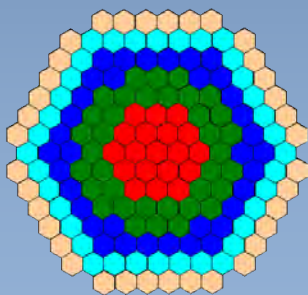
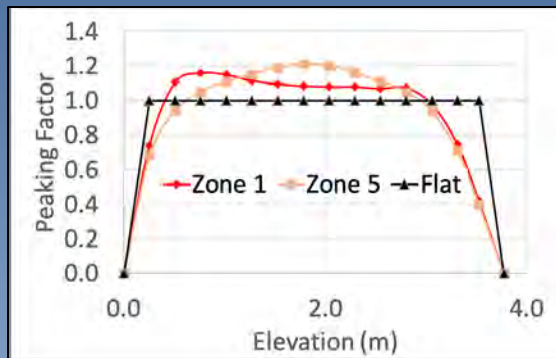
- \* Hydrogen generation occurs primarily during initial heatup ( $T < 2800\text{K}$ )
  - \* Maximum hydrogen rates occur during relocation of melts into water at bottom or below of fuel due to increased steam generation
  - \* *Temporary water addition also shows maximum generation rates consistent with Quench and other integral experiments with water addition)*
- \* Good correlation of exit fluid and maximum assembly temperatures during early heat up until water level drops to bottom of assembly or water addition
  - \* Exit fluid temperatures show clear increase with relocation of melts into water at bottom or below of fuel due to increased flow with assembly with increased steam generation
- \* Water levels will drop asymptotically to bottom of fuel without addition of water
  - \* Depressurization will result
    - \* Temporary cooling due to increased steam generation
    - \* Rapid reduction in water levels
- \* ***Influence of natural circulation not considered but will be addressed using detailed 2D core model (in-vessel) and full plant models (RCS)***



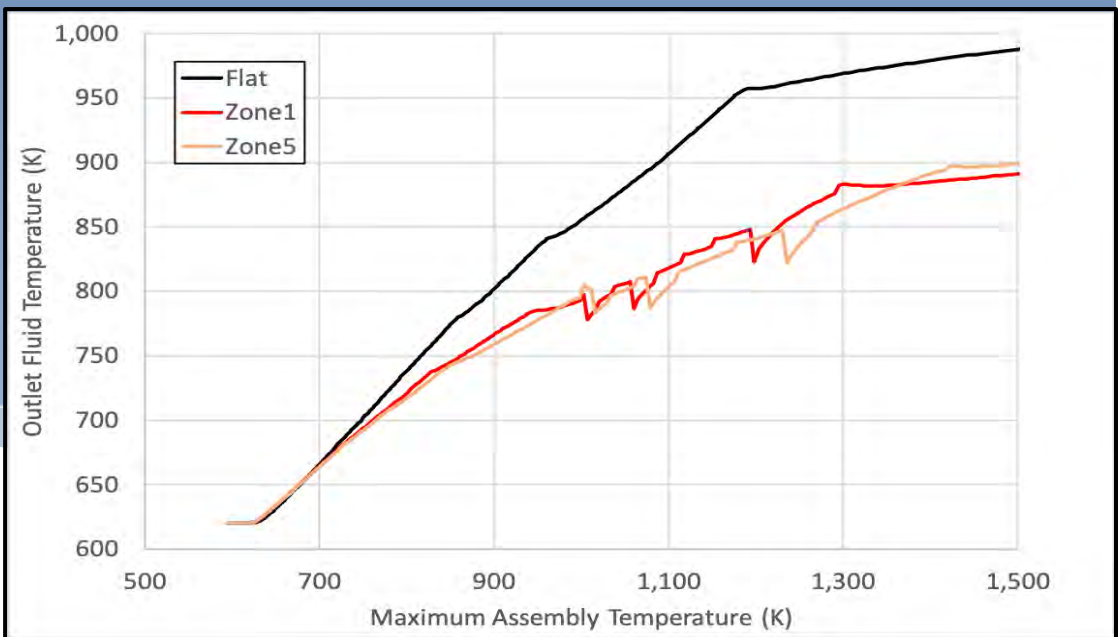
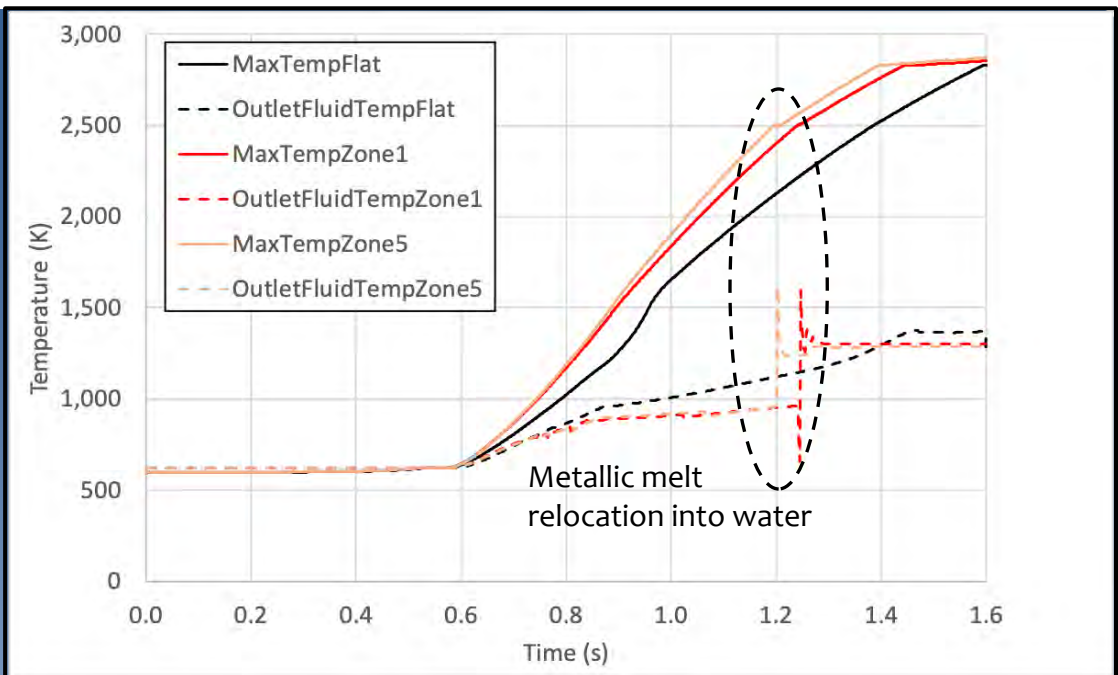
Input models developed and improved through international collaboration  
– ISS, INRNE and Worley-Parsons (Bulgaria), University of Alexandria (Egypt), with input from Energy Safety Group LLC (Ukraine)



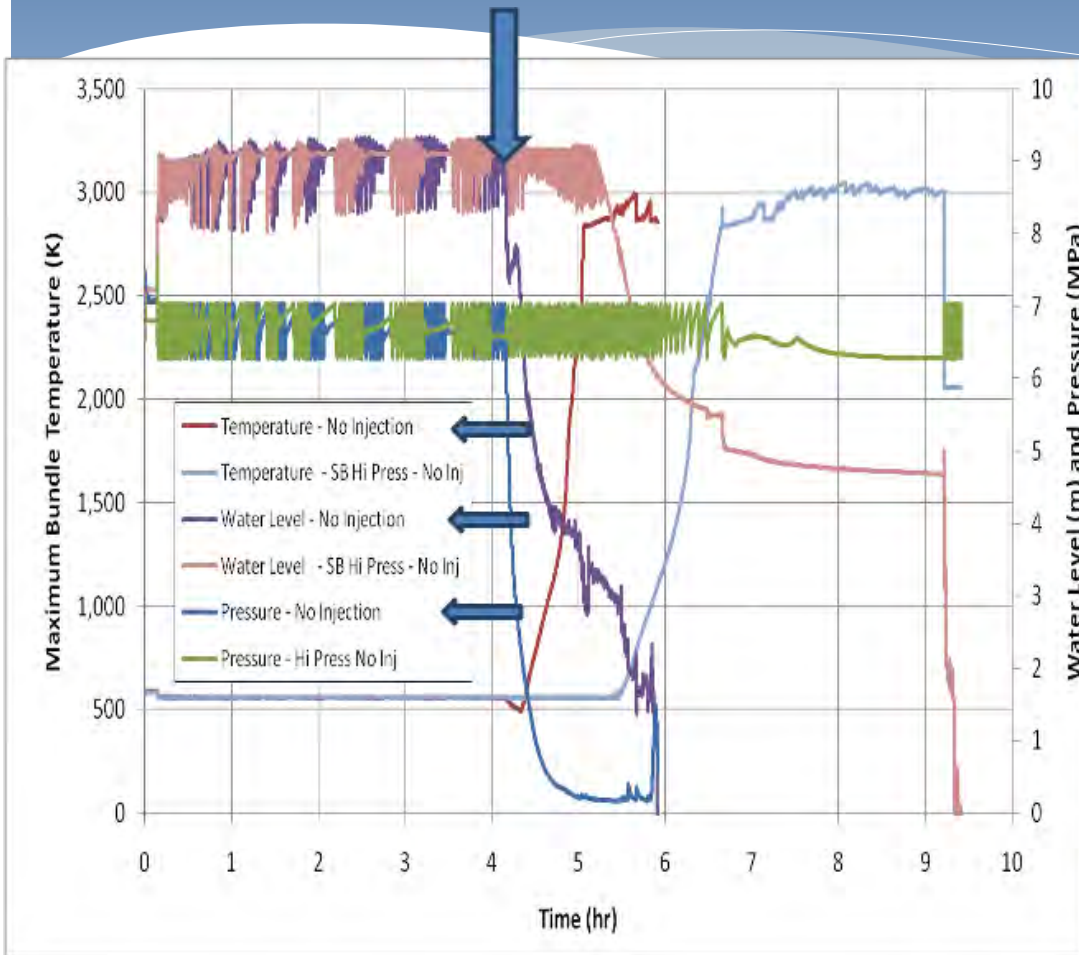
# Good correlation between key parameters and indicators for variation in axial power profiles – Hi-Pressure



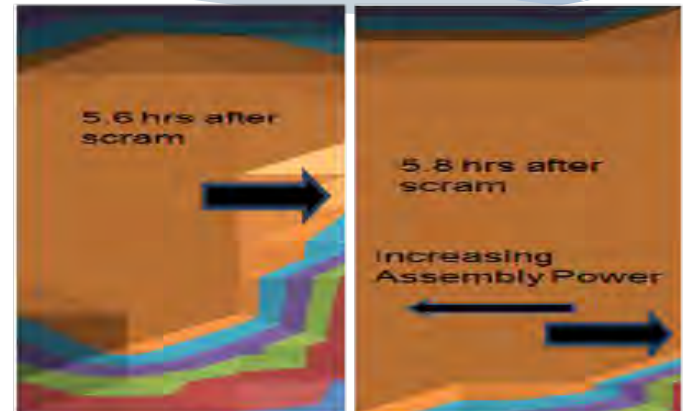
- ZONE 1
- ZONE 2
- ZONE 3
- ZONE 4
- ZONE 5



Fukushima Daiichi analysis using RELAP/SCDAPSIM shows depressurization likely to increase mass of {U-Zr}-O<sub>2</sub> relocating into LP initially (with likely early relocation of control blade/channel box materials)



**Depressurization prior to fuel melting**



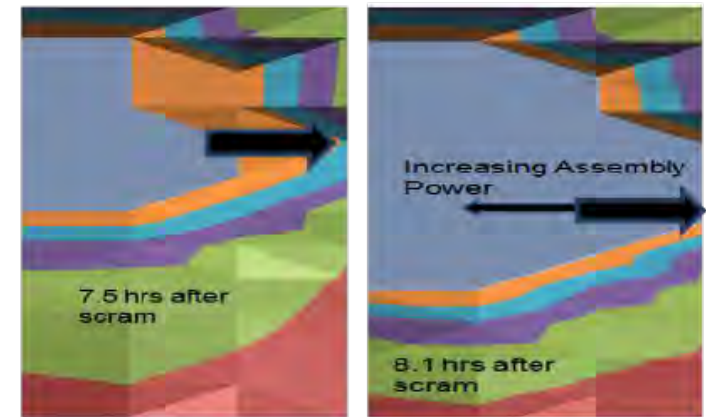
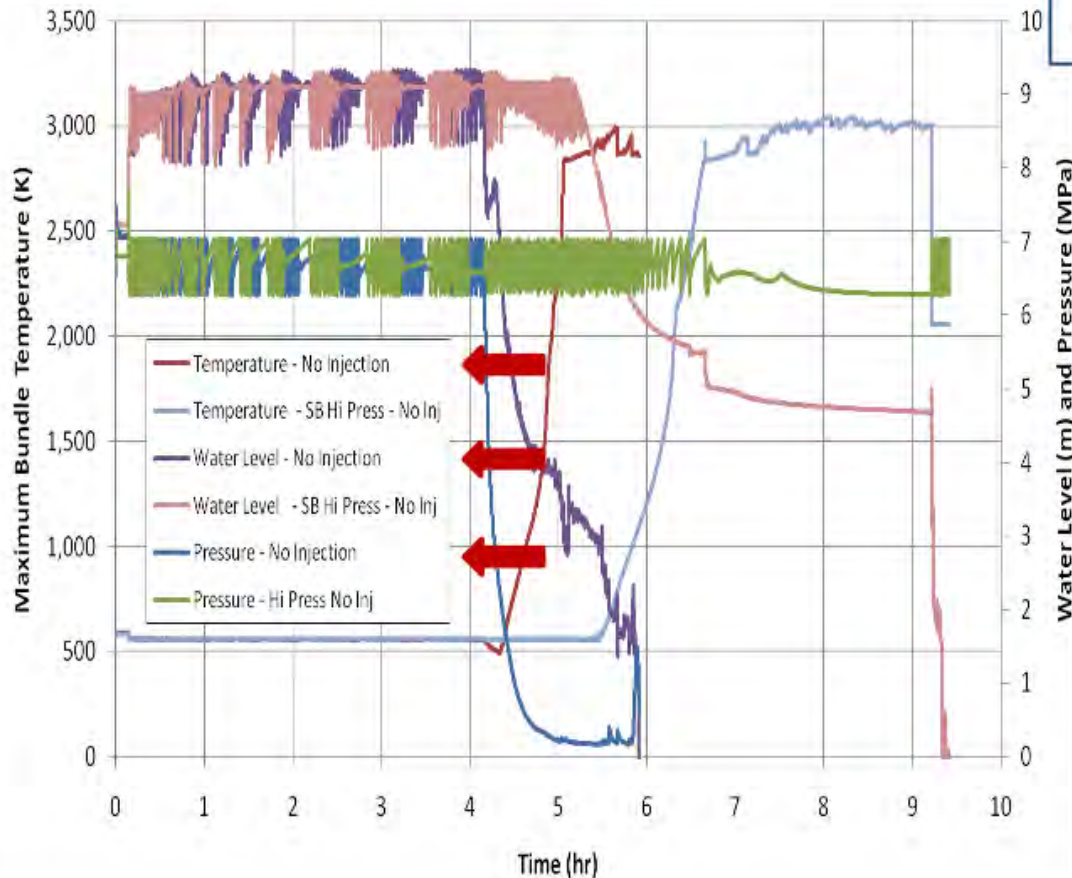
Most likely failure points of crust due to natural circulation in melt





# Fukushima Daiichi analysis using RELAP/SCDAPSIM shows late depressurization make TMI-2-like $\{U-Zr\}-O_2$ relocation into LP more likely (with more retention of metallics in core)

**No depressurization prior to fuel melting**



**Most likely failure points of crust due to natural circulation in melt**







**W. Tromm**  
**KIT**

## **Overview on LWR nuclear safety research at KIT**

Walter Tromm gave an overview on the Reactor Safety research activities at KIT in the framework of the HGF program NUSAFE.

He described the experimental and modeling capabilities for design basis accidents & materials research as well as for beyond design basis accidents & emergency management. Most of the research is embedded in national and international collaborations.

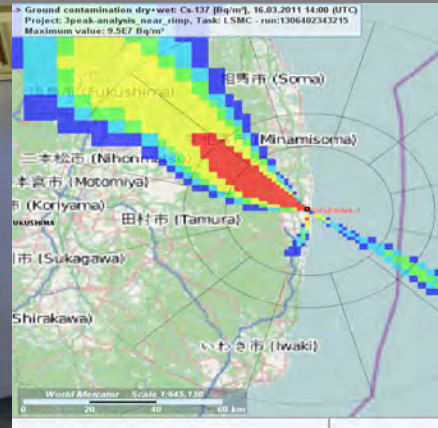
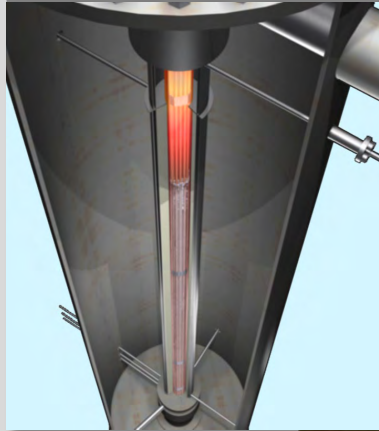
As an integral part of the Helmholtz (HGF) research, the following current and future activities have been described:

- Contributions to immediate and long-term impact on reactor safety
- International cutting-edge research by multidisciplinary and innovation with a long-term perspective
- Competencies for the operation of large-scale facilities
- Enhancement of cooperation with important international players
- Ensure competencies for continuing tasks in nuclear technology for research, industry, and authorities
- Establishment of a wider application in the research field energy

# 27th QUENCH Workshop at KIT

## Overview Programme NUSAFE at KIT and Helmholtz Association

Th. Walter Trome, Programme Nuclear Waste Management, Safety and Radiation Research



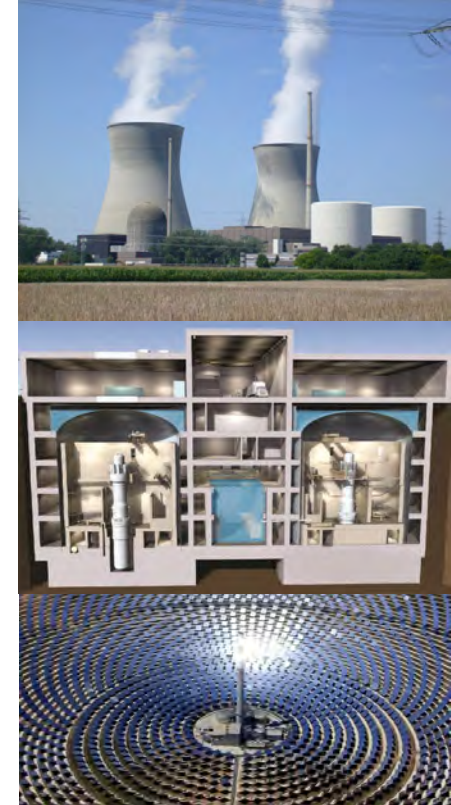
# Structure of the Program NUSAFE

- Topic 1 – Nuclear Waste Management
  - nuclear waste disposal
  - predisposal
  - fundamental scientific aspects
- Topic 2 – Reactor Safety
  - design basis accidents & materials research
  - beyond design basis accidents & emergency management



# Strategy Topic 2: Reactor Safety

- Contribution to and assessment of the international developments in reactor safety technology
  - Lifetime extension for existing reactors
  - New builds and innovative concepts
- Leading edge research on key aspects of reactor safety
  - To remain a competent partner in international projects, bodies and committees
  - To ensure Germany's lasting influence on reactor safety in Europe and worldwide
- Providing an attractive education, training and research hub for next generation experts
- Synergies of scientific expertise within research field energy, e.g.:
  - Liquid metal for MTET program,
  - Hydrogen Safety for MTET program,
  - Agent Based Modelling for ESD program





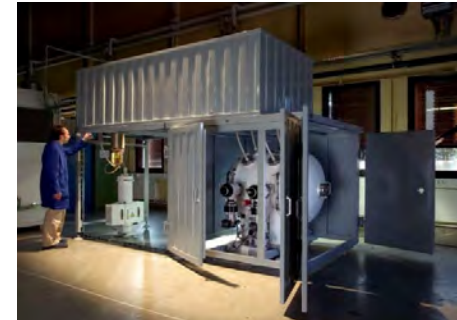
# Objectives Topic 2, Subtopic 1:

## Design Basis Accidents and Materials Research

- Coupled reactor safety simulation tool for the complete calculation chain from the creation of input data over the conduction of core analyses to the analysis of design basis accidents as well as their validation
  - Multiphysics and multiscale approaches
  - Experiments at the high-pressure test facility COSMOS-H
- Safety investigations for liquid-metal-cooled innovative reactor systems and development of advanced corrosion-mitigation strategies
  - Test of devices under real operational and accidental conditions in the KALLA and KASOLA laboratory
  - Corrosion test facilities COSTA and CORRIDA for liquid lead coolant



COSMOS-H



GESA  
Pulsed Electron Beam Treatment

# Development of advanced safety analysis tools for Small Modular reactors (SMR)

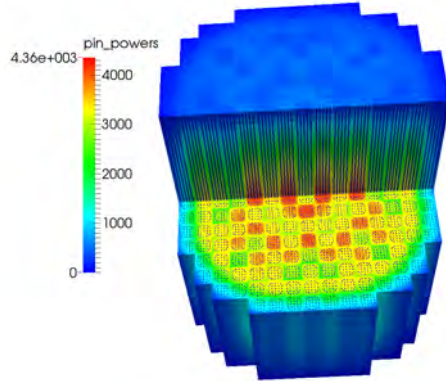


- **EU-project McSAFER:**  
Improving safety analysis methodologies
- Increased deployment of different SMR-design in EU and worldwide
- BMBF-initiative „Innovationspool-Projekts „**Sicherheitsbewertung generischer kleiner modularer Reaktoren (SMR)**“ to support:
  - Develop advanced simulation tools for safety analysis of SMR to be build in Europe
  - Contribute to the validation of numerical simulation tools using experimental data relevant for SMR e.g. data generated at KIT COSMOS-H facility
  - KIT Focus:
    - advanced neutronic (MC and transport) and thermal hydraulics (two-phase, porous-media) for the core and plant behavior of SMR
    - Experimental investigations at COMSOS-H facility (safety-relevant TH phenomena e.g. boiling, CHF)

# Reactor dynamics and accident analysis: Thermal Hydraulics Code Development

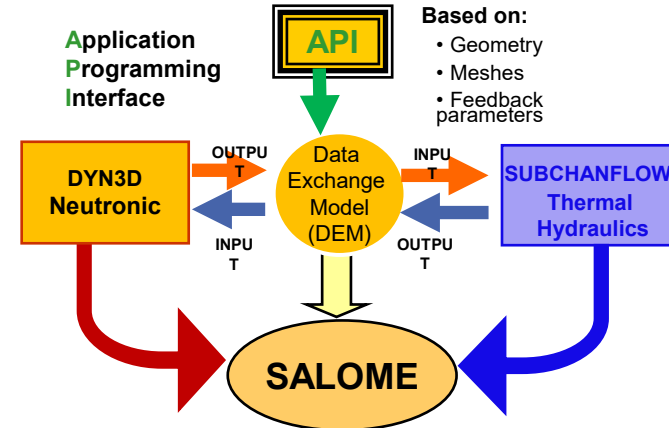
## SUBCHANFLOW Code (In-house):

- Fast running code with flexible geometry
- Diverse working fluids (water, gas, liquid metals)
- Coupled with different neutronics, thermo-mechanic and thermal-hydraulics codes



Full PWR Core SERPENT2/SCF Solution

## Part of the EU NURESIM Platform



## NURESIM- Platform: Code coupling Strategy

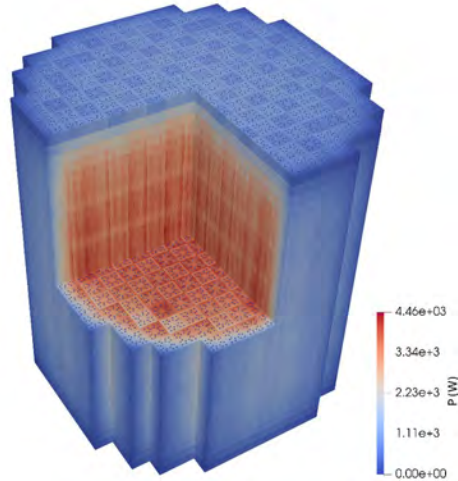


EU NURESAFE (2013-2016)



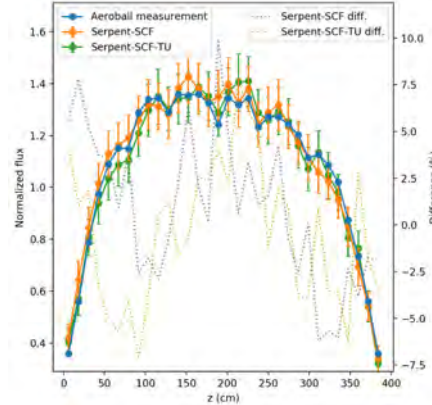
EU McSAFE (2017- 2020)  
coordinated by KIT

# Full Core Depletion of a PWR and VVER (pin-level): SERPENT/SCF/TU



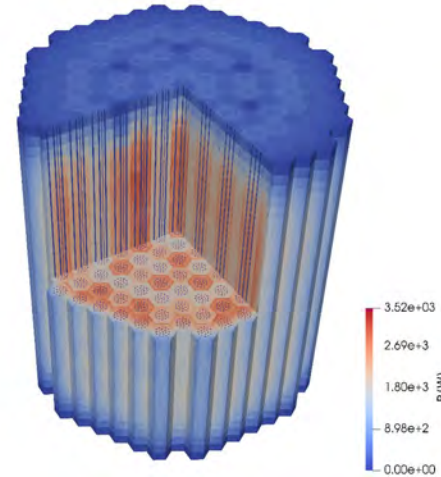
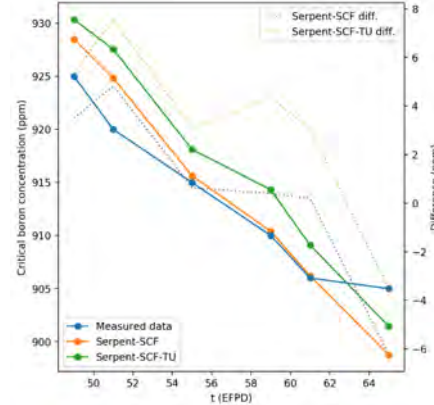
## PWR pin power distribution

- Local feedbacks between N, TH and TM considered
- Pin/subchannel level simulation



## PWR validation with experimental data

- Pin-level neutron flux measurements
- Critical boron concentration



## VVER pin power distribution

- Predicted / measured power distribution

**First-of-a-kind depletion analysis of real LWRs**



# McSAFER: High-Performance Advanced Methods and Experimental Investigations for Safety Evaluation of Generic SMR

■ Start: 1.9.2020 - 1.8.2023

■ KIT Coordinator

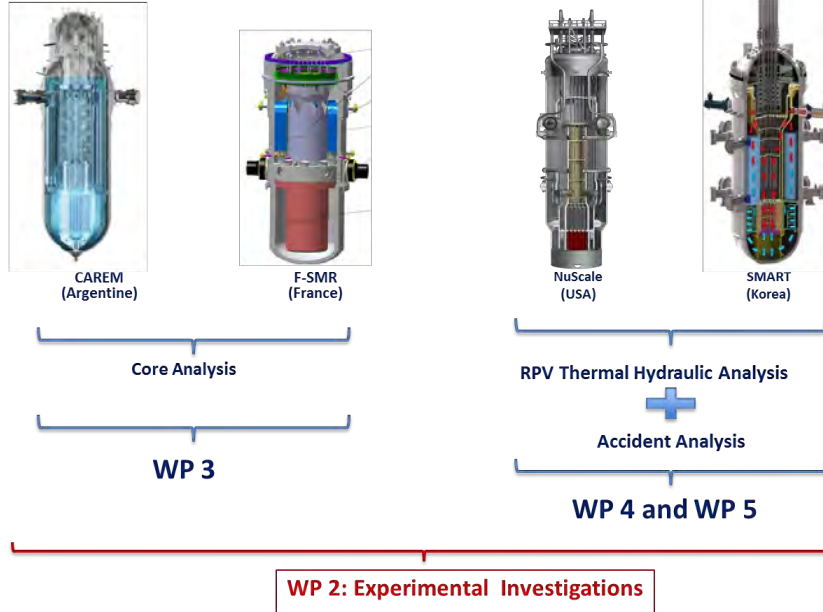
■ Ca. 4 Mio EC (100%)

■ Key-experiments:

- KIT: COSMOS-H
- KTH: HWAT
- LUT: MOTEL

■ 12 EU partners + Argentina

- UNI: KTH, LUT, KIT, UPM
- Research centres: VTT, HZDR, JRC, UJV, CNEA, CEA
- Industry: PEL, TRACTEBEL, JACOBS



## Analysis methodologies:

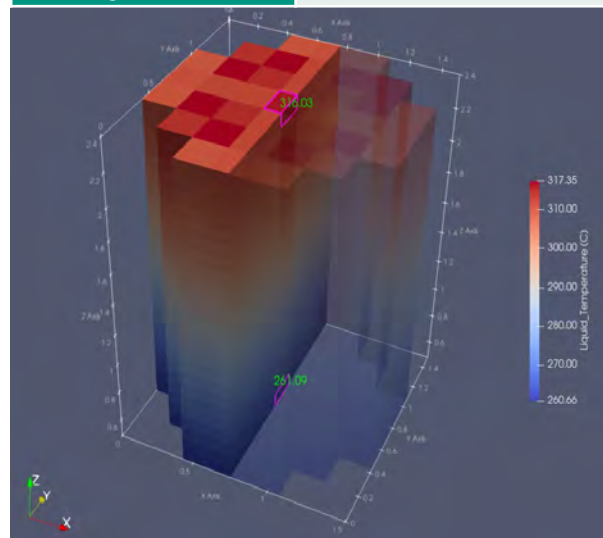
- Core: Multiphysics methods developed at **McSAFE**
- RPV: Multiscale thermal hydraulics: systemTH-Subchannel-CFD
- Plant: Multiscale thermal hydraulics: systemTH-Subchannel-CFD

# In-house code TWOPORFLOW: NuSCALE Core Analysis at FA-Level

## NuScale data:

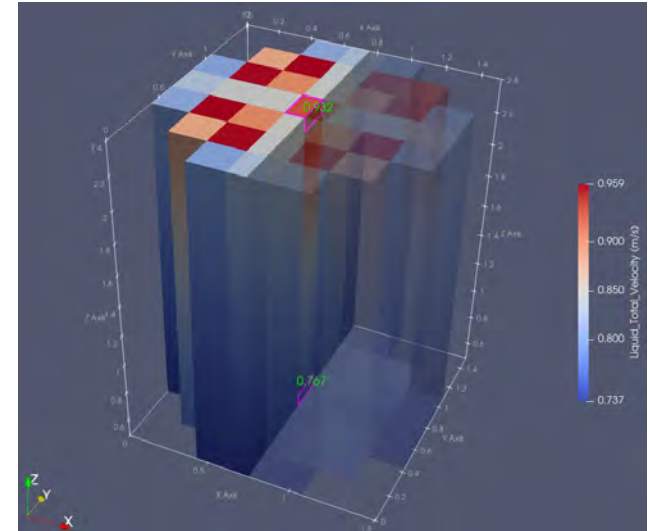
- Power: 160 MWth
- Exit pressure: 12.8 MPa
- Inlet temperature: 258.33 C
- Core flow: 544.29 kg/s

Value	$\frac{ \text{Reference-Value} }{\text{Reference}} \times 100$
$\Delta T_{avg} = 55.56 \text{ K}$	Reference
$\Delta T_{avg} = 55.25 \text{ K}$	0.55795



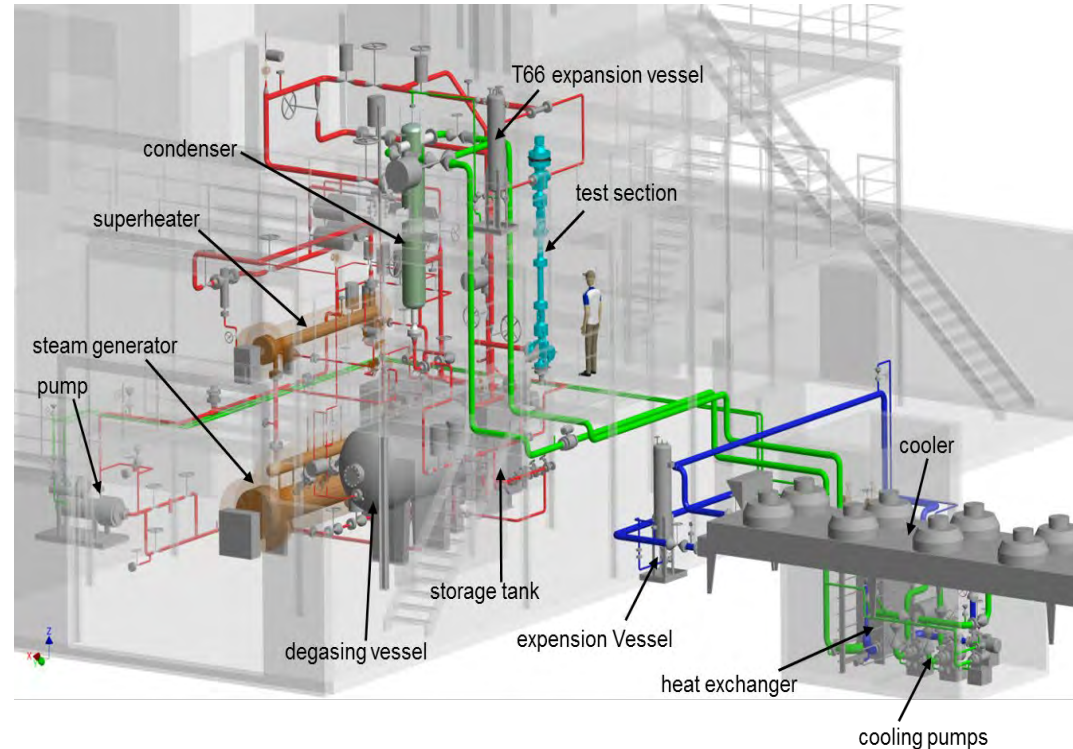
NuScale core: 3D Coolant temperature

Value	$\frac{ \text{Reference-Value} }{\text{Reference}} \times 100$
$Vel_{avg} = 0.82296 \text{ m/s}$	Reference
$Vel_{avg} = 0.87021 \text{ m/s}$	5.7414



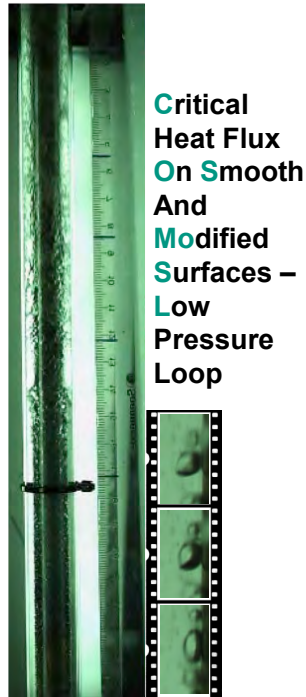
NuScale core: 3D Coolant velocity

- Experiments in McSAFER (High-Performance Advanced Methods and Experimental Investigations for the Safety Evaluation of Generic Small Modular Reactors)
- Two series of experiments are planned to investigate the thermal hydraulics in different SMR concepts
  - Investigation of flow boiling up to the critical heat flux under reactor typical conditions



# Reactor dynamics and accident analysis: Thermal Hydraulics Experimental Facilities

## COSMOS-L



Critical  
Heat Flux  
On Smooth  
And  
Modified  
Surfaces –  
Low  
Pressure  
Loop

CHF at 3 MW/m<sup>2</sup>

- **Scientific objectives**
  - Detailed investigations on Critical Heat Flux (CHF) under reactor typical conditions
  - Measurement data for CFD
- **System parameters**
  - Working fluid: Water
  - System pressure 17 MPa
  - System temperature 360°C
  - System power 2 MW
  - 4 m modular test section (600 kW)
- **High resolution instrumentation**

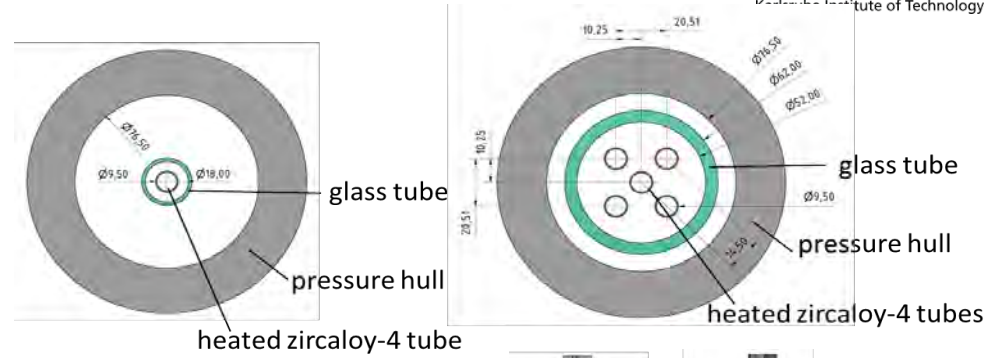
## COSMOS-H

Critical Heat Flux On Smooth  
And Modified Surfaces – High  
Pressure Loop

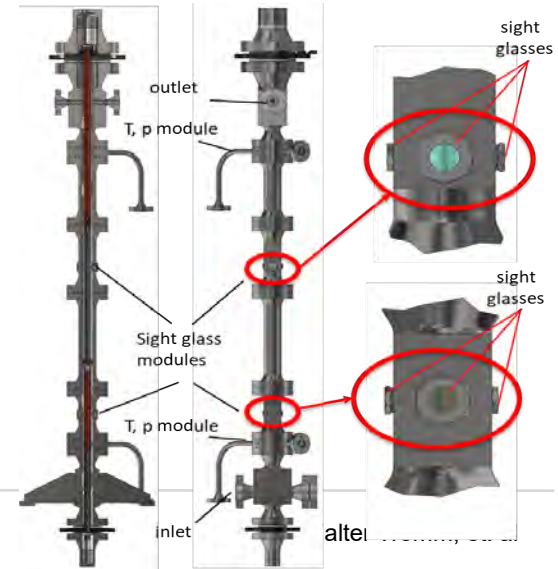




- Two test arrangements are planned: a single heated 1.4 m long zircaloy tube in an annular gap and a rod bundle consisting of five tubes of the same length.



- Instrumentation:
  - pressure sensors, flow sensors, thermocouples, fiber optic sensors and cameras
  - for the relevant boundary conditions and phenomena in the boiling flow at the heated section.



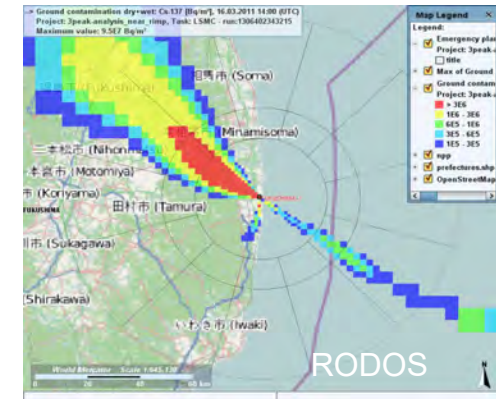
# Objectives Topic 2, Subtopic 2:

## ■ Beyond Design Basis Accidents

- Development and validation of detailed physical models taking profit of the diverse KIT experimental facilities
- Improvement of severe accident integral codes to support Severe Accident Management Guidelines  
MELCOR and ASTEC (Source Code)

## ■ Emergency Management

- Multi-criteria decision analysis (MCDA) as well as agent based modeling (ABM) to improve decision making under high uncertainties in all emergency situations with JRODOS real time online decision support system



# KIT Strategy for SA codes (1/2)

- Fukushima accidents showed necessity for
  - Re-evaluating accident analysis methods, SAMGs, and plant status
  - Improving the numerical simulation tools
  - Codes extension and V&V
  - V&V of SA codes ← Experiments
  - Support to the development of SA codes ← Experiments
- Coupling with other codes, e.g. MELCOR/GASFLOW\*, ASTEC/JRODOS
  - Evaluation of the Radiological Source Term
  - Application of U&S methods to SA codes, e.g. URANIE, SUNSET, DAKOTA, in-House tools ← Experiments
  - Applications of SA Codes for SAMs assessment
  - Use of High Performance computing (HPC)
- Education and Knowledge preservation/dissemination (PhDs and Master programs)

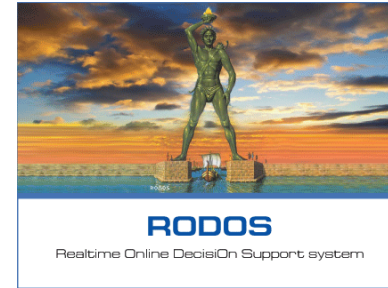
# KIT Strategy for SA codes (2/2)

- ASTEC
  - Support to code development
  - Plant applications
  - U&S
- MELCOR
  - Plant applications
  - Code benchmarking
  - U&S (planned)
- Validation against KIT Experiments
  - QUENCH, LIVE, MOCKA, HYKA

Radiological  
Source Term



- **Emergency Management**
  - **JRODOS (KIT)**



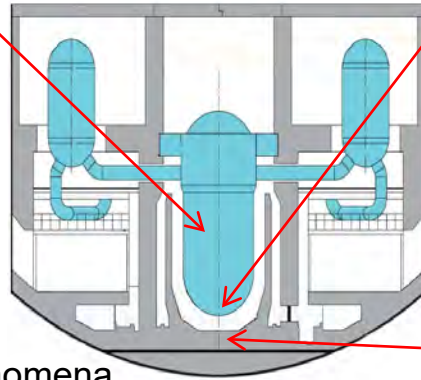
Development of Severe Accident Codes and JRODOS integral part of reactor safety research at KIT!

Large scale test facilities needed!



# Severe Accident Large Facilities @KIT

Core  
coolability and  
debris cooling  
**QUENCH**



In-vessel melt retention



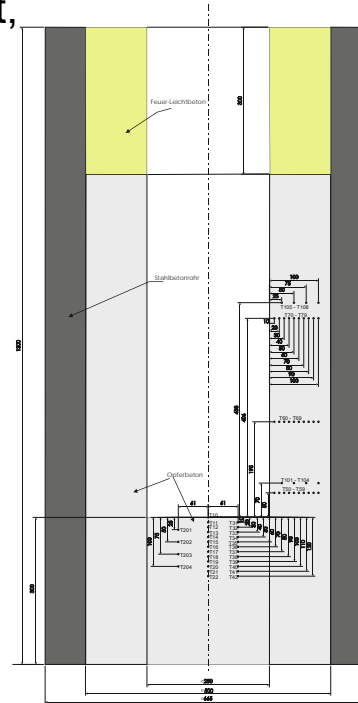
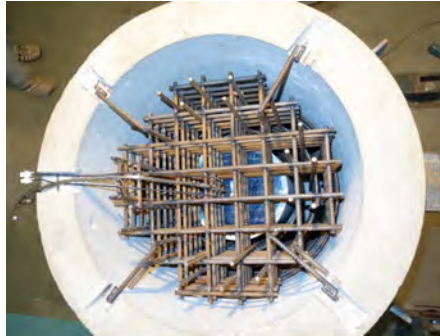
MCCI

Containment phenomena



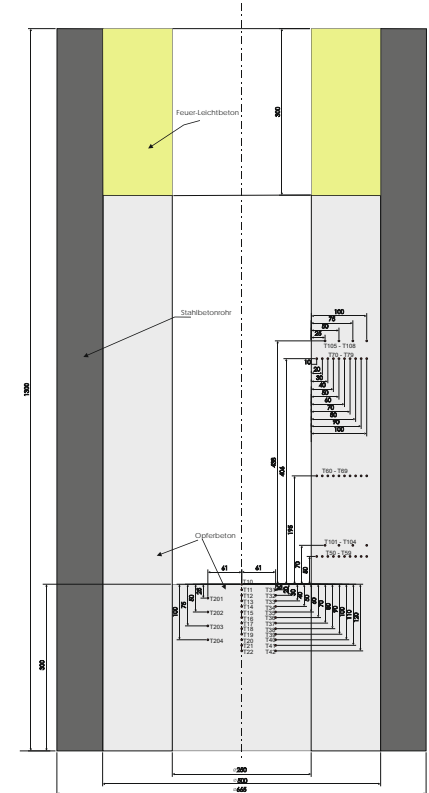
# MOCKA experiments: Ex-vessel molten core concrete interaction (MCCI)

- MCCI on reactor containment basement,
- Siliceous, limestone-common sand (LCS) concretes,
- With and without rebar,
- Addition of thermite and Zr to sustain high power input for 35 minutes.



# (selective) MOCKA: concrete crucible production and instrumentation

## Bottom-up view of the reinforcement





# Summary of MOCKA results



Pure Siliceous concrete

Siliceous concrete with rebar

Limestone common sand (LCS)

- Ablation in siliceous concrete:
  - High axial ablation in metal phase
  - Rebar mitigates the ablation rates
- Ablation in LCS:
  - Pronounced lateral ablation
  - Rebar has no special function
- Zr oxidation promotes
  - axial ablation in siliceous concrete
  - lateral ablation in LCS concrete



# JIMEC: molten Jet impingement in SFR Core-Catcher: a task in EU H2020 ESFR-SMART Project

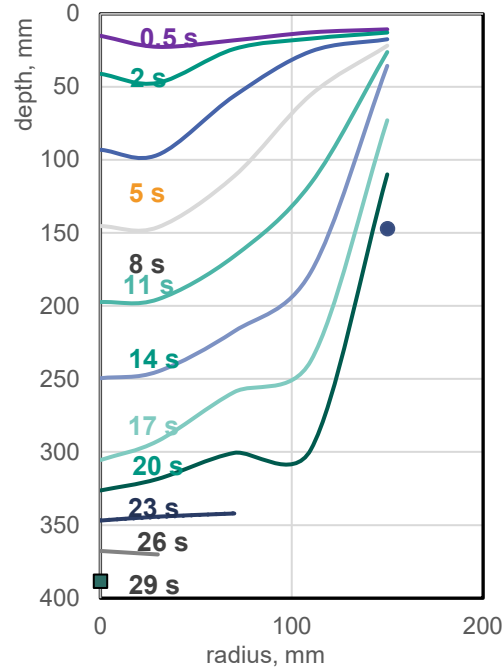
## Ablation of steel core-catcher by steel jet impingement

- Jet mass: 1000 kg
- Jet diameter: 40 mm
- Jet temperature: 2000-2100 °C
- Jet velocity: ~ 5 m/s
- Steel substrate  
D·H: 40 cmx 40 cm.



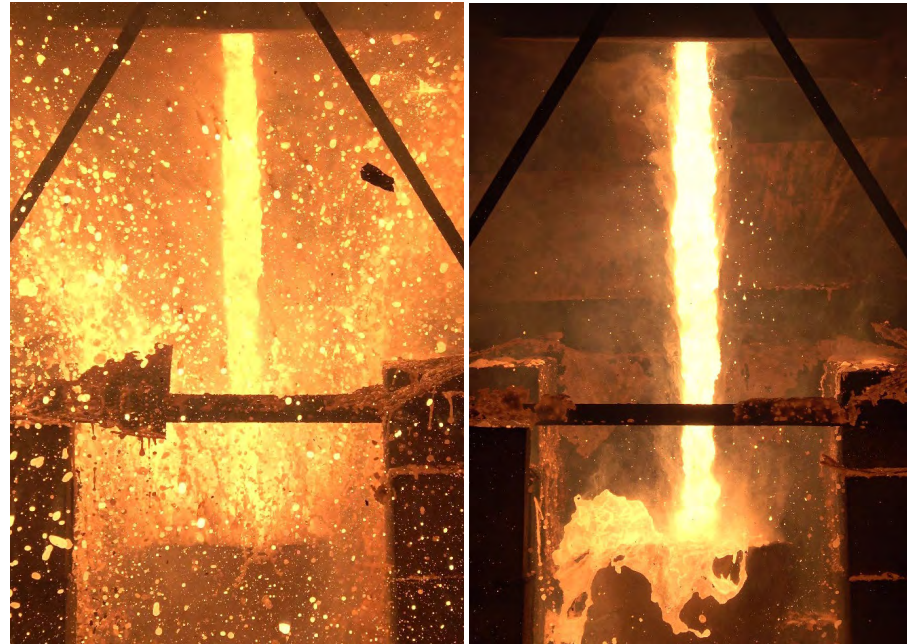
# Ablation dynamics (selective)

## Cavity contour vs. Time



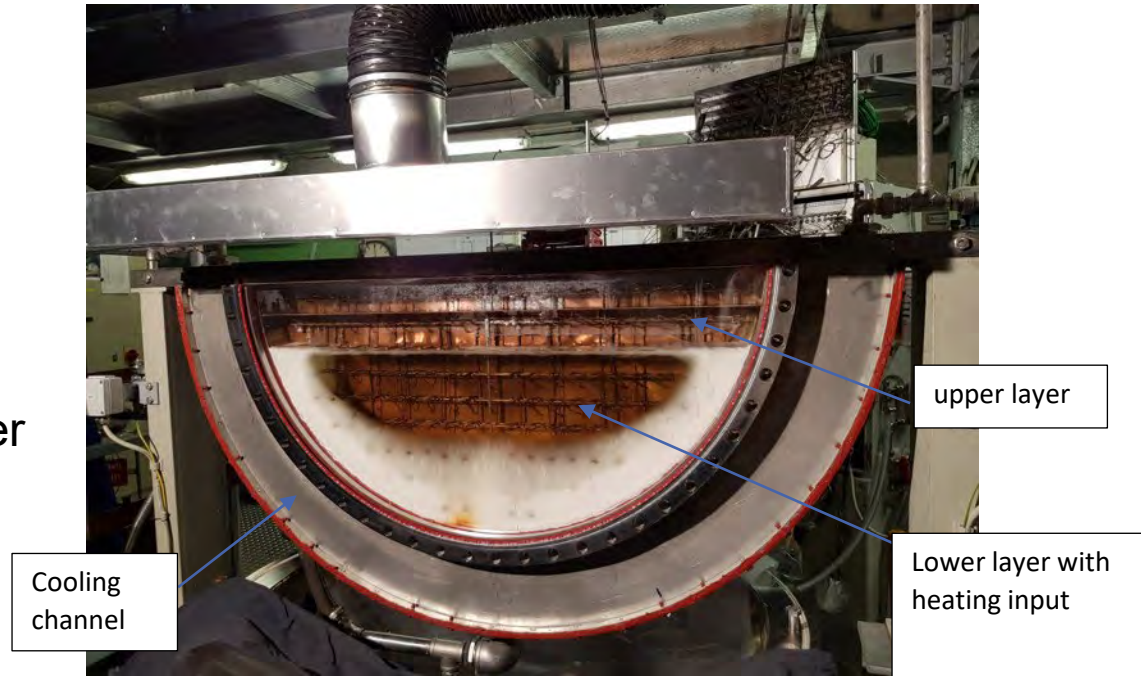
before 18s

after 18s with pool effect



# LIVE2D two-layer corium with nitrate salt mixtures

- A large-scale experiment in EU H2020 IVMR project,
- Heat flux focusing effect in the upper layer,
- Pioneer work on realization of self-separated two-layer corium pool,
- Nitrate mixtures as the lower layer with crust formation,
- External cooling and top cooling concepts.

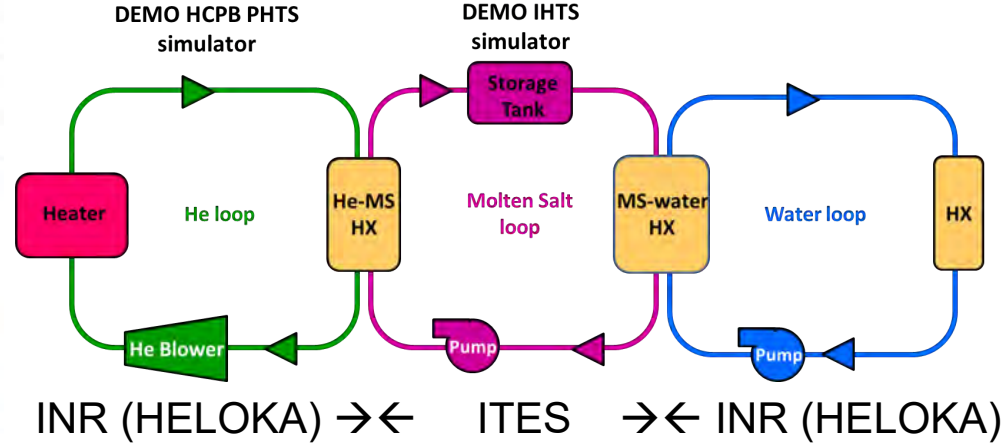
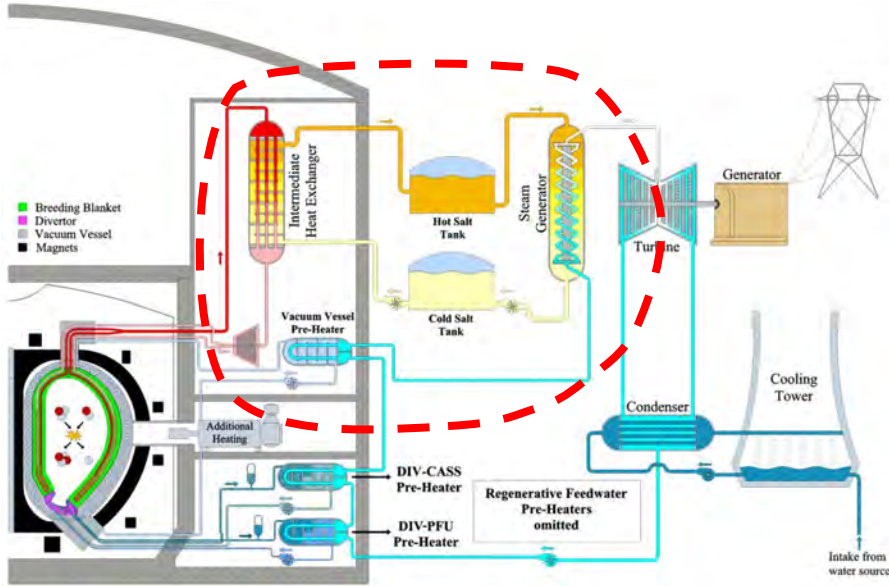


# Results of LIVE-2D Experimentes

- Naturally immiscible two-layers melt pool was created with thermal oil and nature salt mixture in the upgraded LIVE2D test facility.
- Global thermal interactions between the two layers are observed:
  - Pronounced heat flux focusing effect in the upper layer
  - Top cooling mitigates the thermal load of the vessel wall
  - Heat flux in upper layer reduces with increase of layer thickness
  - Interactive heat transfer between the layers
  - Global response of the interlayer crust with the trans-layer heat transfer



# Next step: HELOKA-Upgrade Storage

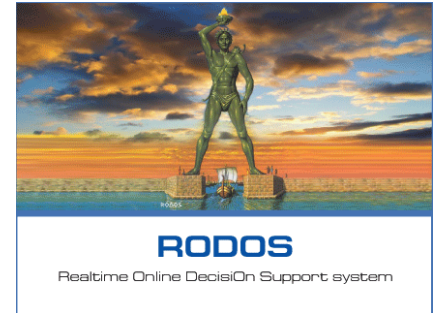
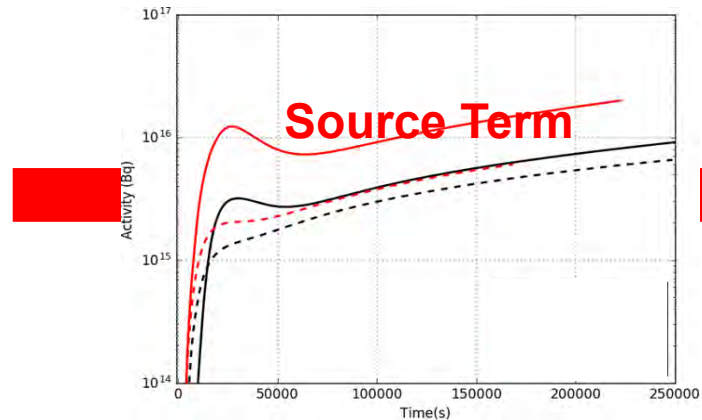
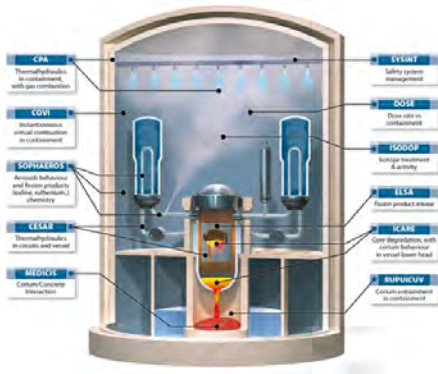


- **NUSAFE - FUSION** cooperation on enhanced flexibility and anti-ageing of power plants to future energy system demand
- **Component level:** performance and operating experience of the various components (blower, IHX, ...)
- **System level:** verify the capability, flexibility and simplicity of the concept to handle transients dwell-pulse and pulse-dwell
- **Experimental data:** qualify numerical models able to evaluate the system and its dynamic behavior
- **Opportunities:** to investigate Power-to-Heat and to identify cost reduction possibilities

# ASTEC – JRODOS Overview

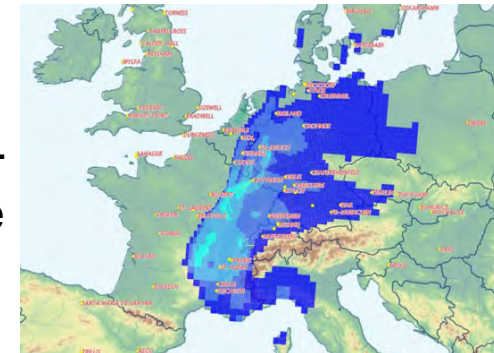
- Evaluation of source term (ST) and fission product (FP) dispersion during a severe accident (SA) in NPPs is one of the major objectives of the nuclear reactor safety research program at KIT.
- Main goal → supporting the emergency and management teams during such abnormal events → **a reliable evaluation of the source term is mandatory.**
- **Reference** codes to be employed for assessing a database of STs during SA scenarios for different NPPs → Realistic fuel inventories, ST evaluation (ASTEC), U&S and ST prediction (FSTC+MOCABA algorithm), FP dispersion (JRODOS).

# Strategy for Source Term Analyses (1/2)



<https://www.ites.kit.edu/english/294.php>

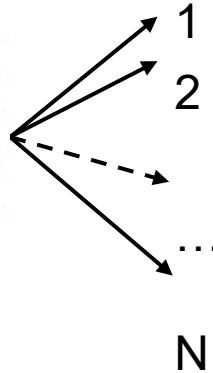
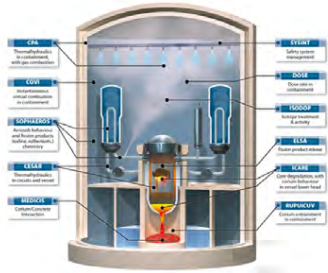
- **European reference Accident Source Term Evaluation Code (ASTEC)**, developed by IRSN and co-developed by KIT since 2020 → SA scenario analyses and ST evaluations.
- ASTEC results employed to analyze the FP dispersion in the environment by means of the **Java based Real-Time On-Line Decision Support system (JRODOS, KIT)**.



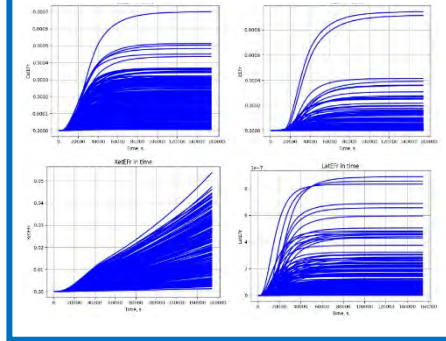
## Strategy for Source Term Analyses (2/2)

Development of in-house **K**arlsruher **T**ool for **U**ncertainty and **S**ensitivity **A**nalysis (KATUSA) (formerly known as FSTC) → **U**ncertainty **Q**uantification (**UQ**) of the **ASTEC ST** results + **t**raining **d**atabase + **e**mployment for **J**RODOS

**Source Term prediction** → Monte Carlo-based Bayesian inference model (**MOCABA** algorithm from Framatome GmbH embedded)



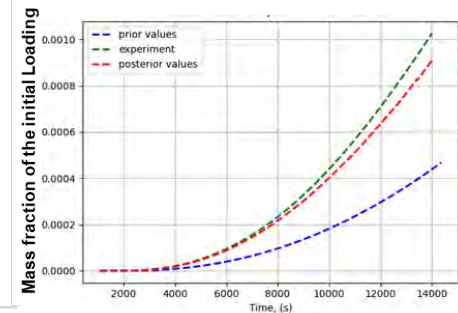
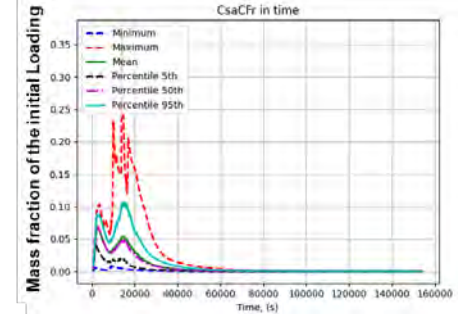
### ST Training Database



ASTEC+UQ

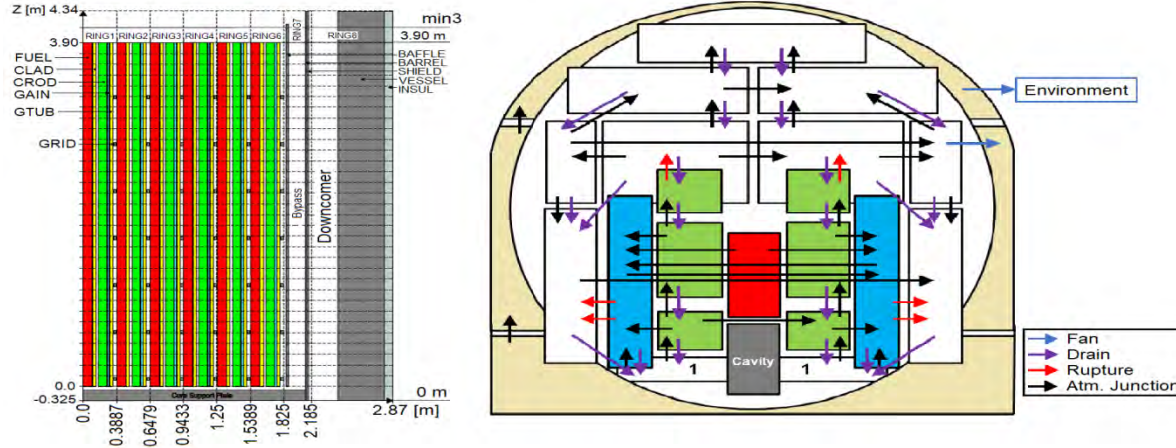


ASTEC+UQ  
+MOCABA

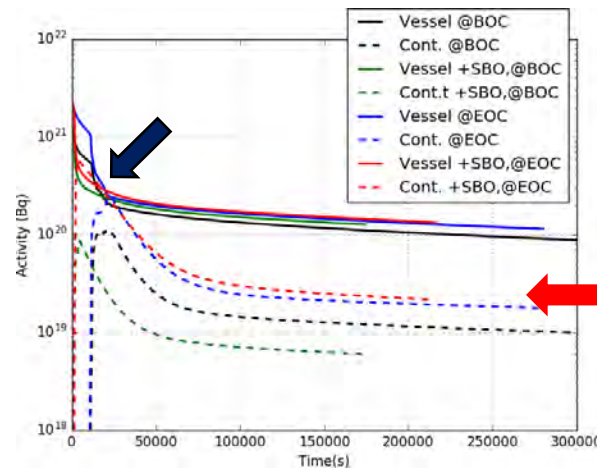
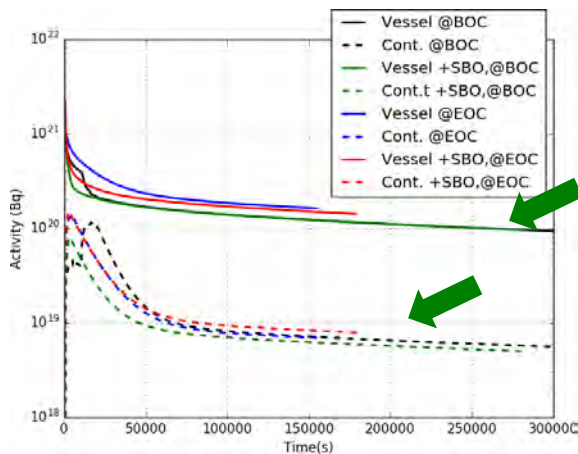




# ASTEC: Severe Accident Analyses in a generic KONVOI NPP



- ASTEC 2.2.0.1 is used
- All ASTEC modules are activated
- Extension and improvement of the generic input deck developed during the EU CESAM project
- Fuel inventories calculated with ORIGEN-ARP code
- Containment leakage to the annulus (based on design data)
- No filtering
- Simulation up to basemat rupture



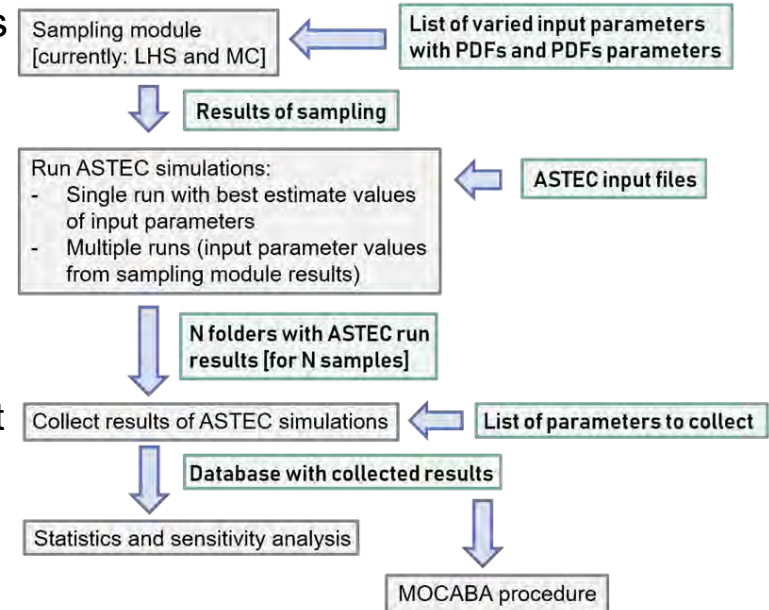
**MBLOCA scenarios** → about 1% of the initial activity of the fuel inventory transported to the containment.

### SBLOCA scenarios more severe

- SBLOCA+SBO (@EOC) → about 3% of the initial activity in the vessel transported to the containment in the long term.
- SBLOCA @EOC → **max. activity release to the containment about 15-20% (no SBO) and 70% (+SBO) of the initial activity.**
- **The release to the containment is almost twice as high for a fuel inventory at EOC as for a fuel inventory at BOC.**

# The KATUSA tool for U&S analyses of the ASTEC ST Results

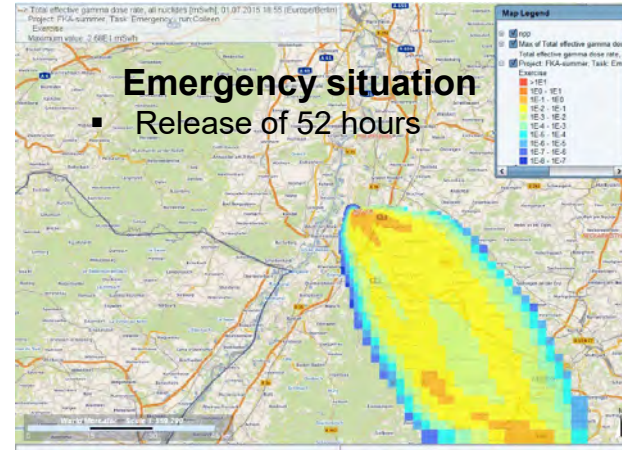
- Source term evaluation affected by the uncertainties still existing on SAs modeling, i.e. MCCI.
- Framework: EU MUSA and German WAME projects.
- Karlsruher Tool for Uncertainty and Sensitivity Analysis (KATUSA) (formerly FSTC) tool developed at KIT Python based
  - Easy to be installed on any machine and environment
  - Two 'modes': UQ and UQ+Prediction
  - Verified against URANIE



# Emergency Management: JRODOS

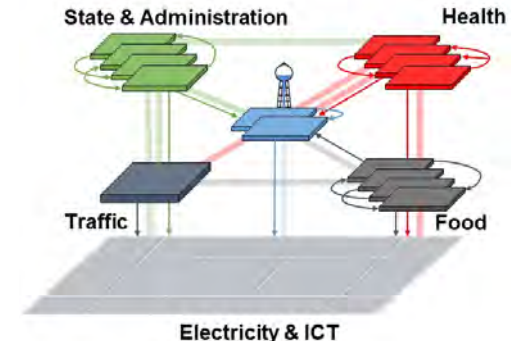
## ■ Real-time on-line decision support system for nuclear and radiological incidents

- Considering releases into water and the atmosphere
- Determining contamination levels in the urban and agricultural environment and doses to the public



## Cross program activity: Security

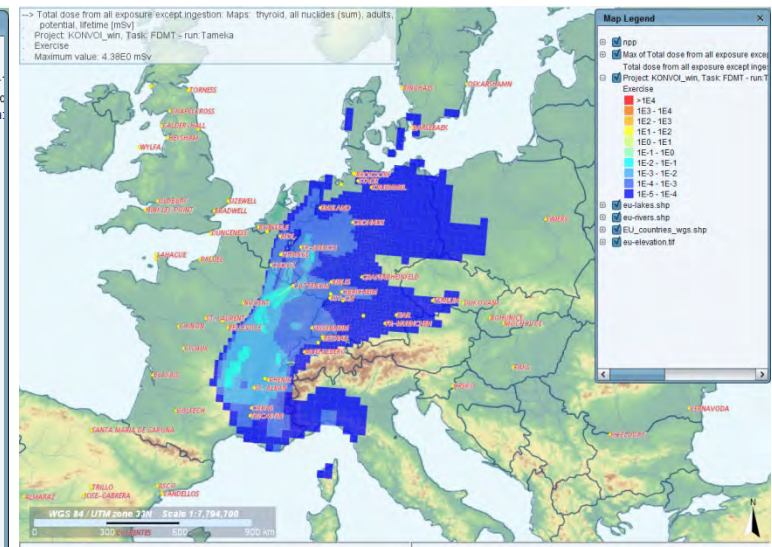
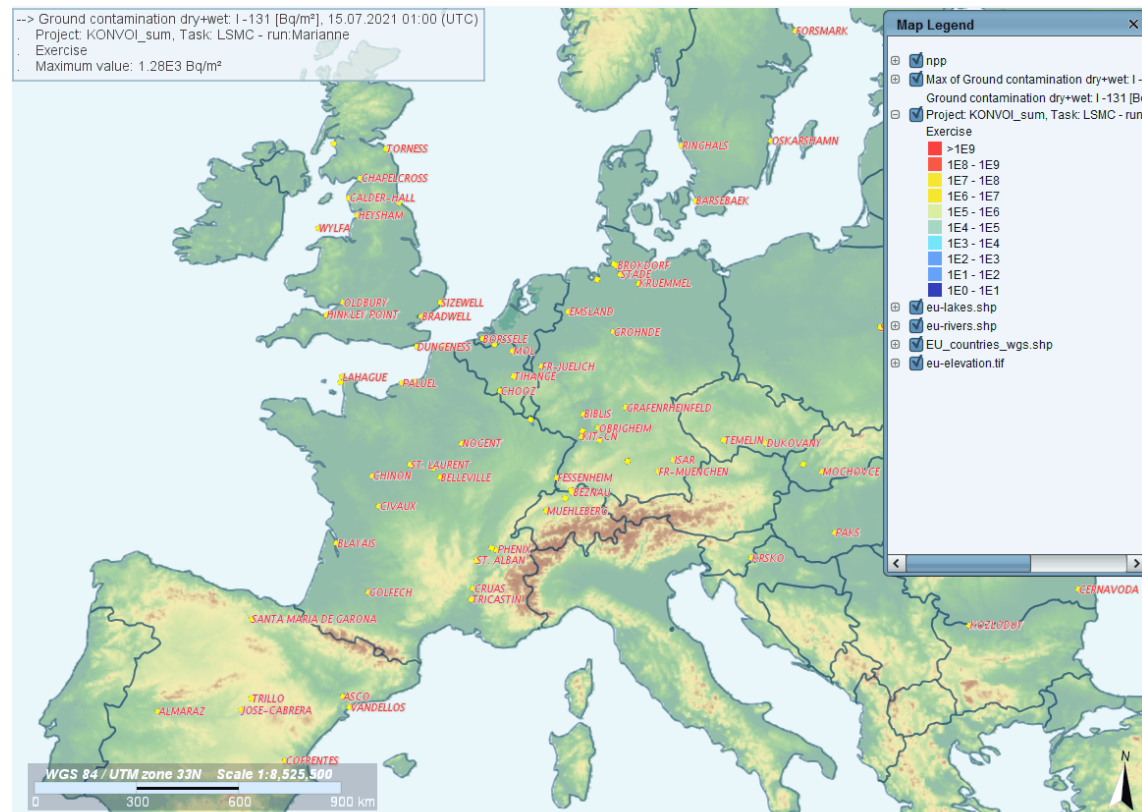
- Combine nuclear and non-nuclear competences and expand activities to the theme “Security”
- Decision support for large crisis situations with critical infrastructures affected
- Use of agent based simulation methods to identify appropriate countermeasures





# JRODOS Results for the MBLOCA Scenario at EOC

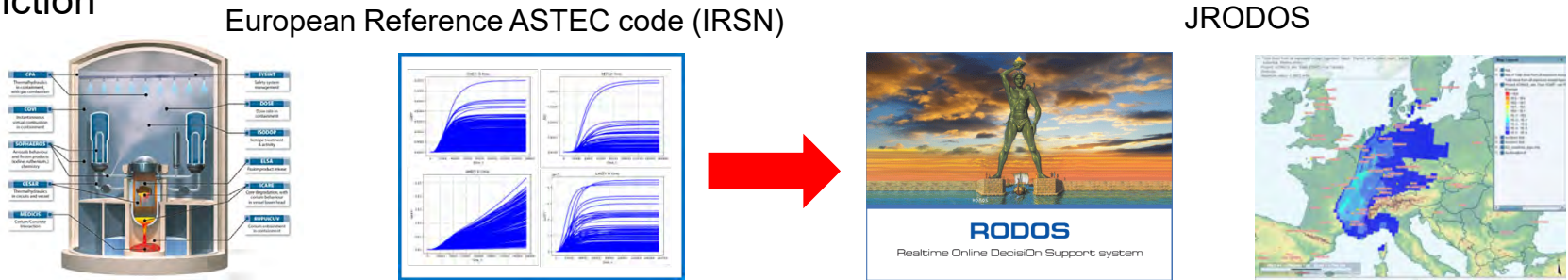
--> Ground contamination dry-wet: I-131 [Bq/m<sup>2</sup>], 15.07.2021 01:00 (UTC)  
 . Project: KONVOI\_sum, Task: LSMC - run:Marianne  
 . Exercise  
 . Maximum value: 1.28E3 Bq/m<sup>2</sup>



- Max. Contamination is over **E5 Bq/m<sup>2</sup>**
- Total thyroid doses is about **4 mSv for an adult lifetime**

# Assessment of the radiological consequences of severe accidents in nuclear power plants

- Data bank with ASTEC source term results → Quantification of uncertainty and prediction accuracy
- Emergency management support for beyond-design-basis events
- Innovative computational platform for realistic assessments of fission product release and dispersion to the environment in case of severe accidents in NPPs, i.e. German PWR, VVER-1000, BWR and SMR
- **Outlook:** Use of artificial intelligence algorithms to improve ASTEC code and source term prediction

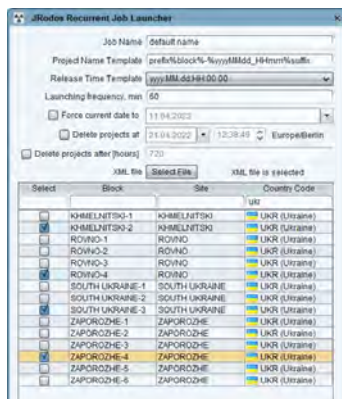


## Application/research needs (selection)

- Ukraine – threat of accidents at the 4 NPP sites, other nuclear installations (e.g. Chernobyl, Neutron source in Kharkov)
- Ukraine – nuclear warheads
- Source term estimation/reconstruction
- Assessment of the uncertainties in the early phase of an emergency
- Optimisation of management strategies for the transition and recovery phase

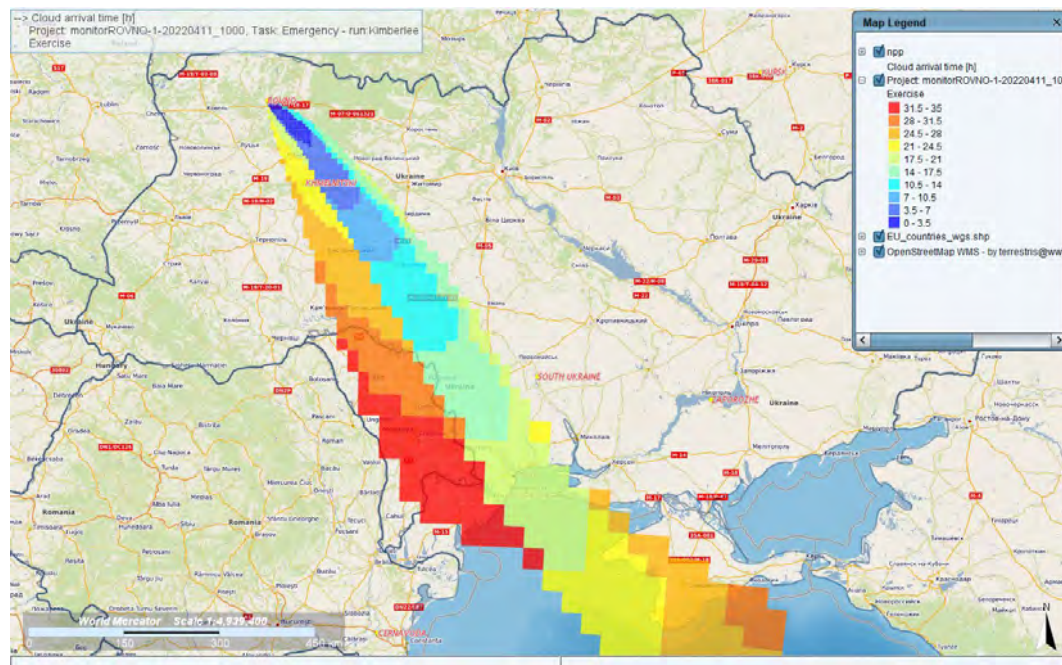
# Ukraine NPP – automated assessments

Typical result: cloud arrival time



Open Project

Project Name	User	Date Created (UTC)	Date Modified (UTC)	Description	Model Chain
monitorZAPOROZHE-1-202...	christoph	11.04.2022 10:32	11.04.2022 10:37	Automatically create...	Emergency
monitorKHMELNITSKI-1-202...	christoph	11.04.2022 10:31	11.04.2022 10:37	Automatically create...	Emergency
monitorSOUTH UKRAINE-1-...	christoph	11.04.2022 10:31	11.04.2022 10:37	Automatically create...	Emergency
monitorZAPOROZHE-1-202...	christoph	11.04.2022 09:32	11.04.2022 09:38	Automatically create...	Emergency
monitorROVNO-1-20220411...	christoph	11.04.2022 09:31	11.04.2022 09:37	Automatically create...	Emergency
monitorKHMELNITSKI-1-202...	christoph	11.04.2022 09:31	11.04.2022 09:37	Automatically create...	Emergency
monitorSOUTH UKRAINE-1-...	christoph	11.04.2022 09:32	11.04.2022 09:37	Automatically create...	Emergency
monitorZAPOROZHE-1-202...	christoph	11.04.2022 08:32	11.04.2022 08:37	Automatically create...	Emergency
monitorROVNO-1-20220411...	christoph	11.04.2022 08:21	11.04.2022 08:27	Automatically create...	Emergency
monitorSOUTH UKRAINE-1-...	christoph	11.04.2022 08:32	11.04.2022 08:37	Automatically create...	Emergency
monitorKHMELNITSKI-1-202...	christoph	11.04.2022 08:31	11.04.2022 08:37	Automatically create...	Emergency
monitorZAPOROZHE-1-202...	christoph	11.04.2022 07:32	11.04.2022 07:37	Automatically create...	Emergency
monitorROVNO-1-20220411...	christoph	11.04.2022 07:31	11.04.2022 07:37	Automatically create...	Emergency
monitorKHMELNITSKI-1-202...	christoph	11.04.2022 07:31	11.04.2022 07:37	Automatically create...	Emergency
monitorSOUTH UKRAINE-1-...	christoph	11.04.2022 07:31	11.04.2022 07:37	Automatically create...	Emergency
monitorZAPOROZHE-1-202...	christoph	11.04.2022 06:32	11.04.2022 06:38	Automatically create...	Emergency
monitorROVNO-1-20220411...	christoph	11.04.2022 06:31	11.04.2022 06:37	Automatically create...	Emergency
monitorSOUTH UKRAINE-1-...	christoph	11.04.2022 06:31	11.04.2022 06:37	Automatically create...	Emergency
monitorKHMELNITSKI-1-202...	christoph	11.04.2022 06:32	11.04.2022 06:38	Automatically create...	Emergency





# Nuclear warheads

- Germany is not prepared for protecting the population against the consequences of nuclear detonations – Radiation Protection Commission
- First attempt in JRODOS, but needs improvement

## Release location and fractions

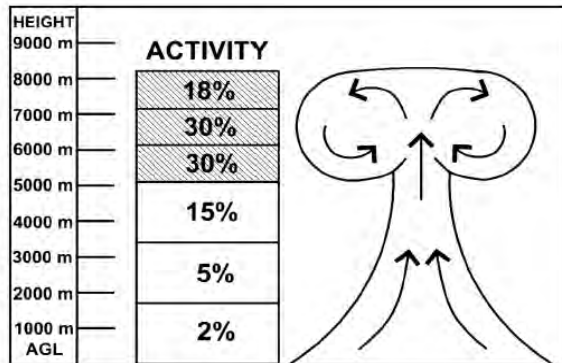


Fig. 1. Model representation of a nuclear mushroom cloud and the total activity fraction in each vertical segment defined by the model for a 10 kT explosion (Hefter, 1969). The shaded region represents the layers defining the cap of the cloud.

## Particle size distribution

$\mu\text{m}$	250	150	100	50	10
%	12	18	20	28	12

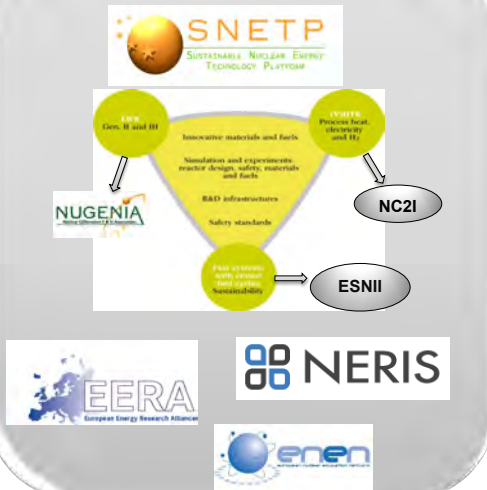
# Networking and cooperations



## NUSAFE Collaborations in Germany

Alliance for Competence in Nuclear Technology (KVKT)  
with universities, authorities and industry

### European collaborations



### Bilateral cooperations

research and industry  
(national & international)



### Advisory boards / Committees in international organisations

- IAEA: TWG-LWR, TWG-FR
- OECD/NEA: NSC, CSNI-WGAMA



## NUSAFE Topic 2, EU-projects

- In the Euratom Call NFRP-2021-2022 in October 2021, a total of 10 proposals with KIT participation were submitted, 1 of which was coordinated by KIT
- Evaluation results in February 2022: 9 of the 10 submitted proposals were approved, including the one coordinated by KIT - success rate: 90%
- Approved funding amount for KIT: about 2.9 million euros over 4 years

Acronym	EC funding for KIT	Full title
<i>bewilligt:</i>		
ANSELMUS	68.719,00	Advanced Nuclear Safety Evaluation of Liquid Metal Using Systems
ASSAS	358.313,00	Artificial intelligence for the Simulation of Severe AccidentS
ENEN2plus	105.000,00	Building European Nuclear Competence through continuous Advanced and Structured Education and Training Actions
ESFR-SIMPLE	578.774,00	European Sodium Fast Reactor - Safety by Innovative Monitoring, Power Level flexibility and Experimental research
INNUMAT (Koord.: KIT)	1.021.986,00	Innovative Structural Materials for Fission and Fusion
OFFERR	42.500,00	eurOpean platForm For accEssing nucleaR R&d facilities
SASPAM-SA	247.032,00	Safety Analysis of SMR with PASSive Mitigation strategies - Severe Accident
SCORPION	249.930,00	SiC composite claddings: LWR performance optimization for nominal and accident conditions
SEAKNOT	192.047,00	SEvere Accident research and KNOWledge management for LWRs
<i>bewilligte Summe</i>	<b>2.864.301,00</b>	
<i>nicht bewilligt:</i>		
ARMSTRONG		Advanced Robust Multiphysics Simulation Tools for Reactors Of New Generation

# Summary and Outlook



## KIT reactor safety research as an integral part of Helmholtz research

- Contributions to immediate and long-term impact on reactor safety
- International cutting-edge research by multidisciplinary and innovation with a long-term perspective
- Competencies for the operation of large-scale facilities
- Enhancement of cooperation with important international players
- Ensure competencies for continuing tasks in nuclear technology for research, industry and authorities
- Establishment of a wider application in the research field energy





# Many thanks for your attention

**Th. Walter Tromm**  
**Karlsruhe Institute of Technology**  
**Programme Nuclear Waste Management,**  
**Safety and Radiation Research**

**walter.tromm@kit.edu**



**T. Wiss**

**JRC Karlsruhe**

## **Overview of spent fuel ageing studies and testing at JRC Karlsruhe**

After storage at reactor sites for initial heat decay of spent fuel elements, and if no reprocessing is foreseen, the spent fuel will be transported and then stored for periods of several decades or even centuries in wet or dry interim storage facilities prior to disposal. The safety assessment of extended storage requires predicting the behaviour of the spent fuel assemblies and of the spent fuel itself over a correspondingly long timescale, to ensure that the mechanical integrity and the required level of functionality of all components of the containment system are retained. Accelerated ageing and basic studies supported by modelling are necessary to predict the long term behaviour of these materials. Updated results from spent fuel experimental studies performed at JRC-Karlsruhe addressing extreme conditions related to handling/transportation and long-term storage issues are presented. The potential consequences of accidents causing spent fuel rod failure involve fuel particles release and dispersion. Impact tests using a hammer drop device and bending tests in hot cell were performed on spent fuel rod segments. Particle size distribution analysis of the coarse fraction released from the rod breakage, which settled by gravity, and of the fine fraction, including fuel particles deposited on a second stage filter of the testing chamber and particles deposited on the walls of the impact test chamber and on the surfaces adjacent the bending setup, were performed. High speed camera video recorded during impacting and related analysis is also presented.

The final goal of these investigations is to determine parameters and conditions governing the response of spent fuel rods to impact loads and other thermo-mechanical solicitations corresponding to normal and off-normal conditions that may be experienced by the rod during handling, transportation, storage, and after extended storage.

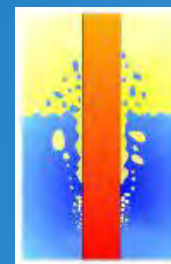
In addition to mechanical loading tests, property measurements as a function of accumulated radiation damage are performed on spent fuel and alpha-doped analogues to determine the long term evolution and the potential effects of ageing processes on the mechanical integrity of the spent fuel rod. Spent fuel rod alterations as a function of time and specific activity, and the alteration kinetics are monitored at microstructural level (defects and lattice parameter swelling) and at macroscopic property level (e.g. hardness and thermal conductivity). In order to reproduce cumulative damage effects expected after extended storage time within acceptable laboratory timescales, accelerated damage build-up conditions are applied by testing unirradiated (U,Pu) oxide with high specific alpha-activity. The results obtained so far show that saturation of macroscopic hardness and thermal conductivity occurs for a simulated timescale corresponding to spent fuel after decades or centuries of storage. Alpha-damage effects that will prevail during storage/disposal has also been studied in old irradiated fuel with high minor actinide content, hence having cumulated radiogenic helium equivalent to extremely old conventional spent fuels. The examination of the microstructure of such fuels has evidenced their very high radiation resistance; a detailed characterization of the defect pattern has been obtained from e.g. Transmission Electron Microscopy investigations. The helium behaviour and its relation to the microstructure in the aged fuel microstructure has been investigated by helium thermal desorption.



# Overview of spent fuel ageing studies and testing at JRC Karlsruhe

T. Wiss, V.V. Rondinella, D. Papaioannou, R. Nasyrow

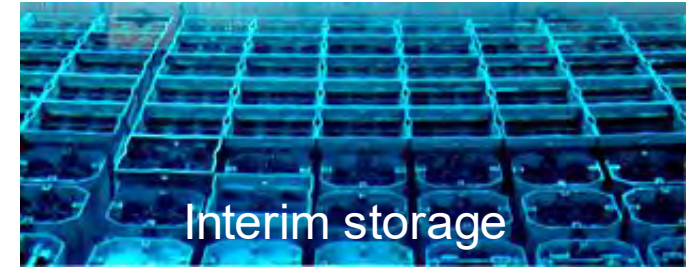
**27<sup>th</sup> International QUENCH Workshop, KIT, 27-29 Sept. 2022**



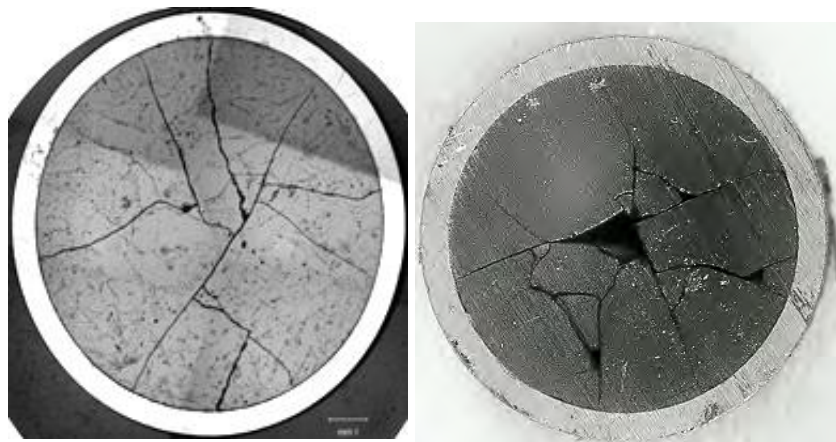


# Outline

- introduction
- spent fuel evolution during storage
- mechanical testing of spent fuel
- new tools and conclusions (so far)



LWR ~55 GWd/tHM





# Extended Spent fuel (SF) storage

In countries where the construction of the geologic repository is delayed, the duration of the interim storage will increase; timeframes of the order of centuries are considered.



Safety assessment of extended SF storage requires:

- demonstration that the SF assemblies and the containers will retain their integrity and functionality, allowing all repackaging and transportation *after* storage;
- if not, indication on how to cope with degradation of any containment system (cladding, canister, cask, welds/sealing, etc.)

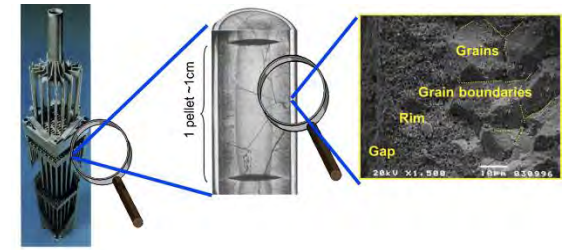


The challenge is to design suitable experimental and calculation tools to be able to predict what will or may happen over an undefined future timescale



This presentation highlights studies performed at JRC to investigate processes related to storage potentially affecting the mechanical integrity of the spent fuel rod.

# Rational



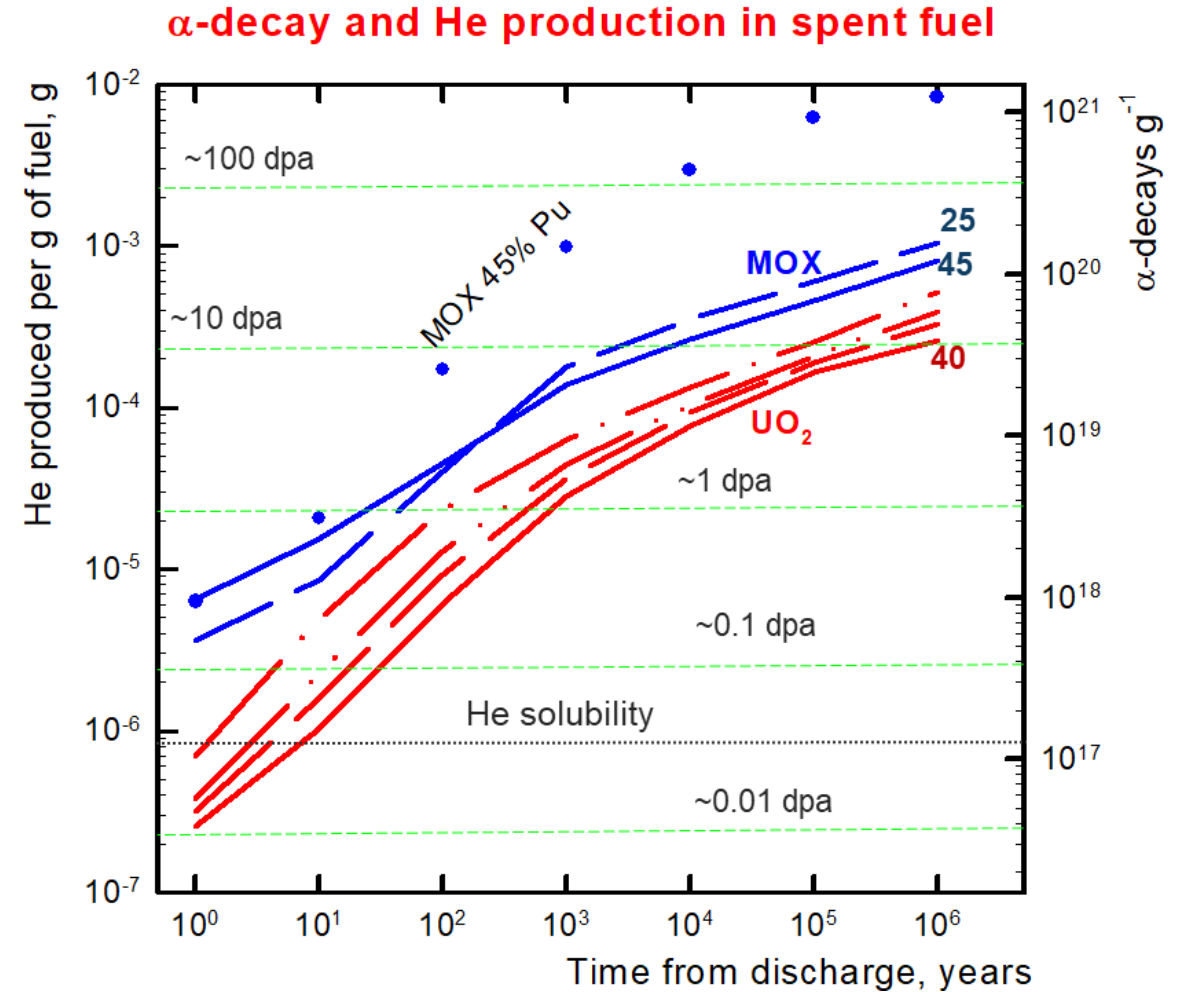
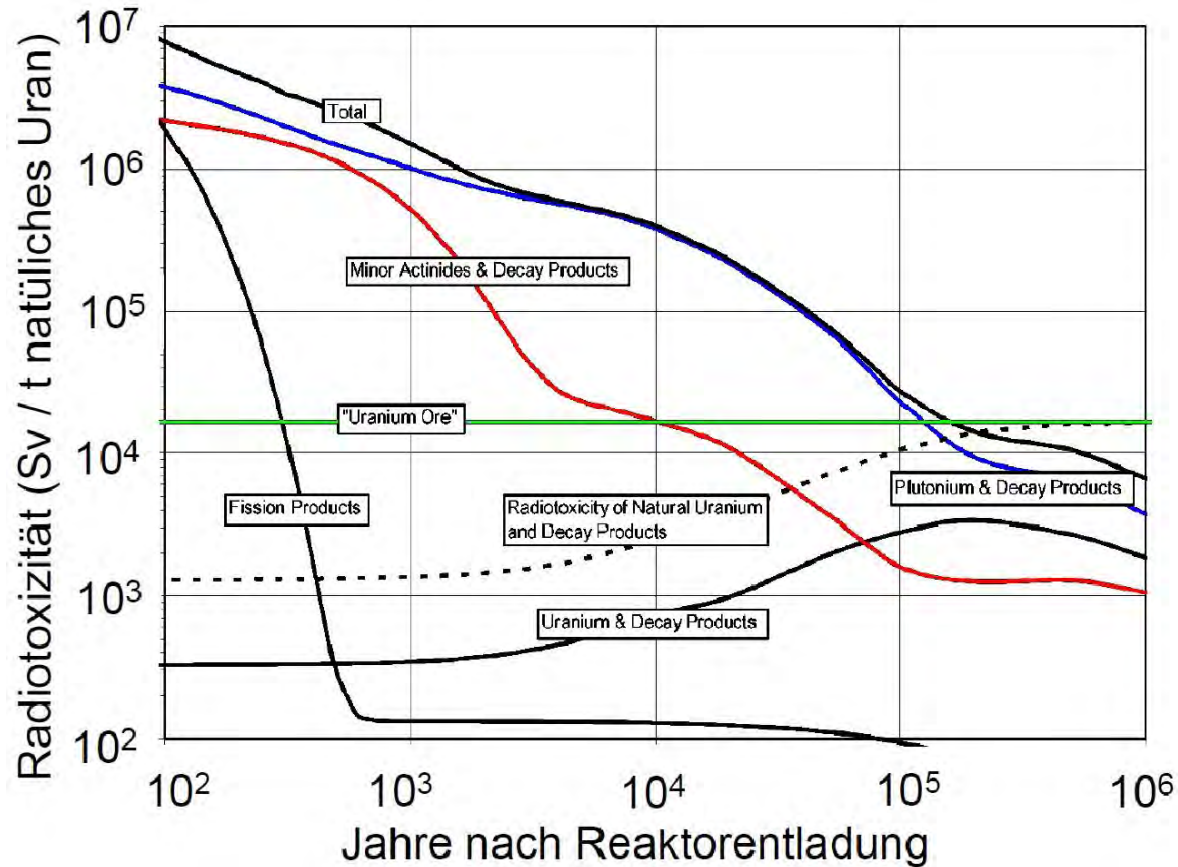
- Decay of fission products and other radionuclides change the composition of the SNF
- Chemical evolution associated to  $\beta$ -disintegration which produces elements with different valence states and the temperature decrease could change the oxygen potential.
- Release of radionuclides from the spent fuel grains by diffusion (radiation enhanced). This process could enhance the inventory of radionuclides rapidly released when water contacts the fuel.
- **Physical evolution associated with helium production and accumulated damage due to  $\alpha$ -decay.**
- **The metal cladding properties may also evolve due to creep under internal pressure and to hydride reorientation during cooling under stress.**

# Spent fuel evolution

Irradiated fuel with high MA content: SUPERFACT

Simulated fuel: alpha-doped

# Alpha-damage in fuels





# Perspectives for SNF studies

- (Severe) accidents

pools, storage, handling, transport:

**mechanical load, impact resistance**; corrosion, loss of cooling; damaged SF, debris

- Degradation of spent fuel by increasing **He accumulation** during final storage?

Total He production in MOX fuel is after  $10^6$  years 4 – 5 times higher than in  $UO_2$

Direct investigation of degradation difficult (too long time span)

- Exist a model system to study the influence of  $\alpha$ -dose in significant shorter time?

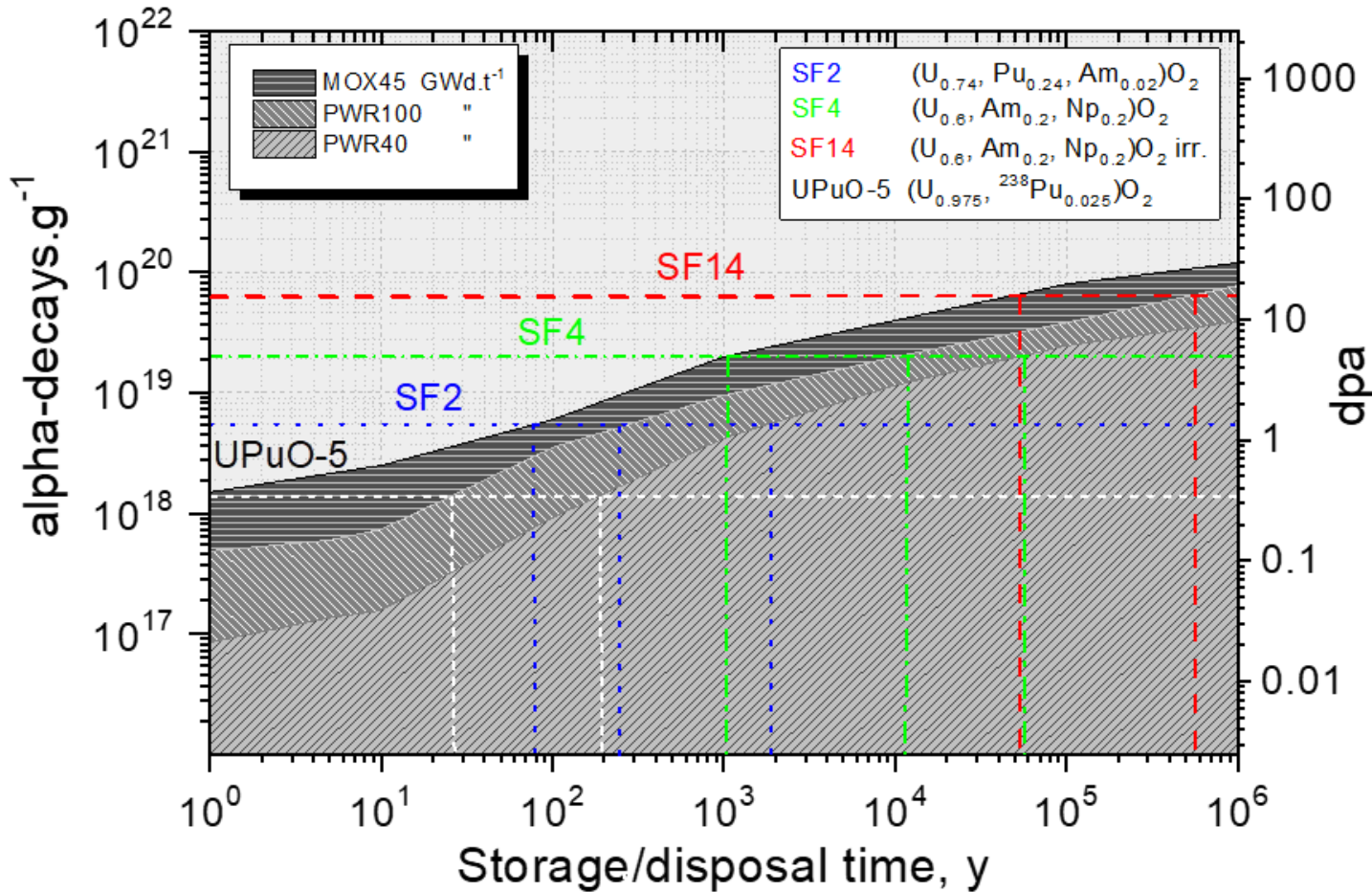
Much faster He build up in (U, Pu, Am, Np) $O_2$  fuel

➡ SUPERFACT fuel, a potential model system

# SUPERFACT irradiated

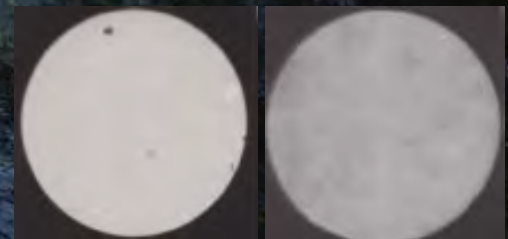
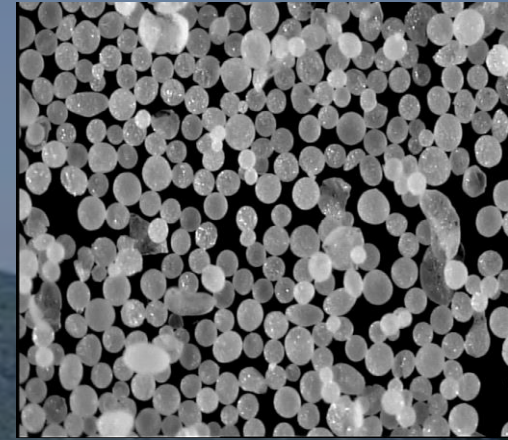
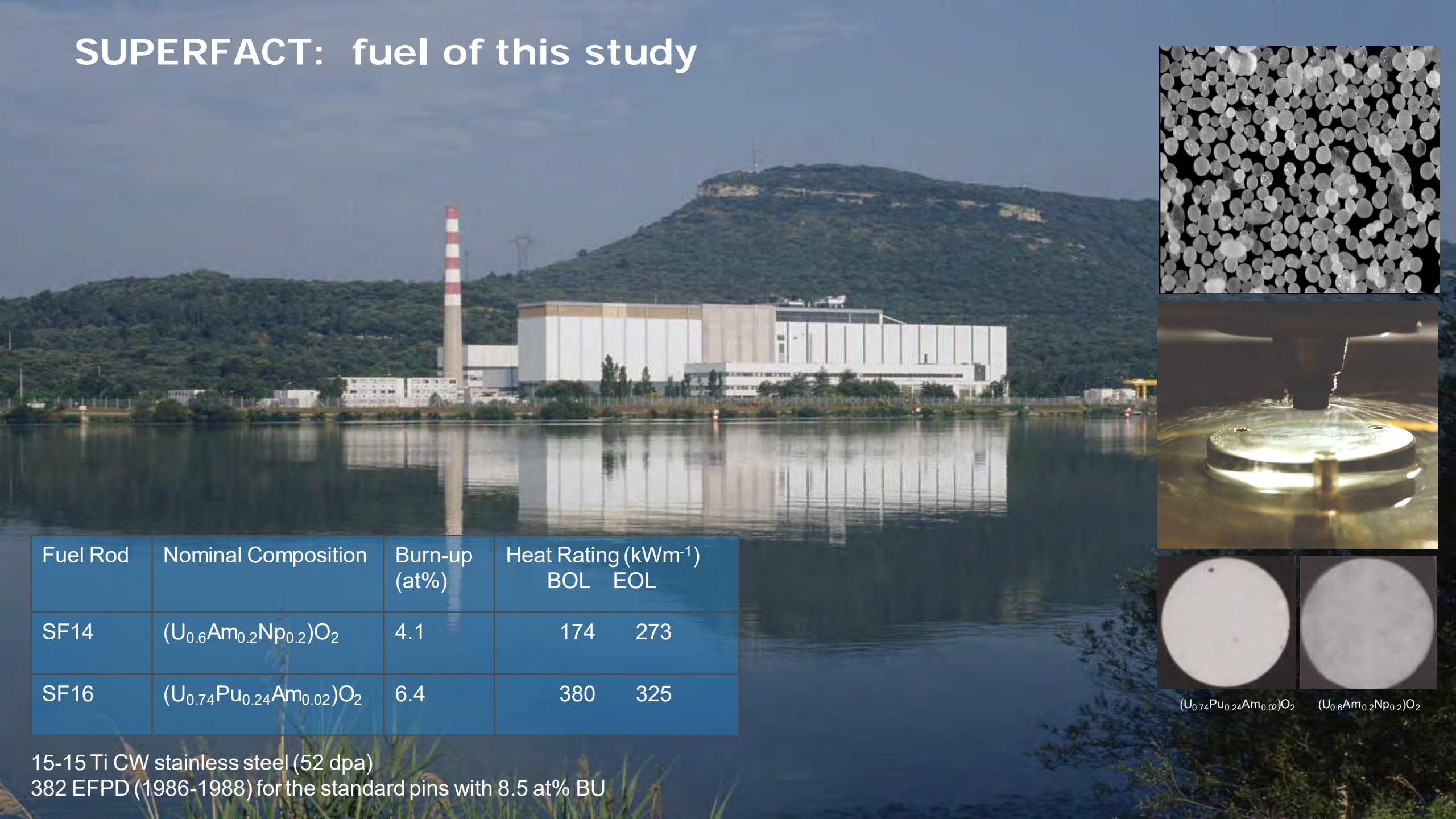
High MA content (SF14)

# Helium and damage in SUPERFACT and alpha-doped $\text{UO}_2$



Sample	$\alpha$ -Decays [ $\text{g}^{-1}$ ]	Dpa	Storage Time (Years)		
			Eq. Standard LWR (40 GWd/t)	Eq. HBU LWR (100 GWd/t)	Eq. MOX LWR (45 GWd/t)
SF2 $(\text{U}_{0.74}, \text{Pu}_{0.24}, \text{Am}_{0.02})\text{O}_2$	$5.5 \times 10^{18}$	1.3	2000	250	80
SF4 $(\text{U}_{0.6}, \text{Am}_{0.2}, \text{Np}_{0.2})\text{O}_2$	$2 \times 10^{19}$	4.9	55,000	12,000	1000
SF14 $(\text{U}_{0.6}, \text{Am}_{0.2}, \text{Np}_{0.2})\text{O}_2$ irr.	$6.4 \times 10^{19}$	15.9	>1,000,000	550,000	60,000
UPuO-10 $(\text{U}_{0.9}, {}^{238}\text{Pu}_{0.1})\text{O}_2$	$1.6 \times 10^{19}$	4	30,000	5000	600
UPuO-5 $(\text{U}_{0.975}, {}^{238}\text{Pu}_{0.025})\text{O}_2$	$1.4 \times 10^{18}$	0.33	200	25	1

# SUPERFACT: fuel of this study



$(U_{0.74}Pu_{0.24}Am_{0.02})O_2$        $(U_{0.6}Am_{0.2}Np_{0.2})O_2$

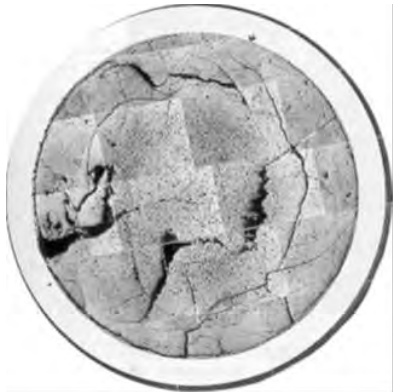
Fuel Rod	Nominal Composition	Burn-up (at%)	Heat Rating ( $kWm^{-1}$ )	
			BOL	EOL
SF14	$(U_{0.6}Am_{0.2}Np_{0.2})O_2$	4.1	174	273
SF16	$(U_{0.74}Pu_{0.24}Am_{0.02})O_2$	6.4	380	325

15-15 Ti CW stainless steel (52 dpa)  
382 EFPD (1986-1988) for the standard pins with 8.5 at% BU

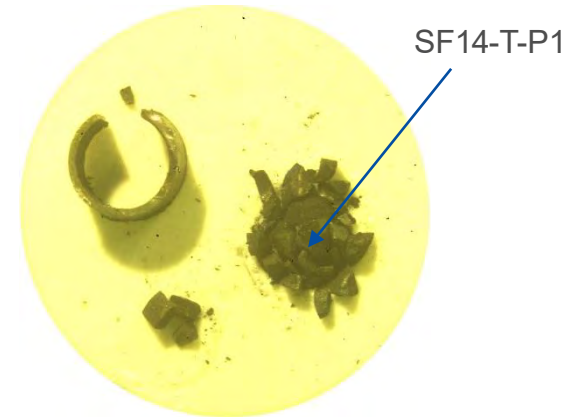


# Optical microscopy – selection of samples

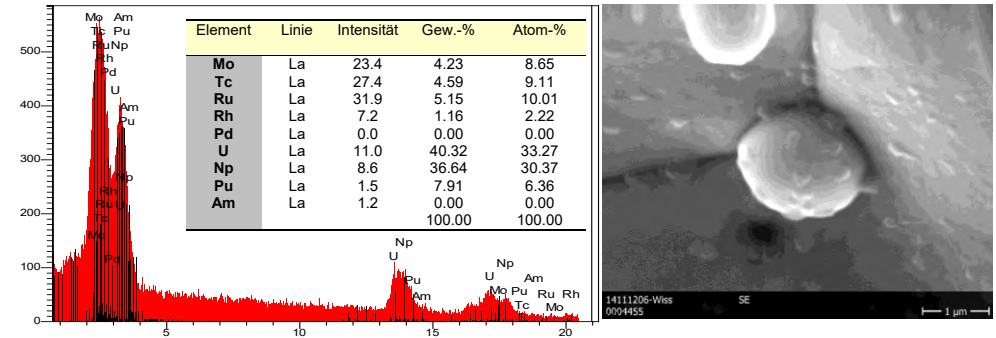
Typical observations for  $(U_{0.6}Np_{0.2}Am_{0.2})O_2$  fuel SF14:



- Actinide transmutation 31%
- Begin of PCMI noted
- **High helium production** (60 times standard pins) and release (high porosity)
- Swelling (axial expansion 2.3%, radial expansion 3.3%)
- No restructuring (low power)



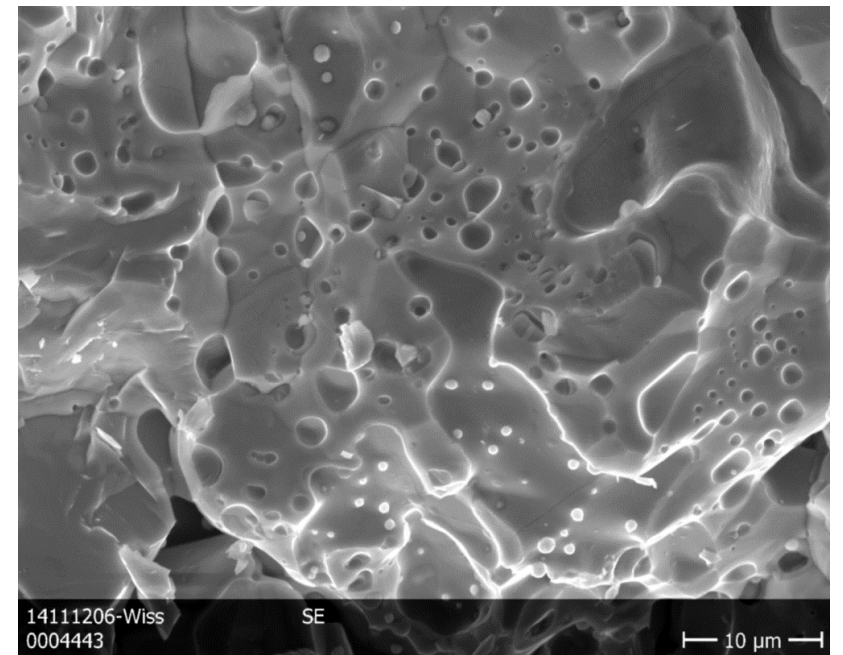
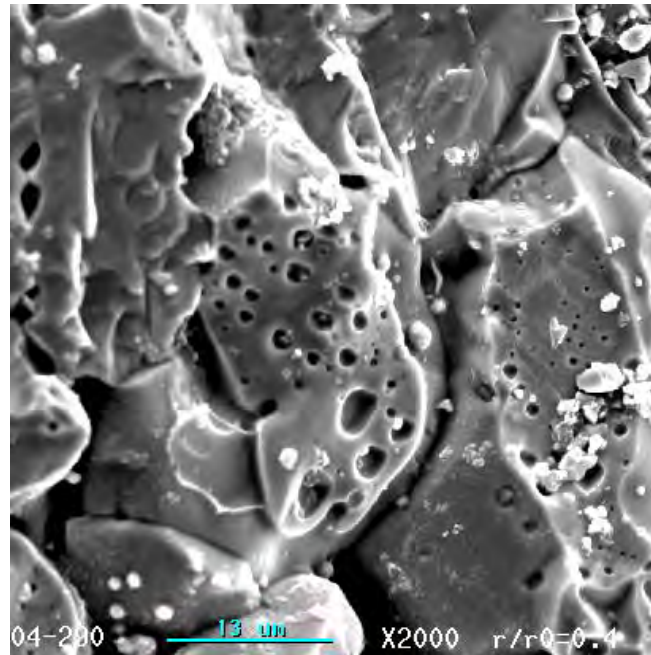
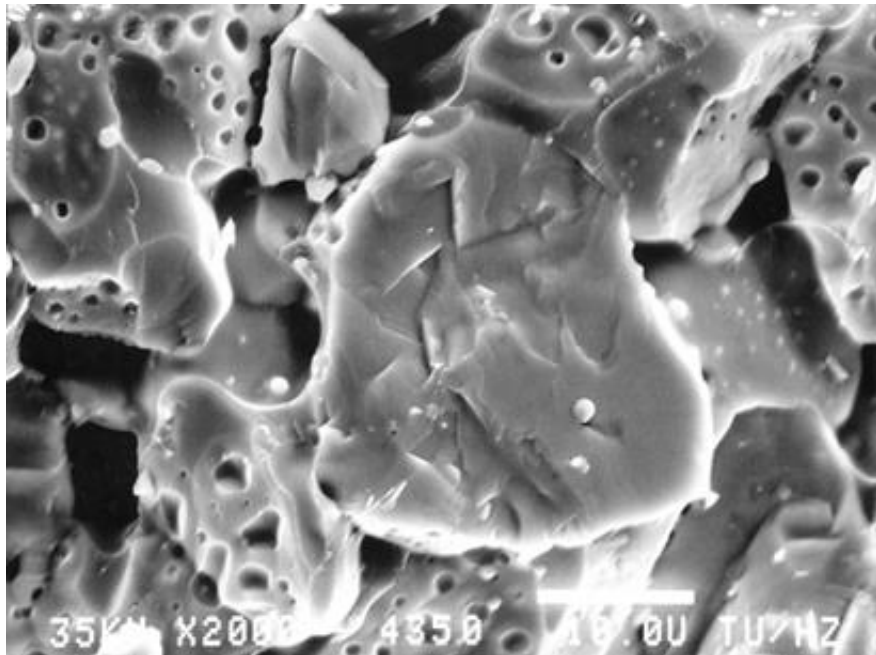
# SEM over time – SF14



1991

2003

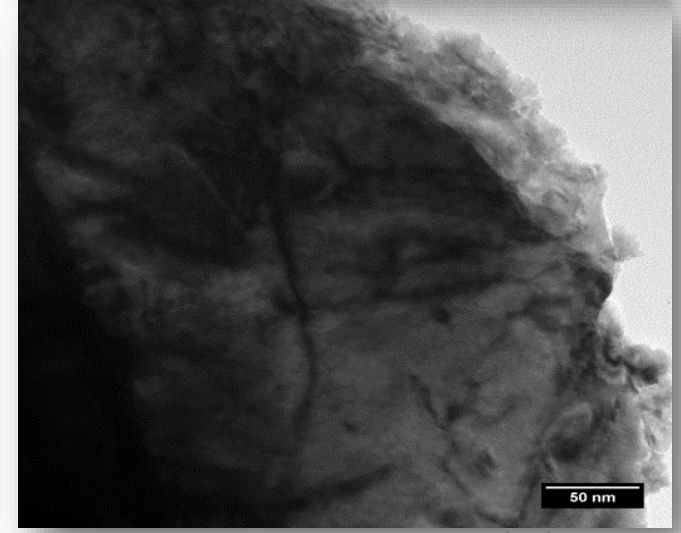
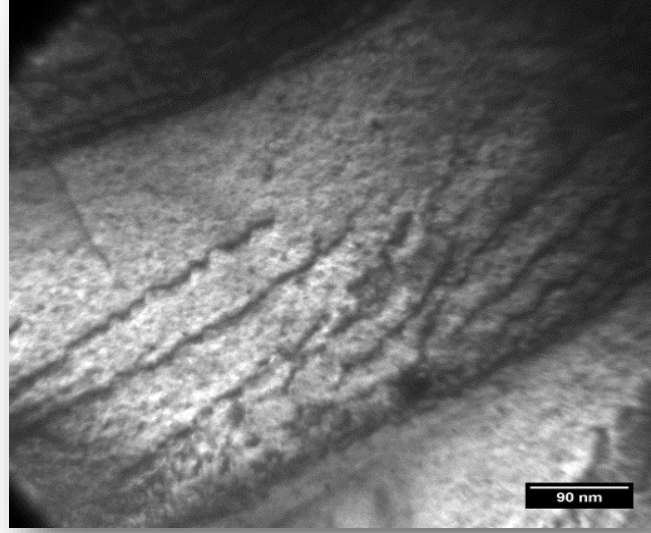
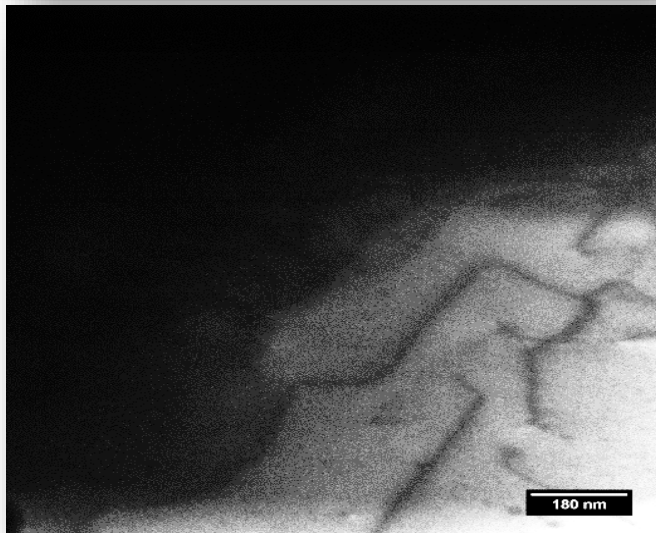
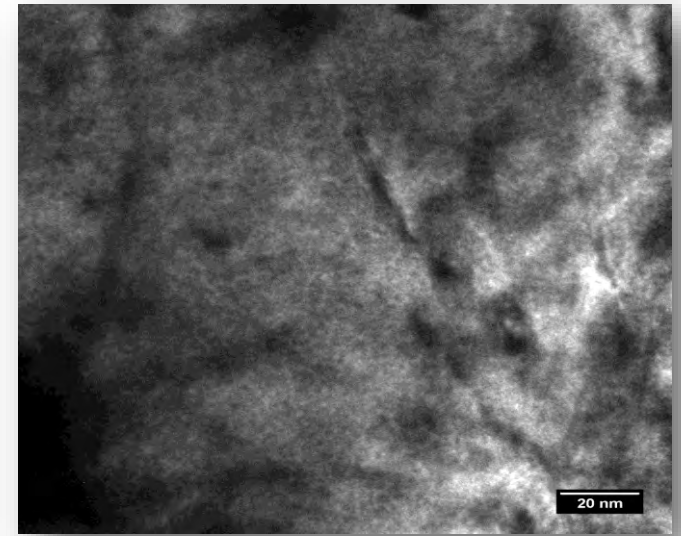
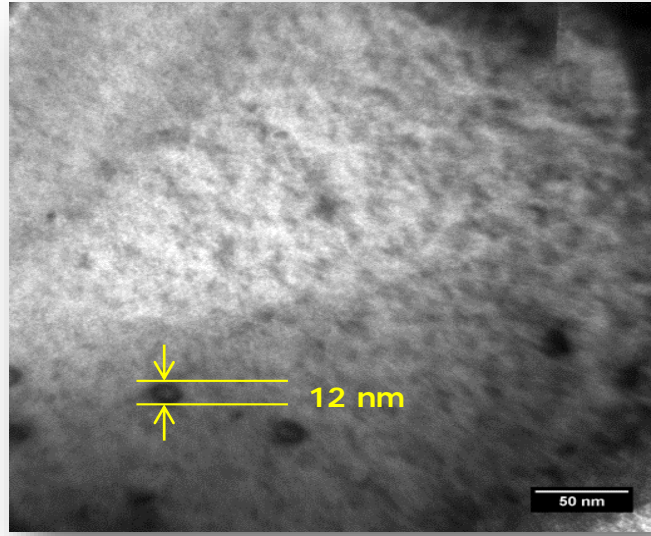
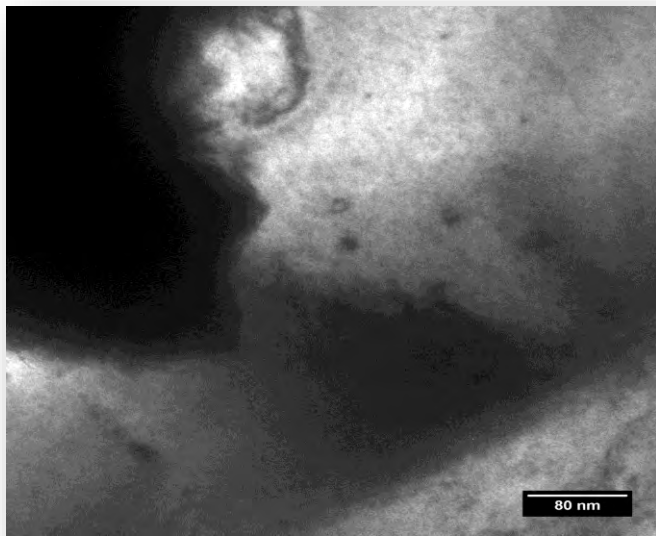
2014



No observable degradation, i.e. GB opening



# SUPERFACT Irradiated SF14-T-P1

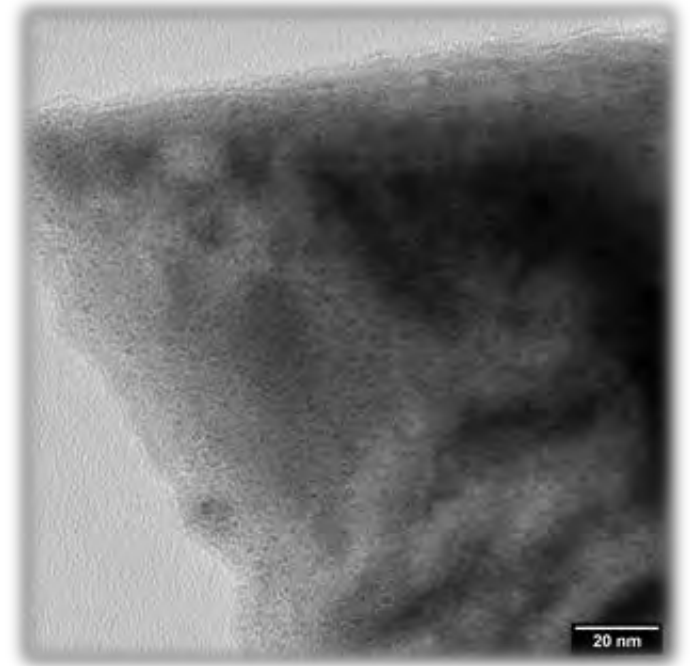
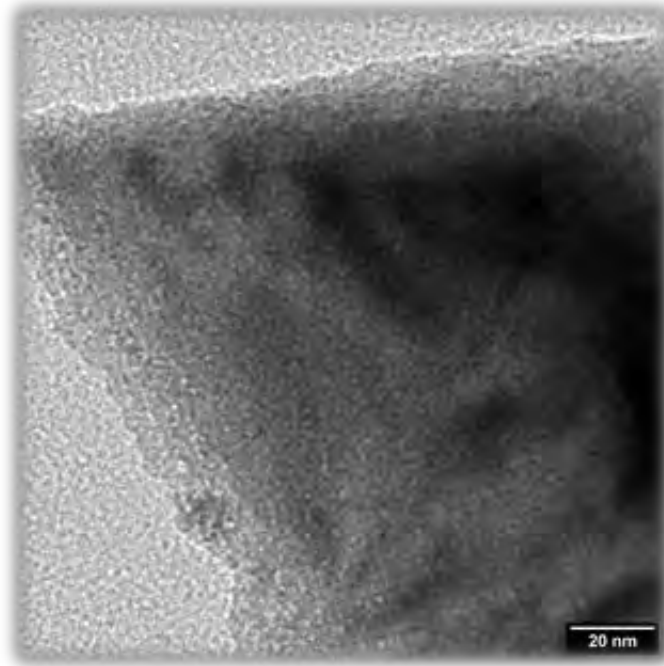
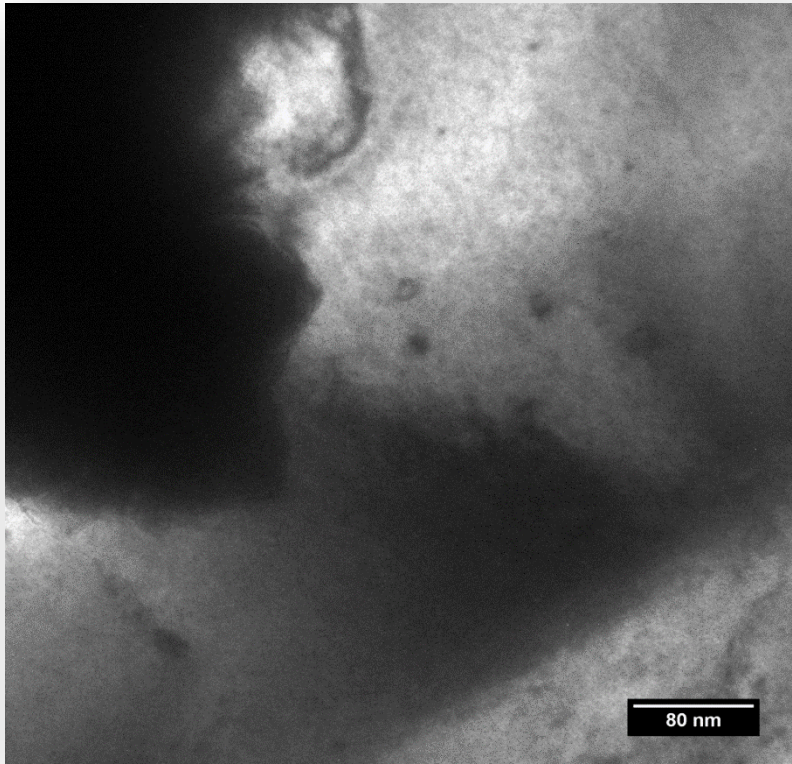


EOI + 16 dpa

$6.3 \times 10^{19} \alpha.g^{-1}$

Dislocation loops and lines

# TEM of SUPERFACT Irr. SF14-T-P1



EOI + 16 dpa

$6.3 \times 10^{19} \text{ } \alpha \cdot \text{g}^{-1}$

Dislocation loops and He bubbles

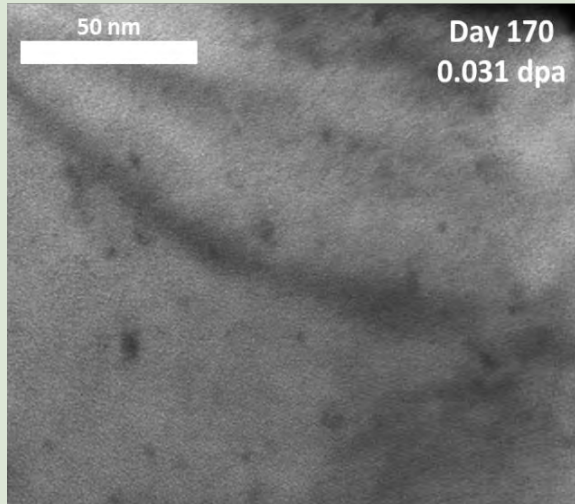


# Alpha-doped $\text{UO}_2$

$^{238}\text{Pu}$  different content

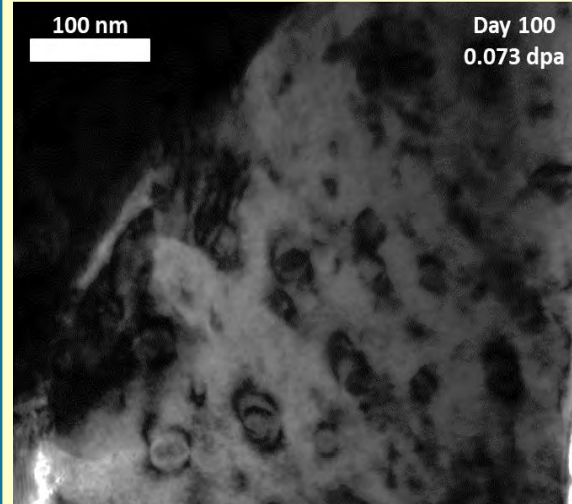
# Periodic characterization – TEM of (U, <sup>238</sup>Pu)O<sub>2</sub>

2.5 % – 0.031 dpa



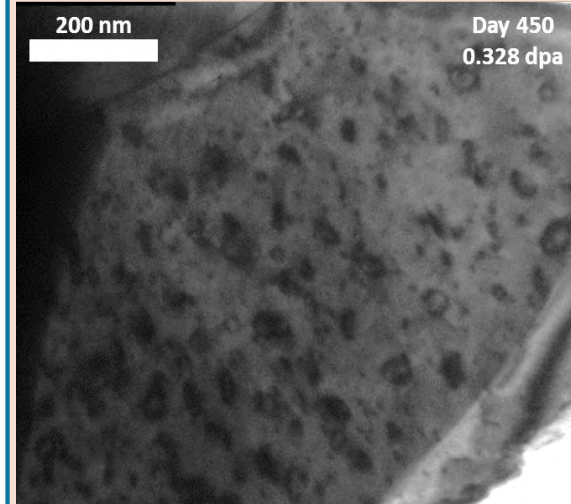
Onset of extended defects population

10 % – 0.073 dpa

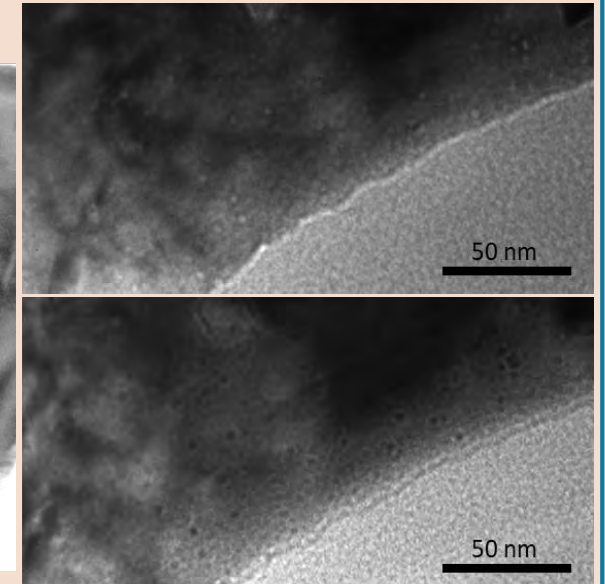


Dislocation loops

10 % – 0.328 dpa

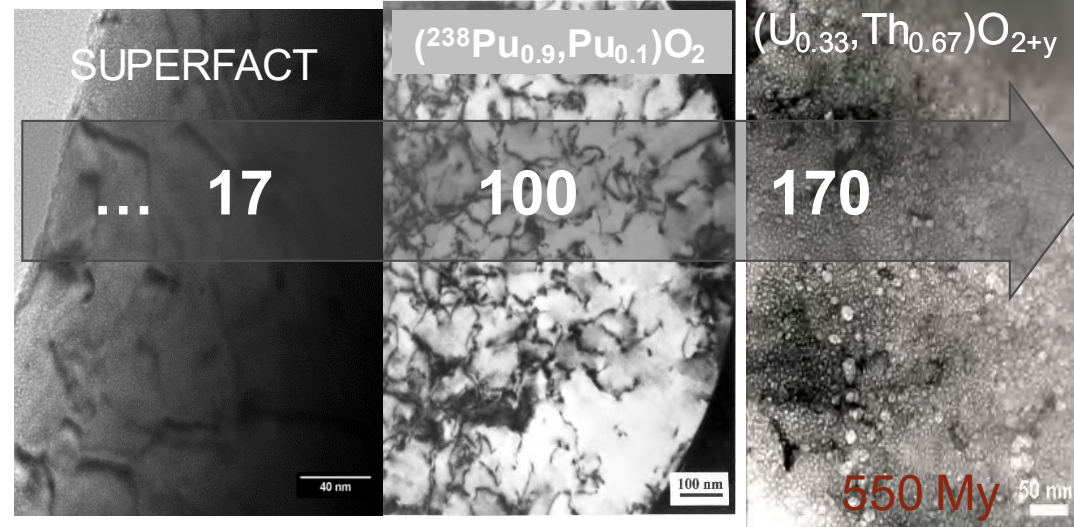
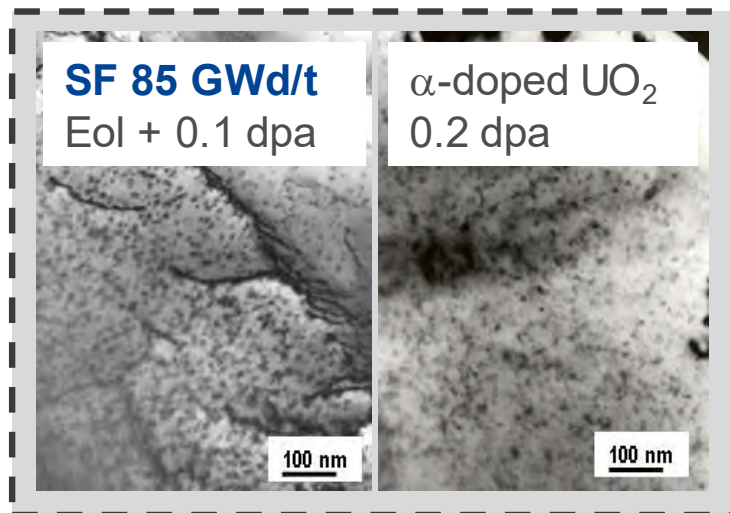
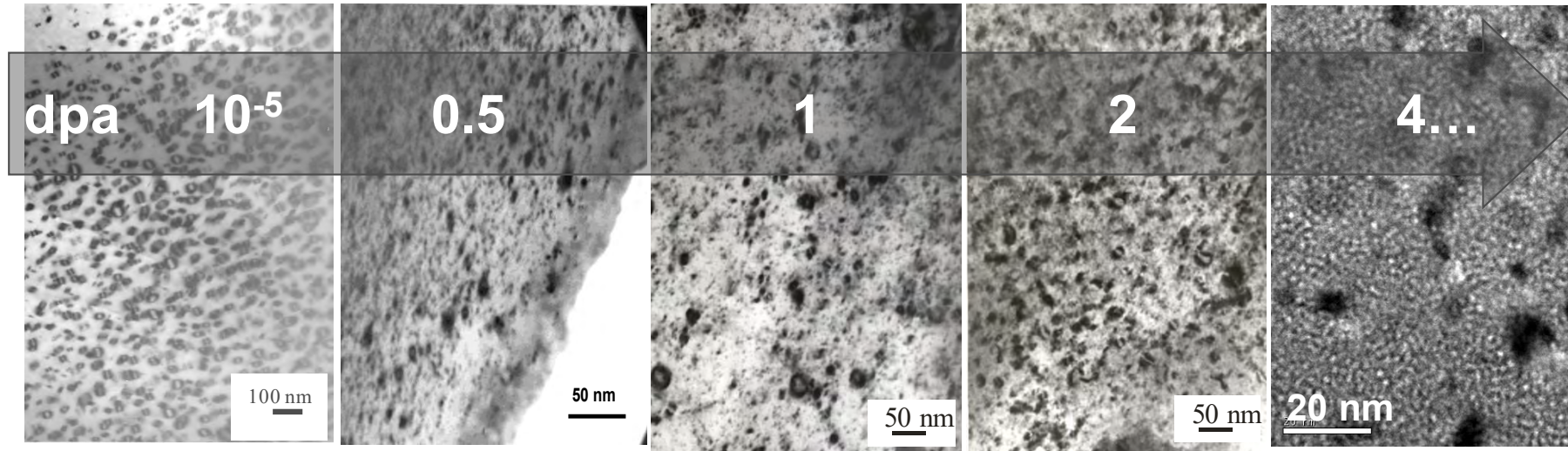


More and larger dislocation loops



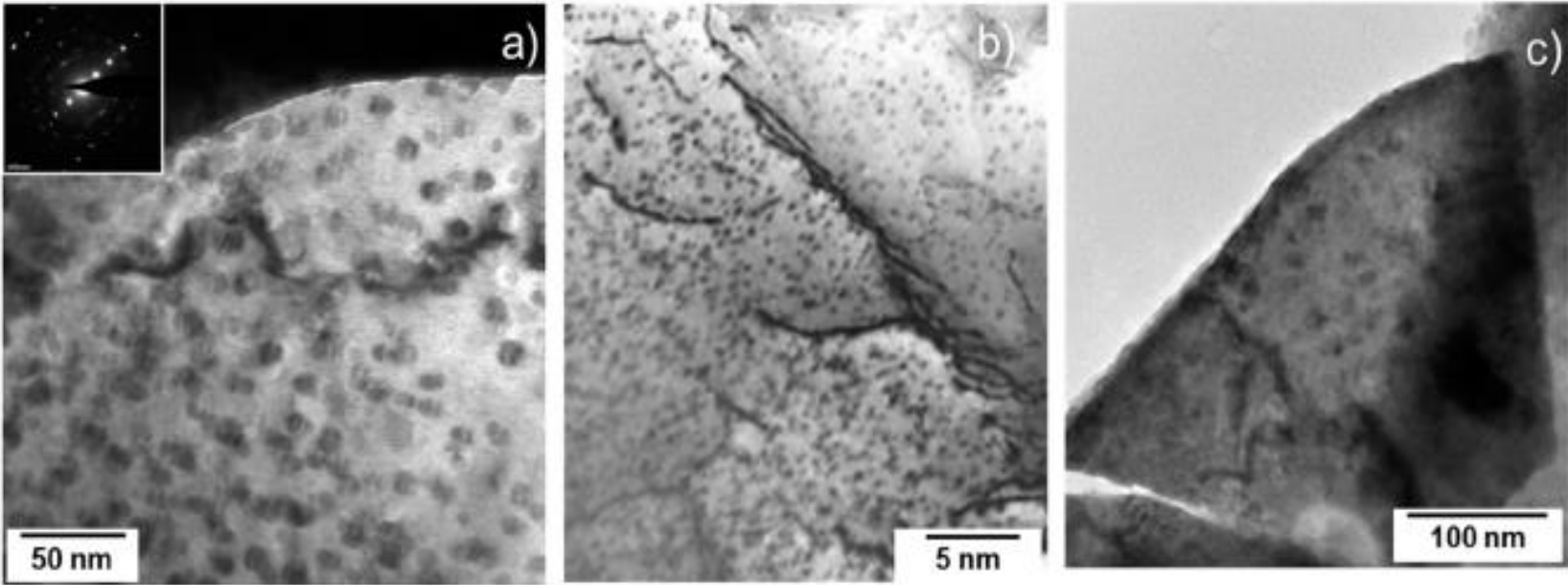
He bubbles

# Microstructure of alpha-damaged samples





# Comparison with irradiated fuel at 0.1 dpa



70 GWd.t<sup>-1</sup>

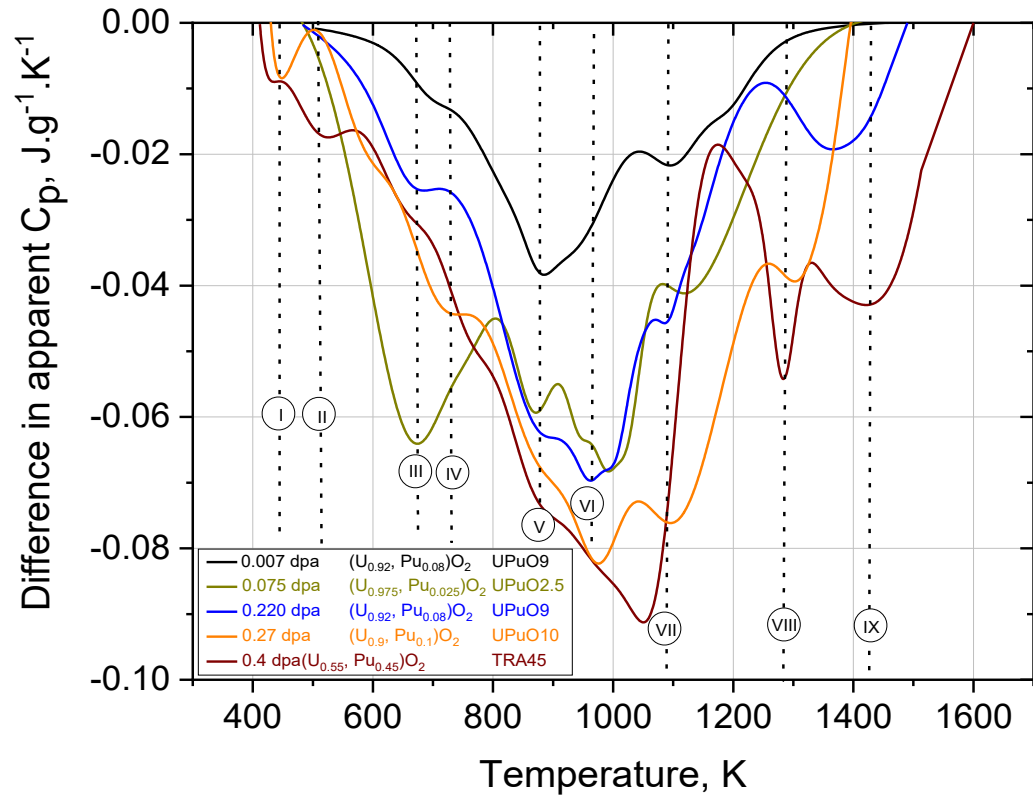
34 GWd.t<sup>-1</sup>

58 GWd.t<sup>-1</sup>

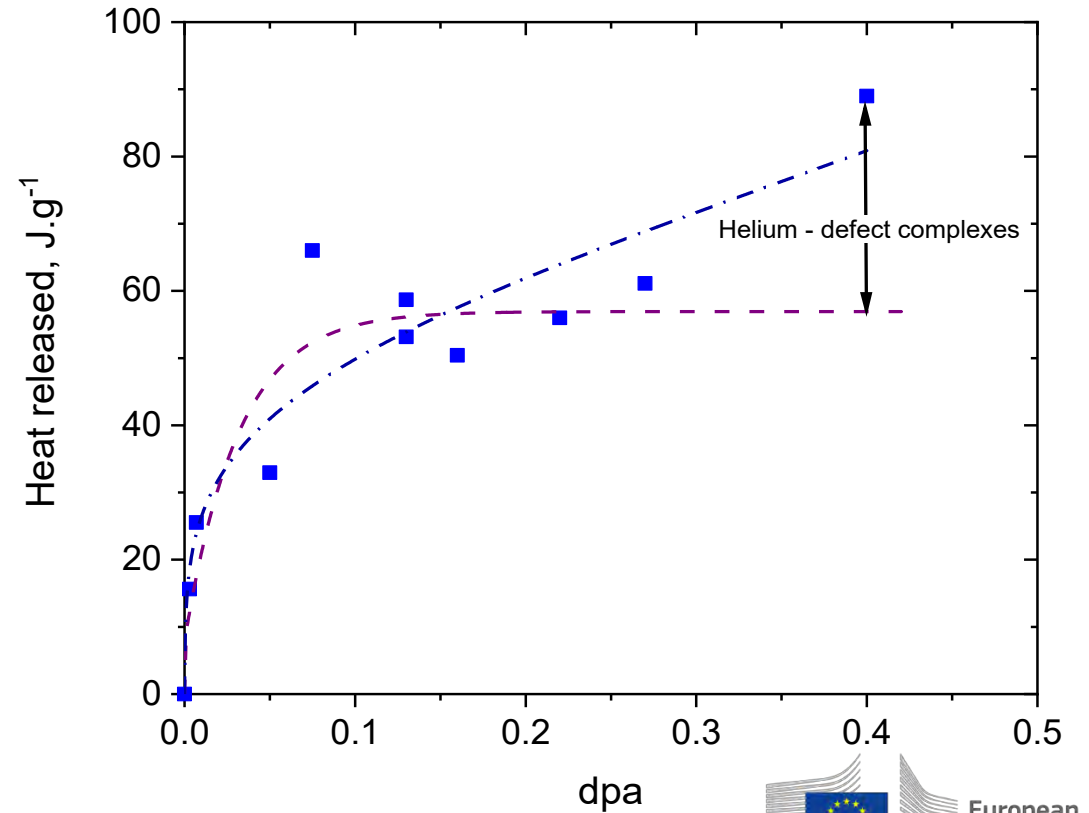


# Defect annealing

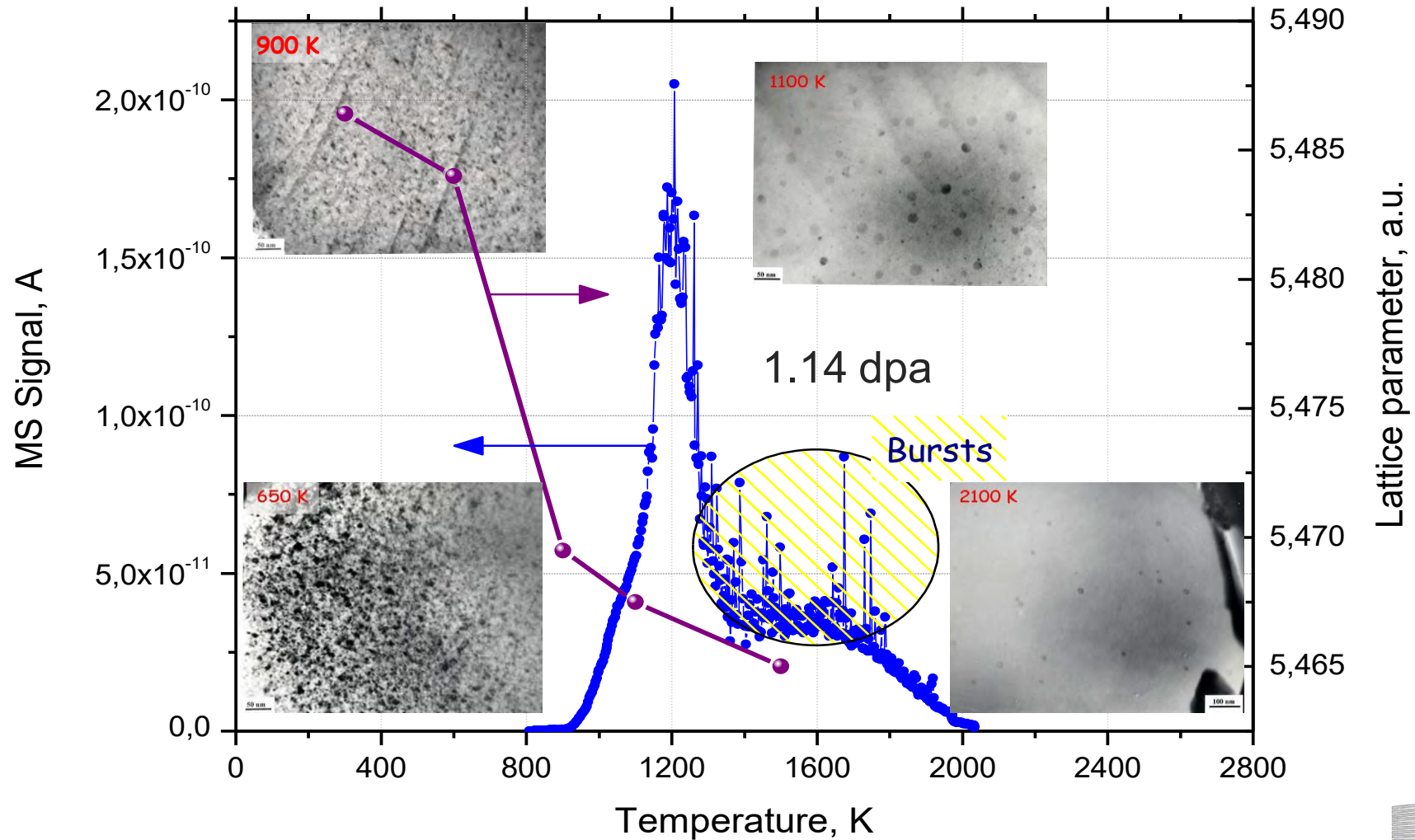
- Apparent  $C_p$



- Total heat (annealing)



# Annealing of alpha-damage + He release

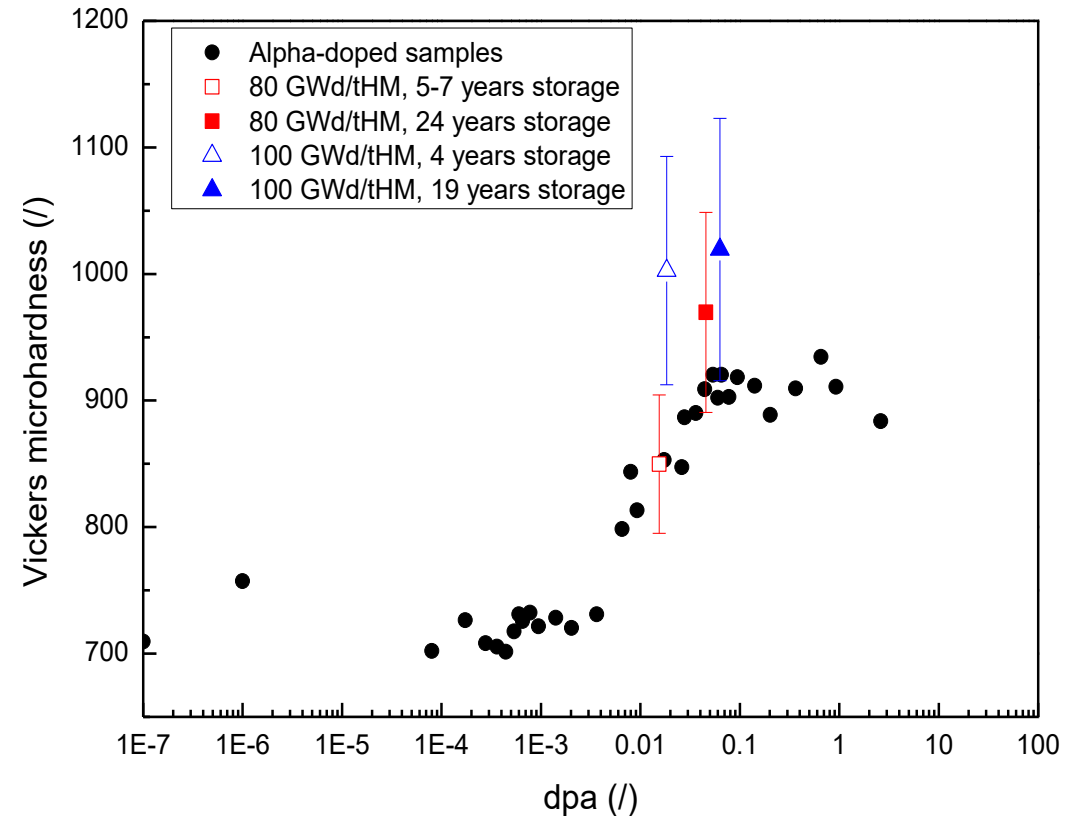


# Reconciling analogues and actual SNF

Example: hardening as a function of accumulated decay damage

Ageing studies performed on spent fuel analogues (alpha-doped  $\text{UO}_2$ ) under accelerated conditions must be validated on spent fuel.

Hardening trends observed on alpha-doped  $\text{UO}_2$  are confirmed by measurements on high burnup fuel after different storage times.



Vickers microhardness as a function of accumulated decay damage

# Takeaway message (SF ageing)

- Actinide dioxides with the fluorite structure can be used for the prediction of LWR spent nuclear fuel behaviour over an extended storage time or even over disposal times.
- It was previously demonstrated that for  $^{238}\text{Pu}$ -doped  $\text{UO}_2$ , a difference of a factor of 100 in activity does not affect the linearity of some properties (XRD, Hardness,...) related to damaging effects. The microstructure evolution follows a similar profile independently of the studied dose, and thus corroborates this finding and extends the range of materials to study from the ageing of spent LWR fuel to minor actinide doped  $\text{UO}_2$ .
- The irradiated SUPERFACT transmutation fuel constitutes an even more representative material because it has been irradiated and hence contains fission products and reactor irradiation damage.



# Takeaway message (ctnd)

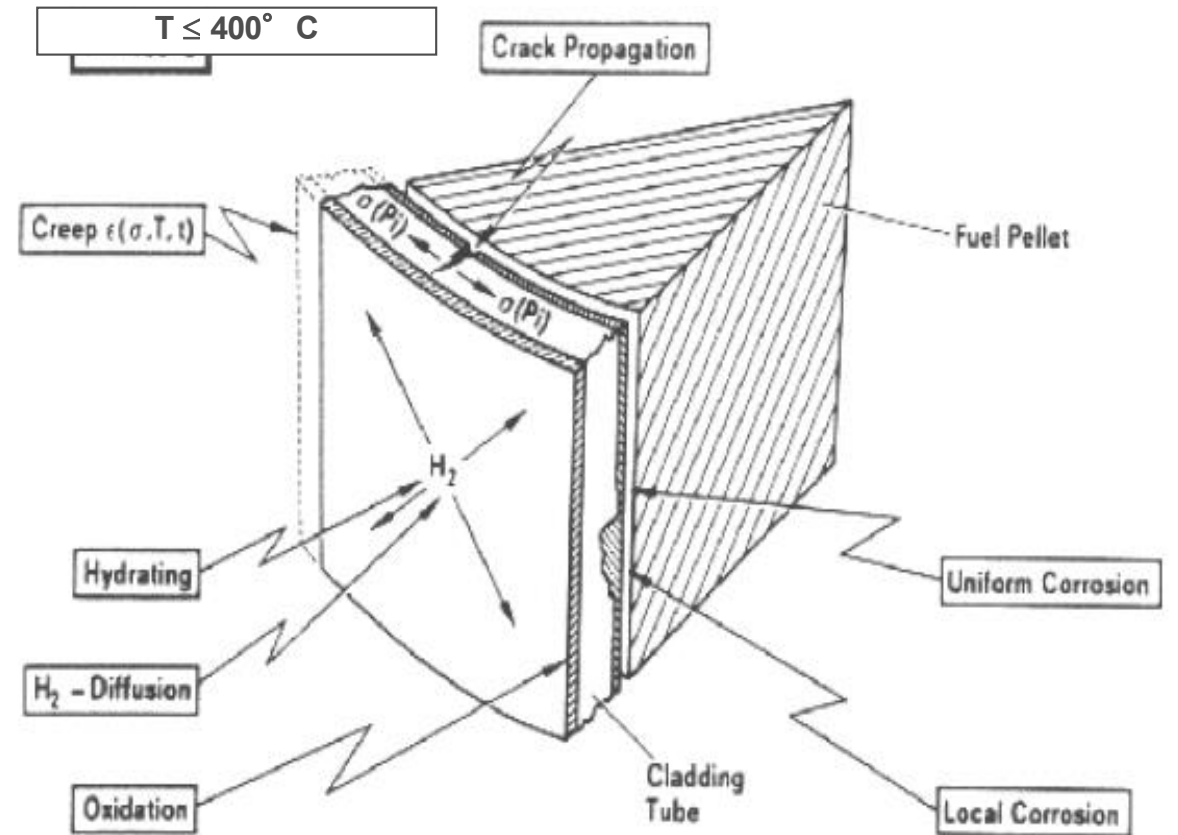
- For the highest dpa studied here, and in particular that of a reactor-irradiated material corresponding to a standard LWR fuel aged more than one million years, it has been shown that the material preserves its integrity and that the microstructure is characterized mainly by the presence of extended defects.
- Some limitations are intrinsic to the studied materials, whose actinide content does not reflect the reality of real spent fuel, particularly in the case of the irradiated SUPERFACT SF14 fuel, which presented a relatively large porosity formed during irradiation that could accommodate a substantial amount of helium.
- Annealing of alpha-damage starts at 500-600 K i.e. dry storage

# Spent fuel rod mechanical integrity during and after storage

# Spent fuel rod (clad) mechanical integrity degradation

## Interconnected processes:

creep, irradiation growth  
corrosion-assisted strength degradation  
burnup effects  
temperature transients: drying-cooling  
hydride reorientation  
embrittlement  
delayed hydride cracking  
mechanical load: pinch/impact, bending,  
fuel swelling/pellet-clad interaction



# Mechanical tests at JRC-Karlsruhe

## Reason:

Assessing the mechanical integrity and level of functionality of spent fuel rods retained during handling, storage and transportation, and behaviour under accident conditions.

## Scope:

Establish a basis of reference data and evaluate the response of spent fuel rods to external solicitations that might occur under various accident conditions.

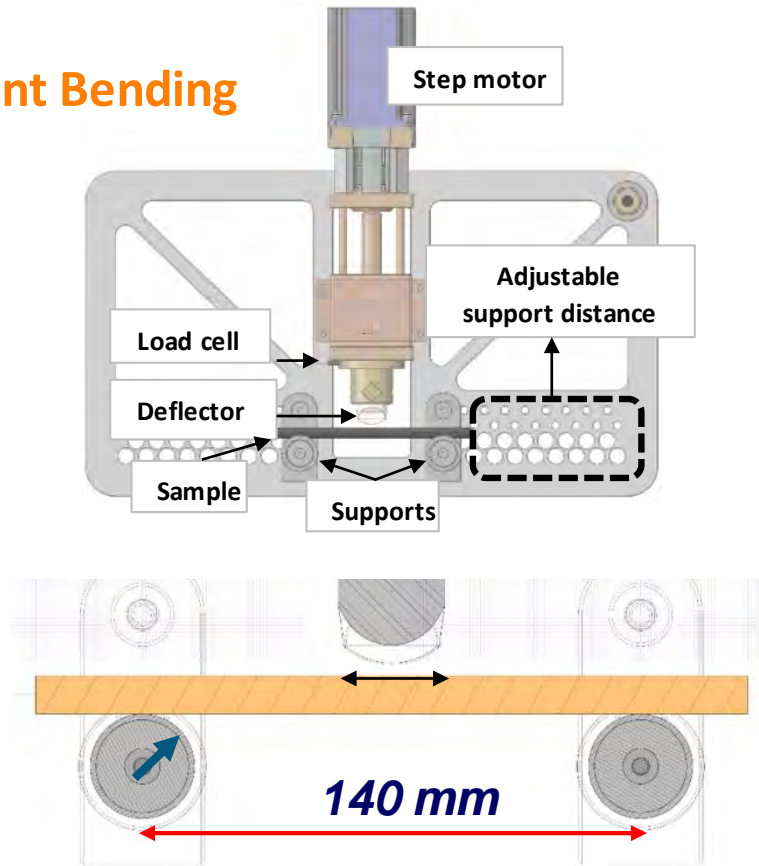
## Approach:

Bending and impact tests on fuel rod segments;

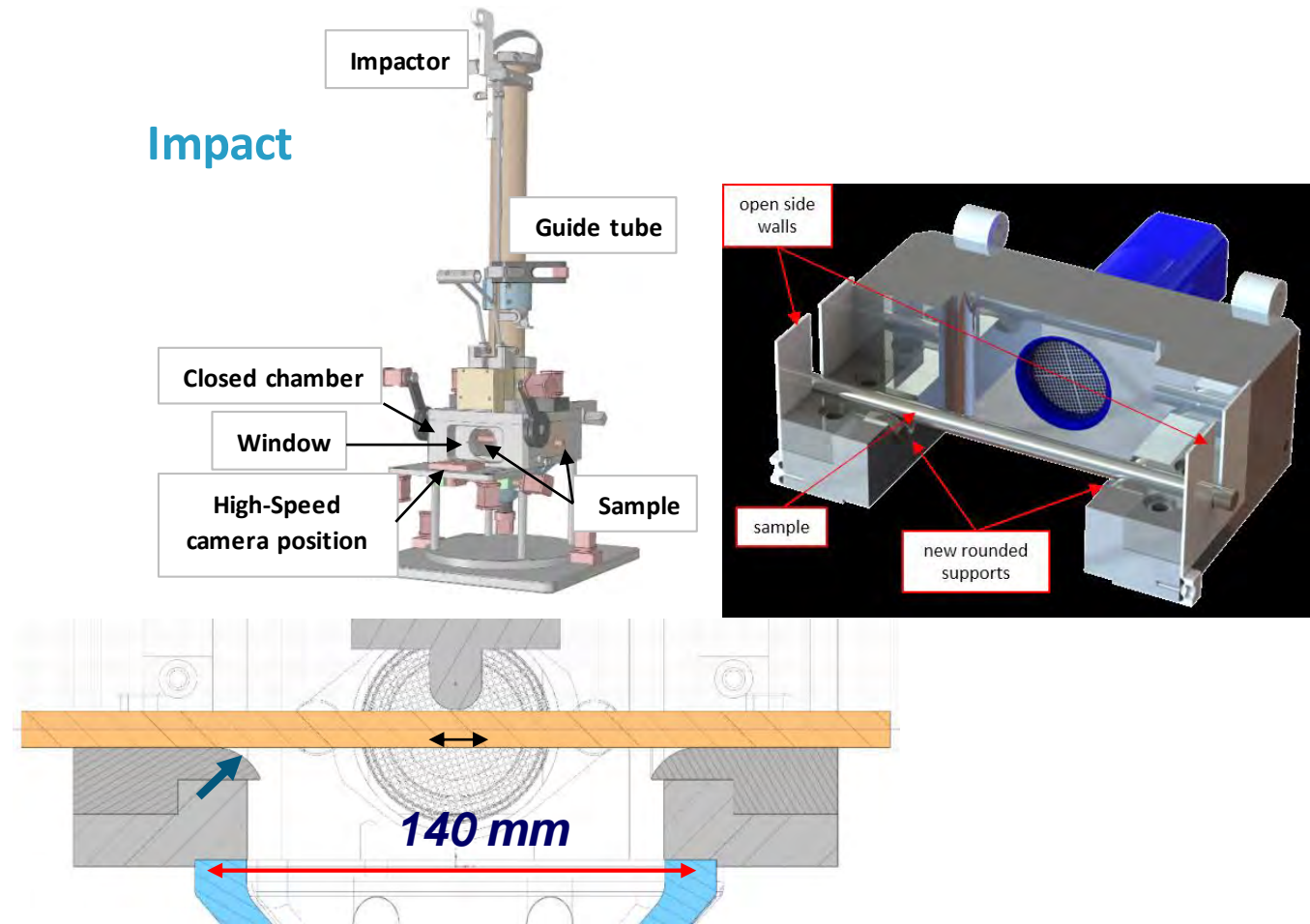


# Setup for bending and impact tests

## Three-Point Bending

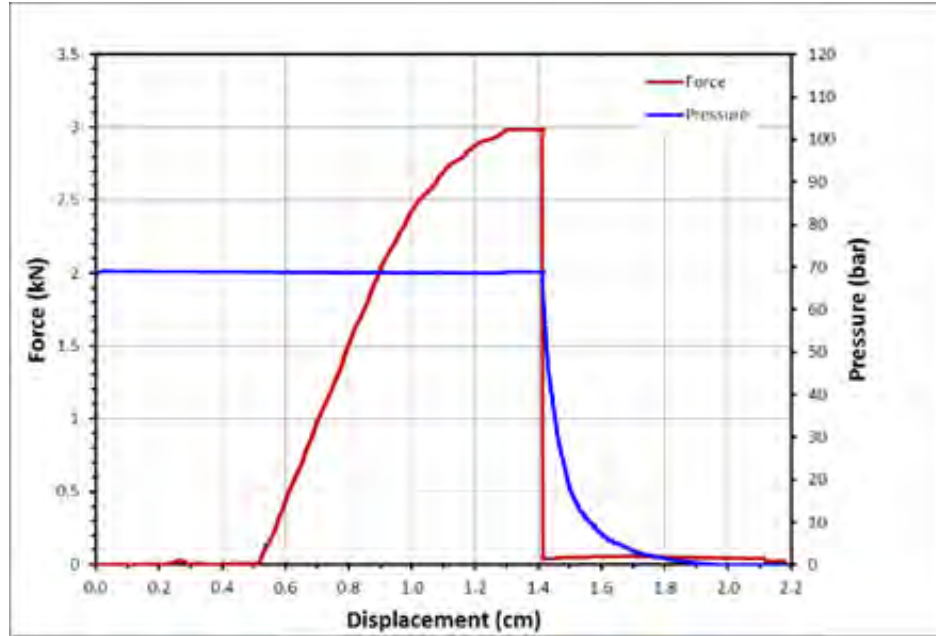


## Impact

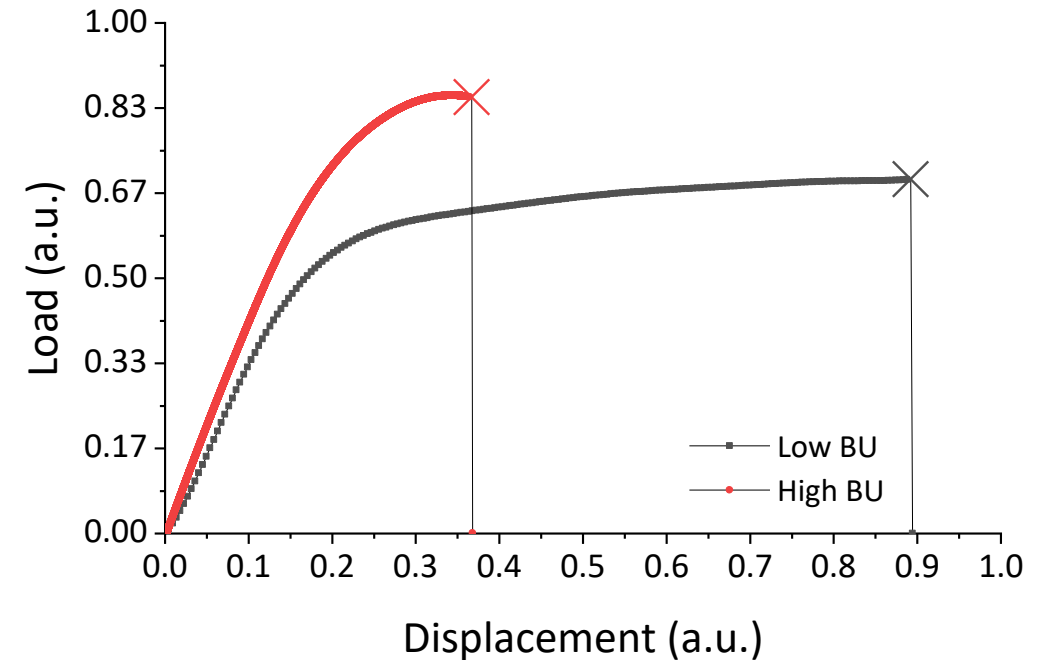


Similar geometrical configuration enables correlation between quasi-static and dynamic loads

# Bending of SNF rod segments

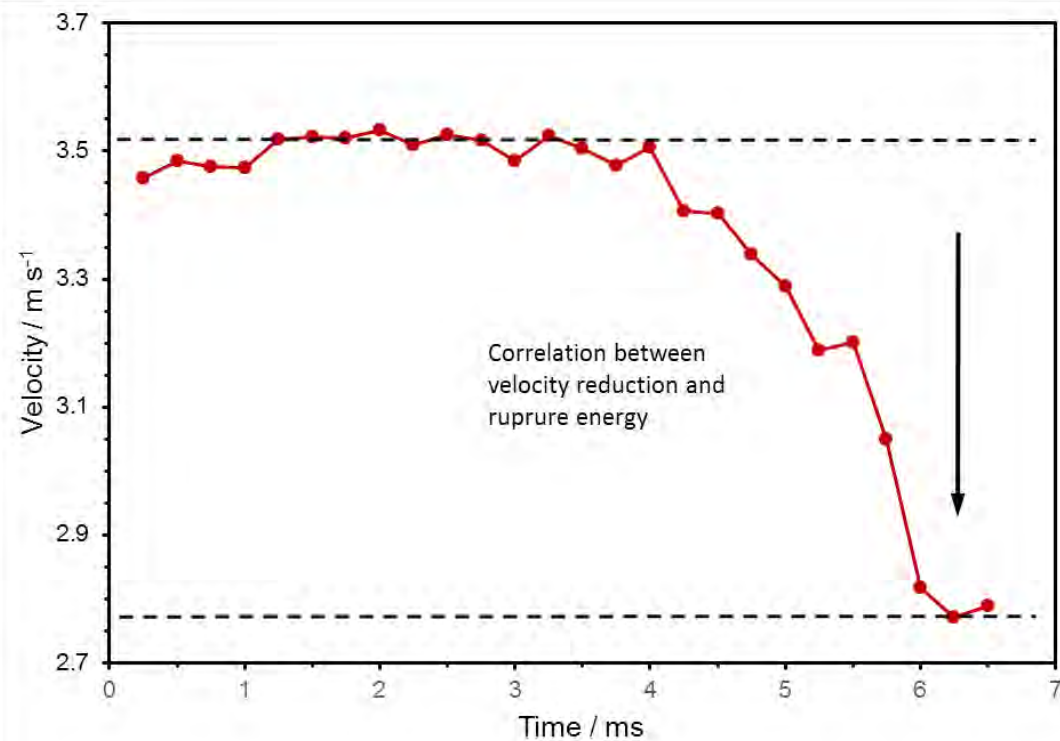
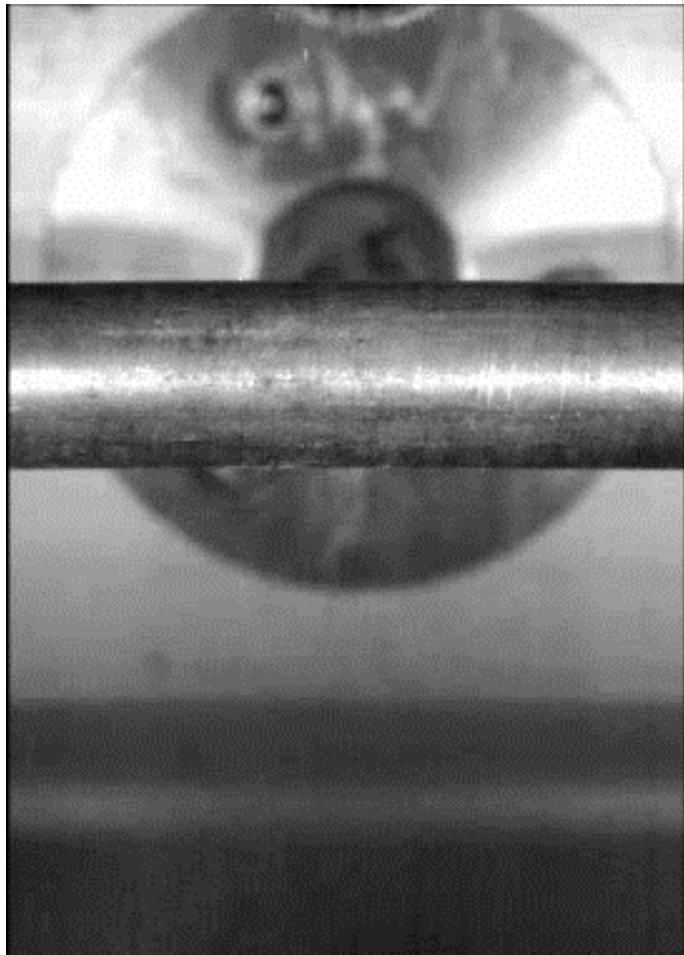


Bending test on a high burn-up SNF rod segment. Instant load drop at crack initiation; the complete depressurization of the segment after the initial drop, requires longer time when PC gap is closed.



- Low BU sample preserves ductility
- High BU sample: high stiffness and strength

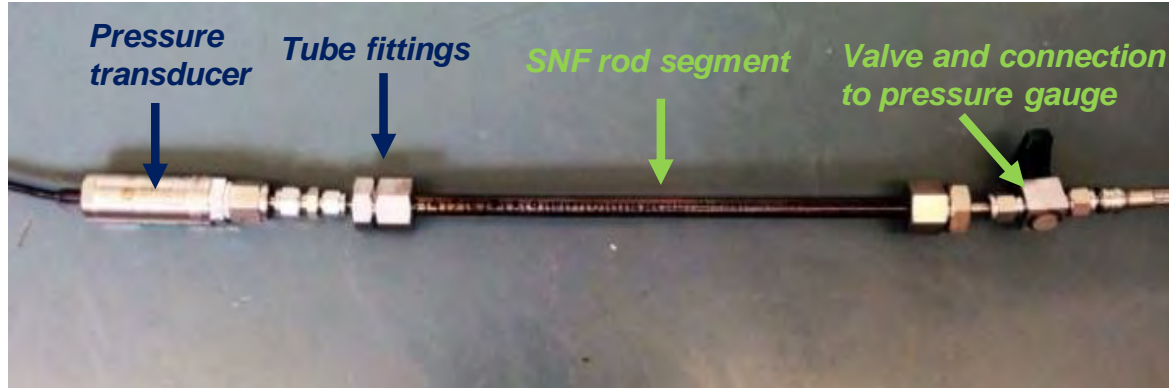
# High speed camera video during impacting



**Video digital analysis is used to calculate the transmitted rupturing energy.**

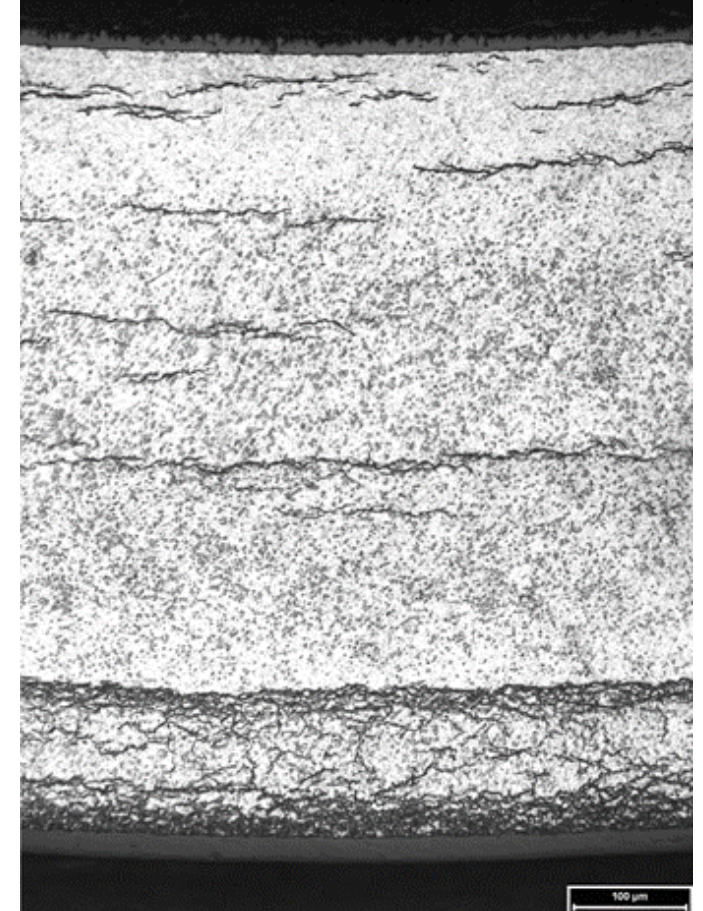


# Mechanical tests of a 59 GWd/t<sub>HM</sub> SNF rod specimen



## Specimen:

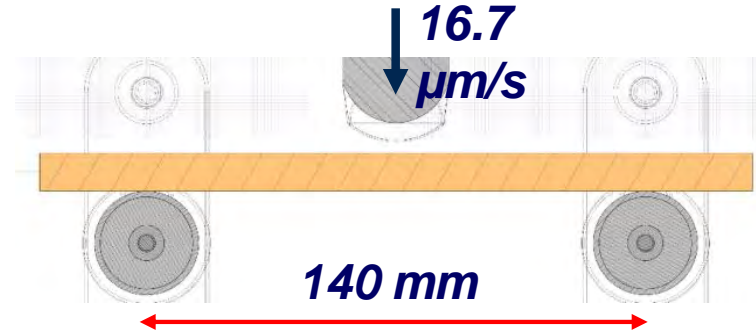
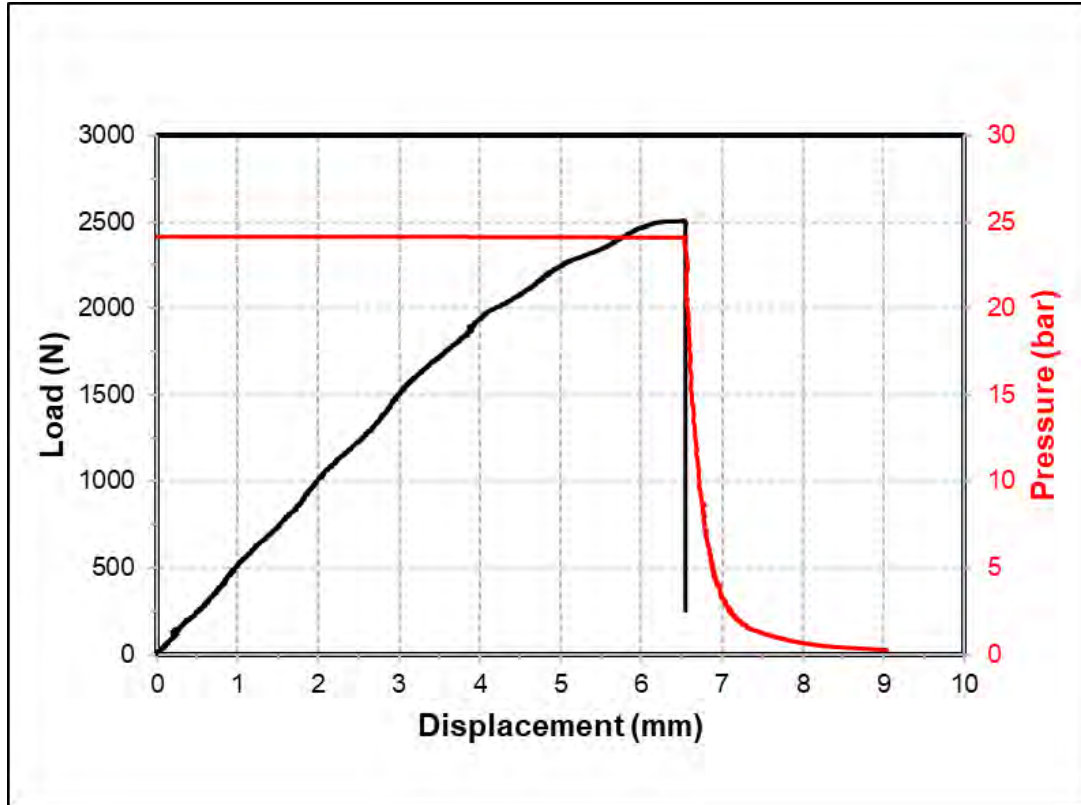
- UO<sub>2</sub>
- Central axial position, away from spacer;
- Cladding: DXD4 duplex (230 ppm Hydr.);
- NPP: PWR Gösgen / Switzerland;
- Average burn-up: 59 GWd/tHM;
- Pressure: 69 bar impact, 29 bar bending.





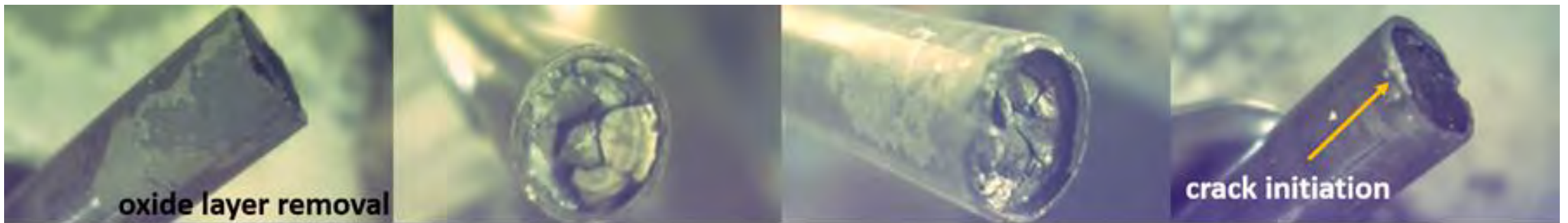
# 3-point bending test on SNF rod segments

59 GWd/tHM



- Deflector translation: 16.7  $\mu\text{m/s}$
- Load, displacement and pressure monitored online.
- Displacement (contact till rupture): 6.6 mm
- Maximum load: 2.5 kN (~9.1 J)
- Fuel mass released: 1.18 g

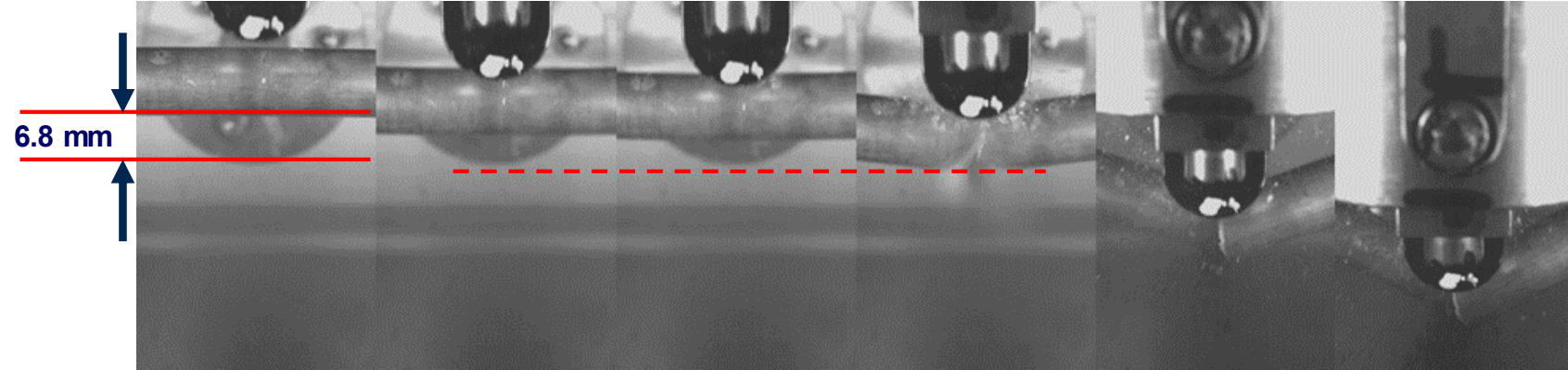
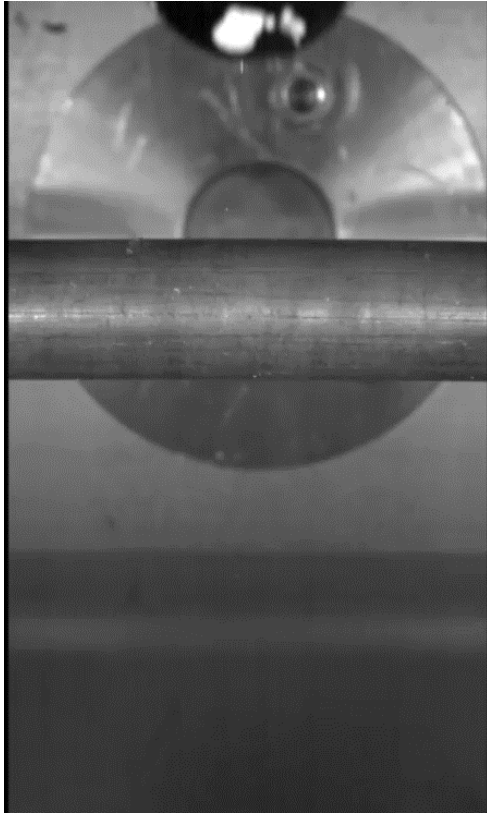
# Images of the broken SNF rod segment



## Fracture surfaces after impacting:

- Only limited fuel amount has been released, as it is strongly bonded with the cladding
- Near the impact location, the outer corrosion layer has been removed from the cladding.

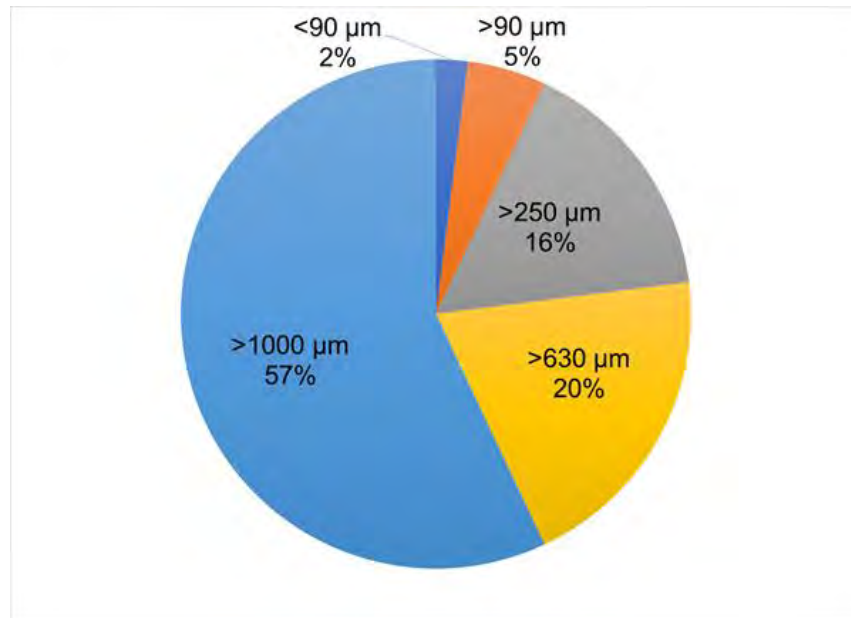
# Impact test on a 59 GWd/tHM SNF rod segment



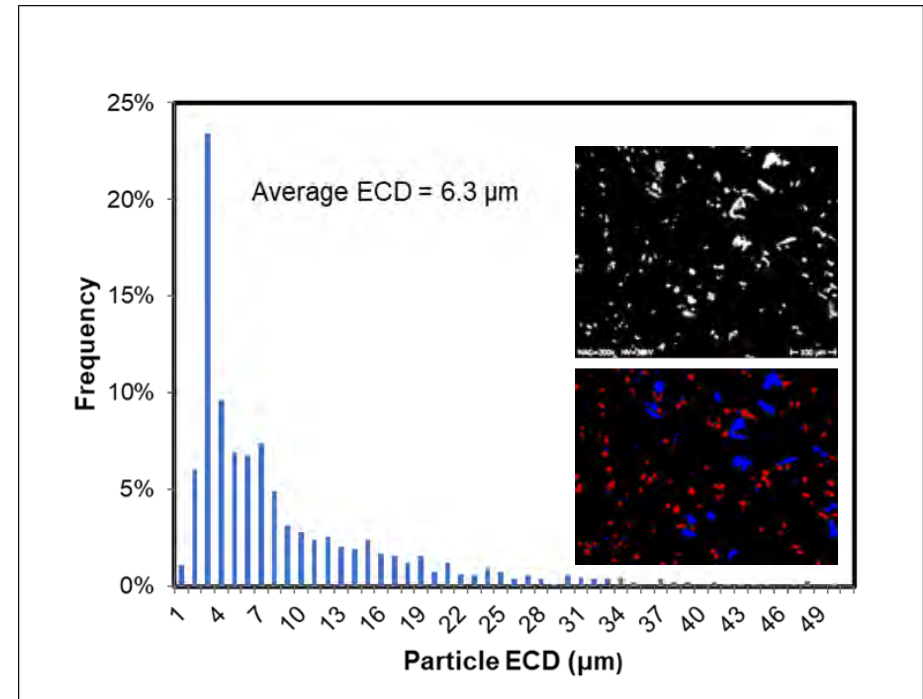
- High speed camera video recorded during impacting
- Splinters from the outer corrosion layer are first detached
- Due to internal pressure, fine particles are released explosively
- Displacement till crack initiation: 6.8 mm
- Absorbed energy upon fracture: 13.5 J
- Fuel mass released: 2.09 g

# Size of released fragments upon SNF rod breaking

- 99.5% of the mass released collected at the bottom of the testing chamber;
- The 0.5% missing fraction is constituted by aerosol and fine particulates.



Size distribution of coarse fragments collected at the bottom of the testing chamber after impact test.

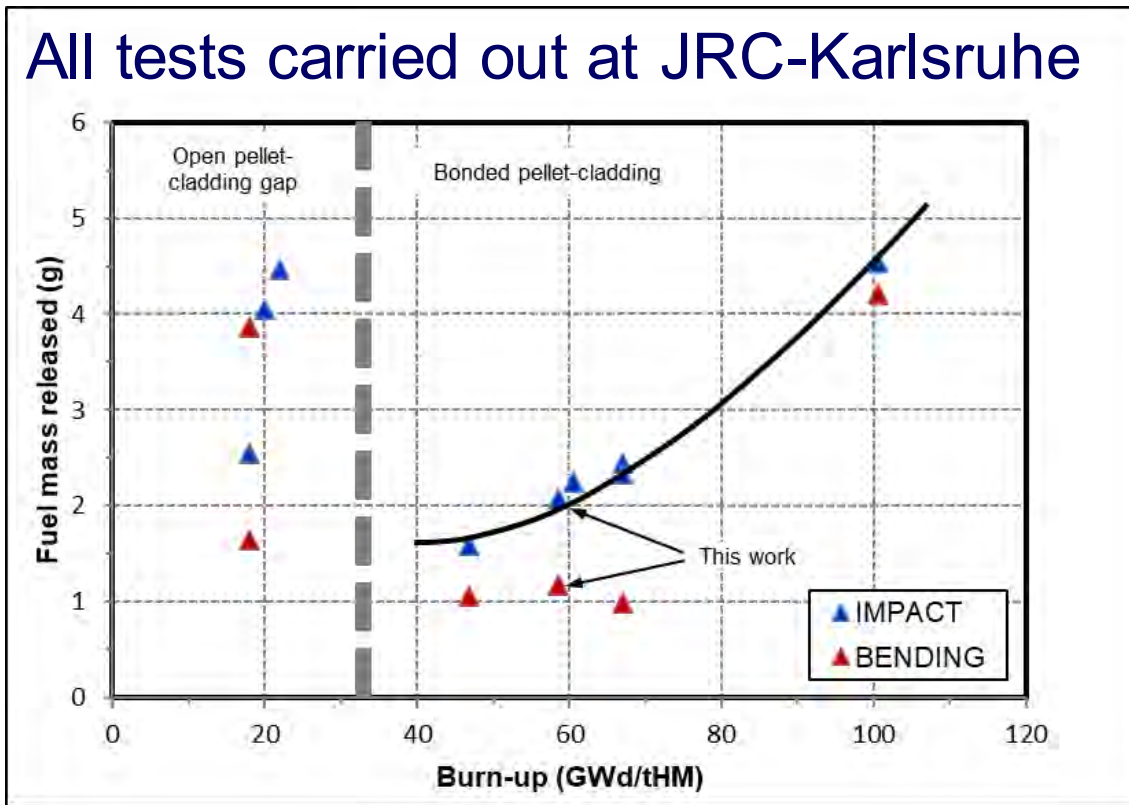


Classification and fractional size distribution of the aerosol particles released after impact test based on their equivalent circle diameter (ECD).



# Mass release during the SNF integrity tests

All tests carried out at JRC-Karlsruhe



Fuel mass released during impact and bending tests as a function of burn-up.

- The released fuel mass during bending or impact tests is of the same order of magnitude
- The higher mass release during impact is attributed to the higher energy transmitted to the specimen
- The released fuel did not exceed the mass of a single fuel pellet
- Increase of released mass with burn up was observed; lower masses of fuel release are expected around 30 GWd/tHM.

# Conclusion

- **In all tests the overall released masses did not exceed the mass of a single fuel pellet.**
- **The slightly higher mass release during impact in comparison to bending is attributed to the higher energy transmitted to the specimen.**
- **The main fraction of the released mass consists of relatively heavy fragments. A small fraction (~0.5%) is constituted by aerosol and fine particulates.**

# Acknowledgements

(spent fuel testing)

## *Collaboration*

*EURAD*

*contributions*

*SNF providers*

## *Other partners*

nagra.



framatome



*Sandia National Laboratories (SNL)*

*Pacific Northwest National Laboratory (PNNL)*

# Thank you for your attention! Questions?



## Stay in touch



JRC Science Hub:  
[ec.europa.eu/jrc](https://ec.europa.eu/jrc)



Twitter and Facebook:  
[@EU\\_ScienceHub](https://twitter.com/EU_ScienceHub)



LinkedIn:  
[european-commission-joint-research-centre](https://www.linkedin.com/company/european-commission-joint-research-centre)



YouTube:  
[JRC Audiovisuals](https://www.youtube.com/JRC_Audiovisuals)



Vimeo:  
[Science@EC](https://vimeo.com/Science@EC)





**F. Boldt**

**GRS**

## **The SPIZWURZ Project – Benchmark Update and Preliminary Results**

After service in operation spent nuclear fuel is stored in wet storage for several years. Dependent on the fuel storage concept, dry storage in dual-purpose casks follows for several decades. During the entire storage period spent nuclear fuel is subject to changes such as decay heat generation as well as continuous helium generation. Specific phenomena occurring during the drying process and the following storage have not been investigated in detail. In particular, the fate of hydrogen inside the fuel rod cladding remains an open question. It is still under discussion, under which conditions circumferential or radial hydrides form and how such precipitates influence the fuel rod's ductility.

The SPIZWURZ project includes a long-term cool-down of an electrically heated fuel rod simulator bundle at KIT's QUENCH facility. The experiment aims to study the hydrogen behaviour in zirconium-based fuel rod claddings assuming boundary conditions in the range of dry storage conditions. The bundle will be cooled from a peak temperature of around 400 °C over 8 months with a cooling rate of approximately 1.0 K/d. Prior to the experiments, the claddings will be loaded with defined hydrogen contents using a furnace at KIT. As experimental results we expect detailed information about the axial distribution of hydrides in fuel rod claddings after cool-down. Furthermore, we aim to analyse the location as well as orientation of hydrides depending on the axial position in the rod.

GRS proposes a benchmark to compare existing fuel rod simulation codes against the SPIZWURZ cool-down experiment regarding the prediction of hydrogen diffusion within fuel rod claddings. The benchmark will be performed as "blind benchmark" providing the necessary boundary conditions to predict the hydrogen behaviour during the experiment. Prior the experiment a preparation phase is launched to predict test the fuel rod simulation code capacities. Preliminary results of the GRS fuel rod code TESP-ROD are presented. It was predicted that hydrogen diffuses from the hot centre to cooler parts where the hydrogen precipitates according to the mechanical stresses in circumferential or radial orientation.

# The SPIZWURZ Project – Progress and Benchmark Update

**Felix Boldt**<sup>1),2)</sup>, Daniel Nahm<sup>1)</sup>, Thorsten Hollands<sup>1)</sup>, Alina Sutygina<sup>1)</sup>, Florian Falk<sup>1)</sup>

<sup>1)</sup>Gesellschaft für Anlagen- und Reaktorsicherheit (GRS) gGmbH

<sup>2)</sup>Technical University of Munich, Chair of Nuclear Technology

**27th International QUENCH Workshop**

**27 - 29 September 2022**

# Content

## Introduction

SPIZWURZ project  
Bundle experiment

## Benchmark overview

Boundary conditions  
Preliminary TESPA-ROD results

## Outlook and Timeline

**Spannungsinduzierte  
Wasserstoffumlagerung in Brennstabhüllrohren  
während längerfristiger  
Zwischenlagerung (SPIZWURZ)**






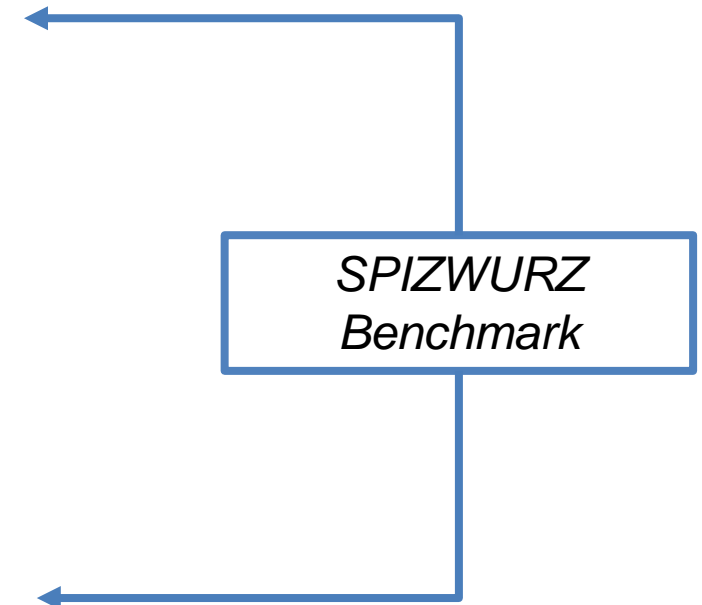
Credit: Audrius Meskauskas

Purple gentian  
(ger. Spitzwurz)

*Stress-induced hydrogen  
rearrangement in fuel rod claddings  
during long-term storage  
(SPIZWURZ)*

## Introduction *SPIZWURZ project*

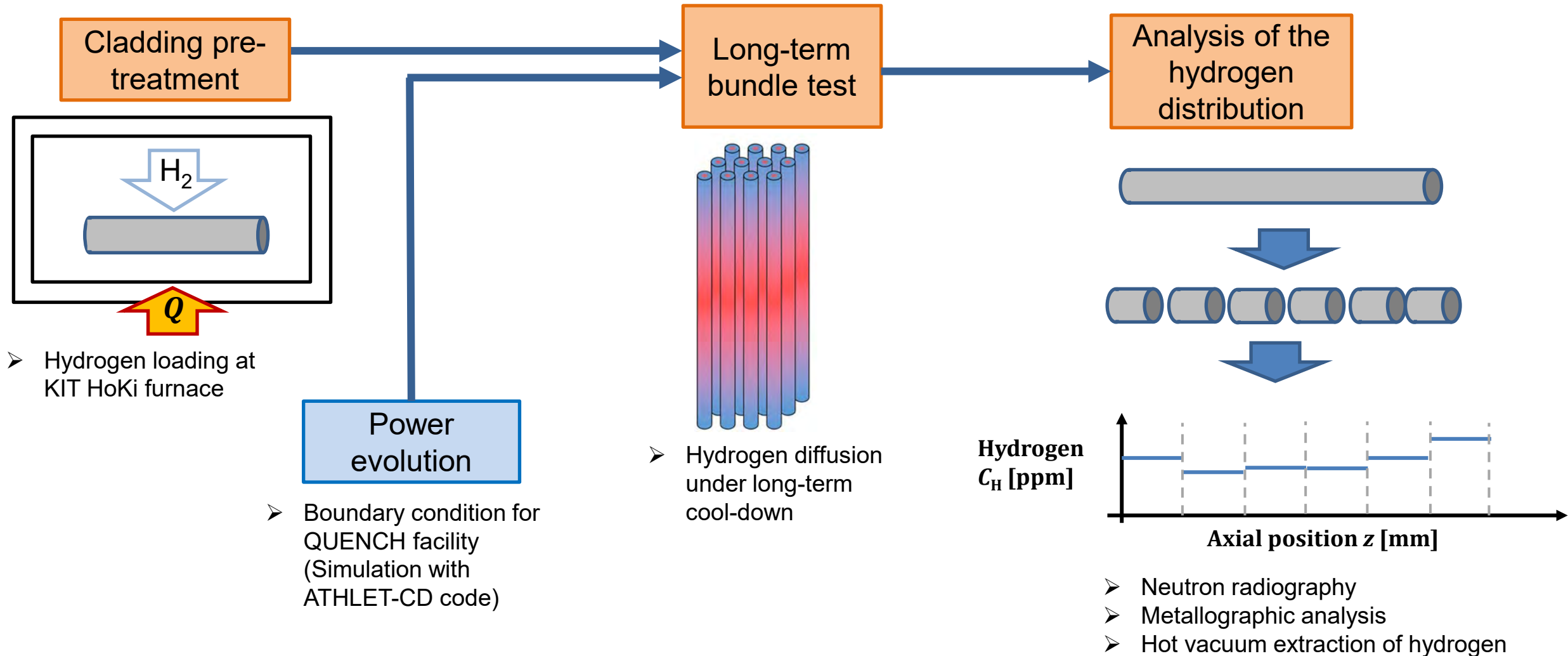
- Joint project of  global research for safety and  1825 1956 2009 Karlsruhe Institut für Technologie and as observer  Gesellschaft für Zwischenlagerung mbH
- Experimental determination and theoretical description of the **solubility and diffusion** of hydrogen in cladding tube materials under long-term storage conditions.
- Qualitative and quantitative description of hydrogen diffusion on a **macroscopic and microscopic scale** for improved prediction of the formation of hydride structures in zirconium alloys
- Improvement of the data on the **pellet-cladding interaction** during spent fuel storage
- Consolidation of all results into a consistent description of real cladding tube materials under conditions of long-term storage with reference to irradiation and slow cooling rates.





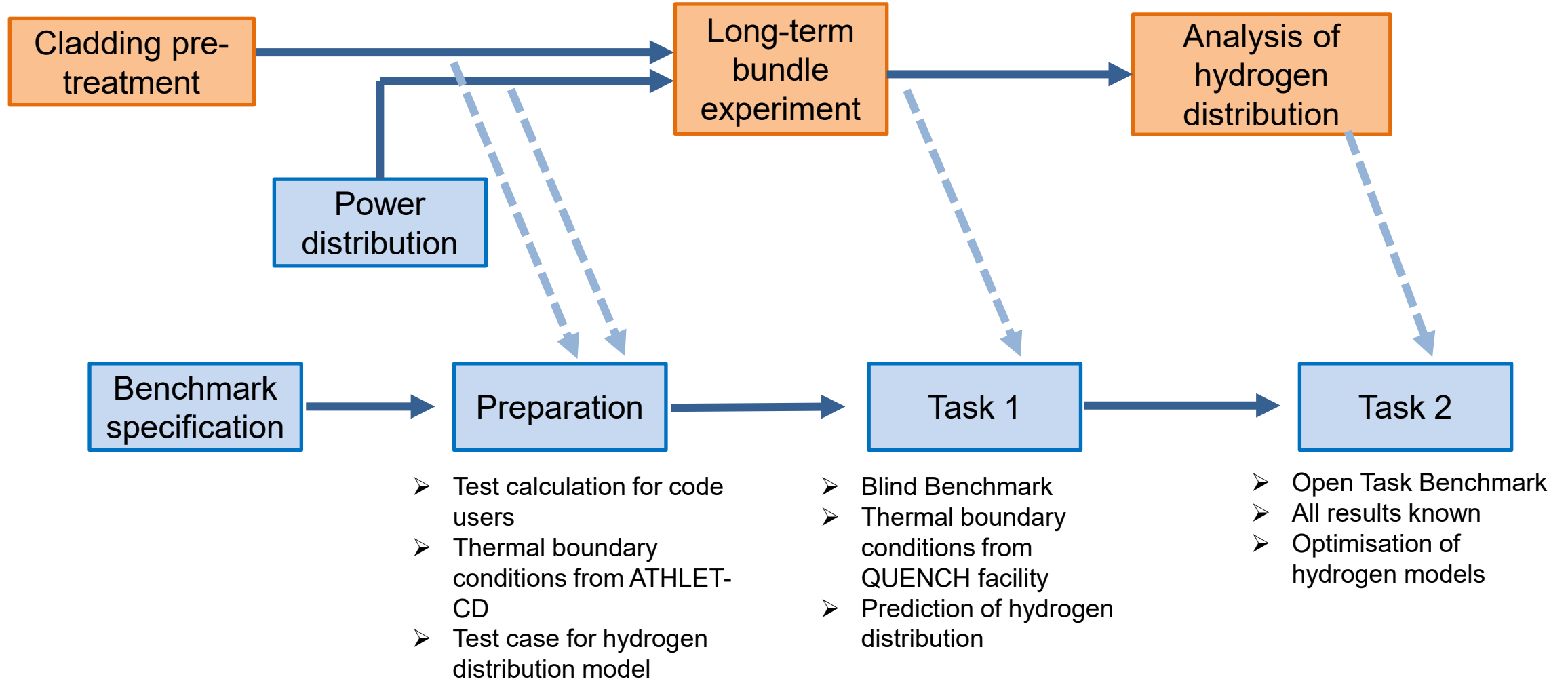
## Introduction *Bundle experiment*

Goal: 8 month long-term cool down of hydrided fuel rod claddings at KIT's QUENCH facility

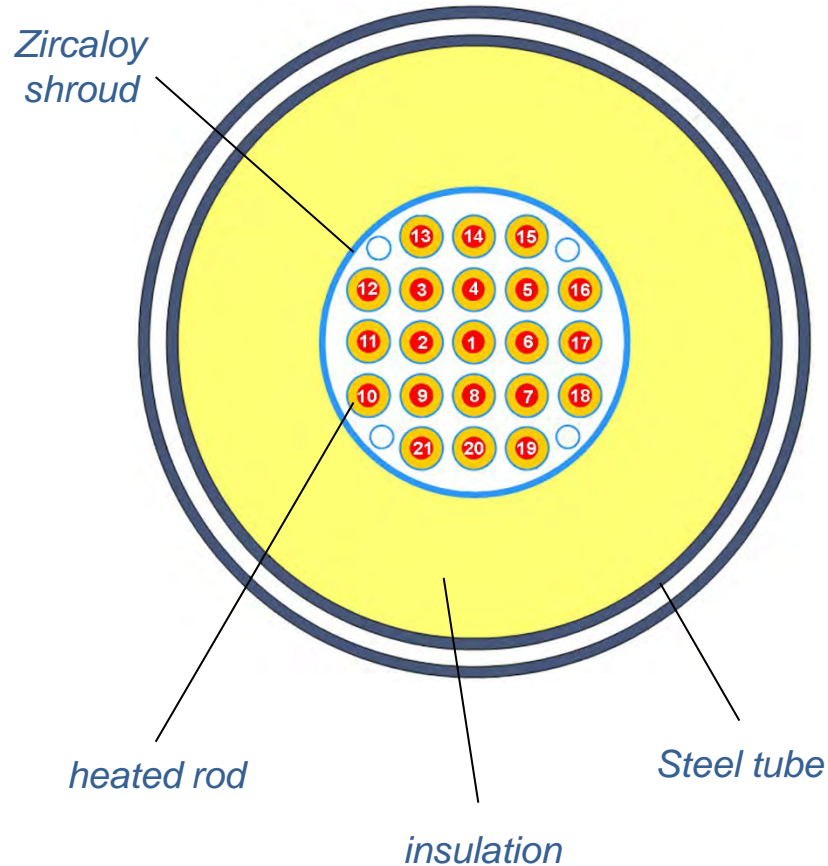


## Introduction *Benchmark*

Benchmark is conducted complementary to the experiment at KIT's QUENCH facility



## Benchmark *Bundle experiment*

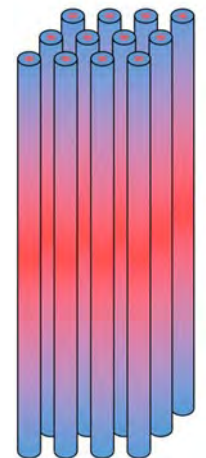


### The SPIZWURZ bundle

- 21 electrically heated fuel rod simulators
- Pressure and heating power control for every rod
- Test matrix involving 3 materials, 2 pressures (resulting in 70 and 100 MPa stress), 2 hydrogen concentrations (100 and 300 wppm)

Material	$p_{\max}, C_{H,\max}$	$p_{\max}, C_{H,\min}$	$p_{\min}, C_{H,\min}$	$p_{\min}, C_{H,\max}$
Zry-4	2x	2x	2x	2x
Zirlo	2x	2x	2x	2x
Duplex DX-D4	2x	1x	1x	1x

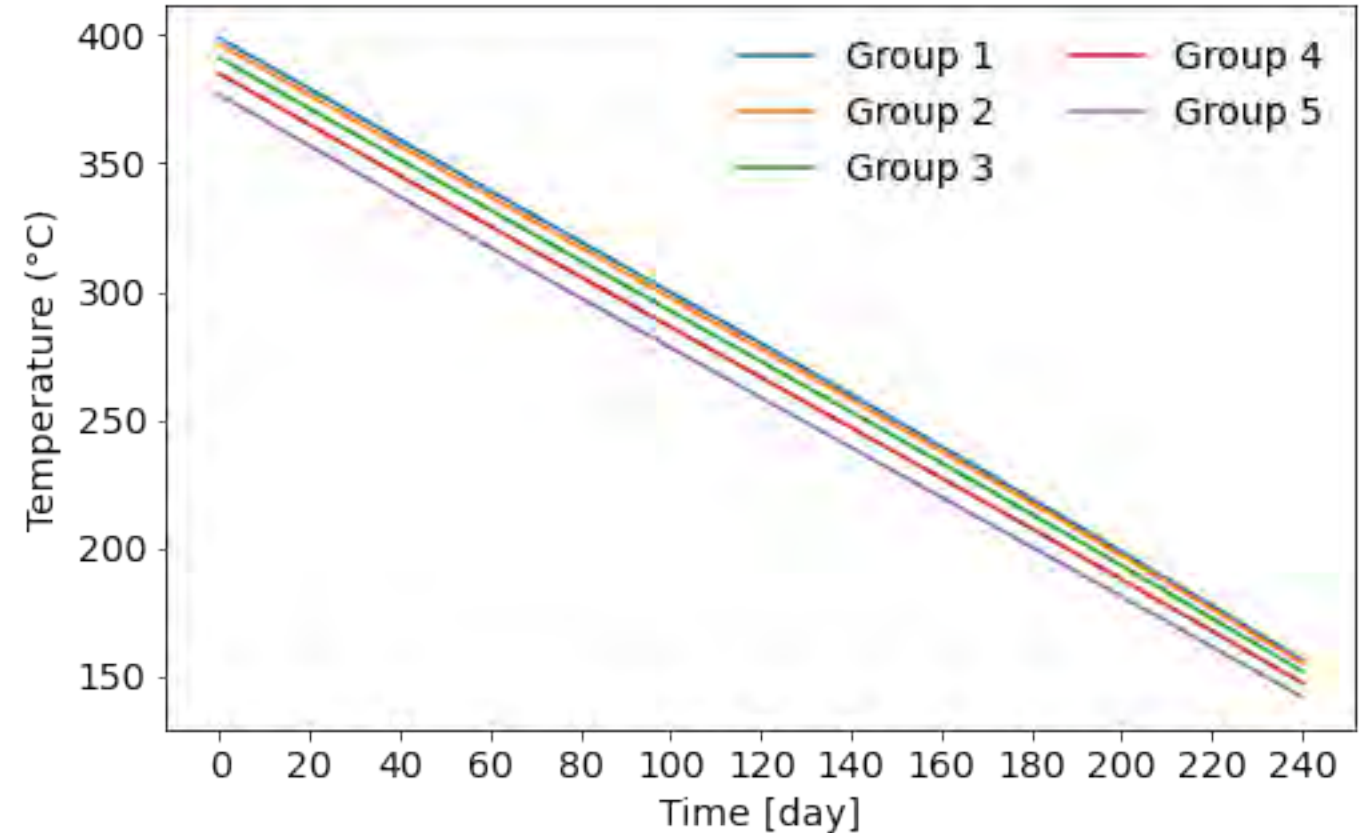
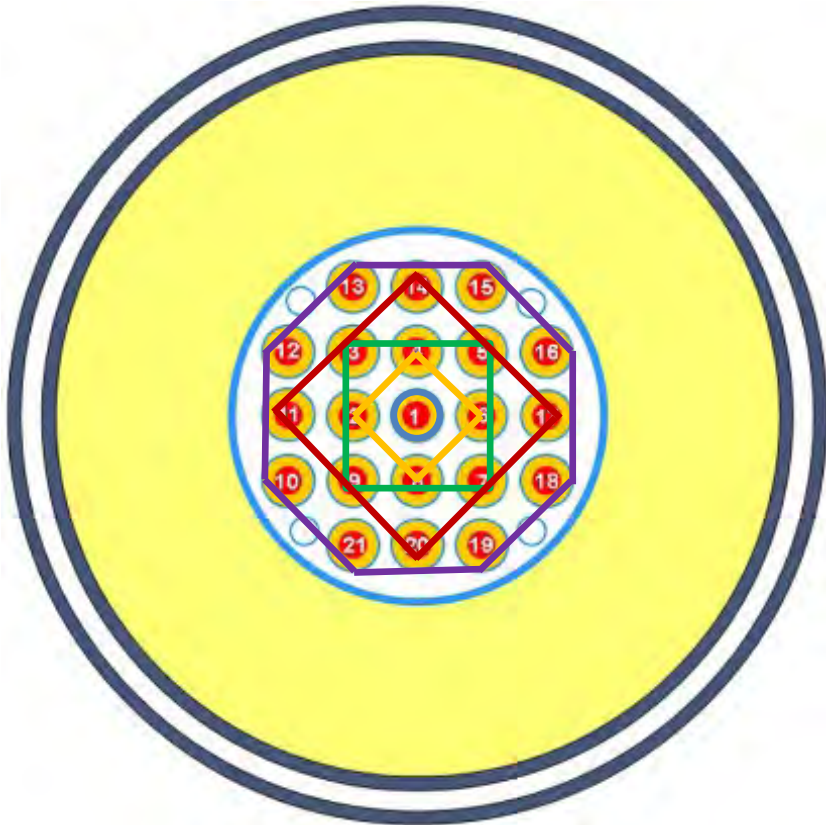
- Start temperature of  $T_{\max} = 400 \text{ }^{\circ}\text{C}$
- Cooling rate of  $\frac{\Delta T}{\Delta t} = 1.0 \frac{^{\circ}\text{C}}{\text{d}}$
- Bell-shaped temperature profile provides every temperature at 2 locations
  - Two samples per rod



## Benchmark *Bundle experiment*

*Specification calculations performed with AC<sup>2</sup>/ATHLET-CD*

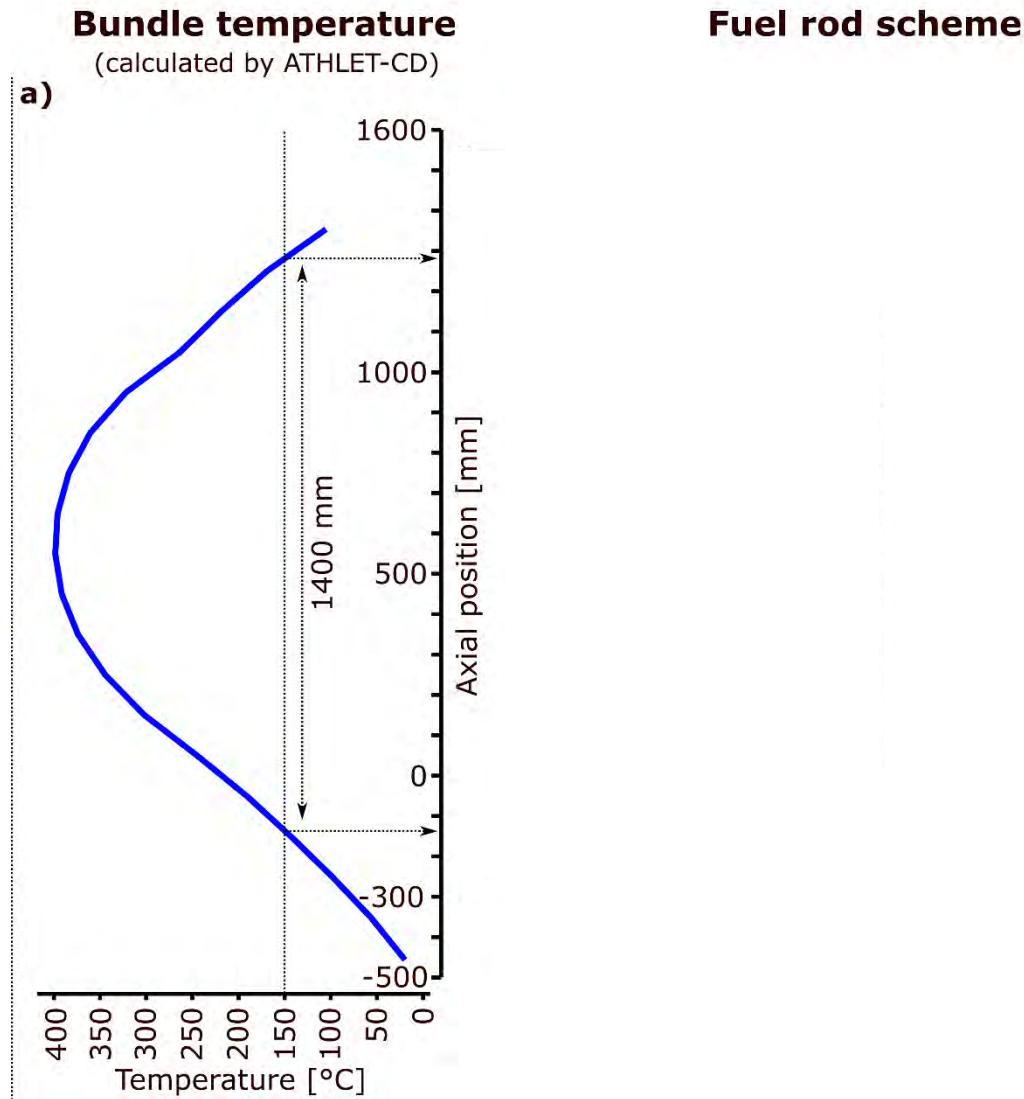
- Five groups of rods
- Constant ambient temperature



- Final set-up of boundary and initial conditions in cooperation with KIT **before** and **during** experiment conduct



## Benchmark *Temperature distribution*



Preparation phase entirely relies on boundary conditions calculated by ATHLET-CD code

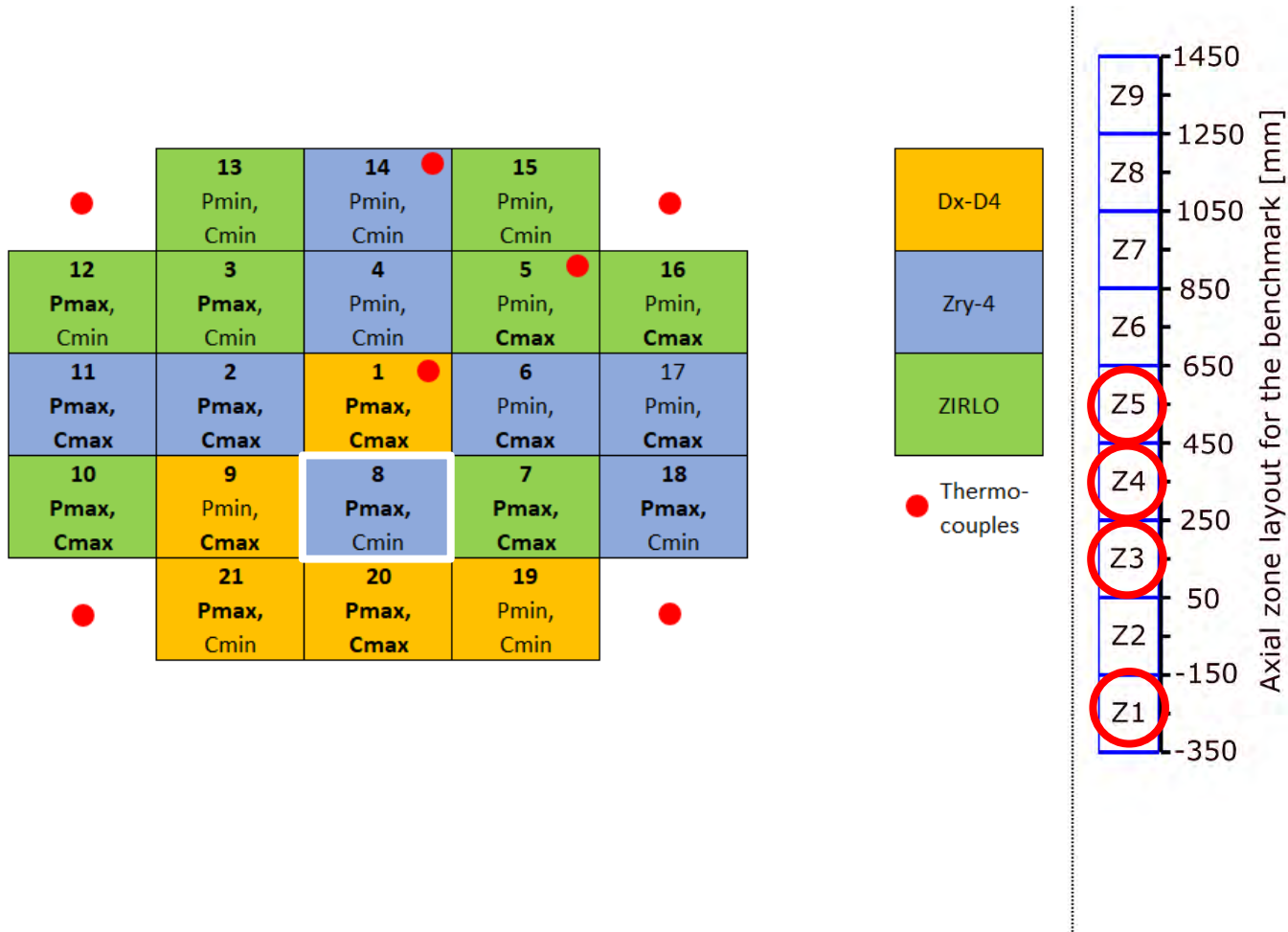
a) The bell-shaped temperature profile defines the diffusion of hydrides

b) 90 % of power is concentrated on the tungsten heater in the fuel rod centre

c) The experiment will have 9 thermocouples along the test rod

d) Fuel rod code nodalisation according to the 9 thermocouple positions

## Benchmark *Temperature distribution*



The bell-shaped temperature profile defines the diffusion of hydrides

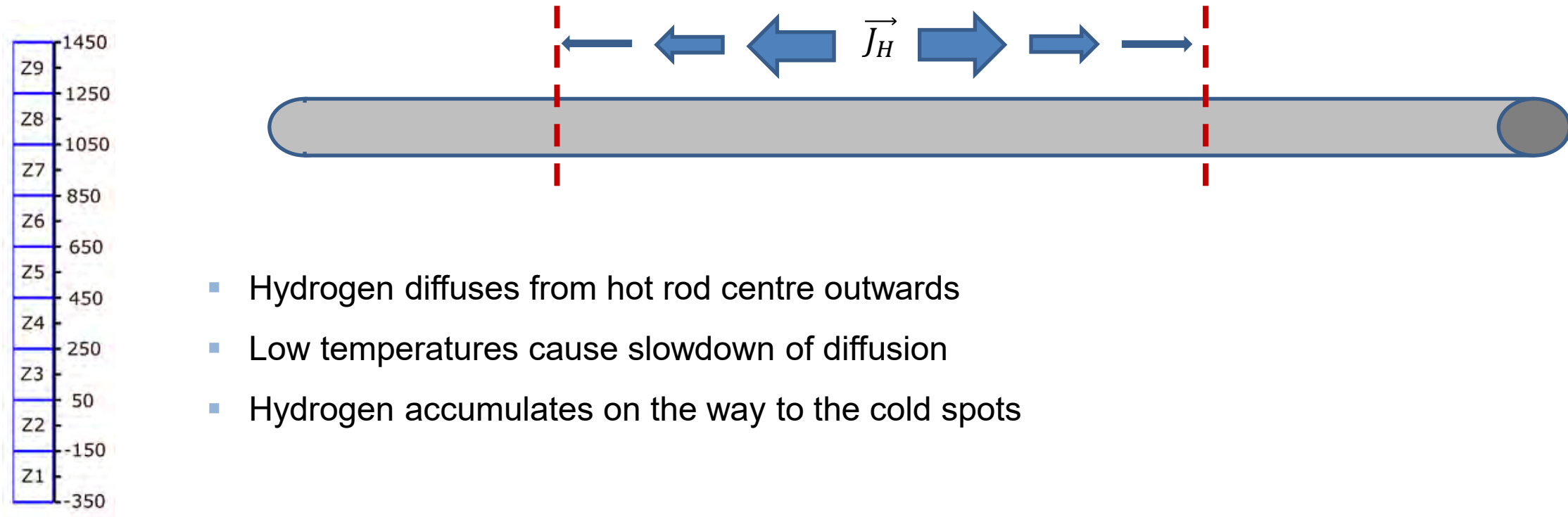
Following preliminary results will show some results based on the boundary conditions with ATHLET-CD

TESPA-ROD results will be presented at 4 different axial zones

Following preliminary results will be shown for rod 8, with lower hydrogen concentration and high pressure

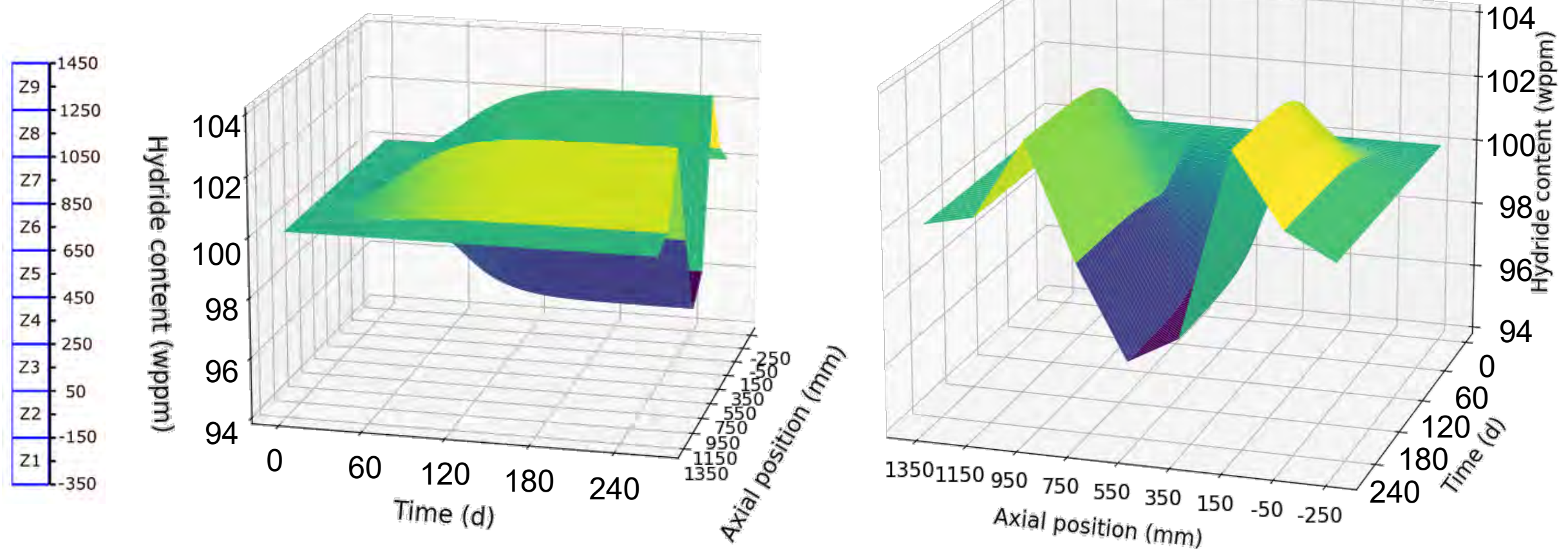
## Benchmark *Preparation Phase – Preliminary TESPA-ROD results*

*Hydride and hydrogen behaviour strongly differs over the axial positions*



## Benchmark *Preparation Phase – Preliminary TESPA-ROD results*

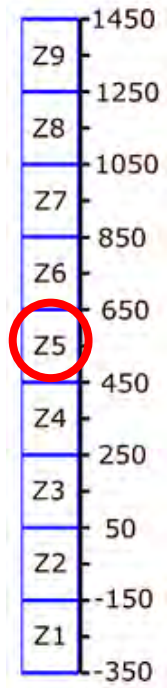
*Hydride and hydrogen behaviour strongly differs over the axial positions*





# Benchmark *Preparation Phase – Preliminary TESPA-ROD results*

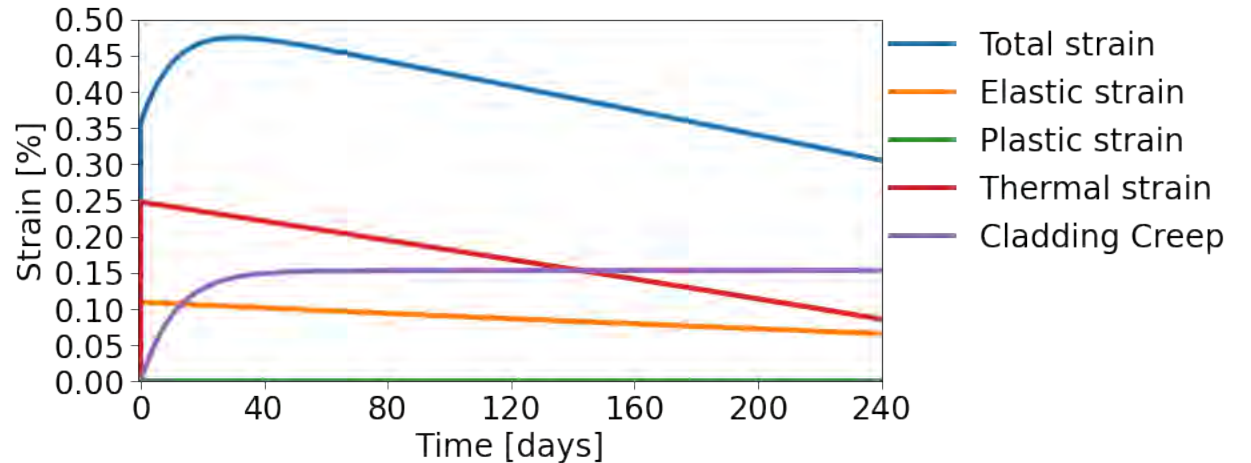
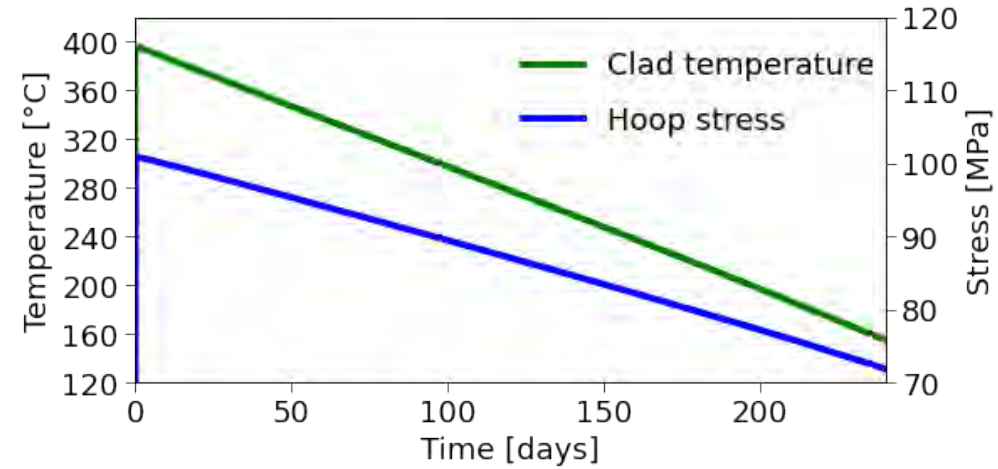
## Results for zone 5



Cladding temperature and pressure decrease

Thermal strain has largest influence on total strain.

Creep strain stagnates with lower temperatures

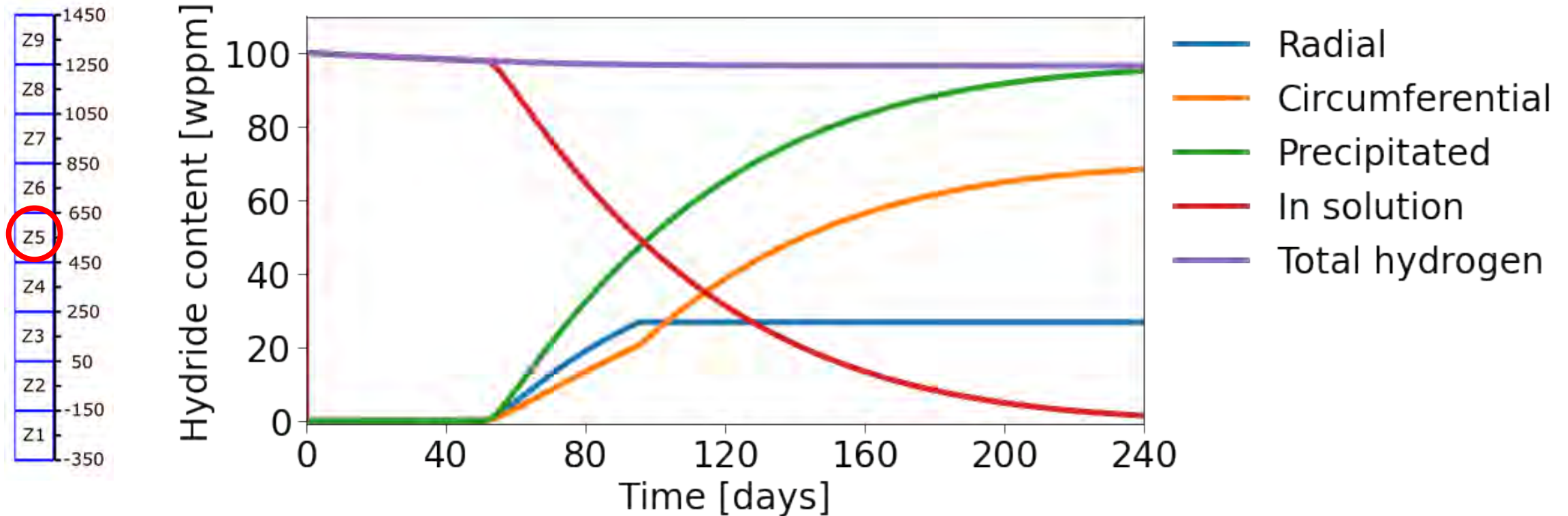


## Benchmark *Preparation Phase – Preliminary TESPA-ROD results*

*Full dissolution of hydrogen during first weeks*

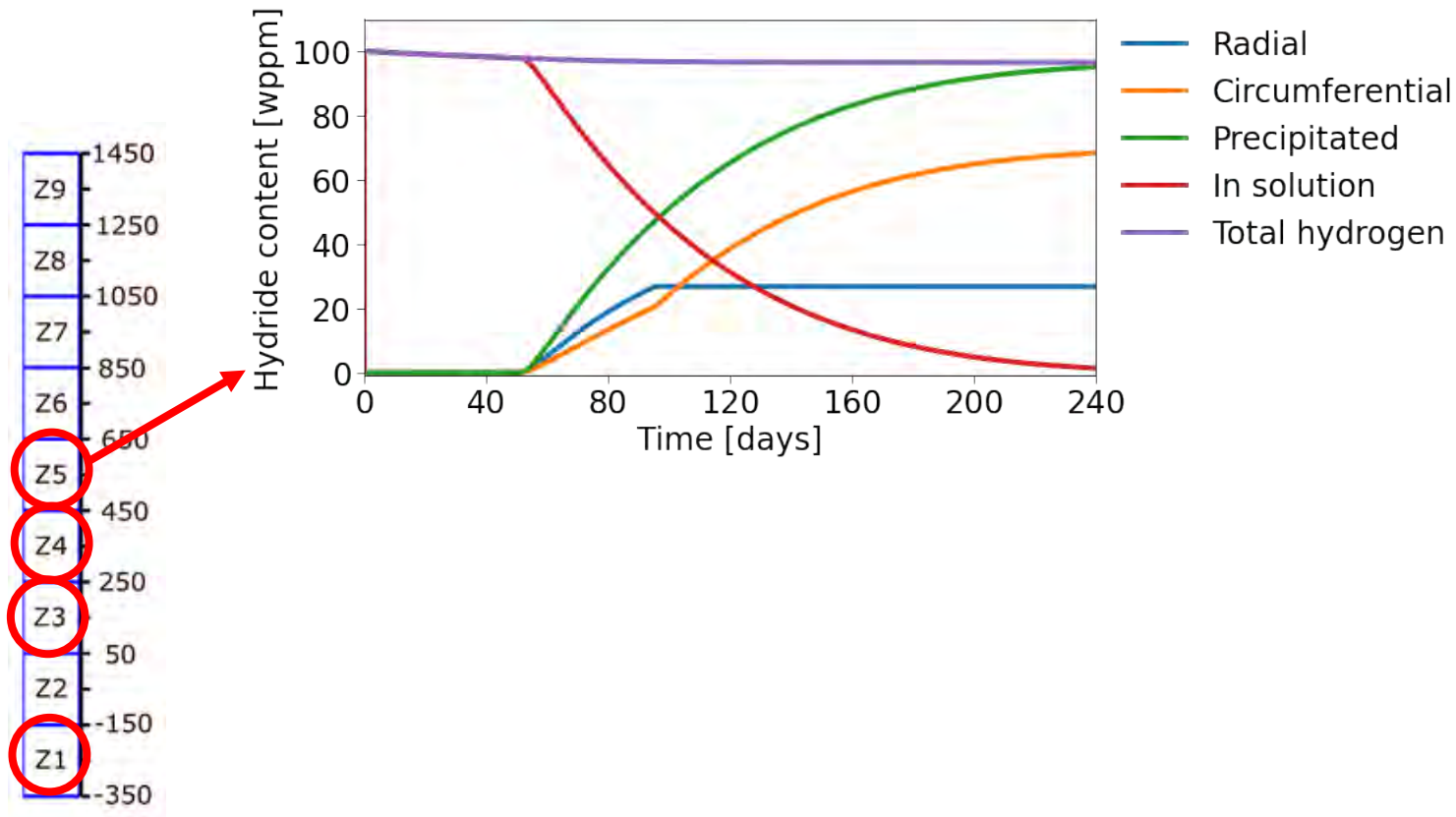
*Hydrides precipitation starts after reaching the Terminal Solid Solubility limit (TSS) at around 50 days*

*Radial hydrides precipitate in the beginning and stagnate when reaching the reorientation threshold*



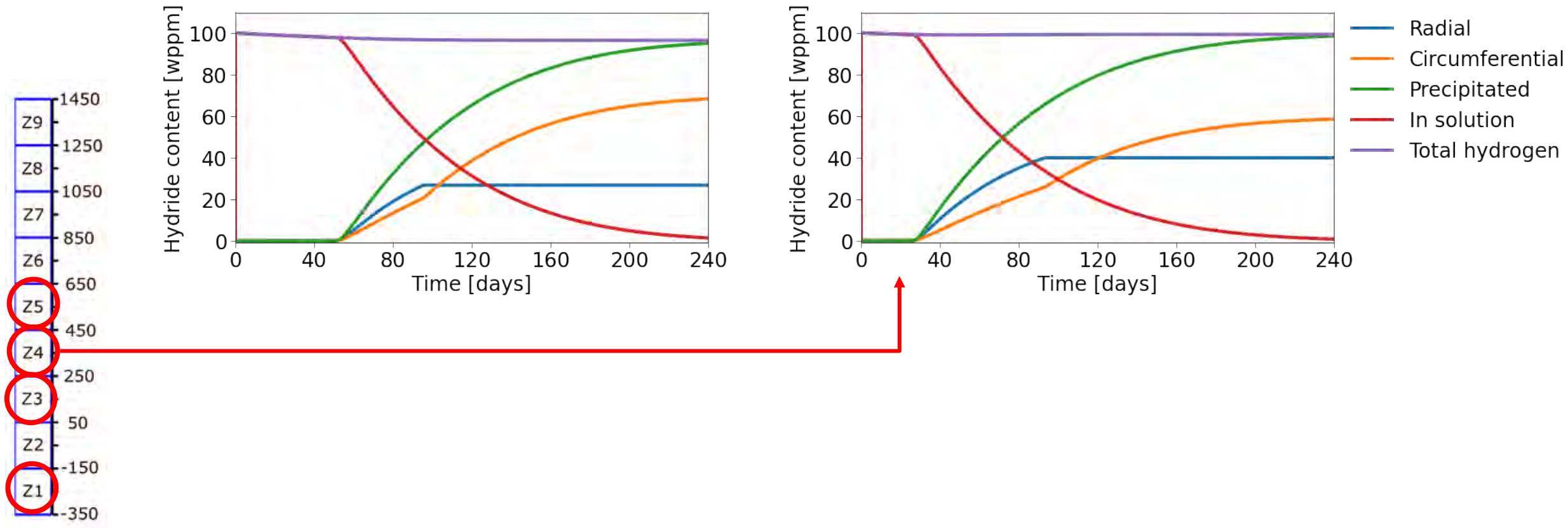
## Benchmark *Preparation Phase – Preliminary TESPA-ROD results*

*Hydride and hydrogen behaviour strongly differs over the axial positions*



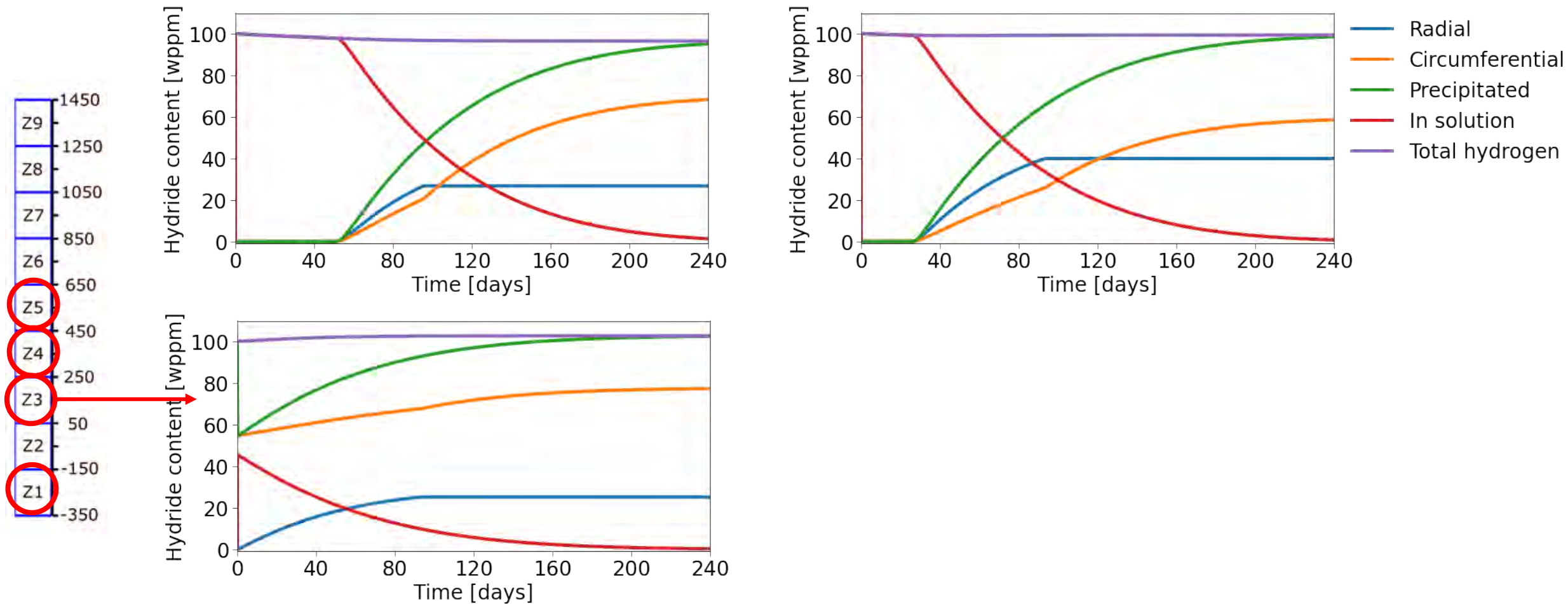
## Benchmark *Preparation Phase – Preliminary TESP-ROD results*

Zone 5 is the hydrogen source for the cooler axial nodes, while the hydrogen diffuses via zone 4 to zone 3



## Benchmark *Preparation Phase – Preliminary TESPA-ROD results*

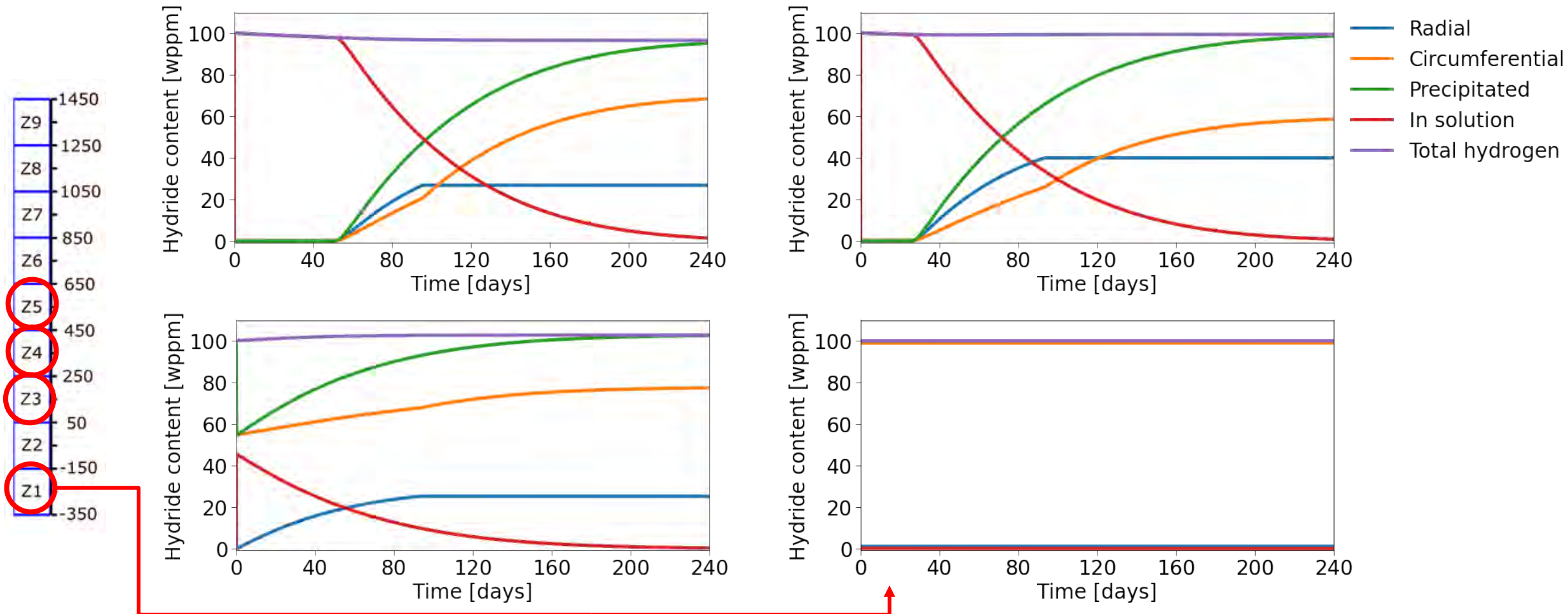
Zone 3 shows slight increase in total hydrogen, while hydrides are never fully dissolved





## Benchmark *Preparation Phase – Preliminary TESPA-ROD results*

Zone 1 exhibits a low temperature, that it's the solid solubility is too low to dissolve hydrogen



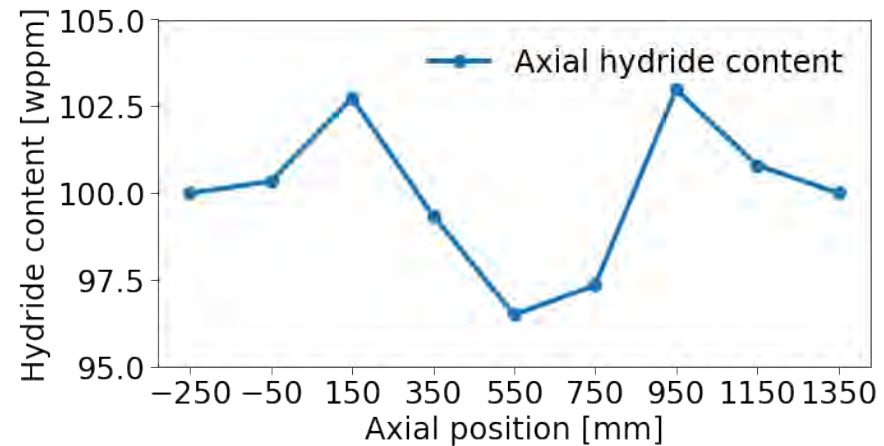
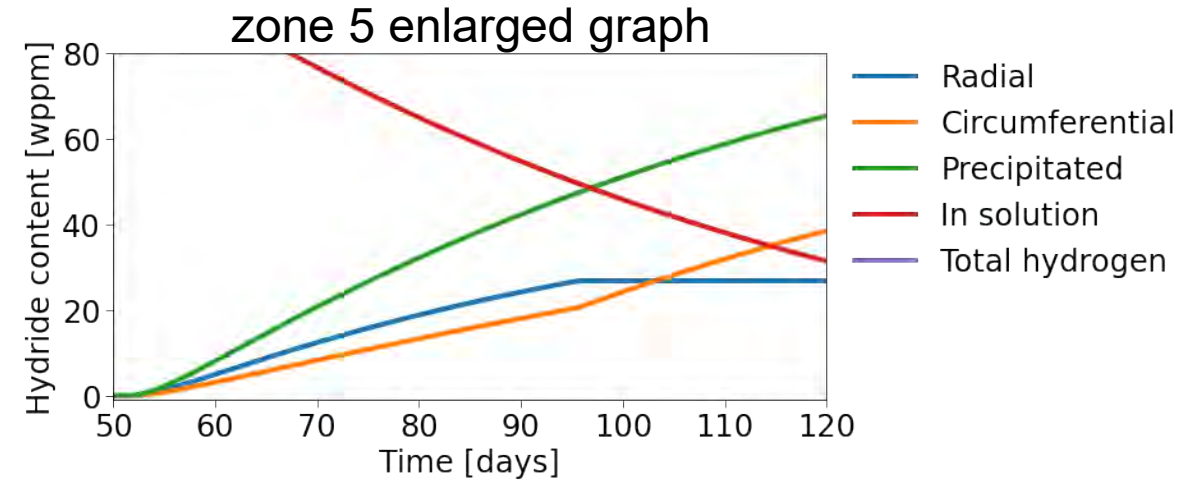
## Benchmark *Preparation Phase – Preliminary TESPA-ROD results*

### Hydrides

- Hydrogen solubility strong effect at beginning
- Radial hydrides precipitate as long pressure is high enough
- At lower pressures SRA Zry-4 tends to build circumferential hydrides

### Diffusion

- Axial diffusion of hydrogen visible, but small effect
- Hydrogen accumulation at two mid-temperature zones at 150 mm and 950 mm
- Cold end zones unaffected



## Benchmark *Preparation phase - discussion*

### *Hydride precipitation*

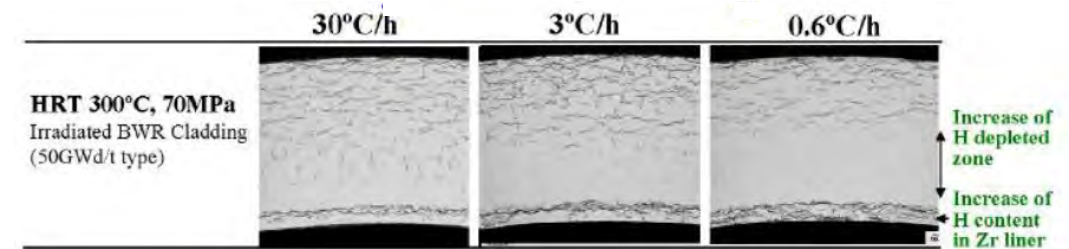
- For sufficient high hoop stresses in the beginning of cool-down code predicts radial hydride precipitation
- Highest share of radial hydrides shown in Zone 4

### *Axial hydrogen diffusion*

- The calculated hydride diffusion is rather low
- The local hydride diffusion may be larger, since nodalisation of this model is rather low
- Number of zones oriented at the planned experiment

### *Radial hydrogen diffusion*

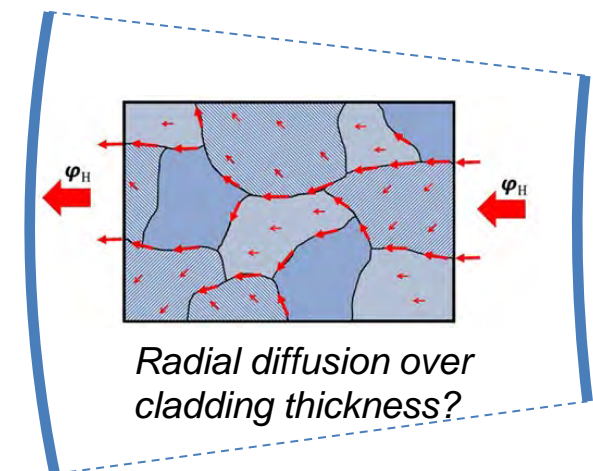
- Until now, TESP-ROD code is not capable of simulating radial hydrogen diffusion or concentration differences inside the cladding
- Flat temperature profile, due to low power generation of approx. 18 W/m
- Differences for materials, especially for Duplex DX/D4?



UNF Dispositon Campaign, SRNL-STI-2015-00256

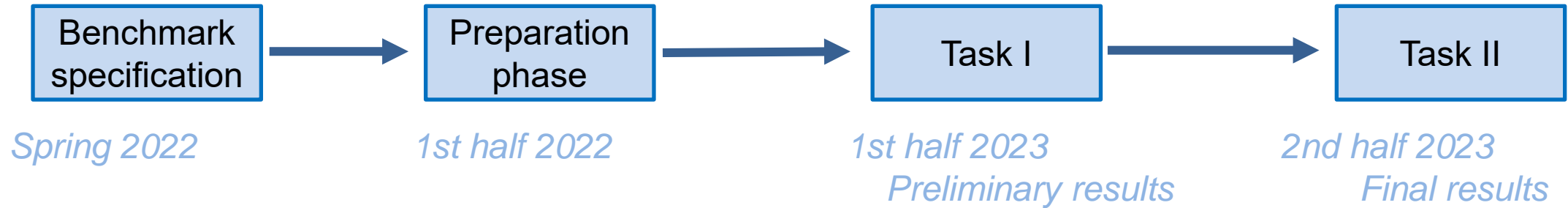
*Questions to answer:*

- *Diffusion type?*
- *Material influence?*
- *Hydride reorientation*



## Benchmark *Outlook and Timeline*

Results for the hydrogen distribution and the hydride characterization are available at the end of the project



### *Benchmark participation*

- Open for everyone
- Published as report
- Participation via email to [felix.boldt@grs.de](mailto:felix.boldt@grs.de) and [daniel.nahm@grs.de](mailto:daniel.nahm@grs.de)

### *SPIZWURZ project contacts*

- Project coordinator: Felix Boldt (GRS)
- Hydrogen experiments and QUENCH-facility: Mirco Grosse (KIT IAM) [mirco.grosse@kit.edu](mailto:mirco.grosse@kit.edu)
- Fuel-pellet interaction: Michel Herm (KIT INE) [michel.herm@kit.edu](mailto:michel.herm@kit.edu)

*Thank you for your kind attention!*

Supported by:



Federal Ministry  
for the Environment, Nature Conservation,  
Nuclear Safety and Consumer Protection

based on a decision of  
the German Bundestag

Acknowledgements to

M. Große, J. Stuckert, S. Weick, M. Herm, M. Marchetti, M. Stuke, P. Peridis and Stefan Mohr





**S. Weick**  
**KIT**

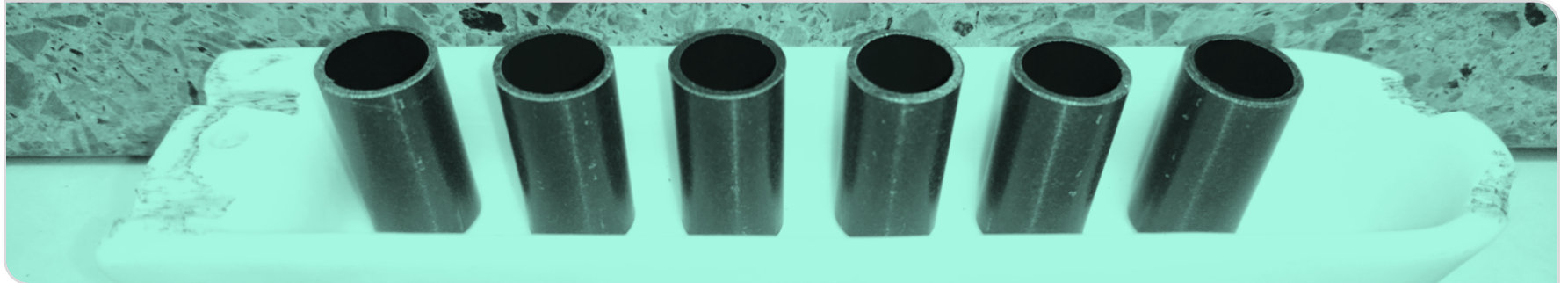
## **Update of the investigations on the hydrogen solubility and diffusivity in cladding tube materials in the framework of the SPIZWURZ project**

The hydrogen and hydride behaviour in zirconium and zirconium-based cladding tubes related to the interim dry storage period of spent nuclear fuel can be investigated non-destructively by means of neutron imaging. In this framework, especially the influence of stress on the hydrogen in solid solution and the precipitated hydrides are of interest during this long-lasting period of slow cooling from up to 400°C.

In this paper, an update of the investigations on the hydrogen solubility and diffusivity in cladding tube materials in the framework of the SPIZWURZ project is presented. Therefore, different cladding tube samples (Zircaloy-4, Dx/D4 DUPLEX) are hydrogenated with variations in loading time and temperature (375-450°C) by different atmospheres (air, argon, hydrogen) three different methods – loading from the gas phase using a Sieverts chamber, loading from a ZrH<sub>2</sub> powder and loading by contact with pre-hydrogenated compact Zry-4. The neutron radiography measurements are conducted with polychromatic neutron beams in the cold energy range at the ICON facility at SINQ at the Paul Scherrer Institute in Villigen, Switzerland. Because of the very low neutron cross section of Zirconium, the metal is nearly invisible for neutrons and the contrarily behaving hydrogen that scatters neutrons strongly, appears as dark contrast in neutron images. The hydrogen content within the samples in dependency of annealing time and temperature and the theoretical correlation of hydrogen diffusion coefficients are presented in this framework. With the KIT's new INCHAMEL facility, which is introduced in this paper, tensile tests are combined with the heating of samples to up to 500°C. Thus, the influence of stress on hydrogenated samples can be investigated on flat samples and on cladding tube samples.

# Update of the investigations on the hydrogen solubility and diffusivity in cladding tube materials in the framework of the SPIZWURZ project

**Sarah Weick, Mara Marchetti, Mirco Große, Martin Steinbrück, Hans Jürgen Seifert**



# Project SPIZWURZ

- **SPIZWURZ** = Spannungsinduzierte Wasserstoffumlagerung in Brennstabhüllrohren während längerfristiger Zwischenlagerung  
(Strain induced hydrogen redistribution in fuel cladding tubes during longterm interim storage)

- KIT/IAM-AWP & KIT/INE & GRS & BGZ



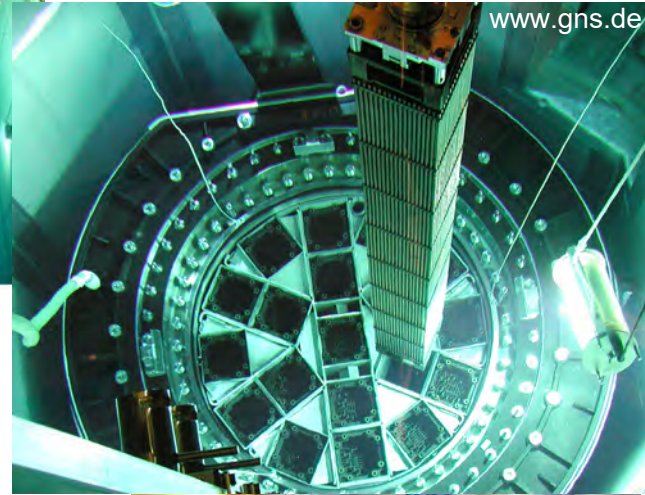
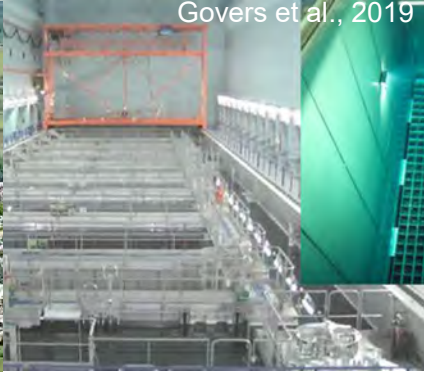
- different cladding tube materials (Zircaloy-4, Dx/D4-Duplex, ZIRLO™)

# Introduction – Spent Nuclear Fuel

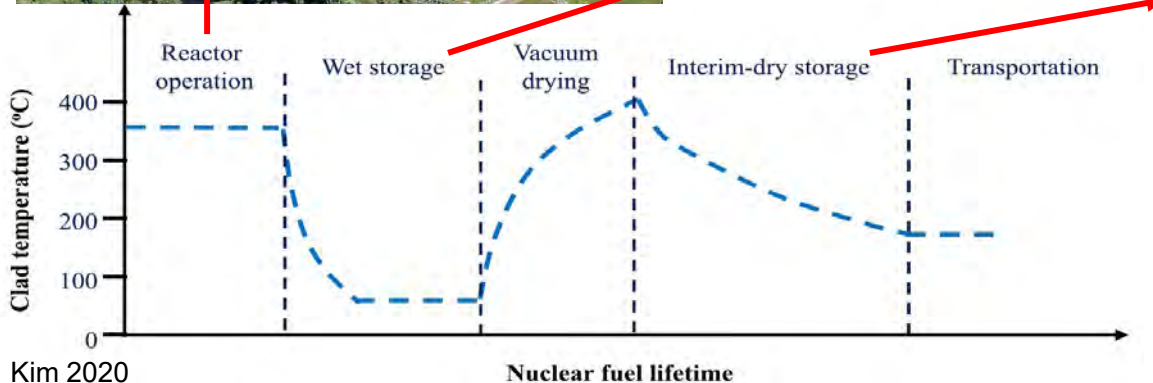
@ EnBW Kernkraft GmbH



Govers et al., 2019



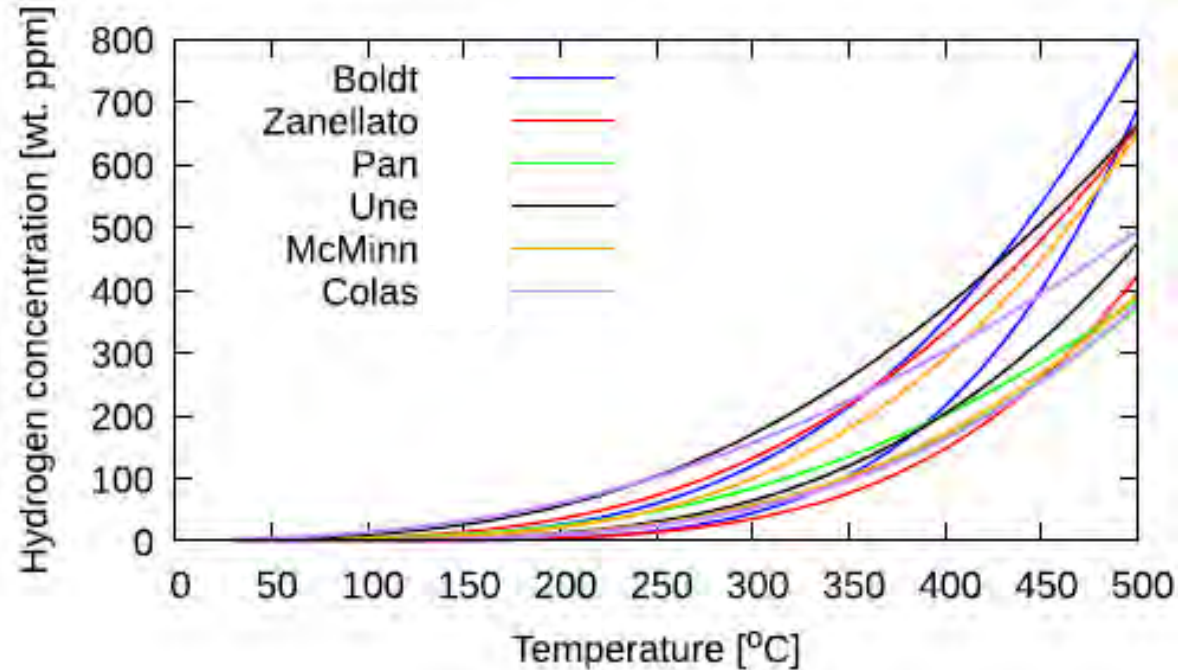
www.gns.de



www.gns.de

# Introduction – H solubility

- **TSSp curves:** precipitation terminal solubility limit
- different experimental data
- extreme variations of up to 400 wt.ppm (500°C)



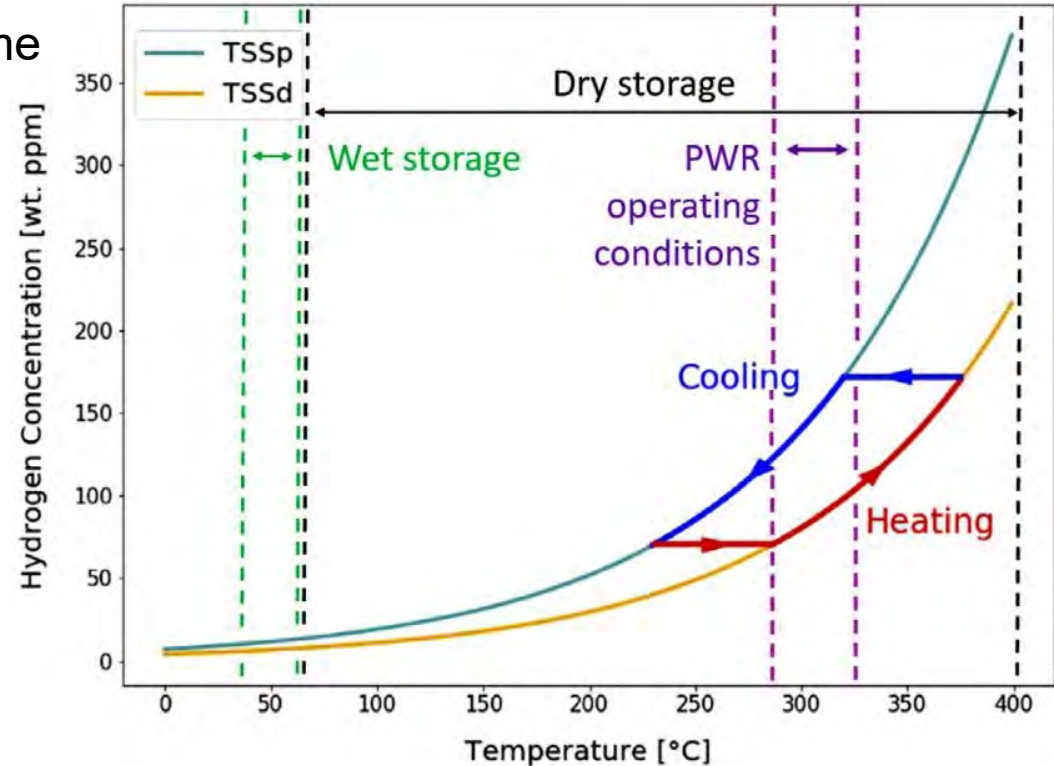


# Introduction – H solubility

- H dissolution-precipitation scheme with modelled **TSS** (terminal solid solubility)

→ **TSSp**: precipitation terminal solubility limit

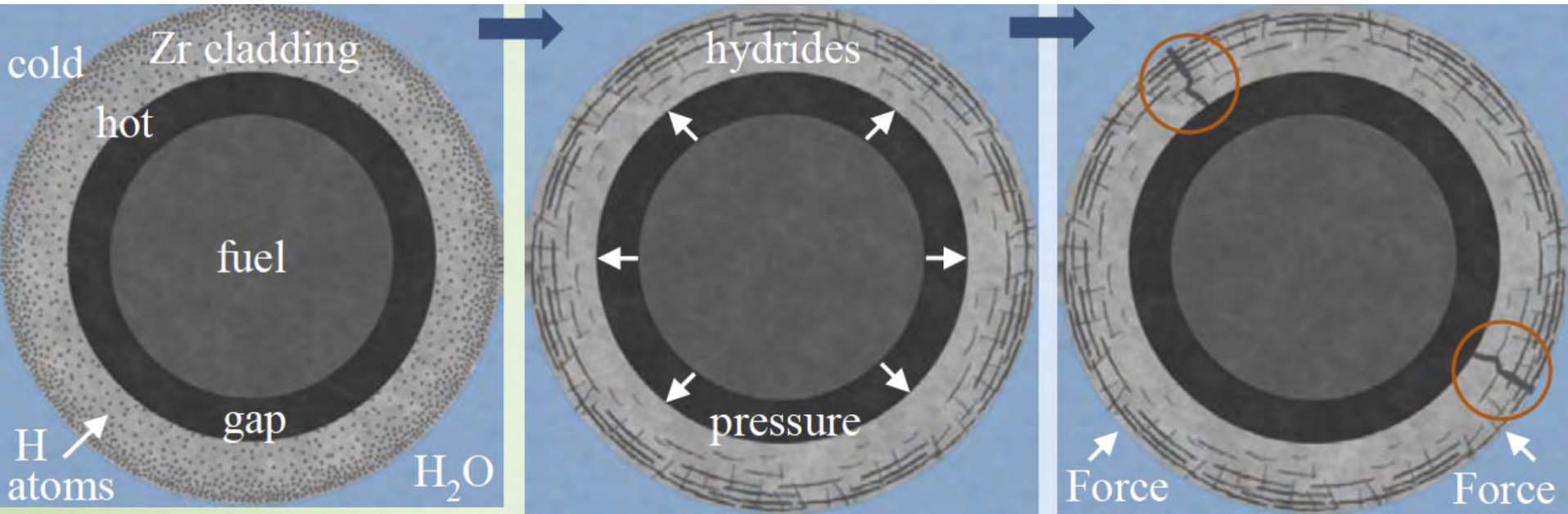
→ **TSSd**: dissolution terminal solubility limit



Kaufholz et al.2018, modified from Konarski 2021

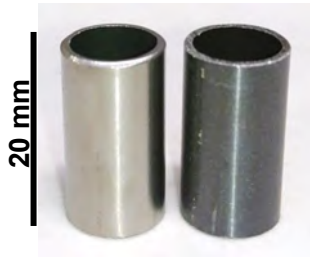
# Introduction – Hydrogen embrittlement

- H uptake ► H precipitation (tangential/radial) ► H embrittlement

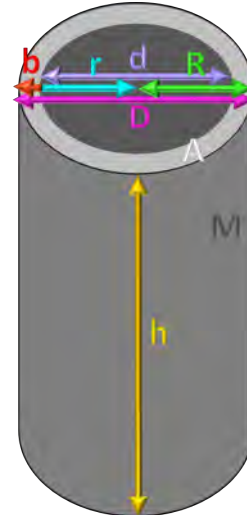


# Samples

- original cladding tubes
- different zirconium alloys: Zry-4 & DX/D4 & Zirlo
- different oxide layer thicknesses (pre-ox.)



cladding tube	h [mm]	b [mm]	D [mm]
Zry-4, Dx/D4	20	0.725	10.75
Zirlo	20	0.5715	9.5

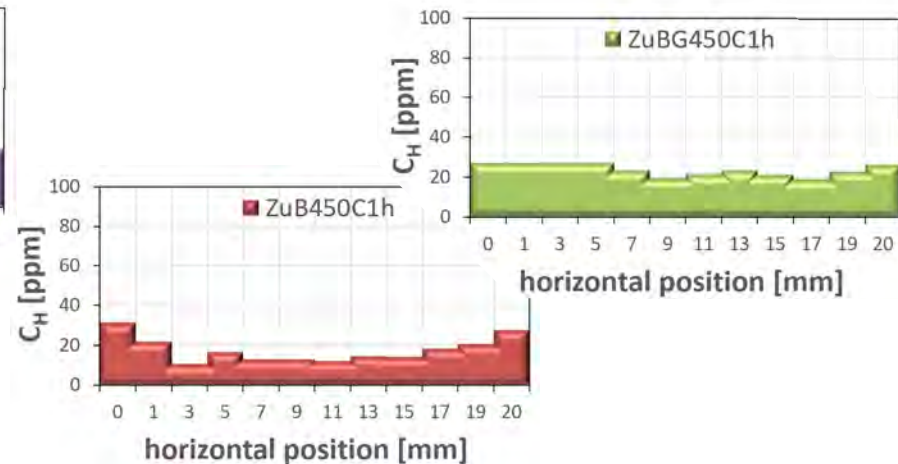
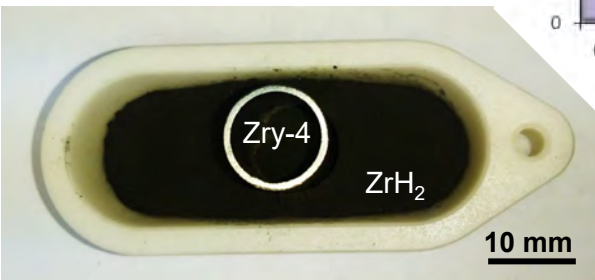
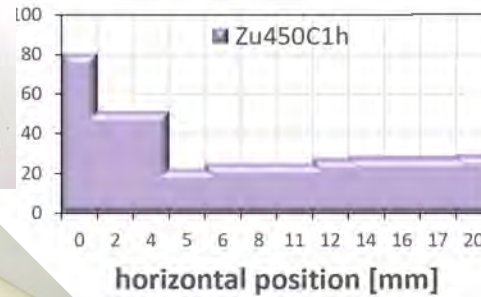
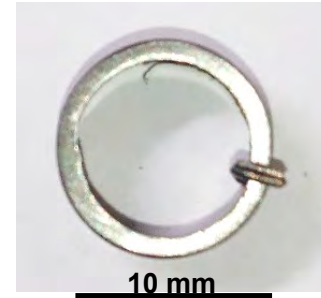
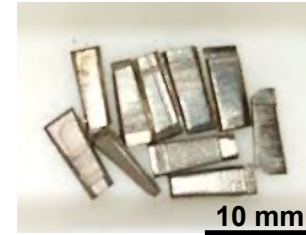


alloy	Sn [wt.%]	Fe [wt.%]	Cr [wt.%]	Nb [wt.%]	O [wt.%]
Zry-4, D4	1.3	0.2	0.1	-	0.13
Dx	0.5	0.5	0.2	-	0.14
Zirlo	0.9	0.1	-	0.9	-

# Hydrogen uptake methods

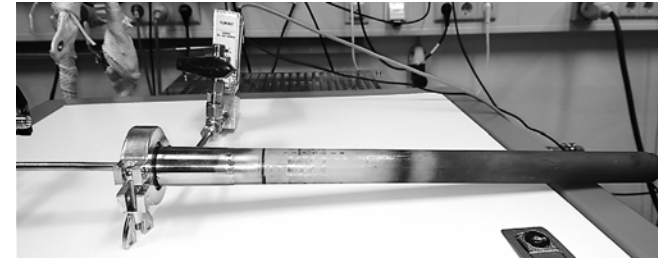
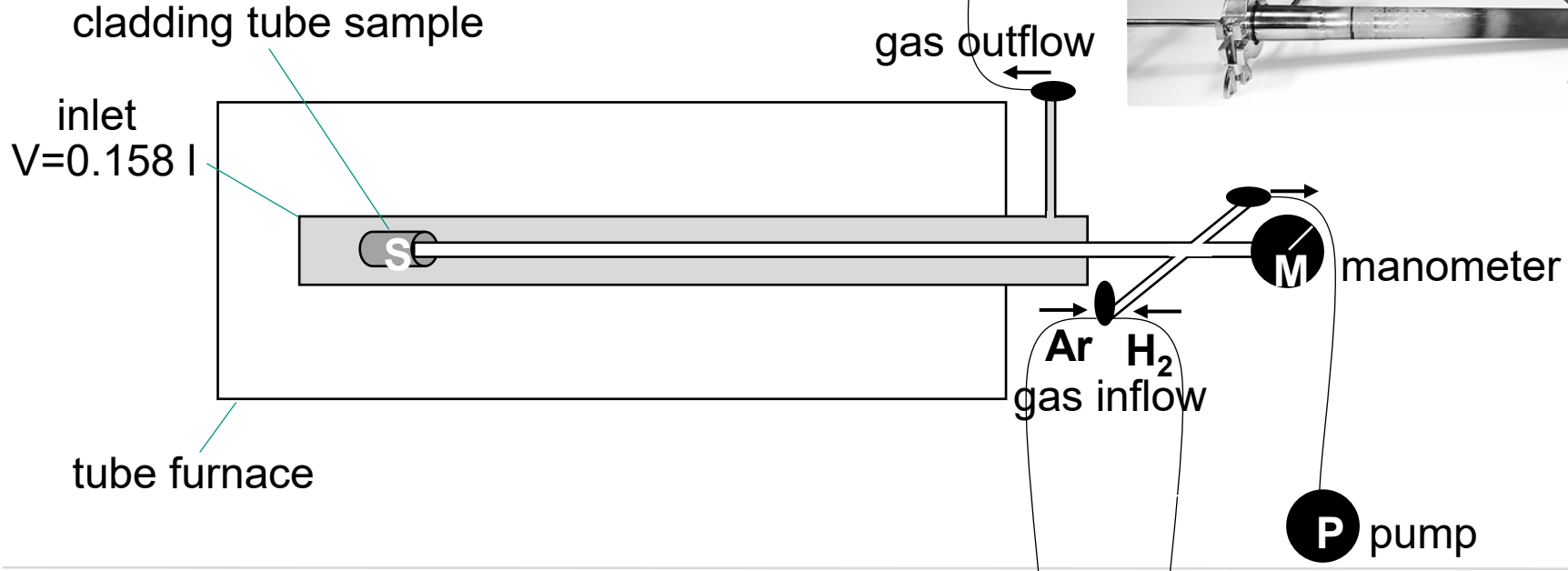
- annealing from gas phase
- contact to  $ZrH_2$  powder
- contact to Zr-plates with 21.000 ppm H

→ diffusion in axial and/or circumferential direction



# Hydrogen uptake – SICHA/ H gas

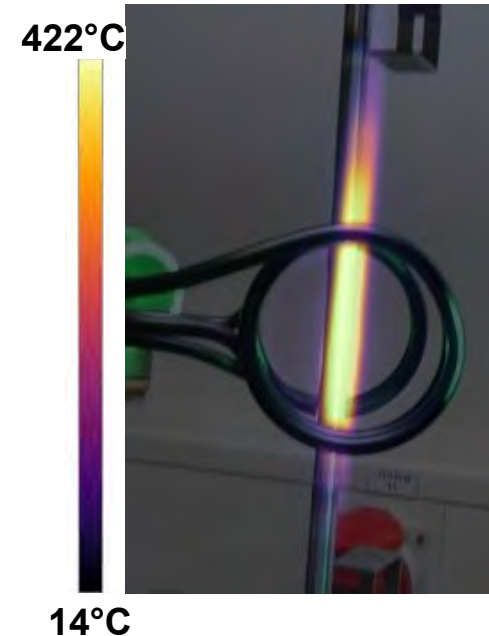
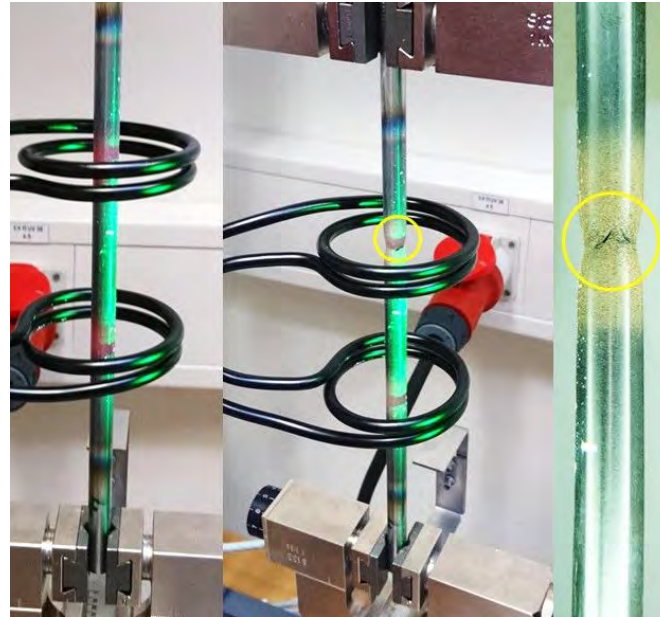
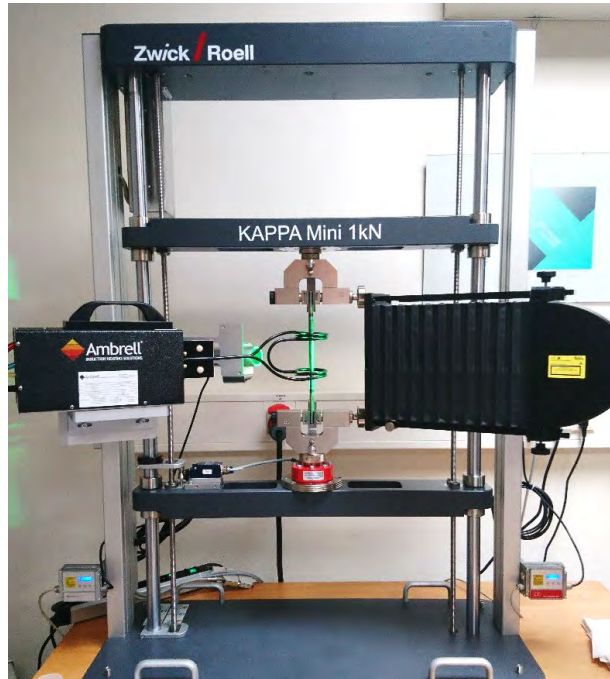
SICHA = Sieverts Chamber for Hydrogen Absorption





# Hydrogen Diffusion - stress influence

INCHAMEL = In-situ Neutron radiography Chamber with Mechanical Load



# Analysis – Image Analysis

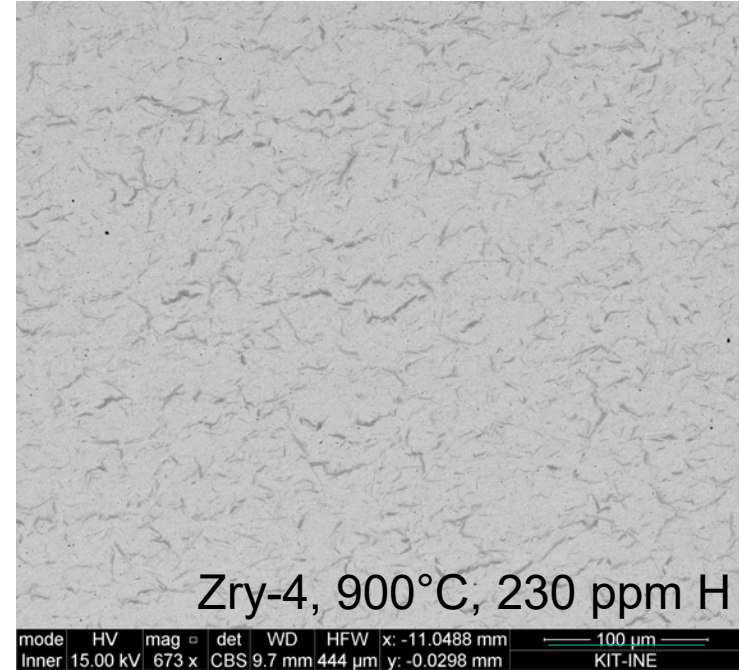
Hydrogen concentration in the fuel cladding can be determined by Image Analysis (I.A.).

The Zircaloy-4 cladding was embedded, ground and polished in several steps with decreasing abrasive cloth /paste size.

Vibratory polishing used for 2 h with amorphous 0.02  $\mu\text{m}$  colloidal silica suspension for stress-free polishing as last step.

Scanning Electron Microscope images  
acquired in backscattered mode with contrast  
based on Z.

Accelerating voltage: 15 kV



# Analysis – Image Analysis

Trainable Weka of ImageJ was used to segment the images and then particle analysis was applied to remove round and small particles (area > 6  $\mu\text{m}^2$  and circularity between 0 - 0.7).

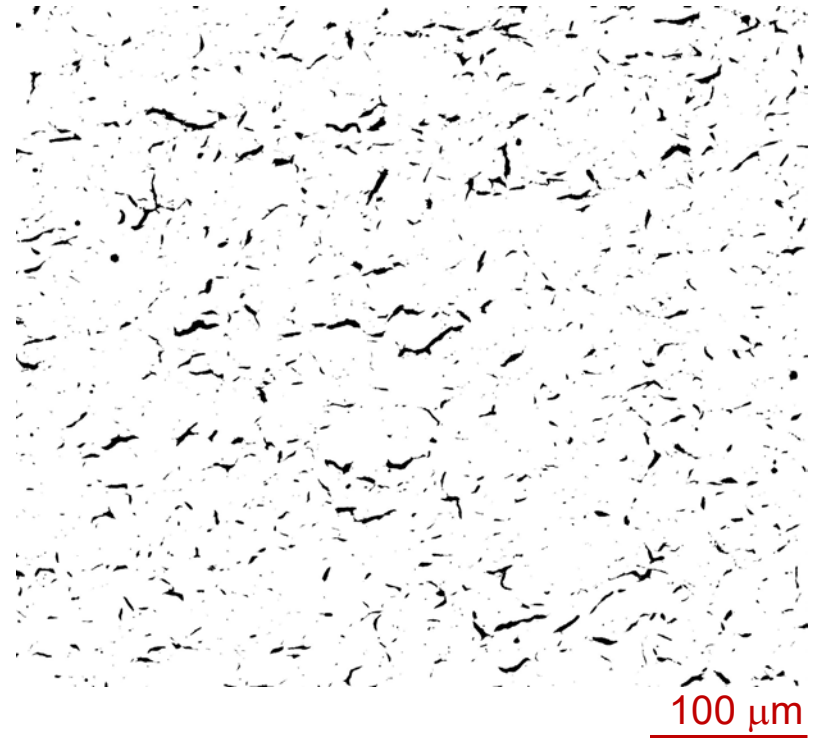
## Results:

H concentration –Hot  
vacuum extraction (ppm)

230

H concentration - I.A (ppm)

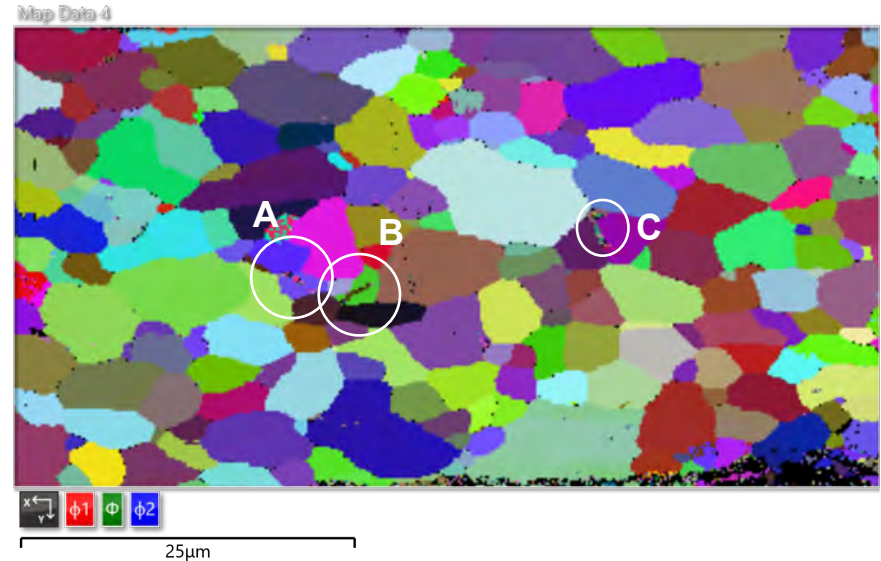
269  $\pm$  77



# Analysis – Electron Backscatter Diffraction (EBSD)

EBSD Layered Image 3

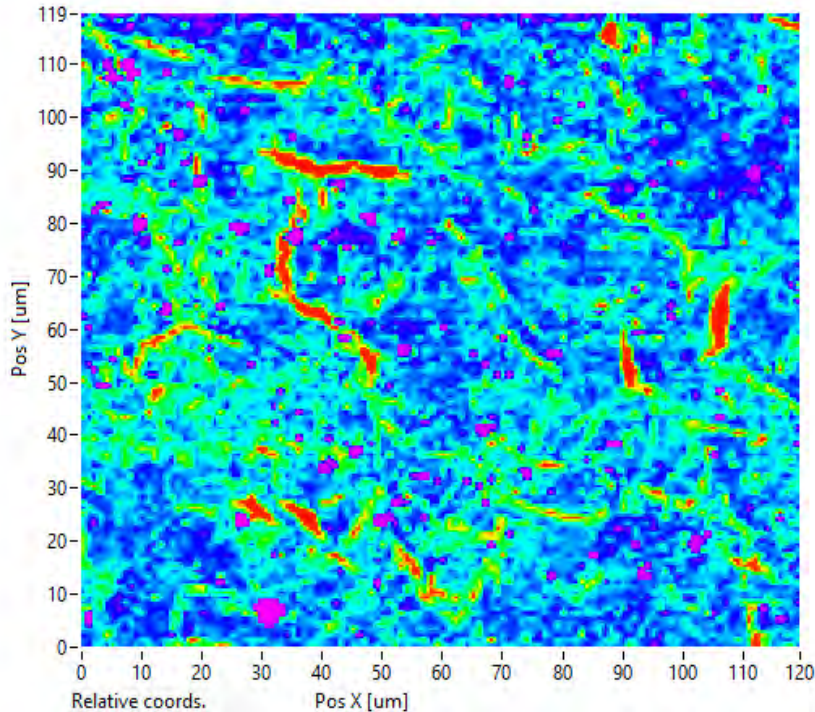
Phase Name	Phase Fraction (%)
Zry-4	97.93
$\gamma$ -ZrHx (metastable)	0.12
$\delta$ -ZrHx	0.22
Zero Solutions	1.73



An area of the specimen was selected for focused ion beam (FIB) cutting and polishing, then the surface was tilted at 70° and an image was acquired with a forward-scattered detector (electron scattered in the forward direction). **Needle-like hydrides growing from the boundaries (A and B) to the grain and at the grain boundary (C) are observable.**



# Analysis – Hardness

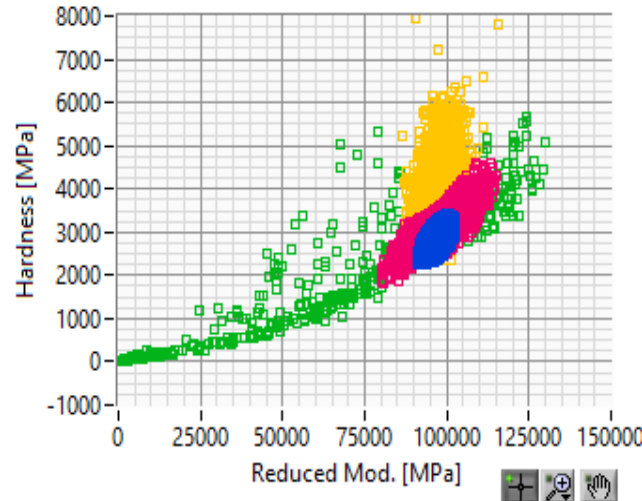
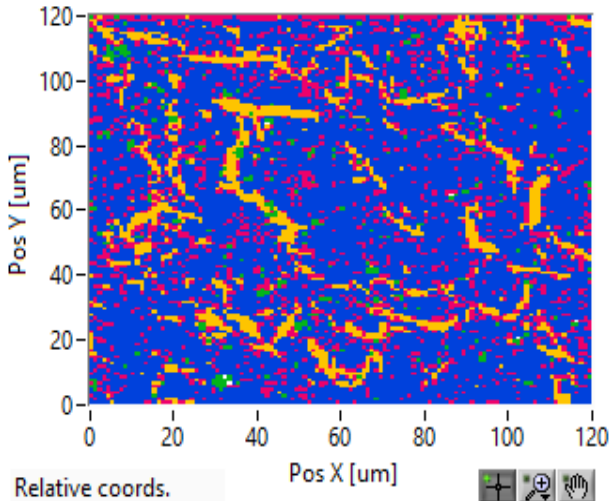


In this colourmap three/four different Hardness values groups can be identified:

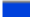



- The Zircaloy matrix in blue (Hardness about 2.8 GPa)
- The  $ZrH_x$  in red/green (Hardness about 4.0 GPa)
- The interface (light blue) between matrix and  $ZrH_x$  with intermediate Hardness.



# Analysis – Hardness



Cluster analysis (4 classes with gaussian mixture algorithm) we observe the group of the Zr matrix, the  $ZrH_x$  platelets/needles, the interface matrix/ $ZrH_x$  and dirt particles. On the average the  $ZrH_x$  are harder than the matrix. The reduced modulus is the same within the experimental uncertainties.

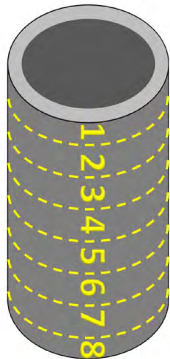
	#	Reduced Mod. [MPa]	Hardness [MPa]	Frac. [%]
	0	96935 +/- 2297	2905 +/- 229.1	69.2
	1	97141 +/- 5302	3140 +/- 417.6	17.4
	2	96971 +/- 3551	3928 +/- 746.2	11.0
	3	64717 +/- 38956	2015 +/- 1541	2.4

$$E_{Zr\text{-matrix}} = 93.6 \text{ GPa} \quad E_{ZrH_x} = 94.3 \text{ GPa}$$

$$H_{Zr\text{-matrix}} = 2.9 \text{ GPa} \quad H_{ZrH_x} = 3.9 \text{ GPa}$$

# Analysis - Carrier Gas Hot Extraction (CGHE)

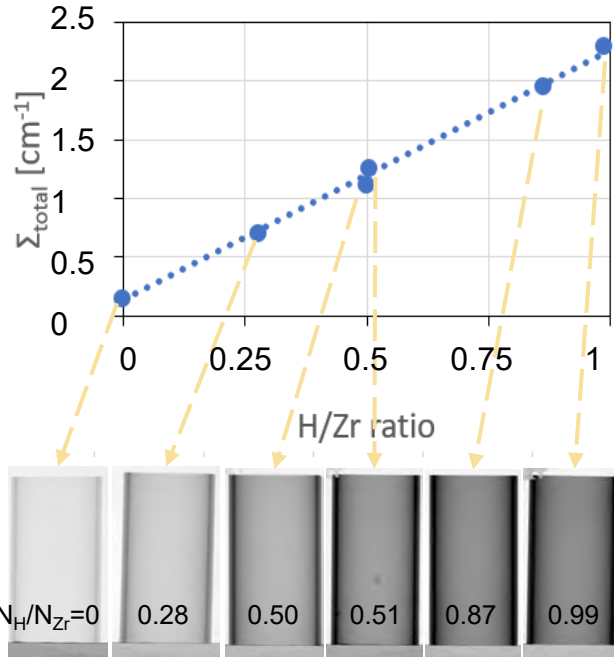
- sample segmentation
- statistical prove
- standards (Zr, Ti)



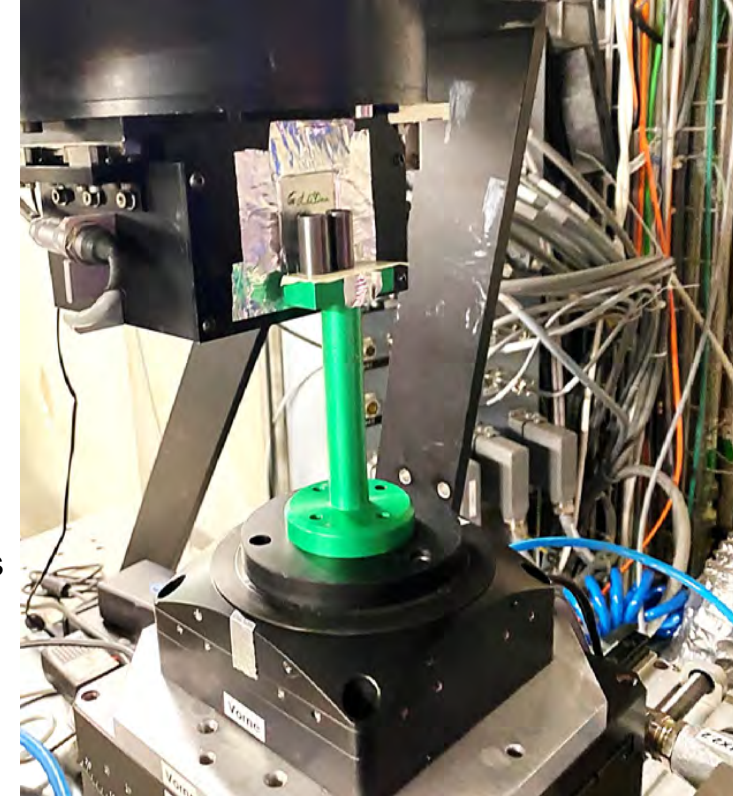
# Analysis - Neutron Radiography (NR)

ICON facility at the PSI

$$I = I_0 \cdot e^{-\sigma Nd} \quad T = \frac{I}{I_0} = \exp(-\Sigma_{total} \cdot s)$$

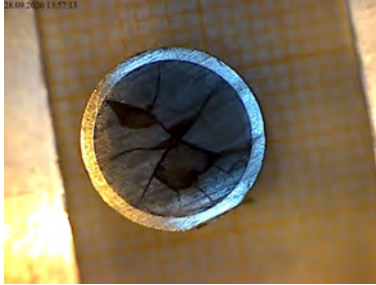


- I: intensity
- T: transmission
- $\sigma$ : microscopic neutron cross section
- N: number density
- d: sample thickness
- s: path length of the neutron beam
- $\Sigma$ : macroscopic neutron cross section

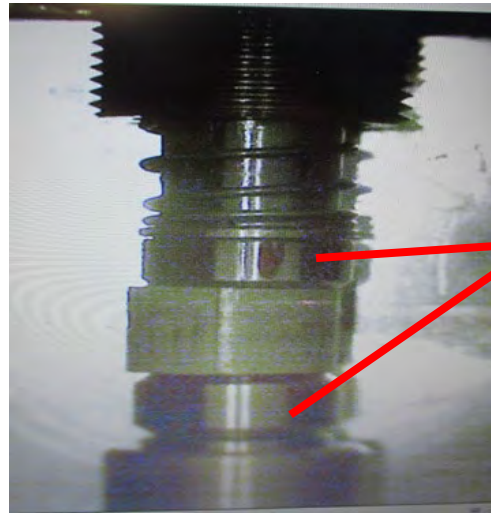
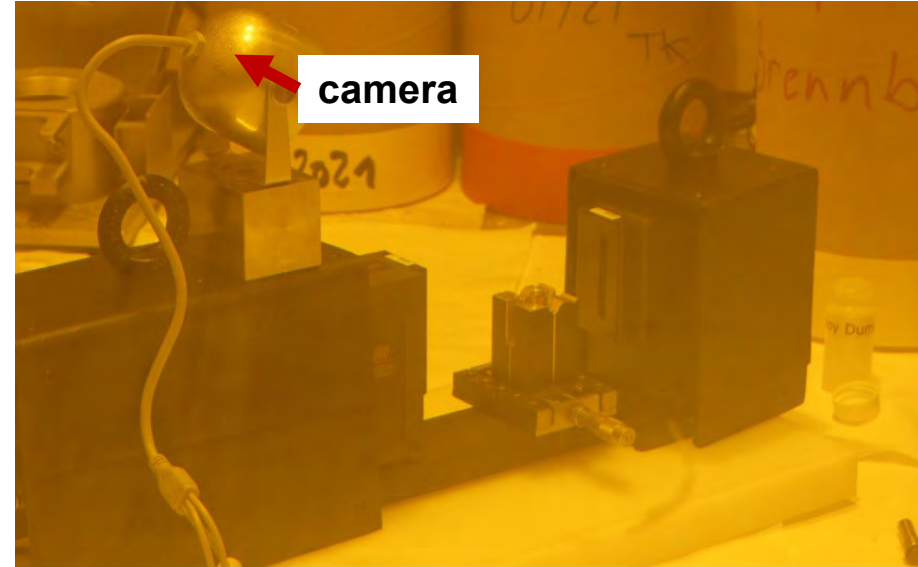


# Analysis – Diameter measurements with $\text{UO}_2$ fuel

Cross section of the  $\text{UO}_2$  pellet segment chosen for diameter variation measurement. Axial length 7.5 mm



Diameter measurement by means of a laser scan micrometre installed in a shielded box.



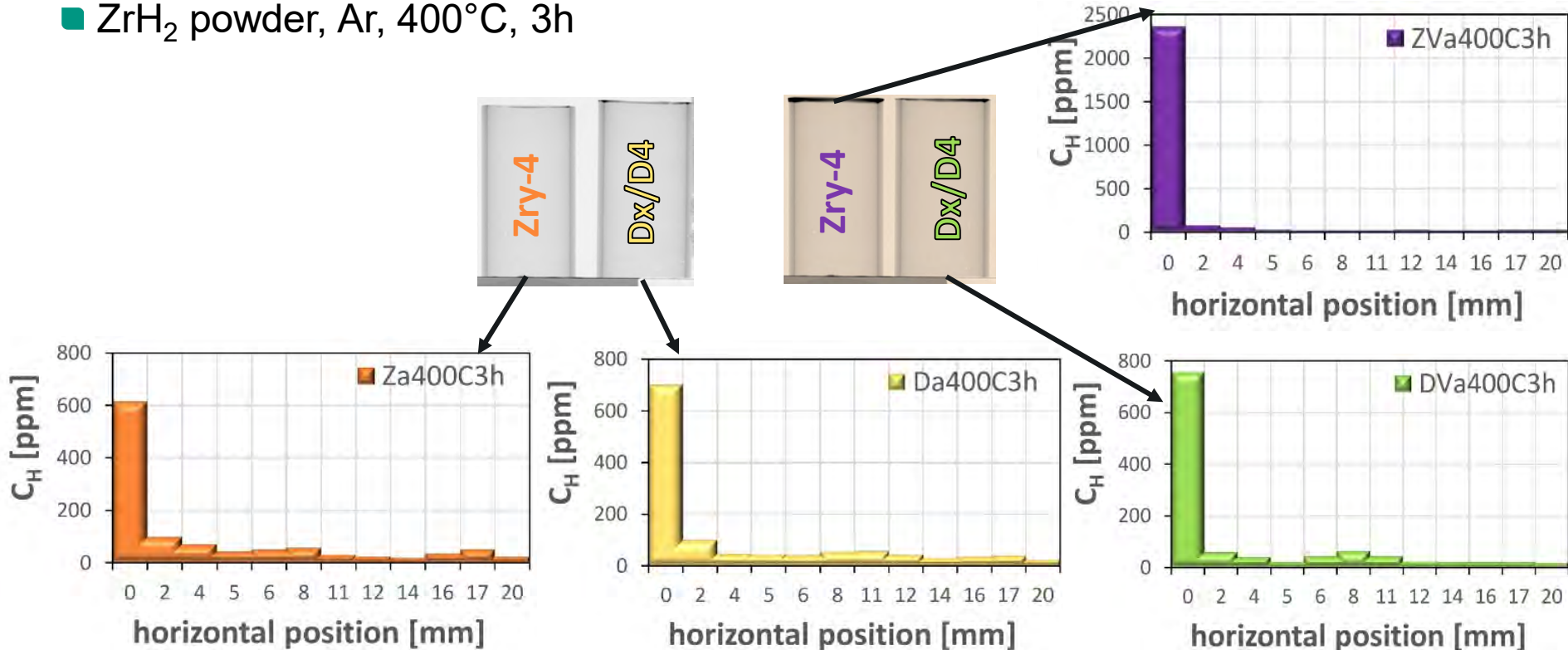
Clumps to rotate  
The pellet

- High accuracy with a linearity of  $\pm 1.0 \mu\text{m}$
- Repeatability of  $\pm 0.1 \mu\text{m}$



# Results – Diff. in axial direction

■ ZrH<sub>2</sub> powder, Ar, 400°C, 3h

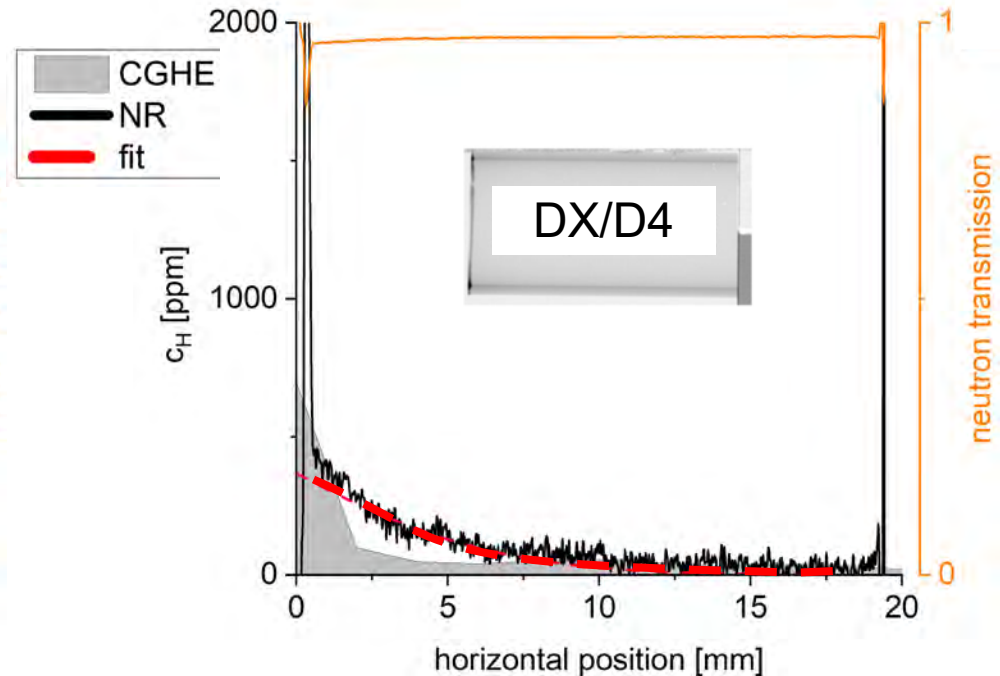
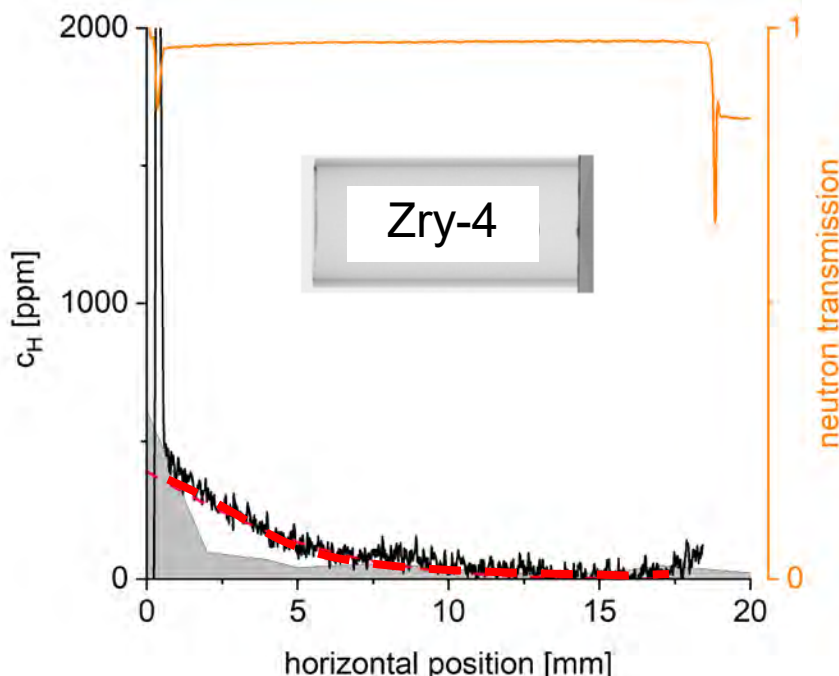




# Results – Diff. in axial direction

■ ZrH<sub>2</sub> powder, Ar, 400°C, 3h

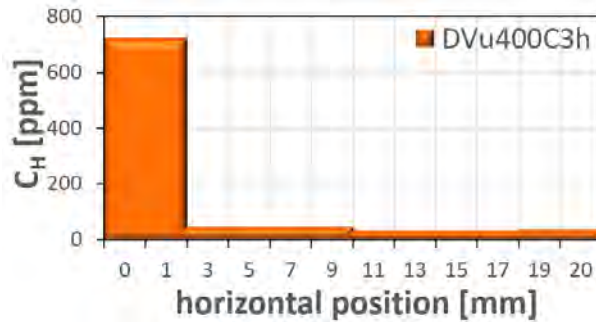
$$c(x, t) = c_0 \left( 1 - \operatorname{erf} \left( \frac{x}{2\sqrt{Dt}} \right) \right) + c_i$$



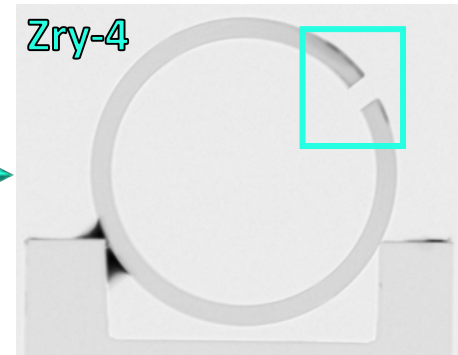
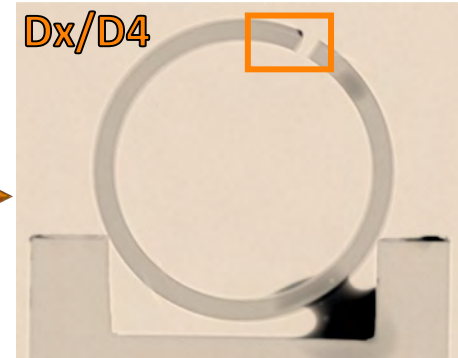
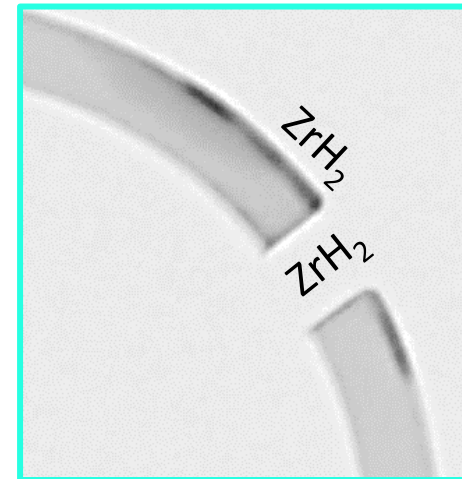
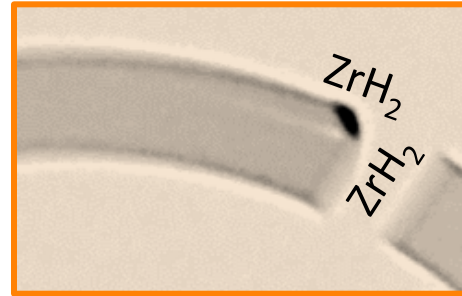
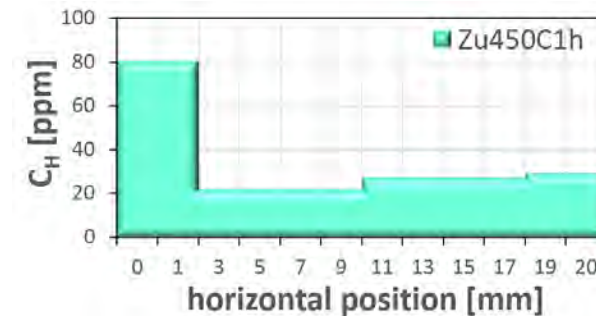
# Results – Diff. in circumferential direction

■ ZrH<sub>2</sub> powder, Ar

DX/D4,  
400°C, 3h,  
pre-ox.



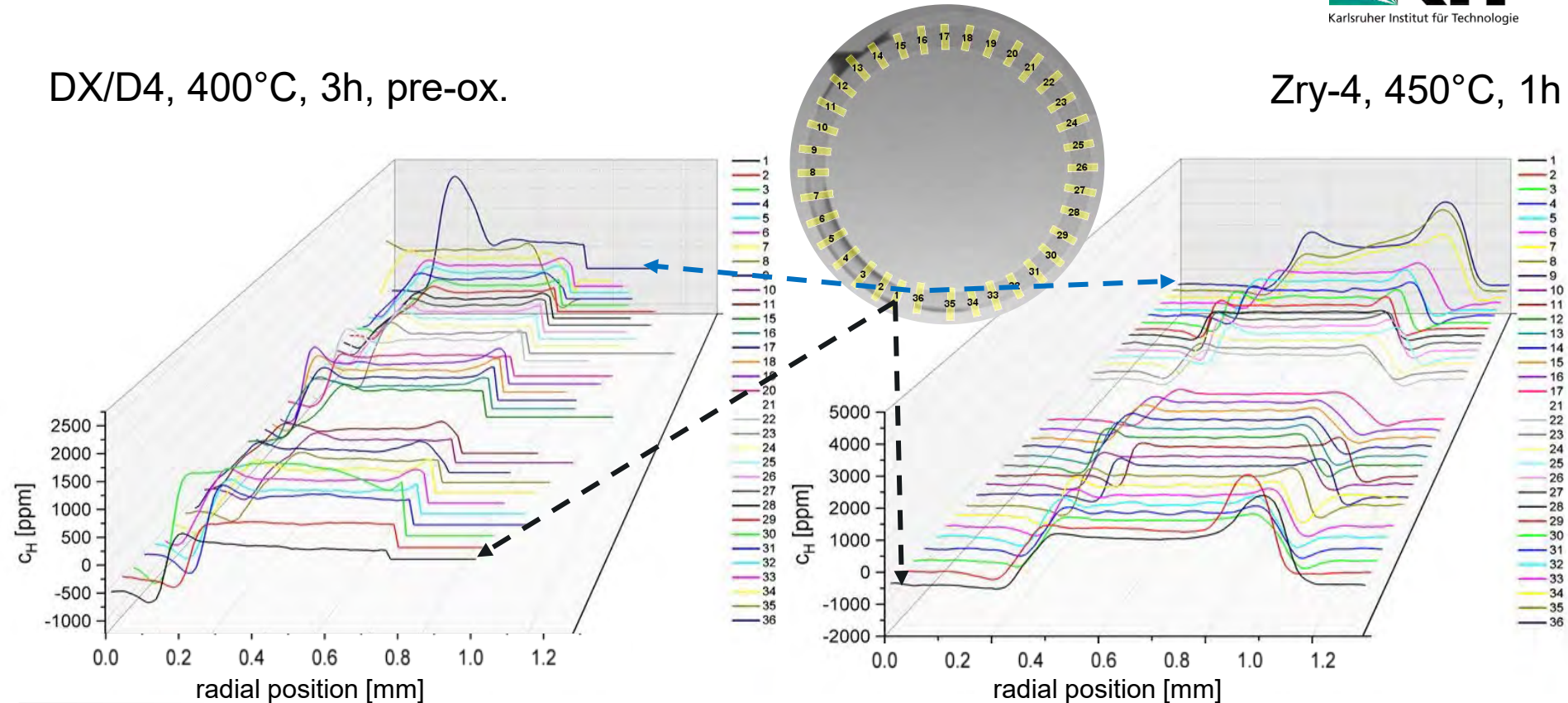
Zry-4,  
450°C, 1h



# Results – Diff. in circumferential direction

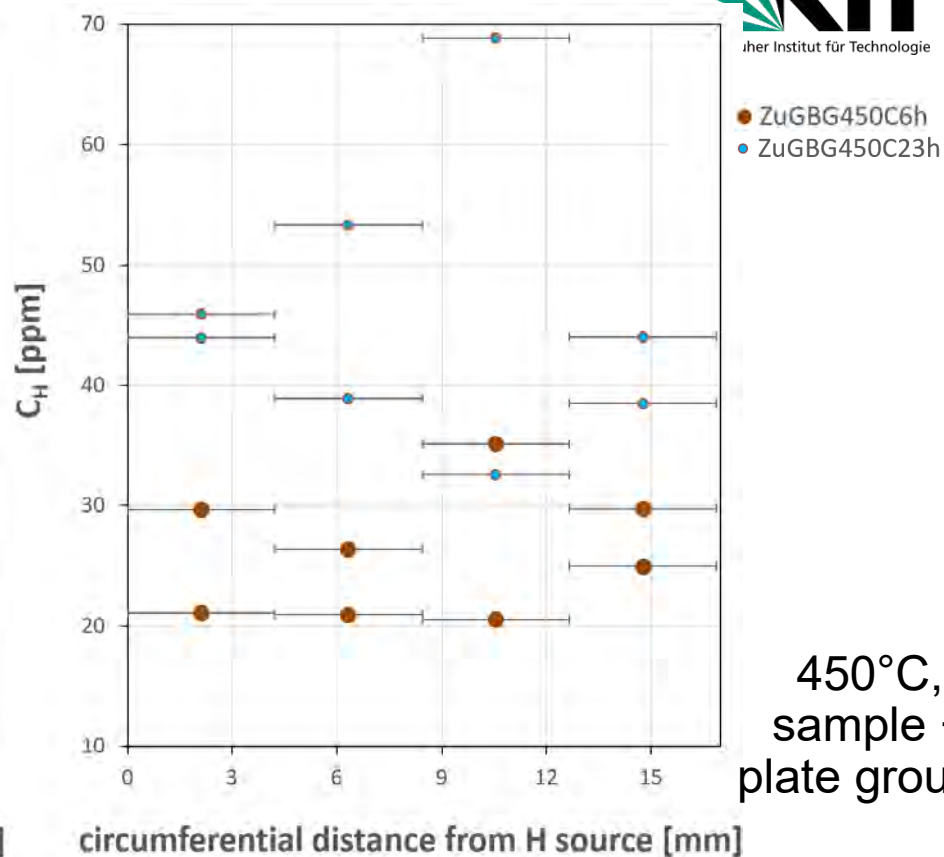
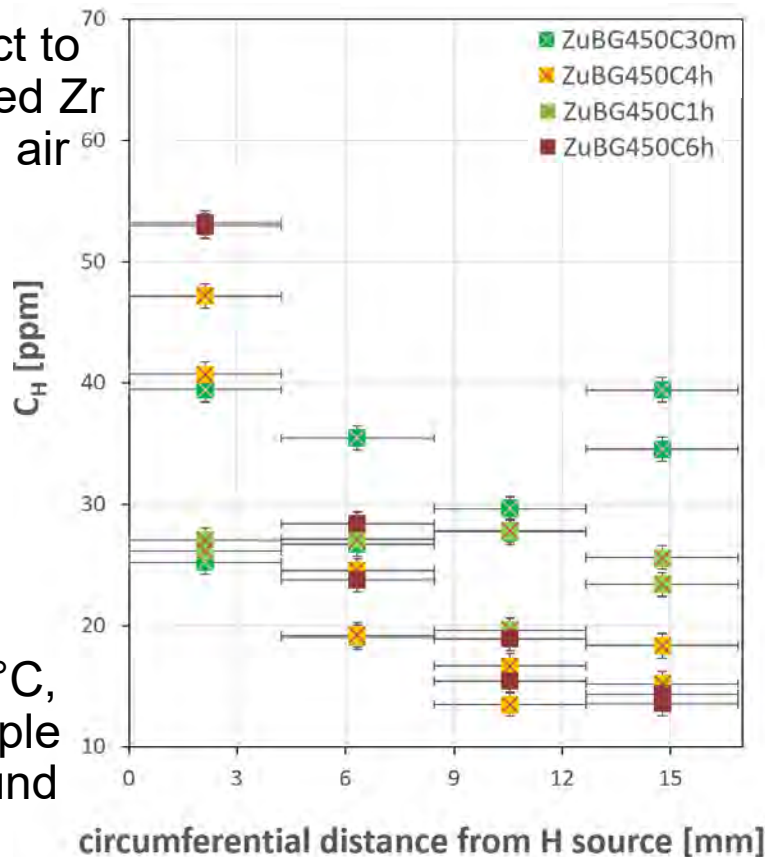
DX/D4, 400°C, 3h, pre-ox.

Zry-4, 450°C, 1h



# Results – Diff. in circumferential direction

Contact to  
hydrided Zr  
plates, air



# Results – Diameter measurements with $\text{UO}_2$ fuel

From preliminary modelling performed by **GRS** the variation induced by the fuel removal is  $\leq 20 \mu\text{m}$ .

Measurements performed after removal of the fuel by chemical digestion in  $\text{HNO}_3$  50% for three days reveal an average variation of the diameter of  $3 \pm 2 \mu\text{m}$ .

However, the variation in the diameter obtained by only moving and rotating the sample is about  $3 \mu\text{m}$  (repeatability test).



# Summary

- H loading: ZrH<sub>2</sub> powder, H-containing Zr-plate, SICHA
- analysis combination CGHE & NR sufficient
- similar results for Zry-4 & Dx/D4
- new INCHAMEL facility for investigations of the stress influence on the chemical potential for H in Zr
  
- Image Analysis method to determine the average content of hydrogen
- Pellet-cladding interaction: the variation of cladding diameter is smaller than predicted by the code
- EBSD analysis shows the presence of needle-like hydrides growing from grain boundaries to the grain or settled at the grain boundaries
- Possible co-existence of two hydride phases (stable FCC  $\delta$ -phase and metastable FCT  $\gamma$ -phase)

# Outlook



HoKi furnace at the KIT

- diffusion experiments will be repeated in-situ
- diffusion experiments will be expanded with an applied stress field in the INCHAMEL facility
- bundle test at the QUENCH facility: 8 months longterm test simulating interim dry storage conditions
- cladding tubes will be loaded with hydrogen from the gas phase in the HoKi-furnace
- results: analysis, then parameter implementation & modelling/ code validation
- Pellet-cladding interactions (INE): Mara Marchetti leaves KIT

QUENCH facility at the KIT



IAM-AWP-HTWC

# Acknowledgements

- the SPIZWURZ project is funded by the Federal Ministry for Economic Affairs and Climate Action (FKZ 1501609B)
- the INCHAMEL facility was funded by the HOVER program of the Helmholtz Association
- PSI for providing beamtime at the ICON facility & colleagues Anders Kaestner & David Mannes for their assistance during the measurements /analysis
- chemical analysis group of Thomas Bergfeldt (IAM-AWP)
- Mara Marchetti & her group at the INE
- QUENCH group & colleagues at KIT





**Y. Lee**

**Seoul National University**

## **Understanding mechanical integrity of hydrided Zircaloy cladding for extended spent fuel management**

This presentation addresses hydride embrittlement of Zirconium based alloy with focus on (1) image analysis for the effect of radial hydride connectivity on mechanical strength of radial hydride, (2) orientation relationship between  $\delta$  hydride and reactor-grade Zircaloy cladding. The presentation demonstrates that the material's strength can increase with increase in circumferential hydrides in the presence of the radial hydrides, and its mechanism was explained using the concept of Radial Hydride Continuous Path (RHCP) via the image analysis using the software PROPHET developed by Seoul National University. For various hydride morphologies, Radial Hydride Fraction (RHF) when greater than 5% was shown to be a power metric that exhibits a strong correlation with the material strength. For RHF < 5%, the amount of hydrogen was shown to be a predominant factor that determines the strength of the material, implying that formation of radial hydrides has limited effect when RHF is less than 5%. The direct observation of orientation relationship between  $\delta$  hydride and reactor-grade Zircaloy cladding via EBSD analyses was successfully conducted. It is shown to significantly improve the prediction of the threshold stress for radial hydride reorientation, and explain suppressed hydride precipitation in the welding zone of Zircaloy cladding tube.

# Understanding mechanical integrity of hydrided Zircaloy cladding for extended spent fuel management

**Department of Nuclear Engineering  
Seoul National University, Korea**

27<sup>th</sup> International QUENCH Workshop  
Karlsruhe Institute of Technology, Germany

**Youho Lee, Sangbum Kim, Dahyeon woo, Chansoo Lee**

[leeyouho@snu.ac.kr](mailto:leeyouho@snu.ac.kr)





# Contents

1. Image analysis for mechanical integrity of hydrided Zircaloy
2. Microstructural effect for hydride embrittlement
3. Conclusions

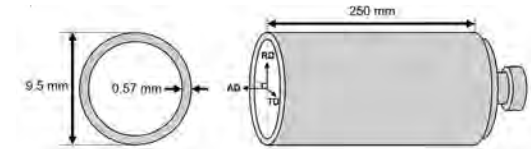


# 1. Image analysis for mechanical integrity of hydrided Zircaloy

# Hydride reorientation and mechanical strength test

## Material : Zr-Nb alloy

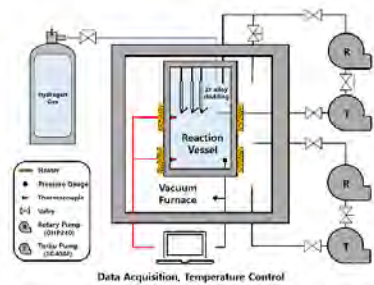
Element	Zr	Sn	Nb	Fe	O
Composition	Balance	0.99 wt%	0.98 wt%	0.1 wt%	0.11 ppm



<Geometry of specimen>

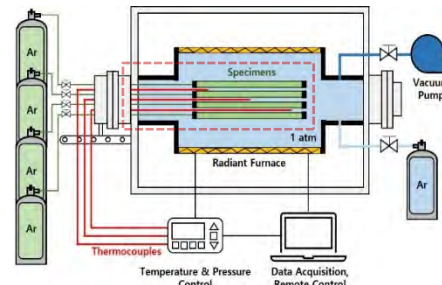
## Experimental protocol

### 1. Hydrogen charging



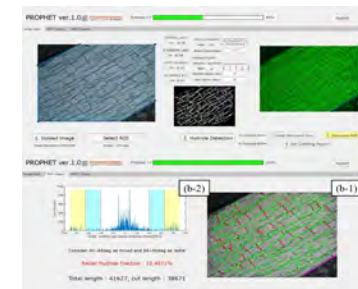
<Hydrogen charging system>

### 2. Hydride reorientation



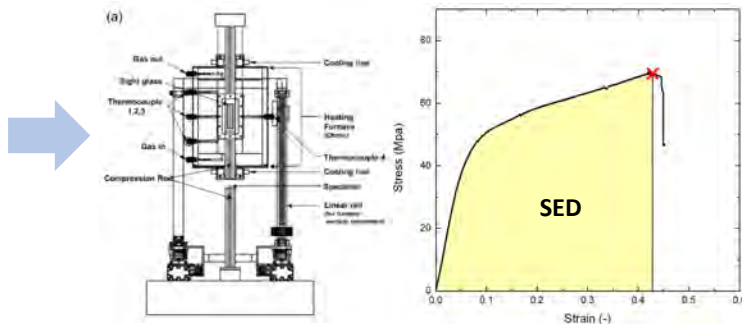
<Multi-axial stress test facility>

### 3. OM & PROPHEC analysis



<PROPHEC analysis>

### 4. Ring compression test



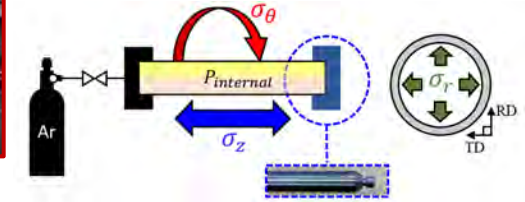
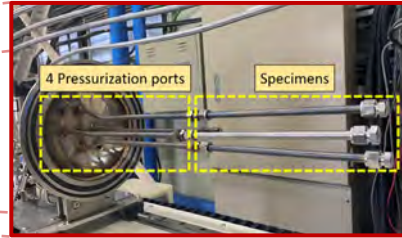
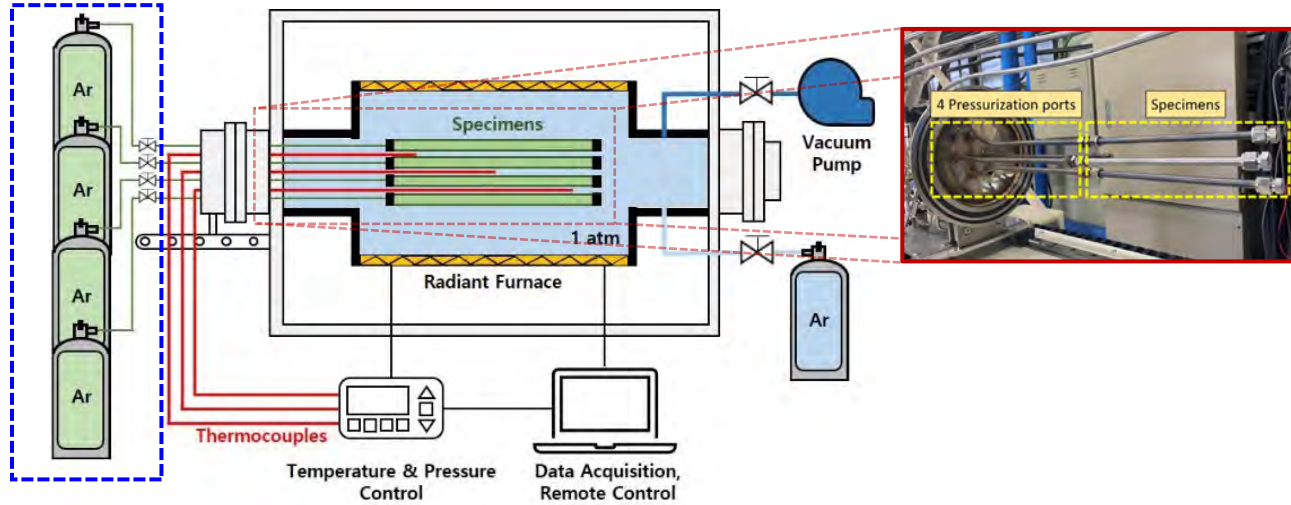
<Strain energy density (SED)>

### 5. H concentration measurement



<H analyzer (ELTRA ONH-2000) >

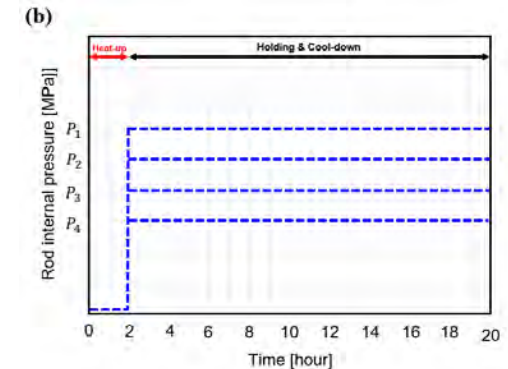
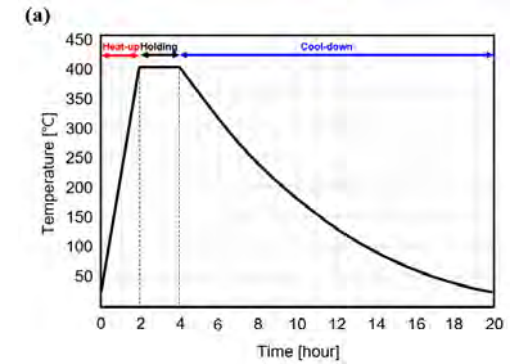
# Hydride-reorientation experiment in detail



<Multi-axial Stress state of internally pressurized cladding>

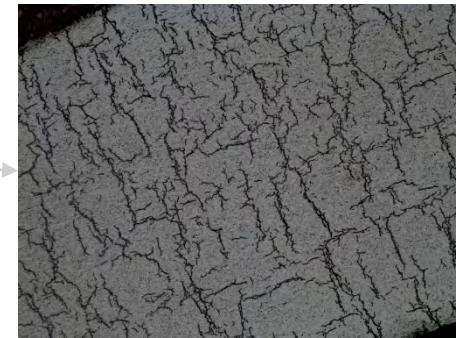
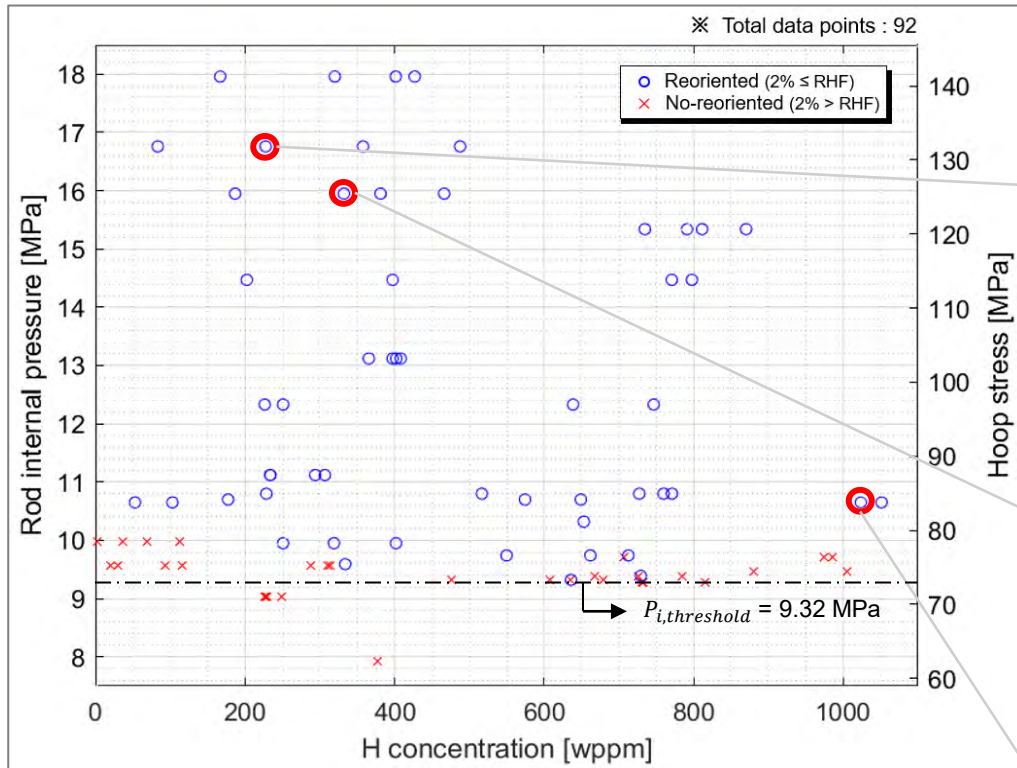
<Multi-axial stress test facility>

- The furnace is filled with Ar gas of 1 atm
- ① Heat-up to 400°C in vacuum furnace
- ② Applying different internal pressures(1-20MPa) in cool-down
  - Cooling rate = 0.396 °C/min
- Stress is generated by the pressure difference between the inside and outside of the cladding.
- Depending on the magnitude of the stress, radial hydride is precipitated during the cool down process.



<Applied temperature and pressure>

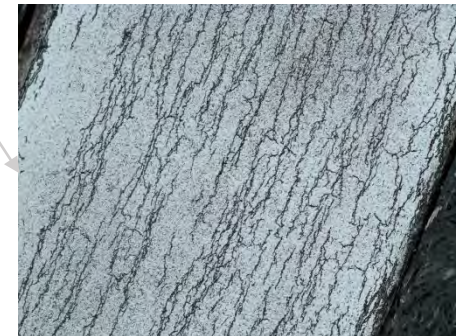
# Hydride reorientation



17.96 MPa, 206.9 wppm, 46.01%



16.76 MPa, 357.9 wppm, 14.05%



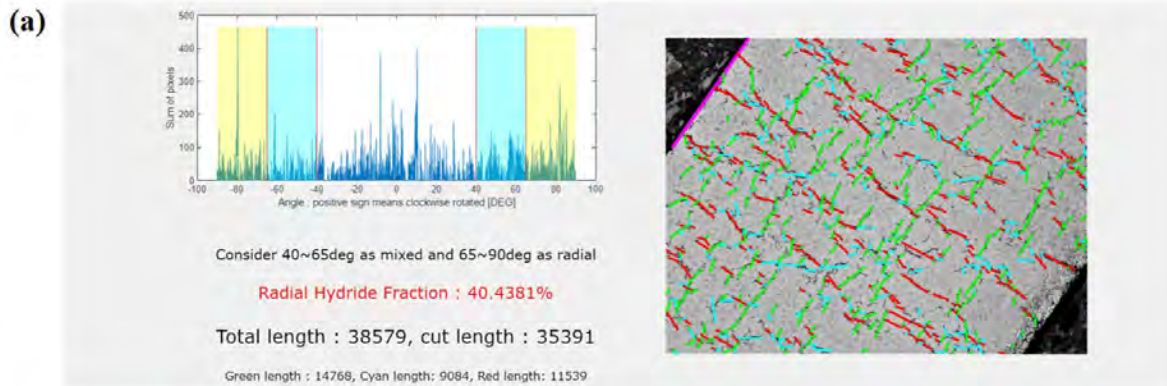
10.8 MPa, 1023.6 wppm, 3.13%

<Hydride reorientation with regard to hydrogen contents and rod internal pressure>

- Hydride reorientation occurs with  $P_i > 9.32 \text{ MPa}$  (>73.3 MPa of hoop stress).
- The slightly early reorientation is considered due to the multi-stress state and constant pressure.



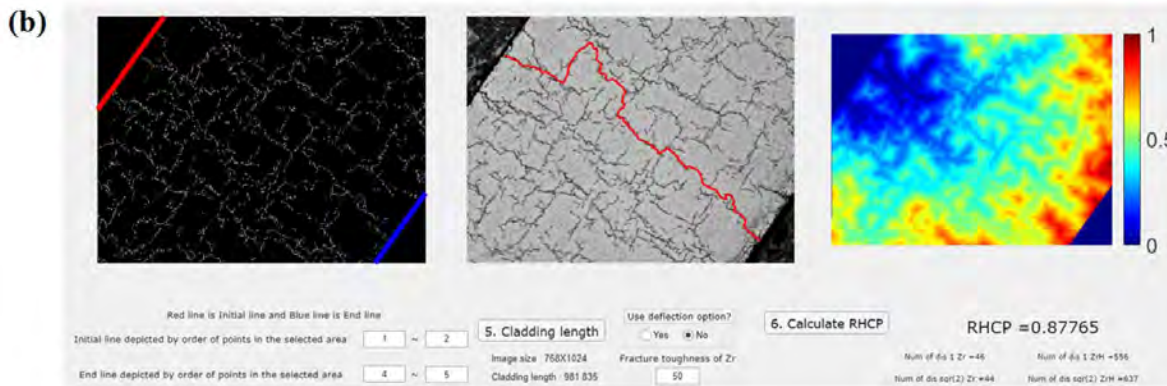
# PROPHET : SNU-developed hydride image analysis code



## Radial Hydride Fraction (RHF)

$$RHF = \frac{\sum_i L_i f_i}{\sum_i L_i}$$

$$f_i = \begin{cases} 0: & 0^\circ \leq \theta < 40^\circ: \text{ circumferential} \\ 0.5: & 40^\circ \leq \theta < 65^\circ: \text{ mixed} \\ 1: & 65^\circ \leq \theta < 90^\circ: \text{ radial} \end{cases}$$



## Radial Hydride Continuous Path (RHCP)

$$RHCP = \frac{Lw_{Zr} - (x_{Zr}w_{Zr} + x_{ZrH}w_{ZrH})}{L(w_{Zr} - w_{ZrH})}$$

Relative cost of Zr matrix and hydride:

$$w_{Zr} = 50 \text{ MPa}\sqrt{m}, \quad w_{ZrH} = 1 \text{ MPa}\sqrt{m}$$

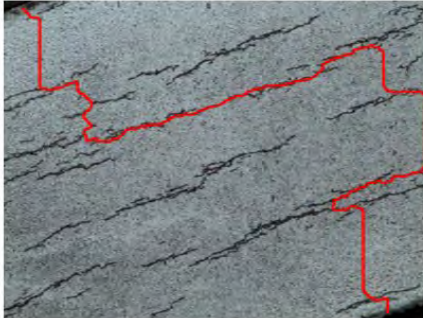
0= Minimum cost path consists of 100% Zr matrix (Straight Zr path)

1= Minimum cost path consists of 100% ZrH (Straight hydride path)

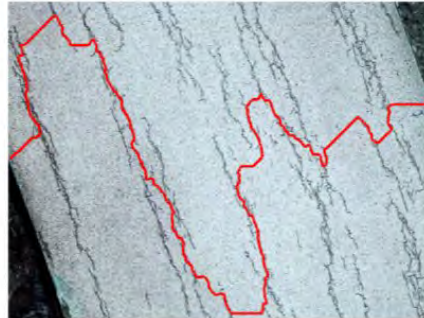
Dijkstra's algorithm:  
Finding the least-cost path

# PROPHET : SNU-developed hydride image analysis code

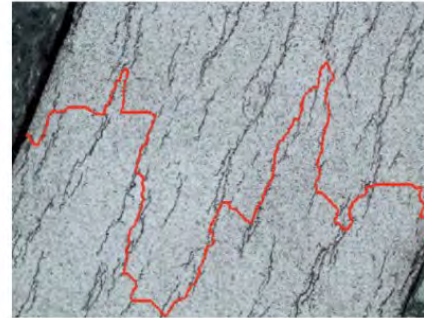
- RHCP assessment of various hydride morphologies



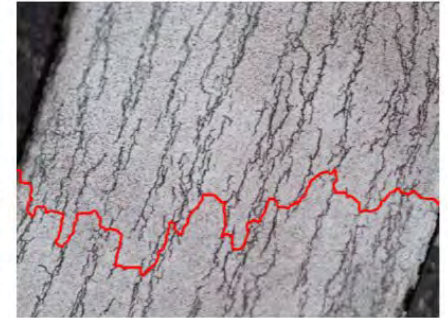
20 wppm / 0.1625



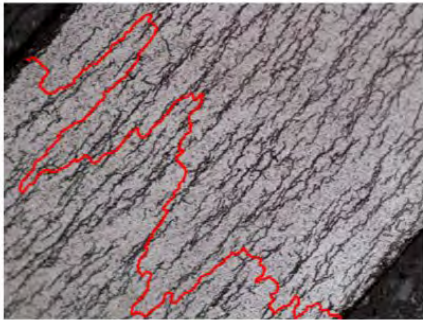
116 wppm / 0.2756



113 wppm / 0.3732



234 wppm / 0.5730



668 wppm / 0.6726



307 wppm / 0.7705



186 wppm / 0.8519

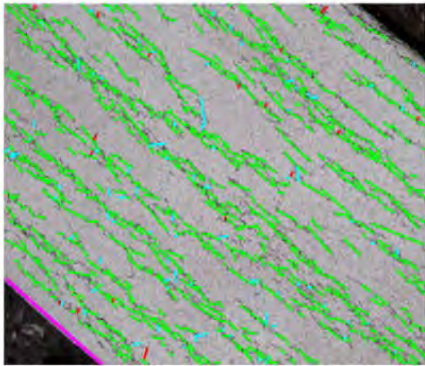


83 wppm / 0.94

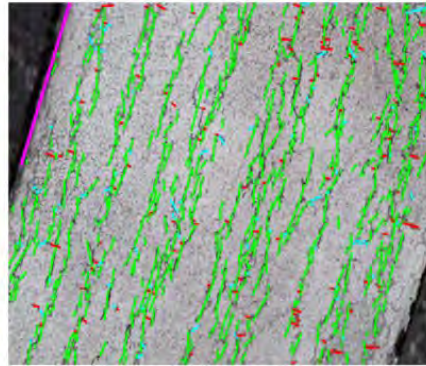


# PROPHET : SNU-developed hydride image analysis code

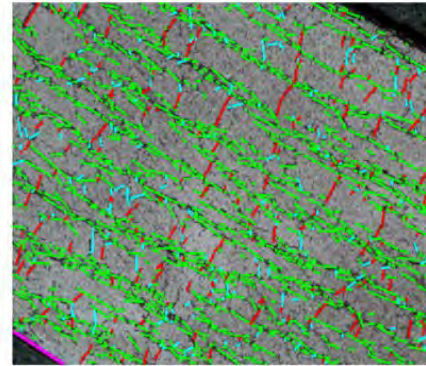
- RHF assessment of various hydride morphologies using PROPHET



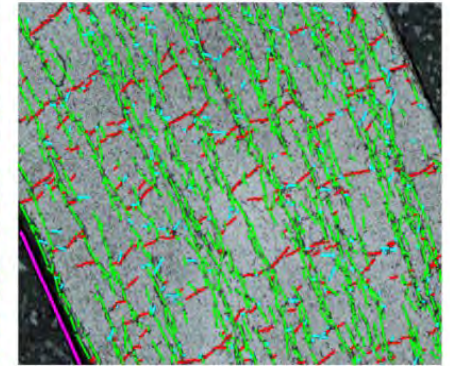
229 wppm / 0%



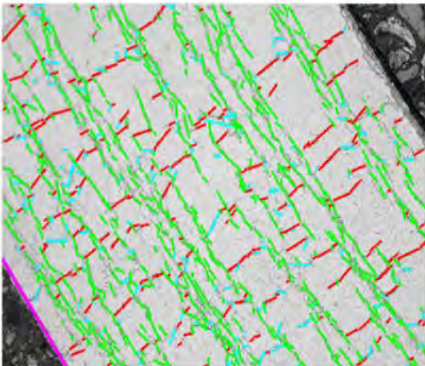
233 wppm / 4.9%



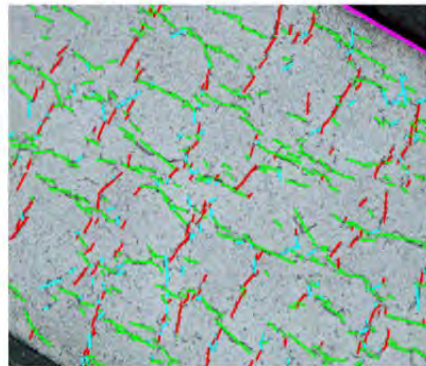
381 wppm / 11.9%



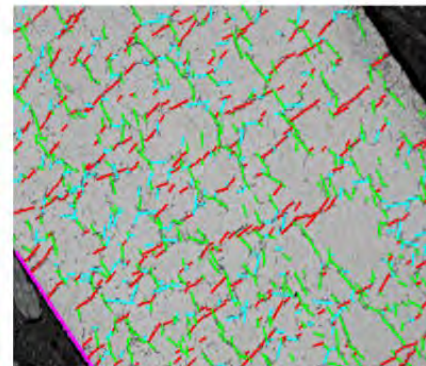
466 wppm / 15.9%



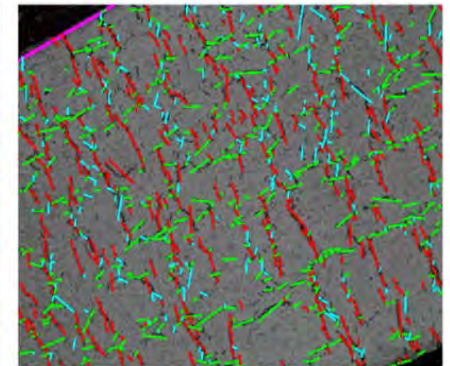
312 wppm / 21.0%



187 wppm / 27.6%



171 wppm / 39.1%



167 wppm / 46.5%

# PROPHET is accessible at our website

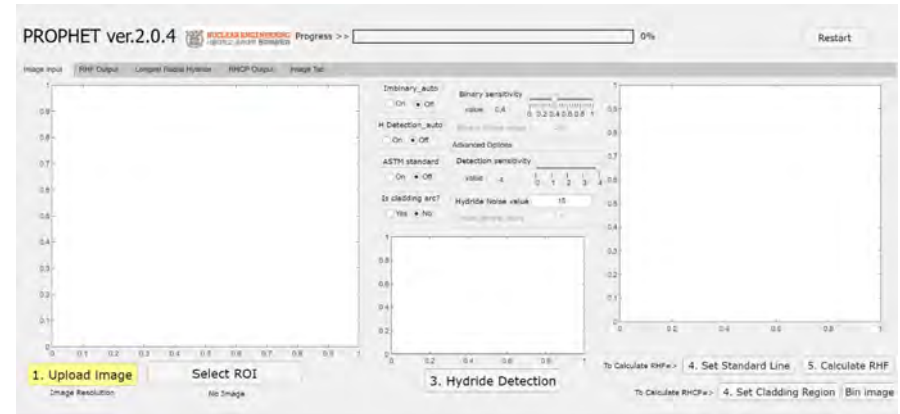
- PROPHET is open to public via <http://fuel.snu.ac.kr>.

Professor Members Research Publications Press Alumni **Prophet**

### Prof. Youho Lee

Prof. Lee studies nuclear fuel materials, reactor safety, and various solid-fluid interface phenomena in extreme environments. His research interests include nuclear fuel design and safety, nuclear fuel mechanical modelling, spent fuel behavior, material compatibility in advanced reactors, material behavior under strong interaction with fluids, and low-power density reactor.

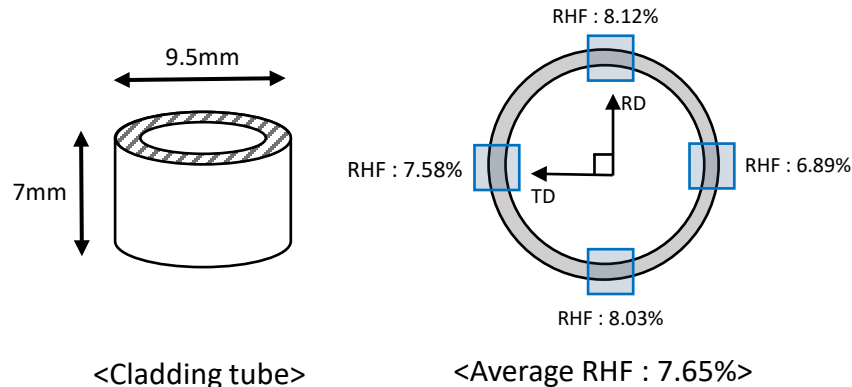
Prof. Lee received a B.S. from the Korea Advanced Institute of Science and Technology (KAIST) in 2009, and an M.S. and Ph.D. in nuclear engineering from the Massachusetts Institute of Technology (MIT) in 2011 and 2013, respectively. Prior to joining Seoul National University, he served as an assistant professor at the



<working screen of PROPHET>

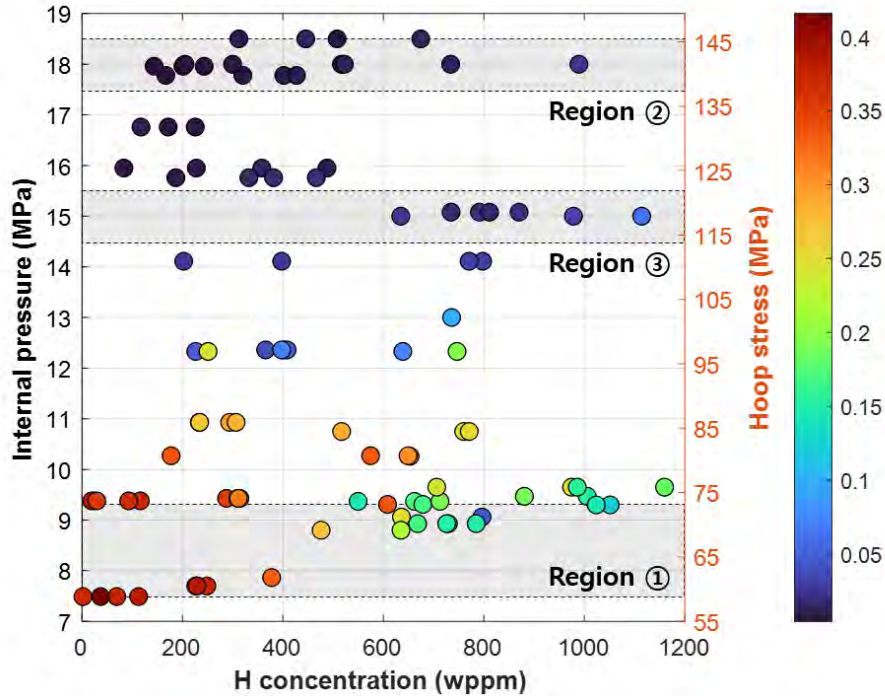
- Statistical nature of image analysis:**

For both RHF and RHCP, the results in four directions were averaged and used.

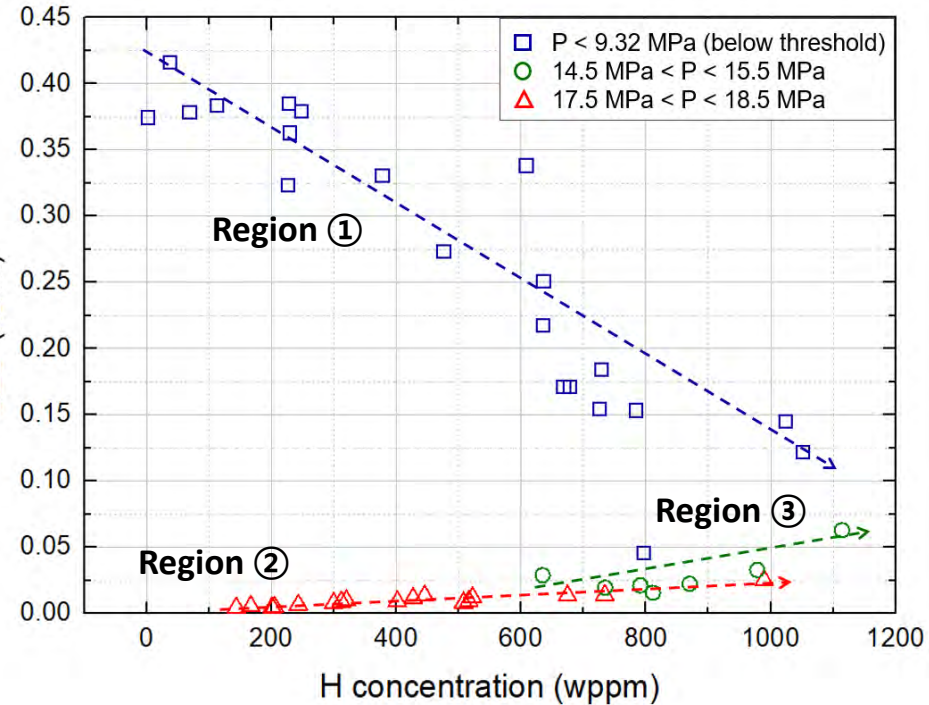




# Structural integrity with various hydride morphologies



<Strain Energy Density (SED) of various hydride morphologies induced by various H concentration and applied pressure >

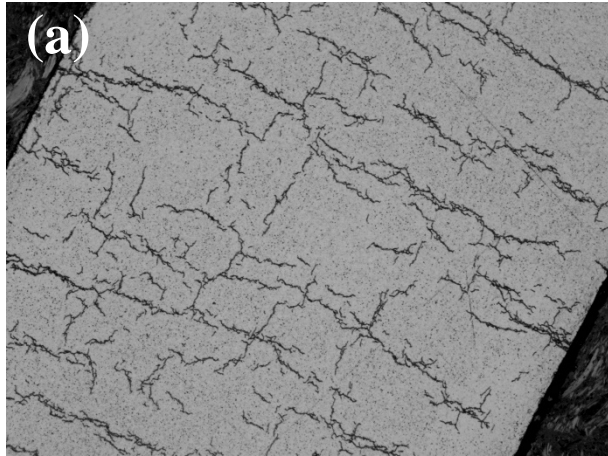


<SED change with H concentration along Region ① (below reorientation threshold) and Region ② (well above reorientation threshold)>

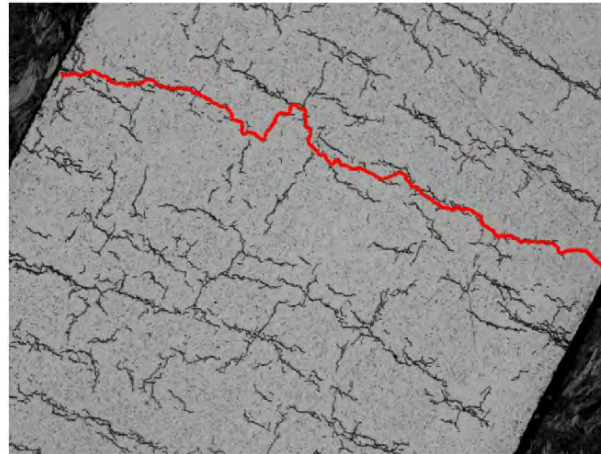
- Hydrogen concentration is a key parameter for Zircaloy without hydride reorientation.
- With a presence of appreciable radial hydrides, the strength exhibits a complex behavior: Increasing H concentration is shown to increase SED (i.e., Region ②)



# Beneficial effect of circumferential hydrides

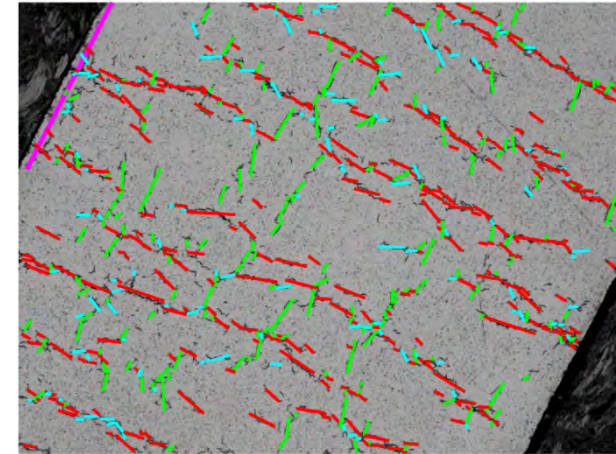


143.7 wppm / 18 MPa

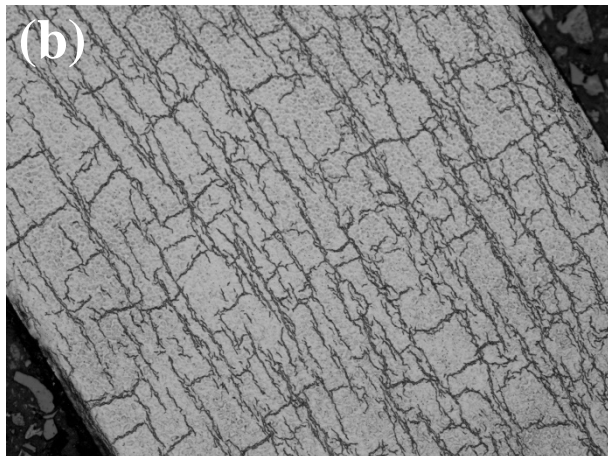


RHCP = 0.902

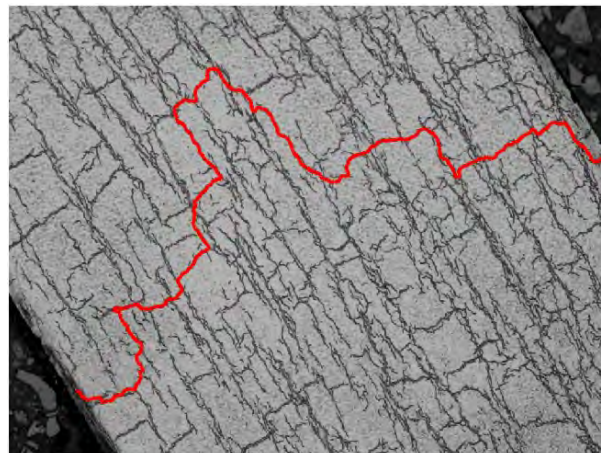
**SED=4 J/m**



RHF = 47.3%

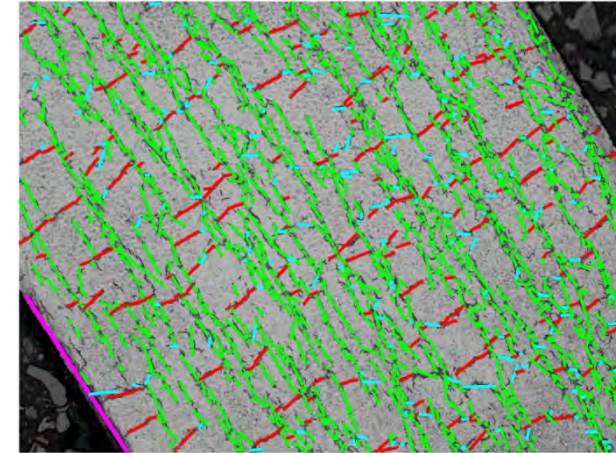


522.4 wppm / 18 MPa / 0.012 kJ/m



RHCP = 0.883

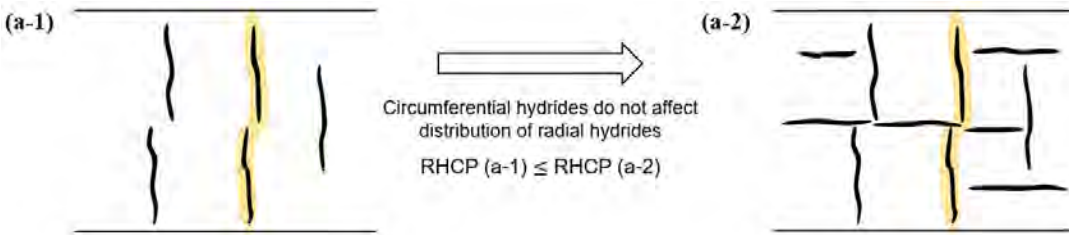
**SED=12J/m**



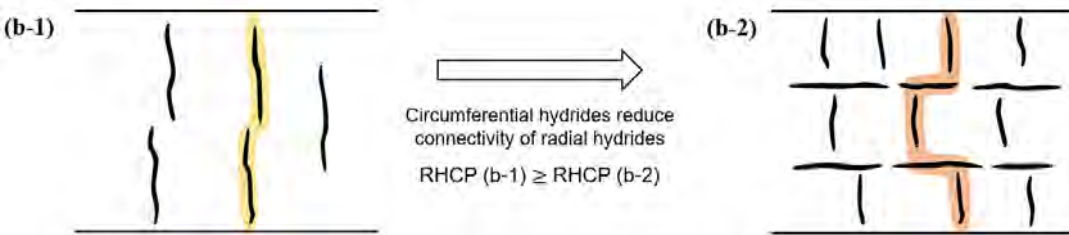
RHF = 15.9%

<OM, RHF, RHCP images for applied pressure of 18 MPa: (a) low total hydrogen case of 143.7 wppm, (b) high total hydrogen case of 522.4 wppm>

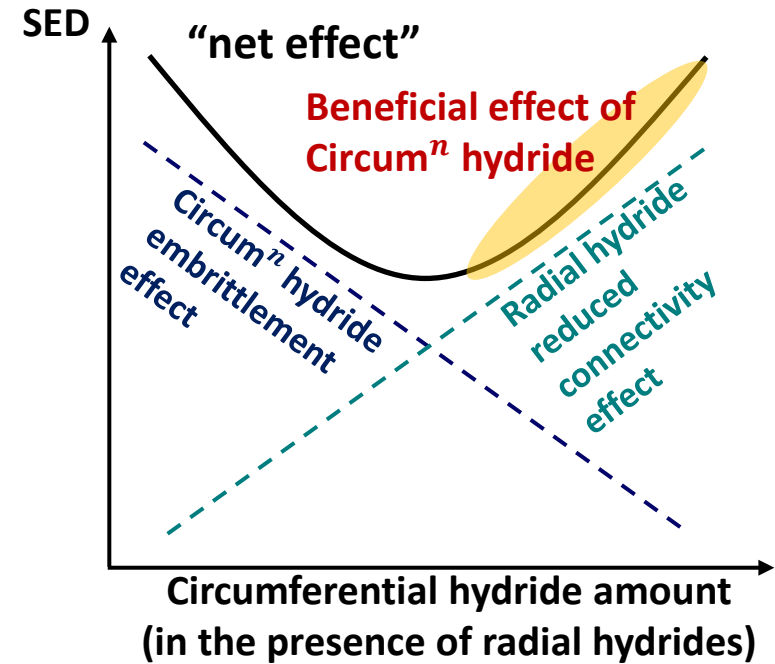
# Mechanisms of circumferential hydride-aided strength



<Ideal case: introduction of circumferential hydrides without affecting radial hydrides>



<Real case: introduction of circumferential hydrides decrease radial hydride connectivity>

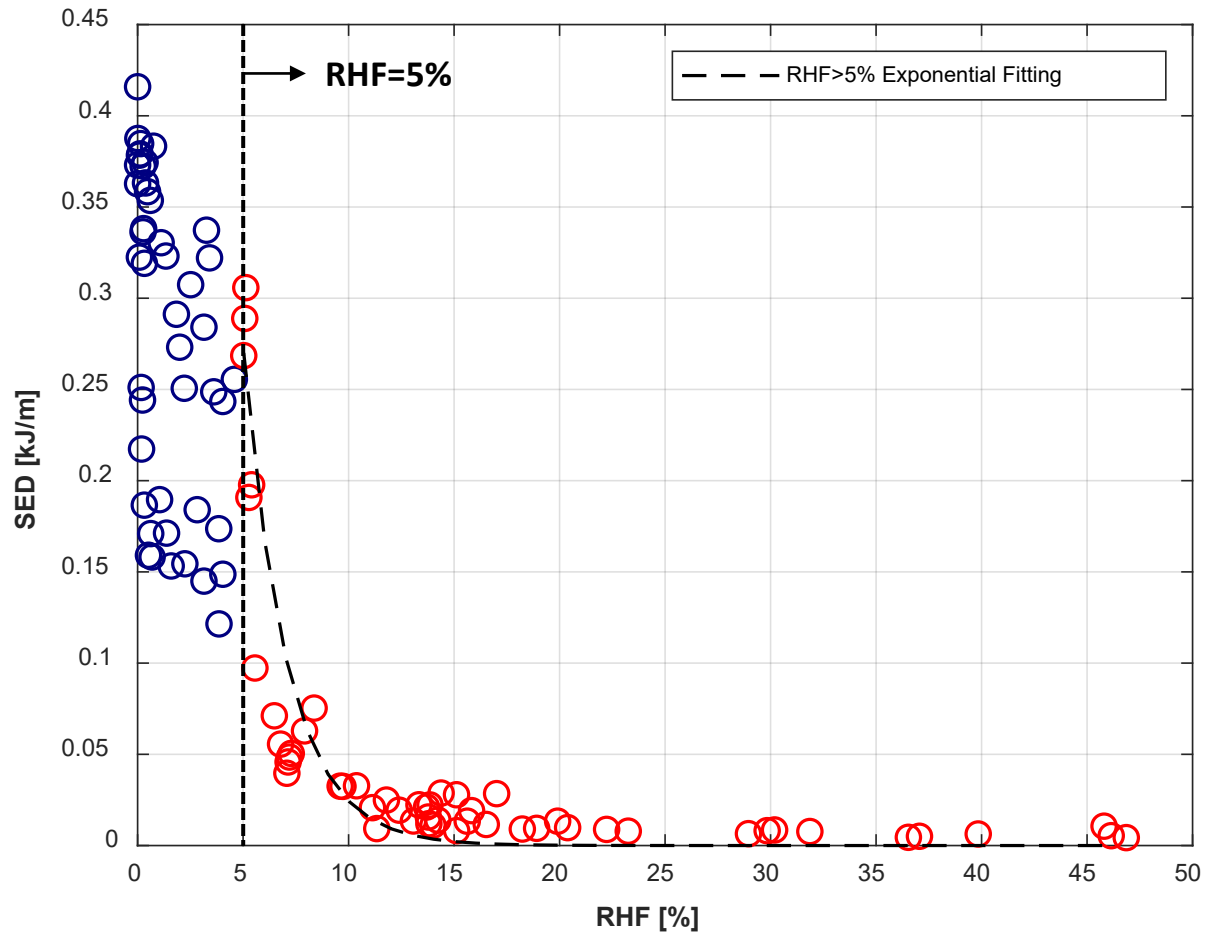


<Schematic diagram of two competing mechanisms of circumferential hydrides on SED in the presence of radial hydrides >

**Effect of increasing circumferential hydrides in the presence of radial hydrides:**

- ①: Increasing embrittlement (strength ↓)
- ②: Decreasing radial hydride connectivity (strength ↑)

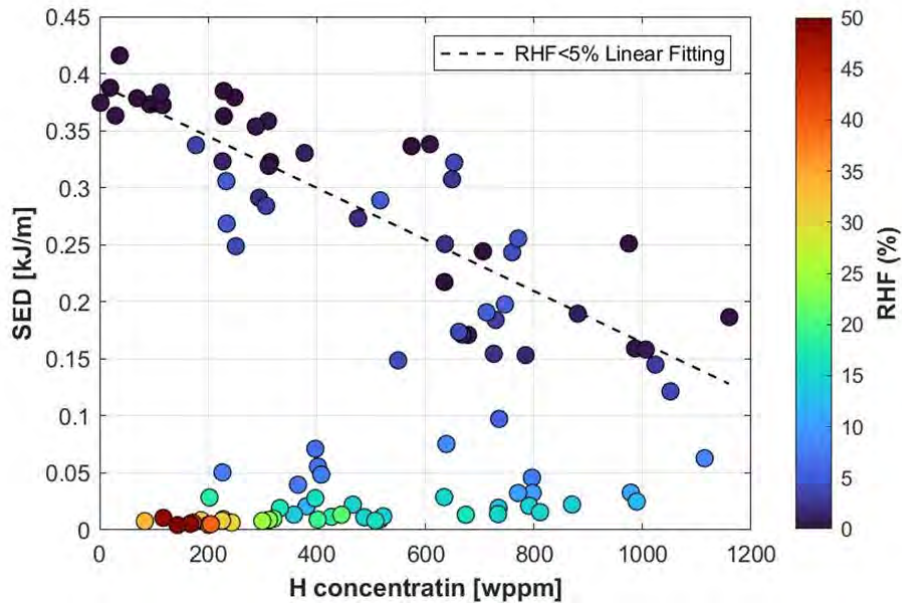
# RHF (>5%) is a powerful metric



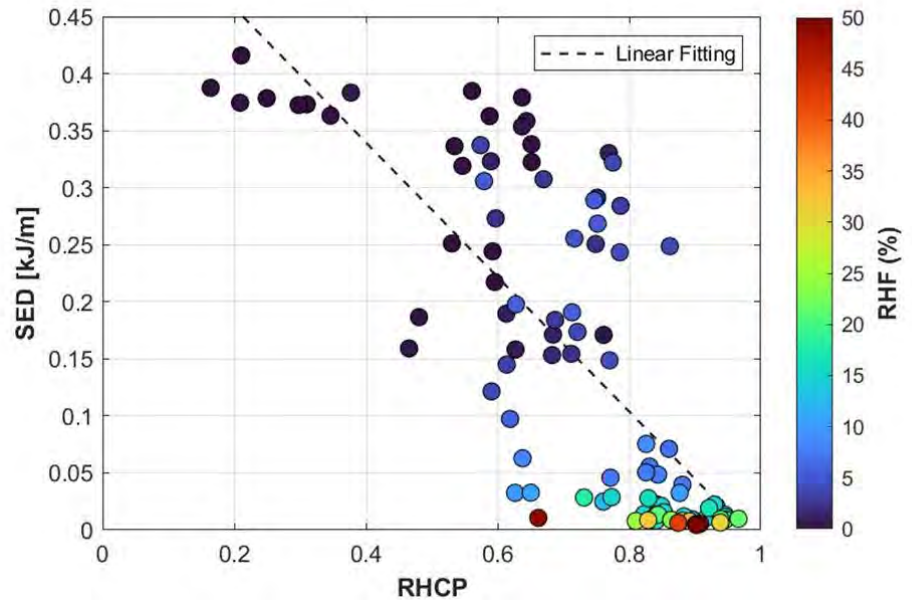
<SED change with RHF>



# Predictability of SED with H concentration and RHCP



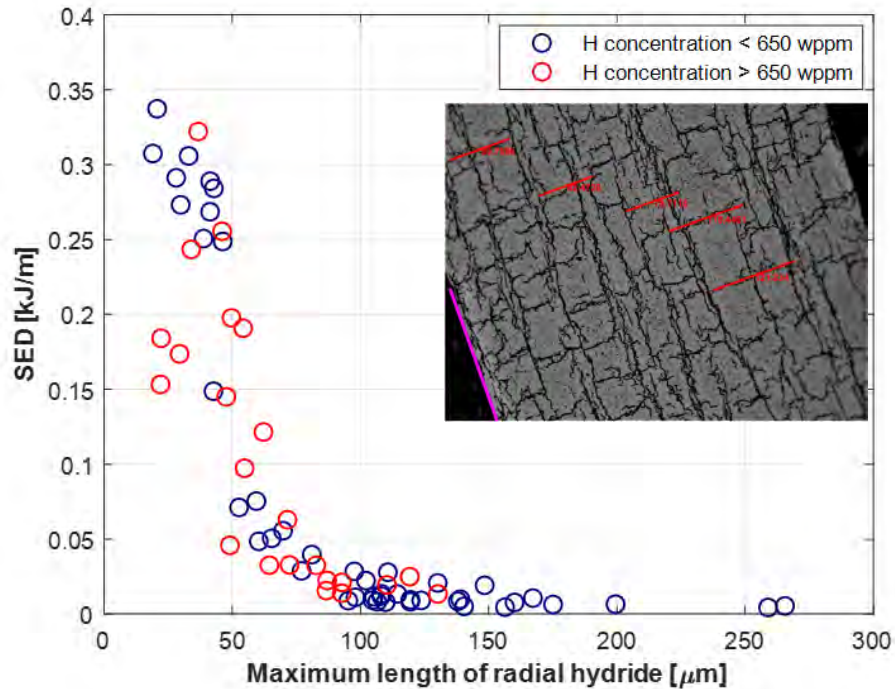
<SED vs. H Concentration>



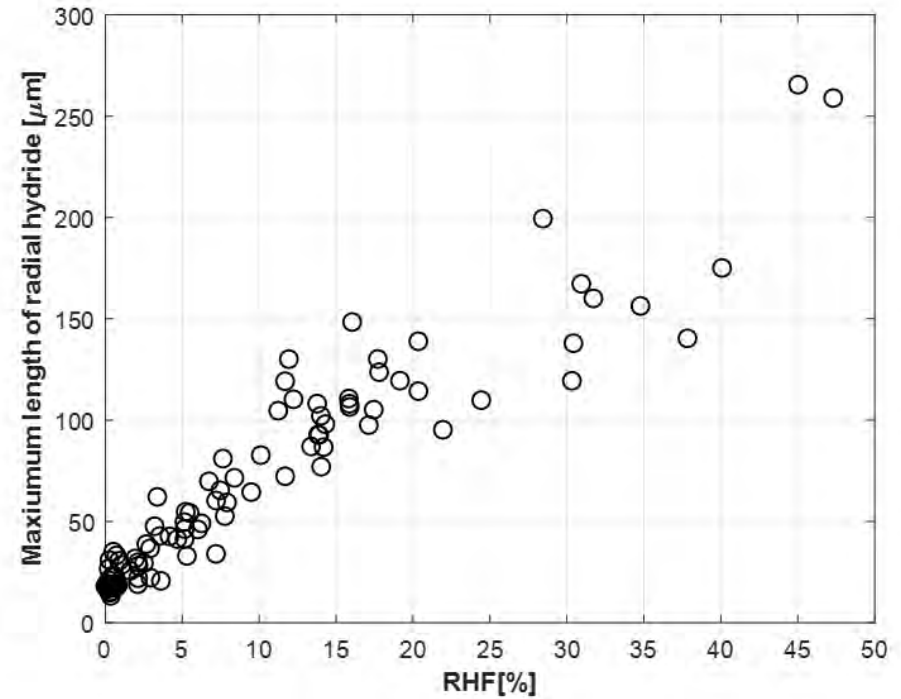
<SED vs. RHCP>

- For RHF < 5% , H concentration plays a predominant role in determining SED.
- RHCP alone presents limited accuracy in predicting SED.

# Maximum radial hydride length is another powerful metric



<SED vs. Max radial hydride length>



< Max radial hydride length vs. RHF >

- Exhibiting a notable correlation with RHF, maximum radial hydride presents a strong correlation with SED. This is consistent with the principle of fracture mechanics which states that the brittle fracture occurs by a critical flaw.





## 2. Microstructural effect for hydride embrittlement

# Hydride reorientation threshold stress prediction

- Limited accuracy of thermodynamic model to predict threshold for hydride reorientation

- Radial hydride nucleation under applied stress : [Qin's thermodynamic model](#) [4], [5]

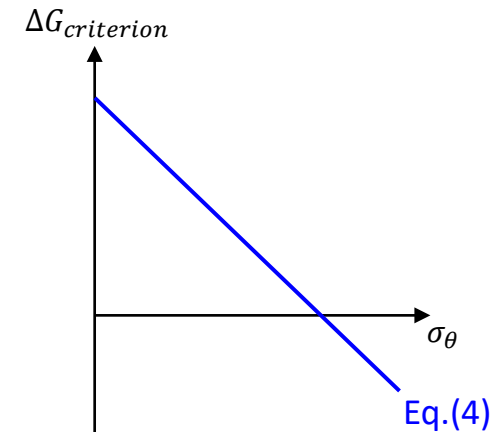
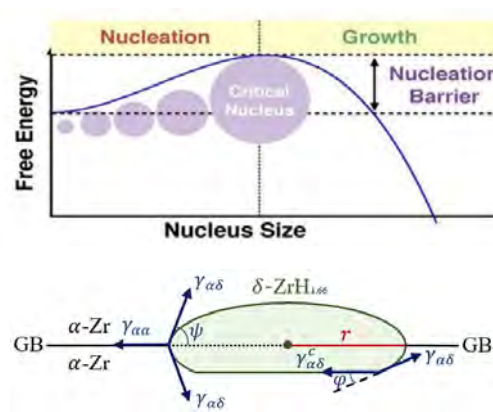
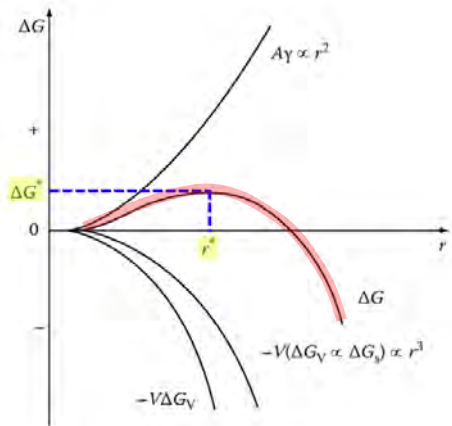
$$\Delta G = -V(\Delta G_{chemical} + P\nu) - V\Delta G_{interaction} + V\Delta G_{strain} + A\Delta G_{interface} - S\Delta G_{GB} \text{----- Eq. (1)}$$

$$\Delta G = (\pi r^3/3)[(2(2 - 3\cos\psi + \cos^3\psi) - (2 - 3\cos\phi + \cos^3\phi))[-\Delta G_{chem} - \left(\frac{x}{\bar{v}_{hyd}}\right)(\sigma_{\theta}\cos\phi/3)\bar{v}_H + \Delta G_{strain} - \sigma_{\theta}\cos\phi\chi] + 4\pi r^2[(1 - \cos\psi) - (1/2)(1 - \cos\phi)]\gamma_{\alpha\delta} + \pi r^2\sin^2\phi\gamma_{\alpha\delta}^c - \pi r^2\sin^2\psi\gamma_{\alpha\alpha} \text{----- Eq. (2)}$$

$$\Delta G^* = \frac{16\pi\gamma_{\alpha\delta}^3 f}{3[-\Delta G_{chem} - \left(\frac{x}{\bar{v}_{hyd}}\right)\left(\frac{\sigma_{\theta}\cos\phi}{3}\right)\bar{v}_H - \sigma_{\theta}\cos\phi\chi + \Delta G_{strain}]^2} \text{----- Eq. (3)}$$

$$\Delta G_{criterion} = -\Delta G_{chem} - \left(\frac{x}{\bar{v}_{hyd}}\right)\left(\frac{\sigma_{\theta}\cos\phi}{3}\right)\bar{v}_H - \sigma_{\theta}\cos\phi\chi + \Delta G_{strain} < 0 \text{----- Eq. (4)}$$

✂ Please refer to the manuscript for the detailed information of parameters



[4] W. Qin et al., "Intergranular  $\delta$ -hydride nucleation and orientation in zirconium alloys," Acta Mater. **59** 18, 7010, Acta Materialia Inc. (2011)

[5] W. Qin et al., "Hydride-induced degradation of hoop ductility in textured zirconium-alloy tubes: A theoretical analysis," Acta Mater. **60** 12, 4845, Acta Materialia Inc. (2012)

# Key assumptions on mi

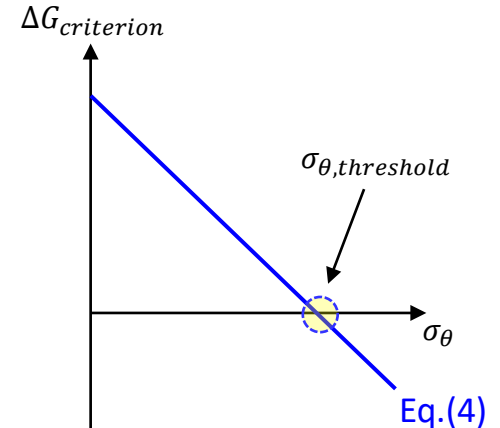
- **Low accuracy of thermodynamic model to predict threshold for hydride reorientation**

- Threshold hoop stress (Qin's thermodynamic model)

$$\Delta G_{\text{criterion}} = -\Delta G_{\text{chem}} - \left(\frac{x}{\bar{v}_{\text{hyd}}}\right) \left(\frac{\sigma_{\theta} \cos \phi}{3}\right) \bar{v}_H - \sigma_{\theta} \cos \phi \chi + \Delta G_{\text{strain}} < 0 \quad \text{Eq. (4)}$$

$$\Delta G_{\text{strain}} = \frac{6\mu\gamma\eta\chi^2}{\eta(\gamma-1)+1} \quad \text{Eq. (5)}$$

$$\sigma_{\theta, \text{threshold}} = \frac{-\Delta G_{\text{chem}} + \Delta G_{\text{strain}}}{\left(\frac{x}{\bar{v}_{\text{hyd}}}\right) \left(\frac{\cos \phi \bar{v}_H}{3}\right) + \cos \phi \chi} \quad \text{Eq. (6)}$$



- Assumptions of the model and overestimation

Assumptions

① Only  $\{10\bar{1}0\}_{\alpha} // \{111\}_{\delta}$  Zr-hydride interface

Maximum  $\chi$  and  $\Delta G_{\text{strain}}$

② Ideal Zr texture (100% radial basal pole)

$\phi : n_{\text{hydride}} \angle \sigma_{\theta}$

$\cos \phi = \cos 0^{\circ} = 1$

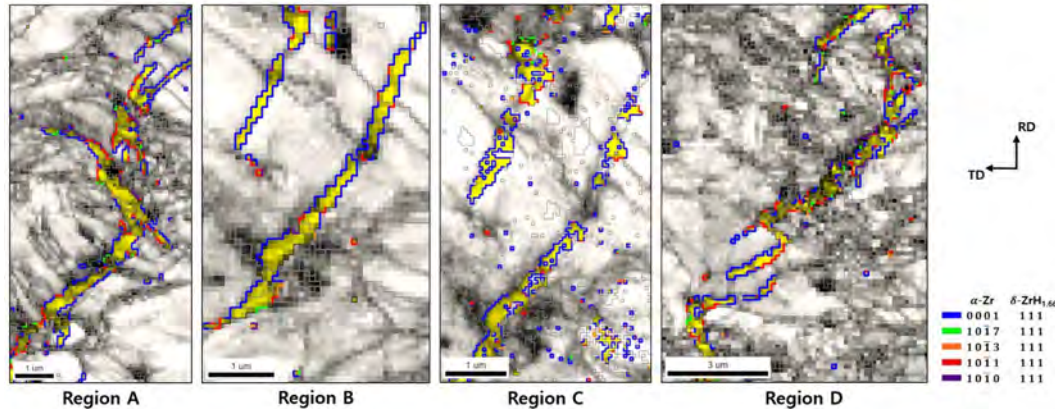
✓ The theoretically predicted threshold hoop stress was **1880 MPa**. (vs. 90 MPa of U.S. NRC)

[4] W. Qin et al., "Intergranular  $\delta$ -hydride nucleation and orientation in zirconium alloys," Acta Mater. **59** 18, 7010, Acta Materialia Inc. (2011)

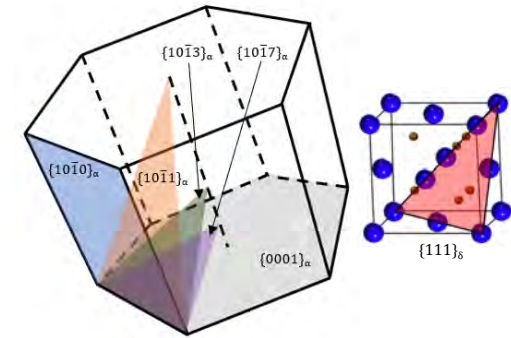
[5] W. Qin et al., "Hydride-induced degradation of hoop ductility in textured zirconium-alloy tubes: A theoretical analysis," Acta Mater. **60** 12, 4845, Acta Materialia Inc. (2012)

# EBSD Analysis of Microstructure – ORs

- Average fraction of 5 orientation relationships analyzed by EBSD (20 regions)



Phase map of radial hydrides (Zircaloy-4, ~458 wppm H, hoop stress 122 MPa)



Orientation relationships of hydride

Orientation Relationship	Plane relationship angle ( $\psi$ )	Angle between hydride plane and hoop stress ( $\phi$ )	Misfit strain ( $\chi$ )	Strain energy ( $\Delta G_{strain}$ )	Average fraction ( $\pm$ standard deviation)
① $\{0001\}_\alpha // \{111\}_\delta$	$\psi_1 = 0^\circ$ (0001) $\angle$ (0001)	$\phi_1 = 47.3^\circ$	0.0520	$2.951 \times 10^8 \text{ J/m}^3$	49.51 % ( $\pm 0.98$ )
② $\{10\bar{1}7\}_\alpha // \{111\}_\delta$	$\psi_2 = 14.7^\circ$ (0001) $\angle$ (10 $\bar{1}$ 7)	$\phi_2 = 32.6^\circ$	0.0537	$3.143 \times 10^8 \text{ J/m}^3$	4.39 % ( $\pm 0.55$ )
③ $\{10\bar{1}3\}_\alpha // \{111\}_\delta$	$\psi_3 = 31.6^\circ$ (0001) $\angle$ (10 $\bar{1}$ 3)	$\phi_3 = 15.7^\circ$	0.0590	$3.801 \times 10^8 \text{ J/m}^3$	4.81 % ( $\pm 1.00$ )
④ $\{10\bar{1}1\}_\alpha // \{111\}_\delta$	$\psi_4 = 61.5^\circ$ (0001) $\angle$ (10 $\bar{1}$ 1)	$\phi_4 = 14.2^\circ$	0.0717	$5.607 \times 10^8 \text{ J/m}^3$	36.73 % ( $\pm 0.28$ )
⑤ $\{10\bar{1}0\}_\alpha // \{111\}_\delta$	$\psi_5 = 90^\circ$ (0001) $\angle$ (10 $\bar{1}$ 0)	$\phi_5 = 24.7^\circ$	0.0775	$6.541 \times 10^8 \text{ J/m}^3$	4.57 % ( $\pm 0.86$ )

$$\Delta G_{strain} = \frac{6\mu\gamma\eta\chi^2}{\eta(\gamma-1)+1} \text{ ---- Eq. (5)}$$

$$\sigma_{\theta,threshold} = \frac{-\Delta G_{chem} + \Delta G_{strain}}{\left(\frac{x}{\bar{v}_{hyd}}\right)\left(\frac{\cos\phi\bar{v}_H}{3}\right) + \cos\phi\chi} \text{ ---- Eq. (6)}$$

- Fraction-weighted  $\phi$ ,  $\chi$ ,  $\Delta G_{strain}$  in real specimen :  $\bar{\phi}$ ,  $\bar{\chi}$ ,  $\bar{\Delta G}_{strain}$

$$\Rightarrow \bar{\phi} = 32.8^\circ \quad \Rightarrow \bar{\chi} = 0.06082 \quad \Rightarrow \bar{\Delta G}_{strain} = 4.1402 \times 10^8 \text{ J/m}^3$$



# Model of Radial Hydride Formation

- **Aggregation of two formation cases (Combinations of texture and two dominant ORs)**

(a) Combination of circumferential basal pole and  $\{0001\}_\alpha // \{111\}_\delta$  orientation relationship : Energetically favorable

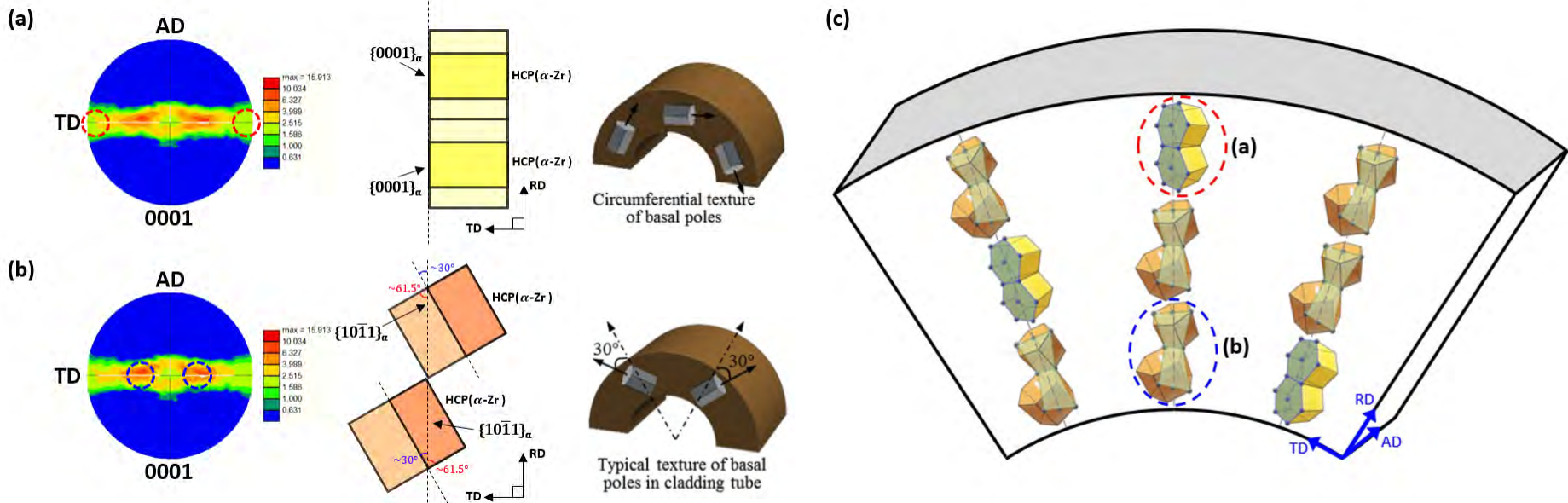
\* Lowest strain energy

(b) Combination of  $30^\circ$  basal pole and  $\{10\bar{1}1\}_\alpha // \{111\}_\delta$  orientation relationship : Statistically favorable

\* Highest angle intensity

\* Plane relationship angle  $(0001) \angle (10\bar{1}1) : \psi_4 = 61.5^\circ$

(c) Typical macroscopic radial hydrides formed by hoop stresses close to the threshold are formed upon an aggregation of two cases in mesoscale.



Schematic illustration of radial hydride formation

# Advancing prediction accuracy with directly measured

- Modified Qin's thermodynamic model

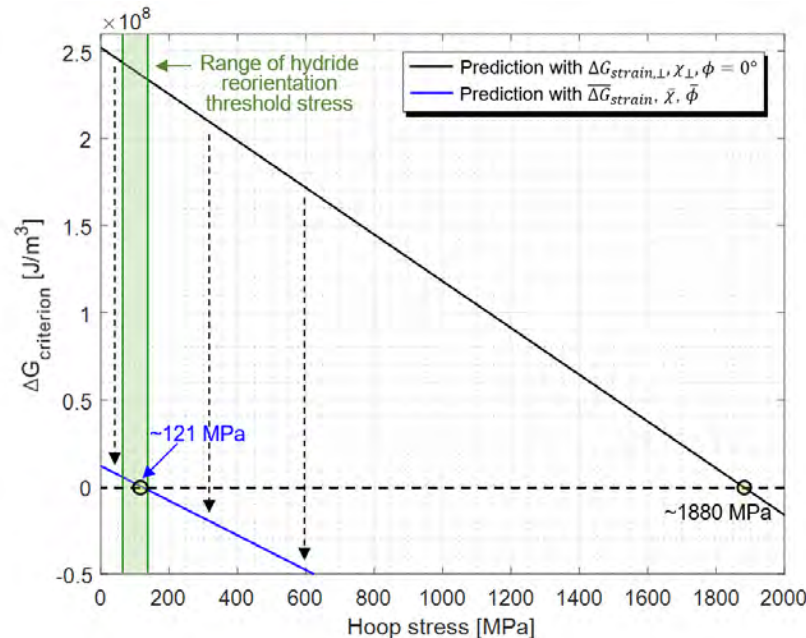
$$\sigma_{\theta,threshold} = \frac{-\Delta G_{chem} + \Delta G_{strain}}{\left(\frac{x}{\bar{v}_{hyd}}\right) \left(\frac{\cos\phi \bar{v}_H}{3}\right) + \cos\phi \chi} \quad \text{Eq. (6)}$$

$$\Downarrow \quad \phi, \chi, \Delta G_{strain} \Rightarrow \bar{\phi}, \bar{\chi}, \bar{\Delta G}_{strain}$$

$$\sigma_{\theta,threshold} = \frac{-\Delta G_{chem} + \bar{\Delta G}_{strain}}{\left(\frac{x}{\bar{v}_{hyd}}\right) \left(\frac{\cos\bar{\phi} \bar{v}_H}{3}\right) + \cos\bar{\phi} \bar{\chi}} \quad \text{Eq. (9)}$$

- Advance of accuracy in prediction for hydride reorientation threshold hoop stress

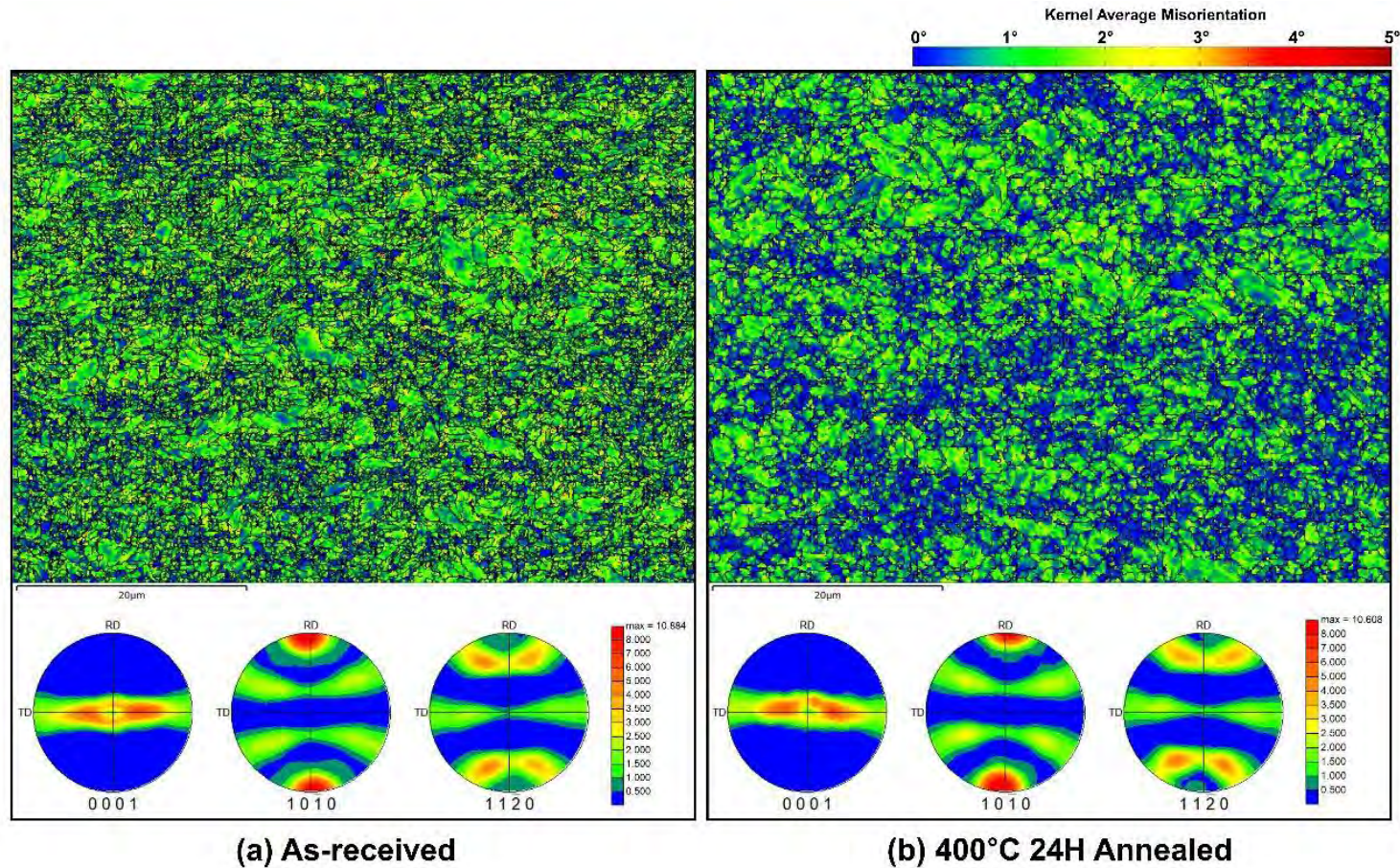
$$\sigma_{\theta,threshold} = 1880 \text{ MPa with Eq. (6)} \quad \Rightarrow \quad \sigma_{\theta,threshold} = 121 \text{ MPa with Eq. (9)}$$



[D. Kim, J. Kang, Y. Lee, Materialia 21 (2022) 101291]

Advanced prediction of threshold hoop stress for hydride reorientation

# Revisiting effect of vacuum drying temperature on microstructure

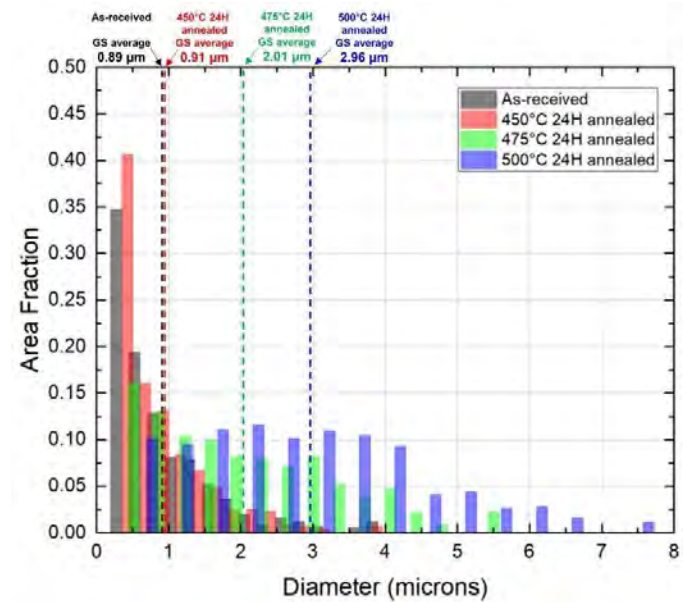
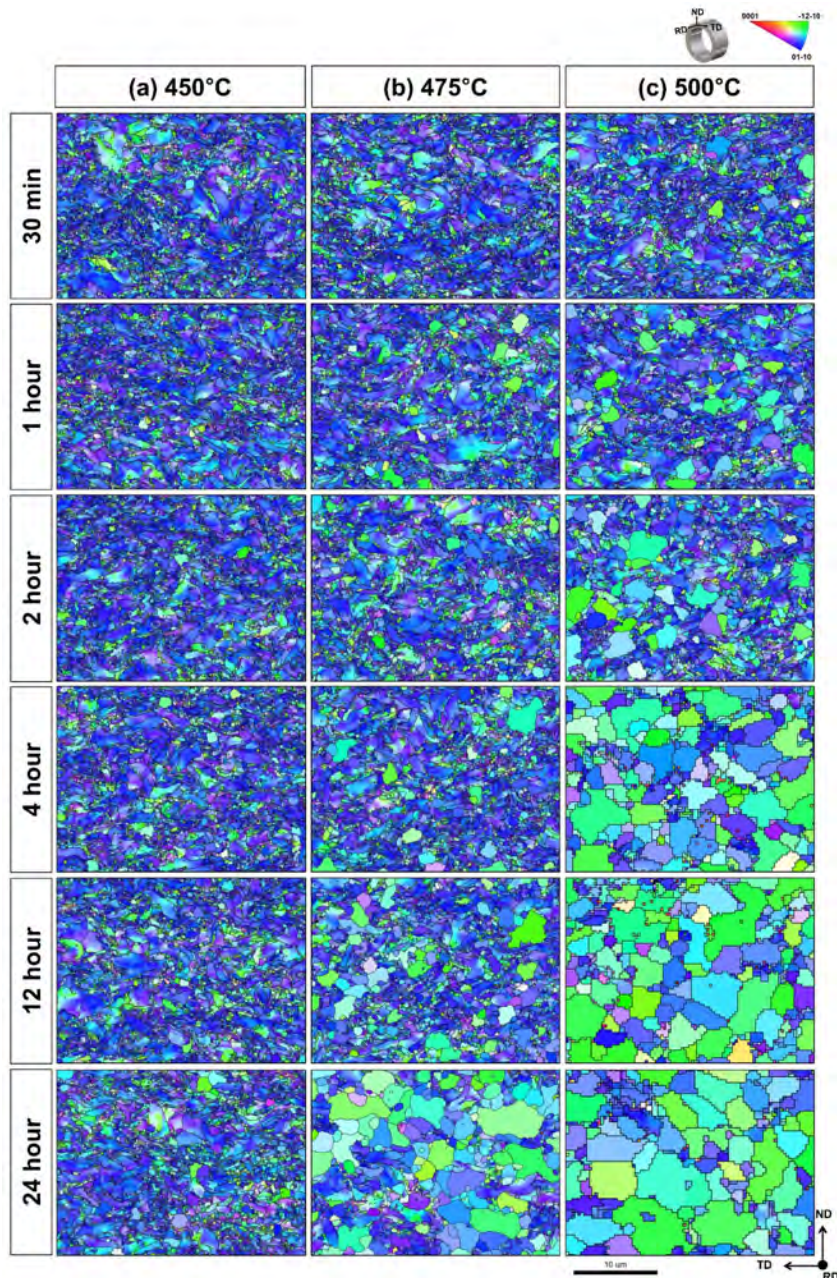


**<Kernel Average Misorientation map (400°C annealing),  
Reactor-grade SRA Zirlo>**

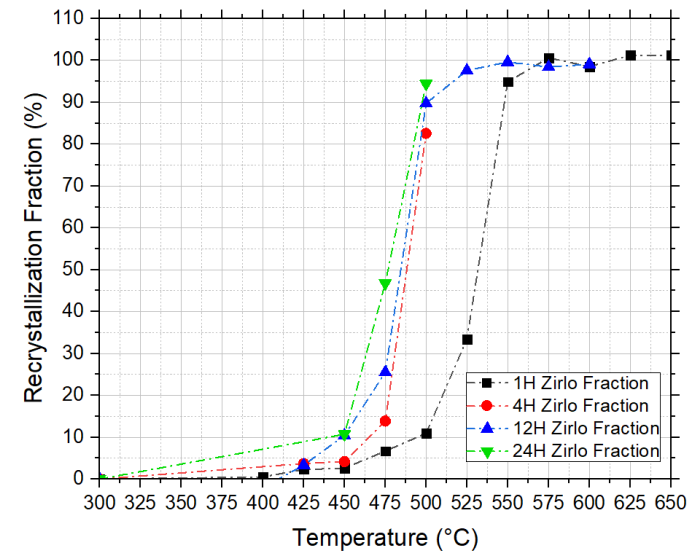
- Recovery of high angle grain boundary was observed without a sufficient change in texture.



# EBSD characterization of annealed texture



<Grain size distribution resulted by various annealing>

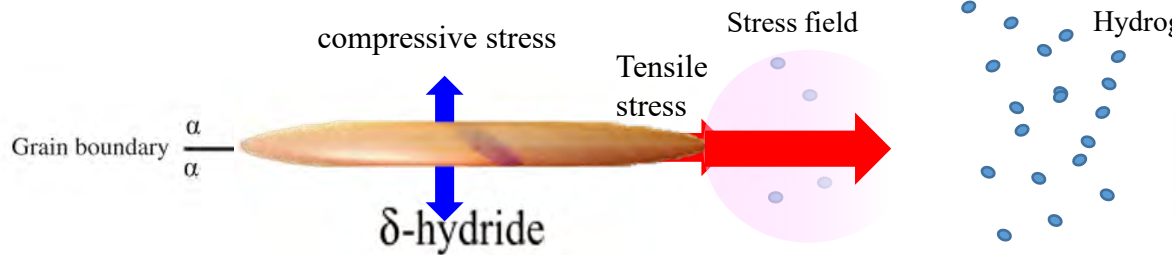


<Recrystallization fraction obtained by hardness measurement> 24

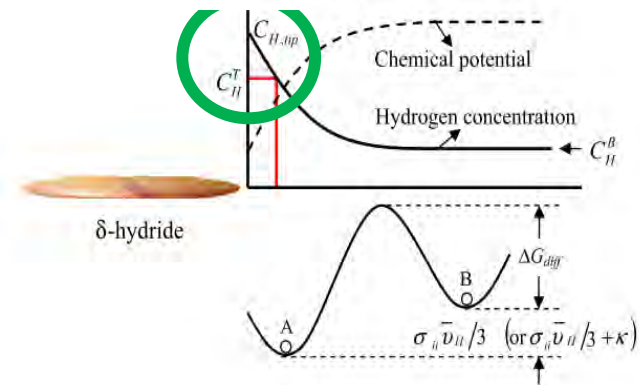
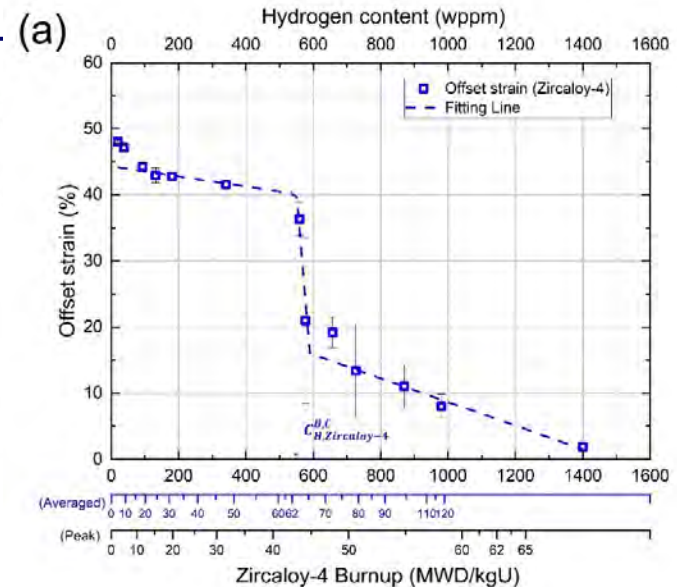


# Hydride Precipitation Thermodynamics and Interlinked-hydride network

## Hydride network theory (by Qin et al. Acta Materialia)



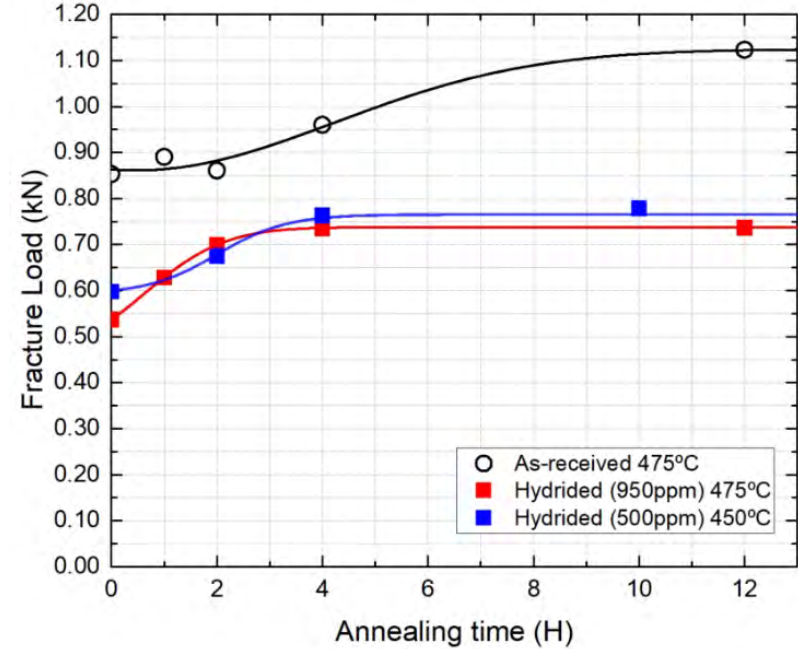
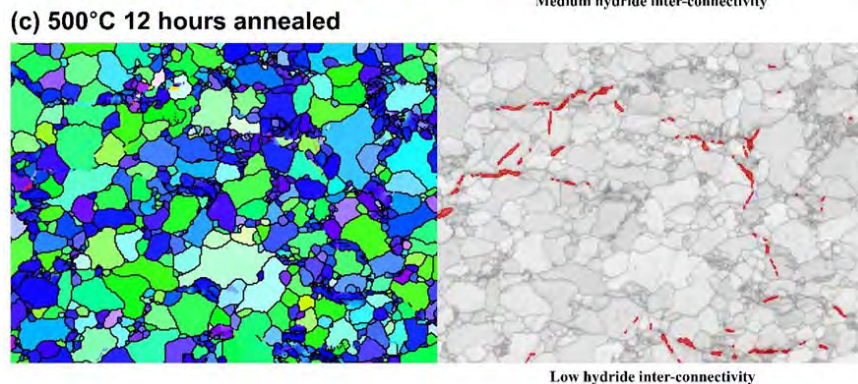
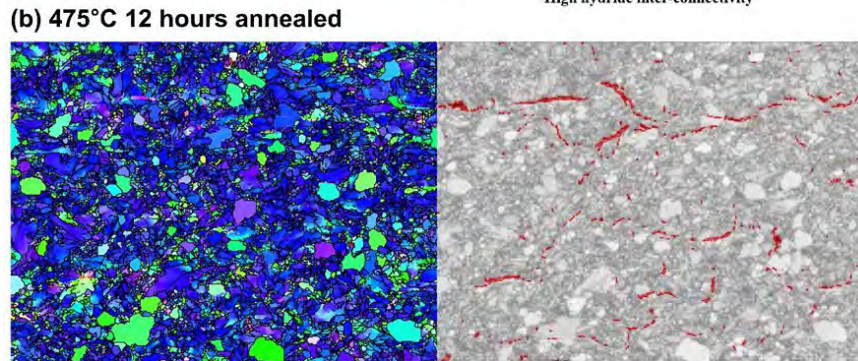
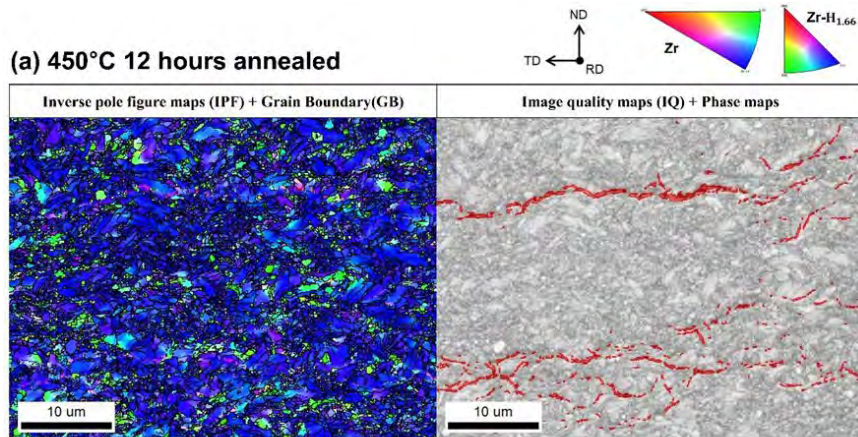
- 1) **Tensile stress lowering the chemical potential of ahead of hydride tip**
- 2) Hydrogen atoms with **higher chemical potential diffuses to the region near the tip** (low potential area), hydrogen accumulation.
- 3) **When  $C_{H,Tip} > C_H^T$  condition satisfies,** the hydride formation ahead of the tip of a pre-existing hydride kicks in
- 4) Hydride growth, **interlinked-hydride network generated**



Chemical potential and hydrogen concentration around the hydride tip

$C_H^T$  the hydrogen terminal solid solubility  
 $C_H^B$  the hydrogen concentration away from the tip and boundaries

# Grainsize-sensitive hydride connectivity and resulting mechanical strength

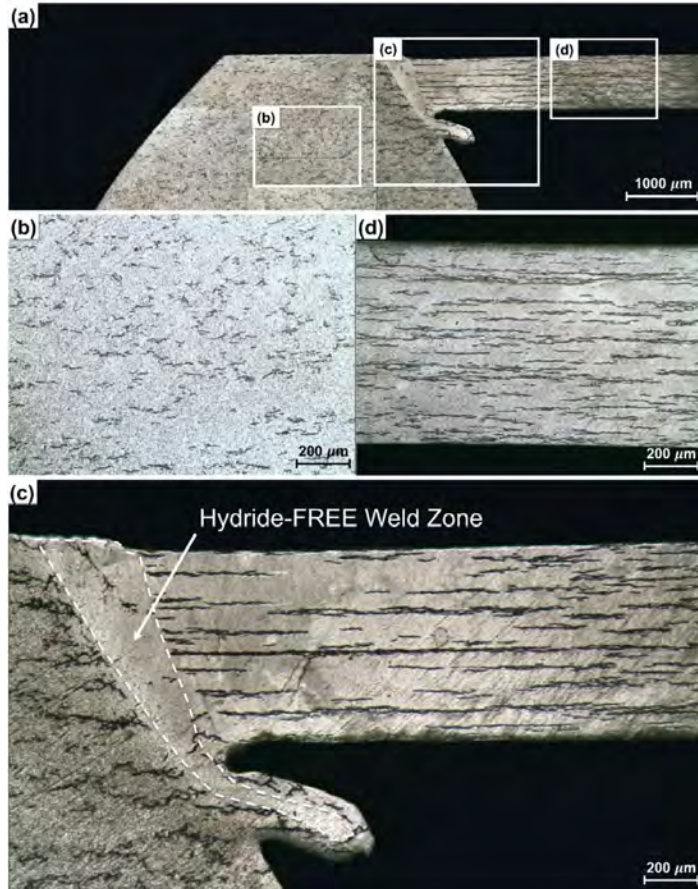


< Fracture load of As-re and hydride specimens resulted by annealing >

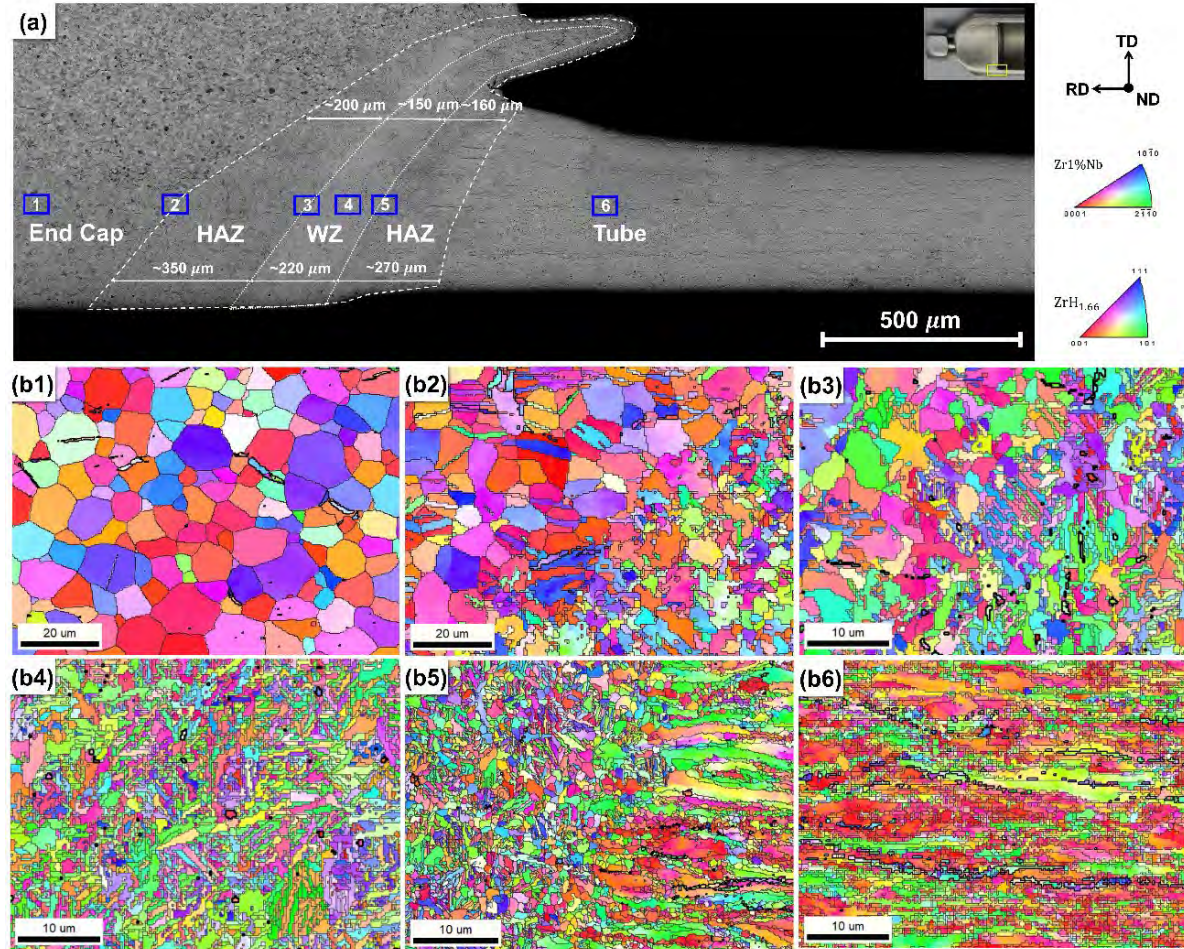
- Annealing (450°C and 475°C) resulted in mechanical strength increase.
- It is due to ① favorable effect of matrix annealing (i.e., recovery of high angle grain boundaries) and ② reduced connectivity of hydrides.
- It beckons the possibility of increasing the vacuum annealing temperature above 400°C.



# Suppressed hydride precipitation in welding zone



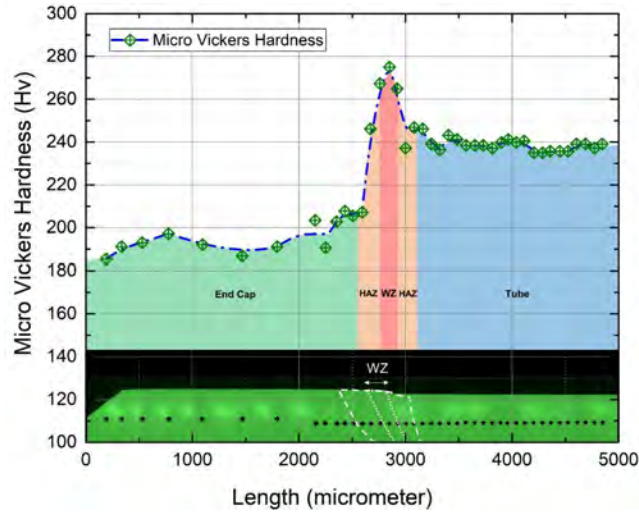
<Hydride free-zone in WZ>



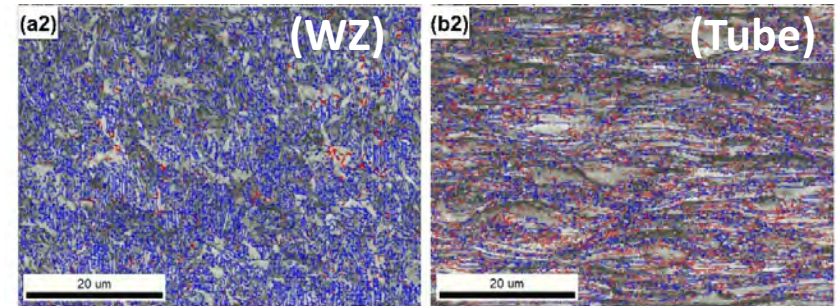
<EBSD characterization>



# Suppressed hydride precipitation in welding zone

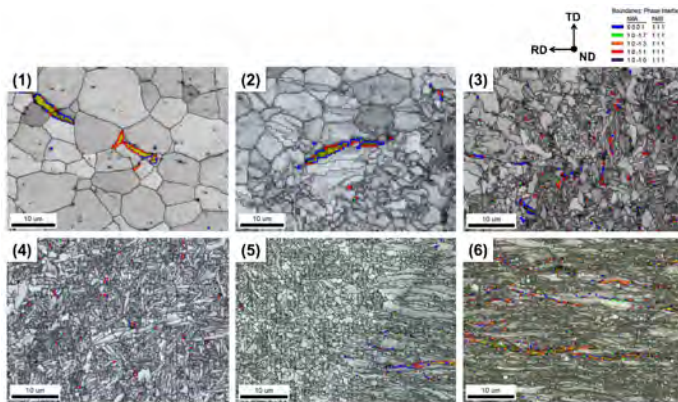


High matrix stiffness in WZ



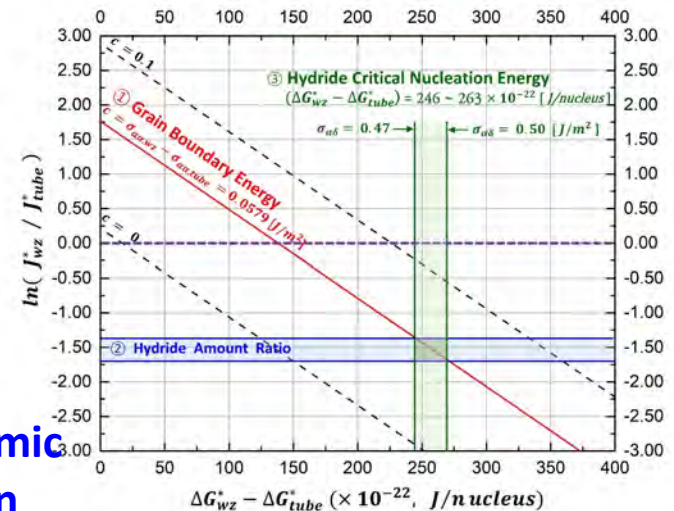
- Grain boundaries (GB), misorientation angles ( $\theta$ )  $\geq 5^\circ$
- Low-angle grain boundaries (LAGB),  $5^\circ < \theta < 15^\circ$
- High-angle grain boundaries (HAGB),  $15^\circ \leq \theta$

Higher grain boundary angle in WZ



Increase misfit strain in WZ

Thermodynamic interpretation

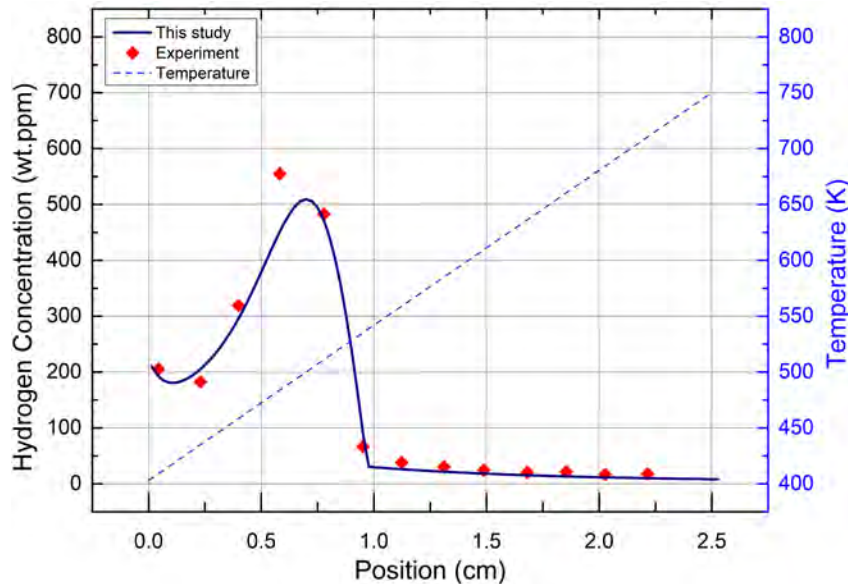


- **Increased resistance of hydride embrittlement in WZ:** Suppressed hydride precipitation in WZ is caused primarily by the combined effects of higher critical nucleation Gibbs free energy of WZ ( $\Delta G_{WZ}^*$ ) due to greater matrix stiffness, and increased misfit strain that outweighs favorable precipitation mechanism resulted by greater grain boundary misorientation angle.

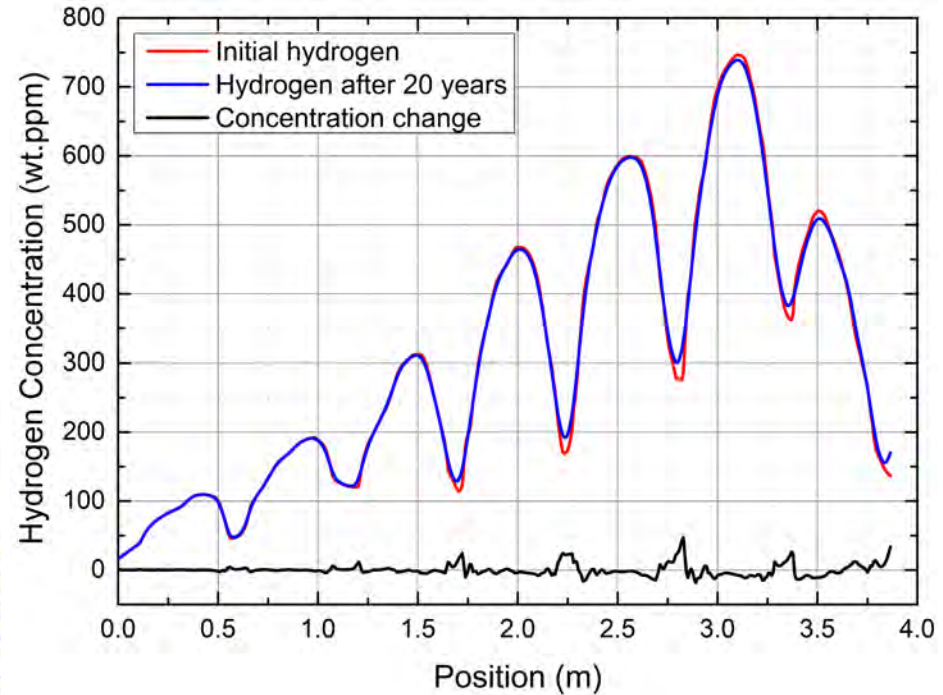
# Hydride migration simulation for a full-length fuel rod in dry storage

$$\frac{\partial C_{ss}}{\partial t} = -\nabla(J_{\text{Fick}} + J_{\text{Soret}}) = -\nabla\left(-D\nabla C_{ss} - \frac{Q^*DC_{ss}}{RT^2}\nabla T\right)$$

+ mHNGD model for hydride phase change kinetics by Penn State and INL



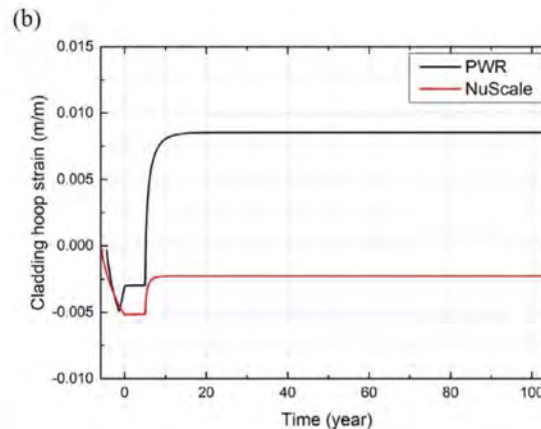
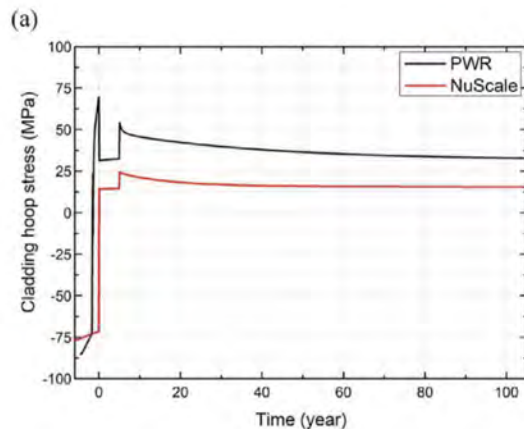
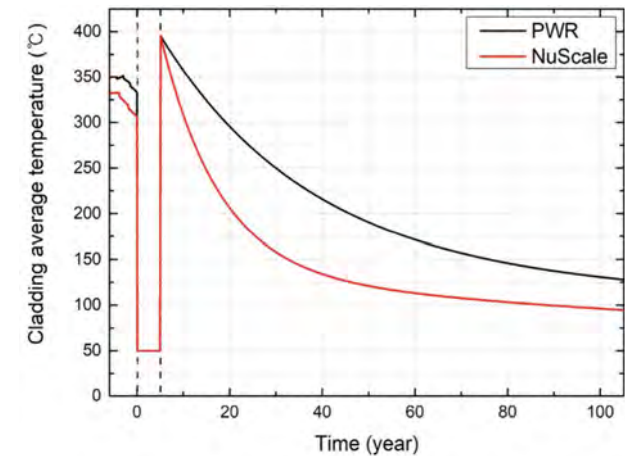
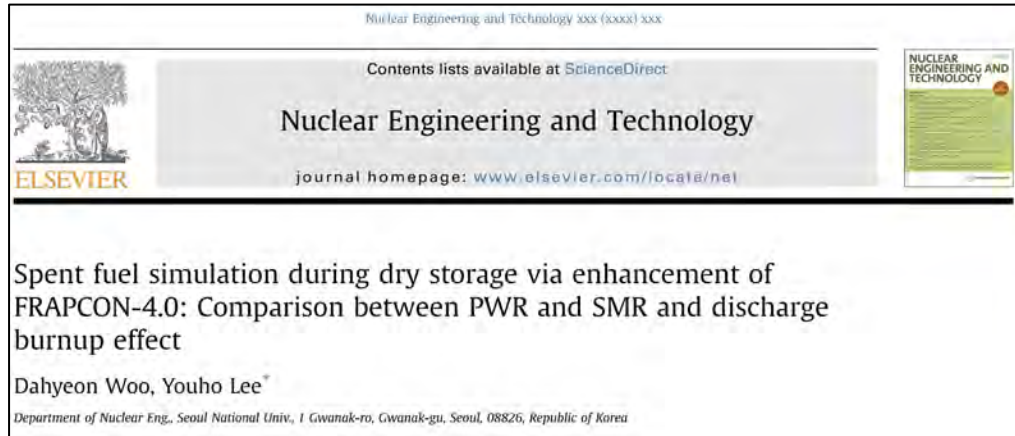
<Validation of the SNU code with Sawatzky's experiment>



Hydrogen concentration of initial and dry storage after 20 years, simulated with a burnup of 50 MWd/kg and initial PCT of 394 °C spent fuel, equal with discharge time after 3.4 years. A small amount of hydrogen migrates from peaks to the spacer grid region and the upper end.



# Spent fuel simulation via modifying FRAPCON-4.0



## FRAPCON-4.0 modified for spent fuel simulation

- Dry storage pellet swelling
  - Dry storage cladding creep (EDF Creep correlation)
  - Dry storage temperature distribution
  - Hydrogen transport model (mHNGD model newly incorporated)
- **Simulation of spent fuel in a continuous manner from the steady-state operation**
  - The increased safety margin of SMRs may be tradable with economic benefits by allowing a larger dry storage cask. It may compensate for the apparently high spent fuel management cost of low burnup SMRs



### **3. Conclusion: key findings**

# Conclusion: key findings 1

---

## ■ Image analysis for mechanical integrity of hydrided Zircaloy

- PROPHET, employing Dijkstra's algorithm, is a software that enables the image analysis of hydrided Zircaloy, and is open to public at <http://fuel.snu.ac.kr>.
- Radial Hydride Fraction (RHF) is a powerful metric for the strength of Zircaloy for  $RHF > 5\%$ . For  $RHF < 5\%$ , strength of the Zircaloy is strongly correlated to hydrogen concentration. Maximum radial hydride length is an alternative, yet effective, metric that can capture the strength of hydrided Zircaloy.
- $RHF < 5\%$  has limited influence on material strength, implying that safety criteria based on the onset of radial hydride precipitation can be conservative (we may be able to allow small amount of RHF if DHC is OK !)
- Our fuel code study shows that radial hydride reorientation is improbable to occur at the current discharge burnup level.
- Circumferential hydrides can play a role in blocking the radial crack shortcut, thereby increasing structural integrity in the presence of radial hydrides.
- It may imply that the low burnup fuels can be more prone to fracture with radial hydride reorientation in comparison with high burnup.

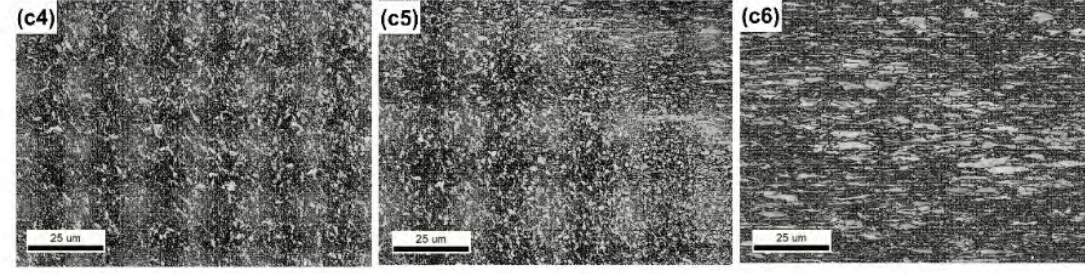
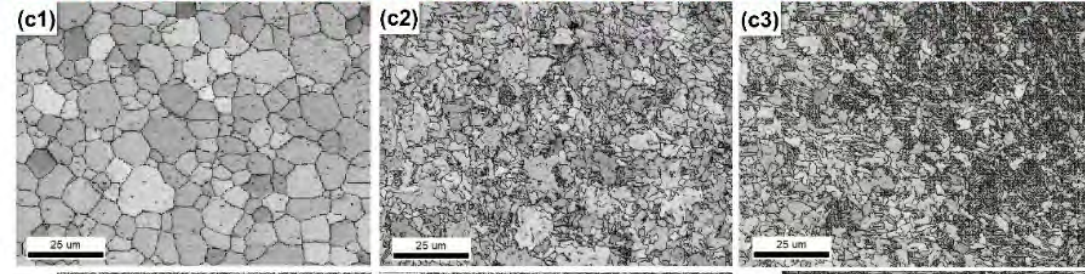
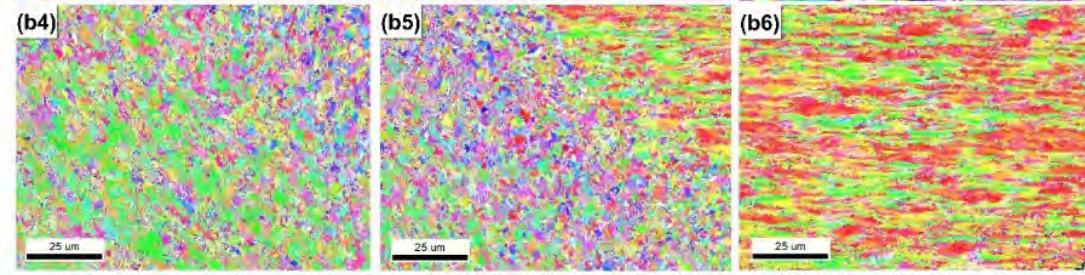
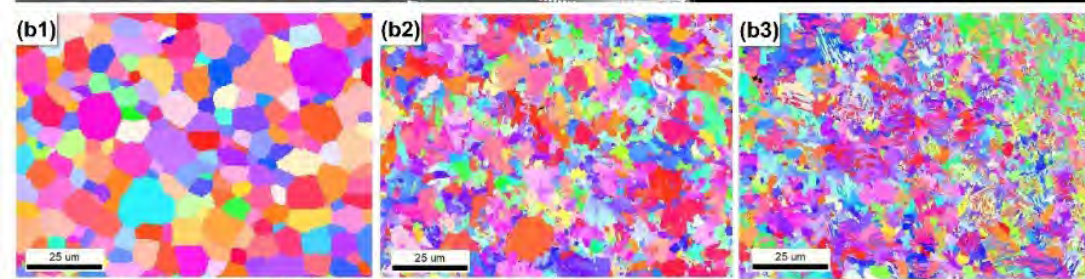
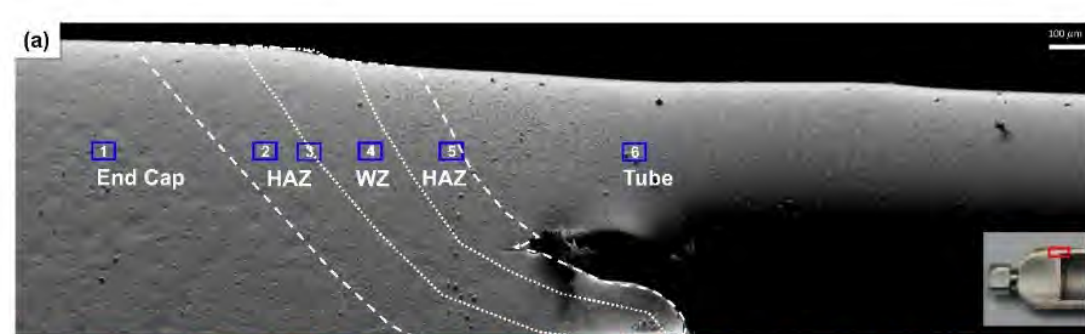
# Conclusion: key findings 2

---

## ■ Microstructural effect for hydride embrittlement

- Using the directly measured orientation relationships and texture information of hydride Zircaloy via EBSD, the accuracy of the thermodynamic model for hydride reorientation significantly improved.
- Recovery of high angle grain boundary without grain growth was observed during annealing at 400°C.
- Vacuum drying process in 400°C - 500°C helps increase structural integrity of hydride Zircaloy. It may beckon the possibility of increasing the vacuum annealing temperature limit above 400°C. A higher PCT limit may allow a larger dry storage.
- However, annealing above 400°C is known to cause radiation damage annealing, adversely increasing creep deformation in dry storage. Hence, a careful tradeoff analysis is needed.
- Hydride precipitation is suppressed in WZ, indicating increased resistance of hydride embrittlement. Suppressed hydride precipitation in WZ is caused primarily by the combined effects of higher critical nucleation Gibbs free energy of WZ due to greater matrix stiffness, increased misfit strain, and greater grain boundary misorientation angle.





<Monet>



Thank you





**A.W. Colldewei**

**Paul Scherrer Institut**

## **Use of advanced imaging methods for characterizing hydrogen related cladding degradation**

Hydrogen uptake in zirconium alloys is a major limiting factor of nuclear fuel cladding as subsequent hydride precipitation can lead to potential cladding failure via cladding embrittlement or delayed hydride cracking (DHC). The specific mechanisms of cladding embrittlement and DHC have been a focus in earlier research, however there is still no clear definition of the resulting crystallography and limiting hydride sizes at various temperatures of crack propagation. In this work, a novel thermo-mechanical testing procedure was used to induce radially propagating DHC cracks in thin-walled cladding in a temperature range from 100°C to 410°C. Additionally, three-point bending, micro- and nano-indentation has been used to study the hydrogen enhanced localized plasticity (HELP) effect, where thermo-mechanical loading has been used to study the hydride reorientation in irradiated material. Focused ion beam (FIB)- prepared lamellae were extracted from samples containing the arrested DHC crack for synchrotron micro-beam X-ray diffraction (XRD) mapping of crystallographic phases.

High-resolution neutron imaging,  $\mu$ XRD, and metallography have been used to investigate hydrogen concentrations, hydride phases, and reorientation. In neutron imaging and metallography, irradiation damage appears to impact hydrogen diffusion, where diffusion seems reduced in irradiated material when compared to unirradiated material. Additionally, hydrogen concentrations in the oxide layer have been investigated in irradiated material. Hydrogen quantification around arrested DHC crack tips shows the trend of hydride diffusion during DHC with respect to temperature, and unveils the influence of the liner on source-hydrogen for DHC. The  $\mu$ XRD phase maps provided information about the required hydride cluster size that would lead to fracture (less than 5  $\mu$ m), i.e. the critical hydride size. Phase mapping shows that DHC-responsible hydrides primarily consist of the  $\delta$  phase, with slightly increased  $\gamma/\delta$  ratios at lower cracking temperatures. In multilayer cladding, the liner material shows significantly increased ratios of  $\gamma$ -hydride, while on average, the  $\delta$ -phase remains predominant. This work also highlights that the  $\gamma$ -hydride is indeed a stable zirconium hydride phase, which can precipitate during DHC propagation and within the inner liner of multilayer cladding. Finally, HELP testing shows that the most pronounced decrease in the yield stress occurs around 300°C in material containing 100 wppm H, where all hydrogen occurs in the solid solution form.

PAUL SCHERRER INSTITUT



QUENCH Programme



**Aaron W. Colldewei**<sup>1</sup>, Francesco Fagnoni<sup>1</sup>, Okan Yetik<sup>1,2</sup>, Robert Zubler<sup>1</sup>, Pavel Trtik<sup>2</sup>, Manuel A. Pouchon<sup>1</sup>, Yong Dai<sup>1</sup>, Liliana I. Duarte<sup>1</sup>, Malgorzata Makowska<sup>1</sup>, Johannes Bertsch<sup>1</sup>

<sup>1</sup>Laboratory for Nuclear Materials (LNM), Paul Scherrer Institut

<sup>2</sup>Laboratory for Neutron Scattering (LNS), Paul Scherrer Institut

# Use of advanced imaging methods for characterizing hydrogen related cladding degradation

September 29<sup>th</sup>, 2022

# Introduction

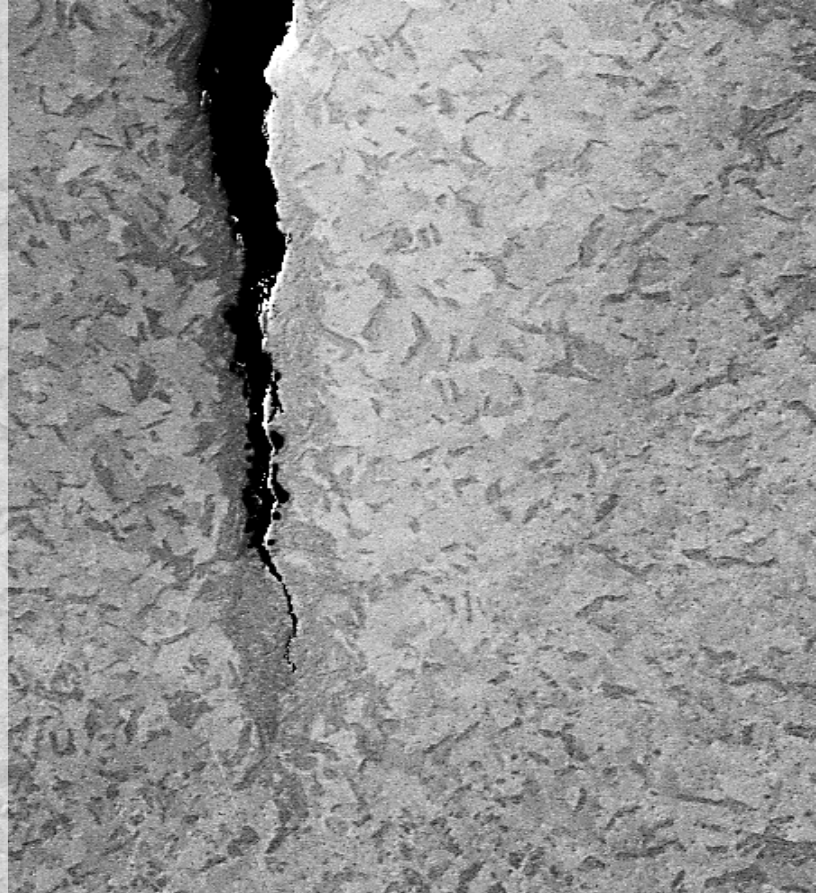
Materials and Tests

n-radiography

Phase Mapping

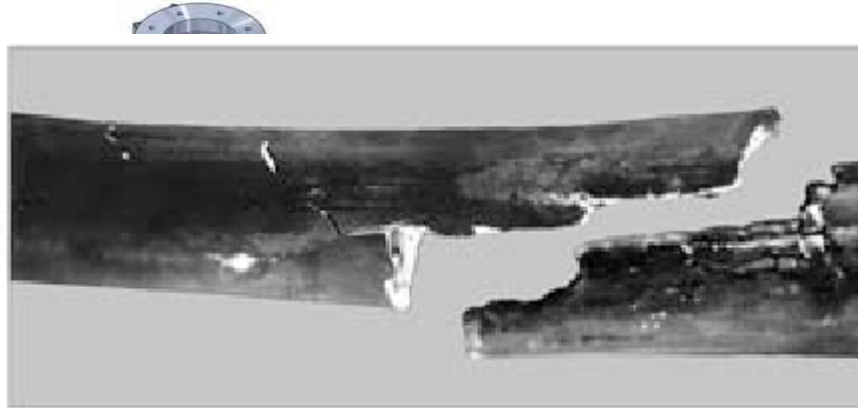
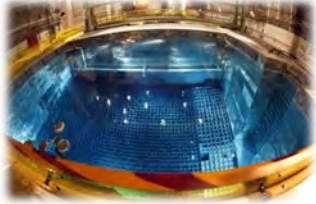
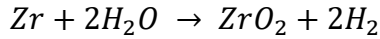
HELP Testing

Conclusions



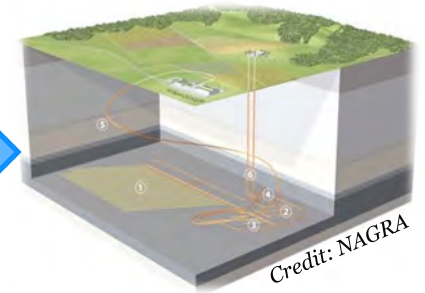


## What is the primary context of hydrogen degradation ? *Transportation and dry storage of SNF*



*Credit: Markov, D., et. al.*

*TN24 cask produced by Orano TN*



Introduction

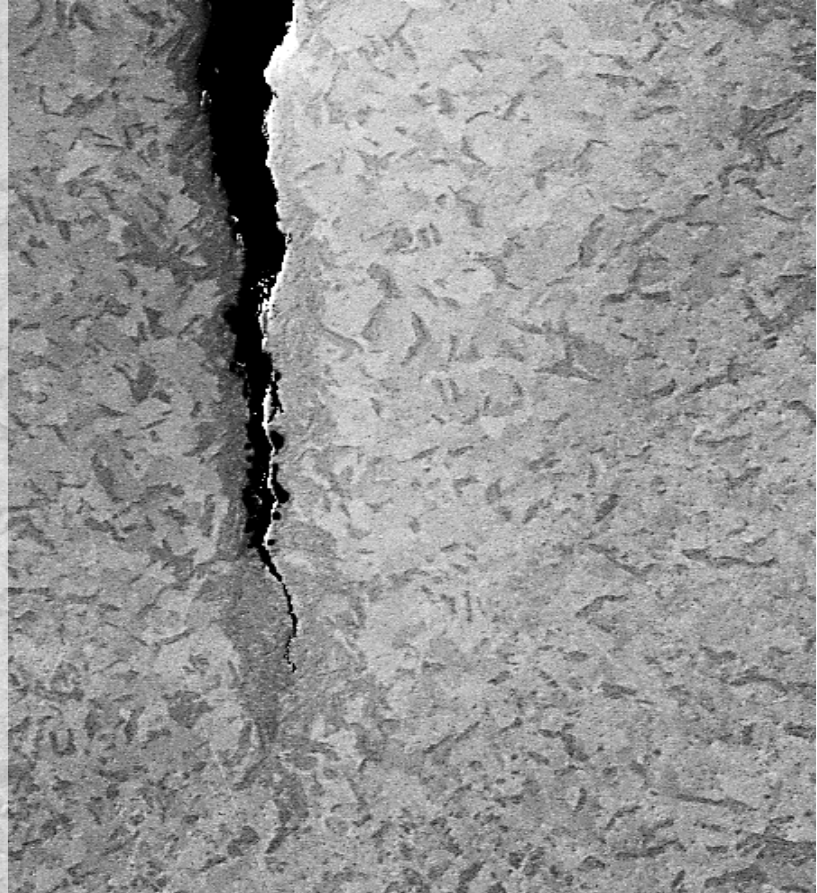
# Materials and Tests

n-radiography

Phase Mapping

HELP Testing

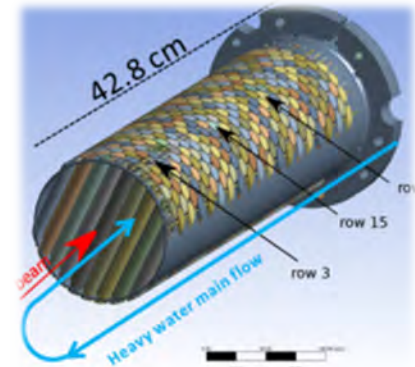
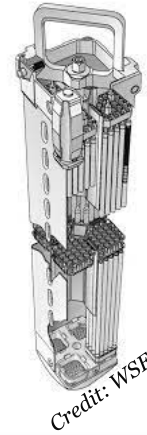
Conclusions



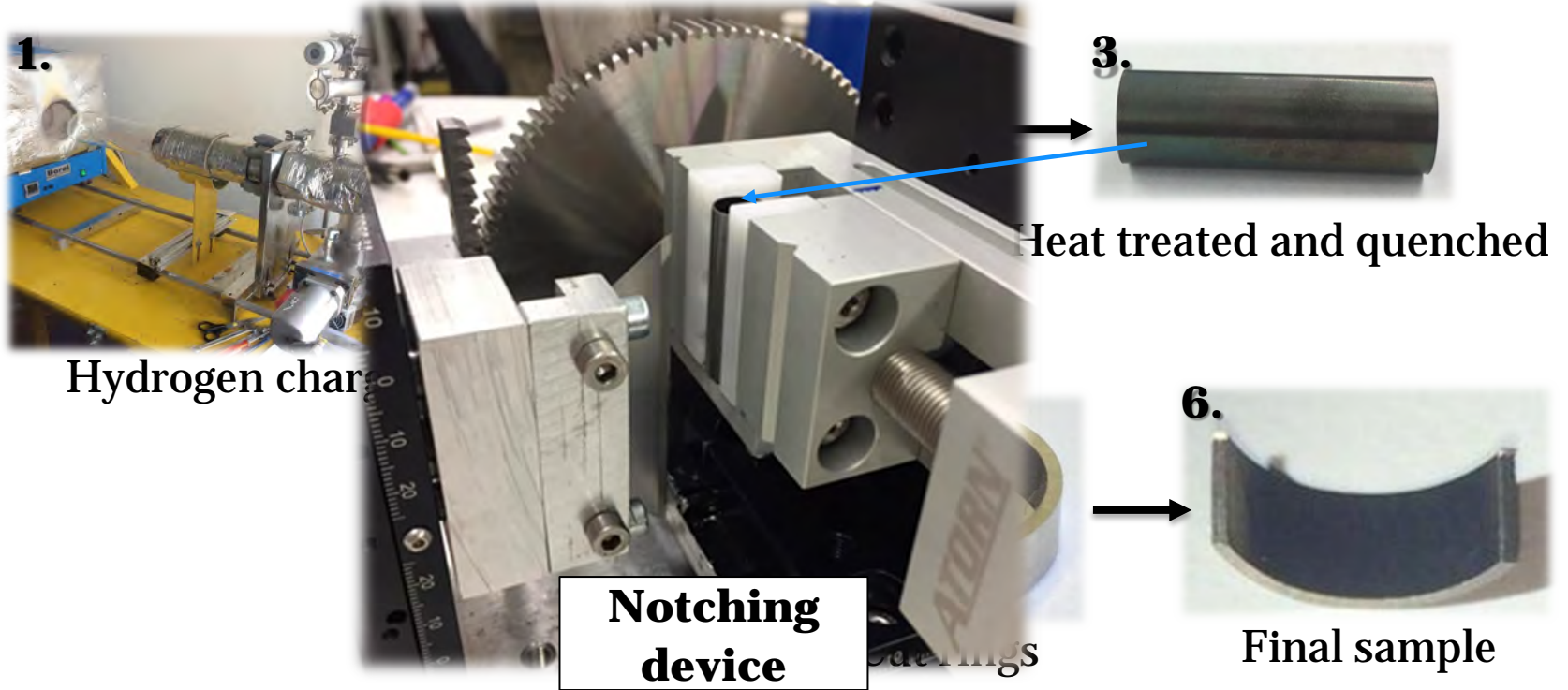
## *Irradiated* and *Unirradiated* Zircaloy-2

Materials	Hydrogen concentration	Rod Av. / Peak Burn-up or dpa
	(wppm H)	
LK3	98 – 328	-
LK3/L	139 - 381	-
LK3/L*	116	57.5 / 65.7 [MWd/kgU]
SINQ Target Rod	401	-
SINQ Target Rod (P0/P1/P19)**	70 / 113 / 143	~25 dpa / 18 dpa / 9.5 dpa
LTP	~200	-
LTP2	~200	-
DXD4	~200	-
DXD4	441	70 [MWd/kgU]
Zry-4	400	60 [MWd/kgU]

\*Irradiated in KKL/KKG \*\*Irradiated in SINQ



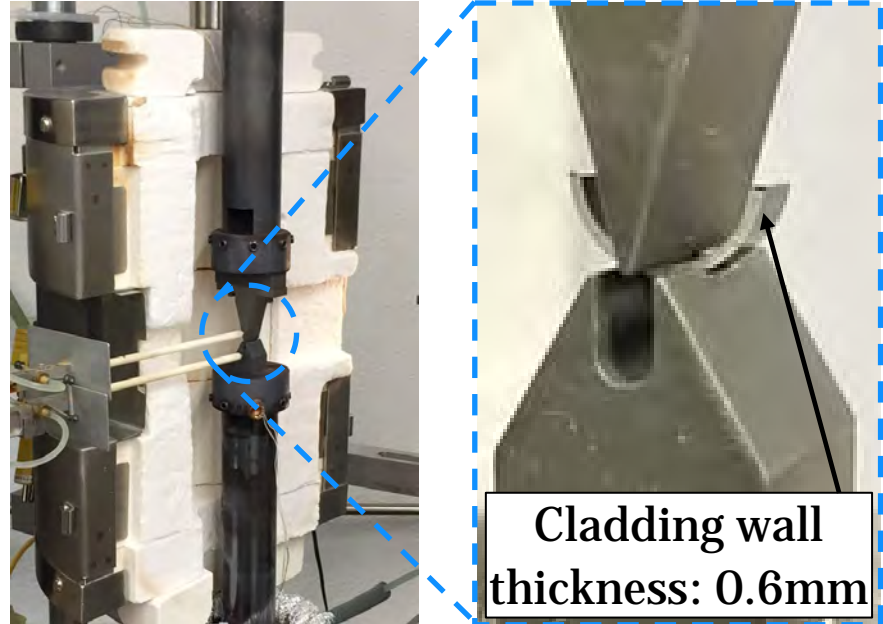
## Sample preparation of unirradiated material





## Three-point bending test

- The most realistic form of crack propagation in a tube, i.e. **outside-in and radially** (as seen in ramp and burst tests)
- Lack of literature data on **radial cracks in fuel cladding**



**Introduction**

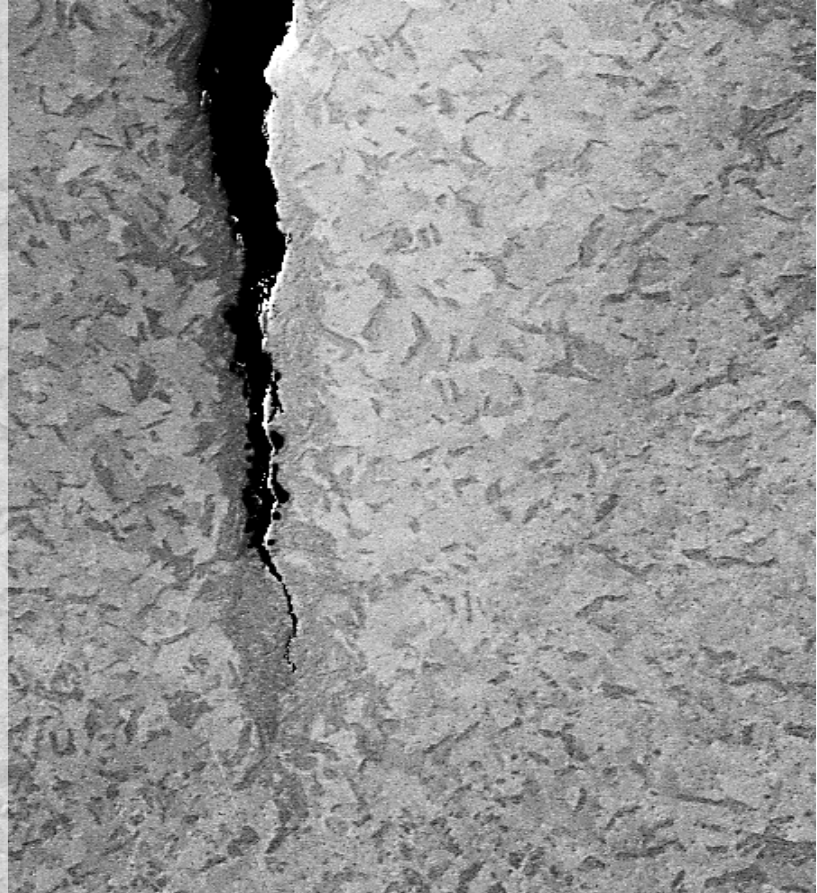
**Materials and Tests**

**n-radiography**

**Phase Mapping**

**HELP Testing**

**Conclusions**



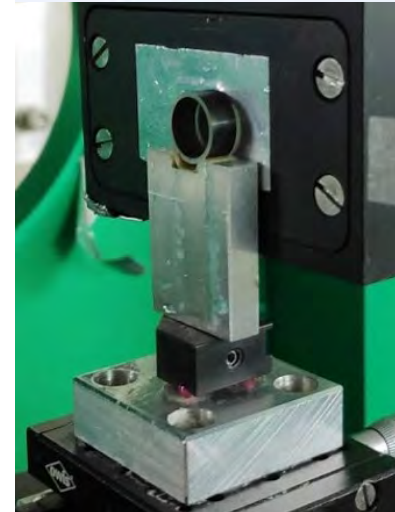
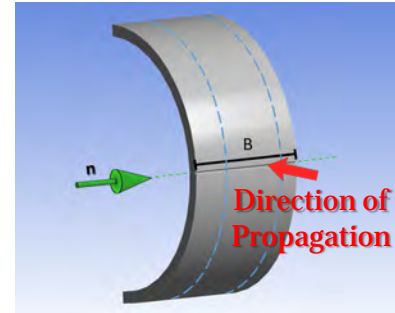
## Objective

Understand the diffusion and precipitation of hydrogen in irradiated material and around the DHC crack tip under various conditions (different hydrogen concentrations, temperature, liner material, irradiated material).

## Importance

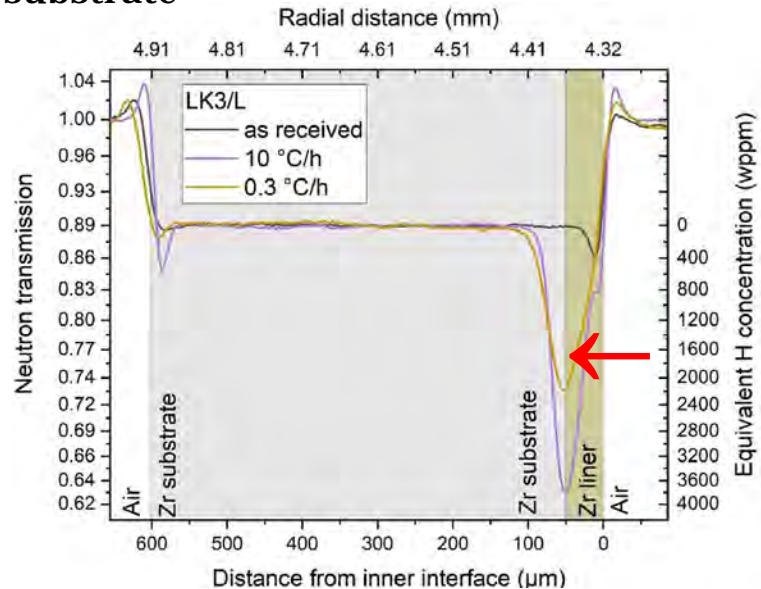
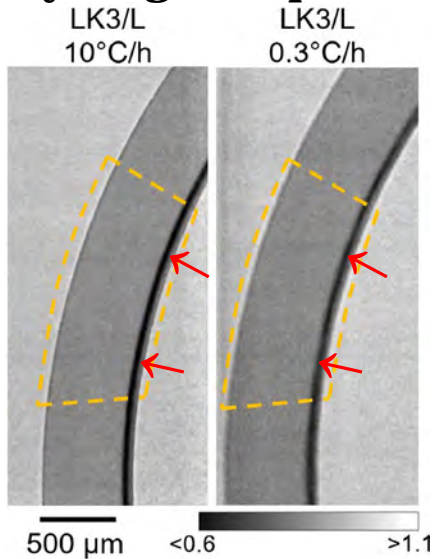
Fundamental understanding of hydrogen diffusion and precipitation can influence how hydrogen diffusion models predict DHC.

**Performed at the POLDI/BOA/ICON beamline of the SINQ at PSI.**  
**Spatial resolution  $<10\mu\text{m}$**



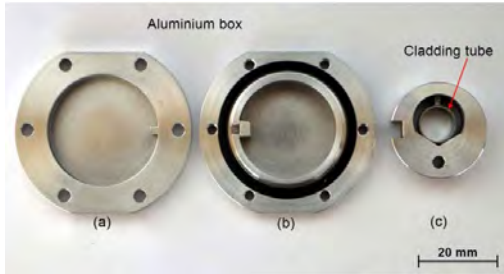
## Inner liner effects

- The liner-substrate interface acts as a **strong hydrogen sink**
- Large **hydrogen depletion** of the substrate

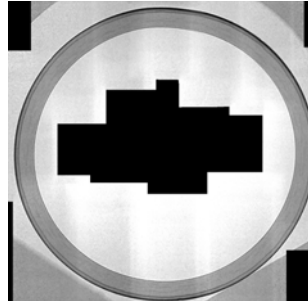




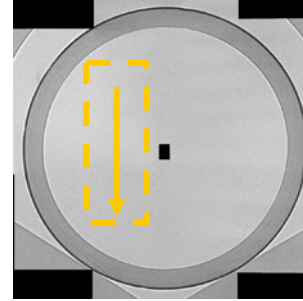
## Active Box design



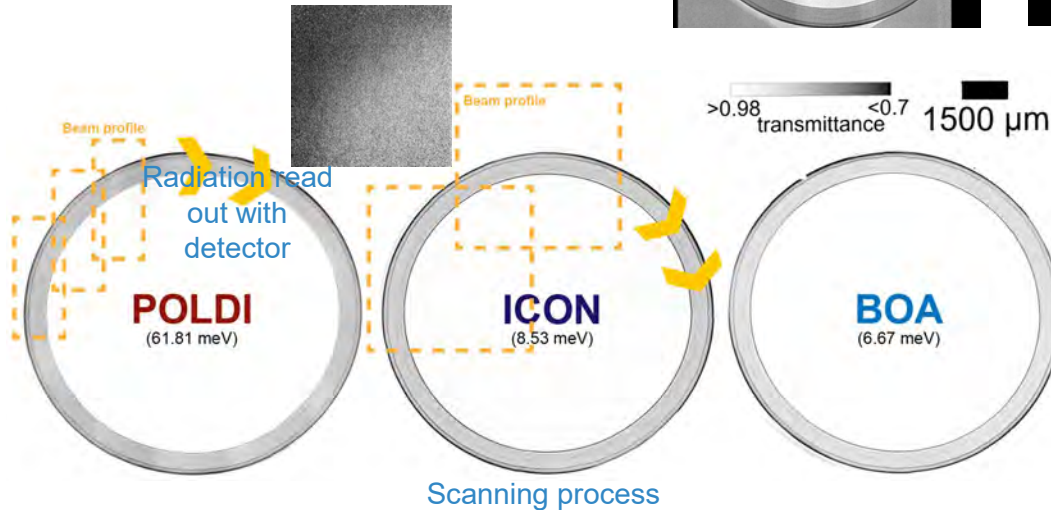
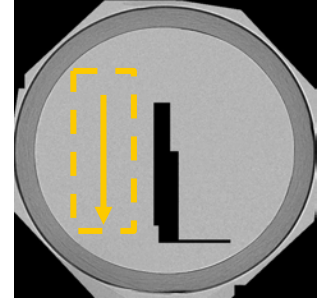
2018



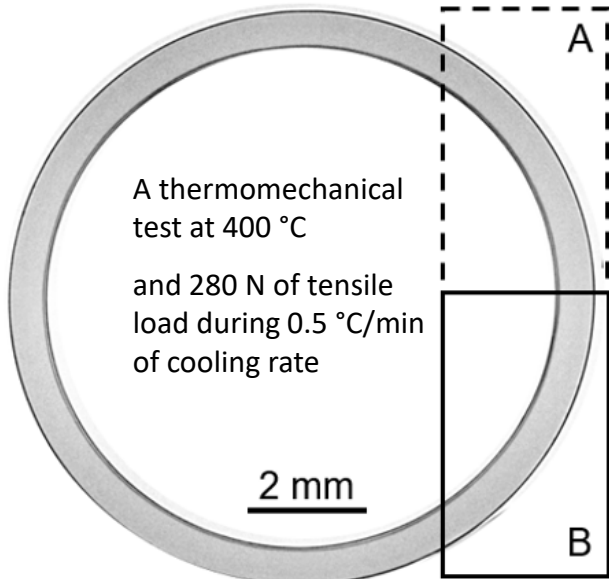
2021



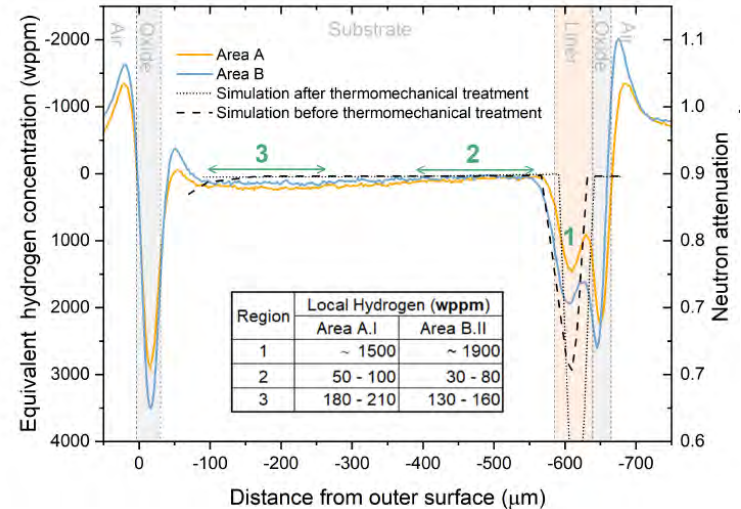
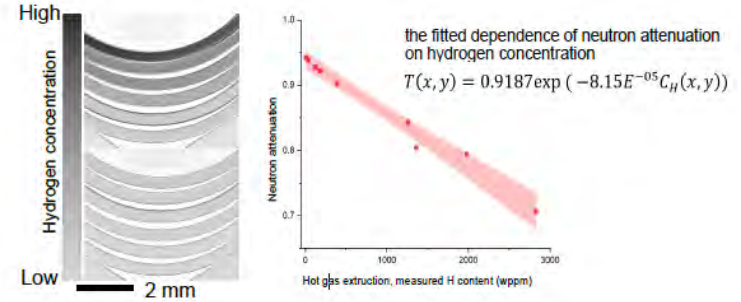
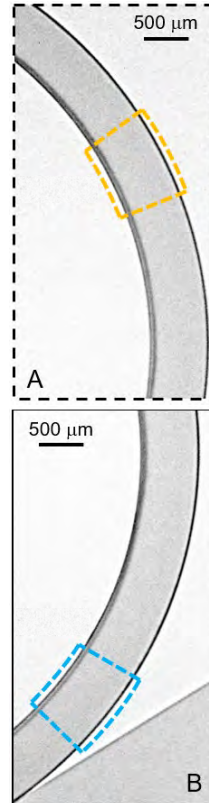
2022



**Irradiated LK3/L**  
 Kernkraftwerk Leibstadt (KKL) (BWR), Switzerland  
 4 reactor cycle, 66 MWd/kgU  
 ~222 wppm H composition (\*HVE)

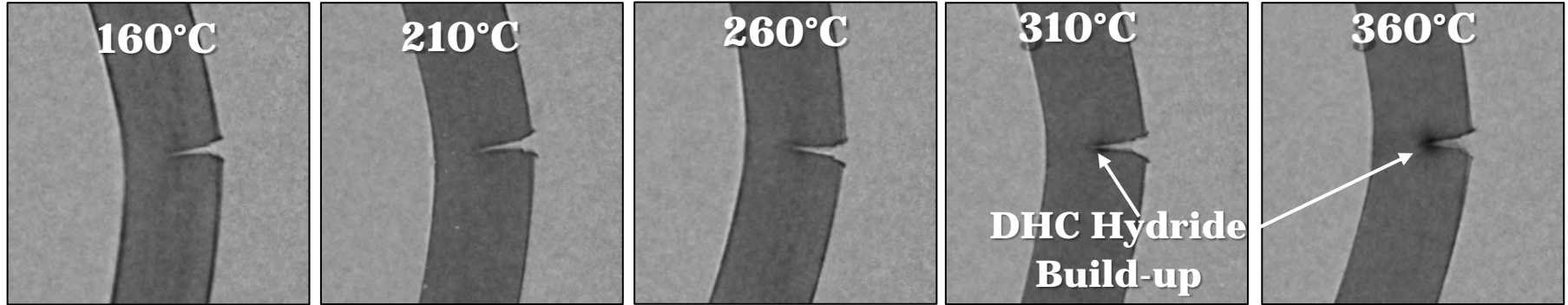


>0.98 Transmittance <0.7

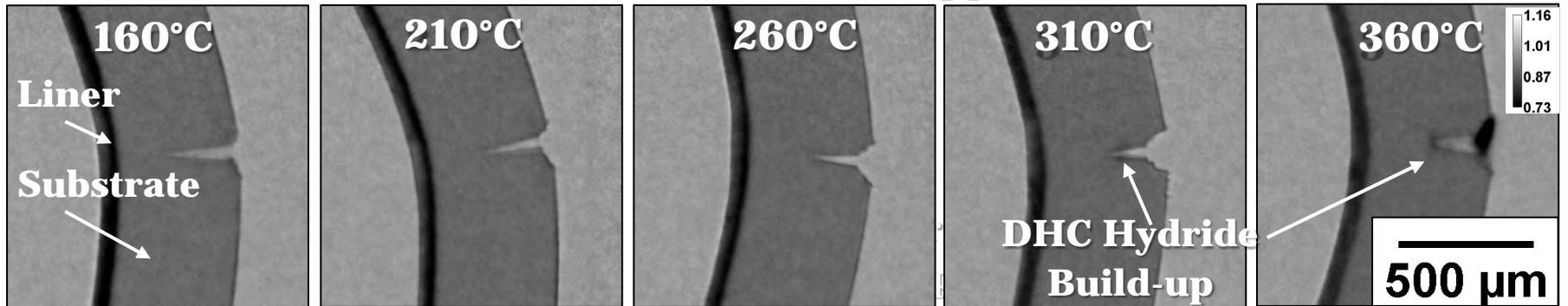


# n-radiography

***without*** inner liner (328 wppm H)

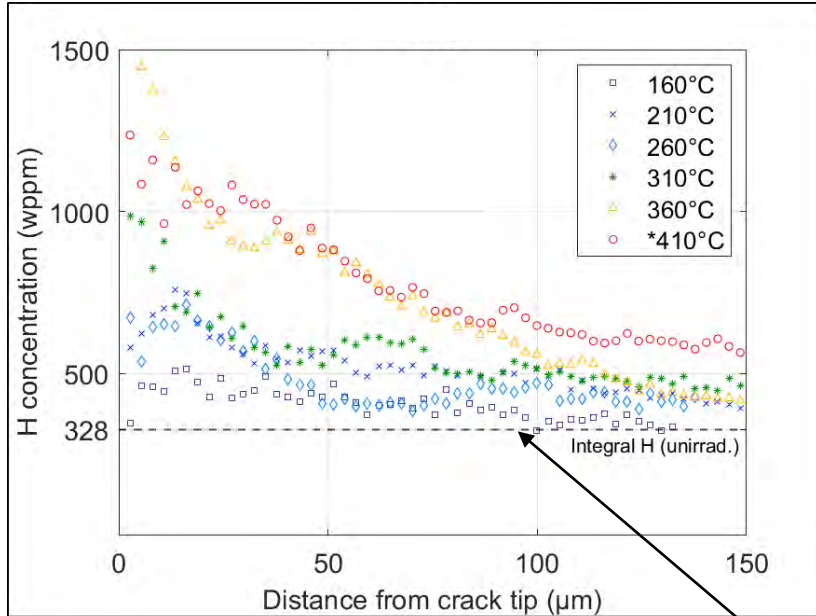


***with*** inner liner (381 wppm H)

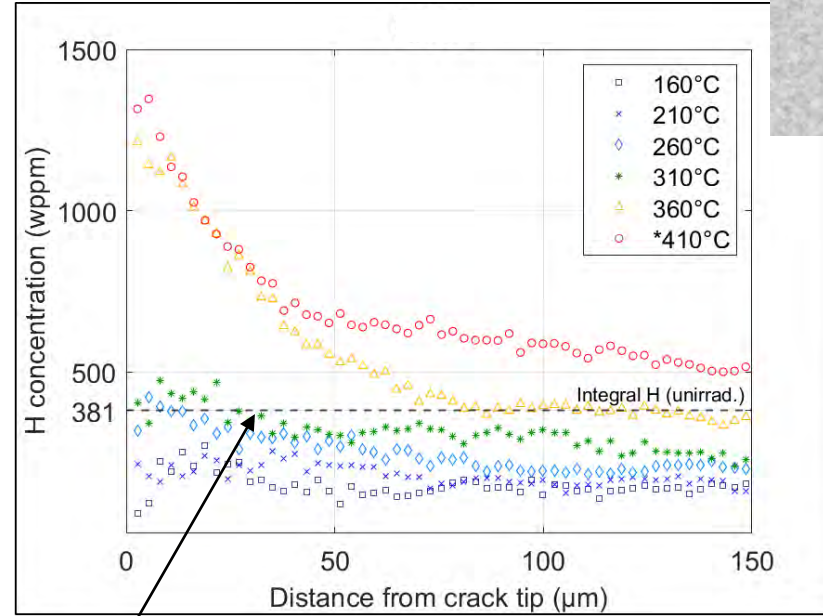


# Hydrogen quantification

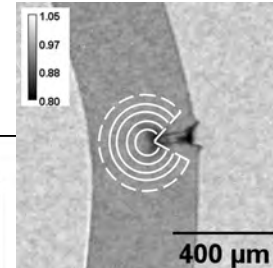
**without** inner liner (LK3)



**with** inner liner (LK3/L)



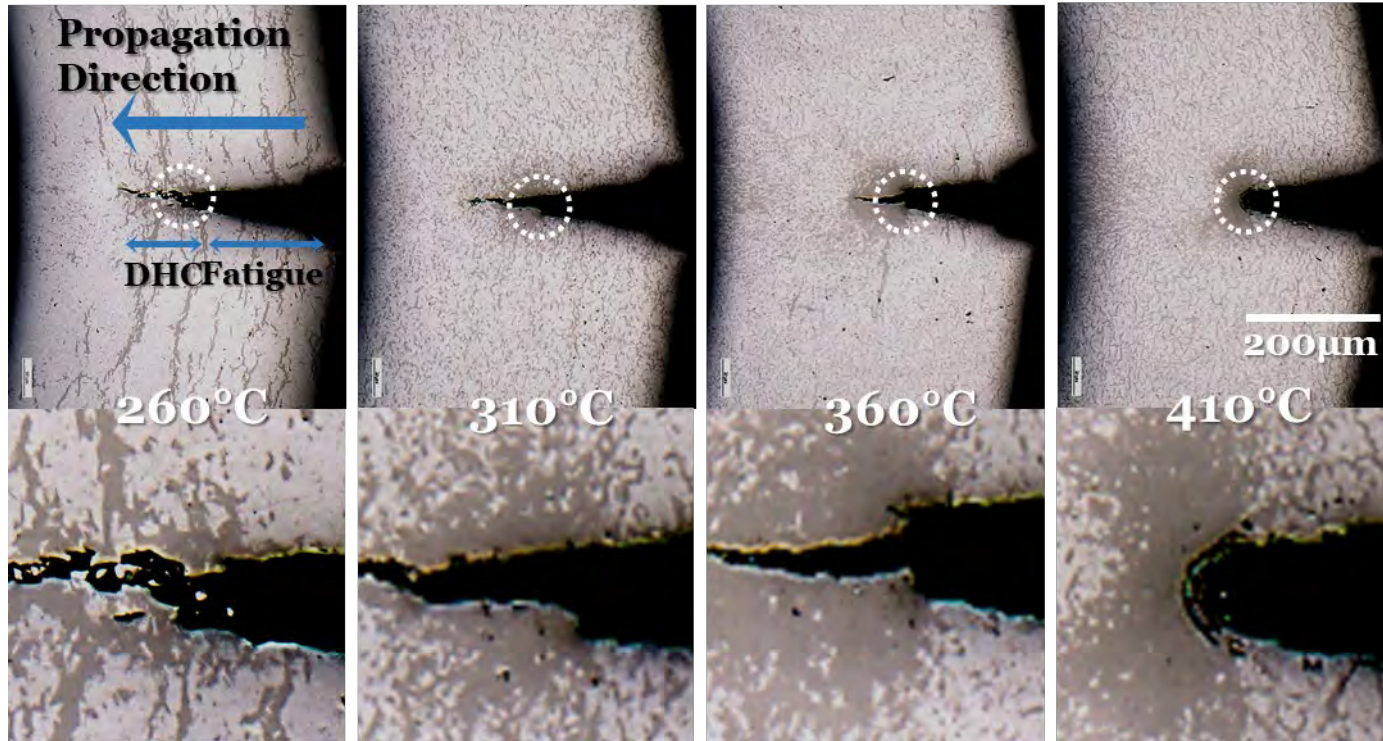
Radial Averaging



Integral sample hydrogen concentration measured with HVE

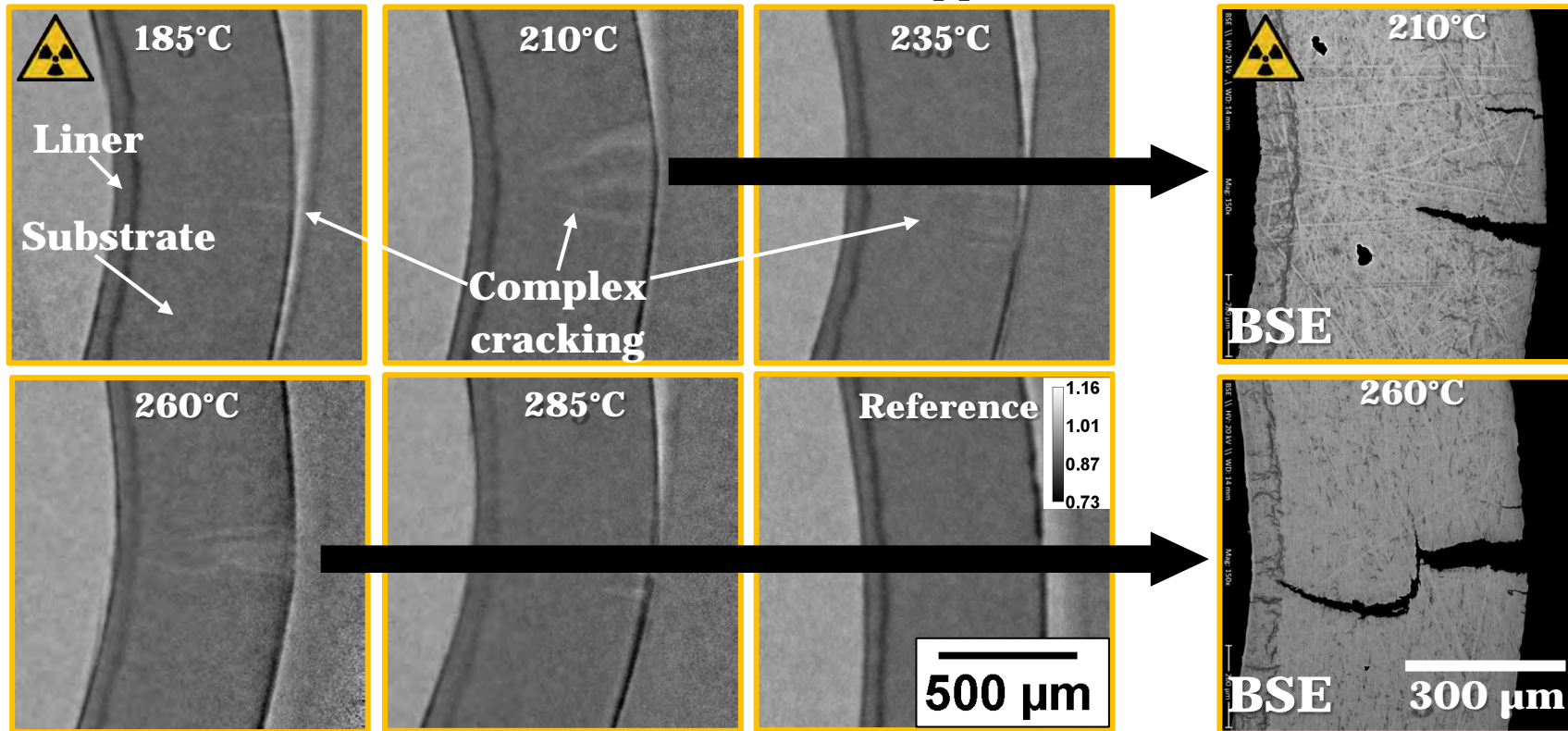


## Blunting above 300°C



# n-radiography

**Irradiated** material *with* inner liner (116 wppm H)



**Introduction**

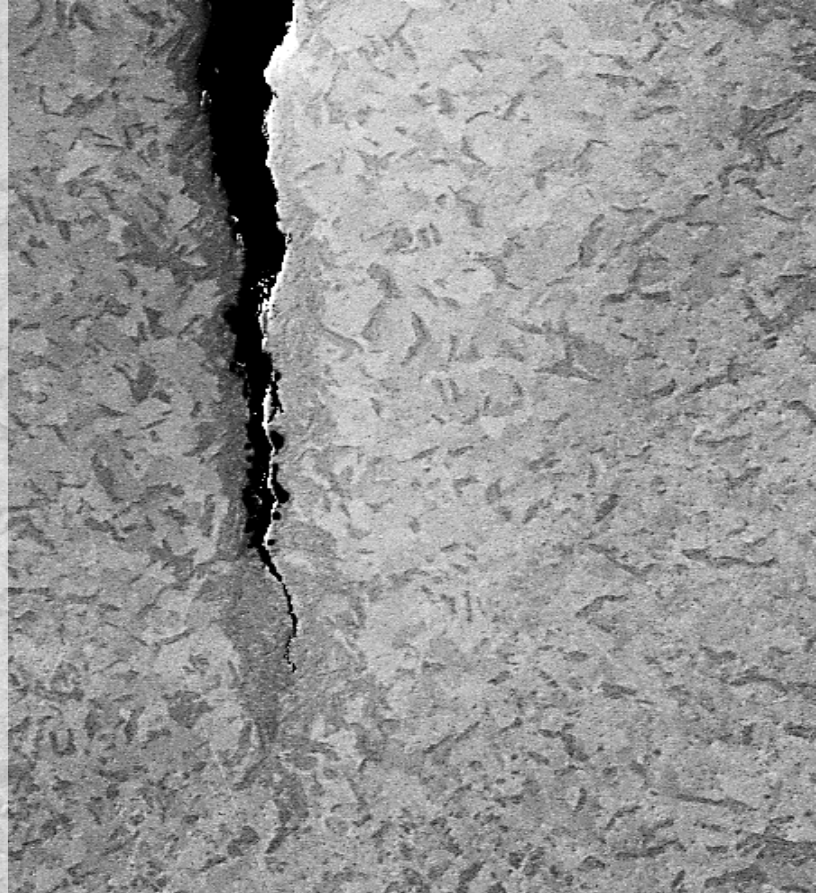
**Materials and Tests**

**n-radiography**

**Phase Mapping**

**HELP Testing**

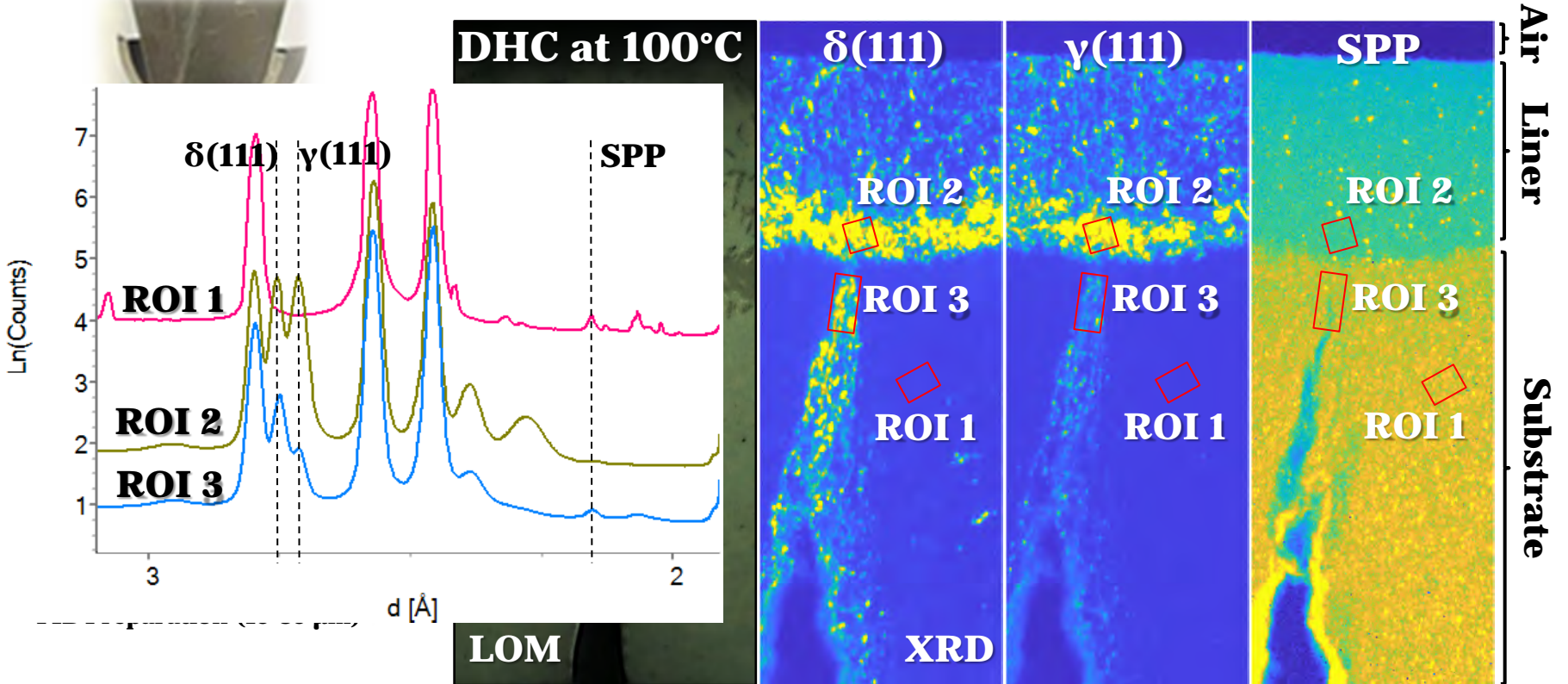
**Conclusions**





# Phase Mapping

XRD-contrast microscopy for phase mapping @ microXAS beamline of SLS





Introduction

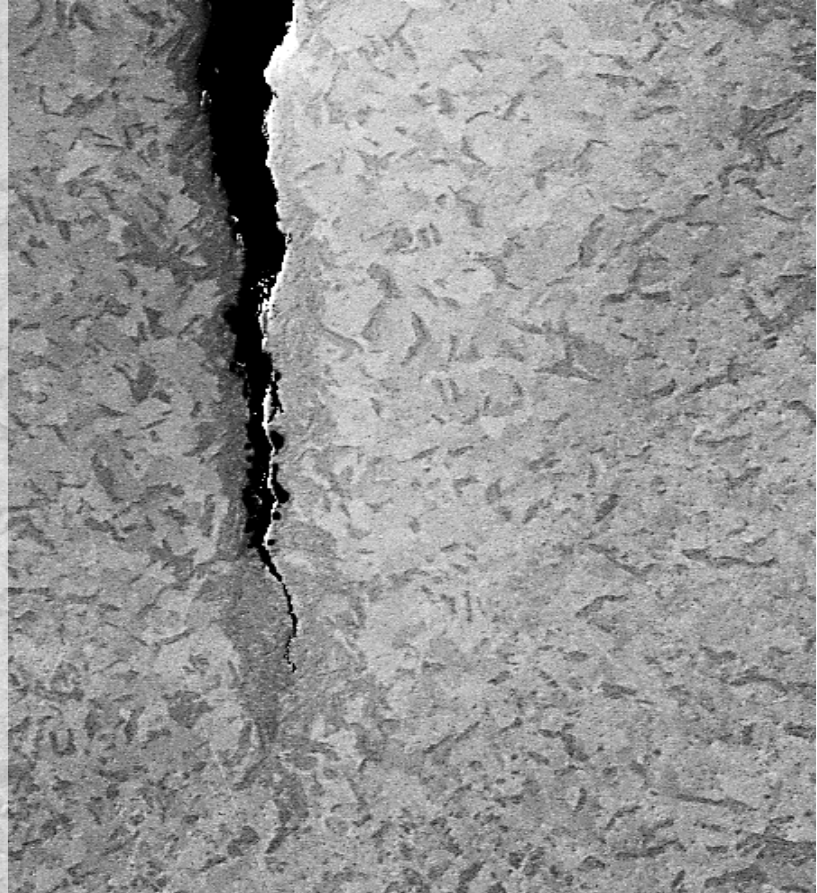
Materials and Tests

n-radiography

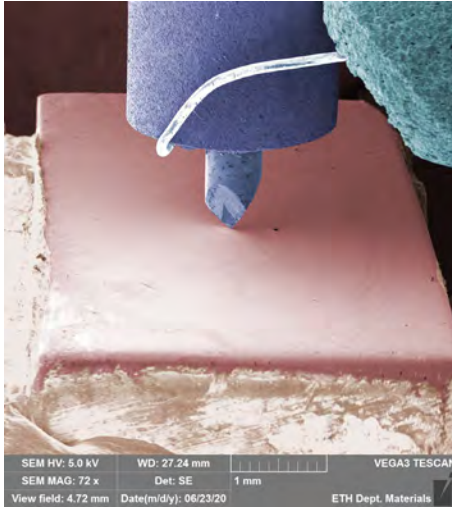
Phase Mapping

**HELP Testing**

Conclusions

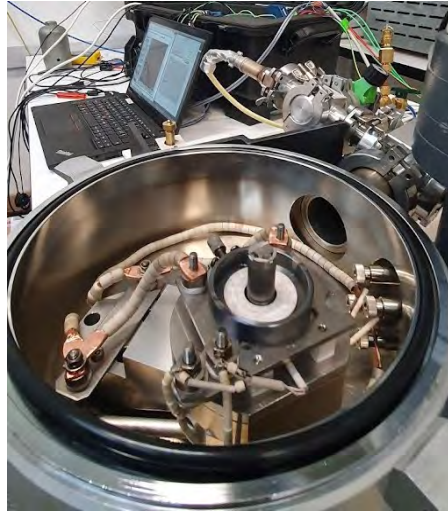


(1) Strain-rate sensitivity



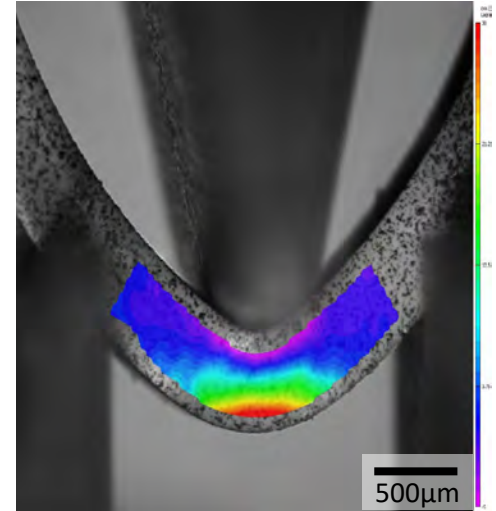
Nano-indenter

(2) Hardness



Micro-indenter

(3) Flexural yield



Macro 3-point bending

# HELP Testing

## Softening due to H in solid solution?

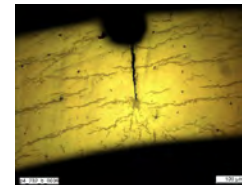
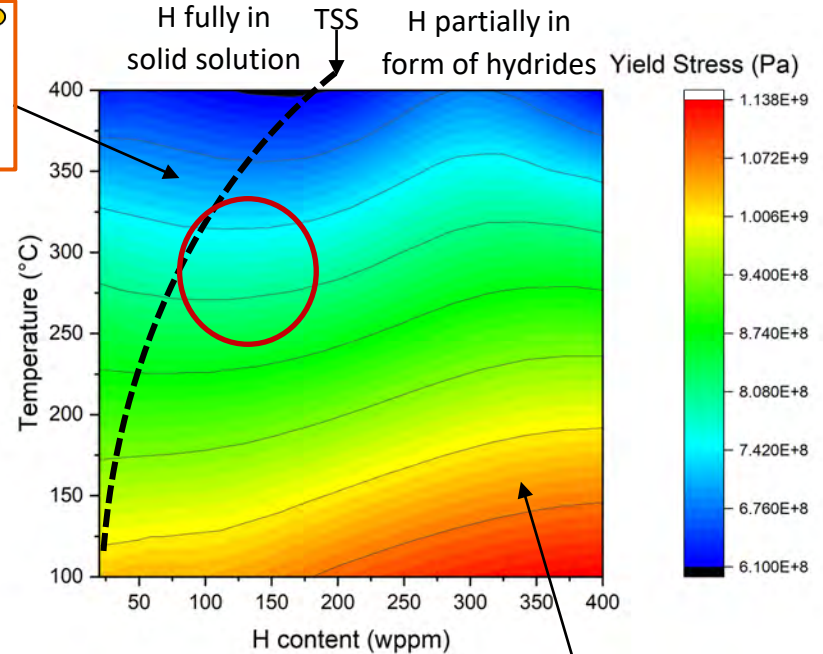
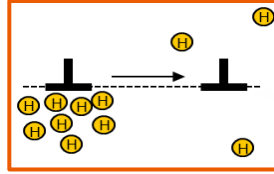
for Zr alloys in nuclear application is an open topic.

H in solid solution tends to decrease yield point. The effect of hydrogen in solid solution is **minor compared to hydrides, but significant.**

The most pronounced softening recorded at 300°C for Zry-4 enriched with 100 wppm of hydrogen with a **decrease of 3% in flexural-yield stress of clad sections.**

Results presented by F. Fagnoni at:

- TopFuel 2021;
- Eurosafe 2021;
- ASTM 2022



**Hardening due to hydrides**  
(image from delayed hydride cracking)

**Introduction**

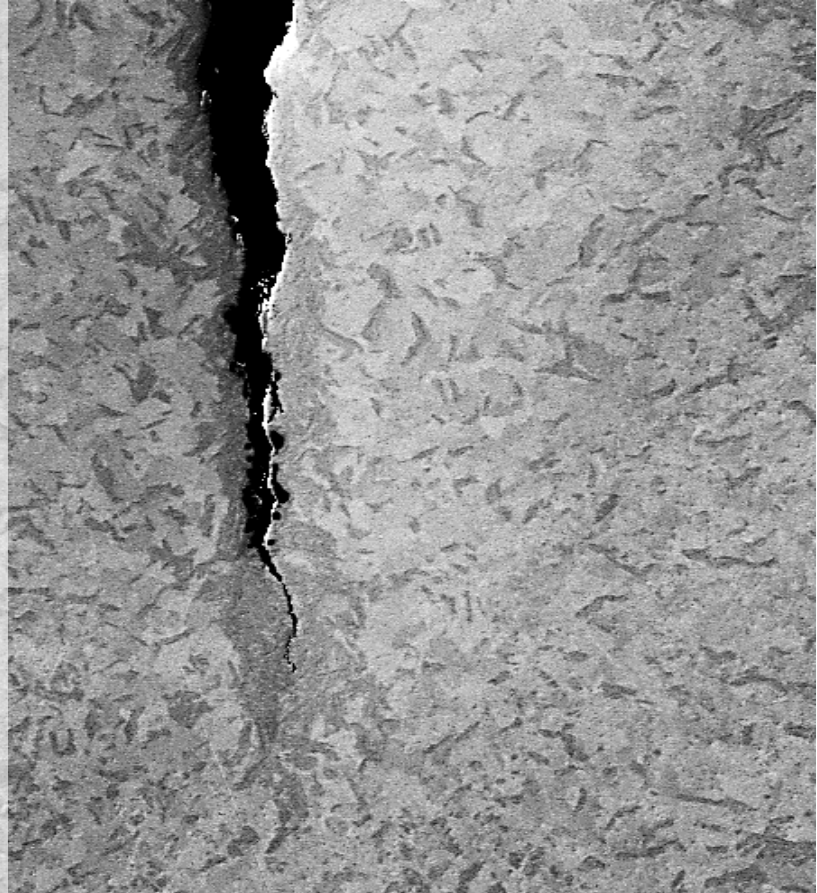
**Materials and Tests**

**n-radiography**

**Phase Mapping**

**HELP Testing**

**Conclusions**





# Conclusions

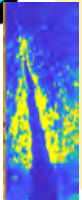
## n-radiography

- Hydrogen quantification
- Liner influence
- Complex cracking of irradiated material

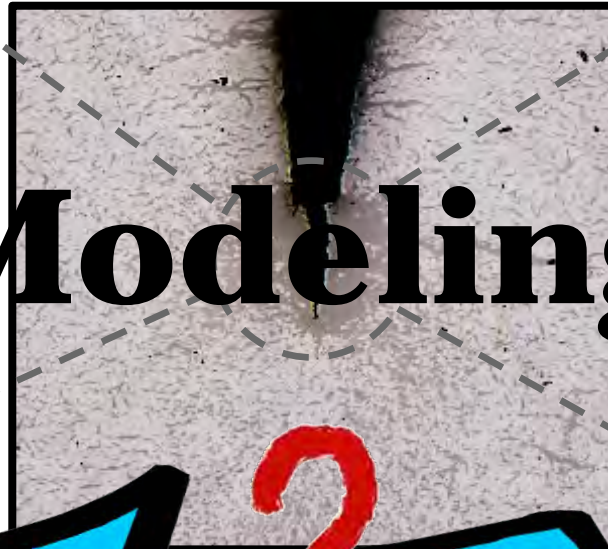


## XRD phase mapping

- Proven method of high-resolution phase mapping
- $\delta$  and  $\gamma$  – hydride phases identified



What has been learned?



# Modeling

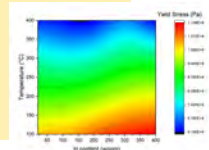
## Mechanical Properties

- $K_{IH}$
- DHC Velocity



## HELP Test

- Reduced Yield Stress with given hydrogen concentration



## Many thanks go to:

- LNM and the Nuclear Fuels Group at PSI
- AHL at PSI
- MIDAS

## Special thanks to sponsors:

nagra

swissnuclear



## Questions to be answered

1. Does DHC propagate **differently** in the **radial direction** versus axial?\*
2. Does the **inner liner affect the propagation** of DHC?
3. Where is the **hydrogen distributed** during DHC?
4. How does **irradiation damage** affect DHC?
5. What are the **threshold loads** (i.e.  $K_{IH}$ ) required for DHC?

## What is delayed hydride cracking?

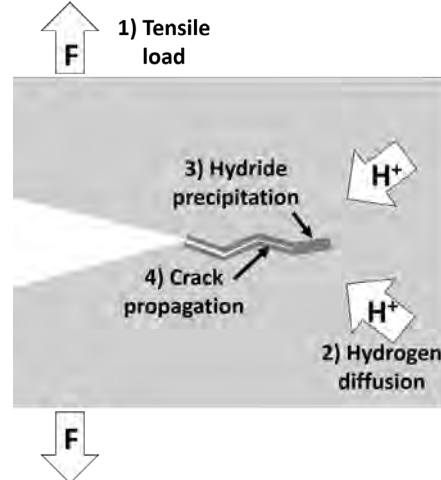
1. a **subcritical crack growth** mechanism in which hydrogen in solid solution
2. hydrogen migrates towards a location of **higher tensile stress**
3. the solvus limit is exceeded resulting in **hydride precipitation**
4. the hydride will **fracture** upon reaching a critical size and shape

**Step 1 and 2:** Stress driven diffusion

$$C_H \approx C_{H_0} \exp\left(\frac{-\Delta\sigma^*\Delta V}{RT}\right)$$

**Step 3 and 4:** Precipitation and fracture

$$C_H > C_{H,Tssp}$$

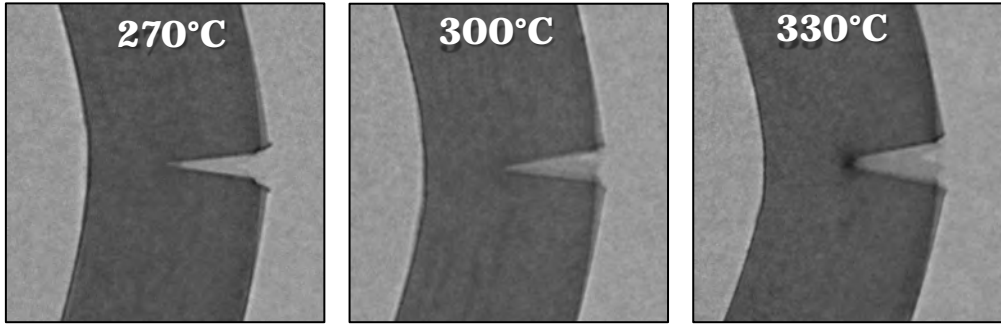


## Critical Factors

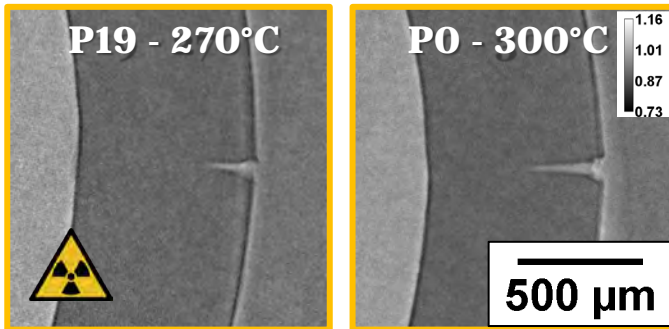
1. *Hydrogen*
2. *Temperature*
3. *Tensile loading*



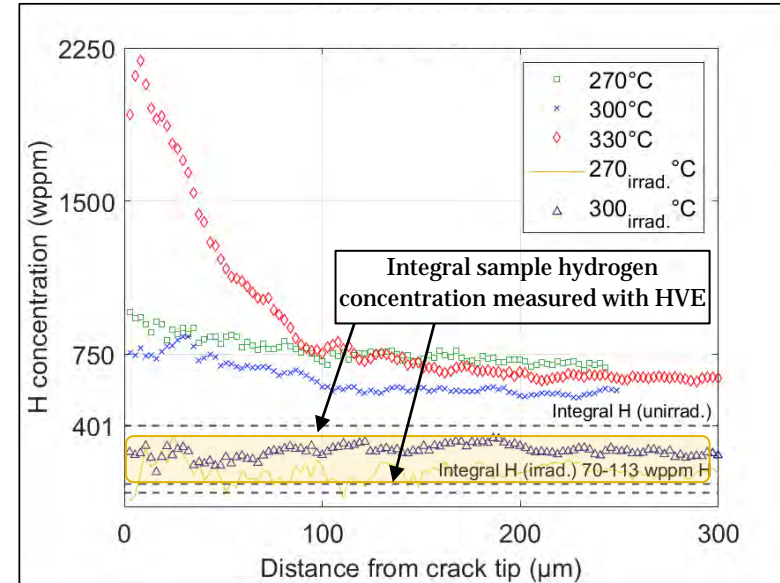
## Unirradiated SINQ target rod (401 wppm H)



## Irradiated SINQ target rod (143/70 wppm H)

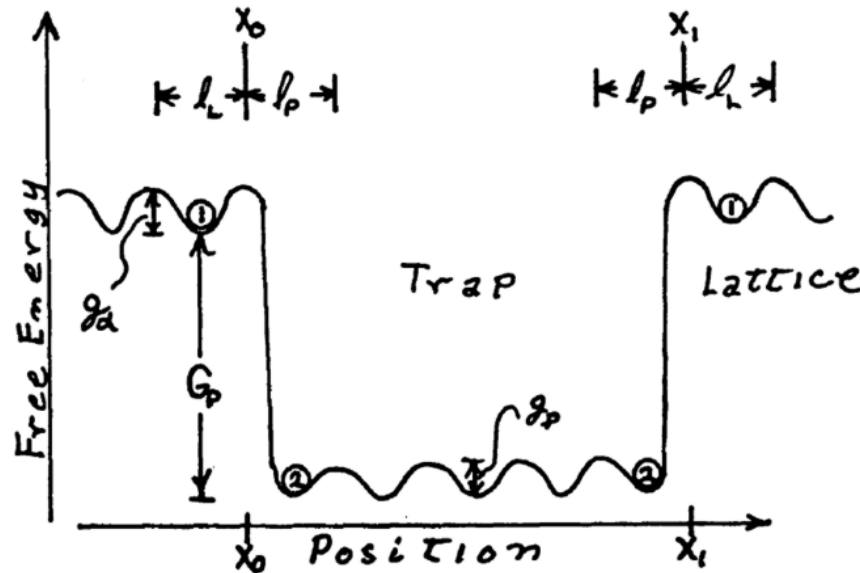


## Hydrogen quantification SINQ target rod



## Irradiation damage effects

- Defects caused by irradiation damage leads to **hydrogen trapping**
- Hydrogen trapping **reduces the mobility** of hydrogen throughout the substrate



$G_p$  = free energy between hydrogen in lattice and trap

$g_{\alpha,p}$  = free energy for hydrogen diffusion barrier within lattice and lattice trap positions

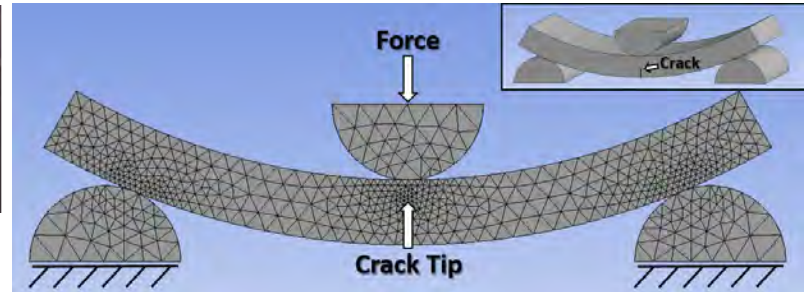
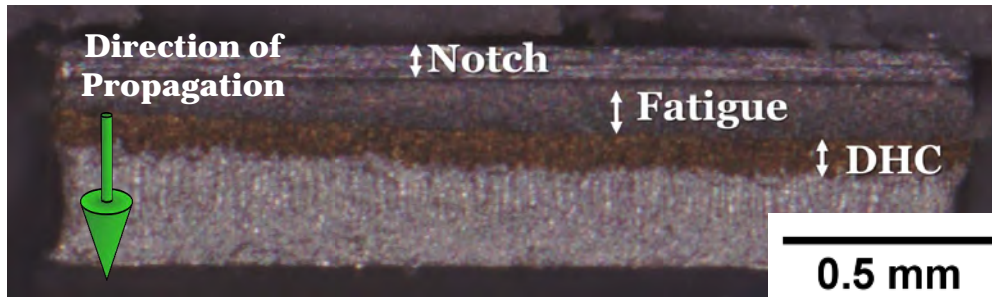
$l_{l,p}$  = thickness of adjacent lattice-trap interface

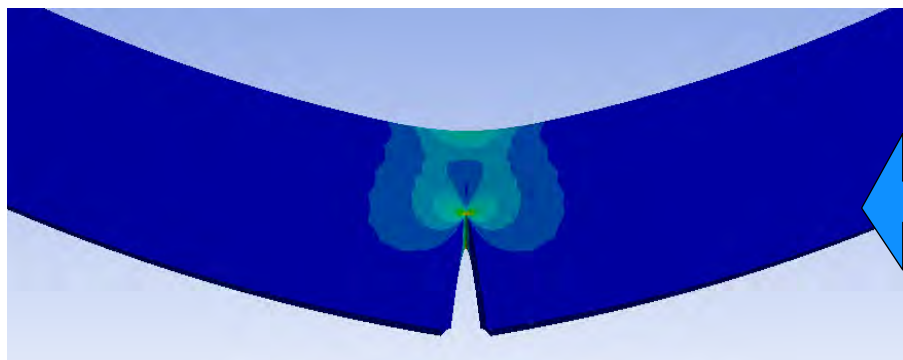
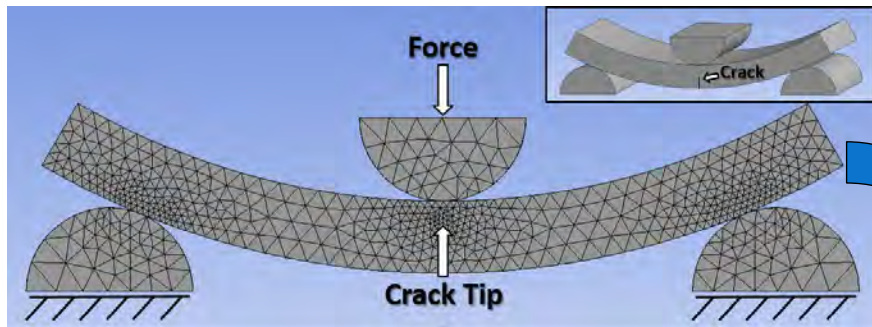
## Objective

Determine the minimum threshold of DHC ( $K_{IH}$ )  
of radially cracked fuel cladding

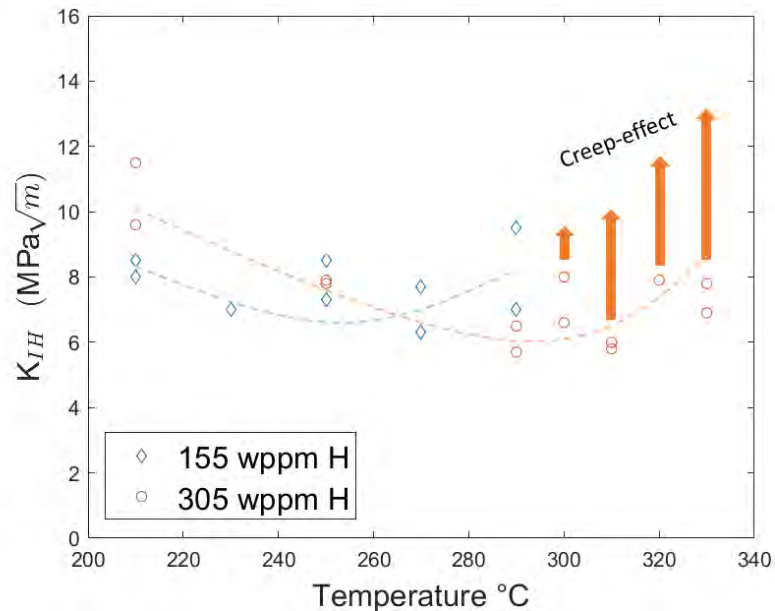
## Importance

Information on  $K_{IH}$  can help to inform the utilities  
on spent fuel handling and safety.





$K_{IH}$  without inner liner



Minimum value ~6 MPa√m

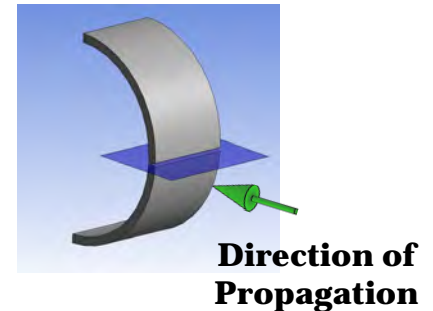
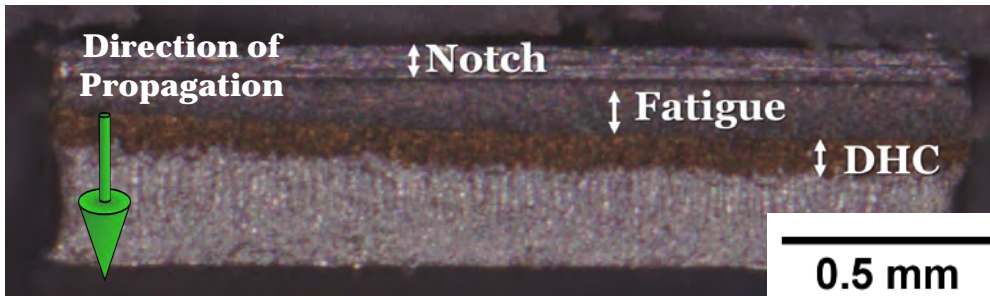


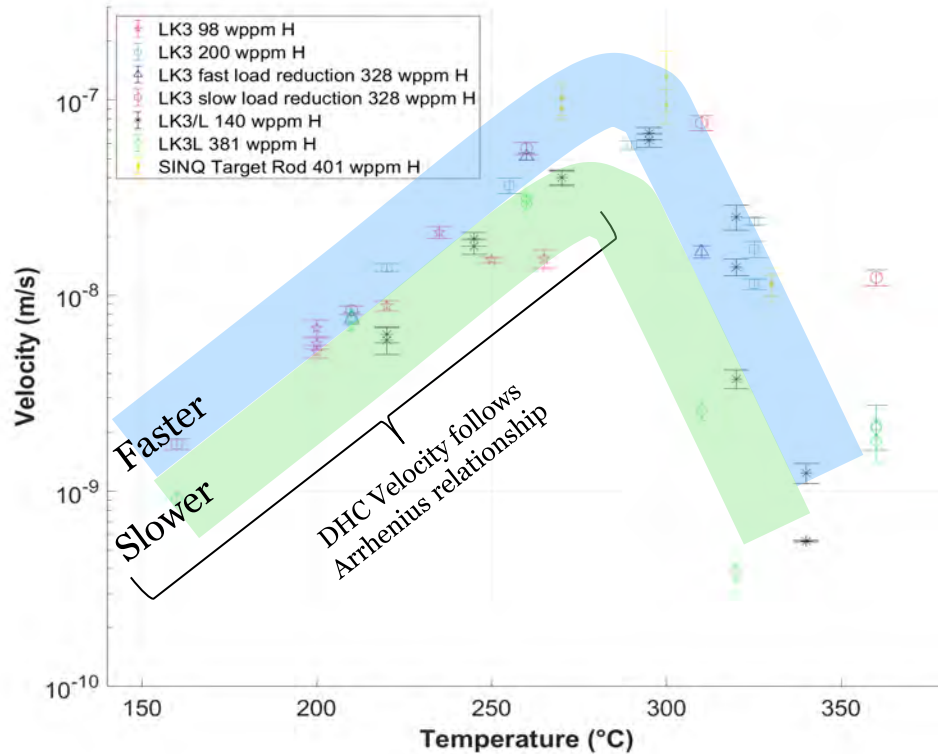
## Objective

Determine velocities of radially cracked fuel cladding and cladding with an inner liner.

## Importance

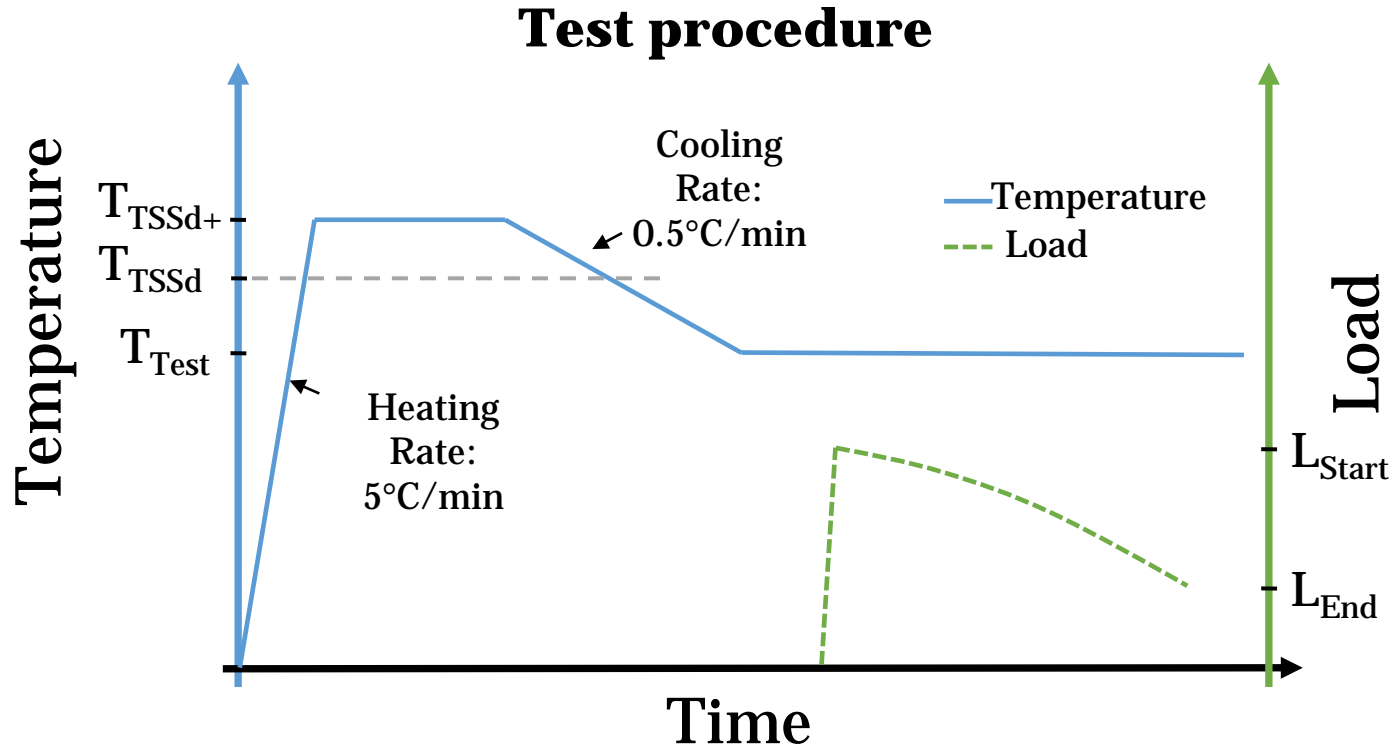
Information on radial cracking is lacking and the liner material has never been studied in the context of DHC.



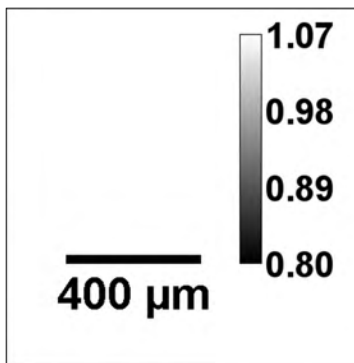
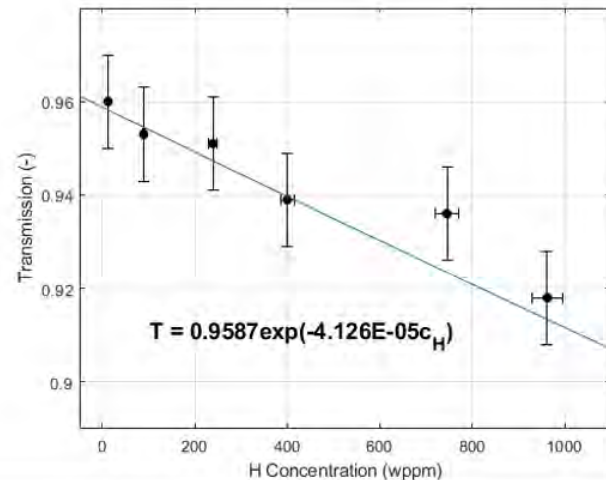
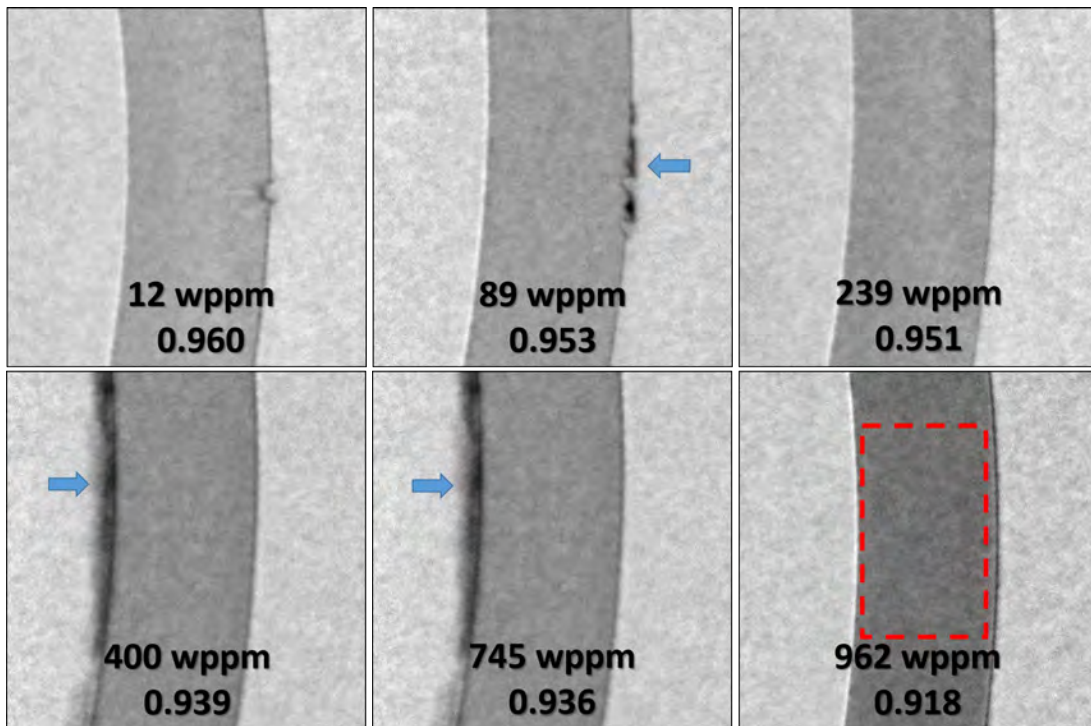


## Activation Energy

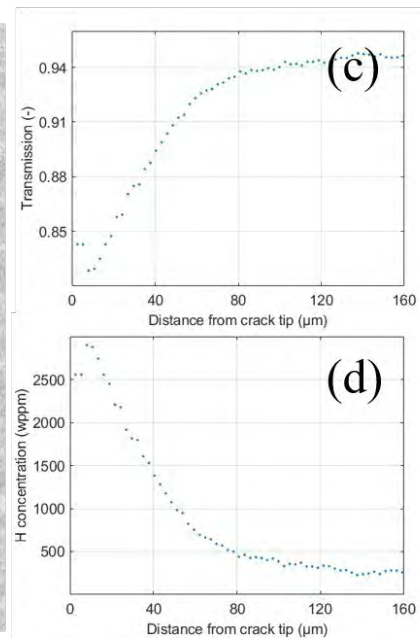
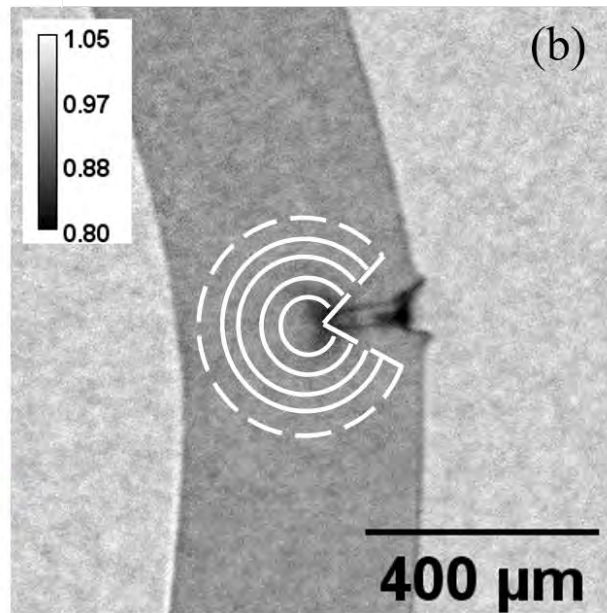
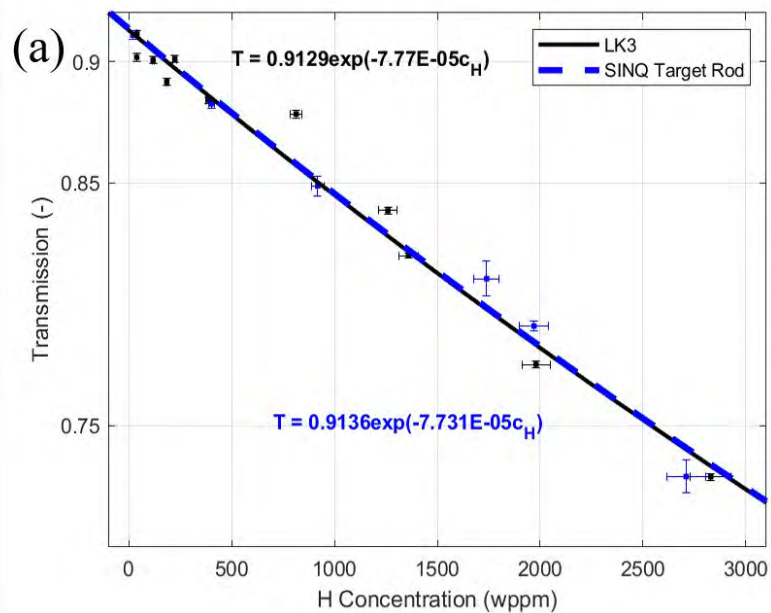
Sample Set	$E_a$ (kJ/mol)
LK3 328 wppm H	67.2
LK3/L 140 wppm H	73.6
LK3/L 381 wppm H	66.7
Literature summary (theoretical)	50-81.5

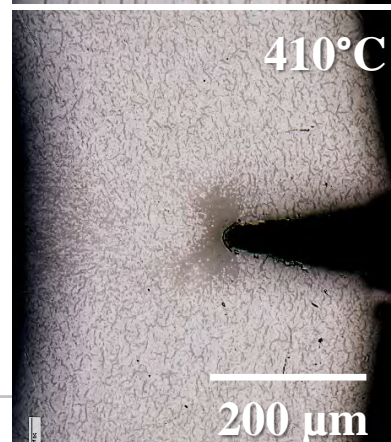
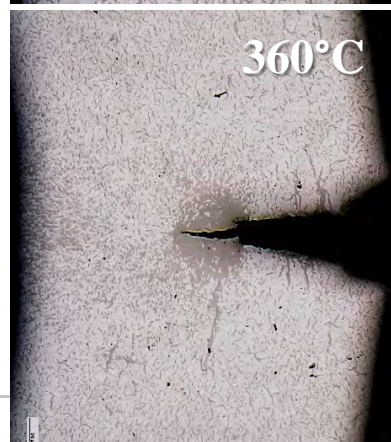
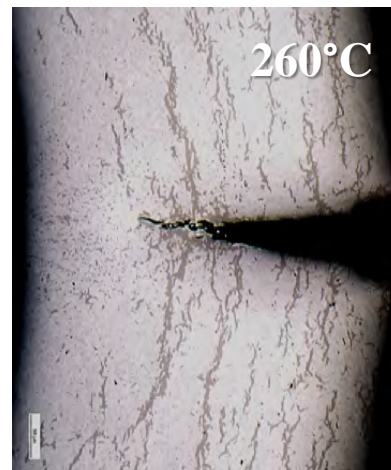


## Hydrogen Quantification

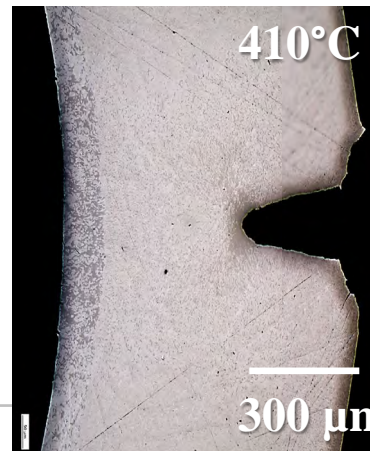
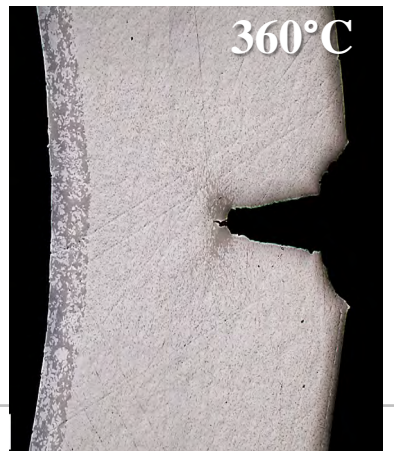
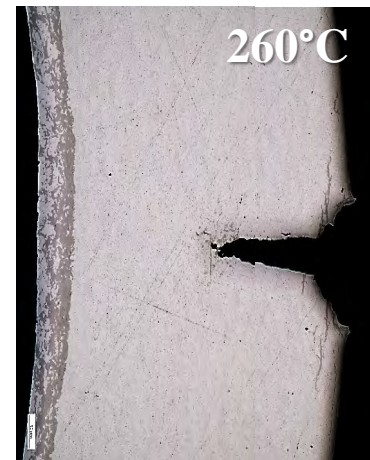




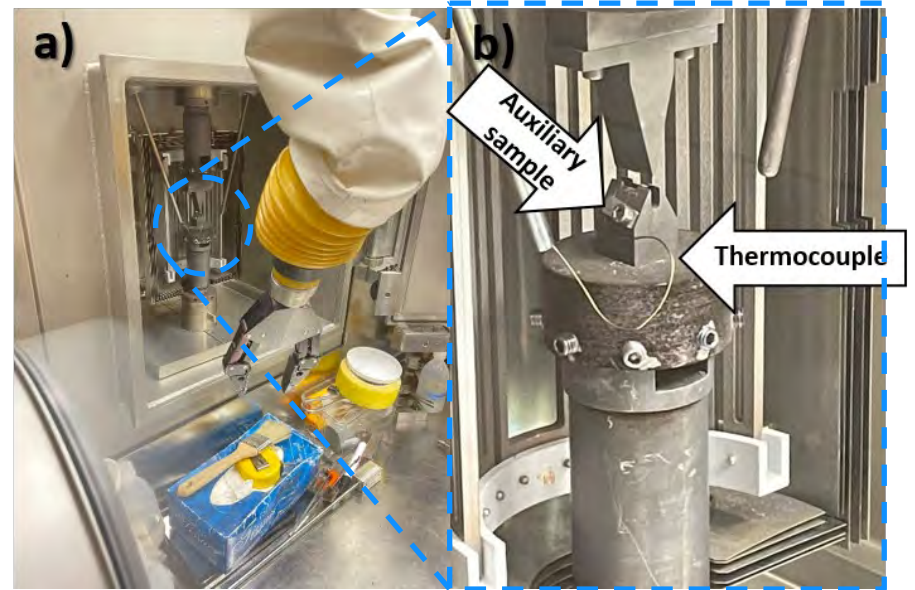
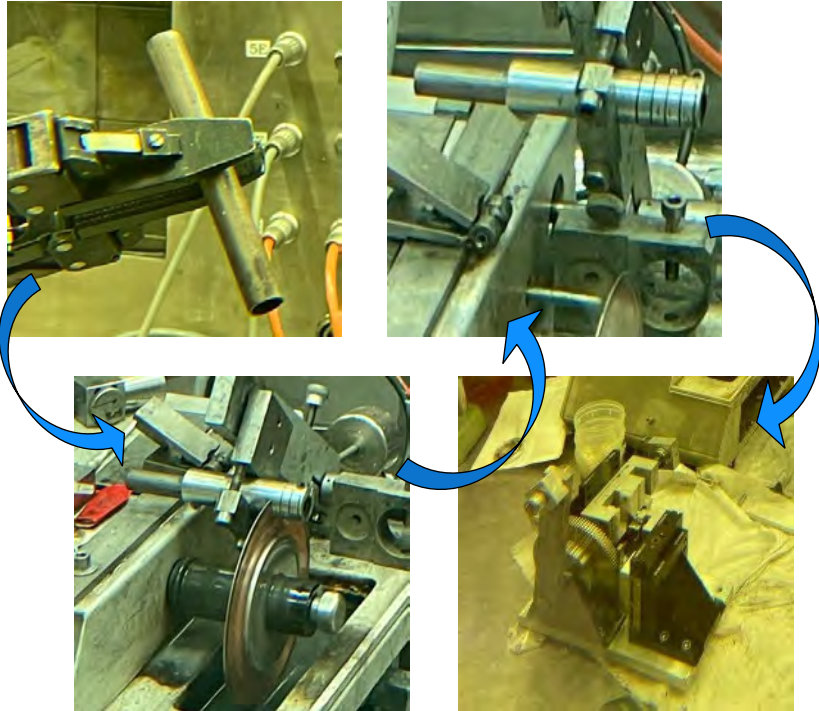




# Metallography LK3/L 4.0 mm

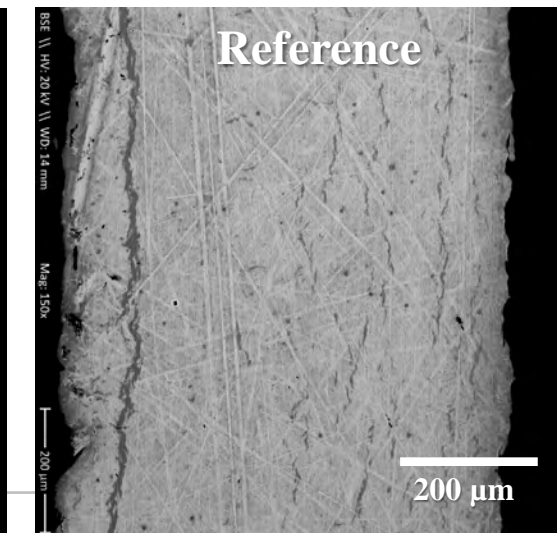
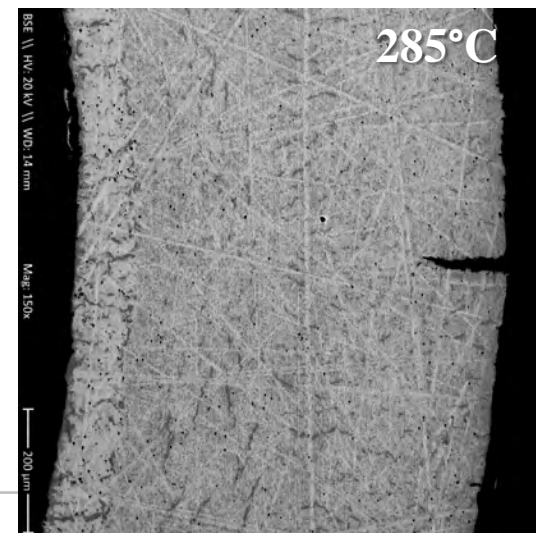
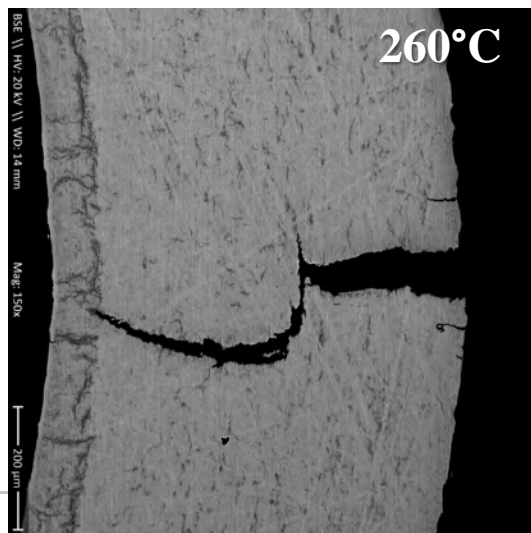
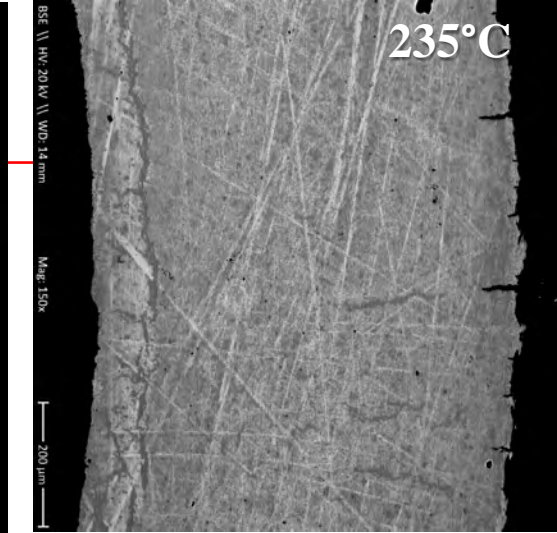
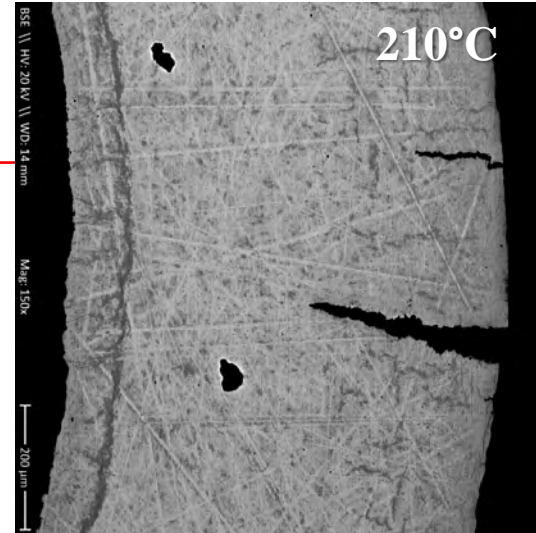


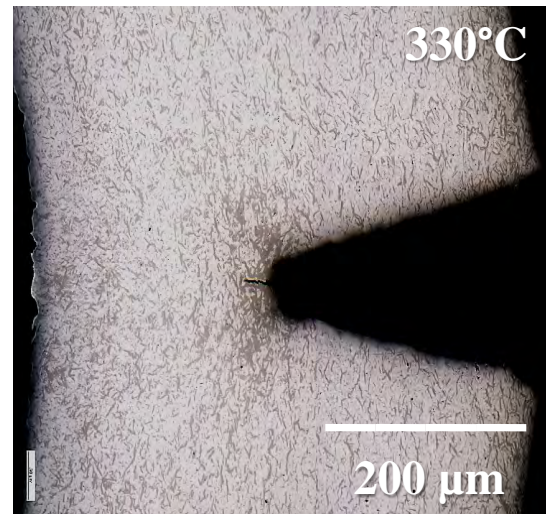
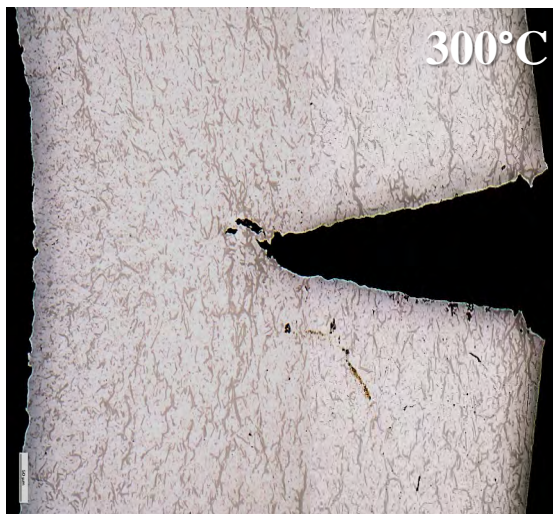
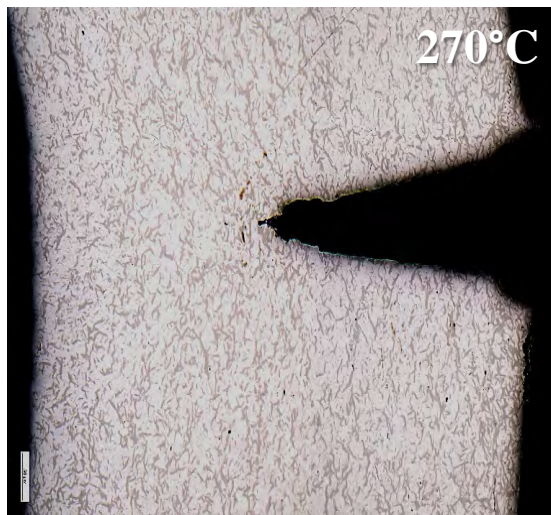




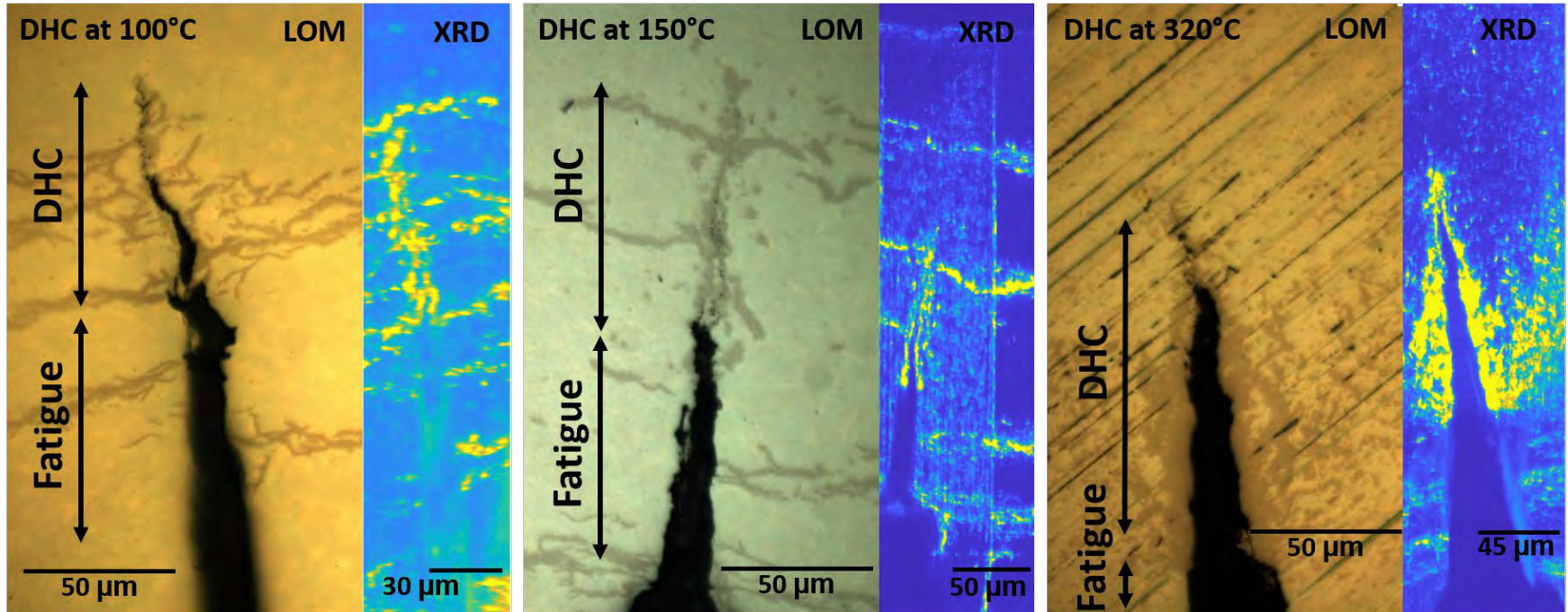
**Irradiated material testing facility**



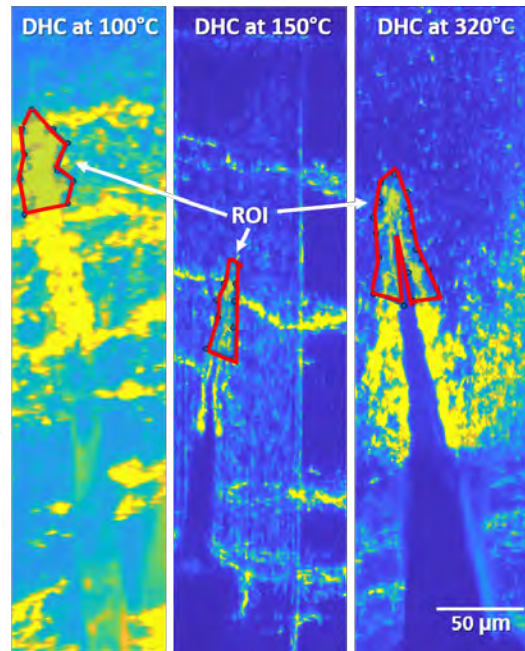
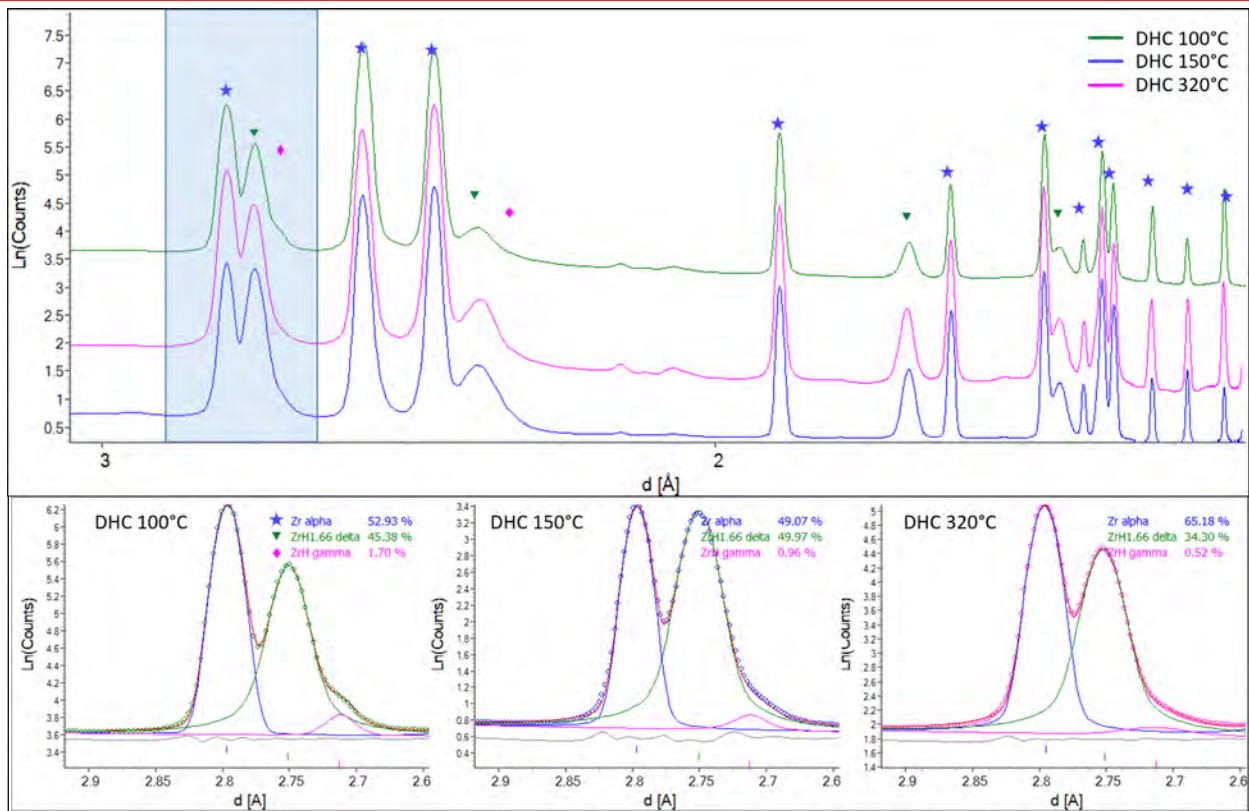






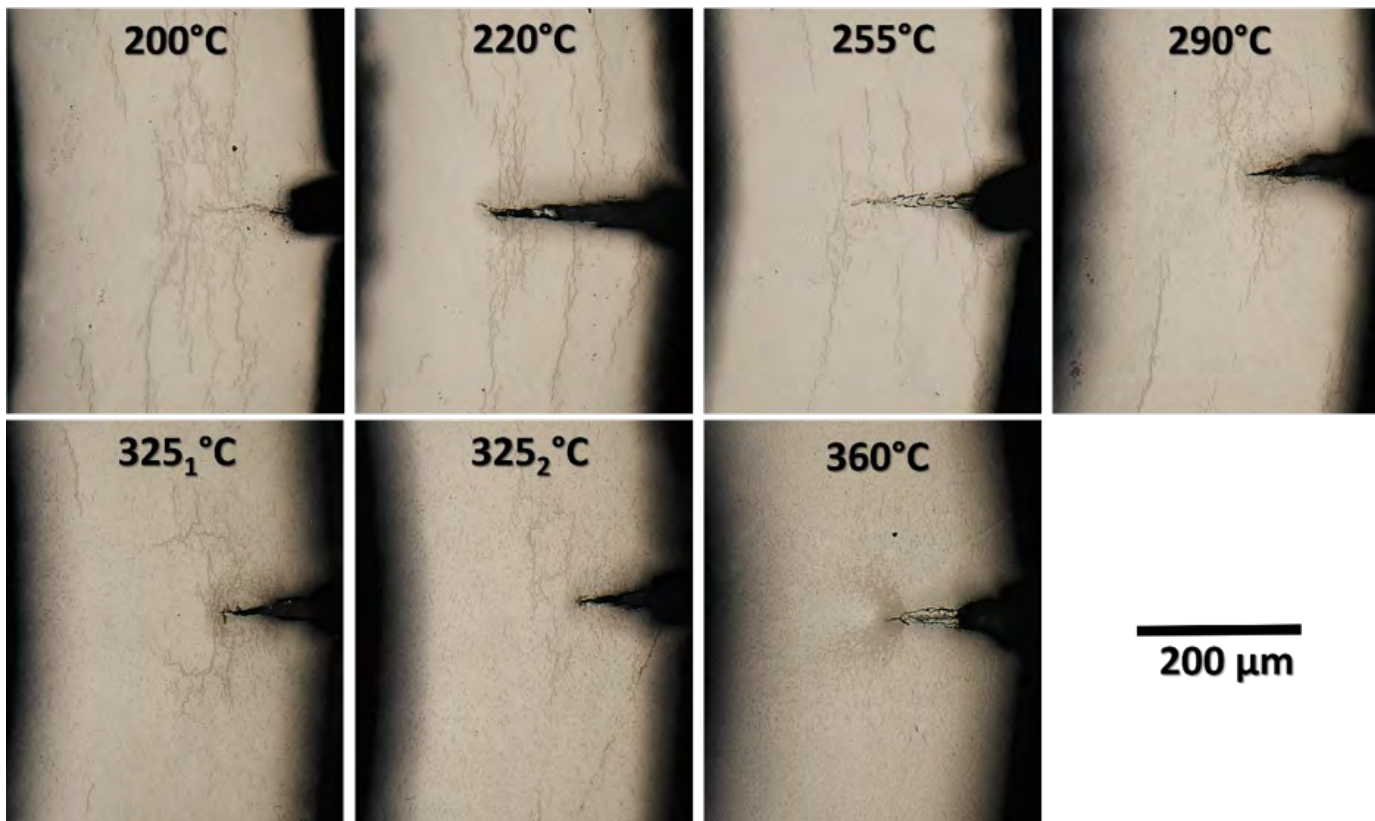


# Synchrotron-XRD Phase Mapping

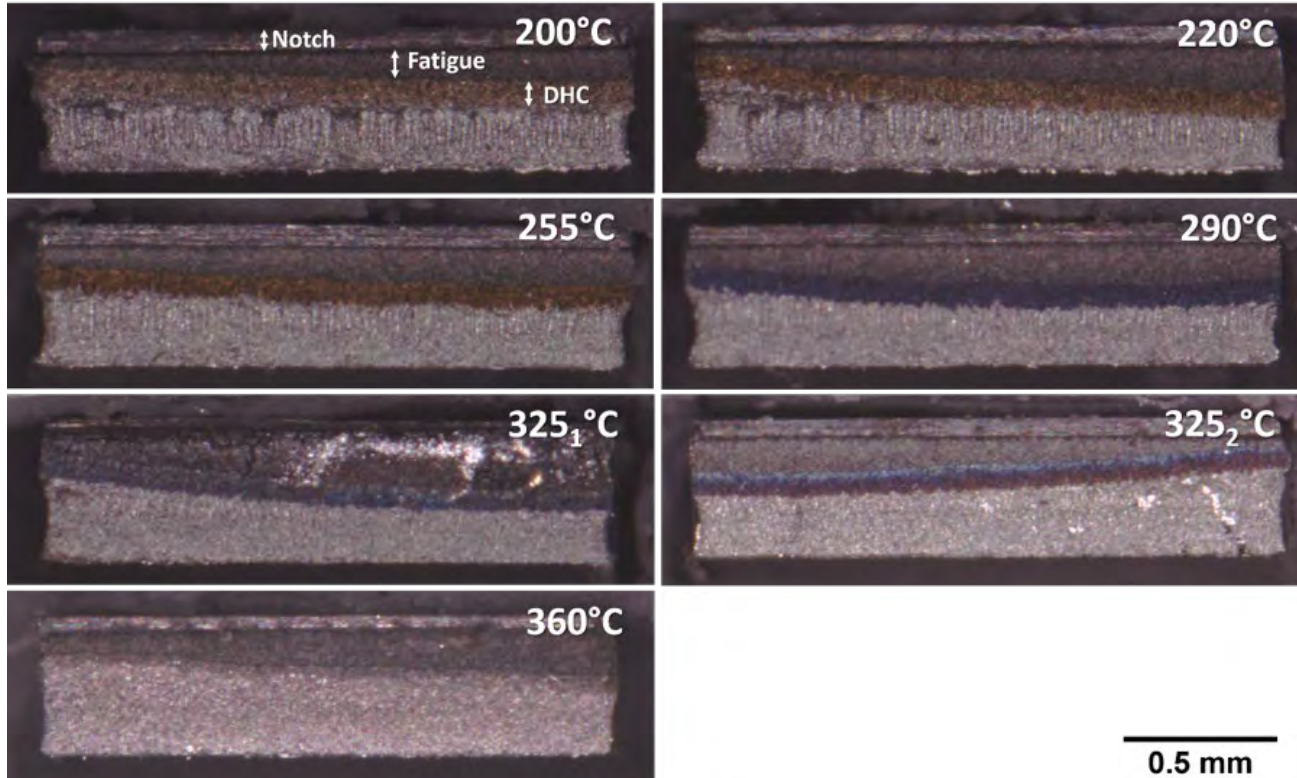




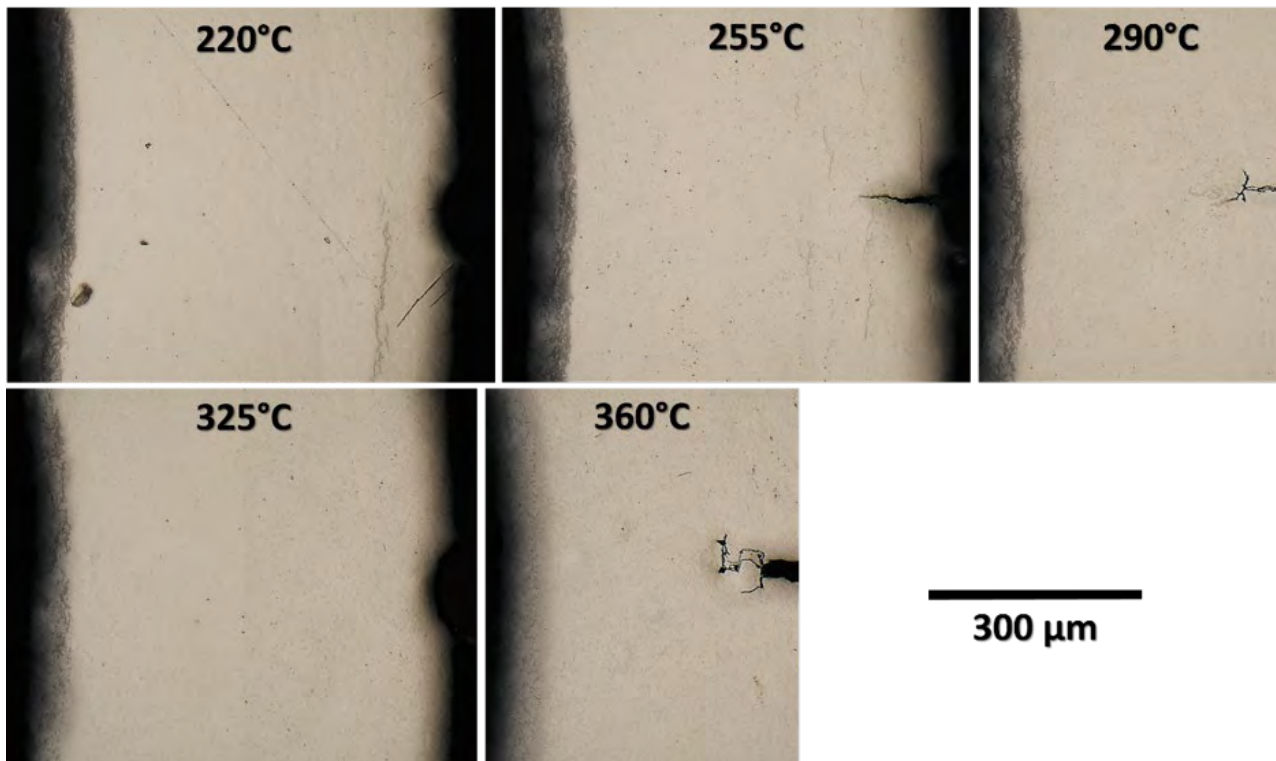
# Metallography LK3 2.0mm



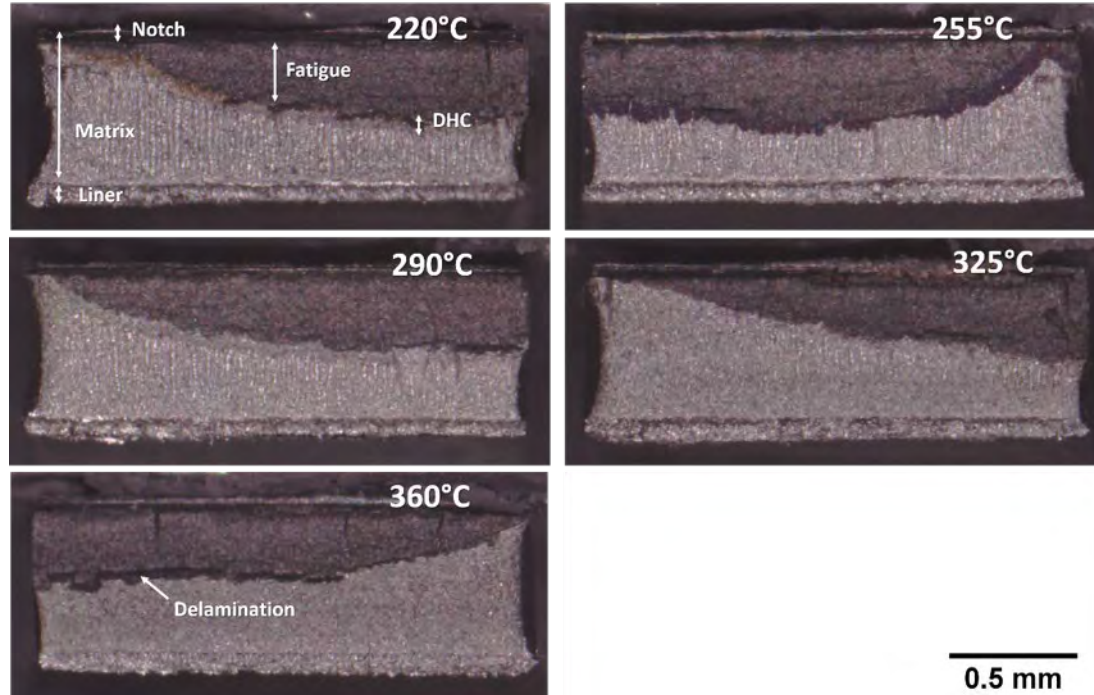
## Fractography LK3 2.0mm



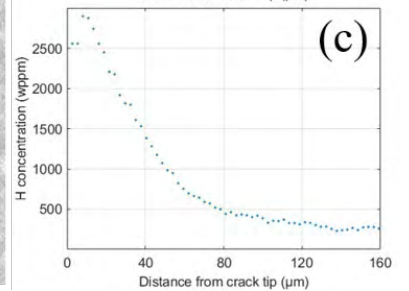
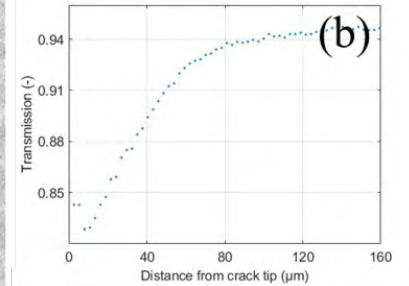
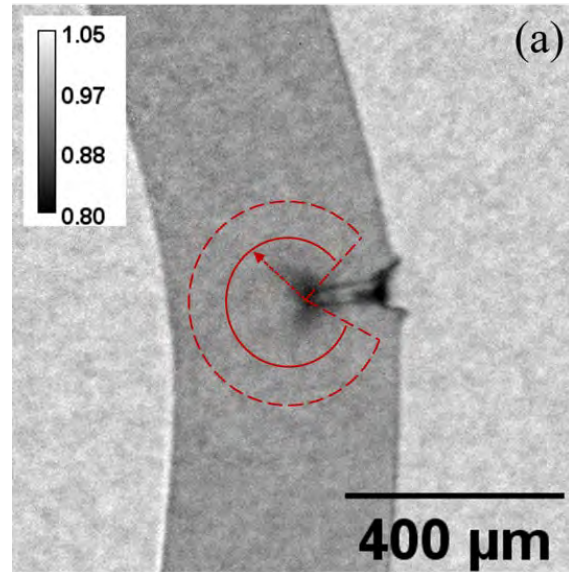
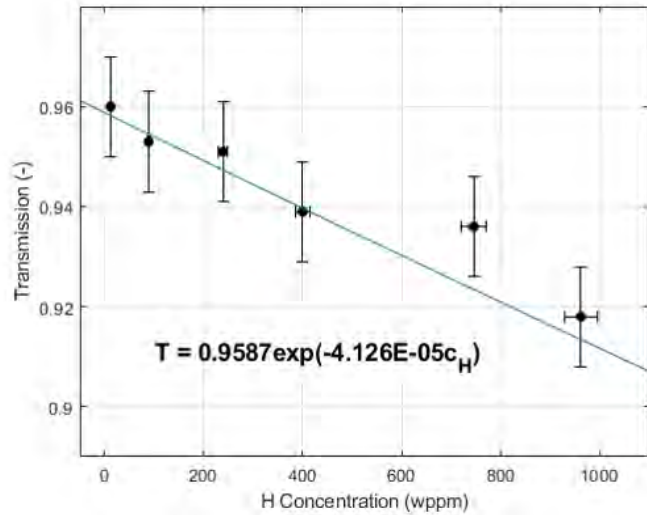
# Metallography LK3/L 2.0mm

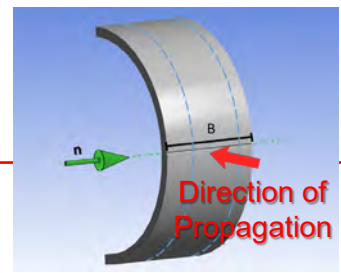


# Fractography LK3/L 2.0mm

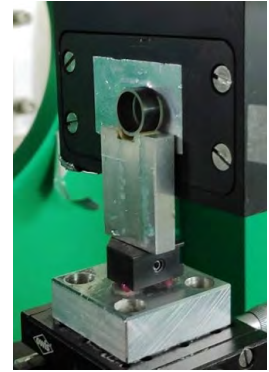
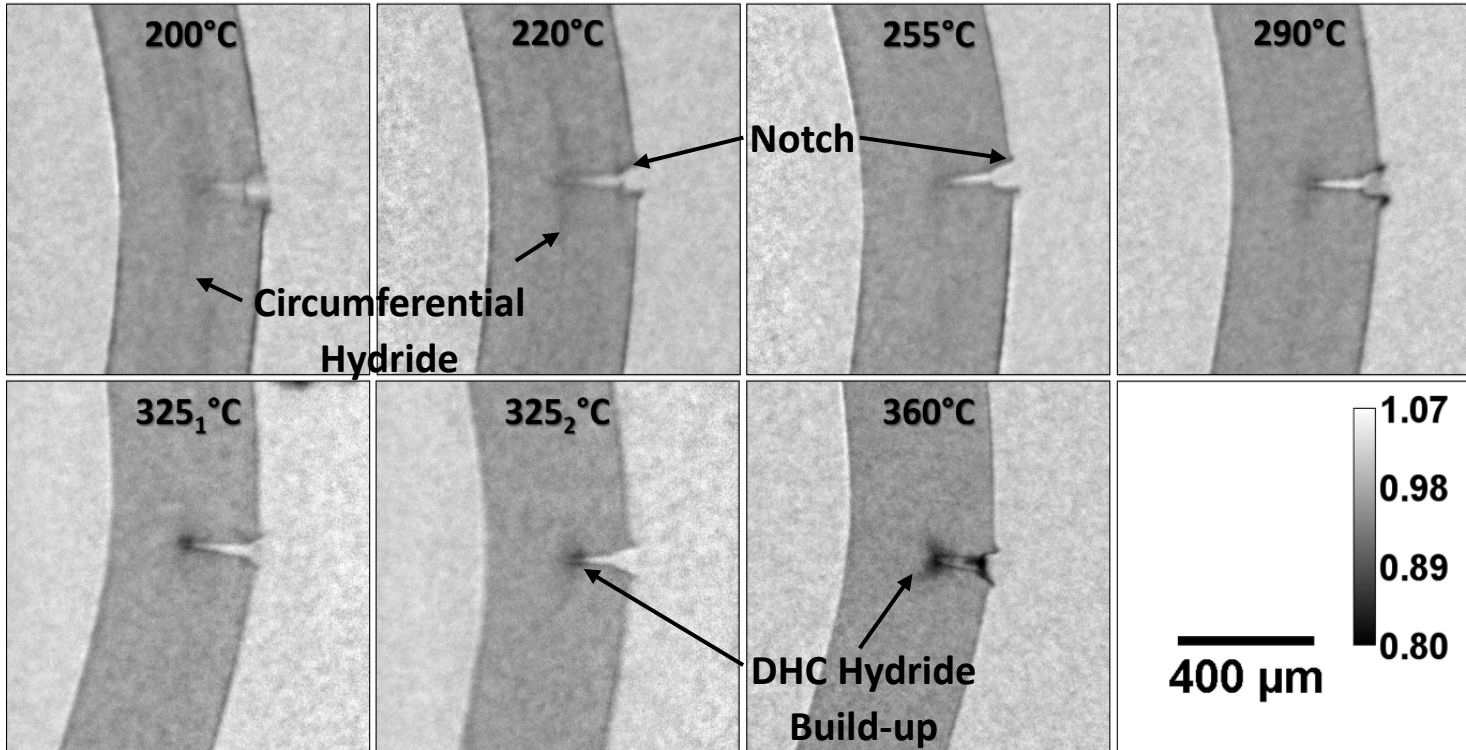


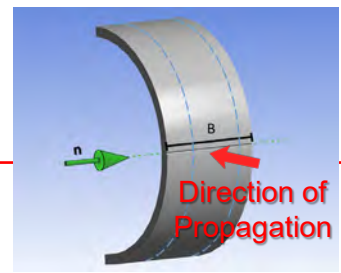




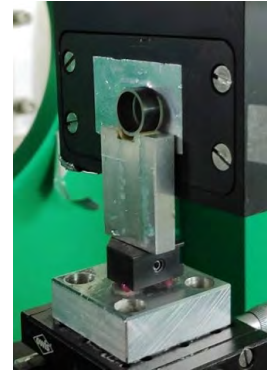
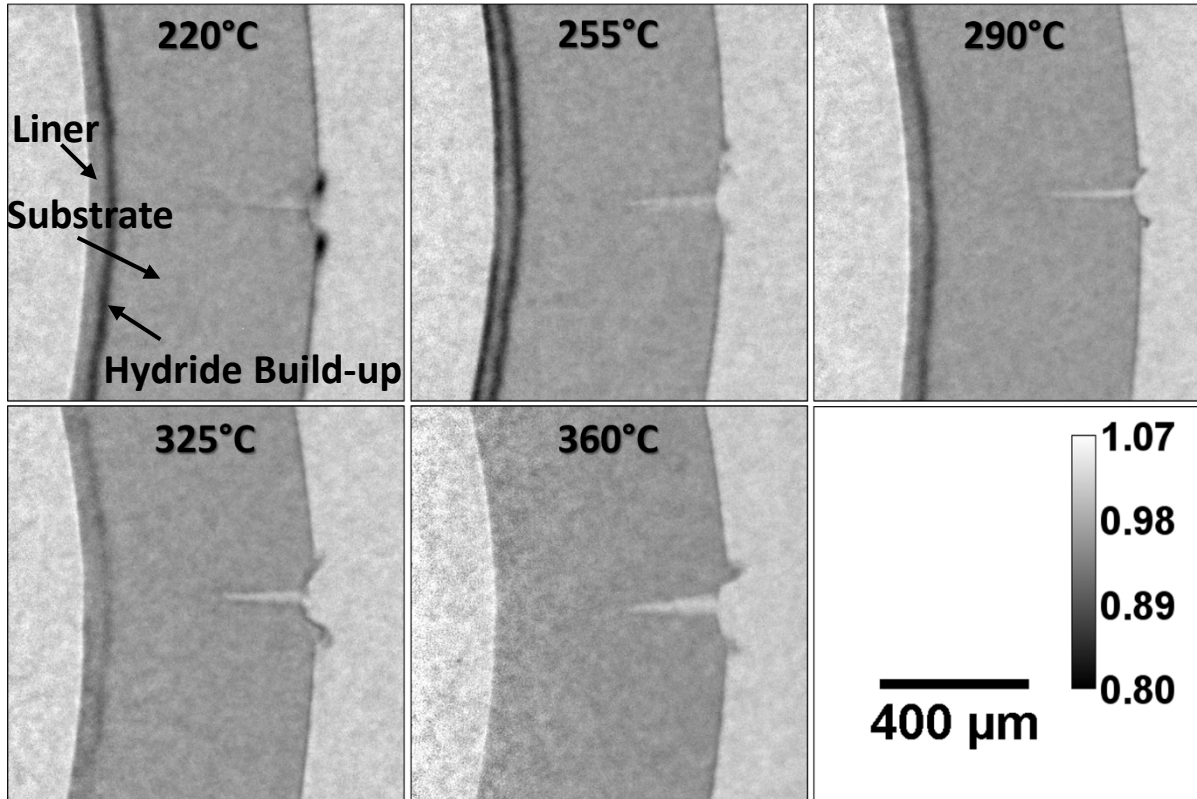


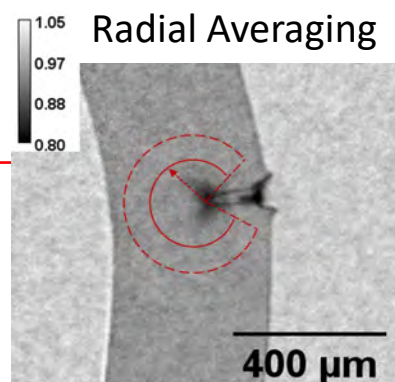
## Zircaloy-2 *without* inner liner (200 wppm H) 2.0 mm



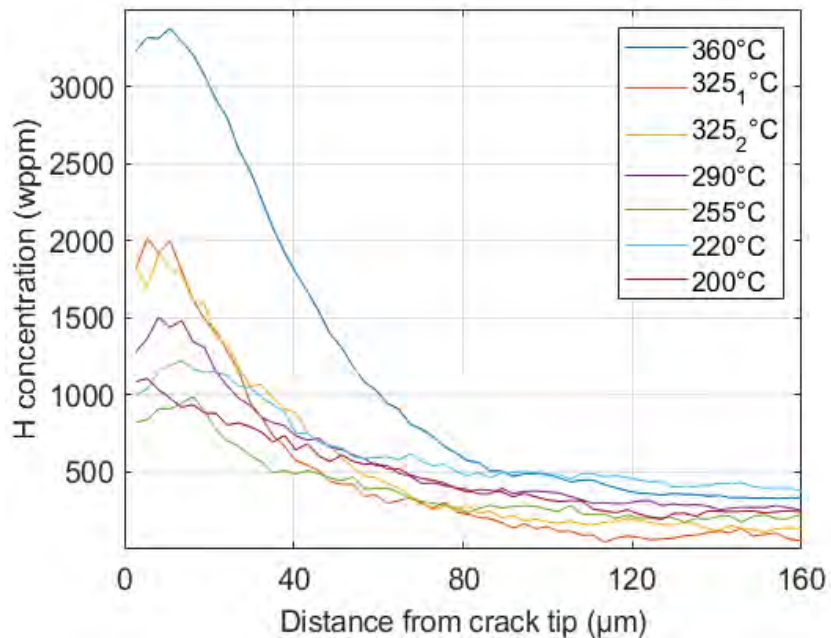


## Zircaloy-2 *with* inner liner (247 wppm H) 2.0 mm

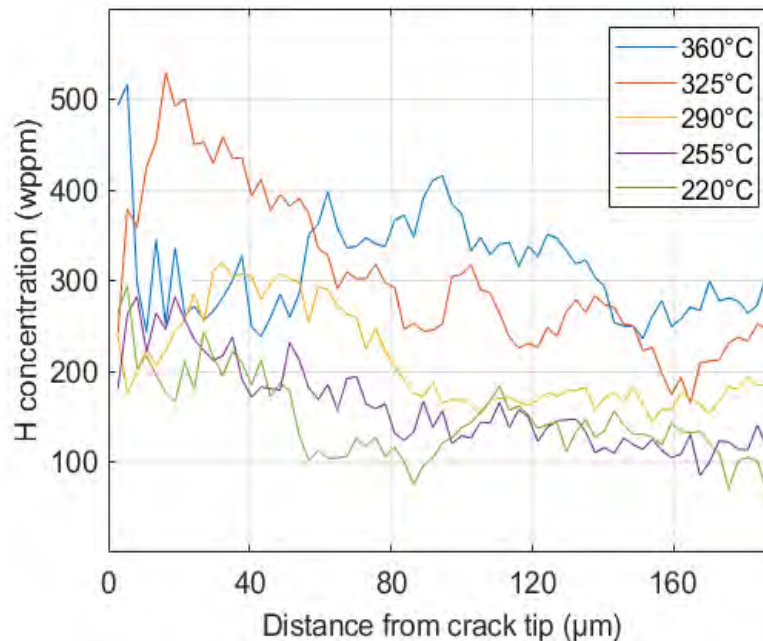




**without** inner liner

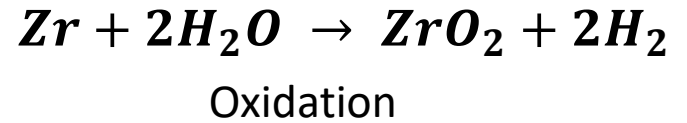
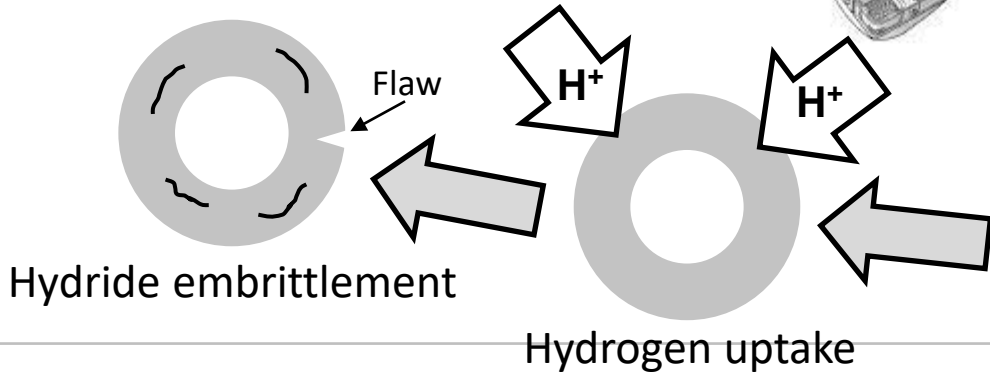
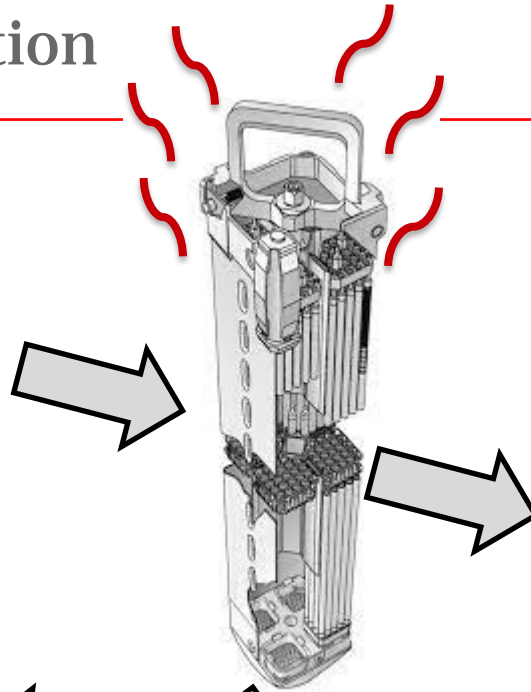


**with** inner liner





# Introduction





**M. Große**  
KIT

## **New test facilities at KIT for investigation of hydrogen/hydride behavior in Zr alloys**

In the framework of the investigations on the material behaviour during long-term dry storage, the experimental capabilities at KIT were improved. Three new or improved facilities were introduced: The SICHA furnace insert, the HoKi furnace and the INCHAMEL facility.

- The SICHA (**S**ieverts **C**hamber for **H**ydrogen **A**bsorption) furnace insert were improved by installation of diaphragm valves. This increases the leak-tightness of the insert. It was demonstrated by a four-week annealing at 450°C of a Zircaloy-4 sample in hydrogen. The hydrogen pressure in the apparatus decreases from 0.45 to 0.05 bar during this time. Even after 28 days an decrease of the total pressure in the SICHA occurs.
- The HoKi furnace was constructed for hydrogen loading of 2.5 m long cladding tubes shall be applied in a QUENCH bundle test. The five-zone furnace (three regular zones and heated flanges at both sides) is actually in the commissioning phase. First loading experiments results in an hydrogen uptake of 180 to 300 ppm depending on the position related to the gas injection system. A better procedure must be found to achieve a more homogeneous hydrogen loading.
- The INCHAMEL (**I**n-Situ **N**eutron Radiography **C**hamber for Tests under **M**echanical **L**oad) was designed together with the ZwickRoell company and constructed by ZwickRoell. The facility was dedicated for neutron radiography experiments under the following boundary conditions:
  - o Mountable on a neutron imaging beamline
  - o As less as possible distortion of the neutron beam by the facility
  - o Less as possible long-term activation of the facility by neutrons

These criteria were fulfilled by the following components

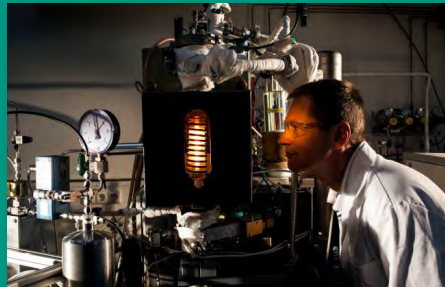
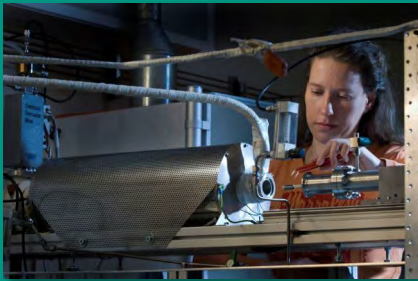
- o an inductive heating system using Helmholtz coils which are completely outside the neutron beam, and
- o contactless measurements of the temperature by two pyrometers and of the strain by a video or a laser extensimeter.

It was achieved that nothing else than the sample is in the beam. No beam windows are needed. The sample was commissioned in a beamtime from September 19-26 at the ICON facility at the Swiss neutron source SINQ at PSI Villigen in Switzerland. The feasibility of the concept of the facility was demonstrated.

# New test facilities at KIT for investigation of hydrogen/hydride behaviour in Zr alloys

**M. Grosse, S. Weick, J. Stuckert, C. Roessger**

KIT / Institute for Applied Materials – Applied Material Physics / Program NUSAFE



# Introduction

For the investigations of the hydrogen and hydride behavior under long term dry storage conditions the following parameters are needed:

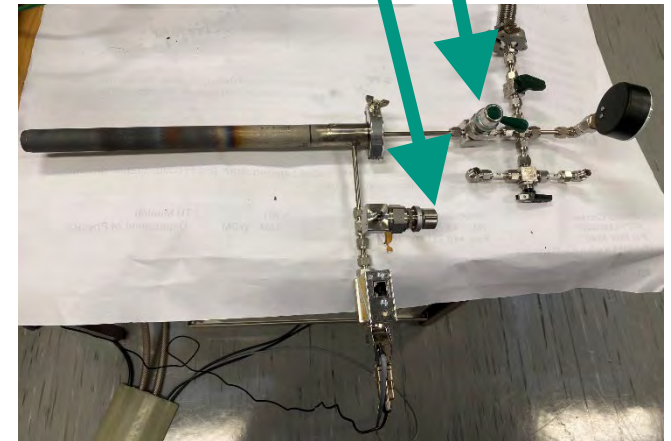
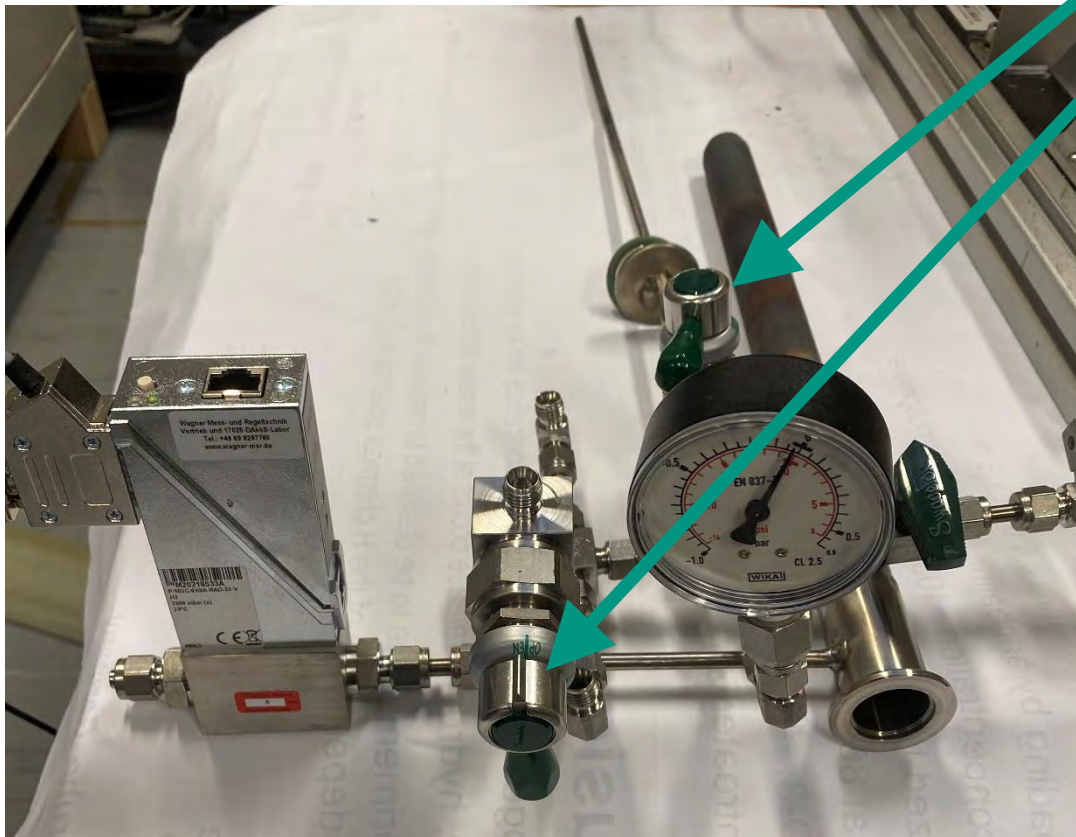
- temperature range between 100 and 500°C
- defined gas pressure (< 1 bar)
- defined mechanical load
- Requirements for neutron radiography experiments (low distortion of the neutron beam by the facility, low activation of the components)

The following experimental equipment achieving this conditions were commissioned or were improved:

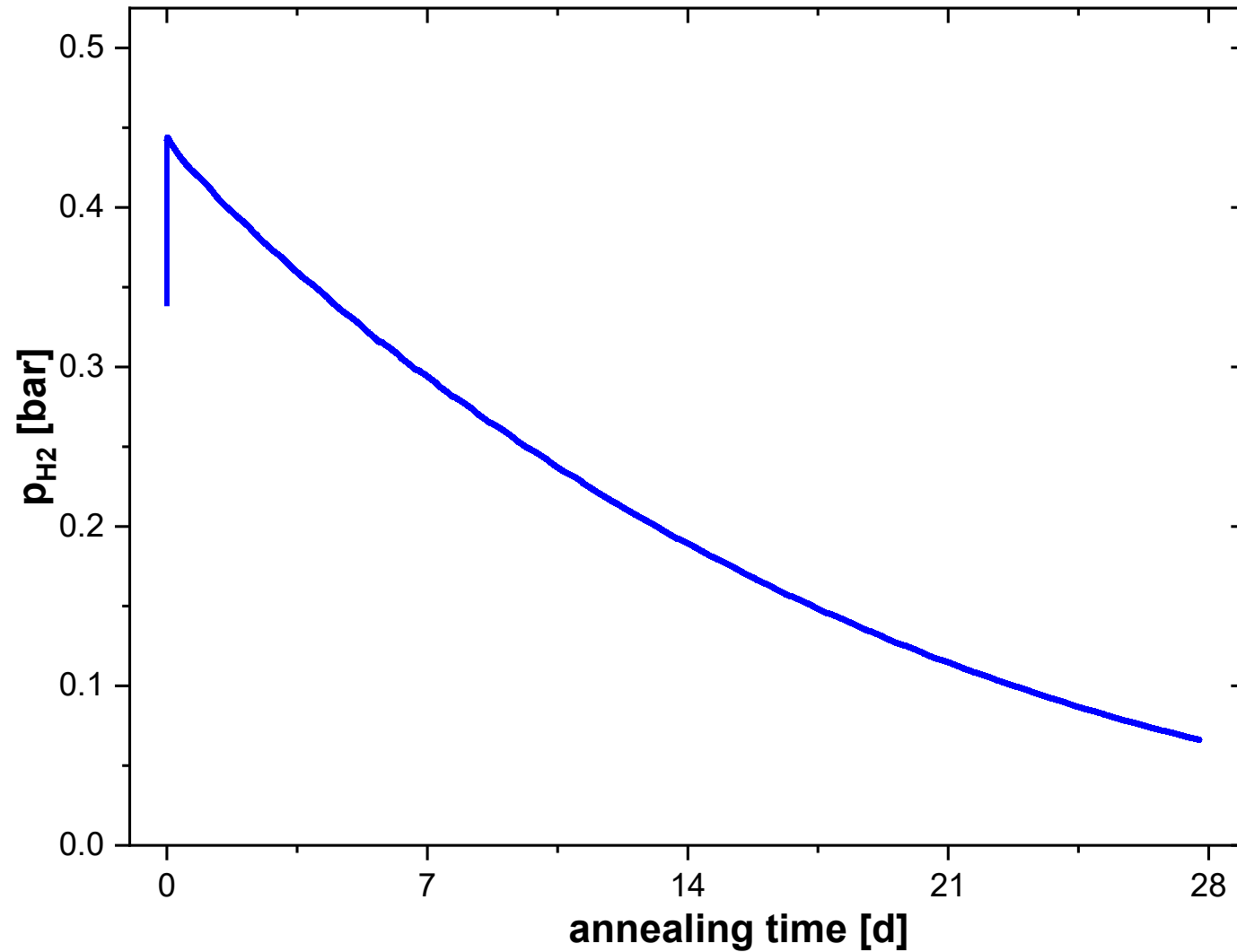
- Commissioning of the HoKi furnace for hydrogenation of long cladding tubes
- Commissioning of the INCHAMEL facility for in-situ neutron radiography investigations under defined temperature and mechanical stress
- Improvement of the SICHA furnace insert for hydrogenation of small samples.



Strong decrease of the leakage rate by mounting of diaphragm valves at both, the gas inlet and outlet tubes.



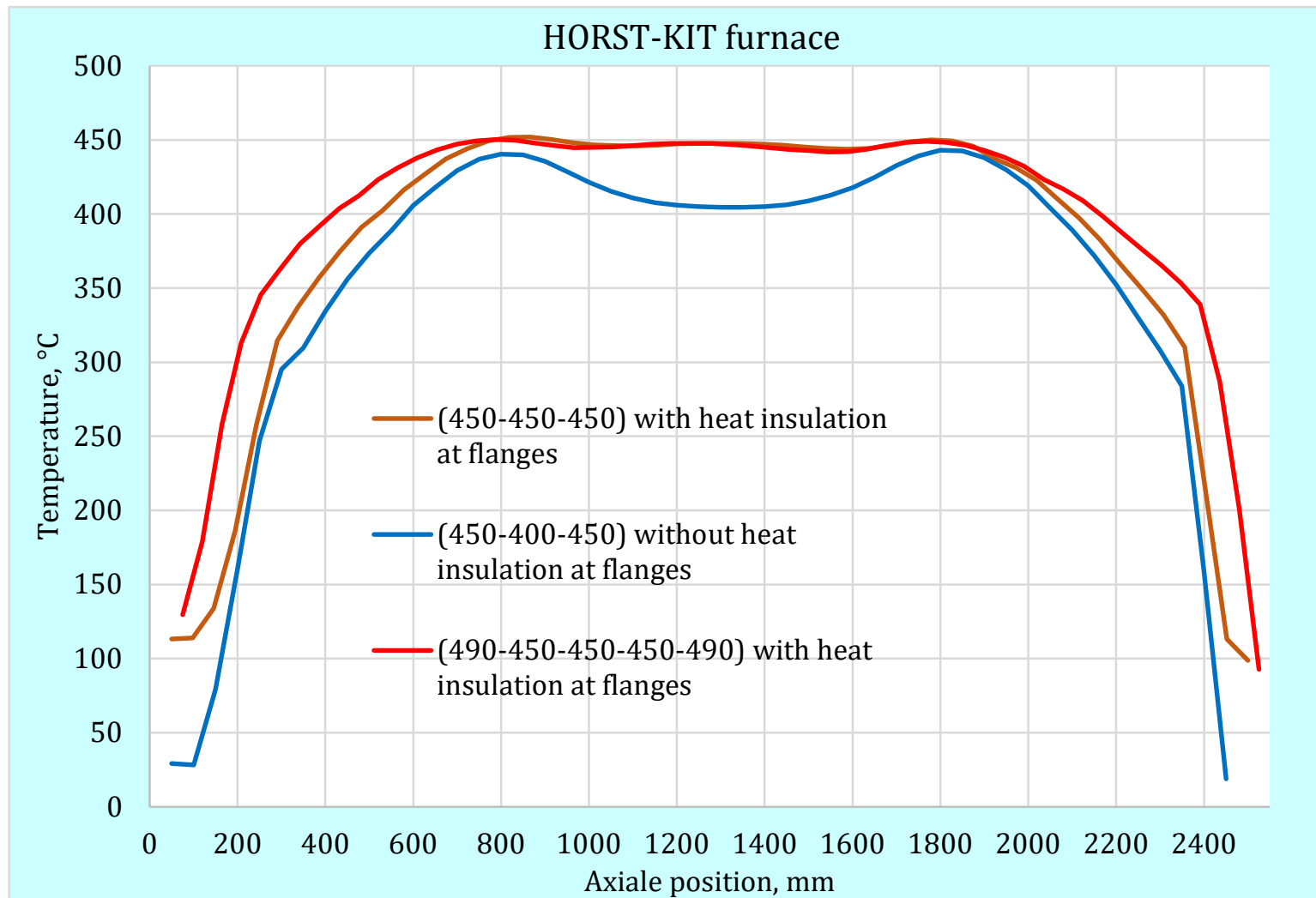
# SICHA – decrease of the hydrogen pressure



# HoKi furnace

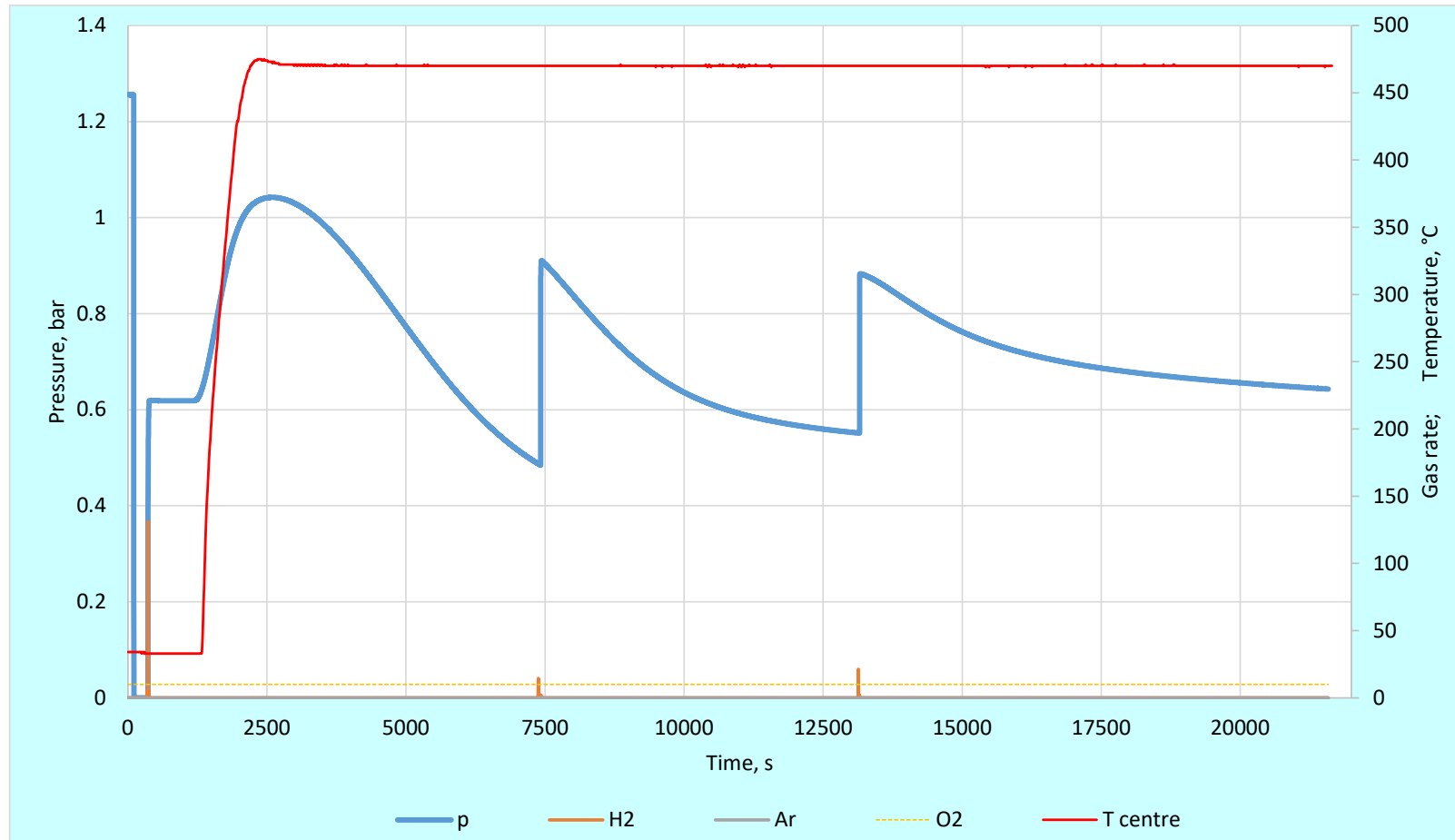


# Axial temperature distribution at the sample in the HoKi furnace





# Sample DUPLEX D-06: hydrogenation with new SWAGELOK diaphragm valve at $p < 1 \text{ bar}$ ; $T = 470 \text{ }^\circ\text{C}$



# First results of the PTE of the test cladding tube

Sample 10 (at gas injection position)

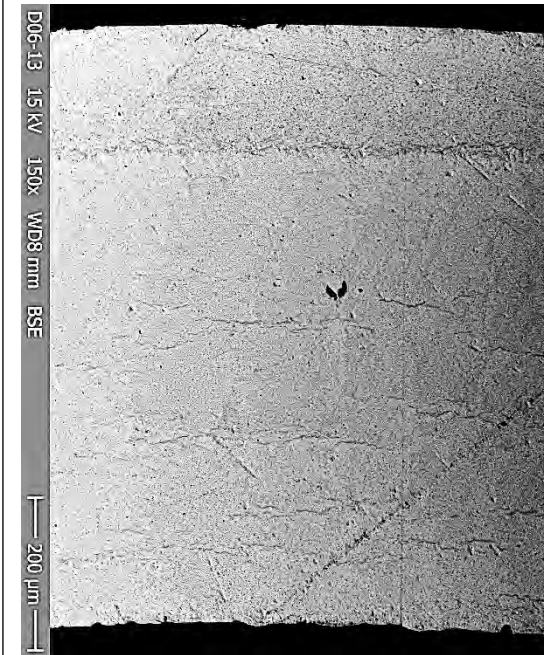
Sample 5 (middle position)

Sample 15 (position opposite to the gas injection position)

Optical view



SEM view



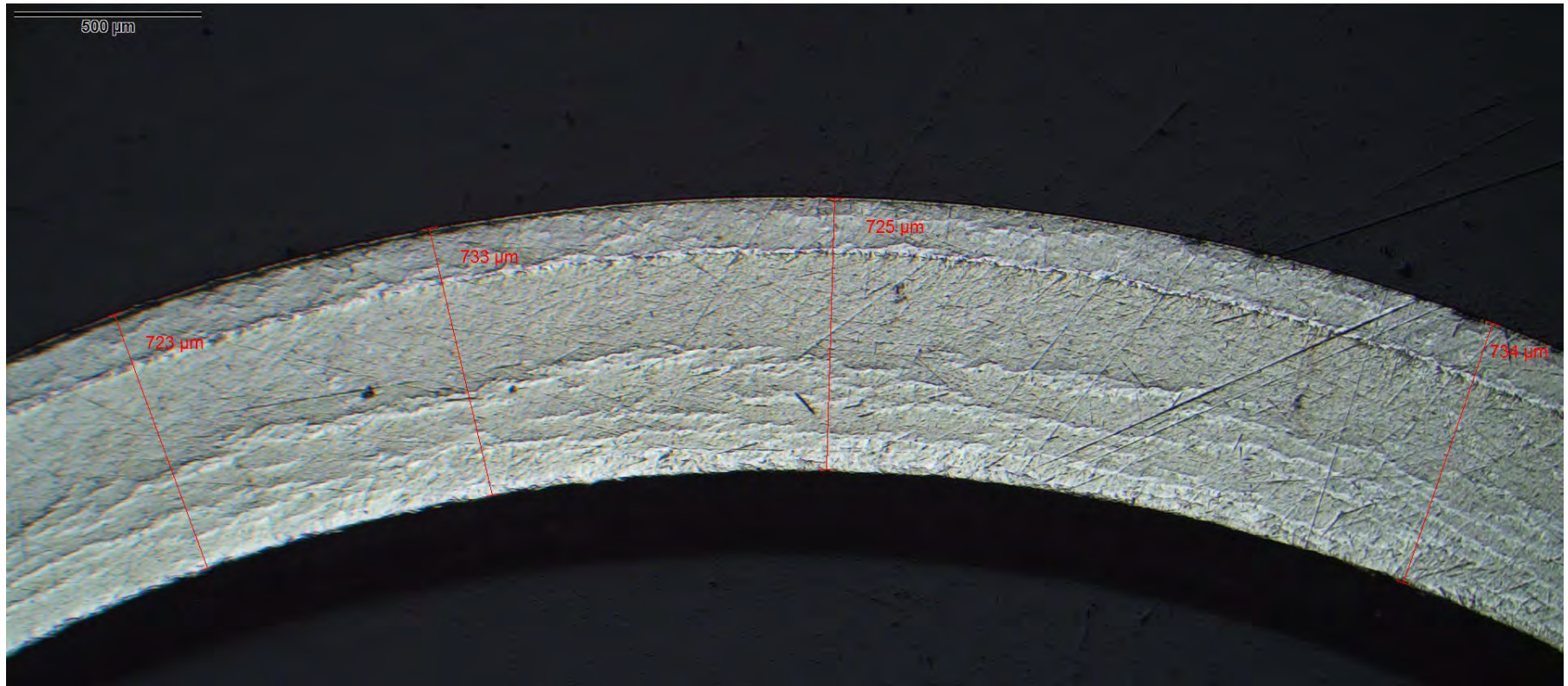
H conc.,  
wppm

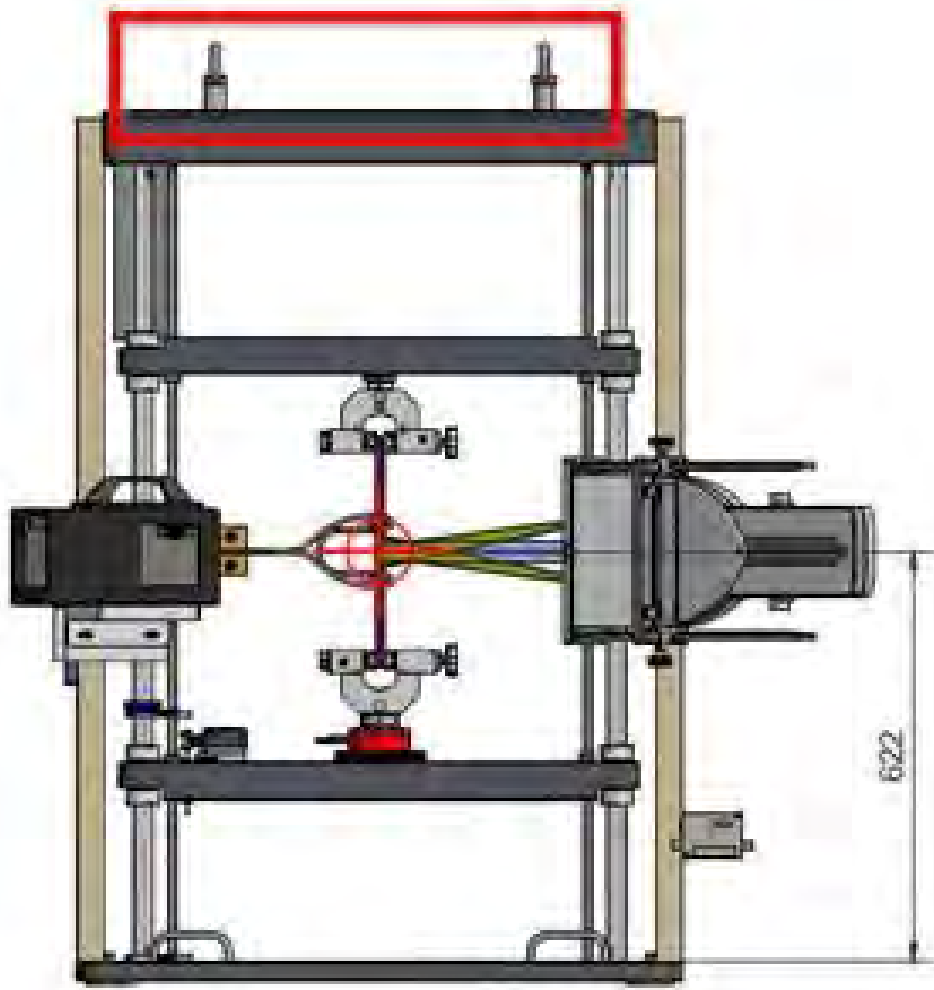
**288**

**199**

**172**

# HoKi furnace – Swelling of the tube wall due to hydrogenation





Nothing else than the sample is in the neutron beam

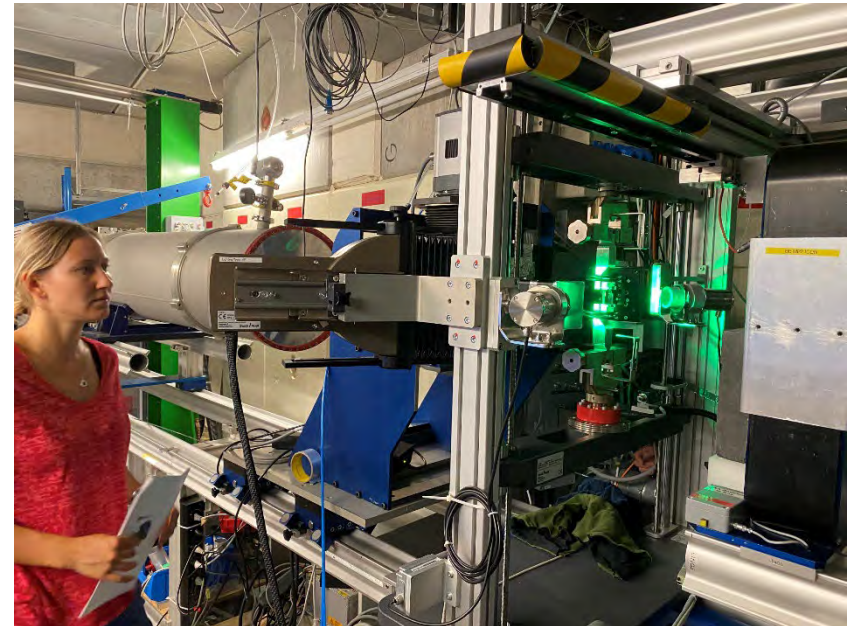
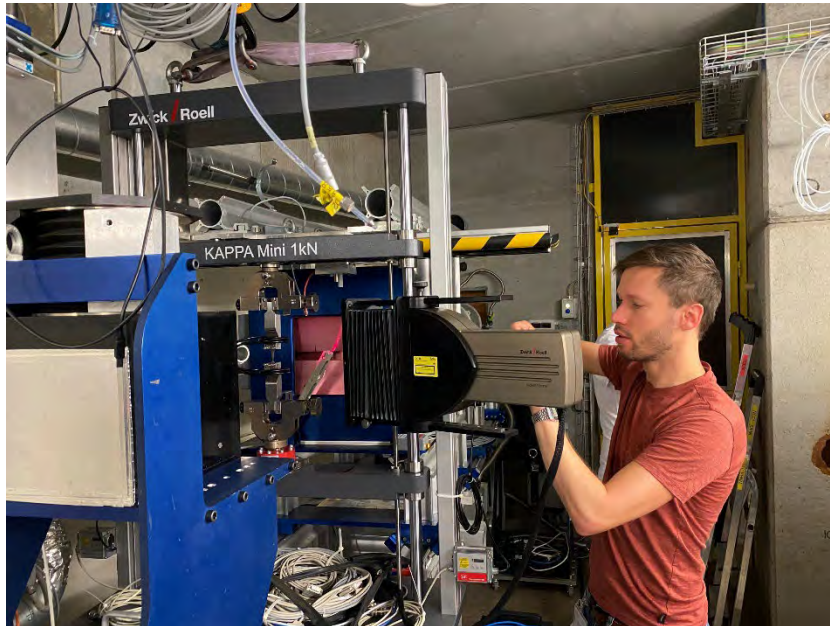
- Contactless measurement of the strain by video extensometer or laser extensometer
- Inductive heating by an Helmholtz coil (no beam window is needed)
- Contactless measurement of the temperature by two pyrometers

**Less activation,  
no distortion of the neutron  
image**

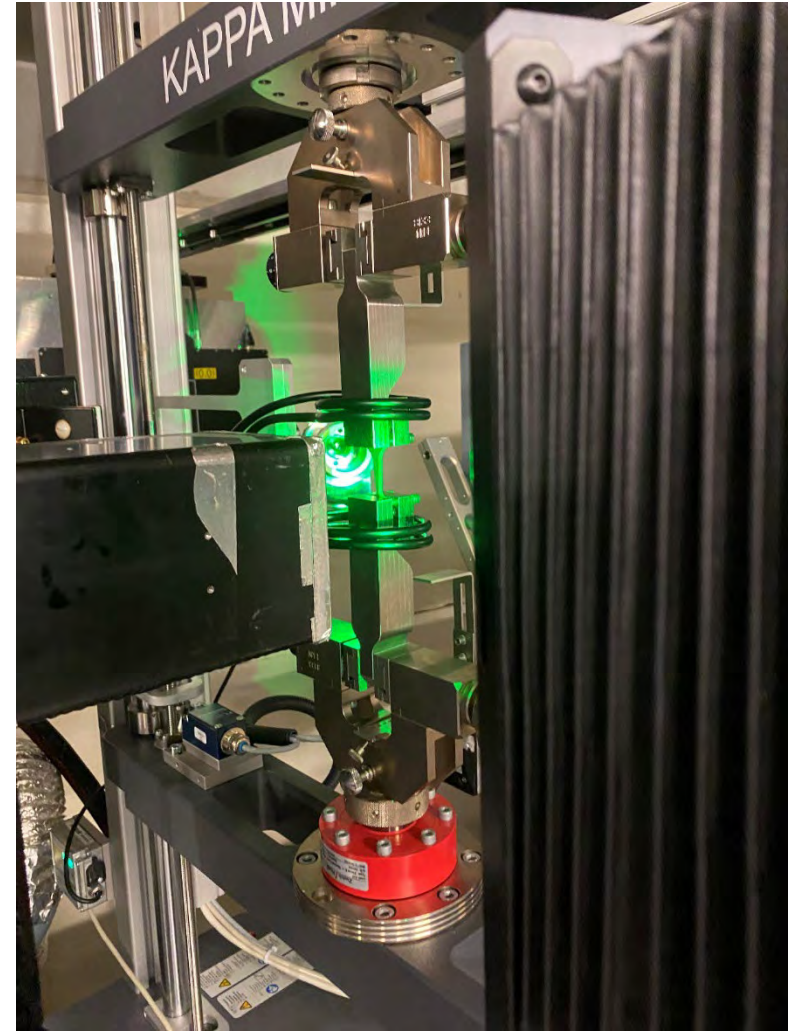
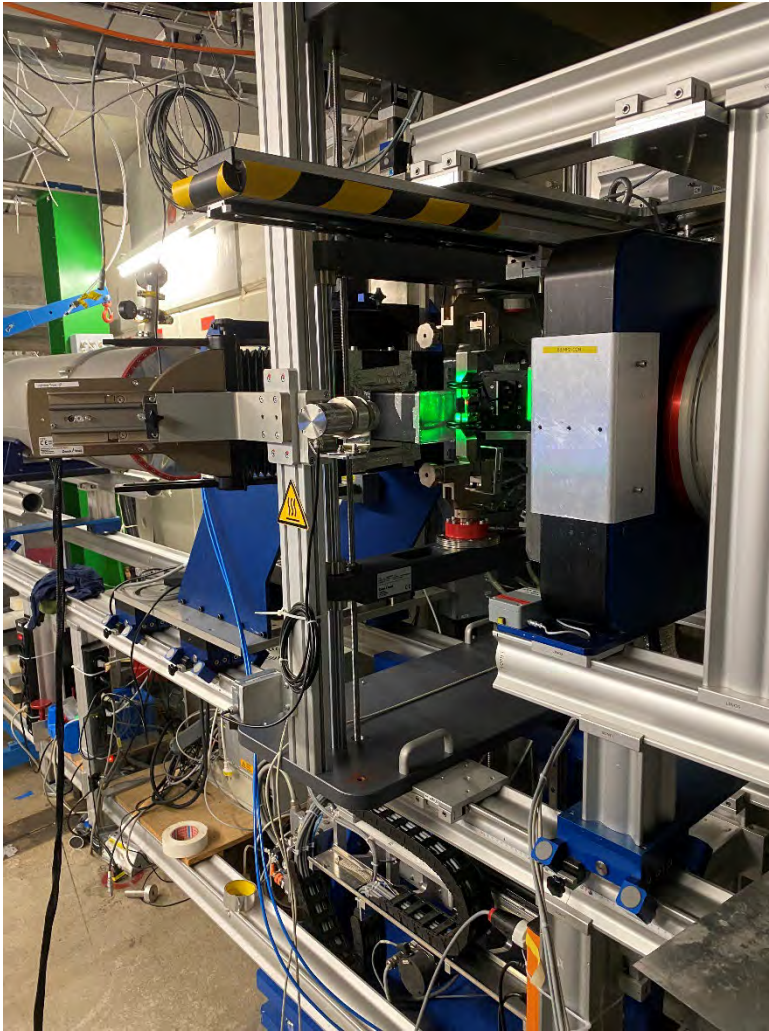


# INCHAMEL facility

- Commissioning tests at September 19 – 26 at the ICON facility (SINQ, PSI Villigen, Switzerland)
- Mounting of the INCHAMEL facility on the sample position of the ICON facility

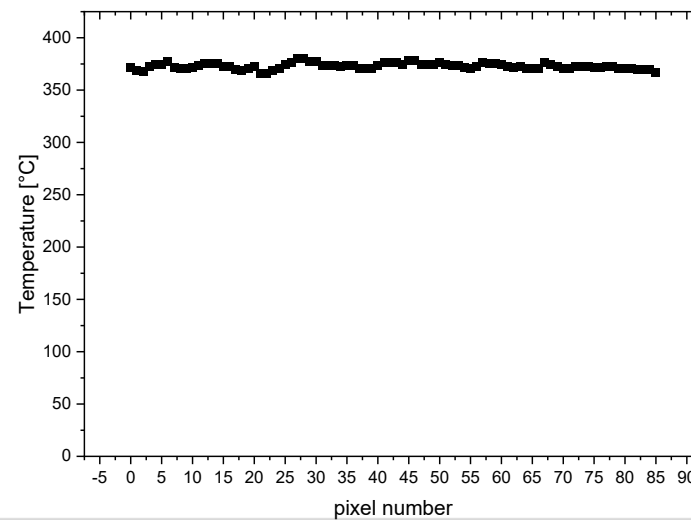
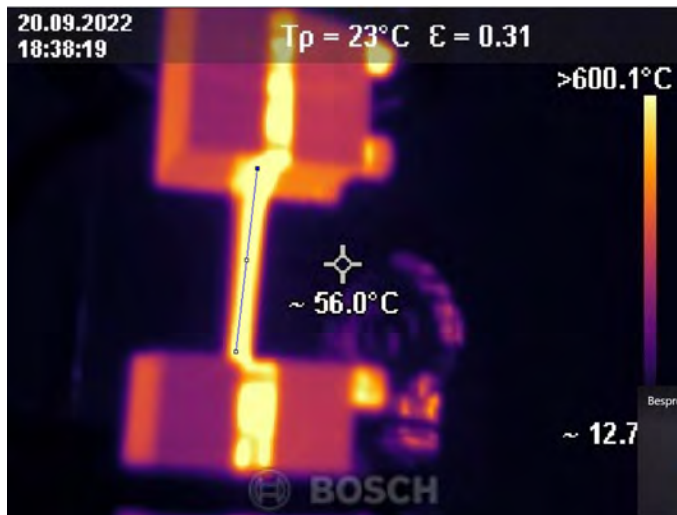
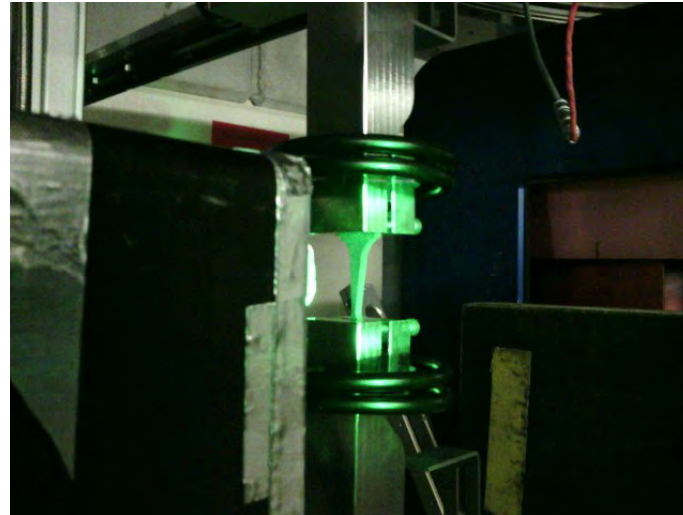
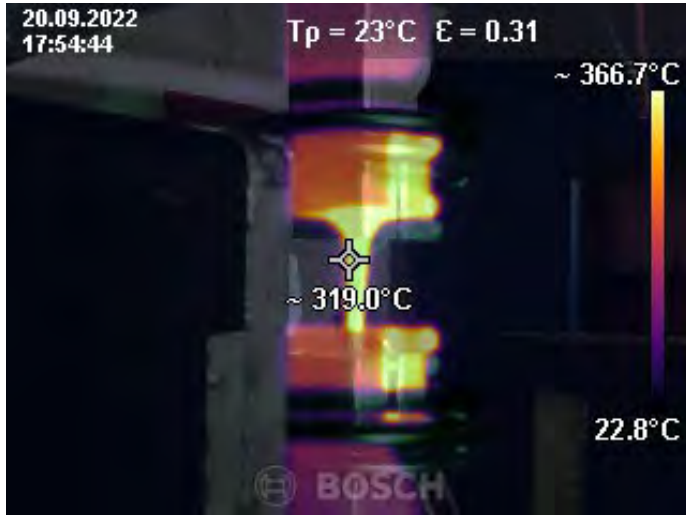


# INCHAMEL facility

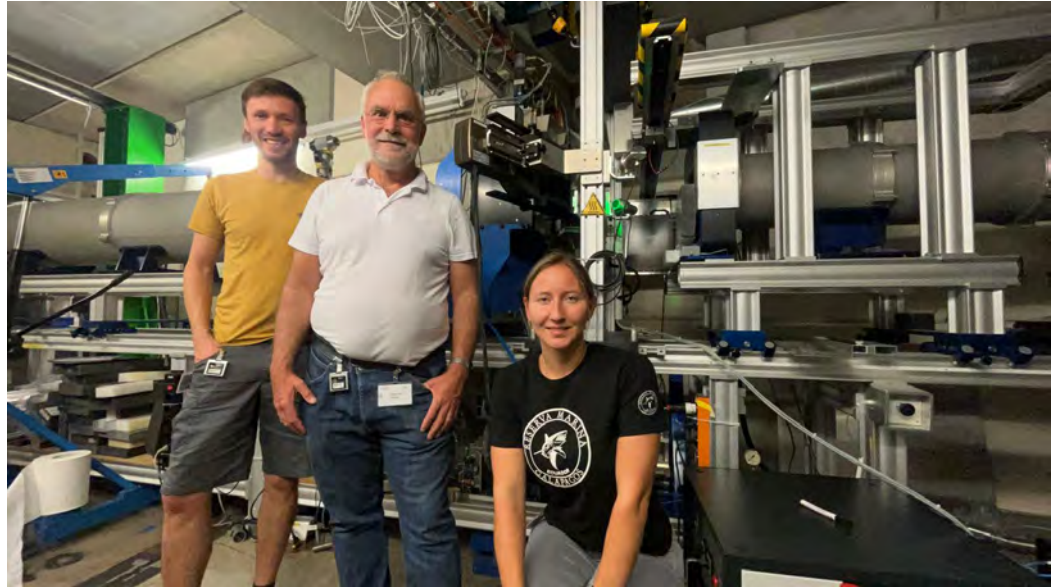
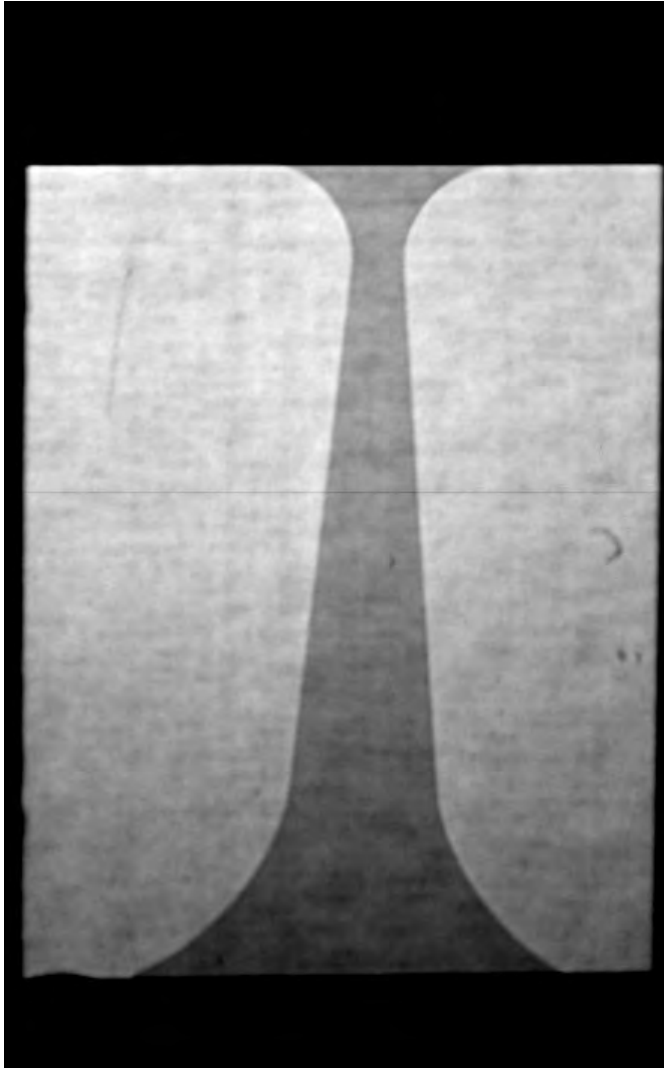




# INCHAMEL facility



# INCHAMEL - First images



Experimental team

Neutron radiograph of sample 20220815  
at 320°C before application of the  
mechanical load.

Data analysis will be started next week.



## Summary and Conclusion

- The SICHA works satisfying
- Commissioning of the HoKi has to be continued
- The INCHAMEL facility has demonstrated the feasibility of the conception. Several possibilities to improve the facility were identified.
- We are on a good way to install a powerful experimental basis for investigating hydrogen related processes occurring under long term dry storage conditions.

## Next steps

- SICHA: - no further improvements are planned
- HoKi: Different hydrogen loading procedures will be tested in the next week
- INCHAMEL
  - Improvement of the inductive Helmholtz coils
  - Fixed installed Al shielding before and behind the sample
  - Improvement of the sample holder
  - Ex-situ tests of the hydrogen redistribution

## Acknowledgement

The HoKi furnace and the INCHAMEL facility were financed by the HOVER project of the Helmholtz society. The SICHA apparatus was constructed using money of the SPIZWURZ budget.

The authors are grateful to the ZwickRoell company for the very good cooperation during the iterative development and construction of the INCHAMEL facility.

PSI for providing beamtime and particularly Anders Kaestner for his support during the measurements

Many thanks to the whole QUENCH team particularly Ulrike Stegmaier, Jutta Laier and Jürgen Moch.

# Thank you for your attention

## 27<sup>th</sup> International QUENCH Workshop - List of participants

	<b>Family Name</b>	<b>First Name</b>	<b>Institution</b>	<b>Country</b>	<b>Remote</b>
1	Afiqa	M	JAEA	Japan	x
2	Alakiozidis	Ioannis	University of Manchester	United Kingdom	
3	Allison	Chris	INNOVATIVE SYSTEMS SOFTWARE, LLC	USA	
4	Ambard	Antoine	EdF	France	x
5	Aryanfar	Asghar	American University of Beirut	Lebanon	
6	Birchley	Jon	PSI retired	UK	x
7	Boldt	Felix	GRS	Germany	
8	Bottomley	Paul David	JRC Karlsruhe retired	Germany	
9	Brachet	Jean-Christophe	CEA, Paris-Saclay University	France	
10	Bratfisch	Christoph	RUB	Germany	
11	Campbell	Shawn	U.S. NRC	United States of America	
12	Colldeweih	Aaron	PSI	Switzerland	
13	Cozzo	Cerdric	PSI	Switzerland	x
14	Czerniak	Luke	Westinghouse Electric Company	USA	
15	Daum	Robert	EPRI	United States	x
16	Duriez	Christian	IRSN	France	
17	Elsalamouny	Noura	Lithuania Energy Institute	Lithuania	x
18	Esmaili	Hossein	U.S. NRC	U.S.A.	
19	Falk	Florian	GRS	Germany	
20	Fargette	Andre	Framatome SAS	France	
21	Gabriel	Stephan	KIT	Germany	
22	Goddard	Dave	NNL	UK	x
23	Grosse	Mirco	KIT	Germany	
24	Guillard	Gaétan	IRSN	France	
25	Haste	Timothy	Imperial College, London	UK	
26	Hollands	Thorsten	GRS	Germany	x
27	Howell	Jutta	KIT	Germany	
28	Jäckel	Bernd	PSI retired	Germany	
29	Jarugula	Rajesh	Research Centre Rez	Czech Republic	
30	Kaji	Yoshiyuki	JAEA	Japan	x
31	Kakiuchi	Kazuo	JAEA	Japan	x
32	Kaliatka	Tadas	Lithuania Energy Institute	Lithuania	
33	Laier	Jutta	KIT	Germany	
34	Lee	Youho	Seoul National University	Korea	



35	Lind	Terttaliisa	PSI	Switzerland	x
36	Martin	Julie-Fiona	OECD NEA	France	
37	Matocha	Vitezslav	UJV Rez	Czech Republic	
38	Nagy	Richard	Centre for Energy Research (EK)	Hungary	
39	Nahm	Daniel	GRS	Germany	
40	Nakamura	Kinya	CRIEPI	Japan	
41	Nemoto	Yoshiyuki	IAEA	Japan	x
42	Ohta	Hirokazu	CRIEPI	Japan	x
43	Pouillier	Edouard	EdF	France	x
44	Roessger	Conrado	KIT	Germany	
45	Sanchez	Victor	KIT	Germany	
46	Sappl	Jonathan	GRS	Germany	
47	Schubert	Arndt	JRC Karlsruhe	Germany	
48	Sevecek	Martin	CVUT	Czech Republic	x
49	Shirzadi	Sahar	LEI	Lithuania	x
50	Sim	Ki Seob	IAEA	Austria	x
51	Stahlberg	Gregor Tobias	Ruhr-University Bochum	Germany	
52	Stegmaier	Ulrike	KIT	Germany	
53	Steinbrück	Martin	KIT	Germany	
54	Stuckert	Juri	KIT	Germany	
55	Sutygina	Alina	GRS	Germany	
56	Tang	Chongchong	KIT	Germany	
57	Tiborcz	Livia	GRS	Germany	
58	Tromm	Th. Walter	KIT	Germany	
59	Usagawa	Yutaka	IAEA	Japan	x
60	Van Uffelen	Paul	JRC Karlsruhe	Germany	
61	Wang	Guoqiang	Westinghouse Electric Company LLC	USA	
62	Wang	Shisheng	KIT	Germany	
63	Weick	Sarah	KIT	Germany	
64	Wiss	Thierry	JRC Karlsruhe	Germany	
65	Wolff	Marc	ENSI	Switzerland	x
66	Yook	Hyunwoo	Seoul National University	Republic of Korea	
67	Zhanal	Pavel	Research Centre Rez	Czech Republic	
68	Zhe	Yuan	U.S. NRC	USA	x



FORSCHUNG  
LEHRE  
INNOVATION



**KIT** FORSCHUNG LEHRE INNOVATION  
Karlsruher Institut für Technologie



**NEA** **QUENCH-ATF Joint Undertaking** **KIT**

- Three bundle experiments with ATF cladding in the QUENCH facility
- Time frame: 2021-2024
- Costs: 1.5 M€ (approx. 500 000 € test) + NEA four
- 50% covered by KIT Germany, 50% covered by contributors















Did I forget anything?

Questions, comments,  
complaints to:  
[martin.steinbrueck@kit.edu](mailto:martin.steinbrueck@kit.edu)

